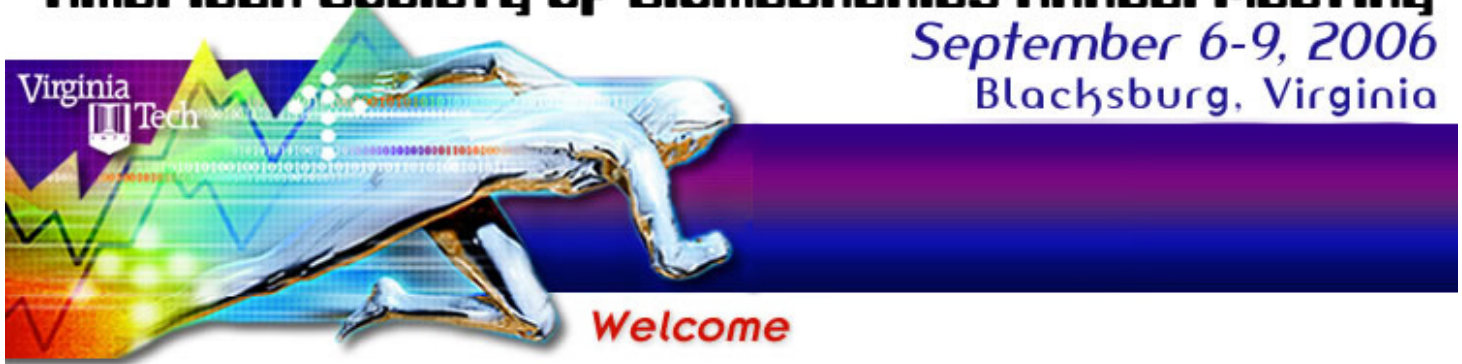


# American Society of Biomechanics Annual Meeting

September 6-9, 2006  
Blacksburg, Virginia



Welcome!

[Home](#)

[Program](#)

[Author Index](#)

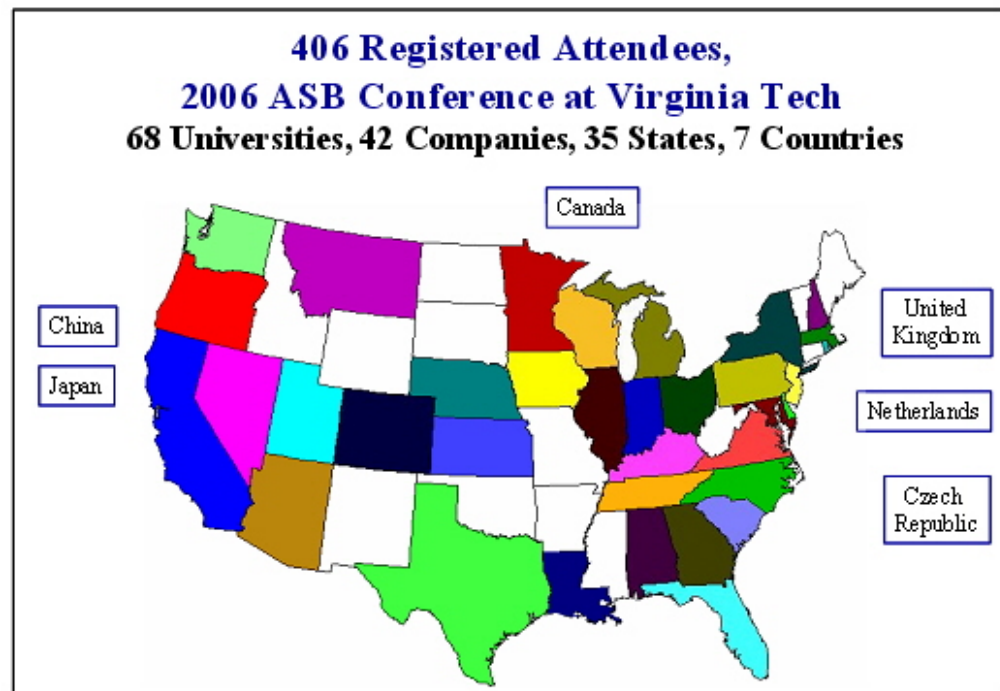
[Search](#)

[Sponsors](#)

[Committees](#)

[CD Tech Support](#)

The Virginia Tech - Wake Forest School of Biomedical Engineering and Sciences is honored to host the 30th Annual Meeting American Society of Biomechanics at Virginia Tech from September 7 – 9, 2006. Over 400 people attended the conference from 68 universities and 42 companies from across the United States and around the world as shown in the illustration below.



The organizers have worked hard to develop an exciting program that is detailed on this CD. In particular, the program was expanded to allow for more podium presentations with approximately 150 slotted for the conference. Also new to ASB this year was six thematic poster sessions that encouraged a lively debate and exchange of ideas on posters with similar topics. In addition to these new ideas, the conference had traditional style poster sessions, invited lectures, symposia, tutorials and lab tours.

The following individuals are to be thanked for developing this exciting conference:

**2006 ASB Meeting Host Committee**

Stefan Duma (Chair)  
Kevin Granata (Co-chair)  
Mike Madigan (Co-chair)

**2006 ASB Program Committee**

Irene Davis (Chair)  
Jack Dennerlain  
Dan Ferris  
Joseph Hamill  
Clare Milner  
Steve Piazza

# GAIT VELOCITY AND SWAY IN ATHLETES AND NON-ATHLETES FOLLOWING CONCUSSION

Tonya M Parker, Louis R. Osternig and Li-Shan Chou

University of Oregon, Eugene, OR, USA

E-mail: [chou@uoregon.edu](mailto:chou@uoregon.edu) Web: <http://biomechanics.uoregon.edu/chou/>

## INTRODUCTION

Much of the current concussion literature has focused on neuropsychological testing. While the use of this type of evaluation has recently been advocated as the “cornerstone” of proper concussion management (Guskiewicz et al., 2004) it does not assess all domains that may be impacted by brain injury. One such domain that has not frequently been investigated is post-concussion recovery of dynamic motor function. Parker and colleagues (*in press*) introduced a method of assessing concussion and recovery that focused on gait as a dynamic functional motor task during conditions of divided and undivided attention. It was found that gait stability, marked by increased sway and sway velocity of the whole body center of mass (COM), decreased when concussed subjects were asked to walk while simultaneously performing a secondary cognitive task compared to walking without mental distraction. A recent study has further suggested that participation in contact sports may produce cognitive impairments without diagnosed concussion (Killiam et al., 2005). Therefore, the purpose of this study was to investigate the extent to which athletes differ from non-athletes in the maintenance of gait stability following concussion.

## METHODS

Fifty-six college-aged men and women served as subjects for this study. The subjects were categorized into four groups according to athlete and concussion status.

The concussed groups consisted of NCAA Division 1 or University Club Sports athletes (CONC-A; n=14) and non-athletes who engaged in no regular sports activities (CONC-NA; n=14). The uninjured control groups consisted of NCAA Division 1 or University Club Sports athletes (NORM-A; n=14) and non-athletes who engaged in no regular sports activities (NORM-NA; n=14). The control subjects were matched to concussed subjects by gender, age, height, weight, and physical activity. All CONC subjects were tested within 48 hours of injury and again at 5, 14, and 28 days post-injury. The NORM participants were tested at the same time intervals.

The gait protocol was the same for each testing day and consisted of level walking with no obstructions and was performed under two conditions: 1) with undivided attention (single-task) and 2) while simultaneously completing simple mental tasks (dual-task). In order to assess gait variables a set of 31 reflective markers were placed on bony landmarks. An eight-camera motion analysis system (Motion Analysis Corporation, Santa Rosa, CA) was used to capture and reconstruct the 3-dimensional trajectory of the surface markers and compute the COM.

Variables were examined in one gait cycle including the medial-lateral COM displacement (MLdisp) and average gait velocity (GV). Repeated measures (4 x 2 x 4) mixed design analyses of variance (ANOVAs) were performed to determine whether differences ( $p < 0.05$ ) existed

between groups and within task and day. An analysis of co-variance was used to identify any effects of between-group GV differences on the COM displacement in the frontal plane.

## RESULTS AND DISCUSSION

The gait velocity of athlete groups was significantly slower than non-athlete groups in both task conditions for all testing days. During the single-task, the concussed and normal athletes walked significantly slower than the concussed ( $p = 0.032$ ;  $p = 0.002$ ) and normal non-athletes ( $p = 0.003$ ;  $p = 0.000$ ). With the addition of the dual-task, the GV was slower for both athlete groups when compared to the normal non-athletes ( $p = 0.002$ ;  $p = 0.001$ ).

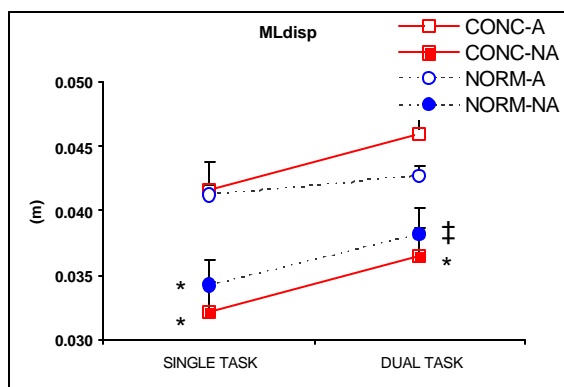


**Figure 1:** Group means and standard errors for medial-lateral displacement in single- and dual-task conditions averaged across testing days. \*\* = Significantly less than CONC-A and NORM-A; ‡ = Significantly less than CONC-A.

For MLdisp the dual-task produced significantly greater sway than the single-task for all groups ( $p = 0.002$ ). Specifically, during the single-task the concussed and non-concussed athletes had significantly greater sway than the concussed ( $p = 0.000$ ;  $p = 0.000$ ) and normal non-athletes ( $p =$

$0.004$ ;  $p = 0.006$ ). For the dual-task condition, the CONC-A group demonstrated significantly more sway than either non-athlete group (CONC-NA,  $p = 0.002$ ; NORM-NA,  $p = 0.001$ ) while the NORM-A subjects showed greater sway than those in the CONC-NA group ( $p = 0.001$ ; Figure 1). Furthermore, the analysis of co-variance showed no significant effect of gait velocity on the medial-lateral COM displacement ( $p = 0.178$ ).

The athletes whether concussed or not, displayed greater sway excursion than the non-athletes. In contrast, the athletes walked slower than the non-athletes. These differences were pronounced during the dual-task compared to the single-task condition and were evident from 2 to 28 days.

## SUMMARY/CONCLUSIONS

The current results suggest that individuals with concussion may maintain their balance through reduced sagittal plane movement in an effort to control for increased coronal plane sway.

## REFERENCES

- Guskiewicz, K.M., Bruce S.L., Cantu R.C., et al. (2004) *J. Ath. Train.* **39**: 280-297.  
 Killam C., Cautin R.L., Santucci A.C. (2005). *Arch Clin Neuropsychol* **20**: 599-611.  
 Parker T.M., Osternig L.R., van Donkelaar P. et al. *MSSE (in press)*.

## ACKNOWLEDGEMENTS

This study was supported by the Centers for Disease Control and Prevention (R49/CCR021735 and CCR023203).

# THE CHARACTERIZATION OF PASSIVE ELASTIC JOINT MOMENT-ANGLE RELATIONSHIPS IN THE LOWER EXTREMITY

<sup>1</sup>Amy Silder, <sup>2</sup>Ben Whittington, <sup>3</sup>Bryan Heiderscheit, <sup>1,2,3</sup>Darryl Thelen,  
Departments of <sup>1</sup>Biomedical Engineering, <sup>2</sup>Mechanical Engineering, and <sup>3</sup>Orthopedics and  
Rehabilitation, University of Wisconsin, Madison, WI, USA  
E-mail: silder@wisc.edu

## INTRODUCTION

Passive elastic joint moments arise from the deformation of connective tissue surrounding a joint. Furthermore, motion at one joint may influence the passive elastic moment at a neighboring joint due to the stretch of bi-articular muscles (e.g. rectus femoris). Methods of describing bi-articulate coupling under active (Herzog, 1991) and passive (Edrich, 2000; Hoang, 2005; Riener, 1999; Vrahas, 1990) conditions have been investigated. However, prior approaches only consider a limited number of joint angle combinations, which limits the robustness of the approach. Furthermore, bi-articulate coupling facilitates the transfer of energy across joints. This coupling requires that passive joint moment-angle models be formulated that properly conserve energy. Finally, the identification of subject-specific moment-angle relationships is often not done, yet is relevant for understanding the role of passive forces during functional movement. The purpose of this study was to develop a comprehensive subject-specific method of describing the passive elastic joint moment-angle relationships about the hip, knee, and ankle while ensuring energy conservation across joints.

## METHODS

**Experimental procedure:** Nine healthy young adults participated in the study. Subjects were positioned side-lying with their dominant limb supported on a table via low friction carts placed under the medial side of the thigh and leg. A padded brace prevented movement of the pelvis during testing. A physical therapist slowly manipulated the limb in 16 unique motion

coupling trials of the hip, knee, and ankle using hand-held 3D load cells. Three-dimensional kinematics of the lower extremity and of the load cells were collected (100Hz) using a passive motion capture system (Figure 1). Load cell forces and moments were simultaneously recorded, and EMG signals from seven lower extremity muscles were monitored to ensure that the muscles remained relaxed.

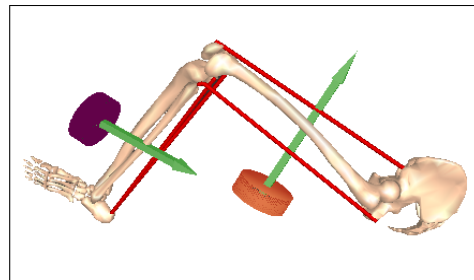


**Figure 1:** The kinematics of reflective markers were monitored to characterize lower-extremity motion as well as the location of two hand-held load cells.

To evaluate the experimental method, eight additional validation trials were performed. Additionally, one trial was repeated three times within each test session (Figure 2).

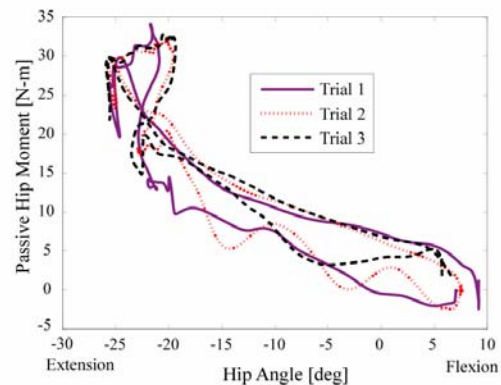


**Figure 2:** Three trials of hip extension followed by knee flexion for the same subject. The graphs demonstrate the repeatability of the collected joint moment-angle measurements between trials.

**Analyses:** Three-dimensional joint moments were computed at the hip, knee, and ankle using the measured load cell forces, body segment kinematics, and joint center positions. A set of eight exponential functions that accounted for the stretch of uni-articular and bi-articular (rectus femoris, hamstrings, gastrocnemius) muscles were used to describe the relationship between the passive hip, knee, and ankle moments, and corresponding joint angles. Uni-articular exponential functions were described by two parameters (offset angle, stiffness). Bi-articular functions included a third parameter (the ratio of moment-arms between neighboring joints), thereby ensuring conservation of energy storage and release. A least squares approach was used to estimate the model parameters using subject-specific measurements. Validity of the parameters was evaluated by using the estimated parameters to calculate joint moments in the eight validation trials not used in parameter estimation.

## RESULTS AND DISCUSSION

Similar trends in model parameter estimates were observed across subjects. Errors between measured and model-predicted joint moments were relatively small (Table 1). Similar results were obtained when applying the model to the unique data sets, thereby increasing confidence in the model validity. Inter-subject variability was apparent at all three joints suggesting subject-specific passive properties (Figure 3).

**Table 1:** Mean (s.d.) root-mean-squared errors (in N-m) between model-predicted and measured joint moments.

RMS Errors	Hip	Knee	Ankle
Identification trials	3.1 (0.5)	1.4 (0.3)	0.7 (0.5)
Validation trials	3.9 (2.5)	1.7 (0.7)	1.2 (0.5)

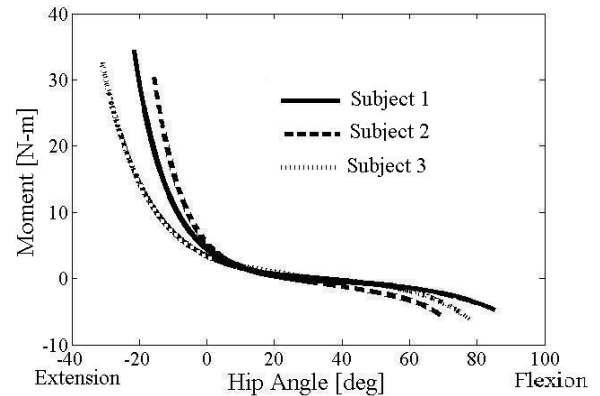


**Figure 3:** Predicted hip joint moments of three subjects. Variation was evident in the passive moment-angle relationship between subjects.

## SUMMARY/CONCLUSIONS

It has been suggested that passive elastic mechanisms may serve as efficient energy storage and release mechanisms during normal gait (Ishikawa, 2005; Muraoka, 2005), and furthermore, that neuromuscular changes with age or injury may alter their usage (McGibbon, 2003; Edrich, 2000). The methods proposed here provide a consistent methodology to be used for quantifying the role of passive joint moments in abnormal gait or in muscle remodeling following surgery or athletic injury. Such analyses may provide new insights into the causes and compensatory mechanisms used to accommodate impairments.

## REFERENCES

- Edrich, T., Riener, R., Quintern, J. (2000). *IEE Trans on Biomed Eng.* **47**, 1058-1065.
- Herzog, W. et al. (1991). *Clin Biomechanics*, **411**, 230-238.
- Hoang, P.D. et al. (2005). *J. Biomechanics*, **38**, 1333-1341.
- Ishikawa, M. et al. (2005). *J. Appl Physiol*, **99**, 603-608.
- McGibbon, C.A. (2003). *Exer And Sp Sci and Rev*, **31**, 102-108.
- Muraoka, T. et al. (2005). *J. Biomechanics*, **38**, 1213-1219.
- Riener, R., Edrich, R. (1999). *J. Biomechanics*, **32**, 539-544.
- Vrahas, M.S. et al. (1990). *J. Biomechanics*, **23**, 357-362.

## ACKNOWLEDGEMENTS

NIH AG023276, NFL Charities, NSF pre-doctoral fellowship (AS).

# The Effects of Extraocular Muscles on the Dynamic Response of the Human Eye under Impact and their Influence on Globe Rupture

Eric Kennedy<sup>1</sup>, Ian Herring<sup>2</sup>, Craig McNally<sup>1</sup>, Stefan Duma<sup>1</sup>  
<sup>1</sup> Virginia Tech – Wake Forest, Center for Injury Biomechanics  
<sup>2</sup> Virginia-Maryland Regional College of Veterinary Medicine  
E-mail: eric\_kennedy@vt.edu Web: www.CIB.vt.edu

## INTRODUCTION

Previous studies have been performed to determine the injury tolerance of the human eye to globe rupture from blunt impact; however, none have investigated the effect that ocular muscles have on the response of the eye. In order to fully understand the biomechanical response of the eye to blunt impact, the effect of these extraocular muscles must be quantified. The purpose of the current study is to investigate the effects of the extraocular muscles to dynamic impact. Specifically, the effects on force-deflection response, and the effect that these muscles may have on the injury response of the eye will be determined.

## METHODS

The effects of the extraocular muscles were determined by matched pair testing on 5 human cadaver heads. The post-mortem human head is mounted in a rigid plastic container using expandable foam. For each specimen, the muscles are transected from one eye, leaving the eye held in place by solely the optic nerve, while the muscles of the other eye are left intact.

The impact tests are performed using a spring-powered dynamic impactor (Figure 1). The impactor is accelerated to a velocity of approximately 10 m/s before it impacts the eye. Force and acceleration data are continually collected at a sampling rate of 100 kHz for the duration of the test on each eye. High speed color video is also taken at a rate of 5,000 frames per second in order to determine the exact time that the impactor

struck the eye. Force-deflection corridors for both groups, with and without extraocular muscles intact, were generated by calculating the characteristic average force-deflection response and standard deviation of the force at each displacement step (Lessley 2004).

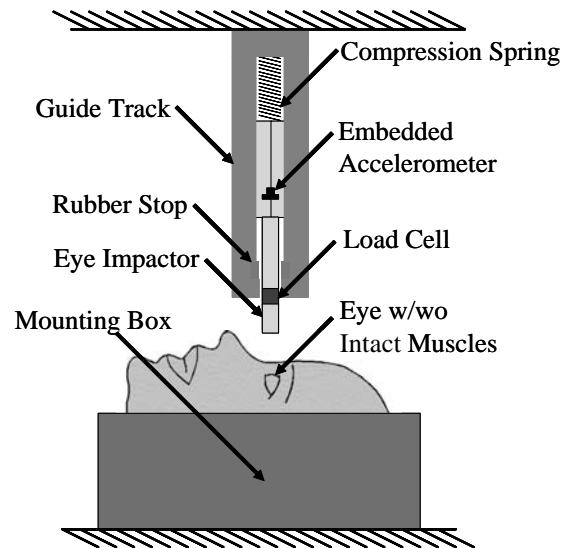


**Figure 1:** Test apparatus for dynamic eye impact tests.

## RESULTS AND DISCUSSION

The average response with the extraocular muscles intact was a peak force of 217 N and 9.9 mm of total displacement. With the muscles transected, the average response was a lower peak force of 161 N and increased displacement of 10.6 mm. Corridors were generated to show the typical force-deflection response both with muscles intact and with the muscles transected (Figure 2).

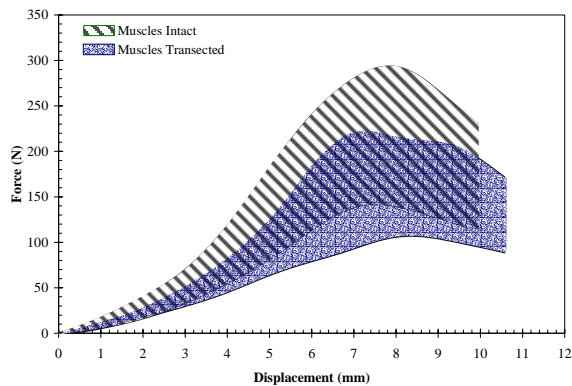


**Figure 2:** Corridors for typical force-deflection response both with muscles intact and with the muscles transected.

Qualitatively, with the extraocular muscles left intact, a slightly stiffer force-deflection response and less translation occurs to the point of the peak force. However, there is much overlap between the two test scenarios, suggesting a region where the response is the same either with the muscles intact or transected. So, while the extraocular muscles increase the resistive force of the eye and lower the posterior translation during impact, it is not sufficient to drastically alter the response of the eye even if the extraocular muscle attachments are not accounted for. This finding is consistent with that of other researchers (Cirovic 2005).

Of the ten dynamic impact tests conducted, there were only three cases of globe rupture observed. All three injuries were similar, and consistent with typically reported cases of globe rupture, spanning from the equator of the eye up to the limbus, at the corneo-scleral interface (Stitzel 2002). Of the three ruptures, two occurred in eyes which the muscles were transected, while one occurred in the eye where the muscles were left intact. Also, of the three injuries, two

occurred in the same test subject, potentially suggesting a weaker overall tolerance to injury in that particular subject. Overall, it was concluded that no appreciable differences were noted in injury outcome (globe rupture) between the eyes with muscles transected versus eyes with muscles left intact. The results indicate that the extraocular muscles do not create an appreciable stress concentration at the muscle insertions to the eye. Therefore, the extraocular muscles do not lead to premature failure of the eye at lower overall loading than enucleated eyes tested in-vitro, for example, in simulated orbits.

## CONCLUSIONS

In summary, this study suggests that during impact testing of human eyes, the extraocular muscles do not have an appreciable effect on eye injury outcome, and that the overall force-deflection corridors are similar with the extraocular muscles left intact or transected. Because of these findings, the results of this study suggest that impact tests performed using a simulated orbit, even without accommodations for the extraocular muscles, can accurately replicate the in-situ response of the eye.

## ACKNOWLEDGEMENTS

We would like to acknowledge the Southern Consortium for Injury Biomechanics for supporting this research project.

## REFERENCES

- Cirovic S, et al. (2005) Computer Methods in Biomechanics and Biomedical Engineering 8(1).
- Lessley D, et al. (2004) Society of Automotive Engineers 2004-01-0288.
- Stitzel JD, et al. (2002) Stapp Car Crash Journal 46.

# DETERMINANTS OF GAIT: APPLIED TO CHILDREN WITH CEREBEL PALSEY

Russell, S.D., Bennett, B.C., Abel, M.F.

Motion Analysis and Motor Performance Laboratory

University of Virginia, Charlottesville VA, USA

E-mail: sdr2n@virginia.edu Web: www.healthsystem.virginia.edu/internet/motion\_lab/

## INTRODUCTION

Saunders, et al. defined pelvic rotation, pelvic obliquity, and single support knee flexion as the three major determinants of gait that serve to minimize and smooth the vertical displacement of the center of mass (CoM). Recent research has modified our understanding of the relative contributions of these determinants on CoM vertical motion. Della Croce, et al. defined 5 new determinants: ipsi-, contra-lateral knee flexion, and heel rise at CoM minimum and leg inclination, and heel rise at CoM maximum, to more completely explain the deviation (both increasing and decreasing) of vertical excursion from compass gait values.

In the present study we quantified the isolated contributions of the above 8 determinants of gait on the vertical CoM displacement of both normal and spastic children. The role of the above 8 determinants of vertical excursion have never been examined for children or children with cerebral palsy (CP). We hypothesized that the relative contributions of the determinants to vertical CoM excursion of children

with CP would be the same as the age-matched controls because the children with CP are employing the same movement strategy as the controls, but are unable to execute it with the same effectiveness.

## METHODS

The kinematic data of 23 children was collected and analyzed. This group consisted of two populations; age-matched controls without known musculoskeletal, neurological, cardiac, or pulmonary pathology. The second group consisted of children diagnosed with spastic diplegic CP. These subjects were community ambulators that did not use walking aids. Subjects walked at their self-selected comfortable walking speed while 3-D kinematic data was collected.

The effect of each determinant of gait was computed using the method described by Della Croce. This method employed two models; 1) a modified compass gait model (Model 1, Figure 1) applied at the instant of time of minimum CoM height, and 2) a simpler model (Model 2, Figure 1) was used to evaluate the decrease of the maximum CoM height. For each trial the model geometry was defined using the 3-D position of each joint center determined from a subject's kinematics at the instant of CoM excursion extrema. The isolated contributions of an individual determinant were computed and normalized by the total vertical excursion.

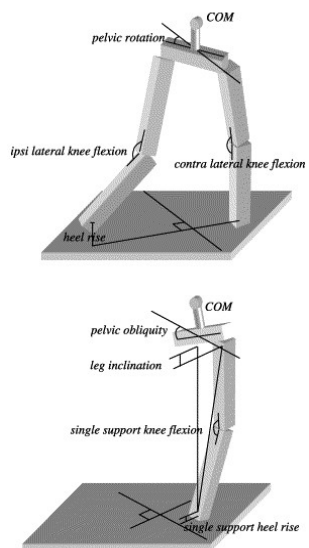


Figure 1. Model 1 (above)  
Model 2 (below)

## RESULTS AND DISCUSSION

Typical of previous research, when asked to walk at their self selected comfortable walking speed the control group had a longer step length and greater speed. Despite walking with longer step lengths the controls also experienced less vertical excursion when normalized by the predicted compass gait excursion.

The average determinant positive (beneficial) and negative (detrimental) contributions in reducing the total vertical CoM displacement computed using the two models are recorded in Table 1. At CoM minimum excursion ipsi- and contra-lateral knee flexion both resulted in an exaggerated increased in CoM excursion for the CP group, both pelvic rotation and heel rise resulted in similar (across groups) reduction in total CoM excursion. The maximum CoM height occurred during single support when leg inclination reduced total CoM excursion for the CP population than the control group. Single support heel rise was also had a different effect on the two groups increasing the total CoM excursion more in the CP subjects than for the controls.

## SUMMARY/CONCLUSIONS

The similarities in the determinants effect on gait between the Controls and adults reflect that children of this age walk with a mature gait. When applied to subjects with CP the determinant analysis found similar, but slightly exaggerated effects of those of the Controls. All determinants that negatively affect CoM excursion were significantly worse in the children with CP, while those determinants that decreased excursion were just as effective in the children with CP as in the Controls. The

main cause for increased vertical excursion of the CoM in the children with CP was the increased knee flexion of both legs during double support. This excessive lowering of the CoM means that extra work is done to raise the CoM over the single support leg. The situation is aggravated by the fact that the CoM was lifted higher than typical because of the heel lifting during single support. The only determinant that had a positive effect and was greater in the children with CP was leg inclination. It is unlikely that this results in a reduction in metabolic cost because the delay in CoM maximum height reduced the effectiveness of energy transfer between kinetic and potential forms, a major energy conserving mechanism in walking (Bennett 2004).

Although these determinants provide some useful information for gait they are limited in their ability to quantify the dynamics and kinetics of gait that are important for individuals with walking disabilities.

## REFERENCES

- Bennett,B. et al (2004), *J Sport Ex Psyc*, **26**, S32-33  
 Della Croce,U (2001), *Gait & Posture*, **14.2**, 79-84  
 Saunders,JB et al (1953), *J Bone Jnt.Surg*, **35A**, 543-58

**Table 1.** Determinants of Gait: Normalized parameters of gait. Step length normalized by leg length, Excursion normalized by predicted compass excursion, determinants normalized by measured excursion.

		CP	Control	P <
		avg ± std	avg ± std	
	<b>Step Length</b>	70.6 ± 7.2	84.1 ± 8.9	0.0023 *
	<b>Excursion</b>	86.08 ± 18.7	52.1 ± 7.9	0.0005 *
<b>M</b>	<b>ipsi lateral knee flexion</b>	-54.9 ± 34.0	-23.6 ± 8.5	0.0269 *
<b>I</b>	<b>contra lateral knee flexion</b>	-45.9 ± 16.7	-17.9 ± 17.1	0.0219 *
<b>N</b>	<b>pelvic rotation</b>	28.8 ± 7.7	41.6 ± 13.5	0.0767
	<b>heel rise</b>	87.4 ± 15.8	83.7 ± 17.7	0.5850
<b>M</b>	<b>single support knee flexion</b>	29.6 ± 24.4	17.8 ± 14.6	0.3335
<b>A</b>	<b>leg inclination</b>	37.0 ± 25.1	16.5 ± 7.2	0.0430 *
<b>X</b>	<b>pelvic obliquity</b>	1.9 ± 4.9	-0.8 ± 4.5	0.3176
	<b>single support heel rise</b>	-28.9 ± 27.6	-4.7 ± 10.0	0.0183 *

# ORBITAL STABILITY OF OVERGROUND VS. TREADMILL WALKING

Hyun Gu Kang and Jonathan B. Dingwell

Nonlinear Biodynamics Lab, Dept of Kinesiology, University of Texas, Austin, TX, USA  
E-mail: [jdingwell@mail.utexas.edu](mailto:jdingwell@mail.utexas.edu) Web: <http://www.edb.utexas.edu/faculty/dingwell/>

## INTRODUCTION

Locomotor stability can be quantified in terms of either “local stability,” how a system responds to very small perturbations *continuously in real time*, or “orbital stability,” how periodic systems respond to small perturbations *discretely from one cycle to the next*. While some studies showed that human walking is orbitally stable (Hurmuzlu 1996), others found significant local instability (Dingwell 2000). Some theoretical limit cycle systems can exhibit locally unstable regions and still remain orbitally stable (Ali 1999). It is not known if this is true for human walking. Thus, both orbital *and* local dynamic stability need to be quantified to fully understand walking stability.

To study walking stability properly, we need to quantify the effects of perturbations over multiple strides. Using treadmills simplifies this task, but treadmill walking may not be equivalent to overground walking. Walking on a rigid treadmill at constant speed is theoretically the same as walking over ground (van Ingen Schenau 1980). Yet, some treadmills can artificially reduce the natural variability and enhance the *local* stability of walking kinematics (Dingwell 2001). This study set out to determine if locally unstable walking kinematics remain orbitally stable and to determine how treadmills affect the orbital stability of human walking.

## METHODS

Ten healthy subjects (age  $27.1 \pm 3.2$ ) walked for 10 minutes on an indoor track at his or her freely chosen pace, and then for 10 min-

utes on a motorized treadmill at the same speed. Anterior-posterior, mediolateral, and vertical trunk accelerations ( $A_{AP}$ ,  $A_{ML}$ ,  $A_{VT}$ ) and hip, knee and ankle joint angles of the right leg were sampled at 66.67 Hz using a custom data logger (Dingwell 2001).

For each of the six time series, an appropriate state-space was generated using delay-embedding (Dingwell 2000). To quantify orbital stability, maximum Floquet multipliers (FM) were computed for each time series using standard techniques (Hurmuzlu 1994). Because Floquet theory presumes the motion is purely periodic, the data for each stride were first time-normalized to 101 samples (0%-100% gait cycle). This let us define a Poincaré section and a Jacobian matrix,  $J^*$ , at each % of the gait cycle. The maximum FM were calculated as the magnitudes of the maximum eigenvalues of  $J^*$ . This maximum FM defined the amount by which a perturbation away from the mean reference trajectory would grow or decay by the next cycle. If the maximum FM has magnitude  $< 1$ , perturbations decay after one stride and the system is orbitally stable.

The largest of all the maximum FM computed across all % of the gait cycle was taken to define “Max FM”. Repeated-measures ANOVA were used to compare Max FM values between treadmill (TM) and overground (OG) walking.

## RESULTS AND DISCUSSION

All subjects exhibited *orbitally* stable walking kinematics (Fig. 1A), even though these same kinematics were previously shown to

be *locally* unstable (Dingwell et al. 2001). Max FM values were not significantly correlated with previously published local stability measures ( $r^2 \leq 20\%$ ;  $p \geq 0.05$ ).

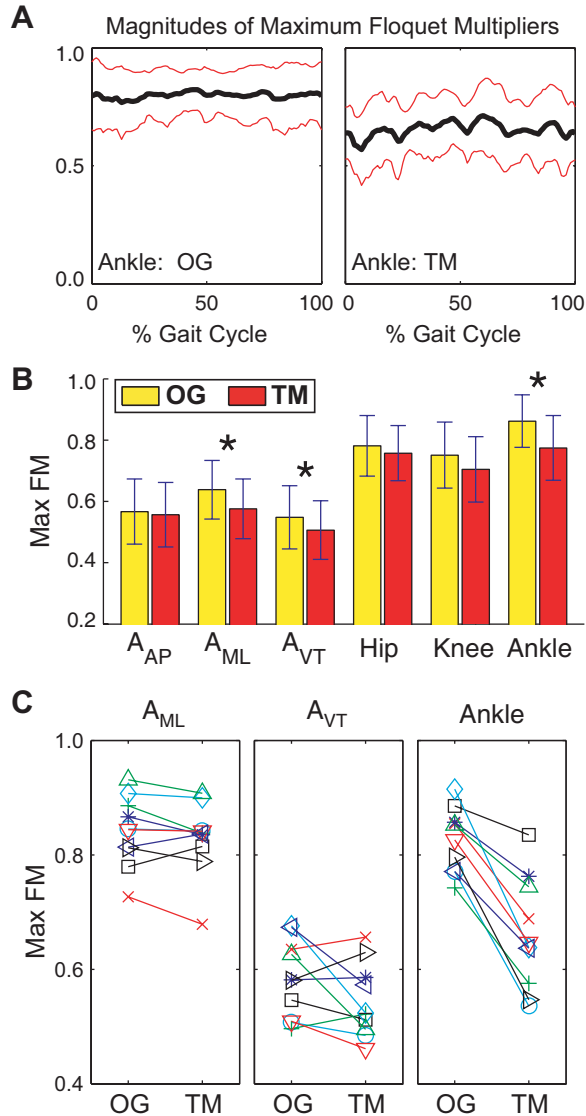


**Figure 1:** **A:** Variations in maximum FM across the gait cycle for Ankle movements. These movements were orbitally stable ( $FM < 1$ ). **B:** Max FM values for OG and TM walking (\* indicates statistically significant,  $p < 0.05$ ). **C:** Subject × Condition interaction plots for A<sub>ML</sub>, A<sub>VT</sub>, and Ankle. Each line/marker represents one subject.

TM walking tended to exhibit slightly better orbital stability than OG walking at the same

speed (Fig 1B). However, for all 3 variables where these differences were statistically significant, significant Subject × Condition interactions were also found ( $p \leq 0.012$ ; Fig 1C). The decreases in Max FM values were not consistent across subjects. TM walking led to small, but inconsistent improvements in orbital stability compared to OG walking. Thus, using a treadmill is not expected to confound orbital stability results.

## SUMMARY / CONCLUSIONS

Humans concurrently exhibited orbital stability and local *instability* in both OG and TM walking. The neuromuscular system corrects any deviations away from the mean reference trajectory, but allows individual strides to diverge away from the path of other strides without compromising overall stability. More work is need to determine exactly how much local instability the locomotor system can tolerate and still remain orbitally stable, and what mechanical and biological mechanisms are used to regulate these processes. Sensory, cognitive, or motor deficits may reduce the amount of local instability that can be tolerated.

## REFERENCES

- Dingwell, J.B., Cusumano, J.P. (2000) *Chaos*, **10**, 848-863.
- Hurmuzlu, Y., Basdogan, C. (1994) *J. Biomech. Eng.*, **23**, 63-74.
- Ali, F., Menzinger, A.C., (1999) *Chaos*. **9**, 348-356.
- Van Ingen Schenau, G.J. (1980) *Med. Sci. Sports Exerc.* **12**, 257-261.
- Dingwell, J.B. et al., (2001) *J. Biomech. Eng.*, **123** 27-32.

## ACKNOWLEDGEMENTS

Supported by Research Grant # RG-02-0354 from the Whitaker Foundation

# CORRELATING DELTA-V TO OCCUPANT INJURY USING EVENT DATA RECORDERS

Douglas Gabauer and Hampton C. Gabler

Virginia Tech, Blacksburg, VA, USA  
E-mail: gabauer@vt.edu

## INTRODUCTION

Delta-V, defined as the total change in vehicle velocity, has traditionally been used as a measure of crash severity and predictor for occupant injury for vehicular crashes. Typically, delta-V is estimated using measured vehicle post-crash damage in tandem with computer codes such as WinSmash or Crash3.

Several researchers have previously correlated this delta-V estimate with risk of occupant injury using logistic regression. Winnicki and Eppinger (1998) developed chest injury risk curves for varying injury and delta-V levels in conjunction with a methodology to evaluate benefits associated with depowering airbags. Similarly, Bahouth et al. (2004) generated a statistical predictive model based on delta-V for all occupant restraint types and crash modalities.

Event Data Recorders (EDRs), installed in many late model vehicles, are an alternate means of obtaining delta-V for a real-world collision. EDRs are similar to “black boxes” in airplanes as they record information in the event of a highway collision, including vehicle change in velocity as a function of time. Current research suggests excellent agreement (within 6 percent) between EDR-recorded delta-V and actual delta-V in frontal collisions (Niehoff et al., 2005).

The objective of this research is to correlate EDR delta-V to occupant injury in real-

world collisions and compare to the results using other methods of estimating delta-V.

## METHODS

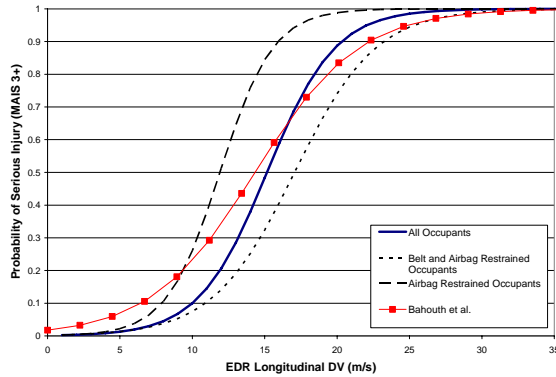
Suitable cases were selected from the National Highway Traffic Safety Administration (NHTSA) EDR database. Currently, the database consists of EDR data for over 1700 cases, all of which are GM vehicles. As these cases were collected in conjunction with NASS/CDS, the corresponding occupant injury information is matched to corresponding EDR data. Suitable cases were limited to frontal collisions with airbag deployment, a single crash event, available EDR data, and known occupant injury. Based on these criteria, there were 191 suitable cases available for analysis; 152 belted and 27 unbelted front seat occupants.

Binary logistic regression models were fit to the entire dataset as well as belted and unbelted data subsets using delta-V as a predictor of serious occupant injury. For this study, serious injury is defined based on the Abbreviated Injury Severity scale (AAAM, 2001).

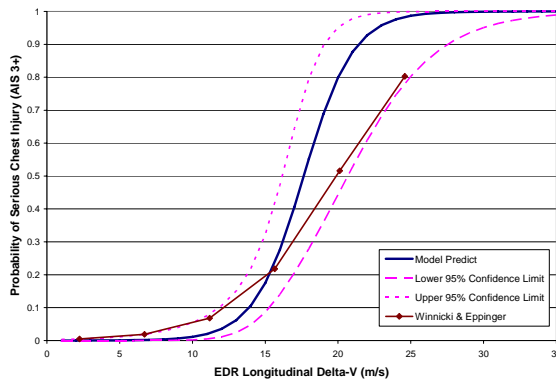
## RESULTS AND DISCUSSION

Figure 1 and Figure 2 show the injury risk curves for overall occupant injury and chest injury, respectively, based on the available data. Note that the chest injury curves only include 179 cases, as injury by body region was not known in 12 instances. For all models, tests of the global null hypothesis

were significant to the 0.0001 level or better. Pearson goodness-of-fit statistics were 0.097 and 0.904 for the belted and unbelted subset data models indicating reasonable fits.



**Figure 1:** Occupant Maximum Injury as a Function of Longitudinal Delta-V.



**Figure 2:** Occupant Chest Injury as a Function of Longitudinal Delta-V.

As expected, for the same delta-V, Figure 1 shows lower injury risk for occupants restrained by both a belt and airbag than for an occupant restrained by an airbag only. For comparison purposes, the Bahouth risk curve is also plotted in Figure 1. There is reasonable agreement for the developed model including all occupants with larger differences evident in the lower delta-V region. This discrepancy is most likely a result of the Bahouth model including all crash modes while the model developed herein is limited to frontal collisions.

For occupant chest injury, Figure 2 shows the developed model with 95% confidence bounds. Since the data set was smaller, no effort was made to split the data by belted and unbelted occupants. Also, the Winnicki and Eppinger risk curve is plotted for comparison purposes. Although there is not exceptional agreement, the risk curve does fall within the confidence bounds of the risk curve developed in this study. Note that the Winnicki and Eppinger risk curve has been based on data collected between 1991 and 1996 while the current study incorporates data from 2000 to 2004.

## SUMMARY/CONCLUSIONS

EDRs offer an alternate means of developing occupant injury risk curves based on injury in real-world collisions. Injury risk curves are generated for overall occupant injury and chest injury using EDR delta-V as the predictor. Reasonable agreement was found with previous work that used vehicle-damage methods to estimate delta-V.

## REFERENCES

- AAAM. (2001) The Abbreviated Injury Scale: 1990 Revision, Update 98.
- Bahouth, G.T. et al. (2004) *Top Emerg Med* 26(2):157-165.
- Niehoff, P. et al. (2005) *Proc. of the 19th Int. Conf. on Enhanced Safety of Vehicles*, Paper 05-0271.
- Winnicki, J, Eppinger, R. (1998). *A Method for Estimating the Effect of Vehicle Crashworthiness Design Changes on Injuries and Fatalities*. NHTSA.

## ACKNOWLEDGEMENTS

The authors would like to thank NHTSA for the provision of the EDR data.

# APPLICATIONS OF THE PERONNET-THIBAUT MODEL OF RUNNING PERFORMANCE

Iain Hunter<sup>1</sup> and John Dallon<sup>2</sup>

<sup>1</sup>Department of Exercise Sciences & <sup>2</sup>Department of Mathematics,  
Brigham Young University, Provo, Utah, USA E-mail: iain\_hunter@byu.edu

## INTRODUCTION

Various mathematical models created and refined over the past 80 years have added to understanding of various capacities of the body, how performances are affected by environmental conditions, and how future performances may be predicted. One of the most accurate models through a wide range of distances was created by Peronnet and Thibault (1989). Their model not only matched world record times very well, but was also tested on a variety of elite athletes with very good accuracy.

With the accuracy of Peronnet's model, further applications may add to current understanding of how the human body functions under various situations. The current study used Peronnet's model to provide the following additional applications not previously reported: 1) How maximal aerobic power, maximal anaerobic power, and the rate of decline of aerobic power change throughout life. 2) How maximal aerobic power, maximal anaerobic power, and the rate of decline of aerobic power change throughout the past since 1920 and how they may change in the future. 3) How maximal aerobic power, maximal anaerobic power, and the rate of decline of aerobic power change with different body masses and heights.

## METHODS

Aerobic and anaerobic capacities and the rate of decline of aerobic capacity were

determined utilizing Peronnet's model through a range of race distances from 60m to the marathon using world record and American age group records. We also modeled how the same capacities have changed over the past 85 years. Finally, the required capacities for people of different heights and weights were estimated.

Peronnet's model estimates the average power required to run maximally for a given amount of time ( $P_T$ , see equation 1). With equation 2, which estimates the power requirement to maintain a given velocity, the model determines the required values for  $A$  (maximum anaerobic power),  $MAP$  (maximum aerobic power), and  $E$  (rate of decline of aerobic power) for any given set of input times, body masses, and body surface areas using an iterative process.

$$P_T = \frac{\left\{ S(1 - e^{-T/k_2}) \right\}}{T} + \frac{\left\{ \int_0^R BMR + B(1 - e^{-t/k_1}) dt \right\}}{T}$$

**Equation 1:**  $S$  is the anaerobic energy store ( $A$ , in J/kg), when  $T < 420$ s, or  $S = A - 0.233A \ln(T/420)$ , when  $T > 420$ .  $B$  is the maximum aerobic power ( $MAP$ , in W/kg) minus basal metabolic rate ( $BMR$ , in W/kg), when  $T < 420$ s; or  $B = MAP - BMR + E \ln(T/420)$ , when  $T > 420$ .

$$P_V = BMR + 3.86v + 0.4BSA(v^3) / BM + 2v^3 / D$$

**Equation 2:** The required power to maintain a given velocity, where:  $BMR$  = basal

metabolic rate,  $BSA$  = body surface area,  $BM$  = body mass, and  $D$  = race distance.

## RESULTS AND DISCUSSION

Aerobic and anaerobic capacities gradually decreased over the lifespan with aerobic capacity showing an increased drop after 80 years old and anaerobic capacity leveling off at the same age (Figure 1).

The rapid decline in maximal aerobic power may be due to the uncoupling of mitochondria sometimes found among those over about age 65. However, the leveling off of maximal anaerobic power may need to be explained by biomechanical or orthopaedic issues which may lead to a need for a change in the mathematical model.

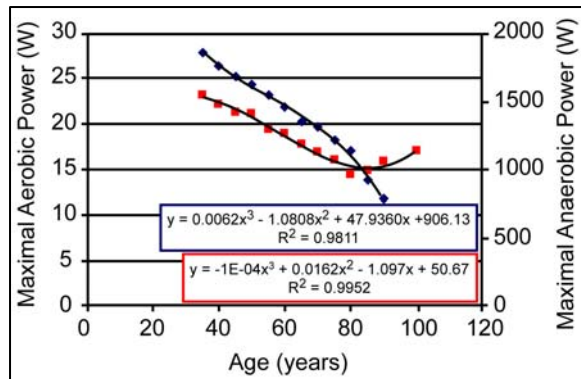


**Figure 1:** Changes in aerobic and anaerobic capacities from 35 to 100 years old.

When considering world record times since 1920, aerobic and anaerobic capacities have increased nearly linearly (Anaerobic capacity =  $2.108 \cdot \text{year} - 2521.6$  ( $R^2 = 0.987$ ), Aerobic capacity =  $0.0456 \cdot \text{year} - 61.4$  ( $R^2 = 0.996$ ). However, the rate of decline of aerobic capacity was much more variable and difficult to predict its future direction, although it seems to be leveling off during the past 20 years (Figure 2). Improvements in all three factors in the

model were expected since performance times have been gradually increasing over the past century. However, over the last ten years, world record times appear to be improving at a lower rate (Nevill, 2005). This may be explained by the rate of decline of aerobic power leveling off.

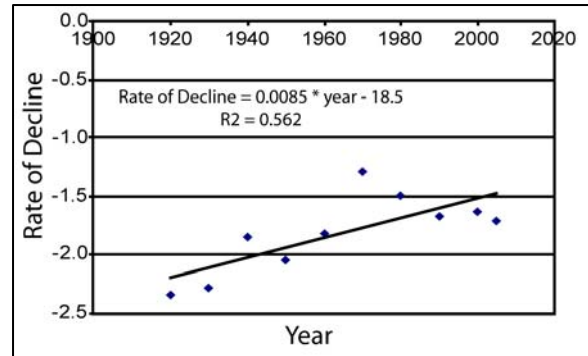


**Figure 1:** The rate of decline of aerobic capacity since 1920 based upon world record performances.

While lighter runners require less power to run any given velocity, the model showed a larger power requirement per kilogram of body mass. Increases in height also increased power requirements. The power requirement per kilogram for lighter runners increased at a greater rate as height was increased. This makes it unlikely to see a very tall slender runner being successful across a large range of races.

## REFERENCES

- Nevill, A.M. & Whyte, G. (2005). Are there limits to running world records. *Medicine and Science in Sports and Exercise*, 4, 1785-1788.
- Peronnet, F. & Thibault, G. (1989). Mathematical analysis of running performance and world running records. *Journal of Applied Physiology*, 67, 453-465.

# THE EFFECT OF LANDING ANGLE ON LOSS OF HORIZONTAL VELOCITY IN THE MEN'S TRIPLE JUMP

Iain Hunter , Laurence Bollschweiler and Kyle Grosarth

Department of Exercise Sciences,  
Brigham Young University, Provo, Utah, USA E-mail: iain\_hunter@byu.edu

## INTRODUCTION

Throughout the history of track and field, a great deal of study has gone into those field events which require a combination of both running and jumping. The triple jump is one such event where excellence in both running and jumping is crucial to success. In performing the triple jump, an athlete must incorporate several specific movements, which, when done correctly will result in greater jumping distances.

It is believed that the most important aspect of the triple jump is the maintenance of horizontal velocity during each jump. The approach plays a major role in the acquisition of horizontal velocity. One study has shown approach running speed to be a determining factor of triple jump results among top European athletes (Viitasalo et al, 1995). However, horizontal velocity acquired during a running approach is not so easily maintained while jumping. It has been previously determined that there is a direct relationship between the gain in vertical velocity acquired during jumping and the subsequent loss in horizontal velocity (Yu, 1999). The challenge lies in creating a high vertical velocity necessary for a greater flight time, while limiting the loss of horizontal velocity.

A few body positions that are believed to play a role in this area are the angle of the leg at landing as well as the angle of the leg at take-off for each of the three jumps. The purpose of this study is, therefore, two-fold. First is to determine if, in fact, horizontal

velocity during the men's triple jump does affect performance. Second is to determine what effect leg angles at landing and take-off have on loss of horizontal velocity in the same event.

## METHODS

Data were collected at the 2006 Mountain West Conference NCAA Indoor Track and Field Championships. Eleven contestants completed a total of 35 successful jumps with an average jump distance of 14.2 (0.40) m.

Horizontal velocity was measured with a laser that measures distance at 100 Hz (LDM 300-C, Jenoptik, Jena, Germany). The laser was placed at the beginning of the approach runway and aimed down the length of the runway. Horizontal velocity was then acquired for all three flights of the triple jump. Loss of velocity was calculated as the difference between each flight.

A 60 Hz digital camcorder (Elura 60, Canon, USA) was placed 45 m away from and perpendicular to the runway.

Leg angles at landing and take-off were determined using Dartfish video analysis. Video captured from a camera located to the side of the runway was used to assess leg angles at the landing of jump 1, the take-off of jump 2, the landing of jump 2, and the take-off of jump 3. These three jumps are commonly referred to as the hop, step and jump. Leg angle at take-off and landing was defined as the angle generated with a line

through the hip, relative to vertical with the ankle as the vertex (Figure 1)..

Two linear regressions were completed. One analysis was done on predicting the distance of the jump using horizontal velocity, with the other being done on predicting the loss of horizontal velocity using landing and take-off angles. Significance was set at  $p \leq 0.05$ .



**Figure 1:** Visual depiction of landing and take-off angles.

## RESULTS AND DISCUSSION

Table 1 shows the results of the four angles measured and the two loss of horizontal velocity measured. Linear regression analysis resulted in two models being produced. The first model is for predicting the distance of the triple jump, and the second is for predicting loss of horizontal velocity. They are as follows:

### Equation 1:

$$\text{Jump distance} = 0.75(V_{fl}) + 7.35$$

$$F\text{-value} = 7.15$$

$$p\text{-value} = 0.018$$

$$R^2 = 0.338$$

Where  $V_{fl}$  is horizontal velocity of flight 1.

### Equation 2:

$$\text{Loss of velocity} = 0.06 (\text{Hop Landing Angle}) + 0.45$$

**Table 1:** Results of the four angles measured as well as loss of horizontal velocity between jumps 1 and 2 and between jumps 2 and 3.

	Hop Landing (deg)	Step Take-off (deg)	Step Landing (deg)	Jump Take-off (deg)	Loss 1-2 (m/s)	Loss 2-3 (m/s)
Mean	-23.20	35.64	-27.35	28.45	-1.03	-0.93
SD	3.54	3.17	2.89	4.15	0.39	0.47

$$F\text{-value} = 12.34$$

$$p\text{-value} = 0.002$$

$$R^2 = 0.349$$

Equation 1 shows that the horizontal velocity of the first flight of the triple jump is a good predictor of jump distance. Equation 2 shows that leg angle at the landing of the hop is a good predictor of how much horizontal velocity is lost. Greater leg angles at landing result in greater loss of horizontal velocity. This indicates that horizontal velocity may be more easily maintained by reducing the leg angle at landing. This can be done by bringing the leg into more of a vertical position upon touchdown.

## SUMMARY/CONCLUSIONS

This data agrees with the current triple jump coaching philosophies. These are that maintenance of horizontal velocity results in greater jumping distances and that landing with the leg near vertical helps to maintain horizontal velocity.

## REFERENCES

- Yu, B. (1999). Horizontal to vertical velocity conversion in the triple jump. *J. Sports Sci.*, **17** (3), 221-229.
- Vuittasalo, J.T. et al. (1995). Approach running speed as a determinant of triple jump results among top European male and female athletes. *Conference: Congress of the International Society of Biomechanics*. Jyvaskyla, Finland.

## HOW RELIABLE IS LUMBAR INTERVERTEBRAL STRESS PROFILOMETRY?

Ralph E. Gay, Brice Ilharreborde, Kristin D. Zhao, Jonathan Bridges, and Kai-Nan An

Biomechanics Laboratory, Division of Orthopedic Research,  
Mayo Clinic College of Medicine, Rochester, MN 55905 USA  
E-mail: rgay@mayo.edu

### INTRODUCTION

Stress measurements in the intervertebral disc have been limited primarily to measuring hydrostatic nuclear pressure with strain gauge techniques and catheter systems. McNally and colleagues developed a technique to measure the distribution of stress in both the nuclear and annular regions. The transducer (OrthoAR Series, Medical Measurements Incorporated, Hackensack, New Jersey) was embedded into the side of a 1.3 mm diameter steel needle which was pulled through the disc at a constant rate producing a “stress profile”. Nuclear pressure measurements were found to be repeatable to  $\pm 1\%$  in all directions (no anisotropy). (McNally 1992) A subsequent study examined the validity of the measures in the anisotropic annulus and concluded that the compressive *force* acting on the disc was proportional to the compressive *stress* perpendicular to the transducer membrane. (McMillan 1996) That study also reported that stress profiles (distance vs. stress curves) varied by less than 20% when large numbers of profiles were recorded on the same disc. Several investigators have now used intradiscal stress profilometry under differing load conditions, but no additional reports of the reliability of this technique have been published. *The objective of this study* was to determine the reliability of stress measurements obtained with the stress profilometry technique in cadaveric lumbar nucleus pulposus and annulus fibrosis during 5 loading conditions (simulating 2

postural loads and 3 distraction therapies). Because negative nuclear pressures could be expected during distracted conditions we also sought to determine the accuracy of the transducer in the potential negative range.

### METHODS

Four fresh frozen human lumbar motion segments of varied degenerative grade were potted in PMMA using a standard technique. A custom testing apparatus was used that allowed application of simultaneous pure moments and axial compression or distraction. Forces and moments were measured with a 6 DOF load cell (JR3, Woodland, CA, USA). The transducer was calibrated and tested for negative pressure in a custom pressure chamber. After a preload of 300 N for 30 minutes, a 1.3-mm spinal needle was introduced into the anterior annulus at the mid-sagittal line, midway between the vertebral endplates and advanced through the posterior outer annulus under fluoroscopic guidance. The needle was removed and the pressure transducer, mounted on a 1.27mm diameter blunt needle, was introduced into the needle track. The transducer, oriented in the horizontal plane to measure vertical stress, was withdrawn at a constant rate of 2 mm/second using a cable and pulley driven by a stepper motor. After 5 repetitions, the transducer was oriented vertically to measure horizontal stresses and 5 more repetitions performed. This process was repeated on each motion segment during 5 conditions in the following order: 1) non-

weight bearing or lying (300 N compression), 2) weight bearing or standing (500 N compression), 3) distraction alone (90 N), 4) distraction combined with flexion (5 Nm) and 5) distraction combined with extension (5 Nm). Discs were then sectioned and graded for degeneration with the scale of Adams (1=normal, 4=severe). (Adams 1996) Profiles were partitioned into nucleus, posterior and anterior annulus regions. Variability (reliability) of the measures was determined using within-specimen coefficients of variation (CV) as a percent.

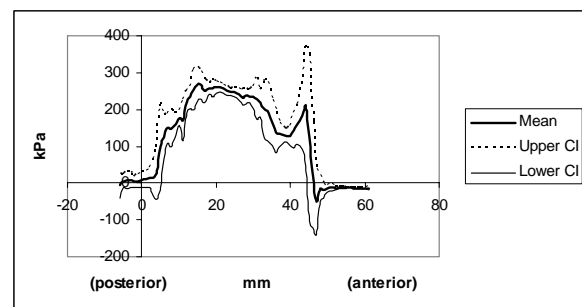
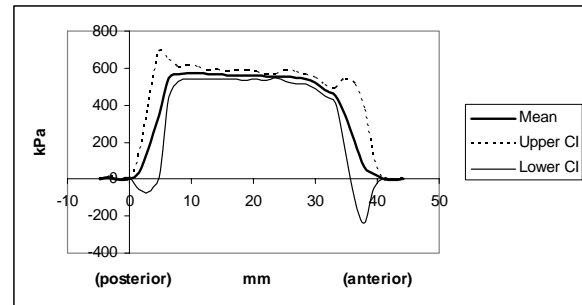
## RESULTS

Vertical profiles were more variable than horizontal profiles and contained more stress peaks. To obtain a conservative estimate of reliability, only CVs of vertical profiles were analyzed. Representative mean vertical stress profiles with 95% confidence intervals for a grade 1 and a grade 3 disc under 500 N compression are shown in figures 1 and 2. CVs were generally smaller for compression conditions than for distraction conditions. Within-specimen CV of nuclear stress during compression ranged from 1.6 to 37.2%. The range for the anterior annulus was 3.9 to 67.4% and for posterior annulus 2.3 to 25.5%. CVs for distraction conditions were often > 100% (standard deviation > mean of measurements) because stress was often near 0. The single motion segment with no degenerative change on visual inspection had the most reliable measures.

## SUMMARY/CONCLUSIONS

The reliability of intradiscal stress profilometry measures is dependent upon test condition and, to some extent, the amount of disc degeneration. Reliability is acceptable for use in studies evaluating within-specimen changes when sample size

and test conditions are appropriately considered.



Figures 1 and 2. Representative mean vertical stress profiles (mean of 5 sequential profiles) and 95% confidence intervals for grade 1 (fig 1, top) and grade 3 (fig 2, bottom) discs under 500 N compression.

## REFERENCES

- Adams MA, McNally DS, Dolan P. (1996) 'Stress' distributions inside intervertebral discs: The effects of age and degeneration. *J Bone Joint Surg Br.* 78:965-972.
- McMillan DW et al. (1996) Stress distributions inside intervertebral discs: the validity of experimental 'stress profilometry'. *J Eng Med (H)* 210, 81-7.
- McNally DS, Adams MA. (1992) Internal intervertebral disc mechanics as revealed by stress profilometry. *Spine.* 17, 66-73.

# EFFECTS OF SPEED ON HAMSTRING KINETICS DURING SPRINTING

Elizabeth S. Chumanov<sup>1</sup>, Bryan C. Heiderscheit<sup>2</sup>, and Darryl G. Thelen<sup>1,2</sup>

Dept of Mech Engr<sup>1</sup> and Orthop and Rehab<sup>2</sup> University of Wisconsin, Madison, WI, USA

Email: easchmerr@wisc.edu

## INTRODUCTION

Acute hamstring strains are commonly associated with maximal speed sprinting activities (Seward, et.al 1993; Hagel 2005). The prevention and rehabilitation of such injuries remains challenging (Orchard, et.al 2002). Therefore, an improved understanding of hamstring musculotendon (MT) dynamics during sprinting may be beneficial to programs aimed at reducing injury rates.

The hamstrings are active and lengthening during the latter half of the swing phase of sprinting (Jonhagen, et.al 1996). Thus, it has been speculated that the hamstrings are at risk for a lengthening contraction injury during swing (Whiting, et.al 1998). We previously found that peak hamstring MT stretch, which occurred just prior to foot contact, is invariant with sprinting speed. However, the dynamic interaction of the muscle and tendon components needs to be considered to determine how this relates to stretch at the fiber level. Furthermore, other factors commonly associated with muscle injury, such as loading and mechanical work (Brooks, et.al 2001) may exhibit substantial dependence on sprinting speed and contribute to injury risk.

The objective of this study was to characterize hamstring MT kinetics during swing phase across sprinting speeds. We hypothesized that 1) peak fiber stretch would be invariant with speed, 2) that both peak hamstring force and negative work would increase with speed.

## METHODS

Nineteen athletes (6 female, 13 male, 16-31 yr old) participated in this study. Whole

body kinematics were recorded at 200 Hz while each subject sprinted on a high-speed treadmill at 80, 85, 90, 95, and 100% of his/her maximum sprinting speed. A subset of 5 athletes had electromyography (EMG) electrodes placed over 5 muscles on their right limb (lateral hamstrings, medial hamstrings, rectus femoris, vastus lateralis, and medial gastrocnemius).

The body was modeled as a linked-segment articulated linkage (Fig 1a). The motion of the pelvis and upper body was prescribed based on experimental data. Twenty-six MT actuators crossing the hip, knee, and ankle were used to drive the lower extremity motion. Each MT unit was represented by line segments connecting the origin to the insertion with wrapping about structures accounted for (Arnold et.al, 2000). MT

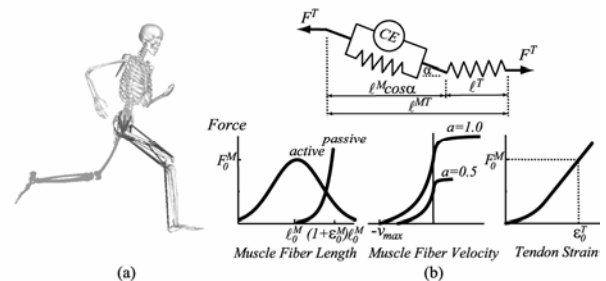


**Figure 1:** (a) Musculoskeletal model shown in the posture of peak hamstring MT stretch. (b) Hill type muscle model used in the forward dynamic simulations

contraction dynamics were represented by a Hill-type model (Fig. 1b, Zajac, 1989). A computed muscle control algorithm (Thelen et al., 2006) was used to determine muscle excitations that drove the limb to track measured kinematics during swing phase. The stretch and power development in the muscle and tendon components were estimated from the simulations. Muscle and tendon stretch were defined as the change in

length relative to the respective relaxed lengths in an upright posture. A repeated measures ANOVA was used to test for significant ( $p < 0.05$ ) effects.

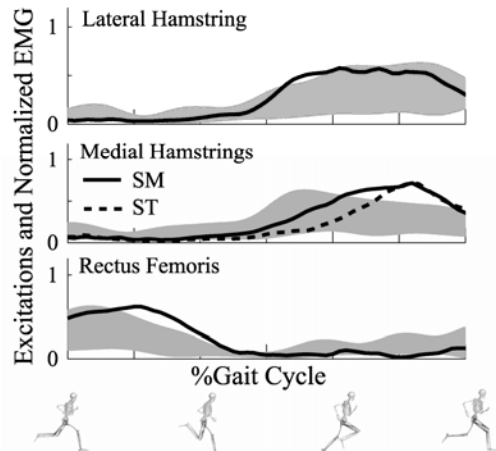


**Figure 2.** Predicted muscle excitations (black line) were consistent with experimental EMG recordings (shaded).

## RESULTS AND DISCUSSION

The computed muscle control algorithm generated simulations that closely tracked the experimental kinematics ( $<2.5^\circ$  average difference). Timing of model-predicted muscle were consistent with the experimentally recorded EMG (Fig. 2). Peak fiber peak stretch was observed to decrease slightly with speed ( $p < 0.05$ ), while peak tendon stretch increased ( $p < 0.05$ ) (Fig 3a). The increased tendon stretch corresponded to an increase in peak MT force ( $p < 0.05$ ). Negative MT and negative muscle work both increased substantially with speed ( $p < 0.05$ ). While peak MT force tended to increase linearly with speed, negative work done by the MT increased  $\sim 40\%$  from 80% to maximal sprinting speed (Fig 3b).

Animal models of muscle injuries have shown that peak fiber strain (Lieber, et.al 1993) and negative work (integral of force times lengthening velocity, Brooks, et.al 2001) are strong indicators of injury potential. Our data support the idea that the

potential for a lengthening strain injury to the hamstrings is substantial during the late swing phase of maximal sprinting. The

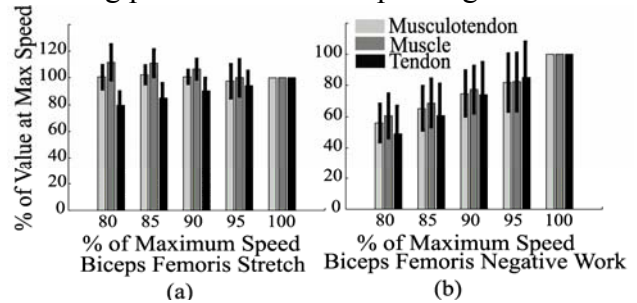


**Figure 3.** (a). Peak stretch for the MT unit is invariant with speed, while muscle stretch decreases and tendon stretch increases with speed. (b) Negative work done by the MT unit, muscle, and tendon increase substantially from submaximal to maximal sprinting speed

hamstrings are active, maximally stretched, and performing a substantial amount of negative work during late swing, presumably to decelerate the limb prior to foot contact. The substantial dependence of negative work on sprinting speed indicates that the work requirements of the lengthening hamstrings may be a factor contributing to injury risk at high speeds.

## REFERENCES

- Arnold, A.A., et al. (2000). *Comp Aided Surg.* **5**: 108-119.
- Brooks, S.V., et.al. (2001). *J Appl Phys.* **91**: 661-666.
- Hagel, B. (2005). *Clin J Sport Med.* **15**: 400.
- Jonhagen, S., et.al. (1996). *Scan J Med Sci Sports.* **6**: 15-21.
- Lieber, R.L., et.al. (1993). *J Appl Phys.* **74**: 520-526.
- Orchard, J., et.al. (2002). *Clin J Sport Med.* **12**: 3-5.
- Seward, H., et al. (1993). *Med J Aust.* **159**: 298-301.
- Thelen, D.G., et.al. (2006) *J Biomech.* **39**: 1107-1115.
- Whitting, W., et.al. (1998). *Biomechanics of Musculoskeletal Injury.* Human Kinetics Publishers.
- Zajac, F.E. (1989). *Crit Rev Biomed Engr.* **17**: 359-411.

## ACKNOWLEDGEMENTS

Contributions of Allison Arnold, Steve Swanson, Li Li, and Michael Young. Support of Aircast Foundation Inc., NFL Charities, and NSF graduate fellowship.

# BIOMECHANICAL EVALUATION OF PROVOCATIVE TESTS FOR SUPERIOR GLENOID LABRUM LESIONS

Seth M. Kuhlman, Michelle B. Sabick, Ronald P. Pfeiffer, Kurt Nilsson, and Kevin G. Shea

Center for Orthopaedic & Biomechanics Research, Boise State University, Boise, Idaho, USA

## INTRODUCTION

Arthroscopic surgery is considered the gold standard for diagnosis of lesions of the superior glenoid labrum (Parentis, 2005). However, arthroscopy is an expensive and invasive diagnostic tool. Consequently, at least 17 different provocative tests have been developed to try to detect superior labral pathology during routine physical examination. Most of the tests aim to elicit labral symptoms by producing tension in the long head of the biceps brachii (LHBB) muscle, which pulls on its proximal labral attachment during contraction, reproducing pain or discomfort (Morgan, 1998).

Clinical evaluations of provocative tests have varied widely, with many showing poor specificity and sensitivity at detecting labral lesions (McFarland, 2002). However, the ability of each of the provocative tests to specifically and effectively activate the LHBB has not been determined. The purpose of this study is to quantify the amount of LHBB muscle activation and the selectivity of muscle recruitment in five clinical tests for superior labral pathology

that were designed to activate the LHBB.

## METHODS

Performance of each provocative test was evaluated using electromyography (EMG). Ten male subjects without history of shoulder pathology were recruited to participate. Six Ag-AgCl surface electrodes were placed over the muscle belly of the LHBB, short head of biceps brachii, anterior deltoid, pectoralis major, latissimus dorsi, and infraspinatus muscles. An intramuscular fine-wire electrode was placed in the supraspinatus due to its deep location.

Subjects performed three repetitions of a maximum voluntary isometric contraction (MVIC) for each muscle. The peak activation level in any of the processed MVIC trials was considered 100% effort and used to normalize the provocative test data

A physician performed three repetitions each of the following five provocative tests on one arm of each subject in random order (Figure 1): Active Compression Test (2 positions) (O'Brien, 1998), Biceps Load

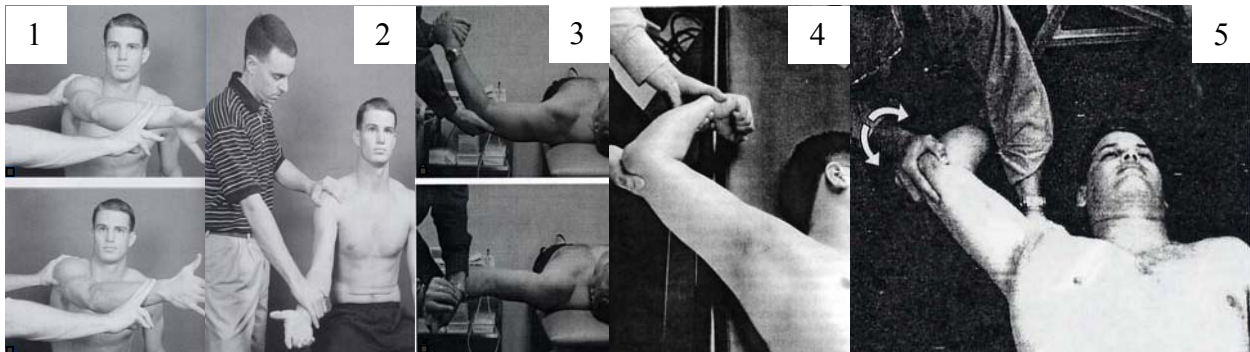


**Figure 1:** Provocative tests for superior glenoid lesions: 1. Active Compression Test 2. Speed's Test 3. Pronated Load Test 4. Biceps Load Test II 5. RSER Test.

Test II (Kim, 2001), Pronated Load Test (Wilk, 2005), Resisted Supination External Rotation (RSER) Test (Myers, 2005), and Speed's Test (Bennett, 1995).

One way repeated measures ANOVA and Tukey HSD post-hoc tests ( $\alpha=0.05$ ) were used to compare peak muscle activation across the five tests. Selectivity, defined as the proportion of EMG signal received from all muscles monitored that is attributable to the LHBB, was compared using the same statistical methods.

## RESULTS

Maximal activation of the LHBB was significantly different between the five tests ( $p=0.004$ ). Post-hoc analysis revealed that the Biceps Load Test II produced a significantly greater activation of the LHBB than the Active Compression Test (palm down) and the Pronated Load Test. Activation in the Biceps Load Test II was not significantly greater than in Speed's Test, RSER Test, or the Active Compression Test (palm up). LHBB activation in the two positions of the Active Compression Test was different. With the palm up, activation was only  $48.5\pm 17.4\%$ ; while in the palm down position it was significantly greater ( $80.0\pm 12.4\%$ ,  $p<0.05$ , Table 1).

Selectivity was also significantly different between the five tests ( $p=0.000$ ). Post-hoc analysis revealed that the RSER Test, Pronated Load Test, and Biceps Load Test II elicited the highest selectivity with no statistical difference between them.

**Table 1:** LHBB activation (%MVIC) and selectivity ratio for each provocative test.

Tests	LHBB Muscle Activation $\pm$ SD	Selectivity $\pm$ SD
Active Compression Test (palm down)	48.51 $\pm$ 17.44	.19 $\pm$ .02
Active Compression Test (palm up)	80.0 $\pm$ 12.42	.13 $\pm$ .01
Biceps Load Test II	93.0 $\pm$ 11.51	.17 $\pm$ .07
Pronated Load Test	65.7 $\pm$ 23.42	.26 $\pm$ .06
RSER Test	74.7 $\pm$ 21.34	.22 $\pm$ .07
Speed's Test	85.9 $\pm$ 8.21	.22 $\pm$ .01

## DISCUSSION

The primary objective of the provocative tests is to elicit symptoms by either passively or actively tensioning the tendon of the LHBB, which, in turn, pulls at its proximal attachment to the superior glenoid labrum. To avoid confounding the test results due to pathologies of the surrounding shoulder muscles, the tests should ideally minimize activity of other muscles.

Analysis revealed that, of the six test positions studied, the Biceps Load Test II, Speed's Test, RSER Test, and Active Compression Test (palm up) maximally activated the LHBB. The RSER Test, Biceps Load Test II and Pronated Load Test displayed the highest selectivity. With their high LHBB activation and selectivity, the Biceps Load Test II and RSER Test should be the most suitable for diagnosing superior labrum lesions. However, a kinematic analysis to study the passive stretching of the LHBB tendon should be conducted to determine whether the tests effectively strain the superior labrum through other means.

## REFERENCES

- Parentis, M.A., et al. (2005). *Am J Sports Med*, **34**(2), 1-4.
- Morgan, C.D., et al. (1998). *Arthroscopy*, **14**(6), 553-565.
- O'Brien, S.J., et al. (1998). *Am J Sports Med*, **26**(5): p. 610-613.
- Bennett, W.F. (1998). *Arthroscopy*, **14**(8): p. 789-796.
- Kim, S.H., et al. (2001). *Arthroscopy*, **17**(2): p. 160-164.
- Myers, T.H., et al. (2005). *Am J Sports Med*, **33**(9): p. 1315-1320.
- Wilk, K.E., et al. (2005). *J Orthop Sports Phys Ther*, **35**(5): p. 273-291.
- McFarland, E.G., et al. (2002). *Am J Sports Med*, **30**(6). P. 810-815.

# THE EFFECTS OF AGE AND STEP LENGTH ON JOINT KINEMATICS AND KINETICS DURING THE MAXIMUM STEP LENGTH TEST

Brian Schulz<sup>1</sup>, Neil Alexander<sup>2</sup>, and James Ashton-Miller<sup>2</sup>

<sup>1</sup> Patient Safety Center, James A. Haley VA Hospital, Tampa, FL, USA

<sup>2</sup> University of Michigan, Ann Arbor, MI, USA

E-mail: Brian.Schulz@va.gov Web: www.patientsafetycenter.com

## INTRODUCTION

The Maximum Step Length (MSL) test is a clinical measure of the maximal distance that can be reached using a single ‘out-and-back’ step with the arms folded across the chest. The MSL test can be used to determine whether the elderly are at an increased risk for falls (Medell and Alexander 2000; Cho et al. 2004), but little is known about the kinematic and kinetic determinants of the known age-related decrease in MSL performance.

## METHODS

Eleven unimpaired young (mean age=24 years) and 10 older (mean age=73 years) women performed the MSL test. Body segment motions were recorded during the MSL at 100 Hz using an Optotrak 3020 system and ground reaction forces were recorded at 1000 Hz using four AMTI force plates. Joint kinematics and kinetics were calculated using an inverse dynamics model (Thelen et al., 1997) in order to determine the effects of age and step length of the biomechanics of maximal length stepping.

## RESULTS AND DISCUSSION

Young subjects stepped 38% farther than the old subjects ( $p < 0.0001$ ) with only one old subject stepping within the range of the young (Table 1). The young used twice the ankle plantarflexion torque and power ( $p < 0.04$ ) to perform the MSL and the ankle rotated faster (PF=13% & DF=24%,  $p < 0.02$ )

**Table 1:** Mean (SD) subject characteristics and maximum step length (MSL)

	Young Women	Older Women
N	11	10
Age (years) <sup>a</sup>	24 (3)	73 (5)
Height (m)	1.63 (0.07)	1.60 (0.05)
Weight (kg) <sup>b</sup>	55 (5)	68 (14)
BMI (kg/m <sup>2</sup> ) <sup>b</sup>	21 (2)	27 (6)
MSL (m) <sup>a</sup>	1.28 (0.09)	0.93 (0.15)
MSL range (m)	1.13-1.43	0.66-1.20

<sup>a</sup> indicates  $p < 0.0001$  and <sup>b</sup> indicates  $p < 0.01$

for longer steps. The young women attained 31% greater knee extension velocities during the double support phase between landing the “step out” and lifting off for the “step in”. Also during this “pushback” phase the young reached their peak knee extension torques during knee flexion, while the old reached their peak knee extension torque during the later knee extension just before step-in foot lift off (Figure 1). Hip joint kinematics and kinetics increased with step length ( $p < 0.0005$ ) regardless of age.

## SUMMARY/CONCLUSIONS

MSL test performance is most strongly related to peak hip kinematics and kinetics. Age, but not step length, was responsible for the delay in peak knee extension torque and reduced peak plantarflexion torque and power used during the double support phase of the MSL test. The correlation between these age-related changes and an inability to prevent a fall using a step should be examined in future research.

## REFERENCES

- Medell J.L., Alexander N.B. (2000). *J Gerontol A Biol Sci Med Sci*, **55**(8):M429-33.
- Cho B.L., Scarpace D., Alexander N.B. (2004). *J Am Geriatr Soc*, **52**(7):1168-73.
- Thelen D.G. et al. (1997). *J Gerontol A Biol Sci Med Sci*, **52**(1):M8-13.

## ACKNOWLEDGEMENTS

The authors wish to acknowledge the support of the GEM consortium, the Michigan Life Science Corridor, the UM Older American Independence Center (AG08808 and AG024824), the NIA Institutional Training Grant T32 AG00114 (Multidisciplinary Research Training in Aging), the Department of Veterans Affairs Research and Development, and the VA Ann Arbor Health Care System GRECC.

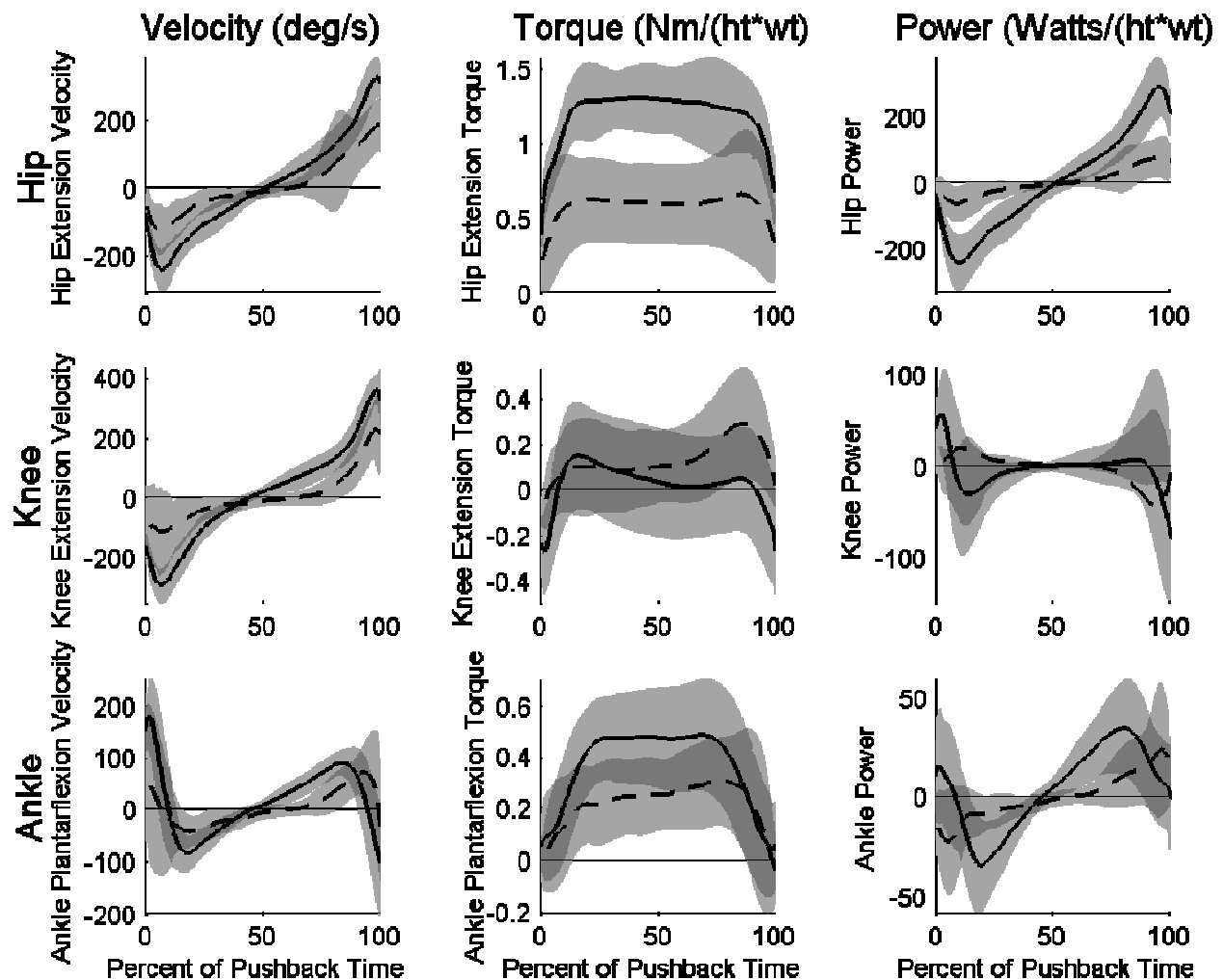


**Figure 1:** Mean hip (top row), knee (middle row), and ankle (bottom row) velocity (left column), torque (middle column), and power (right column) profiles during the ‘pushback’ (dual support with feet apart) phase of the MSL test for young (solid line) and older (dashed line) women averaged across all subjects. Shaded area represents  $\pm 1SD$ . Time is normalized to duration of pushback. Torques and powers are normalized to subject weight and height.

# **PATELLA TENDON GRAFTS MAINTAIN MORE TENSION THAN HAMSTRING TENDON GRAFTS FOLLOWING ACL RECONSTRUCTION**

John J. Elias, William J. Ciccone II, Surya P. Rai, and David M. Weinstein

Medical Education and Research Institute of Colorado, Colorado Springs, CO

E-mail: [elias@meric.info](mailto:elias@meric.info) Web: [www.meric.info](http://www.meric.info)

## **INTRODUCTION**

The primary goal of ACL reconstruction is to limit post-operative anterior knee laxity without over-constraining the knee. Hamstring tendon and patella tendon autografts used for ACL reconstruction are typically harvested early in the procedure and cool to the temperature of the operating room. During reconstruction, initial tension is applied to the grafts to limit knee laxity. Following reconstruction, the grafts stress relax and warm to body temperature at the knee. Post-operative stress relaxation and a temperature increase can decrease the tension and stiffness of the grafts (Ciccone et al., 2006; Johnson et al., 1994). The current hypothesis is that the tension and stiffness decrease is greater for hamstring tendon grafts than patella tendon grafts.

## **METHODS**

Six semitendinosus tendons, six gracilis tendons, and six 10 mm wide patella tendon grafts were harvested from cadaver specimens (mean donor age: 79 years) and stored at -20°C prior to testing. The hamstring tendon grafts were tested in a quadruple strand construct. The free ends of the grafts were sutured together while under tension to minimize the force imbalance between the strands during testing. The free ends of each quadruple strand graft were secured to a polyurethane foam block, which was secured to the base of a material testing machine, with tandem screws and spiked washers. A cross pin secured to the actuator of the testing machine was placed through

the looped end of each graft. The patella tendon grafts were tested with the patella and the tibial bone block secured to the base and actuator, respectively, of the testing machine. Tanks were constructed to submerge the hamstring tendon and patella tendon grafts in saline solution, without submerging the testing fixtures.

Each graft was initially tested with the saline bath at the temperature of an operating room (20 °C). The grafts were preconditioned by applying a load of 105 N, followed by 30 minutes of stress relaxation. Each graft was loaded to 105 N a second time to represent the tension applied during ACL reconstruction. Following 15 minutes of stress relaxation, the actuator force was recorded to represent the graft tension immediately following ACL reconstruction. The graft stiffness was also measured by rising, and subsequently lowering, the actuator by 0.1 mm. Graft tension and stiffness were measured a second time following 4 additional hours of stress relaxation. The saline bath was then heated to 34 °C to represent body temperature at the knee, and the graft tension and stiffness were measured again. Graft tension and stiffness were measured a fourth time after decreasing the temperature back to 20 °C. The four tension and stiffness measurements were compared between the hamstring tendon and patella tendon grafts with a two-way repeated measures ANOVA. The post-hoc comparisons between the four stiffness and tension measurements for each type of graft were performed with a repeated measures Student-Newman-Keuls test.

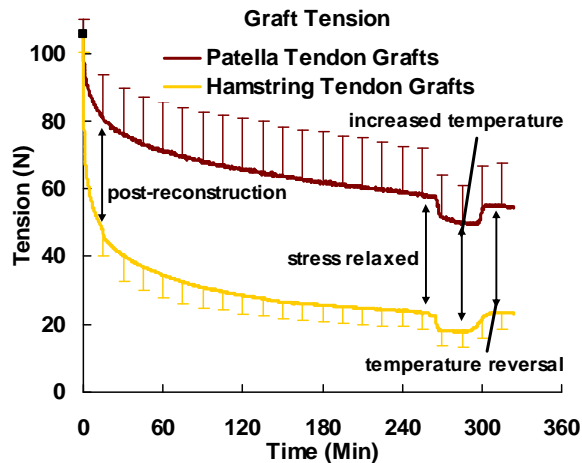


**Figure 1:** Average graft tension ( $\pm$  standard deviation) at 4 time points.

## RESULTS AND DISCUSSION

Over all the time points, the tension in the patella tendon grafts was significantly ( $p < 0.01$ ) larger than the tension in the hamstring tendon grafts (Fig. 1). In addition, for both types of graft, the decreases in graft tension due to stress relaxation (from post-reconstruction to stress relaxed) and due to the temperature increase (from stress relaxed to increased temperature) were statistically significant ( $p < 0.01$ ). For both types of graft, the graft tension values prior to the temperature increase and following the reversal in the temperature increase were not significantly different ( $p > 0.1$ ).

Over all the time points, the stiffness values did not differ significantly ( $p > 0.8$ ) between the patella tendon and the hamstring tendon grafts. For the hamstring tendon (Fig. 2) and patella tendon grafts, the graft stiffness was  $174 \pm 17$  N/mm and  $159 \pm 35$  N/mm, respectively, at the time point representing immediately following reconstruction. The graft stiffness decreased significantly ( $p < 0.01$ ) to  $136 \pm 10$  N/mm and  $140 \pm 39$  N/mm, respectively, following stress relaxation. Increasing the temperature significantly ( $p < 0.01$ ) decreased graft stiffness to  $115 \pm 11$  N/mm and  $129 \pm 35$

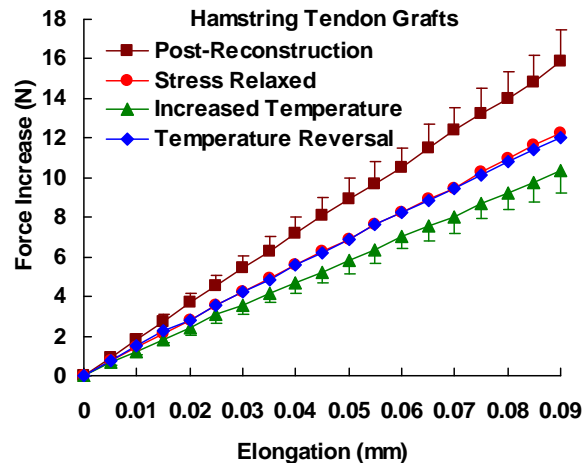


**Figure 2:** Average force increase vs. graft elongation during stiffness tests.

N/mm, respectively. For both types of graft, the graft stiffness values prior to the temperature increase and following the reversal in the temperature increase were not significantly different ( $p > 0.3$ ).

## SUMMARY/CONCLUSIONS

Patella tendon and hamstring tendon grafts lose tension and stiffness following ACL reconstruction due to stress relaxation and a temperature increase. Patella tendon grafts maintain graft tension better than hamstring tendon grafts, although post-operative stiffness levels are similar for the two types of graft. Decreased graft tension could contribute to larger post-operative knee laxity measurements for hamstring tendon grafts than patella tendon grafts (Feller and Webster, 2003; Freedman et al., 2003).

## REFERENCES

- Ciccone, W.J., et al. (in press). *J Bone Joint Surg*
- Johnson, G.A., et al. (1994). *J Orthop Res*, **12**, 796-803.
- Feller, J.A., Webster, K.E. (2003). *Am J Sports Med*, **31**, 564-73.
- Freedman, K.B., et al. (2003). *Am J Sports Med*, **31**, 2-11.

# SHORT LEG WALKING BOOTS INCREASE MUSCLE ACTIVATION OF EXTRINSIC FOOT MUSCLES DURING GAIT

Maria Keefer, Douglas Powell and Songning Zhang

Biomechanics/Sports Medicine Lab, The University of Tennessee, Knoxville, TN, USA  
email: mkeefe2@utk.edu, web: [web.utk.edu/%7Eesals/resources/biomechanics\\_laboratory.html](http://web.utk.edu/%7Eesals/resources/biomechanics_laboratory.html)

## INTRODUCTION

It has been shown that short-leg walking boots alter kinematics and ground reaction forces (GRFs) during gait (Zhang, in press). Short-leg walkers have also been associated with decreased muscle activity compared to barefoot walking and walking in traditional casts (Kadel, 2004). In walking boots, the decreased amplitude of muscle activity would be beneficial to the recovery by limiting the amount of internal loading subjected to the foot. However, Kadel et al. measured muscle activity across the entire stance phase and did not account for muscle activity that is happening prior to and after stance phase (Kadel, 2004). Therefore, the purpose of this study was to determine how short-leg walkers affect muscle activity of major ankle muscles during walking. We examined muscle activity outside of stance phase by using burst duration to analyze muscle amplitude. It was hypothesized that walkers would cause a decrease in ankle muscle activity.

## METHODS

Eleven subjects between ages of 18 and 40 ( $27.4 \pm 7.8$  yrs) participated in this study. Subjects performed five level walking trials in each of three conditions: Gait Walker (DeRoyal Industries, Inc.), Equalizer (Royce Medical Co.) and a pair of lab shoes. Data were collected using an EMG system (600 Hz, Noraxon USA), force platform (600 Hz, AMTI) and a 6-camera motion analysis system (120 Hz, Vicon). EMG data were collected from the Tibialis Anterior (TA),

Peroneous Longus (PER) and Medial Gastrocnemius (MG).

Muscle activity onset and offset were calculated using the raw EMG signal and were defined as the beginning and end of EMG activity. Onset and offset were normalized to heelstrike. TA1 is activation of the TA prior to heelstrike while TA2 is the activation of TA during late stance and initial swing. EMG data were smoothed and rectified using the root mean squared with a 20 ms smoothing window. The integrated and mean EMG values were analyzed between EMG onset and offset and normalized to the maximal integrated EMG (iEMG) value across the three conditions.

A one-way repeated measures ANOVA was used to evaluate selected EMG variables and post hoc comparisons were conducted with an alpha level ( $p < 0.05$ ) adjusted for multiple comparisons through a Bonferroni procedure.

## RESULTS AND DISCUSSION

During the swing to stance transition (IC) the TA was activated 27% of maximal activation while the PER and MG were activated 40% and 36%, respectively. During the stance to swing transition (PS) the TA was activated 36% of maximal activation. The amplitudes of all muscles analyzed were increased during the walker conditions. During IC, wearing Gait Walker and Equalizer increased TA muscle activity by 16% and 9% respectively (Table 1).

During PS, the TA had a two-fold increase in activation intensity for both the Gait Walker and Equalizer. PER muscle activation increased by 28% and 24%, respectively while the MG muscle activation was increased by 34% and 27%, respectively (Table 1).

Kinematic and kinetic data revealed significantly greater maximum knee flexion for the Gait Walker compared to the no walker condition, delayed peak plantarflexor moment for both boots, and a significantly higher peak plantarflexor moment for the Gait Walker compared to the Equalizer (Zhang, in press). These differences in the kinematic and kinetic data may have impacted the EMG data. There was an increase in maximum knee flexion in the Gait Walker, however, the Equalizer did not show this increased knee flexion but still shows significant differences in iEMG except for TA1.

The walkers do not entirely eliminate ankle movements. It was demonstrated that there was a significant decrease in ankle eversion for the Equalizer and ankle range of motion (ROM) for the Gait Walker (Zhang, in press). However, the restriction of ankle movements and the greater weight of the walkers during the boot conditions may contribute to the increased ankle muscle activities due to the need of co-contraction during walking.

The kinetic data collected in this study showed a later peak plantarflexor moment in stance phase for the boot conditions, presumably due to the immobilization of the ankle joint. This peak plantarflexor moment was significantly greater for the boot conditions than the no walker condition. The Gait walker peak plantarflexor moment was also significantly higher than the Equalizer, which is intriguing because the

Gait Walker and Equalizer were not found to have any significant differences in iEMG.

**Table 1.** Integrated EMG values during gait.

	Shoe	Gait Walker	Equalizer
TA1	26.8 ± 8.4	42.6 ± 15.9*	35.3 ± 8.7
PER	39.9 ± 22.9	67.8 ± 14.3*	63.8 ± 12.3*
MG	36.4 ± 15.1	70.5 ± 19.2*	63.2 ± 12.6*
TA2	35.9 ± 22.9	72.1 ± 14.6*	72.9 ± 10.9*

Note: \* - significantly different from Shoe.

## CONCLUSIONS

This study suggests that walking boots cause an increase in ankle muscle activity compared to the shoe condition. This contradicts the literature (Kadel et al., 2004). The discrepancy may be related to how the EMG data were analyzed in this and the previous studies, and the co-activations seen in the ankle muscles in the walker conditions. The subjects in this study were healthy and pain free possibly allowing them to decrease alterations to the gait kinematics at the expense of increased muscle activity. In addition, the muscles examined in the present and previous studies are ankle muscles and may not entirely reflect the internal loading to the foot. Future research is warranted to assess muscle activity in subjects who are prescribed to wear a short-leg walker.

## REFERENCES

- Zhang, S., et al. (In Press). *Gait Posture*.  
 Kadel, N.J., et al. (2004). *Foot Ankle Int.*,  
**25**, 406-9.

## ACKNOWLEDGEMENTS

Funded by DeRoyal Industries, Inc.

# INDEX FINGER JOINT MOTION GENERATED BY INDIVIDUAL EXTRINSIC MUSCLES: A CADAVERIC STUDY

Ashish Nimbarte, Rodrigo Kaz, Zong-Ming Li

Hand Research Laboratory, University of Pittsburgh, PA, USA

E-mail: zmli@pitt.edu

## INTRODUCTION

Index finger joint motion substantially contributes towards hand dexterity. The coordinated phalangeal joint movement by a set of intrinsic and extrinsic muscles has been studied in human subjects (Darling et al., 1994) and also using computer models (Buford et al., 2005). Motion produced by extrinsic muscles at the phalangeal joints greatly depends on their anatomic arrangement. Several cadaveric studies delineating the distribution pattern, anatomic variation and arrangement of extensor tendons were performed. However little is known about the quantitative motion generated by the extrinsic muscles at the phalangeal joints. The purpose of this study was to investigate the index finger joint motion generated by individual extrinsic muscles. In addition, as wrist and finger joints move in synergy (Su et al., 2005), the second purpose was to investigate the effect of wrist position on phalangeal joint motion.

## METHODS

Five cadaver hand specimens, amputated at the mid-humerus and free from apparent musculoskeletal disorders, were used in this study. Upon thawing overnight at room temperature, the specimens were minimally dissected to expose the musculotendinous junctions of the extrinsic muscles: flexor digitorum profundus (FDP), flexor digitorum superficialis (FDS), extensor digitorum communis (EDC), and extensor indicis proprius (EIP). A baseball suture was established at each musculotendinous

junction for tendon loading. The dissected specimen was mounted on a custom made fixture using schanz screws and k-wires drilled into the radius, the metacarpals and middle and distal phalanges of the non-tested fingers (Figure 1). The phalangeal joints of non-tested fingers were stabilized by passing k-wire through them. A set of reflective markers of 5 mm diameter were placed on the dorsal surface of the index finger. Each muscle tendon was loaded manually using a force transducer (Nano 17, ATI Industrial Automation, Apex, NC). Prior to the tendon loading, the index finger was passively moved for 15 seconds through its comfortable motion territory and then placed in a position with minimal resistance to motion. Each tendon was loaded gradually to 10% of their maximal force production capability (Brand et al, 1981) in 10 seconds following a ramp displayed on the screen by custom LabVIEW program. The tests were performed with the wrist at neutral, 45° of flexion, and 45° of extension respectively.



**Figure 1:** A cadaver hand mounted on a custom fixation device for tendon loading and motion recording.

Motion data was recorded using a motion analysis system (Vicon 460, Oxford, UK). The 3 dimensional coordinates of each marker were obtained and processed to determine the flexion-extension angles for the metacarpophalangeal (MCP), proximal interphalangeal (PIP), and distal interphalangeal (DIP) joints.

## RESULTS

At neutral wrist position, the range of motion ratio (MCP:PIP:DIP) generated by the FDP was 1:2.9:2.0 (Table 1). The range of motion at the MCP and PIP joints by the FDS was approximately 2 and 1.5 times of those generated by the FDP. The range of motion ratio (MCP:PIP:DIP) generated by EDC was 6.3:4.4:1. The EIP had motion effects similar to the EDC. Wrist flexion led to increases in the average range of motion at the PIP and DIP joints by the FDP and at the PIP joint by the FDS. The range of motion by the EDC and EIP were not substantially affected by wrist flexion.

**Table 1:** Ranges of motion (°) generated by the individual extrinsic muscles/tendons at different wrist positions.

	Wrist Neutral		
	DIP	PIP	MCP
EDC	-3.07±2.1	-13.7±5.4	-19.6±4.5
EIP	-3.4±1.9	-14.3±3.2	-15.3±9.5
FDS	-1.4±1.5	37.7±6.9	21.9±4.1
FDP	19.6±10.5	27.5±5.7	9.7±6.5
	Wrist Flexion		
EDC	-2.9±1.5	-12.0±2.5	-16.3±5.2
EIP	-3.3±1.7	-13.7±2.3	-16.2±1.3
FDS	-0.5±2.9	45.3±7.4	17.2±5.1
FDP	23.2±10.8	33.4±5.1	8.3±6.1
	Wrist Extension		
EDC	0.2±1.9	-5.9±8.4	-19.3±9.2
EIP	-0.3±1.5	-6.6±6.0	-14.4±9.1
FDS	-1.4±0.8	31.2±11.1	19.5±5.6
FDP	18.8±12.4	24.0±11.8	9.1±7.0

(Note: negative numbers indicate extension range of motion)

Wrist extension decreased the ranges of motion at the DIP joint by the FDP and at the PIP joint by the FDS. The ranges of motion at the DIP joint by the EDC and at the DIP and PIP joints by the EIP also decreased. Wrist posture, in general affected the starting flexion angles of the phalangeal joints (Table 2). In particular, the MCP joint flexion angle increased with wrist extension. The PIP joint flexion angle decreased with wrist flexion and increased with wrist extension. However wrist position had little effects on the DIP joint position.

**Table 2:** The phalangeal joint starting flexion angles (°) at different wrist postures.

Wrist postures	MCP	PIP	DIP
Neutral	31.5±7.4	45.6±8.9	16.1±6.7
Flexion	32.3±5.9	40.4±7.7	16.0±6.6
Extension	37.0±8.5	51.5±9.5	18.0±6.7

## DISCUSSIONS

We studied the index finger phalangeal joint motion generated by individual extrinsic muscles with wrist at neutral, flexed, and extended positions. At a specific wrist position, the two extrinsic extensors generated similar phalangeal movements, but the two extrinsic flexors actuated phalangeal movements in a different manner. The wrist position affected not only the starting phalangeal joint positions, but also phalangeal joint ranges of motion. The results provide insight into the functional manifestation of the index finger by each individual extrinsic muscle.

## REFERENCES

- Brand, P.W. et al. (1981) *J Hand Surg*, **6**, 209-19.
- Buford, W. L. et al. (2005) *J Hand Surg [Am]*, **30**, 1267-75.
- Darling, W.G. et al. (1994) *J Biomech*, **27**, 479-91.
- Su, F.C. et al. (2005) *Clin Biomech*, **23**, 63-74.

# THE COST OF SWINGING THE LEG IN HUMAN WALKING

Brian R. Umberger

University of Kentucky, Lexington, KY, USA  
E-mail: umberger@uky.edu Web: www.coe.uky.edu/~brian

## INTRODUCTION

Swinging the leg forward and placing the foot on the ground in front of the body is a critical component of walking. The energetic cost associated with swinging the leg in human walking is presently unknown, but has recently received much attention in the literature. Early researchers often assumed leg swing to be passive (e.g., Mochon & McMahon 1980), which would imply no cost. Some recent investigators have estimated the cost of swinging the leg to be 10-20% of the net metabolic cost of walking (Gottschall & Kram 2005, Griffin et al. 2003), however, a different estimate based on isolated leg swinging suggested that the cost was closer to 33% (Doke et al. 2005). An intermediate value of 26% was obtained using in vivo measurements in walking guinea fowl (Marsh et al. 2004).

Progress has been limited by the inability to directly measure muscle energy expenditure during walking. Musculoskeletal modeling techniques allow muscle energy expenditure to be estimated during simulated activities, and can complement the experimental procedure used in other studies. The purpose of this research was to estimate the cost of swinging the leg using a computer simulation model of human walking.

## METHODS

A forward dynamics simulation of walking at 1.3 m/s was generated using an existing model that was modified to simulate the foot-ground interface during stance (Fig 1). The model included seven rigid segments

(trunk, thighs, shanks, and feet), and was driven by 12 Hill-type muscle actuators per leg (Umberger et al. 2006). The muscle model yielded both mechanical and thermal energy production, which were summed to obtain muscle metabolic energy expenditure (Umberger et al. 2003). An energy term representing the rest of the body was also included to estimate whole-body energy consumption.

The model was controlled by muscle excitation signals that were defined by three consecutive blocks that could each vary in timing and magnitude. Numerical optimization was used to find muscle excitation patterns that produced walking that: a) was cyclic, b) minimized distance-specific energy expenditure, and c) did not result in knee joint hyperextension. Muscle metabolic energy expenditure was obtained by integrating the rate of energy expenditure (sum of work and heat rates) with respect to time over the stance and swing phases for each muscle. Comparable experimental kinematic, kinetic, and metabolic data were collected on six healthy, young adults walking at the same speed as the model.



**Figure 1:** Planar, seven-segment, nine-degree of freedom musculoskeletal model.

## RESULTS AND DISCUSSION

Numerical optimization resulted in a simulation that reproduced the essential features of human walking. Whole-body energy expenditure was 7% higher in the model than the subject average, but was well within the range of experimental values (Fig 2). Leg muscle energy consumption represented nearly 80% of the whole body energy expenditure. Of the energy expended by the leg muscles, 71% was consumed during the stance phase, and 29% was consumed during the swing phase (Fig 2).

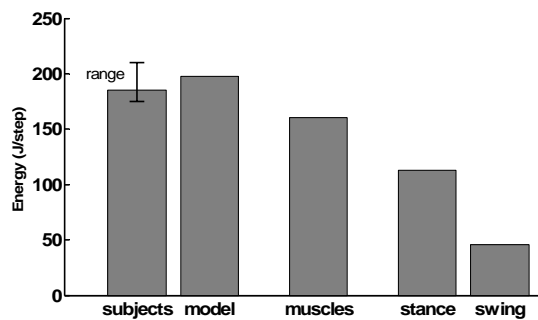


**Figure 2:** Left: subjects and model whole-body energy expenditure. Center: model muscle energy expenditure. Right: model muscle energy expenditure during stance and swing phases.

The greatest consumers of energy during stance were the plantarflexors, hamstrings, gluteals, and quadriceps, which together accounted for 95% of stance phase energy expenditure. Of these muscle groups, the plantarflexors (soleus, gastrocnemius, and the other plantarflexors) consumed the most energy, representing 33% of the stance phase costs. The greatest contributors to swing phase costs were the hamstrings, quadriceps, iliopsoas, and dorsiflexors, which together consumed 91% of the swing phase energy. These four muscle groups made relatively similar contributions to the total cost of swinging the leg. The hamstrings were the only muscle group to

make a meaningful contribution to the costs of both the stance and swing phases.

## SUMMARY

The findings of this simulation study support experimental results that suggest the metabolic cost of swinging the leg represents about one quarter (Marsh et al. 2004) to one third (Doke et al. 2005) of the total lower limb muscle energy expenditure in walking. Together, these results have implications for the continued development of a theory to explain the determinants of the metabolic cost of locomotion. Future work using this modeling and simulation approach will focus on how stance and swing costs vary with speed and stride rate. Additional studies will be conducted to better identify the metabolic costs associated with other aspects of walking, such as supporting body weight and generating propulsion, or producing force and doing mechanical work.

## REFERENCES

- Doke, J. et al. (2005). *J Exp Biol*, **208**, 439-445.
- Gottschall, J.S., Kram, R. (2005). *J Appl Physiol*, **99**, 23-30.
- Griffin, T.M. et al. (2003). *J Appl Physiol*, **95**, 172-183.
- Marsh, R.L. et al. (2004). *Science*, **303**, 80-83.
- Mochon, S., McMahon, T.A. (1980). *J Biomech*, **13**, 49-57.
- Umberger, B.R. et al. (2003). *Comp Method Biomech Biomed Eng*, **6**, 99-111.
- Umberger, B.R. et al. (2006). *J Biomech*, in press.

## ACKNOWLEDGEMENT

The assistance of Karin Gerritsen, PhD, with development of the musculoskeletal model is greatly appreciated.

# ACCURACY OF CONTACT AREA MEASUREMENTS WITH THIN-FILM PRESSURE SENSORS

Elizabeth I. Drewniak, Joseph J. Crisco, David B. Spenciner, and Braden C. Fleming

Department of Orthopaedics, Brown Medical School/Rhode Island Hospital, Providence, RI  
E-mail: Joseph\_Crisco@brown.edu Web: www.brownbiomechanics.org

## INTRODUCTION

To better understand the biomechanics of joint injury and replacement, several methods to measure contact force, pressure, and area have been developed (e.g. Fregly 2003, Harris 1999, Heino Brechter 2003, Matsuda 1997). The thin-film based Tekscan system (Tekscan, Inc., South Boston, MA), which consists of a matrix of semi-conductive ink that creates an electrical resistance at intersection points called sensels, is frequently used.

The purpose of this study was to investigate the accuracy of contact area measurements using a Tekscan Sensor and to introduce a new approach for improving the accuracy of these measurements.

## METHODS

Four flat-ended aluminum circular indenters with differing diameters were used to apply loads to a Tekscan 5076 sensor (Tekscan Inc., South Boston, MA). The indenter contact areas were 1140mm<sup>2</sup>, 2027mm<sup>2</sup>, 3167mm<sup>2</sup>, and 4560mm<sup>2</sup>. Applied loads ranged from 1000 to 7000N in 1000N increments. Quasi-static loads were applied using a servo hydraulic material tester (model 8521-S; Instron Corp., Canton, MA). The experimental setup included the indenter placed on top of a Tekscan sensor with a thin foam-rubber pad inserted between the indenter and the sensor, which was positioned on a rigid steel plate and load cell.

A preload of 100N was applied and then ramped up to the desired load at a rate of 800N/s. Test loads were held for one minute while data were collected at a rate of 25Hz. Each indenter was tested three times at each load for a total of 84 tests.

The contact area data were collected using I-scan software. A MATLAB (The Mathworks, Inc., Natick, MA) program was written to calculate the area recorded with the Tekscan sensor. The program also determined the mean pressure value of the sensels and the pressure value at two standard deviations from the mean. The program then filtered out sensels less than two standard deviations from the mean before calculating the adjusted area. The data were plotted as functions of applied load and percent error between the actual area of the indenter, and the unfiltered and filtered Tekscan areas.

The percent errors in contact area measured by the Tekscan system and computed by the MATLAB filtering program were compared using a Mann-Whitney Rank Sum Test (SigmaStat3.1, Systat Software, Inc., Point Richmond, CA). The significance value of  $P < 0.05$  was set *a priori*.

## RESULTS AND DISCUSSION

Percent errors in the contact area ranged from as low as 5% for the largest indenter at the lowest applied load to 27% for the smallest indenter at the highest applied load

with the 5076 sensor. At all loads, decreasing the indenter size increased the contact area percent error. An unexpected finding was the trend of a greater percent error in contact area with an increase in the applied load (Figure 1).

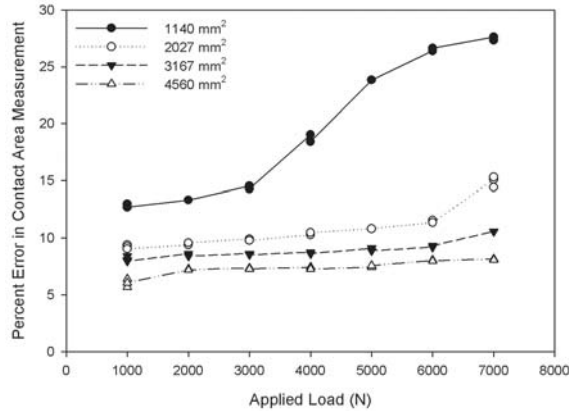


**Figure 1:** Percent error between the actual contact areas of the indenters and the areas recorded with Tekscan 5076 sensor as a function of applied load.

Filtering out the data collected with the 5076 sensor reduced the percent error in contact area to less than 1% for all but one load when using the three largest indenters. The smallest indenter, however, had area percent error ranging from approximately 2 to 14.3% (Figure 2).

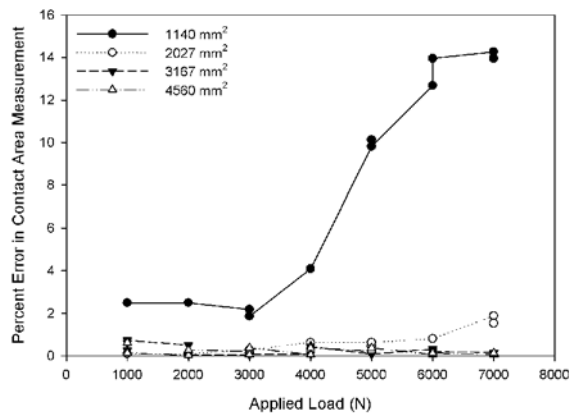


**Figure 2:** Contact areas after filtering out pressure values lower than two standard deviations from the mean pressure value.

Overall, filtering the pressure values before calculating area significantly ( $P < 0.001$ ) reduced percent errors in contact area measurements for all forces and areas using the 5076 sensor.

While our filtering approach improved the accuracy and precision of the contact area measurements, this study still has some limitations. The indenters used in this investigation were circular, so we cannot say if this filtering method would work for other shapes. Only one 5076 sensor was evaluated. Further testing could have investigated variability and fatigue across numerous sensors. Also, results could differ depending on the compliance of the indenter and the underlying surface.

## SUMMARY

In summary, our results show a degree of inaccuracy in contact area measurements when using the Tekscan system with the 5076 sensor. However, when the data were run through a filtering program, accuracy was dramatically improved. Filtering Tekscan output is a viable way to reduce the errors.

## REFERENCES

- Fregly, B.J. et al. (2003). *J. Biomech*, **36**, 1659-1668.  
 Harris, M.L. et al. (1999). *J. Biomech*, **32**, 951-958.  
 Heino Brechter, J. et al. (2003). *Magn Reson Imaging*, **21**, 955-959.  
 Matsuda, S. et al. (1997). *J. Arthroplasty*, **12**, 790-797.

## ACKNOWLEDGEMENTS

This study was funded in part by the RIH Orthopaedic Foundation Inc. and University Orthopedics, Inc.

# ADJUSTMENTS OF PREHENSION SYNERGIES IN RESPONSE TO SELF-TRIGGERED AND EXPERIMENTER-TRIGGERED LOAD AND TORQUE PERTURBATIONS

Jaebum Park<sup>1</sup>, Vladimir M. Zatsiorsky<sup>2</sup>, Mark L. Latash<sup>2</sup> and Jae Kun Shim<sup>1</sup>

<sup>1</sup>Department of Kinesiology, University of Maryland, College Park, MD

<sup>2</sup>Department of Kinesiology, Penn State University, University Park, PA

E-mail: jkshim@umd.edu Web: www.hhp.umd.edu/KNES/faculty/jkshim/neuromechanics/

## INTRODUCTION

Hand action has been often used as an object to study feed-forward mechanism of control in human movements. Previous studies addressed feed-forward changes in the overall performance of the hand in anticipation of changes in the external forces. It was shown that anticipatory adjustments could be achieved in the grip force prior to an action or a perturbation applied to a hand-held object (Gordon et al. 1993).

In this study, we ask a different question: Can the central nervous system adjust multi-digit synergies in a feed-forward manner, in preparation to predictable perturbation, without changing the overt behavior of the multi-digit prehension system?

Based on the principle of superposition, a skilled, complex action can be decomposed into independently controlled sub-actions such as grasping force control and rotational equilibrium control. So, we also expected to see different adjustments in indices of multi-digit synergies stabilizing the total gripping force and the total moment of force.

## METHODS

To address this issue, we studied adjustments in multi-digit synergies associated with applied load/torque perturbations while the subjects held a customized handle steadily.

There were six experimental conditions: two types of perturbations (self-triggered and experimenter-triggered) by three positions of the load (left, center, and right).

Subjects (n=8) performed 12 trials for each condition, and returned the initial handle position as quickly as possible after a perturbation, which consisted of removing one of three loads hanging from the handle. Three-dimensional forces and moments of force recorded from each digit contact were used for the analysis.

Indices of covariation among digit forces and among moments of force, previously applied for studying motor synergies, were computed across trials. (Shim et al. 2004)

## RESULTS AND DISCUSSION

In steady-state conditions, strong positive indices for both digit forces and digit moment were shown over all subjects. Negative covariation of individual digit force and moments of force means the positive value of the indices in order to stabilize the total force and moment acting on the handle.

Under the self-triggered conditions, changes in the indices of digit force and moment covariations were seen about 150 ms prior to the perturbation, while such changes were detected right after the perturbation under the experimenter-triggered conditions (Figure 1).

Immediately following a perturbation, the indices of force and moment covariation rapidly changed to negative revealing the lack of inter-compensation among the individual digit forces and moments.

Later, both indices showed a recovery to positive values; the recovery was faster in the self-triggered conditions than in the experimenter-triggered ones. During the steady-state phase after the perturbation, the indices of force and moment covariation

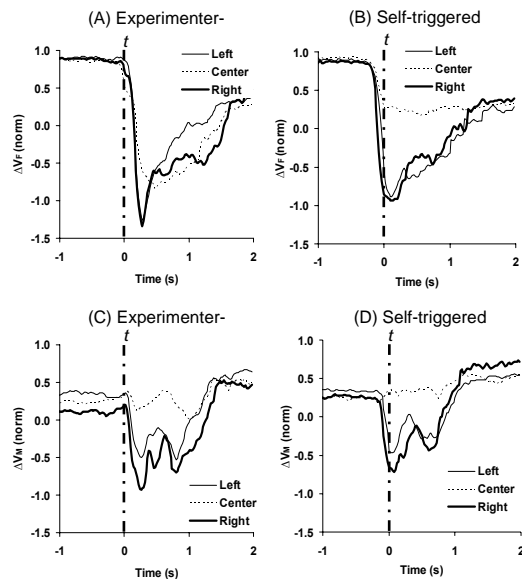


**Figure 1.** Indices of finger force covariation. The load was removed at time  $t_0=0$  s ( $t_0$ ). Different lines show data during lifting the loads at different locations. Note the early shifts in  $\Delta V$  indices for self-triggered conditions.

decreased and increased, respectively, as compared to the indices during the steady-state phase prior to the perturbation.

## SUMMARY/CONCLUSIONS

We conclude that 1) humans are able to adjust multi-digit synergies involved in prehensile tasks in anticipation of a self-triggered perturbation, and 2) Different changes in the indices of force and moment covariation after a perturbation corroborate the principle of superposition.

## REFERENCES

- Gordon AM, Westling G, Cole KJ, Johansson RS (1993). *J. Neurophysiol*, **69**, 1789-1796
- Mason MT, Salisbury KJ (1985). *Robot Hands and the Mechanics of Manipulation (Artificial Intelligence)*. MIT Press,
- Shim JK, Lay BS, Zatsiorsky VM, Latash ML (2004). *J. Appl Physiol*, **97**, 213-224
- Shim JK, Olafsdottir H, Latash ML, Zatsiorsky VM (2005). *Exp Brain Res*, **164**, 260-270

## ACKNOWLEDGEMENTS

NIH grants AG-018751, AR-048563, M01 RR10732, and NS-35032.

# ACTIVE AND PASSIVE MECHANICAL PROPERTIES OF MATURING DYSTROPHIC EDL MUSCLES

Andrew Wolff<sup>1</sup>, Ashley Niday<sup>2</sup>, Kevin Voelker<sup>3</sup>, Jarrod Call<sup>3</sup>, Nick Evans<sup>3</sup>, Kevin Granata<sup>2</sup>, and Robert W. Grange<sup>3</sup>

<sup>1</sup> Department of Mechanical Engineering, Virginia Tech, Blacksburg, VA USA

<sup>2</sup> Department of Engineering Science and Mechanics, Virginia Tech, Blacksburg, VA USA

<sup>3</sup> Department of Human Nutrition, Foods, and Exercise, Virginia Tech, Blacksburg, VA USA

E-mail: wolffan@vt.edu

## INTRODUCTION

Duchenne muscular dystrophy (DMD) is an X-linked degenerative skeletal muscle disease characterized by the absence of the protein dystrophin from the cytoplasmic surface of skeletal muscle cell membranes. Dystrophin associates with a group of proteins collectively known as the dystrophin-glycoprotein complex (DGC) that is localized to the sarcolemma of skeletal muscle fibers. In the absence of dystrophin, the proteins of the DGC are also absent (Durbeej and Campbell, 2002).

In maturing dystrophic mice aged 9-12 days, prior to the overt onset of the disease, absence of dystrophin appears to have minimal effects on muscle stiffness during a stretch-injury protocol (Grange et al., 2002). These data suggest that stiffness in dystrophic muscles may only differ following dystrophic onset and progression. To address this issue, we considered that muscle mechanical properties should be assessed over an age range prior to, during and following onset of the dystrophic process.

The purpose of these studies was to determine (1) if the active and passive mechanical properties (i.e., stiffness and damping) of maturing dystrophic muscles were different from control; and, (2) if

different, when during maturation did these properties change?

## METHODS

At ages prior to and following the overt onset of the dystrophic process (14-35 days), control and dystrophic extensor digitorum longus (EDL) muscles were subjected to two passive stretch protocols at 5% strain with two strain rates (instantaneous and 1.5 L0/s) in vitro. Force profiles at the instantaneous strain rate were fit to a muscle model (Fung, 1993) composed of viscous and linear elastic branches in parallel, combined with a pure linear elastic branch in series (Fig 1). From this model we could determine several mechanical properties of muscle including parallel and series elastic stiffness and damping, C. The same viscoelastic muscle model was used to determine stiffness properties of 28 day old active control and *mdx* EDL muscles at strain rates of 2, 4 and 8 Lo/s. In addition to whole muscle mechanics, we are currently running experiments with an atomic force microscope (AFM) to determine stiffness of the muscle fiber membrane directly. The membranes are probed with the AFM by indenting the surface of the cell with the tip of the cantilever and measuring the force-indentation. Deflection-distance curves are recorded at different points along the length of the muscle fiber membrane.

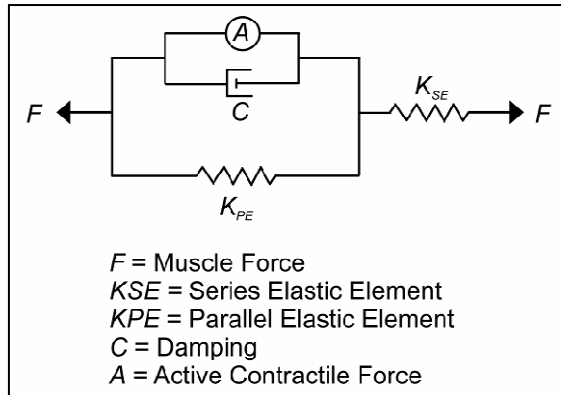


**Figure 1:** Viscoelastic mathematical muscle model with series and parallel components.

## RESULTS AND DISCUSSION

The dystrophic and control EDL muscles exhibited similar passive mechanical properties at each age (14, 21, 28, and 35 days). For example, there was no difference in passive series elastic stiffness between dystrophic and control EDL muscles (Fig. 2). There was no loss in maximum tetanic force before and after the repeated passive stretches indicating that the contractile apparatus was not affected by the stretch protocols. No difference in active stiffness was found between *mdx* and control 28 day old EDL muscles at all three strain rates. These results suggest a functional threshold for dystrophic muscle below which damage may be minimized. Determining this threshold could have important clinical implications for treatments of muscular dystrophy involving physical activity.

## SUMMARY

We observed few differences in passive mechanical properties of 14-35 day old *mdx* and control EDL muscles stretched within their linear elastic range. Although passive stiffness properties of dystrophic muscles appear similar during early maturation (e.g., 9-35 days), it is likely that more severe

stretch perturbations in the nonlinear elastic stretch range will evoke muscle damage as the dystrophic process is initiated and progresses. The absence of dystrophin also showed no effect on the active stiffness of 28 day old EDL muscles. An AFM is currently being used to compare direct stiffness measurements of the muscle membrane with the results from the whole muscle viscoelastic model. Determination of skeletal muscle passive and active mechanical properties may be useful to assess the effects of other muscle diseases including the muscular dystrophies, as well as for determining efficacy of therapeutic treatments.

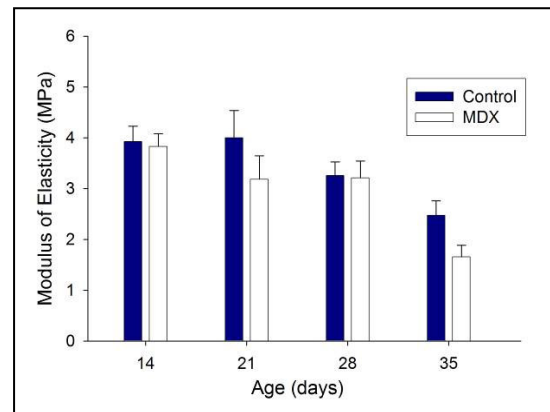


**Figure 2:** No difference in passive series elastic stiffness between genotypes at each age ( $P < 0.05$ ).

## REFERENCES

- Durbeej, M., Campbell, K.P. (2002). *Curr Opin Genet Dev*, **12**, 349-361.
- Grange, R.W. et al (2002). *Am J Physiol Cell Physiol*, **283**, C1090-C1101
- Fung, Y.C. (1993) *Biomechanics: Mechanical Properties of Living Tissues*. Springer-Verlag New York, Inc.

## ACKNOWLEDGEMENTS

This research was supported by NIH grant R01-AR049881 to R.W. Grange.

# THE EFFECT OF JOINT POSITION AND FATIGUE ON AGONIST/ANTAGONIST CO-ACTIVATION DURING ISOMETRIC KNEE EXTENSION

Staci M. Stevens; Naoko Aminaka; Anuradha Mukherjee; Danny M. Pincivero

Human Performance and Fatigue Laboratory, Department of Kinesiology, The University of Toledo; Toledo, OH, USA

Email: [staci.stevens@utoledo.edu](mailto:staci.stevens@utoledo.edu), [danny.pincivero@utoledo.edu](mailto:danny.pincivero@utoledo.edu)

## INTRODUCTION

Agonist/antagonist co-activation has been proposed to be a potential injury prevention mechanism for the anterior cruciate ligament (ACL). However, varying results have been reported throughout the literature, with respect to agonist/antagonist co-activation across various knee positions. As anterior tibial translation is proposed to be greatest at more extended knee positions and if agonist/antagonist co-activation is a mechanism for reducing ACL strain, it may be speculated that co-activation would be greatest near full extension. Furthermore, the level of co-activation may also be limited subsequent to fatigue inducement of the antagonist muscle group. Therefore, the purpose of this study was to investigate the effect of joint position and knee flexor fatigue on agonist/antagonist co-activation during isometric knee extension.

## METHODS

Eight healthy, recreationally active individuals (5 men, 3 women) with no history of lower limb injury volunteered for participation in this study. The subjects visited the laboratory 6 times, with at least 48 hours between sessions. Each testing session occurred at a pre-determined, and randomly ordered knee position (10, 30, 50, 70, 90 deg knee flexion). Electromyography (EMG) was collected from 7 muscles (vastus medialis (VM), vastus lateralis (VL), rectus femoris (RF), medial hamstring

(MH), lateral hamstring (LH), medial gastrocnemius (MG), and lateral gastrocnemius (LG)) during each visit. Subjects sat in the Biodex accessory chair, the lower leg was secured to the resistance adaptor and the knee was then placed in the pre-determined testing position. The subjects first performed 5 manually resisted, plantar-flexion maximal voluntary contractions (MVC), each lasting approximately 5 s with 2 minutes between each contraction. Subjects then performed 5 isometric knee extension MVC's (5 s, 2 min rest). Subjects subsequently performed 5 isometric knee flexion MVC's in a similar manner. The fatigue protocol consisted of sub-maximal and maximal knee flexor contractions and began with the subjects performing a 5 s sub-maximal (50% MVC) contraction, which was followed by a 5 s rest period. Following 5 sub-maximal contractions, the subjects were instructed to perform a 5 s knee flexor MVC. The subjects were considered fatigued when their MVC torque decreased by 50%, or when they were no longer able to maintain 50% MVC for the entire 5 s duration. Immediately following the fatigue protocol, the subjects were asked to perform 5 isometric knee extension MVC's, with 2 min separating each contraction.

## RESULTS AND DISCUSSION

The results of this investigation revealed no significant difference between pre-fatigue and post-fatigue co-activation values for the

MH and LH; however, the MG and LG co-activation values were found to be significantly greater post-fatigue ( $p < 0.05$ ) (Figure 1). An effect of knee angle on co-activation was found to be significant for the MG and LG ( $p < 0.05$ ), as co-activation was greatest at 70 deg knee flexion. However, no effect was revealed for the MH and LH (Figure 2).

With no change in MH and LH co-activation with fatigue, it is suggested that the neural drive to the hamstrings is maintained after the fatigue protocol and the functional ability of the hamstrings as antagonists is not effected by muscular exhaustion. As it has been shown that the gastrocnemius muscle acts as an antagonist to the ACL (Fleming et al., 2001), the results of this study suggest that the function of the gastrocnemius is more apparent with fatigue of the hamstring muscle group.

The lack of a significant change in hamstring co-activation throughout the knee range of motion indirectly suggests that hamstring co-activation is not initiated by strain on the ACL. As research has suggested that ACL strain is greatest with quadriceps femoris muscle contraction at extended positions (Grood et al, 1984), these results indirectly demonstrate that the ACL-hamstring reflex is not the only moderator of hamstring co-activation. It may be that a common drive to the agonist and antagonist muscle groups is responsible for antagonist co-activation (Psek & Cafarelli, 1993).

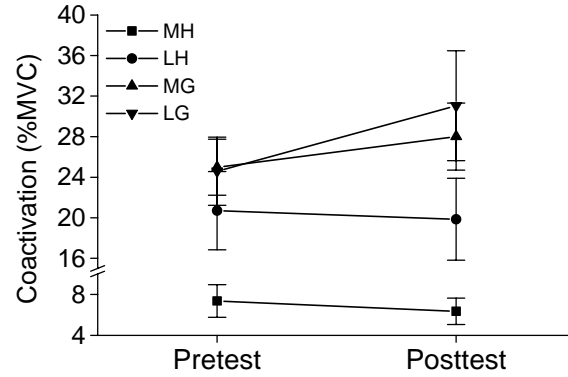


Figure 1. Co-activation levels as a function of pre- and post-fatigue tests, for the MH, LH, MG, and LG.

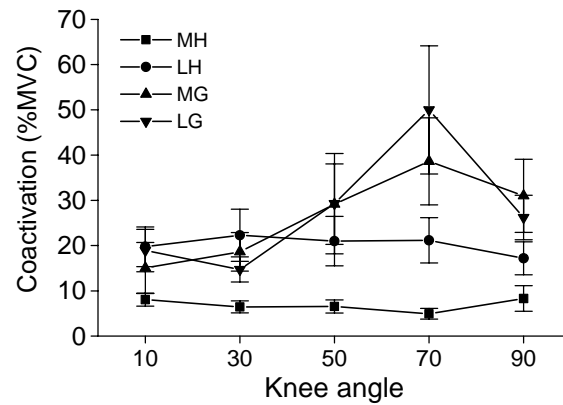


Figure 2. Co-activation levels as a function of knee flexion angle, for the MH, LH, MG, LG.

## REFERENCES

1. Fleming, B.C., et al. (2001) *Journal of Orthopaedic Research*, **19**, 1178-1184.
2. Grood, E.S., et al. (1984) *Journal of Bone and Joint Surgery, Am*, **66**, 725-734.
3. Psek, J.A. & Cafarelli, E. (1993) *Journal of Applied Physiology*, **74**, 170-175.

## ACKNOWLEDGEMENTS

This project was funded by the 2005 American Society of Biomechanics Graduate Student Grant-In-Aid Program.

# PLANTAR PRESSURE VARIATIONS DURING EXERCISE ON FOUR PIECES OF COMMERCIALLY AVAILABLE CARDIOVASCULAR EQUIPMENT

Amy G. Jorde<sup>1,2</sup>, Shannon R. Ogren<sup>1,3</sup>, Tanner R. Augustin<sup>1,2</sup>,  
Tate A. Augustin<sup>1,2</sup>, Gregory R. Bashford<sup>2</sup>, and Judith M. Burnfield<sup>1,2,3</sup>

<sup>1</sup> Madonna Rehabilitation Hospital, Movement Sciences Center, Lincoln, NE, USA

<sup>2</sup> University of Nebraska – Lincoln, Lincoln, NE, USA

<sup>3</sup> University of Southern California, Los Angeles, CA, USA

E-mail: jburnfield@madonna.org

## INTRODUCTION

Plantar pressures during exercise are influenced by variations in forces generated at the foot-floor interface and contact area between the foot and supporting surface (Kernozek & Zimmer, 2000; Burnfield et al., 2004). Recent emphasis on the value of exercise for prevention of secondary medical complications combined with an expansion of the availability of commercial fitness equipment into medically-based fitness facilities has resulted in a wide range of cardiovascular exercise options for persons with acute and chronic medical conditions. As prolonged exposure to elevated plantar pressures can lead to pain and tissue injury in persons with orthopaedic and neuropathic foot disorders, a better understanding of the impact of select exercises on foot pressures appears warranted. The purpose of this study was to explore plantar pressure variations during exercise on four commercially available cardiovascular exercise devices which were selected due to the expected variations in foot-contact patterns and weight-bearing loads on the foot while exercising.

## METHODS

Ten subjects (19-35 years old; 5 male, 5 female) with no known musculoskeletal or neurological disorders were recruited. Each participated in four sessions. During the first three sessions, subjects were familiarized

with the cardiovascular equipment (Life Fitness™ Treadmill 97Ti, Elliptical Cross-Trainer 95Xi, Recumbent Bike 95Ri, Stairclimber 95Si) and instructed to exercise on each at a speed that they could maintain for a thirty minute workout. During the fourth session, plantar pressure variables (Pedar by Novel) and support surface kinematics (Motion Analysis) were recorded simultaneously as subjects performed treadmill walking, treadmill running, elliptical training, recumbent biking, and stairclimbing in self-selected footwear. Each was performed for five minutes, and the order was randomized. Data were recorded during the final minute of each exercise. Mean Maximum Peak Pressure (PP) values in the heel, arch, and forefoot were identified, and their respective Mean Maximum Force (MF) and Mean Contact Area (CA) values were recorded for the dominant limb. Separate one-way analyses of variance with repeated measures determined if PP, MF, or CA varied significantly across activities in each region. A Bonferroni adjusted alpha level of  $P < 0.0167$  assessed significance.

## RESULTS AND DISCUSSION (Table 1)

**Heel:** PP under the heel was significantly higher during walking and running compared to elliptical training, stairclimbing, or recumbent biking ( $P \leq 0.005$ ) owing primarily to a significantly higher MF under the heel during walking

and running compared to the other three conditions ( $P \leq 0.002$ ). Compared to all other activities, biking registered the lowest heel MF ( $P \leq 0.001$ ) and CA ( $P \leq 0.002$ ). Heel CA was also diminished during stairclimbing, registering a significantly lower value than during running ( $P = 0.009$ ).

**Arch:** PP under the arch was significantly higher during running compared to all other activities ( $P \leq 0.010$ ), primarily due to the presence of significantly higher MF during running compared to all other conditions ( $P \leq 0.003$ ). Arch PP was also elevated during walking, exceeding those during biking and stairclimbing ( $P < 0.001$ ). PP under the arch was lowest while biking versus all other exercise conditions ( $P < 0.001$ ) owing primarily to a significant reduction in MF under the arch during biking compared to all other activities ( $P < 0.001$ ). Significantly lower PP during biking occurred despite the reduction in arch CA during biking compared to walking, running and stairclimbing ( $P \leq 0.007$ ). PP was significantly higher during elliptical training compared to stairclimbing ( $P = 0.016$ ) despite insignificant MF and CA variations.

**Forefoot:** PP under the forefoot was significantly higher during running, walking and elliptical training compared to biking and stairclimbing ( $P \leq 0.007$ ), resulting primarily from significantly higher MF in the forefoot during the former three activities ( $P \leq 0.002$ ). Forefoot PP was significantly lower while biking compared to all other activities ( $P < 0.001$ ), owing mainly to a significantly reduced MF during

this activity compared to all other tasks ( $P < 0.001$ ). Forefoot MF during elliptical training was notably lower than that recorded during running ( $P = 0.010$ ). Forefoot CA did not vary significantly across exercise conditions.

## SUMMARY/CONCLUSIONS

In healthy young adults, PPs varied greater than seven-fold under the heel, four-fold beneath the arch, and five-fold under the forefoot across exercises due primarily to variations in MF. While further research is required in persons with pathology, rehabilitation from orthopaedic conditions where protection of heel tissues is important should consider use of the recumbent bike, stairclimber, and elliptical trainer due to the associated low heel pressures and forces. Persons with pain or injury in the arch region or at risk for neuropathic forefoot ulcers should consider use of the recumbent bike and stairclimber due to the associated low arch and forefoot pressures and forces.

## REFERENCES

- Burnfield. J.M. et al. (2004). *Clinical Biomechanics*, **19**, 78-84.  
 Kernozek, T.W., Zimmer, K.A. (2000). *Foot & Ankle International*, **21**, 749-752.

## ACKNOWLEDGEMENTS

Daniels Fund, Denver, CO  
 UCARE Program,  
 University of Nebraska - Lincoln  
 Madonna Auxiliary, Lincoln, NE  
 Gifford Swenson Estate, Lincoln, NE

**Table 1.** Mean Maximum Peak Pressure (N/cm<sup>2</sup>), Maximum Force (N), and Contact Area (cm<sup>2</sup>) on heel, arch, and forefoot regions for five activities during the fifth minute of exercise (mean  $\pm$  SD).

Activity	Heel			Arch			Forefoot		
	PP	MF	CA	PP	MF	CA	PP	MF	CA
Walking	22.4 $\pm$ 3.1	414.4 $\pm$ 139.4	27.9 $\pm$ 8.8	12.2 $\pm$ 1.4	165.7 $\pm$ 44.8	27.6 $\pm$ 4.9	24.9 $\pm$ 8.1	217.3 $\pm$ 45.2	14.5 $\pm$ 2.3
Running	19.9 $\pm$ 4.6	376.9 $\pm$ 149.9	28.2 $\pm$ 9.3	15.4 $\pm$ 2.8	294.8 $\pm$ 92.7	27.3 $\pm$ 5.7	25.2 $\pm$ 4.9	251.8 $\pm$ 61.3	14.5 $\pm$ 2.4
Elliptical Training	10.3 $\pm$ 4.0	215.8 $\pm$ 122.5	29.1 $\pm$ 7.4	10.8 $\pm$ 2.3	186.0 $\pm$ 54.8	29.6 $\pm$ 6.8	18.6 $\pm$ 8.0	181.8 $\pm$ 78.3	15.0 $\pm$ 2.0
Recumbent Biking	3.0 $\pm$ 1.0	25.4 $\pm$ 22.8	10.28 $\pm$ 8.9	3.8 $\pm$ 1.0	52.8 $\pm$ 24.1	19.0 $\pm$ 7.5	4.4 $\pm$ 1.5	36.5 $\pm$ 21.0	11.1 $\pm$ 5.2
Stairclimbing	7.6 $\pm$ 1.6	133.3 $\pm$ 68.8	24.5 $\pm$ 8.9	8.6 $\pm$ 2.3	156.3 $\pm$ 34.2	28.6 $\pm$ 4.3	10.8 $\pm$ 2.0	122.9 $\pm$ 30.8	15.9 $\pm$ 2.0

# DESIGN AND FABRICATION OF ABOVE-KNEE PROSTHESIS FOR AMPUTEES USING EXTERNAL MOTION ASISTANCE SYSTEM

R Bhargav Prasad and Vikram Srinivas

Anna University, Chennai, TN, India  
E-mail: srinivas\_vikram\_10@yahoo.com

## INTRODUCTION

In spite of many path breaking advances in medicine, little has been done to address the needs of amputees who constitute nearly 5% of the population of Third World countries. A majority of the population of these countries are already worn down in their struggle to make ends meet and invariably end up with no means to support themselves upon amputation. The products available to help them lead a normal life require high maintenance and are built with sophistication making them far too expensive. **The paper is a report of the analysis, design and fabrication process of artificial limb for Above-Knee Prosthesis.** We are confident that our design is cost-effective without compromising on gait.

## OVERVIEW

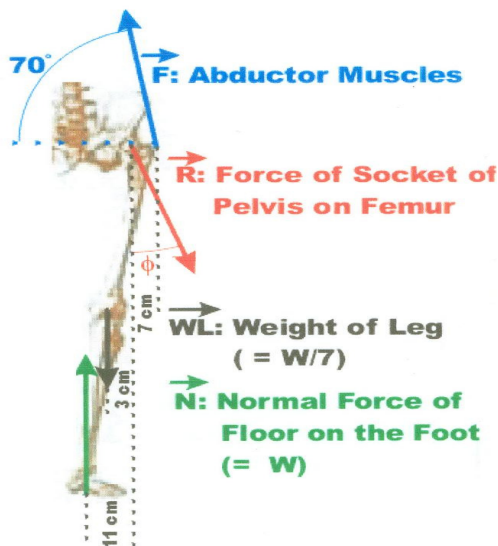


**Figure 1:** Static Force Analysis on leg joints.

**Static force analysis** of an A-K amputee was done to determine the load and their inclinations on the joints (as shown in the figure 1). The horizontal, vertical components of the forces and the torque equations are:

$$\begin{aligned}\sum F_H &= F \cos 70^\circ - R_H \\ \sum F_V &= F \sin 70^\circ - R_V - W/7 + W \\ \sum \tau &= (F \sin 70^\circ)7 + (W/7)3 - 11W\end{aligned}$$

Assuming equilibrium and solving,

$$\begin{aligned}R &= 1.51221 F = 2.43 W \\ \Phi &= 13.071^\circ\end{aligned}$$

## PATIENT SPECIFICATION

**Name** : James Anandan  
**Age** : 28  
**Type of Stump** : Trans-Femoral  
**Amputation Detail** : Lost left leg due to road accident in the year 1992.

## DESIGN AND FABRICATION OF THIGH SOCKET

The socket conforms to the body dimensions of the patient's stump. The socket design was done such that no power loss occurs. The material chosen should be extremely resistant to impact damage, have high strength/weight ratio and cost-effective. It should also be easily moldable into complex shapes. Hence, Fiber-Glass was chosen over other options like Kevlar and Carbon-Fiber. **Adopting negative-casting method using**

**Plaster of Paris, Fiber-Glass socket was fabricated** as shown in figure 2.



**Figure 2:** Fabrication of Thigh Socket.

### DESIGN OF KNEE JOINT

Knee joint is the most important constituent of an A-K type artificial limb. So care should be taken to design and easily operative, light weight and cost effective model. **Standard ALIMCO single axis knee joint** with Indian squat of  $140^{\circ}$  enabled, is a standard component available in the market that satisfied the requirements and was hence purchased.

### DESIGN OF FOOT

The foot with an inbuilt rocker and toe-spring that enables it to move even in the absence of an ankle joint was selected in design process. **PUF (Poly Urethane Foam) foot with inbuilt toe spring system** was thus used.

### OPTIMIZATION

The standard ALIMCO knee setup used in our case has a knee lock which has to be activated prior to walking to clear the ground by moving the limb in an arc like fashion. To avoid this, the knee lock has to be deactivated. When deactivated, there is a possibility of buckling of the knee. Addressing this problem, design and fabrication of an **External Motion Assisted System (EMAS)**, using nylon as the material and spring control of the knee, is

done. Here the bending is controlled by virtue of stiffness of the two springs which use two screws to guide them. The entire setup is attached to the kneecap as shown in the figure 3.



**Figure 3:** EMAS Mechanism.

### FINAL PRODUCT



**Figure 4:** Patient using the Fabricated Artificial Limb.

### CONCLUSION

The limb designed and fabricated costs USD 79.60 and is hence **30% more economical than commercially available limbs** such as ALIMCO (USD 120.00) and OTTO BOCK (USD 160.00) limbs.

### REFERENCE

- Chester, C.H., Atha, T. (1945) *Amputation Prosthesis.*
- Romm, Sharon. (1988) *Plastic and Reconstructive Surgery.*

# CAN HIP JOINT ACTUATIONS BE USED TO CONTROL THE STRUCTURE OF CHAOTIC LOCOMOTION?

Max J. Kurz<sup>1,2</sup> and Nicholas Stergiou<sup>1</sup>

<sup>1</sup>University of Houston, Houston, TX, <sup>2</sup>University of Nebraska at Omaha, Omaha, NE  
E-mail: mkurz@uh.edu Web: [http://hhp.uh.edu/pep/Faculty\\_Pages/MKurz/Mkurz.htm](http://hhp.uh.edu/pep/Faculty_Pages/MKurz/Mkurz.htm)

## INTRODUCTION

Although it is well known that chaos is a central feature of human locomotion, it is not clear what biomechanical factors influence the structure of the chaotic pattern or if it is controllable. Previously, we have used a passive dynamic walking model that has a chaotic locomotive pattern as our foundation to explore these questions (Figure 1; Kurz & Stergiou, 2005). Our simulations indicate that hip joint actuations can be used to transition to stable gaits embedded within the chaotic locomotive attractor. Assisting the motion of the swing leg resulted in the model transitioning to a higher-order gait pattern. For example, a systematic increase in hip joint assistance promoted a period-4 gait pattern to bifurcate to a period-8, and a period-8 gait to bifurcate to a period-16. This suggests that tuning the motion of the swing leg can be used to control the chaotic structure of the gait pattern and may provide a mechanism to transition to stable gaits embedded within the chaotic attractor. Here we explore if these concepts extend to human chaotic gait patterns with a custom built mechanical hip actuator that assists the motion of the swing leg during gait (Figure 2).

## METHODS

The mechanical hip actuator was designed to assist the swing leg during locomotion by applying a linear force at the ankle of the subject via a cable-spring winch system (Figure 2). Similar systems have been developed to explore the contribution of the swing leg to the energetics of locomotion (Gottschall & Kram, 2005). During

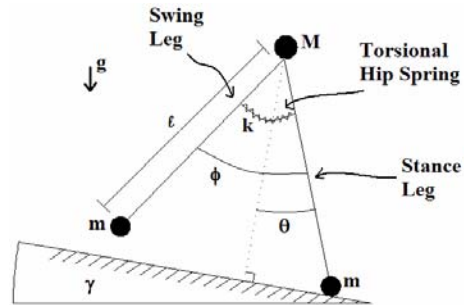


**Figure 1.** Passive dynamic walking model that controls the chaotic structure of the gait pattern with a hip joint actuator (torsional hip spring).

locomotion, the stance leg moved backward due to the treadmill motion and stretched a rubber spring that was in series with the cable. Upon the initiation of the swing phase, the stored potential energy in the spring assisted the forward motion of the swing leg. Nineteen subjects (Age =  $27.68 \pm 4.3$  years, Weight =  $713.05 \pm 188.6$  N, Height =  $1.71 \pm 0.09$  m) walked on the treadmill for five minutes at a self-selected pace while the mechanical hip actuator assisted the motion of the swing leg at forces equal to 0%, 10%, 20% and 25% of the subject's limb weight. A 60 Hz high-speed three-dimensional motion capture system was used to capture the hip, knee and ankle sagittal plane joint angles. The largest

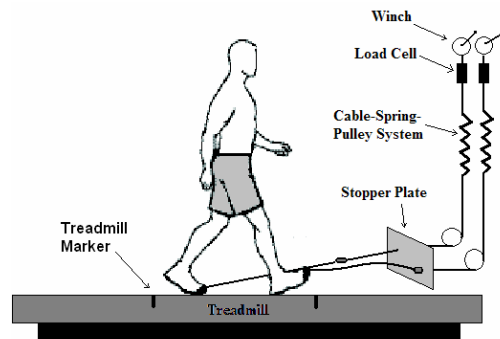


**Figure 2.** Mechanical hip actuator that assists the motion of the swing leg.

Lyapunov exponent (LyE) was used to quantify the chaotic structure of the respective lower extremity joint angle time series. The LyE for a periodic sine wave is zero and random noise is 0.469. Human chaotic locomotion lies somewhere between the two extremes (Stergiou *et al.*, 2004). A systematic increase in the LyE value as hip assistance was increased would indicate a change in the structure of the human chaotic gait pattern that was similar to our model's simulations.

## RESULTS AND DISCUSSION

A significant difference was found in the LyE for the hip ( $p = 0.0001$ ), knee ( $p = 0.0001$ ) and ankle ( $p = 0.0001$ ) joints as the percent of hip resistance was increased (Fig 3). Post-hoc analysis revealed a significant difference between all the assistance conditions and the no assistance condition ( $p < 0.05$ ). A significant ( $p < 0.05$ ) increasing linear trend was found for all of the lower extremity joints as assistance was increased. This indicated that the swing assistance scaled the structure of the human chaotic gait pattern in a similar fashion as our passive dynamic walking model. At the greatest level of hip assistance, the chaotic structure of the hip joint increased by 38%, knee joint increased by 35% and the ankle increased by 25%. Hence, our human experiments and model indicated that the neural control of the swing limb plays an important role in the structure of chaotic gait. Potentially, the inability to properly 'tune' the motion of the swing leg may be related to changes in the chaotic structure seen in the pathological populations such as the elderly (Stergiou *et al.*, 2004). This is the first investigation to demonstrate that the structure of chaos is controllable and that it can be systematically altered. Possibly we may be able to control the chaotic structure of pathological gait patterns. Currently, we

are using the mechanical hip actuator to determine if we can 'tune' the motion of the swing leg in the elderly and control the chaotic structure of their gait. This may lead to therapeutic mechanisms that can restore a healthy and stable chaotic gait pattern.

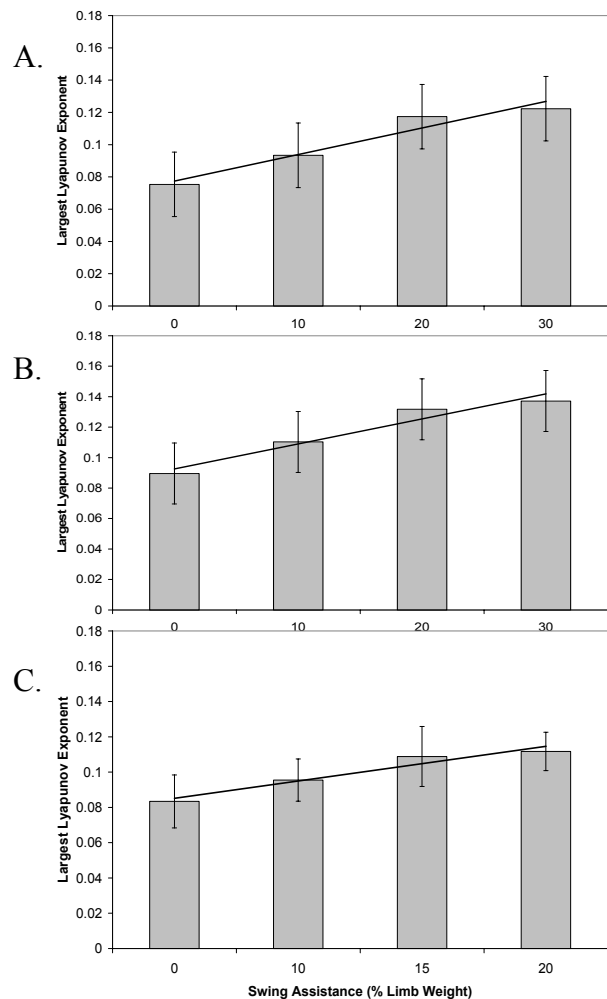


**Figure 3.** LyE values for the hip (A), knee (B) and ankle (C) joints as the percent of swing assistance was increased. The line represents the increasing linear trend.

## REFERENCES

- Kurz MJ & Stergiou N (2005). *Bio Cyber*, **93(3)**, 213-21.  
 Gottschall J & Kram R (2005). *J Appl Phys*, **99(1)**, 23-30.  
 Stergiou N, *et al.* (2004). *Innovative Analysis of Human Movement*. Human Kinetics:Champaign, IL.

# Cerebral Palsy: A 3D *in vivo* Knee Joint Kinematic Study

Frances T. Sheehan, PhD<sup>1</sup>, Andrea R. Seisler, MBE<sup>1</sup>,  
Katharine E. Alter, MD<sup>1</sup>, and Steven J. Stanhope, PhD<sup>1</sup>

<sup>1</sup> National Institutes of Health, Bethesda, MD, USA  
E-mail: fsheehan@cc.nih.gov Web: pdb.cc.nih.gov

## INTRODUCTION

Cerebral Palsy (CP) is the most common disabling condition in childhood, involving a diverse group of movement and posture disorders of varying etiologies. Yet, the analysis techniques used to study this disease have difficulty quantifying kinematic parameters at the joint structure level. Thus, this work focuses on quantifying *in vivo* tibiofemoral (TF) and patellofemoral (PF) kinematics along with the patellar tendon moment arm in a group of individuals with CP during volitional knee extension using fast-PC MRI. Four primary questions were addressed: 1) Can patients with CP perform the repetitive motion required to capture the kinematic data? 2) Does “lever-arm dysfunction” exist in this population 3) Are there significant differences between normal and CP knee joint function and are these differences consistent across the CP population of this study? and 4) Do the current findings relate to clinical observations?

## METHODS

Four subjects diagnosed with CP participated in this study. For one subject both knees were examined, thus 2 subject numbers were assigned in order to represent both limbs (S2=left knee and S3=right knee). Subjects were placed supine in within the 1.5-T MR imager (LX-9.1M4; GE Medical Systems, Milwaukee, WI, USA). Data were acquired using dynamic imaging sequences (fast-PC MRI) while subjects

cyclically extended and flexed their knee through a comfortably attainable range of motion at 35 cycles/minute.

From these data, 3D kinematic translations and rotations were quantified for the PF and TF joints as well as determining the patellar tendon moment arm relative to the TF finite helical axis (TF-FHA). These data were then compared to the normative average (n=34). For consistency in comparing subject data, all translational and moment arm data were normalized by the average epicondylar width (77.7mm) and the individual subject’s epicondylar width.

## RESULTS AND DISCUSSION

The patellar tendon moment arm for 4 out of the 5 CP subjects was greater than the

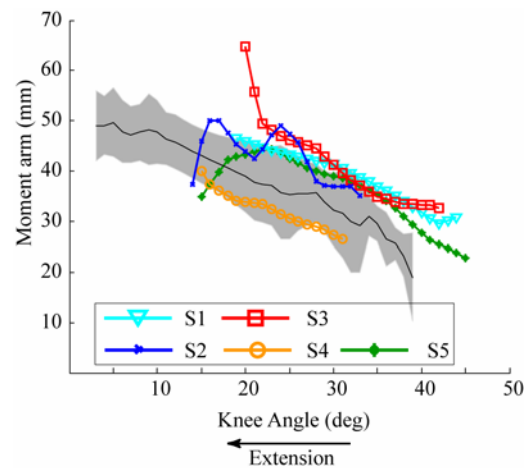


Figure 1: **Moment Arm:** The normative average (n=34) is in black with  $\pm 1$ SD in grey). Each CP knee was assigned a unique color and symbol.

normative average, disagreeing with the theory of lever-arm dysfunction (Figure 1). Though the differences compared to the normative population did not reach significant levels, they remained 1.0-1.5 SD away from the normative average. The only previous direct measure of the PF joint in CP patients has been through the use of sagittal radiographs, in which the TF finite helical axis was assumed to be a fixed point. In both the both populations this was not the case and it appeared that the increased moment arm in the CP patients was due to a finite helical axis that remained more posterior than the normative population.

The strongest commonality in kinematics was found in three most involved subjects (S1, S4 and S5) and agreed well with the clinical findings. These commonalities included decreased PF extension, increased PF varus rotation and increased PF superior translation as compared to the normative population. These three subjects also demonstrated varied PF medial tilt and similar TF varus. The internal tibial rotation for S5 was almost exactly aligned with the normative average, whereas S1 and S4 had significantly internally rotated tibias. This may be influenced by S5's recent distal tibial derotation osteotomy for tibial torsion.

The PF joint was the most affected in CP subjects, which agrees with the clinical observation that individuals with CP often have PF joint dysfunction, limited knee extension strength and spasticity which all contribute to mobility impairments.

Going forward, studying a larger CP population including a variety of functional subtypes, both before and after major surgical interventions will allow correlations between various dynamic quantities, clinical findings, and interventional outcomes to be established. This may allow differentiation of PF and TF function in various functional sub-types of CP, which will provide insights into the management of these specific subpopulations affected by CP.

## SUMMARY/CONCLUSIONS

Fast-PC MRI is a practical tool for acquiring data with which to study the effects of CP at the joint level. There were significant differences between the CP subjects and the unimpaired subjects. However, these differences were not consistent across the CP population, but the results of each individual in this study are supported by clinical findings.

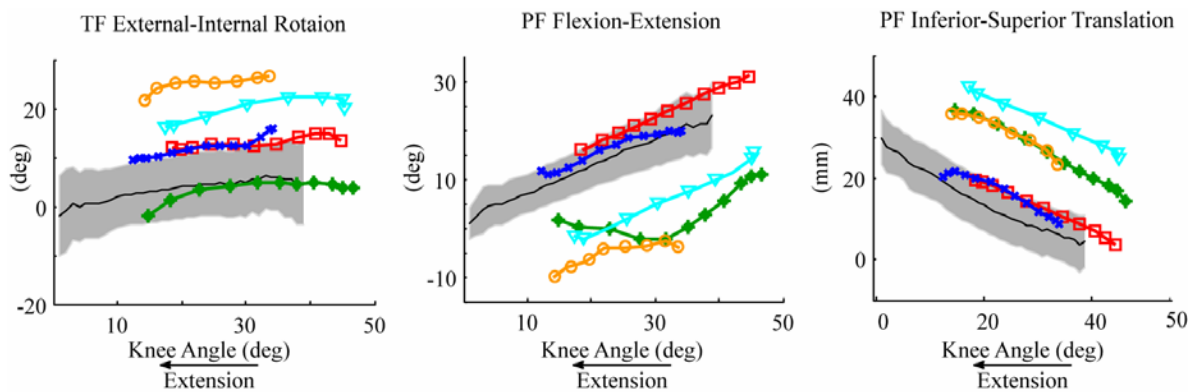


**Figure 2:** Key PF and TF kinematics parameters that demonstrated a relationship with clinical findings. The colors and symbols are the same as in Figure 1.

# A NEW METHOD OF DETERMINING THE STRUCTURE OF BIOLOGICAL TIME SERIES BY USING APPROXIMATE ENTROPY AND CHANGING LAG VALUES

Naomi Kochi<sup>1</sup>, Joan E. Deffeyes<sup>1</sup>, Regina T. Harbourne<sup>2</sup>, Stacey L. DeJong<sup>2</sup>, Wayne A. Stuberg<sup>2</sup>, Anastasia Kyvelidou<sup>1</sup>, and Nicholas Stergiou<sup>1</sup>

<sup>1</sup>University of Nebraska at Omaha, Omaha, NE, USA

<sup>2</sup>University of Nebraska Medical Center, Omaha, NE, USA

E-mail: nkochi@mail.unomaha.edu Web: www.unocoe.unomaha.edu/hper/bio/home.htm

## INTRODUCTION

To better understand the biological implications of the variability present in physiological signals, it is important to use nonlinear tools, as methods of analysis, in addition to conventional linear tools (i.e. standard deviation). Nonlinear tools can assist in obtaining subtle information hidden in very complex physiological signals, which cannot be obtained by using linear tools. One of the most widely used nonlinear tools to detect the presence of chaos in a time series is the Lyapunov Exponent (LyE). Another nonlinear tool that has been used extensively is the Approximate Entropy (ApEn), which can quantify the predictability or regularity of the fluctuations present in a time series (Pincus, 1991; Pincus et al., 1991). The calculation of ApEn is based on conditioning vectors that are used to identify component-wise similar vectors and through which similar patterns that exist in a time series can be detected. The lag parameter value for the calculation of ApEn is defined as the consecutive data points skipped to create conditioning vectors by the algorithm. The purpose of the present study was to describe a technique that can be used to determine the presence of chaos in a time series that is based on the behavior of the ApEn values as the lag parameter value increases. To accomplish this goal, we used both known (chaotic, periodic and random) and biological time series.

## METHODS

We have identified as our known time series the following: the Lorenz, the Baker, the Ikeda and the Henon map as chaotic time series; a simple sine, a double sine and multiple sine waves as periodic time series; and three different fractional Gaussian noises as random time series. For our biological time series, we used Center-Of-Pressure (COP) data obtained from eleven typically developing sitting infants. These infants participated in data collections started at the age of 145.1 days old ( $sd = 15.9$ ) and taking place twice a month for a period of four months. The COP data was collected with an AMTI force plate (Watertown, MA), interfaced to a computer system running Vicon data acquisition software (Lake Forest, CA). LyE was calculated using the Chaos Data Analyzer software (Sprott & Rowlands, 1995). To compute ApEn, custom laboratory software written in Matlab (Mathworks, Natick, MA), with code developed by Kaplan and Staffin (1996), was used. We calculated ApEn of each time series, increasing the lag parameter value from 1 to 20.

## RESULTS AND DISCUSSION

ApEn values for all the chaotic time series except the Lorenz increase rapidly and converge to higher values of ApEn as the lag value increases. Compared with the chaotic time series, the ApEn values of the periodic time series remain lower, and there are relatively small effects of changing the lag

value on the ApEn values. For the random time series, consistent results are obtained, and there is almost no influence of changing the lag value on the ApEn values. These results are explained by the fact that change in the lag value brings rearrangement of conditioning vectors. With small lag values, conditioning vectors stay relatively closer to the structure of an original time series while with large lag values, they do not accurately represent patterns in the original time series. Thus for the case of chaotic time series, as long as conditioning vectors are created in a way that does not destroy subtle structures contained in the time series, similar patterns can be detected, and ApEn values stay lower. Considering the fact that a periodic time series has structures repeating themselves and that whatever the lag value is, a constant number of points is skipped, change in the lag value has little effect on finding similar patterns. As for a random time series, it contains fewer similar patterns to begin with. Therefore, having conditioning vectors with large lag values that do not represent the original time series has little effect on the ApEn values.

For the COP data, LyE and ApEn were calculated for each of 219 trials. LyE was positive for all the data ( $Mean = 0.10$ ,  $sd = 0.02$ ) indicating the presence of chaos. The ApEn values gradually increased and showed a similar behavior as those of the chaotic time series even though the ApEn were smaller than those of the chaotic time series.

## SUMMARY/CONCLUSIONS

We have shown that time series with different structures have unique behaviors in terms of the changes observed on the ApEn values as lag values increase. A converging behavior of a time series as the lag value increases suggests the presence of chaos,

and we have used biological data to also demonstrate this finding. Taking into consideration that ApEn is robust with short and relatively noisy physiological data, we believe that our method is worth being further explored as a new technique to determine the structure of biological time series. This may be important in determining abnormalities in biological time series such as the COP, as well as in evaluating effects of treatment for pathological conditions.

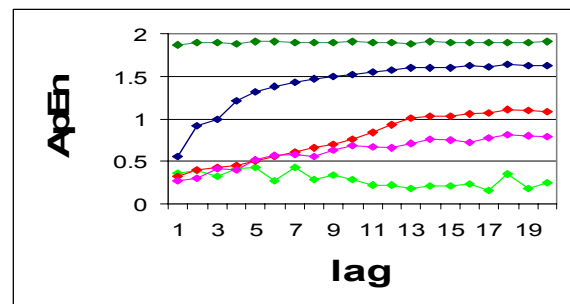


**Figure 1:** Mean ApEn for 3 random time series (dark green), for 4 chaotic time series (blue), for 3 periodic time series (light green), Lorenz (red) and COP (pink).

## REFERENCES

- Pincus, S.M. (1991). *Proc Natl Acad Sci USA*, **88**, 2297-2301.
- Pincus, S.M. et al. (1991). *J Clin Monit*, **7**, 335-345.
- Sprott J.C., Rowlands, G. (1995) *Chaos Data analyzer*.
- Kaplan, D., Staffin, P. (1996). <http://www.macalester.edu/~kaplan/hrv/doc/>

## SECONDARY TASK EFFECT ON GAIT STABILITY DURING OBSTACLE CLEARANCE IN OLDER ADULTS

Ka-Chun Siu, Vipul Lugade, Li-Shan Chou, Paul van Donkelaar, and Marjorie Woollacott

Department of Human Physiology, University of Oregon, Eugene, Oregon, U.S.A  
E-mail: chou@uoregon.edu

### INTRODUCTION

Previous research indicated that balance is greatly perturbed and the fall risk is increased in older adults when simultaneously performing a secondary cognitive task during gait (Shumway-Cook and Woollacott, 2000). Deficits in balance maintenance under dual-task conditions are more prominent in older adults with balance impairments (Shumway-Cook et al, 1997). Previous dual task research in balance-impaired subjects has been limited to the study of balance control during stance; thus the effect of performing a secondary task on stability during challenges to gait is not known. In light of reported findings from studies on stance balance control, one would expect that the ability to properly maintain gait stability could be greatly decreased under dual-task conditions in balance impaired elders. This may explain why inability to recover from slips and trips during gait accounts for the majority of falls in balance impaired older adults (Nevitt et al, 1991).

This study examined how a secondary task affects gait stability during obstacle clearance in the elderly. It was hypothesized that a greater impact on gait stability would demonstrate in older adults with balance impairments while performing two tasks simultaneously.

### METHODS

Twelve healthy young adults (HYA) (5 females and 7 males;  $22.8 \pm 2.7$  years;  $172.3 \pm 14.18$  cm;  $72.2 \pm 14.3$  kg), 12 healthy elderly adults (HOA) (3 males and 9 females;

$74.1 \pm 4.6$  years;  $163.6 \pm 10.3$  cm;  $67.8 \pm 11.4$  kg) and 12 elderly patients with a fall history (BIOA) during walking (4 male and 8 female;  $81.1 \pm 4.3$  years;  $164 \pm 8.9$  cm;  $72.3 \pm 12.7$  kg) were recruited for this study. Subjects were asked to walk at a self-selected pace along a walkway in unobstructed level walking and while stepping over an obstacle set to a height equivalent to 10% of the subject's body height.

Three dimensional marker trajectories were collected at 60Hz with an eight-camera motion tracking system (MotionAnalysis, Santa Rosa, CA). Twenty-nine reflective markers were placed on bony landmarks of the body (Hahn & Chou, 2004). An auditory Stroop task was implemented as a secondary task by SuperLab Pro (Cedrus, San Pedro, CA). Stimuli presenting a word (HIGH or LOW) with high or low pitches were relayed to the subject via two speakers during crossing obstacle. Verbal reaction times (VRT) during the Stroop task were recorded.

Both external markers and estimated joint centers (of both distal and proximal ends) were used to calculate the three-dimensional locations of segmental center of mass (COM). Whole body COM position data was calculated as the weighted sum of each body segment, with 13 segments representing the whole body (head-neck, trunk, pelvis, upper and lower arms, upper and lower legs, feet). The center of pressure position was calculated from the ground reaction forces/moments collected from two

force platforms (AMTI, Watertown, MA) at 960 Hz.

Gait variables and VRT were assessed as dependent measurements by using a three-factor ANOVA with repeated measures of testing conditions and congruency.

## RESULTS AND DISCUSSION

For VRT performance, congruency effect (difference between congruent and incongruent situations) was significantly larger in seated condition compared with two walking conditions in all subjects. The congruency effect was reduced linearly ( $p < 0.05$ ) across three testing conditions. Interestingly, BIOA showed a relative smaller difference between congruent and incongruent situations during obstacle crossing (Fig. 1).

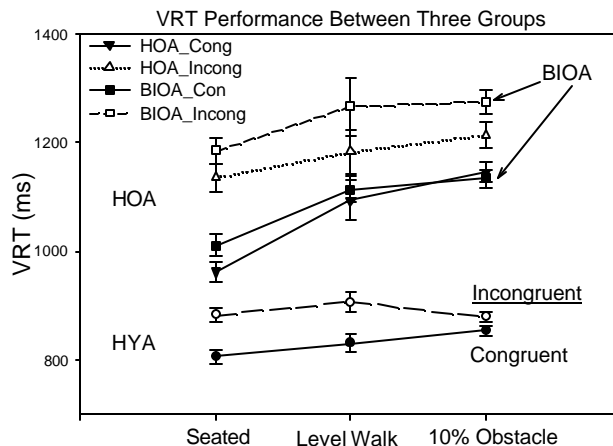


**Figure 1:** This graph illustrates the average VRT performance among three groups in three conditions. Solid lines represent congruent situation and dot lines represent incongruent situation.

During obstacle clearance, when compared to level walking, medial-lateral COM deviations (ML COM) increased significantly in all age groups, especially in the incongruent situation (Table 1). Only elderly individuals with balance impairments showed a significant reduction in ML COM sways between incongruent and control situation, indicating walking strategy was altered to be more stable in order to perform the secondary task in BIOA.

## SUMMARY/CONCLUSIONS

As balance task becomes more challenging, the congruency effect diminishes in HYA and HOA, indicating that obstacle crossing is highly attention demanding. Although BIOA minimize their body sway when performing a difficulty secondary task, they show a smaller reduction in the congruency effect. It suggests that BIOA may have insufficient dual task capacity to perform two tasks simultaneously and tend to prioritize their gait stability in dual task environment.

## REFERENCES

- Shumway-Cook A., Woollacott M. (2000). *J. Gerontology*, **55**, M10-M16.  
 Shumway-Cook A. et al. (1997). *J. Gerontology*, **52**, M232-M240.  
 Nevitt M.C. et al. (1991). *J. Gerontology*, **46**, M164-M170.  
 Hahn M.E., Chou L-S. (2004). *J. Biomech*, **37**, 837-844.

## ACKNOWLEDGEMENTS

This study was supported by the NIH. (R01 AG05317).

**Table 1:** ML COM range of motion in cm (mean  $\pm$  SD)

Groups:	HYA		HOA		BIOA	
Conditions:	Level walk	10%	Level walk	10%	Level walk	10%
Single	3.6 $\pm$ 1.1	4.5 $\pm$ 1.3	3.5 $\pm$ 0.6	5.1 $\pm$ 1.7	5.5 $\pm$ 1.7	8.7 $\pm$ 2.9 <sup>a</sup>
Congruent	3.7 $\pm$ 0.6	4.4 $\pm$ 1.1	3.4 $\pm$ 0.6	5.5 $\pm$ 1.4	5.5 $\pm$ 1.9	7.8 $\pm$ 2.2
Incongruent	3.4 $\pm$ 0.4	4.3 $\pm$ 1.1	4.1 $\pm$ 1.8	5.0 $\pm$ 1.5	5.7 $\pm$ 2.3	7.6 $\pm$ 2.3 <sup>a</sup>

a. significant congruency difference,  $p < 0.05$

# EFFECTS OF MOMENT OF INERTIA ON DIGIT FORCES DURING OSCILLATORY ANGULAR MOVEMENTS OF A CIRCULAR HANDHELD OBJECT

Alexander Hooke, Junfeng Huang, Jae Kun Shim  
University of Maryland, College Park, MD, USA  
E-mail: jkshim@umd.edu

Web: [www.hhp.umd.edu/KNES/faculty/jkshim/neuromechanics/](http://www.hhp.umd.edu/KNES/faculty/jkshim/neuromechanics/)

## INTRODUCTION

Everyday manipulation tasks require static grasping and dynamic translation and/or rotation of a hand-held object such as lifting, holding, drinking a glass of water, etc. (Shim et al. 2005)

Previous studies have investigated static grasping of both rectangular and circular object manipulations. The prismatic grip of rectangular objects has been a favorite topic of research studies on the central nervous system control of hand digit forces and moments. Other studies on pinch or multi-digit grasping of rectangular objects showed that humans increase a grip force (normal force) with object weight (Kinoshita et al. 1995). It has been also shown that the grip force is always larger than the minimally required normal force to prevent slipping of digit tips at contacts (safety margin: Westling and Johansson 1984). Recently, a study on dynamic translational movements of hand-held objects of different weights showed linear increases of grasping forces with the weight of the objects.

However, our knowledge on central nervous system control of digit forces and moments during circular object manipulation is largely limited. In this study, we investigated changes in finger normal and tangential forces and safety margins during oscillatory angular movements of hand-held objects of seven different moments of inertia.

## METHODS

A cylindrical aluminum handle (radius = 4.5 cm) was used in this study. An aluminum beam (69.8cm) was attached to the center

bottom of the handle at its midpoint. A vertical pillar was attached to the bottom of the aluminum beam below the center of the handle. Mounted to the handle were five, six-dimensional sensors, each capable of measuring force and moment in three dimensions. The relative angular positions of the sensors were determined from average angular digit positions across all subjects. Two masses of 262.5 g were attached to the aluminum beam, each an equal distance in a transverse plane.

We manipulated the moment of inertia about the vertical axis for different experimental conditions by changing the load locations in the plane. At the bottom of the vertical pillar, a three-dimensional magnetic sensor was used to provide online feedback of the angular position of the handle about the vertical axis.

Six healthy, young adults volunteered as subjects for this study. Each subject grasped the handle such that each digit tip was placed on the midpoint of a sensor and the aluminum beam was perpendicular to gravity. The subjects were asked to rotate the system about the longitudinal axis for 20 oscillatory cycles covering a range from 45° counter-clockwise to 45° clockwise from the neutral grasping position. We provided auditory feedback (beeps) to subjects to control the period of oscillation. The frequency of oscillations was 1.0 Hz.

## RESULTS AND DISCUSSION

The time profiles of the normal and tangential forces were found over an entire 20 cycle trial. The average maximum values of normal and tangential forces were then

calculated from these profiles over all cycles (Figure 1). Under all of the conditions, the magnitudes of normal and tangential forces were largest in the thumb. The largest safety margin was found in the thumb and the smallest in the index finger.

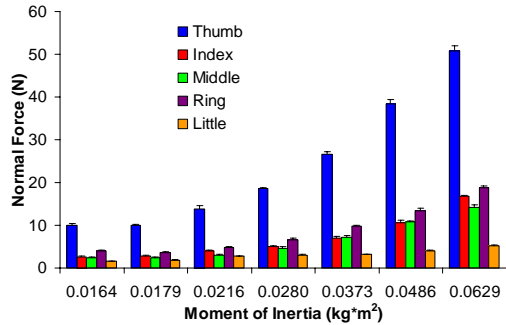


Figure 1: Average maximum value of individual finger normal forces under varying moment of inertia conditions.

The relationship between the normal and tangential forces was also plotted, yielding that the normal force increased with the magnitude of tangential force (Figure 2).

The total normal force was calculated to be the sum of each of the individual digit normal forces. The average total normal force over the entire 20 cycle trial was found to linearly increase with the moment of inertia of the system.

## SUMMARY/CONCLUSIONS

The angular displacement between the thumb and index finger and between the thumb and little finger was significantly greater than the angular displacement between other digits. In this orientation, the thumb opposes the other digits. This opposition accounts for the large magnitude of normal and tangential forces in the thumb.

The safety margin is a measurement of force efficiency. A large safety margin indicates an excessive, and thus less efficient, application of force. From our results we can conclude that the use of thumb force is the least efficient (largest safety margin) and the use of index finger force is the most efficient of all the digits.

Previous studies show that the index finger is the most dexterous of all the fingers. The relatively small safety margin of the index finger found in this study supports these previous findings of high index dexterity.

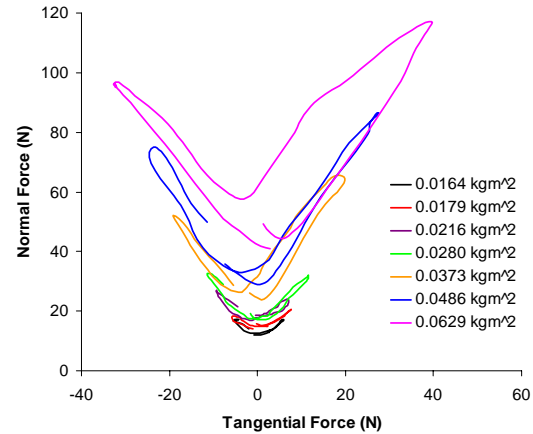


Figure 2: Normal force versus tangential force under varying moment of inertia conditions for a single oscillatory cycle.

Because the moment of inertia is held constant within each set of oscillations, the tangential force changes exclusively with angular acceleration. The normal force increased with the magnitude of tangential force. We can therefore conclude that the normal force increases with the magnitude of angular acceleration.

The recent study mentioned prior of dynamic translational movements of hand-held objects of different weights showed a linear increase of grasping force object weight (Zatsiorsky et al. 2005). Our findings yield a linear increase in grasping force with an increase in moment of inertia.

## REFERENCES

- Kinoshita, H., S. Kawai, K. Ikuta (1995). *Ergonomics* **38**: 1212-30.
- Shim, J.K., M.L. Latash, V.M. Zatsiorsky (2005) *J Neurophysiol* **93**: 3649-58.
- Westling, G. and R. S. Johansson (1984). *Exp Brain Res* **53**: 277-84.
- Zatsiorsky, VM. and F. Gao, M.L. Latash (2005). *Exp Brain Res* **162**: 330-308.

# Exploring *In Vivo* 3D Joint Impairments Using MRI-Based Dynamic Joint Models

Frances T. Sheehan, PhD<sup>1</sup>, Weidong Luo, Neil Weston,  
Andrea R. Seisler, MBE<sup>1</sup> and Steven J. Stanhope, PhD<sup>1</sup>

<sup>1</sup> National Institutes of Health, Bethesda, MD, USA  
E-mail: fsheehan@cc.nih.gov Web: pdb.cc.nih.gov

## INTRODUCTION

The Virtual Functional Anatomy (VFA) project is designed to fill the important knowledge gap that exists in the relationship between functional movement limitations and impaired joint structure and function. Our current focus is to develop and ultimately validate a combined set of tools that will enable the accurate and precise measurement, analysis and visualization of three-dimensional (3-D) static and dynamic musculoskeletal anatomy (i.e., bone shape, skeletal kinematics, tendon and ligament strain, muscle force, and joint space). This project combines MR imaging capabilities with a highly accurate, imaging-based measurement and analysis techniques for the non-invasive quantification of complete joint anatomy and tissue dynamics during functional movements. This requires the development of methodologies for creating 3D digital images of loaded and moving joint tissues (bone, cartilage, and connective tissues) in order to reveal joint contact patterns and tissue loads. The variability of bone shape and the sensitivity of defined joint attitude (translation and rotation of one bone relative to another) to osteo-based coordinate system definition are being evaluated. These capabilities are being developed to document and evaluate the function of normal and impaired joint structures (e.g., Cerebral Palsy, Ehlers Danlos syndrome and patellar maltracking syndrome) under simulated conditions experienced during activities of daily living. Recently, this work has concentrated on four primary project areas: 1) VFA tool

development, 2) *In vivo* normal and impaired knee joint function, 3) *In vivo* ankle joint function and 4) The quantification of bone shape.

## METHODS

The cornerstone of quantifying 3D joint dynamics is the General Electric (GE) fast phase contrast (fast-PC) imaging sequence, which acquires a series of images over time

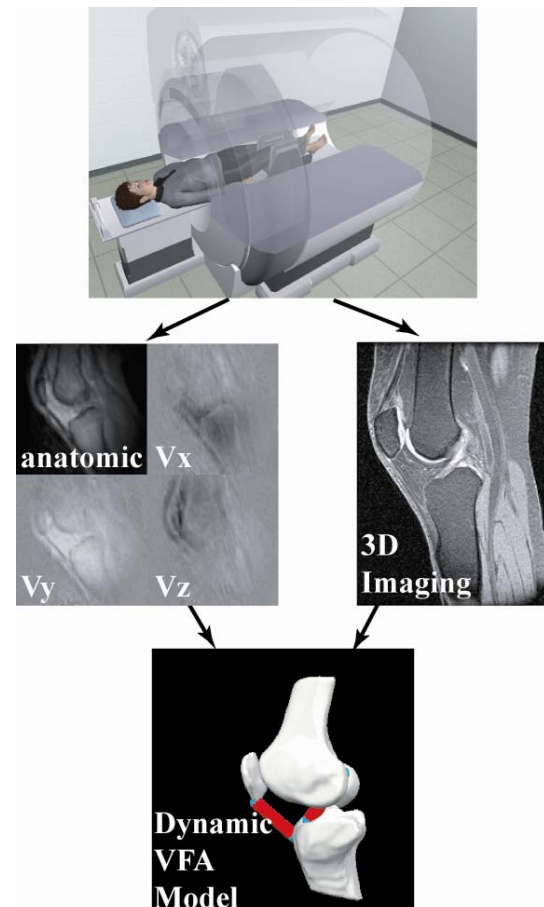


**Figure 1:** Pictorial representation of the creation of a dynamic VFA model

depicting the anatomy with correlated measures of the 3D velocity for each pixel within the imaging plane. During a fast-PC acquisition subjects cyclically move their joint through a specified range of motion at a typical rate of 35 cycles/minute. Next, the 3D attitude for each bone within the joint and muscular displacements over the movement cycle are quantified through integration of the velocity data. Based on the attitude of the bones and muscular displacements; the finite helical axis, tendon moment arms and tendon strain are defined. By registering the dynamic data with high quality static 3D MR images, ligament strains and cartilage contact patterns can be determined. In addition to the dynamic imaging, methods are under development for the 2D and 3D quantification of bone shape.

Currently normative databases for complete knee joint (n=34), inclusive of the patellofemoral and tibiofemoral joints, and for the hindfoot (n=22), inclusive of the talocrural and subtalar joints, have been established. Using these data the finite helical axes of these joints and the strain and moment arm of the patellar and Achilles' tendon have been quantified. Beginning with this baseline, the changes in joint kinematics due to impairments (Cerebral Palsy, Ehlers Danlos syndrome, patellar maltracking, ACL loss) are being explored.

## **RESULTS AND DISCUSSION**

By creating highly accurate and precise databases for knee and ankle joints, specific trends have come to light that have not been seen before. It was determined that the joints of the ankle do follow a coupled rotation (supination or pronation), but primary rotations occur at joints opposite to clinical definitions. It was determined that the knee joints do not follow a coupled rotation and that individual subjects can have variable initial starting attitudes and changes in

attitudes. This variability likely accounts for much of the inter-subject variability and some of the conflicting results reported in different studies. In terms of impairments, it was demonstrated that patellar maltracking was not simply a 2D problem, but alterations in kinematics could be seen in all three directions. In cerebral palsy, a lack of support for the theory of "lever-arm" dysfunction being the source of low joint torque was found. In this population there was good agreement between the kinematic results and clinical findings.

The two dimensional bone shape project defined key definitions for developing anatomical coordinate systems for the knee and ankle joints. It also highlighted potential sources of error in previous static and kinematic MRI studies. It was found that a slight rotation or translation of the knee joint relative to the imaging plane resulted in significant differences in six key parameters typically used in clinical imaging to define patellofemoral impairments. The 3D bone shape project has demonstrated that in order to better quantify local shape variations, the local and global shape variations must be accounted for separately.

## **SUMMARY/CONCLUSIONS**

The VFA toolbox is an accurate and precise tool for acquiring data with which to study the effects of impairments on the musculoskeletal system at the joint level. The fact that direct links have been seen between the VFA outputs and clinical evaluations implies that this tool has the potential for becoming a key clinical analysis package. The bone shape project will allow for more precise average bone models and for the quantification of variations in bones on both the local and global scale.

# SINGLE JOINT VERSUS MULTIPLE JOINT MODELING USING A HYBRID-EMG DRIVEN APPROACH

Daniel N. Bassett<sup>1</sup>, Qi Shao<sup>1</sup>, Daniel L. Benoit<sup>1</sup>, Kurt T. Manal<sup>1</sup>, and Thomas S. Buchanan<sup>1</sup>

<sup>1</sup> Center for Biomedical Engineering Research  
University of Delaware, Newark, DE, USA  
E-mail: bassett@me.udel.edu Web: <http://www.cber.udel.edu/>

## INTRODUCTION

When one is interested in modeling the forces in a joint it is tempting to focus only on that joint. The disadvantage of this approach is that it may not provide a sufficiently powerful representation of the way biarticular muscles contribute to single joints. In this study, our previous single joint model was expanded to include multiple joints. Specifically, we compared estimation of ankle joint moments and muscle forces with results from a combined ankle and knee model.

## METHODS

The data collection for this preliminary comparison of modeling methods was conducted on a subject with healthy gait. The subject performed gait and maximum voluntary contraction trials. The data collected were kinematics, muscle specific electromyography (EMG), and ground reaction forces. Muscles chosen were the semitendinosus, biceps femoris, rectus femoris, vastus lateralis, vastus medialis about the knee (Lloyd & Besier, 2002), the tibialis anterior and soleus about the ankle, and the gastrocnemii as biarticular muscles that span both the ankle and knee.

After the data collection, we averaged the EMGs from the vasti estimating activation for the vastus intermedius. In addition, EMG for the biceps femoris was assumed to

be the same for both the long and short head. EMG data were processed by relieving bias, rectifying, high and low-pass filtering, and finally normalizing by the maximal activation for each muscle. The kinematic data were used to obtain joint angles for the hip, knee, and ankle and subsequently muscle-tendon lengths and muscle moment arms using SIMM. Also, inverse dynamic joint moments were calculated for the knee and ankle from the kinematic data and the ground reaction forces.

Our EMG-driven model is built on a forward dynamic approach using a Hill-type model which includes active, passive, and damping components (Figure 1) (Buchanan et al., 2005). The processed EMG data were passed through a history-dependent recursive filter and then non-linearized to

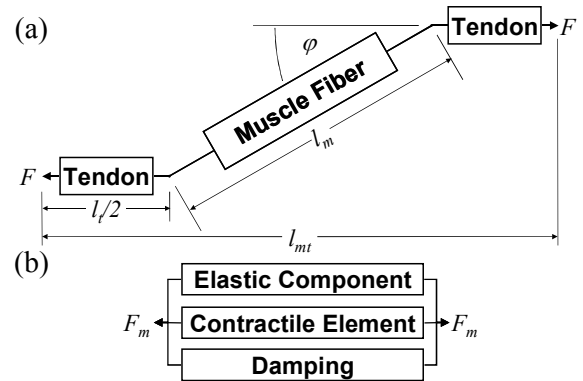


**Figure 1:** Hill-type model: a) muscle-tendon unit, b) muscle fiber unit. Where  $F$  is force,  $l_t$  tendon length,  $l_m$  muscle fiber length,  $l_{mt}$  muscle-tendon length,  $\phi$  pennation angle, and  $F_m$  muscle force.

give muscle activation. The equation relating components of our Hill-type model was integrated to calculate fiber length and tendon length. Tendon force was interpolated from the force-length relationship, which combined with muscle moment arms gave joint moments (Buchanan et al., 2004).

Due to the difficulty of *in vivo* measurement of subject specific muscle parameters, such as tendon slack length, we used a hybrid model. In the tuning process, these parameters were adjusted according to an optimization algorithm (Goffe et al., 1994) using the inverse dynamic joint moments as the standard. Our model was tuned to the ankle and then to the ankle and knee combined for the first trial. The tuned models were then used to predict ankle joint moments for other walking trials.

## RESULTS AND DISCUSSION

The model's ability to predict joint moments was consistent between single and multiple joint calibrations ( $R^2 = 0.97$  and  $0.96$  respectively). RMS values of 7.7% and 8.1% showed a moderate increase in error when the knee was included in the tuning process (Figure 2). The RMS difference between the two predictions was 1.3%, and a 5% reduction in peak error was found by using the multi-joint model. The differences found between our models are seen in the muscle forces. The predictions for the soleus and tibialis anterior varied less than 5% between the two calibrations. On the other hand, the forces were estimated to change up to 20 percent for the gastrocnemii in the combined model.

The study showed consistency in joint moment predictions. More importantly, the deviations in muscle force predictions were more pronounced for the biarticular muscles,

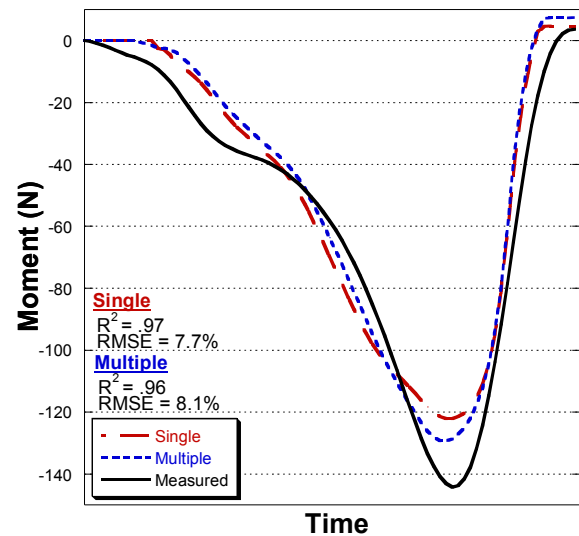


**Figure 2:** Ankle joint moment comparison as expected. Single joint modeling of the ankle neglects contributions of the gastrocnemii at the knee. Multiple joint modeling accounts for more complex and physiological kinetics.

## CONCLUSIONS

The performance of our multiple joint model was consistent with our previous work. The differences found in muscle force estimation are most likely due to increased physiological accuracy of the model.

## REFERENCES

- Buchanan, T.S., Lloyd, D.G., Manal, K.T., Besier, T.F. (2004). *J. App. Biomech*, **20**, 367-395.
- Buchanan, T.S., Lloyd, D.G., Manal, K.T., Besier, T.F. (2005). *Med Sci Sports Exerc.*, 1911-1916.
- Goffe, W.L., Ferrier, G.D., Rogers, J. (1994). *J. Econom.*, **60**, 65-99.
- Lloyd, D.G., Besier, T.F. (2002). *J. Biomech.*, **36**, 765-776.

## ACKNOWLEDGEMENTS

NIH R01-HD38582 and P20-RR16458

# THE EFFECT OF FLATFOOT DEFORMITY AND TENDON LOADING ON THE WORK OF FRICTION MEASURED IN THE POSTERIOR TIBIAL TENDON

Stacie I Ringleb, Kenichiro Arai, Kristin D Zhao, Lawrence J Berglund, Harold B Kitaoka,  
Kenton R Kaufman

Biomechanics Laboratory, Division of Orthopedic Research, Mayo Clinic College of Medicine,  
Rochester, MN, USA

E-mail: [Kaufman.Kenton@mayo.edu](mailto:Kaufman.Kenton@mayo.edu) Web: [mayoresearch.mayo.edu/mayo/research/biomechanics](http://mayoresearch.mayo.edu/mayo/research/biomechanics)

## INTRODUCTION

Posterior tibial tendon dysfunction (PTTD) is the most common cause of acquired flatfoot deformity in adults (Myerson et al., 1996). While numerous etiologies have been proposed, the cause of PTTD and its progression are still unknown. We hypothesized that abnormal gliding resistance and tendon excursion increases the work of friction, which may lead to PTT degeneration and failure. The purpose of this study was to improve our understanding of PTT gliding resistance and excursion: 1) in the intact foot and simulated flatfoot and 2) when the PTT is loaded at different levels.

## METHODS

Seven male fresh-frozen cadaveric lower extremities, disarticulated at the knee, were studied ( $67 \pm 24$  years). The proximal tibia and fibula were potted in PMMA and mounted in a custom testing apparatus. Ring shaped force transducers (diameter 1.5 cm) were attached to distal and proximal ends of the PTT. Distally, a 1.5 cm section of the PTT was removed and a transducer was attached to the tendon on the proximal side and anchored to the navicular. The proximal end of the tendon was attached to a cable, which was placed around a pulley that incorporated a rotatory potentiometer to measure tendon excursion. Static loads (0.5, 1 and 2 kg) were applied to the cable. The foot was moved through the range of motion in the sagittal (plantarflexion/dorsiflexion),

coronal (inversion/eversion) and transverse (internal/external rotation) planes for three trials. Tests were conducted for the intact foot and after a flatfoot deformity was created by sectioning the peritalar soft tissue constraints (Kitaoka et al., 1998). The force in the proximal sensor was subtracted from the force in the distal sensor to calculate the gliding resistance (An et al. 1993; Uchiyama et al., 1995), which was plotted against PTT excursion, to yield a hysteresis curve. The hysteresis curve was truncated such that an equal range of motion was considered for each condition (i.e., 1.5 cm of excursion in the coronal and transverse planes and 0.3 cm in the sagittal plane). The area within the truncated curve was defined as the work of friction (Fig.1). For statistical analysis, a Wilcoxon signed rank test ( $p < 0.05$ ) was used to test differences between intact and simulated flatfoot. A Friedman test ( $p < 0.05$ ) was used to test differences in each tendon loading level.

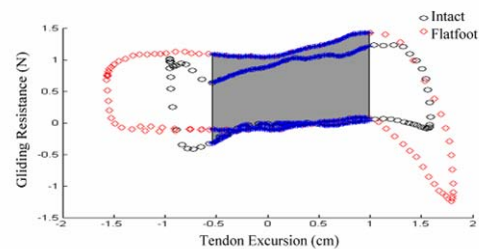


**Fig.1** Sample hysteresis curve in the coronal plane for the intact and flatfoot conditions at 2kg. The shaded areas represent uniform truncation of the curves for all test conditions used to calculate the work of friction values.

## RESULTS AND DISCUSSION

The hysteresis curves were consistent and repeatable for each testing condition. Standard deviations of the calculated work of friction from three cycles of manipulation were less than 6% of mean values. The maximum PTT excursion in sagittal, coronal and transverse planes 1) in the intact condition was  $0.60 \pm 0.13$  cm,  $2.42 \pm 0.18$  cm and  $2.39 \pm 0.44$  cm, respectively and 2) in the flatfoot condition was  $0.68 \pm 0.14$  cm,  $2.95 \pm 0.21$  cm and  $2.84 \pm 0.28$  cm, respectively.

Flatfoot deformity increased the work of friction significantly in the coronal and transverse planes ( $p < 0.05$ ) but did not in the sagittal plane. In all three planes of motion, the work of friction increased between 0.5 kg and 2 kg ( $p < 0.05$ ) (Fig.2).

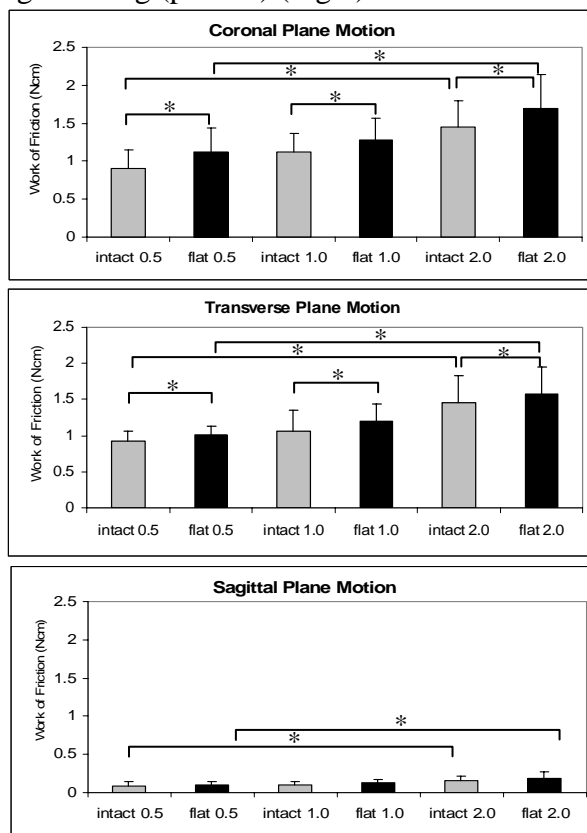


**Fig.2** Work of friction in the intact and flatfoot conditions with the PTT loaded at 0.5, 1 and 2 kg (\* $p < 0.05$ ).

Previous studies examined the change in gliding resistance when the hindfoot was positioned in neutral, maximum dorsiflexion, and maximum planter flexion and the PTT was manually moved 10 mm (Uchiyama et al., 2000). This study showed that the sagittal plane PTT excursion in the physiologic range of motion is smaller ( $6 \pm 1$  mm), while the coronal and transverse plane excursions were significantly larger.

## SUMMARY AND CONCLUSIONS

This study combined both gliding resistance and PTT excursion to assess the work of friction in the PTT during passive motion of the hindfoot. The work of friction increased with tendon loading in all three planes of motion and was greater in the flatfoot condition than the intact condition in the coronal and transverse planes. These results suggested that non-operative treatment should be focused on limiting coronal and transverse plane motions. This may decrease the degenerative effects, while permitting sagittal motion to allow for more normal ambulation.

## REFERENCES

- An, K. et al. (1993). *Biomed Sci Instrum*, **29**, 1-7.
- Kitaoka, H. et al. (1998). *Foot Ankle Int*, **19**, 447-451.
- Myerson, M. et al. (1996). *J Bone Joint Surgery [Am]*, **78**, 780-792.
- Uchiyama, S. et al. (1995). *J Orthop Res*, **13**, 83-89.
- Uchiyama E. et al., (2000). *Proceedings from ORS*, 0191.

## ACKNOWLEDGEMENT

This study was funded by the Mayo Foundation.

# SCAPULAR KINEMATICS IN CHILDREN WITH BRACHIAL PLEXUS BIRTH PALSY

Sudarshan Dayanidhi <sup>1</sup>, Susan V. Duff <sup>2,1</sup>, Scott H. Kozin <sup>1</sup>

<sup>1</sup> Shriners Hospital for Children, Philadelphia, PA, USA

<sup>2</sup> Thomas Jefferson University, Physical and Occupational Therapy, Philadelphia, PA, USA

E-mail: sdayanidhi@shrinenet.org

## INTRODUCTION

Scapular kinematics have been previously studied in adults and healthy children (1,2) and differences have been observed between adults and children (1). Brachial Plexus Birth Palsy (BPBP) often affects the shoulder musculature and these children display impairments in humeral elevation in the affected limb, glenohumeral (gh) joint deformities and compensatory changes in scapulothoracic (st) motion (3,4).

Kinematics of the upper limb has been studied previously in children with BPBP (5), although this analysis did not include scapular kinematics. Since children with BPBP demonstrate scapular compensations during humeral elevation, analysis should include scapulothoracic motion to assess overall shoulder motion. The purpose of this study was to describe the scapular kinematics in children with BPBP on both their involved and their non-involved sides.

## METHODS

Sixteen children with BPBP (8 F/ 8 M), 4-12 years of age participated in this study. Three trials of humeral elevation were collected on both the involved and uninvolved upper limbs. The independent variable was humeral elevation. The dependent variables were the scapular angles and the glenohumeral elevation angles from which the glenohumeral to scapulothoracic ratios (gh:st) were calculated. Kinematic data were collected using a magnetic tracking device

(Polhemus 3Space<sup>®</sup> Fastrak, Colchester, VT). This method has been previously validated in adults (2). Based on the amount of humeral elevation achieved, the children were divided into 2 groups; group 1 able to achieve up to 75° and group 2 able to achieve greater than 75°. 75° was used since clinically it was thought to be functional. The degrees of excursion for GH elevation and for the scapular variables during elevation to 75° were compared between groups and sides using a Repeated Measures ANOVA. A one-way ANOVA was also conducted between sides for children in group 2 during elevation from 15°-135°.

## RESULTS AND DISCUSSION

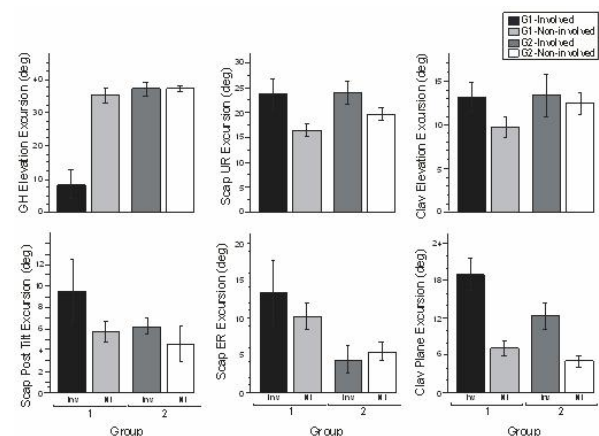
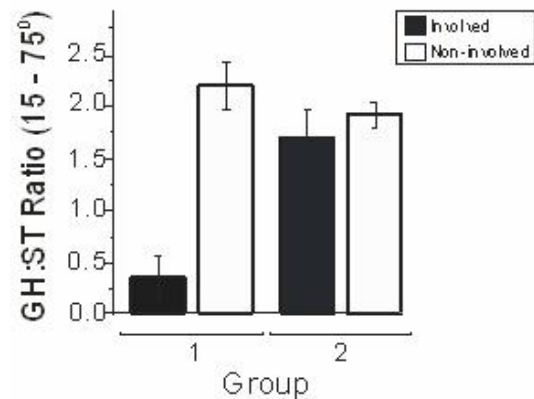


Figure 1- Shoulder Variables

Figure 1 shows the mean excursions for gh elevation and all five scapular variables on the involved and non-involved sides. The results show that for gh elevation significant differences for group ( $p < 0.0001$ ), side ( $p < 0.0001$ ) and an interaction between group and side ( $p < 0.0001$ ) were seen. Significant differences were not found for scapular upward rotation (UR) or clavicular elevation, though the mean excursions for both tended to be higher for the involved sides of both groups. For scapular posterior tilt there was a significant difference between sides only ( $p < 0.05$ ). For scapular external rotation there was a significant difference between groups ( $p < 0.05$ ). Figure 2 shows on the involved sides the average gh:st for the motion from  $15^\circ - 75^\circ$  in group 1 was 0.3:1 and in group 2 was 1.6:1. For the non-involved side the ratio for group 1 was 2.2:1 and for group 2, 1.9:1. The gh:st between sides were not significantly different for group 2 for elevation from  $15^\circ - 135^\circ$ . The average gh:st ratio on the involved side in group 2 was 1.5:1 and on the non-involved side 1.81:1.

Two patterns of scapulohumeral motion were seen among the children with BPBP. In group 1, humeral elevation was limited to less than  $75^\circ$  and greater scapular mobility was noted to enhance elevation capabilities of the affected limb. These children appear to have reduced strength of the rotator cuff muscles and hence are unable to move at their glenohumeral joint appropriately. This combination directly influenced scapular motion as seen by decreased gh:st ratio. In group 2, humeral elevation was greater than  $75^\circ$  and the scapular contribution to overall motion was less resulting in a better gh:st ratio that was even higher than previously reported in children with typical development (1). These children appear to have better strength of the rotator cuff and enhanced glenohumeral joint motion. EMG



**Figure 2**-Mean GH:ST Ratios

## SUMMARY/CONCLUSIONS

This study revealed differences in scapular contribution to humeral elevation between the involved and uninjured upper limbs of children with BPBP. Children with limited humeral elevation ( $< 75^\circ$ ) exhibited greater contribution from the scapulothoracic joint than the children with higher elevation. They also demonstrate the feasibility of using a magnetic tracking device to analyze shoulder motion in children with BPBP which could also be used for pre-operative planning and post-operative evaluations to study the efficacy of treatment.

## REFERENCES

- Dayanidhi S, et al. (2005). *Clinical Biomechanics* 20(6): 600-6
- Karduna, R. A., et al. (2001). *J of Biomech Eng*, 123, 184- 190.
- Strombeck C, et al. (2000). *Develop Med and Child Neuro* 42(3): 148-57
- Waters, P. M. (1997). *J of Amer Acad of Orthopaedic Surgeons*, 5, 205-214
- Mosqueda T et al.(2004). *J of Ped Orthop* 24(6): 695-9

## ACKNOWLEDGEMENTS

Our thanks to Andy Karduna for his insights and assistance with the project.

# EVIDENCE OF ISOMETRIC FUNCTION OF THE FLEXOR HALLUCIS LONGUS MUSCLE IN NORMAL GAIT

Yatin Kirane, Andrew Hoskins and Neil A. Sharkey

Biomechanics Laboratory, The Pennsylvania State University, University Park, PA, USA

E-mail: [nas9@psu.edu](mailto:nas9@psu.edu) Web: <http://www.biomechanics.psu.edu>

## INTRODUCTION

Biarticular and multiarticular muscles are known to possess unique biomechanical and functional characteristics. The activation patterns of multiarticular muscles in multi-joint movements have been studied in the past. These muscles are thought to function as ‘nearly isometric structures’ transferring mechanical energy from one joint to another rather than doing substantial work themselves during certain movements. (Bobbert and van Ingen Schenau 1988). However, the theory of ‘isometric function of multi-articular muscles’ is based on anatomical and geometric considerations, indirect force estimates and electro-myographic (EMG) data. Direct experimental data supporting isometric function in humans are scarce.

The Flexor Hallucis Longus (FHL), a multi-articular muscle, is the major great toe flexor. Originating from the distal third of the fibula and traveling across the entire length of the sole, FHL inserts on the base of the distal phalanx of the great toe. The FHL tendon crosses multiple joints along its path, notably the ankle and the 1<sup>st</sup> metatarso-phalangeal (MTP) joint. Neural drive to FHL is maximal during the push-off phase of the gait cycle. The dynamic coupling of the 1<sup>st</sup> MTP and ankle joints becomes apparent during the early push-off phase when the former is dorsiflexing while the latter is plantarflexing.

We hypothesized that the FHL muscle operates isometrically during the gait cycle, and that, the constant length that is maintained is specific to each individual foot.

## METHODS

Using a custom-made robotic device, called the robotic dynamic activity simulator (RDAS), we created dynamic simulations of the stance phase of walking gait in non-embalmed human cadaver feet. The capacity of RDAS to simulate walking has been previously validated (Sharkey and Hamel, 1998; Hoskins, 2004). Kinematic data of the proximal shank as measured in live subjects during the stance phase of normal, unshod walking, and EMG data (Perry et al., 1992), scaled according to relative muscle cross-sectional area, were used as input for the simulations. Lower extremity specimens with intact tendons were mounted in the RDAS and were loaded under near physiological conditions, i.e. peak vertical ground reaction forces (GRF) of 500 N. A set of three linear actuators was used to recreate the pre-recorded kinematics of the proximal shank. Another set of actuators, linked to the musculo-tendinous junctions via cables and cryogenic clamps, simultaneously prescribed the muscle activity (i.e. ‘target’ muscle force profiles derived from the scaled EMG data). The three components of the GRF, as well as displacements and forces of the major extrinsic tendons of the foot were dynamically recorded over each simulation.

During initial trials, predetermined force profiles for individual tendon units were achieved using force feedback (FFB) control while proximal tendon displacements were recorded. In subsequent trials, FFB control was used for all tendon units except the FHL, which was controlled using displacement feedback (DFB) with the

forces generated in the tendon being monitored. Constant FHL lengths at different positions were prescribed as input. Successive trials were aimed at finding the specific (i.e. ‘neutral’) position at which the recorded FHL force profile matched its ‘target’ force profile as estimated from EMG and anthropometric measures. Subsequently, constant FHL positions 2, 4, 6 and 8 mm proximal to the ‘neutral’ position were prescribed in successive trials to monitor the corresponding changes in the forces generated in the FHL tendon (fig.1).

## RESULTS AND DISCUSSION

The total excursion of the FHL tendon during foot movements alone, without any toe movement, is reported to be 27 mm (Hintermann, 1994); however, we found it to be 6-8 mm on an average, during walking simulations under FFB control. The recorded FHL force profiles under FFB control were identical to the target profiles.

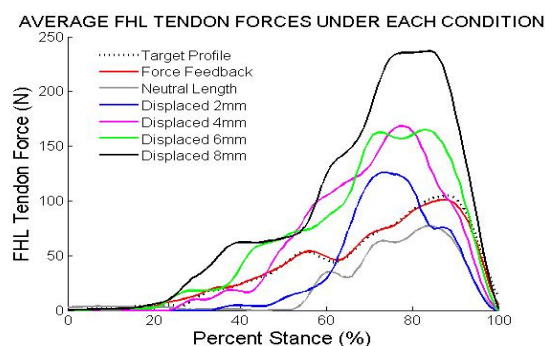


Fig.1: Average FHL tendon force profiles under different conditions.

Likewise, at the ‘neutral position’ under DFB control, the FHL force profiles were comparable to the target force profiles. The neutral position was found to be within the middle of the FHL excursion range and was specific for each specimen. Furthermore, setting the FHL at constant positions located 2, 4, 6 and 8 mm proximal to the defined neutral position produced dramatic and proportional increments in the peak tendon forces. These findings have potentially interesting implications for the control of

locomotion. The central neural drive to FHL possibly seeks to maintain a specific length over the gait cycle and thus contributes to the coupled dynamics between the ankle and 1<sup>st</sup> MTP joints. While central pattern generators (Yamaguchi, 2004) seem to regulate the reciprocal activation of the proximal limb muscles during locomotion, some distal muscles could likely be controlled via length-servo mechanisms. The FHL appears to be one such muscle. The negative feedback provided by the stretch reflex circuit (Matthews, 2004) seems ideally suited for such control; and has previously been postulated to be involved in the control of limb impedance (Granata, 2004). We suggest that locomotion control might employ two mechanisms: reciprocal muscle activations via central pattern generators, and impedance control via length-servo control. This idea has potential implications for the conditions of impaired stretch reflex function, e.g. peripheral neuropathies.

## CONCLUSION

FHL muscle can produce physiological tendon forces during ambulation while operating isometrically.

## REFERENCES

- Bobbert and van Ingen Schenau et al. (1987) *J anat Dec*; **155**:1-5.
- Granata et al (2004) *J Electromyogr Kinesiol Oct*; **14(5)**:599-609
- Hintermann et al. (1994) *Foot & Ankle International Jul*; **15(7)**:386-95
- Hoskins et al. (2004) *28<sup>th</sup> Annual Meeting of American Society of Biomechanics* 238-39
- Matthew PB (1994) *J Physiol Dec* **15**; **481** (pt3):777-98
- Perry J. (1992) *Gait Analysis: Normal and Pathological Function*.
- Sharkey and Hamel (1998) *Clinical Biomechanics* **13**: 420-433.
- Yamaguchi T (2004) *Prog Brain Res* **143**:115-22

# THE INFLUENCE OF FOOTWEAR SOLE HARDNESS ON UTILIZED COEFFICIENT OF FRICTION DURING WALKING

Yi-Ju Tsai and Christopher Powers

Musculoskeletal Biomechanics Research Laboratory  
Department of Biokinesiology and Physical Therapy  
University of Southern California, Los Angeles, CA, USA  
E-mail: yijutsai@usc.edu Web: www.usc.edu/go/mbrl

## INTRODUCTION

Slips have been recognized as a significant cause of falls. Slip events occur when the utilized friction exceeds the friction available from the foot/floor interface and can be influenced by both human and environmental factors (Hanson et al. 1999). The utilized coefficient of friction (COFu) can be used to estimate the slip potential of an individual. For example, a greater COFu value is indicative of a higher friction demand and an increased probability of a slip event (Burnfield et al. 2005). As loading characteristics have been reported to vary when wearing shoes with different sole hardness (McCaw et al. 2000), it is reasonable to hypothesize that sole hardness may have an impact on the COFu, and therefore slip potential. The purpose of this study was to determine the influence of footwear sole hardness on COFu during walking.

## METHODS

Fifty six healthy adults (28 men and 28 women; mean age  $27.7 \pm 3.4$  yrs) participated in this study. Ground reaction forces were recorded at 1560 Hz using three force platforms (AMTI, Watertown, MA) as subjects walked at a self-selected fast walking speed across a high-pressure laminate floor. Full body kinematic data were recorded at 120 Hz using an eight-camera motion analysis system (Vicon

Motion Systems, Lake Forest, CA). Two sets of Oxford style dress shoes with smooth styrene butadiene rubber soles (Bates Footwear Inc., Rockford, MI) that differed only in outsole hardness were provided for each subject. Data were obtained under two footwear conditions: 1) soft sole (Shore hardness 75A) and 2) hard sole (Shore hardness 54D). Following all walking trials, subjects were asked to provide a subjective rating of perceived slipperiness by placing a vertical mark along a 10 cm horizontal scale.

COFu was quantified as the ratio of the resultant shear to vertical ground reaction force throughout stance phase of gait. Peak COFu during weight acceptance was identified, as was the vertical and resultant shear ground reaction forces at the time of peak COFu. The horizontal acceleration of the total body center of mass (COM) and the heel marker was calculated 50 msec prior to and immediately following initial contact. Subjective perception of footwear slipperiness was rated as a continuous variable from 0 (not slippery) to 100 (very slippery). Paired t-tests were used to determine the influence of footwear sole hardness on each of the variables of interest.

## RESULTS AND DISCUSSION

Subjects perceived the hard soled shoes to be more slippery than the soft soled shoes ( $70.0 \pm 19.9$  vs.  $47.1 \pm 21.1$ ;  $P < 0.001$ ). On average, the self-selected fast walking speed

while wearing the hard soled shoes was slightly slower than when wearing the soft soled shoes ( $1.90 \pm 0.16$  m/sec vs.  $1.92 \pm 0.16$  m/sec;  $P < 0.05$ ). The peak COFu was significantly lower when wearing hard soled shoes compared to wearing soft soled shoes ( $0.23 \pm 0.03$  vs.  $0.26 \pm 0.04$ ,  $P < 0.001$ ; Table 1). The vertical ground reaction forces at the time of peak COFu were not significantly different between the two shoe conditions. However, the resultant shear forces were significantly lower when wearing soft soled shoes compared to wearing hard soled shoes (Table 1). In addition, the total body COM acceleration prior to and immediately following initial contact was significantly lower when wearing the hard soled shoes compared to the soft soled shoes (Table 2). No differences in heel accelerations were observed (Table 2).

The finding of reduced peak COFu during weight acceptance implies that for a given surface, a slip would be less likely to occur while wearing hard soled shoes when compared to soft soled shoes. The lower COFu while wearing the hard soled shoes resulted from a decrease in the resultant shear ground reaction force as differences in the vertical forces were not observed. The decreased resultant shear forces at the time of peak COFu can be explained by the

decreased horizontal acceleration of the total body COM prior to and immediately after initial contact. Decreases in the horizontal acceleration of total body COM while wearing harder soled shoes suggests that subjects may have employed behavioral adaptations aimed at reducing COFu. Such an adaptation appears to coincide with the finding that subjects perceived the harder soled shoes to be more “slippery”.

## SUMMARY/CONCLUSIONS

Peak COFu was shown to be lower when wearing hard soled shoes when compared to wearing soft soled shoes. Our data also suggest that the decrease in COFu may have been a behavioral adaptation to wearing shoes that are perceived to be more slippery. Whether or not such behavioral adaptations to wearing hard soled shoes would decrease the potential for slip initiation needs to be examined.

## REFERENCES

- Hanson, J.P., et al. (1999). *Ergonomics*, **42**(12), 1619-1633.  
 Burnfield, J.M., et al. (2005). *Gait & Posture*, **22**, 82-88.  
 McCaw, S.T., et al. (2000). *Med. Sci. Sports Exerc.*, **32**(7), 1258-1264.

**Table 1.** Peak COFu and ground reaction forces (Mean  $\pm$  SD)

	Soft soled shoes	Hard soled shoes	P value
Peak COFu	$0.26 \pm 0.04$	$0.23 \pm 0.03$	< 0.001
Vertical Forces (N)	$651.02 \pm 189.46$	$661.97 \pm 199.39$	0.705
Shear Forces (N)	$168.51 \pm 49.10$	$152.21 \pm 48.36$	0.016

**Table 2.** Horizontal accelerations of the total body COM and heel (Mean  $\pm$  SD)

	Soft soled shoes	Hard soled shoes	P value
COM Acceleration before contact (m/sec <sup>2</sup> )	$0.42 \pm 0.73$	$0.20 \pm 0.74$	0.002
COM Acceleration after contact (m/sec <sup>2</sup> )	$0.73 \pm 1.24$	$0.43 \pm 1.00$	0.004
Heel Acceleration before contact (m/sec <sup>2</sup> )	$-48.04 \pm 7.56$	$-48.45 \pm 8.25$	0.497
Heel Acceleration after contact (cm/sec <sup>2</sup> )	$-29.06 \pm 11.00$	$-29.79 \pm 10.35$	0.362

# GAIT STABILITY DURING STAIR DESCENT IN OLDER ADULTS

Heng-Ju Lee and Li-Shan Chou

Motion Analysis Laboratory, Department of Human Physiology, University of Oregon  
Eugene, Oregon, U.S.A  
E-mail: [chou@oregon.edu](mailto:chou@oregon.edu)

## INTRODUCTION

Epidemiological studies of falls have shown that most falls during some forms of locomotion. Stair negotiation is among the most challenging and hazardous locomotion for older people. There are about 10% of fall related deaths occurred on stairs (National Safety Council, 1992). Stair decent has been reported as a more challenge task during stair negotiation for elderly (Tinetti et al., 1988). Loss of balance and tripping are the primary two reasons that causing fall on stairs in the elderly. Therefore, a better understanding on how stair negotiation perturbs gait stability is critical to reducing the incidence of falls among older people.

Gait stability could be assessed using the motion of the whole body center of mass (CoM) and its relative position to the center of pressure (CoP) of the supporting foot. A greater CoM-CoP separation was reported during stair descent than stair ascent and level walking in young adults (Zachazewski et al., 1993). However, the coordination between CoM and CoP during stair negotiation is still unknown for elderly. A recent study reported that instantaneous CoM-CoP inclination angles could exclude inter-subject variability and better detect gait instability in the elderly (Lee and Chou, 2006). Elderly patients with balance disorders demonstrated a significantly greater medial CoM-CoP inclination angle than healthy elderly adults.

In this study, sagittal and frontal plane CoM-CoP inclination angles were assessed during stair descent in healthy young and elderly adults. It was hypothesized that elderly adults would demonstrate a greater medial

inclination angle than young adults during stair descent.

## METHODS

Twelve healthy elderly adults, (4 males and 8 females;  $72.2 \pm 3.8$  years;  $170.8 \pm 8$  cm;  $80 \pm 17.3$  kg) and thirteen healthy young subjects (6 males and 7 females;  $21 \pm 2.4$  years;  $170.8 \pm 10$  cm;  $72.8 \pm 10$  kg) were recruited for this study. Subjects were instructed to perform stair descent at a self-selected pace while barefoot.

The stair apparatus was composed of three individual steps. Each step had a raise of 7'' and a tread of 12''. A force plate was mounted on the first two steps. The third step included a three-meter extended walkway. The extended walkway allowed subjects reaching steady pace before stepping downstairs. The other two force plates were embedded in series on the level ground and aligned to the first step. This design allowed kinetic data collection during the stair descent phase and the transition phase to the level ground. A complete gait stride was examined for each of the phases. Whole body motion analysis was performed with an 8-camera motion analysis system (Motion Analysis Corp., Santa Rosa, CA). Twenty-nine reflective markers were placed on bony landmarks of each subject. Three-dimensional marker trajectory data were collected at 60 Hz. Whole body CoM position data was calculated as the weighted sum of each body segment, with 13 segments representing the whole body. The CoP position was calculated from the ground reaction forces/moments collected from four force platforms (AMTI, Watertown, MA) at 960 Hz.

Instantaneous inclination angles in the sagittal and frontal planes were defined by the linkage between CoP and CoM, and the vertical line. Effects of subject group on peak sagittal and frontal plane CoM-CoP inclination angles were assessed using a one factor ANOVA analysis with the significance level at 0.05.

## RESULTS AND DISCUSSION

Peak anterior and medial inclination angles occurred right before swing limb heel strike. Peak posterior inclination angles occurred right after swing limb toe off.

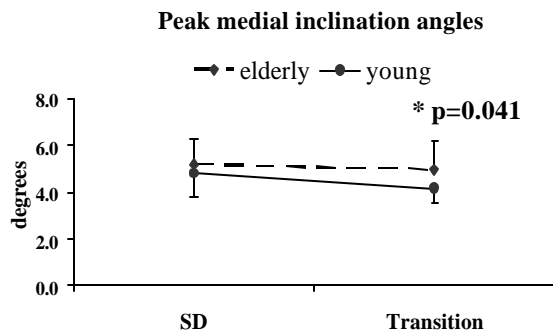


**Figure 1:** SD indicates steady state stair descent phase. Transition indicates transition phase from steps to level ground.

There were no significant group differences on the gait velocity, step width, peak anterior and posterior CoM-CoP inclination angles during both the stair descent and transition phases (Table 1). However, elderly adults demonstrated a significantly greater peak medial CoM-CoP angle and shorter stride length than young adults during transition phase (Figure 1).

**Table 1:** CoM-CoP inclination angles and temporal gait measurements, group means (SD)

Stair descent phase	Steady state descent		Transition (steps-level ground)	
	Healthy elderly	Healthy young	Healthy elderly	Healthy young
Peak medial angles (Deg.)	5.2 (1.1)	4.8 (1.0)	<b>5.0 (1.1)*</b>	<b>4.1 (0.6)*</b>
Peak anterior angles (Deg.)	7.0 (1.1)	6.6 (1.3)	12.5 (3.0)	13.4 (2.4)
Peak posterior angles (Deg.)	5.5 (1.6)	5.0 (1.2)	7.0 (1.6)	5.9 (1.8)
Gait velocity (m/s)	0.6 (0.1)	0.7 (0.1)	0.7 (0.1)	0.8 (0.1)
Stride length (cm)	76.0 (9.0)	78.1 (6.3)	<b>104.7 (15.0)*</b>	<b>112.0 (11.4)*</b>
Step width (cm)	10.5 (4.0)	11.5 (3.5)	9.1 (3.8)	9.8 (3.4)

\* Significant group difference,  $p < 0.05$

Results of this study indicated that, compared to young adults, gait stability of the elderly was perturbed more significantly during the stair-level ground transition phase. Previous study (Lee and Chou, 2005) showed that both healthy elderly and young adults had similar medial inclination angles ( $\sim 4^\circ$ ) during level walking. Stair descent resulted in a greater medial inclination ( $\sim 5^\circ$ ) than level walking for both groups. Young subjects were able to adjust the medial inclination angle back to its normal magnitude during the transition to level ground walking. However, during this transition phase, the frontal plane stability of elderly adults was found to be further perturbed.

## SUMMARY/CONCLUSIONS

The greater medial CoM-CoP inclination angle observed in elderly adults may indicate their deficiency in balance control which could result in a higher risk of accidental falls than young adults during the transition phase of stair descent.

## REFERENCES

- Falls in the home and community, (1992) *National Safety Council*
- Tinetti, M.E. et al., (1988). *N Engl J Med*, **319**, 1071-9.
- Zachazewski, J.E. et al., (1993) *J Rehabil Res Dev*, **30**, 412-22
- Lee, H.J., Chou, L.S. (2005) *Proceedings of ISB'05*
- Lee, H.J., Chou, L.S. (2006, in press) *Archives of PM&R*

# A FEASIBILITY STUDY OF TRIP RECOVERY TRAINING AS A FALL PREVENTION INTERVENTION

Kathleen A. Bieryla, Michael L. Madigan, and Maury A. Nussbaum

Virginia Tech, Blacksburg, VA, USA  
E-mail: kbieryla@vt.edu

## INTRODUCTION

Falls are a major cause of injury and death in adults aged 65+. On average, 5070 older adults are treated every day for a fall-related injury and approximately 37 die every day from a fall-related injury (CDC 2004).

Numerous exercise interventions have been proposed to help prevent falls in older adults (Lord 1995). However, the most effective type, intensity, frequency, and duration of exercise in preventing falls has yet to be identified (Tinetti 2003). An alternative intervention to help prevent falls may be to take advantage of motor learning principles by allowing individuals to practice movements directly related to fall prevention in a safe, controlled setting. The goal of this study was to evaluate the feasibility of trip recovery training as a fall prevention intervention.

## METHODS

Twelve healthy community-dwelling older adults (mean  $73.3 \pm 6.1$  years) participated in the study. The experiment employed a two-group pretest-posttest design. Participants were randomly assigned to either an experimental group or control group while keeping an equal number of males and females in each group. Each group performed one trip before (Trip 1) and one trip after (Trip 2) an intervention.

While in a safety harness, participants walked at a self-selected pace along a walkway and were informed that a trip may

occur. After a minimum of 20 walking trials, a three-inch high pneumatically-driven obstacle in the floor was triggered to elicit a trip which rose in approximately 160 ms from time of activation.

After Trip 1, the experimental group performed trip recovery training on a modified treadmill. Once activated, the treadmill accelerated to 2.0 mph in ~190 ms. Subjects were instructed to step over an obstacle and recover their balance. Twenty trials were performed. The control group walked on the treadmill at 2.0 mph for 15 minutes (the approximate time it took to complete the trip recovery training). After the interventions, both the control and experimental groups were tripped again while walking along the walkway after a minimum of 20 walking trials.

Whole body kinematics, ground reaction forces, and forces applied to the harness were recorded during randomly selected walking trials as well as during Trip 1 and Trip 2. Trip recovery performance was quantified using several measures derived from the kinematic data. Measures included the maximum trunk flexion, maximum trunk angular velocity, minimum hip height, as well as the time to maximum trunk flexion and maximum trunk angular velocity.

To determine the effect of the trip recovery training on trip recovery performance, difference values were calculated between the two trips (Trip 2 - Trip 1), and a t-test was performed between the two groups.

## RESULTS AND DISCUSSION

Nine of 11 participants successfully recovered their balance after both trips, one participant failed only after Trip 1, and one participant failed after both trips.

Several measures of trip recovery performance exhibited changes from Trip 1 to Trip 2 that were consistent with greater improvements in the experimental group compared to the control group. Maximum trunk flexion and time to maximum trunk flexion decreased significantly from Trip 1 to Trip 2 in the experimental group, while minimum hip height increased significantly from Trip 1 to Trip 2 in the experimental group ( $p < 0.05$ ) (Figure 1). No other variables of trip recovery performance were different between groups.

## SUMMARY/CONCLUSIONS

Overall, the results suggested beneficial effects of trip recovery training on actual trip recovery. The trip training showed a decrease in maximum trunk flexion and arresting the forward rotation of the trunk has been shown to be a key factor in successfully recovering from a trip (Grabiner 1993). The beneficial effects of trip recovery training may be due to changes in “neural factors” elicited by motor learning. Trip recovery training may allow modification of muscle activation levels and muscle activation sequences to occur via motor learning to improve balance recovery.

In conclusion, trip recovery training on a treadmill had beneficial effects on recovery from an actual trip. Future studies should further examine the ability to retain improvements in trip recovery performance over extended periods without training or non-exposure to a trip, and optimize the training to maximize the beneficial effects.

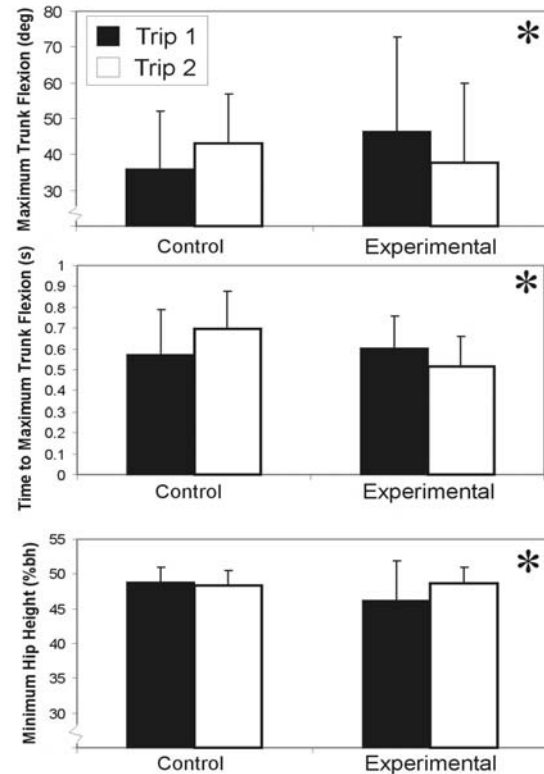


**Figure 1:** Mean participant data. Error bars represent standard deviation and the star indicates significant difference.

## REFERENCES

- Centers for Disease Control and Prevention. (2004) Web-based Injury Statistics Query and Reporting System (WISQARS) [Online].
- Lord S.R. et al. (1995). *J Am Geriatr Soc.*, **43**, 1198-1206.
- Tinetti M.E. (2003). *N Engl J Med.*, **348**, 42-49.
- Grabiner M.D. (1993). *J Gerontol.*, **48**, M97-102.

## ACKNOWLEDGEMENTS

Funding for this work was provided by the Carilion Biomedical Institute (Roanoke, VA) and the Virginia Tech Center for Gerontology.

# A TEST OF THE FUNCTIONAL ASYMMETRY HYPOTHESIS IN WALKING

Matthew K. Seeley, Brian R. Umberger, and Robert Shapiro

University of Kentucky, Lexington, KY, USA  
E-mail: mksee12@uky.edu Web: www.coe.uky.edu/biodynamics/

## INTRODUCTION

Subtle kinematic, kinetic, and electromyography (EMG) asymmetries have been well documented in able-bodied gait, yet the causes of these asymmetries remain unclear (Sadeghi et al. 2000). One prominent theory is that these bilateral discrepancies represent what are commonly referred to as *functional asymmetries*. Functional asymmetry has been defined as the consistent task discrepancy between the non-dominant (ND) and dominant (D) lower limbs (Sadeghi et al. 2000). It is purported that the ND limb is primarily responsible for providing support (vertical acceleration of the center of mass), while the D limb is primarily responsible for propulsion (forward acceleration of the center of mass). Preliminary evidence suggests that gait asymmetries may also be speed-dependent (Goble et al. 2003).

Some studies have provided provisional support for the hypothesis of functional asymmetry, yet many of these studies contain important limitations. As part of a larger effort to evaluate kinematic, kinetic, and EMG asymmetries, we report here on asymmetries in impulses due to the vertical and anterior-posterior (AP) ground reaction forces (GRF) during gait. It was hypothesized that if functional asymmetry is a reasonable explanation for able-bodied gait asymmetries, then: 1) impulses due to the VGRF (V) would be greater for the ND limb, and 2) impulses due to the propulsive portion of the APGRF (P) would be greater for the D limb. Also, it was expected that there would be no speed effect on V

impulses (due to the constancy of the gravitational force), but that P impulses would increase with speed disproportionately on the D side.

## METHODS

Two force platforms were used to measure bilateral GRF during simultaneous gait cycles in 20 young adults walking at three different speeds: preferred, slow (20% slower than preferred), and fast (20% faster than preferred). Five satisfactory trials were recorded at each speed. Trials were time normalized to the gait cycle, normalized to body weight, and then ensemble averaged for each limb, for each speed. V impulse was calculated as the time integral of the normalized VGRF during stance. P impulse was calculated as the time integral of the normalized APGRF, while the APGRF was directed in the anterior direction (approximately the second half of stance).

A repeated measures ANOVA ( $p = 0.05$ ) was utilized to detect effects of limb and walking speed on the dependent variables. Bonferroni adjusted post hoc analyses were performed to detect bilateral differences at each walking speed.

## RESULTS AND DISCUSSION

There was no significant main effect of limb for V impulse ( $p = 0.219$ ), but there was a significant limb  $\times$  speed interaction ( $p < 0.001$ ). Post hoc analyses revealed no significant bilateral differences at the slow ( $p = 0.334$ ) or preferred ( $p = 0.523$ ) speeds. However, V impulse was 2% greater in the

ND limb ( $p = 0.009$ ) at the fast speed (Figure 1). Similarly, there was no significant main effect of limb for P impulse ( $p = 0.753$ ), but there was a significant limb  $\times$  speed interaction ( $p = 0.001$ ). However, there were no significant bilateral differences at the slow ( $p = 0.212$ ), preferred ( $p = 0.675$ ), or fast ( $p = 0.130$ ) walking speeds (Figure 1).

The lack of a bilateral difference in V or P impulses at the slow and preferred speeds does not support the hypothesis of functional asymmetry as an explanation for able-bodied gait asymmetries. However, results at the fast walking speed offered modest support for functional asymmetry. As predicted, V impulses were greater for the ND limb at the fast speed, and there was also a trend towards greater P impulses for the D limb at the fast speed. Perhaps, if subjects had been required to walk faster, still larger bilateral differences may have been observed. However, given the results obtained at the preferred and slow speeds, present support for the concept of functional asymmetry as a general phenomenon is weak at best.

The absence of a limb effect at the preferred speed indicates that the gross kinetics of able-bodied gait are generally symmetrical. This supports the assumption of symmetry that is often made in studies of able-bodied gait. However, this does not guarantee that joint kinetics or neuromuscular patterns will be symmetrical.

## SUMMARY/CONCLUSIONS

The present results, based on impulses generated against the ground, do not support functional asymmetry as a valid explanation for able-bodied gait asymmetries, while walking at or below a preferred speed. Future efforts to clarify this issue should consider joint kinematics, joint kinetics, and EMG data, and more closely examine the issue of walking at speeds greater than preferred.

## REFERENCES

- Goble, D. et al. (2003). *Hum Mov Sci*, 22, 271-283.  
 Sadeghi, H. et al. (2000). *Gait and Posture*, 12, 34-45.

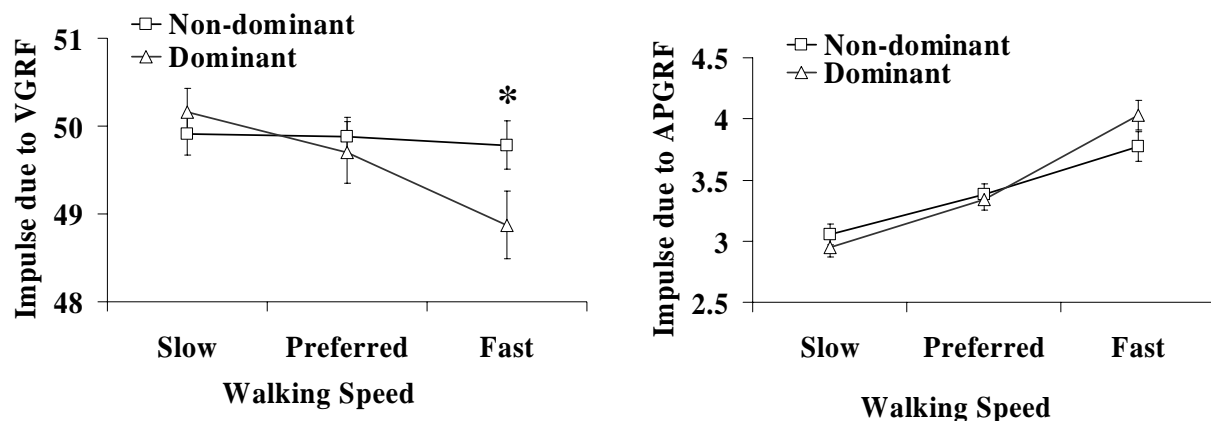


**Figure 1:** Mean impulses due to the VGRF and APGRF for non-dominant and dominant limbs during gait at three different walking speeds; ordinate values are reported as the product of force (N/body weight) and time (% of the gait cycle); the asterisk indicates statistical significance.

# MEASUREMENT OF MUSCLE INDUCED MOTION AND TORQUES AT POSTURES SEEN DURING THE SWING PHASE OF GAIT

Antonio Hernández<sup>1</sup>, Yasin Dhaher<sup>2</sup>, Darryl Thelen<sup>1</sup>

<sup>1</sup>University of Wisconsin-Madison, Madison, WI, USA

<sup>2</sup>Rehabilitation Institute of Chicago, Chicago, IL USA

E-mail: ahernandez2@wisc.edu Web: <http://www.engr.wisc.edu/groups/nmbi>

## INTRODUCTION

Forward dynamic simulation is emerging as a tool to characterize muscle function in normal walking [Neptune, 2001; Zajac, 2002] and to investigate the underlying causes of walking disorders [Goldberg, 2004; Riley and Kerrigan, 1998]. The predictions of forward dynamic models sometimes challenge commonly held views of muscle action [Zajac and Gordon, 1989]. For example, a model of swing phase predicts that the biarticular rectus femoris accelerates the hip into extension [Piazza and Delp, 1996]. However, such predictions have not been experimentally tested in-vivo. In this study, we introduce an experimental setup and methodology that can be used to measure the sagittal joint motion and torques induced by electrical stimulation of lower extremity muscles.

## METHODS

The subject is positioned side lying with his/her pelvis strapped to a padded brace (Fig. 1). Air bearing supports under the thigh and shank allow the limb to slide over a smooth table with negligible friction. Adjustable length bars, fixed to the table edge, hold the extremity in desired configurations. These bars are fitted with load cells for measurement of external forces. In a compliant mode, springs are connected between the load cells and the air bearing supports to allow leg motion (Fig. 2). A fixed-leg mode is also being developed for computation of the joint

torques applied by the muscles in a fixed leg configuration. In this mode, the springs are removed and the bars are extended to attach directly to the air bearing supports.

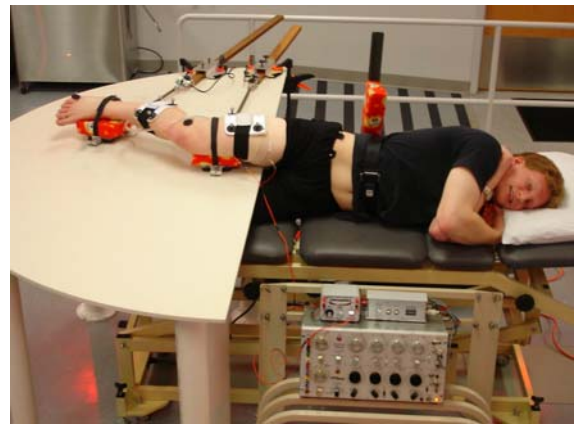


**Figure 1:** Experimental setup for the compliant mode in which springs are used to hold the limb in a desired equilibrium position prior to stimulation.

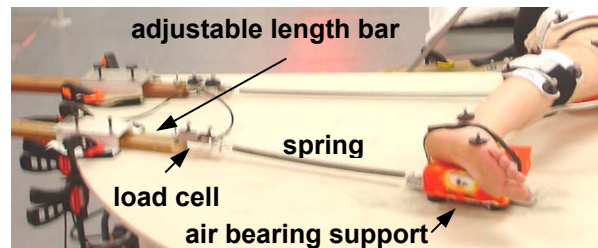


**Figure 2:** Adjustable length bars have load cells at their ends and can be either fitted a spring for compliant operation (as shown) or extended and attached directly to the air bearing leg supports. Markers on each load cell indicate the direction of external forces.

Lower limb position is tracked via 17 reflective markers placed on the pelvis, thigh, shank, and foot. Soft tissue artifacts are minimized by placing the tracking markers of a segment (shank or thigh) on a

rigid plate. Inverse kinematics and dynamics are used to compute lower extremity joint angles and torques from the measured data.

Electrical stimulation of muscles is introduced by fine wires inserted directly into the muscle(s) of interest. A two channel muscle stimulator (Grass S88) delivers current-controlled pulse trains. Short duration trains (<100 ms trains of 300  $\mu$ s pulses at 33 Hz) are used to avoid confounding the stimulus with potential reflex actions. EMG signals on the stimulated and neighboring muscles are simultaneously collected to assess potential stimulation crossover.

## RESULTS AND DISCUSSION

Our experimental setup has proven successful to collect motion data induced by short duration electrical stimulation of lower extremity muscles. For example, a 60 ms pulse train applied to vastus medialis produced 4.5° of knee extension and 0.5° of hip extension 100 ms after cessation of the stimulating pulse train (Fig. 3).

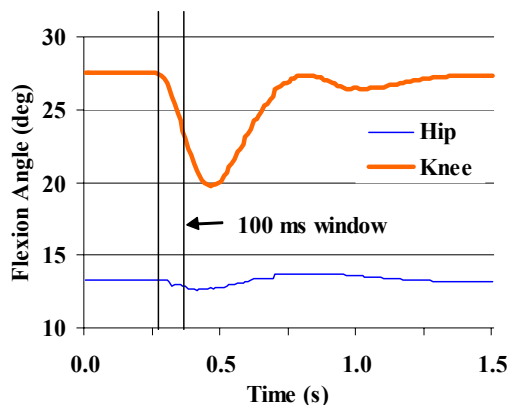


**Figure 3:** Hip and knee flexion angle as a function of time for stimulation of the vastus medialis with a 60 ms pulse train at  $t=0.27$  s. Both the knee and hip extend in the 100 ms window following the train.

We are currently using the setup to characterize the function of the rectus femoris (RF) and vastus medialis (VM) at five postures seen during the swing phase of gait (60%, 70%, 80%, 90% and 100% of the gait cycle). Based on a forward dynamic model of our experimental task, our first hypothesis is that RF generates hip extension motion at a limb posture seen during early swing. This function, which would be opposite to RF's common anatomical classification as a hip flexor, was predicted by Piazza and Delp [1996] using a muscle-actuated simulation. Our second hypothesis is that the effects of stimulating the RF and VM simultaneously will be the sum of their independent effects. This superposition principle is inherently assumed in almost all forward dynamic models of movement.

## SUMMARY/CONCLUSIONS

A new setup and methodology has been demonstrated for measuring muscle-induced motion and forces in the lower extremity.

## REFERENCES

- Goldberg, S., et al. (2004). *J Biomech*, **37**, 1189-96.
- Zajac, F.E., et al. (2002). *GaitPosture*, **16**, 215-232.
- Neptune, R.R., et al. (2001). *J Biomech*, **34**, 1387-98.
- Riley, P.O., D.C. Kerrigan (1998). *J Biomech*, **31**, 835-40.
- Piazza S.J., S.L. Delp (1996). *J Biomech*, **29**, 723-33.
- Zajac, F.E. and M.E. Gordon. (1989) *Exerc Sport Sci Rev*, **17**, 187-230.

## ACKNOWLEDGEMENTS

Contributions of Amy Silder and Betsy Hunter; Support of NIH AG20013, AG023276, and the Midwest Rehabilitation Research Network.

# THUMB KINEMATICS PRODUCED BY INDIVIDUAL EXTRINSIC MUSCLES: A CADAVERIC STUDY

Jie Tang, Matthew C. Chakan, Rodrigo Kaz, Zong-Ming Li

Hand Research Laboratory

Departments of Orthopaedic Surgery and Bioengineering, University of Pittsburgh

Email: zmli@pitt.edu Web: www.pitt.edu/~zmli/handlab/

## INTRODUCTION

The thumb plays a critical role in hand function because of its unique anatomy and numerous associated muscles. Previous studies of thumb biomechanics have examined the moment arms and associated torques about joints (Smutz et al., 1998), thumb tip force (Pearlman et al., 2004), and muscle activation patterns (Kaufman et al., 1999). The relationship between thumb joint kinematics and individual muscles remains relatively unclear. The purpose of this study was to investigate the thumb motion produced by individual extrinsic thumb muscles.

## METHODS

Six fresh-frozen cadaveric arms were used in this experiment. The specimens were prepared by minimal dissection to expose the musculotendinous junctions of the flexor pollicis longus (FPL), abductor pollicis longus (APL), extensor pollicis brevis (EPB), and extensor pollicis longus (EPL). A baseball suture was created at each junction to allow for tendon loading. The specimens were then rigidly mounted on a custom apparatus in neutral forearm position, with the palm vertical to the table and all finger joints fully extended. T-shaped plates with 5 mm diameter reflective markers were attached on the thumb and hand to establish coordinate frames (Figure 1). Before each trial, the thumb was passively moved for 15s and then placed in a position with minimal

resistance to motion (i.e. resting posture). The muscles were individually loaded to 10% of their maximal force capability (Brand et al., 1981) over 10s. The force was applied manually and monitored by a force transducer that interfaced with a customized LabVIEW (National Instruments, Austin, TX) program. Thumb motion was recorded using a motion analysis system (VICON 460, Oxford, UK) at a frequency of 100 Hz. Euler angles were calculated to quantify flexion/extension, abduction/adduction, and axial rotation at the carpometacarpal (CMC), metacarpophalangeal (MCP), and interphalangeal (IP) joints.

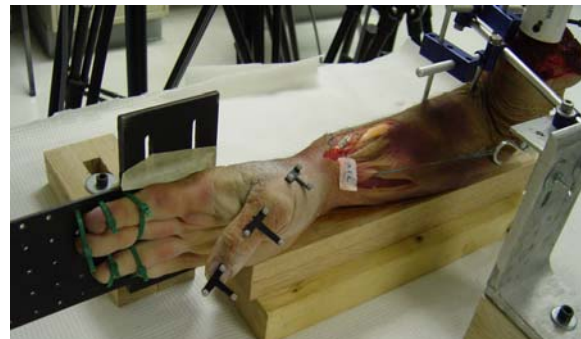


**Figure 1:** A specimen mounted in the custom fixation apparatus for muscle/tendon loading and motion recording

## RESULTS

Each extrinsic muscle produced unique angular trajectories at each joint and generated joint movements in multiple directions. For example, the APL loading caused extension, adduction, and supination at the CMC joint (Figure 2). Ranges of

motion (ROM) for each joint in all directions produced by individual muscles are presented in Table 1. The FPL mainly flexed the MCP and IP joints by 12.1° and 31.8°, respectively. The APL mainly moved the CMC joint by a range of 34.5° extension and 36.3° supination. The EPB produced 19.4° CMC joint extension and 19.0° MCP joint extension, as well as minimal IP extension. The EPL extended all three joints and also produced 16.8° adduction at the CMC joint. Both EPB and EPL rotated the CMC joint with supination of 20.8° and 22.1°, respectively.

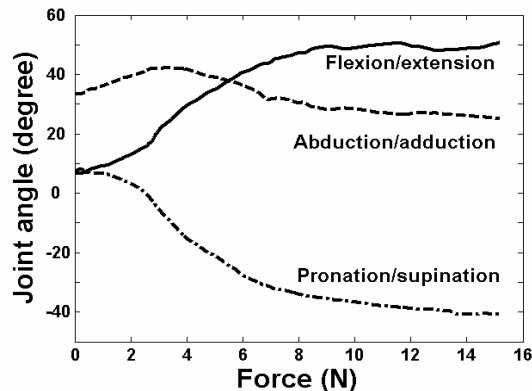


**Figure 2.** Angular trajectories of the CMC joint generated by APL loading. Positive directions are for extension, abduction, and pronation.

**Table 1.** Average joint positions and ranges of motion (degrees) produced by individual muscles.

Tendon		CMC			MCP			IP		
		S	E	ROM	S	E	ROM	S	E	ROM
FPL	EX	6.5	4.8	-1.8	-27.8	-39.9	-12.1	-20.0	-51.9	-31.8
	AB	24.2	23.7	-0.5	0.4	-1.3	-1.7	-0.5	3.3	3.8
	PR	8.0	9.8	1.8	1.4	1.3	-0.1	3.9	8.3	4.4
APL	EX	6.3	40.9	34.5	-28.6	-33.5	-4.9	-16.5	-20.9	-4.5
	AB	25.0	20.7	-4.4	0.5	0.0	-0.5	-0.4	2.3	2.7
	PR	7.9	-28.4	-36.3	1.7	3.0	1.3	1.0	1.2	0.3
EPB	EX	5.8	25.2	19.4	-17.2	1.7	19.0	-12.5	-8.1	4.5
	AB	24.0	22.6	-1.4	0.2	-1.9	-2.1	-0.9	-1.1	-0.2
	PR	7.8	-13.0	-20.8	3.0	3.5	0.5	2.2	3.0	0.9
EPL	EX	6.4	26.8	20.4	-21.1	-1.2	19.9	-9.3	8.9	18.2
	AB	21.3	4.4	-16.8	-2.0	-11.6	-9.6	-1.8	-4.2	-2.3
	PR	5.7	-16.5	-22.1	-1.6	-3.7	-2.1	2.0	-1.7	-3.6

Note: S: starting position; E: ending position at the target load; ROM (range of motion) = E - S. Positive angles indicate extension (EX), abduction (AB), and pronation (PR).

## DISSCUSSION

Our study examined the complex motion of thumb joints produced by each extrinsic muscle. Each muscle produced joint movements in multiple directions. Joint motion did not necessarily correspond to the anatomically implied function of the actuating muscle. For example, the APL mainly generated extension and supination at the CMC joint, and hardly produced joint abduction. Our data provide novel insight into the biomechanical roles of thumb muscles.

## REFERENCES

- Brand, et al. (1981). *J Hand Surg*, **6**, 209-219.  
 Kaufman, et al. (1999). *Clin Biomech*, **14**, 141-150.  
 Pearlman, et al. (2004). *J Orthop Res*, **22**, 306-312.  
 Smutz, et al. (1998). *J Biomech*, **31**, 565-570.

## ACKNOWLEDGEMENTS

The Whitaker Foundation.

# MULTI-SCALE GEOMETRIC MEASUREMENTS OF EXPERIMENTALLY INDUCED OSTEONECROTIC LESIONS IN AN EMU MODEL

Jessica Goetz,<sup>1</sup> Douglas Pedersen,<sup>1</sup> Duane Robinson,<sup>2</sup> Michael Conzemius,<sup>2</sup> Thomas Brown<sup>1</sup>

<sup>1</sup> University of Iowa, Iowa City, IA, USA

<sup>2</sup> Iowa State University, Ames, IA, USA

E-mail: jessica-goetz@uiowa.edu Web: poppy.obrl.uiowa.edu

## INTRODUCTION

Femoral head osteonecrosis (ON) is a disease in which fracture of abnormal bone in the femoral head causes collapse of head contour and subsequent hip joint degeneration. Histologic analysis is the most definitive method of diagnosing osteonecrosis. However, because mechanical collapse occurs at a macroscopic level and is contingent upon the geometric and spatial characteristics of the necrotic lesion, purely histologic determination of the presence of ON is insufficient to draw meaningful conclusions about the true severity of ON.

The outcome of ON is dependent on the size, shape, and orientation of the necrotic lesion within the femoral head (Nishii, 2002). To determine the severity of the necrotic lesions created in the developing emu model of ON, geometric and spatial information about the histologically determined lesions is critical. Making use of three-dimensional paraffin histology methods, geometric information was determined for cryoinsult induced osteonecrotic lesions in the emu femoral head.

## METHODS

Cryoinsult parameters of freeze time, freeze temperature, and number of freeze cycles were varied in an experimental surgical series in a group of adult emus. Following a one-week survival time, the emus were euthanized, and the proximal femora were harvested and fixed in formalin. Two

fiducial holes were drilled through the femoral neck and marked with dowels of potato. The femoral heads were then embedded in paraffin and serially sectioned through the entire thickness of the femoral head.

Sections were scanned into sub-regions on a stepper-motor-driven microscope stage and analyzed individually for percentage

osteocyte viability.

Less than 50%

osteocyte viability

was used to define ON. Once all slides in a given head were analyzed, they were stacked in the third dimension, aligned by the potato fiducial markers and saved into a three-dimensional data array in Matlab (Figure 1) (Goetz, 2005).

The necrotic sub-regions were isolated from the 3D data set and scaled to millimeters, making use of the known size of slice spacing and scan area. To determine the geometric properties of the necrotic lesion, the three-dimensional data were rotated to a coordinate system defined with the x-axis aligned along the major axis of the necrotic lesion.

Moments of inertia were calculated about the x, y, and z-axes of the lesion-based coordinate system. A second order

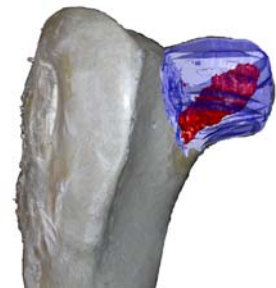


**Figure 1:** Rendering of 3-dimensional histologic data on an emu femur.

polynomial curve was fit to representative two-dimensional slices of the lesion boundary and rotated to enclose a smooth, idealized lesion volume (Figures 2&3). The volume enclosed in this idealized lesion is calculated by the disk method of integration. Volume is then compared to a standard head volume for the emu femoral head, and the maximum radius of the lesion is calculated.

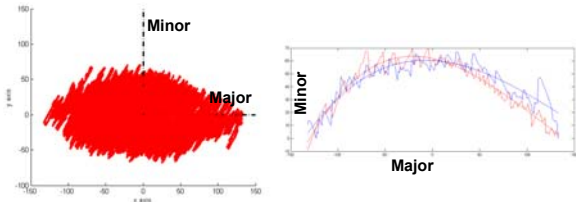


**Figure 2:** (Left) Necrotic lesion rotated to a lesion based coordinate system. (Right) Lesion boundary (red=top; blue=mirror of bottom) and associated polynomial fits.

## RESULTS AND DISCUSSION

The moments of inertia for lesions created by different cryoinsult parameters were similar around the minor axes (in the lesion based coordinate system), indicating some lesion symmetry. This is to be expected because the cryoprobe used to deliver the insult is cylindrical in shape and freezes around its entire circumference.

The lesion volumes calculated for the different freeze parameters ranged up to ~40% of the entire femoral head volume. This is a relevant volume for osteonecrotic lesions. To replicate human cases of ON when lesions can be larger than 40% of the

femoral head volume, variations in more than one freeze parameter can be made to increase the size of the lesion.

Maximum radii of the lesions induced in the femoral head extend beyond the 4mm drill tract made for cryoprobe insertion (up to ~8mm). Lesion diameters indicate that the necrotic lesions being developed are due to the freezing process, and are not simply collateral damage from the creation of the cryoprobe drill tract.

## CONCLUSIONS

In the laboratory setting, detailed multi-scale 3-D geometric information about experimentally induced osteonecrotic lesions can be gathered from histology-based mappings. This method allows for a definitive assessment of functional severity of osteonecrosis based on collapse-predisposing macroscopic biomechanical characteristics of the microscopically defined lesion.

## REFERENCES

- Nishii, T. et al. (2002). *J Orthop Res*, **20**, 130-136.
- Goetz, J.E. et al. (2005). *Proceedings of the XX<sup>th</sup> Congress of the ISB/29<sup>th</sup> Meeting of the ASB*. Cleveland, OH.

## ACKNOWLEDGEMENTS

Funding from NIH AR49919. Scanning assistance from Erich Stoermer, Marie Frenn, Matt Paul.

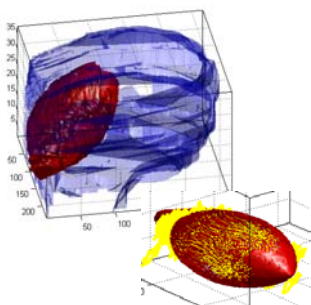


**Figure 3:** Idealized lesion enclosing the actual data, and idealized lesion within the 3D rendering.

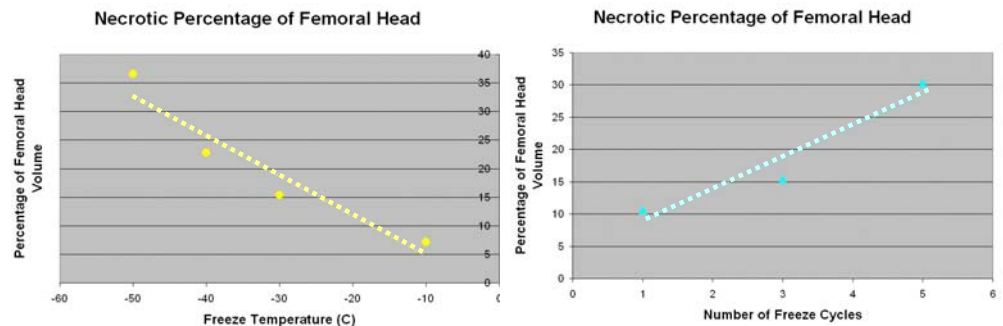


**Figure 4:** Variation in percentage of femoral head volume that is enclosed within the necrotic lesion with change in freeze temperature (left) and number of freeze cycles (right).

# EFFECTS OF FATIGUE ON LOWER EXTREMITY JOINT KINEMATICS DURING A STOP AND GO LANDING TASK

Deborah King<sup>1</sup>, John Sigg<sup>1</sup>, Barb Belyea<sup>2</sup>, Chris Hummel<sup>1</sup>, and Mike Buck<sup>2</sup>

<sup>1</sup>Department of Exercise and Sport Sciences, Ithaca College, Ithaca, NY, USA

<sup>2</sup>Department of Physical Therapy, Ithaca College, Ithaca, NY, USA

Email: [dking@ithaca.edu](mailto:dking@ithaca.edu); Web: [www.ithaca.edu/hshp/ess](http://www.ithaca.edu/hshp/ess)

## INTRODUCTION

Stop and go tasks are involved in the majority of non contact anterior cruciate ligament (ACL) injuries (Arendt and Dick, 1995; Boden, et al., 2000; Gwinn, 2000). Moreover, muscle fatigue can result in noticeable affects on the mechanics of complex motor skills such as walking, running, and jumping (Johnston, et al, 1998; Pinniger, et al., 2000; Rodacki, et al., 2001). However, there is limited literature on the effects of fatigue on the mechanics of landing and cutting tasks (e.g. Chappell, et al., 2005; McNitt-Gray, et al, 1996; Nyland, et al., 1997; Nyland, et al., 1994). Results from these studies suggest that with fatigue, onset of muscle activation is delayed, max knee flexion is decreased, and shear forces are increased (Chappell, et al., 2005; Nyland, et al., 1994).

Considering the link between ACL injuries and stop and go tasks (Arendt and Dick, 1995; Boden, et al., 2000; Gwinn, 2000) and the increased risk for non contact ACL injuries in female athletes (Arendt and Dick, 1995; Delfico and Garrett, 1998; Traina and Bromberg, 1997) it seems that further research is warranted on the effects of fatigue on landing mechanics in male and female athletes. The purpose of this study was to examine joint kinematics in competitive athletes performing stop and go landing tasks in a fatigued state representative of game conditions.

## METHODS

Twenty healthy collegiate athletes participated in this study after giving their

written informed consent. The testing session involved a warm-up, pre-fatigue testing, a fatiguing protocol, and post-fatigue testing. The stop and go task analyzed during pre and post fatigue testing was a 45 degree cut performed off the subject's preferred leg after landing from a 0.5 m high box.

The fatigue protocol consisted of a 10 minute progressive incline treadmill run immediately followed by a 10 by 12 foot footwork pattern of forward, backward and side ways steps with two vertical jumps. The pattern was repeated until 1) lap time slowed to 150% or 2) completion of 10 laps and inability to achieve maximum jump height.

Ground reaction forces (GRF) were measured with two force plates. Two high speed digital cameras captured the motion of the preferred leg during the 45 degree cut. Three dimensional coordinates of marker arrays were computed and 3D kinematics were calculated of the cutting leg. Subjects completed 3 vertical jumps between each post trial to maintain fatigue. This paper will focus only on the lower extremity kinematics, as the GRF data has been reported elsewhere. To date, data of 7 men and 7 women are included in the analysis. Data were analyzed with a two way repeated measures ANOVA at  $\alpha = 0.05$ .

## RESULTS AND DISCUSSION

The only significant effect from the fatiguing protocol was an increase in time to max knee flexion ( $p=0.03$ ), which supports findings from previous studies (Nyland, et

al., 1997). There were no significant changes in ankle or knee angles at contact or in knee range of motion, as has been previously reported (Nyland, et al, 1997; Chappell, et al., 2005). The lack of change in ankle & knee angles with fatigue may be due to the dual emphasis on cardiovascular and muscular fatigue, as compared to studies which focused more on lower extremity muscular fatigue, or the use of competitive athletes versus recreational athletes.

Several male female differences were observed in lower extremity mechanics (Figure 1). At contact, the female athletes were in a position of greater knee flexion and less ankle inversion ( $p \leq 0.002$ ). During the landing phase, the female athletes exhibited less dorsiflexion in their ankle and more valgus in their knee. The increased valgus of the knee for the female athletes is similar to other findings reported in the literature; though the female athletes did not exhibit less knee flexion ROM as has also been reported (Malinzak, et al, 2001). This could be due to the use of competitive collegiate athletes who may be stronger or more powerful than recreational athletes or pre adolescent & adolescent athletes, who are commonly studied (Milinzak, et al., 2001; Chappell, et al., 2002, 2005).

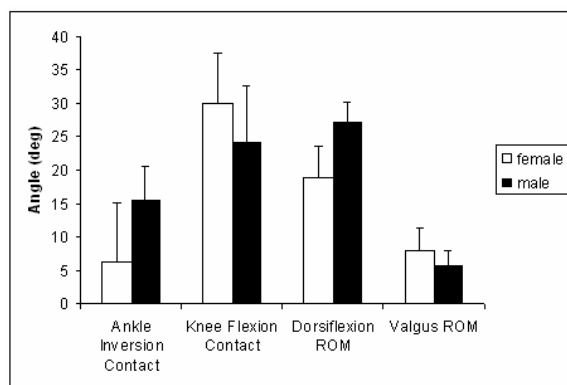


Figure 1. Kinematic variables with significant difference between male and females.

## CONCLUSIONS

The collegiate female athletes had increased knee valgus as compared to the male athletes but did not demonstrate decreased knee flexion. Time to max knee flexion was slower in the fatigued state. Combining these results with previous reported results of changes in GRFs and joint kinetics, future research investigating the relationship between lower extremity mechanics, fatigue, and injury incidence appear to be warranted.

## REFERENCES

1. Arendt E.A., Dick, R. (1995). *Am J Sports Med*, **23**, 694-701.
2. Boden, B.P. et al. (2000). *Orthopedics*, **23**, 573-578.
3. Chappell, J.D., et al. (2002). *Am J Sports Med*, **30**, 261-267.
4. Chappell, J.D., et al. (2005). *Am J Sports Med*, **33**, 1022-1029.
5. Delfico, A.J., Garrett W.E. Jr. (1988). *Clin Sports Med*, **17**, 779-785.
6. Gwinn, D.E. (2000). *Am J. Sports Med*, **28**, 98-102.
7. Johnston, R.B., et al. (1998). *Med Science Sports Exerc*, **30**, 1703-1707.
8. Malinzak R.A., et al. (2001). *Clin Biomech*, **16**, 438-445.
9. McNitt-Gray, et al. (1996). *Proceedings of 23<sup>rd</sup> American Society of Biomechanics Annual Meeting*, 47-48.
10. Nyland, J.A., et al. (1994). *J Ortho Sports Phys Ther*, **20**, 132-137.
11. Nyland, J.A., et al. (1997). *J Ortho Sports Phys Ther*, **25**, 171-184.
12. Pinniger, et al. (2000). *Med Sci Sports Exerc*, **32**, 647-653.
13. Rodacki, A.L., et al. (2001). *Med Sci Sports Exerc*, **33**, 1157-1167.
14. Traina, S.M., Bromberg, D.F. (1997). *Orthopedics*, **20**, 545-549

# APPLYING STATISTICAL PROCESS CONTROL TO IDENTIFY TRANSITIONARY FOOT MOTIONS DURING MANUAL MATERIAL HANDLING TRANSFER TASKS

David W. Wagner and Matthew P. Reed  
University of Michigan, Ann Arbor, MI, USA  
E-mail: [dwwagner@umich.edu](mailto:dwwagner@umich.edu) Web: [www.humosim.org](http://www.humosim.org)

## INTRODUCTION

The transition between cyclical gait and non-cyclical stepping has been well studied during the initiation and termination phases of the gait cycle (Breniere, and Do, 1991; Nissan and Whittle 1990). Progression velocity and step frequency during the initiation, rhythmic, and termination phases of gait have been used to establish the step at which a transition to or from nominal gait occurs (Sparrow and Tirosh, 2005). Research has not focused on the similar transitions in stepping behavior during manual material handling (MMH) tasks.

Statistical process control (SPC) is traditionally associated with monitoring a manufacturing process for unusual causes of variation (i.e. equipment malfunction). A control chart, a primary technique of SPC, is a method for identifying a deviation in the process from a sample of parts produced by the process (Montgomery et al. 2001). A method for applying a Shewhart control chart to monitor stride velocity during a MMH pickup transfer task and identify at which step a deviation from nominal gait occurs is presented.

## METHODS

Whole-body motion data were gathered with a six-camera Qualisys Proreflex 240-MCU optical based motion tracking system sampled at 50 Hz in the Human Motion Simulation (HUMOSIM) laboratory at the University of Michigan. Ground contact times for each heel and toe were captured at 500 Hz with footswitch signals. Participants

were instructed to move a load with two hands between two shelves with a 45-degree delivery angle (Figure 1). Shelf height was scaled to 0.53 times participant stature. Data were obtained from 7 male and 8 female participants between the ages of 20 and 30. The protocol was approved by an institutional review board and all subjects provided written, informed consent.

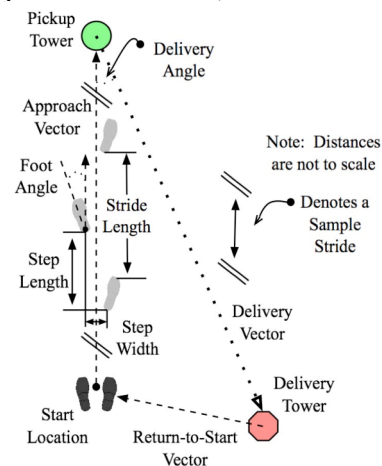


**Figure 1:** Schematic of MMH transfer task and selected spatial gait parameters.

Spatiotemporal parameters of step length, stride length, step width, foot angle, instantaneous velocity of progression, and step frequency were computed for each trial (Figure 1). The gait parameters for a nominal stride were calculated for each trial between the first and third heel contact step events after the trial began (Breniere and Do, 1991). Results for stride velocity are presented here. Stride velocity is defined as the stride length divided by the elapsed time between consecutive ipsilateral heel strikes.

A Shewhart chart was constructed for monitoring instantaneous stride velocity at

each step throughout a trial. The center line (CL) was calculated as the average nominal gait stride velocity across trials for each participant. Upper and lower control limits (UCL and LCL) were calculated as the CL  $\pm 3\sigma$  respectively, where  $\sigma$  is defined from published intra-subject coefficient of variation (CV) values (Beauchet et al., 2005). The transition from the nominal gait cycle is defined when stride velocity for a particular step is outside the range defined by the LCL and UCL.

## RESULTS AND DISCUSSION

Descriptive statistics for stride length and stride velocity (mean  $\pm$  standard deviation) are presented for all the observed trials. The stride length (137.4  $\pm$  13.6 cm) and stride velocity (118.5  $\pm$  12.6 cm/s) were computed for fifteen participants and are consistent with the nominal values published by Beauchet et al, 2005.

A representative control chart for the stride velocity of one trial (subject 10) is presented (Figure 2). Steps 1 and 2 are initialized from the stationary posture. Nominal gait stride velocity is reached by the 5<sup>th</sup> step and consistent with nominal gait until the step after the load is lifted. Trials were excluded if the stride velocity for a nominal gait cycle was not achieved. Thirty-one trials were analyzed. In 77% (90%) of the trials once a nominal gait velocity was achieved, it was maintained until the step (two steps) prior to when load pickup occurred.

The use of statistical quality control as a measure for defining the transition between cyclical gait and non-gait stepping behaviors

has shown promise. However, knowledge of nominal means and variances of gait parameters are crucial to defining accurate control charts. A limitation of the work presented here is that population CVs were used to define the control limits. The use of subject specific variations would improve transition detection by increasing the sensitivity of the control charts over the ones presented here. Identifying transitions between nominal gait and other stepping behaviors during gait initiation, gait termination, turning, stepping over obstacles, and climbing stairs are just a few of the possible applications of this approach.

## REFERENCES

- Beauchet, O. et al. (2005). *J. Neuro-Engineering and Rehabilitation*, **2**:26.
- Breniere, Y., Do, M.C. (1991). *J. Motor Behavior*, **23**, 235-240.
- Montgomery, D.C. et al. (2001). *Introduction to Statistical Quality Control, 4<sup>th</sup> Edition*. John Wiley & Sons, Inc.
- Nissan, M., Whittle, M.W. (1990). *J. Biomedical Engineering*, **12**, 165-171.
- Owings, T.M., Grabiner, M.D. (2004). *Gait and Posture*, **20**, 26-29.
- Sparrow, W.A., Tirosh, O. (2005). *Gait and Posture*, **22**, 362-371.
- Terrier, P., Schutz, Y. (2003). *European Journal of Applied Physiology*, **90**, 554-56.

## ACKNOWLEDGEMENTS

This research was sponsored by the HUMOSIM consortium (GM, Ford, DaimlerChrysler, International Truck, USPS, UGS, and the US Army-RDECOM).

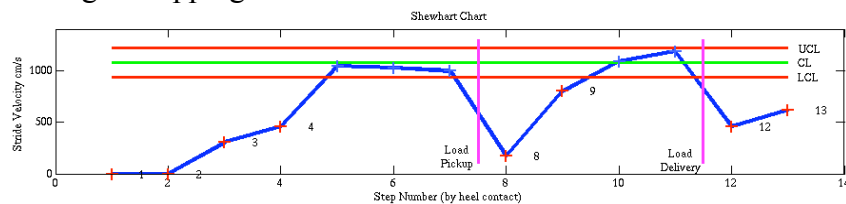


**Figure 2:** Representative Shewhart control chart of stride velocity for a single trial.

# ULTRASOUND MEASURES OF FASCICLE LENGTH ARE SUPERIOR TO THE APONEUROSIS ANGLE INDICATING WHOLE MUSCLE LENGTH CHANGES WITH TWO-JOINT MOVEMENTS

Timothy J. Brindle, Maria K. Lebedowska, Jeri L. Miller and Steven J. Stanhope

\*\* Physical Disabilities Branch, National Institutes of Health, Bethesda, MD 20892  
E-mail: Tbrindle@cc.nih.gov, web: <http://pdb.cc.nih.gov/>

## INTRODUCTION

Change in fascicle length and pennation angle can be reliably measured with ultrasound in-vivo.[1,2] However these measures might not represent changes across the “whole” muscle.[3] We present a measure of the gastrocnemius (GAST) aponeurosis angle ( $\theta$ ), defined as the angle between the superficial and deep aponeurosis of the GAST, which may better represent length changes across the whole muscle opposed to more local changes represented by fascicle length (FL) changes (Figure 1). The purpose of this study was to detect the sensitivity between FL and  $\theta$ , during two-joint movements

## METHODS

Twenty subjects were seated on a Biodex (*Biodex Inc., Shirley NY*) with their legs positioned in a custom-made foot/ankle apparatus, controlled by a linear actuator (*Ultramotion, Inc, Mattituck, NY*), that passively and simultaneously extended knee and plantar flexed the ankle. A 7.5 MHz ultrasound linear transducer (*SonoSite, Bothell, WA*) imaged the mid-third of the GAST in the longitudinal plane. The transducer array was set in a jig, attached to the Biodex arm, and held in place with an elastic wrap to maintain image planes-of-site of GAST targets during data acquisition.[1] As the knee was passively extended ( $60^{\circ}$ - $20^{\circ}$  at  $2^{\circ}/s$ ) the ankle rotated ( $0^{\circ}$ - $5.2^{\circ}$  at  $0.26^{\circ}/s$ )

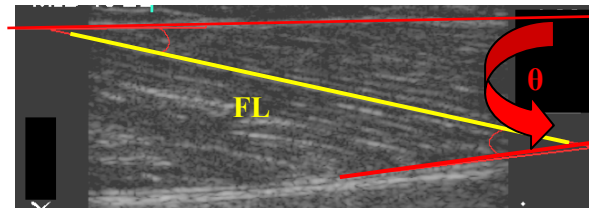


**Figure 1:** Ultrasound image of FL and  $\theta$ .

medial GAST elongation or rotated ( $0^{\circ}$ - $13.0^{\circ}$  at  $0.65^{\circ}/s$ ) for lateral GAST shortening.[4] Off-line ultrasound measures of FL and  $\theta$ , were acquired every  $10^{\circ}$  of knee extension, and included FL and  $\theta$ . Commercial software enabled calculation of muscle fascicle length (*Carnoy, Schols, P. & E. Smets.2001*) and  $\theta$  (*Photoshop8, Adobe, Seattle, WA*) (Figure 1). Separate repeated measures ANOVA were used to determine differences between elongation of the medial GAST and shortening of the lateral GAST for every  $10^{\circ}$  of knee extension. We calculated the minimal detectable difference ( $MDD = (\bar{X}_1 - \bar{X}_2) \pm 1.96 * SEM$ ) between every  $10^{\circ}$  of knee extension for FL and  $\theta$ , and determined an overall MDD average. A linear regression line was fit on each muscle's measure (FL,  $\theta$ ) to represent the rate of change (*slope*) per degree of knee extension. Average MDD for each measure was divided by *slope* to give the minimally detectable knee extension (MDKE) necessary to observe changes in FL or  $\theta$  using ultrasound.

## RESULTS AND DISCUSSION

As expected, there was a significant interaction ( $p < 0.001$ ) between the two conditions at all knee angles for both **FL** and  $\theta$ . Post-hoc analysis demonstrated significant differences among elongation and shortening of the medial and lateral GAST (Figure 2).

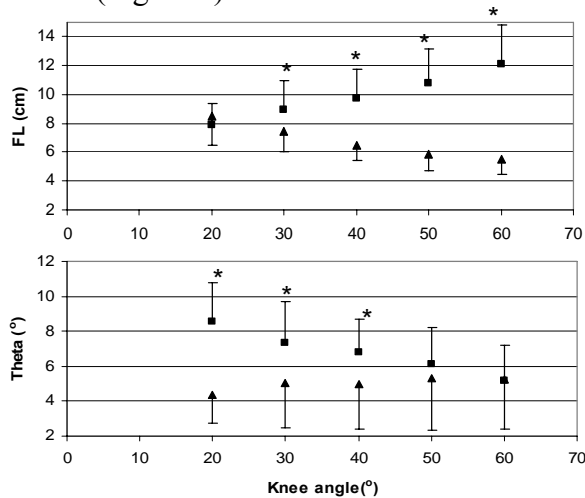


**Figure 2:** Elongation (▲; -1 SD) and Shortening (■; +1 SD) of **FL** (top) and  $\theta$  (bottom), plotted versus knee angle.

\* Significant differences ( $p < 0.05$ ) between the muscles at different knee angles.

**MDD** for every  $10^\circ$  of knee extension, average **MDD**, *slope* and **MDKE** of muscle change for both measures are presented in (Table 1). These data suggest that both **FL** and  $\theta$  are equally capable of detecting changes in the lateral GAST muscle during shortening. However, when using  $\theta$  there needs to be a two-fold increase in extension

prior to reliably detecting changes in medial GAST length. While  $\theta$  may or may not be more representative of whole muscle changes it does not demonstrate a superior ability to detect muscle length changes in the medial GAST. This may be due to the area imaged on the muscle and differences in muscle architecture relative to the lateral GAST. Using both **FL** and  $\theta$  to determine muscle length changes is recommended due to differences between these two measures.

## SUMMARY/CONCLUSIONS

Based on **MDKE** both **FL** and  $\theta$  are can detect elongation and shortening of both the medial and lateral GAST. They also demonstrate equal sensitivity in detecting lateral GAST shortening. **FL** measures can detect elongation of the medial GAST with only  $12.5^\circ$  of knee extension as opposed to  $30^\circ$  of knee extension necessary before  $\theta$  can medial GAST elongation. These results suggest FL may be a superior indicator of whole muscle kinematics.

## REFERENCES

- [1] Chow, et al. *Eur J Appl Physiol.* **82**, 236-244, 2000.
- [2] Herbert et al. *J Physiol.* **539**, 637-645, 2002.
- [3] Aagaard, et al. *J Physiol.* **534** 613-623, 2001.
- [4] Refshauge et al. *J Physiol.* 488 231-241, 1995.

\*\*A collaboration between the NICHD and the Mark O. Hatfield Clinical Research Center, NIH

**Table 1:** **MDD** for every  $10^\circ$  of knee extension, average **MDD**, *slope* and **MDKE** (n=20)

	20-30°	30-40°	40-50°	50-60°	Avg. MDD	<i>slope</i>	<b>MDKE</b>
<b>Elongation</b>							
<b>FL(cm)</b>	1.4	1.2	1.0	0.4	1.0 cm	0.08 <sup>cm</sup> / <sub>deg</sub>	12.5 °
$\theta$ (°)	0.5	0.4	0.8	0.8	0.6 °	0.02 <sup>deg</sup> / <sub>deg</sub>	30.0 °
<b>Shortening</b>							
<b>FL(cm)</b>	1.5	1.2	1.4	1.8	1.5 cm	0.1 <sup>cm</sup> / <sub>deg</sub>	15.0 °
$\theta$ (°)	1.6	1.2	0.9	1.6	1.3 °	0.08 <sup>deg</sup> / <sub>deg</sub>	16.3 °

# CARPAL TUNNEL EXPANSION BY STRETCHING THE TRANSVERSE CARPAL LIGAMENT

Zong-Ming Li, Jie Tang, Matthew C. Chakan, Rodrigo Kaz, Ashish D. Nimbarte

Hand Research Laboratory

Departments of Orthopaedic Surgery and Bioengineering, University of Pittsburgh

Email: [zmli@pitt.edu](mailto:zmli@pitt.edu) Web: [www.pitt.edu/~zmli/handlab/](http://www.pitt.edu/~zmli/handlab/)

## INTRODUCTION

The transverse carpal ligament (TCL) forms the palmar roof of the carpal tunnel and plays a critical role in regulating carpal tunnel mechanics (Brooks et al., 2003; Kiritsis and Kline, 1995). The mechanical constraint of the TCL predisposes the median nerve to compression and the ensuing carpal tunnel syndrome. Transecting the TCL, whether by open or endoscopic carpal tunnel release procedures, is the standard surgical treatment of carpal tunnel syndrome. Even though carpal tunnel release has existed for over 70 years, we have limited knowledge of the mechanical properties of the carpal tunnel and the TCL. Common complications and recurrence associated with TCL transection continues to challenge us to develop alternative CTS treatments without cutting the TCL (Sucher, 1993; Berger, 2005). Yet, understanding carpal tunnel mechanics is critical to the development of such alternatives. The purpose of this study was to investigate the expansion of the carpal tunnel with palmarly directed force on the TCL from within the carpal tunnel.

## METHODS

Five fresh frozen cadaveric hands were dissected to expose the TCL by removing the skin, fascia, and fat while the ligament insertion sites to carpal bones were kept intact. The TCL was recognized by its transverse fibers and insertions at the

pisiform, hook of hamate, tuberosity of scaphoid and ridge of trapezium (Figure 1). The flexor tendons and median nerve were removed to clear the carpal tunnel.

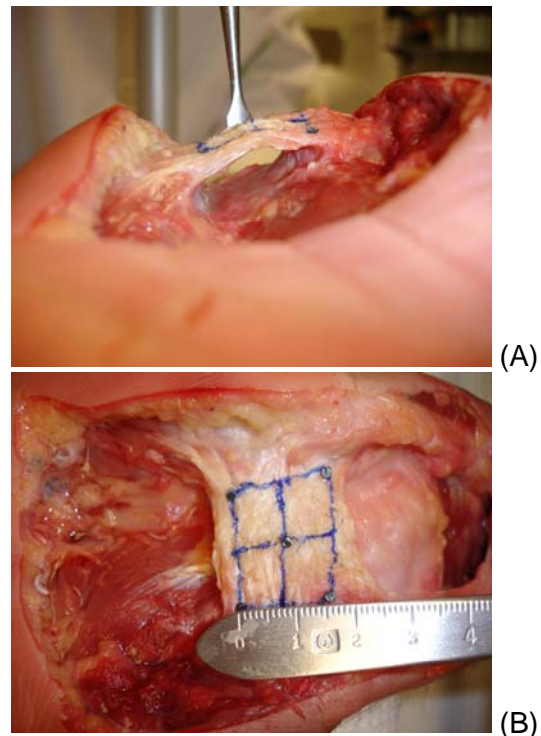


**Figure 1:** Cadaveric preparation of the carpal tunnel (A) and the transverse carpal ligament (B)

The bony surface within the carpal tunnel was digitized to determine the cross-sectional area formed by carpal bones. Then specimen was mounted on a dorsal support in full supination and approximately 20° of wrist extension on a custom platform. A lever, which rotated about a suspended, threaded rod, was inserted under the central

line of the TCL so that the midpoint of the central line located 150 mm from the lever's fulcrum. The lever was then made parallel to the table surface and loaded, at a distance of 450 mm from the fulcrum. With this lever device, the TCL was stretched by a palmarly directed force from within the carpal tunnel. A steel plate was passed through the carpal tunnel to stabilize the hand. The palmar surface of the TCL was digitized while the TCL was being stretched. Eight constant force levels were applied to the TCL, ranging from 10 N to 200 N. The cross-sectional area was determined at the middle level between the trapezium and scaphoid.

## RESULTS

The area defined by the carpal bones without the TCL-formed arch was  $128.2 \pm 24.2 \text{ mm}^2$ . The TCL formed an arch that expanded the carpal tunnel with increasing loading (Figure 2 and Figure 3). With the TCL stretching and arch formation, the cross-sectional areas of the carpal tunnel were  $165.0 \pm 24.9 \text{ mm}^2$  at 10 N, and  $194.3 \pm 21.4 \text{ mm}^2$  at 200 N, representing increases of 28.7% and 51.6%, respectively. The TCL arch heights were  $2.8 \pm 0.3 \text{ mm}$  at 10 N and  $5.4 \pm 0.4 \text{ mm}$  at 200 N.

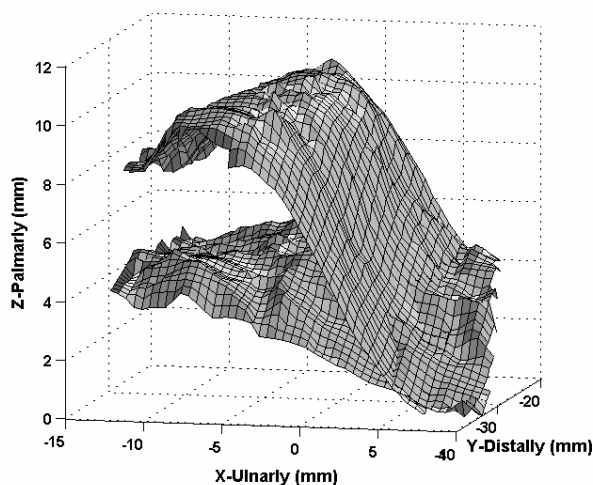


**Figure 2:** Surface plots of the transverse carpal ligament before and after stretching at 200 N

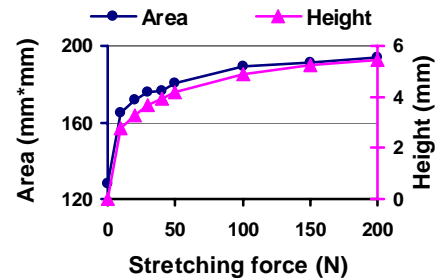


**Figure 3:** Average cross-areas of the carpal tunnel and TCL arch heights with increasing stretching forces

## DISCUSSION

Our study demonstrates the stretchability of the TCL and the resulting expansion of the carpal tunnel. The result of about 30% carpal tunnel expansion by a small stretching force of 10 N suggests that the TCL is accommodating with the variation of carpal tunnel pressure in a physiological environment. Greater than 50% carpal tunnel expansion is available under relatively large stretching force (> 200 N). Future studies are needed to investigate the viscoelastic properties of the TCL and to explore the potential of permanent residual deformation. The mechanical properties of the TCL may be exploited for the development of alternative carpal tunnel syndrome treatments, such as manipulative procedures (Sucher, 1993) and balloon carpal tunnel plasty (Berger, 2005).

## REFERENCES

- Berger (2005), Personal communications.
- Brooks, et al. (2003), *Clin Biomech*, **18**, 685-93.
- Kiritsis and Kline (1995), *J Hand Surg*, **20**, 173-80.
- Sucher (1993), *J Am Osteopath Assoc*, **93**, 1273-8.

## ACKNOWLEDGEMENTS

The Pittsburgh Foundation

# RELATIONSHIPS BETWEEN RECONSTRUCTED HIP CENTER AND HIP FORCES IN SUBJECTS WITH TOTAL HIP REPLACEMENTS

Kharmma C. Foucher, Markus A. Wimmer, Debra E. Hurwitz

Rush University Medical Center, Chicago, IL USA

E-mail: [kharmma\\_c\\_foucher@rush.edu](mailto:kharmma_c_foucher@rush.edu),

Web: [www.ortho.rush.edu/Gait](http://www.ortho.rush.edu/Gait)

## INTRODUCTION

Configurations of joint geometry linked to increased incidence of aseptic total hip replacement loosening include a superior or lateral hip joint center (Yoder et al, 1988, Zahiri et al., 1999). Large hip forces, in particular implant twisting moments, have been linked to implant loosening (Bergmann et al., 1995). The relationship between hip forces and joint geometry has not been investigated *in vivo*. This study tested the hypothesis that there is a significant correlation between the position of the hip joint center and hip forces during walking.

## METHODS

28 subjects with primary hip osteoarthritis underwent gait analysis (Andriacchi et al., 1997) one year after THR surgery. Hip forces were modeled based on the kinematics and external moments collected during walking for each subject. A description of the model has been previously published (Hurwitz et al., 2003). The two peak hip contact forces during stance were each analyzed separately. Peak implant twisting moment, calculated from the hip contact force and the distance to the implant axis, was also analyzed. Horizontal (HP) and vertical (VP) positions of the hip joint center were measured from postoperative anterior-posterior pelvic radiographs. Pearson correlations were calculated when testing for significant relationships between the radiographic parameters and the force parameters.

## RESULTS AND DISCUSSION

VP was significantly correlated with the peak implant twisting moment during walking (Table 1). Increasing VP should increase the moment arm of the implant twisting moment (figure 1). In fact a more superior hip center was associated with a larger implant twisting moment (figure 2). There were no other significant correlations between force parameters and VP.

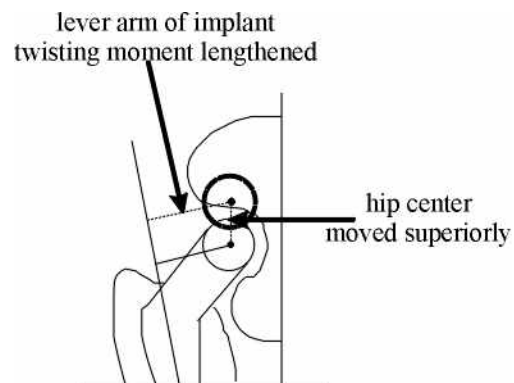


**Figure 1:** Moving the hip center superiorly increases the moment arm of the implant twisting moment.

There were no significant correlations between HP and the force parameters. This was in contrast to the study by Yoder et al., 1988. While the amount of variation (standard deviations) in this measurement was comparable in the two patient groups, the range of measurements was less in the present study (present study 27 to 41 mm; Yoder study 18 to 53 mm). Relationships between the horizontal joint center position

and hip forces may not be seen in this small range.

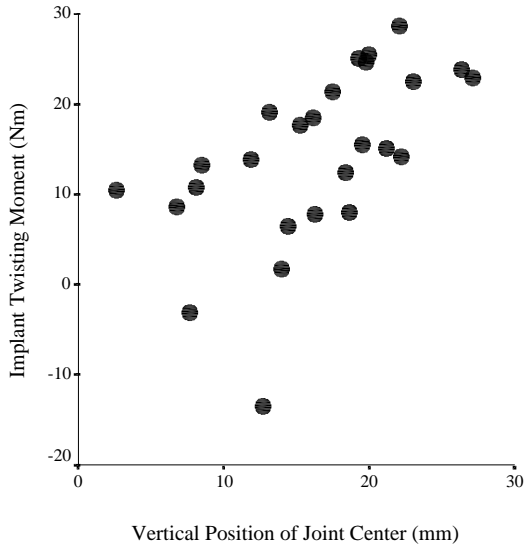


**Figure 2:** The vertical position of the hip joint center was significantly correlated to the implant twisting moment ( $R = 0.574$ ,  $p = 0.002$ ).

### SUMMARY/CONCLUSIONS

A more superior joint center position was related to increased implant twisting moment. No other significant correlations were found between hip loading and superior-inferior joint center position. There

was no relationship between the medial-lateral joint center position and the force parameters. The lack of additional correlations between joint geometry and the hip joint loading environment suggest that it may be more strongly governed by postoperative gait patterns than the simple static mathematical relationships between geometry and hip forces and/or muscle forces. However in turn, gait patterns may be influenced by postoperative joint geometry.

### REFERENCES

Andriacchi et al. (1997). In Basic Orthopaedic Biomechanics 2nd ed. eds. VC Mow and WC Hayes.

Foucher, K.C., et al. *Gait and Posture*, 7(2):158-9, 1998.

Hurwitz DE, et al. *J. Biomech.* 2003 Jan;**36**(1):113-9

Yoder SA, et al. (1988). *CORR*, **288**, 79-87.

Zahiri CA, et al. (1999). *J. Arthroplasty* **14**(3), 326-332.

### ACKNOWLEDGEMENT

Whitaker Foundation

**Table 1:** Pearson correlation coefficients between the joint geometry parameters and the force parameters. The vertical joint center position and peak implant twisting moment (Bold) were significantly correlated.

	First Contact Force Peak	Second Contact Force Peak	Peak Implant Twisting Moment
Vertical Joint Center Position	R = 0.288 p = 0.183	R = 0.216 p = 0.322	<b>R = 0.574</b> <b>p = 0.002</b>
Horizontal Joint Center Position	R = 0.002 p = 0.992	R = 0.013 p = 0.938	R = -0.019 p = 0.787

# CURRENT AUTOGRAFTS USED FOR ACL RECONSTRUCTION DO NOT RESTORE TIBIAL ROTATION DURING PIVOTING

Stavros Ristanis<sup>1</sup>, Vasileios Chouliaras<sup>1</sup>, Constantina Moraiti<sup>1</sup>, Nicholas Stergiou<sup>2</sup> and Anastasios Georgoulis<sup>1</sup>

<sup>1</sup>Orthopaedic Sports Medicine Center of Ioannina, Department of Orthopaedic Surgery, University of Ioannina, Greece

<sup>2</sup>HPER Biomechanics Laboratory, University of Nebraska at Omaha, Omaha, NE, USA  
E-mail: oaki@cc.uoi.gr Web: <http://www.osmci.gr>

## INTRODUCTION

The two most frequently used autografts for anterior cruciate ligament (ACL) reconstruction are the bone-patellar tendon-bone (BPTB) and the quadrupled hamstrings tendon (semitendinosus and gracilis; ST/G). The purpose of this study was to identify the effectiveness of these two autografts, in restoring tibial rotation to normal physiological levels, using *in-vivo* biomechanics.

## METHODS

Eleven male patients, ACL reconstructed with a quadrupled ST/G graft, eleven male patients ACL reconstructed with a BPTB graft and eleven healthy gender- age- height- and mass- matched controls were assessed in this study. Individuals with more than 25% of meniscus damage, chondral lesions, posterior cruciate or collateral ligament injury, symptomatic anterior knee pain or objective instability at the latest follow-up examination (positive pivot-shift test results, positive Lachman-test results and arthrometer side-to-side differences of more than 3 mm) were excluded from our study. Post-operatively the two groups followed the same accelerated rehabilitation program. Return to sports related activities was permitted 24 weeks after reconstruction for both groups.

Kinematic data were collected (50Hz) with a six-camera optoelectronic system (Peak Performance), while the subjects descended stairs and immediately after, pivoted on their landing leg. The descending period was concluded upon initial foot contact with the ground. Following foot contact, the subjects were instructed to immediately pivot (externally rotate) on the landing (ipsilateral) leg at 90 degrees and walk away from the stairway. The pivoting period was identified from initial foot contact with the ground of the ipsilateral leg, until touchdown of the contralateral leg. All subjects performed the activity with both legs. The dependent variable evaluated statistically was the maximum range of motion of the tibial rotation during the pivoting period. All patients were also assessed clinically and with the use of a KT-1000 to examine anterior tibial translation.

## RESULTS AND DISCUSSION

Negative Lachman and pivot-shift tests indicated that the knee joint stability was regained clinically for all ACL reconstructed subjects. For the ST/G reconstructed subjects, the median Lysholm score was 92 (range 87-95) and the Tegner score was 7 (range 6-8), while for the BPTB reconstructed subjects, the median Lysholm score was 94 (range 90-97) and the Tegner score was 8 (range 7-8). KT-1000 results

revealed that the mean difference between the anterior tibial translation of the reconstructed and intact sides in both groups was less than 2 mm.

The statistical analysis performed on the kinematic dependent variable, showed the existence of significant differences between the groups ( $p=0.001$ ). The post-hoc comparisons revealed that both ACL reconstructed groups had significantly increased tibial rotation when compared with the control, while no significant differences were observed within the two reconstructed groups. In other words, the intact knees for both reconstructed groups had similar values with the control.

Therefore, we found that neither graft is able to restore tibial rotation to normal levels during an in-vivo evaluation. This conclusion is supported by *in-vitro* findings from Woo et al [2002], who showed that even though the two grafts are successful in limiting anterior tibial translation, neither is effective in reducing tibial rotation. We believe that our findings are the result of the inability of current ACL reconstruction techniques to restore the actual anatomy of the ACL which is a two bundle ligament. Current techniques, using BPTB and ST/G grafts, anchored in one femoral and one tibial tunnel, seem to only partially achieve this goal. Our results may also provide an intriguing explanation regarding the development of future pathology in ACL reconstructed knees [Daniel et al, 1994; Asano et al, 2004]. It is possible that this increased tibial rotation could result in the application of loads at areas of the cartilage and are not commonly loaded in a healthy knee. Over time this could lead to knee osteoarthritis.

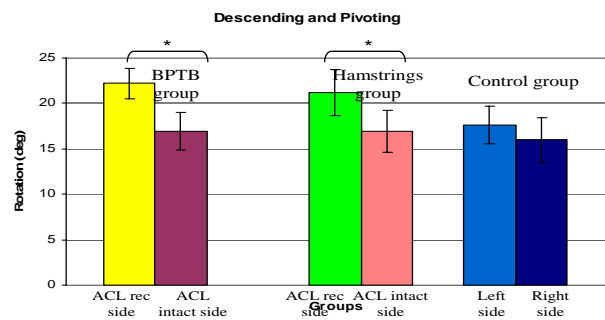


**Figure 1:** Bar graphs that indicate the group means and SD values for tibial rotation maximum range of motion during the pivoting period. (\*)  $p < 0.05$

## SUMMARY/CONCLUSIONS

The two most frequently used autografts for ACL reconstruction can not restore tibial rotation to normal levels during pivoting activities with the current surgical techniques. It is possible that this excessive tibial rotation is the cause of the degenerative changes in the knee joint, which have been noticed in long term follow-ups after ACL reconstruction. The improvement and development of new surgical techniques that can better approximate the actual anatomy and function of the ACL, may be able to provide a solution to this problem.

## ACKNOWLEDGEMENTS

Supported by the Greek Ministry of Sports.

## REFERENCES

- Woo, S.L., et al (2002). *J Bone Joint Surg*, 84A, 907-914.
- Daniel, D.M., et al (1994). *Am J Sports Med*, 22, 632-644.
- Asano, H., et al (2004). *Arthroscopy*, 20, 474-481.

# STRENGTH TRAINING ALTERS THE STRUCTURE OF FORCE FLUCTUATIONS DURING ISOMETRIC QUADRICEPS FEMORIS CONTRACTIONS IN OLDER ADULTS.

Samantha L. Winter and John H. Challis

Biomechanics Laboratory, Department of Kinesiology, The Pennsylvania State University,  
University Park, PA, USA.  
E-mail: slw294@psu.edu

## INTRODUCTION

When the resultant joint moment acting at a joint during an isometric contraction is measured it is not constant but rather it fluctuates (e.g., Lippold et al., 1957). These fluctuations limit the ability of an individual to maintain a desired force or to realize an intended limb trajectory (Harris and Wolpert, 1998). These fluctuations are increased in older adults (Tracy et al., 2004).

The size of the force or moment fluctuations has been quantified using the coefficient of variation (CV) of the force (e.g., Tracy et al., 2004). The time dependent structure of the fluctuations has been analysed using Approximate Entropy (ApEn) (e.g., Challis, 2006), which is a dimensionless measure varying between 0 (indicating a signal with high regularity such as a sine wave) and 2 (a signal with low regularity such as white noise) (Pincus, 1991). The Detrended Fluctuation Analysis (DFA) (Peng et al., 1994) has also been used to determine the fractal scaling index ( $\alpha$ ) of the force signal (e.g., Vaillancourt and Newell, 2003).

A previous study (Tracy et al., 2004) determined that there was no change in the magnitude of the fluctuations quantified using CV during isometric contractions following strength training in older adults. However, force signals produced during isometric contractions have been shown to have fractal scaling index above 0.5 (Vaillancourt and Newell, 2003), indicating

a non-normal distribution. The purpose of this study was to use a non-parametric equivalent of CV to confirm the lack of change in the magnitude of the fluctuations with strength training, and to analyse the time dependent structure of the force signal before and after training using ApEn.

## METHODS

Eight female subjects aged between 65 and 74 years were recruited following screening to ensure absence of obesity, cardiovascular, lung, neurological and musculo-skeletal disorders including osteoporosis. Subjects were familiarised with the procedures and provided written informed consent. The Institutional Review Board at The Pennsylvania State University approved all procedures. At the initial testing session, following a five minute cycle ergometer warm-up and practice contractions, subjects performed isometric knee extension contractions using the right leg at a 90 degree knee angle in a Biodex III dynamometer. Subjects performed three maximal voluntary isometric contractions with five minutes rest between each contraction. Subjects then performed contractions at each of the following levels: 75%, 50% and 25% of maximum, using visual feedback. The Biodex moment signal was sampled at 1600 Hz and low pass filtered at 20 Hz using LabVIEW 7.

Subjects underwent a supervised ten week whole body strength training programme

including: uni-lateral leg extension performed on both legs, bi-lateral leg press, uni-lateral leg curl performed on both legs and bi-lateral calf raises. After the training period the subjects were re-tested.

A 2.2 second window was selected from the joint moment records at each force level for analysis using a minimum variance criterion. The response variables (CV, fractal scaling index, and ApEn) were calculated for this window. A surrogate analysis of the data determined that the ApEn and DFA results were due to signal properties and not measurement system noise. Statistical comparisons were performed using a three way analysis of variance.

## RESULTS AND DISCUSSION

There was no significant change in CV with strength training. The DFA results gave values ranging from 0.9 to 1.7, and a significant increase in the fractal scaling index was seen with increasing force level for each subject ( $F=34.88$ ;  $d.f.=1,7$ ;  $p<0.001$ ). Values in this range reflect non-normal distributions, therefore a non-parametric equivalent to CV was used to confirm that there was little evidence of change in the magnitude of the fluctuations ( $F=2.60$ ;  $d.f.=1,7$ ;  $p=0.151$ ).

ApEn did change significantly with force level ( $F=32.11$ ;  $d.f.=3, 21$ ;  $p<0.001$ ), and following strength training ( $F=6.89$ ;  $d.f.=1,7$ ;  $p=0.034$ ). Post-hoc comparisons showed that the significant change with strength training seemed to be related to changes at the 50% and 75% force levels, though these just failed to be significant at a familywise alpha level of 0.05.

That the magnitude of the fluctuations does not change following strength training agrees with previous results for the

quadriceps (Tracy et al., 2004). However, the present results show that the ApEn value does change significantly such that it tends to increase with strength training, particularly at intermediate force levels.

## CONCLUSIONS

Use of a non-parametric equivalent to the coefficient of variation suggests that there is no change in the magnitude of force fluctuations with strength training of the quadriceps in older adults. However, strength training results in an increase in ApEn particularly at 50-75% of maximum isometric force. ApEn appears to decrease with age (Challis, 2006), possibly as a result of changes in motor unit characteristics such as innervation ratio. The present results indicate that the effects of ageing on force regularity are reversed by strength training.

## REFERENCES

- Challis, J. H. (2006). *J. Biomech.*, (in press).  
Harris, C. M., Wolpert, D. M. (1998). *Nature*, **394**, 725-726.  
Lippold, O. C. et al. (1957). *J. Physiol.*, **137**, 473-487.  
Peng, C-K. et al. (1994). *Phys. Rev. E.*, **49**, 1685-1689.  
Pincus, S. M. (1991). *Proc. Natl. Acad. Sci.*, **88**, 2297-2301.  
Tracy B. L., et al. (2004). *J. Appl. Physiol.*, **96**, 1530-1540.  
Vaillancourt, D. E., Newell, K. M. (2003) *J. Appl. Physiol.*, **94**, 903-912.

## ACKNOWLEDGEMENTS

This research was in part supported by grants from The Gerontology Center (PSU), The Whitaker Foundation, and the National Institute of Health Grants MO1-RR-10732 (GCRC).

# ROBOTIC SURGERY AND TRAINING: DOES AUGMENTED FEEDBACK HELP RETAIN PERFORMANCE?

Timothy N. Judkins<sup>1</sup>, Dmitry Oleynikov<sup>2</sup>, and Nick Stergiou<sup>1</sup>

<sup>1</sup> HPER Biomechanics Lab, University of Nebraska at Omaha, Omaha, NE, USA

<sup>2</sup> Dept of Surgery, University of Nebraska Medical Center, Omaha, NE, USA

E-mail: [tjudkins@gmail.com](mailto:tjudkins@gmail.com) Web: [www.unocoe.unomaha.edu/hper/bio/home.htm](http://www.unocoe.unomaha.edu/hper/bio/home.htm)

## INTRODUCTION

Laparoscopy, a form of minimally invasive surgery (MIS), has revolutionized the treatment of abdominal pathologies. The advent of robotic surgical systems, such as the da Vinci™ Surgical System (dVSS), have further improved MIS by adding three-dimensional viewing (D'Annibale, et al. 2004) and increasing dexterity (Moorthy, et al. 2004). However, it is necessary to train and evaluate surgeons on the usage of the robotic system (Judkins, et al. 2005). The current means of evaluating surgical performance, while using a robotic surgical system, are limited to task completion time and number of errors (Hubens, et al. 2003; Moorthy, et al. 2004) or subjective evaluations. Furthermore, no studies have attempted to provide additional feedback for training and retention of performance. This study seeks to determine how augmented visual feedback affects performance during training and a retention test with dVSS.

## METHODS

Thirty medical students performed with the dVSS three tasks that were designed to mimic actual laparoscopic surgical tasks: bimanual carrying (BC), needle passing (NP), and suture tying (ST). The subjects were randomly assigned to five feedback groups: speed (SP), grip force (GRIP), relative phase between left and right graspers (RP), video (VID) and control (CTRL). They performed 3 pre-training (PRE), 10 training with feedback, 3 post-

training (POST), and 5 retention (RET; 3 weeks later) trials. Prior to PRE, subjects were given verbal instruction on completing the task, but did not practice. SP, GRIP, and RP feedback were displayed real-time during training trials. It was overlaid on the visual display of the dVSS surgeon's console. The VID group watched video of experts performing each task, while the CTRL group received no feedback. Position and velocity of dVSS instruments, sampled at 75 Hz, were used to measure time to task completion (TTC), distance traveled (D), speed (S), path curvature ( $\kappa$ ), and grip force (F) for the left and right instruments. A 5 X 3 ANOVA was used to test for significant differences between conditions and groups.

## RESULTS AND DISCUSSION

Nearly all measures significantly improved when comparing POST and RET to PRE for all tasks (Table 1). While the condition comparisons showed that training improves performance and performance is retained after several weeks, interactions differentiated task-specific effects. For the BC task, TTC and right and left S showed significant interactions. For TTC, the SP group started with a larger TTC during PRE and decreased to the same level as other groups for POST and RET. For right and left S, the SP group started with a smaller S and increased to the same level as other groups for POST and RET. While interactions were found for the BC task, the effect was not significant since the level of performance during POST and RET was the same for all

groups. For the NP task, TTC, right and left D, left S, and right and left F had significant interactions. For TTC, the CTRL group started with a smaller TTC and decreased to the same level as other groups for POST and RET. For right and left D, the RP group did not significantly decrease POST training but decreased to the same level as other groups during RET. For left S, the SP group increased more than other groups for POST compared to PRE but was at the same level as other groups during RET. For right F, the GRIP group significantly decreased more than other groups for POST compared to PRE but returned to the same level as other groups during RET. For left F, the GRIP group significantly decreased POST training compared to PRE and remained at a lower level compared to other groups. While several interactions were found, the data shows that feedback can have an immediate effect POST training, but the benefit is not retained. For the ST task, only right F had a significant interaction. For the GRIP group, right F significantly decreased more than other groups for POST compared to PRE but returned to the same level as other groups during RET. The SP group had a significantly smaller left F for POST compared to PRE and the even smaller F during RET. Similar to the NP task, it appears that the benefits of feedback are not retained even though they are beneficial immediately following training. Secondly, the continued decrease in F for the SP groups during POST and RET shows that a plateau in learning was not reached. More

training trials are necessary to determine if this trend continues.

## SUMMARY/CONCLUSIONS

Real-time augmented visual feedback was found to be beneficial for robotic surgery immediately following training with feedback provided. However, the benefits of feedback do not appear to be retained over a period of time. Further investigation is needed to determine if a longer training regimen with feedback will actually improve retention of skills. GRIP feedback showed the best POST results and may have the greatest potential for improving grip force. This feedback can reduce tissue injury by making the surgeon more aware of the force applied to delicate tissues.

## REFERENCES

- D'Annibale, A.M.D., et al. (2004) *Surg Laparosc Endosc Percutan Tech.* **14**, 38-41.
- Hubens, G., et al. (2003) *Surg Endosc.* **17**, 1595-9.
- Judkins, T.N., et al. (2005) *Stud Health Technol Inform.* **119**, 243-248.
- Moorthy, K., et al. (2004) *Surg Endosc.* **18**, 790-795.

## ACKNOWLEDGEMENTS

Support was provided by the Nebraska Research Initiative.

**Table 1: Pair-wise comparisons of condition for all dependent variables and tasks.**

Task	Comparison	TTC	Right D	Left D	Right S	Left S	Right κ	Left κ	Right F	Left F
BC	PRE-POST	15.4 *	16.1	38.5	-8.5 *	-8.6 *	0.412 *	0.249 *	0.047 *	0.041 *
	PRE-RET	17.6 *	22.1	55.1 *	-10.8 *	-10.8 *	0.439 *	0.243 *	0.047 *	0.068 *
	POST-RET	2.2 *	6.0	16.6	-2.3 *	-2.1 *	0.027	-0.006	-0.001	0.027 *
NP	PRE-POST	47.8 *	319.1 *	194.7 *	-3.4 *	-4.1 *	0.448 *	1.490 *	0.030 *	0.013
	PRE-RET	51.9 *	364.7 *	232.8 *	-3.7 *	-4.3 *	0.398 *	1.501 *	0.033 *	0.022
	POST-RET	4.1 *	45.5	38.1	-0.3	-0.2	-0.051	0.010	0.002	0.009
ST	PRE-POST	58.9 *	389.1 *	391.7 *	-6.8 *	-5.3 *	0.672 *	1.082 *	0.049 *	0.059 *
	PRE-RET	57.5 *	349.3 *	353.5 *	-7.0 *	-5.3 *	0.604 *	0.984 *	0.039 *	0.057 *
	POST-RET	-1.4	-39.5	-38.1	-0.1	-0.02	-0.068	-0.098	-0.009	-0.002

\* indicates a significant difference at the  $p=0.05$  level. All values reported are mean differences between the indicated conditions.

# KINETIC REDUNDANCY ON HAND DIGIT CONTROL IN CHILDREN WITH DCD

Marcio A. Oliveira<sup>1</sup>; Jefferson F. Loss<sup>2</sup>; Ricardo D. S. Petersen<sup>2</sup>; Jane E. Clark<sup>1</sup>; Jae Kun Shim<sup>1</sup>

<sup>1</sup> University of Maryland, College Park, MD, USA

<sup>2</sup> Federal University of Rio Grande do Sul, Porto Alegre, RS, Brazil

E-mail: marcio@umd.edu Web: www.hhp.umd.edu/KNES/faculty/jkshim/neuromechanics

## INTRODUCTION

Motor redundancy in manipulative tasks has been extensively investigated in adults (Zatsiorsky, et al. 2002; Shim, et al. 2004). However, far less attention has been drawn to children, especially, children with motor difficulties such as those with Developmental Coordination Disorder (DCD). Children with DCD have particular impairments in manipulation tasks which affect everyday and school activities such as eating, drinking, writing, drawing, etc.

It has been known that typically developing children increase their finger strength and capability to control finger forces as they grow up (Smits-Engelsman, et al. 2003; Potter, et al. 2006). Previous studies have also shown that children with DCD experience higher variability in controlling isometric finger force (Lundy-Ekman, et al. 1991; Pereira, et al. 2001). However, we know little about how typically developing children and children with DCD regulate force when multiple fingers are involved in a motor task (i.e., motor redundancy).

This study systematically investigates the age-related changes of finger strength and finger force or torque control in typically developing children and children with DCD using motor tasks with different kinetic redundancies.

## METHODS

Forty-eight typically developing children aged 7 ( $7.6 \pm 0.5$  yrs), 9 ( $9.6 \pm 0.3$  yrs), and 11 ( $11.4 \pm 0.6$  yrs) participated in this study: 15 children for each age. Sixteen nine-year-old children with DCD ( $9.6 \pm 0.2$  yrs) also participated in the experiments. All of the subjects were right-handed. All children with DCD had Movement Assessment Battery for Children (MABC) (Henderson and Sugden 1992) scores below the 5<sup>th</sup> percentile – a standard cut-off point for this disorder. All typically developing children had MABC scores above the 35<sup>th</sup> percentile.

Three different experimental settings were used for three isometric force/torque production tasks with different numbers of kinetic redundancy (KR): constant index finger pressing force (KR=0) production, constant thumb-index finger pinching force production (KR=1), and constant thumb-index finger torque production (KR=5). Subjects were asked to perform two main tasks: maximum voluntary force/torque production (*MVC*) and constant isometric force/torque production at 40% of their *MVC* for 20 s (*CONST*).

A fixed horizontal line was displayed on the oscilloscope screen indicating the target force/torque. Another moving horizontal line indicating the force/torque produced by a subject was shown on the same screen as online feedback. Each trial started with a “get ready” signal, and the subjects were instructed to match the line showing the force or torque produced to the target force or torque. For *MVC* tasks, the instant peak

force/torque was selected as the maximum force/torque. From *CONST* tasks, coefficient of variation (CV = standard deviation/mean) was computed over the last 15s as an index of force or torque variability.

## RESULTS

In typically developing children, both *MVC* force and torque all increased with age in typically developing children while CV during constant force and torque production decreased with age.

There was no significant difference between the 9-year old DCD group and their age-matched control group in *MVC* force or torque. In general, 9-year-old children with DCD, as compared to 9-year-old typically developing children, showed larger variability during constant force and torque production tasks (Figure 1). The difference in variability between these two groups was the largest during the torque production task while no significant differences were found for the press and pinch tasks. We also calculated the developmental delays in children with DCD as compared to their typically developing cohorts. The constant torque task showed the largest developmental delay (1.7 yrs) while pressing and pinching force tasks showed relatively small delays (1.0 and 1.1 yrs, respectively).

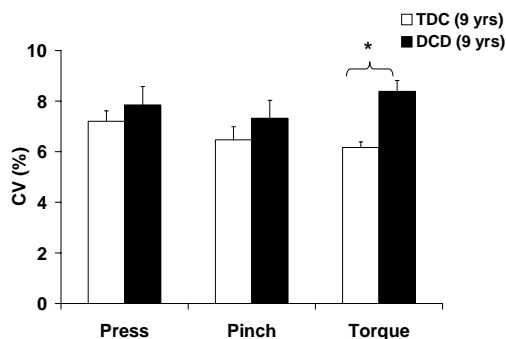


**Figure 1** – Coefficients of variation (CV) for 9-year-old typically developing children (TDC) and 9-year-old children with DCD (DCD) during constant press, pinch and torque tasks. \*  $p < .05$ .

## DISCUSSION AND CONCLUSION

The results from *MVC* tasks compliment the previous studies that showed increases in the maximum force production capability and variability of isometric force with children's age. The unique finding of this study is the large difference in torque variability between typically developing children and children with DCD. This finding may suggest that children with DCD have deficits in controlling movements with a large number of degrees of freedom.

We intentionally used similar tasks with different numbers of kinetic degrees of freedom. However, we should also recognize that the tasks employed were functionally different (i.e., pressing and rotating). Another experiment with a same task involving different numbers of effectors (e.g., same pressing task with different numbers of fingers involved) may strengthen our claim.

## REFERENCES

- Henderson, S. E. and D. A. Sugden (1992). London, The Psychological Corporation.
- Lundy-Ekman, L., R. Ivry, et al. (1991). *Cog. Neuroscience* 3: 367-376.
- Pereira, H. S., M. Landgren, et al. (2001). *Neuropsychologia* 39(5): 478-88.
- Potter, N. L., R. D. Kent, et al. (2006). *Exp Brain Res*: 1-15.
- Shim, J. K., M. L. Latash, et al. (2004). *Exp Brain Res* 157(4): 457-67.
- Smits-Engelsman, B. C., Y. Westenberg, et al. (2003). *Brain Res Cogn Brain Res* 17(1): 68-74.
- Zatsiorsky, V. M., R. W. Gregory, et al. (2002). *Biol Cybern* 87(1): 40-9.

## ACKNOWLEDGEMENTS

NIH grant R01HD42527 to J.E. Clark

# REGIONAL MOTION PATTERNS OF THE HUMAN BRAIN DUE TO IMPACT

Hong Zou<sup>1</sup>, James P. Schmiedeler<sup>1</sup> and Warren N. Hardy<sup>2</sup>

<sup>1</sup> The Ohio State University, Columbus, OH, USA

<sup>2</sup> The Wayne State University, Detroit, MI, USA

E-mail: zou.26@osu.edu

## INTRODUCTION

Relative brain motion with respect to the skull due to impact is recognized as a main cause of brain injuries such as diffuse axonal injury, contusion, and acute subdural hematoma. Although they have been studied for decades, the brain motion patterns are not yet thoroughly understood.

Zou et al. (2006) found that the whole brain follows closely a rigid body displacement under mild impact. As the impact becomes more severe, brain deformation represents an increasing portion of the total brain motion. They concluded that the rigid body displacement of the whole brain is 4-5 mm in translation and  $\pm 5$  deg in rotation under low-severity impact in the sagittal plane.

This study analyzes the experimental data in both the sagittal and coronal planes to identify the regional brain motion patterns, which consist of rigid body displacement and local deformation.

## METHODS

With a high-speed x-ray system tracking neutral density targets (NDTs), Hardy et al. (2001) found that the relative displacement of the brain with respect to the skull has a magnitude of  $\pm 5$  mm under low-severity impacts. The NDTs were implanted in two columns, anterior and posterior, located in the temporoparietal region and in the occipitoparietal region. A total of six tests were performed using two specimens, C755 and C383. Among these tests, three

accelerating impacts were conducted on C755 and three decelerating impacts on C383 in either the frontal or the occipital area for both specimens. The impacts on C383 were more severe in terms of the HIC values and maximum resultant accelerations.

The NDTs at the initial positions before impact are transformed as a rigid body into new positions, called transformed positions, to match the measured NDT positions as close as possible at each time step. The matching is determined by the total squared error between the measured and transformed positions. The difference between these two is the brain deformation for each NDT.

Expressed as a vector in Figure 1, circle  $R_i$  and star  $S_i$  are the initial and measured position of the  $i$ th NDT, respectively. The gray dots  $S_i^*$  are obtained by transforming  $R_i$  as a rigid body through a distance  $d$  and an angle  $\theta$ , so  $S_i^* = AR_i + d$ , where  $A$  is the  $2 \times 2$  transformation matrix. The values  $d$  and  $\theta$  are to be found such that the total squared error  $E_n = \sum_{i=1}^n |S_i^* - S_i|^2$  is minimal, when  $\partial E_n / \partial d = 0$  and  $\partial E_n / \partial \theta = 0$ . It yields,

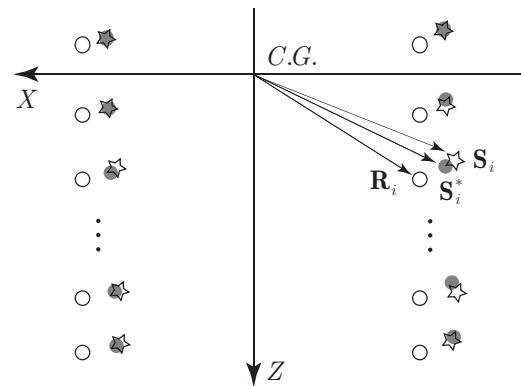


Figure 1: Schematic of NDT positions.

$$\mathbf{d} = \frac{1}{n}(\mathbf{S}_\Sigma - A\mathbf{R}_\Sigma),$$

$$\theta = \tan^{-1} \left( \frac{\frac{1}{n}\mathbf{S}_\Sigma \times \mathbf{R}_\Sigma - \sum(\mathbf{S}_i \times \mathbf{R}_i)}{\sum(\mathbf{S}_i \cdot \mathbf{R}_i) - \frac{1}{n}\mathbf{S}_\Sigma \cdot \mathbf{R}_\Sigma} \right),$$

where  $A\mathbf{R}_\Sigma = \sum A\mathbf{R}_i = A\sum \mathbf{R}_i$ , and  $\mathbf{S}_\Sigma = \sum \mathbf{S}_i$ .

## RESULTS AND DISCUSSION

The brain motion patterns in the sagittal plane in the anterior and posterior columns for test C383-T4 are shown in Figures 2 and 3, respectively. The subfigure on the left contains the measured brain motion, and the one in the middle contains the brain displacement generated using rigid body translation and rotation. The difference between these two at each NDT location is a measure of brain deformation, as shown in the subfigure on the right. For all of the six tests, the measured brain motion, whose magnitude generally varies within  $\pm 5 \text{ mm}$ , and rigid body brain displacement generally coincide in terms of both direction and magnitude for each NDT in both the anterior and posterior columns, where the brain deformation is therefore small, about only  $0.5\text{-}1.5 \text{ mm}$ . Similar patterns are obtained in the coronal plane with smaller magnitudes.

Compared with the whole brain in the previous study (Zou et al., 2006), each individual column in tests on C755 has almost the same rigid body displacement, which has about  $4\text{-}5 \text{ mm}$  in translation and  $\pm 5 \text{ deg}$  in rotation. As the impact becomes more severe on C383, each column still follows closely a rigid body displacement. However, the anterior column maximally translates about  $9.0 \text{ mm}$  along the x-axis,  $5.3 \text{ mm}$  along the z-axis, and rotates  $13.0 \text{ deg}$  about the y-axis, while these values for the posterior column are about  $10.2 \text{ mm}$ ,  $8.4 \text{ mm}$ , and  $14.0 \text{ deg}$ , respectively. Thus, relative motion and therefore brain deformation exist in the region between these two columns in tests on C383.

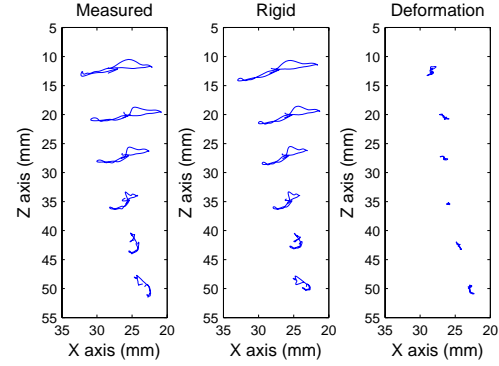


**Figure 2:** Brain motion pattern of anterior column in the sagittal plane in test C383-T4.

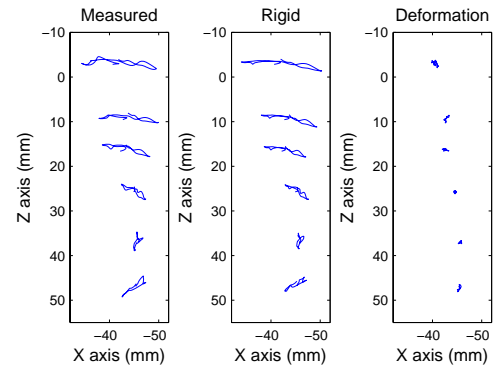


**Figure 3:** Brain motion pattern of posterior column in the sagittal plane in test C383-T4.

## CONCLUSIONS

Similar to the whole brain, the two columns, representing the temporoparietal region and occipitoparietal region, individually follow closely a rigid body displacement in both the sagittal and coronal planes under mild impact. As the impact becomes more severe, each column still follows closely a rigid body displacement, which has a magnitude of  $9\text{-}10 \text{ mm}$  in translation and  $12\text{-}14 \text{ deg}$  in rotation. However, relative motion becomes larger between these two columns, introducing strain deformation.

## REFERENCES

- Zou, H. et al. (2006). *J. Biomech*, submitted.  
 Hardy, W.N. et al. (2001). *Stapp Car Crash Journal*, **45**, 337-368.

# THE EFFECTS OF LOCAL MUSCLE FATIGUE ON SHOCK ATTENUATION FOR FEMALE RUNNERS

Kaori Teramoto, Janet S. Dufek, and John A. Mercer

University of Nevada, Las Vegas, NV, USA

E-mail: [jdufek@unlv.nevada.edu](mailto:jdufek@unlv.nevada.edu) Web: <http://kinesiology.unlv.edu>

## INTRODUCTION

Running is a popular activity for many people to include in their daily exercise since it is a convenient activity and can induce physiological stress to increase general fitness. Unfortunately, many runners experience of running-related injuries in their lower extremities especially overuse injuries (James et al., 1978). Though the exact mechanism of overuse running injuries is not fully understood, this type of injury occurs when runners undergo repetitive forces, which may cause fatigue effects beyond the capabilities of a specific biological structure, and lead to microtrauma in the musculoskeletal system (Messier et al., 1991). One hypothesis addressing overuse running injuries is that muscle fatigue is associated with injury since muscle dissipates the stress on bones by eccentric contraction (Hill, 1962; Nordin et al., 2001). However, it is still unclear how the capability of the system to attenuate impact forces during running is influenced by local muscle fatigue.

In this study, we quantified and examined one biomechanical measure, shock attenuation (SA) which is a parameter used to understand how the impact initiated with foot strike is reduced through the body (Mercer, et al., 2002). The purpose of this study was to examine the effects of local muscle fatigue on SA characteristics for female runners. It was hypothesized that SA would differ between non-fatigued and fatigued ankle dorsiflexor conditions.

## METHODS

Twelve females ( $24.8 \pm 4.5$  yrs;  $64.6 \pm 7.1$ kg;  $163.3 \pm 4.2$  cm) granted consent to participate in accordance with compliance procedures established at the affiliated university and completed treadmill runs at the same (preferred) speed prior to and following a fatigue protocol. Each subject was first securely instrumented with two light-weight uni-axial accelerometers (1000Hz), mounted on the distal aspect of the tibia and the forehead. An initial non-fatigued treadmill run was then completed.

The fatigue protocol was designed to fatigue a local muscle group bilaterally (ankle dorsiflexors). Using a commercial exercise device (DARD®), five sets of maximal concentric and eccentric contractions with 15 s rest between sets were completed. Within a set, repetitions were continued until the ankle range of motion decreased or subjects could not keep up with the rhythm of the metronome (60 bpm).

Following completion of the fatigue protocol, subjects transferred to the treadmill as quickly as possible (within 10 s) and performed a second one-minute run while accelerometer data were obtained.

Head peak acceleration (HdPk) and leg peak acceleration (LgPk; Figures 1 and 2) over 10 consecutive strides per subject-condition were selected and used to quantify SA. SA was calculated as:

$$SA = (1 - HdPk / LgPk) * 100$$

Dependent variables (HdPk, LgPk, SA) were analyzed independently using paired *t*-tests with the level of significance set at 0.05.

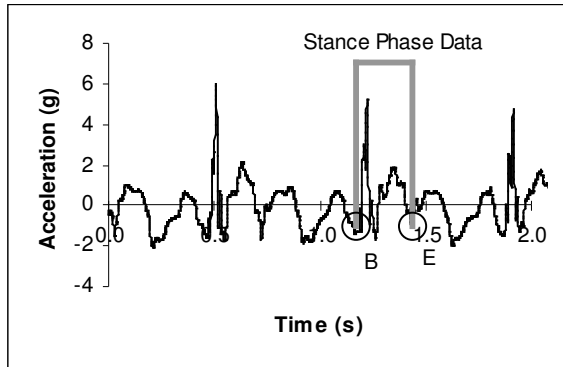


**Figure 1:** Exemplar leg acceleration time history during running.

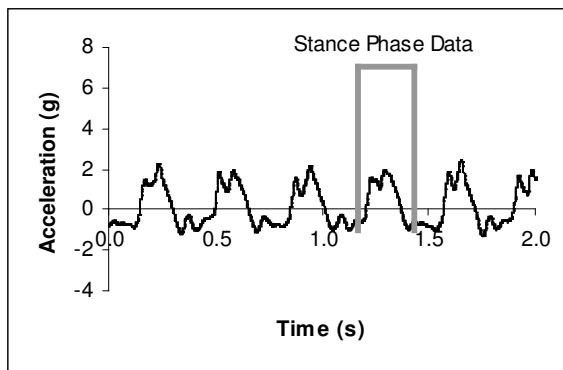


**Figure 2:** Exemplar head acceleration time history during running.

## RESULTS AND DISCUSSION

**Table 1:** Changes in HdPk, LgPk and SA measures with the dorsiflexor fatigue (mean  $\pm$  SD). (\* $p < 0.05$ )

	Non-fatigued	Fatigued
HdPk (g)	1.12 $\pm$ 0.33	1.47 $\pm$ 0.86
LgPk (g)	3.96 $\pm$ 0.78	4.95 $\pm$ 0.47*
SA (%)	71.84 $\pm$ 6.99	75.59 $\pm$ 7.60*

SA and LgPk (75.59% and 4.95g, respectively) were significantly greater following the fatigue protocol ( $p < 0.05$ ; Table 1), while HdPk (1.47g) exhibited no significant difference (Table 1). Results indicated that the impact acceleration

experienced at the leg level increased as well as the impact attenuation through the body (SA) when runners' ankle dorsiflexors were fatigued. These findings suggest that local muscle fatigue contributes to the incapability of the musculoskeletal system to maintain the impact acceleration at the leg segment level. Eight subjects showed increases in SA, while all twelve subjects exhibited increases in LgPk following the fatigue protocol. Increased LgPk may be due to the role that the dorsiflexors play to attenuate impact at the leg. The increased SA following fatigue suggests that runners' systems adjusted to compensate for local fatigue. A possible explanation for increased SA may be that runners modified kinematics between conditions. Further research into the effects of muscle fatigue on running mechanics may lend insight into injuries during running.

## CONCLUSIONS

Results suggest that SA and LgPk were sensitive to local muscle fatigue, with more shock being attenuated through body along with increased LgPk during fatigued running.

## REFERENCES

- Hill, D.B. (1962). *Science*, **131**, 897-903.  
 James, S., et al. (1978). *Am. Orth. Soc. Spts. Med*, **6**, 40-50.  
 Mercer, J.A., et al. (2002). *Eur. Jrl. Appl. Phys.*, **87**, 403-408.  
 Messier, S., et al. (1991). *M.S.S.E.*, **23**, 1008- 1015.  
 Nordin, M., Frankel, V. (2001). *Basic Biomechanics of the Musculoskeletal System*. Lea and Febiger.

## ACKNOWLEDGEMENTS

Partially funded by the Graduate & Professional Student Association, University of Nevada, Las Vegas.

# **bilateral strength and activation characteristics of quadriceps in experienced soccer players: implications on return to play criteria**

John W. Chow, Dana M. Otzel, and Mark D. Tillman

Department of Applied Physiology & Kinesiology, University of Florida, Gainesville, FL, USA  
E-mail: jchow@hhp.ufl.edu Web: www.hhp.ufl.edu/apk/ces/labs/biomech/

## **INTRODUCTION**

Clinicians often use isokinetic strength exercises in the rehabilitation of lower extremity injuries and the resulting test scores are often used as criterion to determine the progression within a rehabilitation protocol as well as the suitability of the patient to return to sport participation. For example, Shelbourne et al. (1995) suggested that once the anterior cruciate ligament (ACL) reconstructed extremity achieves 70% of the strength of the uninjured leg, the patient is allowed to engage in sport-specific activities and begin the progression toward competitive participation. A criterion like this would be a valid standard assuming no strength differences exist between limbs prior to injury. Few bilateral differences in lower extremity strength exist in most sedentary individuals or athletes participating in bilaterally symmetrical lower extremity activities. However, soccer players usually have tendencies to use one leg more than the other for dribbling, shooting and performing long kicks. As a result, soccer can be characterized as an asymmetrical lower extremity activity. If bilateral strength differences exist, then appropriate adjustments should be made for return to activity standards. This study examined whether differences existed in isokinetic knee flexion and extension strength and voluntary activation of the quadriceps between the dominant and non-dominant legs in experienced soccer players.

## **METHODS**

Eleven female (age  $20.7 \pm 0.9$  yrs, height  $164.2 \pm 4.5$  cm, weight  $626 \pm 83$  N,  $7.1 \pm 3.3$  yrs competitive soccer experience) and 15 male ( $21.7 \pm 1.1$  yrs,  $171.5 \pm 10.9$  cm,  $724 \pm 130$  N,  $6.7 \pm 3.6$  yrs) soccer players were tested. Bilateral knee flexion and extension torques were assessed using a KinCom isokinetic dynamometer at speeds of 60 and 180 °/s in a seated position. After a warm up, the subject performed 2 trials of 3 reciprocal extension/flexion repetitions with maximum efforts for each isokinetic speed (3-minute rest period between trials).

Motor unit activation of the quadriceps was evaluated by delivering interpolated supramaximal tetanus twitches to the quadriceps while the subject performed an isometric knee extension at 90° of knee flexion with maximum effort on a KinCom AP125 dynamometer (Stevens et al., 2001). A Grass S48 stimulator was used to deliver a train of electrical impulses (12 spikes, 0.01 s apart, 1/15000 s duration for each spike). The ratio of the force exerted by the subject leading up to the electrical stimulation to the peak force after the stimulation (central activation ratio, CAR) was used to determine the efficiency of the subject in recruiting available motor units. Two CAR trials were completed for each leg.

For each subject, the highest extension and flexion torques for each speed and CAR value for each leg were used in subsequent analyses. The dominant leg was defined as the leg that is often used for dribbling, shooting and performing long kicks (self-

reported). CAR data were analyzed using a 2 x 2 (gender x side) repeated measures ANOVA ( $\alpha = 0.05$ ). Flexion and extension peak torques were submitted to a 2 x 2 x 2 (gender x speed x side) MANOVA with repeated measures in the last 2 factors to test for significant differences between males and females, the dominant and non-dominant legs, and the 2 speeds ( $\alpha = 0.05$ ).

## RESULTS AND DISCUSSION

The MANOVA revealed significant main effects for the gender ( $p = 0.044$ ), speed ( $p < 0.001$ ), and side ( $p = 0.050$ ). As expected, males had significantly greater strength than females and peak torques at 60 °/s were significantly greater than those at 180 °/s. Univariate tests indicated a significant difference between dominant and non-dominant legs only in peak extension torques ( $p = 0.015$ ), but not in peak flexion torques ( $p = 0.314$ ). On average, peak knee extension torques for the dominant leg were 6% and 4% greater than the corresponding values for the non-dominant leg for the 60 and 180 °/s speeds, respectively (Table 1). In other words, isokinetic knee extension strength of the non-dominant leg is about 95% of the dominant leg.

No significant main effects were detected by the ANOVA suggesting that the bilateral difference in knee extension strength is not related to the voluntary activation of the quadriceps. The results suggest that the return to play criteria should be slightly

different for dominant and non-dominant legs in experienced soccer players. We proposed that, as a conservative approach, 74 and 67% of contralateral knee extension strength should be used for the dominant and non-dominant legs, respectively.

Future studies should examine whether differences existed in isokinetic knee flexion and extension strength between the dominant and non-dominant legs in elite soccer players. Investigators should explore additional strength parameters such as eccentric strength and muscular endurance as return to play criteria.

## SUMMARY/CONCLUSIONS

Small but significant bilateral differences in knee extension strength were observed in experienced soccer players. To determine the optimal return to player criteria for individual soccer players, pre-season strength evaluation is highly recommended.

## REFERENCES

- Shelbourne, K.D. et al. (1995). In L.Y. Griffin (ed.), *Rehabilitation of the Injured Knee* (pp. 149-163), St. Louis: Mosby Year-Book, Inc.
- Stevens, J.E. et al. (2001). *Arch. Phys. Med. Rehabil.*, 82, 973-978.

## ACKNOWLEDGEMENTS

We appreciate the assistance of Stacy Colon.

**Table 1:** Mean (SD) peak knee extension and flexion torques (Nm) and CAR values (%).

	Extension				Flexion				CAR	
	60 °/s		180 °/s		60 °/s		180 °/s		D	N
	D	ND	D	ND	D	ND	D	ND		
Females	129.3 (34.8)	122.1 (26.5)	92.8 (26.2)	91.0 (27.5)	88.0 (26.9)	82.0 (28.1)	74.7 (19.7)	74.5 (25.6)	99.3 (2.4)	99.0 (2.8)
Males	154.7 (35.5)	145.6 (38.1)	134.1 (40.2)	128.2 (34.4)	106.2 (29.4)	104.7 (28.5)	101.1 (28.2)	98.0 (22.7)	99.3 (1.1)	99.5 (1.2)

# EMG SIGNAL AMPLITUDE DIFFERENCES DURING MAXIMAL ISOMETRIC AND ISOKINETIC ACTIVITY

Nicole J. Chimera<sup>1</sup>, Daniel L. Benoit<sup>1</sup>, and Kurt Manal<sup>1</sup>

<sup>1</sup>Center for Biomedical Engineering Research,  
University of Delaware, Newark, DE USA  
E-mail: chimera@udel.edu

## INTRODUCTION

The use of maximal voluntary isometric contractions (MVICs) for the purpose of electromyographic (EMG) data normalization is a well accepted practice within exercise and sport science literature. Benoit et al. (2003) reported that treadmill walking in ACL injured subjects elicited normalized medial gastrocnemius surface EMG values of 160% MVIC, indicating muscular activation during dynamic activity generates higher peak EMG values than MVICs. Further, Arsenault et al. (1986) demonstrated normalized soleus EMG values during sub-maximal walking trials of up to 120% MVIC. This peak soleus muscle activity occurred at approximately two-thirds of the stance phase of gait, where ankle plantar flexion velocity is estimated to be 30°/second.

Few authors have proposed explanations for sub-maximal dynamic tasks eliciting greater activation than maximal isometric contractions. Mirka (1991) states that MVC normalization leads to large errors due to movement of the sampled muscle relative to the reference EMG electrodes. The purpose of this preliminary study was to investigate this previously proposed explanation for the large increases in surface EMG muscle

activation observed in dynamic versus static activities.

## METHODS

EMG activity of the soleus muscle was recorded using surface and fine-wire bipolar electrodes while the subject performed multiple trials of isolated isokinetic (30°/second) maximal plantar flexion on a Biodex-3 System. From a starting position of maximal dorsiflexion with 90° knee flexion, the subject extended to maximal plantar flexion. Repeated plantar flexion MVIC trials were also performed on the Biodex at 15° of dorsiflexion and 90° knee flexion. The EMG signal was full-wave rectified and low pass filtered using a 4<sup>th</sup> order Butterworth digital filter with a cut-off frequency of 6 Hz. Dynamic trial EMG data was normalized to the maximal activation recorded during the isometric plantar flexion contraction using the surface or fine-wire EMG signal respectively.

## RESULTS AND DISCUSSION

Results indicated that there is no difference in detection of soleus muscle activation onset regardless of the type of EMG electrode used for recording. Peak normalized surface EMG during the

dynamic trial was at least 20% greater than that obtained during MVIC. However, this increase was only 6% using data from the fine-wire electrodes. While the peak occurred at approximately the same joint angle for both the surface and fine-wire electrodes (Figure 1), this angle differed from the joint position of the isometric trial. This may indicate that we were unable to elicit a maximal contraction at the prescribed angle of isometric contraction.

Potvin & Bent (1997) suggested movement of muscle fibers relative to surface electrodes as a possible explanation for their increased EMG signals recorded during dynamic tasks. Our data suggests that this may contribute to the higher activity recorded during dynamic contractions since the peak EMG from our dynamic trial occurred at a different joint position as compared to the isometric trial.

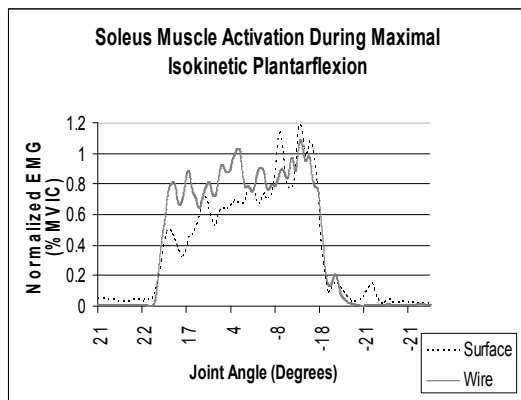


**Figure 1:** Graph illustrates the difference between recording with fine wire and surface electrodes in normalized EMG muscle activation during isokinetic plantar flexion at 30°/s.

Therefore, during the dynamic trial the electrodes may not have been recording from the same muscle fiber region.

Furthermore, the smaller change in activation level recorded using the fine-wire electrodes, which should be recording from the same muscle fiber region during dynamic and isometric contractions, indicates that this difference may not be a physiological issue but rather a methodological one.

## SUMMARY/CONCLUSIONS

In this investigation we find that onset of activation is nearly identical when recording from either surface or fine-wire electrodes; however two different normalized peak amplitudes were recorded from surface compared to fine-wire electrodes. In addition, we may not be able to elicit true maximal activation at one specific joint angle as compared to that elicited throughout the joint's total range of motion.

## REFERENCES

- Arsenault, A.B. et al. (1986). Is there a 'normal' profile of EMG activity in gait? *Med & Biol Eng & Compt* **24**:337-343.
- Benoit, D.L. et al. (2003). The clinical significance of electromyography normalization techniques in subjects with anterior cruciate ligament injury during treadmill walking. *Gait Posture* **18**:56-63.
- Mirka, G.A. (1991). The quantification of EMG normalization error. *Ergonomics* **34(3)**:343-352.
- Potvin, J.R., Bent, L.R. (1997). A validation of techniques using surface EMG signals from dynamic contractions to quantify muscle fatigue during repetitive tasks. *J Electromyogr Kinesiol* **7(2)**:131-139.



# BETWEEN- AND WITHIN-HAND SYNERGIES DURING TWO-HAND FORCE PRODUCTION TASKS

Stacey Gorniak, Vladimir M. Zatsiorsky, Mark L. Latash

Pennsylvania State University  
Department of Kinesiology, Motor Control Laboratory and Laboratory of Biomechanics  
E-mail: mll11@psu.edu

## INTRODUCTION

Several papers have reported multi-finger synergies stabilizing the total force produced by the fingers of a hand during accurate force production tasks (Latash et al. 2002; Shim et al. 2005). In those studies, synergies were defined as co-variations among finger forces across trials that reduced the variability of the total force. One study has shown, however, that a two-hand multi-finger task involving unusual finger combinations was not accompanied by within-a-hand force stabilizing synergies (Kang et al. 2004). In this study, we tested a hypothesis that the central nervous system is limited in its ability to organize within-a-hand multi-finger synergies during two-hand tasks while such synergies are present in comparable one-hand multi-finger tasks.

## METHODS

Subjects (four males and four females) sat in a chair with both arms resting directly on the table in front of them in the prone position. Each forearm was constrained using Velcro straps. A small wooden dome was placed under each hand to assure its stable shape. Eight piezoelectric force sensors measured vertical finger forces.

First, the subjects produced maximal voluntary contractions (MVCs) with pairs of fingers:  $IM_R$ ,  $IM_L$ ,  $RL_R$ , &  $RL_L$  (I=index, M=middle, R=ring, L=little, the subscripts indicate the hand). These MVCs were used to set the magnitude of the trapezoid template for the main experiment.

The main task required subjects to produce force by an instructed set of fingers in order to match a trapezoid template. A 5% MVC baseline was used as a target for before and after the trapezoid. The maximum force was set at 20% of the MVC for the instructed finger set. The duration of the ramps was 1.5 s. The instructed finger sets were  $IM_{RL_R}$ ,  $IM_{RL_L}$ ,  $IM_R$ ,  $IM_L$ ,  $RL_R$ ,  $RL_L$ ,  $IM_R+IM_L$ ,  $IM_R+RL_L$ ,  $RL_R+IM_L$ , and  $RL_R+RL_L$ .

For each point in time the following variables were calculated: total force of instructed fingers ( $F_{TOT}$ ) and its variance ( $V_{TOT}$ ), forces of individual instructed fingers ( $F_i$ ), their variances ( $V_{F_i}$ ), the sum of their variances ( $\sum V_{F_i}$ ) and an index of co-variation ( $\Delta V = (\sum V_{F_i} - V_{TOT}) / \sum V_{F_i}$ );  $\Delta V$  was calculated with respect to 4 fingers (for 4 finger tasks), with respect to 2 separate hands (for 2 hand tasks), and with respect to fingers on one hand.

## RESULTS

During both two-finger and four-finger one-hand tasks, subjects showed predominantly negative co-variation among finger forces across trials that led to much smaller variance of the total force than the sum of the variances of individual finger forces (Fig. 1). This was particularly prominent during steady-state phases with high positive values of the index of co-variation,  $\Delta V$ ;  $\Delta V$  dropped during the ramp phases (Fig. 2).

In contrast, during two-hand tasks, indices of finger force co-variation computed for pairs of fingers within-a-hand were close to zero; these indices were significantly positive when computed for co-variation of forces across all four fingers and when computed for co-variation of forces produced by the two hands (Fig. 3). The differences between  $\Delta V$  indices computed for finger pairs in one- and two-hand tasks were statistically significant ( $p < 0.01$ ). These differences were also significant across the five intervals of the task, the three steady-state portions and the two ramps ( $p < 0.001$ ). The interaction between task and interval was also significant ( $p < 0.05$ ).

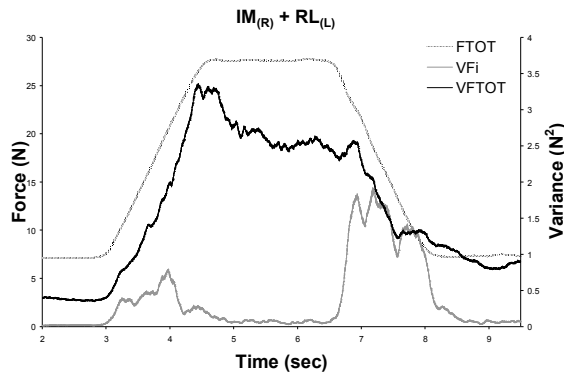


**Figure 1:** A typical force profile ( $F_{TOT}$ ), variance of total force ( $V_{FTOT}$ ), and the sum of individual finger variances ( $\sum V_{Fi}$ ) for one subject in the finger combination of  $IM_{(R)} + RL_{(L)}$ .

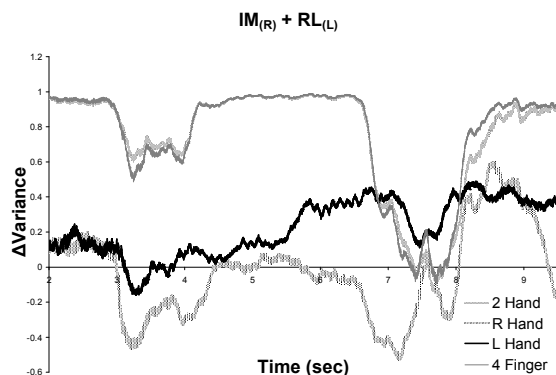


**Figure 2:** Typical  $\Delta V$  time profiles for a representative subject who performed the  $IM_R+RL_L$  task.

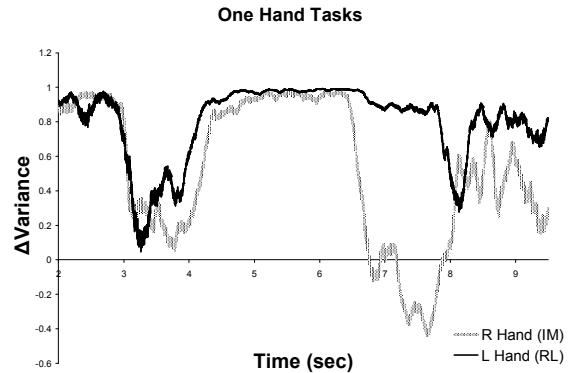


**Figure 3:** Typical  $\Delta V$  time profiles for a representative subject who performed the  $IM_R$  and the  $RL_L$  tasks.

## DISCUSSION AND CONCLUSIONS

High positive  $\Delta V$  indices may be interpreted as a force stabilizing synergy (Shim et al. 2005). The results show that in both one- and two-hand tasks, all fingers taken together formed a synergy. However, in two-hand tasks, the within-a-hand synergy was lost. This may indicate a limitation in the ability of the central nervous system to form force-stabilizing synergies at two levels of the control hierarchy, at the level of hand action and at the level of within-a-hand finger action. Such ability may, however, emerge with specialized training as shown in an earlier study (Kang et al. 2004).

## REFERENCES

- Kang, N. et al. (2004). *Exp Brain Res*, 157, 336-50.
- Latash, M.L. et al. (2002). *Exp Brain Res*, 146, 419-32.
- Shim, J.K. et al. (2005). *Exp Brain Res*, 164, 260-70.

## ACKNOWLEDGEMENTS

NIH grants AG-018751, NS-035032, AR-048563, and M01 RR-1073.

# NON-UNIFORM LAGRANGIAN FINITE STRAIN FIELDS AT THE MUSCULOTENDINOUS JUNCTION OF INTACT SUPRASPINATUS DURING SHOULDER ELEVATION MEASURED WITH CINE PHASE CONTRAST MRI

Hehe Zhou<sup>1</sup> and John E. Novotny<sup>1</sup>

<sup>1</sup> University of Delaware, Newark, DE, USA  
E-mail: novotny@me.udel.edu Web: www.udel.edu

## INTRODUCTION

Intratendinous shear stress and strains in the supraspinatus (SP) tendon are believed to be an important initiator of rotator cuff tears (Fukuda, H., 1994; Bey, M.J., 2002), though there is no dynamic and in vivo data to prove or refute these hypotheses. Recently, non-uniform atrophy within the SP muscle cross section was found after rotator cuff tears (Meyer, D.C., 2005). This implies a functional difference between the superior and inferior portions of the normal SP muscle resulting in non-uniform degeneration. Again, no functional difference has been measured in the SP in vivo. We propose to use Cine Phase Contrast MRI (CPC-MRI) to determine if the superior, middle and inferior portions of the SP muscle, near the SP outlet, exhibit different mechanical behaviors during humeral elevation. We hypothesize: (1) strain within the SP muscle is related to the shoulder joint position; and (2) there is a non-uniform distribution of the strain from superior to inferior, reflecting different behavior within the muscle.

## METHODS

Seven normal shoulders were scanned (four subjects: one female, three males; ages: 24-56) with a 1.5 T MRI clinical scanner (GE, Milwaukee, WI). All subjects provided informed consent by signing a form approved by Human Subject Review Board at University of Delaware. The scanning parameters for the CPC-MRI images were

determined by the anatomy of the shoulder joint and the characteristics of the motion: TR=24 ms, TE=7.2 ms, flip angle = 30°, 256×256 matrix, pixel size = 1.3281 mm, FOV = 34×34 mm<sup>2</sup> and 24 frames. The motion was completed approximately every two seconds (35 cycles per minute) for approximately six minutes. The setup of image plane and a custom-made experimental device were used to achieve a reliable planar motion near the musculotendinous junction of the SP (MTJS) for each subject.

From the magnitude image at the first frame (20° elevation), a six pixels high and nine pixels long ROI was defined (Fig. 1) and divided into three layers in the superior to inferior direction. Each layer was meshed with a modified pattern filling algorithm into four hundred evenly distributed right-angle triangular meshes at 20% of the pixel size. A novel method was developed to interpolate the velocity field, track displacement of meshes at sub-pixel resolution and finally derive the principal strains and strain directions according to displacements (Zhou, H., 2006). To quantify the deformation at the MTJS, strains were averaged across the triangular meshes in each layer, then across seven normal shoulders. A two factor repeated measures ANOVA with a Geisser-Greenhouse adjustment followed by a Tukey-Kramer post-hoc analysis was used to assess the effect of the region and joint angle on the maximum principal strain (PS1) and the maximum in-plane shear strain (PSXY). Significance level was set to be  $p < 0.05$ .

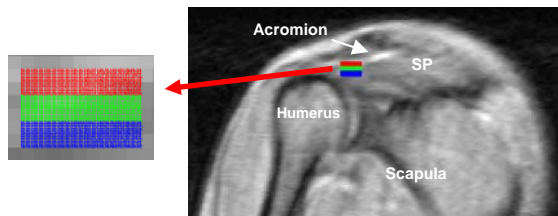


**Figure 1:** Definition of ROIs at MTJS

## RESULTS AND DISCUSSION

PS1 was found to be related to the joint angle ( $p < 0.0004$  with a power 99.7%) with the larger shoulder elevation angle resulting in the larger strain (Fig. 2). Post-hoc analysis showed the maximum principal strain at  $20^\circ$  significantly different from that at both  $35^\circ$  and  $50^\circ$ , and at  $35^\circ$  different from  $50^\circ$  ( $p < 0.05$ ). Similar patterns were found for the PSXY ( $p < 0.0042$  with a power 77.6%) (Fig. 2). A non-uniform strain pattern was seen across the MTJS (Fig. 2). Post-hoc multiple comparison test ( $p < 0.05$ ) indicated that the PS1 and PSXY at the bursal side were significantly larger than those at the middle layer and joint side.

As hypothesized, a non-uniform behavior has been found at the MTJS. This suggested a non-uniform supraspinatus contraction may be necessary for the tendon to be stretched uniformly and thus minimize shear between adjacent layers, a source of possible tear. This implies a certain level of coordination between the layers of muscle contracting at different rates, to various final shortening lengths and perhaps generating different levels of force. Loss of this

coordination could be a possible initiating factor in generating tendon tears or a response that continues tear progression.

## SUMMARY/CONCLUSIONS

A novel method was presented to investigate the dynamic, *in vivo* contraction mechanics in the SP muscle. The non-uniform strain pattern at the MTJS suggested a more complex loading condition rather than uniform force was involved. Furthermore, acromion, clavicle and scapular bone structures and soft tissues like bursa and ligaments also played an important role in the deformation of the supraspinatus. This suggests that the real mechanics in the supraspinatus tendon might be related to more complicated factors than those previously thought.

## REFERENCES

- Bey, M.J. et al. (2002). J Shoulder Elbow Surg, 11, 562-9.
- Fukuda, H. et al. (1994). Clin Orthop, 60-7
- Meyer, D.C. et al. (2005). J Orthop Res, 23, 254-258.
- Zhou, H., Novotny, J.E. (2006). JMRI, *in press*.

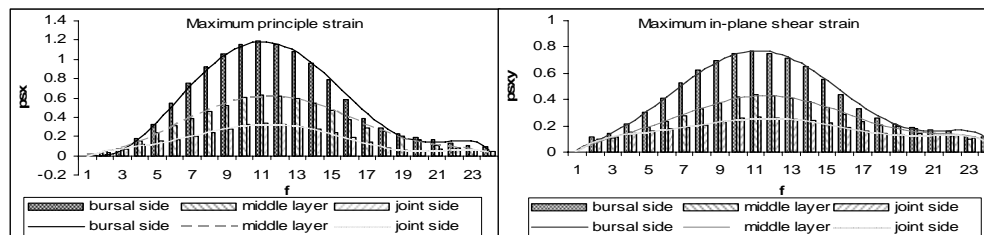


**Figure 2:** Strains at MTJS

# THE EFFECT OF PHARMACOLOGIC THERAPY ON KINETIC GAIT PARAMETERS IN PATIENTS WITH PERIPHERAL ARTERIAL DISEASE

Jessie M. Huisinga<sup>1</sup>, Sara A. Myers<sup>1</sup>, Jason M. Johanning<sup>2,3</sup>, Iraklis Pipinos<sup>2,3</sup>, and Shing-Jye Chen<sup>1</sup>

<sup>1</sup> University of Nebraska at Omaha

<sup>2</sup> University of Nebraska Medical Center

<sup>3</sup> Veterans Affairs Medical Center, Omaha, NE

E-mail: [jhuisinga@mail.unomaha.edu](mailto:jhuisinga@mail.unomaha.edu) Web: [www.unocoe.unomaha.edu/hper/bio/home.htm](http://www.unocoe.unomaha.edu/hper/bio/home.htm)

## INTRODUCTION

Peripheral Arterial Disease (PAD) is a manifestation of atherosclerosis of the leg arteries that affects 10 million people in USA (Antignani, 2003). For these people, walking is a difficult task because the increased metabolic demands of the leg muscles are constrained due to the decreased blood flow. The result is claudication, defined as pain of the leg muscles during ambulation and is present in 40% of all PAD patients (Schainfeld, 2001). With rest, adequate blood flow eventually returns and the pain subsides. Claudication symptoms are treated with behavioral modifications, surgery and pharmacologically (Shainfeld, 2001). The two most prevalent pharmacological therapies use different approaches; the first (Treatment 1; T1) acts primarily by decreasing blood viscosity, while the second (Treatment 2; T2) acts primarily as a vasodilator (Dawson, 2001). Recently, research has examined PAD and the associated claudication as a primary gait disability (Gardner et al., 2001). However, this research has included only temporal and spatial parameters, such as stride length and step time, without exploring joint kinematics and kinetics. Similarly, studies investigating the effects of T1 and T2 also used the same limited approaches (Dawson et al., 2000). Thus, Gardner et al. (2001) suggested that these previous evaluations have been incomplete in their ability to describe the true gait handicap of PAD. Our goal was to further understand PAD gait and the influence of pharmacological therapies on the elimination of gait abnormalities.

## METHODS

Nine PAD patients with diagnosed occlusion, which resulted in claudication, participated in the study. Five patients underwent T1 and four underwent T2. Because some patients were bilateral and some unilateral, we had nine total claudicating limbs affected by T1 and six total claudicating limbs affected by T2. Patients were asked to walk through a 10 meter walkway at self-selected normal walking pace, while ground reaction forces were collected by a Kistler force plate (600Hz). The patient performed five trials while pain free, or with no claudication (C1). The patient rested between each trial to ensure pain free data collection. Patients then walked on a treadmill at a 10% grade and at a speed of 0.67 m/s until the onset of pain. This protocol is common in PAD clinical examination. After pain was induced (C2), patients completed five more trials. Data collection was performed before (PRE) and after (POST) the use of each treatment. Treatment lasted a minimum of three months. Statistical analysis using 2x2 ANOVAs were performed on selected ground reaction force parameters.

## RESULTS AND DISCUSSION

Regarding T1, the local minimum of vertical force experienced at midstance ( $F_{zmin}$ ) was significantly decreased from PRE to POST. This indicates a higher positioning of the center of gravity and possibly a straighter leg at single support during the POST test. The braking impulse (IB) was significantly increased from PRE to POST indicating an

increase in forward momentum after touchdown. No other main effects were found for PRE to POST for T1. The second active loading vertical peak (F2) significantly decreased from C1 to C2 which could illustrate a tendency to better distribute loading between the legs during terminal stance when pain is present. Fzmin significantly increased from C1 to C2, indicating a lower positioning of the center of gravity and possibly a more flexed leg at single support when the patient was walking with claudication. The maximum propulsion force was significantly increased from C1 to C2 in the anterior-posterior direction which could be an adaptive mechanism employed to help carry the leg into swing when pain is present. There was a significant interaction for IB where the braking impulse increased significantly more for C2 than C1 from the PRE to the POST test. This possibly suggests an improvement in the patients' gait under claudication after T1.

Regarding T2, the peak braking force significantly increased from PRE to POST which indicates that after treatment, patients were able to increase the braking force as necessary and possibly control forward momentum. The increased blood flow to the leg could enable improved muscular response leading to increased forward momentum. F2 significantly decreased from C1 to C2, which is similar to the effect seen as a result of T1 and could illustrate a tendency to distribute the vertical force during terminal stance when pain is present. The first active loading vertical peak force showed a significant interaction, where from PRE to POST, an increase was observed for the pain condition while a decrease was observed for the pain free condition. Thus, it

seems that T2 promoted a change in this parameter. It is possible that during the PRE test, the patient was trying to adapt to the decreased blood flow and increased loading by possibly lowering the center of gravity with increased step distance during the first double support. However after the introduction of the vasodilator, the patient promoted a higher positioning of the center of gravity during claudication. Finally, the braking impulse showed significant interaction, which was similar with T1.

## SUMMARY/CONCLUSIONS

The above results indicated that T1 affected a larger number of kinetic gait parameters than T2. The similar results found between the two treatments for F2 and IB indicated that their effects are reproducible for at least these two variables. However, the number of differences found in other variables indicated that the two treatment mechanisms could result in differential effects on kinetic gait parameters on PAD patients. These preliminary findings need to be substantiated with larger samples sizes, and examination of the corresponding kinematic and joint moment data.

## REFERENCES

- Antignani, P.L. (2003). *Curr. Vasc. Pharmacol.*, **1**, 205-216.
- Dawson, D.L. (2001). *Am. J. Cardiol.*, **87**,19D-27D.
- Dawson, D.L. et al. (2000). *Am. J. Med.*, **109**, 523-530.
- Gardner, A.W. et al. (2001). *Vasc. Med.*, **6**, 223-227.
- Schainfeld, R.M. (2001). *J. Am. Board Fam. Pract.*, **14**, 443-450.

# EFFECT OF VISION REMOVAL ON STIFFNESS REGULATION DURING BOUNCING GAIT

Hiroaki Hobara<sup>1</sup>, Koh Inoue<sup>1</sup>, Tetsuro Muraoka<sup>2</sup> and Kazuyuki Kanosue<sup>1, 2, 3</sup>

<sup>1</sup> Graduate School of Human Sciences, Waseda University, Saitama, JAPAN

<sup>2</sup> Consolidated Research Institute for Advanced Science and Medical Care, Waseda University

<sup>3</sup> Faculty of Sports Sciences, Waseda University

E-mail: [h\\_hobara@moegi.waseda.jp](mailto:h_hobara@moegi.waseda.jp) Web: <http://www.f.waseda.jp/kanosue/>

## INTRODUCTION

The center of mass in both humans and animals moves like a bouncing ball during hopping, running and trotting. In these bouncing gaits, the dynamics of body movement can be described with a simple spring-mass model (Fig. 1-A). The stiffness of the overall leg spring (leg stiffness) is modulated depending on the dynamics of the interaction between the leg and the ground (Ferris and Farley, 1997).

Recently, we demonstrated that leg stiffness decreased when vision was removed (Hobara et al., being submitted). However, since the leg stiffness is a function of multiple joint spring stiffness (joint stiffness; Fig. 1-B), we could not gain the information concerning the stiffness of each joint only from the spring-mass model. The purpose of this study was to investigate the relative importance of joint stiffness for leg stiffness regulation in altered visual conditions. Ankle stiffness is considered as a major determinant of leg stiffness (Farley and Morgenroth, 1999). Therefore, we hypothesized that it also plays an important role even when vision is removed.

## METHODS

Seven subjects hopped in one place on a force plate. All subjects hopped bare foot on both legs, matching a metronome beat at 2.2 Hz (approximately preferred frequency).

In this experiment, we utilized two different conditions: eyes-open (EO) and eyes-closed conditions (EC). In the EO, the control condition, subjects were asked to hop repetitively in their preferred manner. In the EC condition, subjects were asked to hop wearing an eye mask and to close their eyes while wearing the mask during hopping.

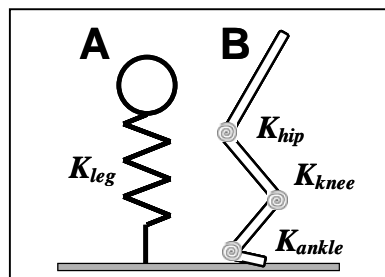


**Fig.1** Behavioral model for bouncing gait. A: Spring-mass model. B: Torsional spring model

Using a spring-mass model (Fig. 1-A), we calculated the leg stiffness ( $K_{leg}$ ) from the ratio of the peak ground reaction force to the maximum leg compression during the ground contact. In additions, using the torsional spring model (Fig. 2-B), we calculated hip, knee and ankle joint stiffness ( $K_{hip}$ ,  $K_{knee}$  and  $K_{ankle}$ , respectively), which is the ratio of the peak joint moment and angular displacement. These calculations were based on the equation of Farley and Morgenroth (1999).

Multiple regression analyses were performed both in the EO and EC conditions, using  $K_{leg}$  as dependent variable and joint

stiffness ( $K_{hip}$ ,  $K_{knee}$  and  $K_{ankle}$ ) as independent variables. Statistical significance was set at  $p < 0.05$ . Within each multiple regression analyses, standardized partial regression coefficient (beta) was used to determine the relative importance of joint stiffness to  $K_{leg}$ .

## RESULTS AND DISCUSSION

Table 1 shows the results of multiple regression analysis. In each groups, regression model resulted statistically significant. It accounted for 86% of the variance of  $K_{leg}$  in the EO, and for 85% in the EC conditions (See Table 1; “Adjusted  $R^2$ ”). Therefore, the model can be likely to explain the  $K_{leg}$  variance with lower extremity joint stiffness in both conditions.

The most important finding of this study is that the relative contribution of joint stiffness to  $K_{leg}$  changes with different visual conditions. In the EO condition,  $K_{ankle}$  was most crucial for regulating  $K_{leg}$  ( $\beta = 0.676$ ). On the other hand, in the EC condition,  $K_{knee}$  was relatively more important for regulating  $K_{leg}$  ( $\beta = 0.572$ ).

**Table 1:** Standardized partial regression coefficient (beta) in eyes-opened (EO) and eyes-closed (EC) conditions.

	EO	EC
Adjusted $R^2$	0.865*	0.856*
$\beta K_{hip}$	-0.311	-0.042
$\beta K_{knee}$	0.068	0.572
$\beta K_{ankle}$	0.676	0.425

\*  $p < 0.05$

We had hypothesized that ankle stiffness played an important role even when vision was removed. But the organism seems to take different control strategy under altered visual conditions. Indeed, if  $K_{ankle}$  decrease to stabilize posture, it would become difficult for the subjects to hop. This is because triceps surae muscle and Achilles tendon behave as a spring during bouncing gait (Alexander, 1988). Therefore, when vision is removed, it is likely that subjects conserve their constant ankle stiffness, which is required to hop repetitively. Alternatively, knee stiffness might be modulated to stabilize dynamic posture. Further research, which includes quantitative evaluation of muscle activity, is required for better address this conjecture.

## SUMMARY

Effect of vision removal on stiffness regulation during hopping was investigated. When vision was removed, human hopper primary conserved constant ankle stiffness, and knee stiffness was modulated to control dynamic postural stability.

## REFERENCES

- Alexander, R.M. (1988). *Elastic Mechanisms in Animal Movement*. Cambridge University Press.
- Ferris, D.P., Farley C.T. (1997). *J. Appl Physiol*, **82**, 15-22.
- Farley, C.T., Morgenroth, D.C. (1999). *J. Biomech*, **32**, 267-273.
- Hobara, H. et al. (*Manuscript Submitted for Publication*)

# USING CINE PHASE CONTRAST MRI TO MEASURE NON-UNIFORM LAGRANGIAN FINITE STRAIN FIELDS IN THE INTACT BICEPS BRACHII DURING ELBOW FLEXION

Hehe Zhou<sup>1</sup> and John E. Novotny<sup>1</sup>

<sup>1</sup> University of Delaware, Newark, DE, USA  
E-mail: novotny@me.udel.edu Web: www.udel.edu

## INTRODUCTION

Few studies have measured how human skeletal muscle deforms *in vivo*, dynamically as a solid material instead of as a line. This is important not only because the function of a muscle in isolation may not reflect how it behaves in the skeletal system. Activation may be non-uniform and deformation may be affected by the surrounding anatomy and by synergistic functional requirements. Therefore the *in vivo* measurement of muscle deformation can allow us to find the crucial connections across various scales of muscle organization from sarcomere, fiber level to *in vivo* muscle behavior. The objective of this study is to apply the CPC-MRI to measure muscle function and derive the Lagrangian strain field for the biceps brachii and to determine its homogeneity (Zhou, H. 2006). An understanding of internal muscle strain *in vivo* will help in the formulation of more complex muscle contraction models.

## METHODS

MRI images were collected with a clinical scanner (GE 1.5 Tesla, Milwaukee, WI) for 8 subjects (one female, seven males, and age 24-34) without history of previous biceps muscle injuries were recruited. All subjects read and signed an informed consent form approved by the Human Subject Review Board at the University of Delaware. The imaging plane was selected to bisect the distal aponeurosis and muscle belly (Pappas, G.P. 2002). Dynamic MRI images (34×34

cm2 FOV, 256×128, TR=24ms, flip angle=30°, VENC=10cm/second) were collected for cyclic motions of subjects' arms. Subjects were guided to keep their motion within a plane with a range of motion from 180° or full extension to 120° with a 5% maximum voluntary isometric contraction (MVIC) resistive force.

A previously developed novel method was used to derive the finite strain fields of biceps with the CPC-MRI (Zhou, H. 2006). The anatomical coordinate system was created according to the functional force center line of biceps from pre-calculated shear strain image (Fig. 1). The middle and anterior portion were divided into an anterior belly part and a center part which included aponeurosis, then further semi-automatic divided into 24 sub-regions (Fig. 1). Each sub-region was then meshed into several hundred 0.2×0.2 pixel triangular meshes. Defining the muscle state in the first frame as reference, longitudinal y-directional strain (SY), transverse x-directional strain (SX), shear strain (SXY), maximum principal strain (PS1), minimum principal strain (PS2) and maximum in-plane shear strain (PSXY) were derived. To quantify the deformation at the different sub-regions in the biceps muscle, strains were averaged across the triangular meshes in each sub-region. A two factor repeated measures ANOVA followed by a Tukey-Kramer post-hoc analysis was used to assess the effect of the location and elbow joint flexion angle on the SY, PS1 and PS2.

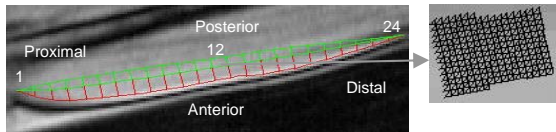


**Figure 1:** Division of Biceps Anterior Half: Green-Aponeurosis, Red-Belly, area ratio between belly and aponeurosis is 3:2.

## RESULTS AND DISCUSSION

A non-uniform spatial distribution of SY, PS1 and PSXY was found across the biceps (Fig. 2). The deformation of the most distal end, the zone most influenced by the internal aponeurosis, was often found significantly different from that of other sub-regions ( $p < 0.05$ ). An obvious transition zone from shortening to stretching can be seen across 15th to 17th sub-regions, indicating a tissue change from myofibrillar to tendinous material close to the distal insertion of biceps tendon. In terms of temporal effect for SY, PS and PSXY, significant differences were found at larger extension angles ( $< 7^{\text{th}}$  frame), and between larger extension angles and lower extension angles ( $> 8^{\text{th}}$  frame). For PS2, the biceps showed a consistent contractile ability throughout the muscle either spatially and temporally ( $p > 0.05$ ). Values are not much different between the belly and aponeurosis. For most regions, a calculation of a pseudo-Poisson's ratio with the ratio PS2/PS1 gives values near 0.5.

Computed strain fields uncovered non-uniform deformation in the biceps when observing the strain in its longitudinal direction. Elongation seen in the distal end perhaps indicates that the proximal muscle may stretch the distal. PS2, assumed to indicate the contractile strain, its values indicate that contraction strain was relatively uniform in magnitude throughout the muscle. PS1 was slightly higher distally perhaps indicating the effects of other structures around the musculotendinous junction or narrowing muscle may alter tensile strains.

The ratio of PS2/PS1 indicates the muscle is generally incompressible during this contraction. Overall internal muscle strains seem to vary somewhat along the length of a muscle but not much between the aponeurosis or mid-line compared to the belly. The differences in values between strains in the longitudinal axis of the muscle and the principal strains represent information on functional muscle architecture rather than just the anatomy.

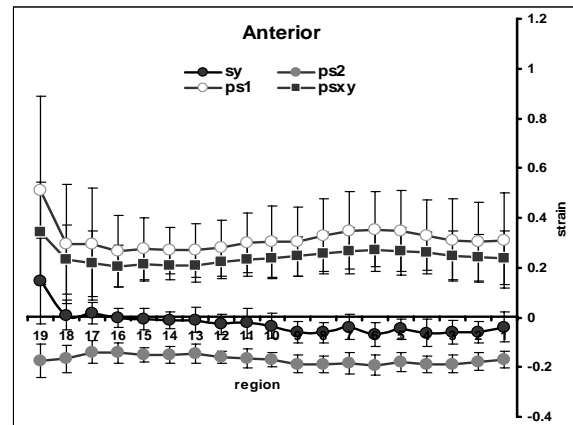


**Figure 2:** Strains vs. Regions

## SUMMARY/CONCLUSIONS

A novel method was presented to derive continuous two-dimensional Lagrangian strains of biceps brachii *in vivo* with the CPC-MRI. Calculated finite strains showed that internal insertion of aponeurosis caused an inhomogeneous deformation pattern in either anterior and center part of biceps brachii muscle, which suggested the importance to consider the muscle structure and organization in muscle modeling.

## REFERENCES

- Pappas, G.P. et al. (2002). *J Appl Physiol*, 92, 2381-2389.  
 Zhou, H., Novotny, J.E. (2006). *JMRI*, *in press*.

# **IN VIVO BICEPS BRACHII MUSCLE MORPHOLOGY: FINITE PRINCIPAL STRAINS AND STRAIN DIRECTIONS MEASURED WITH CINE PHASE CONTRAST MRI AND DYNAMICALLY**

Hehe Zhou <sup>1</sup> and John E. Novotny <sup>1</sup>

<sup>1</sup> University of Delaware, Newark, DE, USA  
E-mail: novotny@me.udel.edu Web: www.udel.edu

## **INTRODUCTION**

Previous studies have observed non-uniform internal architectures in skeletal muscles (e.g. Agur, A.M. 2003), yet few have measured how human skeletal muscle deforms *in vivo*, dynamically as a solid material instead of as a line. Our previous study developed a novel method to calculate 2D Lagrangian strain field of skeletal muscle from the CPC-MRI (Zhou, H. 2006). The objective of this study is to apply the CPC-MRI to quantify the finite principal strains, strain directions and apply those strain data to measure structure information like muscle functional force center line, muscle fiber direction, and pennation angle change of human biceps muscle non-invasively, *in vivo* and dynamically.

## **METHODS**

MRI images were collected with a clinical scanner (GE 1.5 Tesla, Milwaukee, WI) for 8 subjects (one female, seven males, and age 24-34) without history of previous biceps muscle injuries were recruited. All subjects read and signed an informed consent form approved by the Human Subject Review Board at the University of Delaware. The imaging plane was selected to bisect the distal aponeurosis and muscle belly (Pappas, G.P. 2002). Dynamic MRI images (34×34 cm<sup>2</sup> FOV, 256×128, TR=24ms, flip angle=30°, VENC=10cm/second) were collected for cyclic motions of subjects' arms. Subjects were guided to keep their motion within a plane with a range of

motion from 180° or full extension to 120° with a 5% maximum voluntary isometric contraction (MVIC) resistive force.

A previously developed novel method was used to derive the finite strain fields of biceps with the CPC-MRI (Zhou, H. 2006). An effective way was first used to locate the functional force center line of biceps according to pre-calculated shear strain image at 3×3 pixel resolution (black line in Fig. 1) in image coordinates. The direction of the muscle's center line was then used to make the anatomical coordinate which was applied to do the region of interest (ROI) meshing and allowed for calculation of strain along the muscle's functional longitudinal axis. Local strain would be a function of fiber orientation which in the biceps is not along its long axis. In order to quantify the muscle fiber direction in the biceps, maximum principal strain (PS1), minimum principal strain (PS2) and PS2 strain direction were solved by determining to strain matrix's Eigen-values and vectors. The direction of PS2, or most negative strain, would be assumed to be the direction of muscle contraction for a given element.

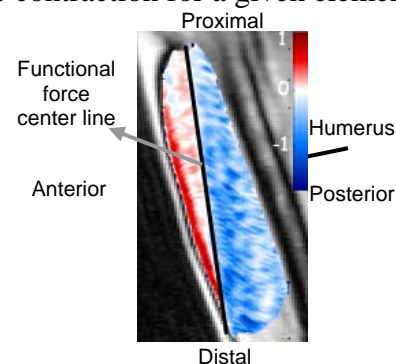


**Figure 1:** Shear Strain Used to Locate Functional Force Center Line

## RESULTS AND DISCUSSION

With the developed novel method in our previous studies (Zhou, H. 2006), *in vivo* deformation of biceps muscle was investigated non-invasively. Derived 2D Lagrangian finite strain fields measures the internal architecture of human skeletal muscle *in vivo* and dynamically. Fig. 1 shows the shear strain distribution in one biceps muscle calculated at  $0.2 \times 0.2$  pixel resolution. The functional force, center line of the biceps can be located due to the different signed shear magnitudes on either side. In addition, this method avoided the manually alignment of the center line of biceps with longitudinal axis of MRI scanner (Pappas, G.P. 2002), therefore reduced the imaging setup time and improved the accuracy of calculation of deformation. Fig. 2 shows the PS2 image mapped to the original magnitude image together with the PS2 direction. According to the ultrasound images collected, the PS2 direction in the muscle belly is approximately aligned with fiber direction, which means that it can be used to track the pennation angle change as a function of muscle contraction and joint position. Non-uniform deformation in the biceps can be seen. In comparison with anterior half, the posterior half has slightly larger deformation. Bands of similar strain values, or iso-strain bands, run perpendicular to the PS2 direction or across fibers. Similar strain across fibers would minimize shear between muscle fibers units. Iso-strain bands give an idea of how muscle may coordinate contraction to minimize shear between fibers. This information will aid and verify the formulation of FEM muscle contraction models.

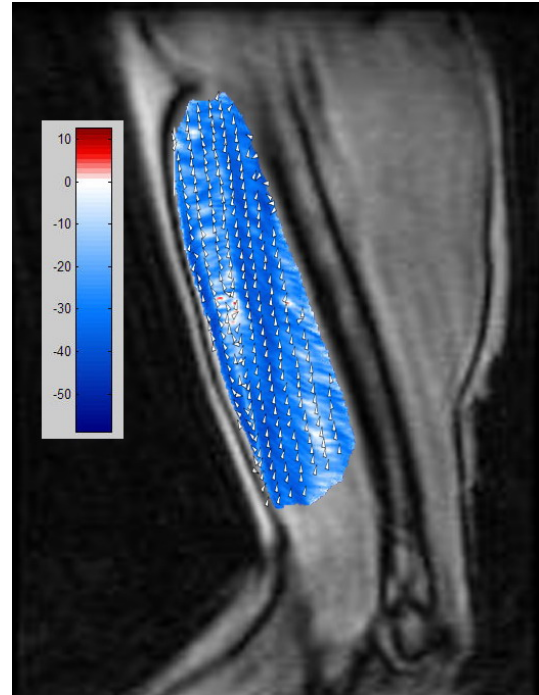


**Figure 2:** PS2 and Strain Direction

## SUMMARY/CONCLUSIONS

A novel method was presented to measure morphology of biceps brachii *in vivo* with the CPC-MRI. This *in vivo* and dynamic information can give us a better understanding of muscle function, verifying and guiding muscle modeling and permitting more sophisticated interpretation of the functional effects of injury.

## REFERENCES

- Agur A.M. et al. (2003). Clin Anat., 16, 285-93.
- Pappas, G.P. et al. (2002). J Appl Physiol, 92, 2381-2389.
- Zhou, H., Novotny, J.E. (2006). JMRI, *in press*.

# INTER-DAY RELIABILITY OF CENTRAL ACTIVATION RATIO FOR THE QUADRICEPS IN HEALTHY YOUNG ADULTS

Dana M. Otzel, John W. Chow, and Mark D. Tillman

Department of Applied Physiology & Kinesiology, University of Florida, Gainesville, FL, USA  
E-mail: dotzel@hhp.ufl.edu Web: www.hhp.ufl.edu/apk/ces/labs/biomech/

## INTRODUCTION

Clinically significant deficits in voluntary activation are of importance, given that joint damage as a result of injury or surgical procedure may cause disruption of the neural drive to the muscle. The technique of superimposing electrical stimulation during a maximal effort voluntary contraction, termed burst interpolation, is commonly used to assess the level of motor unit activation (or the degree of central inhibition) of a muscle. However, the inter-day reliability of the measures has not been evaluated nor has the reliability of using the technique on the quadriceps been determined.

The purpose of this study was to evaluate the inter-day reliability of the burst interpolation technique in young healthy individuals based on the common use of this technique to infer motor deficits of the muscle. Given that the prevalence of knee injury is high and that the knee serves as a crucial link in the weight bearing biomechanical chain, voluntary muscle activation of the leg extensors was evaluated.

## METHODS

Eleven female (age  $21.4 \pm 0.9$  years, height  $165.5 \pm 4.8$  cm, weight  $606.2 \pm 114.1$  N) and 11 male ( $21.8 \pm 1.2$  years,  $179.4 \pm 5.1$  cm,  $861.0 \pm 153.0$  N) volunteers who were physically active and had no lower extremity injuries at the time of participation served as the subjects. Each subject attended 3 testing

sessions within 4 weeks. The average time elapsed between the first and second and between the second and third sessions was  $10.0 \pm 3.7$  and  $7.0 \pm 1.9$  days, respectively.

Motor unit activation of the quadriceps was evaluated by delivering interpolated supramaximal tetanus twitches to the quadriceps while the subject performed an isometric knee extension at  $90^\circ$  knee flexion with maximum effort on a KinCom AP125 dynamometer (Stevens et al., 2001). A Grass S48 stimulator was used to deliver a train of electrical impulses (12 spikes, 0.01 s apart, 1/15000 s duration for each spike). The ratio of the force exerted by the subject leading up to the electrical stimulation to the peak force after the stimulation (central activation ratio, CAR) was used to determine the efficiency of the subject in recruiting available motor units.

Two CAR trials were completed for each leg in each session and the trial with higher CAR value for each leg was used in subsequent analyses. To minimize inter-tester variability, all tests were conducted by the same investigator (DMO). A 2 (gender) x 2 (side) x 3 (session) ANOVA with repeated measures was used to examine the effect of different factors on the maximum isometric knee extension torque prior to stimulation ( $\alpha = 0.05$ ). To evaluate inter-day reliability, intraclass correlation coefficient (ICC) values were computed for these groups – male, female, dominant and non-dominant legs, and overall.

## RESULTS AND DISCUSSION

As expected, maximum isometric knee extension torques for males were significantly greater than their female counterparts (Table 1). No significant differences in strength were found between dominant and non-dominant sides or across the 3 testing sessions. Mean CAR values were above 95% among male and female subjects (Table 2). The CAR values in our study were similar to those found in other studies (Kent-Braun & Ng, 1999; Stackhouse et al., 2000; Stevens et al., 2001). Except for the female dominant group, the ICC values were moderate to good across sample groups of dominant and non-dominant lower extremities (Table 3). The negative ICC found for the female dominant sample may be due to the relatively small between-subject variation compared to the within-subject variation.

## SUMMARY/CONCLUSIONS

Overall, the inter-day reliability of the burst interpolation technique used to assess CAR for the quadriceps in young healthy individuals is considered moderate. The ICC values would have been higher if not for the small between-subject variation relative to within-subject variation. Researchers should feel confident in using the burst interpolation technique over different testing days.

## REFERENCES

- Kent-Braun J.A. & Ng A.V. (1999). *J. Appl. Physiol.*, 87(1), 22-29.  
 Stackhouse S.K et al. (2000). *Muscle Nerve*. 23(11), 1706-12.  
 Stevens, J.E. et al. (2001). *Arch. Phys. Med. Rehabil.*, 82, 973-978.

## ACKNOWLEDGEMENTS

Dr. Jennifer Stevens for her technical assistance.

**Table 1:** Mean (SD) maximum isometric torques (Nm) prior to electrical stimulation.

Session	Female*		Male*	
	Dominant	Non-dominant	Dominant	Non-dominant
1	106.9 (33.5)	102.2 (30.0)	150.7 (46.7)	154.5 (41.4)
2	103.5 (29.3)	95.7 (22.0)	154.1 (48.4)	149.1 (34.1)
3	100.8 (23.8)	100.2 (19.5)	161.3 (42.6)	145.4 (27.6)

\*Significant difference between gender (p < 0.001)

**Table 2:** Mean (SD) central activation ratio (CAR) values.

Session	Female		Male	
	Dominant	Non-dominant	Dominant	Non-dominant
1	99.3 (2.4)	99.1 (1.8)	98.1 (4.1)	98.4 (3.5)
2	99.0 (1.9)	99.0 (2.5)	95.8 (5.3)	97.5 (4.0)
3	99.7 (0.9)	99.7 (0.9)	98.1 (3.1)	98.1 (3.1)

**Table 3:** Intra-class correlation coefficient (ICC) values for different sample groups.

Group	Dominant	Non-dominant	Overall
Female	-.0735	.6273	.4766
Male	.8177	.5892	.6569
Overall	.7764	.6172	.6655

# HAND DIFFERENCE IN MULTI-FINGER QUICK FORCE PULSE PRODUCTION

Wei Zhang<sup>1</sup>, Robert L. Sainburg<sup>2</sup>, Vladimir M. Zatsiorsky<sup>2</sup>, and Mark L. Latash<sup>1</sup>

<sup>1</sup> Motor Control Laboratory and <sup>2</sup> Biomechanics Laboratory, Department of Kinesiology  
Penn State University, University Park, PA, USA

E-mail: wuz107@psu.edu

Web: <http://www.personal.psu.edu/faculty/m/l/ml111/index.htm>

## INTRODUCTION

Several recent studies have suggested that the dominant (D) and non-dominant (ND) hands have different specialization with respect to trajectory and endpoint location control (Sainburg 2002; Sainburg & Schaeffer 2004). In particular, the D hand is assumed to have a better interaction torque compensation. We hypothesize that the control mechanisms for the D and ND hands may differ in their more general ability to create multi-element synergies stabilizing the time profile of a performance variable. This hypothesis was tested in experiments with multi-finger isometric force production that do not involve significant interaction torques.

## METHODS

Eight young male and eight young female right-handed volunteers participated in the experiment. The subjects sat comfortably in a chair; their forearm was secured onto the horizontal board. The fingertips of the hand were placed on unidirectional force sensors. The subjects watched a monitor that showed their total force-time profile computed on-line as the sum of their individual finger forces. There were two tasks, the Pulse and the Step task, performed by both D and ND hands in a balanced order. Each task required the subjects to follow, as closely as possible, a horizontal line shown on the screen corresponding to 5 N of total force for 3 s. Then the subjects were instructed to produce a self-paced quick force pulse over the next 3 s.

The required amplitude of the pulse was  $25 \pm 5$  N (shown on the screen). In the Pulse task, the subjects relaxed after reaching a peak force. In the Step task, they were required to keep the total force at the target level until the end of the trial. The total time of a trial was 8 s. Twenty-four trials were performed at each task.

The trials were aligned by the pulse onset point ( $t_0$ ), defined as the time when  $dF/dt$  reached 5% of its peak value. Average force and its variance profiles were computed over each set of trials. The framework of the uncontrolled manifold hypothesis (Scholz & Schöner 1999) was used to compute an index ( $\Delta V$ ) of total force stabilization at each time sample over sets of trials at each task and for each subject separately (Latash et al. 2001).

## RESULTS AND DISCUSSION

Female subjects produced significantly higher ( $F_{[1,7]}=5.79$ ,  $P<0.05$ ) but slower ( $F_{[1,7]}=22.86$ ,  $P<0.001$ ) force pulses than men. Variance of the total force showed a peak before the peak force; its magnitude was similar for both genders. For both tasks, there were no differences between the D and ND hands for both peak force and peak variance of the total force.

The subjects showed differences between the D and ND hands in the profiles of  $\Delta V$  index. Figure 1 shows the averaged  $\Delta V$  time-profiles for men (A) and women (B).  $\Delta V$  was positive

corresponding to a strong force-stabilizing synergy during the steady-state phase ( $\Delta V_{\text{stst}}$ ). There was a drop in  $\Delta V$  prior to  $t_0$  ( $\Delta V_{\text{pret0}}$ ) followed by a major drop in  $\Delta V$  during the force pulse production ( $\Delta V_{\text{min}}$ ) that typically occurred about the time of peak rate of force change. For both tasks, the  $\Delta V$  drop from  $\Delta V_{\text{stst}}$  to  $\Delta V_{\text{min}}$  was significantly larger in the ND hand than in the D hand ( $F_{[1,15]}=8.41$ ,  $p<0.01$ ). There seem to be gender specific effects. In particular, men showed larger hand-specific differences as compared to women. In particular, the drop from  $\Delta V_{\text{stst}}$  to  $\Delta V_{\text{post}}$  was similar in men and women for the right hand while, for the left hand, men showed significantly lower  $\Delta V_{\text{post}}$  values ( $t=3.2$ ,  $p<0.01$ ).

## SUMMARY/CONCLUSIONS

The results have shown that the D hand avoids major force destabilization during quick force production tasks as compared to the ND hand. This finding supports our main hypothesis that the D hand has an advantage in forming multi-finger synergies that stabilize the total force, and this advantage becomes apparent during quick actions. The findings may be viewed as extending the applicability of the hypothesis on hand specialization to multi-finger isometric tasks. The close to significant gender differences confirm earlier observations on gender effects on multi-finger synergies (Kang et al. 2004).

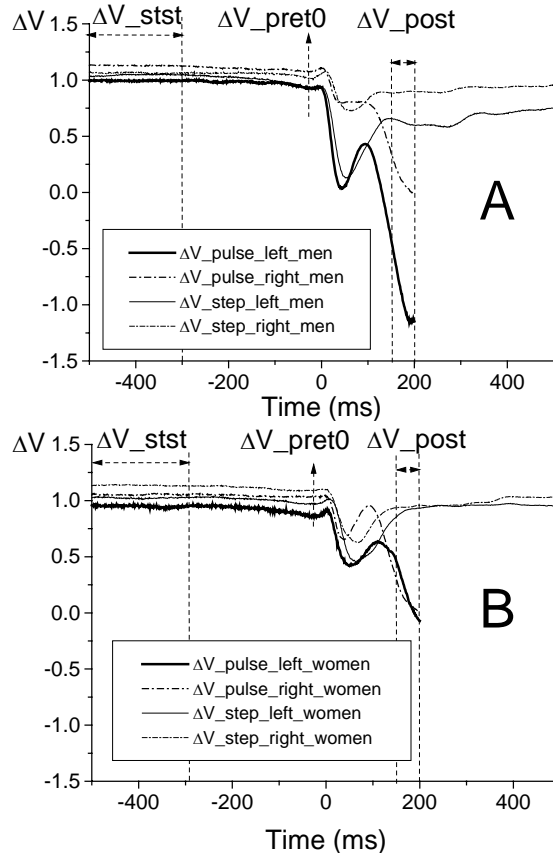


**Figure 1:**  $\Delta V$  time profiles of the Pulse (thick lines) and Step tasks (thin lines) performed by the D (right, dashed lines) and ND (left, solid lines) of men (A) and women (B).

## REFERENCES

- Kang et al. (2004) *Exp Brain Res* **157**: 336-350.  
 Latash et al. (2001) *Exp Brain Res* **141**: 153-165.  
 Sainburg RL, Schaefer SY (2004) *J Neurophysiol* **92**: 1374-1383.  
 Sainburg RL (2002) *Exp Brain Res* **142**: 241-258.  
 Scholz JP, Schöner G (1999) *Exp Brain Res* **126**: 289-306.

## ACKNOWLEDGEMENTS

This research was supported in part by NIH grants AG-018751, NS-035032, and AR-048563.

# THE INFLUENCE OF TAI CHI TRAINING ON LOCOMOTOR ABILITY IN PARKINSON'S DISEASE

Chris J. Hass<sup>1</sup>, Dwight E. Waddell<sup>2</sup>, Steven L. Wolf<sup>3</sup>, Jorge L. Juncos<sup>3</sup>, Robert J. Gregor<sup>4</sup>

<sup>1</sup> University of Florida, Gainesville, FL, USA <sup>2</sup> University of Mississippi, Oxford, MS, USA  
<sup>3</sup> Emory University, Atlanta, GA ; <sup>4</sup> Georgia Institute of Technology, Atlanta, GA, USA  
E-mail: ch2290@columbia.edu

## INTRODUCTION

Postural control during dynamic activities such as initiating gait and locomotion, requires the integration of multiple sensory and motor pathways so that the central nervous system can coordinate the anticipatory/postural and intentional/movement components of the task. Persons with Parkinson's disease (PD) exhibit a marked deficit in maintaining equilibrium during transitions between states of static and dynamic equilibrium, such as during gait initiation, termination, or turning. Indeed, disturbance of gait initiation (GI) is well documented in patients with PD (Hass, 2005). PD is also associated with locomotor disturbances resulting in decreased gait speed, step length, and joint excursions (Morris, 2001).

Several investigators have studied whether pharmacologic administration, task specific external cueing, attentional strategies, movement amplitude training, and/or weight supported treadmill training could improve these deficits in GI and locomotion. However, few studies have evaluated whether exercise therapy can be beneficial for improving movement initiation and gait.

We suggest that Tai Chi (TC) training may be particularly beneficial for improving gait initiation and locomotor deficits in this population. First, TC training can lead to improved anticipatory postural adjustments during gait initiation in transitionally frail older adults. TC improved the mechanism

by which forward momentum is generated and improved coordination during gait initiation, suggesting improvements in postural control (Hass, 2005). Second, Tai Chi has been shown to improve postural stability and musculoskeletal fitness (Klein, 2004), parameters that are known to influence locomotor ability in PD. Thus, the purpose of this study was to evaluate the effectiveness of Tai Chi for improving locomotor function in PD.

## METHODS

Twenty-three sedentary patients with idiopathic PD (mean age 66.6 yrs, *SD* 6.4; mass 79.1 kg, *SD* 15.4; height 174.7 cm, *SD* 8.1; Hohen and Yahr 2.2 *SD* 0.4) were recruited from the metropolitan area. Patients were randomized to receive either Tai Chi training or Qi-Gong meditation twice weekly for 16 weeks. Investigators were blinded to group assignment.

Tai Chi training emphasized physical movements, mind/body coordination, and meditation. Participants performed 8 Tai Chi forms during the 60-minute sessions. The 60-minute Qi-Qong treatments emphasized prolonged, intense contemplative, or deep meditation in two postures, "sitting Chan" and "lying Chan" (seated and lying supine on floor mats.)

Prior to GI and gait analysis, participants were fitted with retroreflective markers according to the Helen Hayes marker

system. Ground reaction forces (GRF) were sampled at 360 Hz from force plates (Bertec Corp., Columbus, OH) embedded within a 8m walkway. Kinematic data were captured at 60 Hz using a six camera 3D Optical Capture system (Peak Performance, Englewood, CO). All data were time synchronized in the Peak Motus analysis system. GRF and kinematic data were exported to in-house software for inverse dynamics calculations.

GI trials began with the participant standing quietly on the force platform with a self-selected stance width. Following a verbal cue, the participants initiated walking and continued walking for several steps. For each participant, six trials were performed at a self-selected pace. The center of pressure trajectory during GI was divided into three periods and five dependent variables were computed: displacement and average velocity in the anterior/posterior and medial/lateral directions and movement smoothness.

For the gait trials, a starting position was selected near one end of the walkway so that foot contact would occur on the force platforms in a normal stride. A trial was discarded if the participant's foot was not completely on the force platform or if the participant made visibly obvious stride alterations. Each subject performed a minimum of eight successful trials.

Our primary hypothesis was that differences would be observed in the dependent variables between the 2 intervention groups over time during the 3 COP trace periods. Three separate 2x 2 (Group x Time) multivariate analysis of variance (MANOVA) were used to test for overall group differences while controlling for type I error. Separate analyses of variance (ANOVAs) were then performed for follow-

up testing when appropriate. The dependent variables of interest during the gait trials (gait velocity, stride length, % stance, % double limb support, and step duration) were compared using a Group x Time repeated measures analysis. We used an a priori level of .05 or less. The Bonferroni procedure was used to adjust the overall type I error rate for the follow-up tests.

## RESULTS AND DISCUSSION

In this single blind study, the statistical evaluation failed to identify any Group x Time interactions or any Group or Time main effects for any of the dependent variables of interest during the GI and gait analyses. This finding is surprising considering that in follow up interview the Tai Chi participants all reported having benefited from the exercise and they perceived their balance had greatly improved. It is possible the twice-weekly exposure to the Tai Chi forms might not have been sufficient to induce a significant adaptive response. Further, the 16-week duration may not have provided sufficient time for learning of the Tai Chi forms.

## SUMMARY/CONCLUSIONS

Based on this preliminary investigation it appears that 16 weeks of Tai Chi training is not effective for inducing improved locomotor ability in patients with PD defined by the magnitude of impairment used in this study.

## REFERENCES

- Hass, C.J. et al. (2005). *Arch Phys Med Rehabil* **86**:2172-6.
- Morris, M.E. et al. (2001). *Clin Biomech* **16**, 459-470.
- Klein, P.J., Adams, W.D.(2004) *Am J Phys Med Rehabil*. **83**,735-45.

# **FLEXION-RELAXATION INDUCED CREEP DEFORMATION ALTERS PARASPINAL REFLEX RESPONSE AND RECOVERY**

Martin L. Tanaka, Ellen L. Rogers, and Kevin P. Granata

Virginia Polytechnic Institute and State University, Blacksburg, VA, USA

E-mail: granata@vt.edu Web: www.biomechanics.esm.vt.edu

## **INTRODUCTION**

Trunk flexion postures are a well recognized risk factor for low back pain.<sup>1,2</sup> Recent investigations link prolonged and/or cyclic trunk flexion to impaired neuromuscular function. Specifically, animal models show that the reflex response in the paraspinal muscles is disturbed following spine flexion.<sup>3</sup> This flexion induced neuromuscular disturbance was attributed to creep deformation of the passive tissue in the spine.<sup>4</sup> During prolonged static and cyclic lumbar flexion, viscoelastic tissues in the spine may provide resistance against flexion loading. This allows the trunk muscles to become deactivated, i.e. flexion-relaxation. The passive tissue load produces tissue laxity and creep deformation. It is indicated by an increase in relative trunk angle over time. Laxity in viscoelastic tissues may cause mechanoreceptors in the ligaments to become desensitized. As a result, their ability to monitor vertebral movements and initiate reflexive muscular action is reduced.<sup>4</sup>

The goal of this investigation was to determine the effect of prolonged flexion-relaxation and recovery time on paraspinal reflex behavior in human subjects.

## **METHODS**

A total of 25 human subjects with no history of lower back pain participated in the study. In order to record trunk muscle response and kinematics behavior, subjects were seated without trunk support in an upright posture.

A restraining belt was strapped around the subject's waist to immobilize the pelvis. A harness and cable system attached the subject to the servomotor at the T10 level of the torso.

The subjects resisted a constant isotonic flexion preload by maintaining an upright posture. Pseudorandom stochastic force perturbations ( $\pm 70\text{N}$ ) were superimposed on the preload to elicit reflexes in the paraspinal muscles. The applied forces were measured by a force transducer and electromyographic (EMG) response was recorded from surface electrodes over the right and left lumbar paraspinal muscles. A trial consisted of two ten-second force perturbation sequences during which reflexes and recorded.

Paraspinal reflexes were recorded prior to beginning static flexion-relaxation. Spinal ligament stretch was induced by having subjects lean forward to a flexion-relaxation posture while remaining seated within the pelvic restraint. This posture was held for four minutes while the trunk angle was recorded using EMG sensors. Then, the subjects returned to the upright posture and a reflex trial was recorded. The cycle was repeated four times for a total of 16 minutes of static flexion-relaxation.

A nonparametric impulse response function (IRF) was calculated from the pseudorandom force input and the rectified EMG output of the erector spinae muscles. Calculation of the IRF was based on

deconvolution techniques for a time delayed linear system response.

$$y(t) = \int_{T_1}^{T_2} IRF(\tau)x(t - \tau)dt = IRF(t) * x(t)$$

Reflex gain,  $G_R$ , was calculated from the peak of the IRF (Figure 1). Reflex gain characterizes the magnitude of muscle reflex response scaled with respect to the time dependent amplitude of the force distribution. High  $G_R$  indicates a large reflex response. The kinematics gain,  $G_K$ , was estimated from a similar analysis relating force input to torso movement.

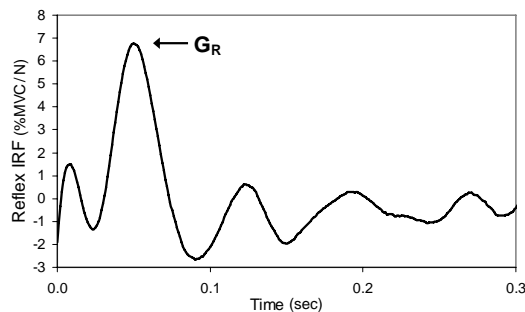


**Figure 1:** Typical IRF computed from applied trunk force (input) and rectified EMG (output). Reflex gain was computed from the peak of the IRF.

## RESULTS AND DISCUSSION

Results showed that prolonged static flexion-relaxation influenced the function of the neuromuscular system in human beings. Relative lordosis angle increased during each four minute flexion-relaxation cycle (Figure 2A) indicating creep deformation of the passive lumbar spine. In addition, lumbar paraspinal reflex gain decreased throughout the flexion-relaxation trials. Significant, but incomplete recovery occurred during the one minute between trials. However, reflex gain declined significantly after 16 minutes of flexion-relaxation (Figure 2B). The decrease in reflex gain follows the change in spinal tissue laxity. Tissue laxity can result in desensitization of neurosensors and explain the noted reduction in reflex gain.

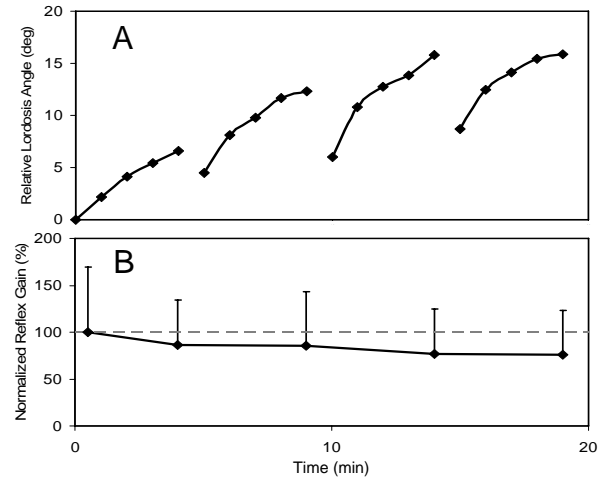


**Figure 2:** Lordosis angle increased during flexion-relaxation with significant, but incomplete recover occurring between trials (A). Reflex gain declined significantly following static flexion-relaxation (B).

## SUMMARY/CONCLUSIONS

Results confirm that prolonged static flexion-relaxation in humans results in passive tissue creep and neuromuscular changes. Reduced reflexes suggest that the spine was less stable following prolonged flexion-relaxation, and therefore, more susceptible to lower back pain and injury. Thus, extended rest may be required for full recovery. Inhibited paraspinal reflexes may contribute to the risk of lower back injury in workers using a flexed posture due to the inability of the neuromuscular system to coordinate an appropriate muscle response to an unexpected load.

## REFERENCES

- Punnett, L, Wegman, D.H., (2004). *J. Electromyogr Kinesiol*, **14**, 13-23
- Marras, W.S. et al. (1993). *Spine*, **18**, 617-28
- Solomonow, M. et al. (2003). *J. Electromyogr Kinesiol*, **13**, 381-96
- Solomonow, M. et al. (1999). *Spine*, **24**, 2426-34

# POSTURAL STABILITY IN THE YOUNG AND ELDERLY AS A CONSEQUENCE OF PERTURBATIONS

John H. Challis, Samantha L. Winter, and Dustin Quig

Biomechanics Laboratory, Department of Kinesiology, The Pennsylvania State University,  
University Park, PA, USA  
E-mail: jhc10@psu.edu

## INTRODUCTION

The elderly are the most rapidly increasing proportion of society (Fuller, 2000). A major problem confronting this cohort is their susceptibility to falls (Jantti et al., 1995). A number of studies have demonstrated a link between postural stability in quiet standing and the ability to avoid falls (e.g., Fernie et al., 1982; Wolfson et al., 1985). During upright stance the maintenance of balance can become problematic, particularly for the elderly, if a simultaneous cognitive task is performed (Rankin et al., 2000). Given that in many everyday activities postural perturbations occur while also performing a cognitive task, understanding more about the response under such conditions is important.

The purpose of this study was to examine stability in both young and older subjects when postural perturbations are combined with a cognitive task. In particular the focus was on how long it takes to re-establish stability after a postural perturbation.

## METHODS

Two groups of 10 subjects were recruited for this study, a young group between the ages of 21 and 25 years old (age -  $22.50 \pm 1.35$  years; height -  $1.70 \pm 0.10$  m; mass -  $70.86 \pm 8.33$  kg), and a young-old group between the ages of 65 and 73 years old (age -  $69.8 \pm 3.05$  years; height -  $1.67 \pm 0.12$  m; mass -  $66.36 \pm 13.6$  kg). All subjects provided informed consent. Subjects were

medically screened to ensure they had no medical problems which could affect their balance.

Subjects performed three trials of four different standing tasks. They adopted the same standardized foot position for all trials on a force plate (Kistler, Model 9287A), from which center of pressure (COP) data were sampled at 500 Hz. The tasks were quiet standing (task 1), a mechanical perturbation achieved by dropping a 1 kg mass (task 2), a cognitive perturbation achieved by performing mental arithmetic (task 3), and finally a task which combined both a mechanical and cognitive perturbation (task 4). The specific conditions for each task were,

**Task 1** – quiet standing on a force plate for 30 seconds.

**Task 2** - quiet standing on a force plate while holding a mass (1.0 kg) at arms length for 20 seconds then on a signal dropping the mass and maintaining balance for a subsequent 40 seconds (Perturbation Task).

**Task 3** – as task 1, but during the task counting backward from 100 in jumps of 3 for 30 seconds (Cognitive Task).

**Task 4** – as task 2, but during the task counting backwards from 100 in jumps of 3 (Perturbation and Cognitive Task)

For tasks 1 and 3 the motion of the COP was quantified in the anterior posterior direction by computing its standard deviation, and range of motion. For tasks 2 and 4 the motion of the COP in the anterior posterior direction, after mass release, was quantified

by computing its range of motion, peak velocity, and time to stability. Time to stability was defined as the time to that instant at which the absolute velocity of the COP was maintained below a criterion value. The criterion value was the mean plus four times the standard deviation of the absolute velocity of the COP during task 1. Repeat measures analysis of variance was used to examine differences between the two groups, and the tasks ( $\alpha = 0.05$ ).

## RESULTS AND DISCUSSION

During quiet standing, task 1, there was no statistically significant difference between the two groups of subjects for the measured parameters. This lack of a difference persisted when the subjects were asked to simultaneously perform a cognitive task. There were statistically significant changes in the COP motion for both groups when the cognitive activity was added to quiet standing. These results indicate that the populations studied responded similarly for these two tasks.

After release of a mass, task 2, the young-old group demonstrated greater peak velocity compared with the young, but had similar COP ranges of motion, and times to obtain a stable stance. When a cognitive challenge was added (task 4), the young-old had a statistically significant different peak velocities, and greater times to stability than

the young group. Time to stability was statistically greater for both subject groups for task 4 compared with task 2.

These results indicate that older subjects are more influenced during quiet standing by perturbations to their stability if they are also performing a cognitive task. When there are simultaneous physical and cognitive challenges it takes much longer for the young-old subjects to return to a stable posture. The time duration for this re-establishment of normal levels of postural stability (30 seconds) may be the source of guidelines for the elderly when being advised about recovering from perturbations. It would be interesting to examine the effect of another perturbation during this period of regaining stability. These results will be of interest to clinicians interested in establishing 'biomarkers' of diminished motor control in the elderly.

## REFERENCES

- Fernie, G. R., et al. (1982). *Age Ageing*, **11**(1), 11-16.
- Fuller, G. F. (2000). *Am. Fam. Physician*, **61**(7), 2159-2168.
- Jantti, P. O., et al., (1995). *Aging (Milano)*, **7**(1), 23-27.
- Rankin, J. K., et al. (2000). *J. Gerontol. A Biol. Sci. Med. Sci.*, **55**(3), M112-119.
- Wolfson, L., et al. (1995). *J. Gerontol. A Biol. Sci. Med. Sci.*, **50** Spec No, 64-67.

**Table 1:** Mean  $\pm$  standard deviation of metrics of the COP motion for the different tasks.

Variable	Task 1		Task 3	
	Young	Young-Old	Young	Young-Old
Standard Deviation (mm)	5.2 $\pm$ 2.3	4.3 $\pm$ 2.26	6.1 $\pm$ 2.1	6.5 $\pm$ 2.4
Range of Motion (mm)	15.5 $\pm$ 7.0	9.4 $\pm$ 4.5	33.9 $\pm$ 12.5	32.5 $\pm$ 11.5
	Task 2		Task 4	
	Young	Young-Old	Young	Young-Old
Range of Motion (mm)	37.3 $\pm$ 18.5	46.8 $\pm$ 15.0	31.5 $\pm$ 12.1	41.2 $\pm$ 14.7
Peak Velocity (mm/s)	81.0 $\pm$ 36.9	162.4 $\pm$ 94.8	72.1 $\pm$ 29.4	114.1 $\pm$ 54.8
Time to Stability (s)	20.2 $\pm$ 11.2	19.6 $\pm$ 13.0	21.3 $\pm$ 10.0	30.1 $\pm$ 10.9

# MEASURING HUMERAL HEAD TRANSLATION USING FLUOROSCOPY: A VALIDATION STUDY

Jun G. San Juan and Andrew R. Karduna

University of Oregon, Eugene, OR, USA  
E-mail: bsanjuan@uoregon.edu

## INTRODUCTION

Humeral translation is an important mechanism believed to be associated with several shoulder pathologies. For example, abnormal superior translation of the humeral head is believed to be one of the major causes of shoulder impingement syndrome (Deutsch, 1996; Wong, 2003). In order to detect abnormal translations of the humeral head, a precise and accurate measurement is necessary.

There are numerous techniques used to monitor humeral head translation. The most common techniques utilized include roentgenogram (X-ray), and magnetic resonance imaging (MRI). Fluoroscopy, which is an imaging technique based on x-ray technology, is also commonly utilized to allow real time digital collection of images (Livyatan, 2003; Pfirrmann, 2002).

There is a scarcity of research looking at the accuracy of imaging techniques in monitoring translations of the humeral head. Therefore, the purpose of this study was to assess the accuracy of fluoroscopy in measuring humeral head translation in cadaver bones. In particular, we wanted to determine projection errors associated with motion perpendicular to the field of view of the fluoroscope.

## METHODS

Eight glenohumeral joints were harvested from two female and two male human cadavers. All the muscles, ligaments, capsules, labrum, and tendons surrounding the shoulder girdle were detached and only the scapula and the humerus were preserved. A GE (OEC) 9800 fluoroscopy unit was used to monitor the translation of the humeral head.

A shoulder jig was utilized to secure the scapula and the humerus (Figure 1). The specifically designed jig enabled the scapula to be manipulated, allowing it to move with three degrees of freedom (i.e. anterior/posterior tilt, upward/downward rotation, internal/external rotation). The humerus was mounted on a translation device that enabled the investigator to move the bone in millimeter increments.



**Figure 1:** Shoulder Jig

During data collection, the scapula was placed in a predetermined position, based on a previous study, which mimics the position of the scapula when the arm is abducted, *in-vivo*. The humerus was superiorly translated in 2 mm increments, and fluoroscopic images were taken. A total of three images per scapular position were collected while the humerus was at 90 degrees of abduction in the scapular plane. An arc on the humeral head was digitized and was used to calculate the geometric center. Additionally, the mid-distance between two digitized points on the glenoid face served as the origin of translation of the geometric center.

## RESULTS AND DISCUSSION

The error for a given translation was defined as the difference between the known translation and the measured translation. The difference between the two translations was then used to calculate the root mean square (RMS) errors.

During humeral head translation, when the scapula was at neutral position the lowest error was recorded at 0.48 mm (Figure 2).

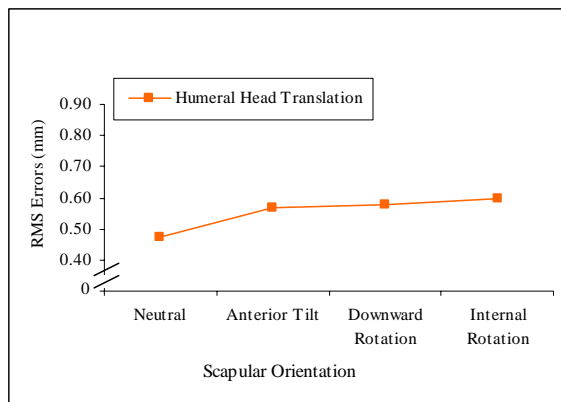


**Figure 2:** Measured humeral head translation root mean square error for different scapular positions.

The largest error was recorded when the scapula was positioned in downward rotation and internal rotation, 0.58 and 0.60 mm, respectively. The results suggest that when the scapula is in plane (i.e. neutral) from the view of the fluoroscope, the amount of measured translation error is less. The amount of error recorded range between 0.48 – 0.60 mm across scapular orientations.

## SUMMARY/CONCLUSIONS

The error measured for this preliminary study is larger than expected. Further analysis will be performed by the investigator to determine the source of error generated by this technique. To our knowledge, this is the only study that has validated the measuring technique using 2-D imaging.

## REFERENCES

- Deutsch, A., et al. (1996). *J Shoulder Elbow Surg*, **5**(3), 186-93.
- Livyatan, H., et al. (2003). *IEEE Trans Med Imaging*, **22**(11), 1395-1406.
- Pfirschmann, C.W., et al. (2002). *Invest Radiol*, **37**(2), 73-76.
- Wong, A.S., et al. (2003). *J Shoulder Elbow Surg*, **12**(4), 360-364.

## ACKNOWLEDGEMENTS

Pain Consultants of Oregon, Eugene, OR for the use of the fluoroscope unit. Annie Fetcher and Linden Lee for technical assistance.

# INSIGHT INTO MUSCLE FUNCTION DURING GAIT PROVIDED BY MUSCLE-INDUCED ACCELERATIONS PER UNIT ACTIVATION

Saryn R. Goldberg, Karen Lohmann Siegel, and Thomas M. Kepple

Physical Disabilities Branch, National Institutes of Health, Department of Health and Human Services, Bethesda, MD, USA

email: [goldbergs@cc.nih.gov](mailto:goldbergs@cc.nih.gov), web: <http://pdb.cc.nih.gov>

## INTRODUCTION

Muscle-induced accelerations provide insight into how individual muscles contribute to an observed motion. In some previous studies, a muscle's action at a joint has been normalized by muscle force to calculate the relative potential of a muscle to contribute to motion per unit muscle force (Arnold et al. (2005), Kimmel et al. (2006)). However, because muscle force is a function of muscle activation, length, and shortening velocity, examining muscle-induced accelerations per unit muscle force does not take into account the relative capacity of individual muscles to produce force and how this capacity changes during a movement. By calculating muscle-induced accelerations per unit activation, the resulting values reflect the capacity of a muscle to produce force throughout a movement, as well as the potential of the muscle to accelerate a joint at each instant due to its moment arm(s) and the dynamics of the system. In the present study, we calculated muscle-induced accelerations per unit activation for the major lower extremity muscles active during normal stance phase. By examining these values together with a subject's EMG data, the strategies that the individual used to execute the movement, as well as feasible alternative strategies, can be analyzed.

## METHODS

Motion capture and force platform data were collected from a single subject (male, 180 cm, 74 kg) walking at a self-selected speed.

Surface EMG was collected for 8 right lower extremity muscles. Three trials were collected and a single representative trial was analyzed from right foot-flat to toe-off.

Segment positions and orientations were obtained from the motion capture data and input into a 3D model that included 8-segments and Hill-type musculotendon actuators representing the major lower extremity muscles (based on Delp et al. (1990)). Using SIMM (Musculographics, Inc.), each muscle was individually given a maximum activation of 1.0 and the resulting joint moments were recorded. These joint moments take into account the force-generating capacity of each muscle at the lengths and shortening velocities reached throughout the measured stance phase.

An identical model (without the muscles but with the same geometry) was created using SDFast (Symbolic Dynamics, Inc.). The model was positioned according to the measured stance phase joint angles, the joint moments corresponding to a unit activation in each muscle were applied individually, and the resulting joint accelerations were calculated. The model was constrained so that each foot was fixed to ground during foot-flat. After heel-off, each foot was allowed to rotate about a medial/lateral pin joint passing through the measured center of pressure. Joint moments corresponding to activations less than 1.0 were also calculated and found to scale with activation within approximately 10%.

## RESULTS AND DISCUSSION

Vasti and soleus have the most potential to accelerate all three major lower extremity joints (Fig. 1a-b, ankle data not shown). This is due to a combination of their large physiological cross-sectional areas (PCSA) and effective configurations for dynamic coupling. Soleus reached its peak potential in mid-stance, when vasti was at its minimum. The gluteus muscles had less potential to accelerate the hip and knee than expected for their PCSA; this is likely due to their less than optimal muscle lengths and shortening velocities in stance. The biarticular muscles were found to have little potential to accelerate the major joints of the body due to the oppositional dynamic coupling of their moment arms at each joint.

Analyzing the calculated muscle potentials in conjunction with the measured EMG data suggest control strategies similar to those found from computer simulation studies that calculated muscle-induced accelerations during gait (Arnold et al.(2005), Neptune et al. (2004)). The current technique provides some insight into muscle function without requiring the complexity of computer simulation and, unlike the unit force approach, the unit activation method takes into account the changing capacity of a muscle to produce force during a movement. While EMG does not scale directly with activation, this technique can provide information about the strategies that an individual used during gait, as well as possible alternative available strategies.

## REFERENCES

- Arnold A.S., et al. (2005) *J Biomech*, **38**, 2181-2189.
- Delp S.L., et al. (1990) *IEEE Trans Biomed Eng*, **37**, 757-767.
- Kimmel S.A., Schwartz M.H. (2006) *Gait & Posture*, **23**, 211-221.

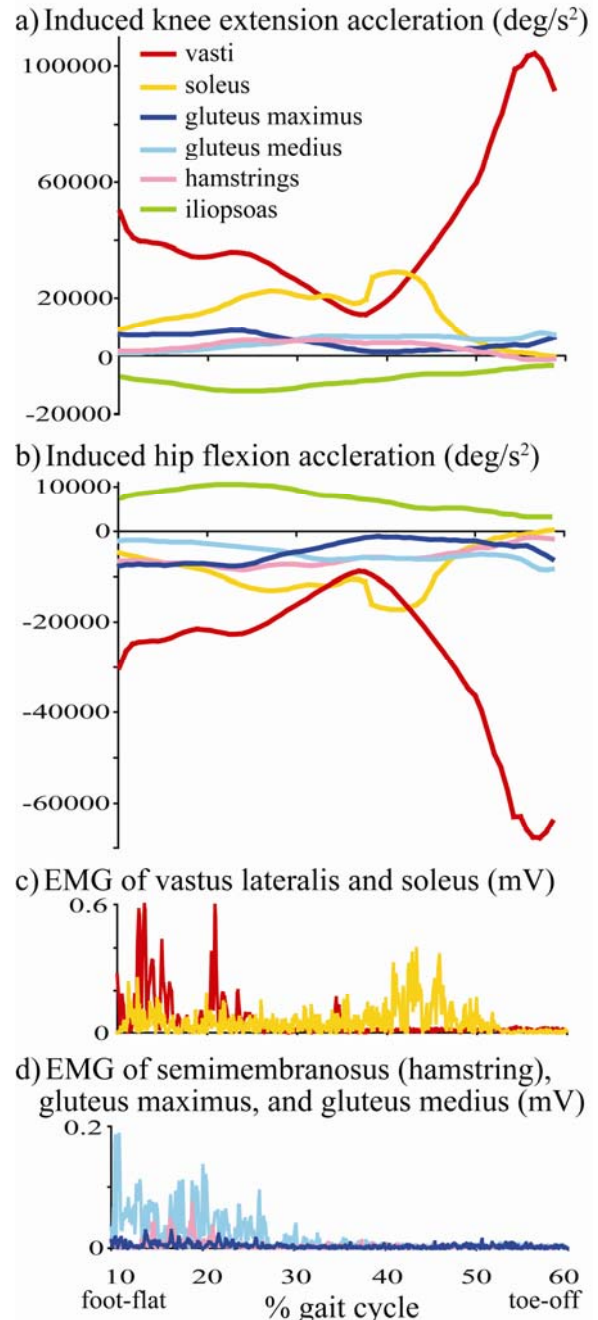


**Figure 1.** a) Knee and b) hip accelerations due to unit activation in each muscle and c-d) measured muscle excitations.

Neptune R.R., et al. (2004) *Gait & Posture*, **23**, 194-205.

## ACKNOWLEDGEMENTS

Thanks to Stephanie Baker and Alex Razzook for assistance with data collection.

# MODELING INVESTIGATION OF BICEPS BRACHII SURFACE EMG

David A. Gabriel

Brock University, St. Catharines, ON, Canada L2S 3A1

E-mail: dgabriel@brocku.ca

## INTRODUCTION

An increase in root-mean-square (RMS) amplitude and a decrease in mean frequency (MNF) of the surface electromyographic (SEMG) signal have been reported for maximal voluntary contractions (MVCs) of the elbow flexors (Bilodeau et al., 1992). This may be due to high levels of rate-coding and/or synchronization of motor units (MUs). An SEMG model was used to investigate the MU firing patterns underlying the biceps brachii (BB) SEMG signal during MVCs.

## METHODS

**Model Description:** The first derivative of the intracellular action potential was convolved with the impulse response function of the anisotropic volume conductor to generate the single muscle fiber action potential (Dimitrov & Dimitrova, 1989). Muscle fiber semilength was 70 mm. Bipolar, square electrodes were placed between the endplate and tendon (Figure 1). There were 5 radial electrode locations above the muscle (0, 2, 4, 6, and 8 mm).

There was variability in muscle fiber activation times ( $17 \pm 5.5$   $\mu$ sec), endplate location ( $\pm 3$  mm) and tendon insertion ( $\pm 6$  mm) within the MU. There were 120 MUs. The numbers of fibers per MU increased exponentially from 26 for MU 1 to 2,510 for MU 120 (Keenan et al., 2005). Conduction velocity was related to MU size and increased exponentially from 2.5 to 5.5 m/s. The MU territories were randomly located without constraint within the circular cross-

section of a muscle (radius=8.67 mm). There were 50 different random locations for each MU within the muscle.

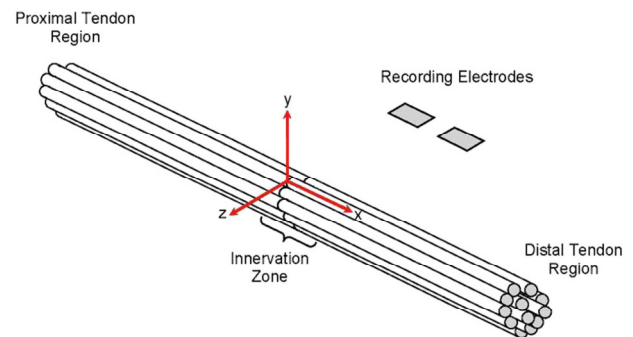


**Figure 1:** Coordinate system used for the generation of muscle fiber action potentials.

The recruitment, rate-coding and synchronization schemes established by Fuglevand et al. (1993) and Yao et al. (2002) were used to generate MU firing times. Recruitment of BB MUs was up to 88% of MVC. Maximum firing rate for MU #1 was 30 Hz; it then decreased so that the peak firing rate difference (PFRD) between low and high threshold MUs was 10 Hz. Firing rate variability was set at 15%. For the synchronization, the time separation between synchronized MUs was  $0 \pm 2$  ms. The MU action potential trains were then summed to create the synthetic SEMGs.

Neural drive was modeled as an excitation level wherein all MUs were assumed to receive the same input. The excitation function increased at a rate that allowed the target level to be achieved within one second; it was then maintained for another two seconds. The target levels were 40, 60, 80 and 100% of excitation. Two MU firing

patterns were evaluated: (1) high rate-coding and (2) moderate rate-coding with low synchronization. The simulations were completed in MATLAB (The Math Works, Natick, MA). Data reduction was the same as that for the experimental data.

**Experimental data:** Thirty-six subjects performed three 5-second isometric actions of the elbow flexors at 40, 60, 80 and 100% of MVC. There was five minutes of rest between each contraction, and the order of presentation was randomized. Force was measured with the JR3 load cell (JR3 Inc., Woodland, CA). Biceps SEMG was monitored with bipolar Ag/AgCl electrodes. The SEMG signals were amplified (1000 $\times$ ) and band-passed filtered (3-1000 Hz) before A/D conversion at 2 kHz on a Pentium III IBM-PC. The RMS and MNF were calculated on a 1-second stationary portion of the signal in MATLAB (The Math Works, Natick, MA).

## RESULTS AND DISCUSSION

The MNF remained stable at  $81 \pm 14$  Hz between 40 and 80% of MVC. It then decreased ( $p < 0.05$ ) to  $73 \pm 14$  Hz at 100% of MVC. This spectral compression was evident in the frequency spectra (Figure 2, right panel, thick line). The RMS values exhibited a quadratic ( $p < 0.05$ ) increase from  $0.28 \pm 0.2$  mV to  $1.28 \pm 0.63$  mV. The MNF and RMS means, and their pattern of change was consistent with the work of Durkin and Callaghan (2005).

High rate-coding was simulated by decreasing the PFRD from 10 to 5 Hz at 100% of MVC. The MNF and RMS for the synthetic SEMGs followed the experimental data, but the decrease in MNF at 100% of MVC was not as pronounced. Moderate rate-coding with low synchronization was simulated by decreasing the PFRD to 7 Hz at 100% of excitation. A synchronization

level of 4% was added at the maximum excitation level. The MNF and RMS for the synthetic SEMGs followed the experimental data from 40 to 80% of MVC. The two superimposed MU firing patterns were further able to reproduce the marked decline in MNF at 100% of MVC.

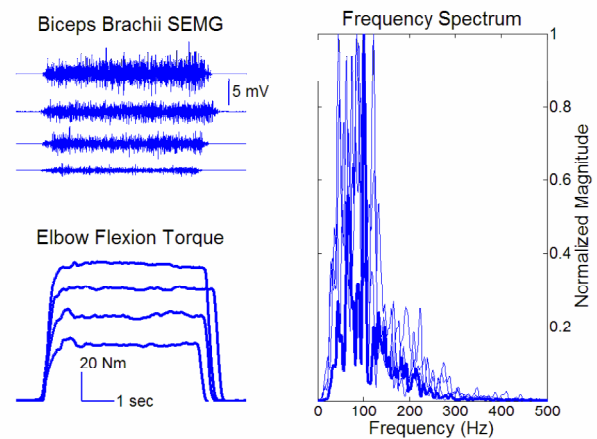


**Figure 2:** Representative data for one subject.

## SUMMARY/CONCLUSIONS

Moderate rate-coding with low synchronization described the experimental SEMG activity better than high rate-coding alone.

## REFERENCES

- Bilodeau M, et al. (1992). *Med. Biol. Eng. Comput.*, **30**, 640-644.
- Dimitrov, GV, Dimitrova, NA (1989). *Med. Eng. & Phys.*, **20**, 371-381.
- Fuglevand AJ, Winter DA, Patla AE. (1993). *J. Neurophysiol.*, **70**, 2470-2488.
- Keenan KG, Farina D, Maluf K, et al. (2005). *J. Appl. Physiol.*, **98**, 120-131.
- Yao W, Fuglevand AJ, Enoka RM. (2002). *J. Neurophysiol.*, 2000, **83**, 441-452.

## ACKNOWLEDGEMENTS

Funded by the NSERC of Canada.

# The Effect of Manipulating Subject Mass on Ground Reaction Force During Locomotion

John K. DeWitt<sup>1</sup>, Ronita L. Cromwell<sup>2</sup> and R. Donald Hagan<sup>3</sup>

<sup>1</sup>Bergaila Engineering Services, Houston, TX, USA; <sup>2</sup>The University of Texas Medical Branch, Galveston, TX, USA; <sup>3</sup>NASA Johnson Space Center, Houston, TX, USA  
email: john.k.dewitt@.nasa.gov

## INTRODUCTION

During spaceflight, astronauts perform locomotive exercise to produce ground reaction forces (GRF) beneficial for maintenance of the musculoskeletal system. However, Schaffner et al. (2005) found that regardless of external load, GRF during walking and running in microgravity are less than those generated during locomotion at similar speeds in normal gravity. Adding mass to an astronaut could increase the GRF by increasing the forces necessary to accelerate and decelerate their center of mass.

To assess the effects of added mass during locomotion, an unweighting system can be used in combination with a weighted vest to create test conditions in normal gravity where effective body weight remains constant while mass is manipulated. Using this approach, Chang et al. (2000) found that when running at  $3.0 \text{ m}\cdot\text{s}^{-1}$ , GRF magnitude did not change with additional masses of up to 125% of normal body mass. However, it is possible that they did not utilize large enough mass increases to illicit changes. Also, it is not known if their results would be similar for walking.

The purpose of this investigation was to examine the effects of increasing mass upon GRF during walking and running. We hypothesized that GRF parameters would increase during walking and running as mass increased.

## METHODS

Vertical GRF was measured for ten subjects (5M/5F) during walking ( $1.34 \text{ m}\cdot\text{s}^{-1}$ ) and running ( $3.13 \text{ m}\cdot\text{s}^{-1}$ ) on a Kistler Gaitway treadmill (Amherst, NY). Each speed condition was completed on separate days. Subjects completed one minute of locomotion at each of 5 added mass (AM) conditions (0%, 10%, 20%, 30% and 40% of body mass) in random order. During each condition, mass was increased by having subjects wear a weighted vest (X-Vest, Perform Better, Cranston, RI) to increase mass. Weight was adjusted to initial body weight using an H/P/Cosmos Airwalk (Nussdorf-Traunstein, Germany) pneumatic unweighting system.

Ten consecutive strides at the beginning of each trial were analyzed. Peak impact force (PI), peak propulsive force (PP), and stride time (ST) were measured for each stride. Loading rate (LR) was computed as the slope of the GRF trajectory between heel strike and PI. Trial means for each variable were computed for each condition.

An analysis of variance with repeated measures was used to determine if PI, PP, ST and LR were affected by AM condition. Tukey-Kramer post-hoc tests were used to determine differences when a significant AM effect was found. Significance was achieved a  $p < .05$ .

## RESULTS AND DISCUSSION

Each dependent variable was affected by AM condition during walking; all variables except PP were affected by AM condition during running. The data suggest that the body reacts to the addition of mass differently depending on gait type (See Figures 1a-1d).

PI and LR were less during walking than during running. PI and LR increased during walking up to 30% AM, and decreased during running up to 40% AM. PP decreased with AM during walking, but remained constant during running. This suggests that during walking, maintenance of ST is an important factor in adapting to AM. However, during running, minimizing PI and maintaining PP appear to be important to adapting to AM.

## SUMMARY/CONCLUSIONS

Our findings suggest that when mass is increased while maintaining body weight, change in GRF are different for walking and running. There may be differing control mechanisms responsible for walking with added mass as compared to running. Further study is necessary to determine if similar differences occur in microgravity.

## REFERENCES

- Schaffner, G. et al. (2005). *NASA/TP-2005-213169*.  
 Chang, Y.H.. et al. (2000). *J. Exp Biol*, **203**, 229-238.

## ACKNOWLEDGEMENTS

Supported by the Exercise Countermeasure Project at NASA Johnson Space Center. Thanks to EXL personnel for their aid during data collection

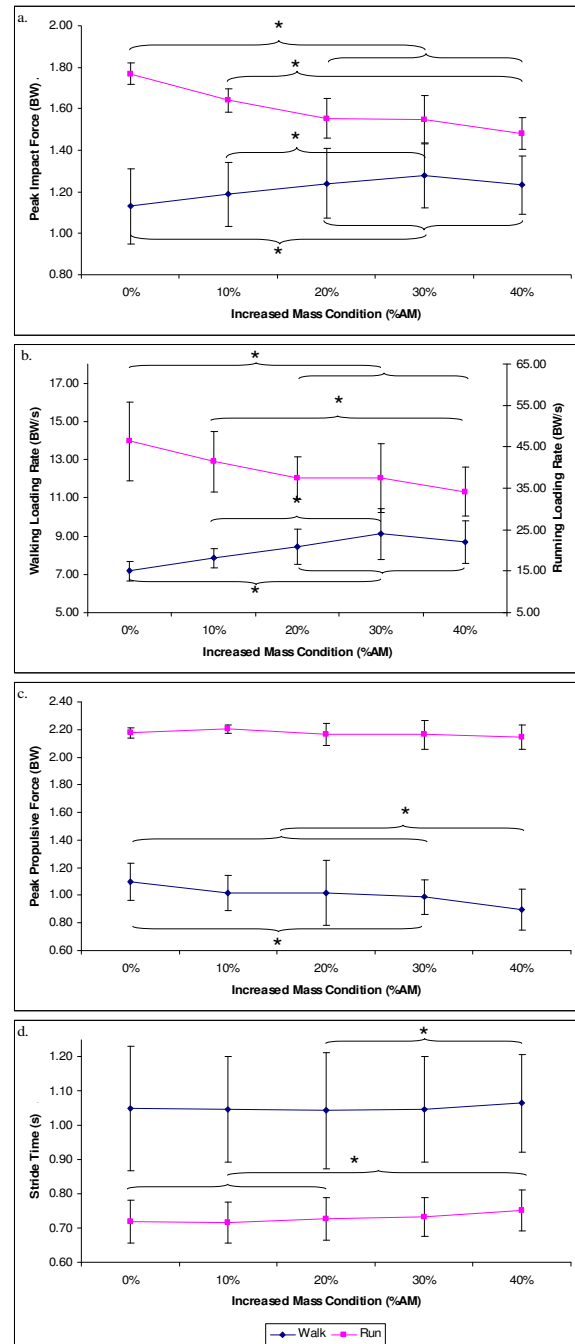


**Figure 1:** Peak impact force (a), loading rate (b), peak propulsive force (c) and stride time (d) during locomotion with increased mass. \*p<.05.

# FOREFOOT, REARFOOT AND SHANK COUPLING: EFFECT OF VARIATIONS IN FOOT STRIKE PATTERN

Michael B Pohl<sup>1</sup> and John G Buckley<sup>2</sup>

<sup>1</sup> Centre of Sport & Exercise Sciences, University of Leeds, UK

<sup>2</sup> Vision & Mobility Lab, Department of Optometry, University of Bradford, UK

Email: pohl@udel.edu

## INTRODUCTION

The coupling between movements of the foot and tibia during gait has been suggested to be linked with lower limb overuse injuries. There is growing evidence that motion at the midfoot contributes significantly to overall foot motion during walking and running (Pohl et al., 2006). Despite this, studies examining both midfoot and subtalar joint coupling during gait are rare. Given the potential link between injury and lower extremity coupling, there is a need to investigate normal coupling patterns from which injured populations can then be compared to.

Foot strike pattern can vary between individuals during running and has been shown to significantly affect rearfoot eversion (Stacoff et al., 1989). If changes in rearfoot eversion alter shank and forefoot kinematics in a similar manner, coupling should not be influenced. The aim of this study was to assess the robustness of coupling between the forefoot, rearfoot and shank as foot strike pattern was altered. It was hypothesized that the kinematic coupling between the forefoot, rearfoot and shank would be similar.

## METHODS

Twelve injury free subjects participated in over-ground running using three different foot strike patterns: a heel strike condition

(HFS) where the heel was the first part of the foot to touchdown; a forefoot strike condition (FFS) where the forefoot was the first part of the foot to touchdown, with the heel subsequently making contact with the ground; and a toe running condition (TFS) where the forefoot was the first part of the foot to touchdown but the heel remained off the floor throughout the whole of stance.

Markers placed on the shank (tibia and fibula), rearfoot (calcaneus) and forefoot (metatarsals) were used to determine 3-D kinematics. Rearfoot motion was expressed relative to the shank (subtalar joint), and the forefoot relative to the rearfoot (midfoot joints). Data were captured using a seven-camera-system (ProReflex).

To examine the continuous coupling between adjacent segments, kinematic data for one segment was compared to kinematic data for the adjacent segment using a cross correlation technique. This approach was used to determine the coupling between the segmental rotations shown in Table 1.

## RESULTS AND DISCUSSION

Coupling between rearfoot EVE/INV and shank IR/ER was consistently high regardless of foot strike pattern (Table 1). This was also the case for coupling between rearfoot EVE/INV and both forefoot PF/DF and forefoot ABD/ADD. This suggested a kinematic link between rearfoot frontal

plane motion and motion about the midtarsal joint. In addition, the coordinated sagittal and transverse movements of the forefoot lend support to the proposed oblique axis of the midtarsal joint (Manter, 1941).

The lack of coupling between rearfoot EVE/INV and forefoot EVE/INV across all foot strike patterns indicates that frontal plane motion of the forefoot has limited affect on the rearfoot frontal plane motion and vice versa. However, this may be due to greater degrees of freedom between the articulations of the midfoot and forefoot in the frontal plane.

Overall there were no differences in cross-correlations between foot-strike conditions. However, during HFS running, there was less rearfoot eversion during the initial 15% of stance compared to both FFS and TFS running (Figure 1). This meant that less rearfoot EVE was transferred into shank IR during this period of stance in the HFS condition. There was also reduced forefoot dorsiflexion excursion occurring during the first 15% of stance (Figure 1), which suggested that the midtarsal joint can influence the transfer of movement between the rearfoot and shank. This altered coupling is masked when taking average cross-correlations across the entire stance phase. We are currently in the process of examining coupling in smaller sub-phases of the stance phase to gain a greater understanding of the relationship.

## SUMMARY

Forefoot PF/DF and ABD/ADD were highly coupled with rearfoot EVE/INV regardless of foot strike pattern. This suggests forefoot motion can influence subtalar joint kinematics and vice versa.

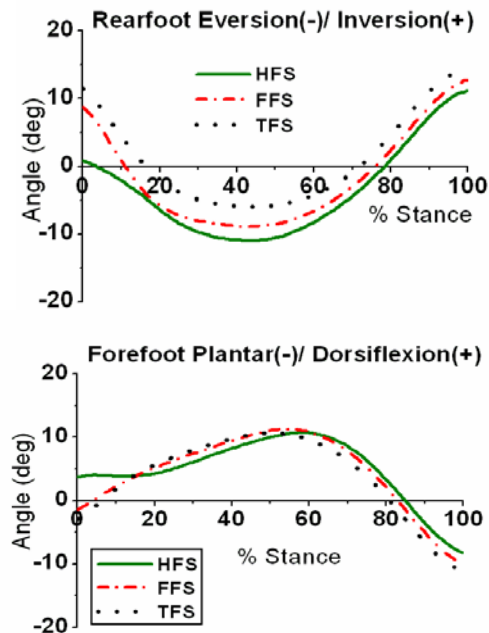


**Figure 1:** Angular displacement curves of rearfoot eversion/ inversion (top) and forefoot plantar/ dorsiflexion (bottom) during heel strike, forefoot strike and toe running conditions. The ensemble means are shown for all subjects.

## REFERENCES

- Manter, J.T. (1941). *Anatom. Rec*, **80**, 397-410.  
 Pohl, M.B. et al. (2006). *Clin. Biomch*, **21**, 175-183.  
 Stacoff, A. et al. (1989). *Int. J. Sp. Biomch*, **5**, 375-389.

**Table 1:** Mean (SD) coupling (cross-correlation) between rearfoot eversion/inversion and shank internal/external rotation and forefoot motion in each plane.

Variables	HFS	FFS	TFS
Rearfoot EVE/INV _ Shank IR/ER	<b>0.930</b> (0.066)	<b>0.918</b> (0.082)	<b>0.961</b> (0.027)
Rearfoot EVE/INV _ Forefoot PF/DF	<b>-0.930</b> (0.066)	<b>-0.939</b> (0.043)	<b>-0.853</b> (0.113)
Rearfoot EVE/INV _ Forefoot EVE/INV	<b>-0.021</b> (0.520)	<b>-0.213</b> (0.452)	<b>0.314</b> (0.396)
Rearfoot EVE/INV _ Forefoot ABD/ADD	<b>0.953</b> (0.039)	<b>0.952</b> (0.043)	<b>0.947</b> (0.048)

# IN VIVO EXAMINATION OF KNEE VARUS/VALGUS STIFFNESS: THE EFFECT OF WEIGHT BEARING

Anastasios D. Tsoumanis<sup>2</sup> and Yasin Y. Dhaher<sup>1</sup>

<sup>1</sup>Department of Biomedical Engineering, Northwestern University, Chicago, IL, USA

<sup>2</sup>Department of Biomedical Engineering, Illinois Institute of Technology, Chicago, IL, USA

E-mail: [tsouana@iit.edu](mailto:tsouana@iit.edu) or [a-tsoumanis@northwestern.edu](mailto:a-tsoumanis@northwestern.edu)

## INTRODUCTION

It has been proposed that increased compression loading at the human knee results in an increased resistance to varus/valgus motion (Olmstead et al, 1985; Markolf et al, 1978). It has also been shown in cadaveric models that an increase in joint compression forces resulted in a significant increase of the joint's intrinsic varus/valgus stiffness (Markolf et al, 1981). It was concluded that increased load bearing at the knee, increases the contribution of the passive structures to joint stiffness. These findings may have been confounded by methodological issues. For example, in all of the aforementioned studies, the moment contribution at the knee joint due to the applied load was not subtracted from the overall torque observed at the knee. It is reasonable to assume that these contributions are small due to the small angular excursions used. However, these contributions may be significant when compared to the contributions of the joint passive tissues to the recorded coronal plane torque especially at or near the physiological range of the joint varus/valgus movements. Accordingly and to the contrary of previously reported effects, we propose that the presence of external compression loads at the joint results in a decrease in the contribution of the passive tissues to the joint's intrinsic varus/valgus stiffness. We further hypothesize that this reduction of the intrinsic joint stiffness can be recovered with an appropriate muscle activation patterns.

## METHODS

We tested 11 healthy subjects. Part of the experimental set-up has been presented previously (Dhaher et al, 2003). In the present study subjects were standing upright with their left leg placed on a customized

position-fixed platform. A customized full body orthosis was fitted to our subjects to minimize possible movements of their upper body (including the hip joints, torso and left leg), during the rapid perturbations applied at the right knee. The subject's right knee was attached to a servomotor system and it was pre-loaded in the valgus direction to ensure initial stretch of passive tissues. Each subject was asked to provide 3 weight-bearing force levels as a percent of their body weight (%BW) (0, 15 & 30%) and 3 different muscle activation levels (0, 10-15 and 25-30% of each subject's MVC). Multiple 7° rapid (60°/s) valgus step inputs were applied at the knee at all load-bearing levels. At least 5 trials per condition were applied. The force and torque signals for each trial were collected using a 6-DOF-load cell. EMG activity was recorded from 8 knee muscles of the perturbed limb, using surface electrodes.

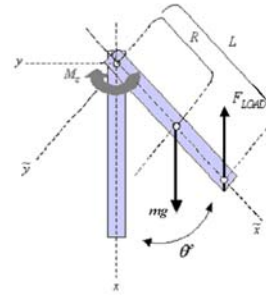


**Figure 1:** Mathematical model of the knee

A 2<sup>nd</sup> order model of the knee and lower limb mechanics was used in the form:

$$I \cdot \ddot{\theta} + B(\eta) \cdot \dot{\theta} + K(\eta) \cdot \theta + mgR \sin(\theta) - F_{load} L \sin(\theta) = M_z \quad (1)$$

where  $\eta$  defines the targeted BW level;  $M_z$  is the joint's measured varus/valgus torque (output), and  $\theta$  is the knee varus/valgus angle (input). The inertia,  $I$ , stiffness,  $K(\eta)$ , and damping,  $B(\eta)$  represent the intrinsic mechanics. In addition  $g$  is the gravitational acceleration,  $m$ ,  $R$  and  $L$  are the mass the radius of gyration and the lower limb length respectively (estimated using predictive

regression equations from Zatriosky and Seluyanov (1985)) while  $F_{load}$  is the force provided by the subject at each BW level. A nonlinear least squares optimization technique was used to estimate  $I$ ,  $B$  and  $K$  at the different load bearing conditions. The model was cross-validated with simulations based on fresh data not used in the estimation procedure. After the completion of the perturbation experiments, subjects were asked to maintain the varus/valgus stiffness estimated at no load during the other load bearing conditions with self-determined muscle activation patterns at the knee.

## RESULTS AND DISCUSSION

Our preliminary results show a significant decrease in joint intrinsic varus/valgus stiffness ( $p < 0.01$ ) as a function of BW force across all subjects (Figure 2).

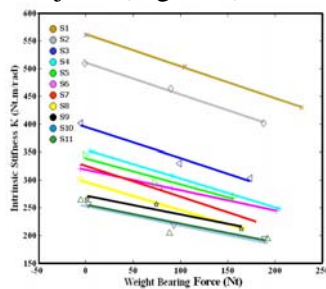


**Figure 2:** Intrinsic joint stiffness estimates as a function of BW force.

Figure 3 shows the group mean fit of the ensemble average data of all subjects. The figure also shows that, for a representative subject (S1), the reduction in joint intrinsic stiffness is recoverable with knee muscle activations. Subject S1 was able to increase its joint stiffness to the level estimated at the no load bearing state for the different loading levels.

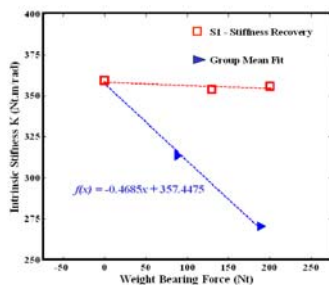


**Figure 3:** Group mean fit and S1 stiffness recovery as a function of BW force.

While there was an equal incremental increase in BW force from the no load

condition (0-15% & 15-30% BW), the subject used two different activation patterns for the different BW forces to maintain the level of joint stiffness similar to the stiffness estimated during the no loading condition (Figure 4).

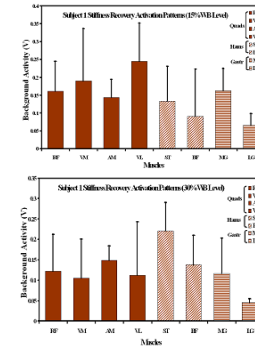


**Figure 4:** Muscle activation patterns for two BW force levels (bars show mean +/- SD).

## SUMMARY

Our results reveal that compressive loads result in a significant decrease of the joint's varus/valgus stiffness. Contrary to earlier findings, we believe that the increase in compression loads results in a decrease in the origin-to-insertion distance of passive tissues in the joint. This decrease can potentially deactivate different portions of the respective tissues and hence compromise the contributions of the tissues to the overall intrinsic joint stiffness. Moreover, we observe that increase in the muscle activation levels can be used as a compensatory mechanism to overcome the reduction in joint stiffness due to load bearing. These findings reemphasize the role of muscular contractions in the active varus/valgus stabilization of the joint under load bearing conditions.

## REFERENCES

- Dhaher et al. (2003), *J.Biomech*, **3**, 199-209
- Olmstead et al. (1986), *J.Biomech*, **19**, 565-77
- Markolf et al, (1981), *JBJS*, **64A**: 570-85
- Markolf et al, (1978), *JBJS*, **63A**: 664-74
- Zatriosky & Seluyanov (1985), *Int. Series in Biomech.*, U. of Illinois, 233-39

## ACKNOWLEDGEMENTS

This work was supported by the National Institute of Health (1-R01-AR049837-01).

# COMPRESSIVE STIFFNESS PROPERTIES OF HUMAN LUMBAR INTERVERTEBRAL DISCS AND THE INFLUENCE OF STRAIN RATE

Andrew Kemper<sup>1</sup>, Craig McNally<sup>1</sup>, Dave McNeely<sup>1</sup>, Fumio Matsuoka<sup>2</sup>, and Stefan Duma<sup>1</sup>

<sup>1</sup> Virginia Tech, Blacksburg, VA, USA

<sup>2</sup> Toyota Motor Corporation, Japan

E-mail: akemper@vt.edu Web: www.cib.vt.edu

## INTRODUCTION

There have been numerous researchers that have investigated the properties of human intervertebral discs. However, there has been no attempt to characterize the effects of loading rate on the stiffness of human intervertebral discs. The purpose of this study was to develop the compressive stiffness properties of individual lumbar intervertebral discs when subjected to various dynamic compressive loading rates.

A total of 44 axial compression tests were performed on 11 individual human lumbar spine intervertebral discs dissected from 6 fresh frozen human cadavers, 5 male and 1 female. Functional spinal units (FSU), defined an intervertebral disc and the two adjacent vertebral bodies, were dissected from the cadavers. The FSU was fixed to a load cell with a custom aluminum pot and then subjected to dynamic compressive loading using a servo-hydraulic Material Testing System (MTS 810, 22 kN, Eden Prairie, MN).

## METHODS

Prior to specimen preparation, lateral view digital radiographs were taken of each spine in order to identify any pre-existing degenerative changes. The intervertebral discs for each spine were graded, by a certified physician, on a scale of 1 to 4 based on criteria presented by Gordon *et al.* (1991). Intervertebral levels with a degenerative grade of 3 or 4 were rejected.

A number of detailed steps were taken in order to ensure the spines were rigidly secured while maintaining the proper testing orientation. After the spine was sectioned into the desired FSU, all the soft tissue except the ligaments was removed from the FSU. Second, a custom potting cup was filled with a bonding compound (Bondo Corporation, Atlanta, GA), and one half of the proximal vertebral body of the FSU was placed into the bonding compound. Special care was taken to ensure that the mid-plane of the disc was parallel with the potting cup, and that the disc was centered in the potting cup. This potting orientation has been used by numerous previous authors (Yoganandan *et al.*, 1989; Lin *et al.*, 1978; Gordon *et al.*, 1991; Brickmann *et al.*, 1989). The potted vertebrae was then attached to the MTS actuator, and the distal potting cup was filled with the bonding compound. Finally, one half of the distal vertebral body was lowered into the distal potting cup. This procedure prevented any induced flexion or extension moments.

Each intervertebral disc was subjected to a four part test battery in which the loading rate was increased with each test. First, the intervertebral disc was preconditioned to a displacement of 0.5 mm at a rate of 1 Hz, which is similar to the frequency of normal walking. Each intervertebral disc was then subjected to two dynamic displacement steps, 0.5 mm and 1.0 mm, at rates of 0.1 m/s and 0.2 m/s respectively. Finally, each intervertebral disc was subjected to a

dynamic failure test at a rate of 1.0 m/s. However, due to the length limitations the failure results are not presented in this paper. After each test, the MTS actuator was returned to the original position of zero strain and the specimen was allowed to relax for 10 minutes. The specimen was kept hydrated during the entire preparation and testing process by spraying saline directly on the specimen.

Points used to calculate stiffness and strain rate values were taken at approximately 25% and 50% of the loading curves. Strain was calculated based on the lateral disc height obtained from the digital X-rays.

## RESULTS AND DISCUSSION

The loading rate for preconditioning, 0.0001 m/s, resulted in an average stiffness and strain rate of  $375.8 \pm 55.8$  N/mm and  $0.01 \pm 0.0$  s<sup>-1</sup>. The loading rate for the first step test, 0.1 m/s, resulted in an average stiffness and strain rate of  $1835.1 \pm 645.6$  N/mm and  $6.8 \pm 1.5$  s<sup>-1</sup>. The loading rate for the second step test, 0.2 m/s, resulted in an average stiffness and strain rate of  $2489.5 \pm 474.1$  N/mm and  $13.5 \pm 2.0$  s<sup>-1</sup>. The loading rate for the failure tests, 1.0 m/s, resulted in an average stiffness and strain rate of  $6551.1 \pm 2017.0$  N/mm and  $72.7 \pm 16.8$  s<sup>-1</sup>.

The results show that the stiffness of lumbar intervertebral discs is highly dependent on the loading rate. Carter (1977) reported that ultimate compressive strength and modulus of human compact and trabecular bone are proportional to the strain rate raised to 0.06 power. Therefore, a relationship similar to the one developed by Carter (1977) was developed. The resulting relationship shows that the stiffness of lumbar intervertebral discs is proportional to the strain rate raised to the 0.29 power (Figure 1).

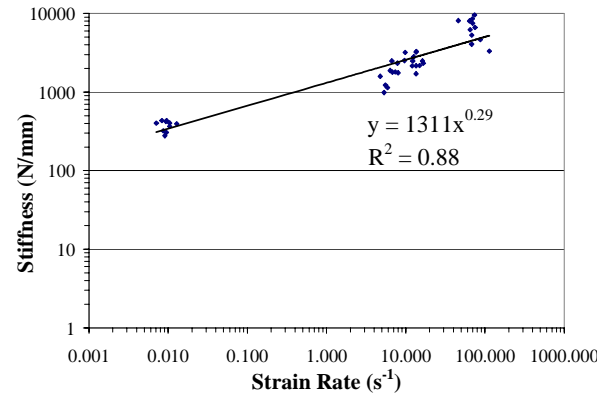


**Figure 1:** Relationship of intervertebral disc stiffness to strain rate.

Note: log-log scale.

## SUMMARY/CONCLUSIONS

The compressive stiffness properties for the individual lumbar intervertebral discs were determined at various loading rates. The results show that the stiffness of lumbar intervertebral discs is highly dependent on the loading rate. It was determined that the stiffness of lumbar intervertebral discs is proportional to the strain rate raised to the 0.29 power.

## REFERENCES

- Brickmann, P. et al. (1989). *Spine* **14**(6): 606-610.
- Cater, D.R., Hayes, W.C. (1977). *J. Bone Joint Surgery*, **J59-A**(7), 954-962.
- Gordon, S.J et al. (1991). *Spine* **16**(4): 450-456.
- Yoganandan, N. et al. (1989). *J. Biomechanics*, **22**, 135-142.
- Lin, H.S. et al. (1978). *J. Bone Joint Surgery*, **60A**(1), 41-55.

## ACKNOWLEDGEMENTS

The authors wish to acknowledge Toyota Motor Corporation for providing the funding for this research.

# Kinematic Differences Between Motorized and Nonmotorized Treadmill Locomotion

John K. DeWitt<sup>1</sup>, Jason R. Bentley<sup>2</sup>, Stuart M.C. Lee<sup>2</sup>, Jason Norcross<sup>2</sup>, Cassie Smith<sup>3</sup>  
and R. Donald Hagan<sup>4</sup>

<sup>1</sup>Bergaila Engineering Services, Houston, TX, USA; <sup>2</sup>Wyle Life Sciences, Houston, TX, USA;  
<sup>3</sup>JES Tech, Houston, TX, USA; <sup>4</sup>NASA Johnson Space Center, Houston, TX, USA;  
email: john.k.dewitt@.nasa.gov

## INTRODUCTION

There are few published literature comparing locomotion on motorized and nonmotorized treadmills. Lakomy (1987) and Gamble et al (1988) reported that forward lean is greater on a nonmotorized treadmill to aid in the generation of horizontal force necessary for belt propulsion, but there are no data concerning lower limb kinematics.

During long-term spaceflight, astronauts use locomotive exercise to mitigate the physiological effects caused by long-term exposure to microgravity. A critical decision for mission planners concerns the requirements for a treadmill to be used during potential trips to the Moon and Mars. Treadmill operation in an un-powered configuration could reduce mission resource demands, but also may impact the efficacy of treadmill exercise countermeasures. To ascertain the most appropriate type of treadmill to be used, it is important to understand biomechanical differences between motorized (M) and nonmotorized (NM) locomotion.

The purpose of this evaluation was to test for differences in lower limb kinematics that occur during M and NM treadmill locomotion at two speeds. It was hypothesized that hip and knee joint angle trajectories would differ between the conditions.

## METHODS

Twenty subjects (10 males/ 10 females; 31±5 yrs, 172±10 cm, 68±13 kg, mean±SD) performed locomotion during M and NM conditions on a ground-based version of the treadmill currently used onboard the International Space Station. Subjects completed three 8-stride trials at 2 velocities (1.34 and 3.13 m·sec<sup>-1</sup>) in each condition. NM and M trials were completed on different days.

Motion capture data were collected (60 Hz) via the Smart Elite Motion Capture System (BTS Bioengineering SPA., Milan, Italy) and smoothed with a 4<sup>th</sup> order digital filter at specific cutoff frequencies chosen for each 3-D point (2-15.5 Hz). Ankle, knee, and hip range of motion (ROM), and trunk sagittal plane angles were computed. Stride time was calculated as the duration between successive heel strikes of the left foot.

Comparisons of joint range of motions were made between M and NM within each speed using paired t-tests. Wilcoxon Rank-Sum tests were used when the data were not normally distributed.

## RESULTS AND DISCUSSION

All subjects chose to walk during the 1.34 m·sec<sup>-1</sup> trials and run during the 3.13 m·sec<sup>-1</sup> trials for both M and NM conditions. M and NM gait styles were different (see Table 1). Figure 1 depicts typical joint positions at

heel strike and toe off for each treadmill mode.

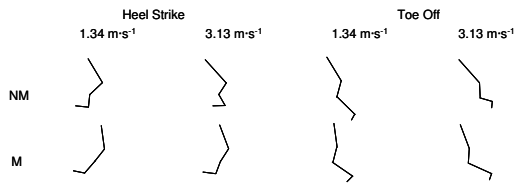


**Figure 1:** Typical limb positions at heel strike and toe off.

Although speed was not different between conditions, the subjects chose differing kinematic patterns. Ankle and hip ROM, as well as maximum trunk lean (with respect to the vertical), were larger during NM. Subjects also took shorter strides during NM.

Hip and knee angle trajectories for each condition at each speed are depicted in Figures 2 & 3. While knee ROM was similar at both speeds (approximately 3° different), coordination strategies between the hip and knee were condition dependent. It appears that the hip operated in different amounts of flexion relative to knee angle. The difference in the hip trajectory was especially apparent during the 3.13 m·sec<sup>-1</sup> trials.

## SUMMARY/CONCLUSIONS

NM treadmill gait requires different lower limb coordination patterns than M locomotion. Therefore, long-term training using NM treadmill modes may result in

different physiological adaptations than M modes.

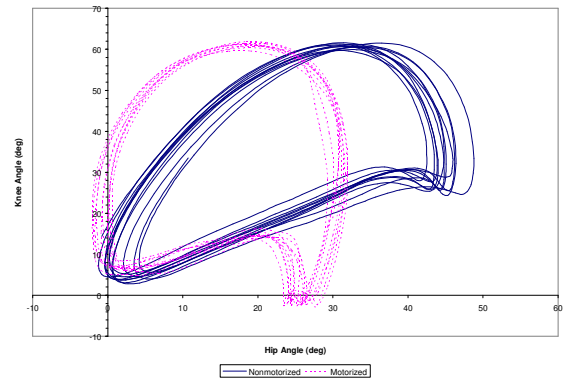


**Figure 2:** Typical Knee-Hip Angle trajectory of nonmotorized (NM) and motorized (M) locomotion at 1.34 m·sec<sup>-1</sup>.

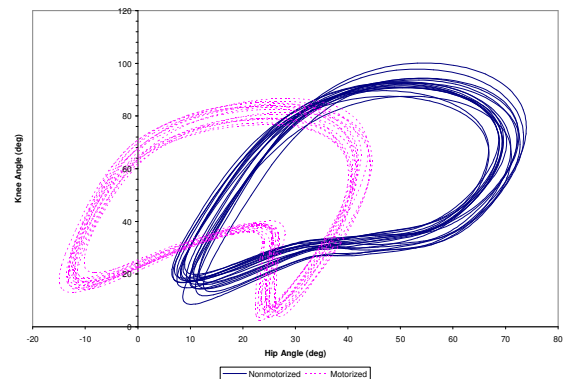


**Figure 3:** Typical Knee-Hip Angle trajectory of nonmotorized (NM) and motorized (M) locomotion at 3.13 m·sec<sup>-1</sup>.

## REFERENCES

- Lakomy, H.K.A. (1987). *Ergonomics*, **30(4)**, 627-637.  
 Gamble, D.J. et al. (1988). *Biomech Sport*, 25-32.

**Table 1:** Stride time and joint ROM for each speed and condition (mean± SD).

Speed (m·sec <sup>-1</sup> )		Stride Time (msec)	Ankle ROM (deg)	Knee ROM (deg)	Hip ROM (deg)	Trunk Lean (deg)
1.34	NM	902.2 ± 56.1*	39.1 ± 5.6**	57.4 ± 4.1*	48.4 ± 4.6**	20.2 ± 4.6*
	M	987.1 ± 52.9	29.8 ± 2.9	60.6 ± 3.8	34.4 ± 3.2	7.6 ± 1.8
3.13	NM	593.1 ± 64.1*	53.5 ± 5.7*	74.4 ± 10.2	62.4 ± 6.0*	27.6 ± 3.5*
	M	685.5 ± 39.6	48.5 ± 4.3	76.9 ± 7.2	49.8 ± 5.4	12.8 ± 3.3

\* p<.05 (paired t-test); \*\*p<.05 (Wilcoxon Rank Sum test)

# ANTICIPATORY LOCOMOTOR ADJUSTMENTS DURING GOAL-DIRECTED WALKING

Angela DiDomenico

Liberty Mutual Research Institute for Safety, Hopkinton, MA, USA  
E-mail: [angela.didomenico@libertymutual.com](mailto:angela.didomenico@libertymutual.com)

## INTRODUCTION

Successful hazard accommodation is an important aspect of maintaining a continuous walking pattern and avoiding slips and falls. Identifying and adapting to observed hazards is one component that leads to this success. Anticipatory locomotor adjustments (ALAs) have been previously investigated with respect to accommodating versus avoiding changes in surface levels (e.g. McFadyen and Carnahan, 1997) and during the circumvention of obstacles in the travel path (e.g. Vallis and McFadyen, 2003). Numerous studies have been completed documenting gait control and evaluating ALAs at the hazard or 'target' (e.g. Cham and Redfern, 2002), that is, the kinetic and kinematic features of step regulation at the time the contingency in the environment is negotiated. The question as to how gait is regulated during the approach is considerably less well documented.

Previous studies have examined approach characteristics in the sport of long jumping where there is a requirement to approach the target at maximum velocity (e.g. Hay, 1988). Fewer studies have examined adjustments while walking towards various types of targets (e.g. Buekers et al., 1999). Step length regulation upon approach appears to be an important feature of successful obstacle negotiation or target accommodation (Bradshaw and Sparrow, 2001). Minimal research, however, has focused on more complex gait adjustments

that occur during multiple steps prior to a target or hazard.

## METHODS

An experiment using a 2x2 repeated measures design incorporated two within-subject variables: walking velocity (normal and fast) and size of target (small-2cm x 2cm and large-33cm x 53cm). To minimize confounding influences related to ordering, the presentation of the conditions was randomly assigned after being blocked by walking velocity. Thirty-six participants (19 females, 17 males) completed this experiment. The means (sd) of ages, heights and weights of the participants were 41.7 (15.1) years, 168.4 (9.4) cm, and 72.5 (14.7) kg, respectively.

A straight runway of approximately 10m was used for all trials, with overhead lights projecting targets towards the end of the runway. Participants were fitted with uniform footwear (athletic shoes). After determining the walking velocities for the participant, each participant performed 50 walking trials at each of the two self-selected velocities to acquire a minimum of ten usable trials per condition. Participants were instructed to completely cover the small target with their foot and center their foot within the large target while walking. The color of the runway was dark gray to provide adequate contrast with the targets.

Kinematic data of the lower limbs were collected using a passive reflective

cinematographic motion tracking system (Eagle Digital camera system, Motion Analysis Corp, Santa Rosa, CA, USA). Position data was collected at 200Hz using 10mm diameter reflective markers placed according to the modified Helen Hayes marker set (Kadaba et al., 1990).

Kinematic data was processed to provide gait parameters for each step within the trials. The initiation of ALAs determined in the analyses were compared across participants to determine the onset of ALAs. ANOVAs were used to determine the effects of walking velocity and target size for each of the dependent measures. Post-hoc statistical analyses (Tukey's HSD test) were used to determine the step at which significant changes were initiated within the trial. All statistical analysis used a significance level of  $p < 0.05$ .

## RESULTS AND DISCUSSION

Target size and gait velocity significantly affected adjustments of step length and step velocity but did not significantly affect step width or step duration. Generally, step length and step velocity decreased during adjustment phases to apparently provide better control of foot placement.

During normal walking velocities, participants made small changes in variables within multiple steps (three or four) while maintaining a relatively normal and uninterrupted gait pattern. This may be possible because visual control onset occurs earlier at lower velocities (Bradshaw and Sparrow, 2001). Adjustments during the faster trials were only made to the two steps prior to stepping on the target. This was similar to findings by Buekers et al. (1999) who found that excessive adjustments in stride length were required for the final step preceding a doorway opening.

Some of the variation in ALA onset can be attributed to the effect of target size. Larger adjustments over an additional step were required for smaller targets because stepping on the small target placed added constraints on foot placement. Similarly, Bradshaw and Sparrow (2001) showed a linear relationship between approach velocity of the whole body and accuracy of foot placement for various targets and obstacles.

## SUMMARY/CONCLUSIONS

Goal-directed walking, represented by the targeting task, involves adjustments to gait parameters over multiple steps. Present findings indicate that future research regarding slips and obstacle negotiation should consider multiple steps during the approach of a hazard, not just the step immediately preceding it.

## REFERENCES

- Bradshaw, E. J., Sparrow, W. A. (2001). *Human Movement Science*, **20**(4-5), 401-426.
- Buekers, M. et al. (1999). *Neuroscience Letters*, **275**, 171-174.
- Cham, R., Redfern, M. S. (2002). *Gait and Posture*, **15**, 159-171.
- Hay, J. G. (1988). *International Journal of Sports Biomechanics*, **4**, 114-129.
- Kadaba, M. P. et al. (1990). *Journal of Orthopaedic Research*, **8**(3), 383-392.
- McFadyen, B. J., Carnahan, H. (1997). *Experimental Brain Research*, **114**, 500-506.
- Vallis, L. A., McFadyen, B. J. (2003). *Experimental Brain Research*, **152**, 409-414.2

# A LABORATORY FOR ANALYSIS OF STANDING EXERTIONS PERFORMED WITH & WITHOUT FEEDBACK ON HAND FORCES

Suzanne G. Hoffman, Don B. Chaffin, and Charles B. Woolley  
University of Michigan, Ann Arbor, MI, USA  
E-mail: [grovess@umich.edu](mailto:grovess@umich.edu) Web: [www.humosim.org](http://www.humosim.org)

## BACKGROUND

Job analysis tools require ergonomists to make assumptions regarding task postures and hand forces. It has been shown that a 10 degree error in the limiting joint angle can result in +/- 30% variations in percent capable predictions (Chaffin & Erig, 1991). Forces exerted at the hands translate into mechanical joint loads; thus, hand force estimation errors also affect job assessment accuracy. The dependency of hand forces on task parameters (de Looze et al, 2000) combined with differences in perceived and actual hand force directions (Kerk et al, 1994) make hand forces difficult to predict.

Biomechanical analysis of standing tasks can provide insight into the postures selected and forces exerted at the hands. Analyses by Gaughran & Dempster (1956) and Kerk et al (1994) show how basic mechanics and task constraints, coupled with knowledge of strength and balance limits may be used to identify preferred postures.

## OBJECTIVE

Based on the preceding, a specialized laboratory and experimental methods were developed to allow a detailed biomechanical analysis of high exertion standing tasks.

## METHODS

The laboratory setup is comprised of four systems: (1) translating force platforms, (2) force handle, (3) force feedback display, and (4) motion tracking system (Figure 1).

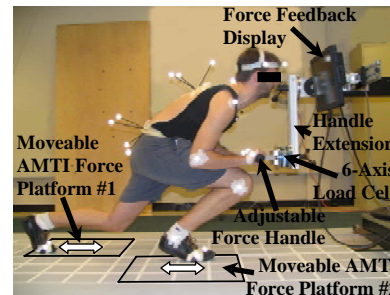


**Figure 1:** Participant in the laboratory.

Since it has been shown that preferred foot placements vary with task parameters (Holbein & Chaffin, 1997), reconfigurable force plates are required to capture ground reaction forces for various stances. Two independently-translatable force plates allow for a range of parallel and split-stances to be accommodated. Also, task parameters have been shown to affect hand force direction and joint torques (Hoozemans, 2004). An adjustable force handle affixed to a 6-DOF load cell provides the ability to study the effect of task parameters on posture and hand forces (Figure 2).

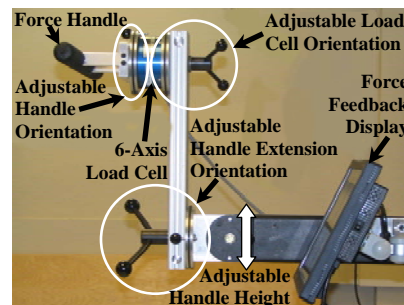


**Figure 2:** Force handle adjustability.

It has been reported that without feedback on hand forces, the measured hand force vector differs from that requested (Kerk, 1992). For our experiments a force feedback display that provides the subject

with real-time feedback on hand forces was developed in LabVIEW 7.1 to control variations in force magnitude and direction (Figure 3). The experimenter has the option to display off-axis forces or not and to indicate the desired force-level with a goal.

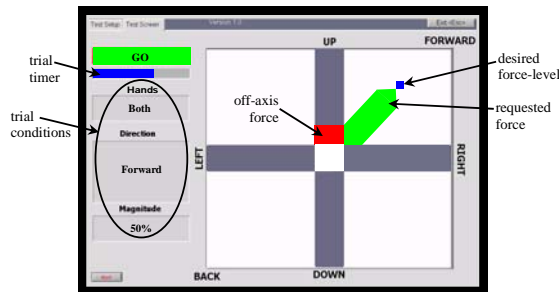


**Figure 3:** Force feedback display.

An eight-camera optical motion tracking system is also provided to quantify whole-body motions and postures (Figure 1).

## RESULTS AND DISCUSSION

A pilot study with one subject performing two-handed exertions in the forward and backward directions on an elbow-height force handle was used to assess the laboratory setup. Force levels of 50% and 75% of the subject's maximum capability in a given direction were exerted. Each exertion was performed with and without a constraint imposed on off-axis forces.

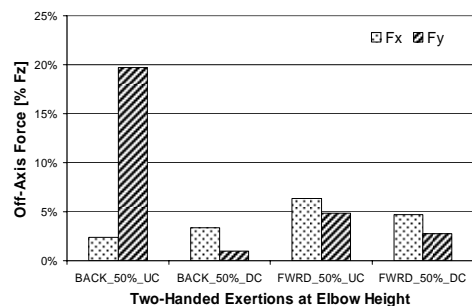


**Figure 4:** Hand forces exerted with force direction constrained (DC) & force direction unconstrained (UC).

Visual feedback provided to the subject via the display allowed the subject to control

hand force magnitude within  $\sim \pm 5\%$  of the requested force level. Off-axis force levels differ between trials performed with and without feedback on the off-axis forces generated (Figure 4). The vertical off-axis force,  $F_y$ , during a two-handed 50% max exertion in the backward direction decreased from 19.7% to 1.0% of the requested force when force direction was constrained.

## SUMMARY

Data collected with this setup will allow for a better understanding of the biomechanics of standing exertions. A set of experiments are currently underway to provide insight into posture selection and the relationship between hand forces, task requirements and posture, allowing for improved ergonomics analysis tools.

## REFERENCES

- Chaffin, D.B., Erig, M. (1991). *IIE Transactions*, **23**(3), 215-227.
- de Looze, M.P. et al. (2000). *Ergonomics*, **43**(3), 377-390.
- Gaughran, G.R.L., Dempster, W.T. (1956). *Human Biology*, **28**(1), 67-92.
- Holbein, M.A., Chaffin, D.B. (1997). *Human Factors*, **39**(3), 456-468.
- Hoozemans, M.J.M. et al. (2004). *Ergonomics*, **47**(1), 1-18.
- Kerk, C.J. (1992). *Doctoral Dissertation*, University of Michigan, Ann Arbor, MI.
- Kerk, C.J. et al. (1994). *IIE Transactions*, **26**(3), 57-67.
- LabVIEW 7.1 (2004). National Instruments Corporation, Austin, TX.

## ACKNOWLEDGEMENTS

Thanks to Robert Hoffman for his help, and to the HUMOSIM consortium (GM, Ford, DaimlerChrysler, International Truck, USPS, UGS, ARC, and the US Army-RDECOM) for their financial support.

# GENDER DIFFERENCES IN GEOMETRIC MEASURES OF KNEE EXTENSOR FUNCTION

Mark D. Tillman, Jeff T. Wight, John D. Garbrecht, Caitlin Reese, and John W. Chow

Department of Applied Physiology & Kinesiology, University of Florida, Gainesville, FL, USA  
 E-mail: mtillman@hhp.ufl.edu Web: www.hhp.ufl.edu/apk/ces/labs/biomech/

## INTRODUCTION

The effective moment arm of the knee extensor mechanism affects the loads on the ligamentous and bony structures of the knee during extension exercises and may be related to the increased rate of anterior cruciate ligament injuries observed in the female athletic population. However, little is known regarding the influence gender on the knee extensor mechanism. One of the primary functions of the patella is to improve the mechanical advantage of the quadriceps muscles for the knee extension. The effective moment arm of the quadriceps muscle is determined by the geometric configurations of the tibiofemoral and patellofemoral articulations (Figure 1). Gender may be associated with alterations in

the geometric configurations of the knee and alter the effective moment arm values at different joint angles.

## METHODS

Sagittal knee radiographs of right and left knees for 19 healthy adults (11 males: age  $21.6 \pm 1.1$  yrs, height  $184.0 \pm 7.1$  cm, mass  $87.2 \pm 16.8$  kg; 8 females: age  $21.6 \pm 0.7$  yrs, height  $167.3 \pm 7.4$  cm, mass  $64.7 \pm 6.9$  kg) were obtained at three different knee flexion angles ( $10^\circ$ ,  $30^\circ$ , and  $50^\circ$ ). Each subject sat on a stool located next to an X-ray film and performed maximum isometric knee extensions when the radiographs were taken (Figure 2). The test stool has an angle iron (with equally spaced holes) fixed to the bottom of the stool to provide anchor sites for an inelastic cable attached to an ankle

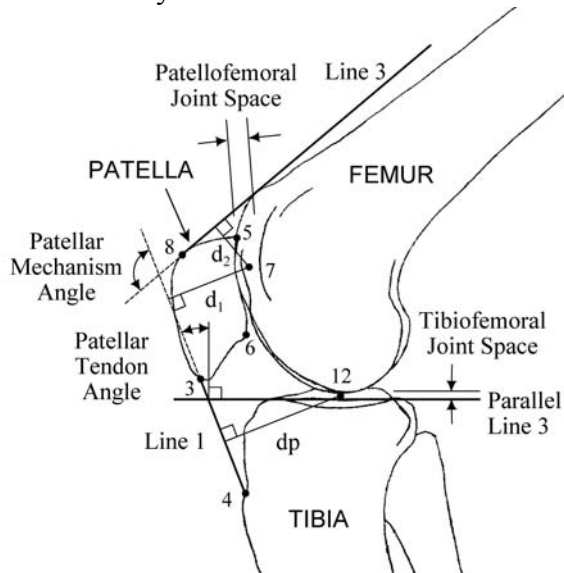


**Figure 1.** The effective moment arm of the patella may be calculated as follows:  $d_e = d_2 d_p / d_1$ .

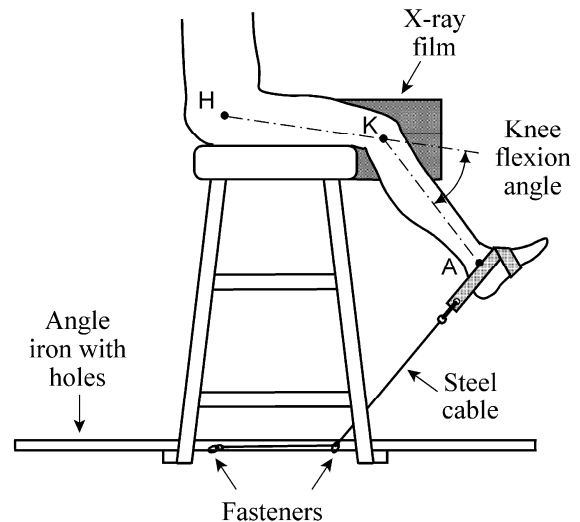


**Figure 2.** Experimental setup for radiographic measurements during isometric knee extensions.

strap. Knee flexion angles were measured goniometrically and were altered by changing the length of the cable. A metal pin with a length of 10.15 cm was placed on the anterior surface of the patella tendon for spatial reference.

Each x-ray was evaluated by two independent analysts using the same procedures/instructions. The digitizing technique has been proven to be very reliable (Chow et al., 2006). Each analyst identified several different bony landmarks on each radiograph and determined the lines of action of the patellar tendon, quadriceps tendon, and patellofemoral joint contact forces and the patellofemoral and tibiofemoral contact points. The effective moment arm of the quadriceps was computed as the product of the moment arm of the patellar tendon force about the tibiofemoral contact point and the mechanical advantage of the patellar mechanism (the ratio of the moment arms of the patellar tendon and quadriceps tendon force acting on the patellofemoral joint) (Grood et al., 1984).

The average values of each dependent variable from the pair of analysts were used in subsequent statistical analyses. More specifically, separate 2: gender x 2: leg x 3: knee flexion angle ANOVA with repeated measures on the last two factors were computed. A traditional level of statistical significance was utilized ( $\alpha=0.05$ ). When appropriate, Bonferroni posthoc analyses were performed.

## **RESULTS AND DISCUSSION**

Nine of the twelve variables tested varied with knee flexion angle, six variables varied between right and left legs, and six varied between males and females ( $p<0.05$ ). Females exhibited significantly shorter

effective moment arm, patellafemoral joint space, patellar tendon length, and patellar heights. Angular and dimensionless measures of knee geometry did not vary between males and females. Therefore, the linear measures were re-analyzed after normalizing for the height of each subject. Patellafemoral joint space was the only variable that remained significantly decreased for the females. Although the effective moment arm was 3% larger in males after normalizing, the difference was not statistically significant.

The extensor torque produced at the knee is dependent on the force generated in the quadriceps muscle, as well as, the effective moment arm of the quadriceps. The small (non-significant) difference between males and females indicates that the greater knee extensor strength common in males may be due to both geometric differences and greater muscular strength.

## **SUMMARY/CONCLUSIONS**

The greater incidence of anterior cruciate ligament injuries in females is a multifactorial problem. Additional research regarding knee geometry is warranted, as well as, analysis of other factors (intrinsic and extrinsic) to provide more insight into gender based injury rate differences.

## **REFERENCES**

- Chow, J.W. et al. (2006). *Knee*. (in press)
- Grood, E.S. et al. (1984). *J. Bone Joint Surg.* **66-A**, 725-734.

# COMPARISON OF VALIDATION TECHNIQUES FOR NEURAL NETWORK ESTIMATION OF JOINT MOMENTS DURING GAIT

Katie B. O'Keefe and Michael E. Hahn

Movement Science Laboratory, Montana State University, Bozeman, MT, USA  
E-mail: mhahn@montana.edu

## INTRODUCTION

Full, three-dimensional gait analysis provides clinically useful measures of normal and abnormal gait patterns. However, costly equipment is a limitation for many clinical settings. A few studies have demonstrated that artificial neural networks (ANN) can accurately map nonlinear relationships between electromyography (EMG) signals and joint torque (Hahn, 2005; Koike and Kawato, 1995; Luh et al., 1999). Only one previous study has estimated lower extremity joint moments from surface EMG (Sepulveda et al., 1993), however current efforts in our laboratory are showing initial success in estimating joint moments during gait using similar ANN models.

The focus of this study was to compare a k-fold cross validation technique within the ANN to the bootstrap re-sampling used previously. K-fold cross validation has become a widely accepted model validation technique because of its ability to reduce computational time (Burman, 1989). Implementing this technique should decrease processing time of the ANNs used in joint moment estimation models, making them more useable in clinical settings.

## METHODS

A three layer feed-forward ANN designed during prior research (Hahn, 2005) was implemented in this study using the Neural Network Toolbox in Matlab 7.0 (The Mathworks, Inc.). The data used for training

and testing the ANN were compiled from nineteen subjects (12 female, 7 male;  $22.3 \pm 1.6$  years). All subjects completed a brief survey regarding physical activity and joint health, allowing screening for neuromuscular or orthopedic pathologies prior to participation.

Each subject performed a series of gait trials at their self-selected pace. Lower limb trajectories were sampled at 200Hz using Workstation® software (ViconPeak, Lake Forest, CA). An AMTI platform was used to collect the ground reaction force data, sampled at 1000Hz. EMG signals were recorded at 1000Hz using a Myopac Jr. (Run Technologies, Inc., Mission Viejo, CA) and passive surface electrodes on seven muscles (gluteus maximus, gluteus medius, biceps femoris, rectus femoris, vastus lateralis, tibialis anterior and medial gastrocnemius).

Seventy-seven total trials (approximately 4 trials per subject) were entered into the ANN for analysis. Analysis involved comparing two different techniques of validation: bootstrap re-sampling and 11-fold cross validation (CV). Each technique was used three times for each joint.

The inputs of the neural network included subject demographics and anthropometrics as well as the kinematic and EMG data. The target, or output layer, was the time-normalized joint moments of the hip, knee, and ankle. The training goal was 0.1 mean-square error between the actual joint moment and the target. Five processing units were used in the hidden layer for mapping

between the input and output. Back-propagated error correction was performed using the Levenberg-Marquardt algorithm.

Bootstrap re-sampling was performed by first randomizing the dataset according to trial, followed by training and testing of the ANN. A proportion equal to 0.7 of the data was selected to train the ANN while the remaining data was used for testing. This process was repeated fifty times to ensure broad re-sampling of trials selected for training and testing.

The 11-fold CV technique also began with randomizing the data according to trial. The data was then divided into eleven equal subsets. Ten of the subsets were used to train the ANN while the sole remaining subset was used to test the neural network. This process was repeated until each of the eleven subsets was used for testing.

For each joint, total processing time was recorded for each validation technique. Correlation coefficients as well as the mean number of epochs to reach the output goal were also recorded. A two-sample t-test assuming equal variance was performed to test mean number of epochs and mean correlation coefficients for significant effect of validation technique ( $\alpha=0.05$ ).

## RESULTS AND DISCUSSION

The 11-fold CV performed faster with comparable accuracy compared to bootstrap re-sampling. For the ankle joint, the average processing time for 11-fold CV was 29.36

seconds whereas bootstrapping took 110.69 seconds. Processing for the knee and hip joints took longer than the ankle. However, the 11-fold CV still performed 2.76 times faster than bootstrapping for the knee joint and 3.1 times faster for the hip (Table 1).

The difference in correlation coefficients between the two re-sampling techniques was not significant for the ankle or the knee. The hip model however, showed a significantly improved accuracy with 11-fold CV. The difference between epochs needed was not significant for any of the joints (Table 1).

## SUMMARY/CONCLUSIONS

Processing time of the ANN decreased considerably using the 11-fold CV technique while no significant difference was found for training epochs required or prediction accuracy for the ankle and knee. The present ANN model has shown initial success in estimating joint moments during gait. However, faster processing times will benefit the clinical application of this model.

## REFERENCES

- Burman, P. (1989). *Biometrika*, **76**, 503-514.  
 Hahn, M.E. (2005). *Proceedings of XXth ISB Congress*, 75.  
 Koike, Y., Kawato, M. (1995). *Biol Cybern*, **73**, 291-300.  
 Luh, J.J. et al. (1999). *J Electromyogr Kinesiol*, **9**, 173-183.  
 Sepulveda, F. et al. (1993). *J Biomech*, **26**, 101-109.

**Table 1:** Results for each of the two validation techniques; Mean value given.

Technique	ANKLE			KNEE			HIP		
	Epoch	R	Time (s)	Epoch	R	Time (s)	Epoch	R	Time (s)
11-fold	4	0.98	29.4	994	0.90	5620.8	721	0.94*	4079.6
Bootstrapping	4	0.98	110.7	992	0.88	21156.0	815	0.93*	16714.3

\* significant technique effect

# ANKLE AND KNEE JOINT KINETICS IN RUNNERS WITH AND WITHOUT LOWER EXTREMITY OVERUSE INJURIES

Alan Hreljac<sup>1</sup>, Rodney Imamura<sup>1</sup>, Rafael F. Escamilla<sup>2</sup>, Toran D. MacLeod<sup>2</sup>, Jason Kawada<sup>1</sup>, Sarah Krogh<sup>2</sup>, and Jennifer Stafford<sup>2</sup>

<sup>1</sup>Kinesiology and Health Science Department, California State University, Sacramento

<sup>2</sup>Physical Therapy Department, California State University, Sacramento

E-Mail: ahreljac@csus.edu

## INTRODUCTION

Running injuries occur at an alarming rate. According to epidemiological studies (e.g. Macera et al., 1989), anywhere from 27% to 70% of distance runners are injured during any one year period. The most common site of overuse running injuries is the knee (Taunton et al., 2002). Although the exact causes of overuse running injuries have yet to be determined, it could be stated with certainty that the etiology of these injuries is multifactorial and diverse (Rolf, 1995; van Mechelen, 1995). Some researchers (e.g. James, 1998) have concluded that there are no specific risk factors that correlate with specific types of injury in a reliable fashion. There are, however, several risk factors which may be associated with a variety of running injuries. These factors could be placed into three general categories: training, anatomical, and biomechanical factors. Biomechanical variables include impact forces, impact loading rates, and peak tibial acceleration (Ferber et al., 2002; Hreljac et al., 2000). Joint kinetics may be more indicative of stress levels to injured structures. One study (Stefanyshyn et al., 1999) found that increased knee joint forces and moments are a factor in developing patellofemoral pain syndrome in runners. The purpose of this investigation was to evaluate the lower extremity overuse injury potential of runners by identifying joint kinetic variables which may predispose a runner to overuse injuries.

## METHODS

A group of five injury free (IF) runners, who had never sustained an overuse running injury (> 3 years experience) were matched in training and anatomical variables with a group of five injured (I) runners who had suffered at least one overuse running injury of the knee. All runners were heel strikers and were pain free at the time of the study. Subjects performed three successful trials of running down a 20 meter runway, and over a floor mounted force platform at a speed of  $3.5 \text{ m}\cdot\text{s}^{-1}$  while being filmed by a single digital video camera (240 Hz) in the sagittal plane. The 2D kinematic data of five reflective markers (right greater trochanter, knee joint center, lateral malleolus, calcaneus, and head of the fifth metatarsal) were synchronized with ground reaction force data (960 Hz). A trial was successful if the speed was within  $\pm 3\%$  of  $3.5 \text{ m}\cdot\text{s}^{-1}$ , the landing foot completely contacted the force platform, and if the stride length did not visibly change. After smoothing, ankle and knee joint reaction forces and moments were determined using a standard inverse dynamics approach. All variables were normalized by dividing by body mass. Dependent variables (DVs) analyzed included maximum knee extensor moment, maximum ankle plantar flexor moment, and maximum knee and ankle power absorption and generation. All DVs were compared between groups using a MANOVA ( $\alpha = 0.05$ ).

## RESULTS AND DISCUSSION

The I group had significantly greater maximum knee extensor moments and knee power absorption than the IF group, while the IF group had significantly greater maximum ankle plantar flexor moments and ankle power absorption than the I group (Table 1). In addition, there was a trend toward greater knee power generation by the I group. Differences between groups occurred most notably during the first half of stance, when the lower extremity joints are acting as shock absorbers. The ratio of knee/ankle joint energy absorption was approximately 3.5 for the I runners, and about 1.3 for the IF runners. More compliant joints have been found to be superior at absorbing energy (Hamill et al., 2000), suggesting that the IF runners had a more compliant ankle joints than the I runners. Since the ankle is more compliant when pronating, it is likely that runners who pronate to a greater extent, provided that it is within physiological limitations, may be at a reduced risk of injury, as suggested in a previous study (Hreljac et al., 2000).

**Table 1:** Value of all DVs (mean  $\pm$  1 SD) for injured (I) and injury free (IF) groups.

Variable	I Group	IF Group
Knee-ExM (N·m·kg <sup>-1</sup> )	3.18 $\pm$ 0.49*	2.23 $\pm$ 0.60
Ankle-PFM (N·m·kg <sup>-1</sup> )	2.11 $\pm$ 0.76	3.10 $\pm$ 0.54*
P-Abs-Knee (W·kg <sup>-1</sup> )	16.73 $\pm$ 3.08*	11.82 $\pm$ 3.53
P-Abs-Ankle (W·kg <sup>-1</sup> )	4.84 $\pm$ 2.45	9.03 $\pm$ 2.24*
P-Gen-Knee (W·kg <sup>-1</sup> )	9.63 $\pm$ 2.56	6.41 $\pm$ 2.46
P-Gen-Ankle (W·kg <sup>-1</sup> )	12.52 $\pm$ 3.78	15.96 $\pm$ 2.86

\*Value of variable is significantly greater for this group.

## SUMMARY

The results of this study demonstrate that runners who had previously sustained overuse injuries rely more heavily on muscles of the knee than of the ankle for energy absorption, while runners who had never sustained an overuse injury utilize the plantar flexors and other muscles of the ankle to a greater extent for energy absorption. This suggests that an excessive reliance upon the knee joint musculature to absorb the energy from impact is a risk factor for overuse running injuries of the knee. More specifically, a high knee/ankle joint ratio of power absorption during running may be indicative of a runner with an increased risk of sustaining an overuse injury of the knee.

## REFERENCES

- Ferber, R. et al. (2002). *Med. Sci. Sports Exerc.*, **34**, S5.
- Hamill, J. et al. (2000). *Arch. Physiol. Biochem.*, **108**, 47.
- Hreljac, A. et al. (2000). *Med. Sci. Sports Exerc.*, **32**, 1635-1641.
- James, S.L. (1998). *AAOS Instr. Course Lect.* **47**, 407-417.
- Macera, C.A. et al. (1989). *Arch. Intern. Med.*, **149**, 2565-2568.
- Rolf, C. (1995). *Scand. J. Med. Sci. Sports*, **5**, 181-190.
- Stefanyshyn, D.J. et al. (1999). *Proceedings of the 4th Symposium on Footwear Biomechanics*, 86-87.
- Taunton, J.E. et al. (2002). *Br. J. Sports Med.*, **36**(2), 95-101.
- van Mechelen, W. (1995). *Sports Med.*, **19**, 161-165.

# PENGUIN WADDLING RESULTS IN REDUCED STEP WIDTH VARIABILITY

Melissa M. Scott-Pandorf<sup>1</sup>, Diane Olsen<sup>2</sup>, Greg Whittaker<sup>2</sup>, and Max J. Kurz<sup>1</sup>  
<sup>1</sup>Laboratory of Integrated Physiology, University of Houston, Houston, TX, USA

<sup>2</sup>Moody Gardens®, Galveston, TX, USA

E-mail: mkurz@uh.edu, Web: <http://www.hhp.uh.edu/faculty/Kurz/research/index.html>

## INTRODUCTION

Previous research indicates that an increased amount of step width variability in humans is associated with an unstable locomotive pattern. For example, the elderly have an increased amount of step width variability compared to their younger counterparts (Ownings & Grabiner, 2004). This notion is further supported by simulations from passive dynamic walking models. Two-dimensional passive dynamic walking models can produce a stable sagittal plane gait pattern based on mechanics alone. However, three-dimensional passive dynamic walking models cannot produce a stable gait and requires additional control in the frontal plane to prevent falls (Kuo, 1999). These scientific observations suggest that the medial-lateral motion of gait must be actively controlled by the nervous system, otherwise falls will occur. Experimental observations indicated that a gait pattern that lacks medial-lateral control will have an increased amount of step width variability (Ownings & Grabiner, 2004). However, it is not currently clear what neuromechanical variables are responsible for controlling the medial-lateral motion of gait.

Historically, scientists have often turned to nature for answers when faced with a problem that is difficult to understand or when a solution to the problem is not readily evident. By studying and comparing species, new insights are often revealed that would not have been gained from traditional laboratory experiments. Compared to other

terrestrial animals, penguins appear to have an excessive amount of medial-lateral motion in their gait, which is characterized as waddling. It is not clear if waddling is an advantageous neuromechanical mechanism for improved stability or if it makes the locomotive system more susceptible to falls. During the breeding period, penguins walk long distances on uneven terrain that offers a stability challenge to their locomotive system (Pinshow *et al.*, 1977). If medial-lateral variability is unfavorable, it would seem that evolutionary pressures would have eliminated a waddling locomotive strategy. No investigations have classified the step width and step length variations in the penguin's locomotive pattern. Possibly, waddling may be an evolutionary mechanism for controlling the medial-lateral motion of the gait pattern. The purpose of our investigation was to explore the unique locomotive pattern of the penguin. Based on previous research with humans, we hypothesized that penguins would have a greater amount of step width variability during locomotion compared to the step length.

## METHODS

The spatial characteristics of the gait of twelve King penguins (*Aptenodytes patagonica*, height:  $68.1 \pm 0.8$  cm, weight:  $11.1 \pm 0.3$  kg) were investigated. Data collection was performed at a local aquarium (Moody Gardens®, Galveston, TX). A custom 15-foot walkway with walls was built to guide the penguins to walk across a pressure mat (GAITRite, CIR Systems, Inc., Hovertown, PA) that collected the right and left foot positions for

every step of the penguin's gait. Each penguin performed 10 walking trials that resulted in ~200 steps. Trials were only accepted for analysis if the penguin stayed within the boundaries of the pressure mat and maintained a constant walking speed.

The coordinate positions of the penguin's feet for each step were used to determine the step length and step width. Standard deviations were calculated to classify the variability in the step length and width. A t-test was performed to determine significant difference between step width and step length variability profiles with an alpha level of 0.05.

## RESULTS AND DISCUSSION

Our results did not support our hypothesis. Step width had significantly ( $p = 0.0001$ ) less variability than step length in penguins' locomotive pattern (Figure 1). Surprisingly, this is opposite of the results found in humans with limited medial-lateral control (i.e., elderly; Ownings & Grabiner, 2004).

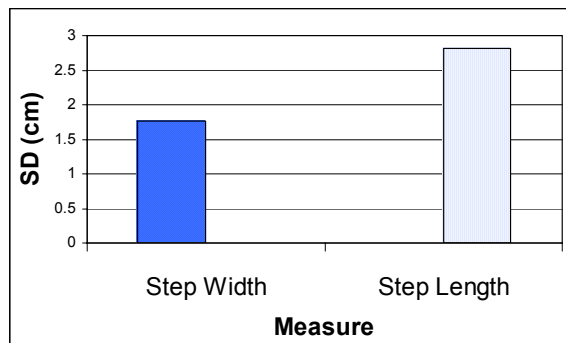


**Figure 1.** Step width and length variability in standard deviations (SD).

It appears that evolutionary pressures have promoted the penguin to develop a unique locomotive strategy that results in the selection of a consistent step width. Possibly waddling may provide a neuromechanical mechanism for the control of a more stable gait in the ever challenging arctic terrain.

Previously, Griffin and Kram (2000) determined that penguin waddling is an

effective mechanism for improving the recovery of mechanical energy.

Encompassing our results with theirs, it appears that waddling is a beneficial locomotive strategy. Potentially, a more consistent step width may also be related to the efficiency of the penguin's gait since a less variable step width is related to a lower metabolic cost (Donelan *et al.*, 2004). We intend to further explore how waddling influences step width variability by using an external stabilizing mechanism that reduces the waddling motion of the penguin's gait pattern.

We foresee that the penguin's movement strategy can be extended to humans. Possibly a waddling pattern can be used to improve the efficiency and the stability of human gait patterns. Currently, we are exploring if step width variability is reduced and the mechanical energy recovery is improved when a human adopts a waddling gait pattern. Understanding the mechanisms in which the penguins use waddling to improve their gait may lead to new rehabilitation techniques that prevent falls and improve the efficiency of pathological gait patterns.

## ACKNOWLEDGEMENTS

We would like to thank Chris Arellano for his assistance during data collection.

## REFERENCES

- Donelan, J.M. *et al.* (2004). *J Biomech* **37**, 827-35.
- Griffin T.M. & Kram R. (2000) *Nature*, **408(6815)**, 929.
- Kuo, A. D. (1999). *Int J Robotic Res.* **18**, 917-930.
- Ownings T.M. & Grabiner M.D. (2004). *J Biomech*, **37(6)**, 935-8
- Pinshow, B. *et al.* (1977). *Science*, **195**, 592-94.

# THE EFFECT OF CLAUDICATION ON JOINT MOMENTS DURING WALKING

Shing-Jye Chen<sup>1</sup>, Iraklis Pipinos<sup>2,3</sup>, Jason Johanning<sup>2,3</sup>, Jessie M. Huisinga<sup>1</sup>, and Sara A. Myers<sup>1</sup>

<sup>1</sup>University of Nebraska at Omaha, NE, USA

<sup>2,3</sup>University of Nebraska Medical Center

<sup>2,3</sup>Veterans Affairs Medical Center, Omaha, NE, USA

E-mail: shingjychen@unomaha.edu

Web: www.unocoe.unomaha.edu/hper/bio/home.htm

## INTRODUCTION

About 10 million people in USA suffer from Peripheral Arterial Disease (PAD) which is a manifestation of atherosclerosis at the leg arteries. For this population, walking becomes a difficult task since the leg muscles metabolic demand is constrained due to the decreased blood flow. The result is claudication which is pain of the leg muscles during walking. Claudication is present in 40% of the PAD patients. With rest, blood flow returns and pain ceases. Claudication symptoms are treated with behavioral modifications, surgery and pharmacologically. However, the efficacy of these treatments has not been investigated. In addition, this gait handicap has only been examined with simple gait parameters (i.e., stride length/time; Gardner et al., 2001; McDermott et al., 2001; McCully et al., 1999). In our previous work, we have expanded this research using joint kinematics and ground reaction forces to better describe the true gait handicap of PAD patients (Scott et al, 2005). However, we have not presented the effect of PAD on gait joint moments. It is well known that joint moments can reveal specific neuromuscular demands of the legs during gait and they have been used to describe the gait handicap of various pathologies (Winter, 2005). Therefore, the purpose of this study was to identify the effect of claudication onset on the joint moments generated at the leg during walking.

## METHODS

Six male PAD patients with bilateral lower extremity claudication (age=62.3±6.0yrs; mass=80.5±12.0kg; height=1.70±0.10m) and no other leg pathologies, walked through a 10 meter walkway at their self-selected pace while kinematics and kinetics of each leg were collected using a 6-camera EvaRT 4.7 system (Motion Analysis Corp., Santa Rosa, California; 60Hz) and a Kistler force plate (600Hz). Data were captured for five trials for each leg for two different conditions; pain free (C1) and with pain (claudication; C2). Pain was induced with a common clinical PAD protocol; walking on a treadmill at 10% grade with a speed of 0.67 m/s until the onset of claudication. Internal joint moments were calculated using the OrthoTrak 6.2.9 version (Motion Analysis Corp.). The maximum flexor and extensor joint moments were identified for the ankle, knee and hip joints during stance. A two-way repeated measures ANOVA was used to test for differences in each joint for these parameters between the right and left leg and between C1 and C2. A post-hoc Bonferroni adjustment was conducted to control for family-wise error setting the  $\alpha$  level at 0.013 while paired t-tests were used to further investigate interaction effects.

## RESULTS AND DISCUSSION

Claudication resulted in a non significant decrease in the walking velocity (C1=1.11 m/s, C2=1.03 m/s,  $p=0.06$ ). There were no significant main effects found, however, significant interaction effects were detected for every joint. During late stance, the

maximum plantar flexor moment of the left leg and the maximum hip flexor moment of the right leg significantly decreased due to claudication (Figure 1). During early stance, the maximum knee extensor moment of right leg significantly increased due to claudication. Therefore, claudication can produce changes in the joint moments of bilateral PAD patients. However, these changes were not the same for both legs. It is possible that this result is due to the severity of PAD in each leg, and/or the small sample size of this preliminary work. Overall, the net effect of the muscular demands of the knee extensors during early stance increased to better stabilize and control the body as the PAD patient gets ready for the challenges of the single support phase. However, the hip flexors and ankle plantar flexors can not produce the necessary muscular contractions to efficiently propel the body forward during push off possibly resulting in a decreased walking velocity in PAD patients.

## SUMMARY/CONCLUSIONS

Our results showed that joint moment analysis can provide with significant findings regarding the effect of claudication on gait. This biomechanical approach can be used to explore the effect of treatments such as pharmacotherapy and surgery on PAD. However, our results need to be further substantiated with larger sample sizes and expanded to include comparisons with healthy controls.

## REFERENCES

- Gardner, AW. et al. (2001). *Vasc Med.* **6**, 31-34.  
 McCully, K. (1999). *J. Gerontol A Biol Sci Med Sci*, **54**, B291-294.  
 McDermott, M.M. et. al. (2001). *JAMA*, **286**, 1599-1606.

Scott, M.M. et al. (2005). *Proceedings of ISB '05*, Cleveland, OH.

Winter, D. (2005). *Biomechanics and Motor Control of Human Movement*. Wiley & Sons.

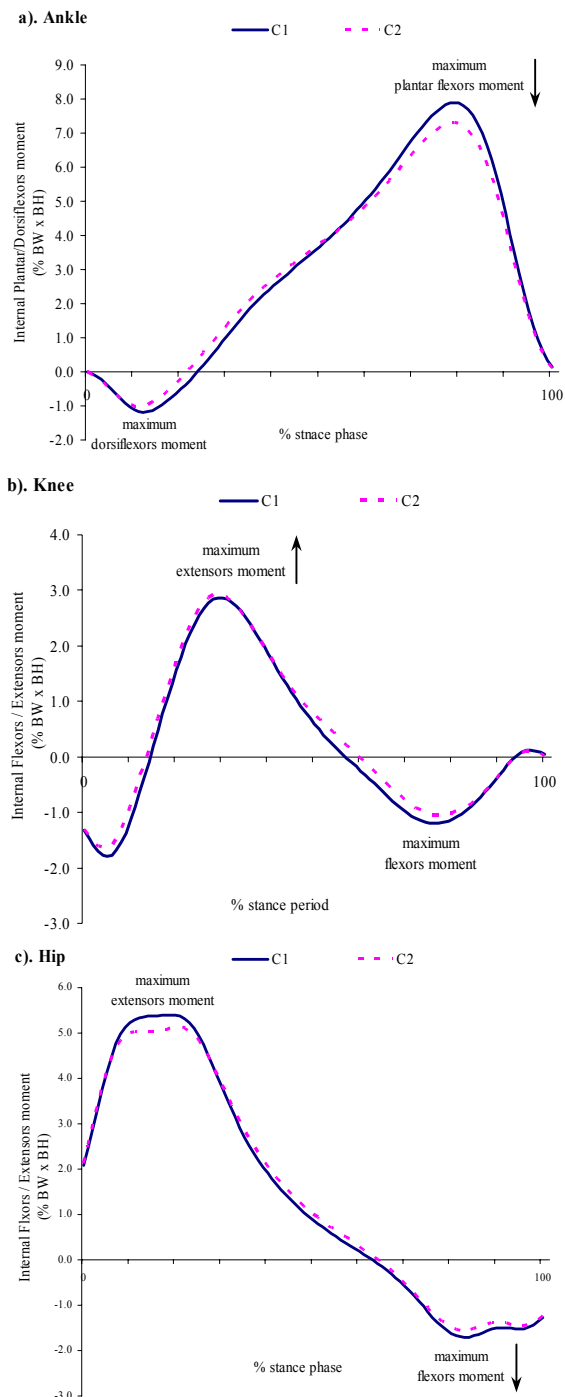


**Figure 1:** Ensemble joint moment curves of the a) ankle, b) knee, and c) hip for the pain free (C1) and pain (C2) conditions during the stance phase of walking.

# A POTENTIAL MECHANICAL PATHWAY FOR THE INITIATION OF OSTEOARTHRITIS IN THE OBESE POPULATION

Annegret Mündermann<sup>1,2</sup>, Seungbum Koo<sup>1</sup>, Lise Worthen-Chaudhari<sup>2</sup>, William J. Maloney<sup>1</sup>, Thomas P. Andriacchi<sup>1,2</sup>

<sup>1</sup> Stanford University, Stanford, CA

<sup>2</sup> Bone and Joint Center, Palo Alto VA, Palo Alto, CA

E-mail: amuender@stanford.edu Web: biomotion.stanford.edu

## INTRODUCTION

Obesity has been identified as a major risk factor for knee OA. Yet, the precise mechanism describing the basis for obesity as a cause of knee OA remains unknown. Recent results (Andriacchi et al. 2004) have indicated that healthy and osteoarthritic cartilage thickness is related to the knee adduction moment during walking. A relationship between cartilage morphology and loading during gait for overweight and obese subjects without osteoarthritis similar to that in patients with knee OA would suggest a mechanical pathway of the initiation of OA in this population. Other mechanical factors may also play a critical role in the initiation of knee OA. For instance, knee hyperextension at heel-strike during walking has been observed in overweight and obese subjects (Messier et al. 2005). The purpose of this study was to test the hypotheses that (a) the ratio of medial to lateral articular cartilage thickness is correlated with the magnitude of the knee adduction moment during walking and (b) the ratio of anterior to posterior articular cartilage thickness in both medial and lateral compartments is correlated with the degree of hyperextension of the knee at heel-strike in overweight and obese subjects and age and gender matched control subjects.

## METHODS

Six overweight and obese subjects (3 male; age  $48.5 \pm 7.7$  yrs; mass  $84.7 \pm 15.1$  kg; height  $1.70 \pm 0.15$  m; body mass index  $29.2$

$\pm 0.3$  kg/m<sup>2</sup>) and six age and gender matched normal-weight control subjects ( $46.5 \pm 10.2$  yrs;  $66.6 \pm 6.3$  kg;  $1.73 \pm 0.05$  m;  $22.3 \pm 1.1$  kg/m<sup>2</sup>) underwent magnetic resonance imaging (MRI) of their knees (fat suppressed 3D spoiled gradient echo sequence) (Koo et al. 2005). Cartilage was segmented in MR images, and three-dimensional thickness models were created. Average cartilage thickness was calculated for anterior, middle, and posterior regions of the medial and lateral femur condyles and anterior and posterior regions of the medial and lateral tibia plateau. Medial/lateral and anterior/posterior cartilage thickness ratios were computed. Then, a six marker link model, optoelectronic system, and force plate were used to collect kinematic and kinetic data for three walking trials at self-selected speed. The knee flexion angle at heel-strike and the first peak knee adduction moment were determined (Schipplein, Andriacchi, 1991). Paired Student's t-tests were used to compare subject characteristics, cartilage thickness, and average gait variables between groups ( $\alpha=0.05$ ). Linear regression analyses were used to relate cartilage thickness ratios to gait variables within each group ( $\alpha=0.05$ ).

## RESULTS AND DISCUSSION

Overweight and obese subjects had a negative correlation between the medial/lateral cartilage thickness ratio for the tibia and the first peak knee adduction moment whereas the control subjects had a positive correlation (Figure 1). This result

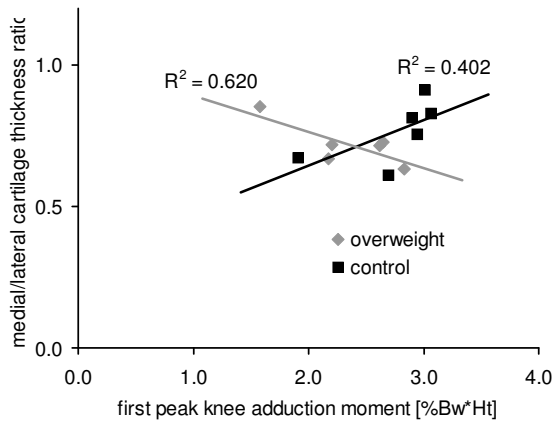


**Figure 1:** Relationship between medial/lateral cartilage thickness ratio for the anterior cartilage region and the first peak knee adduction moment.

indicates that the cartilage thickness at the knee joint in overweight and obese subjects responds to loading during gait in a manner similar to patients with OA as previously reported (Andriacchi et al. 2004). These findings suggest the possibility that increased weight initiates a pathway of cartilage degeneration prior to the emergence of OA symptoms. This result and the previous finding that patients with more severe knee OA have a higher knee adduction moment compared to healthy subjects (Mündermann et al. 2004) supports the interpretation that a higher knee adduction moment may not be the cause of OA but the result of morphological changes associated with the disease. The results of the current study suggest that cartilage of overweight and obese subjects is sensitive to the load distribution at the knee during walking and reacts similarly to higher loads as osteoarthritic cartilage even though the load magnitude is in a healthy range.

Another important finding of this study was that the negative correlation between medial/lateral thickness ratio and adduction moment was more pronounced in the anterior than the posterior tibia region ( $P = 0.032$ ). The anterior/posterior cartilage

thickness ratio for the lateral tibia plateau was higher for the overweight and obese subjects than for the normal-weight subjects (+25.6%;  $P = 0.011$ ). Three of the six overweight and obese subjects had knee hyperextension at heel-strike that would be considered pathological (knee flexion angle  $< -5.0^\circ$ ). The anterior/posterior cartilage thickness ratio showed a strong relationship with knee hyperextension at heel-strike (overweight and obese subjects:  $R^2 = 0.637$ ;  $P = 0.028$ ) suggesting that knee hyperextension at heel-strike may be critical. Thus, it is possible that in subjects with greater knee hyperextension, the femur is in contact with the tibia more anteriorly at heel-strike during walking and that cartilage adapts to these differences in loading area.

This study represents a first step in evaluating a proposed mechanism that involves testing the relationship between variations in *in vivo* functional mechanics and variations in cartilage thickness in an obese population, and thus a potential mechanical pathway for the initiation of OA in the obese population. In addition, these findings suggest the potential benefits of the earlier introduction of a load modifying intervention in this population.

## REFERENCES

- Andriacchi T.P. et al. (2004) *Ann Biomed Eng.* **32**, 447-457.
- Koo S. et al. (2005) *Osteoarthritis Cartilage*, **13**, 782-789.
- Messier S.P. et al. (2005) *Arthritis Rheum*, **52**, 2026-2032.
- Mündermann A. et al. (2004) *Arthritis Rheum*, **50**, 1172-1178.
- Schipplein O.D., Andriacchi T.P. (1991) *J Orthop Res*, **9**, 113-119.

## ACKNOWLEDGEMENTS

NIH grant # AR049792; VA grant # A04-3583R

# SCAPULAR KINEMATIC ALTERATIONS FOLLOWING SERRATUS ANTERIOR FATIGUE

John D. Borstad<sup>1</sup>

<sup>1</sup> Physical Therapy Division, The Ohio State University, Columbus, OH, USA  
e-mail: borstad.1@osu.edu

## INTRODUCTION

Serratus anterior is positioned to control upward rotation, posterior tipping and external rotation of the scapula on the thorax during arm elevation. For individuals with subacromial impingement, altered scapular kinematics including decreased posterior tipping, increased internal rotation and decreased upward rotation have been identified. One potential mechanism for these alterations is serratus anterior fatigue. Individuals with high exposure to repetitive overhead activities are at risk for serratus fatigue.

At the present time, no clinical test is available to test for the fatigability of serratus anterior or to measure the consequences of such fatigue on scapular kinematics. The present study was designed to determine whether a task sufficient to produce serratus anterior fatigue in normal volunteers would lead to altered scapular kinematics consistent with the deficits seen in patients with impingement.

## METHOD

Seven healthy subjects without a history of shoulder pathology volunteered to participate. The fatiguing task consisted of holding a push-up plus position with the feet elevated 30cm until no longer able to continue. This task approximates one previously demonstrated to fatigue serratus anterior. Measured variables during the fatiguing task included time to failure (sec),

and self-report of fatigue (Borg scale).

Three-dimensional motion data of the humerus, scapula and trunk of the dominant arm were also collected on each subject during five repetitions of active arm elevation before and after the fatiguing task using the Flock of Birds electromagnetic system.

Scapular orientation angles relative to the trunk were determined at humerus to trunk angles of 60°, 90°, and 120° before and after the fatiguing task. The arm elevation and arm lowering phases were considered separately. A repeated measures Analysis of Variance was used to determine the effect of the fatiguing task on scapular orientation for each phase, with time (before and after) and angle (60°, 90°, and 120°) the within subject variables.

## RESULTS/DISCUSSION

The mean time to failure during the task was 84.5 sec (SD 27.8), and the mean change in Borg score was 5.5 (SD 2.1). During arm elevation, there was a statistically significant interaction effect between time and angle ( $P < 0.001$ ) for scapular tipping. Post-hoc testing revealed that there was significantly more scapular anterior tipping at 120° after the task (-7.2°) than before the task (-3.9°). There were no other statistically significant results during arm elevation.

During arm lowering, there continued to be a significant interaction effect for tipping ( $P < 0.01$ ) with more anterior tipping after the

task (3.0° greater at 120°; 3.1° greater at 90°) than before the task. There were also statistically significant main effects of the fatiguing task on scapular upward rotation ( $P<0.05$ ) and tipping ( $P<0.05$ ). There was 2.3° less upward rotation and 2.5° more anterior tipping after the task.

Other authors have examined scapular kinematics following fatiguing tasks and have also demonstrated kinematic alterations. These studies, however, did not specifically isolate serratus anterior during their fatigue task. The current findings describe a direct effect of serratus anterior fatigue on scapular kinematics.

This task has potential for use as a clinical test for serratus function. It appears to adequately fatigue serratus and result in scapula kinematic alterations in a young, healthy sample. The task may be able to provide clinicians with a tool to assess scapular stability and a patient's ability to return to repetitive activities using the arms. Further testing on a larger sample is necessary to establish normative data. In

addition, testing on individuals with shoulder impingement is needed to determine whether they perform differently on this task, and whether their scapular kinematics are differentially affected by fatigue.

## **SUMMARY/CONCLUSIONS**

Performing a task designed to fatigue serratus anterior resulted in altered scapulothoracic kinematics in healthy subjects. Scapular posterior tipping was decreased during both elevation and lowering the arm, while scapular upward rotation was decreased during arm lowering only.

## **REFERENCES**

- Ebaugh DD, McClure PW, Karduna AR. (2005). *J Electromyogr Kinesiol*. 23: Epub.
- Ebied AM, Kemp GJ, Frostick SP. (2004). *J Orthop Res*. 22:872-877.
- McQuade KJ, Dawson J, Smidt GL. (1998). *J Orthop Sports Phys Ther*. 28(2):74-80.

# A MECHANISM TO LOWER THE KNEE ADDUCTION MOMENT DURING WALKING: GAIT RETRAINING AS INTERVENTION FOR KNEE OA

Jessica L. DeMarre<sup>1</sup>, Lars Mündermann<sup>1</sup>, Thomas P. Andriacchi<sup>1,2</sup>,  
Annegret Mündermann<sup>1,2</sup>

<sup>1</sup> Stanford University, Stanford, CA

<sup>2</sup> Bone and Joint Center, Palo Alto VA, Palo Alto, CA

E-mail: amuender@stanford.edu Web: biomotion.stanford.edu

## INTRODUCTION

The external adduction moment at the knee during walking has been shown to be a strong predictor for medial compartmental knee osteoarthritis (OA) severity (Mündermann et al. 2004) and rate of progression (Miyazaki et al. 2002). It has been reported (Mündermann et al. 2005) that patients with knee OA adopt a gait pattern that involves a more extended knee at heel-strike, a more rapid increase in the ground reaction force, greater lateral ground reaction force, and greater knee and hip abduction moments. It was speculated that this pattern is caused by a lateral shift of the trunk with the goal to control the peak knee adduction moment. This strategy appeared to be successful only in patients with less severe knee OA as these patients had normal knee adduction moments in contrast to patients with more severe knee OA who had higher moments than matched control subjects. If increasing trunk motion would result in similar gait changes and also reduced knee adduction moments, this method of gait retraining could be used as an intervention to reduce medial compartment load in patients with knee OA. The purpose of this study was to test the hypothesis that when walking with increased medio-lateral trunk motion, control subjects will have more extended knees at heel strike, increased knee and hip abduction moments resulting in reduced knee and hip adduction moments compared to normal walking.

## METHODS

Nineteen subjects (7 female, 12 male; age:  $22.8 \pm 3.1$  yrs; height:  $174.8 \pm 9.7$  cm; mass:  $70.5 \pm 16.3$  kg) participated in this study after giving written consent in accordance with the Institutional Review Board. None of the subjects had previously been treated for any clinical lower back or lower extremity condition or had any activity-restricting medical or musculoskeletal condition. Subjects performed walking trials of normal gait and increased medio-lateral trunk sway. The degree of sway for the increased trunk sway trials and walking speed were self-selected by the subject. Kinematics and kinetics of each trail was analyzed using the 6-marker-link model, ground reaction force measurements, and limb segment mass/inertia properties, and moments were then normalized to body weight and height (% Bw\*Ht) (Schipplein and Andriacchi 1991). Knee angle at heel-strike, loading rate, knee and hip abduction and adduction moments, and lateral ground reaction force were compared between the two conditions using a MANOVA and paired Student's t-tests ( $\alpha = 0.01$ ).

## RESULTS

When walking with increased trunk sway, all subjects had greater hip and knee abduction moments and reduced first peak hip and knee adduction moments (Figure 1). With increased trunk sway, subjects also

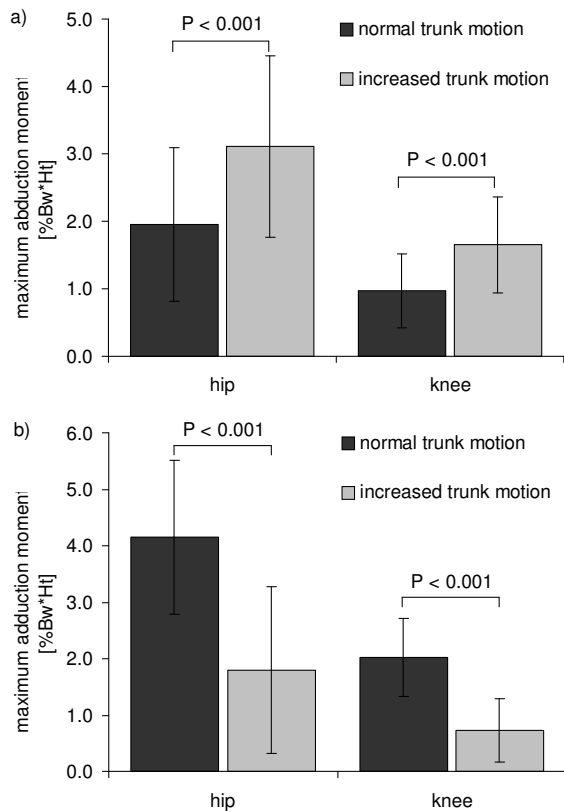


Figure 1: Average (1 standard deviation) external peak hip and knee abduction (a) and adduction (b) moments for walking with two trunk sway conditions (n = 19).

landed with slightly more flexed knees (+3.0°; P=0.009) and similar lateral ground reaction force compared to walking with normal trunk motion. Walking speed was the same for normal and increased trunk sway trials walked at similar speed (1.48 ± 0.17m/s and 1.44 ± 0.15m/s, respectively).

## DISCUSSION

The results support the hypothesis that increased trunk sway in healthy subjects leads to similar changes in hip and knee abduction moments as have been reported for patients with knee OA (Mündermann et al. 2005). In contrast to patients with knee OA, this gait pattern resulted in lower knee adduction moments in all healthy subjects. Interestingly, the healthy subjects tested in

this study also had similar knee flexion angles at heel-strike, loading rates, and lateral ground reaction forces when walking with increased trunk sway and with normal trunk sway. The combined results of this study and our previous work (Mündermann et al. 2005) suggest that patients with knee OA may utilize a strategy to control the knee adduction moment that includes differences in trunk sway but may be constrained by the muscle strength of hip and trunk stabilizers, and thus is only successfully accomplished by patients with less severe knee OA.

Subjects in this study were instructed to merely increase their medio-lateral trunk sway, and required minimal practice (less than three practice trials) to adopt the gait patterns presented here. Thus, increased trunk sway may be a simple yet effective non-invasive intervention in early knee OA that amplifies patients' natural gait changes leading to a reduction in medial compartment load without secondary changes in gait mechanics such as decreased knee flexion angle at heel-strike or increased ground reaction forces and loading rates that may represent increased loads at other joints.

This result supports the concept of developing new methods for gait retraining of patients with knee OA in the medial compartment of the knee.

## REFERENCES

- Miyazaki T. et al. (2002) *Ann Rheum Dis* **61**:617-622.
- Mündermann, A. et al. (2004) *Arthritis Rheum*, **50**, 1172-1178.
- Mündermann, A. et al. (2005) *Arthritis Rheum*, **52**, 2835-2844.
- Schipplein, O.D., Andriacchi, T.P. (1991) *J Ortho Res*, **9**, 113-119.

# DIFFERENT GAIT PARADIGMS DISTINGUISH IMMEDIATE VS. LONG-TERM EFFECTS OF CONCUSSION

Robert D. Catena, Paul van Donkelaar and Li-Shan Chou

Department of Human Physiology, University of Oregon, Eugene, OR, USA  
E-mail: [chou@uoregon.edu](mailto:chou@uoregon.edu) Web: <http://biomechanics.uoregon.edu/chou/>

## INTRODUCTION

Bernstein (2002) has found evidence of prolonged effects of concussions, even up to a year after mild TBI. When still suffering from concussive effects, Cantu (1998) found increased susceptibility to subsequent concussions. The CDC (1997) has reported increased neurological damage and fatalities after multiple concussions. However, current treatment standards for concussion do not adequately account for this sequence of events. A return to pre-injury activities usually occurs long before the effects of concussion have been resolved (Parker et al., in press).

Several dynamic testing protocols have been examined in recent years to distinguish a concussed group from healthy individuals. However, these studies have focused on a comparison between level walking and one other difficult task. With the exception of Parker et al. (in press), longitudinal analyses have not been conducted as well. There is little information comparing the ability of testing protocols to distinguish a concussed group from healthy controls; particularly tracking task performance to a point of recovery. The purpose of this study was to determine a sensitive dynamic measurement of the effects of concussion by comparing previously utilized methods. A longitudinal comparison will aid in the development of a sensitive testing protocol to determine a proper time to return to activity.

## METHODS

Thirty grade II concussed (CONC) subjects were first tested within 48 hours after injury. Each was tested again at 5, 14 and 28 days post-injury. Gender, age, stature and activity level matched controls (NORM, n=30) were also tested at four equivalent intervals. Whole body motion data were collected with an 8-camera motion analysis system. Twenty-nine reflective markers were used to create a thirteen-link model, with the segment center of mass (CoM) defined according to Dempster (Winter, 1990). The whole-body CoM was calculated using the weighted sum of each segment. Center of pressure (CoP) location was found with two force plates. Each day's collection was divided into three parts: single task level walking (Level), Obstacle-crossing at 10% of body height (OB), and level walking with a concurrent cognitive task (Q&A, e.g. subtraction by sevens).

Spatial-temporal parameters and CoM motion in relation to the CoP were examined. A three-way mixed model analysis was used to assess significant differences. A comparison between groups was of particular interest in this project, so post-hoc group comparisons were performed with adjustments for multiple comparisons.

## RESULTS AND DISCUSSION

Spatial-temporal parameters only detected group differences 48 hours after the injury. CONCs walked significantly slower during the Q&A task and OB task (Fig 1). They also had shorter stride times than NORMs during OB. There was no significant

difference between the two groups' spatial-temporal parameters by day 5. These results indicate that concussed individuals adapted a conservative gait strategy immediately following the concussion.

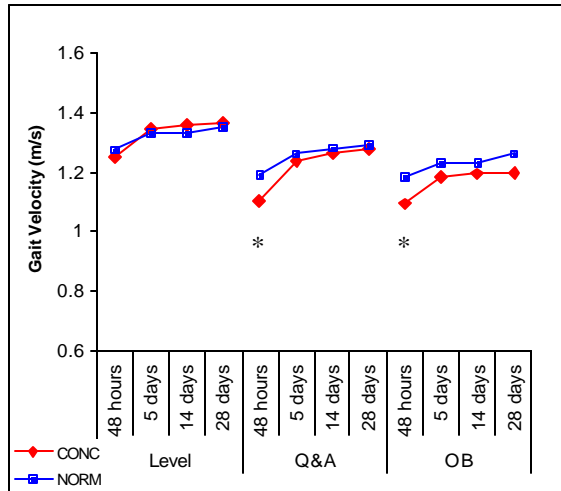


**Figure 1:** Gait Velocity for each condition on each day. An asterisk indicates significant group differences

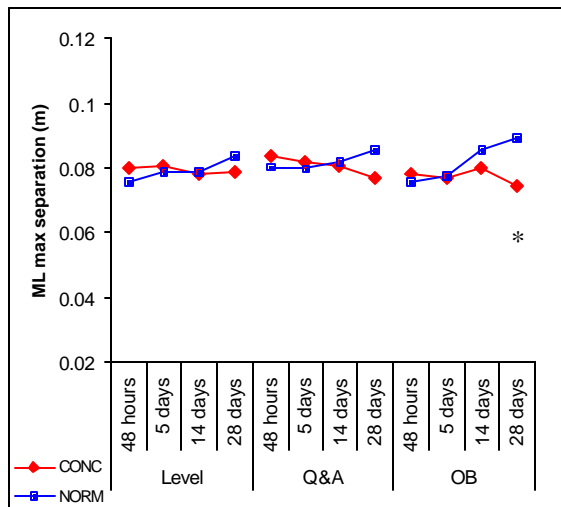


**Figure 2:** Medial-lateral max separation between the CoM and CoP for each condition on each day. An asterisk indicates significant group differences

Anterior-posterior (A/P) range of motion of the CoM was not significantly different

between the two groups during any testing session. Neither was the CoM medial-lateral (M/L) range of motion, through the first three testing sessions. However, by day 28 CONCs demonstrated significantly less separation between the CoM and CoP in the M/L direction, but only during the OB task (Fig 2) indicating possible residual effects of concussion on the CoM and CoP coordination in the frontal plane.

Neither group displayed better cognitive performance. Trailing toe obstacle clearance showed a group by day interaction. In the first two testing sessions CONCs had a greater clearance height. By day 14, CONCs no longer used this conservative strategy.

## SUMMARY/CONCLUSIONS

Initially after a concussion, a concurrent mental task or obstacle during gait can both pinpoint conservative gait strategies. Conservative strategies are not observed by day 5. By day 28, obstacle-crossing was able to distinguish a new strategy following concussion, which allowed for normal gait velocity, but required less medial-lateral CoM-CoP separation.

## REFERENCES

Bernstein DM, 2002, *J. International Neuropsychological Society*, **8**:673-682.  
 Cantu RC, 1998, *CSM*, **17**(1):37-44.  
 CDC, 1997, *MMWR*, **46**(10):224-227.  
 Parker TM, et al., 2006, *MSSE*, in press.  
 Winter DA. 1990. *Biomechanics and Motor Control of Human Movement*. Wiley, New York, pp.56-7.

## ACKNOWLEDGEMENTS

This study was supported by the CDC (R49/CCR021735 and CCR023203).

# MAGNETIC RESONANCE ELASTOGRAPHY: A NON-INVASIVE METHOD TO DIFFERENTIATE BETWEEN HEALTHY AND PATHOLOGIC MUSCLE STIFFNESS

Stacie I. Ringleb<sup>1</sup>, Kenton R. Kaufman<sup>1</sup>, Jeffrey R. Basford<sup>1</sup>, Krista Coleman-Wood<sup>1</sup>,  
Qingshan Chen<sup>1</sup>, Richard L. Ehman<sup>2</sup>, Kai-Nan An<sup>1</sup>

<sup>1</sup>Biomechanics Laboratory, Division of Orthopedic Research, Mayo Clinic College of Medicine,  
Rochester, MN USA

<sup>2</sup>MRI Research Laboratory, Department of Radiology, Mayo Clinic College of Medicine,  
Rochester, MN USA

E-mail: [an.kainan@mayo.edu](mailto:an.kainan@mayo.edu) Web: [mayoresearch.mayo.edu/mayo/research/biomechanics](http://mayoresearch.mayo.edu/mayo/research/biomechanics)

## INTRODUCTION

The underlying cause of functional changes that occur in skeletal muscle as a result of pathology or injury are often difficult to understand. Instead of measuring functional changes, quantification of the elastic properties of skeletal muscle may improve our understanding of the pathophysiology of muscular injury.

Magnetic Resonance Elastography (MRE) is a non-invasive phase contrast MR technique that can directly image induced shear waves in a muscle of interest. Tissue displacements caused by the shear waves are then calculated at each voxel and used to estimate the shear stiffness of the muscle (Manduca et al., 2001). The purpose of this project was to: 1) assess repeatability and reliability of MRE data analysis, 2) identify an asymmetry index in healthy asymptomatic volunteers and 3) to determine if MRE is capable of detecting differences between healthy and pathologic muscle.

## METHODS

Bilateral MRE data were collected from the lateral gastrocnemius in 11 asymptomatic volunteers (8 female, 3 male, age 25±3) and 10 patients (4 female, 6 male, age 54±20) with hemiparesis as the result of stroke.

Data were collected with the ankle positioned at 30° and 10° of plantarflexion, as well as 10° of dorsiflexion while the muscle was relaxed. Additionally, the ankle was positioned at 10° of plantarflexion while internal isometric dorsiflexion moments from 0-20 Nm were applied.

An electromechanical driver placed at the distal end of the gastrocnemius applied shear waves at 100 Hz. A gradient-echo, cyclic motion sensitizing sequence was used to obtain the MRE data (TR/TE of 100ms/min full, 256x64 acquisition matrix, 24cm FOV, acquisition time 68 seconds). Shear stiffness was estimated using a phase gradient technique (Manduca et al., 2001).

The data from the asymptomatic volunteers were used to assess repeatability (n=7), inter- and intra-operator reliability (n=5) of data analysis and an asymmetry index (n=11). The coefficient of repeatability was used to assess repeatability and reliability (Bland and Altman, 1995). The asymmetry index ( $A_x$ ) was calculated (equation 1), where D is the dominant limb and N is the non-dominant limb.

If  $D/N \geq 1$ , then  $A_x = D/N - 1$

If  $D/N < 1$ , then  $A_x = 1 - D/N$  (equation 1)

The asymmetry threshold was determined (equation 2), where  $t_{n-1, \alpha/2}$  was the critical value of a  $t$  distribution,  $n$  is the number of

subjects, and  $s$  is the standard deviation of  $A_x$  (Kaufman et al., 1996).

$$A_{ul} = 0 \pm t_{n-1, \alpha/2} \frac{s}{\sqrt{n}} \quad (\text{equation 2})$$

The asymmetry threshold was used to determine if measured differences between the affected and unaffected limbs in the stroke patients were due to anatomic variations or because of changes in the mechanical properties of the muscle. A Wilcoxon signed rank test was used to compare the bilateral stroke patient data with bilateral age and gender matched healthy volunteers ( $n=3$ ).

## RESULTS AND DISCUSSION

The coefficient of repeatability was  $\pm 7.2$  kPa, the inter-operator reliability was  $\pm 3.55$  kPa and the intra-operator reliability was  $\pm 3.24$  kPa. The asymmetry threshold, indicating that differences in shear stiffness exceeding these limits are not due to anatomic variations, was  $\pm 7.3$  kPa. The asymmetry threshold was exceeded in at least one testing condition for all subjects with hemiparesis ( $10^\circ$  DF  $n=4$ ;  $10^\circ$  PF  $n=5$ ;  $30^\circ$  PF  $n=6$ ; active loading  $n=3$ ).

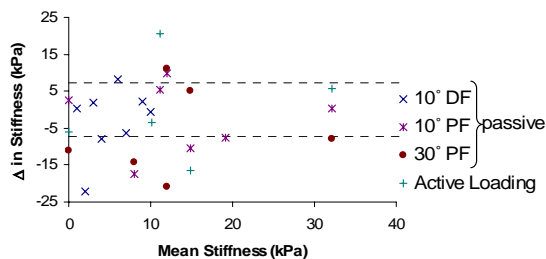


**Fig. 1.** Individual subject difference between affected and unaffected limb in stroke patients ( $n=10$ ). The dashed lines indicate the asymmetry threshold, which was exceeded in at least one testing condition for all subjects with hemiparesis ( $10^\circ$  DF  $n=4$ ;  $10^\circ$  PF  $n=5$ ;  $30^\circ$  PF  $n=6$ ; active loading  $n=3$ ).

Notable differences between the affected limb in the stroke patients and the non-dominant limb in the age matched normals

( $n=3$ ) were found when the ankle was positioned at  $30^\circ$  ( $p=0.07$ ) and  $10^\circ$  ( $p=0.1$ ) of plantarflexion (Fig. 2). Significance may be found with a larger sample size.

MRE is capable of detecting muscle pathology, both by comparing the affected to the unaffected limb in hemiplegic stroke patients as well as in comparison with age and gender matched control subjects. Strength testing and data collection from additional age matched neurologically intact subjects is planned to further interpret these data.

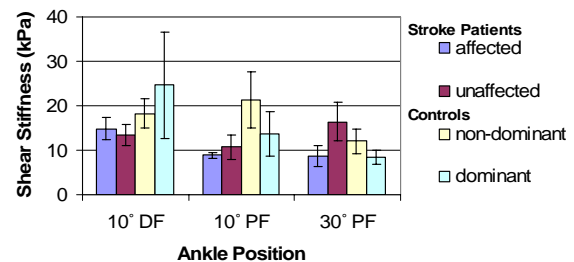


**Fig. 2.** Mean stiffness in hemiplegic stroke patients and age and gender matched control subjects ( $n=3$ ).

## SUMMARY AND CONCLUSIONS

MRE can detect differences in the shear stiffness between healthy and pathologic muscle. Further studies will be designed to interpret these differences.

## REFERENCES

- Bland JM and Altman DG (1995) *Lancet*, **346**, 1085-1087.
- Kaufman, K.R., et al. (1996) *J Ped. Orthop*, **16**, 144-150.
- Manduca, A, et al. (2001) *Med Image Analysis*, **5**, 237-254.

## ACKNOWLEDGEMENTS

This study is supported by NIH grants EB00812, EB01981, CA91959 and HD07447.



# NEUROMUSCULAR CONTROL IS ALTERED IN SIMULATED GAIT WITH ANKLE FOOT ORTHOSIS (AFO)

Charles A. Crabtree and Jill S. Higginson

Department of Mechanical Engineering, University of Delaware, Newark, DE, USA  
E-mail: crabtree@me.udel.edu      Web: www.me.udel.edu/higginson/research.htm

## INTRODUCTION

AFOs are prescribed for ambulatory stroke patients to eliminate foot drop and provide joint stability by restricting range of motion and supplying restorative passive joint torque. Understanding how AFOs mechanically alter muscle activity and synergies could assist orthotists, therapists and patients in device tuning and prediction of muscle utilization.

Previous studies have focused on the effect of AFO use on such parameters as stride length, speed, ground reaction force profile and knee moment (de Wit et al., 2004; Gök et al., 2003). However, none to date have concentrated on the changes in neuromuscular control caused by wearing an AFO during gait. Therefore, the goal of this initial study is to investigate the effects of wearing AFOs on muscle excitation timing and magnitude in healthy gait.

## METHODS

Passive restorative torque was measured from three one-piece AFOs (small, medium, and large). Each AFO (CAMP Healthcare) was secured to an isokinetic dynamometer (Biodex) in passive mode using heavy-duty velcro straps and a 3" pvc insert to stabilize the shank. Torque was measured at a sampling rate of 1 kHz during AFO plantarflexion and dorsiflexion at a rate of 5 deg/s over a range of 50 degrees for five cycles. This process was repeated for speeds of 30 and 120 deg/s. After removing

baseline torque due to the weight of the AFO and footplate assembly, the average torque from 5 cycles was calculated. Each hysteresis plot was then split into two plots to isolate the restorative torques associated with positive and negative joint velocity. By separately interpolating slopes and intercepts to account for rate dependence, a quasi-linear torque-angle relationship was derived:

$$\tau_{AFO} = [-(a)\log(\dot{\theta}) - b]\theta + c\dot{\theta}^d$$

where the coefficients 'a', 'b', 'c' and exponent 'd' depend on the size of the AFO.

A previously developed forward dynamic computer simulation of gait [Neptune 2001] which includes a 9 DOF musculoskeletal model of the human lower extremities was modified to include the AFO models. Masses, inertias and segment centers of mass for eleven rigid body segments were defined according to those of a healthy male (Delp & Loan, 1995). Fifteen muscles from each leg were modeled (Zajac, 1989). Exponential functions were used to model passive stiffness and range of motion limits for each joint (Davy & Audu, 1987). Experimentally-derived passive AFO torque was applied bilaterally to the computer model's ankles. A set of averaged gait data from adult subjects walking at 1.5 m/s was tracked to optimize muscle control parameters and initial conditions for simulation. The cost function tracked errors in kinematics and ground reaction forces. Using a simulated annealing algorithm (Goffe, 1994), the cost function was minimized to obtain plausible muscle timing

and excitation for an entire gait cycle, which were used to drive the simulation. Muscle power was computed as the product of fiber velocity and muscle force.

## RESULTS AND DISCUSSION

For both tibialis anterior (TA) and soleus (SOL), excitation timing for nominal and AFO trials was similar. Figure 1 shows the optimized excitation profiles for SOL, which was allowed to produce three levels of excitation during stimulation. Excitation during the AFO trial was less than nominal during the first two-thirds of stimulation—when SOL eccentrically contracts to control forward progression of the tibia and provide body weight support. During pre-swing, SOL excitation increased with the AFO trial, but this resulted in only a slight increase over nominal in peak muscle power generation.

Figure 2 shows the optimized excitation profiles for TA, which was constrained to a single intensity level during stimulation. The overall effect of lower excitation magnitude in the AFO trial was a 40% reduction of peak muscle power output compared with the nominal trial.

## SUMMARY/CONCLUSIONS

As polypropylene is a viscoelastic material, AFO torque depends on deformation rate as well as shape and size. Wearing an AFO affects mechanical energy distribution even when gait kinematics are closely matched, implying that AFOs induce changes in neuromuscular control.

Comprehensive assessment of an AFO's mechanical effects will require consideration of patient history, gait dynamics and measured torque output from the prescribed AFO. Future research will include extending

current models to asymmetric and 3D motion, concurrent with experimental trials with healthy and stroke subjects.

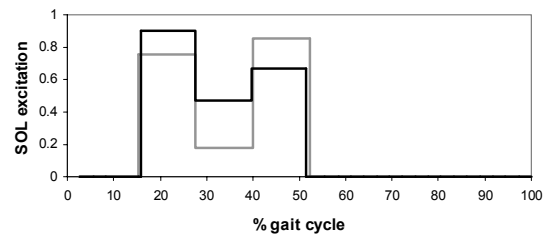


**Figure 1:** Excitation magnitude for SOL is reduced during stance when wearing the AFO (gray line) compared to nominal (black line).

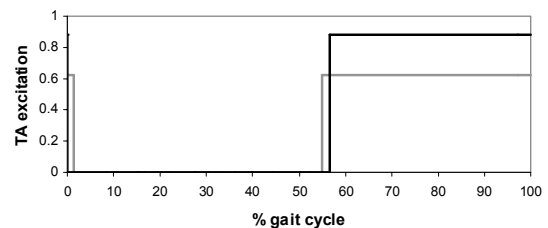


**Figure 2:** Excitation magnitude for TA is reduced when wearing the AFO (gray line) compared to nominal (black line).

## REFERENCES

- Davy D.T., Audu M.L. (1987). *J. Biomech.* **20**, 187–201
- Delp, S.L., Loan, J.P. (1995). *Comp. Biol. Med.* **25**, 21-34.
- De Wit, D.C.M. et al. (2004). *Clin. Rehab.*, **18**, 550-557.
- Goffe, et al. (1994). *J. Econometrics*, **60**, 65-100.
- Gök, H., et al. (2003). *Clin. Rehab.*, **17**: 137-139.
- Neptune, R.R., et al. (2001). *J. Biomech.* **34**, 1387-1398.
- Zajac, F.E. (1989) *CRC Rev. Biomed. Eng.*, **17**, 359-411.

## ACKNOWLEDGEMENTS

Funding provided by the University of Delaware Research Foundation.

# DIABETIC NEUROPATHY IS RELATED TO JOINT STIFFNESS DURING LATE STANCE PHASE

D. S. Blaise Williams,<sup>1</sup> Denis Brunt<sup>1</sup> and Robert J. Tanenberg<sup>2</sup>

<sup>1</sup> East Carolina University, Greenville, NC, USA

<sup>2</sup> Brody School of Medicine, East Carolina University, Greenville, NC, USA

E-mail: williamsdor@ecu.edu

## INTRODUCTION

It has been reported that as many as 35% of ulcers in individuals with diabetes occur on the plantar surface of the first metatarsal head (Birke and Sims, 1986). Increased plantar pressures beneath the metatarsal heads in individuals with diabetes are predictive of ulceration in this region (Veves et al, 1992). Increased plantar pressures are present in individuals with peripheral neuropathy. Since neuropathy affects both sensory and motor function in the diabetic patient (Reiber et al, 1999), neuromuscular compromise likely results in changes in lower extremity biomechanics. It has been previously reported that persons with diabetic neuropathy have demonstrated alterations in general gait parameters (Katoulis et al, 1997). Since the highest forces and pressures are present beneath the metatarsal heads during the second half of the stance phase of the gait cycle, differences in biomechanics should be evaluated during this time. General stiffness is common, especially in the feet, in the diabetic population and has been evaluated statically (Glasoe et al, 2004). Since joint stiffness is a contributor to total lower extremity stiffness, it is possible that individuals with peripheral neuropathy would have increased joint stiffness during gait. Therefore, the purpose of this investigation was to demonstrate differences in ankle and knee joint stiffness between type 2 diabetic individuals with and without peripheral neuropathy.

## METHODS

22 subjects were tested and placed in two groups (Non-neuropathic and neuropathic). All subjects were between the ages of 32 and 70 years and had a current diagnosis of type 2 diabetes. Sensation on the plantar surface of the feet was determined using the method described by Birke and Sims (1986). Kinematic and kinetic data were collected using a 6-camera, motion analysis system combined with a force plate. Each subject was asked to walk along a 60-foot walkway at a speed of 1.25 m/s ( $\pm 5\%$ ). Ten foot strikes were collected and averaged for each subject.

The three-dimensional coordinates of each marker were reconstructed using a direct linear transformation method. Joint moments were calculated employing a standard inverse-dynamic calculation method. Ankle and knee joint stiffness were calculated using the method described by Hansen et al. (2004) during walking. Specifically, ankle joint moment was plotted against ankle joint angle in the sagittal plane during the stance phase of gait. The slope between successive points was determined, averaged over the periods of 50 to 65% and 65 to 80% of stance and compared between groups. 80% is consistent with the propulsive peak of the vertical ground reaction force. Comparisons between neuropathic and non-neuropathic subjects were made using a one-tailed Student's t-test ( $p \leq 0.05$ ).

## RESULTS AND DISCUSSION

Ankle joint stiffness for both neuropathic and non-neuropathic subjects is shown in Figure 1. From 50% to 65% of the gait cycle there is no significant difference in ankle stiffness between the groups. Although there was no group difference for peak dorsiflexion, the peak occurred significantly earlier for the non-neuropathic group.

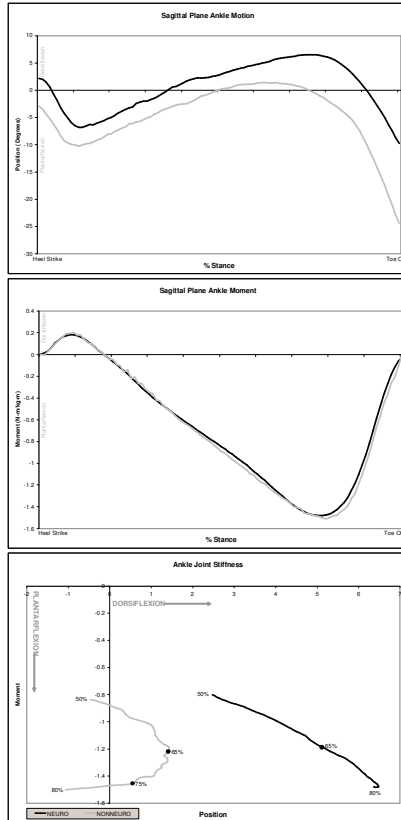


**Figure 1.** Ankle joint motion, moment and stiffness. Note the bimodal nature of the ankle stiffness in the non-neuropathic group.

Unlike the ankle, the pattern of knee moments and joint angle at the knee, and therefore stiffness (Figure 2), are similar for both groups. However, there was a trend for peak knee extension to occur earlier in stance for the neuropathic group. Therefore, knee stiffness becomes negative prior to 65% of stance in the neuropathic group.

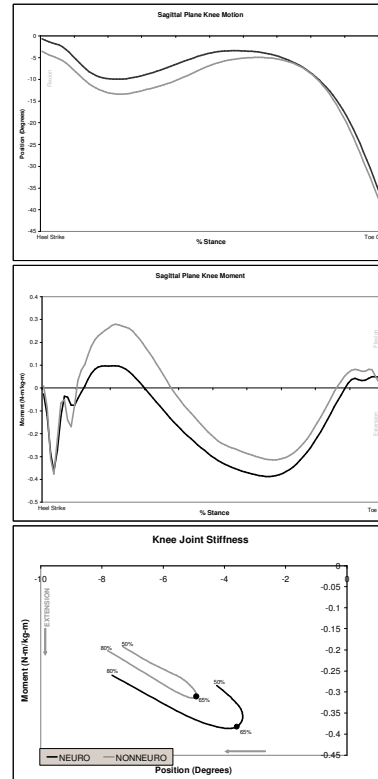


**Figure 2:** Knee joint motion, moment and stiffness. There was no difference in stiffness between groups.

## SUMMARY/CONCLUSIONS

The current data demonstrates clear differences in knee and ankle stiffness between subjects with and without peripheral neuropathy related to type 2 diabetes. The different patterns in joint motion dictated differences in joint stiffness.

## REFERENCES

- Birke, J.A., Sims, D.S., (1986) *Lepr Rev.* 57:261-7.
- Glasoe WM et al. (2004). *Foot Ankle Int.* 25:550-5.
- Hansen AH et al (2004) *J Biomech.* 37:1467-74.
- Katoulis, E. C. et al (1997) *Diabetes Care.* 20: 1904-1907.
- Reiber GE et al (1999) *Diabetes Care.* 22:157-62
- Veves A, et al (1992) *Diabetologia.* 35:660-3.

# THE INFLUENCE OF SELECTED TECHNICAL PARAMETERS ON DISCUS THROWING PERFORMANCE

Steve Leigh and Bing Yu

Center for Human Movement Science, Division of Physical Therapy, University of North Carolina at Chapel Hill, Chapel Hill, NC 27599-7135, USA  
E-mail: stvleigh@email.unc.edu

## INTRODUCTION

The official distance of a discus throw is determined by the speed, angle, and height of release. These release characteristics are altered by each athlete's technique during the throwing procedure. Effective technique maximizes the speed of release and optimizes the angle and height of release. The purpose of this study is to determine the effects of combinations of technical parameters on discus throwing performance.

## METHODS

Videographic data of 288 competitive trials by male and female discus throwers, and a calibration frame specific to each meet, were captured using 2 camcorders operating at a sampling frequency of 60 frames/sec.

Two-dimensional coordinates of 21 body landmarks and the discus were acquired by manually digitizing the video clips of every throw. The calibration frame was similarly digitized. Real-life, 3-D coordinates were obtained from the mathematically synchronized 2-D landmark and calibration coordinates using the direct linear transformation procedure. The technical parameters were reduced at 6 critical instants for each trial. The phase times and release characteristics were also reduced.

Hierarchical, stepwise multiple regression analyses were performed to determine the influence of linear combinations of the

technical parameters on discus throwing performance. The technical parameters were the independent variables, official distance was the dependent variable, and the release characteristics were used as intermediate variables. The order of entry into the regression was established using a deterministic model. Male and female discus throwers were assessed separately.

## RESULTS

For female discus throwers a linear combination of: shoulder-arm separation at left foot down, hip-shoulder separation at left foot down, arm elevation at right foot off, trunk tilt at right foot down, trunk tilt at left foot down, release phase time, and second single support phase time accounted for a significant amount of the discus throwing performance variability ( $R^2 = 0.414$ ,  $F_{7,132} = 13.343$ ,  $p < 0.001$ ). The full model is shown in Table 1.

For male discus throwers a linear combination of: shoulder-arm separation at max back swing, shoulder-arm separation at release, hip-shoulder separation at left foot off, and arm elevation at max back swing accounted for a significant amount of the discus throwing performance variability ( $R^2 = 0.194$ ,  $F_{4,143} = 8.625$ ,  $p < 0.001$ ). The full model is shown in Table 2.

## DISCUSSION

Female discus throwers with large official

distances tended to have greater separation angles after the flight phase, greater arm elevation before the flight phase, sequentially changing trunk tilts during the throwing procedure, and shorter phase times closer to release. This may assist them in achieving long distances by dynamically stretching their muscles, maximizing the horizontal release velocity, increasing the vertical distance traveled by the discus, and increasing the angle of release.

Male discus throwers with large official distances tended to have smaller separation angles before the flight phase, larger separation angles at release, and greater arm elevation before the flight phase. This may assist them by increasing the vertical distance traveled by the discus, and

increasing the angle of release. However, a non-tangential release is not optimal.

These findings suggest that the relative effects of the technical parameters on discus throwing performance are different for males and females. Our data may indicate that elite female discus throwers are more reliant on effective technique throughout the throwing procedure to achieve long throws, while male discus throwers have a greater dependence on physical strength than technique to achieve long throws.

## REFERENCES

- Bartlett, R.M. (1992). *J Sports Scien*, **10**, 467-510.  
 Hay, J.G. and Yu, B. (1995). *J Sports Scien*, **13**, 125-140.

**Table 1: Female Discus Throwing Performance Predictor Model**

Model Variable	Regression Coefficient	<i>p</i> value
Constant	61.148	0.000
Shoulder-Arm Separation at Left Foot Down	0.089	0.002
Hip-Shoulder Separation at Left Foot Down	0.069	0.000
Arm Elevation at Right Foot Off	0.130	0.003
Trunk Tilt at Right Foot Down	0.129	0.017
Trunk Tilt at Left Foot Down	-0.308	0.000
Release Phase Time	-66.186	0.000
Second Single Support Phase Time	-44.516	0.000

**Table 2: Male Discus Throwing Performance Predictor Model**

Model Variable	Regression Coefficient	<i>p</i> value
Constant	63.849	0.000
Shoulder-Arm Separation at Max Back Swing	-0.029	0.049
Shoulder-Arm Separation at Release	0.064	0.047
Hip-Shoulder Separation at Left Foot Off	-0.073	0.000
Arm Elevation at Max Back Swing	0.050	0.004

# VISCOELASTIC PROPERTIES OF THE DISC FOLLOWING PUNCTURE

David A. Ryan and Adam H. Hsieh

University of Maryland, College Park, MD, USA  
E-mail: hsieh@umd.edu Web: www.bioe.umd.edu/orthomechlab

## INTRODUCTION

Low back pain continues to be a leading cause of disability in people of all ages. It is well accepted that biological, genetic, and mechanical factors interact in the degenerative process of the intervertebral disc. However, their precise contributions to disc degeneration remain unclear.

One experimental method that has been used to initiate disc degeneration consists of physically puncturing the annulus. It has been shown that 16- and 18- gauge needle punctures result in a degenerative response in rabbit discs, while 21- gauge needles had little effect (Muehleman et al., 2003). It is not known whether this method induces degeneration due to changes in disc mechanics or to a biological response induced by the laceration.

Interestingly, intradiscal pressure measurements obtained both in vivo (Wilke, 1999) and in vitro for human discs (Cripton, 2001) and in animal discs (Ekstom, 2004) require inserting a pressure sensor through the annulus. This has not been previously studied in rodents because of the small size of their discs. But with the prevalence of experimental rodent models and the advent of sensors on the order of 100  $\mu\text{m}$ , understanding the physical impact of annular puncture will become significant.

Therefore, the aim of this study is to determine what effect, if any, the insertion of a needle into the nucleus has on the load carrying ability of the disc, using a rat tail model. Implications of this study are two-

fold. Not only will we define design constraints on pressure sensor size for use in rodent discs, but we will also gain insight into the physical mechanisms that may be involved in laceration-induced degeneration.

## METHODS

Motion segments (caudal level 6-7) consisting of vertebra-disc-vertebra were isolated from 12 rats and divided into four groups: 18 gauge needle, 22 gauge needle, 26 gauge needle, and control (n=3 each group). Rats were obtained immediately after death, and all skin and soft tissue were removed from the tail. Motion segments were stored at  $-20^{\circ}\text{C}$  until time of testing.

The mechanical test protocol comprised eight cycles, each consisting of 15 minutes of load at  $-0.3\text{ MPa}$ , followed by 30 minutes of rest at  $-0.05\text{ N}$  ( $0.003\text{ MPa}$ ). Between cycles seven and eight, a period of 25 minutes of load controlled rest was followed by 5 minutes of constant displacement, during which a needle was inserted into the center of the disc. Following puncture, the segment was again loaded to  $-0.3\text{ MPa}$ , and allowed to rest for 30 minutes (Fig 1).

Viscoelastic parameters were determined using a trust-region curve fitting algorithm to a stretched exponential function as done previously for motion segments (MacLean, 2006):

$$d(t) = d_{\infty} + (d_o - d_{\infty})e^{-(t/\tau)^{\beta}},$$

where the stretch parameter,  $\beta$ , and time constant,  $\tau$ , are used to describe the transient nature of the mechanical response.

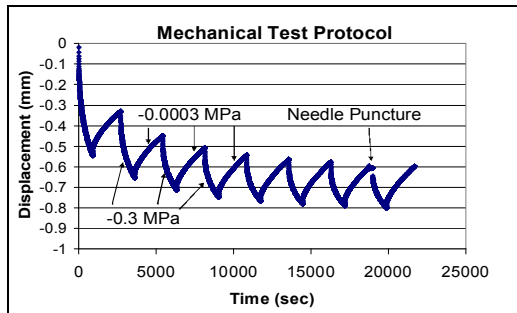


**Figure 1:** Typical displacement data during mechanical test protocol.

## RESULTS AND DISCUSSION

Viscoelastic parameters for all cycles were obtained (Table 1). A significant decrease in time constant,  $\tau$ , occurred following puncture with an 18 gauge needle (Fig 2). No differences were seen for  $\tau$  with other needles, or for stretch parameter,  $\beta$  (Fig 3).

The decrease in  $\tau$  for the 18-gauge needle corresponds to a loss of load carrying ability in the disc, which could in turn lead to degenerative changes. Possibilities exist to use this as an injury model for degeneration.

No significant changes were seen in the 22- or 26-gauge puncture group. Therefore, it is possible that pressure sensors inserted through this gauge needle can be used to measure intradiscal pressure in a rat tail model without affecting disc mechanics. Future work should evaluate the mechanics of the disc with a pressure sensor inserted.

## SUMMARY/CONCLUSIONS

This study demonstrated significant changes

in the time constant of IVD creep after puncture with an 18-gauge needle. Smaller needles did not affect the load carrying capability of the disc.

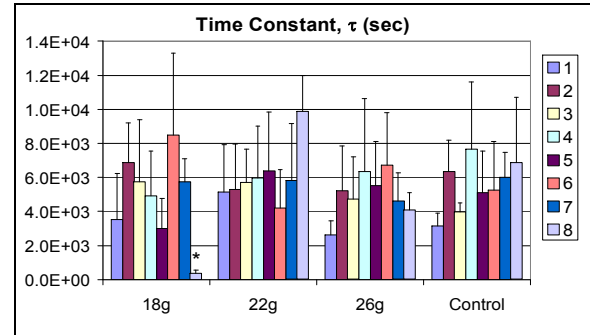


**Figure 2:** Average time constants for each cycle of 0.3 MPa compressive load.

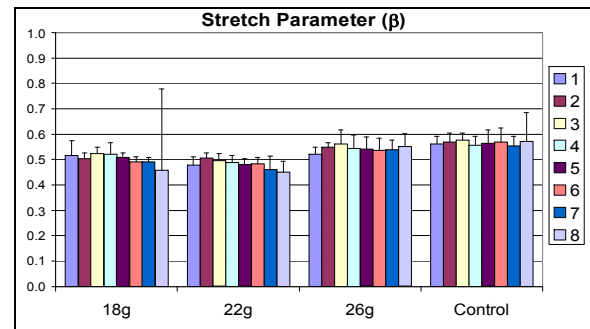


**Figure 3:** Average stretch parameter for each cycle for all test groups.

## REFERENCES

- Cripton, P.A., et al. (2001). *J. Biomech*, **34**, 545-549.  
 Ekstom, L. et al. (2004). *J Spinal Disord Tech*, **17**, 312-316  
 MacLean, J.J. (2006). *J. Biomech*, In Press  
 Muehleman, C. et al. (2003). *49<sup>th</sup> Annual meeting of the ORS*, New Orleans, 2003.  
 Wilke, H-J et al. (1999). *Spine*, **24**, 755-76

**Table 1:** Comparison of viscoelastic parameters (mean $\pm$  SD).

	Cycle	18-gauge	22-gauge	26 gauge	control
Beta	1-7	0.5081 $\pm$ 0.03	0.4848 $\pm$ 0.03	0.5417 $\pm$ 0.04	0.5644 $\pm$ 0.04
	8	0.4577 $\pm$ 0.32	0.4499 $\pm$ 0.04	0.5505 $\pm$ 0.05	0.5711 $\pm$ 0.11
Tau	1-7	5476 $\pm$ 2741	5505 $\pm$ 2792	5109 $\pm$ 2510	5359 $\pm$ 1979
	8	388.4 $\pm$ 158.4 *	9869 $\pm$ 2107	4075 $\pm$ 1039	6857 $\pm$ 3842

\* P<0.05 between different needle sizes and between cycles 1-7 and cycle 8 within the 18-gauge needle.

# RECONSTRUCTION SIMULATIONS BY USING THE INFORMATION OF MOTORCYCLE TRAFFIC ACCIDENT ANALYSIS

Cheolwoong Ko<sup>1,2</sup>, Sadayuki Ujihashi<sup>1</sup>, Koshiro Ono<sup>2</sup>, and Tamotsu Nakatani<sup>2</sup>

<sup>1</sup>Tokyo Institute of Technology (TIT), Tokyo, JAPAN

<sup>2</sup>Japan Automobile Research Institute (JARI), Tsukuba, Ibaraki, JAPAN

E-mail: [cheol-ko@uiowa.edu](mailto:cheol-ko@uiowa.edu) Web: <http://www.hei.mei.titech.ac.jp/>, <http://www.jari.or.jp/>,

## INTRODUCTION

Motorcycle crash-related fatalities and injuries have been increasing in the U.S since 1997 (NHTSA, 2003). Reliable evaluation for safety functions of motorcycle helmets is very crucial for protecting head injuries of motorcyclists. Several computational human body models have been developed to simulate motorcycle-car accidents recently (Wu et al., 2005). However, studies on reconstruction simulations by applying motorcycle traffic accident data have not been extensively reported. In this study, a method to perform reconstruction simulations using real motorcycle traffic accident information was suggested for more effective studies on motorcycle accident-related head injuries.

## METHODS

From the case studies for motorcycle traffic accidents, accident-related data such as collision speed, collision posture, helmet damage (Figure 1), and motorcyclist's head injury pattern (Figure 2) were investigated (ITARDA, 2002). The obtained information was utilized for drop impact tests reconstructing the selected real motorcycle traffic accident (Figure 3a). Also, the reconstruction test was simulated by using deformable helmet and rigid headform FE models (Figure 3b). In this study, ABAQUS/Explicit (HKS) was used as a solver. The computed acceleration response

Estimated Collision Position

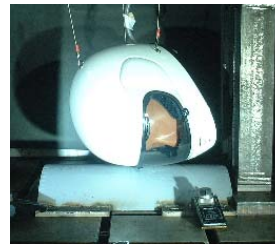


Figure 1: Real Helmet in Traffic Accident

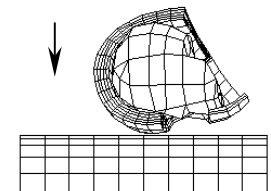
Skull Fracture on Head



Figure 2: CT Image of Injured Head



a) Reconstruction Test



b) Reconstruction Simulation

Figure 3: Comparison of Helmet Collision Posture

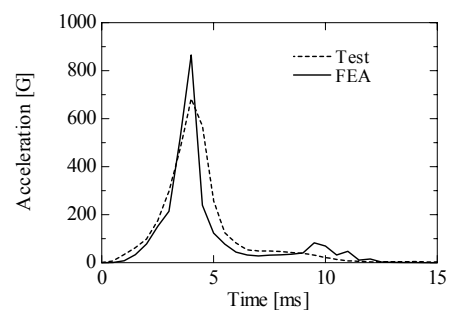


Figure 4: Acceleration Responses of Headform between Test and FEA (Collision V = 11.7 m/s)

of the headform showed good agreement with that of the reconstruction test (Figure

4), indicating the validity of the simulation method in this study. With the same collision posture, the rigid headform FE model was replaced with a human head FE model, in order to investigate the effects of physical parameters in the human head due to impact loadings (Figure 5).

## RESULTS AND DISCUSSION

From the simulation results using the head FE model, very useful information regarding physical parameters in the human head as well as acceleration response was obtained: for example, coup/contrecoup intracranial pressure, brain stress, and skull stress, etc. (Figure 6), which could be used to study head injury mechanisms. The locations of high stress both on the helmet and head model were qualitatively matched with those on the damaged helmet and motorcyclist's injured head, respectively (Figure 7). From this, it was apparent that applying a human head FE model for reconstruction simulations would be very crucial for reliable prediction of head injuries due to impact loadings in motorcycle accidents.

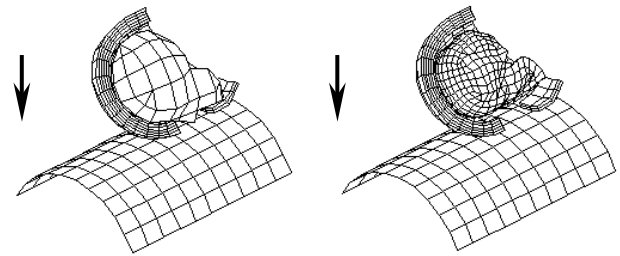
## SUMMARY

In this study, a method to use real motorcycle traffic accident data was established for performing reconstruction simulations using helmet and headform FE models. Also, a head FE model instead of a rigid headform was introduced in the reconstruction simulations, obtaining very useful information necessary for better explaining motorcycle accident situation.

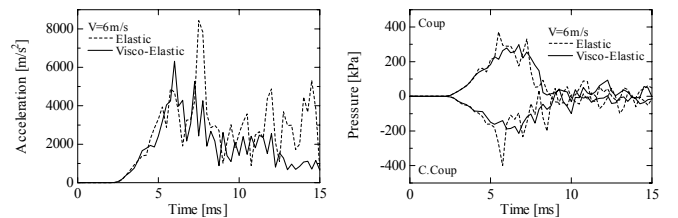
## ACKNOWLEDGEMENTS

The authors appreciate Toyota Central R&D Lab's data assistance for a head FE model.

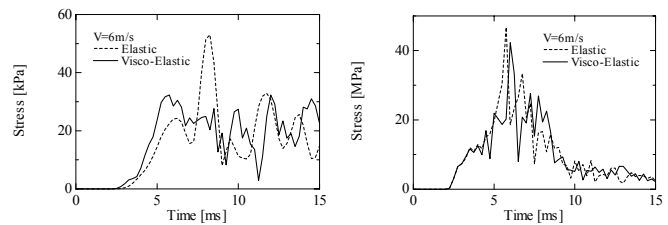
## REFERENCE



a) Helmet and Rigid Headform (b) Helmet and Head  
**Figure 5: Comparison of Reconstruction Simulations of Motorcycle Traffic Accident**

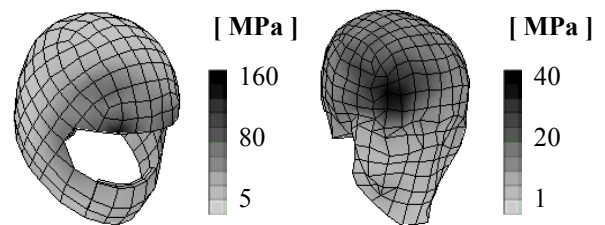


a) Acceleration Responses (b) Intracranial Pressure



c) Max. Brain Stress (d) Max. Skull Stress

**Figure 6: Responses of Reconstruction Simulations by Helmet and Head FE Model**



a) Helmet Shell (b) Skull

**Figure 7: Stress Contour at 6 ms after Collision**

ITARDA, (2002), *Annual Report*, 286-326.  
 NHTSA, (2003), <http://www.nhtsa.dot.gov/>  
 Wu, C.Y. et al. (2005), *ISB XXth Congress-ASB 29<sup>th</sup> Annual Meeting*, 510.

# EFFECT OF FATIGUE ON STABILITY OF DYNAMIC TRUNK MOVEMENT

Pranitha Gottipati and Kevin P. Granata

Musculoskeletal Biomechanics Laboratory

Virginia Polytechnic Institute and State University, Blacksburg, VA, USA

E-mail: granata@vt.edu Web: www.biomechanics.esm.vt.edu

## INTRODUCTION

Low-Back Disorders (LBDs) are the most prevalent source of musculoskeletal disability and the most common musculoskeletal problem in the United States. LBDs are often attributed to tissue strain from spinal instability. Stability is defined as the ability to maintain intervertebral and global torso equilibrium despite the presence of small mechanical disturbances and/or small neuromuscular control errors. Stability of the spine may be impaired by fatigue of the paraspinal muscles (Granata et al., 2001). This may contribute to the risk of LBDs in industrial manual materials handling tasks. Therefore, the goal of this ongoing study was to assess the change in stability of the torso associated fatiguing trunk extension exertions.

Biomechanical models describe how factors including steady-state muscle recruitment, static spinal posture, and external load contribute to stability of the spine. However, they ignore the role of movement dynamics and neuromuscular response. Empirical estimates of stability are an alternative to biomechanical modeling wherein nonlinear analyses quantify the local stability of repetitive dynamic torso flexion movements (Granata et al., *in press*). During repetitive dynamic trunk flexion-extension movements it is reasonable to assume that the kinematics of each cycle could be similar to every other cycle, i.e. the target trajectory. Kinematic variance about this target trajectory is the manifestation of stochastic disturbances and control errors. At any given time the kinematic variance can be represented as an  $n$ -

dimensional sphere where the volume of the sphere describes the magnitude of the kinematic variance and  $n$  is the number of state variables. Neuromuscular response to the kinematic perturbations will cause the movement dynamics to be attracted toward the target trajectory. Thus, as time progresses the  $n$ -dimensional sphere of kinematic variance evolves into an ellipsoid whose principle axes contract (or expand) at rates described by Lyapunov exponents. The largest Lyapunov exponent,  $\lambda_{\text{Max}}$  quantifies the stability of a dynamic movement task and can be used to assess the effects of fatigue.

## METHODS

Five males and five females with no self-reported history of low back pain performed dynamic trunk flexion and extension movements. The task was to touch a target placed near knee level (Thomas et al., 2003) with their hands then return to the upright posture in time with a metronome tone (30 cycles per minute) in a continuously repetitive movement pattern (60 second data trial). 3-D upper-body kinematic data were recorded from electromagnetic motion sensors that were secured with double-sided tape over the vertebral processes of the T10 and S1 (Ascension, Burlington, VT).

Experimental conditions included task asymmetry and fatigue. During the symmetric conditions the subjects touched the target with both hands. During the asymmetric trials they were instructed to touch the target with their dominant hand only. After completing the stability assessment the subjects participated in a low-

back fatigue protocol (Davidson et al., *in press*). They performed repeated dynamic trunk extension exertions on a Roman chair. Trunk extension force was recorded from a load cell during maximum voluntary isometric exertion (MVE) each minute during the fatigue protocol. The exercises continued until the MVE force was 60% of the unfatigued value. Immediately following the fatigue protocol, the subjects repeated the stability assessment. All the subjects provided informed consent approved by the Virginia Tech institutional review.

Stability was determined from the measured kinematic data. Maximum finite-time Lyapunov exponents  $\lambda_{Max}$  were calculated from the distance,  $d_i(t)$ , between kinematic nearest neighbors. Nearest neighbors were found by selecting data points from separate cycles that are closest to each other in the state-space. The maximum Lyapunov exponent,  $\lambda_{Max}$  was approximated as the slope of the linear best-fit line created by the equation,

$$y(t) = \frac{1}{\Delta t} \langle \ln d_i(t) \rangle$$

The time delay for the reconstructed state space was found to be 30 (0.3 sec).

## RESULTS AND DISCUSSION

To date, preliminary data from 5 of the ten subjects has been completed. No significant gender difference was observed for the number of subjects studied. Embedding dimension represents the number of state-space dimensions necessary to represent the dynamics of the measured system.

Movements after fatigue were confined to lower dimensional state space; embedding

dimension was 6 after fatigue whereas it was 7 before fatigue, indicating less dynamic complexity. Neuromuscular control of the movement tasks is considered less stable with increased  $\lambda_{Max}$ .  $\lambda_{Max}$  of the asymmetric movements were significantly ( $p < 0.01$ ) less than those of the symmetric movements, which is consistent with previous studies (Granata et al., *in press*).  $\lambda_{Max}$  of the unfatigued movements were significantly ( $p < 0.01$ ) less than those of the fatigued movements, indicating that the system was dynamically less stable when the muscles were fatigued.

## SUMMARY AND CONCLUSIONS

The maximum Lyapunov exponent  $\lambda_{Max}$  for the trunk movements before the fatigue was found to be less than the  $\lambda_{Max}$  of the fatigued movements. This shows that the local dynamic stability of the torso is impaired by fatigue of the trunk extensor musculature. Further research is warranted to understand the role of this impaired stability behavior in the risk of LBDs associated with fatiguing occupational lifting tasks.

## REFERENCES

- Granata KP. and Wilson SE. (2001). *J.Biomechanics* 16, 650-659  
 Granata, K.P. and England, S.A. *Spine. (In press)*.  
 Davidson BS, Madigan ML, Nussbaum M A. *Eur.J Appl.Physiol. (In Press)*.  
 Thomas JS, Corcos DM, and Hasan Z.E. (2003) *Exp.Brain Res.* 148:377-87.

**Table 1.** Maximum finite-time Lyapunov exponent  $\lambda_{max}$  for trunk flexion angle. Mean (stdev)

Trial type	Before fatigue $\lambda_{Max}$	After fatigue $\lambda_{Max}$
Asymmetric	1.00 (0.08)	1.17 (0.05)
Symmetric	1.07 (0.08)	1.31 (0.09)

# AGING-RELATED DOPAMINE DENERVATION IN THE BASAL GANGLIA AND BALANCE IN SWAY-REFERENCED VISUAL ENVIRONMENTS

Amy McNeal<sup>1</sup>, April J. Chambers<sup>1</sup>, Rakié Cham<sup>1</sup> and Nicolaas I. Bohnen<sup>2</sup>

<sup>1</sup> Department of Bioengineering, University of Pittsburgh, Pittsburgh, PA, USA

<sup>2</sup> University of Michigan, Ann Arbor, MI, USA

E-mail: chamr@upmc.edu

## INTRODUCTION

Parkinsonian-like balance/gait impairments have been implicated in falls reported in the elderly free of neurological conditions (Bennett et al., 1996; Chong et al., 2001). The dopaminergic (DA) activity of the basal ganglia (BG) declines with age (Volkow et al., 1996) and it is unclear whether this effect contributes to parkinsonian-like balance impairments in healthy adults. Findings of balance studies investigating the impact of L-dopa therapies on balance/gait in Parkinson's Disease (PD) cannot be extrapolated to healthy controls with aging-related DA denervation because of the complex neurochemical abnormalities associated with DA fluctuations, non-DA lesions and secondary complications found in PD (Bloem et al., 2001). Thus, the goal of this study is to determine whether aging-related DA levels in the BG explains a proportion of the variability in center of pressure (COP) sway behavior above contributions made by age.

## METHODS

*Subjects and protocol:* Twenty nine adults aged 21 to 83 years old (mean 58, SD 16) and with no diagnosis of neurological condition were recruited for participation. The sensory organization test (SOT) was preformed using the Equitest posture platform (Neurocom, Inc.). In this abstract, we focus on Condition 3, i.e., sway-referenced visual environment and fixed floor, as adaptive postural behavior of PD

patients is known to be impaired when subjected to moving scenes (Bronstein et al., 1990). In-vivo positron emission tomography (PET), specifically <sup>11</sup>C-β-CFT PET, was used to quantify pre-synaptic DA transporters in the BG of all participants.

*Processing:* Anterior-posterior COP velocity (A-P COP VEL) and anterior-posterior COP root mean square (A-P COP RMS) were derived. Three trials were conducted and the average of the last two trials was analyzed. Multivariate regression methods were used to process the PET scans (Ichise, 1996), deriving the binding potential of pre-synaptic DA transporters in the dorsal basal ganglia (DA-DBG) and ventral basal ganglia (DA-VBG). The binding potential reflects pre-synaptic DA nerve terminal density.

*Analysis:* Five regression models were fit using A-P COP VEL/RMS as dependent variables and (i) age only, (ii) DA-DBG only, (iii) VA-DGB only, (iv) both DA-DBG and age, and (v) both DA-VBG and age as independent variable(s). R<sup>2</sup> was noted as a measure of the proportion of variability in COP measures explained by the independent variable(s).

## RESULTS AND DISCUSSION

*Descriptive summary:* Aging-related DA denervation was statistically significant both in the dorsal and ventral BG (Table 1 and Figure 1). This denervation appears more prominent in the dorsal BG than in the

ventral BG. Also, the amount of COP sway (A-P COP RMS) increased with reduced DA-VBG levels (Table 1). Other DA-COP bivariate relationships were modest and not statistically significant (Table 1).

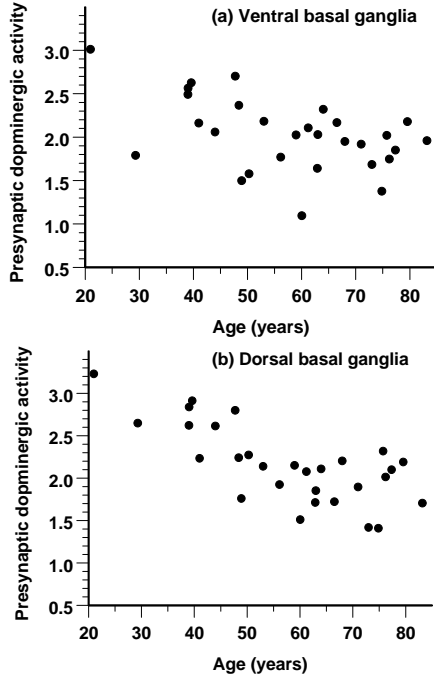


**Figure 1:** Aging-related pre-synaptic DA denervation in the ventral (a) and dorsal (b) BG

An additional 34 and 20% of the variability in A-P COP VEL above contributions made by age alone was explained by including DOP-DBG and DOP-VBG with age, respectively (Models 4-5 vs. 1 in Table 2). Also, the combination of DOP-DBG and age explained an amount of A-P COP VEL variability that is greater than the sum of their individual contributions, suggesting a multivariable dependency of A-P COP VEL on DOP-DBG and age that cannot be explained by bivariate relationships.

**Table 2:** Proportion of the variability ( $R^2$ ) in COP sway characteristics explained by age and pre-synaptic dopaminergic activity alone (Models 1-3) and by the combined effect of age and dopamine (Models 4-5)

Model number →	1	2	3	4	5
Predictors →	Age	DOP-VBG	DOP-DBG	Age, DOP-DBG and interaction	Age, DOP-VBG and interaction
↓ Dependent variables ↓					
A-P COP VEL	0.282	0.051	0.033	0.377	0.337
A-P COP RMS	0.025	0.174	0.070	0.073	0.194

**Table 1:** Pearson correlation coefficients

Age	A-P COP VEL	A-P COP RMS	DA-DBG	DA-VBG
1.00	** 0.53	0.16	** -0.73	** -0.48
	1.00	* 0.40	-0.18	-0.23
		1.00	-0.27	* -0.42
			1.00	** 0.79
				1.00

\*\*  $p < 0.01$ ; \*  $p < 0.05$

In contrast to sway velocity, A-P COP RMS variability was mostly explained by DOP-VBG (Table 2).

## SUMMARY/CONCLUSIONS

Aging-related dopamine denervation in healthy adults, less severe and more symmetric than in PD patients, may be enough to affect the ability to maintain balance in moving visual environments.

## REFERENCES

- Bennett, D.A. et al. (1996). *New England Journal of Medicine*, **334**, 71-76.  
 Bloem, B.R. et al. (2001). *Advances in Neurology*, **87**, 209-23.  
 Bronstein, A.M. et al. (1990). *Brain*, **113**, 767-779.  
 Chong, R.K. et al. (2000). *J. Neurological Sciences*, **175**, 57-70.  
 Ichise, M. et al. (1996), *J. Nuclear Medicine*, **37**, 513-520.  
 Volkow, N.D. et al. (1996). *J. Nuclear Medicine*, **37**, 554-558.

## ACKNOWLEDGEMENTS

VA P01 E2869R

# INFLUENCE OF CHANGE IN SURFACE SUPPORT ON STANDING POSTURAL SWAY IN OLDER ADULTS

Kathryn W. O'Connor<sup>1</sup>, Patrick J. Loughlin<sup>1,2</sup>, Mark S. Redfern<sup>1,3</sup> and Patrick J. Sparto<sup>1,3,4</sup>

<sup>1</sup> Department of BioEngineering, <sup>2</sup> Department of Electrical Engineering

<sup>3</sup> Department of Otolaryngology, <sup>4</sup> Department of Physical Therapy

University of Pittsburgh, Pittsburgh, PA, USA

E-mail: psparto@pitt.edu Web: www.mvrc.pitt.edu

## INTRODUCTION

Older adults exhibit greater postural instability compared with young adults. Of the many causes attributed to this decline in postural control, a defect or slowing of central integration processes may play an important role (Woollacott et al., 1986; Teasdale et al., 1991). As a result, older adults may have more difficulty maintaining balance when confronted with a sudden change in postural demands (Teasdale et al., 1991; Hay et al., 1996).

For example, Hay et al. (1996) found that while both young and older adult subjects were greatly affected by the removal of reliable proprioceptive inputs (in the form of tendon vibration), only the elderly had difficulty maintaining balance when proprioceptive information was reinserted. While the young subjects quickly incorporated the reinserted sensory input, some older adults took over 10 s to readjust.

The purpose of this study was to examine if there was a similar pattern of reduced readaptation to accurate somatosensory input in older adults standing on a posture platform that changed from moving to fixed.

## METHODS

Twenty-five healthy young control (YC) subjects (14 females, mean age = 27 y), and 24 healthy older control (OC) subjects (13 females, mean age = 70 y) completed the study. Informed consent was obtained from each subject before participation.

Subjects stood on a NeuroTest posture platform within a full field of view (FOV) display enclosure (Sparto et al., 2004). The head sway of each subject was recorded using a Polhemus Fastrak<sup>TM</sup> electromagnetic tracking system.

Subjects performed 24 trials, with rests after every 2 to 4 trials. During each trial, subjects viewed 0.4 Hz sinusoidal anterior-posterior (AP) optic flow for 50 s while standing on a fixed or sway-referenced platform. During sway-referenced trials, the platform moved about an axis of rotation aligned with the each subject's medial and lateral malleoli, in proportion to the amount of sway in the pitch plane. For this report, we are reporting on 3 of the trials in which the platform transitioned from sway-referenced to fixed at a random time between 22 and 28 s of the trial duration. These trials were the final three trials that were performed.

The AP head sway was sampled at 20 Hz. The data were lowpass filtered using a 4<sup>th</sup> order, zero-phase digital Butterworth filter with a cutoff frequency of 2 Hz. The sway velocity was computed by differentiating the signal. The instantaneous power of the head sway velocity was determined by squaring the velocity signal. For these trials, we limited our analysis to the 10 s segments of data before and after the transition from sway-referenced to fixed platform. Each 10 s segment was further subdivided into two consecutive 5 s periods. The log of the

average power (dB) during each 5 s interval was computed and statistically analyzed. A mixed factor repeated measures ANOVA was used to test for the effects of subject group (YC and OC), period (1, 2, 3 and 4), and trial (1, 2, and 3).

## RESULTS AND DISCUSSION

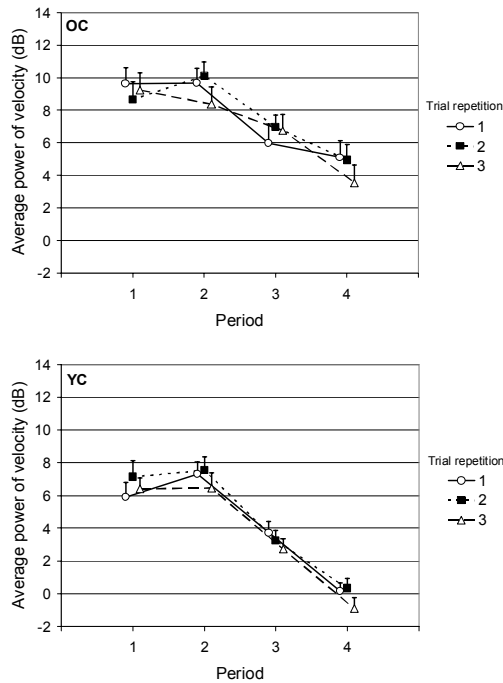


**Figure 1.** Average power of sway velocity in older controls (OC) and young controls (YC) during 3 trials in which the posture platform changed from sway-referenced to fixed in between periods 2 and 3. Each consecutive period lasted for 5 s.

The average power of sway velocity (dB) is shown in Figure 1. A main effect of subject type was present ( $p = 0.001$ ). Across periods, the OC group had a 3.24 dB greater level of sway power than the YC. Furthermore, there was a main effect of period ( $p < 0.001$ ), with pair wise comparisons revealing significant differences between all pairs ( $p < 0.001$ ) except periods 1 and 2 ( $p = 0.625$ ).

As shown in Figure 1, the level of postural sway power decreased from periods 2 to 3 ( $p < 0.001$ ). The amount of decline in sway power was greater in YC (3.88 dB,  $p < 0.001$ ) than in OC (2.83 dB,  $p < 0.001$ ). Sway power continued to decrease in the fourth period. The YC showed a larger reduction, with an average decrease of 3.38 dB from period 3 to 4 ( $p < 0.001$ ), whereas the OC had a 2.83 dB decrease ( $p = 0.026$ ).

Comparison of the sway during period 4 with sway obtained during steady-state, fixed platform conditions revealed that sway power had not returned to baseline levels. The OC subjects had a greater difference (4.99 dB) in comparison with the baseline trials compared with YC subjects (3.30 dB).

## SUMMARY/CONCLUSIONS

The results indicate that healthy older adults do not adapt as quickly as healthy young adults when sensory conditions change from a sway-referenced to fixed surface environment. This finding is likely due to age-related changes in the central nervous system, although the neurophysiological correlates are not yet understood.

## REFERENCES

- Hay, L. et al. (1996). *Experimental Brain Research*, **108**, 129-139.
- Sparto, P.J. et al. (2004). *IEEE Trans. Neural Systems and Rehabilitation Engineering*, **12**, 360-366.
- Teasdale, N. et al. (1991). *Experimental Brain Research*, **85**, 691-696.
- Woollacott, M.H. et al. (1986). *International Journal of Aging and Human Development*, **23**, 97-114.

## ACKNOWLEDGEMENTS

This research was supported in part by the National Institutes of Health under Grants K25-AG01049, P30-DC05205, and by the Eye and Ear Foundation.

# INTERNAL KINETIC FACTORS AND THE PREFERRED TRANSITION SPEED IN HUMANS

Toran D. MacLeod, Alan Hreljac, and Rodney Imamura

California State University, Sacramento, CA, USA  
E-mail: toran\_furch@yahoo.com

## INTRODUCTION

Previous authors (Biewener, et al., 1983, Biewener, et al., 1986, Farley, et al., 1991, Rubin, et al., 1982) have suggested that the preferred gait transition (PTS) of quadrupeds are triggered by internal kinetic factors within the musculoskeletal system. Invasive research on horses, dogs, and goats has demonstrated that musculoskeletal strain decreases when changing gait from a trot to a gallop (Biewener, et al., 1983, Biewener, et al., 1986, & Rubin, et al., 1982). In addition, non-invasive ground reaction force (GRF) data from large horses (Farley, et al., 1991) supported similar conclusions.

Two experiments (Hreljac, 1993, Raynor, et al., 2002) have been conducted on humans, using a non-invasive GRF data collection technique previously used on animals (Farley et al., 1991), to determine if external kinetic variables may have a relationship with the human gait transition. These studies did not support the hypothesis that external kinetic variables have a relationship to gait transitions in humans.

The walk-run PTS has been shown to be triggered by dorsiflexor stress (Hreljac, 1995). Peak dorsiflexor activity occurs just after toeoff. Dorsiflexor muscles during the swing phase were focused on within this study to follow up on previous findings (Hreljac, 1995). The purpose of this investigation was to determine if ankle joint kinematic and kinetic factors, particularly dorsiflexor power during the swing phase

are related to the gait transition speed in humans.

## METHODS

The PTS was determined on 24 male subjects, using a method similar to previous studies (Hreljac, 1993, Raynor, et al., 2002, Hreljac, 1995), under two loading conditions. An unloaded condition did not include an external load, and a loaded condition included a 2 kg load attached to each shoe of the subject about the center of mass of the foot. Each condition was completed twice in a random order for each subject.

After determination of the PTS, subjects walked on a treadmill at three speeds (60, 80, and 100% of the PTS), and ran at one speed (100% of the PTS) for both loading conditions, in random order. Speed for all trials was calculated from the elapsed time of ten belt rotations. Reflective markers were placed on the right greater trochanter, knee joint center, lateral malleolus, calcaneus, and base of the 5<sup>th</sup> metatarsal while a digital video camera (240 Hz) recorded subjects in the right sagittal plane. Ten stride lengths were recorded for each trial.

Raw kinematic data were smoothed using a 4<sup>th</sup> order, zero lag, Butterworth filter. Ankle joint kinetic factors during the swing phase were determined using inverse dynamics. Ankle joint power was calculated as the product of ankle joint moment and ankle angular velocity. All variables were

normalized to body mass before comparisons were made. Dependent variables (DVs) included maximum ankle angular velocity, ankle angular acceleration, and ankle joint power. The PTS under the two loading conditions were also compared in order to assure that the loaded condition affected the PTS. A repeated measures MANOVA compared average values of all DVs between speed and loading conditions. If the hypothesis tested was to be accepted for a DV, the value of the DV would increase as walking speed increased, then decrease when gait changed to a run (at the PTS). For all comparisons,  $\alpha = 0.05$ .

## RESULTS AND DISCUSSION

PTS data are included (Table 1) to demonstrate that the unloaded PTS was significantly faster than the loaded PTS condition. All of the DVs, under both loading conditions, increased as walking speed increased, and decreased with the change to a run (Table 2). Ankle angular velocity and acceleration results support previous findings (Hreljac, 1995). The results of the current study, along with previous findings, indicate dorsiflexor muscle stress has a role in determining the PTS. The ankle joint moments produced by the dorsiflexors may also have a relationship with the PTS. Further study may demonstrate that other internal kinetic factors are determinants of the PTS. Kinetic factors are ultimately responsible for kinematics, so finding an ankle joint moment as a determinant makes sense.

**Table 2:** Value of DVs at all conditions (\*=sig. difference from previous speed under respective loading condition).

Condition	w60u	w80u	w100u	r100u	w60l	w80l	w100l	r100l
$\omega$ (rad/s)	2.69	3.17*	3.83*	2.75*	3.31	3.54*	4.09*	3.42*
$\alpha$ (rad/s/s)	100.33	115.05*	125.51*	62.30*	116.25	130.04*	140.95*	68.10*
P (W/kg)	0.03	0.05*	0.07*	0.05*	0.06	0.09*	0.13*	0.08*

**Table 1:** Gait speed (m/s) at all conditions (\*=significant difference between the loading conditions while walking at the PTS)

Condition	w60	w80	w100 (PTS)
Unloaded	1.24 (0.12)	1.62 (0.09)	2.03* (0.12)
Loaded	1.16 (0.08)	1.55 (0.11)	1.94 (0.13)

## SUMMARY/CONCLUSIONS

Ankle angular velocity, angular acceleration, and joint power appear to have a relationship to the PTS. Dorsiflexion appears to be important to the PTS in humans based on the results of this study and others (Hreljac, 1995, Hreljac, et al., 2001). Further study should be conducted on internal kinetic factors in relationship to the PTS in humans.

## REFERENCES

- Biewener, AA, et al. *J Biomech* **16**, 565-76, 1983.  
 Biewener, AA, et al. *J Exp Biol*, **123**, 383-400, 1986.  
 Farley, CT, et al. *Science*, **253**, 306-8, 1991.  
 Hreljac, A. *Gait Posture*, **1**, 217-23, 1993.  
 Hreljac, A. *J. Biomech* **28**, 669-77, 1995.  
 Hreljac, A, et al. *J Appl Biomech*, **17**, 287-96, 2001.  
 Raynor, AJ, et al. *Hum Mov Sci*, **21**, 785-805, 2002.  
 Rubin CT, et al. *J Exp Biol*, **101**, 187-211, 1982.

# ANALYSIS OF FORCE-LIMITING CAPABILITIES OF FOOTBALL NECK COLLARS

David McNeely, Sarah Manoogian, Kaitlin Wilson, Tracy Ng, Craig McNally, and Stefan Duma

Virginia Tech-Wake Forest Center for Injury Biomechanics, Blacksburg, VA, USA  
E-mail: dmcneely@vt.edu Web: www.cib.vt.edu

## INTRODUCTION

As many as 65% of college football players will suffer a transient brachial plexopathy, commonly called a burner or stinger, at some point (Sallis 1992). Stingers result from a stretching or pinching of the brachial plexus. Symptoms include pain, numbness, and tingling in the shoulder and upper arm, sometimes extending to the forearm and fingers, but are usually transient, disappearing within one or two minutes (Clancy 1977). Brachial plexus axonotmesis is a more serious injury that occurs from the same injury mechanisms. It may present itself as a common brachial plexopathy, but can cause loss of strength and axon degeneration for weeks or months after the injury (Pellman 2003). These injuries are commonly caused by lateral flexion of the neck due to an impact of the player's head with another player or the ground. Studies have found a connection between cervical stenosis and a higher incidence of multiple injuries (Castro 1997). Often, players with multiple occurrences of these injuries will wear accessory cervical orthoses, or neck collars, to reduce the risk of injury. The design and use of these collars is based largely on empirical data (Gorden 2003, Hovis 1994). Previous studies have examined the motion-limiting capabilities of accessory collars, both in passive and active lateral flexion and hyperextension of the neck in a static situation (Gorden 2003, Hovis 1994), but no studies have examined these orthoses in a dynamic environment. The purpose of this study is to evaluate a range of neck collars and determine their

efficiency at limiting head and neck forces in dynamic impacts.

## METHODS

A total of 48 impacts were performed using four different collar/shoulder pad combinations. The control configuration consisted of a set of regular shoulder pads, Douglas model CP25, with no accessory collar. In addition, two collars were tested: the McDavid Cowboy Collar™, and a custom-designed and fitted orthosis worn by a Virginia Tech player called the Bullock collar.



**Figure 1:** Screen capture of high-speed video of impact.

These were fitted onto a Hybrid-III dummy, along with a Riddell VSR-4 football helmet. The Hybrid-III was instrumented with upper and lower neck load cells, as well as head CG tri-axial accelerometers and angular rate sensors. High-speed video of the impacts was recorded at 1,000 frames per second. In addition, the impactor was instrumented with a load cell and a light gate to record impactor load and impact velocity, respectively. Each collar/shoulder pad combination was tested in a normal and a

raised state. The raised state was intended to simulate a player assuming a tackling posture, in which the shoulders are naturally raised in anticipation of an impact. Each padding combination and state was subjected to impacts in three locations: front, side, and an axial loading condition. Impacts were performed at 7.5 m/s and 11 m/s at each test condition, using a linear pneumatic impactor similar to the new proposed NOCSAE impactor (Pellman 2006). These locations and impact velocities were selected to replicate on-field impacts (Pellman 2003).

## RESULTS AND DISCUSSION

Data are presented for selected impacts in Figure 2 and Table 1. In the side position, the Bullock Collar provided a reduction in the lower neck bending moment. The Cowboy Collar, however, did not reduce this moment. In the front position, both collars provided a reduction in the lower neck bending moment, with the Cowboy Collar having the most effect.

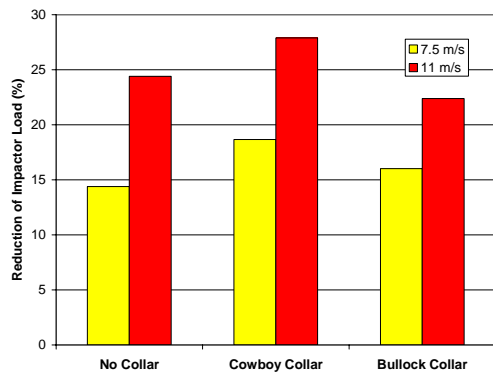


**Figure 2:** Percent reduction of impactor load, axial loading position, raised shoulder pads.

In the axial loading position, the Cowboy Collar provided a larger percent reduction of the impactor load compared to the shoulder

pads alone. The Bullock Collar did not improve the percent reduction of impactor load.

**Table 1:** Impact force and moment data, multiple impact locations.

Test Condition	Side	Front	Axial Loading
	Mx (Nm, positive to left shoulder)	My (Nm, positive to back)	Percent reduction of impactor load (%)
No Collar	222.54	284.10	24.41
Cowboy Collar	223.11	226.11	27.89
Bullock Collar	200.60	254.72	22.38

## CONCLUSIONS

Both collars limited loads at some locations; however, no collar was effective at limiting loads at all locations. Further testing is needed at lower impact velocities that are similar to injurious impacts in the field.

## REFERENCES

- Castro, F.P., et al. (1997). *Am J Sports Medicine*, **25**, 603-608.
- Clancy, W.G., et al. (1997). *Am J Sports Medicine*, **5**, 209-216.
- Gorden, J.A., et al. (2003). *J Athletic Training*, **38**(3), 209-215.
- Hovis, W.D., et al. (1994). *Med Sci Sports Exerc*, **26**(7), 872-876.
- Pellman, E.J., et al. (2003) *J Neurosurgery*, **53**(4), 799-814.
- Pellman, E.J., et al. (2006) *J Neurosurgery*, **58**(1), 7978-96
- Sallis, R.E., et al. (1992). *Phys Sportsmed*, **20**(11), 47-55.

## ACKNOWLEDGEMENTS

The authors would like to acknowledge Dr. Patrick Kerr, who provided materials and funding for this project.

# EFFECT OF MULTIPLE FREEZE-THAW CYCLES ON THE SAGITTAL PLANE MOTION CHARACTERISTICS OF PORCINE LUMBAR SPINE

Michio Hongo<sup>1</sup>, Ralph E. Gay<sup>2</sup>, Jui-Ting Hsu<sup>1</sup>, Kristin D, Zhao<sup>1</sup>,  
Brice Ilharreborde<sup>3</sup>, Lawrence J. Berglund<sup>1</sup>, Kai-Nan An<sup>1</sup>

<sup>1</sup> Orthopedic Biomechanics Laboratory and <sup>2</sup> Dept. of Physical Medicine and Rehabilitation,  
Mayo Clinic College of Medicine, Rochester, MN

<sup>3</sup> Department of Orthopedic Surgery, Robert Debré Hospital, Paris, France

## INTRODUCTION

Fresh frozen cadaver specimens are commonly used in biomechanical investigations of the spine. Although frozen storage of spine specimens has been shown to increase disc hydration resulting in swelling (Pflaster 1997), storing them in a deep freezer (-18 degrees C) did not significantly alter their mechanical properties. (Panjabi 1985; Smeathers 1988) Since many study designs require staged specimen preparation and biomechanical testing, the constancy of spinal motion behavior after multiple freeze-thaw cycles should be understood. However, we found no literature describing the effect of multiple freeze-thaw cycles on the mechanical response of motion segments.

The objective of this study was to determine the effect of multiple freeze-thaw cycles on the range of motion and the biomechanical parameters that reflect stiffness during dynamic motion in the porcine spine.

## METHODS

Ten lumbar functional spinal units were obtained from post-sacrificed female pigs with an average weight of 61.3kg (range 57 to 69kg). Specimens were harvested within 1 hour after death. After harvesting, specimens were screened by x-ray to insure that there were no skeletal anomalies. Single motion segments were then potted in

polymethylmethacrylate in circular acrylic fixtures.

Specimens were tested at baseline (BL), within 3 hours after sacrifice in a custom dynamic spine testing apparatus. Motion was induced with continuous flexion-extension cycles under load control (pure moment of 5 Nm) at 3 degrees/second. Data was collected on the 5<sup>th</sup> trial for analysis. They were then frozen at -20 degrees C. Motion segments were then thawed at room temperature (21 degrees C.) for 12 hours prior to repeat testing and refreezing. They were thawed, tested and refrozen every 24 to 72 hours for a total of 3 post-thaw (PT) tests. Specimens were kept moist with 0.9% saline, toweling, and flexible plastic wrap during all testing and storage.

Force and moment data were recorded during the dynamic motion by a six degrees-of-freedom load cell. Rotations were measured with miniature tilt sensors (Crossbow Technology, San Jose, CA, USA). Moment vs. angle curves were generated for each trial. Motion parameters were determined from the curves, including range of motion (ROM), transitional zone width (TZW), and transitional zone slope (TZS). (Figure 1) Data were analyzed with repeated-measures ANOVA (effect = freeze-thaw cycle), and post hoc test (Wilcoxon signed rank test) for multiple comparisons to determine differences between pairs of cycles.

## RESULTS

All PT cycle ROMs were significantly smaller than BL, but no significant difference was found among PT measures. The TZW also significantly decreased at the first PT measure, as compared to BL, however there was no difference between PT measures. The TZS increased with the first freeze-thaw cycle compared to BL, but with no significant difference among PT conditions. (Figure 2)

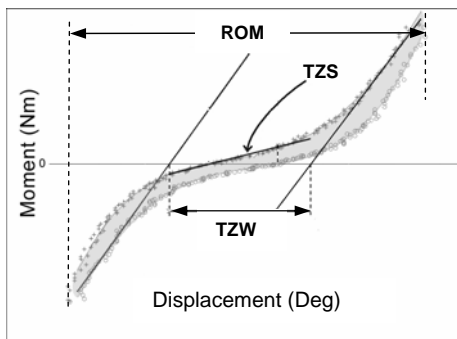


**Figure 1.** Motion parameters

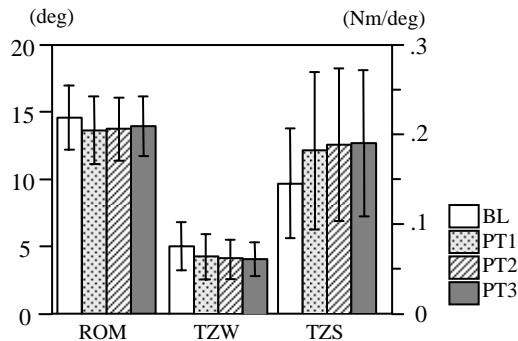


**Figure 2.** Data from dynamic moment-angle curves. (mean  $\pm$  SD)

## DISCUSSION AND CONCLUSION

We found that dynamic motion properties significantly changed after initial freezing but were not altered by subsequent freeze-thaw cycles. Previous studies using human spines found that biomechanical properties were not affected by freezing and thawing. (Smeathers 1988; Panjabi 1985; Dhillon 2001) In a study using porcine lumbar spines, the stiffness and displacement did not change after freezing and thawing, however the measurements under ultimate compressive load and compressive creep behaviors were altered by frozen storage. (Bass 1997; Callaghan 1995) The difference between porcine and human tissue might come from the higher water content in the porcine disc.

Although mechanical properties significantly changed after the first post-thaw measure, our results indicate that the behaviors measured thereafter were reasonably stable in these specimens exposed to 3 freeze-thaw cycles. This suggests that porcine spine specimens which have been frozen and thawed multiple times can be used in biomechanical testing.

## REFERENCES

- Pflaster, D.S., et al., (1997), *Spine*, **22**, 133-139.
- Panjabi, M.M., et al., (1985), *J Orthop Res*, **3**, 292-300.
- Smeathers, J.E. and D.N. Joanes, (1988), *J Biomech*, **21**, 425-433.
- Dhillon, N., E.C. Bass, and J.C. Lotz, (2001), *Spine*, **26**, 883-888.
- Bass, E.C., et al., (1997), *Spine*, **22**, 2867-2876.
- Callaghan, J.P. and S.M. McGill, (1995), *J Orthop Res*, **13**, 809-812.

# CONDYLAR LIFT-OFF DOES NOT OCCUR DURING THE DEEP SQUAT

Dyrby, C O<sup>1,2</sup>; D'Lima, D D<sup>3</sup>; Colwell, C W<sup>3</sup>; Andriacchi, T P<sup>1,2</sup>

<sup>1</sup> Stanford University, Stanford, CA, USA

<sup>2</sup> VA Palo Alto Health Care System, Palo Alto, CA, USA

<sup>3</sup> Shiley Center for Orthopaedic Research & Education, Scripps Clinic, La Jolla, CA

E-mail: dyrby@stanford.edu Web: biomotion.stanford.edu

## INTRODUCTION

A number of single plane fluoroscopic image studies have shown the possibility of condyle lift off during a squat or deep knee bend (Stiehl 1995, Dennis 1998, Insall 2002, Bertin 2002). Lift-off has also been implicated in tibial component wear that can lead to polyethylene failure (Bertin 2002). These studies did not have a way to measure the forces present in the knee during the activities. Retrieval studies (Wimmer et al 1998) of polyethylene components do not show damage patterns that would suggest lift off of one compartment with high loads passing through a single compartment. In addition, the forces and moments at the knee during the deep squat are not conducive to allowing lift-off (Dyrby and Andriacchi 2000, Nagura 2002).

The purpose of this study was to quantify the forces in the medial and lateral compartment of the knee in a subject that has had an instrumented knee prosthesis during the deep squat. The hypothesis tested is that the forces measured at 30°, 60°, 90° and maximum knee flexion, in the medial or lateral compartment will not reduce to zero during the descending phase of the squat. This would indicate that both compartments remain in contact.

## METHODS

A standard Sigma PFC (DePuy J&J) with a standard primary cruciate retaining posterior

lipped prosthesis was implanted in the right knee of an 81-yr-old male (170 cm, 633 N). The upper tibial tray and locking mechanism was the same design as a primary PFC tibial component. The lower part of the tray and the stem was designed to hold custom designed load cells and telemetry system (D'Lima 2005). IRB-approved informed consent was obtained. The instrumented knee transmitted the compressive load in the medial anterior and posterior, lateral anterior and posterior compartments of the knee using four uniaxial load cells embedded in the tibial component at a rate of approximately 70Hz. These transmitted forces were recorded on a laptop computer using custom acquisition software (Labview). The sum of the two measurements in the medial and lateral compartments was used to estimate total medial compartment compressive loading. Compressive loading was normalized to body weight. The subject performed two trials of a deep squat to maximum knee flexion.

Kinematic and kinetic data during the squat were also collected using an optoelectronic system and force plate. An on/off synchronization signal was also collected in order to synch the two systems. Intersegmental moments were calculated using a previously-described 6-marker link method (Andriacchi TP et al. 2004). Data were sampled at 30°, 60°, 90° and maximum knee flexion.

## RESULTS AND DISCUSSION

At no point was the compressive load in the medial or lateral compartment measured to be zero during the trials (Figure 1). The average maximum compressive load seen in the lateral compartment was 0.82 BW and for the medial compartment was 1.8 BW. The majority of the load passes through the medial compartment of the knee.

Calculation of kinetics at each knee flexion angle gave an average external knee flexion moment of 2.9, 5.7, 5.9, and 8.5%BW\*Ht each flexion angle. The maximum flexion moment occurred near the same time as the maximum medial compartment compressive load. The knee had an average external adduction moment of 0.7, 0.6, 0.5 and 0.7%BW\*ht at each flexion angle.

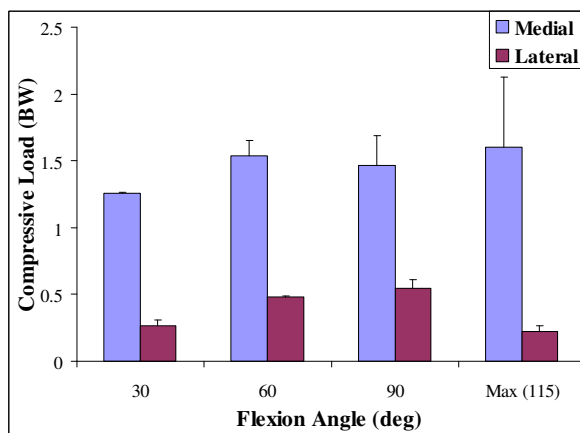


Figure 1: Medial and lateral compartment compressive forces during the squat

## SUMMARY/CONCLUSIONS

The results of this study show that lateral lift off did not occur during the activity studied. Insall et al (2002) had reported variable results for his lift-off study. Their subject's data fluctuated as to which condyle lifted off the tibial plateau when measured at 0°, 30°,

60°, and 90°. Our study show compressive loading during each of the measured flexion angles. The subject studied did not have a 0° knee flexion angle to compare.

A previous study of deep squat stated that a high quadriceps moment, an important determinant in compressive loads at the knee, would produce condition where lift off is not likely to occur (Dyrby and Andriacchi 2000, Nagura 2002). In spite of the maximum adduction moment of 0.7%BW\*Ht, no lateral lift off occurred due to the high external flexion moment.

Wimmer (1998) in a retrieval study of tibial plateaus showed that no plateau had scarring on either the medial or lateral sides, indicative of lift-off. This again shows that lift off is not likely for total knee replacement systems.

## REFERENCES

- Andriacchi TP et al. (2004). In *Basic Orthopaedic Biomechanics, 3rd ed.*, 91.
- Bertin, K.C. (2002) *J. Arthroplasty*, **17(8)**, 1040.
- D'Lima, D.D. et al. (2005). *J Biomechanics* 38, 299.
- Dennis, D.A., et al. (1998). *Clin Orthop* **356**, 47.
- Dyrby and Andriacchi (2000). *Proceeding of ASB 2000*, 7.
- Insall J.N. et al (2002). *Clin Orthop* **403**, 143.
- Nagura et al (2002). *J Orthop Research*, **20(4)**, 881.
- Stiehl, J.B. et al. (1995). *J Bone Joint Surg Br* **77**, 884.
- Wimmer et al. (1998). *J Arthroplasty*, **13(1)**, 8.

# LOWER EXTREMITY COUPLING VARIABILITY DURING AN EXHAUSTIVE RUN IN INDIVIDUALS WITH ILIOTIBIAL BAND SYNDROME

Stacey A. Meardon, Ross H. Miller, Timothy R. Derrick, and Jason C. Gillette

Iowa State University, Ames, IA, USA

E-mail: [rosshm@iastate.edu](mailto:rosshm@iastate.edu) Web: [www.hhp.hs.iastate.edu](http://www.hhp.hs.iastate.edu)

## INTRODUCTION

Disruption of normal lower extremity motion during running has been associated with injury (DeLeo, 2004; Hreljac, 2004). Lower extremity coupling (LEC) evaluates the interaction of displacement, velocity, and timing of segment motions. In the past, joint timing and excursions have been used to evaluate LEC. More recently, dynamical systems theory has been applied to LEC across the running cycle (Hamill et al., 1999). Variability of continuous relative phase (CRP) curves provides insight for spatial and temporal relationships of LEC. Decreased variability of LEC during running has been associated with injury (Hamill et al., 1999, Heiderscheit et al., 2002). Lack of variation of LEC may result in repeated stress to tissues resulting in overuse injury. Iliotibial band syndrome (ITBS) is an overuse running injury attributed to abnormal lower extremity kinematics. Effects of an exhaustive run in ITBS have not been extensively studied.

The purpose of this research was to use continuous relative phase (CRP) values to evaluate LEC variability in individuals with a history of ITBS during an exhaustive run. We hypothesized that ITBS runners would exhibit less variability in LEC at the beginning of a run. Additionally, at the end of an exhaustive run, ITBS would have decreased variability in LEC.

## METHODS

Sixteen recreational runners ( $27 \pm 8.1$  years) were recruited (8 ITBS runners and 8 age-matched controls). ITBS runners had a history of ITBS, but were not currently experiencing symptoms. The runners completed a treadmill run at a self-selected pace until they reached volitional fatigue.

An eight-camera Vicon Peak motion capture system was used to capture 3D kinematic data at 120 samples per second. Twenty-three reflective markers were attached to the lower extremities. Data were sampled every 2 min. for 10 sec. Stance phase segment angles from the first and last 10 seconds were calculated in MATLAB. CRP angles of key LECs were calculated for each individual. Group means of individual CRP standard deviations were analyzed in SPSS using repeated measures ANOVA ( $\alpha < 0.05$ ).

## RESULTS AND DISCUSSION

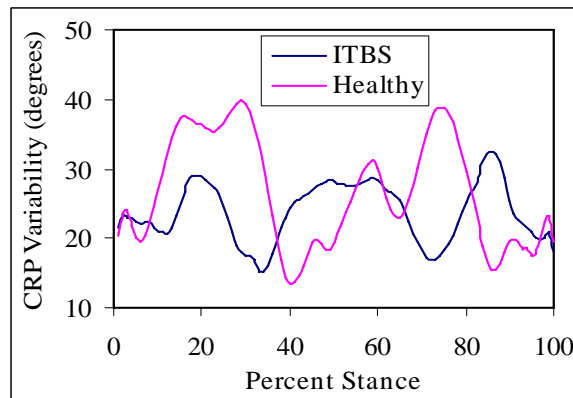


**Figure 1.** CRP variability for Thigh<sub>Abduction/Adduction</sub> - Tibia<sub>Rotation</sub>

At the beginning of the run, Thigh<sub>Abduction/Adduction</sub>-Tibia<sub>Rotation</sub> coupling variability was significantly less in the ITBS group (Figures 1 & 2). Consistent with our hypothesis, summation of all LECs evaluated demonstrated a trend toward overall decreased variability in the ITBS group. At the end of the run, the ITBS runners demonstrated significantly less variability in Thigh<sub>Flexion/Extension</sub>-Tibia<sub>Rotation</sub> coupling (Figure 3). However, Tibia<sub>Rotation</sub>-Foot<sub>Inversion/Eversion</sub> and Thigh<sub>Abduction/Adduction</sub>-Foot<sub>Inversion/Eversion</sub> (Figures 4 & 5) coupling increased.

### SUMMARY/CONCLUSIONS

Consistent with previous research, LEC variability appears to be less in injured runners (Hamill et al., 1999, Heiderscheit et

al., 2002). However, at the end of an exhaustive run, runners demonstrated less variability with couplings involving the knee and greater variability with coupling involving the foot. Overall, differences for between group variability of CRP values with an exhaustive run did not follow a consistent pattern. However, patterns of compensation for altered coupling may be present.

### REFERENCES

DeLeo AT et al. (2004). *Clin Biomech*, **19**, 938-991.  
 Hamill J et al. (1999). *Clin Biomech*, **14**, 297-308.  
 Heiderscheit BC et al. (2002). *J Appl Biom*, **18**,110-121.  
 Hreljac A (2004). *Med Sci Sports Exerc*, **36**, 845-849.

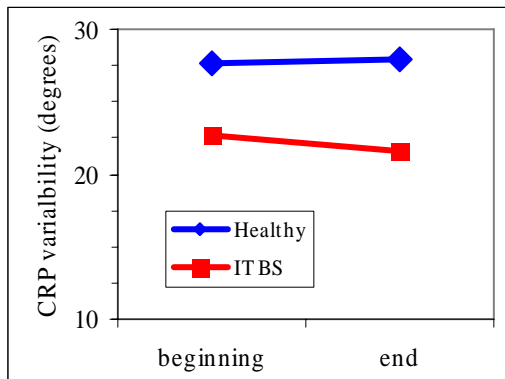


**Figure 2.** Thigh<sub>Abduction/Adduction</sub>-Tibia<sub>Rotation</sub> coupling with significant group effect (p=0.022).

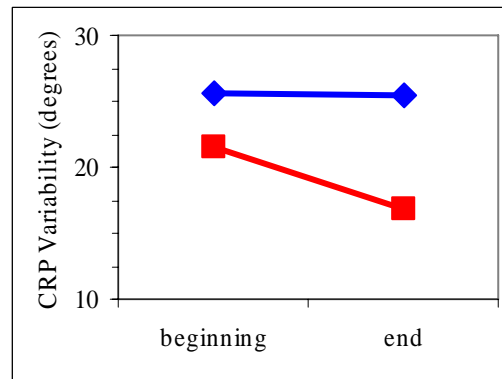


**Figure 3.** Thigh<sub>Flexion/Extension</sub>-Tibia<sub>Rotation</sub> coupling with significant group\*time effect (p=0.014).

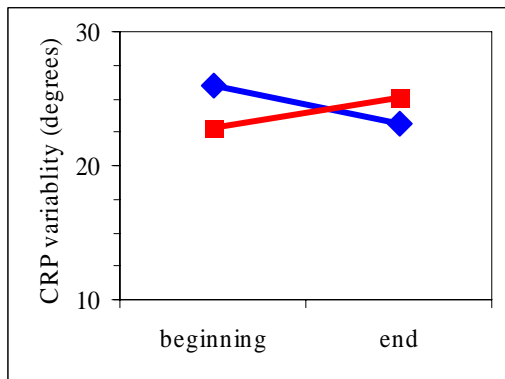


**Figure 4.** Tibia<sub>Rotation</sub>-Foot<sub>Inversion/Eversion</sub> coupling with significant group\*time effect (p<0.001).

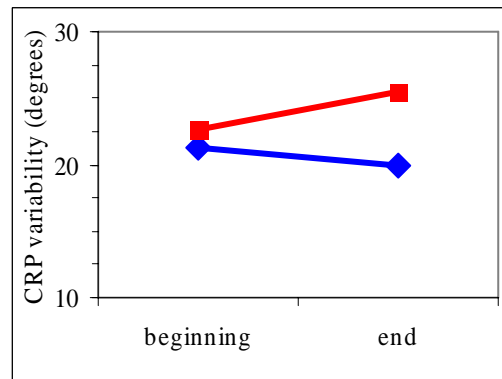


**Figure 5.** Thigh<sub>Abduction/Adduction</sub>-Foot<sub>Inversion/Eversion</sub> coupling with significant group\*time effect (p=0.021).

# CORTICAL BONE REMODELING DECREASES IN HIBERNATING GRIZZLY BEARS TO PREVENT DISUSE OSTEOPOROSIS

Aaron J. Maki,<sup>1</sup> Meghan E. McGee,<sup>1</sup> O. Lynne Nelson,<sup>2</sup>  
Charles T. Robbins,<sup>2</sup> and Seth W. Donahue<sup>1</sup>

<sup>1</sup>Michigan Technological University, Houghton, MI, USA

<sup>3</sup>Washington State University, Pullman, WA, USA

E-mail: swdonahu@mtu.edu

## INTRODUCTION

Disuse unbalances bone remodeling which leads to bone loss. Consequently, prolonged bouts of inactivity result in an increased risk of bone fracture, termed disuse osteoporosis, which may be caused by limb immobilization, spinal cord injury, or space flight. Bears place their bones in a state of disuse (hibernation) for 4-6 months annually, yet trabecular bone volume and mineral content do not decrease (Floyd et al., 1990). In addition, cortical bone porosity does not change and material strength does not decrease with age (Harvey et al., 2005). These observations imply a bone metabolism that is unique to bears. However, the mechanism by which bears are able to mitigate the effects of disuse osteoporosis is poorly understood. The purpose of this study was to quantify the dynamic bone formation properties of hibernating and active grizzly bears using histomorphometric techniques.

## METHODS

Femurs from six age-matched grizzly bears were obtained with approval from the Washington State University Institutional Animal Care and Use Committee. Three bears had been active for at least 14 weeks while three had hibernated for 17-18 weeks. All bears were administered an IV solution of calcein at 5 mg/kg bodyweight 15 and 5 days before sacrifice.

Undecalcified, unstained histological sections were prepared from the mid-diaphysis (20-40  $\mu$ m thick). The samples were viewed under darkfield with an excitation wavelength of 480 nm (Figure 1). Using a digital camera and semi-automated image analysis software (Bioquant OSTEO, Nashville, TN), inter-label width was measured at 5  $\mu$ m intervals between the label midpoints of all double-labeled osteons at 400x magnification. This measurement and the time between calcein injections (10 days) was used to calculate the mineral apposition rate (MAR).

Interlabel area (Ir.L.Ar.) and labeled osteon density (L.On.Dn) were quantified at 400x magnification. Periosteal (Ps.L.Pm) and endosteal (Es.L.Pm) labeled perimeters were measured at 250x magnification.

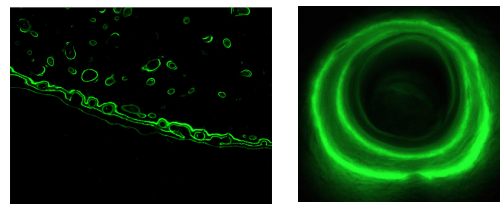


**Figure 1:** Intracortical and periosteal calcein labels at 40x original magnification (left). Calcein-labeled osteon at 400x original magnification (right)

## RESULTS

Mineral apposition rate decreased, and labeled osteon density exhibited a trend towards decreasing in hibernating compared

to active bears (Table 1, Figure 2). Endosteal labeled perimeter decreased, but periosteal labeled perimeter did not change in hibernating compared to active bears (Table 1).

**Table 1:** Dynamic histological properties

Property	Active	Hibernating	p-value
MAR ( $\mu\text{m}/\text{day}$ )	1.0	0.8	.038
Ir.L.Ar. ( $\mu\text{m}^2$ )	2893	1996	.217
L.On.Dn ( $\#/ \text{mm}^2$ )	7.7	2.9	.081
Ps.L.Pm. (mm)	66.1	51.4	.320
Es.L.Pm. (mm)	54.5	38.4	.005

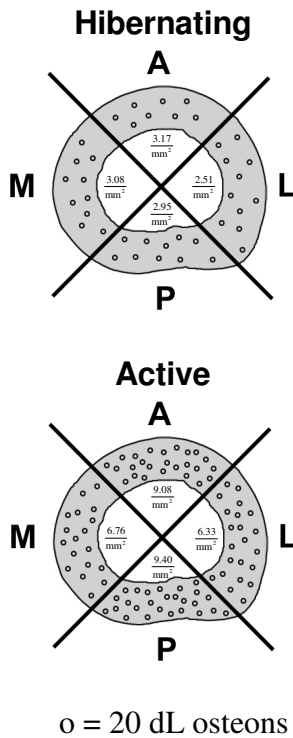


**Figure 2:** Labeled osteon density approached a significant ( $p=.081$ ) decrease in the hibernating bears.

## DISCUSSION

Our study suggests that both bone modeling and remodeling continue during hibernation, but at a slower rate than during active periods. The decreased intracortical remodeling activity (Figure 2) likely explains the previously observed decrease in intracortical porosity in hibernating grizzly bears, despite the decrease in MAR. The continued periosteal and endosteal formation explains why cross-sectional properties like the cross-sectional moment of inertia and whole bone bending strength do not decrease during hibernation. Bone formation remains coupled to resorption during hibernation (Donahue et al., 2006). The ability to maintain bone formation during disuse appears to prevent disuse osteoporosis in hibernating bears. Bears do not eat, drink, urinate or defecate during hibernation, yet they maintain constant serum calcium levels. Therefore, the hormones which control blood calcium homeostasis (e.g., parathyroid hormone) likely regulate these bone formation processes in bears. Future research into these hormones may allow for the development of new drug therapies to treat osteoporosis in humans.

## REFERENCES

- Donahue, S.W. et al. (2006). *J Exp Biol.*, (accepted).  
 Floyd, T., et. al. (1990). *Clin Orthop Relat Res*, 255, 301-309.  
 Harvey, K.B. et al. (2005). *J Biomech*, 38, 2143-2150.

## ACKNOWLEDGEMENTS

Funding from NIH (NIAMS AR050420), the Michigan Space Grant Consortium, and Timothy Floyd, M.D.

# DYNAMIC MULTISENSORY INTEGRATION AT THE BOUNDARY OF INSTABILITY IS EXPLAINED BY A SIMPLE DATA-BASED MODEL

Madhusudhan Venkadesan <sup>1</sup>, John Guckenheimer <sup>2</sup>, and Francisco J. Valero-Cuevas <sup>1</sup>

<sup>1</sup> Sibley School of Mechanical & Aerospace Engineering, Cornell University, Ithaca, NY, USA

<sup>2</sup> Department of Mathematics, Cornell University, Ithaca, NY, USA

E-mail: mv72@cornell.edu Web: www.mae.cornell.edu/nmb1

## INTRODUCTION

Dexterous manipulation is a quintessential dynamic sensorimotor task requiring the nervous system to differentially weigh multiple sensory inputs to estimate task-relevant parameters, such as the orientation of the object being manipulated. Using Bayesian inference methods, past studies of multisensory integration have revealed the effect of noise on multisensory integration in tasks with stationary task goals (Knill and Pouget 2004). The stability of dynamic tasks with sensory feedback depends not only on sensorimotor noise, but also on time-delays that have not been explicitly investigated before. Importantly, real-world tasks like object manipulation are severely nonlinear and evaded even very complex models (Valero-Cuevas 2005). Here we use bifurcation theory of nonlinear dynamical systems to propose a low-order model of the experimental task of dynamic manipulation at the boundary of instability. Combining numerical optimization on this model with experimental data, we find support for the hypothesis that multisensory integration during dynamic manipulation emerges from the interplay between time-delays and noise.

## METHODS

We asked 12 consenting subjects to compress a slender spring maximally using only their thumbpad without letting it slip (**Fig.1**). We tested our hypothesis by altering available sensory modalities (thumbpad

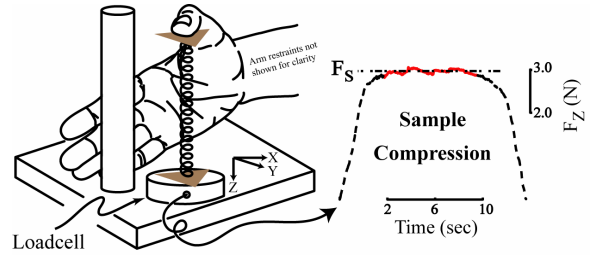


**Figure 2:** Schematic of the manipulation task. A sample compression is shown illustrating the metric of performance ( $F_s$ )

sensation / vision) via a combination of a digital nerve-block and blindfold, during the novel task of object manipulation at the boundary of instability. This allows modeling the system using bifurcation theory that characterizes dynamics at a transition to instability. We modeled spring buckling dynamics as a subcritical pitchfork bifurcation (El Naschie 1990) and sensorimotor control as multisensory (1: thumbpad, 2: non-digital, 3: vision) proportional feedback with time-delays and noise (**Fig.2**). We used time-delays and noise level in our model using values reported in literature. The remaining parameters in the model were obtained based on the mode of failure observed in the experiments.

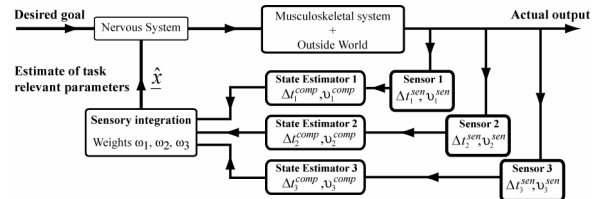


**Figure 1:** The dynamics of the neuromusculoskeletal system + outside world block was modeled as a subcritical pitchfork bifurcation and the feedback law as simple proportional feedback.

## RESULTS AND DISCUSSION

Both experimentally (**Fig.3**) and computationally (**Fig.4**), the loss of thumbpad sensation significantly affected performance since this modality is both accurate and fast. Experimentally, lack of vision degraded performance only when thumbpad sensation was absent (**Fig.3**).

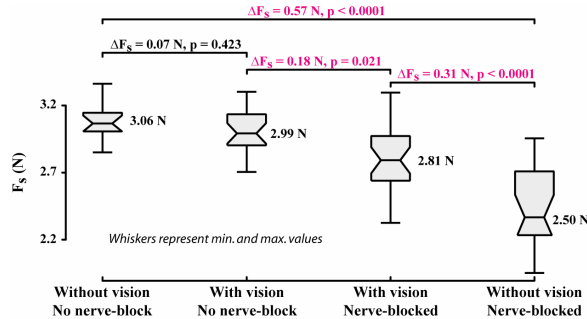


**Figure 4:** Horizontal mid-line is the sample mean, the notches are 95% confidence intervals and the box shows the 25th and 75th percentiles. Whiskers show the min and max values. The differences in shown in magenta are the only significant ones at a significance level of 0.025.

Comparing the optimized models to experimental data shows that sensory weights emerging from a trade-off between time-delays and noise are more realistic than sensory weights accounting for noise alone (**Fig.4**: cyan vs pink markers). Moreover, an extra time-delay for non-digital sensors over and above sensory and nerve-conduction delays (*Model 2* in **Fig.4**) was necessary to explain why lack of vision affected performance only when thumbpad sensation was absent. *Model 1* (crosses), which has no extra time-delay for non-digital sensors, fails to agree with experimental results in the absence of thumbpad sensation (“Nerve-blocked”), since an additional loss of vision (cf. 3rd vs. 4th columns) has either a small effect on performance (blue cross), or an unrealistic increase in performance (magenta cross). *Model 2* (circles) that considers computational time delays shows the same

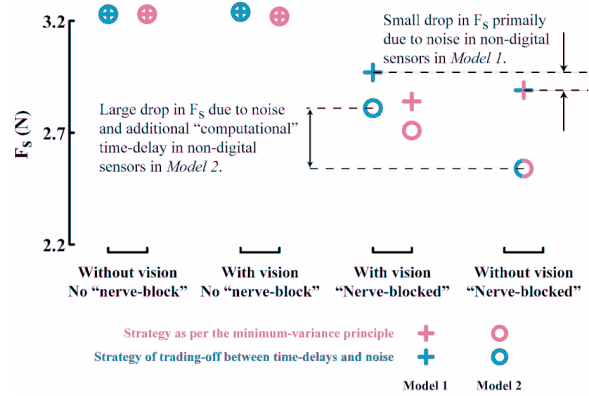


**Figure 3:** The results of simulating both our models, with (‘O’) or without (‘+’) extra time-delay for non-digital sensors) using two alternate strategies – accounting only for noise (pink) or for both time-delays and noise (cyan).

trend as the experimental data (again, cf. 3rd vs. 4th columns). This additional delay can be only due to computational time-delays in sensory processing.

## CONCLUSIONS

To our knowledge, our results demonstrate for the first time that, (i) a simple, yet mathematically rigorous model based on bifurcation theory can characterize very complex neuromuscular behavior such as dynamic manipulation, (ii) neural computational time-delays can measurably affect performance and, (iii) multisensory integration emerges from a trade-off between time-delays and noise.

## REFERENCES

- El Naschie, M.S. (1990). *Stress, stability, and chaos in structural engineering : an energy approach*. McGraw-Hill.
- Knill, D.C. and Pouget, A. (2004). *Trends Neurosci.* **27**. 712-719.
- Valero-Cuevas, F.J. (2005). *J. Biomech.* **38**. 673-684.

## ACKNOWLEDGEMENTS

Work supported by Whitaker Foundation, NSF 0237258, NIH R21HD048566 and NIH R01AR050520 grants to FVC. Drs. Emanuel Todorov and Manoj Srinivasan for their comments.

# A STUDY ON EFFECTS OF CONSTITUTIVE PARAMETERS IN A FLUID-STRUCTURE INTERACTION FE MODEL OF THE CARPAL TUNNEL

Cheolwoong Ko<sup>1</sup> and Thomas D. Brown<sup>1</sup>

<sup>1</sup> Department of Orthopaedics and Rehabilitation, University of Iowa, Iowa City, IA, USA  
E-mail: [cheol-ko@uiowa.edu](mailto:cheol-ko@uiowa.edu) Web: <http://poppy.obrl.uiowa.edu/>

## INTRODUCTION

Carpal Tunnel Syndrome (CTS) is among the most important of the family of chronic nerve compression disorders. Mechanical insult to median nerve is recognized as the proximate cause. However, the potential utility of finite element (FE) analysis of stresses in human carpal tunnel has not been appropriately studied. In this research, human carpal tunnel FE models were constructed based on anatomical information to investigate the effects of pertinent physical parameters on median nerve stress.

## METHODS

An anatomical image of the human carpal tunnel was utilized to build two and three-dimensional FE models (Figure 1, 2). Key attributes were the median nerve and flexor tendons, and the carpal tunnel wall. In this study, ADINA/ADINA-F (Version 8.2, ADINA R&D, Inc.) was utilized as a solver. Visco-elastic material properties (Ruan et al., 1993) for nerve and tendons (Table 1) were applied by using Equation (1). Synovial-like fluid was defined as Newtonian (viscosity  $\mu = 0.02 \text{ Ns/m}^2$ ). Solid contacts were invoked between nerve and tendons, combined with a fluid structure interaction (FSI) boundary condition. The model was driven by volar-ward nerve and tendons displacements.

$$\begin{aligned} G(t) &= G_{\infty} + (G_0 - G_{\infty})e^{-\beta t} \\ K(t) &= K_{\infty} + (K_0 - K_{\infty})e^{-\beta t} \end{aligned} \quad \text{--- (1)}$$

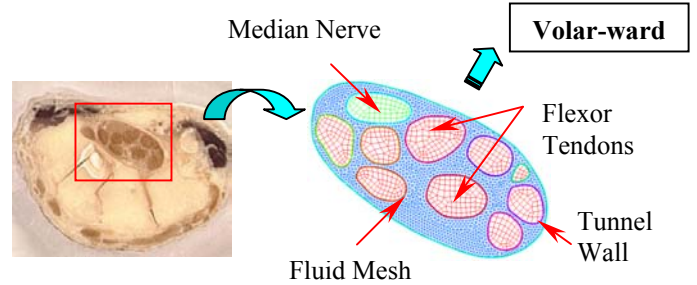
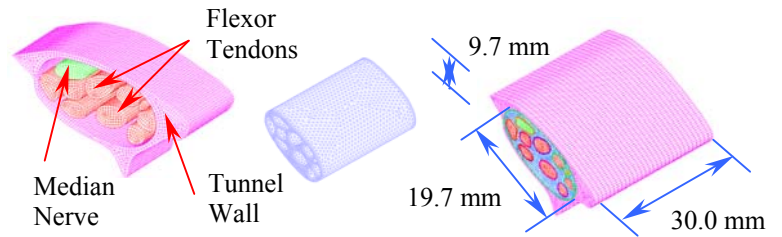


**Figure 1: Human Carpal Tunnel 2-D FE Model**



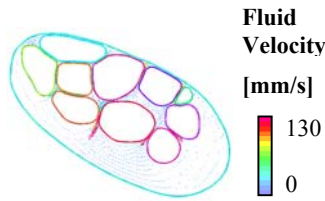
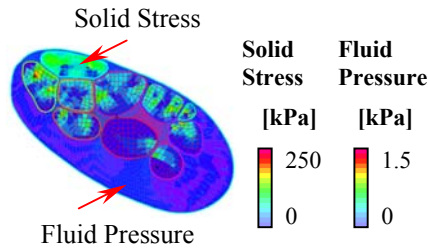
a) Solid Model    b) Fluid Model    c) Combination  
**Figure 2: Human Carpal Tunnel 3-D FE Model**

**Table 1: Material Properties for Baseline Conditions**

$G_{\infty}$	$G_0$	$K_{\infty}$	$K_0$	$\beta$
150 kPa	500 kPa	1,450kPa	4,830 kPa	35 s <sup>-1</sup>

## RESULTS AND DISCUSSION

With the defined baseline analysis conditions for a 2-D FE model with rigid wall, the level of solid stress in the nerve or tendon was far greater than the fluid pressure (Figure 3). When fluid viscosity was varied, the stress in the tendon/nerve and the fluid velocity remained almost unchanged (Table 2). In contrast, the computed fluid pressure showed an



a) Solid Stress and Fluid Pressure      b) Fluid Velocity

**FIGURE 3: Simulation Results with Baseline Analysis Conditions by 2-D Model with Rigid Wall**

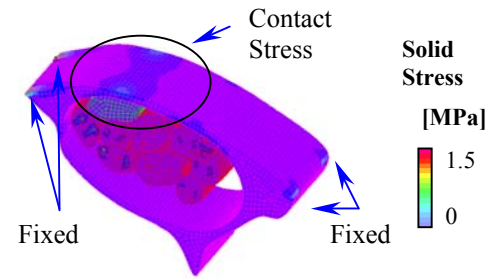


**Figure 4: Simulation Results by 3-D Model under Solid Contact Conditions**

approximately linear relationship with fluid viscosity. Also, to quantitatively investigate the effects of tendon material properties, an elastic condition (assumed Young’s modulus = 65MPa (Dakin et al., 2001) was applied for the tendons. The stress in the tendons showed almost linear relationship with tendon modulus (Table 3). However, fluid pressure and fluid velocity were almost unchanged, while there was a non-linear relationship for nerve stress.

Extending the 2-D multi-body solid contact FE simulation to 3-D FE model with tunnel wall deformation was investigated (Figure 4). Contact stresses on the carpal tunnel wall due to nerve abutment were of the order of the nerve stresses obtained in the 2-D model.

## SUMMARY

It was found that the level of solid stress in the nerve or tendons was far greater than the fluid pressure. From this, it was inferred that mechanical insult from direct structural contact with median nerve could be a far more potent CTS stimulus than fluid pressure. Ongoing work with the 3-D model includes immersed multi-body solid contact analysis.

## REFERENCES

- Dakin, G. et al. (2001). *Journal of Biomechanical Engineering*, **123**, 218-226.  
 Ruan, J. S. et al. (1993). *SAE paper* 933114.

**Table 2: Effects of Fluid Viscosity (Baseline Parameter A3)**

	Fluid Viscosity [Ns/m <sup>2</sup> ]		Max. Tendon Stress [kPa]		Max. Nerve Stress [kPa]		Max. Fluid Pressure [kPa]		Max. Fluid Velocity [mm/s]	
	Ratio		Ratio		Ratio		Ratio		Ratio	
A1	0.001	0.05	258.9	1.000	201.2	1.001	0.080	0.054	131.7	0.971
A2	0.002	0.10	258.9	1.000	201.2	1.001	0.154	0.104	137.5	1.014
A3	<b>0.02</b>	<b>1.00</b>	<b>258.9</b>	<b>1.000</b>	<b>201.0</b>	<b>1.000</b>	<b>1.482</b>	<b>1.000</b>	<b>135.6</b>	<b>1.000</b>
A4	0.2	10.0	259.6	1.003	199.8	0.994	12.78	8.623	127.5	0.940
A5	0.5	25.0	260.3	1.005	198.6	0.988	24.06	16.23	117.9	0.869

**Table 3: Effects of Tendon Young’s Modulus (Baseline Parameter B3)**

	Tendon Y’s Modulus [MPa]		Max. Tendon Stress [MPa]		Max. Nerve Stress [kPa]		Max. Fluid Pressure [kPa]		Max. Fluid Velocity [mm/s]	
	Ratio		Ratio		Ratio		Ratio		Ratio	
B1	0.65	0.01	0.188	0.011	93.70	0.514	0.489	1.043	62.6	1.011
B2	13.0	0.20	2.212	0.200	167.5	0.918	0.455	0.970	62.0	1.002
B3	65.0	<b>1.00</b>	<b>11.06</b>	<b>1.000</b>	<b>182.4</b>	<b>1.000</b>	<b>0.469</b>	<b>1.000</b>	<b>61.9</b>	<b>1.000</b>
B4	325.0	5.00	55.30	5.000	185.7	1.018	0.472	1.006	61.9	1.000
B5	650.0	10.0	110.6	10.00	186.1	1.020	0.472	1.006	61.9	1.000

# Evaluation of Two Methods to Induce Mechanical Injury to Neuronal Cell Cultures

Carolyn Hampton<sup>1</sup>, H. Clay Gabler<sup>1</sup>, Beverly Rzigalinski<sup>2</sup>

<sup>1</sup>Virginia Tech – Wake Forest University School of Biomedical Engineering and Sciences,  
Blacksburg, VA 24061

<sup>2</sup>Edward Via Virginia College of Osteopathic Medicine, Blacksburg, VA 24060  
Email: champton@vt.edu

## INTRODUCTION

Disabilities due to traumatic brain injury are common, and a significant majority occurs as a consequence of automotive accidents (Morrison, 2006). Because this topic is of great interest, there are several methods by which neuronal injury of the brain can be tested. Two such methods are the pressure-driven system used by Ellis et al. (1995) and the biaxial stretch system used by Morrison (2006).

Ellis et al. utilized a pressurized system, where an elastomer-bottomed culture well was deformed outward by a transient pressure pulse. The deformation of the membrane was used to apply stretch injury to cultures of astrocytes, which are glial cells found in the brain or neonatal rat pups.

An alternative system used by Morrison et al. relied on a biaxial mechanism. By deforming the circular membrane along its plane, a uniform biaxial stretch was applied to slices of the hippocampus region of the brain of young rat pups. The slices incorporate all of the cells of the brain, including astrocytes, neurons, and the associated vascular cells.

The objective of this paper is to evaluate, via finite element analysis, the relative merits of each type of injury control system. The local strains induced in the membrane, and

presumably the cell culture, will be examined.

## METHODS

A finite element model was developed to model the two systems. A circular mesh was used to represent the elastomer membrane in both of the models, with the loading conditions differing between the two.

In order to model the system used by Ellis, a pressure was applied to each element. This load pulse was of the form of a sinusoid. The membrane, which lay in the X-Y plane, would then deform in the Z direction. The outer edge of the membrane was restrained from all displacements but allowed to rotate.

The system used by Morrison was modeled by applying prescribed displacements to the nodes making up the outer edge of the membrane. A gravitational force was the only applied loading.

## RESULTS AND DISCUSSION

The model of the pressure driven system was completed and validated against the data published by Ellis (1995). These results are shown in Figure 1. As shown, there was a good agreement between the finite element model and the experimental results ( $R^2$  value of 0.996).

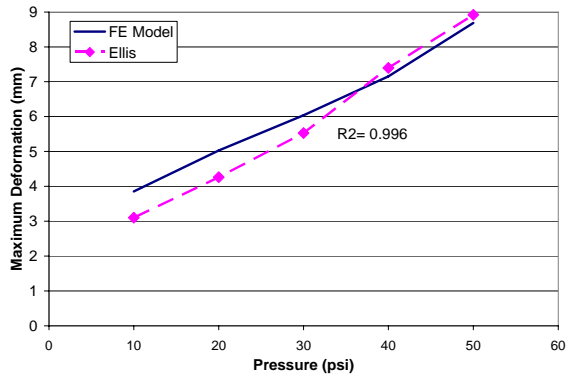


**Figure 1:** Pressure-driven membrane deflection as a function of the pressure pulse magnitude.

The strain profiles for each of the models were of particular interest, as tissue strain is believed to be a predictor of injury. Figure 2 shows a plot of the strain profiles as a function of the radial position on the membrane.

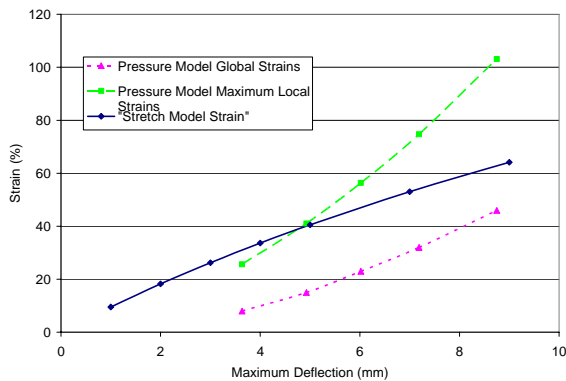


**Figure 2:** Strain profiles for each for the two model types.

The strain profile of the pressure driven system was the most complex. Both the average and maximum strains were non-linear. The strain also varied by the distance from the center.

The biaxial stretch model showed a near uniform distribution of strain across the entire membrane. Small differences in the element strains (< 1%) were attributed to the meshing pattern and considered insignificant.

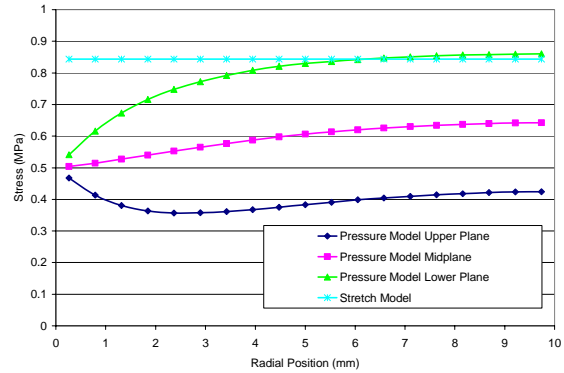


**Figure 3:** Stress profiles for the two models.

The stress profiles of the pressure driven model were found to vary at the different thicknesses. The membrane upper surface, which is in flexion, was under a smaller stress than the lower surface. The stretch model had equal stresses at all levels of thickness due to its lack of deformation in the Z-direction.

## CONCLUSIONS

Two viable methods for inducing injury to cellular cultures were evaluated. The two devices possess differing stress and strain profiles. The strain profiles were uniform in the stretch model and were both variable and non-linear in the pressure driven model.

The virtues of the stretch model include its uniform strain profile and its flat, planar surface that makes video analysis possible. The pressure model is useful for its ease of use. There is no need to transplant cell cultures and the culture medium can be maintained if desired.

## REFERENCES

- Ellis et al. (1995) *Journal of Neurotrauma*, **12**, 3, 325-339
- Morrison et al. (2006) *Journal of Neuroscience Methods*, **150**, 2, 192-201
- LS-DYNA User's Manual*, Livermore Software Technology Corporation

# AGE-RELATED CHANGES IN MUSCULAR EFFORT

Emmanuel B. John<sup>1</sup>, Wen Liu<sup>1</sup>, and Robert W. Gregory<sup>1,2</sup>

<sup>1</sup>University of Kansas Medical Center, Kansas City, KS, USA

<sup>2</sup>University of Kansas, Lawrence, KS, USA

E-mail: [rwg@ku.edu](mailto:rwg@ku.edu)

Web: [www.soe.ku.edu/hses/](http://www.soe.ku.edu/hses/)

## INTRODUCTION

An important factor distinguishing movements that are performed from those that are not is the level of muscular effort associated with movement: movements that are performed generally take less muscular effort than those that are not (Rosenbaum and Gregory, 2002). This insight suggests that sense of muscular effort is an important variable to be assessed in aging populations, since older individuals often have difficulty in performing (or are unable to perform) activities of daily living due to the level of effort that is involved. If one conceives of the individual's state as a ball in a changing effort landscape, the concept of muscular effort can be viewed as the return of the ball to a height corresponding to an acceptable effort level for any task of importance.

Unfortunately, the concept of effort as it relates to movement production in aging populations is not clearly defined; age-related differences in sense of effort are not fully understood and there are contradictory findings (Allman and Rice, 2003). Furthermore, previous investigations that have focused on effort in aging populations have been directed at the physiological and psychological factors that affect sense of effort; no research has been performed to examine the biomechanical factors that influence muscular effort (Borg, 1998). The purpose of this study was to determine age-related changes in biomechanical measures of muscular effort during isometric muscle actions.

## METHODS

Twenty healthy, younger individuals (10 males, 10 females) between 20-40 years of age and 20 healthy, older individuals (10 males, 10 females) between 65-75 years of age participated in this study.

After undergoing informed consent procedures, participants were asked to perform isometric elbow flexion/extension joint actions in the horizontal plane using their dominant arm at three different joint angles (45°, 90°, and 135°). Following a warm-up and measurement of maximal voluntary contraction (MVC) strength for all joint action and joint angle combinations, the participants were required to produce joint torques that corresponded to effort levels of 1 (very light effort), 3 (light effort), 5 (medium effort), 7 (strong effort), or 9 (very strong effort) on a modified Borg CR-10 scale (0 = no effort, 10 = maximal effort). Elbow joint torque was measured using a dynamometer (System 3 Pro, Biodex Medical Systems). The 30 conditions (two joint actions × three joint angles × five effort levels) were presented in random order. Each trial was separated by a period of 2 minutes to minimize the effects of fatigue.

A between-within subjects factorial ANOVA design was used to assess the effects of age, joint action, joint angle, and effort level on elbow joint torque (absolute and normalized to MVC strength). Only the results for the 90° joint angle condition will be presented here.

## RESULTS AND DISCUSSION

There was a significant increase in joint torque (both absolute and relative) as a function of effort level during elbow flexion and extension joint actions for both young and older age groups (see Table 1). In addition, both young and older subjects produced significantly greater absolute joint torques during elbow flexion than elbow extension across all effort levels.

For each effort level, the young subjects produced significantly greater absolute joint torques than the older subjects during both elbow flexion and extension. In addition, except for the very light effort level (1), the older subjects produced significantly smaller relative joint torques than the young subjects at effort levels of 3-9 during both elbow flexion and extension.

The difference in absolute joint torques produced by the young and older age groups as a function of effort was to be expected since we lose muscular strength as we age. Altered processing of the physiological cues for muscular effort due to age-related changes in the brain such as synaptic restructuring or a loss of cortical neurons may have lead to the smaller relative joint torques produced by the older subjects as a function of effort (Allman and Rice, 2003).

## SUMMARY

The purpose of this study was to determine age-related changes in biomechanical measures of muscular effort. It is essential to investigate age-related changes in sense of effort in order to more fully understand changes in physical work capacity due to the aging process and to evaluate changes in muscular effort over time for a given individual. An elevated perception of muscular effort reported by old versus young humans could contribute to impaired movement capabilities with aging.

## REFERENCES

- Allman, B.L., Rice, C.L. (2003). *European Journal of Applied Physiology*, **89**, 191-197.
- Borg, G.V. (1998). *Borg's Perceived Exertion and Pain Scales*. Human Kinetics.
- Rosenbaum, D.A., Gregory, R.W. (2002). *Experimental Brain Research*, **142**, 365-373.

## ACKNOWLEDGEMENTS

This investigation was supported by the University of Kansas General Research Fund allocation #2301572.

**Table 1:** Absolute (Abs) and relative (Rel) elbow joint torques (mean  $\pm$  SD) as a function of age, joint action, and effort level during isometric muscle actions.

Group	Joint Action	Joint Torque	Effort Level				
			1	3	5	7	9
Young	Flex	Abs (Nm)	7.0 $\pm$ 4.9	12.5 $\pm$ 6.5	20.3 $\pm$ 9.3	29.0 $\pm$ 14.2	39.5 $\pm$ 17.7
		Rel (%MVC)	12.9 $\pm$ 5.4	24.7 $\pm$ 7.6	40.2 $\pm$ 10.6	56.5 $\pm$ 11.4	77.1 $\pm$ 12.5
	Ext	Abs (Nm)	4.1 $\pm$ 2.9	7.9 $\pm$ 4.0	13.0 $\pm$ 6.6	17.7 $\pm$ 7.9	23.3 $\pm$ 11.0
		Rel (%MVC)	12.6 $\pm$ 4.9	25.0 $\pm$ 7.7	40.4 $\pm$ 10.6	56.0 $\pm$ 12.4	72.6 $\pm$ 15.6
Old	Flex	Abs (Nm)	4.8 $\pm$ 3.2	8.4 $\pm$ 5.1	13.2 $\pm$ 6.5	17.2 $\pm$ 7.8	23.5 $\pm$ 10.3
		Rel (%MVC)	12.0 $\pm$ 6.8	20.3 $\pm$ 6.8	33.9 $\pm$ 14.1	44.4 $\pm$ 15.9	60.4 $\pm$ 19.5
	Ext	Abs (Nm)	3.1 $\pm$ 2.3	4.9 $\pm$ 2.7	7.2 $\pm$ 3.7	9.1 $\pm$ 4.4	13.6 $\pm$ 6.0
		Rel (%MVC)	12.5 $\pm$ 7.6	20.2 $\pm$ 7.7	30.5 $\pm$ 11.4	39.2 $\pm$ 12.9	57.4 $\pm$ 17.8

# A COMPARISON OF CLINICAL MEASUREMENTS OF ARCH STRUCTURE IN RECREATIONAL ATHLETES

Douglas Powell, Songning Zhang, and Clare Milner

Biomechanics/Sports Medicine Lab, The University of Tennessee, Knoxville, TN, USA  
email: [dpowell4@utk.edu](mailto:dpowell4@utk.edu), web: [web.utk.edu/~Esals/resources/biomechanics\\_laboratory.html](http://web.utk.edu/~Esals/resources/biomechanics_laboratory.html)

## INTRODUCTION

The foot is a complex structure that attenuates shock during load response and acts as a rigid lever during push-off. Mal-aligned and dysfunctional foot structures have been associated with increased risk of injury of the foot as well as ankle, knee and hip joints (Carpintero, Entrenas et al. 1994; Williams, McClay et al. 2001). Thus, it is important to have an assessment tool capable of adequately determining foot dysfunction while being simplistic in nature for use in a clinical setting. Arch index and arch stiffness are two such measurements that are relatively simple in nature and classify foot structure. Normative data for arch index and arch stiffness have been presented previously (Williams and McClay 2000; Zifchock In Press). Other relevant measures of foot function include relative arch deformity (Nigg, Khan et al. 1998; Williams and McClay 2000), classical stiffness and stress-strain ratio. Normative values provide clinicians with a quantitative standard to objectively assess foot function; however, they are all inclusive and may not be accurate for specific subsets of the population. Due to greater activity levels recreational athletes may visit clinicians more often than other populations. The purpose of the current study, therefore, is to provide reference data on a population of recreational athletes and to compare different clinical measurements of arch structure amongst each other.

## METHODS

Seventy-two recreational athletes (34 male and 38 female) between the ages of 18 and 30 ( $21.3 \pm 2.5$  years) participated in the current study. Foot measurements were taken using a custom foot measuring device. The total foot length, truncated foot length and dorsum height were measured. The dorsum height was measured in three conditions, standing on a flat surface as well as standing and seated with the arch unsupported. From these measurements absolute arch deformation (AD), arch index (AI) (Williams and McClay 2000), arch stiffness (AS) (Zifchock In Press), relative arch deformity (RAD) (Nigg, Khan et al. 1998; Williams and McClay 2000), classic stiffness (CS) and stress-strain ratio (SSR) were calculated.

Independent t-tests were used to determine gender differences within each foot measurement (SPSS 14.0). Multiple regression analysis was conducted using AD as the dependent variable to determine the relative contributions of each related measure to the absolute magnitude of arch deformation.

## RESULTS AND DISCUSSION

All subjects were recreational athletes participating in university level club sports or in a recreational league. The mean arch index in the current study was  $0.335 \pm 0.044$  across both genders (Table 1), which is higher than the reported normative value of  $0.316 \pm 0.027$  (Williams and McClay 2000). Mean arch stiffness values were  $3300 \pm 2200$  for males and  $2200 \pm 1800$  for females, respectively (Zifchock In Press). These

values are also higher than previously reported normative values of  $2100 \pm 700$  and  $1200 \pm 500$  for males and females, respectively (Williams and McClay 2000). Mean RAD values in the current study were lower than values previously reported in the literature ( $1.05 \pm 0.51$ ; 1.0-2.0) (Nigg, Khan et al. 1998; Williams and McClay 2000). In addition, a significant gender difference was present in RAD, with males having less deformity than females.

The multiple regression analysis determined that AI, RAD, CS, AS and SSR were significant predictors of arch deformation. Arch deformation was significantly correlated with RAD ( $r=0.89$ ), AS ( $r=-0.77$ ), CS ( $r=-0.77$ ) and SSR ( $r=-0.77$ ). Arch Index was not significantly correlated with AD ( $r=-0.26$ ). While AI, RAD, AS, CS and SSR had significant correlations with arch deformation, collinearity diagnostics revealed that AS, CS and SSR were collinear, thus only SSR was included in the regression analysis to represent these variables. The multiple regression analysis revealed the combination of RAD, AI and SSR was the best model for the prediction. The regression equation ( $r=0.85$ ) is presented below.

$$AD = 0.280 * RAD + 1.084 * AI + 3.6 * 10^{-5} (SSR) - 0.262.$$

Arch index is simple to measure and easy to use in a clinical setting and was the second largest contributor in predicting AD suggesting that it is a good predictor of quasi-dynamic movement of the foot. RAD is a more complex measure of foot function and was the greatest contributor to the prediction of AD in the regression equation suggesting it is also a better predictor of quasi-dynamic foot function. Offering a minor contribution to the prediction equation was SSR. Arch stiffness and

classical stiffness were omitted from the regression equation because they were highly correlated to SSR.

**Table 1.** Mean values of arch structure related variables: mean  $\pm$  SD.

	Male	Female
BMI	24.8 $\pm$ 4.0	22.1 $\pm$ 2.0
AD (mm)	0.257 $\pm$ 0.171	0.267 $\pm$ 0.147
AI (AI units)	0.335 $\pm$ 0.040	0.336 $\pm$ 0.046
AS (BW/AI)	3298 $\pm$ 2205	2183 $\pm$ 1784
RAD (N <sup>-1</sup> )	0.55 $\pm$ 0.33 <sup>a</sup>	0.80 $\pm$ 0.53
CS (N/mm)	5405 $\pm$ 5973	3779 $\pm$ 5085
SSR (N/mm)	1809 $\pm$ 1993	1302 $\pm$ 1806

<sup>a</sup> denotes significant gender difference.

## CONCLUSIONS

Clinicians require measurement tools that are simple in nature yet retain good accuracy and validity. The results from this study showed that both RAD and AI are two best predictors of arch deformation. The most practical measurement for clinicians must also be quick and easy, suggesting AI may be the most clinically useful measurement. The greater mean AI and AS values observed in this study compared to previous studies, indicating higher and stiffer arches, may be related to the unique characteristics of the young and active population involved in the study.

## REFERENCES

- Carpintero, P., R. Entrenas, et al. (1994). *Spine* **19**(11): 1260-3.
- Nigg, B. M., A. Khan, et al. (1998). *Med Sci Sports Exerc* **30**(4): 550-5.
- Williams, D. S., 3rd, I. S. McClay, et al. (2001). *Clin Biomech* **16**(4): 341-7.
- Williams, D. S. and I. S. McClay (2000). *Phys Ther* **80**(9): 864-71.
- Zifchock (In Press). *Foot & Ankle International* (In Press).

# ACHILLES TENDON FORCES DURING A ROUND-OFF BACK HANDSPRING

Christa Piazza and Michael Pavol

Oregon State University, Corvallis, OR, USA  
E-mail: mike.pavol@oregonstate.edu

## INTRODUCTION

Gymnastics has one of the highest rates of severe injury in sports due to its physical demands on its competitors (Kingma and ten Duis, 1998). One severe injury that has begun to occur more frequently is a rupture of the Achilles tendon. Many such ruptures have been observed in the transition from a round-off back handspring to an airborne element during the floor exercise. There is thus a need to understand the factors that influence the forces in the Achilles tendon during this critical period. One factor that may contribute to increased force on the tendon is a greater approach speed. This study therefore investigated the relationship between approach speed and the forces experienced by the Achilles tendon during a round-off back handspring rebound skill.

## METHODS

Twelve women (mean  $\pm$  SD age:  $19.9 \pm 1.8$  years), all advanced-level gymnasts, gave their informed consent to participate. To simulate a competition setting, a 60 cm x 80.5 cm piece of gymnastics spring flooring was mounted to a pair of force plates. An 8.5 m x 1.2 m runway of spring flooring led to the force plates. Mats were placed around and beyond the plates. The flooring was covered with 3.7 cm-thick foam.

After warming up, subjects performed five trials of a round-off back handspring rebound skill from each of three approaches: standing, jump-hurdle, and step-hurdle. In the latter approach types, the round-off was

initiated after a short jump and a step-and-hop, respectively. Subjects were required to land within a marked area over the force plates, then rebound into the air. A motion capture system recorded the positions of 20 markers, attached to the lower limbs and pelvis, at 250 Hz. Force plate data were sampled at 2000 Hz. Trials were blocked by approach type and counterbalanced.

Based on the measured flooring geometry, inertia, and spring stiffness, the ground reaction forces and center of pressure at the spring floor surface were derived from the force plate data. Marker data were low-pass filtered at 15 Hz, and used to determine joint center positions and body segment angles. The bilateral-average ankle plantarflexion moment was computed, with the ground reaction force distributed between the feet based on the center of pressure mediolateral position. The average of the force acting in each Achilles tendon was determined from the ankle moment and the tendon moment arm, and normalized to body weight (BW).

Repeated-measures analysis of variance was used to compare variables between approach types. Analyzed were the peak Achilles tendon force, peak rate of tendon force increase, and approach speed, defined as the forward velocity of the hips over the 100 ms before floor contact. Pearson correlations were computed between the peak Achilles tendon force, the peak ground reaction force, and the minimum foot-floor angle during contact. Positive foot-floor angles correspond to plantarflexion. A significance level of 0.05 was used.

## RESULTS AND DISCUSSION

The peak Achilles tendon force during floor contact ranged from 7.2 to 16.0 BW and occurred either shortly after landing or when the ground reaction force peaked at mid-stance (Figure 1). Neither the peak Achilles tendon force nor the peak rate of force increase differed between approach types, despite greater approach speeds for jump- and step-hurdles than for standing ( $p < .05$ ; Table 1). Peak tendon force was also unrelated to the peak ground reaction force.

A strong positive correlation existed between peak Achilles tendon force and the minimum foot-floor angle during contact ( $r = 0.91$ ;  $p < 0.05$ ; Figure 2). In particular, two subjects whose heels never contacted the floor experienced peak tendon forces 40% greater than average, and 198% of the predicted failure load of 4000 N (Komi, 1987). By staying on their toes, these gymnasts had to rely on their plantarflexors more for energy absorption during landing. They also increased the moment arm of their peak ground reaction force arm about the

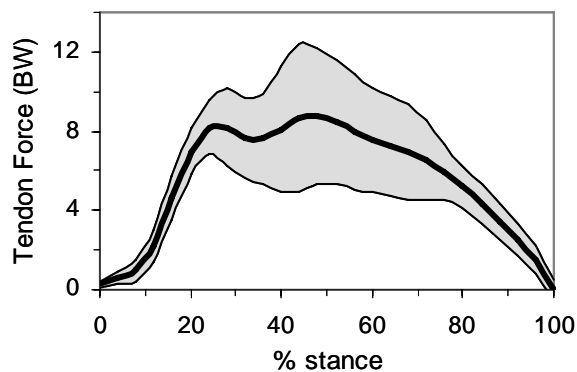


**Figure 1:** Mean  $\pm$  SD Achilles tendon force vs. % stance during floor contact.

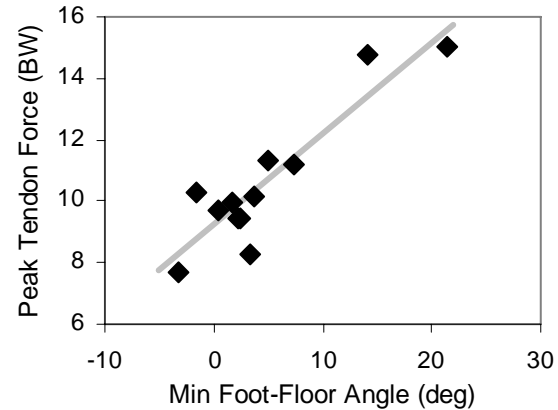


**Figure 2:** Peak Achilles tendon force vs. minimum foot-floor angle.

ankle, increasing the opposing plantarflexor moment needed. Of note, these two gymnasts were very skilled tumblers. This suggests that reducing the foot-floor angle to decrease the injury risk may not be a viable option, as it might impair performance.

## CONCLUSIONS

Landing technique appears to play a far greater role than approach speed in the risk of Achilles tendon injury during a round-off back handspring rebound. Staying on ones toes during landing markedly increases the peak forces in the Achilles tendon.

## REFERENCES

- Kingma, J., ten Duis, H.J. (1998). *Percept Mot Skills*, **86**, 675-686.  
 Komi, P.V. (1987). *Int J Sports Med*, **8**, 3-8.

## ACKNOWLEDGEMENTS

Equipment donated by Palmer Power Springs and the OSU Gymnastics Team.

**Table 1:** Mean  $\pm$  SD approach speed and peak Achilles tendon loading vs. approach type.

		Standing	Jump-Hurdle	Step-Hurdle
Approach speed	(m/s)	3.76 $\pm$ 0.26	4.04 $\pm$ 0.24	4.07 $\pm$ 0.24
Peak force	(BW)	10.6 $\pm$ 2.4	10.8 $\pm$ 2.4	10.4 $\pm$ 2.2
Peak rate of increase	(BW/s)	502 $\pm$ 54	526 $\pm$ 66	533 $\pm$ 57

# TRUNK STIFFNESS REFLEX AS A FUNCTION OF TRUNK POSTURE

Steven W Hanson, Ellen L Rogers, and Kevin P Granata  
Virginia Polytechnic Institute and State University, Blacksburg, VA, USA  
E-mail: granata@vt.edu Web: www.biomechanics.esm.vt.edu

## INTRODUCTION

Spinal instability has been considered a potential risk factor for low back pain (LBP). Stability of the spine has been examined as a function of steady-state muscle recruitment, static spinal posture, and external load. The primary neuromuscular factors that contribute to stability include stiffness of active paraspinal and torso muscles and the reflex response in paraspinal muscles (Moorhouse, 2005). Trunk stiffness during active muscular contraction has been measured as a function of exertion effort and load direction. Flexed postures during manual materials handling is associated with high incidence rates of LBP. However, we are unaware of any studies to characterize the effect of flexion posture on active torso stiffness and reflex response.

This study investigated the influence of torso flexion angle on trunk stiffness and reflex gain. It was hypothesized that trunk stiffness will increase with trunk flexion. It was also hypothesized that reflex gain will decrease with trunk flexion

## METHODS

The experiment allowed for the assessment of trunk stiffness and reflex gain at four trunk angles (0°, 30°, 60°, 90°). To avoid confounding between trunk angle and gravitational moment, lumbar flexion was achieved by rotating the lower body up to the desired angle while the torso remained upright. The subject was attached to a servomotor via a harness and cables system such that anteriorly directed horizontal loads were applied at the T10 level of the trunk. The servomotor applied isotonic loads of

15% and 30% MVE. The subject maintained an unsupported upright isometric trunk posture against the loads with their pelvis strapped to a fixed structure for support and to limit movement to the torso.

During the exertions, pseudorandom binary perturbations (PRBPs) of  $\pm 70\text{N}$  were superimposed on the isotonic preload. PRBP were chosen to eliminate problems with voluntary responses to predictable stimuli. At each trunk angle, twenty second trials were performed at each preload, approximately 50 perturbations per trial. Applied forces were measured with a force transducer (Omega, Stamford, CT) attached to the motor. Trunk kinematics were recorded with two six degree of freedom electromagnetic position sensors at the S1 and T10 levels of the trunk (Ascension, Burlington, VT). Muscle activity was recorded with bipolar surface electrodes (Delsys, Boston, MA) attached over the left and right lumbar paraspinal muscles.

System identification techniques were used to identify the dynamic relationship between applied force and position data. Separate analyses evaluated the dynamic relationship between applied force and EMG response. Correlation methods were used to identify the impulse response functions (IRF) of the respective systems.

$$IRF = \frac{1}{\Delta t} C_{xx}^{-1} C_{xy}$$

Where  $C_{xx}$  is the input autocorrelation,  $C_{xy}$  is the input/output cross-correlation, and  $\Delta t$  is the sample period. This method of solving for the IRF was used in finding the trunk stiffness (input: force; output: position) and the reflex gain (input: force; output: EMG).

A second order equation was fit to the IRF describing the force/position relationship:

$$H(s) = \frac{1}{ms^2 + bs + k}$$

Where  $m$  is the effective mass,  $b$  is the effective damping, and  $k$  is the effective stiffness of the system.

## RESULTS AND DISCUSSION

Trunk stiffness increased with trunk flexion angle despite the fact that flexion moment was held constant across all angle conditions. Changes in passive stiffness may have contributed to the increase in dynamic stiffness in flexed postures. Evidence suggests that a fully flexed spine results in a reduced moment arm for the trunk extensor muscles and load redistribution to passive tissues (Kippers and Parker, 1984). If passive tissues play a larger role in load sharing there may be greater passively-induced stiffness in large angles of trunk flexion.

Reflex gain decreased with trunk flexion. It has been demonstrated previously that

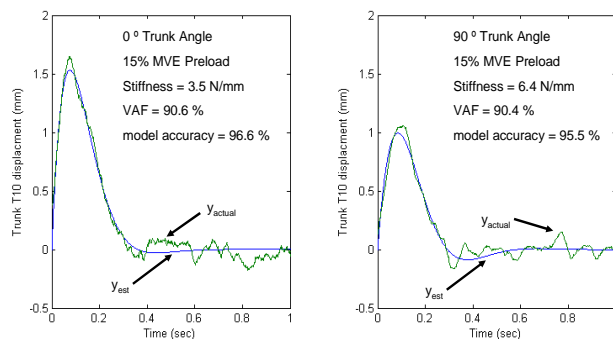


Figure 1. This illustrates the difference in trunk stiffness,  $k$ , due to trunk angle for a subject with the same preload.

paraspinal reflex gain is altered following prolonged static and flexion (Granata, 2005). Mechanoreceptors in passive tissues presumably become desensitized by tissue creep and therefore become unable to initiate reflexive muscular action (Solomonow et al, 1999). Muscle spindle excitability is also altered with repeated and prolonged stretch.

## SUMMARY/CONCLUSIONS

The results of this investigation demonstrate trunk stiffness and paraspinal reflex behavior are affected by trunk posture. Increased trunk stiffness in concert with decreased reflex gain is a possible explanation for high incidence rates of LBP in manual materials handling tasks that involve flexed posture.

## REFERENCES

- Granata, K.P., et al (2005). *Clin Biomech*, **20**, 16-24.  
 Kippers, V., Parker, A.W. (1984). *Spine*, **9**, 740-745.  
 Moorhouse, K.M. (2005). Ph.D dissertation, Virginia Tech.  
 Solomonow, M., et al (1999). *Spine*, **24**, 2426-2434.

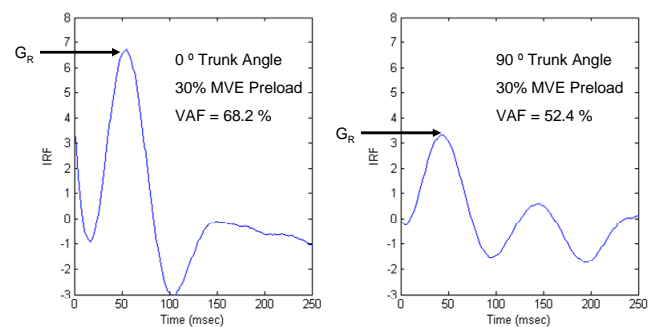


Figure 2. This illustrates the reflex gain,  $G_R$ , due to trunk angle for a subject with the same preload.

# BIOMECHANICAL MEASURES OF MUSCULAR EFFORT: ISOMETRIC MUSCLE ACTIONS

Emmanuel B. John<sup>1</sup>, Wen Liu<sup>1</sup>, and Robert W. Gregory<sup>1,2</sup>

<sup>1</sup>University of Kansas Medical Center, Kansas City, KS, USA

<sup>2</sup>University of Kansas, Lawrence, KS, USA

E-mail: rwg@ku.edu

Web: [www.soe.ku.edu/hses/](http://www.soe.ku.edu/hses/)

## INTRODUCTION

One of the challenges that biomechanists face is to simply and effectively describe the muscular effort expended (or the metabolic cost associated with producing muscle tension) during a wide range of human activities (Andrews, 1983). Although a number of investigators have asked individuals to report the effort they experience while performing different tasks, there has been very little research in which effort ratings have been used to investigate the biomechanics of human movement. Two exceptions are studies by Burgess et al. (1995) and Rosenbaum and Gregory (2002) in which individuals gave effort ratings for isometrically and isotonicity generated torques, respectively.

Given the importance of effort as it relates to the biomechanics of human movement, it is important to develop a method for relating judgments of muscular effort to biomechanical quantities during isometric muscle actions. The first purpose of this study was to develop such a method.

In addition, the establishment of the reliability and validity of a method for relating judgments of muscular effort to biomechanical quantities is critical for its use as an accepted measurement tool. The second purpose of this study was to determine the reliability and validity of the methodology developed in this study for evaluating muscular effort.

## METHODS

Twenty healthy individuals (10 males, 10 females) between 20-40 years of age participated in this study.

After undergoing informed consent procedures, participants were asked to perform isometric elbow flexion/extension joint actions in the horizontal plane using their dominant arm at three different joint angles (45°, 90°, and 135°). The participants were required to produce joint torques that corresponded to effort levels of 1 (very light effort), 3 (light effort), 5 (medium effort), 7 (strong effort), or 9 (very strong effort) on a modified Borg CR-10 scale. Elbow joint torque was measured using a dynamometer (System 3 Pro, Biodex Medical Systems). The 30 conditions (two joint actions × three joint angles × five effort levels) were presented in random order. Participants were asked to return 7-10 days after the initial evaluation to repeat the same procedure.

A within-within subjects factorial ANOVA design was used to assess the effects of joint action, joint angle, and effort level on elbow joint torque. Between-day reliability was determined by calculating an intra-class correlation coefficient for the joint torques obtained during the first and second test sessions for all conditions. Validity was determined by calculating the correlation coefficient between joint torque and the effort level associated with each combination of joint action and joint angle.

## RESULTS AND DISCUSSION

There was a significant increase in joint torque as a function of effort level across all combinations of joint action and joint angle (see Table 1). For each effort level, significantly greater joint torques were produced during elbow flexion than elbow extension. In addition, for both elbow flexion and extension joint actions across all effort levels, there were significantly smaller joint torques produced at the 135° joint angle than those produced at the 45° and 90° joint angles.

The intra-class correlation coefficients for assessing reliability across all conditions ranged between 0.82-0.99. As a general rule, values above 0.90 are considered high and values between 0.80-0.90 are considered moderate for physiological data, while values between 0.70-0.80 are considered acceptable in the behavioral sciences (Vincent, 2005). Therefore, the methodology developed in this study is reliable for assessing muscular effort.

The correlation coefficients used for assessing the relationship between joint torque and effort level across all joint action and joint angle conditions were all at or above 0.90. Values above 0.90 are considered high (Vincent, 2005). Therefore, the methodology developed in this study is valid for assessing muscular effort.

## SUMMARY

The purpose of this study was to develop a methodology that can be used to examine biomechanical measures of muscular effort during isometric muscle actions. The methodology developed in this study is both reliable and valid for this purpose. Based on these findings, it seems reasonable to recommend the method for future research. By determining the relationship between joint torque and muscular effort (the slope of the function relating joint torque to muscular effort), it should be possible to evaluate changes in muscular effort as a function of movement task conditions. This could be a boon for both basic and clinical research.

## REFERENCES

- Andrews, J.G. (1983). *Medicine and Science in Sports and Exercise*, **15**, 199-207.
- Burgess, P.R. et al. (1995). *Somatosensory and Motor Research*, **12**, 343-358.
- Rosenbaum, D.A., Gregory, R.W. (2002). *Experimental Brain Research*, **142**, 365-373.
- Vincent, W.J. (2005). *Statistics in Kinesiology*. Human Kinetics.

## ACKNOWLEDGEMENTS

This investigation was supported by the University of Kansas General Research Fund allocation #2301572.

**Table 1:** Elbow joint torques (Nm; mean ± SD) as a function of joint action, joint angle, and effort level during isometric muscle actions.

Joint Action	Joint Angle	Effort Level				
		1	3	5	7	9
Flexion	45°	6.4±4.0	14.2±10.3	23.4±13.4	30.2±15.0	36.5±15.8
	90°	7.0±4.9	12.5±6.5	20.3±9.3	29.0±14.2	39.5±17.7
	135°	5.4±3.7	9.5±6.2	14.1±7.9	18.8±8.8	27.0±11.3
Extension	45°	4.8±3.7	9.5±6.6	15.3±9.4	18.5±9.2	24.0±12.1
	90°	4.10±2.9	7.9±4.0	13.0±6.6	17.7±7.9	23.3±11.0
	135°	3.1±2.2	6.1±3.8	9.5±5.9	12.7±6.7	17.7±9.4

# KINEMATIC AND KINETIC INDICATORS OF MOVEMENT DURING SIT-TO-STAND IN HEALTHY YOUNG AND OLDER ADULTS

Catherine A. Stevermer and Jason C. Gillette

Iowa State University, Ames, IA, USA  
E-mail: ktsteve@iastate.edu

## INTRODUCTION

Sit-to-stand (STS) is an essential transition for daily activities, which may be challenging for older adults with functional limitations to perform without upper body momentum, upper extremity assistance or external support (Schenkman, et al., 1996). Slow performance of the STS movement is associated with fall risk in older adults (Nevitt, et al., 1989).

Sit-to-stand may be divided into four phases: initiation, ascension, stabilization and termination. To evaluate the duration of STS, it is necessary to determine the point of initiation and termination of movement. In order to compare STS patterns in different populations, normalizing movement curves to a reference of the start of ascension (seat-off) is also essential. There is variation among authors regarding movement indicators for the beginning and ending points of each phase of STS movement (Schenkman, et al. 1996; Mourey, et al. 2000; Gross, et al. 1998).

Depending on laboratory instrumentation, there may also be variation in the available kinematic and kinetic measurements of STS performance. The purpose of this project was to determine which kinematic variables are appropriate to use as movement indicators for the analysis of sit-to-stand in healthy older adults in the absence of seated kinetic measures.

## METHODS

Two young adults ( $35.0 \pm 1.4$  yrs) and two healthy older adults ( $70.5 \pm 2.8$  yrs) participated. An eight-camera system was used to track reflective markers for 3-D kinematic analysis. Subjects were positioned on a bench-mounted force platform at a height of 46.5 cm to measure seated reaction forces. With their feet at a comfortable width on separate force platforms to record ground reaction forces (GRFs), subjects performed sit-to-stand with initial foot placements of 90° of knee flexion, 100° of knee flexion, right-staggered and left-staggered. Subjects performed three trials in each condition. Kinematic variables included marker positions, marker velocities, joint angles and joint angular velocities.

Individual trials were evaluated using MATLAB for thresholds in kinematic variables and kinetic variables as indicators for sit-to-stand movement initiation, seat-off and movement termination (Figure 1). Comparisons were completed between young and older adults in terms of timing variation between movement indicators.

## RESULTS AND DISCUSSION

Based on seated GRFs, trunk angular velocity exhibited a time lag ( $0.04 \pm 0.18$ s) from initiation for all subjects. Hip marker positions showed timing leads with respect to seat-off ( $-0.14 \pm 0.06$ s and  $-0.11 \pm 0.07$ s for horizontal and vertical positions, respectively) for both groups.

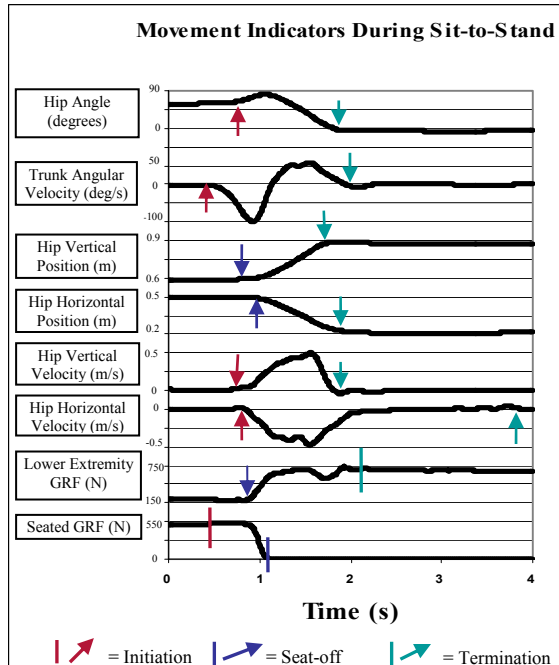


**Figure 1:** Variables analyzed as STS indicators, with GRF reference points (lines). Arrows denote threshold levels.

Movement indicators of STS termination were similar for both groups, although variables demonstrated positive and negative timing shifts (Figure 2). Hip angle was delayed for all subjects ( $0.05 \pm 0.52s$  for younger adults;  $0.11 \pm 0.35s$  for older adults). Hip vertical position showed a timing lead for both groups ( $-0.15 \pm 0.26s$  for older adults;  $-0.25 \pm 0.42s$  for younger adults).

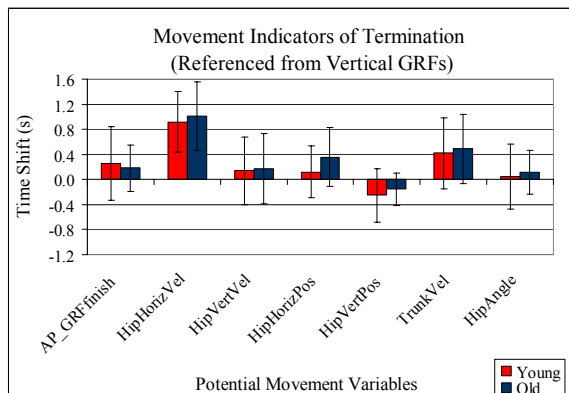


**Figure 2:** Movement variables for STS termination with reference to vertical GRF.

## CONCLUSIONS

It appears that the movement indicators for STS are consistent in both healthy young and older adults. Trunk angular velocity appears to indicate initiation and hip marker positions appear to indicate seat-off for both groups.

Indicators for STS termination may be less consistent due to high variability. In terms of kinematic variables, hip angle and hip vertical position may have the greatest potential as indicators of STS termination due to small time shifts and relatively small standard deviations. Hip marker horizontal velocity may require a higher terminal threshold, as the time lag for this indicator was larger than all other variables. Anterior-posterior GRFs may be a kinetic indicator of termination with similar timing shifts to the kinematic variables.

High variability in the termination indicators may also be representative of an inappropriate reference variable. Vertical GRF from the lower extremities may not be an appropriate determinant of STS termination, due to the oscillations during the stabilization phase of STS. Further research should investigate alternate kinetic and kinematic measures as potential determinants of STS termination.

## REFERENCES

- Gross, M.M. et al. (1998). *Gait and Posture*, **8**, 175-185.
- Mourey, F. et al. (2000). *J. Gerontology*, **55A(9)**, B425-B431.
- Nevitt, M.C. et al. (1989). *J. American Medical Association*, **261(18)**, 2663-2668.
- Schenkman, M. et al. (1996). *J. American Geriatric Society*, **44**, 1441-1446.

# **Familiarization to walking on a split-belt treadmill: kinetics, kinematics and spatio-temporal parameters**

Joseph Zeni and Jill Higginson

Biomechanics and Movement Science Program  
Department of Mechanical Engineering  
University of Delaware, Newark, DE USA  
Email: Jzenijr@udel.edu

## **INTRODUCTION**

The use of a split-belt treadmill with dual force plates provides a convenient means of collecting multiple gait cycles of motion and force data in a small volume. Subjects unfamiliar to walking on a split-belt treadmill may alter their normal gait pattern until they become accustomed to walking on such a treadmill. Previous familiarization studies on a conventional treadmill suggest that trunk kinematics stabilize after 4 minutes of walking at self-selected speed (Taylor et al., 1996) but that healthy young adults require a 10-minute warm-up period before stride length is reproducible (Van de Putte et al., 2006). The purpose of this study was to determine which gait variables are altered when initially walking on the treadmill as well as to examine the changes in these gait variables over a nine minute period of treadmill walking.

## **METHODS**

Nine healthy subjects were recruited to participate in the study (average age 24.1 yrs; range 20-32). Each subject participated in a single session of treadmill walking which lasted for nine minutes. Kinematic and kinetic data were collected from the first thirty seconds of each minute, beginning when the treadmill reached full speed. Walking speed was set at 1.25 or 1.30 m/s to allow for a comfortable walking pace.

Subjects were instructed to walk on the treadmill without using the handrails. They

were asked to walk as they normally would while keeping each foot on a separate belt. None of the subjects had prior experience with walking on a split-belt treadmill.

Force data was collected at 600 Hz via two force plates integrated in the treadmill (Bertec Corp., Worthington OH). Kinematic data was collected at 60 Hz from reflective markers (Helen Hayes set) with a six camera system (Motion Analysis, Santa Ana, CA) and analyzed using Motion Analysis software. Differences between step width, step length variance and ground reaction forces between trials were determined using paired t-tests.

## **RESULTS AND DISCUSSION**

A significant reduction in step width as well as a reduction in the variability of step length was seen as the subjects walked for a longer period of time on the treadmill. No significant changes were seen with step length, vertical ground reaction force, posterior ground reaction force (GRF) or knee flexion at heel strike for each subject throughout the nine minutes.

The reduction in average step width (Fig. 1) was found to be significant ( $p < .01$ ) at the third minute. After five minutes, though, the average step width plateaued and remained constant. The variability of step length (Fig. 2) followed a similar trend, with the variability showing a significant change ( $p < .02$ ) at minute three, but again leveling

off at after that. The average variability of step length increased again at the seventh minute. It is possible that this increase at the end of the session was associated with fatigue. Figure 3 demonstrates the lack of change in kinetic gait variables.

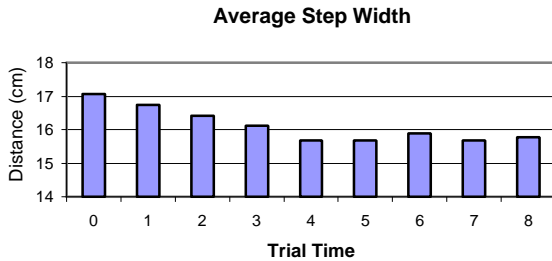


**Figure 1.** Trend of decreasing step width over the first four minute of walking

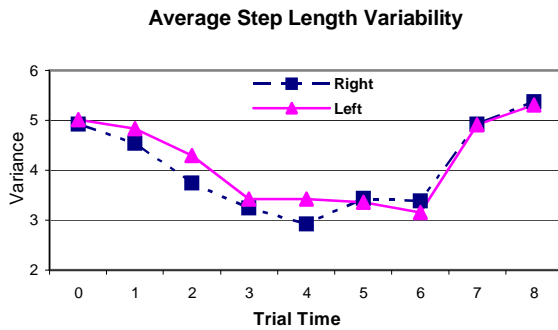


**Figure 2.** Average variability of step length decreasing over the first four minutes.

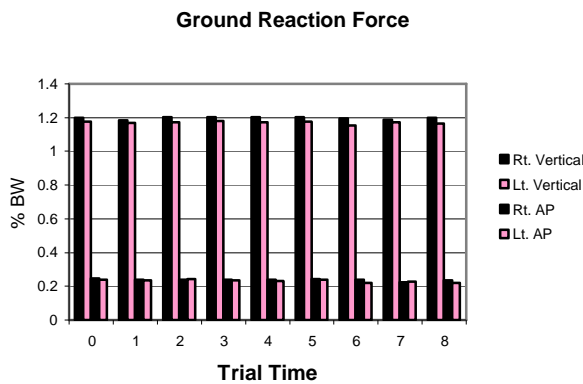


**Figure 3.** Vertical and AP GRF showing no familiarization trend with respect to time.

## SUMMARY

The results of this study suggest that in order to collect accurate data for gait analysis, subjects should be familiarized to the treadmill prior to data collection. The amount of time that should be spent with familiarization to the treadmill is likely subject dependent, but the changes we found in step width and step length variability suggest the time should be at least four to five minutes. The results from this study support the findings of Matsas et al. (2000) who determined that there was no difference between sagittal plane kinematics in overground and treadmill walking after a six minute familiarization period. Even though variability persists throughout the nine minutes, we suspect the variability of step length is similar to what would be seen in overground walking.

Step width is a factor that should be given significant attention when using a split-belt treadmill. It is possible that a subject's initial anxiety of walking on a split-belt treadmill would result in an initial large step width. An elderly or injured population may have increased anxiety about the treadmill and proper precautions should be taken to allow for more accurate data collection. Verbal cues and enough practice time on the treadmill should be incorporated into future studies using a split-belt treadmill.

## REFERENCES

- Matsas et al., *Clin Biomech* 11:46-53, 2000.  
 Taylor et al., *Clin Biomech* 11(8): 484-486, 1996.  
 Van de Putte et al., *Biomed Mat Eng* 16(1): 43-52, 2006.

## ACKNOWLEDGEMENTS

We are grateful for the assistance of Debra George during data collection. This research was funded by NIH P20-RR16458.

# POROELASTIC FINITE ELEMENT ANALYSIS OF UNSTABLE MOTION OF AN INCONGRUOUSLY REDUCED INTRA-ARTICULAR FRACTURE

Curtis M. Goreham-Voss<sup>1</sup>, M. James Rudert<sup>1</sup>, Thomas D. Brown<sup>1</sup>

<sup>1</sup>University of Iowa Orthopaedic Biomechanics Research Laboratory.  
E-mail: curtis-voss@uiowa.edu

## INTRODUCTION

One of the goals of intraarticular fracture repair is the prevention of post-traumatic arthritis by avoiding mechanical environments that increase the stresses in cartilage. A previous cadaver study has shown that contact pressures in the ankle increase significantly under quasi-physiological loading in the presence of an articular incongruity (step-off) (McKinley, 2006). Of particular interest from that study are results in which the talus subluxated from the beneath the tibia in an unstable motion. This study investigates the biphasic response of cartilage to such transient loading. Contact stress transients from the cadaver study are applied to a poroelastic finite element model to investigate the influence of an unstable motion on the stress distribution throughout the cartilage depth.

## METHODS

A sagittal cross-section of a portion of tibial cartilage was modeled as a two-dimensional, plane-strain layer as shown in Figure 1.

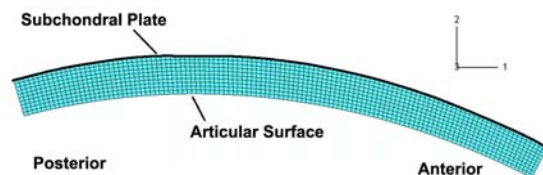


**Figure 1:** Tibial cartilage represented by a plane-strain layer.

A transversely-isotropic, poroelastic material model was developed for this study using the ABAQUS finite element software

(ABAQUS, Inc., Providence, RI). Material properties were derived from various published mechanical tests of articular cartilage. The permeability used was  $1.14 \times 10^{-15} \text{ m}^4/(\text{N}\cdot\text{s})$  (Athanasίου, 2005). The transverse (1-3) plane is the plane of isotropy. The transverse and out-of-plane moduli of elasticity were 33 MPa and 0.55 MPa, respectively (Boschetti, 2004; Charlebois, 2004). The Poisson's ratio characterizing the transverse response to a transverse load was 0.146 (Federico, 2005) and the Poisson's ratio characterizing the transverse response to an out-of-plane load was 0.074 (Athanasίου, 2005). Values for the out-of-plane shear modulus ( $G_{12}$ ) range from 0.5 to 4 MPa in literature (Oakley, 2004). However, Oakley's values are measured in the superficial or middle zones while the dominant shearing action in the present study occurs at the cartilage subchondral plate interface. Since the deep layer of cartilage generally has a compressive stiffness about twice that of the superficial layer, a shear modulus of 10 MPa was used for this analysis. The remaining material properties were determined according to the relationships governing transversely isotropic material. The material model was validated for the case of cylindrical plugs in axial compression.

For this analysis, the cartilage was considered fixed to a rigid subchondral plate. The step-offs were created by translating the anterior third of the cartilage proximally. Transient contact pressures were obtained from the McKinley study (McKinley, 2006) and applied on the

articular surface in the form of time-varying distributed surface loads. The contact pressures used were taken from four combinations of geometry and motion: (1) Intact cartilage with stable motion, (2) Fragmented, anatomically reduced cartilage with stable motion, (3) 2mm step-off with nearly unstable (metastable) motion, (4) 2mm step-off with unstable motion. Figure 2 shows the loading profile for the fourth case.

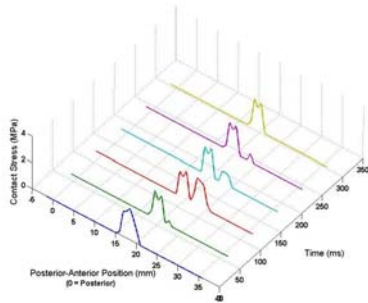


**Figure 2:** Time-varying loading profile for unstable motion.

## RESULTS AND DISCUSSION

Stress distributions from stable and unstable motion are shown in Figure 3. The unstable motion results in higher stress and more severe, transient stress conditions.

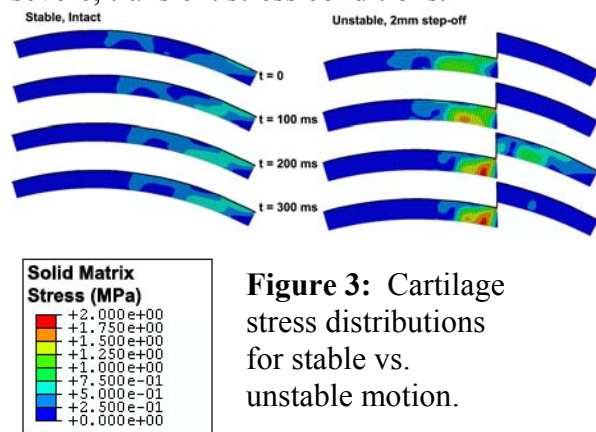


**Figure 3:** Cartilage stress distributions for stable vs. unstable motion.

The maximum stress transients in the cartilage solid matrix are shown in Figure 4. The fully unstable model has maximum transients 4-5 times higher than the maximum stress transients in any other simulations.

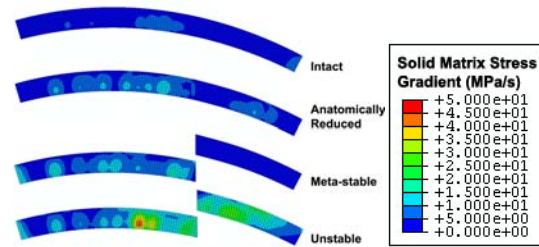


**Figure 4:** Maximum cartilage stress transients for varying loading conditions.

## SUMMARY/CONCLUSIONS

Unstable ankle motion appears to have a severe effect on the cartilage stress transients throughout the cartilage depth. Such a transient “shuck” situation strongly pre-disposes a joint to post-traumatic osteoarthritis, for reasons presently not well-understood. This formulation provides a vehicle by means of which temporal and spatial anomalies of cartilage stress can be quantified for the situation of joint instability due to a surface incongruity.

## REFERENCES

- McKinley et al. (2006). *J Biomech*, **39**(4), 647-626.
- Boschetti et al. (2004). *Biorheology*, **41**(3-4), 159-166.
- Charlebois et al. (2004). *J Biomech Eng*, **126**(2), 129-137.
- Federico et al. (2005). *J Biomech*, **38**(10), 2008-2018.
- Athanasίου et al. (1991). *J Orthop Res*, **9**(3), 330-340.
- Oakley et al. (2004). *Osteoarthritis Cart*, **12**(8), 667-679.

## ACKNOWLEDGEMENTS

Supported by grants from the NIH (AR47653), the CDC (R49CCR, 721745) and an NSF fellowship (CMGV). Drs. Y. Tochigi, D.R. Pedersen, D.D. Anderson and T.O. McKinley provided assistance/advice.

# AUGMENTING PLANTARFLEXION POWER: EFFECTS ON PREFERRED WALKING SPEED & METABOLIC COST OF TRANSPORT

James Norris<sup>1</sup>, Melanie Mitros<sup>2</sup>, Erica Byrne<sup>2</sup>, Anthony Marsh<sup>2</sup> and Kevin Granata<sup>1</sup>

<sup>1</sup> Virginia Tech, Blacksburg, VA, USA

<sup>2</sup> Wake Forest University, Winston-Salem, NC, USA

E-mail: granata@vt.edu Web: www.biomechanics.esm.vt.edu

## INTRODUCTION

We recently developed a pair of powered ankle-foot orthoses (PAFOs) based closely on the design by Ferris, *et al.* (2005). We are focusing on the ankle because during push-off the ankle plantarflexor muscles are the single most important source of positive muscle work (Meinders *et al.*, 1998). Furthermore, for a given gait speed, the power generated by these muscles is smaller for an aging compared to a young healthy population (DeVita and Hortobagyi, 2000). Others have suggested impaired lower extremity muscle power is associated with poor physical function and peak power is predictive of disability in older adults.

Our long-term goal is to use PAFOs to systematically control power at the ankle joint. This research will contribute to understanding how ankle power is related to physical function in the elderly. In this study, we present a control algorithm to augment push-off power using PAFOs, and the effect of augmenting power on preferred walking speed and metabolic cost of transport in young adults.

## METHODS

**PAFO construction.** We built a pair of ankle-foot orthoses for a subject representative of our target population. The orthoses were made of 3/16<sup>th</sup>-inch polypropylene and fitted with aluminum attachment brackets (Figure 1). The polypropylene was stretched over a

removable foam liner to accommodate different subjects. Foot and shank angular velocities were measured with MEMS gyroscopes, and pneumatic muscle force was measured using a load cell.

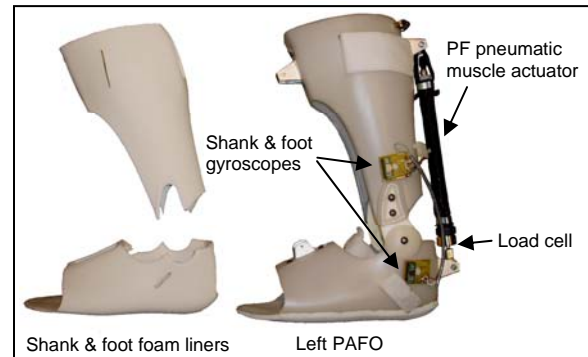


**Figure 1:** The left PAFO brace and removable foot and shank foam liners.

**Control algorithm.** We designed a simple algorithm to actuate the pneumatic muscles to add power during push-off. First, foot-flat on the ground was detected if the absolute value of the foot angular velocity had been below 20 deg/s for 100 ms. After foot-flat was determined, the algorithm detected when the heel began to lift off the ground. The control signal was turned on after a fixed time delay (60 ms) following heel lifting such that the pneumatic muscle contracted, creating a plantarflexion moment, during push-off. During push-off, the pneumatic muscle acted concentrically, i.e., it was actively shortening. The control signal was turned off after 200 ms, to ensure it had emptied by toe-off.

**Overground data.** Two young adults (21 & 23 years) completed overground walking trials. For warm-up, subjects walked a minimum of five minutes on a treadmill for two PAFO conditions: inactive and active. A short break followed while 22 reflective markers were placed on their bodies in the Helen Hayes configuration. The remainder of the experiment was completed on the overground walkway. Subjects were instructed to “walk at a comfortable pace.” Kinematic data were recorded at 60 Hz using a 6-camera Motion Analysis system. Kinetic data were recorded at 500 Hz with a 6-channel AMTI force plate. We recorded data until subjects completed three right-foot force plate contacts for each condition.

**Treadmill data.** Nine young adults ( $23.3 \pm 1.6$  years) completed treadmill trials to determine preferred walking speed for the two PAFO conditions: inactive and active. Subjects returned for a second session to measure metabolic cost of transport (MCOT). MCOT is the steady-state rate of oxygen consumption, i.e.  $\text{VO}_2$ , divided by walking speed.

The Wake Forest University Institutional Review Board approved this investigation and all subjects gave their informed consent.

## RESULTS AND DISCUSSION

**Overground.** Each subject’s kinematic and kinetic data were averaged for their inactive and active trials. Table 1 summarizes the walking speed and peak ankle power, calculated from inverse dynamics. The walking speed results suggest that the additional PF moment provided by the active PAFOs resulted in an increase in overground walking speed. Additional power provided by the PAFOs increased net ankle power from  $2.45 \pm 0.2$  to  $3.35 \pm 0.6$  W/kg.

**Table 1:** Overground walking speed and peak ankle power.

Measure	ID	Inactive	Active
		(avg $\pm$ SD)	(avg $\pm$ SD)
Walking speed (m/s)	Y1	$1.28 \pm 0.04$	$1.42 \pm 0.04$
	Y2	$1.23 \pm 0.01$	$1.30 \pm 0.03$
Peak Net Ankle Power (W/kg)	Y1	$2.7 \pm 0.2$	$3.5 \pm 0.8$
	Y2	$2.2 \pm 0.2$	$3.2 \pm 0.1$

**Treadmill.** The treadmill preferred walking speed results agreed with the observed increase in overground walking speed. The augmented power resulted in subjects increasing preferred walking speed by  $0.08 \pm 0.09$  m/s (Table 2). Additionally, walking in the active PAFOs reduced MCOT by  $0.03 \pm 0.02$  ml  $\text{O}_2$ /kg/m.

**Table 2:** Treadmill preferred walking speed and MCOT. *p*-values are for within subject changes.

	Inactive	Active	<i>p</i>
Walking speed (m/s)	$1.18 \pm 0.16$	$1.25 \pm 0.16$	0.031
MCOT (mL $\text{O}_2$ /kg/m)	$0.19 \pm 0.02$	$0.16 \pm 0.02$	0.009

## SUMMARY

In summary, we used a pair of PAFOs to increase plantarflexion push-off power and showed young adults increased their preferred walking speed with augmented power. This research will be useful for addressing how plantarflexor power influences physical function in older adults.

## REFERENCES

- DeVita, P. and Hortobagyi, T. (2000). *J. Appl. Physiol.*, **88**, 1804-1811.  
 Ferris, D.P., et al. (2005). *J. Appl. Biomech.*, **21**, 189-197.  
 Meinders, M., et al. (1998). *Scand. J. Rehabil. Med.*, **30**, 39-46.

## ACKNOWLEDGEMENTS

We would like to thank Dan Ferris for his guidance, Jovita Jolla for assistance with gait analysis, and BioTech Prosthetics.

# GRIZZLY BEARS MAINTAIN CORTICAL AND TRABECULAR BONE MINERAL, STRUCTURAL, AND MECHANICAL PROPERTIES DURING DISUSE (HIBERNATION)

Meghan E. McGee<sup>1</sup>, Aaron J. Maki<sup>1</sup>, Alesha B. Castillo<sup>2</sup>, O. Lynne Nelson<sup>3</sup>, Charles T. Robbins<sup>3</sup>, Seth W. Donahue<sup>1</sup>

<sup>1</sup>Michigan Technological University, Houghton, MI, USA

<sup>2</sup>Indiana University School of Medicine, Indianapolis, IN, USA

<sup>3</sup>Washington State University, Pullman, WA, USA

E-mail: swdonahu@mtu.edu

## INTRODUCTION

Disuse causes unbalanced bone remodeling which leads to bone loss and reduced bone strength. The remobilization time required to completely recover lost bone is typically 2-3 times longer than the unloading period (Weinreb et al., 1997). However, bears from northern climates experience annual periods of disuse (hibernation) and remobilization that are approximately equal in length, yet they do not lose cortical bone material properties with age (Harvey et al., 2005). Furthermore, trabecular architecture and mineral content are not different in bears before and 2 weeks after hibernation (Pardy et al., 2004). It is not known whether bears completely prevent bone loss during hibernation, or if bone is lost and recovered at a faster rate than most animals. Thus, we investigated bone properties in hibernating and active grizzly bears to determine if bone loss occurs during hibernation.

## METHODS

Six age-matched grizzly bears were used for this study; four bears were 1 year old, and two bears were 18 years old. All handling and treatment procedures were approved by the Washington State University Institutional Animal Care and Use Committee. At the time of death, three bears had hibernated for 17-18 weeks and the others had been active following hibernation for at least 14 weeks. One

femur from each bear was histologically prepared with basic fuchsin, and porosity (**Por, %**) was quantified from a cortical section distal to midshaft using semi-automated image analysis software (Bioquant OSTEO, Nashville, TN) (n=6).

The contralateral femur (if available) was loaded to failure in three-point bending (n=5). After fracture, cross-sectional properties at midshaft including cross-sectional area (**CSA, mm<sup>2</sup>**), section modulus (**SM, mm<sup>3</sup>**), and maximum moment of inertia (**I<sub>max</sub>, mm<sup>4</sup>**) were measured using Scion Image (Scion Corporation, Frederick, MD). Mechanical properties including ultimate stress (**σ<sub>U</sub>, MPa**), modulus of toughness (**u, J/mm<sup>3</sup>**), and energy to failure (**U, J**) were calculated with beam bending theory. Mineral content (**ash frac.**) was quantified by ashing a diaphyseal section proximal to midshaft (n=6).

Trabecular cores (7.6 mm diameter) were removed from the distal femoral metaphysis and epiphysis (n=6 for each site).

Trabecular bone architecture was evaluated using a fan-beam microCT system (μCT40, Scanco Medical AG, Basserdorf, Switzerland). The central region (~1.2 mm) of each core was scanned at 6-9 μm isotropic voxel size and evaluated for morphometric parameters. Bone volume fraction (**BV/TV, %**), trabecular number

(**Tb.N**,  $\text{mm}^{-1}$ ), trabecular thickness (**Tb.Th**, **mm**), trabecular separation (**Tb.Sp**, **mm**), structure model index (**SMI**), degree of anisotropy (**DA**), and tissue mineral density (**M.Dn**,  $\text{mgHA}/\text{cm}^3$ ) were computed.

## RESULTS

Cortical porosity was lower in the hibernating bears ( $p = .003$ ). No differences were detected between the ash fraction, cross-sectional, or mechanical properties of hibernating and active bears (Table 1).

**Table 1: Cortical bone properties**

<i>Property</i>	<i>Active</i>	<i>Hib.</i>	<i>p-value</i>
Por	7.5	5.3	.003
CSA	389	458	.855
SM	2.2 E3	2.0 E3	.935
$I_{\max}$	4.3 E4	5.3 E4	.873
$\sigma_U$	185	214	.308
u	7.0	5.6	.623
U	47.1	57.0	.827
ash frac.	.664	.675	.407

There were no differences between the trabecular properties of hibernating and active bears (Table 2, Figure 1).

**Table 2: Trabecular bone properties**

<i>Property</i>	<i>Active</i>	<i>Hib.</i>	<i>p-value</i>
BV/TV	15.8	14.2	.750
Tb.N	2.79	2.21	.440
Tb.Th	0.101	0.109	.611
Tb.Sp	0.414	0.472	.649
SMI	2.03	2.19	.542
DA	1.42	1.49	.388
M.Dn	1005	1056	.562

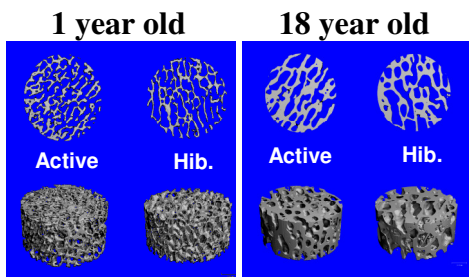


**Figure 1: Representative microCT scans**

## DISCUSSION

Disuse causes unbalanced bone remodeling in most animals, leading to increased cortical porosity, decreased trabecular architecture, loss of mineral, and reduced mechanical properties. However, hibernating grizzly bear femurs were less porous than in active bears. Additionally, the structural and mineral properties of hibernating grizzly bear femurs were not significantly different from active bears. Our findings suggest that grizzly bears do not experience a temporary loss of cortical or trabecular bone during hibernation, possibly because bears maintain balanced bone remodeling during hibernation (Donahue et al., 2006). Serum parathyroid hormone concentrations are positively correlated with serum concentrations of the bone formation marker osteocalcin in hibernating bears (Donahue et al., 2006). Thus, bone formation may be maintained by the anabolic influence of endogenous parathyroid hormone. Further research on the biological mechanism by which bears maintain bone integrity during disuse (e.g., targeting hormones that are differentially expressed between humans and bears during disuse) may provide insight regarding pharmaceutical treatments for human osteoporoses.

## REFERENCES

- Donahue, S.W. et al. (2006). *Transactions of ORS*, **31**, 93.
- Harvey, K.B. et al. (2005). *J Biomech*, **38**, 2143-50.
- Pardy, C.K. et al. (2004). *J Zool Lond*, **263**, 359-64
- Weinreb, M. et al. (1997). *Virchows Arch*, **431**, 449-52.

## ACKNOWLEDGEMENTS

Funding from NIH (NIAMS AR050420), NSF GRFP, and Timothy Floyd, M.D.

# COMPARISON OF LOWER EXTREMITY SAGITTAL PLANE KINEMATICS DURING OVERGROUND GAIT, TREADMILL WALKING, AND ELLIPTICAL TRAINING

Thad W. Buster<sup>1</sup>, Lori M. Ginoza<sup>1,2</sup>, and Judith M. Burnfield<sup>1,2</sup>

<sup>1</sup> Madonna Rehabilitation Hospital, Movement Sciences Center, Lincoln, NE, USA

<sup>2</sup> University of Southern California, Los Angeles, CA, USA

E-mail: jburnfield@madonna.org

## INTRODUCTION

Regaining walking function is frequently a goal in the rehabilitation setting, with therapy sessions often focusing on gait either overground (OG) or on a treadmill (TM). Expansion of commercial fitness equipment into the rehabilitation environment has created opportunities for refining gait mechanics on alternative devices. The elliptical trainer (EL) has been marketed as a piece of equipment that promotes a movement pattern simulating walking. To date, however, the extent to which elliptical training movements emulate the normal motion demands of OG and TM walking has not been systematically explored. The purpose of this study was to compare lower extremity sagittal plane kinematic patterns during overground gait, treadmill walking, and elliptical training activities in young healthy adults.

## METHODS

Seven individuals (19-31 years of age; 3 male, 4 female) with no known musculoskeletal or neurological disorders participated in a multi-session study. During the first three sessions, subjects exercised on a treadmill (Life Fitness™ 97Ti) and Elliptical Cross-Trainer (Life Fitness™ 95Xi) for familiarization purposes. During the fourth session, dominant limb lower extremity kinematics (Motion Analysis) and stride characteristics (B&L Engineering) were recorded as subjects ambulated OG

across a 10m walkway at a self-selected speed, walked on a TM at a speed matched to the self-selected OG pace, and exercised on the EL at a speed approximating ( $\pm 5\%$ ) that obtained during OG walking. The TM and EL activities were performed for three minutes in a randomized order and data were recorded during the final minute. Footswitch (OG and TM) and footplate data (EL) were used to define gait cycle phasing. For each activity, peak angles associated with critical events during gait at the ankle, knee, and hip were identified (Perry, 1992). Separate one-way analyses of variance with repeated measures determined if the critical event angles varied significantly across the three conditions at each joint. A Bonferroni adjusted alpha level of  $P < 0.0125$  assessed significance.

## RESULTS AND DISCUSSION (Table 1)

Consistent with the study design, the average speed at which the tasks were performed varied only minimally (OG = 79 m/min; TM = 82 m/min; EL = 82 m/min).

**Ankle (Figure 1A):** During EL training, trends towards reduced plantar flexion during Loading Response ( $P = 0.047$ ) and increased dorsiflexion during Terminal Stance ( $P = 0.031$ ) compared to the other two walking tasks were recorded. In Mid Swing, dorsiflexion was significantly greater during EL training compared to both OG ( $P < 0.001$ ) and TM walking ( $P < 0.001$ ).

**Knee (Figure 1B):** At Initial Contact, the knee was significantly more flexed during EL training compared to both OG ( $P < 0.001$ ) and TM walking ( $P < 0.001$ ). During Loading Response, the knee remained in significantly greater knee flexion during EL training compared to OG ( $P = 0.002$ ) and TM walking ( $P = 0.008$ ). In Terminal Stance, a trend towards significantly greater knee flexion during EL training was identified ( $P = 0.046$ ).

**Hip (Figure 1C):** At Initial Contact, significantly greater hip flexion was registered during EL training compared to OG ( $P = 0.001$ ) or TM walking ( $P = 0.003$ ). Hip flexion was also greater during TM compared to OG walking ( $P = 0.003$ ). Terminal Stance hip extension was significantly reduced during EL training compared to OG ( $P < 0.001$ ) and TM walking ( $P < 0.001$ ). During Mid Swing, hip flexion was significantly greater during EL

training compared to OG ( $P < 0.001$ ) and TM walking ( $P < 0.001$ ).

## SUMMARY/CONCLUSIONS

During EL training, there were notable differences in ankle, knee and hip critical event positions compared to OG and TM walking, with subjects generally postured in greater flexion during EL training. The impact of these kinematic differences on the muscular demands associated with EL training requires further study.

## REFERENCES

Perry, J. (1992). *Gait Analysis: Normal and Pathological Function*. Slack, Inc.

## ACKNOWLEDGEMENTS

Daniels Fund, Denver, CO

**Table 1.** Peak joint angles (degrees) associated with the critical events of the gait cycle for overground walking, treadmill walking, and elliptical training.

Joint	Phase	Overground degrees (SD)	Treadmill degrees (SD)	Elliptical degrees (SD)	Main Effect P-Value
Ankle	IC	1 DF (2.8)	1 DF (2.9)	1 PF (5.6)	0.357
	PF LR	7 PF (4.0)	6 PF (3.5)	1 PF (5.5)	0.047
	DF TSt	14 DF (2.9)	15 DF (2.6)	20 DF (5.8)	0.031
	DF MSw	2 DF(1.6)	2 DF(1.6)	19 DF (4.8)	< 0.001
Knee	IC	4 Ext (4.1)	3 Ext (4.5)	32 Flex (4.3)	< 0.001
	Flex LR	11 Flex (10.5)	15 Flex (12.6)	32 Flex (4.3)	< 0.001
	Ext TSt	1 Ext (4.0)	1 Flex (2.9)	26 Flex (29.2)	0.046
	Flex ISw	66 Flex (2.5)	66 Flex (1.9)	70 Flex (5.0)	0.131
Hip	IC	31 Flex (4.4)	33 Flex (4.9)	42 Flex (5.4)	0.002
	Ext TSt	10 Ext (3.4)	9 Ext (3.8)	4 Flex (5.7)	< 0.001
	Flex MSw	34 Flex (3.9)	35 Flex (4.4)	51 Flex (5.5)	< 0.001

**Key:** IC=Initial Contact; LR = Loading Response; TSt = Terminal Stance; ISw = Initial Swing; MSw = Mid Swing; PF = Plantar Flexion; DF = Dorsiflexion; Flex = Flexion; Ext = Extension.

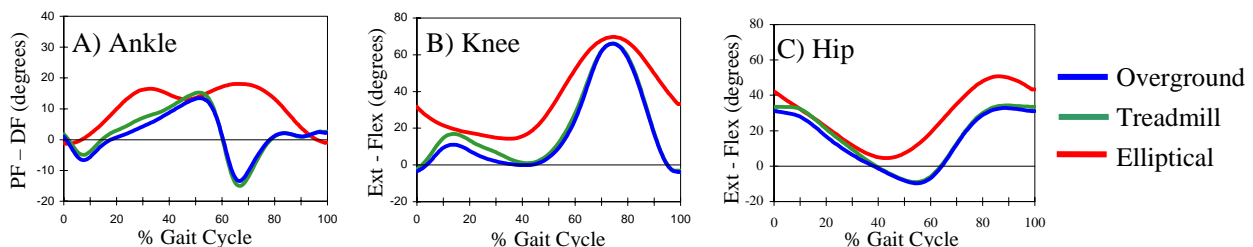


**Figure 1.** Ankle (A), Knee (B), and Hip (C) sagittal plane kinematics during Overground (blue), Treadmill (green) and Elliptical (red) training.

# DEVELOPMENT OF FATIGUE TESTING PROTOCOL AND IMAGE BASED ANALYSIS OF SMALL FRAGMENT CORTICAL BONE SCREWS

Suneel Battula MS <sup>1</sup>, Emily M.Njus <sup>2</sup>, John Konicek <sup>1</sup> and Glen O. Njus PhD <sup>1</sup>

<sup>1</sup> Department of Biomedical Engineering, The University of Akron, Akron, OH, USA

<sup>2</sup> Department Biology, The University of Akron, Akron, OH, USA

E-mail: bsuneel@uakron.edu

## INTRODUCTION

Self-tapping cortical bone screws (STS) have been used as effective tools for osteosynthesis but there have only been a few studies comparing the biomechanical and fatigue properties of these screws. Fatigue characteristics of small fragment screws haven't been extensively studied as they involve time and resource intensive testing. But fatigue is an important characteristic as the implants are subjected to cyclic loading. Fatigue is the result of cumulative process consisting of crack initiation, propagation and finally fracture of the component/construct. During cyclic loading localized plastic deformation may occur at the highest stress site. This plastic deformation induces permanent damage to the component and a crack may develop. As the component experiences an increased number of loading cycles, the length of the crack increases and after a certain number of cycles, the crack will cause the component/construct to fail. Hence arises a need for failure analysis of the whole construct and the each component by itself.

The purpose of this study is to design an efficient testing protocol and use image analysis as a tool for fatigue analysis of small fragment screws. The main objectives of this study are to determine the effect of the screw design parameters and geometry on the fatigue characteristics and to analyze

the effect of the screw material on fatigue properties for screws with similar design.

## METHODS

The fatigue life analysis of 4 different types of screws was conducted using a fatigue-tester designed according to the American Society of Testing and Material (ASTM) standards. The tested screws were all 3.5mm cortical screws (specifications given in Table 1) and included both stainless steel and titanium screws.

**Table 1.** Significant measurements of the screws from the four vendors.

	OD (mm)	ID (mm)	Pitch (mm)	Head Dia (mm)	OD/ID
V1	3.51	2.64	0.78	6.32	1.33
V2	3.53	2.21	1.30	4.60	1.59
V3	3.48	2.39	1.28	5.92	1.46
V4	3.48	2.39	1.28	5.92	1.46

Thirty-two screws were categorized into two test groups (sixteen per group), one group was used to determine the fatigue characteristics based on screw design and the other group was tested to analyze the effect of material on the fatigue life. The screws were tested in cantilever bending mode using the fatigue tester on an Instron 8511 (Canton, MA), material testing system. The testing was performed under load-control mode with an R-ratio of 0.1 with appropriate safety limits for load and

displacement. The tested specimens were then analyzed using microscopic images.

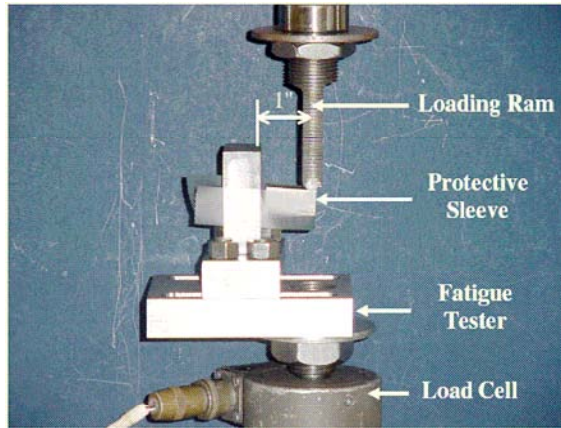


**Figure 1:** Experimental Set-up

## RESULTS AND DISCUSSION

All the tests ended in failure with a broken screw specimen. The fatigue lives of the screws from vendors V1 and V4 (SS) were longer than the screws from vendors V2 and V3 respectively. The screws with lower OD/ID ratio had longer lives than those with higher OD/ID ratio demonstrating that the core (minor) diameter is a principal factor determining the fatigue life.

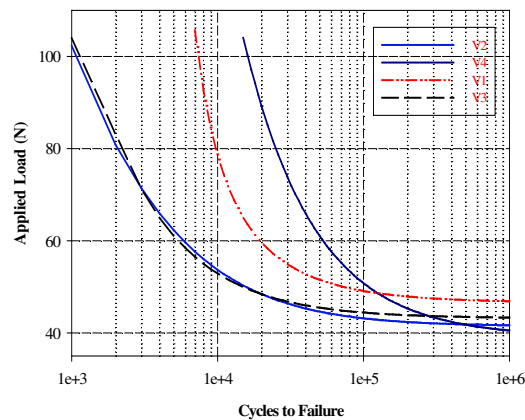


**Figure 2:** S-N Curves illustrating the fatigue life in number of cycles for applied loads.

The results also show that the screws with finer threads (lower pitch) have longer fatigue life. Stainless steel screws had a longer fatigue life than the titanium screws with similar screw geometry demonstrating

the effect of the material properties on the fatigue life.

The image analysis yielded a stable propagation area of 49% for V1 as compared to 44% of V2 and 42% for V4 as compared to 37% of V3. The correlation values between the applied load and stable propagation area weren't very high. Testing of more samples might yield a higher correlation that might aid in the analysis of the failed samples retrieved from the patients.

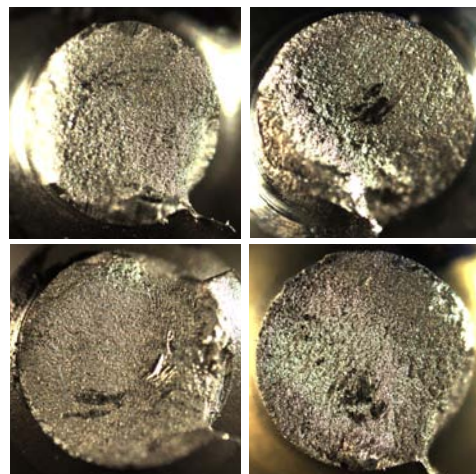


**Figure 3:** Fracture surfaces of the screws after their failure. (a) V2 (b) V4 (c) V1 & (d) V3.

## SUMMARY/CONCLUSIONS

The analysis supports OD-to-ID ratio as the principal factor determining fatigue life as results paralleled implant geometry. But a design modification to improve bending and fatigue strength based on a decreased OD/ID ratio (and decreased pitch) might affect the pullout strength. It was also observed that stainless steel screws had better fatigue characteristics (more cycles to failure) than pure titanium screws in spite of similar geometric designs

## REFERENCES

Merk. B, Stern. S, et al. (2001). *Journal of Orthopaedic Trauma*, 494-99.

# Study of Finger Movement for Normal Gripping and Pinching Using a Quasi-Static Model

Jaewon Choi, R. Brent Gillespie and Thomas J. Armstrong

University of Michigan, Ann Arbor, MI, USA  
E-mail: jaewonc@umich.edu

## INTRODUCTION

Dynamic models have been developed by many investigators [1-3] that explain free finger movements. Most of the models were based on dynamic equations of multi-body system including inertial effects. Some of the models included passive moments at each joint by considering the passive properties of tissues such as muscles and ligaments. Passive moments are caused by cartilage, ligaments, joint capsules and inactive muscle-tendon units. Kamper measured static passive moments, joint damping and stiffness for varying joint angles[4]. These measurements can be used for predicting passive torques in free finger movement.

The purpose of this study is to apply quasi-static model to various work situations. In the quasi-static model, the inertia effect was neglected because the finger has small inertia at normal finger velocities. Grasping movements and pinching movements for differently sized objects were analyzed using the model.

## METHODS

### *Quasi-static model development*

Index finger was modeled using the passive characteristics measured by Kamper[4]. Other terms representing inertia, centrifugal, coriolis and gravity effects were assumed to be negligible in normal speed movement. The equations could be formed for each joint as the following equation.

$$-\tau_{static}(\theta_i) + B_i \dot{\theta}_i + K_i(\theta_i) = \tau_i \quad i=1,2,3 \quad (1)$$

where,  $\tau$  is the torque,  $\tau_{static}$  is the static passive torque,  $B$  is the damping constant,  $K$  is the elastic coefficient (function of  $\theta$ ) and  $\theta$  is the joint angle.

EDC (extensor digitorum communis), FDP (flexor digitorum profundus), FDS (flexor digitorum superficialis), interosseus(palmer and

dorsal), lumbricalis muscles were included in the model. Muscle force-joint torque matrix was made using tendon excursion and moment arms from Armstrong[5] and Buchner[2]. Kinematic constraints followed Buchner's model. To find feasible solutions, the criterion that maximized the endurance was chosen. The MATLAB system and its optimization toolbox was used to implement the model.

### *Experiment*

Two healthy subjects participated the experiment. Markers were secured on dorsal side of index finger and wrist joint. OptoTrak® Certus™ motion tracking system (Northern Digital Inc.) was used to acquire the motion data. Surface EMGs were attached to measure EDC, FDP and FDS muscle activities. Subject was asked to grasp three differently sized objects (diameters: 38 mm, 51 mm, 76 mm) in normal speed using light grip. Subject was also told to pinch the object. A sample plot of DIP (distal interphalangeal), PIP (proximal interphalangeal) and MCP (metacarpophalangeal) joint angles is shown for a subject whose hand started from relaxed to gripping a cylindrical object of 38 mm diameter (figure 1). The acquired data were filtered with 5 Hz low-pass filter, which is reasonable cut-off frequency in human movement. The MATLAB system was used to analyze the data.

## RESULTS AND DISCUSSION

The quasi-static model was compared with dynamic model developed by Buchner. For the given free movement, the quasi-static model estimated larger joint torques than dynamic model, especially in DIP joint. For the movement shown in figure 1 (a), the ratio of peak joint torques by the quasi-static model and the dynamic model was 2.01 for MCP joint, 6.93 for PIP joint and 63.02 for DIP joint.

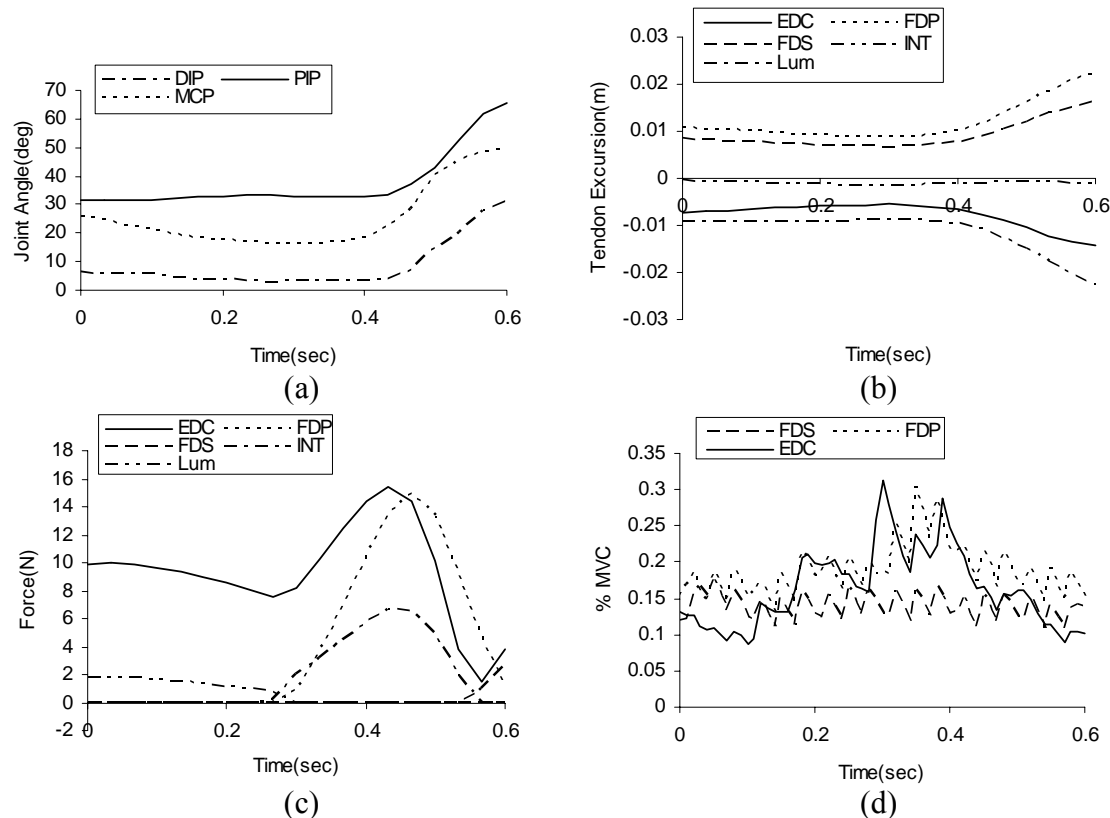


Figure 1 Example of free movement ( pinch) (a) joint angle profile (b) tendon excursion (c) predicted muscle forces (d) % MVC measured by EMG

This resulted from the fact that the finger mass is small and movement speed was not fast. The passive element of the muscle was not modeled because passive element was already included in the quasi-static model by lumped measurement.

Figure 1 showed tendon excursion, predicted muscle forces and EMG measurement for one sample movement. Muscle force patterns were similar to EMG observation. In the extension period, EDC muscle force was largest, while FDP and FDS muscles were not activated. In the flexion motion, FDP and EDC muscle forces increased. This result showed good agreement with other EMG studies[6,7] that observed EDC muscle activation during flexion movement.

Even though large amount of differences in joint torques were estimated between the quasi-static model and the dynamic model, it should be noted that the joint torques in forceful exertion are much larger than the joint torques in free movement. Our pilot study of measuring index finger strength indicated that the joint torques were up to 6.04 Nm in MCP joint, 2.84 Nm in

PIP joint and 0.99 Nm in DIP joint which are 3.67 to 50 times of joint torques in free movement.

## SUMMARY/CONCLUSIONS

The quasi-static model gave a reasonable prediction of muscle forces during free movement of normal tasks. The analysis of grasping and pinching movement for differently sized object will follow.

## REFERENCES

- [1] Sancho-Bru, J.L. et al. (2001) *J. Biomechanics*, 34, 1491-1500
- [2] Buchner, H.J. et al. (1988) *J. biomechanics*, 21(6), 459-468
- [3] Esteki, A. et al. (1997) *Annals of Biomedical Engineering*, 25, 440-451
- [4] Kamper, D.G. et al. (2002) *J. Biomechanics*, 35, 1581-1589
- [5] Armstrong, T.J. et al. (1978) *J. Biomechanics*, 11, 119-128
- [6] Long, C. et al. (1964) *J. Bone Jt Surg.*, 46, 728-733
- [7] Darling, W.G. et al. (1994) *J. Biomechanics*, 27(4), 479-491

# **BIOMECHANICAL MEASURES OF MUSCULAR EFFORT: ISOKINETIC MUSCLE ACTIONS**

Patrick G. Moodie, Zachary D. Schluender, and Robert W. Gregory

University of Kansas, Lawrence, KS, USA

E-mail: [rwg@ku.edu](mailto:rwg@ku.edu)

Web: [www.soe.ku.edu/hses/](http://www.soe.ku.edu/hses/)

## **INTRODUCTION**

The musculoskeletal system is the physiological entity that allows us to move within our environment. The voluntary muscles drive the system's kinematic behavior. Therefore, a thorough understanding of how these muscles behave is of great importance in analyzing the performance of the musculoskeletal system. Because of this, it is essential to effectively describe the muscular effort expended (or the metabolic cost associated with producing muscle tension) during a wide range of human activities (Andrews, 1983).

Although a number of investigators have asked individuals to report the effort they experience while performing different tasks, there has been very little research in which effort ratings have been used to investigate the biomechanics of human movement. Two exceptions are studies by Burgess et al. (1995) and Rosenbaum and Gregory (2002) in which individuals gave effort ratings for isometrically and isotonicly generated torques, respectively.

Given the importance of effort as it relates to the biomechanics of human movement, it is important to develop a method for relating judgments of muscular effort to biomechanical quantities during isokinetic muscle actions. The purpose of this study was to develop such a methodology, as well as to critically examine those biomechanical measures that may provide direct measures of muscular effort.

## **METHODS**

Ten healthy individuals (5 males, 5 females) between 20-40 years of age participated in this study.

After undergoing informed consent procedures, subjects performed isokinetic elbow flexion/extension joint actions in the horizontal plane using their dominant arm at two different angular velocities (60°/s and 240°/s) for five movement cycles. Subjects were required to produce joint torques that corresponded to effort levels of 1 (very light effort), 3 (light effort), 5 (medium effort), 7 (strong effort), or 9 (very strong effort) on a modified Borg CR-10 scale (0 = no effort; 10 = maximal effort). Elbow joint torque and surface EMG data for the biceps brachii and triceps brachii muscles were measured using a dynamometer (Kin-Com 125AP, Chattanooga Group, Inc.). The 10 conditions (two angular velocities × five effort levels) were presented in random order. All subjects performed one trial for each condition in two rounds. The first round was designed to allow subjects to experience the full range of efforts and velocities. The second round was used for data collection.

A within-within subjects factorial ANOVA design was used to assess the effects of joint action, angular velocity, and effort level on joint torque and integrated surface EMG data. The iEMG data for all conditions was normalized with respect to maximal voluntary contractions at both the 60°/s and 240°/s angular velocities.

## RESULTS AND DISCUSSION

There was a significant increase in joint torque as a function of effort level for elbow flexion and extension joint actions and both 60°/s and 240°/s angular velocities (see Table 1). For effort levels 3-9, significantly greater joint torques were produced during elbow flexion than elbow extension during both 60°/s and 240°/s angular velocities. In addition, for both elbow flexion and extension joint actions across all effort levels, there were significantly smaller joint torques produced at the 240°/s angular velocity than those produced at the 60°/s angular velocity. The normalized iEMG demonstrated similar patterns to those obtained for elbow joint torques as a function of effort level for elbow flexion and extension joint actions and both 60°/s and 240°/s angular velocities (see Table 1).

Based on the relationship between both elbow joint torque and iEMG with muscular effort, it has been shown that joint torque and iEMG increase as a function of muscular effort. While it is reasonable to hypothesize that muscular effort is directly proportional to biomechanical quantities involved in movement production, the results of this study provide a quantitative link between biomechanical measures (joint torque, iEMG) and muscular effort.

## SUMMARY

The purpose of this study was to develop a method that can be used to examine biomechanical measures of muscular effort during isokinetic muscle actions. Based on these findings, it seems reasonable to recommend the method for future research. By determining the relationship between joint torque and muscular effort (the slope of the function relating joint torque to muscular effort when joint torque is plotted against muscular effort), it should be possible to evaluate changes in muscular effort as a function of movement task conditions. This could be a boon for both basic and clinical research.

## REFERENCES

- Andrews, J.G. (1983). *Medicine and Science in Sports and Exercise*, **15**, 199-207.  
 Burgess, P.R. et al. (1995). *Somatosensory and Motor Research*, **12**, 343-358.  
 Rosenbaum, D.A., Gregory, R.W. (2002). *Experimental Brain Research*, **142**, 365-373.

## ACKNOWLEDGEMENTS

This investigation was supported by the University of Kansas General Research Fund allocation #2301474.

**Table 1:** Elbow joint torques (mean  $\pm$  SD) and normalized iEMG values (mean  $\pm$  SD) as a function of angular velocity, joint action, and effort level during isokinetic muscle actions.

Ang. Vel.	Joint Action		Effort Level				
			1	3	5	7	9
60°/s	Flex	Torque (Nm)	10.3 $\pm$ 0.8	18.8 $\pm$ 3.1	23.2 $\pm$ 7.9	31.1 $\pm$ 9.0	36.7 $\pm$ 9.7
		EMG (%MVC)	14.8 $\pm$ 9.0	26.4 $\pm$ 11.5	36.8 $\pm$ 15.5	49.4 $\pm$ 12.8	73.6 $\pm$ 27.7
	Ext	Torque (Nm)	9.7 $\pm$ 3.8	14.7 $\pm$ 3.6	18.2 $\pm$ 2.5	22.9 $\pm$ 4.0	25.6 $\pm$ 3.4
		EMG (%MVC)	15.4 $\pm$ 8.2	35.2 $\pm$ 10.6	58.0 $\pm$ 37.4	71.8 $\pm$ 37.8	77.8 $\pm$ 25.4
240°/s	Flex	Torque (Nm)	7.8 $\pm$ 1.8	15.3 $\pm$ 3.7	20.0 $\pm$ 5.9	24.2 $\pm$ 5.4	31.9 $\pm$ 7.1
		EMG (%MVC)	25.6 $\pm$ 6.4	41.8 $\pm$ 14.4	56.2 $\pm$ 21.9	68.2 $\pm$ 24.5	86.2 $\pm$ 15.3
	Ext	Torque (Nm)	6.3 $\pm$ 1.6	12.1 $\pm$ 3.0	15.5 $\pm$ 3.6	18.2 $\pm$ 2.9	23.3 $\pm$ 3.2
		EMG (%MVC)	24.8 $\pm$ 7.6	41.8 $\pm$ 9.8	55.4 $\pm$ 7.4	73.8 $\pm$ 18.8	86.2 $\pm$ 19.3

# CADAVERIC GAIT SIMULATION

Patrick M. Aubin,<sup>1,2</sup> Matthew S. Cowley,<sup>1</sup> William R. Ledoux<sup>1,3,4</sup>

<sup>1</sup>RR&D Center of Excellence, VA Puget Sound, Seattle WA, Departments of <sup>2</sup>Electrical Engineering, <sup>3</sup>Mechanical Engineering and <sup>4</sup>Orthopaedics and Sports Medicine, University of Washington, Seattle, WA  
E-mail: wrledoux@u.washington.edu, Web: www.seattlerehabresearch.org

## INTRODUCTION

The relationship between foot structure and foot function has received much recent study. Often, static cadaveric models are employed. However the relationship between dynamic bony alignment and plantar pressure during gait is not well understood. To further investigate the relationship between foot structure and foot function, we are developing a Cadaveric Gait Simulator (CGS), capable of generating neutrally aligned and pathologic foot kinematics, kinetics, ground reaction forces (GRFs) and plantar pressures. The CGS will be used to generate pathologic pre- and post-surgical gait simulations, as well as conservative treatment simulations. This will serve as a tool for clinicians to explore more efficacious treatment strategies for patients with pathological feet.

Existing dynamic, cadaveric gait simulators are potentially limited by the following: scaled gait simulation speeds, simplified rigid body motion of the tibia, or scaled GRFs (Kim *et al.*, 2001; Hurschler *et al.*, 2003; Ward *et al.*, 2003; Hamel *et al.*, 2004). To overcome these challenges, a novel six degree of freedom parallel link hexapod robot (R-2000, Parallel Robotic System, Inc; Hampton, NH) was used (Figure 1).

Our future work will use cadaveric limbs, but to date we have only employed a prosthetic foot and pylon as an initial step.

## METHODS

The prosthetic limb was mounted to a rigid frame that is mechanically grounded to the floor while the robot simulated the motion of the “ground” relative to the limb. Thus the pylon (or tibia) was stationary while the “ground” was moved by the robot to accurately reproduce the relative pylon - ground rigid body motion. In the future, nine linear actuators will supply force via tendon clamps to the extrinsic muscle tendons of the foot.

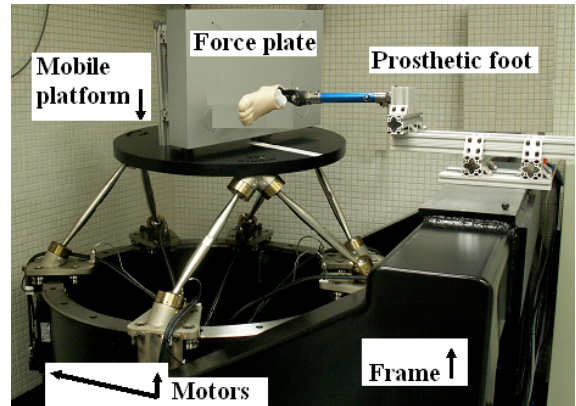


**Figure 1:** The Cadaveric Gait Simulator.

The rotational rigid body motion of the tibia with respect to the ground will be recorded from living subjects (normal and pathologic) with a Vicon twelve camera retro-reflective motion analysis system. To date, we have collected gait data from one transtibial amputee. The robotic “ground” was constrained to recreate the sagittal, coronal, and transverse plane rotations of the *in situ* prosthetic limb. The three translations of the robotic “ground” were adjusted between gait simulations using a proportional iterative

learning controller in order to reproduce the recorded *in situ* GRFs. Changes to the “ground” trajectory were limited to incremental displacements along the vertical ground axis. This ensures that the simulated rotational kinematics of the tibia matched the recorded *in situ* gait data while also achieving the target GRFs. The motion of the prosthetic foot was not directly constrained but rather a function of the “ground” kinematics and kinetics, GRFs, and, in the future, tendon forces.

During the simulation, a force plate attached to the robot measured the GRFs. In the future, a Peak six-camera retro-reflective motion analysis system will measure the rotation of eight bones (the calcaneus, talus, navicular, cuboid, medial cuneiform, and 1<sup>st</sup> and 5<sup>th</sup> metatarsals) via bone pins and marker triads. Further, a plantar pressure measurement device will be mounted in series with the force plate.

## RESULTS AND DISCUSSION

Simulating transtibial prosthetic gait has been the first step to implementing the Cadaveric Gait Simulator. To date, pylon kinematics and GRFs (scaled to 3 seconds and approximately 50% body weight) were simulated and compared to *in situ* gait data (Figure 2). The scaled vertical GRF during the stance phase of transtibial prosthetic gait had an RMS error of 14 N between the *in situ* and simulated gait. The iterative learning controller took 14 gait iterations to reduce the RMS error from 232 N to 14 N. Further improvements to the RMS error require an increased force plate signal to noise ratio as well as compensation for the inertial effects of the moving force plate.

The R-2000’s typical positional error is only 50  $\mu\text{m}$ , meaning the “ground” kinematics will have insignificant amounts of error.

Thus the simulated versus *in situ* “ground” kinematics are identical except for errors due to data collection noise and foot mounting inaccuracies. The data collection noise was estimated to be on the order of a few degrees and a misaligned prosthetic foot only shifts the simulated rotational kinematic curves but accurately maintains their range of motion and rate of change.

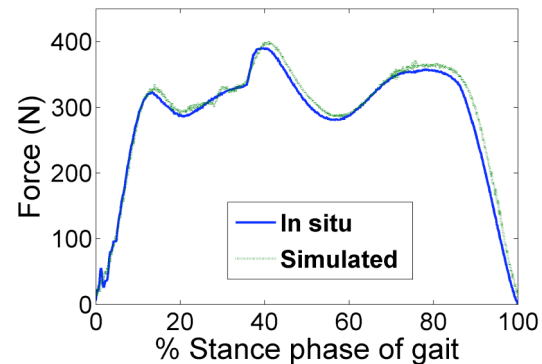


**Figure 2:** *In situ* and simulated vertical GRF.

Future work includes increasing forces to 100% body weight and decreasing the simulated time of stance phase to 0.75 sec by optimizing the “ground” trajectory within the working volume of the R-2000. Cadaveric simulations with active “muscle” forces will follow.

## REFERENCES

- Hamel, A.J., et al. (2004). *Gait and Posture*, **20**(2), 147-153.
- Kim, K.J., et al. (2001). *J Musculoskeletal Research*, **5**(2), 113-121.
- Hurschler, C., et al. (2003). *Foot & Ankle International*, **24** (8), 614-629
- Ward, E.D., et al. (2003). *J. Am Podiatric Med Assoc*, **93**(6), 429-442.

## ACKNOWLEDGEMENTS

This work was supported in part by the Dept. of Veterans Affairs, RR&D Service grant numbers A2661C and A3923R.

# EFFECT OF UNI- AND BI-CORTICAL SCREW ANGULATION ON THE STABILITY OF MULTI-LEVEL CORPECTOMY CONSTRUCT – A FINITE ELEMENT MODEL STUDY

Mozammil Hussain<sup>1</sup>, Amir H. Fayyazi<sup>2</sup>, Raghu N. Natarajan<sup>1,3</sup>, Gunnar B.J. Andersson<sup>3</sup>, Howard S. An<sup>3</sup>

<sup>1</sup> University of Illinois at Chicago, Chicago, IL, USA

<sup>2</sup> State University of New York, Syracuse, NY, USA

<sup>3</sup> Rush University Medical Center, Chicago, IL, USA

E-mail: hussmoz@iit.edu

## INTRODUCTION

Cervical corpectomy and fusion with an anterior screw-plate system is a common surgical technique to treat spondylotic disorders. The dynamic plates are load-sharing in nature that requires bi-cortical screws. In comparison, the rigid plates are load-bearing device that requires uni-cortical screws. Despite excellent immediate-postoperative results, clinical failures of such multi-level construct and adjacent segment disease have been observed due to the load-bearing nature of rigid plates during late-postoperative stages. The objective of the present study was to investigate the stability of the construct using the rigid plates by placing the uni- and bi-cortical screws at an oblique angle with respect to the endplates. Furthermore, the direction of propagation of the adjacent segment disease was determined.

## METHODS

A three-dimensional finite element (FE) model of a healthy C3-T1 segment was developed from the CT scan of a 38-year old woman. Two-level corpectomy was performed and a graft was centrally placed in between the C4 and C7 covering up to 50% area of the opposing endplates. An anterior plate with rigid screw trajectory was used. Five models were built with the screws at an oblique cephalad-caudal screw angle

with respect to the endplates. Four of these models were built with an oblique cephalad-caudal screw angle of 0°, 5°, 10°, and 15°, while the fifth model was built with an oblique cephalad screw angle of 15° and a caudal screw angle of 0°. Uni- and bi-cortical screws of 16 and 18 mm length with an outer and inner diameter of 3.5 and 2.5 mm were used. The material properties were adopted from the literature. The moment loads were created by applying equal and opposite loads on the superior surface of C3 keeping the inferior surface of T1 fixed. A constant preload of 73.6 N was applied using two temperature truss elements connecting the lateral edges of the vertebral bodies to mimic the follower load technique. The analysis was performed using the commercial FE software, ADINA. The stability of the construct and adjacent segments using uni- and bi-cortical angulated screws were compared under a moment of 1.5 Nm with preload.

## RESULTS AND DISCUSSION

The healthy C3-T1 model was validated with the *in vitro* study (Panjabi *et al* 2001 and Wheeldon *et al* 2006) under a moment of 1.0 Nm with preload (figure 1). Some motion results over predicted the *in vitro* data, but they were within the *in vivo* range of motion (Penning *et al* 1978). Moreover, Panjabi *et al* 2001 did not mention the age group of cadavers, while Wheeldon *et al*

2006 used the cadavers with an age range 20-51 years. The above *in vitro* studies using the cadavers represented some degenerative pathology due to the older specimens, while the FE model used the material data of the healthy spine. The two-level corpectomy construct with parallel, uni-cortical screws and anterior rigid plate was validated with the *in vitro* study (Cagli *et al* 2004) during immediate-postoperative condition under a moment of 1.5 Nm with preload (figure 2).

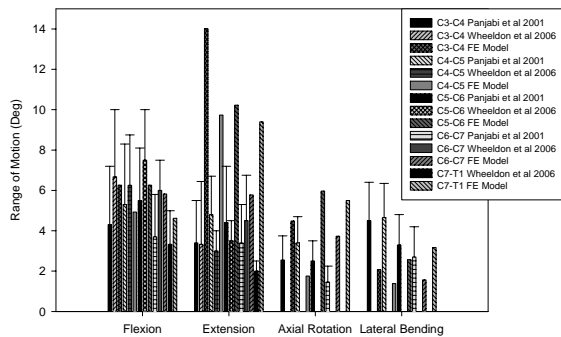


**Figure 1:** Validation of a healthy C3-T1 intact model with the *in vitro* studies.

The range of motion was not dependent upon screw angulations and types of screws. Although bi-cortical screws provided a negligible enhanced stability as compared to the uni-cortical screws during immediate-postoperative condition, but no such effect was observed during late-postoperative condition. Lehmann *et al* 2004 observed the similar results.

Higher percentage reduction in the range of motion of the superior motion segment was observed as compared to the inferior motion segment except for the lateral bending motion. The corpectomy construct was more stable during late- than immediate-postoperative condition due to progressive fusion of the bone graft with the endplate. This stable state of fusion was achieved with the reduction in range of motion of the adjacent segments (figure 3).

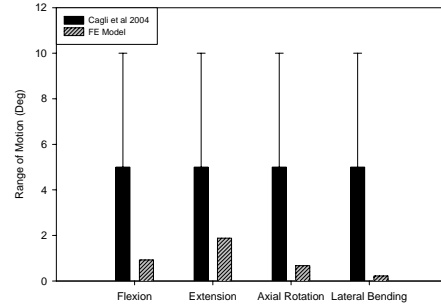


**Figure 2:** Validation of the C4-C7 corpectomy construct with the *in vitro* study.

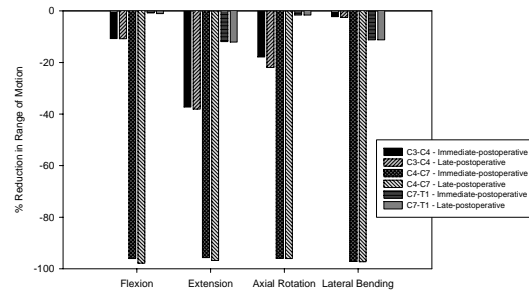


**Figure 3:** Percentage reduction in the range of motion of the corpectomy construct and adjacent segments.

## SUMMARY

The stability of the corpectomy construct and adjacent segments are independent of the angular placement and types of screws. The adjacent segment degeneration was found to propagate superior to the corpectomy construct.

## REFERENCES

- Panjabi, M.M., Crisco, J.J. et al. (2001). *Spine*, **26**, 2692-2700.
- Wheelon, J.A., Pintar, F.A. et al. (2006). *J. Biomech*, **39**, 375-380.
- Penning, L. (1978). *Am J. Roentgenol*, **30**, 317-326.
- Cagli, S., Chamberlain, R.H. et al. (2004). *Spine*, **29**, 1420-1427.
- Lehmann, W., Blauth, M. et al. (2004). *Eur Spine J.*, **13**, 69-75.

# CARTILAGE CONTACT STRESS ABERRATION DURING UNSTABLE JOINT MOTION

Yuki Tochigi, M. James Rudert, Todd O. McKinley,  
Douglas R. Pedersen, and Thomas D. Brown

University of Iowa, Iowa City, IA

E-mail: [yuki-tochigi@uiowa.edu](mailto:yuki-tochigi@uiowa.edu) Web: <http://poppy.obrl.uiowa.edu/>

## INTRODUCTION

Mechanical abnormalities after intraarticular fractures have been implicated in subsequent joint degeneration leading to posttraumatic arthritis. Incomplete reduction of these fractures, “incongruity”, reduces articular contact area, leading to elevated local cartilage contact stresses. Furthermore, the altered surface geometry may impact joint stability, allowing unstable joint motion. During episodes of unstable joint motion, cartilage may experience rapidly increasing stresses (temporal stress gradients) that would not be seen under normal conditions.

Most mechanical studies have involved fixed-position static loading of articular surface incongruities and have found relatively modest increases in local contact pressure. However, static testing does not account for the viscoelastic nature of cartilage and may mask important transient stress elevations that occur during motion. We have developed a dynamic testing system that measures transient contact stress throughout ankle plantar/dorsiflexion and that can concurrently permit unstable joint motion. This study aims to characterize dynamic contact stress aberration during unstable joint motion, by measuring cartilage contact transient pressure in an experimental ankle incongruity model.

## METHODS

Soft tissue was removed from eleven cadaver ankles, allowing access to the tibio-talar joint while preserving all major ligaments. To reproduce clinically possible

unstable motion (transient subluxation event), 30% of the anterior tibial articular surface was osteotomized, displaced proximally (step-off height: 2 mm), and rigidly secured using internal fixation (Fig. 1). The anterior talofibular ligament also was transected as needed. The hindfoot, forefoot, and tibial diaphysis were potted in PMMA and mounted in the testing device (Fig. 2). Specimens, held under a 300 N axial load, were subjected to simulated stance phase ankle motion (flexion angle:  $10^\circ \rightarrow 15^\circ \rightarrow -10^\circ \rightarrow 10^\circ$ ) at 0.5 Hz.

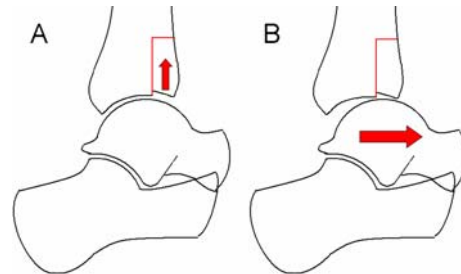


**Figure 1:** Step-off displacement of the anterior tibial surface fragment (A), and anterior talar subluxation (B)



**Figure 2:** The MTS-mounted loading fixture allows free ankle inversion/eversion while controlling flexion-extension angle.

Anterior-posterior loads were applied to the tibia via a pneumatic actuator. While an anteriorly directed baseline constant “stabilizing” load (30 N) was applied in every test, a superimposed “subluxating” load pulse, directed posteriorly, ranging from 0 to 120 N in 10 N increments, was applied at 45 - 70% of the motion cycle (corresponds to heel-off phase.)

Contact stresses between the tibial and talar surfaces were continuously recorded using a thin flexible sensor (TekScan Inc., Boston, MA) inserted into the joint. Designed for the ankle, this sensor incorporates a 32 x 46 (1472) array of pressure-sensing sensels and has a maximum recording frequency of 132 Hz. In our protocol, a motion cycle takes 2 seconds - thus, a data recording for a single cycle consists of a 262-frame “movie”, each frame consisting of 1472 discrete pressure measurements. From these contact stress data, temporal gradients (instantaneous stress change) were calculated by a custom program implemented in Matlab, based on algorithms described elsewhere. [1, 2]

## RESULTS

When a 100 N subluxation pulse was applied, unstable ankle motion (identified by distinct talar contact on the anterior tibial fragment on the stress sensor movie) occurred in seven of eleven specimens. These unstable motions involved an expanded range of contact stress temporal gradients, by increases of both high positive and negative instantaneous stress changes. Ninety-fifth percentile highest positive and negative magnitude across the contact area, during the subluxation event, were  $39.7 \pm 9.5$  and  $-48.6 \pm 13.5$  MPa/sec (average and standard deviation, across the seven specimens), both significantly greater than the corresponding data in the intact (no osteotomy, no ligament sectioning) condition,  $16.9 \pm 3.4$  and  $-18.5 \pm 4.4$  MPa/sec ( $p = 0.002$ ).

The greatest elevations of contact stress temporal gradients occurred on the slightly medial region of the anterior displaced surface and on the lateral region of the posterior surface (Fig. 3). Peak magnitudes in these areas reached  $181.0 \pm 72.1$  and  $156.8 \pm 63.7$  MPa/sec, respectively.

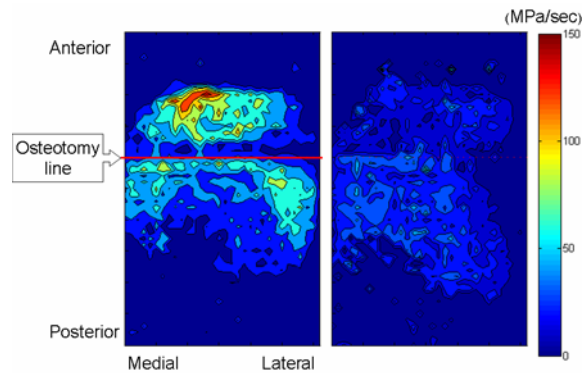


**Figure 3:** Distribution of peak positive contact stress temporal gradient during unstable motion (left, subluxation pulse = 100 N) and during corresponding stable motion (right), in a single specimen.

## CONCLUSIONS

In this displaced intraarticular fracture model, ankle cartilage experienced elevated contact stress temporal gradients during instances of unstable joint motion. Excessive elevation occurred on the displaced anterior fragment surface when the talus transiently subluxated from beneath the tibia, and on the lateral region of the posterior surface when the subluxation was reduced. The results demonstrate that unstable joint motion can cause extreme mechanical demands that articular cartilage never experiences during stable joint motion. Such contact stress aberrations may cause cartilage damage on a chronic basis, exacerbating the propensity for post-traumatic osteoarthritis.

## REFERENCES

1. McKinley TO, et al. OA Cartilage 2006
2. Baer TE, et al. ISB/ASB 2005, Cleveland, Ohio

## ACKNOWLEDGEMENTS

CDC grant R49 CCR721745

# Patellar Tendon Is Extensible During Maximum Effort Knee Extensions

John W. Chow, Ryan A. Mizell, Jeff T. Wight, and Mark D. Tillman

Department of Applied Physiology & Kinesiology, University of Florida, Gainesville, FL, USA  
E-mail: jchow@hhp.ufl.edu Web: www.hhp.ufl.edu/apk/ces/labs/biomech/

## INTRODUCTION

Knee joint models are commonly used to estimate knee joint forces during physical activities. One of the common features of existing knee models is the assumption that the patellar tendon is an inextensible link between the patella and tibia. In other words, the patellar tendon is treated as having constant length at all knee angles (Gill & O'Connor, 1996; Shelburne & Pandy, 1997; van Eijden et al., 1986; Yamaguchi & Zajac, 1989). However, the validity of such an assumption has not been examined. Thus, the purpose of this study was to compare patellar tendon lengths at a relaxed state and during maximal effort isometric knee extensions.

## METHODS

Six males (age  $22.2 \pm 1.0$  yrs, height  $179 \pm 7$  cm, weight  $824 \pm 104$  N) and 6 females ( $22.7 \pm 2.7$  yrs,  $166 \pm 8$  cm,  $740 \pm 131$  N) who had no history of major knee injuries or surgery served as the subjects. A total of 12 sagittal knee radiographs were obtained from each subject (6 from each knee). While sitting on a stool located next to an x-ray film, 5 radiographs were captured at 5 different knee flexion angles ( $25^\circ$  to  $85^\circ$  at intervals of  $15^\circ$ ) for each knee when the subject performed knee extensions with maximum effort (MVIC conditions). To provide the resistance to knee extension, a steel cable with one end connected to an ankle strap and the other end fastened to an angle iron fixed to the bottom of the stool was used. A metal pin with a length of

10.15 cm was placed on the anterior surface of the knee for spatial reference. To determine the unstretched length of the patellar tendon, a radiograph was taken for each knee when the subject sat on the stool with the leg relaxed.

Each radiograph was analyzed by 3 analysts independently using the same guidelines. Specifically, each analyst identified 4 points on a radiograph (Figure 1):

- Ends of the metal pin.
- The proximal attachment of the patellar tendon – the midpoint between the most inferior point of the anterior surface of the patella and the most inferior aspect of the patella.
- The distal attachment of the patellar tendon – the midpoint between the deepest superior tibial indentation and the farthest tibial protrusion.

The patellar tendon length is the shortest distance between the proximal and distal attachments. The average values over 3 analysts were used in subsequent statistical analyses. A one-way ANOVA with repeated measures was performed to determine if significant differences in patellar tendon length existed among different MVIC and relaxed conditions ( $\alpha = 0.05$ ). When a significant difference was found, within group paired t-tests were performed to compare different pairs of MVIC/relaxed conditions. Since there were 15 pairs, the alpha level was set at 0.0067 ( $0.1/15$ ) to adjust for multiple tests.

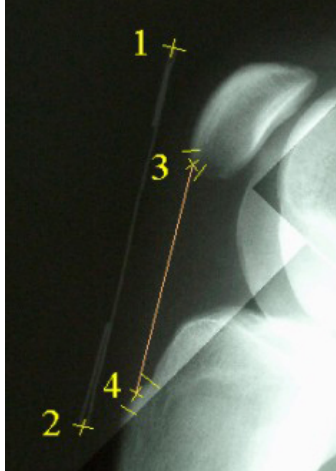


**Figure 1:** Points identified on each X-ray.

## RESULTS AND DISCUSSION

Significant differences were found among different experimental conditions ( $p < 0.001$ ) (Table 1). Within group t-tests indicate that patellar tendon lengths during MVIC conditions are all significantly greater than the unstretched length. In addition, significant differences were also found in the 25-55°, 25-85°, and 40-55° pairs (Table 2). The actual differences (in cm) among different MVIC conditions are relatively small and may not carry any practical significance.

Large ranges of patellar tendon length were observed in different experimental conditions and the variation does not seem to be gender related. For example, the average unstretched patellar tendon lengths for males ( $5.04 \pm 0.55$  cm) and females ( $5.05 \pm 0.58$  cm) were about the same.

Using the knee model they developed (van Eijden et al., 1986), van Eijden et al. (1987) investigated the influence of patellar tendon length on selected knee geometric characteristics and joint forces. They concluded that the patellar tendon length appeared to influence the mechanical behavior of the patellar articulation considerably.

## SUMMARY/CONCLUSIONS

The significant differences between relaxed and MVIC conditions and the large range of patellar tendon length suggest that cautions should be taken when interpreting results obtained from the use of a generic knee model. To increase the validity of different measures given by a knee model, personalized patellar tendon length should be used whenever possible.

## REFERENCES

- Gill, H.S., O'Connor, J.J. (1996). *Clin. Biomech.*, **11**, 81-89.  
 Shelburne, K.B, Pandy, M.G. (1997). *J. Biomech.*, **30**, 163-176.  
 van Eijden, T.M.G.J. et al. (1986). *Acta Orthop. Scand.*, **58**, 560-566.  
 van Eijden, T.M.G.J. et al. (1987). *J. Biomech.*, **19**, 219-229.  
 Yamaguchi, G.T., Zajac, F.E. (1989). *J. Biomech.*, **22**, 1-10.

## ACKNOWLEDGEMENTS

We appreciate the assistance of Stacy Colon, Lindsay Dole, and Kim Fournier.

**Table 1:** Patellar tendon lengths.

	Relax	25°	40°	55°	70°	85°
Mean	5.05	5.46	5.39	5.33	5.39	5.35
SD	0.55	0.59	0.59	0.59	0.57	0.61
High	6.00	6.28	6.59	6.38	6.38	6.39
Low	3.43	4.62	4.68	4.52	4.50	4.31

**Table 2:** P-values of within group t-tests.

	25°	40°	55°	70°	85°
Relax	<.001	<.001	<.001	<.001	.004
25°		.071	.002	.056	.005
40°			.002	.775	.286
55°				.349	.833
70°					.225

# PROPRIOCEPTIVE ERROR CAN BE REDUCED WITH TRAINING

Chris Mizelle,<sup>1,2</sup> Timothy J. Brindle,<sup>2</sup> and Steven Stanhope<sup>2</sup>

<sup>1</sup> Physical Therapy and Rehabilitation Science, University of Maryland School of Medicine

<sup>2</sup> Physical Disabilities Branch\*\*, National Institutes of Health

E-mail: cmizelle@som.umaryland.edu

## INTRODUCTION

The term proprioception refers to the afferent information throughout our bodies that our central nervous system (CNS) uses to locate limb segments in space.

Measures of proprioception characteristically have high variability between different measurement techniques and also between subjects within the same measurement technique,<sup>1</sup> making objective comparisons of baseline joint position sense (JPS) scores difficult between subjects.

It is well known that training reduces movement variability and increases movement accuracy. However, training paradigms in the literature cross multiple physiological systems and are not specific to the proprioceptive system.<sup>2</sup>

In an attempt to specifically enhance JPS accuracy, we developed a passive training paradigm based on motor learning principles. While this type of paradigm has been recommended in the literature, it not been performed.<sup>2</sup>

This pilot work was performed to determine if it is feasible to improve proprioception through a novel training paradigm designed to specifically enhance JPS acuity.

## METHODS

Twenty-six healthy volunteers were seated in a Biodex (Biodex Medical Systems, Shirley, New York) and positioned with the

hip in 75° of flexion and the knee in 90° of flexion. All subjects were trained to reproduce a target position of 20° of knee flexion during passive rotation of the knee at different, randomly presented speeds (Table 1). A thumb-switch was used to end the passive motion when subjects perceived the knee was at the target position. Knowledge of results were presented to the subject at the completion of each trial to aid in training and to provide motivation. We used off-line visual feedback via a video monitor as well as kinesthetic feedback by passively rotating the knee joint to the exact target position when subject performance fell outside of an error tolerance threshold ( $\pm 1^\circ$  for slow and medium speeds;  $\pm 2^\circ$  for the fastest speed). Performance was assessed as absolute error (AE) from the target position in degrees. AE values were subjected to a repeated measures analysis of variance having three levels of movement speed (0.5°/s, 2.0°/s, and 10.0°/s) and two levels of time (initial and terminal 15 % of trials). Bonferroni corrected t-tests were used to compare change in JPS from the initial to the terminal 15% of trials within each movement speed.

**Table 1:** Knee rotational velocities, movement times, and movement magnitudes randomly presented subjects during training.

		Knee Rotational Velocity		
		0.5°/s	2.0°/s	10.0°/s
Time	4s	2°	8°	40°
	5s	2.5°	10°	50°
	6s	3°	12°	60°

## RESULTS AND DISCUSSION

Subject performance was analyzed over 40 trials. A training effect is supported by the results of a 3x2 ANOVA, where there was a statistically significant speed by time interaction effect,  $F(2, 50) = 4.85, p < .005$ . Main effects of speed ( $F(2, 50) = 70.87, p < .001$ ) and time ( $F(1, 25) = 9.85, p < .001$ ) were also statistically significant.

Comparison of the initial to the terminal trials demonstrates improvement in both the 0.5°/s and 10°/s ( $p < 0.01$ ), but not in the 2.0°/s conditions (Figure 1).

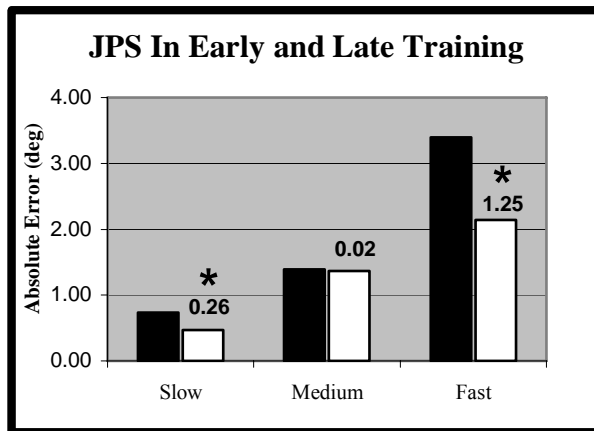


**Figure 1:** Absolute JPS error is reduced following training at the slow (0.5 °/s) and fast (10.0 °/s) speeds, but not at the medium (2.0°/s) speed. Filled bars represent early training and white bars represent late training. \* indicates statistically significant differences at  $\alpha < 0.01$ .

Though passive training of knee joint proprioception produces variable results, this data does support enhanced JPS through a speed-specific training response. We speculate this graded response is a result of enhanced information being made available to the CNS through increased stimulation of specific peripheral receptors at the higher joint rotational velocity.

Much of the proprioceptive information ascending to the CNS at the slowest speed is likely derived from slowly adapting receptors in knee joint and group II afferents. The greater error reduction observed at the highest movement velocity may be a result of the CNS adapting to predict knee location from velocity-specific information from the more dynamic group Ia afferents.

The lack of a training effect at the intermediate speed may be the result of a sensory conflict, where CNS interpretation of JPS is based on both quasi-static and dynamic receptors, making knee position during movement at this speed less certain.

## SUMMARY/CONCLUSIONS

The results of this work demonstrate that the CNS may be trained, through a passive movement paradigm, to enhance JPS acuity. These results have implications for patients with neurological diseases affecting motor skill and accuracy.

## REFERENCES

1. Grob, et al. (2002). J. Bone Joint Surg {Br}, **84-B**, 614-618.
2. Ashton-Miller et al. (2001). Knee Surg, Sports, Traumatol, Arthrosc, **9**, 128-136.

## ACKNOWLEDGEMENTS

This work was supported by the Advanced Rehabilitation Research Training Program, NIH/ National Center for Medical Rehabilitation Research (NCMRR), T32 HD041899-01A1.

\*\* A collaboration between the National Institute of Child Health and Human Development and the Mark O. Hatfield Clinical Research Center, NIH.

# BIOMECHANICAL STABILIZATION OF THE MULTI-LEVEL CORPECTOMY CONSTRUCT USING ANTERIOR AND POSTERIOR INSTRUMENTATION – A FINITE ELEMENT MODEL STUDY

Mozammil Hussain<sup>1</sup>, Ahmad N. Nassr<sup>2</sup>, Raghu N. Natarajan<sup>1,2</sup>, Gunnar B.J. Andersson<sup>2</sup>, Howard S. An<sup>2</sup>

<sup>1</sup> University of Illinois at Chicago, Chicago, IL, USA

<sup>2</sup> Rush University Medical Center, Chicago, IL, USA

E-mail: hussmoz@iit.edu

## INTRODUCTION

Long segment decompression and strut reconstruction with either an anterior or posterior instrumentation have been shown to promote arthrodesis and minimize bone graft related problems. Numerous surgical techniques to supplement the stability of the multi-level construct have been well documented in the literature using the anterior screw-plate system or posterior screw-plate/rod system. These surgical techniques have their own advantages and disadvantages that should be decided by the surgeon carefully before operating on the patients. Anterior instrumentation is a preferred traditional technique due to good neural decompression, strengthening of anterior column, and excellent arthrodesis rate. However, recent failures associated with the multi-level strut reconstruction using anterior screw-plate advocated the need to supplement the construct with posterior instrumentation.

The objective of the present study was to compare the stability of the construct using the rigid anterior screw-plate and/or posterior screw-rod system. Furthermore, the stability of superior motion segment was compared to the inferior motion segment to determine the direction of propagation of the adjacent segment disease.

## METHODS

A three-dimensional finite element (FE) model of a healthy C3-T1 segment was developed from the CT scan of a 38-year old woman. Two-level corpectomy was performed and a bone graft was centrally placed in between the C4 inferior endplate and C7 superior endplate covering up to 50% area of the opposing endplates. A contact gap of 0.1 mm was used to simulate the immediate-postoperative condition. Three types of stabilization models were built from the two-level corpectomy model. Firstly, an anterior stabilization model was created by using an anterior plate with rigid screw trajectory from C4 to C7. Two uni-cortical screws each at the cephalad and caudal ends of the anterior plate were placed parallel to the endplates. Secondly, the posterior stabilization model was enhanced by using a vertical rod with rigid screw trajectory from C4 to C7. Two uni-cortical screws at each segment were placed in the posterior lateral mass. Thirdly, the combined anterior-posterior stabilization model was created by using an anterior screw-plate together with the posterior screw-rod system. The anterior and lateral mass screws of 16 mm length with an outer and inner diameter of 3.5 and 2.5 mm were used. The material properties of the spinal structures and instrumentations were adopted from the literature. The moment loads were created by applying appropriate equal and opposite loads on the superior surface of C3 keeping the inferior surface of T1 fixed. A constant preload of 73.6 N was applied using two

temperature truss elements connecting the lateral edges of the vertebral bodies to mimic the follower load technique. The analysis was performed using the commercially available finite element code, ADINA. The range of motion of the corpectomy construct and adjacent segments using three stabilization models were compared under a moment load of 1.5 Nm with preload.

## RESULTS AND DISCUSSION

The validation studies of the healthy C3-T1 intact segment and two-level corpectomy with anterior instrumentation were described previously (Hussain *et al* 2006).

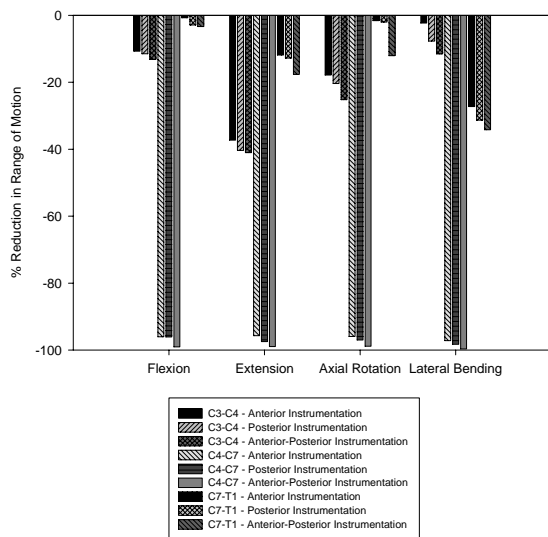


**Figure 1:** Comparison of the percentage reduction in range of motion using the anterior and/or posterior instrumentation for the corpectomy construct and adjacent segments.

The stability of the construct was highest by using the combined anterior-posterior instrumentation. When anterior instrumentation was compared to the posterior instrumentation alone, the former

was found to be less stable (figure 1). This finding was consistent with the cadaveric study of Singh *et al* 2003. However, they found no significant statistical difference between the biomechanical stability of the combined instrumentation and posterior instrumentation alone which was not true with our results.

Higher percentage reduction in the range of motion of the superior motion segment was observed as compared the inferior motion segment except for the lateral bending motion. The increased stability of the construct with the increased instrumentation was simultaneously accompanied by the increased stiffness of the adjacent segments which might lead to disc degeneration.

## SUMMARY

The stability of the corpectomy construct and adjacent segments follows the order as: combined anterior-posterior instrumentation, posterior instrumentation alone, and anterior instrumentation alone. The adjacent segment degeneration was found to propagate superior to the corpectomy construct. The possibility of adjacent segment degeneration follows from the enhanced stability of the corpectomy construct.

## REFERENCES

- Hussain, M., Fayyazi, A.H. et al (2006). *30<sup>th</sup> Annual Meeting of the American Society of Biomechanics*, submitted.
- Singh, K., Vaccaro, A.R. et al. (2003). *Spine*, **28**, 2352-2358.

## ACKNOWLEDGEMENTS

This study was supported by the Department of Orthopedic Surgery, Rush University Medical Center, Chicago, Illinois.

# FOOT MOVEMENT RESTRICTIONS WITH THE USE OF FOOT FORCE TRANSDUCERS DURING BIOMECHANICAL ASSESSMENTS OF PATIENT TRANSFER ACTIVITIES

Brent Carmichael<sup>1,2</sup>, Tilak Dutta<sup>1,2</sup> and Geoff Fernie<sup>1,2</sup>

<sup>1</sup> Institute of Biomaterials and Biomedical Engineering, University of Toronto, Toronto, Canada,

<sup>2</sup> Toronto Rehabilitation Institute, Toronto, Canada

E-mail: brent.carmichael@utoronto.ca

## INTRODUCTION

Caregiving involves a considerable amount of handling, both of equipment and of patients. Many assistive devices have been designed to lessen the stress on caregivers (Plamondon et al. 1996; Schibye et al. 2001). However, even with these devices in place, caregivers continue to be injured (Santaguida 2001). To understand why injuries persist, these devices need to be biomechanically assessed. Often these assessments make use of stationary force platforms which can be problematic when studying bedside activities, such as patient transfers, for three reasons: (1) if the participants are cognisant of the force platforms, their actions may be constrained or biased; whereas, (2) if the participants are unaware of the force platforms, then their movements often exceed the measurable area of the force platforms, and (3) the lack of portability of force platforms prevents clinical measurement. Thus, a study was conducted to investigate whether the use of portable multi-axis force transducers, “forceshoes”, would allow participants to move their feet freely about a region larger in size than that afforded by the force platforms and to see whether these movements would approach those of the natural or free case.

## METHODS

Seven female caregivers (mean age: 26.3yrs, mass: 59kg, height: 166cm, experience: 1.8yrs) were asked to insert a Hoyer U-sling

(Hoyer Model 7000, size XL) under a 93kg non-helpful patient actor given three foot conditions: (1) while wearing their regular work shoes and without any foot placement constraints (the free case); (2) while wearing the forceshoes and without any foot placement constraints (the forceshoe case); and (3) while wearing their regular work shoes and while keeping each foot within the boundaries of its respective AMTI OCR-6 force platform (Advance Mechanical Technology, Inc, Watertown Massachusetts) (the force platform case). The order of the experimental conditions was as above and remained the same for each participant to ensure that participants did not know that they would be using either the forceshoes or force platforms until it was time to use them. While this may have led to some order effects, it was felt that knowledge of the measurement systems prior to the experiment would have biased the caregivers’ actions.

The design of the forceshoes (Fig. 1) is similar to a child’s swing set. Each forceshoe consists of a rigid external aluminium frame that contacts the ground (the frame of a swing set). The subject’s foot is suspended from this external frame by a 6-axis load cell (AMTI MC3A-6-1000 (Advanced Mechanical Technology, Inc., Watertown, Massachusetts) that is coupled to a rigid internal aluminium frame (the swing). The forceshoe supports a standard running shoe 15mm above the ground.

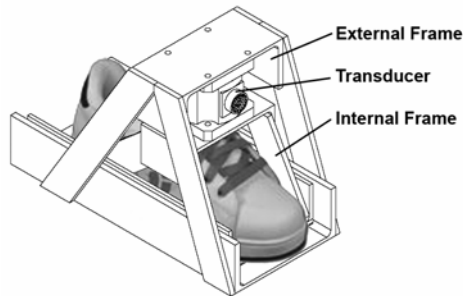


**Figure 1:** The forceshoe

This setup allows the forceshoes to collect force/moment data while minimizing the overall floor to sole height of the forceshoes. Previous results showed no significant difference between the forceshoes and the AMTI force platform system ( $p \leq 0.05$ ) (Carmichael, 2006).

## RESULTS AND DISCUSSION

Participants changed their foot placement patterns when asked to keep their feet within the boundaries of the force platforms. The foot motions for all participants were tracked and the amount of lateral (bedside) movement for each subject for each condition is shown in Fig. 2.

When foot placement was unconstrained (free case), 6 of 7 participants moved their feet significantly more than during the forceshoe ( $p \leq 0.05$ ) and force platform ( $p \leq 0.01$ ) cases. No significant difference in lateral foot movement was found between the forceshoe and force platform cases.

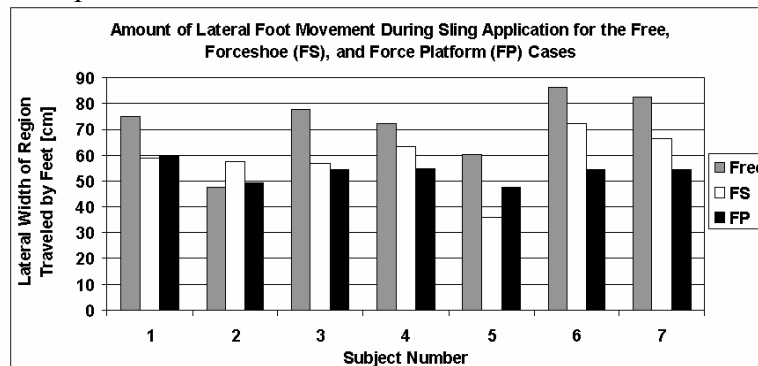


**Figure 2:** Amount of lateral foot movement for each subject for the free, forceshoe, and force platform cases during sling application.

These results suggest that modifications to the design of the forceshoes are required to observe significant impacts on movement constraints.

## SUMMARY/CONCLUSIONS

Two conclusions can be taken from these data: (1) force platforms constrain the user's feet unnaturally during bedside biomechanical tests and (2) the forceshoes still constrain movement unnaturally in their present form although they do grant users increased freedom to move beyond the boundaries of traditional force platforms and they are portable. With the design of lighter and less cumbersome portable foot force transducers, it is hoped biomechanical assessments of activities involving foot travel will be possible in the laboratory as well as in clinical environments.

## REFERENCES

- Carmichael, B. (2006). *Development and testing of a portable force sensing system* Master's Thesis, University of Toronto.
- Plamondon, A., et al. (1996). *Clinical Biomechanics*, **11**, 101-110.
- Santaguida, P. L. (2001). *Efficacy of powered mechanical lifting devices to minimize loads to the low back*, PhD Thesis, University of Toronto.
- Schibye, B., et al. (2001). *Clinical Biomechanics*, **16**, 549-559.

# ANATOMY-BASED MODEL OF NORMAL EMU DURING GAIT

Jessica Goetz,<sup>1</sup> Timothy Derrick,<sup>2</sup> Douglas Pedersen,<sup>1</sup> Duane Robinson,<sup>2</sup> Michael Conzemius,<sup>2</sup> and Thomas Brown<sup>1</sup>

<sup>1</sup> University of Iowa, Iowa City, IA, USA

<sup>2</sup> Iowa State University, Ames, IA, USA

E-mail: jessica-goetz@uiowa.edu Web: <http://poppy.obrl.uiowa.edu>

## INTRODUCTION

The emu (*Dromaius novaehollandiae*) is a large, bipedal bird that weighs an average of 40 kilograms and stands up to 2 meters tall. Because the emu is bipedal and approximates the size of a human, it is attractive for use as an animal model of human pathological conditions where load protection of the affected limb would negate the usefulness of the model.

The emu is being explored as an animal model for femoral head osteonecrosis. In human osteonecrosis, the normally round contour of the femoral head collapses due to fracture of the fragile, necrotic bone. Due to the ability to load-protect the affected limb, quadrupedal animal models of osteonecrosis do not develop femoral head collapse.

To compare the potential attractions and variations that can be expected due to gait when employing the emu as an animal model for human conditions, joint contact forces during gait should be quantified. A scaleable, anatomic emu model is important for accurate calculation of joint reaction forces during normal gait.

## METHODS

Kinematic data capture was performed on two adult emus, raised from hatchlings to be acclimated to human interaction in a gait



**Figure 1:** (Left) Anatomic locations monitored during gait analysis. (Right) Emu over the force platform during a walking trial.

laboratory setting. Eleven anatomic locations were tracked by three synchronized cameras during level walking trials over a carpeted force platform embedded in the floor (Figure 1). A third emu was euthanized and dissected to obtain lower limb muscle location and geometry. Muscle length, weight, and pennation angle were measured prior to muscle removal. Metallic screws were placed at each muscle origin and insertion during the dissection, and following dissection, each bone was placed inside a wire calibration cage for imaging by two orthogonal x-rays (Figure 2). Three-dimensional coordinates relative to bones were obtained for each muscle insertion and origin (Pedersen, 1991).

Computed tomography scans were made of each leg bone, and periosteal surfaces were

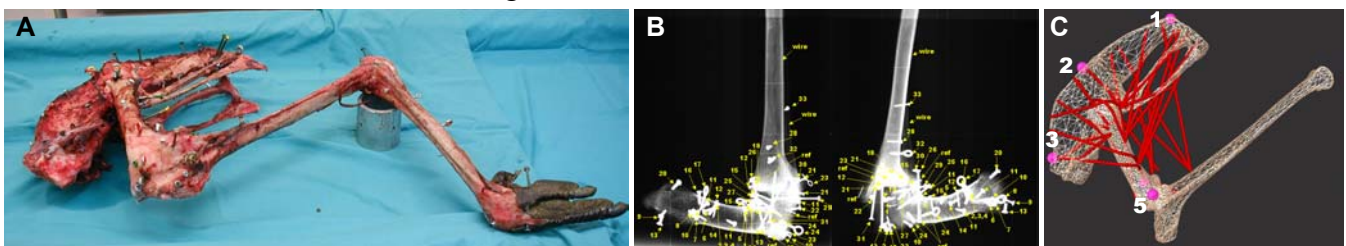


**Figure 2:** (A) Dissected limb segments with screw markers. (B) Orthogonal x-rays of screw-marked emu femur and tibia. (C) Hip musculature in the SIMM program (see Fig 1 for pink marker location).

segmented, smoothed, imported into SIMM, and assigned to a local bony coordinate system. Muscle attachments and kinematics were also imported into SIMM to determine muscle moment arms during the stance phase of gait.

Center of mass, segment length, and segment weight were measured from frozen cadaver segments taken from two additional emus. Moments of inertia and radii of gyration around each of the three principal axes were measured by torsion pendulum.

## RESULTS AND DISCUSSION

The emus used for gait analysis had body weights of 294 N and 361 N and average walking velocities of  $1.01 \pm 0.16$  m/s and  $1.39 \pm 0.27$  m/s. Hip flexion was extremely small and knee flexion much larger ( $\sim 55^\circ$ ) for both birds (Figure 3). Average hip abduction was  $18^\circ$  and decreased to  $13^\circ$  in the knee.

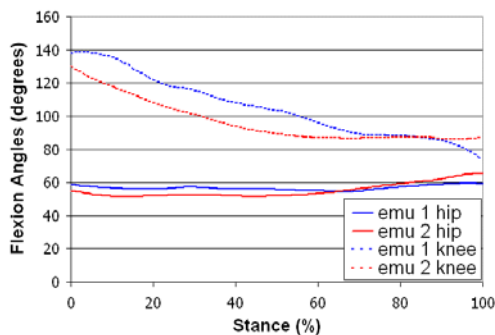


**Figure 3:** Five trial averages of flexion angles in the emu hip (solid) and the emu knee (dashed) during normal level walking.

The majority of the hip musculature was located lateral to the joint. Flexor, extensor, and abductor muscles were large and well developed. The adductor muscles were few and small.

Limb segment measurements were scaled to limb segment weight or length and averaged for the two birds (Tables 1 & 2).

**Table 1:** Selected segment measurements: segment length, weight, and moment of inertia.

Segment	Length		Weight % BW	Moment of Inertia (Kg/m <sup>2</sup> )		
	cm	in		Med/Lat	Sup/Inf	Ant/Post
Foot	19	7	0.8	0.0004	0.0001	0.0005
Tarsus	41	16	1.8	0.0093	0.0002	0.0093
Tibia	42	16	8.7	0.0306	0.0076	0.0271
Femur	25	10	7.9	0.0166	0.0090	0.0096

**Table 2:** Center of mass locations relative to joint centers as a percentage of segment length.

Segment	% of Segment	Direction on Segment
Phalangeal Segment	30	Anterior to joint center
	-7	Laterally to joint center
	33	Superior to bottom of foot
Tarsal Segment	38	Distal to hock center
	2	Medially to hock center
	32	Posteriorly to hock center
Tibial Segment	29	Distally to knee center
	24	Laterally to knee center
Femoral Segment	6	Anteriorly to knee center
	33	Distally to femoral head
	0	Anteriorly to femoral head
	34	Laterally to femoral head

## CONCLUSIONS

An anatomically scaled model of emu gait has been developed. Captured kinematics indicate small non-sagittal motions during walking gait. This model is used for calculations of joint forces and moments and subsequent comparison with human gait characteristics.

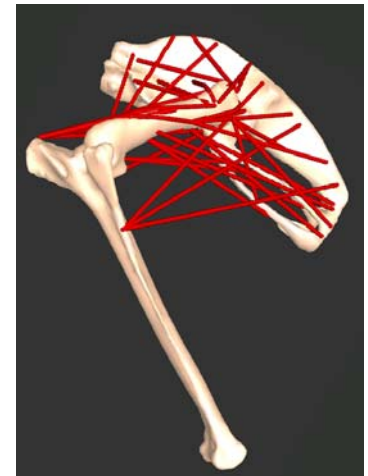


**Figure 4:** SIMM model of the emu hip and knee musculature. Each muscle is marked in red and only the pelvis, femur, and tibia are shown.

## REFERENCES

Pedersen, D.R., Feinberg, J.H., Brand, R.A. (1991). *Acta Anat* (Basel) **140**(2), 139-45.

## ACKNOWLEDGEMENTS

Funding from NIH AR 49919; Matt Frank for implementation of CT data.

# LARGE PATELLAR LIGAMENT INSERTION ANGLE FOLLOWING ACL INJURY CAUSES LARGE QUADRICEPS REDUCTION DURING WALKING

Choongsoo S. Shin<sup>1</sup>, Ajit M. Chaudhari<sup>1</sup>, Chris O. Dyrby<sup>1,2</sup>, and Thomas P. Andriacchi<sup>1,2</sup>

<sup>1</sup> Stanford University, Stanford, CA, USA

<sup>2</sup> VA Palo Alto Health Care System, Palo Alto, CA, USA

E-mail: scslove@stanford.edu Web: biomotion.stanford.edu

## INTRODUCTION

Functional adaptations in gait patterns have been observed following anterior cruciate ligament (ACL) injury. In particular, a reduction in the peak quadriceps moment has been reported following ACL injury (Berchuck, 1990). It has been suggested that reduced quadriceps contraction may be an adaptation to prevent anterior tibial translation in ACL-Deficient (ACL-D) knees. However, the level of quadriceps reduction varies between individuals (Noyes, 1992; Robert, 1999). One potential factor causing these differences may be the anatomical variations in the knee extensor mechanism, because the patellar ligament insertion angle (PLIA) determines how quadriceps force is decomposed into anterior and superior components.

This study tested the hypothesis that the reduction in peak external knee flexion moment (balanced by net quadriceps moment) of ACL-D knees compared to their contralateral knees during walking is negatively correlated to the PLIA in individuals with large PLIA, while no relationship would be observed in individuals with small PLIA.

## METHODS

Nineteen unilateral ACL-Deficient subjects (40.3±12.5 yrs, 12 male, 2~432 months past injury) were tested after IRB consent. Sagittal-plane MRIs (3D-SPGR) were taken in a supine, non-weight-bearing, fully

extended position. PLIA of the ACL-D knee was measured as the angle between the patellar ligament and the tibial shaft, as described previously (Fig. 1) (Shin, 2004). Individuals were divided into a large-PLIA group and small-PLIA group based on the median PLIA observed for all ACL-D knees.

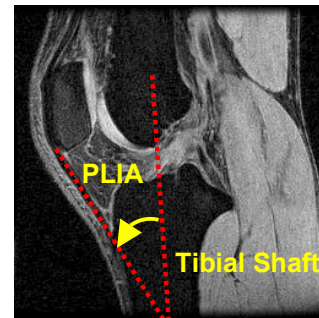


**Figure 1:** Measurement of patellar ligament insertion angle (PLIA) relative to tibial shaft.

Kinetics was measured using an opto-electronic motion capture system (Qualisys, Gothenburg, Sweden) with a force plate (Bertec, Columbus, OH) using a previously-described 6-marker link protocol (Berchuck, 1990). All subjects walked at three self-selected speeds (fast, normal, slow), three trials each. Peak external knee flexion moments (% body weight \* height) corresponding to the average walking speed (1.35m/s) were estimated from each individual's speed vs. peak knee flexion moment regression equation, since peak knee flexion moment is known to be strongly correlated with walking speed ( $R^2=0.73$ ) (Lelas, 2003). The reduction in peak knee flexion moment of ACL-D sides compared to subjects' uninjured contralateral sides was calculated. Linear

regression analysis was performed to study the relationship between PLIA ( $^{\circ}$ ) and the reduction in peak knee flexion moment for each of the two groups.

## RESULTS AND DISCUSSION

The reduction in the peak knee flexion moment was associated with an increased PLIA for subjects in the large PLIA Group (Fig. 2). In the large-PLIA group of ACL-D knees, a significant negative correlation was observed between PLIA and reduction of peak external knee flexion moment ( $R^2=0.81$ ,  $P<0.001$ ). However, in the small-PLIA group of ACL-D knees, no significant correlation was observed ( $R^2=0.03$ ,  $P=0.65$ ). The median value of PLIA was  $20.1^{\circ}$ .

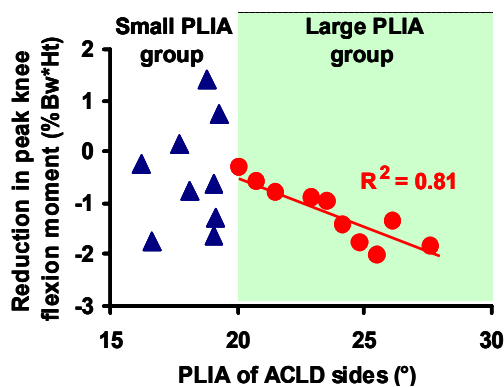


**Figure 2:** Peak knee flexion moment during walking vs. patellar ligament insertion angle (PLIA). Only the large-PLIA group ( $\bullet$ ) showed a significant correlation ( $p<0.001$ ).

The strong negative correlation in the large-PLIA group suggests that these subjects adapt their walking actively following ACL injury. As previously hypothesized (Berchuck, 1990), these patients may perceive instability due to the anterior drawer effect of quadriceps contraction. The quadriceps reduction in this group appears to be a proportional adaptation in response to needs.

In the small-PLIA group, the lack of a correlation suggests that the anterior drawer

effect of quadriceps contraction is small enough not to be perceptible to all individuals. Some may perceive instability and reduce quadriceps usage, whereas others do not. Other factors may also influence a quadriceps adaptation in this group, leading to the large variability observed.

Adapting gait by reduced flexion moment has been shown to result in a more normal tibiofemoral position (Andriacchi, 2005). Thus, this adaptation in the large PLIA group may be beneficial for reducing secondary changes in the meniscus or articular cartilage, thereby slowing down the rate of osteoarthritis following ACL injury.

## SUMMARY/CONCLUSIONS

This study has shown that the anatomy of the knee extensor mechanism provides a possible explanation for the variability previously observed in the adaptation of a quadriceps reduction strategy following ACL injury. In the future, individually-tailored treatment and rehabilitation protocols that include information about the individual's own knee extensor anatomy may improve patient outcomes.

## REFERENCES

- Berchuck, M. et al. (1990). *J. Bone Joint Surg. Am.*, **72**, 871-77.
- Noyes, F. R. et al. (1992). *AJSM*, **20**, 707-16.
- Robert, C. S. et al. (1999). *Gait & Posture*, **10**, 189-99.
- Shin, C. S. et al. (2004). *Proceedings of ASB 2004*, 525-26.
- Lelas, J. L. et al. (2003). *Gait & Posture*, **12**, 106-12.
- Andriacchi, T. P. and Dyrby, C. O. (2005). *J. Biomech.*, **38**, 293-98.

## ACKNOWLEDGEMENTS

Funding from NIH R01-AR39212.

# VALIDATION OF A PATIENT-SPECIFIC FINITE ELEMENT MODEL OF THE ANKLE

Jane Goldsworthy,<sup>1</sup> Donald Anderson,<sup>1</sup> Jim Rudert,<sup>1</sup>  
Yuki Tochigi,<sup>1</sup> Douglas Pedersen,<sup>1</sup> and Thomas Brown<sup>1</sup>

<sup>1</sup>University of Iowa, Iowa City, IA, USA  
E-mail: jane-goldsworthy@uiowa.edu

## INTRODUCTION

Patient-specific finite element (FE) modeling of the ankle has provided a unique opportunity to study the relationship between articular surface anatomy and contact stress (Anderson et al., 2006). Understanding this relationship will help elucidate the mechano-pathology of post-traumatic osteoarthritis. Validation of the FE modeling approach by comparison with measurements from a cadaveric loading test is an important step toward this objective.

## METHODS

Validation testing was performed using a fresh-frozen cadaveric ankle loaded in a custom fixture. A materials testing machine was used to apply a 600 N compressive load across the ankle, establishing a neutral loaded apposition. The ankle was transferred to a plastic mounting fixture in which the neutral loaded apposition was reproduced, and it was then CT scanned.

The ankle was returned to the materials testing machine, a high-resolution custom pressure sensor (Tekscan; Brown et al., 2004) was inserted between the tibia and talus, and the 600 N load was again applied. Two metal pins were drilled through the loaded construct and sensor, and bi-planar radiographs of the ankle and pins were obtained (Figure 1).

CT data were segmented, and the resulting surfaces were imported into a medical data visualization program (DataManager) for registration. Layers of uniform 1.5 mm thick

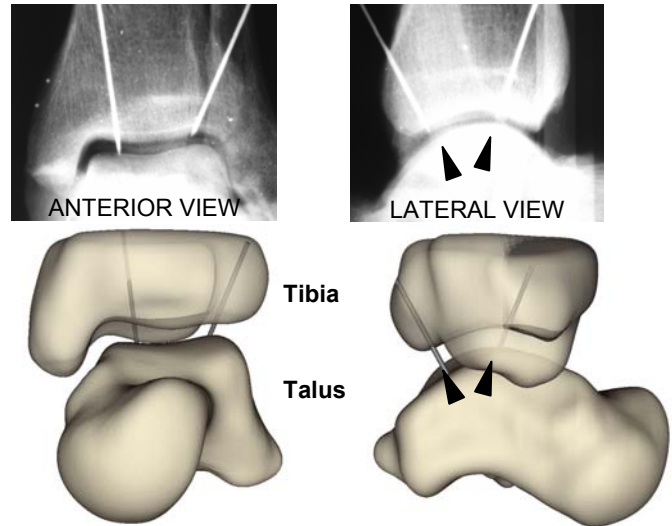


**Figure 1:** Top: anterior and lateral radiographs of loaded cadaver tibia and talus with registration pins indicated by arrows. Bottom: resulting surfaces with registration pins as placed.

articular cartilage were extruded from the distal tibia and proximal talus along surface normals. The articulating surfaces were meshed, and an FE simulation of the joint contact was carried out (ABAQUS v6.51), with boundary conditions to match the experiments. Pressure sensor geometry was imported into DataManager for registration. As the sensor had been pierced by the metal pins, its orientation relative to the bones was known, enabling registration of the datasets.

## RESULTS AND DISCUSSION

The maximum contact stresses from the pressure sensor and FE model were 3.69 and 3.86 MPa, respectively (Figure 2). Contact areas from the sensor and FE model were 295.1 and 378.6 mm<sup>2</sup>, respectively.

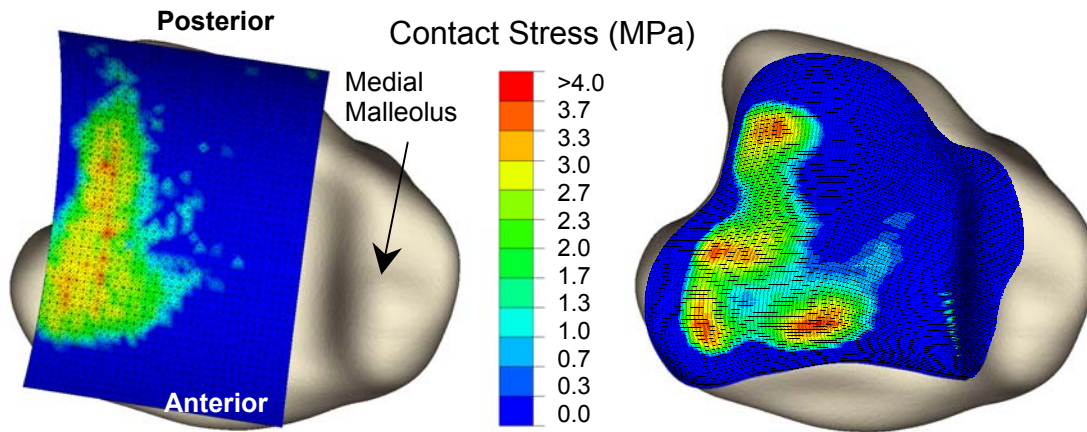


**Figure 2:** Inferior view of the tibia, overlaid with pressure sensor results (left) and FE results (right).

In addition to agreement in the magnitude of peak contact stresses, there was general agreement in the distributions of contact areas across the contact stress levels measured / predicted (Figure 3).

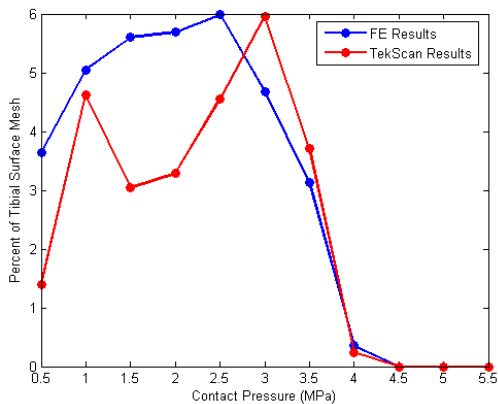


**Figure 3:** Distributions of percentage of tibial surface mesh experiencing various contact pressure values for FE and TekScan results.

While the articulating surface of the tibio-talar joint is nearly cylindrical in nature, there was no evidence of sensor crinkling artifact in the experimental testing. Since the sensor is very thin, and easily conformed to the joint, it was deemed unlikely to interfere with normal joint loading. The sensor was, therefore, not included in the FE model.

## SUMMARY/CONCLUSIONS

This preliminary validation shows reasonable agreement between experimental and computational stress results. While FE articular joint contact stress computations have occasionally been validated in terms of nominal patterns and magnitudes in the past, this is the first instance, to our knowledge, of a formal spatial registration, opening the way for objective statistical measures of regional correlation.

## REFERENCES

- Anderson, D.D. et al. (2006). *Biomech Model Mechanobiol*, [Epub ahead of print].
- Brown, T.E. et al. (2004). *Clin Orthop and Related Research*, 423, 52-58.
- DataManager, [www.tecno.ior.it/research/biomechcomp/projects/multimod/DataManager/dm\\_home.html](http://www.tecno.ior.it/research/biomechcomp/projects/multimod/DataManager/dm_home.html).

## ACKNOWLEDGEMENTS

Funded by the NIH (AR46601 & AR048939). Mr. Thaddeus Thomas and Drs. Fulvia Taddei and Marco Viceconti provided technical assistance.

# FOOT BONE MOTION DURING CIRCUMDUCTION

Michael J. Fassbind,<sup>1</sup> Eric S. Rohr,<sup>1</sup> Bruce J. Sangeorzan,<sup>1,3</sup> William R. Ledoux<sup>1,2,3</sup>

<sup>1</sup> Department of Veterans Affairs, RR&D Center of Excellence, VA Puget Sound, Seattle WA, Departments of <sup>2</sup> Mechanical Engineering and <sup>3</sup> Orthopaedics and Sports Medicine, University of Washington, Seattle, WA  
Email: wrledoux@u.washington.edu Web: <http://www.seattlerehabresearch.org>

## INTRODUCTION

There have been many studies that have quantified foot bone motion or described foot joint kinematics. Manter (1941) and Inman (1976) used mechanical methods for examining the motion of the subtalar and midtarsal joints on cadaveric feet. Lundberg *et al.* (1989) used tantalum balls and stereophotogrammy to study the motion of foot bones in response to single plane foot rotations. Stindel and Udupa *et al.* (2001) used foot MR scans to quantify hindfoot motion in response to motion about a single universal fixed axis of subtalar joint motion. Numerous other studies have used retro-reflective marker systems to study foot motion. However, due to the large number of small bones requiring multiple markers, it is difficult to accurately measure foot bone motion without invasive means or expensive CT or MR scans. Alternatively, externally mounted electromagnetic sensors can record bone motion with a single sensor. The purpose of this study was to explore the use of electromagnetic sensors to track motion of foot bones as the foot went through a range of circumduction. It is expected that this method will be a rapid, inexpensive means of quantifying foot motion.

## METHODS

Five subjects ( $53.4 \pm 4.4$  years) were enrolled in this IRB-approved study. Subjects were included if they had a neutrally aligned foot and were free of any

lower extremity pathology. Subjects were excluded if they could not self ambulate, or had a current ulcer or partial foot amputation.

Data was gathered using six sensors; five sensors placed on the foot at the tibia, calcaneus, navicular, 1<sup>st</sup> metatarsal and 5<sup>th</sup> metatarsal and one that was attached to the foot plate. After instrumenting with the electromagnetic motion sensors, the foot was moved through full circumduction three times while data were recorded with the Liberty system at 240 Hz (Figure 1). A pilot study demonstrated intra-rater differences with this method, so a single rater was used for all data collection. The sensor position data were fit with two methods. First the data were flattened to the XY plane and fit with an ellipse (Figure 2). Second, the data were ordered and evenly distributed about one loop and a 4<sup>th</sup> order Fourier series was fit to the data (Figure 3).

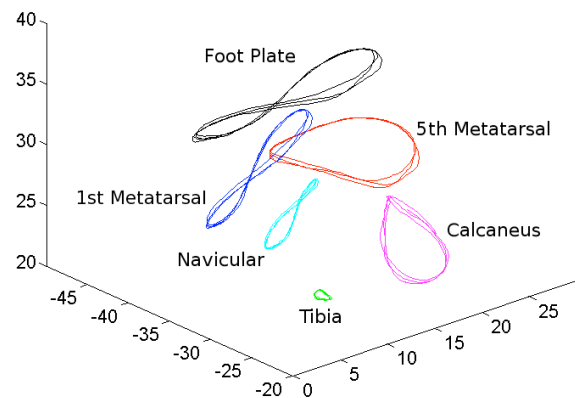


**Figure 1:** The raw data for each sensor.

The following parameters were obtained for each sensor: 1) the area of the ellipse, 2) the aspect ratio of the ellipse axes, 3) the 3D arch angle calculated from the centroid of the 1<sup>st</sup> metatarsal, navicular and calcaneus data, 4) the Z-error (the largest normal distance of any point away from the XY plane used in the ellipse fitting), and 5) the coefficients of the Fourier series expansion. Note that area, major axis, minor axis and Z-error were all normalized by foot length; the numbers presented are unitless.

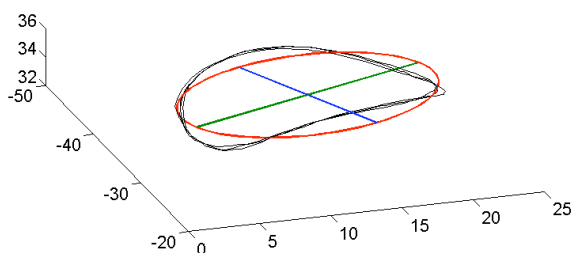


**Figure 2:** The ellipse fit (red line) of the circumduction data (black lines). green line = major axis, blue line = minor axis

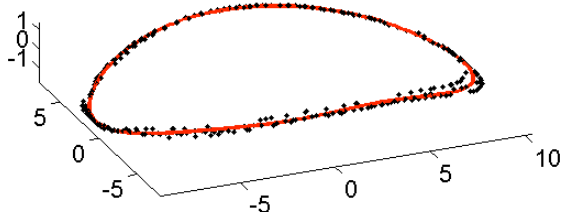


**Figure 3:** The Fourier fit (red line) of the circumduction data (black dots).

## RESULTS AND DISCUSSION

The foot plate, as expected, had the largest ellipse area (0.369), followed by the 1<sup>st</sup> metatarsal (0.195), 5<sup>th</sup> metatarsal (0.186), calcaneus (0.53), navicular (0.034) and finally the tibia (0.002), which was fixed. In general, the short axes were more variable between subjects than the long axes. The coefficient of variation of the short axis (foot plate: 0.153, calcaneus: 0.103, tibia: 0.195, 1<sup>st</sup> metatarsal: 0.210, 5<sup>th</sup> metatarsal: 0.089 and navicular: 0.387) was greater than

the long axes (foot plate: 0.073, calcaneus: 0.104, tibia: 0.201, 1<sup>st</sup> metatarsal: 0.090, 5<sup>th</sup> metatarsal: 0.074 and navicular: 0.098) with the exception of the calcaneus and the tibia. The 3D arch angle measurement from our five initial subjects was  $135.4 \pm 5^\circ$ . Further, the Z-error followed the same trend as the ellipse area, except the calcaneus and navicular were switched. Finally, for the five initial data sets a 4<sup>th</sup> order fit was found to be the minimum order resulting in a fit with less than a 1% root mean square (RMS) error. Excluding the zero<sup>th</sup> fit level (DC component) this fit resulted in 24 coefficients for each sensor or 144 coefficients per subject.

## SUMMARY/CONCLUSIONS

While previous studies have focused primarily on foot motion during gait or motion in a single plane at a time, this work allowed for subject specific measurement of maximum range of motion. Rather than a motion analysis laboratory, we only required an electromagnetic motion analysis system. The motion of the foot bones was quantified with a small number of parameters allowing for comparison between bones in the same foot or between subjects.

## REFERENCES

- Manter J.T., (1941). *Anat. Rec.* 80: 397.
- Inman V., (1976). *The Joints of the Ankle*, Williams & Wilkins Co.
- Lundberg A., (1989). *Acta. Orthop. Scand*, 60, suppl 233.
- Stindel E., *et al.*, (2001). *IEEE Trans. on Medical Imaging*, 48(2).

## ACKNOWLEDGEMENTS

This work was supported in part by the Dept. of Veterans Affairs, RR&D Service grant numbers A2661C and A3030R.

# METHOD FOR MOTION TRACKING INSIDE THE LOKOMAT ROBOTIC ORTHOSIS

Nathan D. Neckel<sup>1</sup> and Joseph M. Hidler<sup>1,2</sup>

<sup>1</sup> Catholic University of America, Washington, DC, USA

<sup>2</sup> National Rehabilitation Hospital, Washington, DC, USA

E-mail: 06neckel@cua.edu Web: <http://cabrr.cua.edu>

## INTRODUCTION

Motion tracking systems are readily used by researchers to track the position of limb segments in space. These systems rely on the placement of markers directly onto the subjects limbs, and that these markers are visible from the recording cameras. This system becomes less convenient when subjects need the use of assistive devices that can block the markers. One such device, the Lokomat robotic orthosis (Colombo et al., 2000), allows for even the most impaired subjects to ambulate on a treadmill. However, tracking the motion of patients inside the Lokomat has proven difficult due to the robotic limbs obscuring the markers from view and the straps around the subject's limbs that hold them in the device leave little room to attach motion tracking markers. Presented here is a method to track the kinematics of a subject's lower limbs as they walk with the aid of the Lokomat robotic orthosis with a motion tracking system.

## METHODS

In order to track the limb segments, groups of four or more markers need to be rigidly attached to the limb segments and any three markers must be seen by the camera at all times. To facilitate experimental set-ups reusable clusters of four markers were designed for each limb segment. A Codamotion motion analysis system (Charnwood Dynamics LTD, UK) was used to track limb position in the Lokomat.

### Thigh Clusters

The clusters used to track the thigh segment were composed of two parts; a base that would slip under the Lokomat leg cuffs, and a cap that would mount on top of both the base and cuff strap. The base was constructed from two layers of 3mm thick Aquaplast thermoplastic cut in the shape of the letter "I", melted together and slightly curved to match the contour of the limb segments. A 2cm thick layer of foam padding on the underside provided comfort and a tighter fit onto the limb segment. When the Lokomat leg cuffs were properly tightened over the narrow portion of the cluster base, the top and bottom of the base provided tabs to mount the caps onto (Figure 1 A). These tabs had eyelits carved into them so additional straps could be tightened around the subjects leg. The caps were similarly constructed from 2 layers of 3mm thick Aquaplast thermoplastic melted together and curved. However the caps were rectangular in shape and had a raised center to account for the thickness of the



Fig 1A. Cluster base

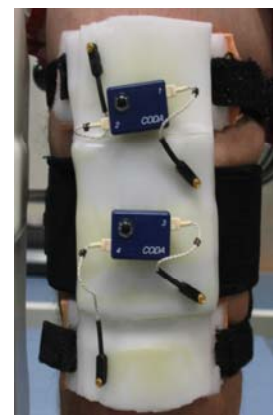


Fig 1B. Cluster cap

Lokomat cuff straps. The loop end of Velcro tape was fixed on the base tabs and the hook end was placed on the corresponding underside of the caps. Hook end Velcro straps were also fixed to the underside of the cap that contacts the Lokomat cuff strap to provide additional security to the subject's thigh. Motion tracking markers were attached to the top face of the cap which was securely fixed onto the base (Figure 1B).

### Shank Clusters

Clusters to track the movement of the shank segment were constructed in a very similar fashion. Instead of an "I" shaped base a thinner, elongated "T" shaped base was used. This base was longer so it could slip under both the upper and lower Lokomat shank cuffs and the bottom tab was removed to accommodate for the variability in shank cuff spacing. The shank cluster cap had two raised sections for both cuff straps. On the shank cluster base loop end Velcro tape was fixed to the upper tab and the region between the two cuff straps. Likewise, hook end Velcro straps were fixed to the corresponding underside of the shank cluster cap as well as the raised surfaces that contacted the Lokomat cuff straps.

## RESULTS AND DISCUSSION

A healthy male subject was tracked as he walked inside the Lokomat at 2.5 km/h. The subject's mean left hip angle and the Lokomat mean left hip angle in the sagittal plane are plotted in Figure 2. Throughout each step the angular difference between the subject's thigh and Lokomat thigh in the sagittal plane was calculated. Figure 3 shows the mean angular difference (with 95% confidence interval) of 14 consecutive steps over the gait cycle.

This data demonstrates that when subjects ambulated inside the Lokomat robotic

orthosis, substantial leg motion occurs within the device, and that this motion is consistent across the gait cycle.

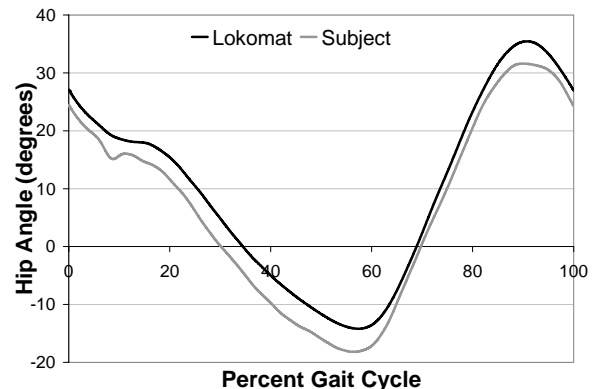


**Fig 2.** Mean hip angle of both the Lokomat and subject over the gait cycle.

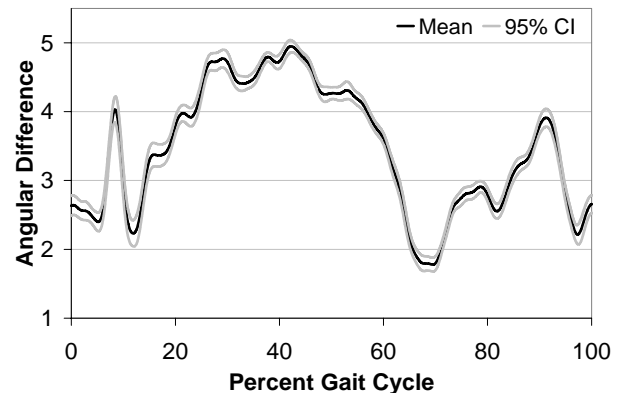


**Fig 3.** Mean angular difference between the Lokomat thigh and the subjects thigh over the gait cycle.

## SUMMARY/CONCLUSIONS

With the re-usable motion tracking marker cluster design presented here, it is possible to accurately track the motion of a subject's lower limbs in space as they walk on a treadmill with the help of the Lokomat robotic orthosis. This allows researchers to perform a wide range of additional experiments with the Lokomat robotic orthosis.

## REFERENCES

- Colombo, G., Joerg, M., Schreier, R., Dietz, V. Treadmill training of paraplegic patients using a robotic orthosis. *J Rehabil Res Dev.* Vol. 37, pp. 693-700, 2000.

# RISK FACTORS FOR LOW-BACK INJURY DURING DEPENDENT TRANSFERS ON AN AIRCRAFT

Brian Higginson, Lisa Welsh, and Michael Pavol

Oregon State University, Corvallis, OR, USA  
E-mail: mike.pavol@oregonstate.edu

## INTRODUCTION

The ability for people with disabilities to travel by commercial aircraft is important for their full participation in society, but poses challenges to airline and airport personnel. An area of great concern, from an ergonomics standpoint, is the process of transferring a traveler with disabilities between a wheelchair and an aircraft seat when the traveler is unable to do so. Such dependent transfers place the transferors at risk of a disabling injury to the lower back, a risk that may be increased on board aircraft due to the confined space in which the transfer takes place. This study investigated the effects of transferee size and spatial constraints on kinematic risk factors for low-back injury during transfers on an aircraft.

## METHODS

Thirty-three pairs of men ( $n = 42$ ) and women ( $n = 24$ ) worked to transfer two anthropometric dummies between a wheelchair and an airplane seat using a “front-and-rear” transfer technique (Pelosi & Gleeson, 1988). The mean  $\pm$  SD age, mass, and height of the subjects were  $24.1 \pm 6.4$  yr,  $68.8 \pm 13.3$  kg, and  $172.0 \pm 9.4$  cm, respectively, for the front transferors, and  $23.6 \pm 4.2$  yr,  $78.0 \pm 13.7$  kg, and  $178.0 \pm 7.7$  cm for the rear transferors. Informed consent was provided.

The transfers were performed in a laboratory simulation of an aircraft interior. A standard economy-class airplane seat was mounted to

the floor with the armrests raised. An aircraft aisle wheelchair was placed side-by-side with the seat. A small (mass: 57 kg; height: 165 cm) and a large (mass: 78 kg; height: 178 cm) anthropometric dummy served as the transferee. Removable frames were utilized to simulate the spatial constraints imposed by the surrounding rows and aisles of seats and overhead bins.

After instruction, warm-up, and practice, subjects transferred each dummy once for each transfer direction (wheelchair-to-seat, seat-to-wheelchair) under unconstrained and constrained conditions. Transfer positions were self-selected and remained the same. The trajectories of 74 reflective markers attached to the subjects and the dummy were recorded at 60 Hz by a motion capture system, and low-pass filtered at 8 Hz.

Dependent measures computed from the marker data consisted of those found by Marras et al. (1995) to increase the risk of low-back injury during lifting tasks. These included peak lumbar (i.e. trunk vs. pelvis) angles ( $\theta$ ) and angular velocities ( $\omega$ ), and the peak load moment arm. Load moment arms were computed as the horizontal distance between a “lumbar joint center” at L<sub>3</sub>L<sub>4</sub> and either a marker on the chest of the dummy for the rear transferor or the point directly between both wrists for the front transferor. Three-way repeated measures ANCOVA were used to test the effects of dummy size, constraint, and transfer direction on the dependent variables, with the height of the transferor used as a covariate. Effects were considered significant at  $\alpha < .05$ .

## RESULTS AND DISCUSSION

Transferee size influenced the lumbar kinematics of both transferors (Table 1). Notably, flexion in the rear transferor was greater for the small dummy, likely due to its stature. In contrast, flexion and lateral bending velocities in the front transferor were greater for the large dummy.

The constraints imposed by the aircraft interior had the greatest effect on the front transferor, resulting in greater peak flexion, bending, and twisting (Table 2). These differences, resulting from the need to reach around the row of seats in front, are all consistent with increased risk of injury. Transfer direction affected only the flexion velocity of the rear transferor ( $p < 0.001$ ).

Taller transferors exhibited larger load moment arms, regardless of transfer position ( $p < 0.001$ ; Figure 1). Shorter rear transferors bent faster laterally and twisted both farther and faster. Among the effects observed, the increases in moment arm would increase injury risk the most (Marras et al., 1995).

## SUMMARY/CONCLUSIONS

The results indicate that transferee size, the spatial constraints imposed by the aircraft interior, and transferor height all affect the risk of low-back injury during transfers of travelers with disabilities on an aircraft. These factors appear to affect the front transferor to greater degree. Interventions should be developed to address these risks.

## REFERENCES

- Pelosi, T., Gleeson, M. (1988). *Illustrated transfer techniques for disabled people*. Melbourne: Churchill Livingstone.
- Marras, W.S., Lavender, S.A., Leurgans, S.E., et al. (1995). *Ergonomics*, **38**, 377-410.

**Table 1:** Effects of dummy size on peak lumbar angles and velocities (Mean  $\pm$  SD).

	Small	Large
Rear transferor:		
$\theta_{\text{FLEXION}}$ (deg) <sup>†</sup>	60.5 $\pm$ 9.7	55.3 $\pm$ 10.1
$\theta_{\text{LAT.BEND}}$ (deg) <sup>*</sup>	7.4 $\pm$ 2.7	8.3 $\pm$ 2.4
$\omega_{\text{EXTENSN}}$ (deg/s) <sup>*</sup>	28.8 $\pm$ 8.7	25.4 $\pm$ 8.1
Front transferor:		
$\theta_{\text{BEND}}$ (deg) <sup>*</sup>	7.9 $\pm$ 2.8	8.7 $\pm$ 2.8
$\omega_{\text{FLEXION}}$ (deg/s) <sup>*</sup>	19.8 $\pm$ 6.9	22.3 $\pm$ 6.7
$\omega_{\text{LAT.BEND}}$ (deg/s) <sup>†</sup>	18.9 $\pm$ 6.9	23.3 $\pm$ 10.4

<sup>\*</sup>  $p < 0.05$ ; <sup>†</sup>  $p < 0.001$

**Table 2:** Effects of spatial constraints on peak lumbar angles (Mean  $\pm$  SD).

	Unconstr.	Constrained
Rear transferor:		
$\theta_{\text{FLEXION}}$ (deg) <sup>*</sup>	57.1 $\pm$ 10.1	58.6 $\pm$ 10.0
Front transferor:		
$\theta_{\text{FLEXION}}$ (deg) <sup>†</sup>	55.9 $\pm$ 15.4	63.4 $\pm$ 12.6
$\theta_{\text{LAT.BEND}}$ (deg) <sup>†</sup>	6.6 $\pm$ 2.0	10.0 $\pm$ 4.0
$\theta_{\text{TWIST}}$ (deg) <sup>†</sup>	3.8 $\pm$ 1.5	4.9 $\pm$ 2.3

<sup>\*</sup>  $p < 0.05$ ; <sup>†</sup>  $p < 0.001$

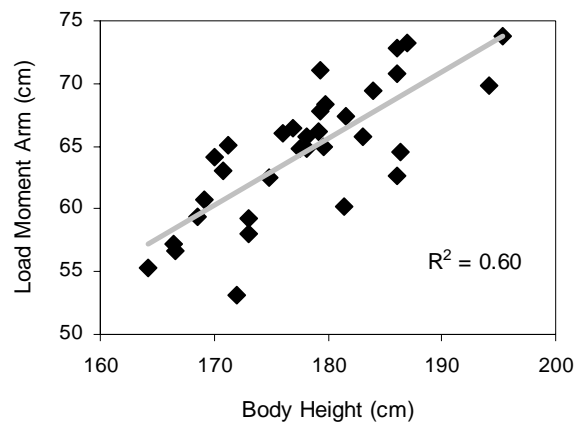


**Figure 1:** Relationship between rear transferor height and load moment arm.

## ACKNOWLEDGEMENTS

Funded by grant H133E030009 from the U.S. Dept. of Education, NIDRR.

# ESTIMATION OF JOINT MOMENTS DURING GAIT USING NEURAL NETWORKS

Michael E. Hahn, Joshua R. Allen and Katie B. O'Keefe

Movement Science Laboratory, Montana State University, Bozeman, MT, USA  
E-mail: mhahn@montana.edu

## INTRODUCTION

A number of studies have used surface electromyography (EMG) with Hill-based models to estimate joint forces and moments during gait (Hof et al, 1987; Olney and Winter, 1985; Bogey et al., 2005). Currently, these models are not well applied in the general clinical environment, specifically in rural settings, perhaps due to expense and space requirement of key equipment and the need for specially-trained technical staff. A model is needed for joint moment estimation which would facilitate the application of current joint dynamics research in general clinical practice. The purpose of this study was to develop a model for estimating joint moments of the hip, knee and ankle during normal gait using easily measured gait descriptors as model input. A set of artificial neural networks (ANNs) were used for this purpose.

## METHODS

Nineteen healthy young adults (12 female / 7 male; 22.3yrs, 173.7cm, 72.0kg) performed a series of walking trials at self-selected speed. Muscle activation was recorded using passive surface EMG collected at 1000Hz from the gluteus medius, gluteus maximus, biceps femoris, rectus femoris, vastus lateralis, medial gastrocnemius, and tibialis anterior using the Myopac Jr. (Run Technologies, Inc., Mission Viejo, CA). EMG signals were bandwidth filtered (10-1,000Hz), full wave rectified and enveloped with a 4<sup>th</sup> order Butterworth filter (low pass cutoff = 5Hz). Processed EMG signals were normalized for

each gait cycle to the maximal activation occurring within that cycle.

Three-dimensional marker trajectory data were collected at 200Hz using a six-camera digital capture system (Vicon 460; ViconPeak, Inc., Lake Forest, CA), and smoothed using Woltring filtering (MSE = 30). Virtual marker positions were estimated to represent internal segment endpoints from the external markers, and the relative positions of the segmental centers of mass based on the Plug-In Gait software (ViconPeak).

Ground reaction force data were synchronized with the motion capture and collected at 1000Hz using two force platforms (AMTI, Watertown, MA) embedded into the walkway. The center of pressure position was computed for each stance foot based on the three measured components of the resultant GRF and three components of the moment about the origin of the force platform. Three-dimensional resultant joint moments were then calculated for the ankle, knee and hip using the inverse dynamics approach.

Three unique 3-layer ANNs (one each for hip, knee, ankle) were designed to estimate joint moments for every point of a time-normalized gait cycle. The input layer consisted of subject-specific demographic (age, gender) and anthropometric data (body height, body mass, segmental moments of inertia), normalized/filtered EMG, and joint kinematics (position, velocity, acceleration). The middle layer consisted of a variable number of hidden units (5 – 30). The output

layer contained one unit representing joint moment data. Back-propagated error correction was conducted with a Levenberg-Marquardt algorithm. Training data proportion was set to 0.7, and the training error goal was tested for settings of 0.1 and 0.01. The ANNs were trained until the error goal was met, or until 1000 epochs. Bootstrap re-sampling (50 training attempts) was used for model validation.

## RESULTS AND DISCUSSION

With all complete trials from each subject, over 7,500 cases were entered for ANN training/testing. Results were promising, with joint moment prediction reaching R-values greater than 0.94 for the hip, knee and ankle when the error goal was set at 0.1., and greater than 0.97 when the error goal was set to 0.01 (Figure 1). Increasing the number of hidden units resulted in greater model accuracy, especially with an error goal of 0.01.

ANN training time (# of epochs) increased to the point of non-convergence for all joint models when the error goal was 0.01 (Table 1). This indicates that while producing highly fit training sessions, the end results may not be as accurate when generalized to a broader population.

## SUMMARY/CONCLUSIONS

These results show initial success in estimating joint moments during gait with ANN models. Further validation of these model estimates will involve time domain analysis of case-specific outcomes in laboratory and clinical settings.

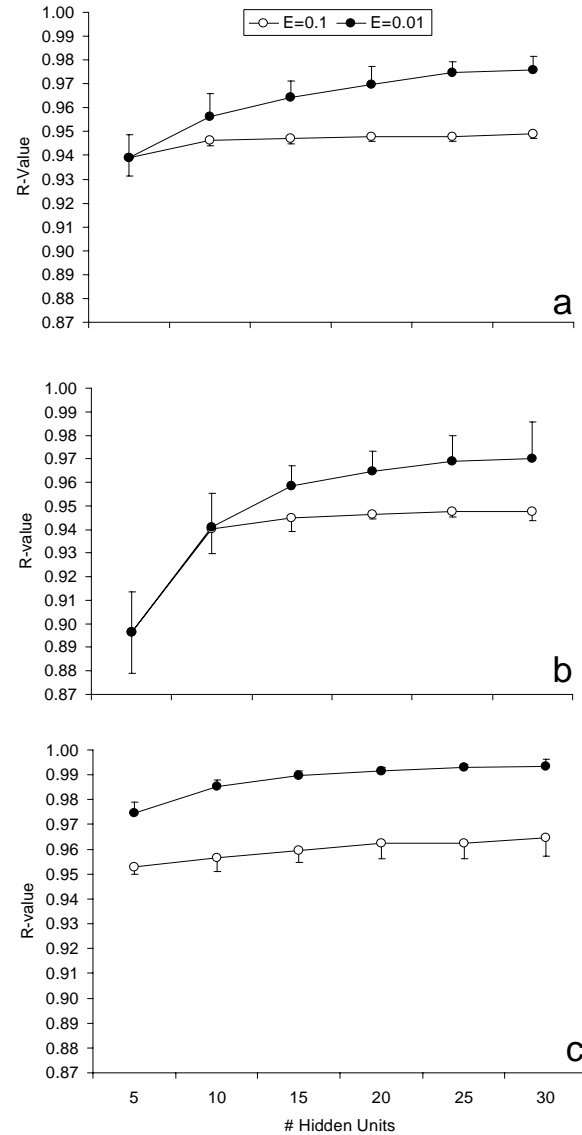


**Figure 1:** Correlation coefficients of the hip (a), knee (b) and ankle (c) models.

## REFERENCES

- Bogey, R.A. et al. (2005) *IEEE Trans Neural Syst Rehabil Eng*, **13**, 302-310.  
Hof, A.L. et al. (1987). *J Biomech*, **20**, 167-178.  
Olney, S.J., Winter, D.A. (1985) *J Biomech*, **18**, 9-20.

**Table 1:** ANN training time for hidden units of 10, 20 and 30; Mean epochs.

Error Goal	Hip			Knee			Ankle		
	10	20	30	10	20	30	10	20	30
<b>0.1</b>	240	15	12	696	37	46	7	7	6
<b>0.01</b>	1000	1000	1000	998	1000	1000	1000	1000	463

# Hand Digit Control in Children: Age-related Changes and Flexion-Extension Differences in Digit Interaction during MVC Tasks

Jeffrey Hsu, Marcio Oliviera, Jane E. Clark, Jae Kun Shim

University of Maryland, College Park, MD, USA

E-mail: [jkshim@umd.edu](mailto:jkshim@umd.edu) Web: [www.hhp.umd.edu/KNES/faculty/jkshim/neuromechanics](http://www.hhp.umd.edu/KNES/faculty/jkshim/neuromechanics)

## INTRODUCTION

Everyday manipulation tasks require some level of independency among hand digits (Mason and Salisbury, 1985; Murphy, 2000) and their synergical actions (Shim et al., 2005a,b). However, it has been documented that humans are incapable of complete independent control of individual digits. Humans can neither move a single digit without affecting the others (Li et al., 2004; Schieber and Santello, 2004) nor produce one digit force without producing forces with the other digits (Li et al., 1998b; Reilly and Hammond, 2000b).

There are both biomechanical and neural factors contributing to this observed incapacity for independent digit control. The biomechanical factors include anatomical connections of hand and forearm and neural factors, including interdependent digit control by the CNS due to overlapping digit representation in the hand area of the primary motor cortex, synchronous firing of cortical cells, and common neuronal input to multiple muscles (Bremner et al., 1991; Matsumura et al., 1996).

Although there have been many studies on finger independency, our knowledge on how it changes with children's development is largely limited. The experimental paradigm of the previous studies was also limited to finger flexion without proper consideration of finger extension.

The aims of this study is to investigate (1) age-related changes and (2) flexion-

extension differences in maximum voluntary force (MVF) production and finger interaction indices such as finger inter-dependency, force sharing, and force deficits.

## METHODS

Twenty-five typically developing children (ages 6-10 with 5 in each age group) participated in this study. The Movement Assessment Battery for Children (MABC) (Henderson and Sugden, 1992) was used as the main exclusion criteria. All children scored above or equal to the 20<sup>th</sup> percentile on the MABC and were right-handed in their daily tasks (e.g. brushing teeth, using fork, and writing).

The experimental setup included four one-dimensional piezo-electric sensors (for the 2<sup>nd</sup>-5<sup>th</sup> digits) attached to a customized aluminum frame which has four slits for the sensor positions to match the individual hand sizes of subjects (Figure 1). C-shaped thimbles were attached inferior to the sensor for subjects to insert their finger tips. The frame was tilted at 25° with respect to the anterior-posterior axis, such that the finger joints were slightly flexed when the distal phalange was inserted into the thimble. Signals from the sensors were amplified, conditioned and digitized at 1000 Hz with a 16-bit A/D Board and a customized LabVIEW program. MatLab programs were written to process and analyze data.

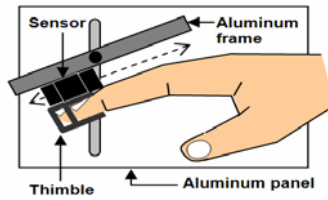


Figure 1. Experimental setup

All subjects sat facing a computer with the forearm resting in a customized wrist-forearm brace. The subjects were instructed to produce maximal voluntary forces (MVF) with five conditions (index-I, middle-M, ring-R, little-L, and four finger- IMRL) in two directions (flexion and extension). Finger interaction measures including force enslaving (FE: unintended finger forces produced by non-instructed fingers during force production of an instructed finger), force deficit (FD: force difference between single finger MVF and the force of the same finger at four-finger MVF), and force sharing (FS: percentage contributions of individual finger forces to the total force at four-finger MVF) were calculated.

## RESULTS

The results showed that 1) MVF increased with age, 2) FE decreased with age, 3) there was greater change in flexion than extension for MVF and FE (as shown by the slopes in Figure 2), 4) MVF and FD were larger in flexion than extension, 5) FS patterns were similar across age but different for flexion and extension (Figure 3).

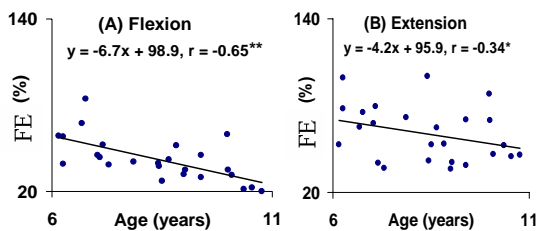


Figure 2. Finger force enslaving *FE* showed decreases with age for both flexion and extension, indicating increases in digit independency.

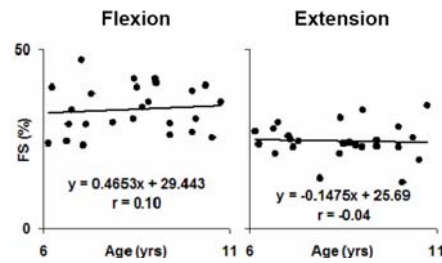


Figure 3. Finger force sharing remains constant across age

## CONCLUSION

The results provide evidence to conclude that (a) the development of finger strength and independency increase with age, while being more evident in flexion than in extension, (b) finger strength and finger independency is greater in flexion than in extension, and (c) force sharing patterns remain constant with age.

## ACKNOWLEDGEMENTS

NIH Grant-R01HD42527 to J. E. Clark

## REFERENCES

- Bremner FD, Baker JR, Stephens JA (1991) *J Neurophysiol* 66:2072-2083.
- Henderson SE, Sugden DA (1992) *Movement Assessment Battery for Children*. The Psychological Corporation, London
- Li ZM, Dun S, Harkness DA, Brininger TL (2004). *Motor Control* 8:1-15.
- Li ZM, Latash ML, Newell KM, Zatsiorsky VM (1998b). *Exp Brain Res* 122:71-78.
- Mason MT, Salisbury KJ (1985). Cambridge, MA: *MIT Press*.
- Matsumura M, Chen D, Sawaguchi T, Kubota K, Fetz EE (1996) *J Neurosci* 16:7757-7767.
- Reilly KT, Hammond GR (2000a). *Neurosci Lett* 290:53-56.
- Schieber MH, Santello M (2004). *J Appl Physiol* 96:2293-2300.
- Shim, JK, Latash ML, Zatsiorsky VM (2005). *J Neurophysiol* 93: 766-776.
- Shim, JK, Latash ML, Zatsiorsky VM (2005). *J Neurophysiol* 93: 3649-3658.

# MODELING CONTROL AND DYNAMICS OF ACTIVITIES INVOLVING IMPACT

Joseph Munaretto<sup>1</sup>, J.L. McNitt-Gray<sup>1,2,3</sup>, and Henryk Flashner<sup>4</sup>

<sup>1</sup>Department of Biomedical Engineering, <sup>2</sup>Kinesiology, <sup>3</sup>Biological Sciences

<sup>4</sup>Aerospace and Mechanical Engineering

University of Southern California, Los Angeles, CA, USA

E-mail: munarett@usc.edu

## INTRODUCTION

During weight bearing activities, humans implement control strategies that take advantage of inherent features of the musculoskeletal system and contact surface. Characterizing how individuals control reaction forces during the impact phase immediately after contact provides insight into how humans regulate external forces associated with injury. Human motion is representative of the ongoing interaction between the musculoskeletal system, the nervous system, and the environment. Modeling how an individual anticipates and controls the reaction force during activities involving impact allows us to simulate movements and independently modulate variables that cannot be manipulated experimentally.

Experimental evidence indicates that humans performing landings do not behave as rigid bodies in that segment motion and muscle control activity are both observed both prior to and during contact. One way of modeling this is to represent the human body as a system comprised of segments connected by joints. Some models represent each body segment as a rigid segment visco-elastically coupled with wobbling masses. Wobbling masses have been incorporated to account for soft tissue motion relative to the bones and as a means of improving the agreement between simulated and experimentally measured reaction forces. Other models incorporate nervous system control logic which regulates segment motion via joint torques. Both modeling

approaches improve the match between simulated and experimentally measured reaction force time histories. However, inclusion of nervous system control law motivated by experimental results is expected to reflect regulation of reaction forces observed during diverse landing conditions

## METHODS

A four segment dynamic model of the human body was created using a dynamic simulation software package (MSC ADAMS). Each segment was modeled as two rigid bodies representing bone and soft tissue connected at their centers of mass by a pair of nonlinear and torsion spring-damper assemblies (Gruber et al. 1998).

Foot-first drop landings were simulated from a height of 0.5 m using three different models. First, the body segments were modeled using wobbling mass model parameters found in literature (Gruber et al. 1998). Next, the body segments were modeled as essentially rigid links in that the stiffness of the spring-dampers assemblies between rigid bodies of each segment was increased by 5 orders of magnitude. Finally, a model of the neuromuscular control during the flight phase, represented by torques at the hip and knee, was incorporated with the rigid link version of the model. Vertical ground reaction forces were computed and kinematics of the system were compared.

Experimental drop landings were performed by a subject (n = 1) from a height of 0.5 m.

The subject was instructed to land as soft as possible and as hard as possible. Three trials of each task were performed. Sagittal motion (200 Hz), ground reaction forces (1200 Hz), and electromyographic (1200 Hz) of the gluteus maximus, semitenosus, rectus femoris, and soleus were recorded.

## RESULTS AND DISCUSSION

Peak vertical reaction forces simulated using the wobbling mass and the torque-controlled model resulted in comparable results (Figure 1) that were approximately 50% less than determined using the (~ rigid link) model. Reduction of force compares favorably with previous model simulations (Gruber et al. 2001; McNitt-Gray et al., 2004) and experimental results (McNitt-Gray et al. 2001). The similarity in the magnitude of peak reaction force observed between wobbling mass and torque control models illustrates that modification of either soft tissue stiffness or joint torques can achieve this reduction in force.

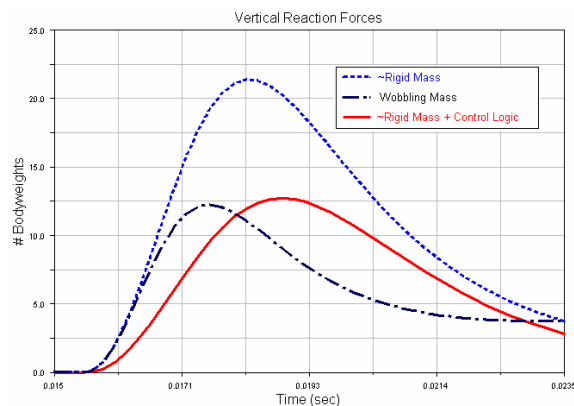


**Figure 1:** Vertical ground reaction forces under 3 simulation conditions

Experimental results also demonstrated the ability of a recreational athlete to reduce the magnitude of the peak vertical reaction force by 60% by simply choosing to land as hard or as soft as possible. Difference in segmental motion was observed pre-contact and during peak vertical force. EMG results

indicated pre-contact muscle activation of all recorded muscles as well as differences in activation levels between soft and hard landings. These results provide experimental evidence that both feedback and feedforward control are being applied by the nervous system to regulate the reaction force during landings.

## SUMMARY/CONCLUSIONS

These experimental and modeling results indicate that a physiologically relevant model of human body behavior during the impact phase of landings warrants inclusion of control logic, particularly when modeling landing performance under diverse conditions (e.g. hard, soft). Future work will model flight phase control logic based on muscle activation patterns used by individuals use to regulate reaction forces during impact.

## REFERENCES

- K. Gruber, H. Ruder, J Denoth, & K. Schneider, 1998. A comparative study of impact dynamics: wobbling mass model versus rigid body model. *Journal of Biomechanics* 31, 439-444
- J.L. McNitt-Gray, D.M. Hester., W. Mathiyakom, & B.A. Munkasy, 2001. Mechanical demand and multijoint control during landing depend on orientation of the body segments relative to the reaction force. *J Biomech*, 34(11), 1471-1482
- J.L. McNitt-Gray, 2000. Subject specific coordination of two- and one-joint muscles during landings suggests multiple control criteria [comment]. *Motor Control*, 4(1), 84-88
- J.L. McNitt-Gray, P.S. Requejo, H. Flashner, & L. Held, 2004. Modeling the Musculoskeletal Behavior of Gymnasts During Landings on Gymnastics Mats.

# VALIDITY OF HAND-HELD HEEL PAD INDENTOR FOR DETERMINING HEEL PAD PROPERTIES

Daniel J. Gales<sup>1,2</sup> and John H. Challis<sup>1</sup>

<sup>1</sup> Biomechanics Laboratory, Department of Kinesiology, The Pennsylvania State University, University Park, PA, USA

<sup>2</sup> Lock Haven University of Pennsylvania, Lock Haven, PA, USA

E-mail: djg153@psu.edu

## INTRODUCTION

The heel pad is composed of fat globules enclosed by fibrous septa designed to cope with impact loading (Jahss et al., 1993). The orientation of the collagen framework allows the heel pad to quickly respond and become stiffer on impact to adapt to applied forces (Spears and Miller-Young 2006).

Heel pad properties have been measured using a variety of techniques including pendulum tests (Aerts 1995), drop testing (Kinoshita et al., 1993) and servo-hydraulic testing (Bennett and Ker 1990). These methods give different results, and are not generally applicable in live populations particularly when soft tissue motion can corrupt estimates of heel pad properties (Pain and Challis, 2001). Many of these problems were overcome by the device designed by Rome and Webb (2000), which is a hand-held indentation device. However, as highlighted by Spears and Miller-Young (2006) different methods of measurement on the same heel pad yield different estimates of heel pad mechanical properties.

This study examines the validity, using cadaver heel pads, of the hand-held indentation device for determining the mechanical properties of human heel pads. The purpose of this study was to compare the mechanical properties of heel pads in cadaver specimens using a servo-hydraulic compression device and a hand-held indentation device.

## METHODS

Eight fresh-frozen cadaver feet were obtained from eight cadaver specimens, and thawed before all procedures. All tissues superior to a 45 mm horizontal line marked on the foot above the uncompressed heel were removed using blunt dissection. Heel pads remained fixed to the calcaneus and the foot and toes and overlying skin remained intact throughout the testing procedures.

The mechanical properties of all specimens were determined using both a hand-held heel pad indentation device, and servo-hydraulic testing apparatus. The heel pad load-deformation data were fitted with the following equation (Fung, 1967),

$$F = k_2 \cdot (e^{k_1 \cdot x} - 1)$$

where F - force causing deformation,  $k_1$ ,  $k_2$  - model coefficients, and  $x$  - amount of deformation. The model coefficients were computed using the Levenberg-Marquardt non-linear least squares algorithm (More, 1977).

The hand-held heel pad indentation (HHI) device was constructed similar to the device described by Rome and Webb (2000). The operator axially loaded the heel pads at an approximate frequency of 0.1 Hz. The diameter of the indenter head was 6 mm.

Dynamic mechanical testing of the heel pads was completed using a servo-hydraulic material test system (MTS model 858). The MTS was operated in displacement control

with axial loading of the heel pad occurring at a frequency of 0.1 Hz to a depth of 5 mm. Testing was completed using a 65 mm diameter indenter (MTS-65) as used in Aerts et al. (1995), and a 6 mm indenter to reflect the hand-held indenter (MTS-6).

For all conditions applied force and obtained displacement were collected at 500 Hz, and five trials were obtained from each heel pad. Only the fifth loading cycle was used for subsequent analysis.

## RESULTS AND DISCUSSION

There was no statistically significant difference ( $\alpha = 0.05$ ) in the amounts of heel pad displacement (MTS-65: 5.0 mm  $\pm$  0; MTS-6: 5.0 mm  $\pm$  0; HHI: 4.3 mm  $\pm$  0.4). The applied loads were significantly different across testing conditions (MTS-65: 709.4 N  $\pm$  82.5; MTS-6: 48.9 N  $\pm$  7.2; HHI: 22.6 N  $\pm$  1.2). The sizes of the indenters, and non-precise control of loading with the HHI account for these force differences.

Heel pad stiffness was computed when the heel pads were loaded to a force equivalent to 5% of each cadaver's body weight. Significant differences were found between MTS-65 and the other two measures, but not between MTS-6 and HHI. The same results were obtained when the heel pad was loaded to one body weight.

Hysteresis was quantified and was not statistically different between the two MTS measures, but was different between both MTS and the HHI. Imprecise control of the HHI after peak deformation was achieved could account for these differences.

## SUMMARY/CONCLUSIONS

In a computer simulation Spears and Miller-Young (2006) have highlighted how different testing conditions can result in different estimates of heel pad mechanical properties. Their results have been confirmed in the present study in cadaver specimens.

Encouragingly the hand-held heel pad indenter gave statistically equivalent results to the loading applied by an MTS with the same size indenting surface. Given the important physiological changes which occur in heel pad properties under certain disease conditions (e.g., Kao et al., 1999), the validity of the hand-held device provides an important tool to track the disease process.

## REFERENCES

- Aerts, P., et al. (1995). *J. Biomech.*, **28**(11): 1299-1308.
- Bennett, M. B., Ker, R.F. (1990). *J. Anat.*, **171**: 131-138.
- Fung, Y.C. (1967). *Am. J. Physiol.* **213**:1532-1544.
- Jahss, M. H., et al. (1992). *Foot & Ankle*, **13**(5), 233-242.
- Kao, P. F., et al. (1999). *Magn. Reson. Imaging.*, **17**(6), 851-857.
- Kinoshita, H., et al. (1993). *Int J Sports Med.*, **14**(6), 312-319.
- More, J.J. (1977). In: *Numerical Analysis*. G.A. Watson (Ed.), Springer-Verlag, New York.
- Pain, M. T. G., Challis, J. H. (2001). *J. Biomech.*, **34**(3), 327-333.
- Rome, K., Webb, P. (2000). *Clin Biomech.*, **15**(4): 298-300.
- Spears, I. R., Miller-Young, J.E. (2006). *Clin. Biomech.*, **21**(2): 204-212.

# HEAD MOTION DURING PITCHING AMONG PROFESSIONAL BASEBALL PITCHERS

Shouchen Dun, Glenn S. Fleisig, David Kingsley, Jeremy Loftice, James R. Andrews

American Sports Medicine Institute, Birmingham, AL, USA

Email: shouchen@asmi.org

## INTRODUCTION

The head holds the two most important perceptual systems for detection of self-motion relative to space, the visual and vestibular systems. These two systems provide important information for the control of postural orientation and equilibrium (Horak and Macpherson, 1996). Baseball pitching is a very rapid human motion, where pitching shoulder internal rotation velocity can reach 7000°/s in elite pitchers (Dillman *et al.*, 1993). Maintaining head stability is therefore maximally challenged during baseball pitching. To date, little is known about how the head moves during baseball pitching. The purpose of this study was to characterize the head motion during baseball pitching among professional baseball pitchers.

## METHODS

Nine healthy professional baseball pitchers volunteered to participate in this study. The subjects' age was  $22.9 \pm 2.8$  years. Signed informed consents were collected before the testing.

An 8-camera, 3-dimensional motion analysis system (Eagle Digital System, Motion Analysis Corporation, Santa Rosa, CA) was employed to track the pitching motion. Fifteen reflective markers (1.27 cm in diameter) were attached on the anatomical landmarks of the subject's body (Barrentine *et al.*, 1998; Dillman *et al.*, 1993). In addition, three markers, Front Head (FH),

Top Head (TH), and Rear Head (RH), were placed to track head motion (Fig. 1). The sampling rate of each camera was 240 frames/s. After normal warm-up routine, the subject pitched 10 fastballs with maximal effort from an indoor pitching mound towards a strike zone target located 18.4 meters away from the pitching rubber.

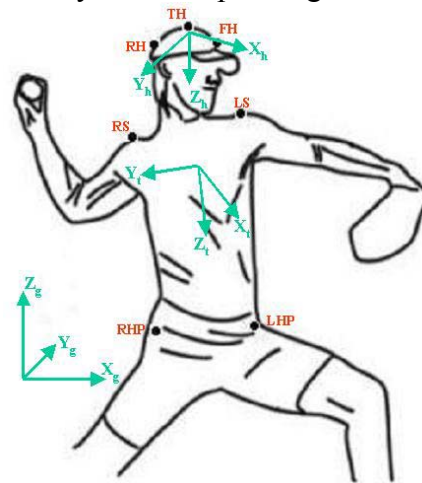


Fig.1. Marker placement and coordinate frames on the head and trunk.

Local head and trunk orthogonal coordinate frames were created. The X-axis of the head frame pointed from marker TH to FH (Fig. 1), Y-axis was the cross product of vector (TH→RH) and X-axis and pointed to the right and Z-axis pointed downwards. The Y-axis of the trunk frame was in the direction from left shoulder marker (LS) to right shoulder marker (RS), X-axis was the cross product of the trunk vector (a vector pointed from mid hip to mid shoulder) and Y-axis, and Z-axis pointed downwards. Head orientations in the trunk frame were calculated as Y-X-Z Euler angles which

represented pitch, roll, and yaw angles, respectively. Neutral roll and yaw positions were defined as 0° roll and yaw angles. A static trial was collected with the subject standing upright and looking straight ahead. The pitch angle during the static trial was defined as neutral pitch position. The head orientation angles in the global inertial frame (space)  $X_g Y_g Z_g$  were calculated using similar methods. For each subject, data from the four highest velocity pitches that hit the strike zone were averaged and analyzed. Results from stride foot contact (FC) to ball release (BR) were time-normalized from 0 to 100% and presented. The head orientation angular velocities were calculated using the five-point central difference method.

## RESULTS

In the trunk frame, the average motion of roll, pitch, and yaw were 42.8°, 27.2°, and 78.4°, respectively (Fig.2); the maximum angular velocities were 1403.2, 1155.7, and 1869.0°/s for roll, pitch, and yaw, respectively (Fig.3). In space, the average motion of roll, pitch, and yaw were 20.3°, 5.5°, and 29.3°, respectively (Fig.2); the maximum angular velocities were 536.5, 183.1, and 794.2°/s for roll, pitch, and yaw, respectively (Fig.3).

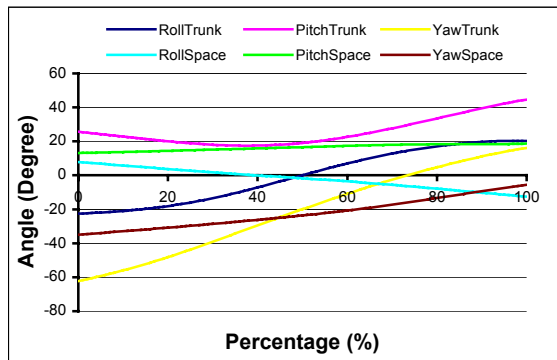


Fig. 2. Head orientation angles from FC (0%) to BR (100%).

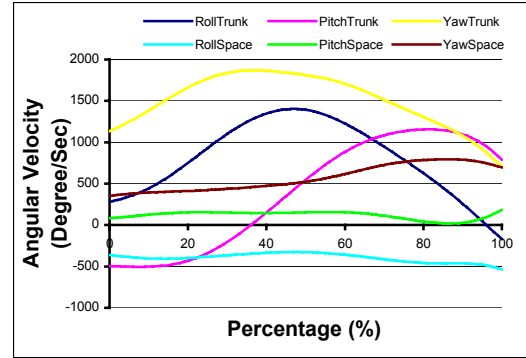


Fig. 3. Head angular velocities from FC (0%) to BR (100%).

## DISCUSSION

Both head ranges of motion and angular velocities were greater in the trunk frame than in space, which may be explained by the fact that the head motions in the trunk frame were the combinations of both head and trunk motions. The large ranges of motion and high angular velocities suggested that maintaining head stability during baseball pitching is a very demanding task. In future studies we will try to correlate head motion patterns with other biomechanical characteristics of the pitchers and compare the head motion patterns during different pitch types, which may help us better understand baseball pitching biomechanics.

## REFERENCES

- Barrentine, S.W. et al. (1998). *J.Orthop.Sports Phys.Ther.* **28**, 405-415.
- Dillman,C.J. et al. (1993). *J.Orthop.Sports Phys.Ther.* **18**, 402-408.
- Horak,F.B. and Macpherson,J.M. (1996). *Regulation and integration of multiple systems.* 255-292. Oxford University Press.

# PROBABILISTIC SHAPE-BASED FINITE ELEMENT ANALYSES OF BABOON FEMURS

Todd L. Bredbenner<sup>1</sup>, Keith A. Bartels<sup>1</sup>, Lorena M. Havill<sup>2</sup>, Jason B. Pleming<sup>1</sup>, and Daniel P. Nicoletta<sup>1</sup>

<sup>1</sup> Southwest Research Institute, San Antonio, TX, USA

<sup>2</sup> Southwest Foundation for Biomedical Research, San Antonio, TX, USA

E-mail: todd.bredbenner@swri.org

## INTRODUCTION

The construction of finite element models that accurately represent the complex morphology of biological structures is a major challenge. Uncertainty and variability exist in the input variables (i.e. bone geometry and density, loading, etc.) to the models and, accordingly, the predicted model response will also be uncertain.

A finite element model describing a set of baboon femurs was developed using statistical shape modeling methodology. Probabilistic finite element analyses were used to investigate the effects of variability in bone geometry and apparent density distribution along with the error in determining elastic modulus from the apparent density on FE model predictions.

## METHODS

Three fresh-frozen right femurs were obtained from baboons that had died due to natural causes (Southwest National Primate Research Center/Southwest Foundation for Biomedical Research, San Antonio, TX). The proximal third of each femur was scanned along with a density calibration phantom in a micro-CT system (Explore RS, GE Healthcare) and 96  $\mu\text{m}$  dimensionally isotropic voxels were reconstructed.

An iterative thresholding scheme was used to extract the bones from the imaging data (ImageJ, NIH) and triangulated surfaces

were defined to describe the outer cortical boundary for each femur (MicroView, GE Healthcare). Surfaces were aligned using Procrustes analyses (ImageJ, NIH).

A computational finite element mesh was defined (TrueGrid, XYZ Scientific Applications, Inc.) and projected to each femur surface to produce a set of volumetric mesh geometries, each consisting of 11,824 8-node hexahedral continuum elements. Using a linear relationship between densities in the calibration phantom and corresponding image intensities, nodal intensity values were converted to apparent density (Taddei, et al., 2004).

A random field description of the geometry and bone density distribution was defined by forming a joint point and density distribution model for the proximal femurs (Pepin, et al., 2002). A Principal Components Analysis (PCA) of this shape model resulted in a set of eigenvalues and eigenvectors, with each eigenvalue,  $\lambda$ , giving the variance of the femur geometry and bone density from the mean along the corresponding eigenvector,  $\mathbf{q}$ . PCA demonstrated that 99.94% of the model variation was explained by a single eigenvalue (Bredbenner, et al., 2006)

Variation in the geometry and density distribution of the femur set was described in terms of the average description and the dominant eigenvalue as:

$$\mathbf{p}_v = \bar{\mathbf{p}} + m\sqrt{\lambda}\mathbf{q},$$

where  $\mathbf{p}_v$  is a vector containing the spatial location and apparent density value for all nodes,  $\bar{\mathbf{p}}$  is a similar vector describing the average femur, and deviation from the average femur was determined as the product of a scalar,  $m$ , and model standard deviation,  $\sqrt{\lambda}$ , along the  $\mathbf{q}$  direction. The parameter  $m$  was modeled as a random variable with a mean of 0.0, a standard deviation of 0.4, and a normal distribution.

Apparent densities were determined for each element as the mean of the included nodal densities and were binned into a total of 7 apparent density levels to reduce computational requirements. Isotropic elastic moduli were determined as a function of apparent density for all bone elements using an empirical relationship given as:

$$E [GPa] = 1.99(\rho_{\text{apparent}} [g/cm^3])^B,$$

where  $B$  was modeled as a random variable with a mean of 3.46 and a standard deviation of 0.12 (Keller, 1994).

Distal nodes in each model were fixed and a 1.0 mm displacement was prescribed to a set of 8 nodes on the proximal side of the femoral head. Finite element models were solved using LS-DYNA (LSTC) on a Linux-based cluster. Femur stiffness was determined by dividing the distal reaction force by the applied displacement.

Using commercially-available probabilistic code (NESSUS, Southwest Research Institute), the effects of shape ( $m$ ) and bone property ( $B$ ) variation and uncertainty were determined using the Latin Hypercube analysis method.

## RESULTS AND DISCUSSION

The assumed variability in geometry and bone density distribution and the error

associated with determining modulus resulted in predicted femur stiffness values ranging from 2085 to 2866 N/mm (Fig. 1). There is a 90% probability that femur stiffness is within this range.

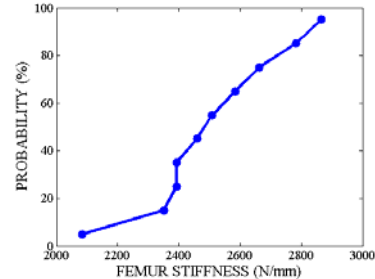


**Figure 1:** The cumulative distribution function demonstrates the effects of input variability on predicted femur stiffness.

## SUMMARY/CONCLUSIONS

High-fidelity finite element models were developed using shape modeling methodology to describe the variability in geometry and material property distribution determined from imaging data for a set of baboon femurs. Probabilistic methods were used to demonstrate the variability in femur model stiffness associated with variation in geometry and bone density distribution and the error associated with determining elastic modulus from the apparent density.

## REFERENCES

- Bredbenner, T.L., et al. (2006). *Proceedings of ASME Summer Bioengineering Conf.*
- Keller, T.S. (1994). *J. Biomech.*, **27**, 1159-1168.
- Pepin, J.E., et al. (2002). *Proceedings of 43<sup>rd</sup> SDM, AIAA-2002-1641.*
- Taddei, F., et al. (2004). *Med. Eng. Phys.*, **26**, 61-69.

## ACKNOWLEDGEMENTS

Support was provided by the Internal Research Program of Southwest Research Institute.

# LOAD-MODIFYING FOOTWEAR INTERVENTION DOES LOWER KNEE ADDUCTION MOMENT IN SUBJECTS WITH SYMPTOMS OF MEDIAL COMPARTMENT KNEE OSTEOARTHRITIS

Jennifer Erhart<sup>1</sup>, Chris Dyrby<sup>1</sup>, Barbara Elspas<sup>2</sup>, Nicholas J. Giori<sup>1,2,3</sup>  
and Thomas P. Andriacchi<sup>1,2,3</sup>

<sup>1</sup> Department of Mechanical Engineering, Stanford University, Stanford, CA, USA

<sup>2</sup> Bone and Joint Center, Palo Alto VA, Palo Alto, CA, USA

<sup>3</sup> Department of Orthopedic Surgery, Stanford University, Stanford, CA, USA  
E-mail: jerhart@stanford.edu      Web: [www.stanford.edu/group/biomotion/](http://www.stanford.edu/group/biomotion/)

## INTRODUCTION

A high maximum adduction moment at the knee during walking has been associated with the treatment outcome (Andriacchi 1994) and rate of progression (Miyazaki et al. 2002) of medial compartment knee osteoarthritis (OA). Consequently, many interventions for knee OA are aimed at reducing the maximum knee adduction moment. While footwear modifications, using wedged insoles or shoes (Crenshaw 2000 and Fisher 2002) have been shown to reduce the knee adduction moment, subjects often find such interventions uncomfortable to wear. Fisher *et al.* 2004 reported that a variable stiffness shoe reduced the knee adduction moment in healthy individuals. However, it has not been shown that a variable stiffness shoe can reduce the adduction moment in subjects with medial compartment knee OA, or if there are certain patients that are not responsive to a variable stiffness shoe. The purpose of this study was to test the following hypothesis: the variable stiffness shoes will lower the knee adduction moment in the affected leg of individuals with symptoms of medial compartment knee OA, compared to the subjects' personal shoes and control shoes.

## METHODS

26 subjects (17 male, 9 female; age:  $58.2 \pm 10.4$  yrs; height:  $1.72 \pm 0.09$  m; mass:  $80.6 \pm 15.8$  kg) with symptoms of medial compartment knee OA participated in this

study after giving written consent in accordance with the Institutional Review Board. Inclusion criteria included the presence of medial compartment knee pain, and exclusions included serious back, hip, ankle, or foot problems; the use of shoe inserts, rigid knee braces, walking aids, or narcotic medications; age less than 18 or greater than 80 years; body mass index greater than  $35 \text{ kg/m}^2$ ; total knee replacement; and gout. Each subject performed 3 walking trials at self-selected slow, normal, and fast speeds in each of 3 shoes: their personal walking shoe, a control shoe (constant-stiffness sole), and an intervention shoe (variable-stiffness sole). In the intervention shoe the lateral sole stiffness was greater than the medial sole stiffness.

Kinematic and kinetic data were collected using an 8-camera optoelectronic system and reflective markers (Andriacchi 1998). External inter-segmental forces and moments were calculated for the lower limb using previously described methods (Andriacchi 2004). The first peak knee adduction moment was calculated for each trial. Average values for each shoe, speed, and subject were determined for each subject's more affected leg (determined by self-reported pain). Paired one-tailed Student's T-tests were used to compare the different shoes ( $\alpha = 0.05$ ).

## RESULTS AND DISCUSSION

The knee adduction moment of the subjects' more affected leg was significantly reduced at all walking speeds for both the intervention vs. personal and intervention vs. control shoe cases (Figure 1).

The amount of reduction in the adduction moment varied from more than a 20% reduction to a 7% increase with the intervention shoe relative to the control, with 4 of the 26 subjects having an increase in the adduction moment with the intervention shoe (Figure 2).

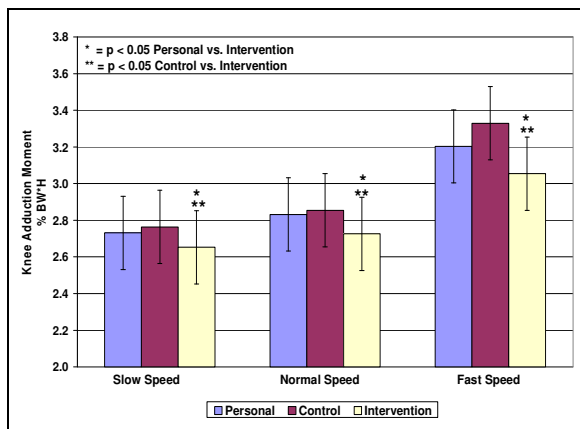


**Figure 1:** Average knee adduction moments ( $\pm$  SEM) for all subjects' affected legs.

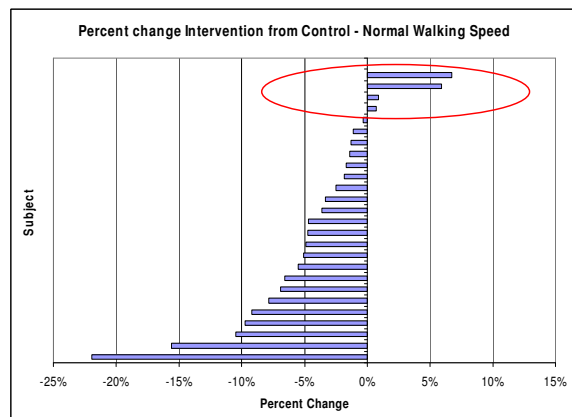


**Figure 2:** Patient responses to the intervention shoe had substantial variation. Red circle indicates non-responders.

## SUMMARY/CONCLUSIONS

The intervention shoes successfully reduced the knee adduction moment in nearly all subjects with symptoms of medial compartment knee OA.

However, as shown in Figure 2, the amount of reduction varied substantially among the population, with a small percentage of the population having an increase in loading with the intervention shoe.

Future work identifying factors to explain the non-responders' increase in knee adduction moment will be important to implement the intervention shoes clinically. By identifying responders vs. non-responders, physicians will be able to accurately prescribe a footwear intervention to slow the progression of medial compartment knee osteoarthritis.

## REFERENCES

- Andriacchi, T.P. et al. (1994). *Orthop. Clin. North Am.*, **14**, 289-295.
- Andriacchi, T.P. et al. (1998). *J. Biomech. Eng.*, **120**, 743-749.
- Andriacchi, T.P. et al. (2004). *Basic Orthopaedic Biomechanics* 3rd ed., 91-121.
- Crenshaw, S.J. et al. (2000). *Clin. Orthop.*, **375**, 185-192.
- Fisher, DS et al. (2002). *48th Meeting of the ORS*, 27, 0700.
- Fisher, DS et al. (2004) *50th Meeting of the ORS*, 50, 1026.
- Miyazaki, T. et al. (2002). *Ann. Rheum. Dis.*, **61**, 617-622.

## ACKNOWLEDGEMENTS

This study was supported by VA grant # A02-2577R.



# SHOULDER MAXIMUM EXTERNAL ROTATION IN THE TENNIS SERVE IS NOT RELATED TO SHOULDER PASSIVE EXTERNAL ROTATION FLEXIBILITY

Jeff T. Wight, Guy B. Grover, John W. Chow, and Mark D. Tillman

Department of Applied Physiology & Kinesiology, University of Florida, Gainesville, FL, USA  
E-mail: [jwight@ufl.edu](mailto:jwight@ufl.edu) Web: [www.hhp.ufl.edu/apk/ces/labs/biomech/](http://www.hhp.ufl.edu/apk/ces/labs/biomech/)

## INTRODUCTION

Shoulder external rotation (ER) is extreme in overhand athletics (figure 1). Both costs and benefits are associated with excessive shoulder ER. The cost is injury potential. Pitchers and tennis players have a high incidence of elbow and shoulder injuries. The potential benefit is the performance enhancement. Shoulder maximum ER in the baseball pitch is positively correlated with throwing velocity (Matsuo et al., 2000). It is important to understand factors that influence shoulder ER.

In this study we attempted to determine if shoulder passive ER flexibility is related to the shoulder ER achieved in the tennis serve. Analysis of shoulder passive ER flexibility is limited for overhand athletics. Previous studies have focused on passive range of motion (ROM) measures exclusively. The rotational resistance associated with acquiring the passive ROM has yet to be quantified. Resistance measures may help to more thoroughly describe shoulder passive ER flexibility. Novotny et al., (2000) demonstrated that it is possible to quantify shoulder passive ER rotational resistance using a custom device. We developed a similar device catered to overhand athletics. To our knowledge, relationships between ER passive flexibility measures and end ROM in overhand athletics have yet to be examined. The purpose of this study was to determine if relationships exist between shoulder ER flexibility measures and the end ROM in the tennis serve.



**Figure 1:** This tennis player is approaching 180° of shoulder external rotation.

## METHODS

Twenty-six advanced (NTPR rating > 5.0) male tennis players (age =  $22.4 \pm 7.0$  yrs) participated in the study. Kinematic data were collected using a 7-camera Hawk Digital Motion Analysis system at 200 frames per second. A custom program was written in LabView software to analyze the shoulder maximum ER during the serve. The torso was modeled using a triad of markers on the upper back (Wight et al., 2004). The upper arm and forearm were modeled using markers placed upon the medial and lateral humeral epicondyles and the medial and lateral wrist.

Shoulder passive ER flexibility measures were collected using a custom device (figure 2). Measures included the resistance onset angle (ROA), defined as the ER angle at 1 N·m of resistance, the passive end ROM (end ROM), and the stiffness (slope of torque vs. ER angle best fit line).

Passive flexibility measures variables were first analyzed singly for all subjects. Pearson product moment correlations were used to determine if relationships existed between the flexibility measures and serving ROM. The two resistance measures (ROA and stiffness) were then assessed simultaneously to form a flexible (n=5) and inflexible (n=5) group. The flexible group consisted of individuals that had a late ROA ( $>95^\circ$ ) and a low stiffness ( $< 0.37 \text{ N}\cdot\text{m}/^\circ$ ). The inflexible group consisted of individuals that had an early ROA ( $<85^\circ$ ) and high stiffness ( $>0.41 \text{ N}\cdot\text{m}/^\circ$ ). Independent T-tests (alpha set at 0.05) were used to determine if differences in passive and serving end ROM occurred between the groups.



**Figure 2:** The researcher slowly pulled on a rope to externally rotate the subject's arm. The rope ran through a pulley that was attached to a load cell (to measure rotational resistance). A potentiometer was mounted to the bicycle wheel (to measure ROM).

## RESULTS AND DISCUSSION

Means and standard deviations were calculated for all individuals (ROA =  $94.0 \pm 14.7^\circ$ , stiffness =  $0.41 \pm 0.9 \text{ N}\cdot\text{m}/^\circ$ , passive end ROM =  $121.1 \pm 17.2^\circ$ , serving end ROM =  $164.9 \pm 17.9^\circ$ ).

The 3 flexibility measures did not significantly predict the shoulder maximum

ER in the serve (ROA:  $r = 0.14$ ,  $p = 0.51$ ; passive ER ROM:  $r = 0.29$ ,  $p = 0.15$ ; ER stiffness:  $r = 0.11$ ,  $p = 0.58$ ). No significant differences ( $p=0.9$ ) were detected in the serving end ROM between the flexible ( $164.4 \pm 6.2^\circ$ ) and inflexible ( $166.4 \pm 33.8^\circ$ ) groups. This data suggests that both flexible and inflexible players were able to obtain excessive ROM during the tennis serve.

A significant group difference was approached ( $p=0.09$ ); the flexible group achieved a greater passive end ROM ( $136.6 \pm 17.3^\circ$ ) than the inflexible group ( $106.8 \pm 12.2^\circ$ ). This data demonstrates the potential to gain further insight about shoulder flexibility properties by accounting for multiple flexibility variables.

## SUMMARY/CONCLUSIONS

A thorough analysis of shoulder passive external rotation was completed by measuring the resistance to rotation. Both flexible and inflexible athletes were able to obtain excessive shoulder ER during the tennis serve. Future research should attempt to determine if ER flexibility influences the shoulder and elbow loads experienced while externally rotating the shoulder during overhand athletics.

## REFERENCES

- Matsuo, T., et al., (2001). *Journal of Applied Biomechanics*, **17**(1), 1-13.
- Novotny JE. et al., (2000). *J Orthop Res* **18**(2): 190-194.
- Wight, J.T. et al., (2004). *Sports Biomechanics*, **3**(1), 67-83.

# ANALYSIS OF GAIT CHARACTERISTICS IN MENTALLY HANDICAPPED INDIVIDUALS

Prakriti Parijat , Jian Liu, Thurmon E Lockhart and Courtney Haynes  
Virginia Tech, Blacksburg, VA, USA  
E-mail: pparijat@vt.edu

## INTRODUCTION

Physical and motor dysfunctions in mentally handicapped individuals predispose them to a higher risk of slip and fall accidents. It is estimated that over 60 million people are currently suffering with some level of developmentally related cognitive impairment (American Disability Act ADA, 2000). Mental retardation occurs in 2.5-3% of the general population. About 6-7.5 million mentally retarded individuals live in the United States alone (ADA, 2000). Slip induced fall accidents are a primary source of injury in people with mental retardation (MR). Often, the incidence of falls among this population is compounded by other disabilities such as autism, seizure, and impulse control disorders. These individuals already have a certain level of physical disability which makes it necessary to predict their tendency of falling in-order to prevent further physical disability. Due to improvements in the health care and assisted living services available to them, many more individuals with MR are reaching old age. In fact, there are between 200,000 and 500,000 older adults with MR in the United States (World Health Organization, 2000). As this population continues to grow, it is important to identify individuals who are at an elevated risk of slip induced fall accidents.

While gait characteristics have been documented for a variety of disabled and non-disabled populations, there is little reliable data on the gait patterns of individuals with MR. Understanding the gait

patterns of this population would be helpful in identifying the factors that might relate to their incidence of falls and eventually developing intervention strategies to minimize the injuries due to falls. Therefore, the purpose of this study was to examine the gait characteristics in mentally impaired individuals with various degrees of MR (Mild, Moderate, Severe and Profound).

## METHODS

Twenty mentally retarded individuals were recruited from Southwest Virginia Training Center (SWVTC). Informed consent was approved by IRB in both the SWVTC and Virginia Tech. The participant's information is summarized in Table 1. The experimental protocol was very similar to previous literature [1]. Participants were instructed to walk along a linear walkway (1.5m x 15.5m), and were protected by an overhead harness system. Two force-plates and a six-camera ProReflex system were used to collect kinetic and motion data. SWVTC staff helped the experimenters to subjectively judge if the way the participants walked was consistent with their daily walking style.

Table 1: Participants Information

n = 20		
MR Status (IQ)	No. of Subjects	Age Range
Mild (55-69)	1	34
Moderate (40-54)	5	23-37
Severe (25-39)	11	24-64
Profound (below 25)	3	31-42

Totally 8 normal walking trials were collected per participant. Step length (SL), heel contact velocity (HCV), and whole-body COM speed (SP) were determined in custom-made MATLAB program [2]. All the parameters were compared with the control group of 20 younger healthy participants, whose data were collected previously using similar experimental protocol. Paired-t tests were performed to assess group effect (mentally retarded group (MR) and healthy younger group (N)) on SL, HCV, and SP. Significant level  $p < 0.05$  was adopted for all the tests.

## RESULTS

Figure 1 demonstrates the summary of the differences in gait parameters between the MR and the control group. The paired-t tests indicated that the MR group walked slower than the control group ( $p < 0.0001$ ). Also, younger adults horizontal heel contact velocity was faster and their step length significantly longer ( $p < 0.0001$ ) than the MR group.

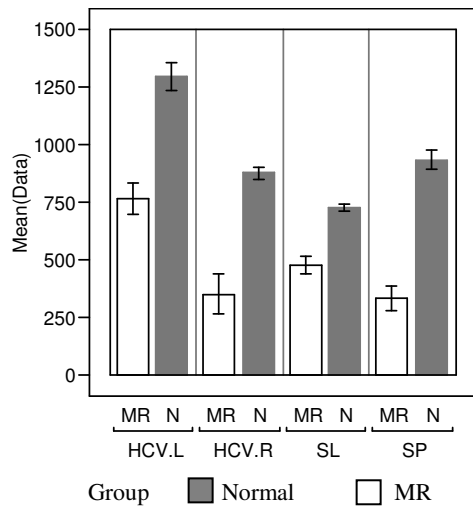


Figure1: Mean and standard deviation of HCV (mm/s) right (R) and Left (L), SL (mm), and SP (mm/s) in mentally retarded group and control group

## DISCUSSION AND CONCLUSION

The objective of the study was to evaluate gait characteristics of the mentally impaired individuals and relate them to their propensity of falls. Previous literature [1] suggested that SP, HCV and SL were major predictors of likelihood of slips and falls. The results obtained in this study indicate that the gait of mentally impaired individuals is similar to that of older individuals with high frequency of falls [3]. The higher heel contact velocity is a predictor variable of the required coefficient of friction (RCOF) which affects the slip initiation. Though there were differences between the HCV of young and the MR group, the results suggest that the evaluated parameters might not affect the slip initiation process of these individuals. However, slower whole body COM velocity has been recognized as a contributing factor for falls [3]. This indicates that mentally impaired individuals might be at a risk of fall when their gait is perturbed, as their whole body COM transfer will be slower which might affect their recovery process. These results warrant further investigation of gait parameters which affect the recovery from slips in mentally impaired individuals.

In conclusion, the present study indicated that the gait characteristics of the MR group were significantly different from the younger individuals which might affect their reactive recovery from a fall.

## REFERENCES

1. Liu, J. et al. (2004). *Proceedings of HFES 48th Annual Meeting*.
2. Lockhart, T. E. et al.(2002). *ASTM STP 1424, Metrology of Pedestrian Locomotion and Slip Resistance*.
3. Kim, S. et al. (2005). *Safety science 43: 425-436*

# Prospective Study of the Biomechanical Factors Associated with Iliotibial Band Syndrome

Brian Noehren<sup>1</sup>, Irene Davis<sup>1,2</sup> and Joseph Hamill<sup>3</sup>

<sup>1</sup> University of Delaware, Newark, DE, USA

<sup>2</sup> Drayer Physical Therapy institute, Hummelstown, PA, USA

<sup>3</sup> University of Massachusetts, Amherst, MA, USA

E-mail: bnoehren@udel.edu

## INTRODUCTION

Iliotibial Band syndrome (ITBS) is the leading cause of lateral knee pain in runners. The Iliotibial band (ITB) originates proximally from the facial attachments of the gluteus medius, gluteus maximus and the tensor fascia late. Distally, the ITB has attachments at the lateral femoral condyle, the lateral patella and at gerdy's tubercle on the lateral tibia. ITBS is thought to result from friction of the ITB sliding over the lateral femoral condyle. The mechanics that increase friction and exacerbate ITBS are not well understood, with few studies having been done to date.

It has been suggested that ITBS is related to a sagittal plane mechanism, whereby repetitive knee flexion causes friction between the ITB and the femoral condyle. However, Orchard et al. (1994) assessed knee flexion at initial contact, maximum knee flexion and time spent in knee flexion in runners with ITBS. They found no differences between the injured leg and uninjured leg in a group of runners.

It has also been suggested that a transverse plane mechanism may be at fault. Ferber et al. (2003) reported that runners with ITB exhibited a 7 deg increase in knee internal rotation compared with a control group. Increased knee internal rotation may be a result of increased ankle eversion due to the coupling between these joints. In fact, Messier et al. (1994) found that the runners with ITBS exhibited greater peak eversion as compared to controls. In addition, in a

prospective study, Ferber et al. (2003) found that runners who went on to develop ITBS had greater peak eversion, greater peak eversion velocity and excursion.

A hip mechanism for developing ITBS has been proposed as well. Weakness of the hip abductors has been associated with ITBS (Fredrikson 2000). Weakness of the hip abductors has been shown to be related to increased hip adduction in runners with patellofemoral pain syndrome (Dierks 2005). However, there are no studies of the role of increased hip adduction in ITBS. It is possible that increased hip adduction combined with knee internal rotation, increases ITB tension. This could increase contact of the ITB with the lateral femoral condyle and lead to irritation with repeated exposure

The purpose of this study was to prospectively compare running mechanics in a group of female runners who went on to develop ITBS compared to healthy controls. It was hypothesized that runners who go on to develop ITBS would exhibit greater hip adduction, knee internal rotation and rearfoot eversion.

## METHODS

This is an ongoing study where, to date, 17 female runners have developed ITBS prospectively. All injuries were confirmed by a medical professional such as a physician, physical therapist or an athletic trainer. They were compared to a control group of 17 age and mileage matched

uninjured runners. In both groups all runners were free from any previous or current hip and knee pathology.

Subjects ran over ground along a 25m runway at 3.7m/s wearing standard laboratory shoes. Five running trials were collected during the stance phase of running. Kinematic data was captured using a 6-camera motion capture system at 120Hz (Vicon, Oxford metrics, UK) and kinetics were captured using a force platform (Bertec OH, USA). Kinematic and kinetics were calculated using visual3D software (Visual 3D, C motion, MD, USA). Variables of interest were compared between groups using an independent, one tailed t-test.

## RESULTS AND DISCUSSION

Comparison of the variables of interest between groups is presented in Table 1. Hip adduction and knee internal rotation curves are presented in figures 1 and 2.

**Table 1 Variables of Interest**

	ITBS	CON	P
Peak EV (deg)	9.7	11.6	0.035
Peak Knee Int Rot	4.49	.021	0.001
Peak Hip Adduction	14.1	10.6	0.009

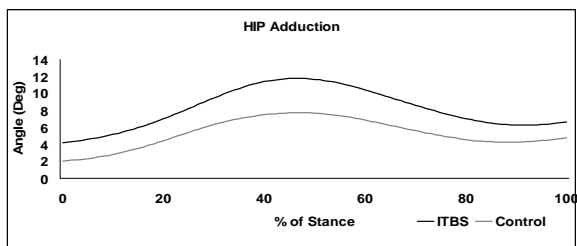


Figure 1. Comparison of hip adduction between groups

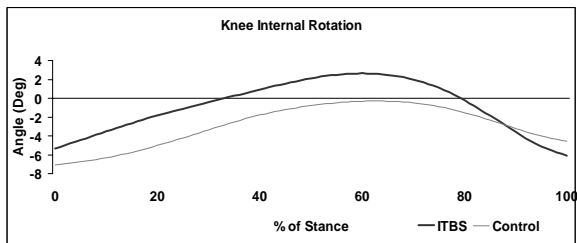


Figure 2. Comparison of knee internal rotation between groups

As hypothesized, hip adduction was greater in the ITBS group. This suggests that hip weakness noted previously in runners with ITBS may result in excessive hip adduction. This could increase the tension on the ITB and, with repeated exposure, lead to ITBS.

The ITBS group also exhibited a 4 deg. increase in knee internal rotation. These findings are in support of Ferber et.al. (2003). Increased knee internal rotation could further elongate the ITB as its attachment at gerdy's tubercle is moved anteriorly. Along with the hip adduction, this is likely to further increase ITB tension.

Unexpectedly, peak eversion was significantly lower in the ITBS group. This is contrast to Messier et al. (1995) and Ferber et al. (2003) who found greater peak eversion. However, it is possible that increased knee internal rotation noted was associated with increased talonavicular pronation, rather than subtalar pronation. Unfortunately, we were unable to measure talonavicular motion with our standard motion analysis techniques.

## SUMMARY/CONCLUSIONS

Results from this prospective study suggest that individuals who go onto to develop ITBS exhibit greater hip adduction and knee internal rotation. These results suggest that interventions should be directed at controlling these motions.

## REFERENCES

- Messier et.al (1995). *MSSE* , **27**, 951-60
- Fredericson et al. (2000) *Clin J St Med*, **10**, 169-75
- Ferber et.al (2003) *MSSE* **35** s91
- Orchard et.al (1996) *AJSM* **24** 375-379
- Dierks et.al (2005) ASB

## ACKNOWLEDGEMENT

Supported by Dept of Defense grant DAMD17-00-1-0

# EFFECT OF TOTAL KNEE REPLACEMENT ON GAIT STABILITY

David Mandeville, Li-Shan Chou, Louis Osternig  
Motion Analysis Laboratory, University of Oregon, Eugene, OR, USA  
Email: chou@uoregon.edu

## INTRODUCTION

A deleterious relationship between knee osteoarthritis (OA) and standing balance has been well established. Hassan et al. (2001), report knee OA patients with increased body sway during quiet standing relative to control. Static stability impairments are thought to be the result of proprioceptive deficits, muscle weakness, and knee pain brought about by the articular degeneration of the knee joint. Leveille et al (2002), suggest that reflex muscle inhibition due to chronic pain could compromise the lower limb muscular response to perturbation. Pain may also decrease an elder's confidence in their physical abilities which may contribute to the relationship between pain and instability. However, assessments of standing postural control are not representative of the dynamic stability requirements of daily living.

Chou et al (2003), reported a dynamic stability assessment which distinguished imbalanced elderly subjects from healthy age-matched controls. The gait protocol involved obstacle crossing at self-paced velocity. Elderly imbalanced subjects were shown to cross the obstacle with increased medio/lateral (M-L) range and peak M-L velocity of the COM. Healthy younger subjects were shown to have invariant M-L motion during obstacle crossing effectively avoiding sideways balance perturbation.

Evaluation of knee OA balance deficits need to reflect the dynamic nature of ADLs in the frontal plane, where elderly fallers are at risk for hip fracture. Understanding the gait stability challenges faced by knee OA and

total knee replacement (TKR) patients may enhance the functional goals of rehabilitation protocols. Therefore, the aim of this study was to assess the effect of TKR on pain and frontal plane gait stability relative to controls during level walking and obstacle crossing. Additionally, the relationship of pain to gait stability was assessed.

## METHODS

Forty-four volunteer subjects were recruited into two experimental groups: 1) TKR, n = 22; and 2) healthy age-matched control, n = 22. All subjects' pain, stiffness, and physical function (ADLs) were assessed via the self-administered, activity based WOMAC questionnaire (Table 1). Subjects were tested twice, pre-operatively (P1) and six months later (P2).

Subjects were fitted into a fall arrest harness for self-selected level and obstacle crossing gait. An array of 29 reflective markers defined a thirteen link model of the human body. Spatio-temporal and whole body kinematic data were obtained using an eight camera motion analysis system. Ground reaction forces were obtained from 2 AMTI force plates embedded in series along a 10 m walkway. Inverse dynamic calculations were computed using Orthotrak 6.2 software. A complete stride for the TKR involved limb and the dominant limb of control were analyzed from each trial. For obstacle crossing, the involved/dominant limb was the trailing or supportive limb. The obstacle was positioned vertically at 10% of body height and placed in the walkway.

Whole body COM was computed as the weighted sum of the 3-D segment COM position. Position derivatives of whole body COM were estimated with the generalized cross-validated spline algorithm. Variables analyzed include: gait velocity, stride length, M/L COM range, peak M/L COM velocity, and self-reported pain. Within and between group differences were assessed using a mixed model ANCOVA with gait velocity as a covariate. Pearson correlation coefficients were assessed via SPSS 12.0.

## RESULTS AND DISCUSSION

Across period, TKR patients report significantly decreased pain ( $P = .0001$ ), yet remain significantly greater than control at P2 ( $P = .002$ , Table 1). Though TKR level gait velocity and stride length increased significantly across period ( $P < .0001$ ,  $P < .0001$ ) respectively, P2 values remained significantly less than control ( $P = .0004$ ,  $P = .0002$ , Table 2) respectively. Across period, TKR M/L COM range values decreased ( $P = .0841$ ) along with peak M/L COM velocity values ( $P = .120$ ). Between group differences for these values were not found at either period.

For obstacle crossing, TKR gait velocity increased significantly across time ( $P < .0001$ , Table 3) and remained less than control at P2 ( $P = .0644$ ). Both groups showed increased M/L COM range and M/L COM peak velocity for obstacle crossing compared to level walking, but significant within or between group differences were not seen for these values.

Both groups display M/L COM range and M/L COM peak velocity values in the range previously reported for healthy elders (Chou et al., 2003). A significant correlation ( $P < .01$ ) was found between M/L COM range and WOMAC ADL ( $r = .478$ ) and pain ( $r =$

.363) scores. Peak M/L COM velocity was also significantly correlated ( $P < .01$ ) to WOMAC ADL ( $r = .416$ ) and pain ( $r = .332$ ) scores. Although significant between group differences for the gait stability parameters were not found, the pain scores relate to stability in that subjects with increased pain show increased sway.

## References:

- Hassan, et al., Ann Rheum Dis, 2001. **60**.  
 Leveille, et al., JACS, 2002. **50**.  
 Chou, et al., G & P, 2003. **18**

**Table 1:** Mean WOMAC/VAS pain, stiffness, and pain subscale scores for TKR and control across time (standard error).

Period	TKR		Control	
	P1	P2	P1	P2
Pain (out of 100)	46.691 <sup>†</sup> (4.867)	14.735 <sup>††</sup> (3.295)	3.224 (0.597)	4.061 (0.82)
Stiffness (out of 100)	57.685 <sup>†</sup> (5.396)	25.825 <sup>††</sup> (5.256)	6.33 (2.157)	6.542 (1.972)
ADLs (out of 100)	46.902 <sup>†</sup> (5.114)	15.439 <sup>††</sup> (2.654)	4.345 (0.841)	3.962 (0.775)

<sup>†</sup>Indicates significant within group difference ( $P < .05$ ).

<sup>††</sup>Indicates significant between group difference ( $P < .05$ ).

**Table 2:** Adjusted mean M/L range and peak velocity of COM during level walking for TKR and control across time (standard error).

Period	TKR		Control	
	P1	P2	P1	P2
M/L COM range (m)	0.041 (0.003)	0.036 (0.002)	0.041 (0.002)	0.038 (0.002)
Pk M/L COM velocity (m/s)	0.140 (0.006)	0.132 (0.005)	0.145 (0.005)	0.133 <sup>†</sup> (0.004)

<sup>†</sup>Indicates significant within group difference ( $P < .05$ ).

<sup>††</sup>Indicates significant between group difference ( $P < .05$ ).

**Table 3:** Adjusted mean M/L range and peak velocity of COM during obstacle crossing for TKR and control across time (standard error).

Period	TKR		Control	
	P1	P2	P1	P2
M/L COM range (m)	0.060 (0.004)	0.059 (0.003)	0.059 (0.003)	0.054 (0.003)
Pk M/L COM velocity (m/s)	0.171 (0.009)	0.166 (0.007)	0.173 (0.007)	0.161 (0.006)

<sup>†</sup>Indicates significant within group difference ( $P < .05$ ).

<sup>††</sup>Indicates significant between group difference ( $P < .05$ ).

# ON CHANGES IN HAMSTRING LENGTH DURING A SIMULATED JUMP LANDING: AN *IN VITRO* STUDY

Erin McIntyre, Alaa Ahmed, Youkeun Oh, Jennifer Kreinbrink,  
Riann Palmieri, Edward Wojtys, James Ashton-Miller

University of Michigan, Ann Arbor, MI, USA  
E-mail: jaam@umich.edu

## INTRODUCTION

Non-contact anterior cruciate ligament (ACL) injuries often involve a one-footed jump landing and may be associated with excessive ACL strain. ACL strain has been measured *in vivo* using a DVRT (Beynon & Fleming 1998). ACL strain correlates with quadriceps force (Torzilli 1994; Dürselen 1995), and a rapid increase in quadriceps force > 6 bodyweights (BW) can rupture the ACL (Dikeman 1998, DeMorat 2004). In an *in vitro* model of a simulated 2-BW jump landing, using knees constrained only by pretensioned springs (7 kN/cm spring rate) representing preactivated quadriceps, medial and lateral hamstring and gastrocnemius muscle forces, the increase in the DVRT-measured relative ACL strain was proportional to the increase in tension in the quadriceps muscle-equivalent as the knee flexed under the impulsive compression and flexion knee moment loading (Withrow 2006a). However, when the hamstring muscle equivalents were instead arranged to lengthen as the knee flexed, then a significant (70%) reduction in peak relative ACL strain was found (Withrow 2006b).

It is not known whether the hamstring muscles shorten or lengthen when landing a jump on one or two legs. We therefore designed a cadaver experiment to test the hypothesis that hamstrings can indeed lengthen during a simulated jump landing. The significance of a “lengthening” muscle contraction (used in lieu of “eccentric”, per

Faulkner 2003) is that the muscle force can exceed 1.6 times the maximum isometric value (or shortening muscle contraction). As Withrow (2006b) showed, a lengthening hamstring muscle contraction helps limit peak ACL strain by limiting quadriceps-induced anterior tibial translation; an isotonic hamstring force provided no such protection.

## METHODS

Three older adult cadavers (two female) were dissected to expose the origins and insertions of the three major hamstring muscles: semimembranosus (SM), semitendinosus (ST) and biceps femoris (BF). With the cadaver torsos and one limb supported in the prone position, Certus (Northern Digital, Inc., Waterloo, Canada) optoelectronic triads were mounted on the posterior aspect of the sacrum, and the anterior aspects of the femur and tibia of the other limb. The locations of the triads, the muscle origin and insertion locations, and standard anatomic landmarks on the pelvis, femur, tibia and foot were hand digitized using Certus. The knee and hip joints were then each flexed through 90 and 75 degrees in the neutral plane, as well as in  $\pm 10^\circ$  hip ab- and adduction. Finally, the hip and knee were flexed simultaneously by protracting and retracting the ankle joint from the hip joint. Kinematic data were recorded at 100 Hz. The Euclidian distance between each muscle-tendon unit (MTU) origin and insertion was then calculated for each hip and knee angle.

## RESULTS AND DISCUSSION

Isolated knee flexion caused all three hamstring MTUs to shorten but, because lever arms are larger at the hip than the knee, isolated hip flexion caused all three MTUs to lengthen to a greater degree (Fig. 1). If hip and knee angles both increase by 15 and 21° from initial hip and knee angles of 30° at foot touch down (landing data from Pflum 2004), then all three MTUs will lengthen (from 'a' to 'c', Fig. 1). Similar results were found with the other cadavers. However, landing and falling backward may preclude a lengthening hamstring contraction due to insufficient hip flexion, thereby placing the ACL at risk. Landing jumps with adequate hip flexion should reduce peak ACL strains (via a hamstring lengthening contraction), and vice versa.

## SUMMARY/CONCLUSIONS

Hamstring lengthening can indeed occur

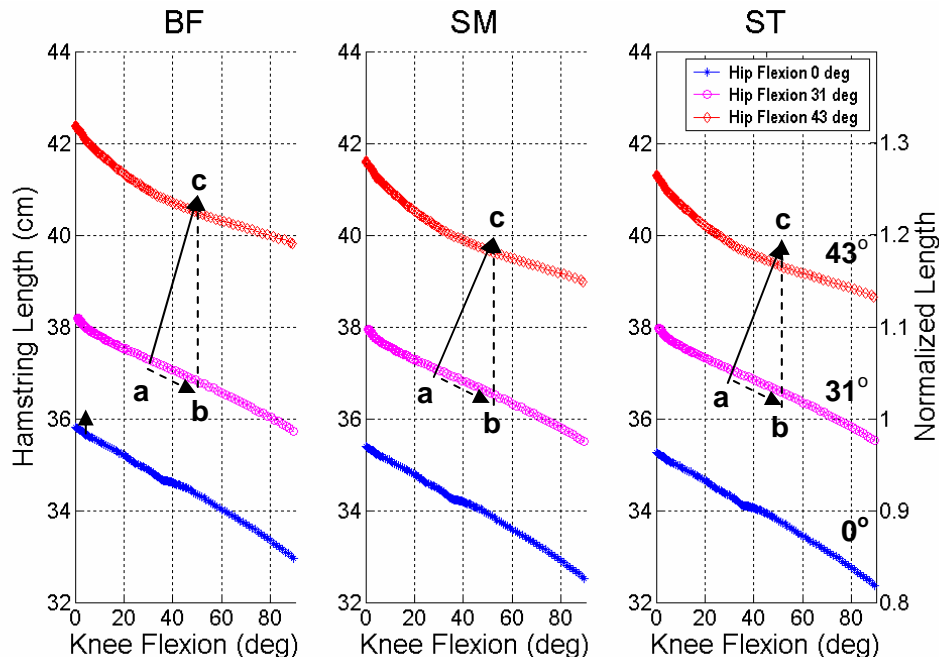


**Figure 1:** Effect of knee and hip flexion on the three hamstring MTU lengths (in cm) in a 92 year-old female cadaver. The BF, SM & ST MTUs would lengthen, from points 'a' to 'c', when hip and knee joints are both flexed through 15 and 21 degrees, respectively, from initial landing angles of 30° each (jump landing data from Pflum 2004).

during a jump landing, but only with adequate hip flexion (>10% knee flexion).

## REFERENCES

- Beynon B.D., Fleming B.C. (1998) *J Biomech.* **31**:519-525.  
 DeMorat G. *et al.* (2004) *Am J Sports Med.* **32**:477-483.  
 Dikeman J.S. (1998) MS thesis, North Carolina State University, Raleigh.  
 Dürselen L. *et al.*, (1995) *Am J Sports Med* **23**:129-136.  
 Faulkner J.A. (2003) *J App Physiol* **95**:455-459.  
 Pflum M.A. (2004) *Med Sci Sports Exerc* **36**:1949-1958.  
 Torzilli P.A. (1994) *Am J Sports Med.* **22**:105-12.  
 Withrow T. (2006a) *Am J Sports Med* **34**: 269-274.  
 Withrow T. (2006b) *Proceedings of 2006 ORS Annual Meeting.*

# SWAY INDUCED MOTION ON AN OSCILLATING PLATFORM

W. Thomas Edwards<sup>1</sup>, Venkata Gade<sup>1</sup>, Nitin Moholkar<sup>1</sup>, David Tung<sup>2</sup>, and Senthil Nakappan<sup>1</sup>

<sup>1</sup> Kessler Medical Rehabilitation Research and Education Corporation, West Orange, NJ, USA

<sup>2</sup> University of Medicine and Dentistry of New Jersey, Newark, NJ, USA

E-mail: tedwards@kmrrec.org Web: www.kmrrec.org

## INTRODUCTION

The task of standing on a translating surface occurs in various transportation environments and can be used for assessing balance. For this reason, it is important to determine how postural coordination and balance is maintained under such conditions. Prior studies have attributed observed responses to the application of balance strategies, without fully considering the inherent physical dynamic response (Buchanan 1999). It can be demonstrated that such experimental observations are a physical consequence of the dynamic response of the biomechanical system, not solely a balance strategy. The objective of this study was to examine and interpret the response of an individual standing on a sinusoidally translating platform.

## METHODS

Seven healthy adult subjects participated. The subjects were screened to eliminate internal pathologies or medications affecting balance. Informed consent was obtained from each participant.

A NeuroCom Research Balance Platform system provided anterior-posterior oscillations, monitored the platform position, and gathered ground reaction forces. Subjects were exposed to sinusoidal translations with a 6 cm amplitude. A Vicon system gathered motion and analog data. The motion data measurements provided segment positions and joint angles.

Data were collected for fixed frequencies (0.1, 0.25, 0.5, 0.75, 1.0, and 1.25 Hz) of platform oscillation and a frequency sweep 0-1.25-0Hz. Each condition was repeated three times. The eighteen trials and the three frequency sweeps were repeated for eyes-open (EO) and eyes-closed (EC). Subjects rested between trials and between the three repetition sets. Subjects were protected from falling by a safety harness system.

The patterns of motion were described on the basis of the displacements and relative phase of joints to the platform motion. The magnitude of motion of the head, clavicle, hip, and knee were calculated across five cycles of data for the fixed frequencies and for each cycle of the frequency sweep. The positions of the head, clavicle, hip, and knee were normalized against the ankle motion.

## RESULTS AND DISCUSSION

The response for the six test frequencies and the frequency sweep trials show different patterns-of-motion as frequency increased. Of five motion patterns observed, three have been reported previously (Buchanan 1999).

- Head, trunk and lower body all move together in phase
  - Trunk out of phase with the lower body
  - Head and trunk steady in space while the lower body moves with the platform
- Two additional motion patterns were found that have not been described before.
- Head and trunk remain steady and out of phase with the lower body as it moves with the platform

- Head, trunk and knee remain relatively steady in space while the lower leg moves with platform

At all frequencies, subjects tended to select strategies that minimize the motion of the head and the upper body. This is consistent with earlier studies. At lower frequencies (0.10 and 0.25 Hz), all subjects moved in phase with the platform. As frequency increased the motion of the head and upper body decreased. Subjects appeared to select different postural control strategies to accomplish this. At frequencies above 0.75 Hz, no subject was able to sustain either of the first two motion patterns, which involve the most head and upper body motion.

In addition to the knee motion pattern, the study provided two new findings. First, at 0.5 Hz with EO, subjects could stabilize their heads using one of the last three patterns, but not with EC. Subjects appeared more rigid with EC. Second during the frequency sweep trials, the motion of the upper body was always less at the end of the sweep, comparing the same frequency, Figure 1. This demonstrates that subjects were able to tune the stiffness of the ankle, knee, and hip to reduce motion during the trial. Models used earlier to investigate this,

show that joint stiffness can be used to adjust the frequency of the body's first two modes to avoid an excitation frequency (Edwards, 2001). The change in amplitude and phase of the motion patterns with frequency appears to reflect this "tuning" effect.

## SUMMARY/CONCLUSIONS

These results suggest that under different dynamic conditions there are postural control strategies that enhance stability and reduce effort. It is hoped that new diagnostic and treatment techniques can be derived from these studies using whole body oscillations and other balance therapies for improving balance rehabilitation

## REFERENCES

- Buchanan, J. J., and Horak, F. B., 1999, *J Neurophysiol.*, **81**(5), 2325-39.  
 Edwards, W. T., 2001, *J Biomechanics*, **34**(6), 831-832.

## ACKNOWLEDGEMENTS

Support by the Henry H. Kessler Foundation

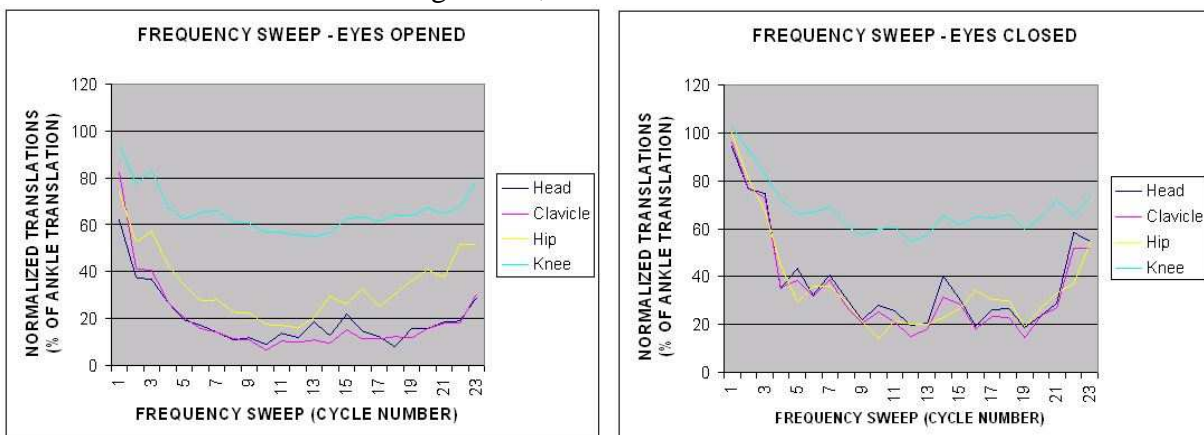


Figure 1a,1b: Mean response (seven subjects) of the head, hip and knee for each of the 23 cycles of the frequency sweep. The platform was stationary at the beginning and the end of the trial and linearly increased in frequency over time to 1.25 Hz at cycle 12. The knee and hip motions are similar for both the EO and EC conditions. With EO, head motion was about 50% of EC.

# BIOMECHANICS OF UPPER EXTREMITY DURING WHEELCHAIR PROPULSION

Shashank Raina<sup>1</sup>, Jill L. McNitt-Gray<sup>1,2,3</sup>, Philip S. Requejo<sup>4</sup>

<sup>1</sup>Department of Biomedical Engineering, USC, Los Angeles, CA, Email:sraina@usc.edu

<sup>2</sup>Department of Kinesiology, USC, Los Angeles, CA

<sup>3</sup>Biological Sciences, USC, Los Angeles, CA

<sup>4</sup>Pathokinesiology Laboratory, Rancho Los Amigos National Rehabilitation Center, Downey, CA

## INTRODUCTION

Of the 1.6 million wheelchair users in the US, only 150,000 use an electric wheelchair (NHIS-D, 1994). A large percentage of wheelchair users are individuals with spinal cord injury. Wheelchairs are the primary means of mobility and for such individuals and hence an essential component of their daily life. Depending on the level of the injury the user possesses varying degree of strength and control of the upper body.

Wheelchair propulsion is a highly repetitive task which is primarily controlled by the upper extremity. This places excessive demands on the shoulder joint which is anatomically not designed to handle such loads for an extended period of time. This causes wear and tear at the shoulder and other joints of the upper limb and can eventually lead to debilitating secondary injuries. There is a need for new designs to lower these loads and consequently reduce the likelihood of injuries. Previous investigations have tried to quantify forces and moments at the shoulder under varying conditions of propulsion (Kulig et al., 1998). The aim of this study is to determine how mechanical loads are distributed among the wrist, elbow, and shoulder under two conditions, which are self-selected fast and slow propulsion. We hypothesized that the distribution of mechanical load across the wrist, elbow, and shoulder joints will be the same across speeds.

## METHODS

Participants in this study exhibited various levels of spinal injury and provided informed consent in accordance with the Institutional Review Board at the Rancho Los Amigos Medical Center, Downey, California. Reflective markers were placed on the hand, forearm, upper arm and the trunk segments, and the right wheel to track segment and wheel kinematics during self-selected fast and slow wheelchair propulsion (six camera Vicon® 3D tracking system). The force applied to the wheelchair by the hand while propelling was measured using SMART<sup>WHEEL</sup> pushrim force collecting system. A four segment 3D upper extremity model (Visual 3D) was used to calculate the joint forces and moments in the upper extremity during the propulsion of the wheelchair. Fine wire EMG was also recorded from eight shoulder and scapular muscles (lower and middle trapezius, anterior and middle deltoids, pectoralis major, subscapularis, supraspinatus and the rhomboids). EMG data was used to determine the role of the upper extremity muscles in controlling the shoulder girdle and joint during fast and slow propulsion.

## RESULTS AND DISCUSSION

The distribution of the mechanical demand imposed on the wrist, elbow, and shoulder was found to be different between tasks at the time of the first ( $Z_1$ ) and second ( $Z_2$ )

peaks in the vertical component of the reaction force (Figure 1).

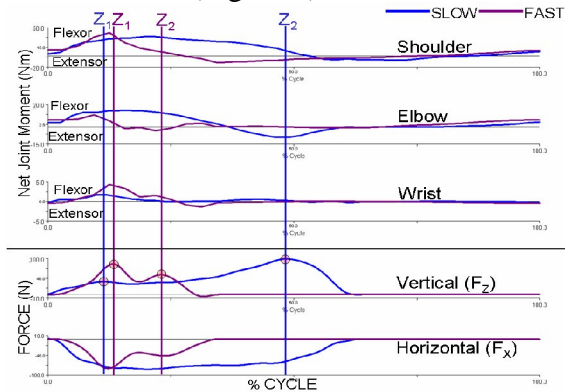


**Figure 1:** The Net Joint Moments (NJM) at the wrist, elbow and shoulder during one propulsion cycle for an exemplar participant: 37 year old male with a T12 spinal injury, 57kg, 1.78m, 15 years post injury.

In the case of the exemplar participant, fast propulsion imposed greater relative demand on the shoulder whereas slow propulsion a more equal distribution between the shoulder and elbow (Figure 2). Wheelchair users with cervical levels of spinal cord injury exhibited different segment kinematics in conjunction with less trunk control. In general, the NJMs were dependent on the magnitude of the reaction forces and Net Joint Forces (NJF) in relation to the segment orientation and the adjacent NJMs. As the segments became more aligned with the reaction and NJFs the magnitude of the NJMs declined. During fast propulsion, the relative angles between the segments and the joint forces were large as compared to slow propulsion. This between-task difference in segment orientation at the time of peak vertical reaction forces contributed to higher wrist and shoulder NJMs during fast propulsion and higher elbow NJMs during slow propulsion. Increase in muscle force requirements increases the potential for muscle fatigue and detrimental loading overtime.

During both the fast and slow propulsion trials, a flexor NJM was required at the elbow and shoulder at  $Z_1$ . In contrast, at  $Z_2$ , a flexor NJM was required at the shoulder whereas an extensor NJM was required at the elbow. This shift in NJM requirements between  $Z_1$  and  $Z_2$  indicates a different set of upper extremity muscles may have been used during the early and late phases of propulsion.



**Figure 2:** Distribution of the NJMs as a percentage of the sum total of wrist, elbow and shoulder moments at  $Z_1$  and  $Z_1$ . Elbow NJM at  $Z_1$  is a flexor; at  $Z_2$  is an extensor).

During fast propulsion, the upper extremity NJMs were sustained for a shorter duration than during slow propulsion. These between task differences in impulse duration may influence the set of muscles used to generate the NJMs required to perform the task.

By understanding how individual patient populations distribute mechanical load during wheelchair propulsion, wheelchair designs can be customized so that individual users can better utilize their muscle force generating capabilities without sustaining an injury.

## REFERENCES

- National Health Interview Survey on Disability, (1994-95) National Center for Health Statistics.
- Kulig, K. et al., (1998) Clinical Orthopedics and Related Research, **354**, 132-143.

# Interpretation of Human Balance Control Based on an Optimal Control Model

Xingda Qu, Maury A. Nussbaum and Michael L. Madigan<sup>1</sup>

<sup>1</sup> Virginia Tech, Blacksburg, VA, USA  
E-mail: xingdaqu@vt.edu

## INTRODUCTION

Upright stance is inherently unstable (Maurer et al. 2005), with maintenance of upright balance performed by the postural control system. Of interest in biomechanics is understanding the control mechanisms involved, both in health and disease.

The objective of this study was to model human balance control under the assumption that the CNS adopts an optimal control strategy. Further, the ability of the model to reflect age-related differences in spontaneous sway was determined, and model parameters were examined to identify potential internal mechanisms responsible for these effects.

## METHODS

An inverted pendulum model was used to determine human body dynamics for the upright posture, and sway was assumed to be restricted to the sagittal plane. Figure 1 illustrates a human postural control system model, in which we assume that spontaneous sway is caused by both the torque generated by the neural controller and a random disturbance torque. In the figure,  $\hat{\theta}$  is the delayed sway angle received by the CNS and approximated by  $\hat{\theta} \approx \theta - \tau_d \dot{\theta}$ , where  $\tau_d$  is the delay time.

The combination of human body dynamics and time delay was considered as the controlled part, the state equations of which can be determined in the standard form.

$$\dot{x} = Ax + Bu \quad (1)$$

where  $x$  and  $u$  present states and control respectively.

It was assumed that the neural controller was an optimal controller which minimized a performance index of the standard form

$$J = \int_0^{\infty} (x^T Qx + u^T Ru + 2x^T Nu) dt \quad (2)$$

where  $Q$ ,  $R$  and  $N$  are time-invariant weighting matrices. These are chosen by regulating relevant physical quantities, including ankle torque change rate and delayed body orientation measures. The optimal controller's performance index in this case is defined by

$$J = \int_0^{\infty} (a_1 \hat{\theta}^2 + a_2 \dot{\hat{\theta}}^2 + a_3 \ddot{\hat{\theta}}^2 + a_4 u^2) dt \quad (3)$$

where  $a_1$ ,  $a_2$ ,  $a_3$ , and  $a_4$  are the weights of different relevant physical quantities. The weighting matrices  $Q$ ,  $R$ , and  $N$  were easily determined by converting the performance index (3) into standard form (2). After knowing the weighting matrices and state equations (1), we obtained the optimal state feedback gain  $K$  by solving the Riccati equation (Naidu, 2003). An optimization procedure, whose objective was to minimize a scalar error function of COP measures, was used to determine the values of model parameters so that the simulation results could best match the experimental results.

## RESULTS AND DISCUSSION

COP measures derived from the model-based simulations matched, in general, experimental data given by Prieto et al. (1996) for young and older adults (Table 1),

indicating that the simulations could yield reasonable estimates of sway behaviors.

The weight of the sway angular acceleration ( $a_3$ ) was significantly smaller in older adults. In contrast, the random disturbance gain ( $Kn$ ) was significantly larger in this group. No significant differences were found in the other parameters. Statistical relationships found in the simulation results could be used to illustrate trends with age. According to these trends, appropriate values of the model parameters might be estimated for the prediction of sway motions in different age groups.

### SUMMARY/CONCLUSIONS

Modeling the neural controller as an optimal controller can help to analyze spontaneous sway from a physiological perspective. In addition, this model can help identify different postural control mechanisms among groups of subjects by comparing

associated model parameters. As a result of the optimization procedure, the model-based simulations reflected experimental data in most cases. Hence, the proposed model may be an effective tool for analysis and interpretation of human balance control, though some limitations still exist. Future work will need to: assess additional individual level effects (e.g. fatigue); develop a more realistic multi-link body model for larger amplitudes of sway motion; incorporate other physical quantities into a performance index; and use additional physical measures to validate the model.

### REFERENCES

- Maurer, C. and Peterka R.J. (2005). *J Neurophysiology*, **93**, 189-200.  
 Naidu, D.S. (2003) *Optimal Control Systems*. CRC Press.  
 Prieto, T.E. et al. (1996). *IEEE Trans Biomed Engin*, **43**, 956-966.

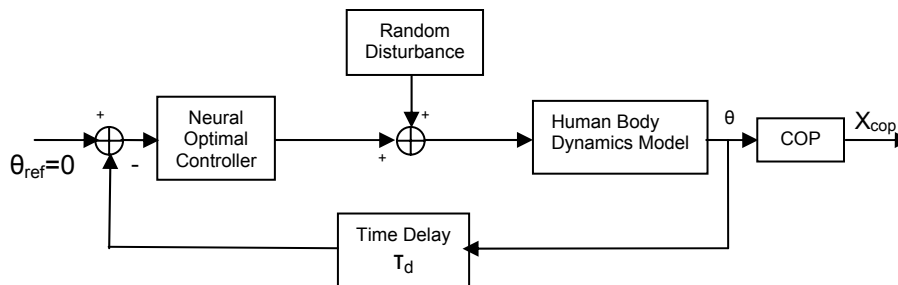


**Figure 1:** Model of the human postural control system

**Table 1:** Simulated and measured (from Prieto et al. 1996) COP values

COP Measures	Young adults				Older adults			
	Measured		Simulated		Measured		Simulated	
	Mean	±SD Range	Mean	±SD Range	Mean	±SD Range	Mean	±SD Range
MD(mm)	2.42	1.45-3.39	2.54	2.10-2.98	3.19	2.18-4.20	3.23	3.05-3.41
RMS(mm)	2.95	1.87-4.03	2.91	2.54-3.28	3.98	2.76-5.20	3.88	3.69-4.07
MV(mm/s)	4.92	3.58-6.26	5.18	4.36-6.00	9.86	6.23-13.49	9.63	8.38-10.90
P50(Hz)	0.275	0.190-0.360	0.210	0.190-0.230	0.355	0.214-0.496	0.245	0.202-0.288*
CFREQ(Hz)	0.509	0.418-0.600	0.607	0.530-0.677*	0.659	0.492-0.826	0.671	0.629-0.712
P95(Hz)	0.928	0.724-1.132	1.175	0.100-1.350*	1.29	0.941-1.639	1.37	1.24-1.50

\* range of simulated measure is not completely within range of the corresponding measured value.

# Digit Inter-dependency during Oscillatory Flexion-Extension Isometric Force Production Task

Qi Li, Jeff Hsu, Marcio Oliveira, Jae Kun Shim  
University of Maryland, College Park, MD, USA

E-mail: jkshim@umd.edu Web: www.hhp.umd.edu/KNES/faculty/jkshim/neuromechanics

## INTRODUCTION

Previous studies on finger force interactions during finger flexion force production have used inter-finger matrix (enslaving matrix) to determine the finger dependency (Zatsiorsky et al. 2000). The inter-digit matrix has been considered as a constant source of positive covariations between finger forces during pressing in uncontrolled manifold hypothesis (Scholz et al. 2004). However, our knowledge is limited in terms of the inter-digit matrix during finger force production in extension and a task involving both flexion and extension.

The aim of this study was to (1) investigate effects of finger force direction (flexion and extension) on finger enslaving, (2) differences in enslaving between tasks of unidirectional force production and continuous changes of finger force directions, and (3) validity of proximity hypothesis (fingers closer to a task finger produce larger involuntary forces).

## METHODS

**Apparatus:** Two-directional (tension and compression) force sensors for four fingers (Index, middle, ring, little) with amplifiers (Models 208 M182 and 484B, Piezotronics, Inc.) were used. The frame was attached to an aluminum panel with a vertical slit (14.0 cm). C-shaped aluminum thimbles were attached on the bottom of each sensor. The frame was tilted at  $25^\circ$  with respect to the antero-posterior axis such that all finger joints were slightly flexed when the distal

phalanges were positioned inside the thimbles. The forearm and hand was fixed in a brace.

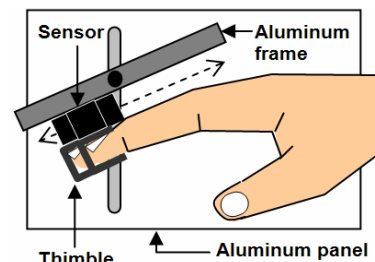


Figure 1. Experiment setup

**Procedure:** Each subject ( $n=18$ ) performed two tasks: individual finger maximum force production (MVF task) and oscillatory flexion-extension force production (oscillation task).

The MVF task was composed of 8 conditions: 4 conditions for task fingers (I, M, R, and L for single-finger tasks) in 2 finger force directions (flexion and extension). During each trial, all fingers were in the thimbles, and subjects were asked to produce maximum isometric force with a task finger in flexion or extension over a 3-s interval. The subjects were instructed to concentrate on the task finger and not to pay attention to non-task fingers.

The oscillation task was composed 4 task finger conditions. For each finger oscillation task, subjects performed 20 flexion-extension cycles for each finger tasks for 20 seconds (1 Hz). The target forces (20% of MVC's in flexion and extension) and the force produced by the task finger were

shown on a computer screen. This was used for visual feedback of finger forces. A metronome was also used to control the frequency of finger force oscillations. The four conditions were performed at 120 beats per minute. The forces produced in either direction were 20% of the task finger's MVC. The conditions lasted 20 seconds (for a total of 20 cycles). A cycle is a flexion force production continued with an extension force production.

For MVF tasks, regression analysis was performed between the task finger force and non-task finger force. The data ranged from 0 to 20% of the task finger MVF were used for the regression analysis. The slopes of the regression lines were used to determine the ratios of non-task finger force to task finger forces. For oscillation tasks, the data were separated into flexion part and extension part. We used frequency response function to calculate the gains. Task finger force was used as an input signal and non-task finger force was used as output signals. The slope ratios and gains were used as the measures of finger inter-dependency (so-called enslaving) for MVF and oscillation tasks, respectively.

## RESULTS

In MVF task, finger enslaving in flexion was smaller than that of extension. In oscillation task, however, difference between finger enslaving effects of flexion and extension was minimal. In MVF task, neighboring fingers showed larger enslaving effects during middle and ring fingers tasks than during index and little fingers tasks. In oscillation task, neighboring fingers showed larger enslaving effects during ring and little finger tasks than during index and middle fingers tasks. Enslaving effects are significantly larger in task of MVF (unidirectional force production) than in task of oscillation.

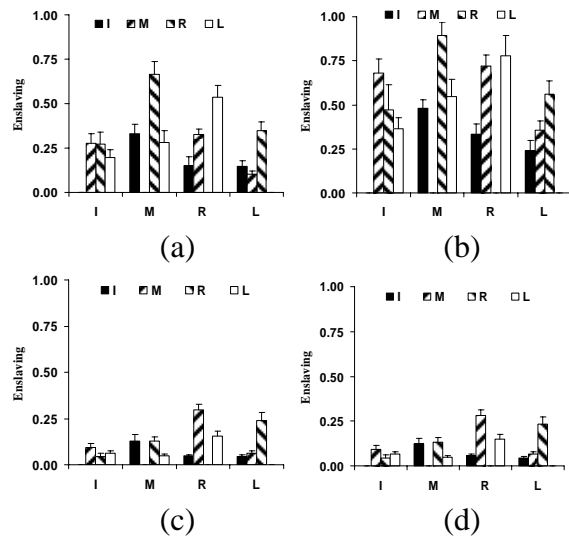


Figure 2. Enslaving during (a) flexion and (b) extension in MVF tasks and during (c) flexion and (d) extension in oscillation tasks.

## CONCLUSIONS

The larger enslaving of fingers closer to task fingers found in our study support the proximity hypothesis. The difference of enslaving effects in MVF and oscillation tasks shows that force production pattern has effect on finger enslaving. These observations also show that finger force direction has influence on enslaving effects in unidirectional force production but has no influence on enslaving effects in force production of continuous changes of finger force directions. We conclude that inter-digit matrix is dependent on force production patterns.

## REFERENCES

- (1) Zatsiorsky VM, Z-M Li, ML. Latash. *Exp Brain Res.* 2000 131:187–195.
- (2) Scholz JP, Kang N, Patterson D, Latash ML. *Exp Brain Res.* 2004 156:282-92.

# PATIENT-SPECIFIC ANALYSIS OF THE INFLUENCE OF VMO TRAINING ON PATELLOFEMORAL FORCES AND PRESSURES

John J. Elias, Surya P. Rai, David M. Weinstein, and David L. Walden

Medical Education and Research Institute of Colorado, Colorado Springs, CO  
E-mail: elias@meric.info Web: www.meric.info

## INTRODUCTION

Physical therapy regimens for treating patellofemoral pain commonly emphasize training the vastus medialis obliquus (VMO), in an attempt to strengthen the muscle and decrease the activation time. The goal of VMO training is to reduce the load applied to the lateral cartilage of the patellofemoral joint and thereby reduce the pressure applied to overloaded cartilage. Because the influence of VMO training on the patellofemoral force and pressure distributions has yet to be established, the current study was performed to characterize the biomechanical benefit of VMO training for patients with patellofemoral pain.

## METHODS

Computational models were developed to represent the knees of five patients who were scheduled for surgical treatment for patellofemoral pain (Fig. 1). The study was approved by the IRB of the Medical Education and Research Institute of Colorado. The models were constructed using MRI images obtained with the knee extended, to reconstruct surface models of the bones and cartilage, and with the knee passively flexed to 45°, to characterize patellofemoral alignment with the knee flexed. Cartilage lesions were identified at locations where the surface models indicated the cartilage thickness decreased dramatically, and the locations were confirmed based on notes from arthroscopic evaluation. The stiffness of the cartilage at each lesion was decreased by 75%. The models were also analyzed

with normal cartilage at the lesion sites. Force vectors represented the muscles of the quadriceps group and the patella tendon. Knee function from 30° to 90° of flexion was simulated for a constant knee extension moment of 30 N-m. A normal quadriceps force distribution, with approximately 10% of the quadriceps force applied by the VMO, and one typical of patients with patellofemoral pain, with approximately 5% of the quadriceps force was applied by the VMO, were simulated (Zhang et al., 2003; Makhssous et al., 2004). Delayed VMO activation was also simulated by eliminating the VMO force.

At each flexion angle, the patellofemoral force and pressure distributions were quantified using the discrete element analysis technique, as described previously (Elias et al., 2004 and 2006). Patellofemoral cartilage was represented by a surface of springs midway between the cartilage on the patella and the femur. In response to the force vectors applied to the patella, the patella translated and rotated with respect to

the trochlear groove in a pattern that minimized the total potential energy stored within the springs. The patellofemoral force and pressure distributions were determined by the deformation of each spring and the spring properties.

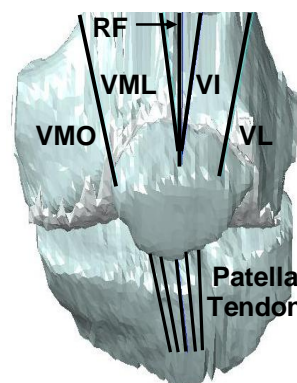


**Figure 1:** Knee model at 45° of flexion.

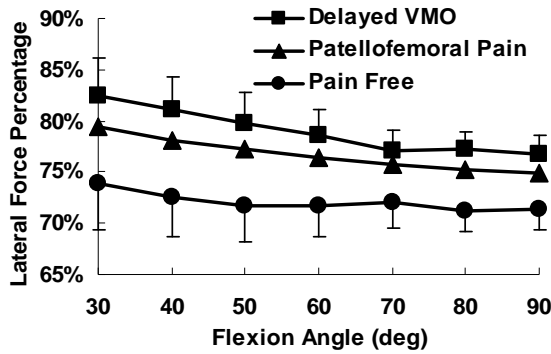


**Figure 2:** The average ( $\pm$  standard error) lateral force percentage.

## RESULTS AND DISCUSSION

Simulated VMO training decreased the lateral force and lateral tilt moment acting on the patella, which decreased the percentage of the total compressive force applied to the lateral cartilage (Fig. 2). The decrease in the lateral force percentage from the “patellofemoral pain” quadriceps force distribution to the “pain free” quadriceps force distribution was statistically significant ( $p < 0.05$ , repeated measures ANOVA and Student-Newman-Keuls post-hoc test) from 30° to 90° of flexion. The decrease from the “delayed VMO” quadriceps force distribution to the “patellofemoral pain” quadriceps force distribution was significant at every angle but 40° and 70°.

The maximum pressure decrease due to simulated VMO training was not as dramatic (Fig. 3). The decrease in the maximum pressure from the “patellofemoral pain” quadriceps force distribution to the “pain free” quadriceps force distribution was only statistically significant at 80°. The decrease from the “delayed VMO” quadriceps force distribution to the “patellofemoral pain” quadriceps force distribution was not significant at any flexion angle. Restoring normal cartilage at the lesion sites decreased the maximum pressure by an average of 8% across all flexion angles, but did not dramatically alter the noted trends.

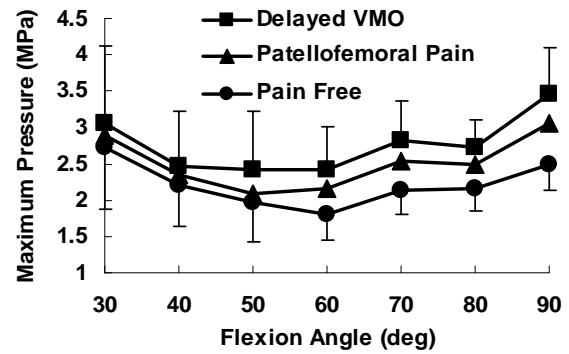


**Figure 3:** The average ( $\pm$  standard error) maximum cartilage pressure.

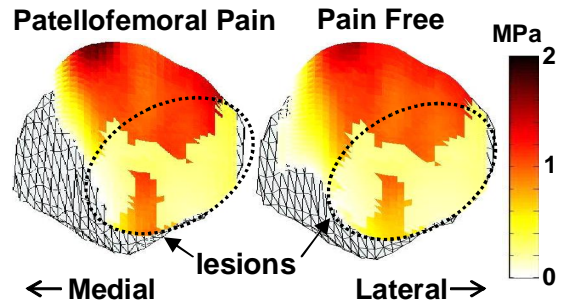


**Figure 4:** Patellofemoral pressure distribution at 80° for one knee.

## SUMMARY/CONCLUSIONS

Improving VMO function consistently reduced the force applied to lateral cartilage. The decrease in the maximum pressure was less consistent due to factors including the presence of lesions, unloading regions away from the position of maximum pressure (Fig. 4), and patellofemoral dysplasia. Additional computational modeling can help characterize the anatomical parameters that influence the biomechanical benefit of improving VMO function.

## REFERENCES

- Zhang, L.Q., et al. (2003). *J Orthop Res*, **21**, 565-71.
- Makhsous, M., et al. (2004). *Med Sci Sports Exerc*, **36**, 1768-75.
- Elias, J.J., et al. (2004). *Am J Sports Med* **32**, 1202-8.
- Elias, J.J., et al. (2006). *J Biomech* **39**, 865-872.

# EFFECT OF TOTAL KNEE REPLACEMENT ON JOINT MOMENTS DURING LEVEL WALKING AND STAIR ASCENT

David Mandeville, Li-Shan Chou, Louis Osternig  
Motion Analysis Laboratory, University of Oregon, Eugene, OR, USA  
Email: chou@uoregon.edu

## INTRODUCTION

Studies assessing changes of gait function due to knee osteoarthritis (OA) and total knee replacement (TKR) have primarily focused on kinematic and kinetic descriptions of the knee joint. Few reports address the role of the ipsilateral hip and ankle joints in these gait compensation strategies (Simon et al. 1983, Benedetti et al. 1999).

Anderson et al. (2003), described muscle forces as major contributors to the vertical ground reaction force (Fz), and concluded that muscle support generating potential is described by its contribution to Fz. Winter (1980) defined the moment of support (Ms) as the summation of the net joint moments at the knee, hip and ankle, representing the extensor synergy of the lower extremity to prevent collapse of the lower limb.

Estimating Ms at the 1<sup>st</sup> peak Fz provides a description of lower limb moment patterns relative to weight acceptance. During stair ascent, the 1<sup>st</sup> peak Fz includes net extensor moments greater than those of level walking. Quantifying intra-limb moment patterns in this manner at pre and post-surgery collections may help characterize the change of lower limb support synergy in response to TKA.

Thus, the aim of this study was to describe the effect of TKR on the involved limb moment patterns during level walking and stair ascent.

## METHODS

Forty-four volunteer subjects were recruited into two experimental groups: 1) TKR, n = 22; and 2) healthy age-matched control, n = 22. Subjects were tested pre-operatively (P1) and 6 months later (P2).

Subjects were fitted into a fall arrest harness for self-selected level and stair gait. An array of 29 reflective markers defined a thirteen link model of the human body. Spatio-temporal and whole body kinematic estimates were obtained using an eight camera Real Time Motion Analysis system. Ground reaction forces were obtained from 3 AMTI force plates located in a 10 m walkway. For stair climbing, the third force plate comprised the surface of an independent first step of a stair assembly. The third plate and stair case were placed in series with the floor-mounted plates for stair climbing trials. Inverse dynamic calculations were computed using Orthotrak 6.2 software. A complete stride for the TKR involved limb and the dominant limb of control were analyzed from each trial. A stair ascending stride was defined as foot contact of the involved/dominant limb on the instrumented first step and ending on the 3<sup>rd</sup> step/platform. Variables analyzed included: gait velocity, stride length, Ms, hip, knee, and ankle net joint moments. Within and between group differences were assessed using a mixed model ANCOVA with gait velocity as a covariate.

## RESULTS AND DISCUSSION

The TKR patients increased their gait velocity ( $P < .0001$ ) and stride length ( $P <$

.0001) for level walking across period, yet these values were significantly less than control values at both periods. The TKR Ms values significantly decreased across periods ( $P = .0091$ , Table 1), due primarily to a knee contribution to the Ms(-12.6%) at P2 which was significantly different ( $P = .0005$ ) than the extensor contribution shown by controls (12.4%). Across period, TKR hip extensor moment values were 68.9% and 72.9% of Ms, which were non-significantly larger than control hip contributions across period by 10.4% and 15.8%, respectively. The TKR ankle plantarflexor moment contribution increased non-significantly across period from 28.4% to 36.8% of Ms, which were similar to control values at P1 but 6.6% greater at P2.

For stair climbing, TKR gait velocity, stride length, were significantly less than control values at P1 and P2; and the Ms values were significantly less than control values at P1 and P2 ( $P < .0001$ , Table 2). As with level walking, TKR Ms values decreased significantly across period ( $P < .0001$ ) and were primarily the result of decreased knee extensor contribution to the Ms from 20% at P1 to 12% at P2. The TKR P2 values were significantly less ( $P < .0001$ ) than the control P2 values of 26.5%. The TKR hip extensor moment values were 5.1% and 12.8% greater than control values at P1 and P2. Patient ankle plantarflexor moment values showed little change across period and were similar to control values.

At P2 testing, patients displayed an extensor moment synergy relative to weight acceptance which was similar to their pre-operative synergy than that of control. The TKR patients showed significantly less knee flexion angle at weight acceptance than control at both periods and appeared to use the knee more as a strut than as a dampening element in the involved kinetic chain. These

results are consistent with the stiff-legged gait previously reported for knee OA and post TKR patients (Andriacchi 1982, Benedetti 1999). The hip extensor contribution to Ms for TKR likely compensates for diminished knee extensor contribution at weight acceptance.

## References:

- Simon et al., 1983. JBJSA, **65**.  
 Benedetti et al., 1999. IEEE TRE. **9**.  
 Anderson, Pandy. 2003. G&P, **17**.  
 Winter 1980. JBmech. **13**.  
 Andriacchi et al., 1982. JBJSA. **64**

**Table 1:** Adjusted mean Ms, hip, knee, and ankle net joint moments<sup>†</sup> and knee angle 1<sup>st</sup> peak Fz during level walking for TKR and control across time (standard error).

Period	TKR		Control	
	P1	P2	P1	P2
Ms (Nm/kgm)	0.893 (0.071)	0.695 <sup>††</sup> (0.058)	0.962 (0.064)	0.939 (0.058)
Hip moment (Nm/kgm)	0.615 (0.053)	0.507 (0.043)	0.563 (0.048)	0.536 (0.043)
Knee moment (Nm/kgm)	0.023 (0.052)	-0.069 <sup>†</sup> (0.037)	0.149 (0.049)	0.120 (0.037)
Ankle moment(Nm/kgm)	0.254 (0.034)	0.256 (0.029)	0.251 (0.030)	0.284 (0.030)
Sagittal knee angle (degrees)	13.747 (1.230)	10.633 <sup>††</sup> (1.155)	15.684 (1.194)	16.092 (1.150)

<sup>†</sup>Extensor moments are positive, flexor moments are negative.

<sup>††</sup>Indicates significant within group difference ( $P < .05$ ).

<sup>‡</sup>Indicates significant between group difference ( $P < .05$ ).

**Table 2:** Adjusted mean Ms, hip, knee, and ankle net joint moments<sup>†</sup> and knee angle at 1<sup>st</sup> peak Fz during stair ascent for TKR and control across time (standard error).

Period	TKR		Control	
	P1	P2	P1	P2
Ms (Nm/kgm)	1.825 <sup>†</sup> (0.119)	1.707 <sup>†</sup> (0.104)	2.513 (0.105)	2.358 (0.103)
Hip moment (Nm/kgm)	0.896 <sup>†</sup> (0.077)	0.890 (0.059)	1.105 (0.067)	0.927 <sup>†</sup> (0.059)
Knee moment (Nm/kgm)	0.364 (0.061)	0.204 <sup>††</sup> (0.048)	0.500 (0.054)	0.625 (0.048)
Ankle moment(Nm/kgm)	0.560 <sup>†</sup> (0.054)	0.606 <sup>†</sup> (0.048)	0.919 (0.046)	0.816 <sup>†</sup> (0.047)
Sagittal knee angle (degrees)	39.909 <sup>†</sup> (2.596)	33.572 <sup>††</sup> (2.505)	50.523 (2.298)	50.547 (2.560)

<sup>†</sup>Extensor moments are positive, flexor moments are negative.

<sup>††</sup>Indicates significant within group difference ( $P < .05$ ).

<sup>‡</sup>Indicates significant between group difference ( $P < .05$ ).

# IMPACT ATTENUATION CHARACTERISTICS FOR COLLEGE-AGE AND POST-MENOPAUSAL FEMALES DURING RUNNING

John A. Mercer, Janet S. Dufek, Kaori Teramoto, and Brent C. Mangus

University of Nevada, Las Vegas, Las Vegas, NV, USA

E-mail: [jmercer@unlv.nevada.edu](mailto:jmercer@unlv.nevada.edu) Web: <http://kinesiology.unlv.edu>

## INTRODUCTION

Current literature has documented the fact that physically active females experience a greater percentage of non-contact knee joint anterior cruciate ligament (ACL) injuries than their male counterparts in comparable impact activities (Cowling and Steele, 2001; Ireland, 1999). It has been hypothesized that the reason(s) for this gender-related injury bias are related to one or several of the following: 1) anatomical differences, 2) hormonal factors, and 3) biomechanical and/or neurological considerations (Hewitt, 2000). Research investigating hormonal factors as an explanation for these greater non-contact ACL injuries in females has been non-conclusive. However, an investigation examining knee joint kinematics during a dynamic activity for pre- and post-pubescent females has documented differences between the groups (Hass, et al., 2005). It is possible that this indirect, non-invasive method of categorizing individuals based upon physiological maturation (differences in hormonal levels) may be a viable approach to understanding functional changes in performance characteristics across the lifespan, specifically with respect to occurrence of injury.

Lower extremity non-contact injuries are the result of one of several possible scenarios including higher than normal force generated in a normal direction which exceeds the tolerance of the biological tissue or force exerted in an abnormal direction

which exceeds the tissue tolerance. A measure of g-forces to which body segments are exposed may provide insight to the forces acting on the structure in vivo, with respect to injury potential. Therefore, the purpose of the study was to examine the impact acceleration characteristics at selected anatomical sites between normally menstruating (N) and post-menopausal (P) women during treadmill running. This aim indirectly examined hormonal factors as a possible explanation for the prevalence of non-contact ACL injuries in females.

## METHODS

Fourteen healthy, normally menstruating (age:  $24.9 \pm 4.0$  yrs; ht:  $163.6 \pm 3.3$  cm; mass:  $63.1 \pm 8.6$  kg) and ten healthy, post-menopausal (age:  $56.1 \pm 6.6$  yrs; ht:  $162.9 \pm 10.0$  cm; mass:  $64.8 \pm 13.2$  kg) women granted consent to participate in accordance with the procedures approved by the Institutional Review Board at the affiliated university. Subjects were instrumented with uniaxial, lightweight accelerometers (tibia, low back, forehead) and were asked to run on a treadmill at their preferred speed (PS) followed by a speed 10% faster (FS) while accelerometer data were obtained (1000 Hz). Peak acceleration values were identified at each measurement site (LgPk, HdPk, BkPk) for 10 strides of running per subject-condition. Three two-way (group x speed) repeated measures analyses of variance (ANOVAs;  $\alpha = 0.05$ ) were

conducted to examine the peak impact values. In addition, shock attenuation (SA:  $[1 - \text{HdPk} - \text{LgPk}] * 100$ ) was computed and similarly evaluated.

## RESULTS AND DISCUSSION

Mean and standard deviation values for each dependent variable (DV)-condition as well as running speed are given in Table 1. One significant group x condition interaction was identified (BkPk). LgPk, HdPk, and BkPk were different across conditions ( $p < 0.05$ ). There were no identified group differences for any of the DVs evaluated ( $p > 0.05$ ).

**Table 1:** Peak acceleration (Gs), shock attenuation (%) and velocity (m/s) values by group-condition (mean; *SD*)

	LgPk	HdPk	BkPk	SA	Vel
<b>N:PS</b>	4.24	1.11	2.85	74.6	2.63
	<i>1.26</i>	<i>0.31</i>	<i>1.11</i>	<i>5.7</i>	<i>0.41</i>
<b>P:PS</b>	3.06	0.86	2.31	70.8	1.88
	<i>1.59</i>	<i>0.45</i>	<i>1.20</i>	<i>7.7</i>	<i>0.56</i>
<b>N:FS</b>	4.62	1.27	2.99	73.0	2.91
	<i>1.43</i>	<i>0.40</i>	<i>0.90</i>	<i>7.6</i>	<i>0.46</i>
<b>P:FS</b>	3.36	1.03	2.97	68.1	2.13
	<i>2.30</i>	<i>0.64</i>	<i>1.59</i>	<i>7.6</i>	<i>0.61</i>

Results of the study support previous research (Mercer, et al., 2002) indicating that SA, or the body's ability to attenuate leg impact, decreases with an increase in running speed. Despite the lack of group differences for the impact measures, results suggest that there may be a difference between groups in BkPk during running. The experimental protocol was designed to produce a slightly greater shock wave via an increase in running speed. N reduced HdPk (relative to LgPk) an average of 73.1% vs 70.6% for P between conditions (Figure 1). Similarly, BkPk reductions were 34.0% and 18.0% for N and P, respectively, with BkPk

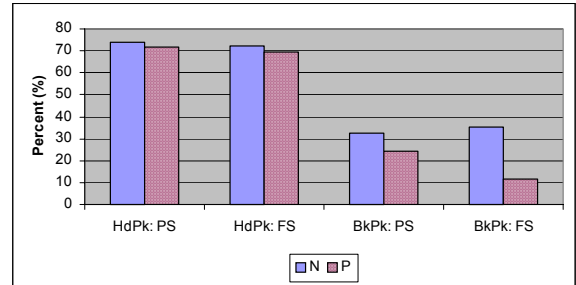


**Figure 1:** Average reduction in impact values (relative to LgPk) for each group-condition.

reductions for P only 1/3 those of N at FS. This may suggest that P reached a limit of impact attenuation at PS, and was not able to accommodate added system stress at FS.

## SUMMARY/CONCLUSIONS

This study sought to explore maturation as a possible defining characteristic relative to impact attenuation and injury potential in females. Results did not support this hypothesis; however BkPk results suggest a source of possible differences between N and P during running.

## REFERENCES

- Cowling, E.J., Steele, J.R. (2001). *J. Elect. Kines.*, **11**, 263-268.  
 Hass, C.J., et al. (2005). *MSSE*. **35**, 100-107.  
 Hewitt, T. (2000). *Sports Med.*, **29**, 313-327.  
 Ireland, M.L. (1999). *J. Athl. Train.* **34**, 150-154.  
 Mercer, et al. (2002). *Eur. Jrl. Appl. Phys.*, **87**, 403-408.

## ACKNOWLEDGEMENT

Partially funded by the Center for Excellence in Women's Health, School of Nursing, University of Nevada, Las Vegas.

# EFFECT OF GENDER AND ORAL CONTRACEPTIVE USE ON FRONTAL PLANE KNEE JOINT STIFFNESS: A PILOT STUDY

Martha Loehr<sup>1,2</sup>, Jennifer Moore<sup>2</sup>, Anastasios Tsoumanis<sup>2,3</sup>, Yasin Dhafer<sup>1,2</sup>

<sup>1</sup> Department of Biomedical Engineering, Northwestern University, Chicago, IL, USA

<sup>2</sup> Sensory Motor Performance Program, Rehabilitation Institute of Chicago, Chicago, IL, USA

<sup>3</sup> Department of Biomedical Engineering, Illinois Institute of Technology, Chicago, IL, USA

E-mail: y-dhafer@northwestern.edu

## INTRODUCTION

The menstrual cycle and the fluctuation of female sex hormones (mainly estrogen) have been implicated in affecting ligamentous laxity of the knee (Hewett, 2000). Indeed, it has been reported that females exhibit greater joint laxity than males in both the transverse (Wojtys, et al. 2003) and sagittal (Granata et al. 2002) planes. One study demonstrated that female athletes using oral contraceptives (OC) had significantly decreased anterior-posterior joint laxity as compare to non-users (Martineau et al. 2004). The authors attribute this result to the stabilization of hormones in OC users rather than the absolute hormone concentrations in the body at any time.

It is not clear as of yet if hormonal stabilization mediated by OC has a significant effect on knee joint stiffness in the frontal plane. The significance of this study stems from emerging findings which associate the incidences of ACL injury to abnormal abduction loading in female athletes (Hewett et al. 2005). In this prospective study, Hewett et al. suggested that abnormal abduction loading at the knee can be used as the primary predictor for ACL risk of injury in female athletes. Accordingly, the purpose of this pilot study was to examine gender differences in frontal plane joint stiffness as well as the effect of different types of OC (monophasic and triphasic) on female joint laxity in this plane of motion.

## METHODS

Ten male and ten female subjects with no history of neurological or musculoskeletal disorders were tested. Female subjects were placed into three groups based on OC usage: F1 - non-users (N = 2), F2 - monophasic OC users (N = 6), and F3 - triphasic OC users (N = 2). All subjects reported a moderate level of activity, which mainly included running/jogging or recreational sports.

Subjects were seated in an experimental chair with the knee fully extended. The subject's right ankle was placed in a cast and then secured to a servomotor actuator, via a rigid cantilever beam. A six degrees-of-freedom load cell was used to record the force and torque signals and brackets were securely fastened around the knee to prevent medial/lateral translation of the knee during the mechanical perturbation. Torque-angle relationships were obtained for each subject by stretching the joint  $\pm 7^\circ$  in the abduction-adduction direction starting and ending at the neutral position at a constant velocity ( $3^\circ/\text{s}$ ) under a volitionally relaxed state (Figure 1). Stiffness was estimated as the average slope of the torque-angle relationship (Dhafer et. al. 2005). Abduction midrange stiffness was estimated between  $0^\circ$  and  $-5^\circ$  and the terminal stiffness was estimated between  $-5^\circ$  and  $-7^\circ$ . Similar estimates for the adduction stiffness were used.

Independent sample 2-tailed *t* tests were performed on the stiffness estimates between males, all females, and the female

subgroups. Statistical significance was set at  $p < 0.05$ .

## RESULTS AND DISCUSSION

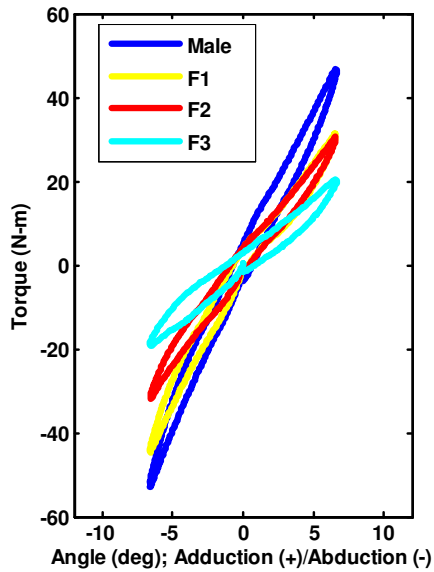


**Figure 1.** Representative torque-angle relationships obtained during passive stretching of the knee in the frontal plane for each experimental group.

Abduction and adduction stiffness estimates for all groups are presented in Table 1. Males exhibited significantly ( $p < 0.05$ ) greater midrange and terminal abduction and adduction stiffness than all female groups, except the F1 (non-users) group. The F1 group tended to have greater stiffness than the F2 group, which in turn exhibited greater stiffness than the F3 group. However, there were only significant differences between female groups in the terminal stiffness comparisons. The F2 group was significantly stiffer than F3 in

abduction and F1 was stiffer than F3 in adduction.

## SUMMARY/CONCLUSIONS

Our preliminary results suggest that usage and type of OC are important factors in determining joint stiffness in the frontal plane. However, our findings were contrary to published results which demonstrated decreased A-P laxity in female OC users (Martineau et al. 2004). These differences may suggest that OC use affects joint stiffness differently in the frontal plane than in the transverse and/or sagittal planes. However, further investigation on a larger sample size is warranted before fair comparisons are made.

We believe that the changes in joint stiffness impose a greater burden on the motor control system to compensate for the contraceptive induced laxity and these changes should be considered when designing neuromuscular training programs.

## REFERENCES

- Dhafer et al. (2005). *J. of Neurophysiology*, **93**(5):2698-709.  
 Granata, KP et al. (2002). *J Electromyogr Kinesiol*, **12**(2):119-26.  
 Hewett, TE (2000). *Sports Med*, **29**(5):313-27.  
 Hewett, TE et al.(2005). *Am J. Sports Med*, **33**(4):492-501.  
 Martineau,PA et al.(2004). *Clin J Sport Med*, **14**(5):281-6.  
 Wojtys, EM et al.(2003). *J Bone Joint Surg Am*, **85-A**(5):782-9.

## ACKNOWLEDGEMENTS

This work was supported by the National Institute of Health (1-R01-AR049837-01)

**Table 1:** Midrange and terminal joint stiffness in abduction and adduction. (Mean  $\pm$  SD, units of N-m/ $^{\circ}$ )

	Males	Females	F1	F2	F3
Midrange Abduction	6.03 $\pm$ 1.13	4.36 $\pm$ 1.08 <sup>a</sup>	5.51 $\pm$ 0.84	4.57 $\pm$ 0.59 <sup>a</sup>	3.45 $\pm$ 1.25 <sup>a</sup>
Terminal Abduction	9.39 $\pm$ 1.98	6.01 $\pm$ 1.36 <sup>a</sup>	7.57 $\pm$ 1.31	6.31 $\pm$ 0.75 <sup>a</sup>	4.59 $\pm$ 0.64 <sup>a,c</sup>
Midrange Adduction	4.43 $\pm$ 1.11	3.35 $\pm$ 0.69 <sup>a</sup>	3.87 $\pm$ 0.12	3.51 $\pm$ 0.28 <sup>a</sup>	3.18 $\pm$ 0.91 <sup>a</sup>
Terminal Adduction	4.77 $\pm$ 0.85	3.31 $\pm$ 0.73 <sup>a</sup>	4.08 $\pm$ 0.23	3.50 $\pm$ 0.47 <sup>a</sup>	2.69 $\pm$ 0.01 <sup>a,b</sup>

a – Female groups exhibiting significantly lower ( $p < 0.05$ ) stiffness than male subjects; b – F3 significantly lower ( $p < 0.05$ ) stiffness than F1; c – F3 significantly lower ( $p < 0.05$ ) stiffness than F2.



# APPROXIMATE ENTROPY AS A MEASURE OF SITTING POSTURAL DEVELOPMENT IN INFANTS

Joan E. Deffeyes<sup>1</sup>, Regina T. Harbourne<sup>2</sup>, Stacey L. DeJong<sup>2</sup>, Wayne A. Stuberg<sup>2</sup>,  
Anastasia Kyvelidou<sup>1</sup>, Nicholas Stergiou<sup>1</sup>

<sup>1</sup> Biomechanics Laboratory, University of Nebraska at Omaha, Omaha, NE, USA

<sup>2</sup> Munroe-Meyer Institute, University of Nebraska Medical Center, Omaha, NE, USA

E-mail: [jdeffeyes@mail.unomaha.edu](mailto:jdeffeyes@mail.unomaha.edu) Web: [www.unocoe.unomaha.edu/hper/bio/home.htm](http://www.unocoe.unomaha.edu/hper/bio/home.htm)

## INTRODUCTION

Upright sitting is one of the first developmental milestones an infant achieves in normal development. This seemingly static posture involves considerable subtle movement as the weight shifts, requiring some type of control strategy to keep the body upright. Center-Of-Pressure (COP) data obtained from a force platform is used to gain insight into these control strategies. In infants COP data gives insight into the development of control strategies as they learn to sit (Harbourne & Stergiou, 2003). The COP data contains information about postural control, but suitable mathematical techniques must be employed to quantify the postural control information. Techniques such as path length or range of movement can be used to describe how much the center of pressure moves around (quantity of movement), but these techniques don't give any information about how well coordinated the movement is (quality of movement). Approximate entropy (ApEn) is a measure of the randomness in a time series (Pincus, 1991) and can be used to assess quality of movement. However, it is necessary to select key parameters used by the algorithm, such as lag time. Here, we present a novel method of lag time selection. In addition, high levels of randomness in postural sway will make maintaining upright posture difficult. We hypothesized that older infants who are better at sitting will have less randomness in postural sway than younger infants who do not sit as well.

## METHODS

Infants were recruited when they were just developing the ability to sit upright (started at age 145.1 days old,  $sd=15.9$  days,  $n=11$ ). Infants were screened for normal development by a physical therapist prior to admission into the study, being excluded if they failed to score above 0.5 standard deviations below the mean on the Peabody Developmental Motor Scales (Folio & Fewell, 2000). Infants came to the laboratory twice per month for a period of four months, until they were beginning to crawl, and would thus no longer sit still for data acquisition.

For data acquisition, infants sat on an AMTI force plate (Watertown, MA), interfaced to a computer system running Vicon data acquisition software (Lake Forest, CA). COP data was analyzed using custom MatLab software (MathWorks, Nantick, MA), and ApEn was calculated using code developed by Kaplan and Staffin (1996), implementing the methodology of Pincus (1991) and Kaplan, et al. (1996). Stage of sitting was assessed by a physical therapist on a scale of 1 to 3 (1=prop sitting, 3=extended time, upright sitting) based on length of time the infant was able to maintain upright sitting without a fall. ApEn was calculated for the COP data from the anterior-posterior axis for each of 244 trials, using various lag times. The ApEn results were then correlated with 1) age of the

infant at data acquisition, and 2) stage of sitting.

## RESULTS AND DISCUSSION

In all cases the correlations were negative, but the strongest correlations were for a lag time of 4. We believe this is due to the fact that we acquired data at 240 Hz, and found a small 60 Hz signal in our data, presumably from 60 Hz AC electrical interference. Thus every fourth data point would be at the same position in the 60 Hz noise cycle. As shown in Figure 1, all lag times with a multiple of 4 had stronger correlations than those which were not multiples of four. Filtering data before calculation of ApEn was not done, because filtering can alter nonlinear analysis results in an unintended manner (Rapp, 1994).

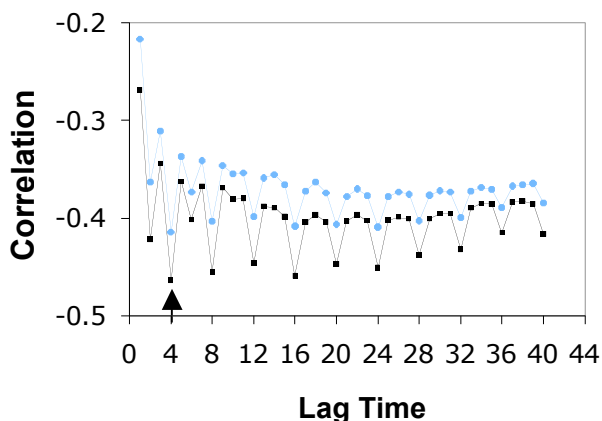


**Figure 1:** Correlation of ApEn with age (circles, lighter curve) and with stage of sitting (squares, darker curve). Arrow indicates lag = 4, the strongest correlation.

We also found a negative correlation coefficient for the correlation of ApEn both with age ( $r = -.414$ ) and with stage of sitting ( $r = -.464$ ). Lower values of ApEn indicate less randomness. Thus we find lower randomness in postural sway is associated with older infants who have higher levels of sitting ability.

## SUMMARY/CONCLUSIONS

Using an optimized lag time parameter in the calculation of ApEn, we found that ApEn values for COP data from infant sitting were negatively correlated with both age of the infant and with stage of sitting. Our results are consistent with the hypothesis that higher randomness in postural sway is associated with earlier stages of growth and development.

This paper also presents a new method of dealing with high frequency noise in nonlinear analysis, namely the selection of an appropriate lag, such that the lag time of the analysis is equal to the data collection frequency/main frequency component of noise. The sampling frequency must be an even multiple of the fundamental frequency of the noise to use this method. Selection of the best lag was made by maximizing the correlation of approximate entropy with age of the infant and with stage of sitting.

## REFERENCES

- Harbourne, R.T., Stergiou, N. (2003) *Dev Psychobiol.* **42**, 368-77.
- Folio M.R., Fewell R.R.(2000). *Peabody Developmental Motor Scales, 2nd Edition*. Pro-ed, Inc., Austin, TX,
- Kaplan, D. et al. (1991). *Biophys.J.* **59**, 945-949.
- Pincus SM. (1991) *Proc Natl Acad Sci USA*, **88**, 2297-2301.
- Rapp, P.E. (1994). *Integr Physiol Behav Sci.* **29**, 311-327.
- Kaplan, D., Staffin, P. (1996). <http://www.macalester.edu/~kaplan/hrv/doc/>

## ACKNOWLEDGEMENTS

This work was supported by NIH (K25HD047194) and NIDRR (H133G040118).

# A NEW TECHNIQUE FOR EXPEDITED FRACTURE SEVERITY ASSESSMENT

Thaddeus Thomas, Donald D Anderson, J Lawrence Marsh, and Thomas D Brown

The University of Iowa, Iowa City, IA, USA  
e-mail: thaddeus-thomas@uiowa.edu

## INTRODUCTION

Intra-articular fractures often portend secondary osteoarthritis, chronic disabling pain, and decreased joint function. Clinical decision-making in treating such complex articular injuries requires assessment of injury severity. Until recently, there has been no means to objectively measure comminution and injury severity, preventing clinicians from compiling a body of literature and collective experience to guide advances in the care of these patients.

A new CT-based methodology has provided objective quantification of injury severity, based upon the amount of interfragmentary surface area [1], and it has been shown to agree with expert subjective opinion [2]. However, translation of these methods to clinical use has been limited by its extended processing time (4-8 hours per case). Thus an expedited technique for fracture severity assessment has been developed based upon textural image analysis.

## METHODS

CT studies were obtained from twenty tibial pilon fracture cases. Interfragmentary surface areas (the established fracture severity metric) were calculated as the difference between free bone surface areas on fractured and intact tibias for each patient, using existing methods for accurate segmentation of bone and its fragments [1].

The expedited technique was developed using the same twenty fracture cases. In lieu

of delineating bone margins, the new method quantified disorder in a given CT slice using texture analysis, based on the gray level co-occurrence matrix (GLCM). The GLCM describes the relative spatial organization of pixel intensities within a given image, a textural feature disrupted on CT images of a fracture. GLCMs were constructed on a slice-by-slice basis for both the intact and fractured tibias using MATLAB. The GLCM was reduced to a scalar value reflecting the heterogeneity of each slice, calculated using statistical methods (Figure 1).

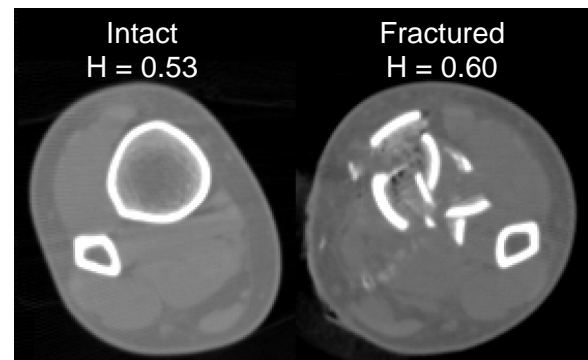


**Figure 1:** Axial CT slices taken from the same level of a fractured and intact contralateral limb illustrate the degree of disorder following a fracture. Heterogeneity scalars (H) are shown for these two slices.

For a given fracture case, the expedited fracture severity metric was calculated by summing the differences in heterogeneity between the intact and fractured limbs over comparable lengths of the distal tibia. The agreement between this expedited metric and the existing validated fracture severity metric was assessed using linear regression.

## RESULTS AND DISCUSSION

The expedited technique reduced the time required to obtain an objective fracture severity assessment to roughly 10 minutes, while maintaining excellent agreement with the existing metric (Figure 2). Linear regression between the heterogeneity measure and interfracture surface area yielded an  $R^2$  value of 0.80 (Figure 3).

In addition, the expedited technique was able to be fully automated, requiring no user intervention once CT scans were obtained.

## SUMMARY/CONCLUSIONS

A new CT-based technique was developed to objectively quantify fracture severity in an expedited manner. Areas for future work include the analysis of additional fracture cases and further algorithm refinement.

Reducing the reliance of present methods upon a CT scan of the intact contralateral limb, not generally available, is a logical next target for refinement. Progressive development of this expedited technique will deliver a practical solution into the clinical setting, providing a new tool to aid in improving patient treatment.

## REFERENCES

1. Beardsley C et al. (2002)  
J Biomech 35:331-8.
2. Anderson D et al. (2004)  
Trans 50th ORS Meeting, 29:488.
3. Thomas T et al. (2006)  
Trans 52nd ORS Meeting, 31:1896.

## ACKNOWLEDGEMENTS

Funded by grants from the NIH (AR46601 and AR048939), The AO Research Fund, and the Orthopaedic Trauma Association.

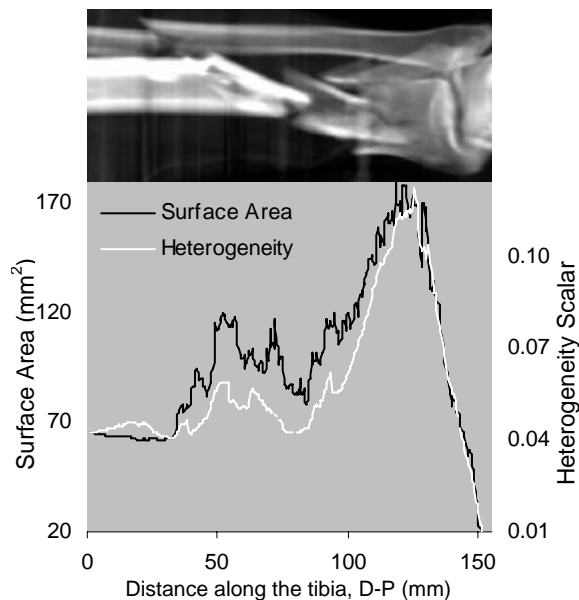


**Figure 2:** GLCM derived scalars identify discontinuity along the length of the tibia e.g. comminution, displaying similar trends to that of surface area liberation.

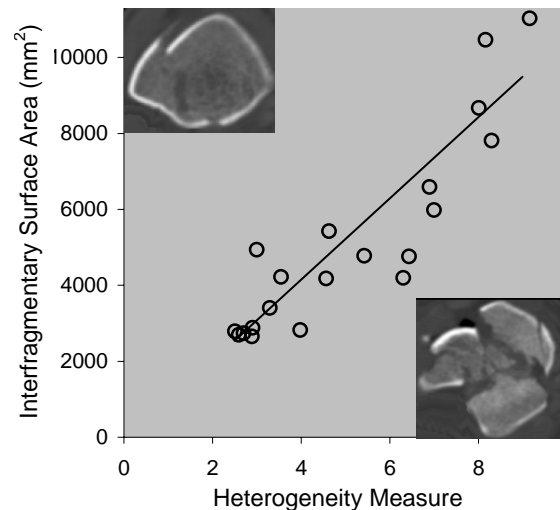


**Figure 3:** The heterogeneity measure agreed well with the established fracture severity metric. Inset images show slices from the least severe (upper left) and most severe (lower right) fracture cases.

# FRONTAL PLANE MECHANICS DURING WALKING IN PATIENTS WITH LATERAL COMPARTMENT TIBIOFEMORAL OSTEOARTHRITIS WITH AND WITHOUT A MEDIALLY WEDGED ORTHOSIS

Joaquin Barrios<sup>1</sup>, Todd Royer<sup>2</sup>, Jeremy Crenshaw<sup>2</sup>, and Irene S. Davis<sup>1</sup>

<sup>1</sup> Department of Physical Therapy, University of Delaware, Newark, DE, USA

<sup>2</sup> Department of Health and Exercise Science, University of Delaware, Newark, DE USA

Email: joaquin@udel.edu

## INTRODUCTION

Tibiofemoral (TF) osteoarthritis (OA) is a progressive disease process affecting millions of Americans. It can affect the medial, lateral or both compartments of the TF joint. Medial TF OA is more common and has received the most attention in the literature. However, lateral TF OA is equally as debilitating and costly to those that suffer from it. Little work has been done to understand and conservatively manage lateral TF OA.

Recently, laterally wedged orthoses have been shown to be beneficial in the management of medial TF OA. These orthoses are designed to alter frontal plane knee mechanics by realigning the foot. Crenshaw et al reported a 7% decrease in the external adduction moment in normal subjects when wearing a laterally wedged insole. Furthermore, Kerrigan et al reported that laterally wedged insoles reduced the external adduction moment in patients with medial TF OA by 6-8%.

Despite the support generated for laterally wedged orthoses and medial TF OA, there is little evidence to support the use of medially wedged orthoses in the treatment of lateral TF OA. Previous studies suggest that patients with lateral TF OA demonstrate smaller peak external adduction moments in comparison to both healthy controls and patients with medial TF OA. The goal of a medially wedged device would be to augment the external adduction moment so it more closely resembles the frontal plane profile of a healthy adult.

Therefore, the purpose of this study was to compare frontal plane knee angles and moments in patients with lateral TF OA during walking with and without a medially wedged orthoses. We hypothesized that patients with lateral TF OA will demonstrate increased peak knee external adduction moments and decreased peak knee abduction angles during walking in a medially wedged orthoses as compared to a no-wedge condition.

## METHODS

This is an ongoing study of which ten subjects (8 women and 2 men) with lateral TF OA have been recruited. Subjects were included after being classified with a Kellgren-Lawrence grade of 2-4, based on an anterior-posterior 30° flexed knee radiograph. The degree of wedging was individually prescribed for each subject so as to maximally reduce knee pain during an 8" lateral step-down test, and was constrained between 5-15 degrees. The wedging was added to a non-custom, contoured orthosis. A 6-camera VICON motion analysis system and a Bertec force plate were used to collect three dimensional kinematics and kinetics during walking at a self-selected speed. A wedge and a no-wedge condition were collected for each subject in a randomized order.

The variables of interest included the peak knee external adduction moment and the peak knee abduction angle during the first half of stance. Due to the small sample size, descriptive statistics will be reported at this time.

## RESULTS AND DISCUSSION

Results are reported in Table 1 and Figures 1-2.

**Table 1.** Mean and (SD) values for variables of interest in the no-wedge (NW) and the wedged (W) conditions

	NW	W	% diff
<b>Pk Add Mom</b> (Nm / kg*m)	0.181 (.10)	0.219 (.17)	21.0%
<b>Pk Abd Angle</b> (degrees)	10.34 (4.07)	10.49 (4.19)	1.45%

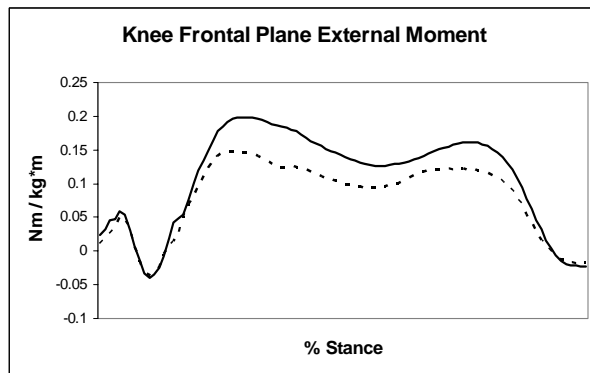


**Figure 1.** Ensemble curves of frontal plane moments in the wedged (solid) and no-wedge (dashed) conditions

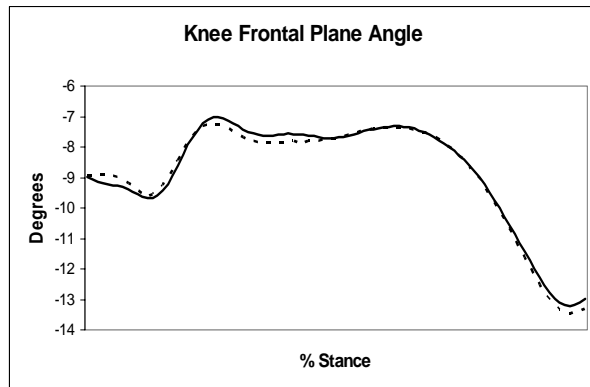


**Figure 2.** Ensemble curves of frontal plane angles in the wedged (solid) and no-wedge (dashed) conditions

Contrary to our hypotheses, it appears that the peak frontal plane angles are similar in patients with lateral TF OA when comparing a wedged condition to a no-wedge condition. This result is similar to the results reported by Butler et al. (2004) when investigating the effects of laterally wedged orthoses on frontal plane angles in medial

TF OA. In support of our hypotheses, the peak external adduction moment did increase. This suggests that medially wedged orthoses can have an immediate beneficial impact on frontal plane knee mechanics.

For these subjects with lateral TF OA, the order of magnitude of change in the external adduction moment was greater than expected. Based on previous work investigating laterally wedged orthoses in medial TF OA, a percent difference of over 10-15% could be considered a positive result. The 21% increase demonstrated in this preliminary study is promising and warrants further research into the biomechanical and clinical efficacy of medially wedged orthoses in lateral TF OA.

## SUMMARY

The results of this study suggest that patients with lateral TF OA exhibit an increased external adduction moment at the knee during walking with a medially wedged orthoses compared to a no-wedge condition. These increased values are closer to the values exhibited by healthy subjects without TF OA. One-year follow-up data are also being collected. We hope those results will elucidate the long-term effects of medial wedging in patients with lateral TF OA.

## REFERENCES

- Rudolph K, et al (in review). *Arthritis Care and Research*.
- Butler RJ, et al (2004). *Proceedings from ASB*.
- Cashen CM, et al (2004). *Proceedings from CBER 2004*.
- Crenshaw SJ, et al (2000). *Clin Orthop and Related Research*, 375,185-192.
- Kerrigan DC, et al (2002). *Arch of Physical Med and Rehab*, 83:889-893.

## ACKNOWLEDGEMENTS

This study has been supported by NIH grant# P20 RR16458.

# EFFECT OF CONFLICTING SOMATOSENSORY AND VISUAL INFORMATION ON CHILDREN'S BODY SWAY

Paula Favaro Polastri<sup>1,2</sup>, Thatia Regina Bonfim<sup>1,3</sup> and Jose Angelo Barela<sup>1</sup>

<sup>1</sup> University of Sao Paulo State, Rio Claro, SP, Brazil

<sup>2</sup> University of Sao Paulo State, Bauru, SP, Brazil

<sup>3</sup> Pontific Catholic University of Minas Gerais, Poços de Caldas, MG, Brazil

E-mail: paulafp@rc.unesp.br Web: www.rc.unesp.br/ib/efisica/lem/principal.htm

## INTRODUCTION

Postural control is influenced by sensory information (visual, somatosensory and vestibular systems) and body orientation and balance are achieved through a dynamic relationship between sensory information and muscular activity (Horak & Macpherson, 1996). However, it seems that young children are not able to use sensory information as adults are in order to maintain a desired postural orientation and equilibrium, especially when sensory cues are conflicting (Forssberg & Nashner, 1982; Shumway & Woollacott, 1985). It has been suggested that young children are more dependent on vision (Woollacott, et al., 1987) and that only about the end of the first decade of age they can integrate all available sensory information similarly to adults (Forssberg & Nashner, 1982; Shumway & Woollacott, 1985).

Previous studies have shown that vision manipulation induces coherent postural responses in children (Schmuckler, 1997) and infants (Barela et al. 2000; Bertenthal et al., 1997). Recently, several studies have showed that light touch to a rigid surface can also induce coherent body sway in children (Barela et al. 2003) and even improve postural control performance in infants (Barela et al. 1999) and toddlers (Metcalf et al. 1995). However none of these studies has investigated the effect of the light touch on children's body sway during manipulation of the visual information.

The aim of this study was to examine the effect of light touch on children's body sway when vision information is manipulated by a moving room.

## METHODS

Eight 8-year-old children and eight young adults were asked to maintain upright stance inside a moving room which was used to manipulate visual information. The room was controlled by a servo mechanism (Compumotor) which allowed forward and backward oscillation at frequency of 0.2 Hz (amplitude of 1 cm and constant peak velocity of 0.6 cm/s). A touch bar device [4-cm-diameter metal plate attached to a load cell (Alfa Instruments, S5)] provided information about the vertical force applied on the sensor. The force application was limited to 0.98 N. The touch bar was placed in front and at the right side of the participant reachable of his/her right index finger.

Mean sway amplitude and gain between visual information and body oscillation were calculated through the IRED markers (Optotrak 3020 ND Inc.) placed on the participant's head, between the scapulas (6<sup>th</sup> thoracic vertebra), and lumbar region (3<sup>rd</sup> vertebra level) and in the moving room. Six experimental conditions were used: with and without vision, with and without light touch and with and without room oscillation. Each trial lasted 60 seconds with a sampling rate acquisition of 100 Hz.

## RESULTS AND DISCUSSION

The results showed that visual information provide by the moving room induced coherent body sway in children and adults. However, when a light touch was added, children and adults' body sway was significantly reduced, independent of the room movement.

Despite the effectiveness of light touch for both, children and adults, mean sway amplitude and gain values showed that light touch effect was larger in adults than in children under the influence of the moving room.

These results indicated that additional somatosensory information (light touch) can be used by the 8-year-old children to reduce body sway even when vision is manipulated by the moving room. However, although children can use somatosensory information to overcome visual influences, they are not as effective in doing it as adults are. Barela et al (2003) have suggested that children seem not be able to ignore available sensory information, even if it is unreliable, prevent them from coupling to the useful sensory information. Embedded in the process of integrating information from different sensory modalities is a reweighing process that involves reducing the effect of sensory information which is present, but unreliable or irrelevant (Oie et al. 2002). It seems that children are not as precise as adults in reweighing the effects of all sensory information to control body sway, and one may speculate that experience would provide basis for the nervous system to learn more accurately how to do it.

## SUMMARY/CONCLUSIONS

In conditions that the visual stimulus is manipulated by a moving room, light touch contact reduces children and adults' body oscillation, indicating that, in this situation, somatosensory information overcomes sensory information provided by the visual system. Although, 8 year-old children use somatosensory information to reduce body sway when vision is manipulated, they are not as effective as adults are. It may be speculated that experience may play an important role in order to provide basis to ignore inaccurate information and focuses on that which is relevant to the task.

## REFERENCES

- Barela, J.A. (1999). *Infant Behavior and Development*, **22**, 87-102.
- Barela, J.A. et al. (2000). *Infant Behavior and Development*, **3-4**, 285-297.
- Barela, J.A. et al. (2003). *Exp. Brain Research*, **150**, 434-442.
- Bertenthal, B.I. (1997). *J. Experimental Psychology*, **23**, 1631-1643.
- Forsberg, H., Nashner, L.M. (1982). *J. Neuroscience*, **2**, 545-552.
- Horak, F.B., Macpherson, J.M. (1996). *Handbook of Physiology*. Oxford University Press.
- Metcalf, J.S. (2005). *Exp. Brain Research*, **161**, 405-416.
- Oie, K.S. (2002). *Cogn. Brain Research*, **14**, 164-176.
- Shumway-Cook, A., Woollacott, M. (1985). *J. Motor Behavior*, **17**, 131-147.
- Schmuckler, M.A. (1997). *J. Experimental Psychology*, **23**, 528-545.
- Woollacott, M. Debu, B., Mowatt, M. (1987). *J. Motor Behavior*, **19**, 167-186.

## ACKNOWLEDGEMENTS

Supported by:  
CAPES #3133/05-2 to the first author  
FAPESP #03/13970

# BIOMECHANICAL CLASSIFICATION OF TAEKWONDO KICKS

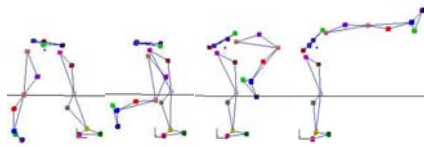
Young-Kwan Kim and Richard N. Hinrichs

Arizona State University, Tempe, AZ, USA

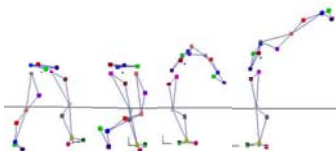
E-mail: Young-Kwan.Kim@asu.edu

## INTRODUCTION

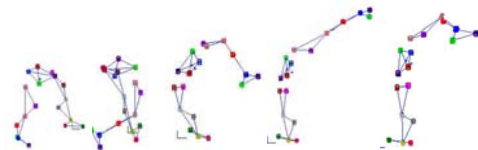
Taekwondo is one of the martial arts and is so popular that it has been an official Olympic event from the 2000 Olympics in Sydney. The popularity of Taekwondo mainly comes from its dynamic kicks during sparring. There are many kinds of kicking techniques in Taekwondo, such as front kick, roundhouse kick, side kick, back kick, swing kick, hook kick, back spinning hook kick, and axe kick, depending on the plane of movement and joint action of lower extremities.



Front Kick (Swing Kick)



Side Kick (Thrust Kick)



Hook kick (Combined kick)

**Figure 1:** Graphical representation of three style kicks in Taekwondo.

There are a few biomechanical studies on front kick and roundhouse kick but the other styles of kicking have not been studied so far (Sorensen et al., 1996). The main goal of kicking is to hit a target correctly with

decent power for getting points in sparring. Therefore, the fast and forceful kick is very important to reach high power of kicking. Even though there are various kicking techniques in Taekwondo, it is hypothesized that there are three distinctive styles of kicking depending on kinematic characteristics of kicking (see Figure 1). The swing kick is used to maximize the speed of the foot at impact. The thrust kick is used to generate large forces at impact. The combined kick is used to generate both a large speed and large forces.

The purpose of this study was to collect kinematic data of six different techniques of Taekwondo kick and to classify their patterns of kicks into three groups depending on their kinematic characteristics.

## METHODS

Six subjects were recruited from the ASU Taekwondo club and off-campus Taekwondo schools. They had a minimum of three years of Taekwondo training and participated in practice on a regular basis.

Eighteen reflective markers were placed on the body segments and 10 CCD cameras (Motion Analysis System, Santa Rosa, CA, USA) with sampling rate of 200 Hz were used to record body marker position data.

Subjects were asked to execute randomly ordered six different kicks in the air and five trials for each kick. The six kicks were front kick (FR), roundhouse kick (RH), side kick (SD), back kick (BA), hook kick (HO), and back hook kick (BH).

Saved body position data were used for kinematic data analysis and pattern analysis following 2<sup>nd</sup> order zero-lag Butterworth filter (cutoff frequency 10 Hz). Repeated measures ANOVA on the maximum kicking speed of each kick were performed. Angle-angle plot for hip and knee flexion/extension angles were investigated.

## RESULTS AND DISCUSSION

Roundhouse kick (RH) showed significantly higher speed ( $13.9 \pm 0.72$  m/s) than SD, BA, and HO. Side kick (SD) speed ( $8.55 \pm 0.53$  m/s) was significantly lower than FR and RH (see Figure 2).

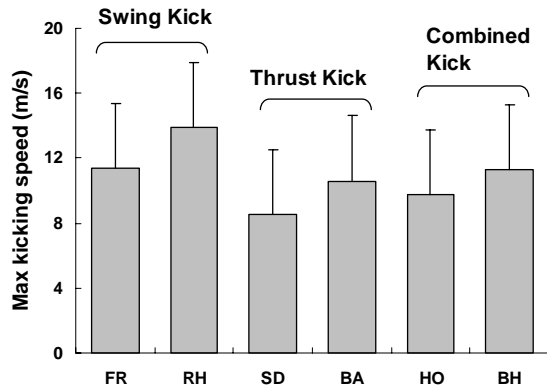


**Figure 2:** Swing kicks generally showed the highest kick speeds while the thrust kicks generally showed the lowest kick speeds.

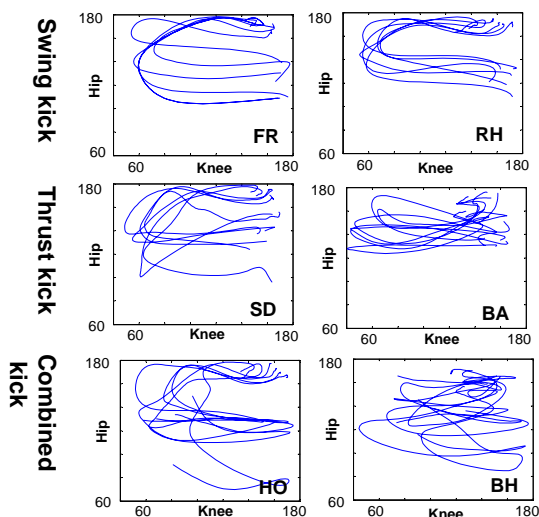


**Figure 3:** Angle-angle plot (hip-knee) indicates the complexity of the combined kick.

Overall mean of combined kick was between swing kick and thrust kick.

The angle-angle plot (hip flexion/extension–knee flexion/extension) showed the qualitative pattern of each kick and the complexity of movement of the kicking leg (see Figure 3). RH showed the consistency across individuals. Combined kick (HO and BH) indicated the complexity of joint movement.

## SUMMARY/CONCLUSIONS

This study indicates that swing kicks (FR and RH) generally achieve the highest kicking speeds of all the types of Taekwondo kicks. The swing kicks use the open kinetic chain principle in an attempt to maximize the distal end linear velocity (Putnam, 1991). Hence, they have a velocity advantage in reaching high mechanical power. Thrust kicks (SD and BH) are performed by opposite torque directions between hip and knee joints to thrust the foot segment toward a target. They have lowest kicking velocities but force advantage due to co-activations of flexors and extensors at hip and knee joints. This indicates force advantage in generating kicking power. Combined kicks (HO and BH) have decent velocities as well as co-activations of flexor and extensor muscles. Therefore, they have both velocity and force advantages in power generation during kicking. However, the complexity of leg motion does not allow the beginners to learn them easily. The highest kicking speed and consistent pattern of angle-angle plot support the popularity of roundhouse kick (RH) among various kicks in Taekwondo.

## REFERENCES

- Putnam, C. (1991). *Med. Sci. Sport Exerc.*, **22**, 130-144.
- Sorensen et al. (1996). *J. Sports Sciences*, **14**, 483-495.

# DOES MIT-MANUS UPPER EXTREMITY ROBOT TESTING CREATE A LEARNING EFFECT IN HEALTHY ADULTS?

Margaret A. Finley<sup>1,2</sup>, Laura Dipietro<sup>3</sup>, Jill Ohlhoff<sup>2</sup>, Jill Whitall<sup>2</sup>,  
Hermano I. Krebs<sup>3</sup> and Christopher T. Bever<sup>1,2</sup>

<sup>1</sup>VA Maryland Healthcare System, Baltimore, MD

<sup>2</sup>University of Maryland School of Medicine, Baltimore, MD.

<sup>3</sup>Massachusetts Institute of Technology, Cambridge, MA

Email: [mfinley@som.umaryland.edu](mailto:mfinley@som.umaryland.edu)

## INTRODUCTION

Robotic devices are capable of moving, guiding or perturbing movements of a patient's upper limb and can record motions and mechanical quantities such as the position, velocity, and forces applied. An important potential benefit of using robotics and information technology for neurological rehabilitation evaluation is that it permits new measurements that may provide deeper insight into the severity of impairments or degenerations and the sensory motor consequences in patients with neurological impairments (Roher, 2002; Finley, 2006).

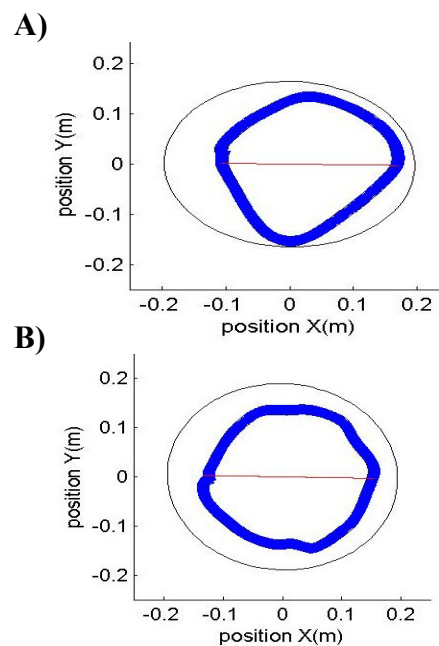
Soon the device will be applied to interventions of persons with musculoskeletal disorders. If these outcome measures are to be utilized it is important to demonstrate the sensitivity of the measures to a learning effect. Therefore, the purpose of this study was to develop descriptive profiles of performance and to assess if a learning effect occurs in robotic testing measures in normal, healthy individuals.

## METHODS

In an effort to test reliability, ten healthy, unimpaired, subjects (age range = 41.1 to 67.8 years) naïve to the robot performed six repeated evaluations (2x/day for three separate days) on the MIT MANUS (Hogan, 1995). Testing consisted of point-to-point reaching and circle drawing with and

without a visual guidance. Outcome variables for reaching were aiming error, mean and peak speed, movement smoothness (mean-to-peak speed ratio) and movement duration. Outcomes for circle drawing were axis ratio metric and shoulder-elbow joint angles correlation metric. The goodness of a circle was characterized by the axis ratio metric (a value from 0 to 1) and increased as the fitted ellipse approximated a circle (Figure 1).

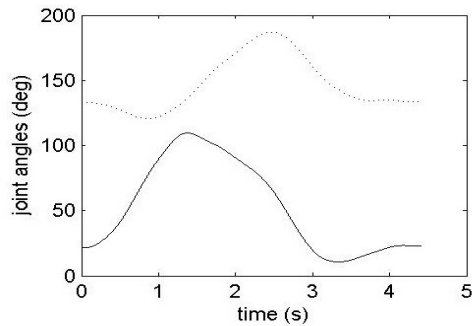
**Figure 1: Circles fitted w/ ellipse**  
**A) no template, B) with Template**



The joint angle correlation metric was based on a two link model of the human arm, shoulder and elbow joint angles with the correlation calculated from the hand path, and characterized the independence of the subjects' shoulder and elbow joint movements (Figure 2).

**Figure 2: Joint Angles during Clockwise Circle Drawing**

(Dotted line= elbow w/ (-) = extension;  
Solid = shoulder with (+) = adduction)



Repeated measures ANOVA ( $p \leq 0.05$ ) determined if difference existed between the six testing session. Intraclass correlations (R) were calculated.

## RESULTS AND DISCUSSION

Reaching and circle drawing variables were reliable, without a learning effect across numerous testing sessions. All intraclass correlation values for the reaching task outcomes were good with the circle variables demonstrating high reliability (Table1).

It was determined that the axis ratio metric and joint correlation metric demonstrated better performance with the use of a visual guidance template, however, in general the use of this template did not carry-over to improved performance of circle drawing in its absence. Lower joint correlation expressed the ability of subjects to move the

shoulder and elbow joints independently, as would be expected in healthy individuals

**Table 1: Robotic Outcome Measures (n=10)**

	Mean (sem)	R
Aiming error (rad)	1.00 (0.02)	0.85
Mean speed(m/sec)	0.11 (0.01)	0.84
Peak speed (m/sec)	0.24 (0.01)	0.83
Mean-peak speed ratio	0.48 (0.01)	0.86
Movement duration (sec)	1.47 (0.05)	0.82
Axis ratio without template	0.77 (0.01)	0.98
Axis ratio- with template	0.83 (0.01)	0.90
Joint correlation without template	0.36 (0.01)	0.91
Joint correlation with template	0.29 (0.01)	0.94

## CONCLUSION

The outcome measures of the MIT-MANUS are reliable and stable in normal, healthy adults. Motor learning does not occur over the course of repeated exposure. The use of a visual guide in normal adults does not stimulate improvements in circle drawing in its absence.

## REFERENCES

- Rohrer B, et al. (2002). *J Neurosci* 22(18):8297-304.  
 Finley, MA<sub>2</sub> et alr, CT, Krebs, HI, Hogan. *J Rehab Res Dev.* (in press)  
 Hogan N, et al inventors (1995); *Interactive Robot Therapy.* USA patent 5,466,213.

## ACKNOWLEDGEMENTS

This research was funded by grant V512(P)P-521-02 and Career Development Grant #B3827V from the VA Rehabilitation and Development Service.

# SECONDARY KNEE KINEMATICS DURING CYCLING ARE GOVERNED BY MUSCLE ACTIVITY

Idubijes L. Rojas, Kharma C. Foucher, and Markus A. Wimmer

Rush University Medical Center, Chicago, IL, USA

E-mail: Markus\_A\_Wimmer@rush.edu      Web: www.ortho.rush.edu/Gait/

## INTRODUCTION

During flexion and extension of the knee, the joint undergoes a complex pattern of motion with six degrees of freedom. The relationship between secondary knee motions (anterior-posterior (AP) translation and internal-external (IE) rotation) and knee flexion angle during weight bearing activities has been demonstrated and attributed to muscle forces acting across the knee joint (Dyrby, 2004). This study investigates the specific influence of muscle force on secondary knee motions by measuring muscle activity during cycling.

## METHODS

Four healthy subjects volunteered for this study: three males and one female (age:  $31 \pm 9$  years; height:  $175 \pm 12$  cm; body mass:  $70 \pm 14$  kg). The subjects were tested while riding an upright stationary bicycle without being clipped to the pedals. Subjects were given the opportunity to adjust the height of their seats for maximum comfort. Two, five-second, trials were obtained for each subject at medium resistance (level 7 from max 15) and a self-selected cadence. Kinematic and surface electromyography (sEMG) data was collected from one side, selected randomly. The motion was captured using a four-camera optoelectronic system (Qualisys). Twenty-one retro-reflective markers were used to obtain kinematic measurements using a previously developed point cluster technique (PCT) (Andriacchi, 1998). A fixed tibial reference system is used to describe the kinematics. Muscle

activity was collected from the marked leg being tested using a transmitter and receiver (Noraxon TeleMyo 2400T and 2400R). The sEMG data was collected from five lower limb muscles or muscle groups: bicep femoris (BF), semimembranosus/ semitendinosus (SM/ST), rectus femoris (RF), vastus medialis (VM), and vastus lateralis (VL). Additionally, single joint hip muscles were tested (data not reported). Self-adhesive dual electrodes (Ag/AgCl electrodes, Noraxon USA, Inc.) were placed on the palpated bellies of the five lower limb muscles. In order to reduce inter-electrode impedance the skin was shaved and cleaned using antimicrobial skin wipes. The sEMG signals were pre-amplified (500x) near the electrodes. The signals were band pass filtered between 10 and 500 Hz and sampled at a rate of 1200 Hz. (Konrad, 2005) The raw sEMG signals, for each subject and each muscle, were rectified and the root-mean-square (RMS) calculated (De Luca, 2002).

## RESULTS AND DISCUSSION

With regard to knee flexion angle (primary kinematics), quadriceps (RF, VM, VL) are active during maximum flexion angles and hamstrings (BF, SM/ST) are active during minimum flexion angles. Maximum anterior translation and external rotation of the femur occurs when quadriceps are active. Minimum anterior translation and internal rotation of the femur occurs when hamstrings are active. At about  $60^\circ$  of knee flexion the patellar ligament becomes posterior rather than anterior to the femur (Ahmed, 1987).

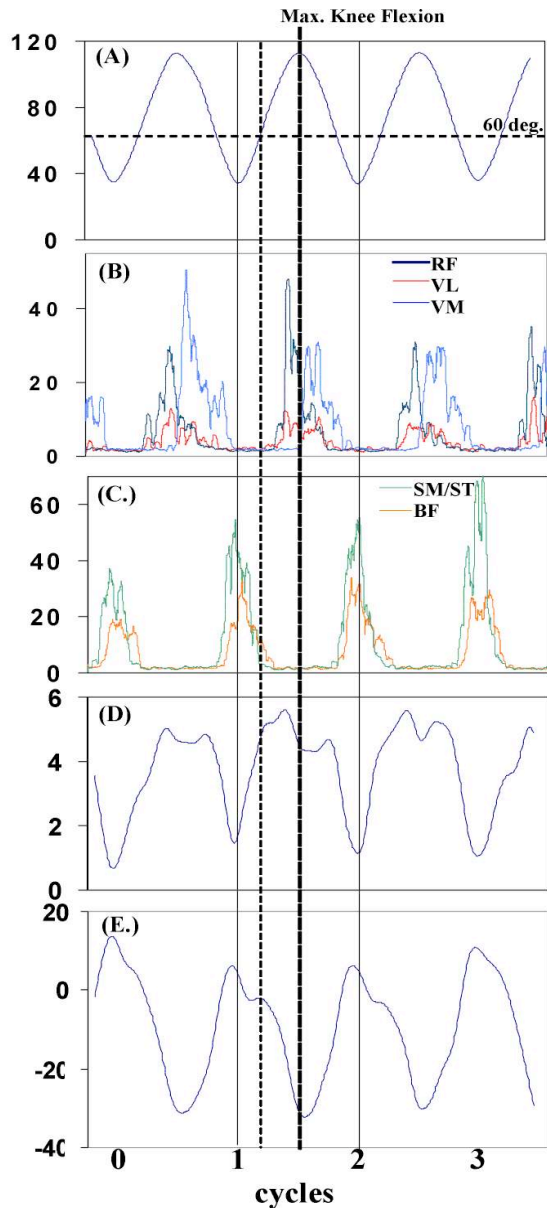


**Figure 1.** Representative of one five-second cycling trial of a male subject. (A) Knee flexion/extension (deg) (B) Quadriceps sEMG (uV) (C) Hamstrings sEMG (uV) (D) Femur AP translation (cm) (E) Femur IE rotation (deg)

Quadriceps onset and hamstrings offset occur near this point (dashed lines). The boundaries of the secondary motion envelope of AP translation and IE rotation during knee flexion – extension activity while cycling (Table 1) are comparable to earlier reports (Caudhari, 2001).

## CONCLUSIONS

This study demonstrated that secondary knee kinematics are governed by muscle activation when cycling. Since the muscle line of action is influenced by the knee flexion angle, the latter plays an important role in describing the overall motion envelope.

## REFERENCES

- Ahmed, A.M., Burke, D.L., Hyder, A. (1987) *J. Orthop Res*, **5**, 69
- Andriacchi, T.P., Alexander, E.J., Toney, M.K. et al. (1998) *J. Biomech Eng*, **120**, 743-749.
- Chaudhari, A.M., Dyrby, C.O., Andriacchi, T.P. (2001) ASB
- De Luca, C.J. (2002) *Surface Electromyography: Detection and Recording*. DelSys Incorporated
- Dyrby, C.O., Andriacchi, T.P. (2004) *J. Orthop Res*, **22**, 794-800
- Konrad, P. (2005) *The ABC of EMG: A Practical Introduction to Kinesiological Electromyography*. Noraxon Inc. USA

**Table 1:** Femur AP Translation and IE Rotation at Max/Min Knee Flexion (mean  $\pm$  SD)

Subject	Max Flexion (deg)	AP Translation (cm)	IE Rotation (deg)	Min Flexion (deg)	AP Translation (cm)	IE Rotation (deg)
1	112.84 $\pm$ 0.18	4.55 $\pm$ 0.15	-31.10 $\pm$ 0.86	34.40 $\pm$ 0.47	1.38 $\pm$ 0.73	5.82 $\pm$ 5.74
2	118.60 $\pm$ 0.42	2.81 $\pm$ 0.55	-30.34 $\pm$ 2.64	36.89 $\pm$ 2.14	0.25 $\pm$ 0.21	-1.71 $\pm$ 1.04
3	106.10 $\pm$ 1.24	3.43 $\pm$ 0.24	-17.20 $\pm$ 1.38d	23.98 $\pm$ 1.26	1.26 $\pm$ 0.09	0.86 $\pm$ 0.72
4	118.93 $\pm$ 0.21	1.81 $\pm$ 0.04	-9.57 $\pm$ 0.51	30.01 $\pm$ 0.49	0.99 $\pm$ 0.01	-4.36 $\pm$ 0.57

# FINITE ELEMENT SIMULATION OF THE MRTA TEST OF A HUMAN TIBIA

Jared Ragone<sup>1</sup> and John Cotton<sup>1,2</sup>

<sup>1</sup> Virginia Tech-Wake Forest, School of Biomedical Engineering and Sciences (SBES)

<sup>2</sup> Virginia Tech, Department of Engineering Science and Mechanics (ESM)

E-mail: j cotton@vt.edu

## INTRODUCTION

The mechanical response tissue analyzer (MRTA) tests long bone quality through low frequency, low amplitude vibration *in vivo* (Fig.1). It is less expensive and more portable than DXA, and is a direct measurement of mechanical response, which indicates a potential for greater accuracy. MRTA measures complex stiffness over a range of low frequencies, offering a wealth of information on bone material and structural composition. Previous MRTA data interpretation used lumped parameter algorithms (Fig.1) focused on reliably estimating the bone's bending stiffness (EI). We present here the first FE simulation of the MRTA test of a human tibia, with an ultimate goal of determining 1) accurate lumped parameter models for determining the EI of the tibia, and 2) the ability of MRTA to estimate other parameters of interest to bone integrity such as damping.



**Figure 1: MRTA Setup for Tibial Strength Assessment and 12-Parameter Algorithm for Tibia**

## METHODS

We created a FE tibia mesh from the *CT\_Fronzen\_TIBIA\_DX\_RI* solid model on the BEL repository (Viceconti, 2003) using PATRAN (v2005). We meshed the cortex

with 2760 linear hexagonal elements and the epiphyses with 8228 linear tetrahedral elements. To simulate the small layer of soft tissue between the forcing probe and tibia, we created 6 linear hexagonal elements on the cortex surface that were 2mm thick (Fig. 2).

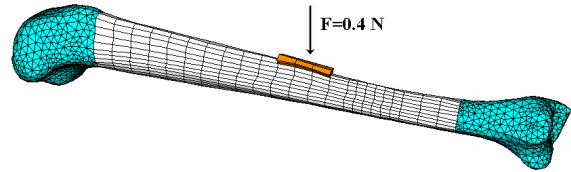


**Figure 2: FE Model for Human Tibia**

The epiphyses were considered cancellous bone while the diaphysis was considered cortical bone. We assigned linear viscoelastic (LVE) properties to cancellous, cortical, and skin elements using frequency-dependent loss and storage moduli taken from the literature (Lakes, 1981; Garner, 2000; Dong, 2003; Periera, 1996). Nodes were clamped at the extreme proximal and distal ends, to simulate physiologic constraints.

The structural bending modes of the tibia under free-free and pinned-pinned boundary conditions were determined using natural frequency analysis in ABAQUS (v6.5). These bending modes were compared to previous experimental and computational results to verify our model.

To simulate the low frequency, low amplitude vibration of the MRTA, we applied a concentrated force of 0.4 N (Fig.

2) at the midshaft over the range of 40 to 500 Hz using the direct steady-state dynamics (DSSD) procedure in ABAQUS. ABAQUS calculated the real and imaginary stiffness versus frequency response at the midshaft of the tibia.

Our FE model was developed in stages by adding complexity. We began with only the diaphysis modeled as a solid cortex with linear elastic (LE) properties. In sequence, we added a medullary canal, LVE properties to cortical bone, linear elastic epiphyses, and then LVE properties to the epiphyses. We use results of earlier models to determine which aspects dominate the characteristic stiffness response.

**RESULTS AND DISCUSSION**

We show in Table 1 that our FE model reproduces reported values of the resonant frequencies for a human tibia under different boundary conditions.

Figure 3 illustrates the effects of various complexities on the dynamic stiffness response. We noted that a solid, LE cortex roughly matches the dominant frequency for the MRTA. Adding the medullary canal and LVE properties to cancellous and cortical bone did not greatly spread the peak or shift the resonant frequency. The addition of the LVE skin layer broadened the peak response to more closely match the MRTA experimental response.

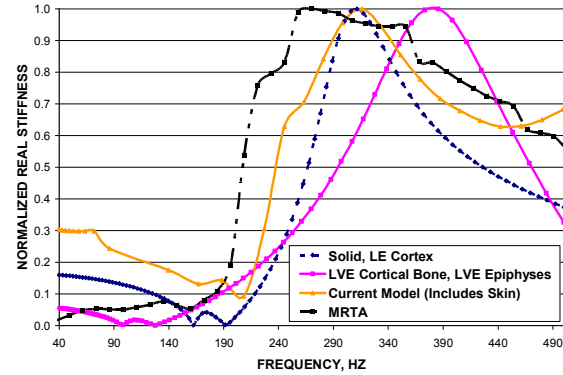


**Figure 3: Stiffness versus Frequency Responses**

**SUMMARY**

These results demonstrate a simulation of the MRTA response based upon published geometries and material data that captures the essence of the instrument.

**REFERENCES**

- Viceconti, M, *International Congress on Computational Bioengineering*, M. Doblaré, et al, Eds., Zaragoza, Sept. 24-26,(2003) and: [http://www.tecno.ior.it/VRLAB/researchers/repository/BEL\\_repository.html](http://www.tecno.ior.it/VRLAB/researchers/repository/BEL_repository.html)
- Lakes, R.S., (1982), *J. Biomech. Eng.* 104:6-11
- Garner E., et al, (2000), *J. Biomech. Eng.* 122:166-172
- Dong, X.N., et al. (2004), *J Biomed Mater Res* 68A: 573–583
- Pereira, J, et al. (1991), *J. Biomech* 24: 157-162
- Van Der Perre, et al, (1983), *J. Biomech. Eng.* 105
- Christensen, et al, (1986), *J. Biomech* 19: 53-60
- Lowet, et al, (1996), *J. Biomech* 29 (8)

**Table 1: Model Comparison to Previous Computational and Experimental Results for Human Tibia**

Computational and Experimental Studies	Pinned-Pinned Bending Mode	Free-Free Bending Mode
FE Tibia Model	408 Hz	455 Hz
Lowet (1996)	-	403 Hz
Van der Perre (1983) <i>Dry, excised human tibiae</i>	-	Natural Frequency Range: 424-690 Hz
Christensen (1986) <i>Wet, excised tibia- Lower limb in vivo-</i>	337 Hz -	476 Hz 470 Hz

\*Blank spaces represent no reported results.

# EFFECTIVENESS OF BOXING HEADGEAR FOR LIMITING INJURY

Nathan Dau, Hai Chun Chien, Don Sherman, and Cynthia Bir

Wayne State University, Detroit, MI, USA

E-mail: nate.dau@wayne.edu Web: [www.bioengineeringcenter.org/home/labs/sports/](http://www.bioengineeringcenter.org/home/labs/sports/)

## INTRODUCTION

The goal in amateur boxing is to outscore your opponent. Points are given for the number of punches landed on an opponent. In an effort to limit head injuries for amateurs, heavily padded gloves and headgear were introduced. Both are designed to provide cushion and energy absorption. USA Boxing, the national governing body for amateur boxing, maintains the safety standards for both gloves and headgear

In 2004, a study was conducted involving a biomechanical surrogate (Walilko, et al. 2005). As part of this effort, the Hybrid III head, neck, and torso was impacted by trained amateur boxers instrumented with hand accelerometers. The results of this study provided a realistic input and a response with high level of biofidelity. The upper portion of a Hybrid III dummy provided the ability to concentrate on the area of greatest concern; the head. By using a Hybrid III, the interaction of the head and neck can more accurately be observed.

The purpose of this study is to evaluate the effectiveness of currently manufactured headgear. The recently established methodology involving the Hybrid III surrogate was utilized.

## METHODS

The punch force of 27 amateur boxers was recorded using the test methodology

established by Walilko et al. (2005). A Hybrid III head, neck, and torso system was fastened to an adjustable height table. Head linear and angular acceleration, head injury criteria (HIC), and punch force were used to evaluate the severity of the impacts. The surrogate was impacted by each of the boxers with a dominant hand hook. The punches were delivered with and without protective headgear.

The hand of each boxer glove was instrumented with three Endevco 7264-2K accelerometers. The three accelerometers were fastened to an aluminum fixture in an orthogonal array. The Hybrid III headform was instrumented with 12 Endevco accelerometers, nine linear and three angular. The upper and lower neck of the surrogate was instrumented with a six-axis load cells (Denton, Inc). The data was collected using a TDAS data acquisition system, at a sampling rate of 20 KHz.

Four criteria were used to analyze the difference in head impacts: peak rotational head acceleration, peak linear head acceleration, peak punch force, and HIC. Since the boxers were of different height, weight, and sex, the averages of these four criteria were compared.

The punch forces are calculated using a summation of forces. The punch force ( $F_p$ ) is set equal to the mass of the headform ( $m$ ) times its acceleration ( $A$ )

and the upper neck forces ( $F_n$ ). The equation is:

$$F_p = mA + F_n$$

This equation is used in all three axes and a resultant force is calculated from the  $F_p$  in the X, Y, and Z directions.

## RESULTS AND DISCUSSIONS

For all criteria, there was a significant decrease with the headgear in place. The average peak rotational acceleration decreased from 9,164.10 to 5,534.78  $\text{rad/s}^2$ . The peak resultant acceleration went from 78.04 to 51.79  $g$ 's. The punch force decreased from 4,260.51 to 2,815.59 N. HIC decreased from 79.23 to 47.34, although both were below the newly proposed threshold of 250 (Viano, et al. 2005). (See Table 1) Paired T tests were performed on each set of variables, and showed that the differences were statistically significant.

The punch velocities were obtained using the integration of the triaxial accelerometer in the gloved hand. The average velocities obtained were 9.57 and 8.43 m/s for impacts with and without headgear respectively.

This study is limited in the type of punch delivered to the dummy. It shows that the headgear lessens the blow of a hook, but does not give any information about

the protection provided for other punches.

In addition, this study only examined one set of headgear. Further studies should be done using different types of headgear and/or different materials.

## CONCLUSIONS

The utilization of boxing headgear significantly reduces the peak punch force delivered to an opponent. In addition, both angular and linear acceleration values are decreased when the headgear is in place. Thus, the resulting HIC is also diminished for the hook punch. Based on the current effort, the currently designed headgear and gloves are effective in reducing the risk of injury.

## REFERENCES

- Viano, D. C., et al. (2005). *Neurosurgery* **57**(6): 1154-72.
- Waliko, T., et al. (2005). *Br. J. Sports Medicine*. **39**(10):710-719.

## ACKNOWLEDGEMENTS

This study would not have been possible without the support of Marilyn Boitano, M.D. and USA Boxing. The authors would also like to thank all of the boxers who participated in the study.

**Table 1:** Data summary

Criteria	With Headgear	Without Headgear
Peak Angular Acceleration ( $\text{rad/s}^2$ )	5534.78	9164.10
Peak Linear Acceleration ( $g$ 's)	51.79	78.04
HIC	47.34	79.23
Punch Force (N)	2815.59	4260.51
Punch Velocity (m/s)	9.57	8.43

# RETROSPECTIVE IDENTIFICATION OF SUBJECT ANTHROPOMETRY USING COMPUTED TOMOGRAPHY OF THE LEG

**M. Daly<sup>1,2</sup>, S.M. Duma<sup>2</sup> and J.D. Stitzel<sup>1,2</sup>**

1. Wake Forest University School of Medicine, Medical Center Blvd, Winston-Salem, NC 27157
  2. Virginia Tech – Wake Forest University Center for Injury Biomechanics, Medical Center Blvd, Winston-Salem, NC 27157
- Email: mdaly@wfubmc.edu

## INTRODUCTION

Lower extremity injuries from car crashes are associated with decreased quality of life. This research effort is motivated by a need to identify CT scans of a 5<sup>th</sup> female and a 50<sup>th</sup> and 95<sup>th</sup> male leg for use in finite element model development. Our goal is to outline a method for obtaining retrospective data on skeletal anthropometry and relate this data to the population when subject anthropometry is unavailable and use this information to create models that can predict injury in humans of all shapes and sizes.

## METHODS

### Developing Normal Distribution Curves

Data from Schneider *et al.* was used to determine leg lengths for a 5<sup>th</sup> percentile female, a 50<sup>th</sup> percentile male, and a 95<sup>th</sup> percentile male [1]. In this study the distance from the lateral femoral condyle to the lateral malleolus defined the length of the leg (Figure 1).

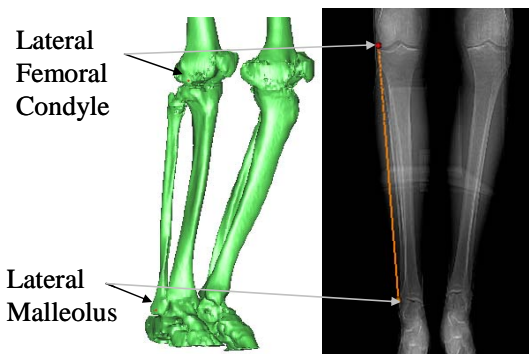


Figure 1. Picture of 3D reconstruction of CT slices (left) and CT scout film (right)

The length of the leg for the 50<sup>th</sup> percentile male model from Schneider *et al.*

was used as the mean leg length to determine normal distribution coefficients (Table 1, Equation 1) [1]. To find the normal distribution curve parameters for leg length in women, normal distribution curve parameters for height were determined from Schneider *et al.* [1]. It was assumed that leg length and overall height scale similarly: i.e. if overall height increases by five percent so does leg length.

$$f(x) = \frac{1}{\sqrt{2\pi\sigma^2}} e^{-\frac{(x-\mu)^2}{2\sigma^2}} \quad (1)$$

Leg length was calculated to be 23% of overall height, thus, the standard deviation of leg length was determined to be 23% of the standard deviation of height. The resulting normal distribution curves for males and females were plotted for +/-3 standard deviations (figure 2).

### Determining 5<sup>th</sup>, 50<sup>th</sup> and 95<sup>th</sup> Percentile Study Scans

Z-scores were determined for each

Table 1. Mean lower leg length and standard deviation of lower leg length in humans.

	Mean Leg Length	Standard Deviation of Leg Length
Males	423mm*	16.0mm
Females	378mm	15.6mm

study scan using Equation 2. The probability associated with the z-score was calculated using Equation 3. This equation was used to determine the percentile rank of all study scans so scans closest to the 5<sup>th</sup>, 50<sup>th</sup> and 95<sup>th</sup> percentile models could be identified

$$z = \frac{x - \mu}{\sigma} \quad (2)$$

$$\Phi(z) = P(Z \leq z) = \int_{-\infty}^z \frac{1}{\sqrt{2\pi}} e^{-\frac{u^2}{2}} du \quad (3)$$

## RESULTS and DISCUSSION

Developing ATDs and computer models that are the correct size and shape is very important because this allows for more accurate predictions by the computer model or ATD of what an occupant will experience during a crash event. The goal of the research described in this paper was to create a method for using CT scans retrospectively to garner information on human anthropometry, specifically leg length. The information presented in Tables

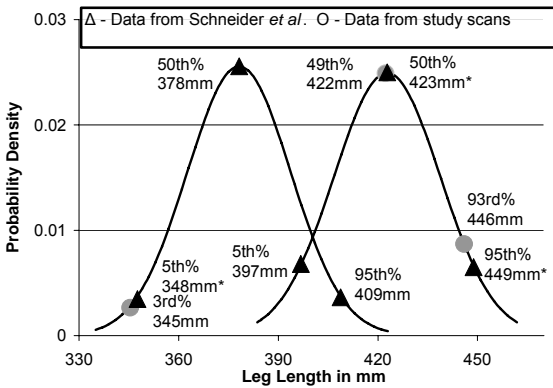


Figure 2. Male and female study scans, superimposed on the normal distribution graph for males and females \*Data from Schneider *et al.* [1]

1 and 2 and Figure 2 allows for a comparison between the 5<sup>th</sup>, 50<sup>th</sup>, and 95<sup>th</sup> percentile models from the normal Table 2. Model leg lengths and patients' leg lengths.

Percentile (%)	Model Length	Model %	Scan Length	Scan %
5 <sup>th</sup>	348mm*	5 <sup>th</sup>	345mm	3 <sup>rd</sup>
50 <sup>th</sup>	423mm*	50 <sup>th</sup>	422mm	49 <sup>th</sup>
95 <sup>th</sup>	449mm*	95 <sup>th</sup>	446mm	93 <sup>rd</sup>

\*Data from Schneider *et al.* [1]

distribution curves and the study CT scans

found to approximate these percentiles. Approximating the 5<sup>th</sup>, 50<sup>th</sup> and 95<sup>th</sup> percentile models with the 3<sup>rd</sup>, 49<sup>th</sup> and 93<sup>rd</sup> percentile study scans is justified because of the inherent lack of accuracy in the measuring system. Cheung et al found intra-observer variation for placing probes to measure length was 3.3mm [2]. Table 2 shows all three study scans have leg lengths that are within 3mm of the 5<sup>th</sup>, 50<sup>th</sup> and 95<sup>th</sup> percentiles respectively.

## CONCLUSIONS

Leg injuries are not often life threatening; however, they can have a large impact on quality of life. While this study took into consideration the gender of the individual other variables such as height, weight and age were left out. This study also considered only the length of the leg; other aspects such as tibia and fibula shape were ignored. The ultimate goal for this research is to create a comprehensive model that can accurately measure stress and strains in models representative of the anatomy of a wide range of individuals.

## ACKNOWLEDGEMENTS

We would like to acknowledge Toyota Motor Corporation for funding this research.

## REFERENCES

- [1] L. W. Schneider, D. H. Robbins, M. A. Pflug, and R. G. Synder, *Anthropometry of Motor Vehicle Occupants: Volume 1- Procedures, Summary Findings and Appendices*: University of Michigan, 1983.
- [2] J. Cheung, D. Weaver, A. Veldhuizen, J. Klein, B. Verdonck, R. Nijluning, J. Cool, and J. Van Horn, "The reliability of quantitative analysis on digital images of the scoliotic spine " *European Spine Journal* vol. 11, pp. 535-542, 2002.

# FALLS CAN BE DETECTED BY COMBINING VELOCITY AND ACCELERATION FEEDBACK IN BIPEDAL-TO-UNIPEDAL TRANSITION

Jaebum Son and James A. Ashton-Miller

University of Michigan, MI, USA  
E-mail: jaebum@engin.umich.edu

## INTRODUCTION

Human postural balance and detection of falls have been interesting topics over decades. The sensory estimator theory suggests that visual, vestibular, and somatosensory information is combined with proper gain set to detect falls, but it's not easy to track the values since the gains of estimator could be modified internally.

In this study, we pick up the instance of balance transition from bipedal to unipedal status, and show how the sensory combination may serve to detect falls, or precisely, to detect the condition to *surrender* of transition.

In the bipedal-to-unipedal (BU) transition in the unipedal balance test, double-stepping followed by simple surrender occurs frequently even though it's not allowed by the test protocol; after surrendering people tend to try the transition again right away. Under this condition, even healthy young people may show surrender of the balance. This could be interpreted as a specific type of falls that the postural controller recognizes the transition will not be successful with the body center of mass (COM) position and velocity (i.e., state) *at the lift-off instance*.

For this kind of *surrender falls*, we hypothesize and test that falls may be detected by combining velocity and acceleration feedback in the eigenvector direction.

## METHODS

11 healthy young and 21 healthy old people volunteered to participate in the test. The experimental setup included two AMTI<sup>TM</sup> force plates and amplifiers, an OPTOTRAK kinematic measurement system and a microprocessor to collect data (100Hz).

Each subject was instructed to stand outside of force plate for 5 seconds, and moved onto force plate with given signal. The subject placed arms cross the chest and stood still while distributing the body weight to each foot evenly for 10 seconds. With verbal signal, the subject transitioned from bipedal to unipedal stance, and tried to stand as still as possible up to 30 seconds. We define the surrender of transition as the trial with the unipedal balance time <1s.

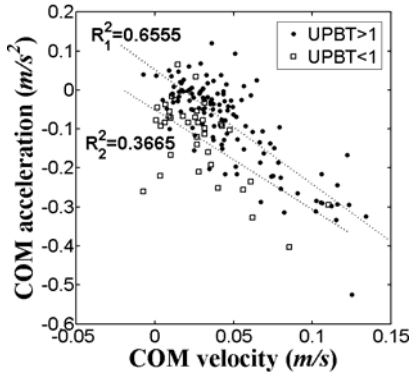
## RESULTS AND DISCUSSION

Thirty-eight trials resulted in unipedal balance time (UPBT) <1s among total 161 trials. To ensure the precise location of COM, the calculated value was verified by cross-validation with two methods: force integration and kinematic estimation by body segments ( $R^2=0.8553$ ).

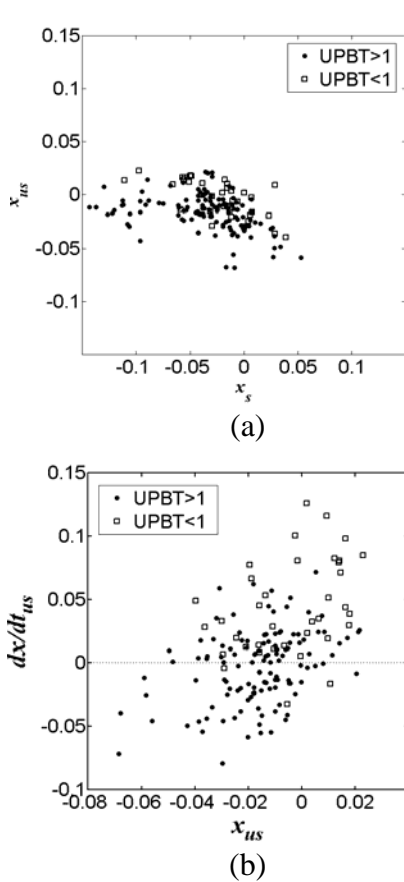
The velocity and acceleration in Cartesian coordinate showed clear difference between two groups with same directional trend (Figure 1).

Figure 2 proves that this direction matches with the eigenvector of the body was performed by assuming the 1-DOF inverted pendulum properties with standard human body distribution. It also shows that the rate of the unstable eigen-coordinate is the better discriminator of the successful

transition than the unstable eigen-coordinate ( $x_{us}$ ).



**Figure 1:** COM velocity and accelerations at the lift-off instance in Cartesian space.



**Figure 2:** Eigenvalue-decomposition of the state and rate of state contrasts the successful transition and unsuccessful transitions.  $x_s$  ( $x_{us}$ ): the component in the direction of stable (unstable) eigenvector.

Even though the normal state space (angular position and velocity of COM) could show minor significant difference of two groups, the derivative of the state space could show much clear contrast (mean  $\dot{x}_{us} = -0.003$  (SD=0.0290) for failure, whereas  $\dot{x}_{us} = 0.0435$  (SD=0.0374) for success,  $p < 1.0e-8$ ). This might imply that the subjects in this test surrendered and fell not because of mechanical constraint of dynamic stability but because of the velocity and acceleration feedback information.

The directional combination of velocity and acceleration suggests that the feedback from joint proprioception may not be necessary to detect falls. This is supported by the facts that it's hard to estimate the precise COM position using joint proprioception, and that the velocity and acceleration information is readily available from visual and vestibular feedback with shorter delay time. It also suggests that the condition for the feasible dynamic stability of balance (Pai,2000) may not necessarily match with the condition of perception of falls.

This result supports that the internal model suggested by Ahmed (2004) (which can be approximated by an inverted pendulum in this case) is utilized at the instance of lift-off.

## CONCLUSIONS

The human postural controller may detect falls without proprioceptive feedback by combining the velocity and acceleration feedback to match the internal model in BU transition.

## REFERENCES

- Ahmed, A.A., Ashton-Miller, J.A. (2004). *Gait & Posture*, **19**(3), 252-62.  
 Pai, Y.C. et al. (2000). *J. Biomechanics*, **33**(3), 387-92.

# AN EXPERIMENTAL AND FINITE ELEMENT STUDY OF THE PORCINE CAROTID ARTERY UNDER DYNAMIC LOADING

F. Scott Gayzik<sup>1,2</sup>, Ola Bostrom<sup>3</sup>, Stefan M. Duma<sup>2</sup>, Joel D. Stitzel<sup>1,2</sup>

<sup>1</sup> Wake Forest University School of Medicine, Medical Center Blvd, Winston-Salem, NC 27157

<sup>2</sup> Virginia Tech – Wake Forest University Center for Injury Biomechanics, Medical Center Blvd, Winston-Salem, NC 27157

<sup>3</sup>Autoliv Research, 447 83 Vargarda, Sweden

E-mail: [sgayzik@wfubmc.edu](mailto:sgayzik@wfubmc.edu)

## INTRODUCTION

An internal carotid artery dissection (ICAD) begins as a tear or defect of the intimal lining of the artery, and can lead to luminal occlusion and cerebral ischemia (Schievink 2001). Arterial injuries such as ICAD are most commonly encountered in automobile accidents (Stemper, Yoganandan et al. 2005). While the incidence of these injuries is low (present in roughly 1% of trauma admissions) the associated mortality and long term neurological morbidity are estimated at 40% and 40-80% respectively (Stemper, Yoganandan et al. 2005).

Our aim is to use the finite element method to characterize the behavior of the carotid artery under dynamic loading conditions, such as those that a vehicle occupant may experience in a car crash. In this study, the outcomes of three dynamic impact tests on porcine carotid arteries are compared to the results of finite element simulations of the same impacts. Specifically, we compare the incidence of intimal damage to the peak stress and strain experienced by the artery during the simulated impact.

## METHODS

Ten porcine carotid arteries were harvested, pressurized, and encased in polyethylene foam. A 2.4kg steel indenter was mounted on a vertically sliding guillotine and released from three heights, striking the carotid

sample perpendicularly at its midpoint. The drop heights of 30, 50 and 70mm above the sample resulted in impact speeds of 2.4, 3.1, and 3.7 m/s respectively. Two samples were tested at 30mm, and four were tested at the remaining two drop heights. The carotid samples were subsequently examined for intimal tearing.

The finite element model was constructed from video of the impacts and analyzed using LS-Dyna (LSTC, Livermore, CA). The foam was modeled using solid brick elements. Quadrilateral shell elements were used to model the carotid artery. An Eulerian flow field was implemented to model the motion of fluid within the carotid artery during the impact. The carotid artery material model used a direct curve fit of a one-dimensional force-deflection test of porcine descending aorta (PDA). The motion of the indenter was recorded with ImageJ (Nation Institutes of Health, <http://rsb.info.nih.gov/ij/>) and applied as a prescribed motion boundary condition.

## RESULTS AND DISCUSSION

The incidence of intimal injury found in the guillotine experiments increased with drop height, with 100% incidence of intimal tearing at 70mm. No intimal tearing was reported at 30mm. The simulation results show that the peak first principal stress on the section of the artery below the indenter increased 48% between the 30mm and

70mm drop, compared to an increase in stress of only 13.6% between the 30mm and 50mm drop. This difference may be of importance since the results of the guillotine study suggest that a threshold in stress or strain may be crossed between the 50mm and 70mm drop. The results of the study are summarized in Table 1.

Previous research characterizing the failure mechanics of PDAs found intimal failure occurred at stress and strain values of 1.24 MPa and 63% respectively (Stemper, Stineman et al. 2005). With regards to the LS-Dyna simulation, this level of stress is only surpassed during the 70mm drop simulation; recall that at this drop height 100% of the carotid artery samples exhibited intimal damage. The peak first principal strains from the all simulation results were less than the average strain to intimal failure reported by Stemper, Stineman, et al, 2005. It should be noted however that this data is the result of quasi-static testing of carotid specimens at <1 strain/sec. Figure 1 shows the first principal strain in the region below the indenter versus time from the LS-Dyna simulation at each drop height. The simulation indicates that the artery experiences a 37% increase in strain in 5 msec, equating to a strain rate of 74 strain/sec. It is well documented that biological materials such as the carotid artery are viscoelastic, and therefore exhibit a rate-dependent response to loading. This finding underscores the need to incorporate dynamic PDA stress-strain data in future finite element models of the carotid artery.

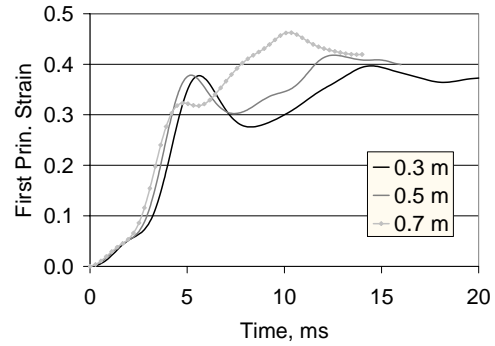


**Figure 1.** First principal strain versus time of region of carotid under the indenter.

## SUMMARY/CONCLUSIONS

A finite element model of a porcine carotid artery under dynamic loading is presented. The results suggest that loads resulting in local stress and strain values of 1.30MPa and 46% may cause intimal damage. However the study underscores the need examine failure mechanics of PDA at strain rates up to 75strain/sec.

## REFERENCES

- Schievink, W. I. (2001). *N Engl J Med* **344**(12): 898-906.
- Stemper, B. D., M. R. Stineman, et al. (2005). *IRCOBI*, Prague, Czech Republic.
- Stemper, B. D., N. Yoganandan, et al. (2005). *J Biomech* **38**(12): 2491-6.

## ACKNOWLEDGEMENTS

Thank to Drs. Frank Pintar and Brian Stemper of Medical College of Wisconsin for the use of PDA data from their lab.

**Table 1:** Summary of guillotine experiment outcome and finite element results

Drop Height(mm)	Guillotine Experiment Outcome		Finite Element Study Results	
	Intrusion depth (mm)	Intimal injury incidence	Peak first. principal stress (MPa)	Peak first. principal strain
30	34	0%	0.88	0.40
50	36	25%	1.00	0.42
70	38	100%	1.30	0.46

# CONTRIBUTION OF VISUAL, VESTIBULAR, AND SOMATOSENSORY SYSTEMS TO GAIT TERMINATION STRATEGY

Zinat Shafaei-Shirazi<sup>1</sup> and Aftab E. Patla<sup>2</sup>

<sup>1,2</sup>Department of Kinesiology, University of Waterloo, Waterloo, ON

<sup>1</sup>[zshafaei@ahsmail.uwaterloo.ca](mailto:zshafaei@ahsmail.uwaterloo.ca)

## INTRODUCTION:

During human locomotion, availability of the online information about the environment and the body limbs (relative to each other and to the environment) is an important issue for the central nervous system (CNS) to modulate the motion strategies to control and maintain the postural balance. There are three main feedback systems, which update the CNS about the environmental and the body position relative to the surrounding space during performing any task, such as Gait Termination (GT). Those controlling systems are: visual, vestibular, and somatosensory systems (Dietz, 1992, Patla, 2003). Visual system contributes in feed-forward control as an anticipatory strategy for dynamic stability for navigation in the environment (Patla, 2003). In reactive control, however, the information from the visual system is not fast enough to recover the body equilibrium from an unexpected perturbation such as slip (Patla, 2003). The vestibular system, detect the perturbation by head acceleration and activate extensor synergies to support the body. Moreover, the somatosensory information from the foot mechanoreceptors and load sensitive afferents in the joints provide feedback from the perturbation and send signal to initiate a polysynaptic response (Patla 2003; Oates et al., 2005). The focus of this study was to have a better understanding about the role of each of the three sensory systems in postural control during GT strategy.

## METHODS

Seven females were asked to walk with their normal speed along an 8 meters walkway and stop within one stride with their both feet side-by-side following an auditory stop signal. A visual target was mounted at the eye level of the participants at a distance of 10 meters straight ahead from the starting position and the participants were asked to fix their eyes on the target during trials performance. A total of 120 trials, including 33% of termination trials were performed. The experimental conditions were performed in 8 conditions of 15 trials: 1) No Vision (NV), 2) Galvanic Vestibular Stimulation (GVS), 3) stepping on 'foam', for somatosensory manipulation, 4) NV+GVS, 5) NV+foam, 6) GVS+foam, 7) NV+GVS+foam, and 8) control condition (no sensory manipulation) GT trials. Whole body kinematics and EMG data were collected and analyzed.

## RESULTS AND DISCUSSION

During somatosensory manipulation the amount of body sway (is shown as Center of Mass (COM) RMS) in anteroposterior direction increased significantly comparing to the control condition. Due to lack of correct perception about the location of the Center of Pressure (COP) under the plantar surface of the feet, the step width was reduced, which resulted in closer location of the COM to the Base of Support (BOS) boundaries ( $P < .0001$ ) (table 1). As a result the time to fall outside the BOS was decreased significantly ( $P = 0.0007$ ). The

onset latencies of the muscle activities were shown to have delay from 70 to 104 msec during manipulation of this sensory system. The visual and vestibular manipulation did not affect the COM trajectory; however, they affected the trend of muscle activation and caused some delays in their latencies.

## SUMMARY/CONCLUSIONS

During stepping on the soft surface, the mechanoreceptors of the plantar surface of the feet cannot predict the COP position under the feet. As the COP has a dominant role in controlling the COM, uncertainty about the position of the COP grants a great challenge to the CNS in dynamic control of the body. Thus, the most effective information in GT control comes from the somatosensory system. The reason is that the manipulation of this system by itself or in conjunctions with other sensory manipulation has the most effect on the GT strategy and postural stability. According to our results, the individuals with somatosensory deficit (eg. individuals with diabetic neuropathy) have to pay extra attention during tasks such as termination of gait. The manipulated vestibular information has the least effect on dynamic stability control comparing to the two other sensory systems. However, when the vestibular inputs are not reliable during unusual somatosensory information or unavailable visual information, the difficulty of the postural control is aggravated. Therefore, the vestibular system has a complementary role with the aid of the two other sensory systems in controlling the postural stability during GT. Absence of visual information delays the action that is required to arrest the forward momentum of the body and causes delay in GT completion.

Table 1: A change in postural stability was found due to sensory manipulation. a, b)The COM was located closer to the BOS edges due to unusual sensory inputs. c) Measurement of COM RMS was conducted to estimate the amount of body sway. The data are shown as average value and the P value for the bold data is less than 0.05.

	Step width (cm)	a) COM-BOS left (m)	b) COM-BOS front (m)	c) COM RMS
GVS	11.79	5.82	5.38	102.91
NoVision	11.89	5.97	5.95	103.52
Foam	<b>10.37</b>	<b>4.85</b>	<b>2.99</b>	104.13
GVS+ NoVision	12.57	<b>6.18</b>	5.95	103.10
GVS+ Foam	<b>10.83</b>	5.14	<b>3.05</b>	<b>104.59</b>
NoVision+ Foam	11.38	5.69	<b>3.40</b>	<b>105.67</b>
G+NV+F	11.08	5.51	<b>3.08</b>	<b>105.43</b>
Control	11.93	5.57	5.23	102.77

## REFERENCES

- Dietz V (1992). *Physiol Rev* **72**:33–69.  
 Oates AR et al. (2005). *J Neurophysiol* **93**(1):64-70, 2005.  
 Patla A E (2003). *IEEE Eng Med Biol Mag.* **22**(2):48-52, 2003.

## ACKNOWLEDGEMENTS

Special thanks to Farzad Khalvati and Michael Greig for MATLAB programming.

# Kinetic finger inter-dependence in a kinematic task

Sun Wook Kim<sup>1</sup> Jae Kun Shim<sup>2</sup> Vladimir M. Zatsiorsky, Mark L. Latash<sup>1</sup>

<sup>1</sup> Penn State University, University Park, PA USA

<sup>2</sup> University of Maryland, College Park, MD USA

E-mail: mll11@psu.edu

## INTRODUCTION

Studies of finger actions in kinetic and kinematic tasks have shown that fingers are not independent force/motion generators (Schieber and Santello 2004). These effects (termed “enslaving”) have been studied both in static force production tasks (Zatsiorsky et al. 1998) and during finger movements (Hager-Ross et al 2000; Li et al 2004). The purpose of this study has been to link enslaving effects between the kinetic and kinematic variables.

## METHODS

Five male and five female healthy, right-handed volunteers participated in the experiment. During the test, the participants sat on a chair with their right lower arms strapped onto the table with a set of Velcro straps. A wrist-lower arm brace was used to prevent the movement of the palm and immobilize the wrist joint. Wooden bars were placed on the dorsal side of all fingers and were wrapped from the proximal to the distal interphalangeal joint with Velcro straps. They were used to restrict movement of the task finger to the metacarpophalangeal (MCP) joint. An electronic goniometer (Sensor SGw65 Biometrics Ltd.) measured the angular movement of the MCP joint in the task finger. Piezoelectric sensors were used to measure the force produced by the other, non-task fingers (Fig. 1). The sensors could be moved in horizontal direction on the aluminum panel to adjust for individual subject’s hand anatomy. The hand and wrist

were kept in a fixed neutral position; the aluminum panel was moved vertically to allow motion of different fingers.

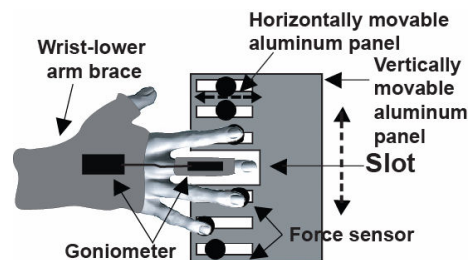


Figure 1. Experimental setup

Before each trial, subjects were instructed to extend all finger joints into approximately 180° with the thumb pointing upward. The subjects had to produce consecutive cycles of flexion and extension by a task finger through the slot along the guide template line on the screen. Forces produced by the other fingers were measured by the force sensors.

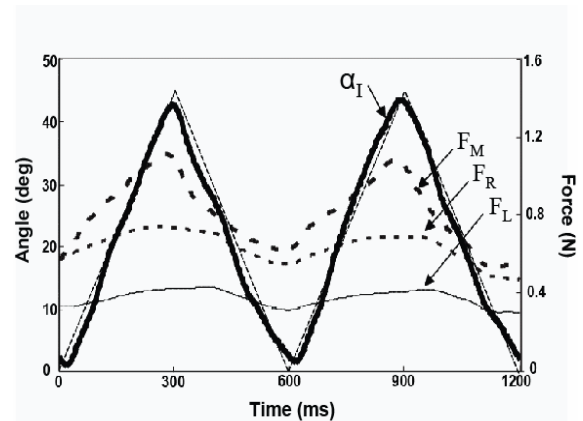


Figure 2. Subject’s performed angular and force production. .

The forces produced by the non-task fingers and the angular position of the task finger

were measured and their ratios calculated to quantify the enslaving effect separately for the up (UP), peak, and down (DN) phases (Fig 2). The data were time normalized. UP direction is defined from onset of flexion to maximal flexion while DN direction is defined from onset of extension to end of extension. To estimate the magnitude of the enslaving (E), the force produced by non-task fingers was divided by the angular displacement of the task finger.

$$E_{ij} = \frac{\Delta F_i}{\Delta \alpha_j}$$

Force and angular deviations were quantified between the 10% and 90% of the peak-to-peak movement amplitude.

## RESULTS AND DISCUSSION

Finger motion was associated with cyclic force production by the non-task fingers (Fig. 2). Figure 3 shows the average enslaving effect for the three phases averaged over the subjects. The largest enslaving effects were observed when the subjects were close to the most flexed finger position (open bars in Fig. 3). The effects did not differ between the flexion and extension phase of the movement. The index finger showed the least enslaving, while there were no significant differences across the other three fingers. Mixed-effects ANOVA with factors *Direction* and *Finger* confirmed these results with significant main effects of each of the factors ( $F[1,10]=69.6$ ;  $p < 0.001$ ,  $F[1,10]=8.9$ ;  $p < 0.001$ ), and no significant interaction)

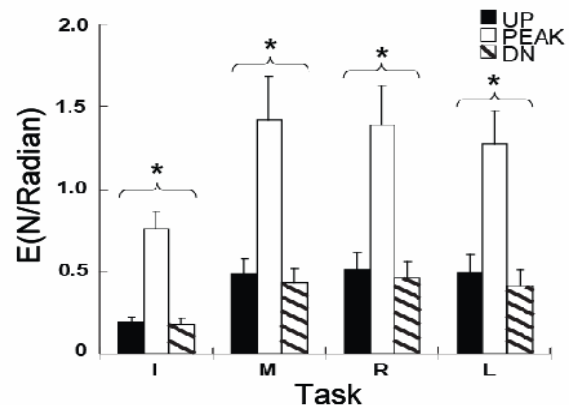


**Figure 3:** Enslaving Effect during UP, Peak, DN phases. Average group data are presented with standard error bar. \* signify significant ( $P < 0.05$ )

## SUMMARY/CONCLUSIONS

This is the first study to provide a link between the well known phenomena of finger inter-dependence during kinetic and kinematic tasks. The index finger is confirmed to be best controlled individually. Enslaving effects seem to be independent on the movement direction by the task finger. In contrast to previous studies, we observed significantly different magnitudes of these effects when the finger approached an extreme flexed position. These results suggest that studies of finger inter-dependence have to consider the range of variables produced by instructed fingers.

## REFERENCES

1. Schieber and Santello. *J Appl Physiol* **96**(6) :2293-2300, 2004.
2. Zatsiorsky VM et al. *Exp Brain Res* **131**:187-195,1998.
3. Hager-Ross CK et al. *J Neurosci* **20**:8542-8550, 2000.
4. Li et al. *Motor Control* **8**:1-15, 2004

## ACKNOWLEDGEMENTS

AG-018751, NS-035032, and AR-048563.

# CHANGES IN PEDAL AND JOINT KINETICS AFTER LEARNING TO DIRECT PEDAL FORCES

Christopher J. Hasson, Richard E.A. Van Emmerik, and Graham E. Caldwell  
Biomechanics & Motor Control Laboratories, University of Massachusetts, Amherst, MA  
cjhasson@excsci.umass.edu

## INTRODUCTION

While it has been suggested that biarticular muscles have a specialized role in directing external reaction forces (van Ingen Schenau, 1989), it is unclear how humans learn to coordinate their muscles in force-directing tasks. Recently, we examined the ability of subjects to learn to specifically direct pedal forces during one-legged cycling, and found that subjects could significantly improve targeted pedal force direction when given real-time feedback (Hasson et al., 2006a). In the present abstract, we describe the changes in pedal and joint kinetics that took place over the learning process. After quantifying these changes, alterations in mono- and bi-articular muscle coordination were studied using electromyography, described in a companion abstract (Hasson et al., 2006b).

## METHODS

Nine male subjects (age:  $25 \pm 4$  yrs; mass:  $83 \pm 13$  kg; height:  $1.77 \pm 0.07$  m) performed one-legged cycling on a ten-speed bicycle mounted on a computerized ergometer. Pedal kinetics were measured using a piezoelectric force pedal mounted on the left crank arm. The angular positions of the crank arm and pedal were measured with digital optical encoders. The force and angle data were sampled at a rate of 200 Hz.

Subjects were instructed to apply their pedal forces such that the resultant force was always perpendicular to the crank arm (target force direction), and to maintain a constant pedaling speed. During pedaling, real-time visual feedback (Fig. 1A) concerning the applied and target force directions and crank angular velocity (vertical bar) was displayed on a computer

monitor. The crank cycle was divided into 16 sectors of equal arc length. For each sector the average error between the target and applied force directions was calculated and displayed as a vector, colored to indicate the error magnitude. After each trial, the results were displayed in summary form as the average root-mean-squared error (RMSE) in each of the four crank cycle quadrants (Fig. 1B).

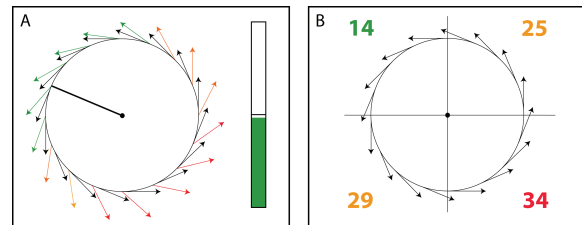


Fig. 1. A: Example of instantaneous feedback. B: Summary feedback (RMSE).

Subjects performed an initial baseline trial without feedback, followed by 16 trials with real-time feedback. Each trial consisted of a 15 s two-legged pedaling warm up, followed by pedaling with only the left leg for 30 s, during which data were collected.

Kinematic and kinetic data were digitally filtered (3 Hz low-pass zero-lag fourth-order Butterworth filter), and expressed as functions of crank angle ( $1^\circ$  resolution) using cubic spline interpolation. Pedal forces were transformed to the global coordinate system. The RMSE between the applied and target force directions was calculated for each crank cycle and trial. The bicycle and rider were modeled as a five-bar linkage (Fig. 2) with two mechanical degrees-of-freedom (Hull and Jorge, 1985). Segment lengths were measured; segment masses and inertial properties were estimated using regression equations from the literature.

Segment linear and angular accelerations were calculated numerically. Joint reaction forces and moments were computed using a standard inverse dynamics approach.

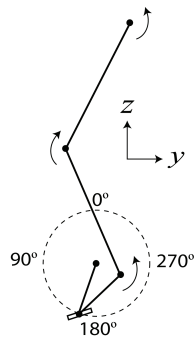


Fig. 2. Schematic of bicycle-rider system. Positive joint moments are shown.

## RESULTS AND DISCUSSION

As reported in Hasson et al. (2006a), subjects showed a significant improvement in their ability to direct applied forces over the entire crank cycle (decreased RMSE from  $59.7 \pm 10.9^\circ$  to  $21.2 \pm 5.5^\circ$  [pre-post,  $p < 0.001$ ]), with the greatest improvement in RMSE in the second half of the crank cycle. The signed mean force-direction error across subjects is shown in Fig. 3A, where a positive mean error reflects an applied force directed radially outward with respect to the target force direction.

With learning, the net ankle, knee, and hip extensor joint moments decreased, while the flexor moments increased (Fig. 3B). Small changes in timing were observed for the ankle and hip moments, but subjects showed a much earlier transition from a knee extensor to flexor moment with learning. These moment changes caused the shapes of the vertical and anterior-posterior (AP) applied pedal forces (Fig. 3A) to become more like the “ideal” patterns of the target force direction.

In the baseline trial, the large extension moments in the first half of the crank cycle produced a large downward pedal force and crank torque. This caused an acceleration of the crank arm, which may have made it difficult for subjects to direct the force accurately at the bottom of the crank cycle and in the second half. After training, subjects demonstrated a reduced crank

torque in the range of  $\sim 0$ - $180^\circ$ . This in turn caused a more uniform crank torque and therefore a more constant crank angular velocity. Without the crank acceleration in the first half of the crank cycle, subjects were better able to direct the pedal forces correctly in the range of  $\sim 160$ - $340^\circ$ .

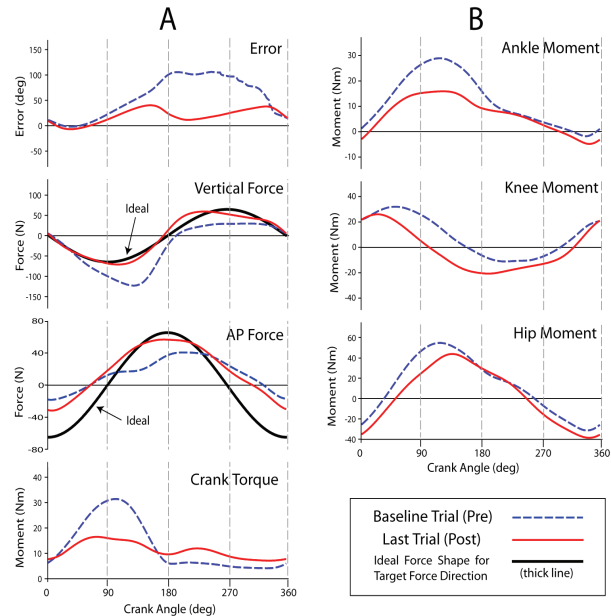


Fig. 3. A: Mean force-direction error, applied pedal forces, and crank torque as a function of crank angle. B: Net joint moments. See Fig. 2 for force and moment definitions. Means are across subjects.

## SUMMARY

Subjects were able to improve their performance of the force-directing task significantly. With training, joint extensor moments decreased, flexor moments increased, and the knee joint moment became flexor earlier in the crank cycle. These changes lead to a much less variable crank torque over the crank cycle.

## REFERENCES

- Hasson CJ, et al. (2006a) CSB 14<sup>th</sup> Meeting.
- Hasson CJ, et al. (2006b) ASB 30<sup>th</sup> Meeting.
- Hull ML, et al. (1985) *J Biomech* 18:631-44.
- van Ingen Schenau GJ (1989) *Hum Mov Sci* 8:301-37.

## ACKNOWLEDGEMENTS

This work was supported by a graduate student grant-in-aid from the American Society of Biomechanics.

# SOFT TISSUE ARTIFACT ERROR CAN BE REDUCED BY USING MULTIPLE REFERENCE POSITIONS

Bo Gao, Naiquan (Nigel) Zheng

University of Florida, Gainesville, FL, USA  
E-mail: nigelz@ufl.edu Web: www.ortho.ufl.edu/BMAL

## INTRODUCTION

When using optoelectronic stereophotogrammetry and skin-mounted markers to study human body movements, errors will be produced by soft tissue artifact (STA), which is caused by muscle and skin's movement relative to the bone underneath. STA error has been proved to be a major problem of this technique and researchers have worked diligently both experimentally and computationally on this challenging issue in recent years (Alberto *et al.*, 2005). To analyze bone's motion from captured markers' motion, a reference position (such as T-pose) is often used to obtain the local coordinates of each marker in its corresponding bone's local coordinate system. However, markers' local positions are normally different from the values obtained from the reference position due to the STA when adjacent joints are not in the T-pose position. This discrepancy propagates as errors in further bone motion calculation. To reduce the discrepancy of marker's local coordinate values caused by STA, a multiple reference positions (MRP) approach is proposed and its validation is demonstrated by knee-joint kinematics calculations during simulated walking.

## METHODS

Eight subjects were tested during level walking using an IRB approved protocol. Eleven markers were put on the thigh and 10 on the shank of each leg. Markers' motions were captured during a gait cycle. For each leg, motions of the femur and the tibia were calculated using point cluster technique (Andriacchi *et al.*, 1998). This set of data

was used to simulate a real motion of the bones while the subject was walking (*true motion*). With the position of markers and specific reference positions, we calculated other sets of bone motion (*calculated motion*) and compared them with *true motion*.

Four positions during gait (heel strike, middle stance, toe off, and maximum flexion) were selected as reference positions. Using each of these reference positions, knee joint kinematics was calculated based on rigid body optimization (Spoor *et al.*, 1980).

For MRP approach, a set of *varying local coordinates* was created by interpolation using the values at the 4 reference positions for each marker. These *varying local coordinates* were used in every timeframe's optimization. Unlike constant values used in single-reference-position method, these *varying local coordinates* are not constant during motion and include part of STA's effect.

To compare the results of MRP approach with the commonly used single-reference-position method, average STA error is

$$\text{defined as } E = \frac{\sum_{nf} \sum_{nm} |[R]^{-1}(\vec{p}_i^g - \vec{O}) - \vec{p}_i^l|}{nm \times nf},$$

where  $\vec{O}$  and  $[R]$  are the origin and the rotation matrix of the bone's coordinate system, and  $\vec{p}_i^g$  and  $\vec{p}_i^l$  represent a skin marker's global and local positions. This error can represent the residue of the optimization and finally determine the accuracy of kinematics calculation. The repeated measures ANOVA was used to test

the differences (SPSS Inc., Chicago, IL, USA).

## RESULTS AND DISCUSSION

A comparison of the STA error using single reference positions and using MRP for all the subjects is shown in Fig.1. The MRP approach reduced the error in both thigh and shank's calculation. There were significant difference ( $p < 0.01$ ) between the thigh and shank and between single and multiple reference positions.

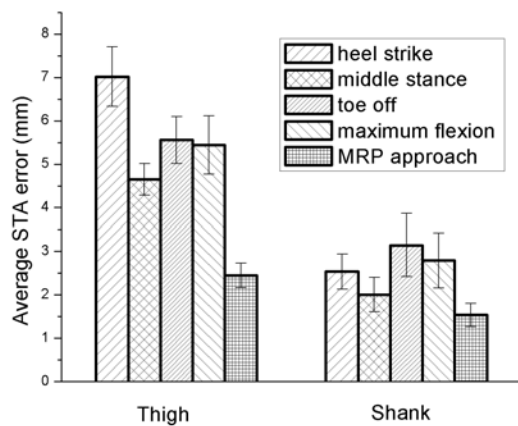


**Fig.1** Average STA errors using MRP approach and using single reference positions when calculating thigh and shank motion.

Because the employment of *varying local coordinates* essentially takes into account part of the STA, it reduces the non-rigid artifact during optimization. As a result, the calculation accuracy of the segmental motion and the joint kinematics are improved. Using average errors relative to *true motion* during the whole motion, the accuracies of MRP approach and single-reference-position method can be compared. As examples, Fig.2 shows the results of knee joint axial-rotation and anterior-posterior (AP) translation calculation. The MRP approach was more accurate than using any single reference position and reduced the error up to 43% for axial

rotation and 77% for AP translation. The differences were statistically significant ( $p < 0.01$ ) among five methods. The MRP approach had the lowest errors.

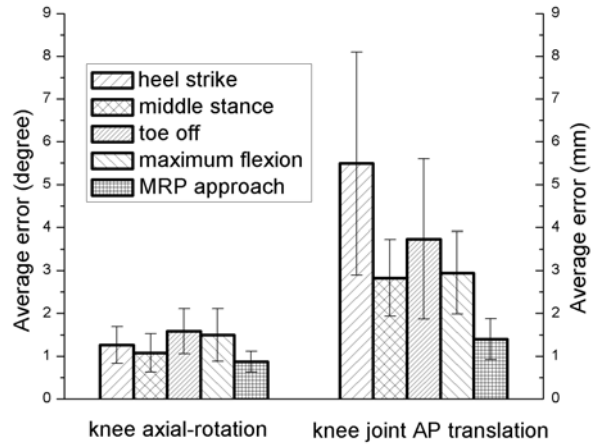


**Fig.2** Average errors using MRP approach and using single reference positions when calculating knee joint axial-rotation and anterior-posterior translation.

## CONCLUSIONS

By introducing *varying local coordinates* to replace the constant local coordinates of markers, the MRP approach can reduce the non-rigid error caused by STA significantly and make the calculation of segmental motion and joint kinematics more accurate. Comparing with other STA compensation methods such as dynamic calibration, this approach is easier for it only needs to calibrate a few reference positions instead of the whole multi-dimensional degree-of-freedom space. Future studies will be focused on the validation of MRP approach in clinical applications.

## REFERENCES

- Alberto L. et al. (2005). *Gait and Posture*, **21**, 212–225.
- Andriacchi T.P. et al. (1998). *J Biomech Eng*, **120**, 743–9.
- Spoor C.W. et al. (1980). *J. Biomech*, **13**, 391–393.

# THE EFFECT OF GENDER ON FINGER ANGLES DURING KEYBOARDING

Nancy A. Baker<sup>1</sup>, James Cook<sup>2</sup>, and Mark Redfern<sup>2</sup>

<sup>1</sup>Department of Occupational Therapy, University of Pittsburgh, Pittsburgh, PA, USA

<sup>2</sup>Department of Bioengineering, University of Pittsburgh, Pittsburgh, PA, USA

E-mail: [nab36@pitt.edu](mailto:nab36@pitt.edu)

## INTRODUCTION

Female gender has been associated with increased risk for computer-related musculoskeletal disorders of the upper extremity (WRMSD-UE). Researchers have hypothesized that this association may be related to anthropometrics, hormones, and differential exposures to occupational practices than males (Tittiranonda et al., 1999). One possible explanation is that females may work in postures which cause greater biomechanical stressors than males.

There is considerable variability in postures between computer users during keyboarding (Simoneau et al., 1999). There has been considerable research that has examined joint angles of the wrist during keyboarding, but few that have examined finger angles (Baker et al., in press; Sommerich et al., 1996). There has been almost no research, however, that compared these joint angles between genders.

The purpose of this paper is to describe the differences in male and female flexion/extension (f/e) and abduction/adduction (ab/ad) joint angles of the metacarpophalangeal (MCP) joints, and the f/e angles of the proximal phalangeal (PIP) joints during keyboarding.

## METHODS

Twenty subjects, 14 females and 6 males, between the ages of 20 and 54 were recruited. All subjects reported using a computer an average of 6 hours per day.

Kinematics data were collected using 5

VICON<sup>TM1</sup> motion measurement system cameras positioned around a computer workstation. The finger movements were derived by tracking 21 passive markers positioned on the dorsal surface of each hand (Baker et al., in press). Data were collected at 60 Hz. Subjects were instructed to type at their normal rate, using their usual keyboarding methods. Subjects typed for 15-minutes to acclimate to the workstation. Three 1-minute trials of motion data were captured at 15-minutes, 20-minutes and 24-minutes of keyboarding.

Joint angles were derived as described in Cook et al. (in press). The three trials' data were combined together and means and standard deviations were calculated for the angles. We used 3-way ANOVAs with 2 within-subject measures, hand and digit, and 1 between-subject measure, gender, to examine the differences between MCP f/e, MCP ab/ad, and PIP f/e. If an overall ANOVA was significant, we used post hoc analyses to examine potential differences in kinematics between the males and females

## RESULTS AND DISCUSSION

Figures 1 – 3 show the mean finger joint angles during keyboarding. There was no significant differences between genders for MCP ab/ad ( $p = .86$ ) and PIP f/e ( $p = .41$ ). There was a significant difference between genders for MCP f/e ( $p = .05$ ). An examination of the means suggested that males had a significantly larger mean MCP flexion angles than females, particularly for the right hand (Figure 1).

---

<sup>1</sup> VICON Motion Systems Inc, Lake Forest, CA, USA - <http://www.vicon.com/jsp/index.jsp>

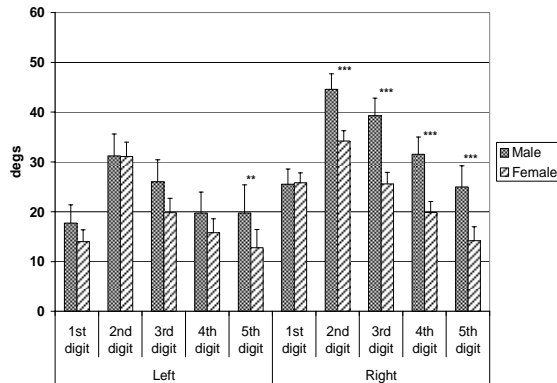


**Figure 1:** Mean male & female MCP flexion angles during keyboarding (\*\*  $p < .05$ ; \*\*\*  $p < .001$ )

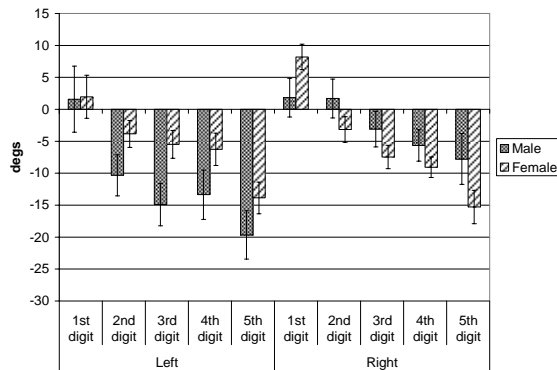


**Figure 2:** Mean male & female MCP adduction<sup>(+)</sup> & abduction<sup>(-)</sup> angles during keyboarding

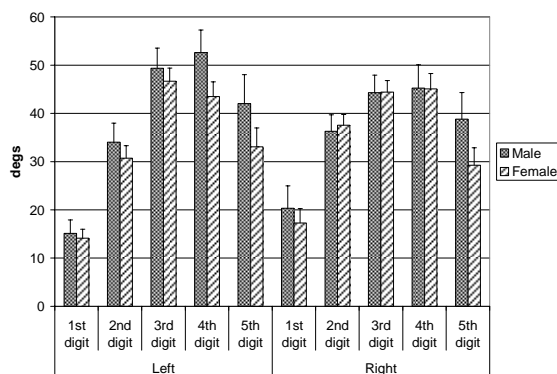


**Figure 3:** Mean male & female PIP flexion angles during keyboarding

Observations of keyboard users suggest that some users maintain their MCP joints in hyperextension when not striking the keys (Baker et al., in press). One possible interpretation of the greater mean flexion of the males is that females, being generally

more flexible than males, may be more likely to hold their MCP joints in hyperextension while in the resting posture. Whether this posture is a gender related risk factor for WRMSD-UE needs to be examined further.

## SUMMARY

This study examined the differences in finger joint angles between genders during keyboarding. Males have significantly larger mean MCP flexion angles than females, suggesting that females may maintain their MCP joints in hyperextension more than males during keyboarding.

## REFERENCES

- Baker, N. A., et al. (in press). Kinematics of the fingers and hands during computer keyboard use. *Clinical Biomechanics*.
- Cook, J., et al. (in press). Measurements of wrist and finger postures: A comparison of goniometric and motion capture techniques. *Applied Biomechanics*.
- Simoneau, et al. (1999). Wrist and forearm postures of users of conventional computer keyboards. *Human Factors*, **41**, 413-424.
- Sommerich, C. M., et al. (1996). A quantitative description of typing biomechanics. *Journal of Occupational Rehabilitation*, **6**, 33-55.
- Tittiranonda, et al. (1999). Risk factors for musculoskeletal disorders among computer users. *Occupational Medicine: State of the Art Reviews*, **14**, 17-38.

## ACKNOWLEDGEMENTS

The authors would like to acknowledge the support of the Competitive Medical Research Fund of the UPMC Health System, the Central Research Development Fund, and Grant # 1 K01 OH007826 – 01A1 from the National Institute for Occupational Safety and Health.

# Lower limb joint work during running on level and up or down a sloped surface

Darren Dutto<sup>1</sup>, Donald Hoyt<sup>2</sup> and Steven Wickler<sup>2</sup>

<sup>1</sup> Eastern Oregon University, La Grande, OR, USA

<sup>2</sup> California State Polytechnic University, Pomona, CA, USA

E-mail: ddutto@eou.edu

## INTRODUCTION

When running up a sloped surface, the mechanical work done at the hip increases (Roberts and Belliveau, 2005). Work is done in order to increase the potential energy of the body. When running down a slope, one might expect the opposite, as energy must be absorbed and dissipated as the potential energy of the body decreases. Hip musculature may be suited to this task, due to the relatively larger muscle volume.

Another reason that one might expect the hip to be absorbing energy during downhill running is from the large braking forces produced (Gottschall and Kram, 2004). Large braking forces might be the result of net flexor moment at the hip during stance. The combination of a flexion (negative) moment and hip extension (positive) results in negative work done on the hip flexor muscles.

The purpose of this study was to determine the amount of work done by the ankle, knee, hip and total leg when running on level, and up (incline) and down (decline) a sloped surface. We hypothesize that work done by the hip would increase when running up the slope. When running down the slope, work would be done on the leg with the hip a likely site to absorb energy.

## METHODS

Six subjects participated in this study (3 men and 3 women). All participants were recreational runners (minimum of 10

mi/week over a minimum of 3 days). Participants signed an informed consent document describing the test protocol approved by an Institutional Review board. Prior to each test, the hip, knee, and ankle joints were identified via palpation and marked with reflective adhesive tape.

Testing occurred in two different locations. Both sites consisted of 30 m long cement runways covered by black rubber matting. One runway was level and the other had a 10% slope. A 60 x 90 cm force measuring platform (model 9287BA, Kistler Instruments) was situated in the middle of each runway (the same platform was used) to record forces (1000 Hz). Video records of each run were taken with a high speed (250 Hz) digital camera (PCI 250; Redlake Imaging Corp.). Video and force recordings were synchronized using LabView (National Instruments).

During a trial participants ran through the testing area at a constant pace. Trials where speed varied between the beginning and end of the recording area by more than 5% were excluded. Average speed across all subjects and trials was 4.0 m/s for all three conditions (level, incline, and decline).

From the kinematic data, joint angles and were determined. Kinematic and kinetic data were combined using inverse dynamics. Joint moments, power, and work were calculated for the hip, knee and ankle. To assess differences between slope conditions, a repeated measures ANOVA was used ( $\alpha = 0.05$ ).

## RESULTS AND DISCUSSION

In all three sloped conditions, the largest amount of work was observed in the hip (Table 1). In the level condition, the hip did more work than that observed by Roberts and Belliveau (2005). Unlike Roberts and Belliveau we did not find significant increases in work done by the hip on the incline. On the decline, energy was absorbed by the hip as seen in the observed negative work. In general the work done by (or on) the hip determined the total work done by the limb.

The change from energy generation on the level and incline to energy absorption on the decline in the hip was from a change in the hip moment. Peak moments were largely extensor (positive) on the level and incline (Lvl:  $6.07 \pm 1.02$  and Inc:  $5.43 \pm 0.97$  Nm/kg) and flexor (negative) on the decline (Dec:  $-6.81 \pm 0.80$  Nm/kg). The amount of work done by the knee increased on the decline due primarily to increased extensor moment (Lvl:  $1.97 \pm 0.43$ , Inc:  $2.07 \pm 0.27$ , Dec:  $5.77 \pm 0.85$  Nm/kg).

Each joint maintained the same ROM across the three slope conditions, however the work done by the ankle was greater for the incline due to a combination of a non-significant increase in both moment and ROM.

We recently presented that knee stiffness increased significantly from 5.5 to 12.9 Nm/kg/rad when going from the level to decline in this group of runners (Dutto, et al. 2005). The knee may be more stiff to allow

energy absorption in the flexor musculature of the hip as opposed to the smaller muscles of the knee and ankle. Increased knee stiffness and negative work done on the musculature of the hip when running down a sloped surface may create the large observed braking forces. Further investigation is necessary to confirm this observation.

## SUMMARY/CONCLUSIONS

Work done by the limb increased slightly when running up a slope compared to running on the level. When running down a sloped surface, the hip absorbs large amounts of energy, resulting in negative work done on the limb. The negative work done on the hip and the large extension moment at the knee may be related to large braking forces found with downhill running.

## REFERENCES

- Dutto, D., et al. (2005). *Med. Sci. Sports Exerc.*, 37(5), S392.  
Gottschall, J.S., Kram, R. (2004). *J. Biomechanics*, 38, 445-452.  
Roberts, T.J., Belliveau, R.A. (2005). *J. Exp. Biol.*, 208, 1963-1970.

## ACKNOWLEDGEMENTS

Holly Greene, M.S. Equine Research Technician was significant in the organization and implementation of data collection. Supported by NIH # 2S06 GM53933 to DH & SW.

**Table 1:** Work (J/kg) done at or on each joint and the limb for the three conditions (mean± SD).

Joint:	Ankle	Knee	Hip	Total
Incline	$0.56 \pm 0.11^a$	$0.11 \pm 0.09$	$1.75 \pm 0.56$	$2.42 \pm 0.67$
Level	$0.23 \pm 0.11$	$0.03 \pm 0.16$	$1.46 \pm 0.33$	$1.72 \pm 0.44$
Decline	$0.12 \pm 0.03$	$0.42 \pm 0.22^b$	$-2.70 \pm 0.56^c$	$-2.17 \pm 0.44^c$

a = Inc > Lvl and Dec (p < 0.05), b = Dec > Lvl (p < 0.05), c = Dec < Lvl and Inc (p < 0.05)

# CHANGES IN DISTAL POSTURAL CONTROL ACCURACY NEAR THE LIMITS OF THE BASE OF SUPPORT

Manuel E. Hernandez MS<sup>1,3,4</sup>, Neil B. Alexander MD<sup>2,4,5</sup>, and James Ashton-Miller PhD<sup>1,3</sup>

<sup>1</sup>Department of Biomedical Engineering, <sup>2</sup>Institute of Gerontology, <sup>3</sup>Biomechanics Research Laboratory, <sup>4</sup>Mobility Research Center, Division of Geriatric Medicine, Department of Internal Medicine, The University of Michigan, <sup>5</sup>VA Ann Arbor Health Care System Geriatric Research, Education and Clinical Center, Ann Arbor, Michigan.

E-mail: manueleh@umich.edu Web: www.med.umich.edu/geriatrics/moblab/

## INTRODUCTION

Balance is an integral part of daily living. The ability to maintain Center of Mass (COM) stability during tasks such as reaching or stooping reduces the risk of falling and suffering injury.

Balance control requires accurate and rapid control of the Center of Pressure (COP) upon the detection of a loss of balance. A loss of balance can be considered to occur when the center of mass falls outside of the base of support and is not actively accelerating towards a state of equilibrium (i.e., stable gait).

Fitt's law introduced a theoretical framework for the trade-off between accuracy and speed in upper extremity reaching tasks, such as reciprocal tapping (Fitts, 1954). To our knowledge, these principles have not yet been applied to distal postural control or the control of the COP by the ankle musculature. We propose a 1-DOF distal postural control (DPC) task, to evaluate speed-accuracy tradeoffs in the reciprocal movement of the COP in the anteroposterior plane.

## METHODS

*Subjects.* Twenty healthy young adults (Age < 30 yrs., males = 10, females = 10) are to be recruited for this study, out of which 2

have been recruited thus far, and are used for this analysis (N=2, males =1, females = 1, Age = 20 and 25 yrs).

*Protocol.* In order to determine the relationship between reciprocal COP movement accuracy and the COP excursion amplitude and target width, a modification to the Functional Base of Support (FBOS) test is proposed (King et al., 1994, Fitts 1954). Participants stand upright and then lean maximally forward and backward to determine their FBOS. FBOS is defined as the limits between the maximal forward and backward excursion of the COP from a steady upright stance. Participants are instructed to shift their COP signal as fast and as accurate as possible between a pair of target COP positions using visual feedback in a 15 second trial. Specific target width and COP excursion amplitude combinations are repeated five times. Outcome measures of this task include COP excursion, COP velocity, and limits of the FBOS.

## RESULTS AND DISCUSSION

Changes in the mean percentage of correct reciprocal movements during the performance of the distal postural control task are shown in Figure 1 and summarized in Table 1. The 28 trials analyzed from the two subjects suggest a change in COP control accuracy, depending on the COP excursion and target width.

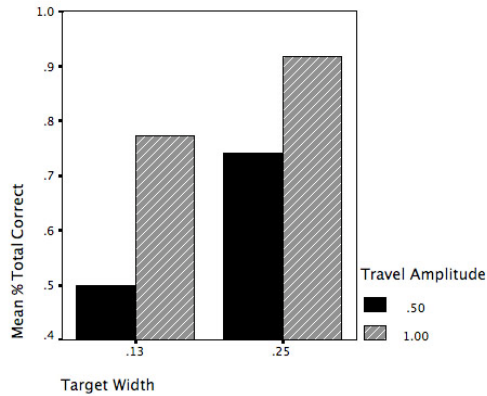


**Figure 1:** Mean Percentage of Correct Reciprocal Movements in the Distal Postural Control Task (Travel Amplitude and Target Width are reported as a percentage of the FBOS)

**Table 1:** Summary of total percentage of correct reciprocal movements

Target Width	Travel Amplitude	
	0.5	1
0.25	0.74 ± 0.23	0.92 ± 0.13
0.125	0.50 ± 0.21	0.77 ± 0.19

The proximity of the large amplitude reciprocal tasks to the edge of the FBOS, might explain the higher accuracy rate observed, when compared to tasks requiring smaller amplitude COP excursions. As the edge of the FBOS is approached, the consequences of a perturbation become more significant (i.e., falls) and thus the detection of a loss of balance becomes increasingly important. Subjects more attuned their position in space relative to their limits of stability may be less likely to fall.

A question remains as to the theoretical framework underlying difficulty imposed by a greater travel of the COP or narrow target width, as analysis has not yet revealed a relationship between accuracy rate and difficulty. Figure 2 illustrates the inverse

relationship between time and the number of correct reciprocal movements.

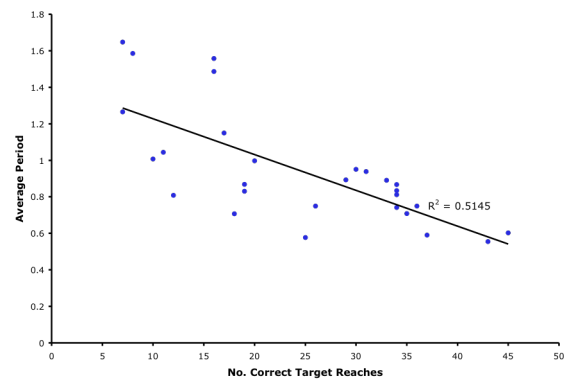


**Figure 2:** Inverse relationship between the Mean Period between reciprocal movements and the total number of correct reciprocal movements in the Distal Postural Control Task

## SUMMARY/CONCLUSIONS

Preliminary findings suggest that COP accuracy rate may depend on the COP excursion and target width. Group sizes are presently too small to draw any conclusions.

## REFERENCES

- Fitts, P.M. (1954). *J. Exp Psychol*, **47**, 381-91.
- King, M.B., Judge, J.O., Wolfson, L. (1994). *J. Gerontol*, **49**, M258-63.

## ACKNOWLEDGEMENTS

We would like to thank the following collaborators, which provided us assistance in collecting data: Ravinder Goswami, Eric Pear, and Lindsey Dubbs. We are grateful to the National Institutes of Health for NRSA Grant Number 1 F31 AG024689-01, which support this project.

# **A GRF COMPARISON BETWEEN LANDING FROM A COUNTERMOVEMENT JUMP AND LANDING FROM STEPPING OFF A BOX**

Mostafa Afifi and Richard Hinrichs  
Arizona State University, Tempe, AZ, USA  
e-mail: mostafa.afifi@asu.edu

## **INTRODUCTION**

Injuries occurring during landing from a jump are common in sports, particularly anterior cruciate ligament (ACL) injuries, which among college athletes are three times more common in females than males (Ireland, 1999). Thus, many studies have investigated the different biomechanical aspects of landing as well as compared differences between males and females.

A common practice among researchers is to have participants step off a box of a certain height to the ground. The purpose of this practice is to make sure participants are landing from the same height (Swartz et al, 2005). An assumption made that stepping off a box to the ground is similar to landing from a jump may be based on another assumption that touchdown velocity of the center of mass from a certain height is always the same.

If the two landings are found not to be the same, then this would cast a doubt on the validity of those studies that have used a box to mimic the landing from a vertical jump. Thus, the purpose of this study was to investigate if there are any biomechanical differences between landing from a countermovement jump and landing from stepping off a box.

## **METHODS**

Eighteen active college students (9 males, 9 females) volunteered to participate in the study. Participants were excluded if they did not take part in sports that involved jumping

at least 2 to 3 times a week or if they had any orthopedic condition that would prevent them from jumping.

Each participant performed three maximal effort countermovement jumps (CMJs) on a force platform (1200 Hz, AMTI). Landing impulse was used to calculate an equivalent landing height (the fall height of the body center of mass prior to touchdown). A box was then set to an appropriate height to match the landing height from the countermovement jump. The participants then stepped off the box with their right foot. If the step off (SO) equivalent landing height did not match any of the CMJ landing heights, the box height as adjusted and procedure repeated until a matching height was reached.

A comparison was then made between the two trials of similar height. Although EMG and video data were collected as part of a larger study, only vertical ground reaction force (GRF) data are presented here.

A mixed design two-way ANOVA with repeated measures (condition  $\times$  gender) with condition as the within-subjects factor was used to analyze the time to peak GRF, peak GRF, and maximum loading rate (maximal slope in GRF curve between contact and peak force; Bus, 2002); see Figure 1.

## **RESULTS AND DISCUSSION**

A significant main effect for condition was seen for time to peak GRF,  $F(1,16) = 6.7$ ,  $p < .05$ , with no significant condition  $\times$  gender

interaction,  $F(1,16) = .10$ ,  $p = NS$ . The SO landings produced significantly shorter times to peak GRF than did the CMJ landings (see Figure 1 and Table 1). Both peak GRF and maximal initial loading rate showed a significant jump type  $\times$  gender interaction. A test of simple effects showed the SO produced larger GRF and loading rates than the CMJ for males only,  $F(1,16) = 17.65$ ,  $p < .01$  and  $F(1,16) = 12.95$ ,  $p < .01$ , respectively.

A shorter time to peak GRF suggests that individuals were less prepared for impact during the SO compared to the CMJ. The difference between the two landings was more pronounced in males. The gender difference may be related to the landing height as the males jumped significantly higher than the females (means of 0.31 m and 0.22 m, respectively),  $F(1, 16) = 19.02$ ,  $p < .001$ .

Results from this study suggest true countermovement jumps should be used to study landings and not stepping off a box, as the two landing conditions produced significantly different force profiles.

Although not part of the original investigation, it was noticed that the equivalent landing heights when stepping off a box were on the average 0.10 m lower than the actual box height as participants tended to lower their foot, thus, lowering body center of mass prior to becoming airborne. This fact alone is troublesome for

all those prior studies that have assumed that the equivalent landing height and the box height are the same.

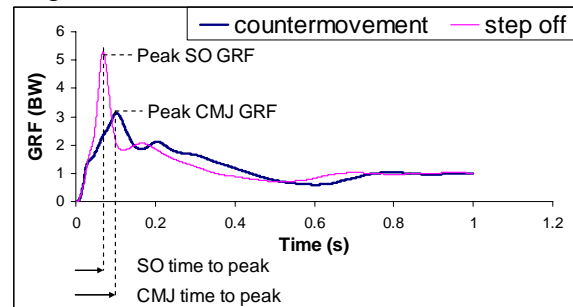


**Figure 1.** GRF in BW for both CMJ and SO landings for a typical male participant.

## SUMMARY/CONCLUSIONS

A comparison was made between vertical GRF when landing from a countermovement jump and stepping off a box. Results suggest that these landings are not similar to each other. Compared to the CMJ, SO landings produced earlier peak GRF in both genders and greater peak GRF and loading rates only in males. Additional work needs to be done to see how these force differences are reflected in patterns of muscle activity and kinematics of landing.

## REFERENCES

- Bus, S.A. (2003). *Medicine and Science in Sports and Exercise*, 35, 1167-1175.  
 Ireland, M.L. (1999). *Journal of Athletic Training*, 34, 150-154.  
 Swartz, E.E. et al. (2005). *Journal of Athletic Training*, 40, 9-14.

**Table 1.** Mean values  $\pm$  SD for dependent variables for conditions and genders.

	Time to CMJ peak GRF (ms)	Time to SO peak GRF (ms)	CMJ peak GRF (BW)	SO peak GRF (BW)	CMJ max loading rate (BW·s <sup>-1</sup> )	SO max loading rate (BW·s <sup>-1</sup> )
Females	82.1 $\pm$ 16	67.4 $\pm$ 11.3	3.68 $\pm$ 0.3	3.63 $\pm$ 0.4	123 $\pm$ 40	144 $\pm$ 54
Males	83.0 $\pm$ 14	63.8 $\pm$ 5.7	4.45 $\pm$ 0.8**	5.5 $\pm$ 0.9**	186 $\pm$ 97**	304 $\pm$ 167**
All participants	82.5 $\pm$ 14*	65.6 $\pm$ 8.9*	4.09 $\pm$ 0.7	4.6 $\pm$ 1.2	158 $\pm$ 77	224 $\pm$ 145

\*  $p < .05$ , significant main effect for condition

\*\*  $p < .05$ , significant simple effect for condition

# LOADING TO FEMALE PLAYERS DURING BASKETBALL CUTTING MOVEMENTS

Songning Zhang<sup>1</sup> and Kurt Clowers<sup>2</sup>, Douglas Powell<sup>1</sup>

<sup>1</sup> Biomechanics/Sports Medicine Lab, The University of Tennessee, Knoxville, TN, USA

<sup>2</sup> Anthropometry and Biomechanics Facility, Johnson Space Center, NASA, Houston, TX, USA

E-mail: szhang@utk.edu Web: web.utk.edu/%7Esals/resources/biomechanics\_laboratory.html

## INTRODUCTION

Prolonged basketball competition and training seasons lead to tremendous amount of injuries. A 69% injury rate for all players was reported over a seven-year period (Henry 1982). The ankle joint had highest amount of injury at 18.2% of all injuries whereas knee injuries caused most games missed at 66%. Arendt and Dick (Arendt 1995) reported that similar knee injury rate for men's and women's soccer and basketball players over four seasons whereas a different study (Hutchinson 1995) showed more knee related injuries of NCAA basketball players than lacrosse, volleyball, ice hockey and softball counterparts.

Comprehensive biomechanical studies on basketball movements are rare in the biomechanical literature. McClay et al. (McClay 1994a, McClay 1994b) conducted the only complete 2D kinematic and kinetic analyses on major biomechanical movements. To the knowledge of the authors, no documentation of comprehensive 3D biomechanical tests can be found in the literature. Therefore, the objectives of the study were to examine characteristics of 3D kinematics, ground reaction forces and lower extremity joint kinetics in major basketball movements by female basketball players and to examine the effects of basketball footwear on the biomechanics in the basketball movements.

## METHODS

Six female basketball players from the women's basketball team of a NCAA Division I school participated in the study.

The subjects performed five trials of following movements in each pair of two basketball shoes (A: DunkFest & B: 4SIGHT II, adidas) in a random order: single-leg jump, two-leg jump, landing from jump-stop, landing from a two-leg vertical jump with pivot, V cut, and lateral cut. These movements were identified based upon the results of a previous study examining the frequency and intensity of major basketball movements during three regular season games. Simultaneous recording of 3D kinematics by a 6-camera Vicon system (120 Hz), ground reaction forces (GRF) (600 Hz, AMTI), and EMG signals was conducted during the testing. Only the data from the two cutting movements are reported in this abstract.

Visual3D (C-Motion, Inc.) was used to compute 3D kinematic and joint kinetic variables. A  $2 \times 2$  (movement  $\times$  shoe) repeated measures ANOVA was used to evaluate selected GRF, joint kinematic and kinetic variables (SPSS, 12.0).

## RESULTS AND DISCUSSION

The results did not show any shoe effects. The data were then combined to run a one-way ANOVA to test the movement differences. An apparent peak mediolateral

(ML) GRF was seen in both cutting movements; the peak ML loading were 1.1 and 1.0 BW for the lateral cut and the v cut respectively (Table 1). The peak vertical GRFs were twice as large compared to the peak ML GRFs. The ML and vertical GRF impulses for the lateral cut were significantly greater than the v cut (Table 1).

During the lateral cut movement, the ML loading applied to the ankle, knee and hip joints were significantly greater than the v cut movement (Table 2). The v cut requires the subject to cut both laterally and anteriorly whereas the lateral cut requires only lateral cutting movement thus causes greater lateral loading to the lower extremity joints. Basketball players executed large amount of cutting movements during competition and also showed greater number of knee related injuries than several other sports (Hutchinson 1995). The high adduction loading applied to the knee joint may play a role in the greater number knee injuries seen in the sport.

### SUMMARY/CONCLUSIONS

The results from this study showed no difference between the two tested models of basketball shoes. The major differences are found in the ML impulses and the vertical impulses in GRF and peak adduction/abduction moments of the lower

extremity joints. High mechanical loading applied to the joints may pose increased risks to the female basketball players. To the knowledge of the authors, this is the first comprehensive 3D biomechanical study of high-loading basketball movements. Information obtained through this study may provide insight on loading applied to the lower extremity joints in various basketball movements. This information coupled with frequency information of the movements during actual competition may provide complete loading profiles of basketball players during a competitive season.

### REFERENCES

- Arendt, E., Dick, R. (1995). *Am J Sports Med*, **23**, 694-701.
- Henry, J. H., et al. (1982). *Am J Sports Med*, **10**, 16-18.
- Hutchinson, M. R., Ireland, M. L. (1995). *Sports Medicine*, **19**, 288-302.
- McClay, I. R., et al. (1994a). *J. Applied Biom*, **10**, 222-236.
- McClay, I. S., et al. (1994b). *J. Applied Biom*, **10**, 205-221.

### ACKNOWLEDGEMENTS

Supported by a grant from Adidas International.

Table 1. Average peak GRF (N/kg) and Impulse (Ns/kg): mean± SD

Movement	ML Max	ML Impulse	Vertical Max	Vertical Impulse
Lateral Cut	-11.3 ± 3.2	-3.4 ± 0.6*	21.4 ± 3.7	6.1 ± 1.1*
V-Cut	-10.4 ± 3.0	-2.5 ± 0.4	21.2 ± 2.8	5.3 ± 1.0

Note: \* - significantly different between the movements.

Table 2. Average peak adduction (+)/abduction moments (Nm/kg): mean± SD

Movement	Ankle	Knee	Hip
Lateral Cut	-0.64 ± 0.3*	1.03 ± 0.5	2.23 ± 0.7*
V-Cut	-0.56 ± 0.2	0.83 ± 0.3	1.70 ± 0.7

Note: \* - significantly different between the movements.

# EVALUATION OF THE MECHANICS OF AMBULATION WITH STANDARD AND SPRING-LOADED CRUTCHES

Adriana Segura, BS<sup>1</sup> and Stephen J. Piazza, PhD<sup>1,2,3</sup>

Departments of <sup>1</sup>Kinesiology, <sup>2</sup>Mechanical Engineering, and <sup>3</sup>Orthopaedics and Rehabilitation,  
The Pennsylvania State University, University Park, PA, USA  
E-mail: steve-piazza@psu.edu

## INTRODUCTION

Many long-term crutch users prefer axillary (underarm) crutches over elbow crutches because they find that axillary crutches offer increased stability and control during gait. Walking with axillary crutches can be problematic, however, because of complications known to be associated with their sustained use, including crutch palsy and denervation (Raikin and Froimson, 1997; Subramony, 1989). One potential means for modifying injurious forces transmitted between the ground and the body is to fit the crutches with spring-loaded tips.

Pariziale and Daniels (1989) found decreases in both initial and maximum force at the handgrips when using spring-loaded crutches when compared to standard crutches. Shoup (1980) instrumented standard and spring-loaded crutches with strain gauges in order to estimate impact forces, anecdotally reporting reduced forces in some subjects. Neither of these studies considered ground reaction forces or their variation with time throughout the gait cycle.

The purpose of this study was to investigate differences in ground reaction force, impulse, initial rate of force rise, and spatiotemporal variables between standard and spring-loaded crutches.

We hypothesized that use of the spring-loaded crutches will produce lower peak forces, lower impulses, and lower initial rates of force rise than those found for

standard crutches. Additionally, we predicted that walking with spring-loaded crutches causes the user to take a longer stride than would be taken with standard crutches because of a potentially enhanced push-off provided by the springs (Shoup, 1980).

## METHODS

Ten healthy females no known musculo-skeletal problems (21-28 yrs; 167.6-175.3 cm; 54.5–72.7 kg) volunteered as subjects. None had used any type of walking aid within the last six months. All procedures were approved by the Institutional Review Board of The Pennsylvania State University.

Two pairs of standard axillary crutches (Sunrise Medical Guardian Red Dot; Carlsbad, CA) were used. One pair was unaltered, but the other was modified by the addition of helical compression springs (22400 N/m) into the shafts near the crutch tips.

All data were collected in the Biomechanics Laboratory at Penn State University. Five reflective markers were placed on the left crutch and seventeen reflective markers were placed on the crutch user. The motion of the markers was monitored using a 6-camera Eagle motion analysis system (Motion Analysis Corporation; Santa Rosa, CA).

Each subject practiced for 15 minutes with each pair of crutches prior to data collection. Subjects were asked to perform ten good trials with each crutch pair by walking over

the force plate with a single-support swing-through crutch gait at self-selected walking speed. A trial was acceptable if the left crutch struck the force plate and the subject cleared the plate without striking it again with the crutch or either foot.

One-way ANCOVAs ( $\alpha = 0.05$ ) with repeated measures were performed with average walking velocity as a random covariate to investigate the effect of crutch type on each outcome variable of interest.

## RESULTS AND DISCUSSION

Of the spatiotemporal measures examined, significant differences between crutch types were found only for the period of crutch stance phase and the duration for one gait cycle. Both were slightly longer for the spring crutches than for the standard crutches. Our hypothesis that the stride length would be increased when using the spring crutches was not supported.

Contrary to our expectations, the maximum ground reaction forces were slightly higher for spring crutch trials than the standard crutch trials, perhaps due to “bottoming out” of the spring. The maximum rate of force rise over any 10 ms interval was significantly lower for the spring crutch than for the standard crutch (Fig. 1). Lower rates of force rise indicate that during the loading phase, forces are transmitted to the crutch user’s body more slowly which may lessen the risk of overuse injury.

The total impulse over the first 50, 100, and 200 ms were all lower for the spring-loaded crutches than for the standard crutches (Fig. 2). These lower impulses may indicate that the spring crutches are less likely than standard crutches to cause injury.

## SUMMARY/CONCLUSIONS

The lower rates of force rise and lower impulses during the loading phase indicate

that spring crutches may reduce skeletal loads and muscle forces, thus lessening the risk of injury during crutch walking.

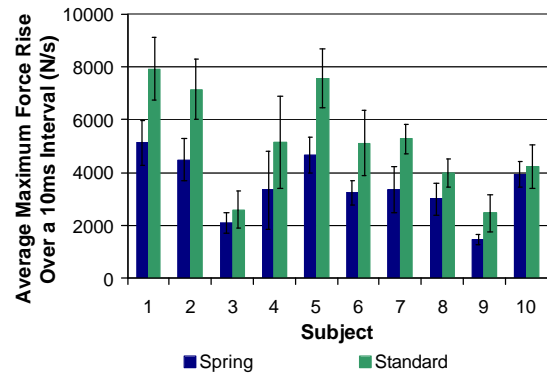


**Figure 1:** The maximum rate of force rise over a 10 ms interval was lower ( $p < 0.0001$ ) for the spring crutches.

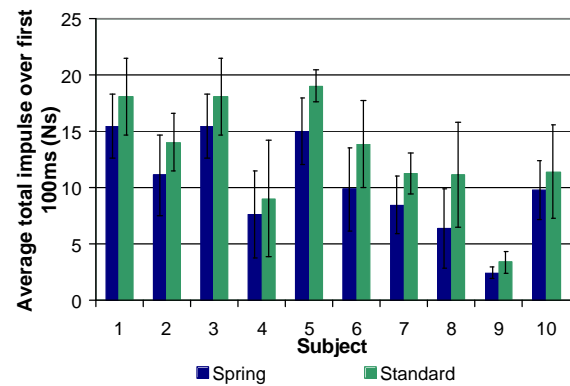


**Figure 2:** The total impulse over the first 100 ms was lower ( $p < 0.0001$ ) for the spring crutches than for the standard crutches.

## REFERENCES

- Pariziale, J., & Daniels, J. (1989). *Am J Phys Med Rehabil*, 68(4), 193-195.
- Raikin, S., Froimson, M. (1997). *Journal of Orthopedic Trauma*, 11(2), 136-137.
- Shoup, T.E., Fletcher, L.S., & Merrill, B.R. (1974). *Journal of Biomechanics*, 7, 11-19.
- Subramony, S.H. (1989). *Electromyogr. clin. Neurophysiol.*, 29(5), 281-285.

## ACKNOWLEDGEMENT

This work was supported by NSF BES-0134217.

# PHASING OF TRUNK MOTION IS CRITICAL FOR THE EFFICACY OF GAIT RETRAINING AIMED TO REDUCE KNEE LOADS

Lars Mündermann<sup>1</sup>, Annegret Mündermann<sup>1,2</sup>, Stefano Corazza<sup>1</sup>, Ajit M.W. Chaudhari<sup>1</sup>, Thomas P. Andriacchi<sup>1,2</sup>

<sup>1</sup> Stanford University, Stanford, CA, USA

<sup>2</sup> Bone and Joint Research Center, VA Palo Alto, Palo Alto, CA  
E-mail: lmuender@stanford.edu Web: biomotion.stanford.edu

## INTRODUCTION

Gait retraining may be a potential non-invasive intervention for patients with knee osteoarthritis (OA). For instance, it has been shown (Mündermann et al. 2006) that the amplitude of trunk sway has a strong negative correlation with the external peak knee adduction moments during walking for healthy subjects. However, it has also been observed that some subjects had very small reductions in the knee adduction moment despite a large increase in trunk sway (Mündermann et al., unpublished data). Mechanically, sway is described not only by the amplitude but also by the frequency and phasing of segment motion. Sway frequency is predetermined by the cadence of walking and will thus not change unless cadence changes. The purpose of this study was to test the hypothesis that both the magnitude and phasing of medio-lateral trunk sway contribute to the reduction in the adduction moment.

## METHODS

Eleven physically active adults (4 female, 7 male; age:  $29.0 \pm 7.0$  yrs; height:  $178.2 \pm 10.1$  cm; mass:  $73.4 \pm 19.7$  kg) participated in this study. None of the subjects had previously been treated for any clinical lower back or lower extremity condition or had any activity-restricting medical or musculoskeletal condition. Subjects performed walking trials at a self-selected normal speed in their own low top,

comfortable walking shoes with a) normal and b) increased medio-lateral trunk motion. Subjects were instructed to shift their trunk more in the medio-lateral direction without changing their walking speed. The external knee adduction moment was calculated from the position of the markers, ground reaction force measurements, and limb segment mass/inertia properties and normalized to body weight and height (% Bw·Ht) (Schipplein and Andriacchi 1991). Medio-lateral trunk motion was calculated as the medio-lateral sway amplitude of the upper trunk segment relative to the vertical axis. Medio-lateral trunk sway phasing was calculated as the time of heel-strike relative to time of peak medial and lateral position of the upper trunk segment. The relationship between the change in first peak knee adduction (KAM), change in medio-lateral trunk sway amplitude (SA) and medio-lateral trunk sway phasing (SP) was tested using multiple regression analysis ( $\alpha = 0.05$ ) using the model equation

$$\Delta KAM = b_0 + b_1 * \Delta SA + b_2 * \cos(SP)$$

where negative (positive) phasing means that heel-strike occurs before (after) the trunk crosses the vertical.

## RESULTS

Increased medio-lateral trunk sway typically resulted in a substantial reduction in the first peak knee adduction moment during walking. On average, subjects increased

their medio-lateral trunk sway by  $7.9 \pm 3.9^\circ$  ( $P = 0.002$ ) with an average phasing of  $82.0 \pm 116.0\text{ms}$  resulting in an average reduction of the first peak knee adduction moment of  $47.1 \pm 31.8\%$  ( $P < 0.001$ ). Subjects with greater increase in medio-lateral trunk sway experienced greater reductions in the first peak knee adduction moment (Figure 1a). Differences in trunk sway amplitude alone explained 28.4% of variability in peak knee adduction moment. 74.5% of variability in peak knee adduction moment was explained by both differences in trunk sway amplitude and trunk sway phasing (Figure 1b;  $P < 0.001$ ). The optimum phasing occurred at 0.201 radians which corresponds to approximately 33ms after heel-strike. Subjects walked at similar speeds for both conditions (normal trunk sway:  $1.46 \pm 0.13\text{m/s}$ ; increased trunk sway:  $1.47 \pm 0.16\text{m/s}$ ;  $P > 0.999$ ).

## DISCUSSION

The results of this study showed that both the magnitude and phasing of the medial-lateral shift contribute to the reduction in the adduction moment. The role of trunk sway phasing appears to be more important than trunk sway amplitude. Thus, a greater increase in trunk sway may not be reflected in a reduced knee adduction moment if the trunk is shifted to the ipsilateral side too early or too late. The results also suggest that there is an optimal phasing (trunk position at heel strike) for maximum reduction of the adduction moment. Subjects with a phasing of around 50ms (upper trunk segment vertical or slightly passed vertical at heel-strike) experienced the greatest reductions in the first peak knee adduction moment. Therefore, care should be taken when introducing increased trunk sway as gait retraining for patients with knee OA as both sway amplitude and correct sway phasing are important.

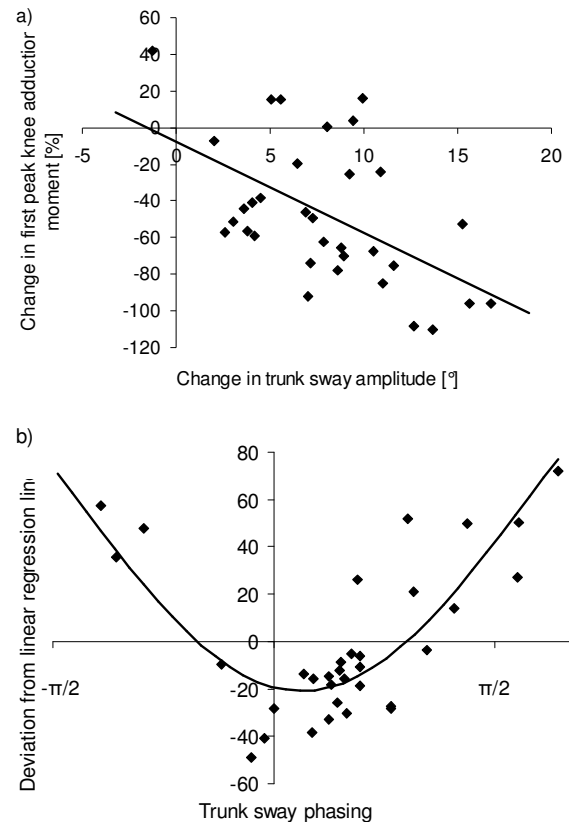


Figure 1: Contribution of a) change in trunk sway amplitude and b) trunk sway phasing to variability in the change in first peak knee adduction moment.

In summary, the results of this study showed that increased medio-lateral trunk sway may be a powerful non-invasive intervention with the goal to reduce medial compartment loads at the knee during walking. However, correct phasing of trunk sway is critical for the efficacy of this method of gait retraining.

## REFERENCES

- Mündermann L. et al. (2006) *Trans Orthop Res Soc*, **52**, 170.  
 Schipplein, O.D., Andriacchi, T.P. (1991) *J Ortho Res*, **9**, 113-119.

## ACKNOWLEDGEMENTS

NSF grant # 03225715.

# MECHANICAL CHARACTERIZATION OF SUBRUPTURE FATIGUE DAMAGE IN TENDONS

David T. Fung, Vincent M. Wang, Jennifer L. Elderbroom, Karl J. Jepsen, Mitchell B. Schaffler and Evan L. Flatow

Leni and Peter May Department of Orthopaedics, Mount Sinai School of Medicine, New York, NY; E-mail: david.fung@mssm.edu

## INTRODUCTION

Despite the high prevalence of tendon injuries, the etiology of tendon rupture is poorly understood. Degeneration due to cumulative microtrauma resulting from overuse has been widely discussed as a major contributor to tendon failure. However, existing biomechanical models of fatigue have largely focused on the relationship between the applied stress and the number of cycles to failure (Wang et al, 1995), identifying stiffness loss as an index of damage. The purpose of the present study was to assess alternate parameters as indices of mechanistic, sub-rupture changes that may underlie the tendon fatigue *process*.

## METHODS

Flexor digitorum longus (N=18) tendons from adult female Sprague-Dawley rats were dissected immediately following euthanasia and underwent fatigue loading in a PBS bath maintained at 39°C. The ends of the tendons were clamped using sandpaper-covered plates. The upper and lower plates were secured to custom grips that were aligned with the test actuator (Instron 8872). Tensile force was measured using a 50-lb load cell attached between the grips and the actuator.

Each sample was allowed to equilibrate to the PBS bath, preloaded to establish its initial length, and loaded cyclically according to a novel damage accumulation protocol (Lee et al, 2006) which consisted of, sequentially, a preconditioning period,

Diagnostic test I (D1), Damage Induction phase, Diagnostic test II (D2), Recovery phase, and Diagnostic test III (D3) (Fig. 1). The tendon was cyclically loaded at 20% maximum load for 300 cycles in the preconditioning period and for 120 cycles each in D1, D2 and D3. In the Damage Induction phase, six tendons were loaded at ~50% maximum load to a mechanical endpoint of 20% decline in secant stiffness, while the remaining twelve tendons were loaded to endpoint grip-to-grip strain of 15% or less. The tendon was unloaded for 4500 sec in the Recovery phase to allow transient effects of the cyclic loading to dissipate (Jepsen and Davy, 1997). Secant stiffness ( $S_1, S_2, S_3$ ), elongation at peak cyclic load ( $\epsilon_1, \epsilon_2, \epsilon_3$ ) relative to the initial length, and hysteresis ( $E_1, E_2, E_3$ ) were determined as the mean of the last five cycles of D1 to characterize the tendon in the pre-fatigue state, D2 in the post-fatigue state, and D3 in the post-recovery state, respectively.

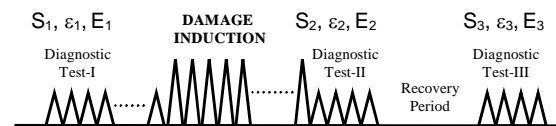


**Figure 1.** Schematic diagram of the loading protocol.

## RESULTS AND DISCUSSION

Tendons were grouped based on their endpoint strain observed during Damage Induction. In tendons that were loaded to 'high' (>11% strain, N=6) and 'mid' (9%-11% strain, N=5) fatigue levels, hysteresis ( $E_1 \rightarrow E_2$ ) ( $p \leq 0.07$ ) increased and stiffness

**Table 1:** Changes in stiffness (S), elongation ( $\epsilon$ ) and hysteresis (E) from D1→D2 (mean±SD). \*  $p \leq 0.05$ ; #  $p = 0.07$ .

	'low' fatigue	'mid' fatigue	'high' fatigue
$S_1 \rightarrow S_2$ (%)	-6.6±6.6	-13.8±14.5 <sup>#</sup>	-11.1±8.4 <sup>*</sup>
$\epsilon_1 \rightarrow \epsilon_2$ ( $\times 10^{-3}$ )	+12.3±8.1 <sup>*</sup>	+34.0±18.4 <sup>*</sup>	+49.3±30.7 <sup>*</sup>
$E_1 \rightarrow E_2$ (%)	+2.2±5.7	+26.0±29.8 <sup>#</sup>	+30.0±27.1 <sup>*</sup>

( $S_1 \rightarrow S_2$ ) ( $p \leq 0.07$ ) decreased following Damage Induction (Table 1), and did not change significantly following Recovery ( $E_2 \rightarrow E_3$ ,  $S_2 \rightarrow S_3$ ). In tendons that were loaded to a 'low' level of fatigue (<9% strain), both hysteresis and stiffness did not change significantly from one diagnostic test to the next. Increases in tendon elongation ( $\epsilon_1 \rightarrow \epsilon_2$ ) were consistent with their respective fatigue levels (from low to high), but did not show a significant amount of recovery ( $\epsilon_2 \rightarrow \epsilon_3$ ) at any fatigue level.

In the tendons that were loaded to an endpoint of 20% secant stiffness loss, post-fatigue stiffness declined by  $21.2 \pm 4.0\%$  ( $S_1 \rightarrow S_2$ ) ( $p < 0.001$ ), indicating that the dynamic assessment of stiffness during Damage Induction in the loading protocol accurately characterized the state of tissue fatigue of the tendon. Changes in strain and stiffness among these tendons during the Damage Induction phase exhibited consistent patterns (Fig. 2). Stiffness remained constant before it declined rapidly,

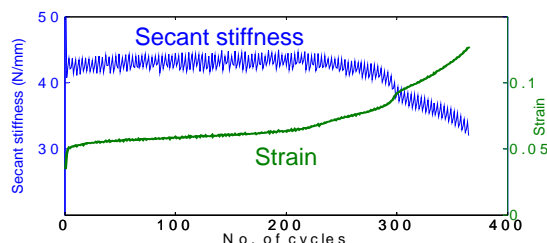


**Figure 2.** Typical stiffness and strain behavior seen in Damage Induction.

while strain concurrently showed a gradual followed by more rapid rate of increase.

Mechanical characterization of the tendons during Damage Induction and all diagnostic tests is consistent with a fatigue mechanism by which loading is supported by shorter fibers initially and redistributes to the lesser-loaded longer fibers as the loading exceeds the shorter fibers' capacity. These events, which do not appear to cause stiffness loss, are characterized by increases in elongation. Continued loading leads to the initiation and accumulation of microtears, resulting in stiffness loss, which is also seen in bone and other composite material resulting from the formation of small voids during fatigue. Such damage in tendons altered the viscous response, as reflected by the coupling of changes between stiffness and hysteresis at increasing levels of fatigue. Histological evaluation on these tendons is underway to examine the morphological manifestations of mechanical fatigue and damage.

## SUMMARY/CONCLUSIONS

The evaluation of mechanical parameters at various stages of tendon fatigue showed that a low level of fatigue is characterized by changes in the tendon's elongation without compromise in the stiffness. The varying responses of elongation, stiffness and hysteresis at increasing levels of fatigue reflect the mechanistic changes that may underlie the *process* by which the tendon degenerates from subrupture loads.

## REFERENCES

- Jepsen KJ, Davy DT (1997). *J Biomech*, **30**(9), 891-4.  
 Lee H et al (2006). *Trans ORS*, **31**, no. 1058.  
 Wang XT, Ker RF (1995). *J Exp Biol*, **198**, 831-45.

## ACKNOWLEDGEMENTS

NIH AR052743 (Flatow)

# AN INVESTIGATION OF SOFT TISSUE ARTIFACT DURING WALKING: TRANSLATION AND ROTATION OF SKIN MARKERS

Bo Gao, Bryan Conrad, Naiquan (Nigel) Zheng

University of Florida, Gainesville, FL, USA  
E-mail: nigelz@ufl.edu Web: www.ortho.ufl.edu/BMAL

## INTRODUCTION

Soft tissue artifact (STA), caused by movement of muscle and skin with respect to the bone underneath, has been proved to be a major source of error when the optoelectronic stereophotogrammetry technique is used in body movement studies (Alberto *et al.*, 2005). Most previous studies of STA focused on skin-marker translation but did not consider marker rotation.

However, a marker is normally more than 10 mm over the skin and attached to an area greater than 3 cm<sup>2</sup>. The marker has a rotational movement relative to the bone's coordinate system. Consideration of this rotational component of STA is essential when using marker rigid-arrays (such as marker pairs or marker triads) because these rigid-arrays can reduce the translation component of STA but cannot reduce the rotation component.

Although STA is considered as a subject-dependent artifact, we hypothesize that STA is also joint movement-dependent. In this study both translation and rotation of skin markers during walking were investigated.

## METHODS

Eight subjects (5 males and 3 females) were tested during level walking using an IRB approved protocol. An 11-camera motion analysis system was used (Motion Analysis Co., CA). Seven single markers and 4 marker-triads were placed on both thighs; 6 single markers and 4 marker-triads were put on the shanks. Their positions are shown in Fig.1. Marker-triads had same attaching areas as single markers so their center points could also serve as single markers.

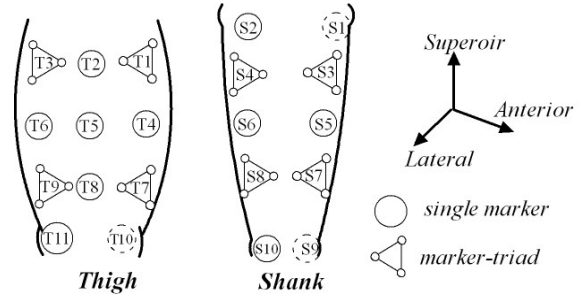


**Fig.1** Marker placements on thigh and shank from anterolateral views.

Motions of femur and tibia were calculated using point cluster technique (Andriacchi *et al.*, 1998). Every marker's translations in bone's coordinate system was calculated by

$$p_i^{trans} = [R]^{-1} (\bar{p}_i^g - \vec{O}) - \bar{p}_i^l,$$

where  $\vec{O}$  and  $[R]$  are the origin and the rotation matrix of bone's coordinate system, and  $\bar{p}_i^g$  and  $\bar{p}_i^l$  are the skin marker's global and local positions. Every triad's rotation relative to the bone underneath was obtained by

$$[R]_i^{rotation} = [R]^{-1} \times [R]_i,$$

where  $[R]_i$  represents the rotation matrix of the triad. The repeated measures ANOVA was used to test the differences (SPSS Inc., Chicago, IL, USA).

## RESULTS AND DISCUSSION

The translation and rotation of each marker or triad on the 16 legs during walking were analyzed. We found that subject-independent patterns of translation and/or rotation could be identified easily for each marker or triad. As an example, Fig.2 shows the means and standard deviations of triad T1's translation and rotation (N=16). The translation and rotation of STA were

dependent on the adjacent joint positions (position in gait cycle). However, there were significant difference of translation and/or rotation among markers and/or triads ( $p < 0.01$ ).

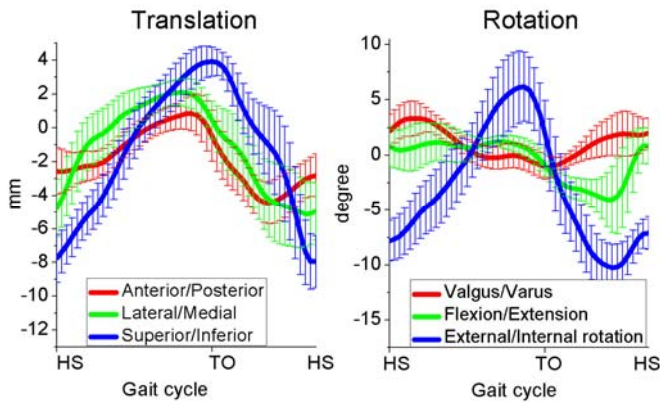


**Fig.2** Means (SD) of triad T1's translation and rotation.

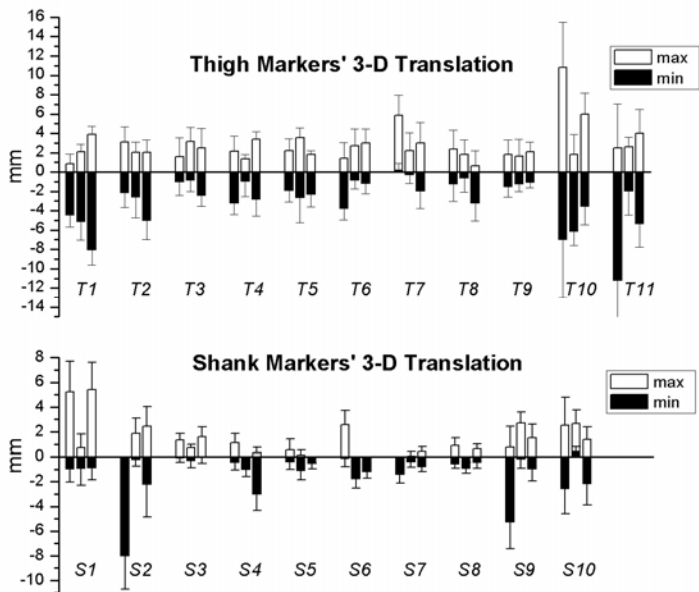


**Fig.3** Markers' translations. From left to right: anterior /posterior, lateral/medial, superior/inferior.

Figure 3 shows the maximum and minimum translations in gait cycle for each marker, with much smaller standard deviations than previously published data (Rita S. *et al.* 2005). Markers on the epicondyles had the greatest translation artifact than other markers. This is due to greater skin

movement over the epicondyles. Figure 4 shows the three rotations of each triad. Rotations could be up to 10 degrees for the thigh triads. Overall, the markers on the thigh had greater translation and rotation STA ( $p < 0.01$ ).

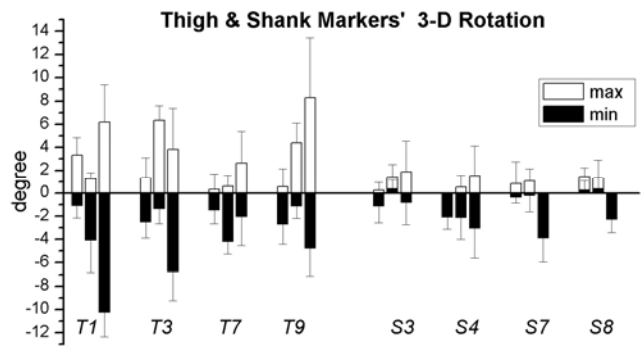


**Fig.4** Triads' rotation. From left to right: valgus/varus, flexion /extension, external/internal rotation.

## CONCLUSIONS

Though STA is often considered subject-dependent, our study shows both translation and rotation of skin markers were location-specific and related to the adjacent joint angles. The patterns of STA translation and rotation were similar for each subject. Thigh markers had greater translation and rotation STA than shank markers. The translation STA had similar values with smaller standard deviations when comparing with published data. Markers' rotational STA are reported here for the first time and the results suggest that rotational STA can not be removed or reduced by using extended wand markers or marker rigid-arrays normally used to calculate the rotations of a segment and joint.

## REFERENCES

- Alberto L. *et al.* (2005). *Gait and Posture*, **21**, 212–225.
- Andriacchi T.P. *et al.* (1998). *J Biomech Eng*, **120**, 743–9.
- Rita S. *et al.* (2005). *Clinical Biomechanics*, **20**, 320–329.

# THE EFFECT OF FATIGUE ON MOVEMENT VARIABILITY DURING RUNNING

Dimitrios Katsavelis, Anastasia Kyvelidou, and Nicholas Stergiou  
HPER Biomechanics Laboratory, University of Nebraska, Omaha, NE, USA  
E-mail: [nstergiou@mail.unomaha.edu](mailto:nstergiou@mail.unomaha.edu) Web: [www.unocoe.unomaha.edu/hper/bio/home.htm](http://www.unocoe.unomaha.edu/hper/bio/home.htm)

## INTRODUCTION

The effect of fatigue on running performance has been investigated in the past for various sport activities, including running (Williams *et al.*, 1991). It has been proposed that fatigue can diminish the ability of the musculoskeletal system to absorb shock and thus, increase susceptibility to injury (Verbitsky *et al.*, 1998). However, the exact mechanisms that underline such a relationship remain unclear. Recently, the relationship between variability and running injuries has received increased attention (Hamill *et al.*, 1999; Stergiou *et al.*, 2001). Changes in variability in running mechanics have been suggested to relate to susceptibility to running injuries (Stergiou *et al.*, 2001). It has also been speculated that a certain amount of inherent variability can provide the system with certain flexibility to avoid injuries (Dufek, 2002; James, 2004).

Taking the aforementioned findings into consideration, we can theorize that changes in the variability of running mechanics, as a result of fatigue, can be associated with increased susceptibility to running injuries. This may be one of the mechanisms that underline the relationship between fatigue and running injuries. However, to explore this hypothesis a first and crucial step is to determine the effects of fatigue on the variability of running mechanics. Therefore, the purpose of this study was to examine the effects of fatigue on kinematic variability during running. We hypothesized that fatigue will affect variability in the system.

## METHODS

Ten healthy active college age females participated in a two-session experiment. The first session consisted of the determination of their ventilation threshold (VT) speed as well as their self-selected pace (SSP) (Table 1). The VT speed was added in the experimental design because it is a tempo that runners seem to prefer in order to improve their strength speed and stamina. In the second session, the subjects underwent a graded exercise test (GXT) to exhaustion (Table 1). In this latter session, three-dimensional lower extremity kinematics were acquired with a high-speed optical capture system (60 Hz) while the subjects ran on a treadmill for at least two minutes. Lower extremity kinematics were collected before and after the application of fatigue at both the SSP and VT speed. Speed order was randomized. Joint angle variability was determined from the kinematics and was evaluated with a linear (coefficient of variation; CV) approach. One minute of continuous running – comprising of approximately 78 to 90 strides – was analyzed. Minimum and maximum joint angles and range of motion (ROM) for each stride were identified and used to calculate the CV values for all strides evaluated. Dependent t-tests were used to identify significant differences between pre- and post-fatigue runs.

## RESULTS AND DISCUSSION

The results revealed significant increases for the knee and the hip flexion CV values at the VT speed (knee flexion,  $P = 0.021$ ; hip

flexion,  $P = 0.020$ ), as well as an increase in the knee flexion CV values at the SSP speed ( $P = 0.031$ ). These results are in accordance with our hypothesis. The location of the occurrence of the identified differences can possibly be explained by considering the size of the muscle involvement, since at the hip and the knee there are larger muscle groups that are contributing to running.

It also seems that the higher speed – VT speed – induced a larger number of significant differences. This is probably expected since the subjects were running at control speed right after a maximal effort protocol. Furthermore, all differences were related with joint flexion which is directly associated with shock absorption during running. This provides some support for connecting fatigue with diminished ability for shock absorption through changes in variability. Possibly the increased variability reflects uncertainty in the neuromuscular system in selecting the proper movement pattern. This may be a result of lactic acid accumulation in the muscle.

## SUMMARY/CONCLUSIONS

The results of the present study showed that fatigue can affect joint kinematic variability during running, since a number of increases were found. However, such results need to be further substantiated by using runners with specific musculoskeletal problems. In

addition, the nature of these variability changes needs to be further investigated. For example, it is possible that they reflect an increase of noise in the system. It is also possible that our findings are due to a deterioration of the long range correlations that have been found during running for stride-to-stride variability (Jordan et al, 2005). These long range correlations have been associated with neuromuscular health (Hausdorff *et al.*, 2003). Thus, it is possible that their deterioration due to fatigue will lead to increased susceptibility to running injuries. However, this hypothesis needs to be further investigated.

## REFERENCES

- Dufek, J.S. (2002). *ACSM's Health and Fitness Journal*, **6**, 18-23.
- Hamill, J. *et al.* (1999). *Clin Biomech*, **14**, 297-308.
- Hausdorff, J.M. *et al.* (2003). *J Geriatr Psychiatry Neurol*, **16**, 53-58.
- James, C.R. (2004). In: *Innovative Analyses of Human Movement*, Human Kinetics.
- Jordan, K. *et al.* (2005). *Gait Posture*, in press.
- Stergiou, N. *et al.* (2001). *Clin Biomech*, **16**, 213-221.
- Williams, K.R., Snow, R., Arguss, C. (1991). *Int J Sport Biomech*, **7**, 138-162.
- Verbitsky, O. *et al.* (1998). *J Appl Biomech*, **14**, 300-311.

**Table 1:** Physical measures for the ten female recreational runners (mean± SD).

	<b>Age (yr)</b>	<b>BW (kg)</b>	<b>Height (m)</b>	<b>SSP (m/s)</b>	<b>VT speed (m/s)</b>	<b>GXT (sec)</b>
Mean (SD)	20(±1)	62.1(±7)	1.68(±.9)	2.5(±.3)	3.0(±.3)	897(±201)

# OFF-AXIS LOADS CAUSE FAILURE OF THE DISTAL RADIUS AT LOWER MAGNITUDES THAN AXIAL LOADS: A FINITE ELEMENT ANALYSIS

Karen L. Troy<sup>1</sup> and Mark D. Grabiner<sup>1</sup>  
<sup>1</sup>University Illinois at Chicago, Chicago, IL USA  
E-mail: klreed@uic.edu

## INTRODUCTION

Distal radius fractures are among the most common fall-related injuries in older women. Numerous studies have quantified upper extremity fall biomechanics with the goal of identifying possible interventions to reduce the peak force on the wrists, thereby reducing the number of fractures [1-3]. Fracture initiation depends both on the force applied to the bone and upon the strength of the bone itself; thus, poor bone quality has been implicated as a factor in distal radius fractures. Generally, an intervention to improve bone quality (such as anti-resorptive therapy) is considered successful if bone mineral density (BMD) can be increased by 2-4% [4].

Cadaver and finite element studies have previously quantified the force required to cause a distal radius fracture [5]. To date, however, only simple axial loads on the radius have been considered. Because most falls onto the hands result in off-axis loads, we considered the possibility that a combination of loading modes would significantly influence the fracture strength of the distal radius. Here, we used a validated finite element model of the distal radius, scaphoid, and lunate, to explore the effects of loading direction and changes in BMD on predicted fracture strength.

## METHODS

The right wrist of a 53 year old female volunteer was imaged with computed tomography. Geometrical and density data for the radius, scaphoid, and lunate were extracted using custom-written software (Matlab 7.01) and a finite element model was built using ANSYS 10.0.

Bone material properties were assigned to each element based on the average Hounsfield value (HU) for those voxels located in the vicinity of the element using the following equations [6-8]:

$$\text{Cortical: } \rho = 1.09 + 0.000445 * \text{HU} \\ E = 2065 * \rho^{3.09}$$

$$\text{Cancellous: } \rho = 0.0012 * \text{HU} + 0.17 \\ E = 1904 * \rho^{1.64}$$

A cut-off value of 672 HU was assigned to distinguish cortical (HU>672) from cancellous (HU<672) bone. A 2.5 mm-thick layer of cartilage was created on the distal articular surface of the radius. The ligaments that directly attach the radius, scaphoid, and lunate were included in the model as non-linear springs (Figure 1).

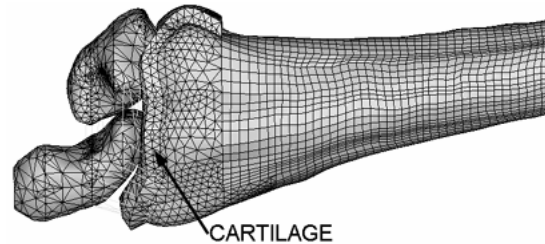


**Figure 1** Dorsal view of the FE mesh

A total of 26 models were run in which bone density and loading direction were varied. In each model a ramped 3000 N load was applied to the radius via the centroids of the scaphoid (1800 N) and lunate (1200 N). Series 1 consisted of all models to which an axial load was applied. BMD was changed from its baseline value in either the cancellous bone only, the cortical bone only, or all bone of the radius, by -4%, -2%, +2%, or +4%. Combined with a model in which no change of BMD was simulated, this resulted in 13 total simulations. Series 2

was identical to Series 1 except that the loading direction was changed to simulate a worst-case off-axis load, described by a unit vector  $[-0.1385 \ -0.3562 \ -0.9241]$  in the [lateral, volar, axial] directions [9]. (A negative axial load indicates the force is directed from the wrist towards the elbow).

For each simulation, each element's first and third principal stress ( $s_1$  and  $s_3$ ) were recorded during the ramped load, and element failure was determined using the Mohr-Coulomb criterion of:

$$s_1/\sigma_{ty} - s_3/\sigma_{cy} \geq 1 \quad [10]$$

where  $\sigma_{ty}$  and  $\sigma_{cy}$  are the material's tensile and compressive yield stresses, respectively. Once element failure was determined for a given load, a custom written algorithm (Matlab 7.01) determined the total volume of contiguous failed elements. A crack large enough to propagate was assumed to have developed after a total volume of  $350\text{mm}^3$  failed [11].

## RESULTS AND DISCUSSION

Loading direction had a strong influence on predicted fracture strength. For the unchanged (baseline) BMD model, an axial load caused fracture at 2752 N. In contrast, the off-axis load applied to the same unchanged BMD model predicted fracture at 1448N (Figure 2).

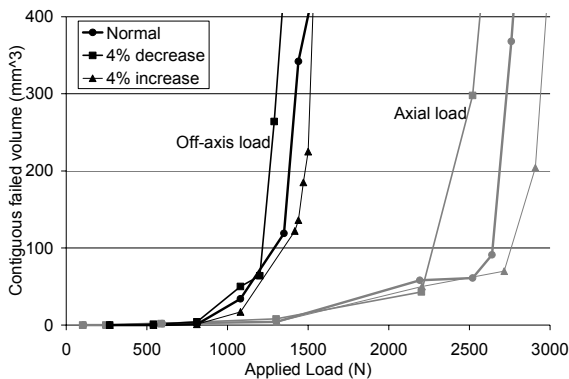


**Figure 2** Load versus failed contiguous volume for on- and off-axis simulations. BMD changes for all bone (cortical and cancellous) are shown. Fracture was assumed at  $350\text{mm}^3$ , however fracture load appears to be somewhat insensitive to the specific volume cut-off.

Changes in BMD caused small but nonlinear changes in predicted fracture strength. Increasing or decreasing cortical bone density did not make a large difference in fracture strength compared to changes in either cancellous or all bone (Figure 3).

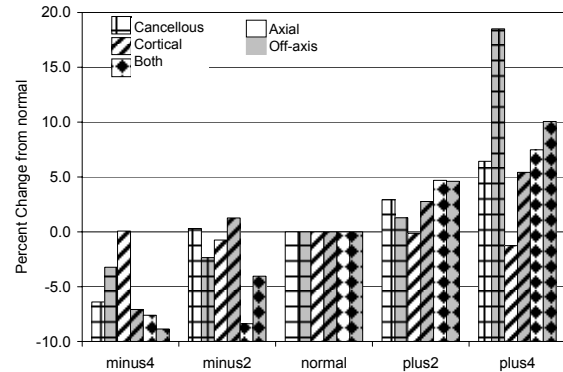


**Figure 3** Percent change in fracture strength compared to the normal BMD values after changes in cancellous, cortical, or all bone.

## SUMMARY/CONCLUSIONS

Loading direction had a strong effect on predicted fracture strength. In contrast, systematic changes in bone mineral density had a much smaller affect on fracture strength. It is possible that changes in BMD in more structurally important locations, such as those that may be initiated through functional loading or through local application of bone growth factors, may cause more substantial enhancements in bone strength. Just as it is possible for people to minimize peak ground impact forces on the hands during a fall, it may be possible to voluntarily influence the direction of ground impact on the wrist.

## REFERENCES

- [1] DeGoede, K.M. and J.A. Ashton-Miller, J Biomech, 2002. 35 p. 843-8.
- [2] Chou, P.H., et al., Clin Biomech, 2001. 16 p. 888-94.
- [3] Chiu, J. and S.N. Robinovitch, J Biomech, 1998. 31 p. 1169-76.
- [4] Liberman UA et al. N Engl J Med 1995.333 p 1437-1443
- [5] Pistoia, W., et al., Bone, 2002. 30 p. 842-8.
- [6] Lotz, J.C. et al., J Comput Assist Tomogr, 1990. 14 p. 107-14.
- [7] Wirtz, D.C., et al. J Biomech, 2000. 33 p. 1325-30.
- [8] Snyder, S.M. and E. Schneider J Orthop Res, 1991. 9 p. 422-31.
- [9] Troy, KL and MD Grabiner. *ISB Proc.* 2005. Cleveland, OH
- [10] Keyak JHet al. J Biomech 1998.31 p125-133
- [11] Keyak JH and Rossi SA. J Biomech 2000.33 p209-214

## ACKNOWLEDGEMENTS

Funding source: F32 AG25619-02 (KLT)

# ALTERATIONS IN MONO- AND BI-ARTICULAR MUSCLE ACTIVITY PATTERNS AFTER LEARNING TO DIRECT PEDAL FORCES

Christopher J. Hasson, Richard E.A. Van Emmerik, and Graham E. Caldwell  
Biomechanics & Motor Control Laboratories, University of Massachusetts, Amherst, MA  
cjhasson@excsci.umass.edu

## INTRODUCTION

Mono- and bi-articular muscles may have separate roles in tasks where the direction of an external reaction force must be controlled. Previously, we reported that with training subjects could improve their ability to direct pedal forces in a specified direction, and that this improvement was accompanied by changes in pedal, crank, and joint kinetics (Hasson et al., 2006a,b). Changes in magnitude and timing of joint moments were found, with the most important at the knee. The present report focuses on the changes in muscle activity patterns from pre- to post-learning. Because biarticular muscles may have a unique role in “tuning” joint moments to control the applied force direction, we hypothesized that activity of the biarticular muscles would demonstrate more learning-related changes than the monoarticulars.

## METHODS

Nine male subjects (age:  $25 \pm 4$  yrs; mass:  $83 \pm 13$  kg; height:  $1.77 \pm 0.07$  m) performed one-legged cycling on a bicycle mounted on a computerized ergometer and instrumented for pedal kinematics and kinetics. Subjects were instructed to direct their pedal forces perpendicular to the crank arm (target force direction), and to maintain a constant pedaling speed. Real-time visual feedback of both applied and target force direction and crank angular velocity was displayed to the subject. Subjects performed an initial baseline trial without the feedback, followed by 16 trials with the real-time feedback. Each trial consisted of 30 s of pedaling using only the left leg after a 15 s warm-up. Task performance was characterized by the RMS

error between the applied and target force directions, and it was shown that subjects significantly reduced the error over these trials (see Hasson et al., [2006a,b] for more details).

Surface electromyographic (EMG) data were collected at 1 KHz from three monoarticular (tibialis anterior [TA], soleus [SO], and vastus lateralis [VL]), and three biarticular (rectus femoris [RF], semitendinosus [HAM], and medial gastrocnemius [GA]) muscles of the left leg. For each muscle, an EMG linear envelope was computed using bias removal, rectification, and smoothing with a 6 Hz low-pass Butterworth filter, and expressed as a function of crank angle using cubic spline interpolation. For each subject and muscle, the EMG linear envelopes were normalized to their maximum values.

In pilot work, the timing of muscle activity was determined by a traditional threshold detection method (Hasson et al., 2004). However, this method could not characterize some of the changes in coordination that were observed (e.g. some muscles remained active for the entire crank cycle). A more advanced method of evaluating changes in coordination of multiple muscles was desired; the structural EMG analysis method of Jansen et al. (2003) was used. For each crank cycle, two 3-dimensional EMG trajectories were defined: a monoarticular trajectory from the TA, SO, and VL, and a biarticular trajectory from GA, RF, and HAM. For each 30 s trial, a similarity matrix was computed to measure the common structure between all cycles for each

trajectory. A clustering algorithm was used to select a primary template (PT), which is a representative cycle that accounts for most of the variability in the data. For each subject, the similarity between the pre-learning baseline PT and the last trial PT (post) for the monoarticular muscles was compared. The same procedure was used to compare the pre- and post-training PTs for the biarticular muscles. A paired t-test was used to determine if the mono- and bi-articular similarity scores were significantly different from each other.

## RESULTS AND DISCUSSION

PTs for one subject, decomposed into their constituent muscle linear envelopes, are illustrated in Fig. 1.

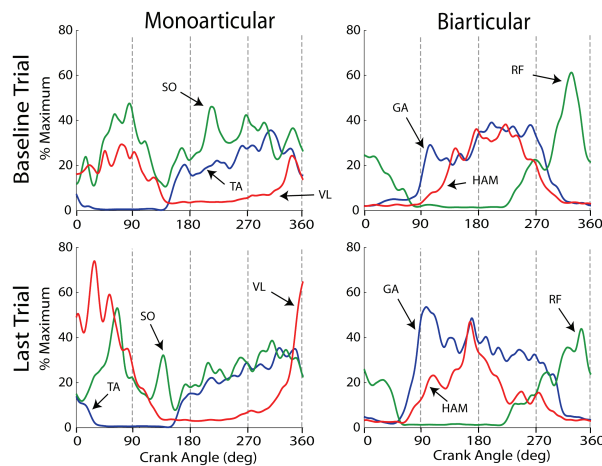


Fig. 1. Decomposed PTs for one subject.  $0^\circ =$  top-dead-center.

Each PT chosen represented the majority of cycles ( $>60\%$ ) within each trial for each subject (Table 1). The similarity scores for both the mono- and bi-articular muscles were different from zero ( $p < 0.05$ ), indicating that the activity of both groups of muscles changed from pre- to post-learning. However, the similarity measures for the

mono- and bi-articular PTs were not significantly different from each other ( $p > 0.05$ ; Table 1). There was a large amount of variability, with some subjects showing more change in the monoarticular PTs and others showing more change in the biarticular PTs. This may indicate that subjects used different strategies for learning the task. Studying changes throughout the entire learning process may lead to further insight. In addition, other multidimensional analysis techniques, such as recurrence quantification analysis, may be useful in discovering more about the nature of the changes in coordination that occurred over the learning process.

## SUMMARY

The present analysis showed that the PTs of both mono- and bi-articular muscle activity patterns changed after learning a force-directing task. However, the amount of change was not significantly different between mono- and bi-articular trajectories. This may be due to the relatively large amount of between-subjects variability. Further analysis on changes in individual subjects as well as across the entire learning of the task may be needed before the roles of mono- and bi-articular muscles can be fully elucidated.

## REFERENCES

- Hasson CJ, et al. (2004) CSB 13<sup>th</sup> Meeting.
- Hasson CJ, et al. (2006a) CSB 14<sup>th</sup> Meeting.
- Hasson CJ, et al. (2006b) ASB 30<sup>th</sup> Meeting.
- Jansen BH, et al. (2003) IEEE Trans Neural Syst Rehabil Eng 11:294-300.

## ACKNOWLEDGEMENTS

This work was supported by a graduate student grant-in-aid from the American Society of Biomechanics.

Table 1. Statistics (Mean  $\pm$  Standard Deviation).

Measure	Monoarticular		Biarticular	
	Pre	Post	Pre	Post
Average % Cycles Matching PTs	60.0 $\pm$ 5.8	66.0 $\pm$ 6.8	60.1 $\pm$ 4.6	61.3 $\pm$ 11.7
Similarity Between PTs (pre vs. post) <sup>†</sup>	82.0 $\pm$ 68.3		53.2 $\pm$ 45.9	

<sup>†</sup>A similarity value of zero would be a perfect match.

# THE USE OF ACCELERATION AND EXTERNAL FORCES TO ESTIMATE BONE STRAIN

W. Brent Edwards<sup>1</sup>, Stacey A. Meardon<sup>1</sup>, Erin D. Ward<sup>2</sup>, and Timothy R. Derrick<sup>1</sup>

<sup>1</sup> Iowa State University, Ames, IA, USA

<sup>2</sup> Central Iowa Foot Clinic, Perry, IA, USA

E-mail: edwards9@iastate.edu Web: www.hhp.hs.iastate.edu

## INTRODUCTION

Mechanical loading from repetitive impacts during locomotion has the potential to stimulate bone adaptation and contribute to overuse injury. Although bone strain can be directly measured using strain gages (Milgrom et al., 2000), this technique requires invasive surgical procedures. Whalen et al., (1988) used the ground reaction force (GRF) as an indirect measure of bone strain, but the collection of GRF is only practical in a laboratory setting.

Accelerometry may be a more convenient means for quantifying bone strain, as it allows for the continuous measurement of impacts in a non-invasive and portable manner.

The purpose of this study was to determine if GRF and tibial accelerations can be used as a measure of bone strain during impact activity.

## METHODS

Four cadaver feet, with tibia/fibula osteotomy 20 cm above the malleoli were subjected to impact force loading. Each foot was thawed at room temperature and an axial strain gage (Vishay Micro-Measurements, CeA-06-06UW-350, Raleigh, NC) was mounted to the anterior-medial tibial bone 10 cm above the medial malleolus. A uni-axial piezoelectric accelerometer (PCB Piezoelectronics, Model 353B, Depew, NY) was also mounted to the skin of the distal anterior-medial tibia 2-3

cm above the medial malleolus. An Exeter impact testing system (Exeter Research, Inc, Exeter, NH) was placed on top of four telescopic jacks and situated over a force platform (AMTI, Watertown, MA). An intra-medullary rod was used to connect the proximal end of the tibia to a custom made missile head at the distal end of the impacting shaft. The two anterior jacks were raised slightly to direct some of the impact in the posterior direction. Ankle angle was controlled prior to impact by applying tension to the anterior tibialis tendon.

Each foot was dropped six times during four conditions, consisting of two separate drop heights (3 and 5 cm) with two different masses (9 and 11 kg). The 3 cm drops were used to simulate impacts during walking, while the 5 cm drops were used to simulate impacts during running. Vertical ground reaction force (vGRF), tibial acceleration (TA) and bone strain (BS) data were collected concurrently at a sampling frequency of 3600 Hz (Figure 1).

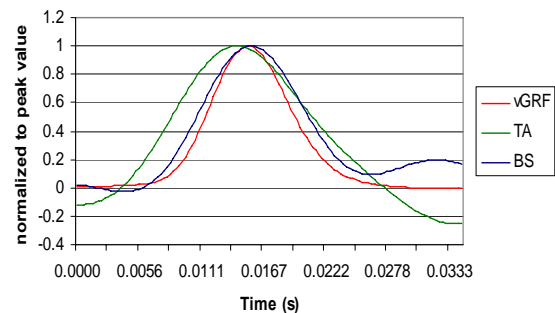


**Figure 1:** Typical vGRF, TA, and BS normalized to peak value.

A 2 x 2 factorial repeated measure ANOVA with Tukey's post hoc test was used to examine the effects of impact mass and drop height on peak vGRF, TA, and BS ( $p < 0.05$ ).

## RESULTS AND DISCUSSION

All main effects of impact mass and drop height were significant for each variable (Table 1). Peak vGRF behaved in a similar manner to peak BS during impacts. Increased mass and increased drop height caused both vGRF and BS to increase (Figure 2a). Peak TA also behaved in a similar manner to peak BS with increased drop height, however increased impact mass had the opposite affect. Increasing the impact mass caused peak TA to decrease (Figure 2b).

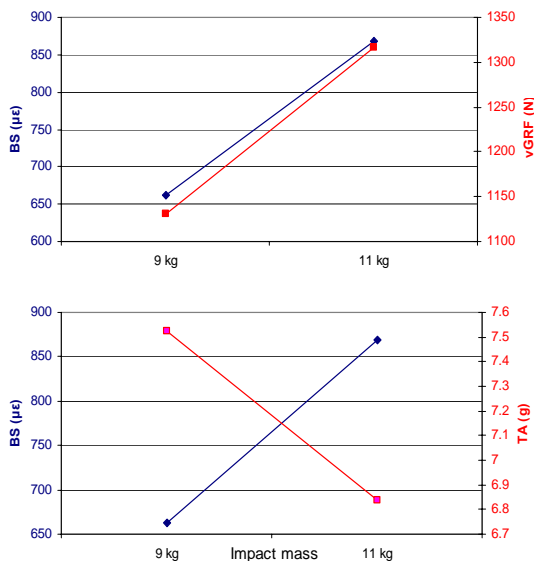


**Figure 2:** Peak BS vs. vGRF (a) and peak BS vs. TA (b) averaged over drop heights.

Larger masses require greater forces to accelerate. The increased mass condition

was associated with a greater force, but this was not enough to produce a subsequent increase in TA. During human walking and running, the mass that responds to an impact force is typically not the mass of the entire body. Rather only a portion of the lower extremity is affected. This portion is called the effective mass and it can be altered by changing the lower extremity geometry at contact (Derrick, 2004). For instance, increasing the knee flexion angle at heel contact has been shown to alter the effective mass of an impact (Denoth, 1986).

## SUMMARY/CONCLUSIONS

Our results suggest that the vGRF can be used as an estimate of bone strain, but TA can only be used when effective mass is constant. If an estimate of bone strain can be derived from external transducers a direct measure of the external force must be included or a second variable that is related to effective mass must be used. Perhaps, a second accelerometer mounted further up the skeletal system could be used to estimate the effects of altered mass from the calculation of impact attenuation.

## REFERENCES

- Milgrom, C. et al. (2000). *Br. J. Sports Med.*, **34**, 195-199.  
 Whalen, R.T. et al. (1988). *J. Biomech.* **21**(10), 825-937.  
 Derrick, T.R. (2004). *Med. Sci. Sports Exerc.*, **36**(5), 832-837.  
 Denoth, J. (1986). In: *Biomechanics of running shoes*, Human Kinetics.

**Table 1:** Mean peak BS, vGRF, and TA values (all main effects were significantly different).

Drop Height (cm)	BS (µε)		vGRF (N)		TA (g)	
	9kg	11kg	9kg	11 kg	9kg	11kg
3	531.1	744.9	944.2	1131.0	6.6	6.1
5	793.9	992.6	1317.9	1502.3	8.5	7.6

# A STATISTICAL MODEL FOR PROXIMAL TIBIOFIBULAR JOINT MOTION

Jacob Scott<sup>1,2</sup>, Wael Barsoum<sup>3</sup>, Antonie J. van den Bogert<sup>1,2,3</sup>

<sup>1</sup>School of Medicine, Case Western Reserve University, Cleveland, OH, USA

<sup>2</sup>Department of Biomedical Engineering, Cleveland Clinic Foundation, Cleveland, OH, USA

<sup>3</sup>Department of Orthopaedic Surgery, Cleveland Clinic Foundation, Cleveland, OH, USA

E-mail: bogerta@ccf.org

## INTRODUCTION

The proximal tibiofibular joint (PTFJ) and its relationship to overall knee joint mechanics has been largely unexplored. The proximal fibula serves as the insertion for several anatomic structures integral to knee stability – the lateral collateral ligament (LCL), arcuate ligament, posterolateral capsular complex, and biceps tendon all insert onto the proximal fibula.

Our group is working on elucidating this joint's functional role in overall knee joint mechanics. We have previously presented data on maximum translation of the PTFJ during discrete loading conditions (Scott et al., 2005). Here we present data on three additional specimens and general conclusions obtained with help of a mathematical modeling technique.

## METHODS

Four fresh-frozen cadaveric knee specimens were tested with the knee joint fully intact. The tibia was mounted vertically on a six degree of freedom force/torque sensor (SI-2500-400, ATI Industrial Automation, Apex NC) mounted to the floor. Two reflective markers were mounted on pins driven into the tibial plateau and the head of the fibula at the proximal tibiofibular joint, respectively. Motion was recorded by a digital video camera at 10 frames per second. Load cell data was synchronized to the video data and recorded at 10 Hz. Specimens were subjected to manual loading conditions in each of four flexion

angles (0, 30, 60, 90 degrees as established by a manual goniometer). Varying loads were applied manually to a “handlebar” on the femur, in combination with a static compressive load of 40 lb to simulate weight bearing (Mizuno et al., 2004). At each flexion angle, the operator loaded the joint in varus, valgus, internal tibial rotation, and external tibial rotation. Peak moments were approximately 20 Nm for internal-external rotation and 50 Nm for varus-valgus.

Video images were digitized using custom Matlab software. The displacement of the fibula marker relative to the tibia marker was computed to quantify PTFJ motion in the sagittal plane. Each specimen's data were entered into custom MATLAB software to obtain a second order regression model for PTFJ motion as a function of the tibiofemoral joint loading state:

$$y = a_0 + \sum_{i=1}^7 b_i x_i + \sum_{i=1}^7 \sum_{j=1}^i c_{ij} x_i x_j \quad ,$$

where  $y$  is the dependent variable (anterior-posterior or inferior-superior PTFJ motion) and  $x_{1-7}$  are the independent variables: flexion angle, 3-D tibiofemoral force vector, and 3-D tibiofemoral moment vector. After a model was created for each specimen, it was used to predict PTFJ motion in nine specific physiological loading conditions: combinations of varus and internal tibial rotation torques (10, 0 and -10 Nm), combined with 250 N compression. The model outputs were then compared across specimens.

## RESULTS AND DISCUSSION

PTFJ joint motion was largest in the anterior-posterior direction. In all specimens, the regression model was able to fit the measured data well. In the anterior/posterior axis, which will be reported here, the RMS fit error ranged from 0.17 mm-0.35 mm, and the correlations of the models ranged from 0.941-0.971.

In all specimens, anterior fibula motion was seen during external tibial rotation. This is consistent with previous observations that LCL force is greatest in this loading condition (LaPrade et al., 2004). We also found anterior fibula translations during varus loading, and combined varus and external rotation (Fig. 1). There was more variation between specimens in pure varus loading. When in pure varus, even small variations in orientation of the articular surface of the PTFJ could drastically affect the motion.

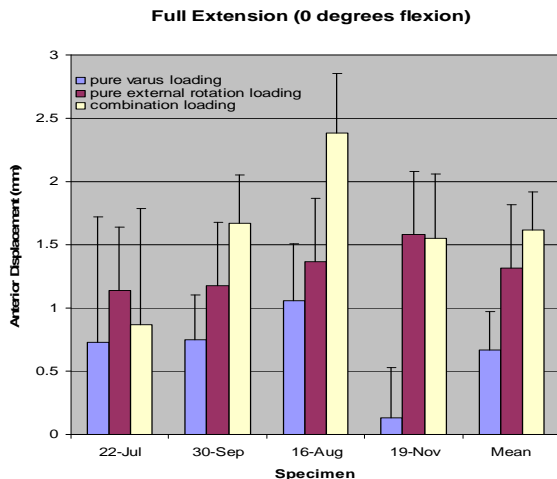


**Fig 1:** Anterior fibula translation in four specimens and three loading conditions.

Results were consistent across specimens at full extension, with increasing variability as the flexion angle increased. This effect is possibly due to changes in knee joint geometry from changing angle of

ligamentous forces as the femur rolls back on the tibial plateau.

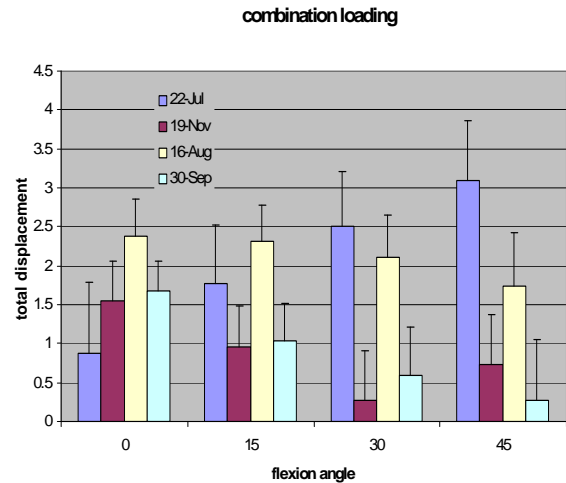


**Fig. 2:** Inter-specimen variability increases with flexion angle.

We present a statistical method of analysis for complex joint loading scenarios. Our model allowed us to interpolate the data within the seven-dimensional space of tibiofemoral joint loading states, such that hypothetical loading conditions could be simulated and compared between specimens. This has allowed us a deeper understanding of the complex behavior of the PTFJ.

## REFERENCES

- LaPrade RF, et al. (2004) *Am J Sports Med* 32: 1695-1701.
- Mizuno K, et al. (2004) ORS 50th Annual Meeting, Paper #240.
- Scott JG, et al. (2005) ISB XXth Congress. Cleveland, OH.

## ACKNOWLEDGEMENTS

We acknowledge Stryker Corporation and NIH 1P30AR050953 and 1T32AR050959-01 for financial support

# MODELING THE EFFECTS OF FOOT PLACEMENT DURING SIT-TO-STAND USING A STABILIZATION STRATEGY

Jason C. Gillette and Catherine A. Stevermer

Iowa State University, Ames, IA, USA  
E-mail: gillette@iastate.edu

## INTRODUCTION

Sit-to-stand movements are required for initiation of gait, upright reaching, and self-care tasks. Older adults with osteoarthritis may find sit-to-stand difficult or impossible without external assistance. It remains unknown how to systematically recommend an optimal seated posture based on individual physical capability.

Reduced strength and increased pain in the lower extremity joints are barriers to the completion of sit-to-stand transfers. Individuals who are unable to perform sit-to-stand without assistance or who perform sit-to-stand slowly ( $> 2$  s) have greater than two times the risk for falls (Nevitt et al., 1989). Arthritic pain was another factor that appeared to compound the risk of falls.

The effects of foot placement on lower joint torques when using a momentum strategy have been simulated (Gillette et al., 2005). We are developing a technique to optimize foot placement using individualized measures (Gillette and Stevermer, 2006). However, if video/force platform data are not available, then the optimization needs to consider multiple sit-to-stand strategies.

Our long-term goal is to extend sit-to-stand optimization to a clinical environment. Individualized measures would include strength, anthropometrics, and sit-to-stand time. Specifically, this study focuses on simulating the effects of foot placement on sit-to-stand when using a stabilization strategy (Scarborough et al., 1999).

## METHODS

The stabilization strategy was simulated with no upper body momentum generation. The initial knee flexion was  $90^\circ$  for foot-back and  $106^\circ$  for foot-neutral, trunk flexion was  $135^\circ$  for both, and ankle dorsiflexion was determined geometrically. Knee extension was initiated at 10%, hip extension at 12%, and ankle plantar flexion at 30% of the sit-to-stand cycle (STS).

Seated forces were simulated by unloading the upper body and thighs at 12% STS for seat-off. Hand support forces were applied, then unloaded at 30% STS if needed to maintain the center of pressure within the base of support. Ground reaction forces were calculated using segment inertias, seated forces, and hand support forces.

For comparison, a female older adult (75 yr) with bilateral total knee replacements performed sit-to-stand transfers from a 41 cm bench. She was observed utilizing a stabilization strategy from foot-back and foot-neutral placements. An eight-camera system tracked reflective markers, and each foot was placed on a separate force platform.

## RESULTS

Hand support forces were not needed to complete the sit-to-stand from the foot-back placement. However, hand support forces at 40% body weight (BW) were required to maintain the center of pressure within the base of support for foot-neutral.

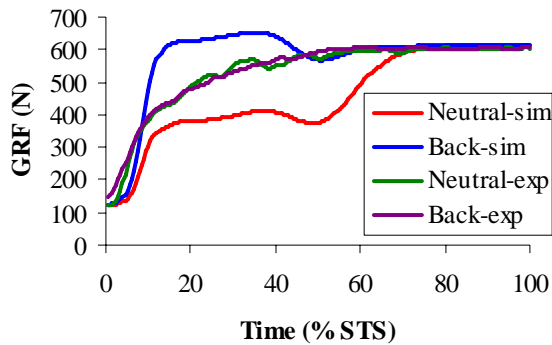


**Figure 1:** Simulated and experimentally measured ground reaction forces.

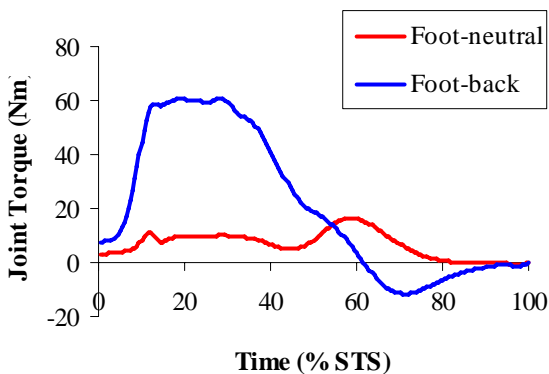


**Figure 2:** Knee extension torques using the foot-neutral and foot-back placements.

Maximum simulated ground reaction forces were greater with the foot-back (108% BW) than with the foot-neutral placement (101% BW). Maximum experimentally measured ground reaction forces were 100% BW for both foot placements (Figure 1).

Maximum ankle plantar flexion (37 Nm vs. 1 Nm), knee extension (61 Nm vs. 16 Nm), and hip extension torques (48 Nm vs. 45 Nm) were greater with foot-back (0% hand support) than with foot-neutral (40% BW hand support) placement (Figure 2).

## DISCUSSION

There were several differences between the simulated and experimentally measured sit-to-stand movements. First, the older adult

did not achieve full extension during upright standing (38° final experimental knee flexion). Second, the ground reaction forces did not change appreciably during the experimental trials. It appeared that the older adult used a similar amount of hand support force regardless of foot placement.

Using the stabilization strategy, high hand support forces were required to complete the sit-to-stand movement with foot-neutral. Previous simulations using the momentum strategy did not require hand support forces with foot-neutral, but high hip extension torques resulted instead. Therefore, an older adult would need either sufficient upper body strength or hip extensor strength depending upon movement strategy.

These results imply that an intermediate foot placement with moderate joint torques and hand support forces may be preferable. The next analysis step toward foot placement optimization would be to compare sit-to-stand torque requirements with strength capability (Gillette & Stevermer, 2006). Since the ground reaction forces displayed left-right asymmetry, staggered foot placement options also merit further consideration.

## REFERENCES

- Gillette, J.C., et al. (2005). *Biomed. Sci. Instrum.*, **41**, 7-12.
- Gillette, J.C. & Stevermer, C.A. (2006). *Biomed. Sci. Instrum.*, **42**, in press.
- Nevitt, M.C., et al. (1989). *JAMA*, **261**, 2663-2668.
- Scarborough, D.M., et al. (1999). *Gait Posture*, **10**, 10-20.

## ACKNOWLEDGEMENTS

This study was funded by a University Research Grant from Iowa State University.

# SYMMETRY IN LANDING MECHANICS OF GYMNASTS AND NON-GYMNASTS

Michelle B. Sabick, Rachael K. Goetz, Seth M. Kuhlman, and Ronald P. Pfeiffer

Center for Orthopaedic & Biomechanics Research, Boise State University, Boise, ID, USA  
E-mail: [MSabick@boisestate.edu](mailto:MSabick@boisestate.edu) Web: [coen.boisestate.edu/cobr](http://coen.boisestate.edu/cobr)

## INTRODUCTION

Experienced gymnasts are considered by many to be landing experts, because they are able to successfully land from heights of 3m or more (McNitt-Gray, 1993). Although gymnasts may be landing experts, their landing mechanics cannot be determined solely by optimal landing strategies because the judging system places constraints on how a landing is to be performed. Gymnasts spend many years perfecting their landings to fulfill these judging requirements, likely affecting their landing mechanics.

Asymmetry in knee joint loads during landing has recently been implicated in the etiology of anterior cruciate ligament (ACL) injuries (Hewett et al., 2005). However, symmetry during landing has not been described in gymnasts or in non-competitive adult athletes. The purpose of this study was to compare symmetry and lower extremity landing mechanics between collegiate gymnasts and non-gymnasts.

Our hypothesis was that collegiate gymnasts would employ a landing strategy with increased ground reaction forces due to restrictions imposed by the scoring system, but that they would also exhibit more symmetry in kinematics and kinetics between dominant and non-dominant legs due to their experience in landings.

## METHODS

Thirteen female collegiate Division I gymnasts and 12 female non-gymnast college students volunteered to participate in

this study. The subjects wore tight-fitting shorts and tops and performed five trials of a two-footed landing task from a height of 72 cm onto two floor-mounted force platforms.

The participants stood on a raised platform located 20-cm away from the force platforms and were instructed to step out with the preferred leg and land with one foot on each force plate. Lower extremity position data were recorded at 250 Hz using a six-camera motion capture system. Twenty retroreflective markers were placed over bony landmarks on the pelvis and lower extremity so that three-dimensional kinematics of the pelvis and the ankle, knee, and hip joints could be computed during landing. Two force platforms level with the surrounding floor and synchronized with the motion capture system sampled ground reaction forces during landing at 1250 Hz. Ground reaction force (GRF) data was normalized to the subject's body weight (BW). To quantify landing symmetry, a ratio of GRF values in the subjects' dominant leg to her non-dominant leg was established. A ratio of 1.0 indicated both legs experienced equal GRFs.

The 3-D marker coordinate data were smoothed using a 4<sup>th</sup> order zero-lag Butterworth filter with a cutoff frequency of 17 Hz. Kinematics of the pelvis, hip, knee, and ankle were calculated using Euler angles as described by Cappozzo et al. (1997). Internal joint resultant forces and moments for the hip, knee, and ankle of both lower extremities were calculated using custom inverse dynamics routines and expressed in

a local joint coordinate system as described by Grood and Suntay (1983). Comparisons between the two groups were made using a Student's two-tailed t-tests with  $\alpha=0.05$ .

## RESULTS AND DISCUSSION

Peak GRF was significantly greater in gymnasts in the vertical and anterior directions for both dominant and non-dominant legs (Table 1). For the vertical GRF component, gymnasts displayed a lower symmetry ratio than the non-gymnasts ( $1.04\pm 0.18$  vs.  $1.40\pm 0.56$ ,  $p=0.041$ ). Joint kinematics were similar in both groups. Gymnasts tended to demonstrate less peak knee flexion in the non-dominant leg ( $80\pm 8^\circ$ ) than non-gymnasts ( $92\pm 15^\circ$ ), but the difference was not significant ( $p=0.08$ ). A similar trend was noted for the dominant leg ( $75\pm 19^\circ$  vs.  $89\pm 13^\circ$ ,  $p=0.06$ ). Joint kinetics were also similar between the two groups, although gymnasts demonstrated higher dominant leg peak hip extension moments than non-gymnasts. Gymnasts also absorbed more energy with the non-dominant hip during landing compared to the non-gymnasts, as evidenced by larger negative power values.

As expected, gymnasts demonstrated more symmetry in GRF during landing than the untrained subjects, and higher peak ground reaction forces overall. The increased peak GRF is likely due to adaptations by the athletes to the gymnastics scoring system, in

which athletes are encouraged to land upright and with relatively straight legs. Improved symmetry between the legs in the gymnasts compared to the non-gymnasts is likely due either to 1) improved strength in the non-dominant leg from training, or 2) to a need to distribute load equally among the lower extremities to decrease the chance of injury due to the high GRFs encountered.

## SUMMARY

Gymnasts landed with significantly higher peak GRF and but more symmetry between dominant and non-dominant legs than did non-gymnasts. There was a trend toward less peak knee flexion in gymnasts, suggesting a stiffer landing strategy, but the between-group differences were not statistically significant.

## REFERENCES

- Cappozzo, A., Della Croce, U., Lucchetti, L. (1997). *Three-dimensional analysis of human locomotion*. John Wiley & Sons Ltd.
- Grood, E.S., Suntay, W.J. (1983). *J Biomech Eng*, **105**, 136-44.
- Hewett, T.E. et al. (2005). *Am J Sports Med*, **33**, 492-501.
- McNitt-Gray, J.L. (1993). *J Biomech*, **26**, 1037-1046.
- Winter, D.A. (1990). *Biomechanics and Motor Control of Human Movement: Second Edition*, John Wiley & Sons, Inc.

**Table 1:** Normalized GRF in the vertical and anterior directions for each leg (mean $\pm$ SD).

	Vertical GRF Component		Anterior GRF Component	
	Mean (BW)	p	Mean (BW)	p
<b>Dominant Leg</b>				
Gymnast	4.31 $\pm$ 0.71	0.037	0.67 $\pm$ 0.23	0.009
Non-gymnast	3.67 $\pm$ 0.71		0.40 $\pm$ 0.22	
<b>Non-dominant Leg</b>				
Gymnast	4.20 $\pm$ 0.70	0.007	0.61 $\pm$ 0.19	0.005
Non-gymnast	2.88 $\pm$ 0.95		0.33 $\pm$ 0.25	



# Mechanical Analysis of Percutaneous Sacroplasty using CT Image based Finite Element Models

Dennis E. Anderson and John R. Cotton

Virginia Tech, Blacksburg, VA, USA  
Email: dennisa@vt.edu

## INTRODUCTION

Vertebroplasty is a widely used procedure for treatment of vertebral compression fractures. It consists of the injection of polymethylmethacrylate (PMMA) bone cement into the cancellous core of the vertebral body. Recently a similar technique, called sacroplasty, has been used in the treatment of sacral insufficiency fractures. Early clinical results, such as presented by Pommersheim et al (2003), indicate sacroplasty is effective in relieving pain and improving daily function. We present here a finite element analysis that examines the mechanical effects of sacroplasty: namely the stiffening effects on the whole sacrum, as well as the redistribution of strain energy in and around the cemented area.

## METHODS

Finite element models were constructed based on Computed Tomography (CT) images from a cadaver in a bilaterally sacroplasty was performed. The model geometry, which included the sacrum and the upper portions of the ilia, was defined from the CT image. MSC.Patran (MSC Software, Santa Ana, CA) was used to create finite element meshes based on the defined bone geometry (Anderson and Cotton, 2006).

In addition to geometry, the CT image was used to create non-homogeneous material properties for the bone in the finite element model. This was done using Bonemat, developed by Taddei et al (2004), and by

estimating reasonable values for mineral density and bone modulus for the sacrum. Cement areas were brighter on the CT image than bone and were assigned a value of 2.5 GPa. Figure 1 shows the resulting modulus variation in the model, where the cement can be clearly seen.

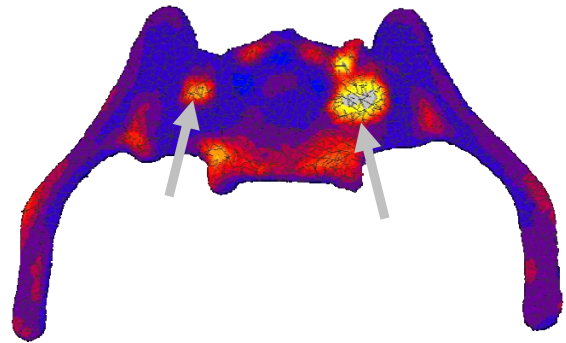


**Figure 1:** Modulus variation in a coronal section of the sacral model. The arrows indicate the bilateral locations of the cement.

To examine the sacroplasty effect, the above model was compared to the same model except the cemented elements were replaced by elements assigned representative values of cancellous bone.

## RESULTS AND DISCUSSION

Principal strain magnitudes and directions were compared in both the cemented and uncemented models. In both, compressive strains were the largest, although tensile and shear strains were also significant. In the locations of the cement, strains were reduced (Figure 2). This local effect was sizeable, reducing strains an average of 30%, some by as much as 70%. While a few

element strains increased, highly strained elements uniformly saw their strains drop.

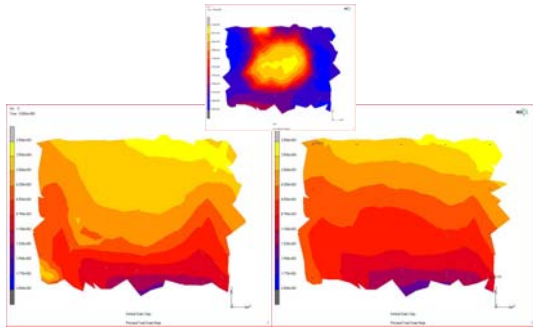


**Figure 2.** Comparison of right cemented area with cement (left) and no cement cases (right). Major principle strains ranging from 250 to  $-2000 \mu\epsilon$ . Inset is the modulus for the cement case, showing cement location.

Despite this local effect, under identical loads the cemented case deflected roughly 2% less. Therefore, the cemented case has slightly less energy to cause damage or pain. Figure 3 shows how this strain energy is redistributed. The stiffer cement elements absorb more energy. However, the volume of cemented elements is not great. Overall, the strain energy in the putative cemented areas increases from 0.73 to 1.84% of the total strain energy by the addition of cement.

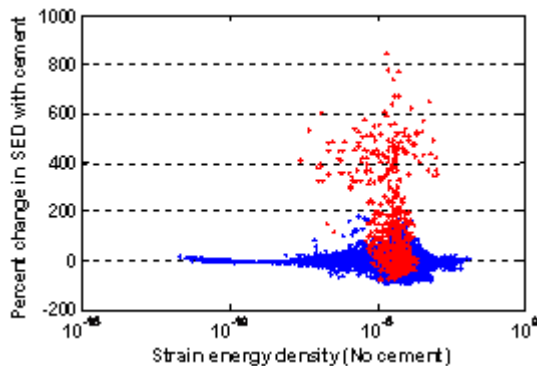


**Figure 3.** The uncemented strain energy in each element changes with sacroplasty. In red are cemented elements, while uncemented elements are blue.

In contrast, examinations of vertebroplasty have shown that it can significantly increase

vertebral body strength and stiffness. The increase is greater for larger amounts of cement. Liebschner (2001) predicted with finite element models that cement could increase vertebral body stiffness by almost 50% over the intact stiffness. Heini (2001) found stiffness increases of 174% in osteoporotic vertebrae. In these cases, the volume of cement injected was 25–50% of the vertebral body volume. In this study, the cement volume was estimated at about 1% of the sacral volume. To obtain percent fills comparable to vertebroplasty would require significantly more cement, as the sacrum is larger than a vertebral body. If the sacrum is limited to small percent fills, the effects of sacroplasty will be primarily limited to the local areas around the cement, as was seen in this model.

## SUMMARY

Sacroplasty acts to reduce the strains in the sacrum, especially in the regions where the cement is present. The overall model was only stiffened slightly.

## ACKNOWLEDGEMENTS

Thanks to Pearse Morris, Wake Forest University School of Medicine, for providing the CT images.

## REFERENCES

- Anderson, D.E., and Cotton, J.R. (2006) *Med. Eng. & Phys.*, In Press.
- Heini, P.F. et al. (2001). *Eur. Spine. J.*, **10**, 164–171.
- Liebschner, M.A.K. et al. (2001). *SPINE* **26** (14), 1547-1554.
- Pommersheim, W. et al. (2003). *Am. J. Neuroradiol.*, **24**(5), 1003-1007.
- Taddei, F. et al. (2004). *Med. Eng. & Phys.*, **26**(1), 61-69.

# ROLE OF REFLEX DYNAMICS IN SPINAL STABILITY

Kevin P. Granata and Kevin Moorhouse

Musculoskeletal Biomechanics Laboratory

Virginia Polytechnic Institute and State University, Blacksburg, VA, USA

E-mail: granata@vt.edu Web: www.biomechanics.esm.vt.edu

## INTRODUCTION

Reflexes play an important role in the control of spinal stability. Three sub-systems contribute to stability including: 1) passive spinal ligaments, discs and bone, 2) intrinsic viscoelastic stiffness of muscles during steady-state activation, and 3) neural feedback including reflex and voluntary responses. Existing biomechanical models assume spinal stability is maintained by intrinsic stiffness of active muscle. However, it is unclear whether intrinsic stiffness alone can sufficiently compensate for the gradient in gravitational moment at each vertebra. Reflex response also contributes to spinal stability; they provide restorative forces similar to intrinsic stiffness but are time-delayed by response latency. The reflex response in the torso and paraspinal muscles may contribute significantly to the stabilizing control spine. Therefore, the goal of this study was to quantify the role of reflexes in spinal stability during voluntary isometric extension exertions.

## METHODS

Eleven healthy males with no history of low back pain participated after signing informed consent. Subjects generated isometric trunk extension exertions (20, 35, 50% MVE) while pseudo-random binary position disturbances,  $\pm 2$  mm amplitude, were applied to the T10 level of the torso. Measured force was represented as the sum of intrinsic stiffness and reflex responses (Figure 1). The intrinsic pathway  $H_{INT}$  described the viscoelastic response to disturbances.  $H_{INT}$  duration was fixed at less than 40 msec, i.e.

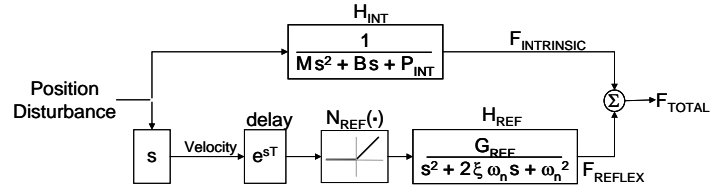


Figure 1. Systems identification of reflex and intrinsic components of torso dynamics.

less than measured reflex delay, to ensure that reflex mechanisms would not influence the estimated,  $H_{INT}$ . Force not accounted for by the intrinsic dynamics was attributed to reflex, i.e. force at  $t > 40$  msec. The reflex pathway was modeled as a delayed Hammerstein series with dynamic linear element,  $H_{REF}$ .  $H_{INT}$  and  $H_{REF}$  were iteratively computed until successive cycles failed to improve model accuracy.

Intrinsic compliance was parametrically modeled as a 2<sup>nd</sup> order behavior (Figure 1,  $H_{INT}$  box).  $P_{INT}$  was operationally defined as the proportional intrinsic response coefficient

$$P_{INT} = k_{INT} - M g h^{-1}$$

in the model and included intrinsic stiffness,  $k_{INT}$ , as well as gravitational contributions to measured force. The reflex impulse response function,  $H_{REF}$ , was parameterized using a model of a standard 2<sup>nd</sup> order system in series with a reflex delay (Figure 1).

$$H_{REF}(s) = \frac{G_{REF}}{s^2 + 2\zeta\omega_n s + \omega_n^2} e^{-sT} \quad (\text{eqn 2})$$

Reflex conduction delay was determined from visual inspection of  $H_{REF}$ . Parameters were computed by least-mean-square fit to measured data, Levenberg-Marquardt algorithm. ANOVA were performed to determine the effect of independent variables of trunk extension exertion on the proportional intrinsic response,  $P_{INT}$ , and reflex parameters

## RESULTS AND DISCUSSION

Nonlinear system identification procedures predicted the total force response to the pseudorandom position perturbations with accuracy of  $80.9 \pm 3.6\%$ . Typical intrinsic force response exhibited large inertial force at the onset of the movement perturbation, i.e. acceleration phase (Figure 2). This was followed by a steady-state force proportional to the position disturbance. Mean value of proportional intrinsic response,  $P_{INT}$ , was not significantly different than zero (Table 1). Gravitational contribution to  $P_{INT}$  was  $-1695 \pm 249$  N/m. Therefore, from equation 1 the mean intrinsic stiffness was  $k_{INT} = 1281 \pm 240$  N/m during the 20% MVE exertions. This increased significantly up  $k_{INT} = 2116 \pm 710$  N/m during 50% MVE. exertions.

Intrinsic stiffness alone was insufficient to stabilize gravitational effects of torso mass. When the spine and torso are disturbed from the equilibrium then intrinsic stiffness,  $k_{INT}$ , provided restorative forces that tend to return the posture toward the equilibrium state, i.e. positive contribution to  $P_{INT}$ . Conversely, gravitational mass contributes destabilizing forces that tend to drive the posture away from the equilibrium state following a small disturbance, i.e. negative contribution to  $P_{INT}$ . The negative contribution of gravitational mass was often greater than the positive contribution of the intrinsic muscle and passive tissue stiffness.

Mean value of reflex gain,  $G_{REF}$ , was  $221 \pm 84$  N-s/m and increased ( $p < .05$ ) with exertion. Mean reflex natural frequency and damping ratio were  $9.13 \pm 2.1$  Hz and  $0.58 \pm 0.12$  N-s<sup>2</sup>/m respectively. These were not

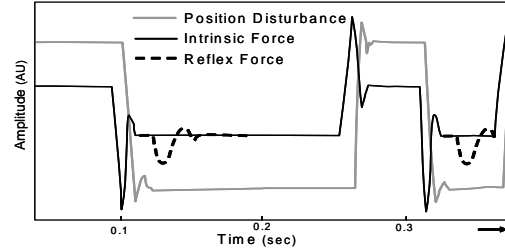


Figure 2. Typical sample of position disturbance, intrinsic and reflex force components.

significantly influenced by exertion effort.

The contribution of reflexes to the total stiffness behavior was estimated from equation 2. Recall that  $H_{REF}$  describes the transfer function from disturbance velocity to reflex force. Hence, the proportional response to describe reflex stiffness

$$\text{is } k_{REFLEX} = \frac{G_{REF}}{2\zeta\omega_n} e^{-sT}. \text{ Standard first-order}$$

Pade approximation was used to account for the reflex delay. Mean reflex stiffness was  $1398 \pm 963$  N/m (Table 1). Therefore, 42% of the total trunk stiffness can be attributed to the reflex response. There was no statistical difference in the reflex contribution to trunk stiffness between exertion levels.

## SUMMARY / CONCLUSIONS

This study provided insight into the significant role that reflexes play in trunk dynamics and spinal stability. Without reflex response the system was often unstable. Recognizing that reflexes may account for up to 42% of the stabilizing dynamics of the torso future models should include reflexes. Results also indicate that individuals with disturbed reflex response may be more susceptible to spinal instability injuries.

Table 1. Mean (standard deviation) values of intrinsic and reflex parameters. Superscript represent significant differences ( $p < 0.05$ ) between exertion conditions.

	Force [N]	$P_{INT}$ [N/m]	$k_{INT}$ [N/m]	$G_R$ [N s/m]	$\zeta$ [N s <sup>2</sup> /m]	$\omega_n$ [Hz]	$k_{Reflex}$ [N/m]
<b>20% MVE</b>	96 (20) <sup>A</sup>	-415 (354) <sup>A</sup>	1280 (240) <sup>A</sup>	197 (96) <sup>A</sup>	0.66 (0.14) <sup>A</sup>	8.69 (2.74) <sup>A</sup>	1205 (990) <sup>A</sup>
<b>35% MVE</b>	155 (38) <sup>B</sup>	43 (637) <sup>B</sup>	1738 (600) <sup>B</sup>	221 (79) <sup>A</sup>	0.55 (0.08) <sup>B</sup>	9.54 (2.23) <sup>A</sup>	1368 (926) <sup>A</sup>
<b>50% MVE</b>	208 (65) <sup>C</sup>	421 (796) <sup>B</sup>	2116 (710) <sup>B</sup>	248 (77) <sup>B</sup>	0.53 (0.12) <sup>B</sup>	9.16 (1.43) <sup>A</sup>	1619 (1024) <sup>A</sup>



# A FRAMEWORK FOR THE FUNCTIONAL IDENTIFICATION OF JOINT CENTERS USING MARKERLESS MOTION CAPTURE, VALIDATION FOR THE HIP JOINT.

Stefano Corazza<sup>1</sup>, Lars Mündermann<sup>1</sup>, Ajit W. Chaudhari<sup>1</sup> and Thomas Andriacchi<sup>1,2</sup>

<sup>1</sup> Stanford University, Stanford, CA, USA

<sup>2</sup> Bone and Joint Research Center, VA Palo Alto, Palo Alto, CA

E-mail: stefanoc@stanford.edu Web: biomotion.stanford.edu

## INTRODUCTION

The accurate identification of joint centers is in general a very important issue in biomechanics for the calculation of human body kinematics and kinetics. The hip joint center (HJC) for example is used in the kinematics to define the anatomical frame of the femur and in the kinetics for the calculation of hip moments generated by external loads. Many previous studies in literature pointed out the importance of an accurate identification of the HJC [Camomilla, 2006] demonstrating how it affects kinematics and kinetics of both hip and knee joint. Many algorithms have been developed in the past for the estimation of hip joint center using marker based kinematics (an exhaustive review can be found in [Camomilla, 2006]) under the hypothesis of spherical joint.

In this paper a framework for the accurate identification of the hip joint centers using markerless motion capture (MMC) method [Corazza, 2006, Mündermann, 2006] is presented. The theory behind is general and can be applied to every joint of the human body. In this work authors focus on the HJC since its representation as spherical joint is a generally accepted hypothesis. An experimental implementation of the method is reported together with validation results in virtual environment, showing errors in the on the order of one centimeter (i.e. the system spatial resolution).

## METHODS

The idea underneath the presented functional joint center algorithm is based on the hypothesis that, for two rigid bodies connected with a ball and socket joint, there exists a *pivot* point  $p$  for which the motion can be described identically by either of the motions of the two rigid bodies.

The complete algorithm was applied to hip joint center identification, in both a virtual and experimental environment, through the following steps (Figure 1):

- i) A 3D representation (visual hull) of the subject was reconstructed for every captured frame. The 3D representation has 1 cm spatial resolution (voxel size).
- ii) Motion is tracked using a rough model and the method described in [Corazza2006]. Through a proximity-check the points of the visual hull belonging to the lower limb are identified (segmentation).
- iii) The segmented lower limb is treated as a rigid body and the transformation matrices for the rigid body registration of couples of different frames were calculated, using Iterative Closest Point and Levenberg-Marquardt minimization based algorithm.
- iv) The hip joint center is given by a least square solution of the (1) where  $R$  and  $t$  are the 3x3 rotation matrix and the 3x1 translation matrix derived from the 4x4 transformation matrixes of the rigid body registration.

$$\begin{bmatrix} R_1^A - I \\ \dots \\ R_n^A - I \end{bmatrix} [JC] = \begin{bmatrix} -t_1^A \\ \dots \\ -t_n^A \end{bmatrix} \quad (1)$$

In equation (1)  $I$  is the identity matrix,  $n$  is the number of frames and index  $A$  refers to the segment of interest, which points coordinates are expressed in the system of reference of the proximal segment. For the validation with synthetic data, a virtual character performed a functional start-arc motion through hip flexion-extension and ab-adduction as described in [Camomilla, 2006]. The 3D reconstruction was obtained by capturing from 8 VGA virtual cameras around the character, same setup used in the experimental trial.

## RESULTS AND DISCUSSION

Results in the virtual environment are presented (Figure 2). After few iterations the error converges to sub-voxel or voxel level accuracies (voxel size=1 cm). The error with marker based technique for equivalent conditions is within 1 mm, on simulated data and not taking into account marker location estimation errors. Figure 2 also demonstrates the stability properties of the method with respect to large initialization errors. Experimental trials were collected and the method implemented as shown in Figure 1.

## SUMMARY/CONCLUSIONS

The presented work defines, in the context of MMC, a framework for the accurate

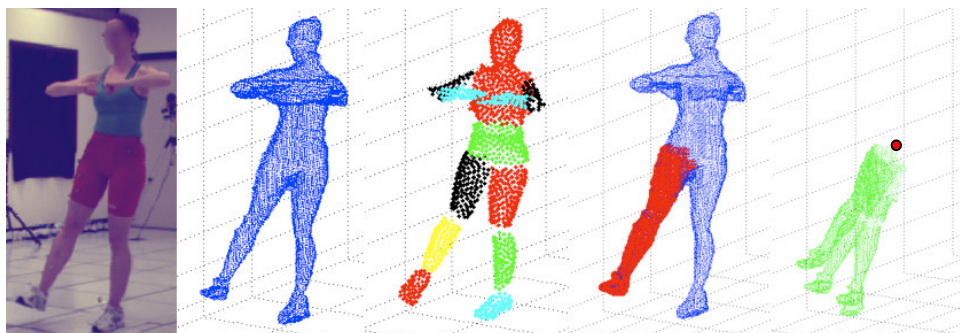


**Figure 1:** From the left: data acquisition, reconstruction of 3D representation, tracking result, segmentation, joint center estimation.

functional identification of joint centers. The method applies well to the case of the HJC for which a validation is provided.

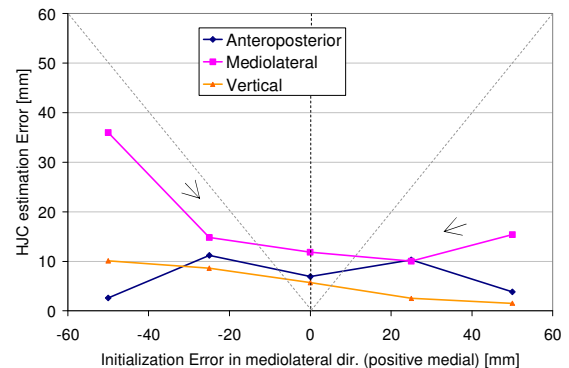


**Figure 2:** Algorithm stability diagram for large initialization error in joint center location in medio-lateral direction (worst case scenario).

Even though in simulated data marker based techniques [Camomilla, 2006] provide slightly more accurate results, the authors believe the presented method has greater potential in the experimental scenario where skin artifacts play a prevalent role, and with the advantage of no marker placement.

## ACKNOWLEDGEMENT

Funding provided by NSF#03225715 and VA#ADR0001129.

## REFERENCES

- Camomilla et al. (2006) *J.Biomech.* **39**(6):1096-106.
- Mündermann et al. (2006) *J.Neuroeng.Rehab.* **3**:6.
- Corazza et al. (2006) *Annals Biomed. Eng.* In press.

# BIOMECHANICAL EVALUATION OF SUPRASPINATUS TENDON WITH DIFFERENT DEGREES OF PARTIAL THICKNESS TEAR

Hyung-Soon Park<sup>1</sup>, Steven Flores<sup>2</sup>, Scott Yang<sup>2</sup>, Jason L. Koh<sup>2</sup>, and Li-Qun Zhang<sup>1,2</sup>

<sup>1</sup> Rehabilitation Institute of Chicago, Chicago, IL, USA

<sup>2</sup> Northwestern University, Chicago, IL, USA

## INTRODUCTION

Partial thickness rotator cuff tears are common sports and age related phenomena (Ticker et al. 1995). Although the majority of previous work has looked at full thickness tears, increasing attention is being turned toward these types of injuries because partial thickness rotator cuff tears are seen much more frequently than full thickness rotator cuff tears (Matsen et al. 1998).

However, there is a lack of quantitative evaluations of different degrees of partial thickness tear and choice of surgical and conservative treatments (Zhang et al. 2002). The purpose of this study is to quantitatively examine the changes in strain of the supraspinatus tendon with different degrees of partial thickness tear under simulated muscle loading, which may help choose appropriate surgical and conservative treatments.

## METHODS

*Specimen:* Seven fresh-frozen upper extremities were used for the study (4 male and 3 female). The average age was 65.3 (ranging from 52 to 77) years.

After the removal of all overlying soft tissue, cables were sutured to individual muscle through fiberglass mesh wrapped around the proximal ends of the dissected muscles, including the anterior, medial, and posterior portions of the deltoid, supraspinatus, upper, middle, and lower portions of the subscapularis and infraspinatus, teres minor and the distal end of the long head of biceps. The muscle bellies were then loaded along their line of action through the cable affixed to the mesh. Muscles were loaded to a predetermined

weight that provided for about 2% of the maximum muscle force.

*Experimental Setup:* The scapula was mounted rigidly onto a Teflon plate with several pairs of bolts and nuts and the glenoid surface was oriented vertically (Fig. 1). The humerus was fixed into an aluminum tubing by sharpened screws and the glenohumeral abduction was set at 30° (~45° shoulder abduction).

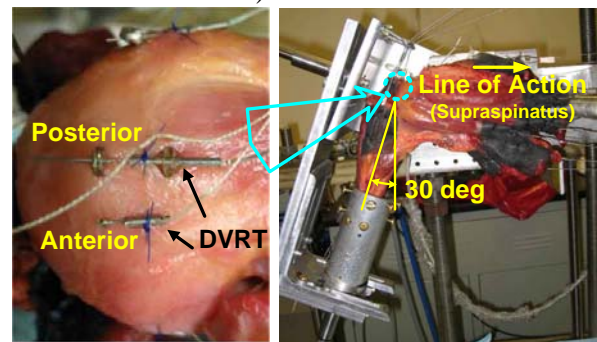


**Figure 1.** Experimental Setup.

Two differential variance reluctance transducers (DVRTs) were mounted onto the tendons using both barbs and suture to measure strains at the posterior and anterior edges of supraspinatus tendon (Fig. 1). The initial length between the two attachment points of the DVRT was measured with a caliper, and a reading of the DVRT was taken at that initial position so that all changes in the DVRT output represented a change in the length between the two attachment points of the DVRT. Strain was then calculated by dividing the changes in length by the initial length.

A load cell was used to measure the force applied to the supraspinatus muscle. The pulling force was generated by a servo motor which was controlled to pull the muscle with a loading rate of 3 N/sec.

*Protocol:* The supraspinatus tendon was pre-loaded for twenty cycles to 10 N. The supraspinatus tendon was then loaded up to 50 N for five cycles with a constant loading rate of 3 N/sec. Partial thickness tears were then created by cutting the supraspinatus tendon from its anterior border for approximately three quarters of the tendon width at 1 mm increments. The controlled supraspinatus loading was repeated after each cut. After the completion and loading of a full thickness tear, the thickness of tendon was measured to calculate the percentage of each cut.

## RESULTS AND DISCUSSION

As the partial thickness tear of the supraspinatus tendon increased, the strain in the remaining intact portion of the tendon, the posterior edge, increased monotonically (Fig. 2). At the 30 N loading, an intact supraspinatus tendon in a representative case showed a strain of 2.3%. The strain increased to 4.3, 4.9, 5.5, 5.8, and 6% at 14, 41, 68, 82, and 100% partial/full thickness tears, respectively. On the other hand, strain in the torn anterior edge of the supraspinatus tendon decreased with the tear thickness.

To evaluate the rate of increase/decrease in strain as a function of the tear thickness, the strain ratio was defined as follows

$$R = (\varepsilon - \varepsilon_I) / |\varepsilon_F - \varepsilon_I|$$

where,  $\varepsilon_I$  and  $\varepsilon_F$  denote the strain at intact and full thickness tear conditions, respectively. A 2<sup>nd</sup> order polynomial was fit to interpolate the strain ratio across different percentages of partial thickness tear.

The strain at the intact portion of the tendon increased as the thickness of tear increased while the strain at torn portion decreased with the thickness of the tear.

## SUMMARY/CONCLUSIONS

The strain at the intact portion increased more rapidly at the lower percentage of thickness tears, indicating the need for early

and proper treatment (Fig 3.). The strain at the torn portion decreased with the tear thickness.

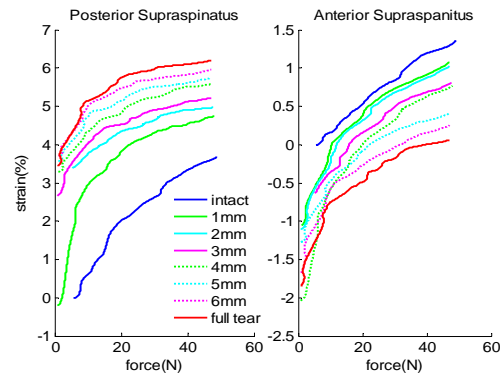


**Figure 2:** The strain changes in the posterior (upper plot) and anterior (bottom plot) supraspinatus tendon with 1 mm increment of tear thickness.

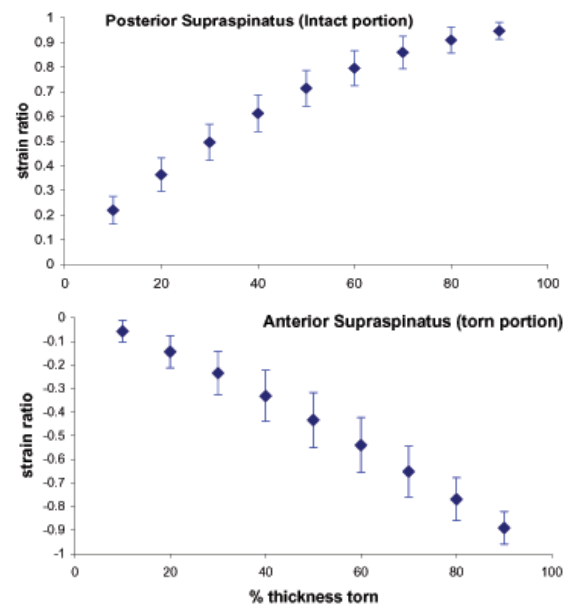


**Figure 3:** The rate of increase/decrease in strain at posterior/anterior edge with increasing % of partial thickness tears.

## REFERENCES

- Ticker, J. et al. (1995). *Sports Medicine*, 19, 418-426.
- Matsen, F.A. et al. (1998). *The Shoulder*. Sauder.
- Zhang, L.Q. et al. (2002). *Proc. of ISG*

# MECHANICAL ANALYSIS AND COMPUTER SIMULATION OF THE STRUCTURE OF FEMORAL NECK

Jing-Guang Qian <sup>1</sup>, Yia-Wei Song <sup>1</sup>, Xiao Tang <sup>1</sup>, Songning Zhang <sup>2</sup>

<sup>1</sup> Nanjing Institute of Physical Education, Nanjing, China

<sup>2</sup> The University of Tennessee, Knoxville, TN, USA

## INTRODUCTION

The femoral neck-shaft angle is formed between long axes of the neck and shaft of the femur. Its range is normally between 125 -135°. This femoral neck angle is a necessary for normal functions of the hip joint. When the femoral neck-shaft angle is less than 110° or greater than 140°, it may disturb normal mechanics and functions of the joint (Ping 2003).

The fracture of the femoral neck is rather common and its etiology and prevention have been widely examined. However, research on the dynamical loading to the structure of femoral neck using computer simulation is still relatively scarce. Therefore, the purpose of this study was to examine the effect of varying the femoral neck-shaft angle on stress levels of the region and provide useful information for fracture prevention and rehabilitation.

## METHODS

X-ray (Chen 2004) and dual-energy x-ray absorptiometry (DEXA, Lunar Expert) (Massin 2000) were used to obtain the femoral neck angle and the bone mineral density (BMD) on both sides of normal participants (53 females & 23 males) and the healthy side of patients with femoral neck fracture (left side females – 11, right side females – 4, left side males – 5). The bone density was measured at following five sites: neck region, upper shaft, ward's triangle,

greater trochanter, and mid shaft of the femur.

A finite element analysis (ANSYS, IMAG) was used to analyze the relationship between the femoral neck angle and stress applied in the femoral neck region (Cody 1999). By examining the stress distribution diagrams obtained through computer simulations, Von Mises stress distribution and its relationship with the change in the femoral neck angle changed from 115 – 140° were obtained.

T-tests were used to exam the difference of the femoral neck angles between the normal and the fractured femurs and the difference between the left and right femurs ( $p < 0.01$ ). The connection between the density of femoral neck, angle of femoral neck and the characteristics of the fractured patients was examined.

## RESULTS AND DISCUSSION

The femoral neck angle for the left side of the male patients was significantly smaller than their normal counterparts (Table 1). A similar but non-significant trend was observed between the other two comparisons. These results may suggest that the fracture of femoral neck may be linked to a smaller femoral neck-shaft angle. No difference between males and females were observed. An examination of individual data showed that some subjects had a greater than 10° difference between the left and right femoral neck angles. The BMD data obtained through DEXA showed that the density at the Ward's

triangle reached its peak at ages of 30 – 39 years and 20 -29 years for males and females, respectively. The density decreased gradually afterwards for females. For the males, the BMD reversed its declining trend at ages of 50 – 59 years and remained at the same level thereafter. The BMD values (0.663) for the normal subjects were significantly greater than the patients' BMD (0.569). This may be related to the high incidence rate of femoral neck fractures in older, especially female population.

Table 1. Mean femoral shaft-neck angle (°): mean ± SD

	Female Left	Female Right	Male Left	Male Right
Normal	134±5	134±5	134±5*	133±5
Fracture	133±4	131±4	124±7	

Note: \* - significant from the fractured femur.

The simulation results from the finite element analysis showed that the stress level increased dramatically with the decreased of the femoral neck angle (Table 2). The highest stress concentration was found in the mid lower region of the posterior femoral neck. The sharpest increase of stress was seen between 125 –120° of the neck angle (Figure 1). These results suggest that under similar loading, the patient may reach their stress limit sooner and increase risks of femoral neck fractures.

Table 2. Simulation results of the femoral neck (°) angle and maximum stress (MPa).

Angle	115	120	125	130	135	140
Stress	3.98	3.81	2.71	2.46	1.97	1.47

## SUMMARY/CONCLUSIONS

The results showed that the patients had a smaller femoral neck angle and BMD in the Ward's triangle compared to the normal

participants. The left side of the male patients had a smaller femoral neck angle compared to the same side of their normal counterparts. The simulation results showed a sharp increase in the maximum Mises stress with the decrease of the neck angle from 125 - 120° and therefore increase the risks of injuries. These results provide a screening criterion for physical examinations. When a person's femoral neck angle falls below 125° and is coupled with a decrease in BMD (i.e. osteoporosis), she/he can be classified into a high-risk group. For a patient with osteoporosis, if the femoral neck angle on one side is far smaller than the angle of the other limb and is below 125°, this affected limb should be considered as a high-risk limb and special attentions should be paid. These results may provide important information in prevention of femoral neck fractures.

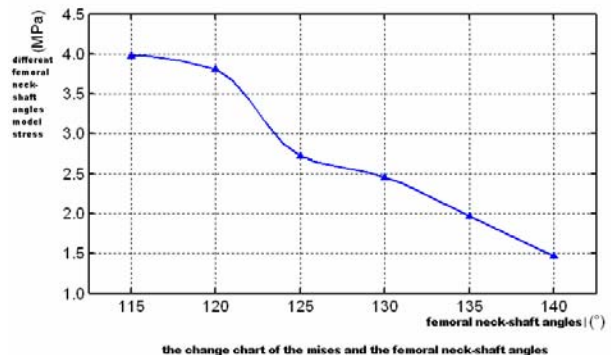


Figure 1. Maximum Mises stress and femoral neck angle.

## REFERENCES

- Ping B. (2003). *J. Tianjin Medical University*, **9**: 475-478.  
 Chen W.P. et al. (2004). *Clin Biomech*, **19**: 255~262.  
 Massin, P.C. et al. (2000). *J Arthroplasty*, **15**: 93-101.  
 Cody D.D., et al. (1999). *J BIOMECH*, **32**: 1013 -1020.

# EFFECTS OF IMPLANT DESIGN PARAMETERS ON FLUID INGRESS DURING THA IMPINGEMENT/SUBLUXATION

Hannah J. Lundberg<sup>2</sup>, Douglas R. Pedersen<sup>1,2</sup>, John J. Callaghan<sup>1,2</sup>, Thomas D. Brown<sup>1,2</sup>

<sup>1</sup> Department of Orthopaedics and Rehabilitation, University of Iowa, Iowa City, IA, USA

<sup>2</sup> Department of Biomedical Engineering, University of Iowa, Iowa City, IA, USA

E-mail: hannah-lundberg@uiowa.edu

Web: mnypt.obrl.uiowa.edu

## INTRODUCTION

Aseptic loosening from polyethylene wear debris remains the leading cause of failure for metal-on-polyethylene total hip implants. Wear is exacerbated by 3<sup>rd</sup> body debris, leading to femoral head roughening, but the manner by which 3<sup>rd</sup> bodies gain access to the very closely congruent bearing surface is unknown. One possibility is that ingress of 3<sup>rd</sup> body debris is facilitated by fluid transport during sublaxation. The high prevalence of indentation damage found on the rim of retrieved acetabular liners from femoral neck impingement (Shon W Yong et al., 2005) suggests that sublaxation events are frequent. To study sublaxation-induced particle ingress, a computational fluid dynamics (CFD) model has been developed to quantify the ensuing fluid motions. The focus of the present study was on the effects of variations in implant design parameters on fluid velocity.

## METHODS

CFD model geometry was created using Truegrid v2.1.5, and solutions were obtained using ADINA v8.2. The region of interest for the CFD model was the capsule-enclosed joint space, plus the bearing region between the femoral head and acetabulum (Figure 1). Kinematics for femoral head movement were taken from output data from a finite element model of leg-cross dislocation (Nadzadi ME et al., 2002) from the beginning of hip sublaxation (impingement initiation). The leg-cross sublaxation event

corresponded to ~0.60 mm separation after .012 seconds. Four variables were parametrically studied: femoral head diameter, bevel angle and face width of the chamfer, and thickness of clearance between the femoral head and acetabulum. The baseline case consisted of a 28mm femoral head diameter, 0.1 mm clearance between the femoral head and acetabular component, a chamfer consisting of 25% of the polyethylene liner thickness at an angle of 30°, and fluid modeled as Newtonian and incompressible (viscosity of 1.0 Pa·s (Mazzucco D et al., 2002). Outer capsule boundaries were modeled as rigid with no-slip conditions, and the femoral head was modeled as a moving rigid boundary.

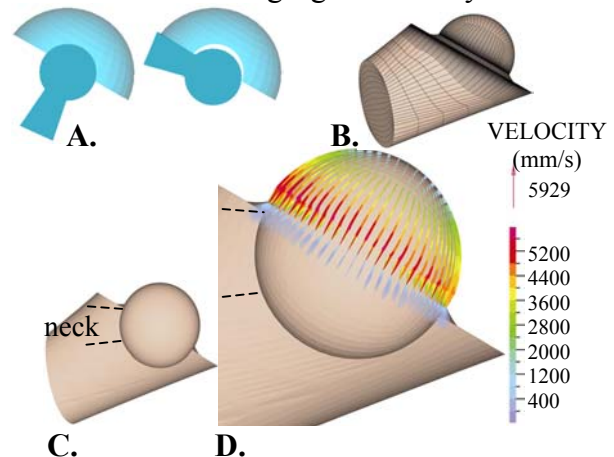


**Figure 1.** 3D CFD model (frontal view for a right hip). A. Schematic indicating sublaxation. B. Outer model view with visible mesh. C. Transparent view of the model with visible femoral head surface. D. Fluid velocity vectors at the beginning of the sublaxation for a 28 mm femoral head.

## RESULTS AND DISCUSSION

As seen in Figure 1, the subluxation resulted in very high fluid velocity along the entrance to the gap between the femoral head and acetabular cup (maximum 5929 mm/s for a 28 mm head, ~120 times the femoral head velocity). This fluid velocity decreased from the gap entrance to the pole of the cup. Fluid velocity at the beginning of subluxation was compared for three head sizes and three clearance widths along an equatorial line in the model (Figure 2). The greatest ingress velocities were seen on the anterosuperolateral acetabular cup edge (~300°-0°, Figure 2), and lowest ingress velocities were seen posteriorly (~120°-180°). Larger head sizes and smaller gap widths resulted in greater fluid velocity (Figure 2).

Fluid pathlines were calculated by integrating the velocity solutions, to determine sites to which suspended 3<sup>rd</sup> body particles could be transported during leg-cross subluxation. As an example, fluid initially just outside the entrance to the gap between the femoral head and acetabular cup at point (1) (Figure 3) moved into the gap at the beginning of the subluxation, and moved towards the pole of the cup throughout the subluxation. At the end of the subluxation, the end of the pathline was 11° away from the pole of the cup.

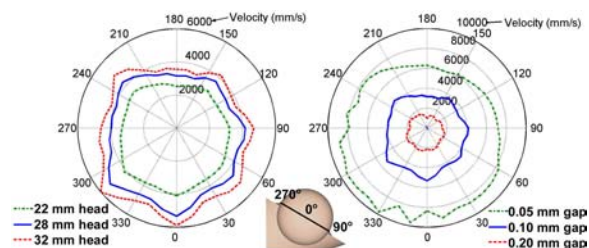


**Figure 2.** Ingress velocity magnitude at an equatorial line around the femoral head at the entrance to the gap between the femoral head and acetabulum, for the beginning of the subluxation.

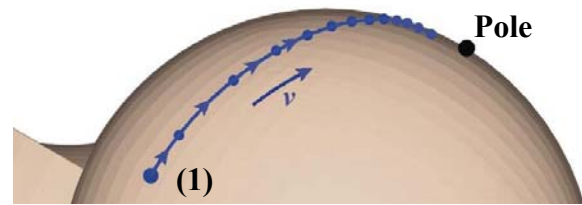


**Figure 3.** Pathline for fluid beginning at location (1) during the leg-cross subluxation. Each dot along the pathline indicates the position of the fluid for successive time points, in 0.001-second increments, up to the end of the subluxation (0.012 s).

## SUMMARY

The data indicate that 3<sup>rd</sup> body debris suspended in joint fluid could be drawn nearly to the pole of the cup with even very small separations of the femoral head (<0.6 mm). Debris suspended near the entrance to the cup just before the subluxation begins can reach a “latitude” of 79°. Larger head diameters and smaller clearance widths had increased fluid velocity at all points around the entrance to the gap compared to smaller head sizes and larger clearance widths, respectively. Fluid velocity was greatest along the anterosuperolateral cup edge for all head sizes and clearance widths. Although absolute fluid velocity was greater, however, fluid pathlines indicated that suspended debris would reach nominally similar angular positions on the cup with larger head sizes.

## REFERENCES

- Shon, W. Yong et al. (2005). *J. Arthroplasty*, **20**(4), 427-435.  
 Nadzadi, M.E. et al. (2002). *Clin. Biomech.*, **17**(1), 32-40.  
 Mazzucco, D. et al. (2002). *J. Orthop. Res.*, **20**(6), 1157-1163.

## ACKNOWLEDGEMENTS

Supported by grants from the NIH (AR44106, AR47653), DePuy, Inc., and an NSF graduate research fellowship.

# A LIQUID CRYSTAL MODEL FOR BILAYER LIPID MEMBRANES

Raffaella De Vita, David Hopkinson, Donald J. Leo  
 Center for Intelligent Material Systems and Structures  
 Mechanical Engineering Department  
 Virginia Tech, VA, USA  
 E-mail: devita@vt.edu

## INTRODUCTION

Bilayer lipid membranes (BLMs) constitute the base component of cell membranes. They exhibit orientational order like crystal solids but they flow like amorphous liquids. Their rigidity permits confining the cell contents and preserving the cell shape while their ordered structure regulates the transport of substances in and out the cell. Their fluidity enables the transport phenomena to occur rather quickly. These peculiar properties are typical of liquid crystals. Indeed, BLMs are recognized to be Smectic liquid crystals since their molecules form layered structures with defined interlayer spacing. In particular, BLMs are classified as Smectic A liquid crystals due to the fact that their molecular axes are normal to the layers.

At CIMMS (Center for Intelligent Material Systems and Structures), preliminary experiments have been conducted to evaluate the maximum pressure that synthetic BLMs can withstand (Hopkinson et al., 2006). Together with experiments, constitutive models need to be developed not only to help the interpretation of the experimental results but also to guide the design of these experiments.

A mathematical model that describes the small deflections of a circular BLM under constant pressure will be presented. The model is formulated within the theoretical framework of the continuum theory of liquid crystals set forth by de Gennes (de Gennes and Prost, 1993).

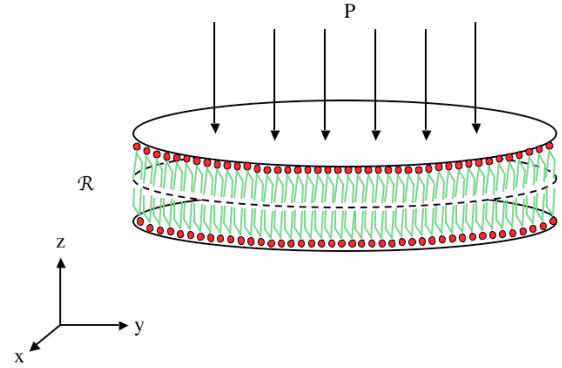


**Figure 1:** Coordinate system for the BLM.

## MATHEMATICAL MODEL

Let  $R$  be the region occupied by the BLM and  $\mathbf{n}$  a unit vector, called director, which defines the average alignment of the lipid molecules. Let consider a coordinate system as shown in Figure 1. If the BLM is assumed not to bend very much from the  $x$ - $y$  plane and not to strongly compress, the bulk elastic energy has the form (de Gennes and Prost, 1993)

$$F = B \left( \frac{\partial u}{\partial z} \right)^2 + \frac{K_1}{2} \left( \frac{\partial^2 u}{\partial x^2} + \frac{\partial^2 u}{\partial y^2} \right)^2 + 2K_1 \left( \left( \frac{\partial^2 u}{\partial x \partial y} \right)^2 - \frac{\partial^2 u}{\partial x^2} \frac{\partial^2 u}{\partial y^2} \right), \quad (1)$$

where  $u(x, y, z)$  is the vertical displacement of the layer,  $B$  and  $K_1$  are constants with energy length<sup>-3</sup> and energy length<sup>-1</sup> dimensions, respectively. The first term in equation (1) defines the compressive (dilatational) energy while the other terms define the elastic splay energy.

It is assumed that for small displacements to the initial alignment the director  $\mathbf{n}$  is given by

$$\mathbf{n} \approx (-u_x, -u_y, 1), |u_x|, |u_y| \ll 1.$$

In the experimental study, the BLM is reconstituted over a polycarbonate substrate with cylindrical pores and, subsequently, subjected to hydrostatic pressure. For this reason, the energy integral that results from the sum of the bulk elastic energy and the work done by the constant pressure  $P$  per unit area acting on the BLM is considered. It has the form

$$\int_R B \left( \frac{\partial u}{\partial z} \right)^2 + \frac{K_1}{2} \left( \frac{\partial^2 u}{\partial x^2} + \frac{\partial^2 u}{\partial y^2} \right)^2 + 2K_1 \left( \left( \frac{\partial^2 u}{\partial x \partial y} \right)^2 - \frac{\partial^2 u}{\partial x^2} \frac{\partial^2 u}{\partial y^2} \right) - Pu \, dR \quad (2)$$

The functional (2) need to be minimized to derive the equilibrium equations for the BLM by using variational methods

## RESULTS AND DISCUSSION

The predictions of the model are obtained by assuming that the compression of the BLM is negligible and that the deflection of the circular BLM has radial symmetry. Under these assumptions, the solution of the equilibrium equations in polar coordinates with the origin in the center of the BLM is

$$u(r) = \frac{P}{64hK_1} (r^2 - R^2)^2, \quad (3)$$

where  $h$  is the thickness of the BLM and the edges of the circular BLM are considered to be clamped. In Figure 2, solution (3) is plotted for  $P=-1$  kPa,  $R=0.4$   $\mu\text{m}$ ,  $h=5$  nm as dictated by preliminary experimental studies and for different values of elastic constant  $K_1$ .

Additional theoretical and computational studies are being performed to model the

mechanical behavior of the BLMs under less restrictive assumptions on the form of the deflection. In addition, new experiments are being designed to accurately measure the pressure that the BLMs can withstand.

## CONCLUSIONS

A continuum model that describes the small deflections of BLMs under constant pressure by accounting for their Smectic A liquid crystalline structure is proposed. The predictions of the model are obtained by assuming that the deflections have radial symmetry and by using values of the material parameters that are suggested by preliminary experimental observations.

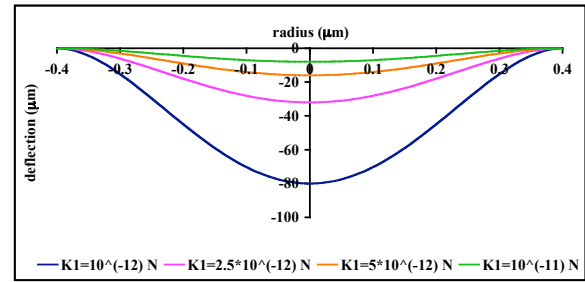


**Figure 1:** Deflection  $u$  of a circular BLM plate of radius  $r$  under constant pressure.

## REFERENCES

- de Gennes, P.G., Prost, J.Y. (1993). *The Physics of Liquid Crystals*, Oxford Science Publications, second edition.  
Hopkinson, D., De Vita R., Leo, D.J. (2006) *Proceeding of SPIE*.

## ACKNOWLEDGEMENTS

This research was carried out with the support of the DARPA contract no. WN11NF-04-1-0421. R. De Vita was supported in part by the Special Projects Office at DARPA through a NASA contract. The authors gratefully acknowledge the support.

# MULTIAXIAL RESPONSE OF HUMAN CEREBRAL ARTERIES

Monson, K. L., Barbaro, N. M., Manley, G. T.

Department of Neurological Surgery, University of California, San Francisco, USA  
Email: kmonson@me.berkeley.edu

## INTRODUCTION

Head trauma frequently involves damage to the cerebral blood vessels (Graham, 1996), and even when the vessels are not damaged, evidence from recent studies suggests that they contribute to the overall response of the brain as a vital piece of its composite structure (Zhang et al, 2002; Parnaik et al, 2004). Thus, characterization of cerebral vessel mechanical response is a necessary step in the development of more accurate models of traumatic brain injury (TBI). Though it was limited to tests in the axial direction, a recent study of these vessels found that the arteries are significantly stiffer than the veins, and that they fail at a lower level of stretch (Monson et al, 2003). On the subject of TBI, then, the arteries are believed to be the more important vessel to characterize – outside of the critical role of the bridging veins in the production of subdural hematoma – and are the focus of this study.

Previous investigations of the mechanical behavior of human cerebral arteries are few and generally focus on a single direction of loading, usually consistent with the particular problem motivating the study, rather than on multi-axial response. While it is believed that axial stretch is the primary mode of vessel deformation in TBI, it is important to define how stretch is influenced by internal pressurization. Data reported here define this effect and pave the way for the development of constitutive relations appropriate for study of TBI as well as other problems involving the cerebral vasculature.

## METHODS

Five arteries were obtained from the surface of the temporal lobe in patients undergoing temporal lobectomy for the treatment of epilepsy. Accompanying tissue was carefully dissected away under a microscope, and vessel branches were occluded by tying with suture. Microspheres were positioned along the length of each specimen to allow tracking of deformation through video. The ends of each vessel were then cannulated with needles and attached to a custom device capable of controlling both axial stretch and internal pressure and were subjected to various load combinations within the physiological range. All experiments were conducted at quasi-static rates.

Axial force and internal pressure data, along with cross-sectional information and video measurements of axial motion and diameter, were used to calculate mean stretch and Cauchy stress values in the axial and circumferential directions. The radially-cut, zero-stress section was used as the reference configuration, and incompressibility was assumed. Stiffness values – defined as  $\Delta(\text{stress}) / \Delta(\text{stretch})$  – around in situ loading conditions were calculated and compared for the two directions of loading.

## RESULTS AND DISCUSSION

Data from experiments consisting of tests both where axial stretch was held constant at various levels while internal pressure was increased and where internal pressure was

held approximately constant while axial stretch was increased demonstrate an interdependence between the axial and circumferential behaviors (**Figure 1**), with increased constant stretch in one direction

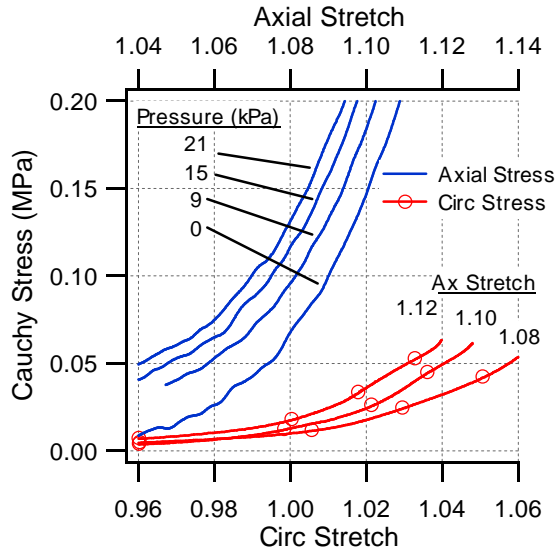


**Figure 1** Cauchy stress-stretch response in the axial and circumferential directions for various combinations of physiological loading conditions

resulting in a shift upward and/or to the left for the direction of increasing stretch.

Because the figure is scaled so as to allow direct comparison of response for the two directions, it is also clear that when these vessels are deformed from in situ conditions, they are more resistant to increases in length than diameter. As Table 1 demonstrates, axial stiffness was higher than circumferential stiffness for all five specimens, though there is significant variation in the degree to which this is true.

**Table 1** Individual and mean in situ circumferential and axial stiffness values, and their ratio.

Specimen	Stiffness Circ, $E_c$ (MPa)	Stiffness Axial, $E_z$ (MPa)	$E_z / E_c$
1	0.72	2.22	3.08
2	0.82	8.62	10.51
3	0.95	3.35	3.53
4	0.60	3.81	6.35
5	0.92	2.71	2.95
<b>Mean</b>	<b>0.80</b>	<b>4.14</b>	<b>5.28</b>

While stiffness variations and interdependence between directions of loading are both expected findings for vasculature in general (Humphrey, 2002), the relative magnitudes of these characteristics have not been previously reported for human cerebral arteries. These multi-axial response data are vital for the construction of constitutive equations for use in models investigating a variety of problems involving the cerebral arteries.

## SUMMARY/CONCLUSIONS

The reported multi-axial data for human cerebral arteries confirm the interdependence of loading directions and reveal that, under in situ loading conditions, the vessels are stiffer in response to extension than to circumferential stretch.

## REFERENCES

- Graham, DI (1996). In: Nrayan et al (eds) *Neurotrauma*, McGraw-Hill, pp. 43-59.
- Humphrey, JD (2002). *Cardiovascular Solid Mechanics*, Springer-Verlag.
- Monson, KL, et al (2003). *J Biomech Eng* 125(2): 288-294.
- Parnaik, Y, et al (2004). *Stapp Car Crash Journal* 48: 259-277.
- Zhang, L, et al (2002). *Stapp Car Crash Journal* 46: 145-163.

## ACKNOWLEDGEMENTS

This work was supported by a grant from the CDC (R49 CE000460).

# EFFECT OF LIMITING THE NUMBER OF STEPS ON THE THRESHOLD OF BALANCE RECOVERY

Marc-André Cyr and Cécile Smeesters

Research Center on Aging, Sherbrooke, QC, Canada  
Department of Mechanical Engineering, Université de Sherbrooke, Sherbrooke, QC, Canada  
E-mail: Cecile.Smeesters@USherbrooke.edu Web: www.cdrv.ca

## INTRODUCTION

There are only a dozen or so studies that have used sufficiently large postural perturbations that balance recovery and avoiding a fall is not always possible. Moreover, there are few results and several controversies among these studies at the threshold of balance recovery. In particular, the effect of limiting the number of steps on the threshold of balance recovery has not been quantified, despite experimental evidence that older adults often take more than one step to recover balance following small and medium postural perturbations (Hsiao and Robinovitch, 2001; Luchies et al., 1994; Maki et al., 2000; McIlroy and Maki, 1996). The purpose of this study was to determine the effect of limiting the number of steps on the ability to recover balance to avoid a fall.

## METHODS

Balance recovery following sudden release from an initial forward lean was performed by 28 healthy younger adults, 14 males and 14 females ( $24.8 \pm 2.5$  yrs,  $1.73 \pm 0.11$  m,  $71.3 \pm 13.8$  kg).

The maximum forward lean angle from which each participant could be suddenly released and still recover balance was determined using i) only a single step, ii) no more than two steps and iii) no limitations on the number of steps. The forward lean angle was sequentially increased until the

participants failed to recover balance twice at a given forward lean angle and the limitations on the number of steps were randomly ordered.

Maximum forward lean angles, reaction times, weight transfer times, step times, step lengths and step velocities were measured using force platforms (OR6-7, AMTI, Newton MA) and a motion measurement system (Optotrak, NDI, Waterloo ON). Data were analysed using one-way analyses of variances with repeated measures (SPSS Version 12, Chicago IL).

## RESULTS AND DISCUSSION

Limiting the number of steps did affect the threshold of balance recovery (Figure 1 and Table 1). In particular, it significantly affected the maximum forward lean angles but only by 1.1 deg.

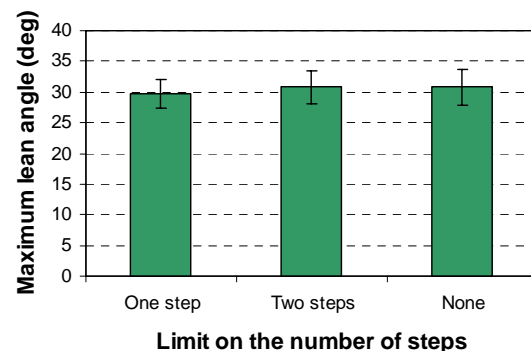


**Figure 1:** Effect of limiting the number of steps on the threshold of balance recovery ( $p = 0.013$ )

At the maximum forward lean angles, limiting the number of steps significantly affected (Table 1):

- Reaction times but only by 4 ms;
- Weight transfer times, step lengths and step velocities of the first step but only by 9 ms, 0.103 m and 0.18 m/s, respectively;
- Step velocities of the second step by 0.69 m/s.

However, at the maximum forward lean angles, limiting the number of steps did not affect (Table 1):

- First step times;
- Weight transfer times, step times and step lengths of the second step.

Therefore, despite the significant effect of limiting the number of steps on the threshold of balance recovery, the differences are very small and all within the experimental standard deviations.

## CONCLUSIONS

The results have shown that restricting balance recovery to only a single step does

not affect ones ability to recover balance to avoid a fall. Moreover, it does not affect kinematic performance measures of the first step of balance recovery. Future studies are needed to confirm these results in healthy older adults.

## REFERENCES

- Hsiao, E.T., Robinovitch, S.N. (2001). *J. Gerontol.* **56**(1), M42-47.
- Luchies, C.W., et al. (1994). *JAGS* **42**(5), 506-512.
- Maki, B.E., et al. (2000). *J. Gerontol.* **55A**(5), M270-277.
- McIlroy, W.E., Maki, B.E. (1996). *J. Gerontol.* **51A**(6), M289-296.

## ACKNOWLEDGEMENTS

We gratefully acknowledge the assistance of Hugo Bastien, Sandra Demers and Mathieu Hamel along with the support of grant 298229-04 from the Natural Sciences and Engineering Research Council of Canada as well as a graduate scholarship from the Canadian Institutes of Health Research.

**Table 1:** Effect of limiting the number of steps on the threshold of balance recovery  
N = 28 unless indicated (mean  $\pm$  SD)

Limit on the number of steps	One step	Two steps	None	p
<b>Maximum lean angle (deg)</b>	29.7 $\pm$ 2.3	30.8 $\pm$ 2.8	30.8 $\pm$ 2.9	<b>0.013</b>
<b>Reaction time (ms)</b>	83 $\pm$ 12	87 $\pm$ 7	86 $\pm$ 10	<b>0.028</b>
<b>First step</b>				
Weight transfer time (ms)	160 $\pm$ 21	151 $\pm$ 20	154 $\pm$ 21	<b>0.034</b>
Step time (ms)	195 $\pm$ 23	180 $\pm$ 29	185 $\pm$ 26	0.063
Step length (m)	0.984 $\pm$ 0.136	0.881 $\pm$ 0.151	0.903 $\pm$ 0.155	<b>0.008</b>
Step velocity (m/s)	5.06 $\pm$ 0.51	4.91 $\pm$ 0.47	4.88 $\pm$ 0.50	<b>0.043</b>
<b>Second step (N = 20)</b>				
Weight transfer time (ms)	n/a	54 $\pm$ 20	52 $\pm$ 36	0.778
Step time (ms)	n/a	272 $\pm$ 54	347 $\pm$ 165	0.052
Step length (m)	n/a	1.132 $\pm$ 0.282	1.076 $\pm$ 0.327	0.309
Step velocity (m/s)	n/a	4.23 $\pm$ 0.98	3.54 $\pm$ 1.38	<b>0.010</b>

# EFFECT OF WALKING POLES ON DYNAMIC GAIT STABILITY

Young-Hoo Kwon<sup>1</sup>, Tobin Silver<sup>1</sup>, Joong-Hyun Ryu<sup>1</sup>, Sukhoon Yoon<sup>1</sup>,  
Robert Newton<sup>2</sup>, and Jae Kun Shim<sup>3</sup>

<sup>1</sup>Texas Woman's University, Denton, TX, USA

<sup>2</sup>Edith-Cowan University, Joondalup, WA, Australia

<sup>3</sup>University of Maryland, College Park, MD, USA

E-mail: [YKwon@mail.twu.edu](mailto:YKwon@mail.twu.edu)

## INTRODUCTION

Decreased balance is a major contributor to accidental falls in the elderly. Ninety percent of hip fractures are caused by these falls and 12% to 20% of the fractures are fatal (Carter et al., 2001).

Gait stability is affected by mechanical factors such as mass, size of the base of support (BOS) and the relative position of the center of mass (COM) to the boundary of the BOS. Age-related adaptations occur in walking to create a more stable, but less efficient walking pattern (Cromwell & Newton, 2004) due to diminished balance. Methods used to assess stability and/or balance include COM trajectory, BOS size, limits of stability (LOS), and gait stability ratio.

Falls can be prevented by improving balance and increasing stability. Although exercise can improve balance, physical weakness and fear of fall prevents the frail elderly from exercising. Assistive walking devices are often prescribed for these individuals to increase stability and to provide a sense of safety. Telescope-style walking poles (T-poles) (Yoon et al., 2005) are an assistive device intended to provide additional support and a wider BOS, thus increasing stability. The purpose of this study was to examine the effect of T-poles on dynamic gait stability parameters. It was hypothesized that T-poles would

significantly alter gait stability parameters, increasing gait stability.

## METHODS

A total of ten healthy elderly volunteers (65+ years old) participated in this study (5 male and 5 female;  $67.1 \pm 6.1$  yrs.;  $169.8 \pm 7.4$  cm;  $78.2 \pm 13.8$  kg). All participants were required to enroll in a 2-month long pole walking program using telescope-style walking poles (Martin Van Breems, Inc., Norwalk, CT). The walking program consisted of mandatory weekly pole training sessions (1 hr/wk) and a minimum of 120-min/wk voluntary pole walking. Participants were tested at the end of the walking program.

Three-dimensional video motion analysis (DLT method) was performed to obtain the whole body COM position and the positions of the toe and heel markers. Hand drawn footprints marked with the locations of the toe and heel markers were videotaped and the contour was then digitized to obtain the real-life coordinates of the contour based on the 2-D DLT. In dynamic BOS computation, the heel and toe markers from the footprint were matched to the actual heel and toe marker positions at heel-strike and toe-off, respectively, obtained through motion analysis.

Participants performed gait trials in 4 different conditions: 2 pole conditions

(with/without poles) x 2 walking speeds (preferred and 15% faster). The COM trajectory was projected to the ground in computing dynamic gait stability parameters. The gait cycle was divided into phases based on the support types (normal walking: 4 phases, single to double supports; pole walking: 8 phases, double to quadruple supports) and the location of the COM with respect to the BOS (in-phase and out-phase). The computed stability parameters included max attainable BOS (MABOS), in-phase time (T), minimum COM distance to the closest inner edge of the MABOS during the in-phase ( $D_{min}$ ), and maximum COM distance to the closest outer edge during the out-phase ( $D_{max}$ ). In the MABOS computation, it was assumed that the entire foot is in contact with the ground in each phase.

Two-way (2 pole conditions x 2 speed conditions) RM ANOVA ( $p < .05$ ) was performed for statistical analysis followed by post-hoc comparisons (Sidak adjustment), if necessary.

## RESULTS AND DISCUSSION

Pole walking resulted in significantly larger mean MABOS than normal walking in both

speed conditions (Table 1). T-poles also increased  $D_{min}$  significantly with no effect on  $D_{max}$ . T significantly increased due to the use of the T-poles.

MABOS almost tripled on the average by the use of the T-poles. Pole walking was also characterized by an increased in-phase time.  $D_{min}$  reflects the magnitude of the gravitational torque that helps maintaining the equilibrium during the in-phase, while  $D_{max}$  reflects the magnitude of the gravitational torque that facilitates loss of equilibrium (forward motion of the COM) during the out-phase. T-poles increased  $D_{min}$  while not affecting  $D_{max}$ .

## SUMMARY AND CONCLUSIONS

The T-poles provided increased gait stability at both preferred and fast speeds in general by mainly increasing MABOS, T, and  $D_{min}$ .

## REFERENCES

- Carter, D. N. et al. (2001). *Sports Medicine*, **30**, 427-437.  
 Cromwell, L.R., Newton, A. R. (2004). *J. Aging and Physical Activity*, **11**, 90-100.  
 Yoon, S. et al. (2005). *Proceedings of the XXth ISB Congress*, 825.

**Table 1.** Comparison of the Dynamic Gait Stability Parameters ( $p < .05$ )

		Pole		Speed		Pole-Speed			
		W/O	W	P	F	W/O-P	W/O-F	W-P	W-F
Mean MABOS (cm <sup>2</sup> ) <sup>‡</sup>	M	493.6	1,448.1	927.5	1,014.2	496.3	490.8	1,358.6*	1,537.6* <sup>†</sup>
	SEM	14.1	53.4	31.8	31.1	15.1	14.4	56.1	54.5
$D_{min}$ (cm)	M	2.8	4.5*	3.7	3.7	3.0	2.7	4.4	4.7
	SEM	0.4	0.6	0.5	0.5	0.3	0.5	0.8	0.6
$D_{max}$ (cm)	M	20.4	20.7	18.8	22.2 <sup>†</sup>	19.3	21.4	18.3	23.0
	SEM	0.9	1.6	1.1	1.3	2.2	1.5	1.6	2.6
T (%)	M	39.4	61.2*	53.2	47.4 <sup>†</sup>	41.7	37.1	64.8	57.6
	SEM	3.2	2.0	2.1	2.3	2.7	4.0	2.2	2.1

\* Significantly different from the matching normal walking condition

<sup>†</sup> Significantly different from the matching preferred walking speed condition

<sup>‡</sup> Significant interaction

# PRINCIPAL COMPONENT ANALYSIS DEMONSTRATES TRUNK MUSCLE ACTIVATION PATTERN VARIATION WITH FALL DIRECTION

Timothy D Craig and Sara E Wilson

University of Kansas, Lawrence, KS, USA  
E-mail: sewilson@ku.edu

## INTRODUCTION

Falls are a risk factor for both low back injury in working aged adults and vertebral fractures in the elderly. Slips and falls have been found to be associated with low back injuries in studies of injury rates in industry (Bigos, 1986, Manning, 1984, Manning, 1981). Studies have also shown that falls play a role in the etiology of age-related vertebral fractures (Myers, 1997, Cooper, 1992).

Trunk muscle activation during a fall is not well understood. In particular, there has been little research on how falls in different directions may influence trunk muscle activation. Principal component analysis facilitates examination of overall patterns in data such as electromyographic data. In this study, principal component analysis was used to examine the influence of fall direction on lumbar erector spinae (ES) muscle activation in order to be able to understand some of the factors that influence trunk muscle activation during descent.

## METHODS

18 subjects (9 male and 9 female) between 19 and 34 yrs old were tested with the approval of the human subjects committee at the University of Kansas. 8 surface electromyographic (EMG) sensors (Delsys, Boston, MA) were used to assess the trunk muscle groups (ES/RA/IO/EO). Data from these sensors was collected at 1500 Hz, filtered to remove electrical noise, rectified

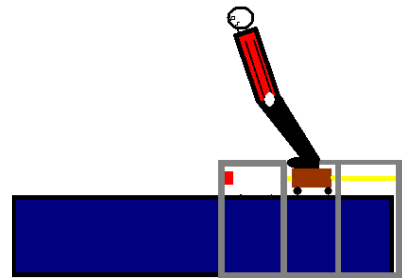


**Figure 1.** Experimental design - a narrow platform on wheels, initially positioned over the mat, slides horizontally, accelerating the lower portion of the body until center of mass is outside the area of stability.

and integrated with a Hanning, 100 point, window filter. Pelvis motion was also collected at 100Hz with 4 electromagnetic sensors located around the subject's pelvis (Ascension, Burlington, VT).

To analyze the muscle activation in the trunk due to falls, a slipping fall was created. A subject stood on a platform as it moved out from under the subject causing the subject to fall onto a soft padded mat. Although falls are commonly associated with gait, this approach removes influences of gait and allows direction to be controlled. Subjects were instructed to remain motionless on the platform and avoid attempting to maintain balance once the slider began moving. Subjects completed 4 block-randomized trials facing 8 directions on the slider representing falls in every 45° orientation from the anterior direction.

The data was examined between platform release and impact on level ground. Trials were removed if the power spectrum and the

raw EMG signal indicated a loss of the sensor during collection. Principal component analysis (PCA) was used to examine the integrated EMG data. The data was rotated from the parameter space to orthogonal planes through the use of eigenvectors of the covariance matrix. This allowed reduction while maintaining account for a high percent of the within data variability.

## RESULTS AND DISCUSSION

The 958 PCA modes for the erector spinae muscle groups could be reduced while still explaining a high percentage of the within data variance. Examining the first 5 and 10 PCA modes explained 80% and 95% of the variability. PCA 1 described 29.7% of the variance with a distinct activation at 550ms. PCA 2 described 20.5% of the variance with a peak at 350-400ms. PCA 3 described 16.7% of the variance with a distinct activation peak at 190ms.

Examination of PCA 3 demonstrated the earliest, reflex-like response followed by a preparatory response for impact. This mode was influenced by fall direction (Figure 3) with increased activation of the response in the right ES with left lateral falls and in the left ES with right lateral falls.

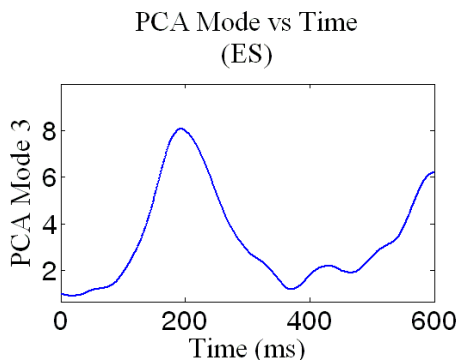


**Figure 2.** Examining PCA mode 3 vs time there is a distinct activation peak at 190ms.

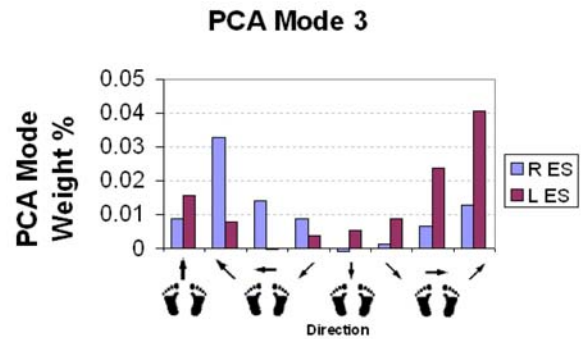


**Figure 3.** Examination of PCA mode 3 shows a difference based on fall direction where falls to the opposite side of the muscle will elicit a greater reflex response.

## SUMMARY/CONCLUSIONS

Trunk muscle response to sudden slips and falls is not well understood. This research suggests that using principal component analysis allows for a reduction of data while maintaining an explanation of a high percentage of the data variation. Analysis demonstrates early muscular response is influenced by fall direction. Erector Spinae activity opposite the fall direction elicited a greater initial response during falls.

## REFERENCES

- Bigos, S.J., et al. (1986), *Spine*, Vol. 11, pp. 246-51.
- Manning, D.P., et al. (1984), *Spine*, Vol. 9, pp. 734-9.
- Manning, D.P. and Shannon, H.S. (1981), *Spine*, Vol. 6, pp. 70-2.
- Myers, E.R. and Wilson, S.E. (1997), *Spine*, Vol. 22, pp. 25S-31S.
- Cooper, C., et al. (1992), *J Bone Miner Res*, Vol. 7, pp. 221-7.

## ACKNOWLEDGEMENTS

Part of the work upon which this publication is based was performed pursuant to the National Institute on Aging grant number 2R44-AG018667-02 under agreement to Barron Associates, Inc.

## MULTI-DIGIT MANIPULATION OF A CIRCULAR OBJECT

Junfeng Huang<sup>1</sup>, Mark L. Latash<sup>2</sup>, Vladimir M. Zatsiorsky<sup>2</sup>, Jae Kun Shim<sup>1</sup>

<sup>1</sup>Department of kinesiology, University of Maryland, College Park, MD

<sup>2</sup>Department of kinesiology, Pennsylvania State University, University Park, PA

E-mail: [jkshim@umd.edu](mailto:jkshim@umd.edu) Web: [www.hhp.umd.edu/KNES/faculty/jkshim/neuromechanics](http://www.hhp.umd.edu/KNES/faculty/jkshim/neuromechanics)

### INTRODUCTION

Manipulation of a circular object is common in daily activities such as opening a door knob, a jar cap, etc. Previous studies of multi-digit prehension mainly focused on a prismatic precision grip, i.e. the grip by the tips of the digits in which the thumb and the fingers oppose each other (reviewed in Zatsiorsky, Latash 2004). While several previous studies have addressed the manipulation of circular objects, they have been limited to force exerted by single digit (Fowler et al. 1999, Kinoshita et al. 1996). As in any multi-digit manipulation, the studied task is mechanically redundant. In particular, due to the kinetic redundancy, the sharing of the total force among the individual digits cannot be predicted solely from mechanical considerations. This study focuses on the individual digit-tip forces and moments during a torque/moment production on a mechanically fixed circular object.

### METHODS

*Experiment:* A circular aluminum handle and five six-component sensors (Nano-17, ATI Industrial Automation, Garner, NC) were used in the experiment. The sensors were attached to the handle with their centers positioned at the preferred angular positions of fingers measured in a prior all-digit natural prehension test. The whole circular handle with the sensors was mechanically fixed to the head of a heavy tripod. The position of the handle could be adjusted by adjusting the tripod head.

*Procedure:* Ten healthy, right-handed volunteers participated in the experiment.

The subjects sat on a chair and placed their right upper arm in a forearm brace that was fixed on a table. The forearm was secured with Velcro straps. The subjects produced maximum moment about a horizontal axis perpendicular to the grasp plane (the plane passing through the centers of all five digit force sensors). X- and Y- axes were horizontal and vertical axes in the grasp plane, respectively. The tasks included isometric maximum torque production about anterior-posterior axis and medial-lateral axis, both in the clockwise and counterclockwise directions.

*Data Processing:* Average normal forces, tangential forces, and moments of tangential force from each digit were calculated. The safety margin (SM) of normal force was calculated as the magnitude difference between applied normal force and minimal normal force required to prevent slipping of digit tips from contact surface (Kinoshita et al. 1996). The internal force and resultant force (the force which cancels out each other due to the opposite directions and the net force which will cause translation effect if the object is not mechanically fixed, Gao et al. 2005) were also calculated. Regression analysis and repeated measures ANOVA with within-subject factors of DIGIT [5 levels: thumb (T), index (I), middle (M), ring (R), and little (L)], AXIS [2 levels: AP and ML axes], DIRECTION [2 levels: opening (OP) and closing (CL) directions of a jar/valve] and COORDINATE [2 levels: anteroposterior (X) and vertical (Y) axes] were performed.

## RESULTS

### 1. Individual digits normal force and moment

Larger moments were found in CL direction than in OP. At the maximum moment production, the thumb and little fingers showed the largest and smallest normal forces, respectively. The ranks of sharing of the total moment by individual digits were in the order of anatomical digit alignments from the thumb to the little, Table 1.

Table 1. Individual digits sharing of normal force and moment at the time of maximum resultant torque production

Sharing	Thumb	Index	Middle	Ring	Little
Normal Force	40.8%	15.5%	18.0%	18.8%	6.9%
Moment	38.8%	21.8%	15.6%	15.2%	8.6%

### 2. Internal and Resultant force

Subjects produced about twice as large an internal force along the X-axis than the Y-axis. This reflects that the internal force was larger in the direction of thumb normal force than in the direction orthogonal to it. The internal force was 20% larger in CL than in OP and 14% larger in ML axis than AP axis. All subjects showed negative resultant forces along the X-axis during moment production in CL and positive resultant forces along X-axis and Y-axis for all other conditions. In other words, the thumb force along the X-axis was smaller than the resultant force of four fingers along the X-axis for the CL direction, but larger for the OP direction. No significant effect in resultant force, however, was found in single factor: AXIS, DIRECTION, or COORDINATE. Significant interactions in resultant force magnitudes were found in AXIS×DIRECTION.

### 3. Safety margins of forces and force angles

The thumb showed the largest safety margin of normal force and little finger showed the smallest one. The safety margin of normal

force for the ML axis was larger than for the AP axis. No significant DIRECTION effect was found, however, a significant effect of DIGIT×DIRECTION was observed. The relative values of the safety margins (percent of the exerted normal forces) showed the largest and smallest values in the ring and index finger, respectively. There were significant effects of AXIS and all factor interactions, but no significant effect of DIRECTION.

The safety margins of individual digits' force angles showed different results. The safety margins of force angles were larger for the ML axis than for the AP axis. A significant DIRECTION effect was not found, but there were significant effects of all factor interactions.

## CONCLUSIONS

No equilibrium requirements are needed when manipulating a mechanically fixed object in contrast with manipulating a free object. In this situation, the pattern of force sharing might be different from the results previously found in a mechanically-free environment. From this study on five-digit maximum torque productions on a circular object, we conclude that: (1) the maximum torque in the closing direction is larger than in the opening direction, (2) the thumb and little finger have the largest and the smallest sharing for both total normal force and total moment, respectively, and (3) the normal force safety margins have the largest values in the thumb and the smallest values in the little finger, respectively.

## REFERENCES

1. Zatsiorsky et al. (2002). *Bio Cybern*, 87:50-7.
2. Fowler et al. (1999). *Clin Biomech*, 14:646-52,
3. Kinoshita et al. *Ergonomics* 39:1163-76, 1996
4. Gao et al. *Exp Brain Res* 165:69-83, 2005

## ACKNOWLEDGEMENTS

NIH grants AG-018751, AR-048563, M01 RR10732, and NS-35032



# HIP STRENGTH AND RUNNING MECHANICS IN FEMALES WITH AND WITHOUT PATELLOFEMORAL PAIN SYNDROME

John D. Willson<sup>1</sup> and Irene Davis<sup>1,2</sup>

<sup>1</sup> Department of Physical Therapy, University of Delaware, Newark, DE, USA

<sup>2</sup> Drayer Physical Therapy Institute, Hummelstown, PA, USA

Email: willson@udel.edu

Web: [www.udel.edu/PT/davis/index.htm](http://www.udel.edu/PT/davis/index.htm)

## INTRODUCTION

Patellofemoral pain syndrome (PFPS) remains a common orthopedic complaint, especially among active females. Females with PFPS possess decreased hip strength than healthy females, which may contribute to a tendency to perform weightbearing activities with greater hip adduction and internal rotation (Ireland et al., 2003). These rotations are believed to increase retropatellar pressure and may lead to PFPS symptoms (Li et al., 2004).

Long term studies of PFPS suggest that pain and functional limitations may persist for years after traditional conservative care (Kannus et al., 1999). Persistent abnormal mechanics associated with high retropatellar pressure during weightbearing may be responsible for these prolonged deficits. Additionally, such mechanics may lead to early degeneration of PF joint articular cartilage and premature PF osteoarthritis (Utting et al., 2005).

The purpose of this ongoing study is to compare hip strength and LE mechanics during running among females with and without PFPS. We expect that females with PFPS will possess decreased hip abduction and external rotation strength than healthy female control subjects. Additionally, we hypothesize that females with PFPS will run with greater contralateral pelvic drop, hip adduction, hip internal rotation, and knee external rotation. Finally, we believe that decreased hip strength will be inversely

associated with these kinematic differences between groups.

## METHODS

To date, hip strength and running mechanics of 2 females with PFPS and 4 healthy female control subjects have been collected. All isometric strength measurements were taken using a hand-held dynamometer and straps to eliminate the influence of tester strength. Hip abduction strength was measured in sidelying with the hip extended and the dynamometer just proximal to the lateral femoral condyle. Hip external rotation strength was measured in prone with the knee flexed to 90° and the dynamometer just proximal to the medial malleolus.

Subjects ran along a 23m. runway at 3.7 m/s ( $\pm 5\%$ ). The stance phase of five trials were collected for each subject. Reflective markers were placed on the subject's foot, lower leg, thigh, and pelvis and recorded at 120 Hz using a six camera motion analysis system. V3D software was used to calculate three-dimensional LE mechanics. Custom software was written to identify LE joint angles at peak knee extension moment (PKEM) as this is the instance with the potential for greatest retropatellar pressure. Excursion data is based on change in joint angle from initial contact to PKEM.

## RESULTS AND DISCUSSION

Results of our preliminary data are promising. Females with PFPS produced

21% less hip external rotation strength and 34% less hip abduction strength compared to females without PFPS. Females with PFPS tend to demonstrate greater peak hip internal rotation and adduction during running than healthy female control subjects (Figure 1,2).

Initial results also suggest an inverse association between hip strength and lower extremity joint rotations during running known to increase retropatellar pressure. Specifically, decreased hip external rotation strength appears correlated with increased anterior pelvic posterior rotation excursion ( $r= 0.88$ ), hip internal rotation excursion ( $r= 0.76$ ), and knee internal rotation excursion ( $r= 0.89$ ). Similarly, hip abduction strength appears correlated with increased peak contralateral pelvic drop ( $r= 0.66$ ) and hip adduction ( $r= 0.86$ ) angles (Figure 3).

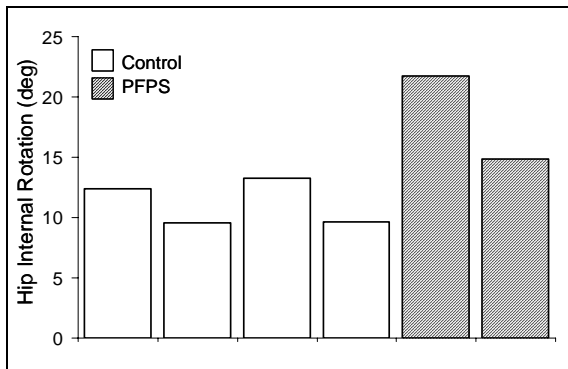


**Figure 1. Individual subject data for peak hip internal rotation during running.**

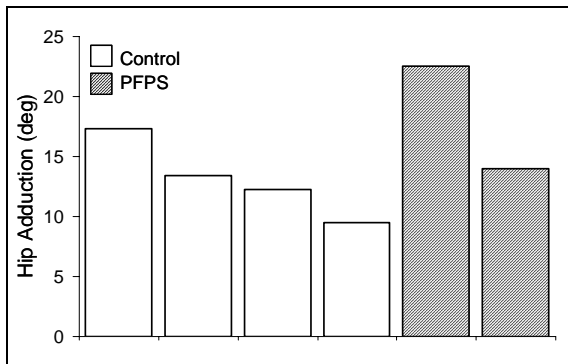


**Figure 2. Individual subject data for peak hip adduction during running.**

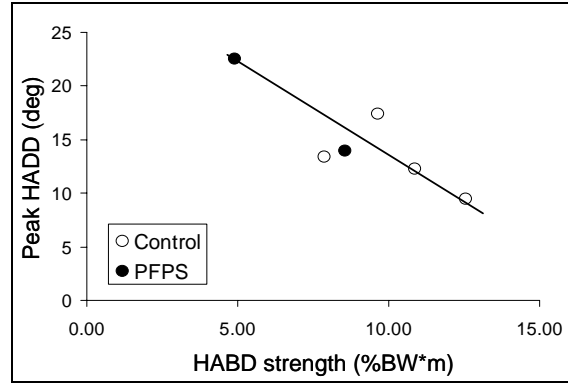


**Figure 3. Hip abduction strength and peak hip adduction in females with and without PFPS during running.**

These preliminary data suggest females with PFPS may possess decreased strength with which to resist hip adduction and internal rotation moments. Decreased strength appears to increase the tendency to run with LE alignment known to increase retropatellar pressure. Thus, efforts to increase hip strength in active females with PFPS may be an important component of their rehabilitation.

## SUMMARY/CONCLUSIONS

The early results of this small sample should be interpreted with caution. We hope that, as subjects are added, the relationship between strength and LE mechanics will be further elucidated. This information will provide important insight regarding treatment measures that may improve long-term patient outcomes and reduce the incidence of future patellofemoral OA.

## REFERENCES

- Kannus, P., et al. (1999) *JBJS, Am*, **81**, 355-363.
- Ireland, M.L., et al. (2003). *JOSPT* **33**, 671-6.
- Li, G. et al. (2004). *J Orthop Res*, **22**, 802-6.
- Utting, M.R., et al. (2005). *Knee*, **12**, 362-5.

## ACKNOWLEDGEMENTS

Support for this project was provided in part by the Foundation for Physical Therapy, Inc. and Drayer Physical Therapy Institute

# BIOMECHANICS OF DROP LANDING: SENSITIVITY OF SINGLE VERSUS MULTIPLE TRIALS ANALYSIS

Rhonda L. Boros

Biomechanics Laboratory, Texas Tech University  
Email: [rl.boros@ttu.edu](mailto:rl.boros@ttu.edu), web: [www.hess.ttu.edu/rboros](http://www.hess.ttu.edu/rboros)

## INTRODUCTION

The kinematics and kinetics of landing from a vertical drop have been studied extensively (Kovacs et al., 1999; McNitt-Gray et al., 1993 & 1994). Comparison of results between studies is complicated by variation in methodological protocol, data analysis and calculations, as well as by the process of trial selection for analysis. Several studies examining drop landing biomechanics had subjects perform multiple trials, yet only utilized either the “subject preferred” or “subject selected” trial for analysis. Other studies (Boros & Challis, 2005) analyzed parameters across repeated trials.

Subject selected trial analyses of drop landing have reported significant gender effects (Cowling & Steele, 1991; McNitt-Gray et al., 1993), while only a few studies have analyzed repeated trials (Boros & Challis, 2005) with few significant findings reported. The present emphasis by peer-reviewed journals on statistically significant findings and effect sizes (i.e., statistical power) begs the question: Are significant findings related to trial selection?

The purpose of this study was to determine if within the same data set, the trials selected for analysis influence the observance of statistically significant findings.

## METHODS

Ten subjects (five males and five females) performed five trials of two types of landings, onto flat feet and toes, from a

nominal drop height of 0.4 m. Kinematic (240 Hz, ProReflex, Qualisys) and kinetic data were collected as subjects performed two-footed hanging drop landings onto a Bertec force plate (1920 Hz). The instant of impact was considered time zero for all parameters, and served to time-synch the kinetic and kinematic data. For each trial, kinetic parameters (normalized peak VGRF, loading rate, landing phase duration, and resultant joint moments - RJM for hip, knee and ankle) and kinematic parameters (hip, knee and ankle joint angle, angular velocity, range of motion - ROM, and soft tissue marker displacement) were determined.

Two methods of statistical analysis were used to determine the sensitivity of results to single versus repeated trials selection. Analysis of variance tests were performed on two data sets as follows: Repeated trials analysis (RTA) utilized the average of all five repeated trials for each subject and landing style (flat and toe); Single trial analysis (STA) utilized for each subject only the trial resulting in the greatest peak VGRF for each landing style. A level of 0.05 denoted statistical significance.

## RESULTS AND DISCUSSION

### *Repeated Trials Analysis*

Males exhibited greater VGRF peaks across landing styles compared with females (Flat: 7.4 and 6.5 bodyweight - BW; Toe: 4.9 and 4.2BW), and demonstrated more rapid rates of loading ( $P < 0.05$ ). Flat-footed landings in general resulted in more rapid onsets of peak RJM compared with toe landings. Males

exhibited greater RJM at the hip during toe landings ( $P < 0.05$ ), and these moments occurred later in the landing phase when compared with females.

Males demonstrated greater knee extension at impact and at the time of peak VGRF compared with females ( $P < 0.05$ ). Females demonstrated significantly greater knee flexion at the bottom-most center of mass position compared with males ( $P < 0.05$ ). Ankle joint angular velocities were greater during toe compared with flat-footed landings, and males demonstrated greater angular velocities at the ankle during the toe landings compared with females ( $P < 0.05$ ).

Soft tissue marker displacement (relative motion of two markers placed on the quadriceps region of the thigh) was greater in females across landing style ( $P < 0.05$ ). No additional statistically significant findings were observed from the RTA.

#### *Single Trial Analysis*

STA similarly revealed larger peak VGRF during flat-footed landings for all subjects ( $P < 0.05$ ). Males demonstrated greater peak VGRF across landing style (Flat: 8.02 and 7.35BW, Toe: 5.51 and 4.82BW), albeit not statistically significant, along with higher loading rates compared with females. No additional significant differences were observed for kinetic parameters.

Females displayed greater knee and hip ROM, and knee flexion angle at the bottom-most position during flat-footed landings ( $P < 0.05$ ). No other statistically significant findings were observed from the STA.

#### **SUMMARY/CONCLUSIONS**

The purpose of this study was to determine the effect of trial selection (multiple versus single) on the statistical comparison of

biomechanical drop landing data. Results support the hypothesis that trial selection does influence statistical comparison of kinetic and kinematic variables. Both trial selection methods (RTA and STA) detected statistically significant findings, albeit for different biomechanical parameters, for a group of subjects performing two landing styles. The high variability observed with single trial selection (STA) appeared to hinder the occurrence of significant findings.

RTA accounts for variability within a subject, and thus may better represent true subject or group mean biomechanics. Argument in favor of STA (e.g. max VGRF trial), however may be warranted as knee injury (e.g. ACL) is likely to occur during a high impact landing (Lephart et al., 2002); and hence biomechanics associated with such landings are of interest. Subject selected trial analysis is cautioned, as a preferred trial may be inconsistent with regard to between-subject kinetics (e.g. peak VGRF).

The two trial selection methods utilized in the present study resulted in different statistical findings. Comparison of results across studies where different trial selection protocols are used, therefore is cautioned.

#### **REFERENCES**

- Boros, R.L., Challis, J.H. (2005). *Proceedings of ASB 2005*.
- Cowling, E.J., Steele, J.R. (2001). *J. Electromyogr. Kinesiol.*, **11**, 263-268.
- Kovacs, I. et al. (1999). *Med. Sci. Sports Exerc.*, **31**, 708-716.
- Lephart S.A. et al. (2002). *Curr. Opin. Orthopedics*, **14**, 168-173.
- McNitt-Gray, J.L. et al. (1993). *J. Appl. Biomech.*, **9**, 173-190.
- McNitt-Gray, J.L. et al. (1994). *J. Appl. Biomech.*, **10**, 237-252.

# ULTRASONIC AND BIOMECHANICAL EVALUATIONS OF MEDIAL GASTROCNEMIUS: BIOMECHANICAL CHANGES IN HYPERTONIC STROKE SURVIVORS

Fan Gao<sup>1</sup> and Li-Qun Zhang<sup>1,2</sup>

<sup>1</sup> Rehabilitation Institute of Chicago, Chicago, IL, USA

<sup>2</sup> Northwestern University, Evanston, IL, USA

E-mail: l-zhang@northwestern.edu

## INTRODUCTION

Stroke patients usually experience considerable spasticity and/or contracture around the ankle joint and this may be attributed to the changes in mechanical properties of muscles, especially the plantar flexor muscles. A better understanding of the changes of muscle properties *in vivo* may provide guidance to the rehabilitation and other treatments. Ultrasonography has been used to study muscle function as a powerful *in vivo* tool (Magagaris et al. 1998; Maganaris 2003; Narici 1996). However, few ultrasonic studies have been done on the hypertonic muscles in stroke survivors. Furthermore, most published studies only examined muscles as a functional group and rarely distinguished individual muscles and their specific contributions.

In the current study, electrical stimulation was used to activate the medial gastrocnemius (MG) selectively to examine the mechanical properties *in vivo*. To overcome the limited field of view, an extended-view-of-field technique, LOGIQview, implemented in the GE LOGIQ-9 ultrasound machine was used to register the muscle images. The purpose of this study is to quantify *in vivo* mechanical properties of MG in both stroke patients and normal subjects. In order to do so, muscle architectures including the pennation angle, fiber length and muscle thickness in the MG and joint torques with the changes in both

ankle position and knee configurations were evaluated.

## METHODS

Ten male subjects (34±6 yr) without neuromuscular injury and ten male stroke patients (55±8 yr) participated in the study, under an approved IRB protocol and with informed consent.

Subjects were seated upright on a custom chair with thigh strapped to the seat using Velcro™ straps and the knee and ankle joints were aligned to the centers of two JR3 force/torque sensors (JR3, Inc., Woodland, CA, USA), which were mounted on a customized leg-foot linkage. Four knee configurations, starting from fully extended position with increment of 30 degrees in flexion, were tested. Ankle angle was also systematically varied with an increment of 10 (dorsi-flexion) /15(plantar flexion) degrees in the range of motion.

A Compex™ electrical stimulator was used to produce trains of biphasic pulses with pulse width of 300 μs and frequency of 40 Hz. The duration of each electrical train was 600 msec and the interval between two consecutive electrical pulse trains was 3 seconds. Each stimulation trial lasted 50 seconds and there were around 10 contractions induced in each trial.

All ultrasound images were collected by an experienced operator using a B-mode ultrasonography scanner with 12 MHz, high-

resolution linear array probe (GE LOGIQ-9 with an M12L probe, Waukesha, WI). Working in the LogiqView mode, the probe was placed perpendicular to the skin and moved smoothly along the middle line of the MG starting from proximal and moving to distal.

Data analysis was conducted by custom MATLAB programs (The MathWorks Inc., MA, USA). The data were digitally low-pass filtered with a 4<sup>th</sup>-order Butterworth filter at 5 Hz. Two-way ANOVA was performed and the significant level was set at  $P<.05$ .

## RESULTS

Compared to normal subjects, stroke patients exhibited significantly shorter muscle fibers (Figure 1), smaller muscle thickness and lower posterior pennation angles under passive condition ( $P<.05$ ). The fiber level changes were correlated closely with joint level changes. The ankle resting angle in the stroke patients was significantly more into plantar flexion than that in normal subjects (Table 1) ( $P<.05$ ). Similar shift of ankle resting angle into PF was observed for both stroke and normal groups as the knee was gradually extended. With hypertonia, stroke patients had much reduced range of motion, especially in dorsiflexion. When knee was fully extended the mean ankle angle is  $0.6^\circ$  in stroke patients compared to  $20^\circ$  in normal subjects. Stroke patients with hypertonia showed higher resistance torques ( $6.2\pm 5.4$  Nm) at  $0^\circ$  dorsiflexion than healthy subjects ( $0.7\pm 0.7$  Nm) with the knee flexed at  $30^\circ$  ( $P<.05$ ).

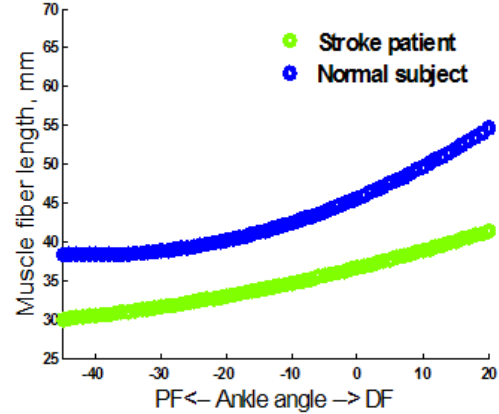


**Figure 1:** Passive muscle fiber length for both normal subjects and stroke patients with a knee flexion of  $60^\circ$ .

## CONCLUSIONS

Results on muscle architectures of normal subjects in this study agree with previously published data. One novelty of this study is that an extended-view-of-field technique, implemented in the state-of-the-art GE ultrasound device, was used to record the complete length of muscle fiber length. To the best of our knowledge, this is also the first study to examine muscle architecture changes in both passive and actively contracting muscle in stroke survivors. Further study is being carried out to analyze the relationship between the muscle architectural and biomechanical changes at the joint and fiber levels.

## REFERENCES

- Narici MV et al. (1996). *J Physiol* **496** (Pt 1): 287-297  
Maganaris CN et al. (1998). *J Physiol* (Lond) **512**: 603-614  
Maganaris CN (2003). *Clin Anat* **16**: 215

**Table 1:** Resting angles of ankle under different knee configurations (mean±Std)

Knee configuration	Fully extended	Flexed $30^\circ$	Flexed $60^\circ$	Flexed $90^\circ$
Stroke patient	$-22.0\pm 7.1$	$-16.6\pm 6.24$	$-17.7\pm 3.56$	$-15\pm 4.69$
Normal subject	$-13.4\pm 2.68$	$-12.9\pm 2.77$	$-12.5\pm 2.76$	$-12.5\pm 2.01$

# STABILITY OF FUSED VS. NONFUSED THA FEMORAL IMPACTION GRAFTS

Anneliese Heiner, John Callaghan, Thomas Brown

Department of Orthopaedics and Rehabilitation, University of Iowa, Iowa City, IA  
E-mail: [anneliese-heiner@uiowa.edu](mailto:anneliese-heiner@uiowa.edu) Web: <http://poppy.obrl.uiowa.edu/>

## INTRODUCTION

Impaction grafting for THA involves impacting morselized cancellous bone (MCB) into a cavitory defect, to build up bone stock. Ideally, the MCB is remodeled into a new cancellous lattice contiguous with the host bone. Although many investigators indicate that this remodeling of the impaction graft is desirable, others have questioned whether this bone remodeling is actually necessary for clinical success.

The purpose of this study was to determine the relative stability of femoral impaction graft constructs in which the MCB has fused (using a recent laboratory model of MCB fusion (Heiner et al., 2005)), versus the freshly-impacted nonfused condition. The hypothesis was that fused impaction graft constructs would have less micromotion and migration as compared to nonfused constructs. Clinically, this would translate to a more stable construct: the prosthesis would be more likely to stay in one position, construct interfaces would be less likely to fail, and cement fracture would be less likely to occur.

## METHODS

Composite femurs were prepared in a standardized manner. A nylon abductor strap was attached to each femur. Cavitory defects were simulated by overdrilling the femoral diaphysis and removing all proximal cancellous bone. Impaction grafts constructs were then created by impacting human MCB into the femur (Figure 1a). A polished,

collarless, triple-tapered femoral stem was then cemented into the impaction graft.

The MCB was either nonfused or fused. The nonfused MCB was defatted, typical of that used surgically. The fused MCB was defatted, dehydrated, and mixed with an amine-based epoxy adhesive just before the impaction grafting process; after the impaction grafting (and cementing) process is complete, the MCB-epoxy mixture fuses into a contiguous structure biomechanically equivalent to intact cancellous bone (Heiner et al., 2005), simulating the desired end-stage of an impaction graft.

Each impaction graft construct was loaded to 500,000 complete physiologic level walking and stair climbing cycles (with both axial and torsional loads) at 50% full-scale loading (Figure 1b). Three-dimensional motion between the femoral stem and the femur was measured at the proximal and distal stem with DVRTs. Micromotion and migration were calculated.

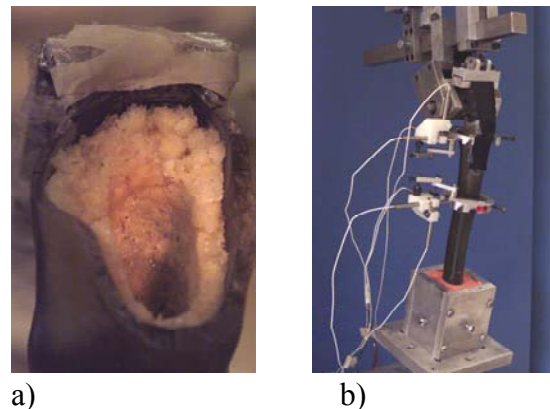


**Figure 1:** Femoral impaction graft a) before cementation and b) testing set-up.

## RESULTS

At the proximal stem location, final level walking micromotion for the fused impaction grafts was 13.1 times less than for the nonfused grafts (1.9 vs. 25  $\mu\text{m}$ ;  $p = 0.018$ ), and final migration was 12.6 times less (45 vs. 565  $\mu\text{m}$ ;  $p = 0.0007$ ) (Figure 2, top). At the distal stem location, final level walking micromotion for the fused impaction grafts was 1.3 times less than for the nonfused grafts (2.2 vs. 2.8  $\mu\text{m}$ ;  $p = 0.19$ ), and final migration was 2.7 times less (305 vs. 828  $\mu\text{m}$ ;  $p = 0.001$ ) (Figure 2, bottom).

## DISCUSSION

The measured migrations for the nonfused graft constructs at 250Kcyc and 500Kcyc were comparable to two 3- and 6-month clinical impaction grafting studies, for which <1mm average migration was recorded (Nelissen et al., 2002; van Doorn et al.,

2002). Although for this study, the applied loads were 50% full-scale, in clinical studies weight bearing is typically restricted 6-12 weeks postoperatively.

The fused femoral impaction grafts were much more stable than the nonfused grafts at the proximal stem location, but MCB fusion had a much smaller effect on distal stem stability. This indicates that most of the opportunity to reduce femoral stem micromotion and migration is proximal, and that steps to enhance MCB fusion (e.g., BMP augmentation) are most effectively focused proximally.

## REFERENCES

- Heiner, A.D., et al. (2005). *J Biomechanics*, **38**, 811-818.  
Nelissen, R.G., et al. (2002). *J Arthroplasty*, **17**, 826-833.  
van Doorn, W.J., et al. (2002). *J Bone Joint Surg Br*, **84**, 825-831.

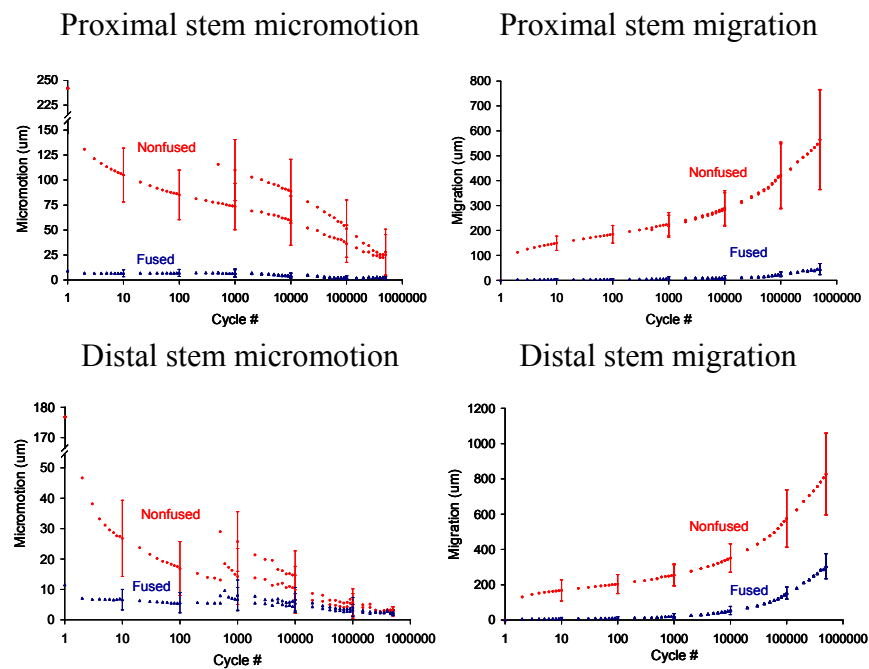


**Figure 2:** Series-average micromotion and migration results for fused vs. nonfused impaction graft constructs ( $n = 6$ ), for the proximal and distal stem locations. For stem micromotion, the higher lines of dots for the fused and nonfused grafts indicate stair climbing cycles.

# A TIBIO-FEMORAL JOINT KINETICS COMPARISON OF THE OLYMPIC AND TRAP BAR SQUATS BETWEEN MALES AND FEMALES

Francis A. Forde, John W. Chow, and Mark D. Tillman

Department of Applied Physiology & Kinesiology, University of Florida, Gainesville, FL, USA  
E-mail: faforde@gmail.com

## INTRODUCTION

An Olympic bar squat is typically performed with the Olympic bar placed across the back of the shoulders. Other squatting techniques such as the trap bar squat are performed with the bar held at the hands (Fig. 1). A trap bar is a rhomboid-shaped metal frame with two plate loading sleeves positioned at opposite corners. Two handles positioned at the same corners of the plate loading sleeves allow a person to hold the bar. The mass and plate loading sleeves of the trap bar are identical to the Olympic bar.

The purpose of this study was to compare tibio-femoral joint kinetics of males and females during the Olympic and trap bar squats. It was hypothesized that mean maximum compressive knee joint forces would be greater in the female subjects and mean maximum anterior shear knee joint force would be greater during the trap bar squat.

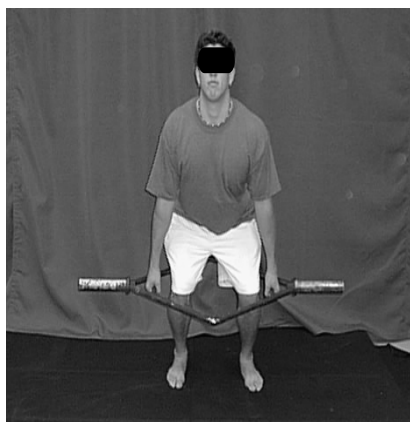


**Figure 1:** Trap bar squat.

## METHODS

Twenty-two trained subjects (11 males and 11 females) performed two 3-repetition trials using the two bars with a load of approximately 75% of their body mass. Trained subjects were used because these subjects have more consistent kinematics during testing (Escamilla, 2001). Subjects were required to perform a self selected warm up.

A Bertec force platform (Type 4060-10, Bertec Corporation, Columbus, OH) sampling at 900 Hz was used to collect ground reaction force data. The size of the top surface of the force platform was 0.6 m x 0.4 m.

Three JVC video cameras (Model # TK C1380) sampling at 60 Hz were used to collect all analog video data. Each camera was strategically positioned to allow for full view of all passive reflective markers. Seven reflective markers were placed on the left leg: second metatarsal head, lateral malleolus, heel, femoral epicondyle, greater trochanter, and at mid-shank and mid-thigh. The descending and ascending phases of a repetition were determined by the vertical location of the left hip marker using a video-based Peak Motus® system. The second repetition of each trial was analyzed and the average of the two repetitions for each bar type was used in subsequent statistical analysis. Resultant knee joint forces were determined using the inverse dynamic approach. Two 2x2x2 (Gender\*Bar type\*Phase) repeated measures ANOVAs

with a Bonferroni adjustment for multiple comparisons that resulted in an adjusted level of significance of  $p = .025$  ( $.05/2 = .025$ ) were performed.

## RESULTS AND DISCUSSION

The trap bar showed a higher mean maximum anterior shear value at the knee which supported the hypothesis that the mean maximum anterior shear force would be greater during the trap bar squat (Fig. 2). The hypothesis that the mean maximum compressive knee joint force would be greater in the female subjects was not supported by the results of this investigation, however the trap bar resulted in a higher normalized mean maximum compressive force than the straight bar squat (Fig. 3).

The trap bar squat (TB) appears to be an adequate variation of the Olympic bar (OB) squat because it provides the same range of motion and a comparable compressive force at the knee which is accepted as a protective

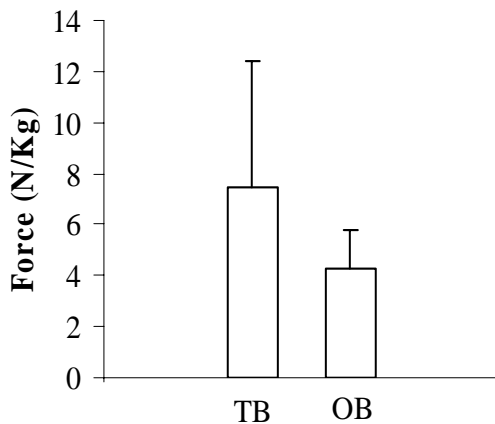


**Figure 2:** Mean maximum anterior shear force. ( $F = 9.573$ ,  $p < .025$ )

mechanism (Escamilla et al., 1998). Additionally, the bar is not placed across the shoulders or lifted from a rack in the upright position, thus a beginner is less likely to lift an uncontrollable mass. Furthermore, the trap bar is lifted from the floor using handles. These features serve as a self-spotter in two ways. First a mass the hands cannot support cannot be lifted and second the weakest position in a squat is the end of the descent phase therefore when lifting from the floor the lifter is less likely to lift a mass that may cause injury.

## REFERENCES

- Escamilla, R.F. (2001). *Med. Sci. Sports Exerc*, **33**(1), 127-141.  
 Escamilla, R.F. et al. (1998). *Med. Sci. Sports Exerc*, **30**(4), 556-569.

## ACKNOWLEDGEMENTS

We appreciate the assistance of Christopher Hasler and Dileep Ravi.

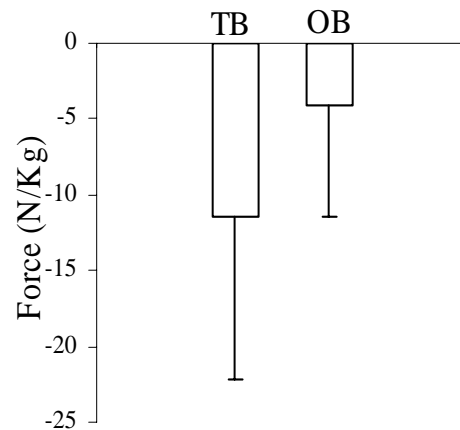


**Figure 3:** Mean maximum compressive force. ( $F = 6.458$ ,  $p < .025$ )

# **CONTROL OF THE REACTION FORCE RELATIVE TO THE CENTER OF MASS DURING THE TAKE-OFF PHASE OF THE FORWARD TRANSLATING TASKS PERFORMED WITH DIFFERENT DIRECTIONS OF ROTATION**

Witaya Mathiyakom <sup>1</sup> and Jill L. McNitt-Gray <sup>2</sup>

<sup>1</sup> Andrus Gerontology Center, University of Southern California, CA, USA

<sup>2</sup> Department of Kinesiology, University of Southern California, CA, USA

E-mail: mathiyak@usc.edu

## **INTRODUCTION**

Achievement of goal-directed tasks requires coordination of multiple body segments to accomplish the desired total body center of mass orientation (CM) relative to the reaction force (RF) during the interaction with the environment. Determining the changes between tasks performed under various conditions advances our understanding of the structure of human movement control. During the take-off phase of platform dives, the lower extremity joints undergo similar motion regardless of differences in direction of translation. However, muscle activation patterns (EMGs) used to control the RF relative to the CM are different (Mathiyakom et al., 2006). These results suggest that regulation of backward angular impulse at the total body influences control of the lower extremity system.

In this study, we compared two forward translating tasks with forward (FS) and reverse (backward) somersault (RS) requirement during the flight phase. We hypothesized that the set of muscles responsible for generating the linear and angular impulse during the take-off phase of FS and RS would be different. We expected that between-task differences in RF orientation relative to the CM would alter the RF orientation relative to the lower extremity segments and require differences in EMGs.

## **METHODS**

Six national level divers performed a series of single rotation of FS and RS from a springboard using a running approach as performed during a competition. Sagittal plane kinematics (60 fps) and EMGs of the lower extremity muscles (1,200 Hz) were acquired and synchronized at the time of departure. Thirteen body landmarks were digitized, filtered using a 4<sup>th</sup> Butterworth filter and used to calculate the CM. The acceleration of the CM in vertical and horizontal directions was used to estimate the RF (Miller, 1983). EMGs were filtered (10-400 Hz). The EMGs were quantified using root-mean-squared values and normalized to maximum values obtained during isometric manual muscle tests

## **RESULTS AND DISCUSSION**

Between-task differences in the RF orientation relative to the CM were attributed to between-task differences in activation patterns of muscles crossing the knee and hip (Figure 1). For example, during springboard depression (-0.5 – 0.25 s) of the task performed in a piked position during the flight, greater activation of the semitendinosus (ST) was observed during RS as compared to the FS. During springboard recoil (- 0.25 s to departure), activation of the vastus lateralis (VL) was significantly larger during the RS as

compared to the FS. In contrast, activation of the ST was significantly larger for the FS as compared to the RS.

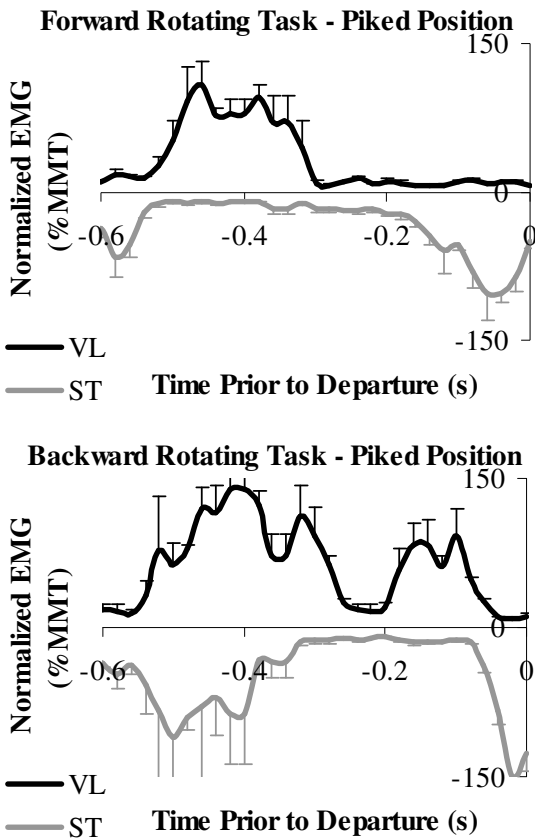


**Figure 1:** EMGs of the knee and hip muscles of an exemplar subject during the tasks performed in a piked position.

Between-task differences in magnitude of angular impulse generated also influenced the EMGs of the muscles crossing the knee and hip (Figure 1 and 2). For example, during springboard recoil of the FS somersault performed in both a tucked and piked position during the flight, the RF was directed posterior to the CM. The relative orientation between the RF and the shank, however, was significantly larger during the FS performed in a tucked position during the flight phase as compared to a piked position. As a result, significantly larger activation of the VL and smaller activation of the ST were required to control the shank motion during the FS performed in a tucked position

as compared to a piked position. Between-task differences in EMGs and relative orientation between the RF and lower extremity segment were also observed in the RS tasks.

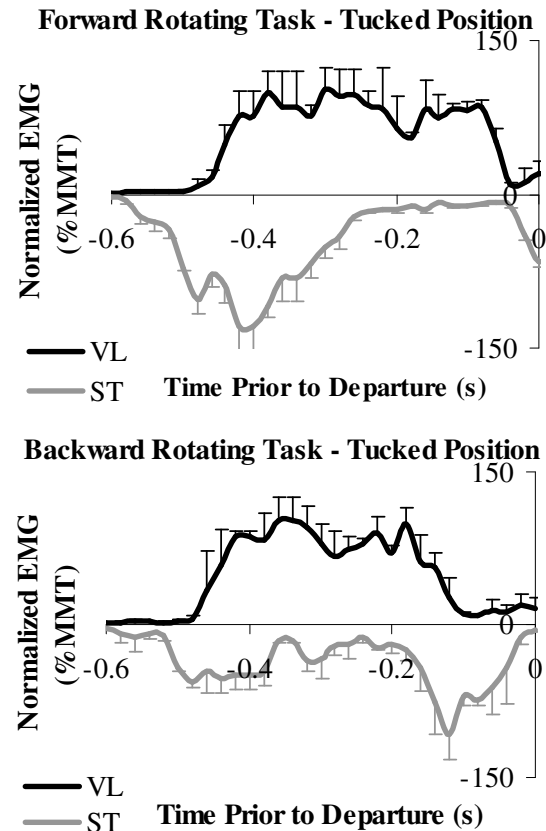


**Figure 2:** EMGs of the knee and hip muscles of an exemplar subject during the tasks performed in a tucked position

## SUMMARY

The set of knee and hip muscles used to generate impulse during the take-off phase of forward translating tasks are influenced by direction and magnitude of angular impulse and are sensitive to the orientation of the RF relative to the lower extremity segment motion

## REFERENCES

- Mathiyakom, W. (2006). *J. Biomech*, **39**, 990-1000.
- Miller, D.I. (1983). *Biomechanics VIII-B*. Champaign Human Kinetics.

# INTRASESSION RELIABILITY OF TRUNK POSTURAL STABILITY

HyunWook Lee, Greg Slota, Kevin P. Granata

Musculoskeletal Biomechanics Laboratory  
Department of Engineering Science & Mechanics  
School of Biomedical Engineering & science  
Virginia Tech

Email: [Granata@vt.edu](mailto:Granata@vt.edu)

web: <http://www.biomechanics.esm.vt.edu/msbiolab/>

## INTRODUCTION

Nonlinear dynamic analyses have been proposed for empirical assessment of neuromuscular control of spinal stability. In a study by Cholewicki (2000) subjects were asked to maintain seated balance on a wobbly chair. The equilibrium state was a zero-velocity, upright seated posture. However, small biomechanical and/or neuromotor disturbances are manifest that continuously disturb the system causing kinematic variance. The neuromuscular control system maintains a stability posture by actively working to return the disturbed posture toward the equilibrium state. Hence, stability can be measured by recording the rate at which the kinematics are attracted toward the posture of static equilibrium.

We plan to use this stability protocol in future studies to document within-subject changes in stabilizing control of the torso. Therefore, the purpose of the current study was to characterize the day-to-day repeatability of the stability assessment.

## METHODS

Eight subjects with no previous history of low back pain were tested after giving informed consent approved by the Virginia Tech, IRB. Subjects included 6 males and 2 females, age 26.8 (std 4.8) yrs, body mass 71.6 (std 14.7) kg, height 179 (std 11.6) cm. They were required to maintain seated balance with arms-crossed over the chest while on a chair that freely pivoted under the

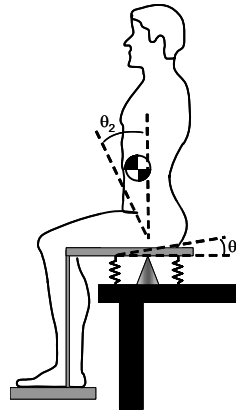


Figure 1. Seated torso stability task. Adapted from Cholewicki 2000

seat-pan. Foot support attached to the seat pan linked the lower extremity to the seat movement whereas the torso was free to move independent of the seat.

Potential energy about the neutral posture is represented as

$$V = \frac{1}{2} k_{\theta} \theta_1 - G(\theta_1, \theta_2)$$

where  $\theta_1$  is the 2-D (sagittal, lateral) angle of the seat pan with respect to horizontal and  $\theta_2$  is the 2-D torso angle with respect to vertical.  $G(\theta_1, \theta_2)$  is the gravitational potential energy of the subject's body mass with respect to the seat-pan center-of-rotation. Adjustable springs with rotational stiffness,  $k_{\theta}$ , applied elastic restorative moment to the seat.  $k_{\theta}$  was adjusted to achieve neutral stability about the base of support,  $k_{\theta} = \frac{\partial}{\partial \theta_1} G(\theta_1, \theta_2)$ , where the linearized gradient in gravitational moment was recorded in static calibration measurements when the subject and seat were tilted  $\pm 10^\circ$  (Bertec, Columbus, OH). Hence, the stability assessment accounted for subject specific anthropometry.

Seat movement in response to the corrective neuromuscular control of the torso moments were recorded from the forceplate (Bertec, Columbus, OH) and the center of pressure (CoP) was calculated. Each trial was 60 sec. in duration. Separate conditions were tested wherein the seat response,  $k_{\theta}$  was adjusted to be neutrally stable (100%), and unstable

(75% and 50% of neutrally stable  $k_{\theta}$ ). Thus, active neuromuscular response was necessary to maintain asymptotic stability of the seated task. Identical test protocols were performed during two separate experimental visits (48 hrs between visits).

Analysis included summary statistics, i.e. maximum (MAX) and root mean square (RMS) displacement of the CoP in lateral and anteroposterior directions, total path length traveled per second (PATH), and 95% confidence ellipse area (EA) of the CoP. Intra-class correlation coefficient, ICC (2, k), were calculated for summary statistics based on a repeated measures ANOVA.

## RESULT AND DISCUSSION

All summary statistics showed significantly increased kinematic variability with smaller  $k_{\theta}$  (Table 1). Previous assessments of spinal stability report limitations due to subject differences in anthropometry. This is related to the fact that the subject mass and center-of-mass location contribute to the potential energy of the system  $G(\theta_1, \theta_2)$  when balancing on an unstable seat. By adjusting the proportional restorative moment of the seat in response to a seat-pan tilt,  $k_{\theta}$ , we were able to accommodate subject differences in anthropometry. This permits between-subject comparisons on stabilizing control of the torso.

Repeatability test for all summary statistics were moderate to very high scores, over 0.9. The ICC scores in this study were comparable to some other seated postural stability measures with ICC values 0.64 – 0.94 (Kerr and Eng 2002). These values suggest that this assessment protocol may be used to record within-subject, time-dependent changes in neuromuscular control of spinal stability.

## CONCLUSIONS

The repeated measures of the unstable seated postural stability demonstrated very good reliability. This ICC results suggested summary statistics were excellent parameters for investigation of torso neuromuscular control of stability. In future studies, we will apply these techniques to healthy individuals and low back pain patients to study the deficits in postural control of the lumbar spine.

## REFERENCE

Kerr HM and Eng JJ (2002) *Clin.Biomech* 17 555-557.  
Cholewicki J, Polzhofer GK, and Radebold A (2000) *J Biomechanics* 33 1733-1737.

## ACKNOWLEDGEMENT

This study was supported by a grant R01 AR46111 from NIAMS of the National Institute of Health.

Table 1. Mean (standard deviation) and ICC summary statistics results during balance performances from three different stability conditions (spring positions).

Spring Stiffness $k_{\theta}$	MAX <sub>x</sub> (mm)	MAX <sub>y</sub> (mm)	RMS <sub>x</sub> (mm)	RMS <sub>y</sub> (mm)	PATH (mm/sec)	EA (mm <sup>2</sup> )
Neutrally stable = 100%	6.2595 (1.0938)	7.7822 (3.2093)	1.4371 (0.2353)	1.8476 (0.4742)	25.1866 (6.8292)	53.8493 (21.2679)
75%	8.6989 (1.8017)	10.0677 (2.2953)	1.9789 (0.2970)	2.4892 (0.5515)	33.0034 (9.1369)	95.8998 (33.4220)
50%	14.9318 (5.6798)	18.7687 (4.2869)	3.4706 (1.0571)	4.1957 (0.8336)	61.8169 (19.3223)	265.3819 (127.6553)
ICC	0.95	0.95	0.97	0.95	0.93	0.94

Subscript x – anteroposterior direction, subscript y – lateral direction.

# QUANTIFYING LOWER EXTREMITY JOINT AXES AND ALIGNMENT USING A QUATERNION PARAMETERIZATION

L. Held<sup>1</sup>, J. L. McNitt-Gray<sup>1,2,3</sup>, H. Flashner<sup>3,4</sup>

Biomechanics Research Lab, Departments of Biomedical Engineering, Kinesiology, Biological Sciences, and Aerospace and Mechanical Engineering  
University of Southern California, Los Angeles, CA, USA  
E-mail: held@usc.edu

## INTRODUCTION

During three-dimensional (3D) tasks involving changes in momentum, control of knee motion requires coordinated control of all three joints of the lower extremity subsystem. As the mechanical demand imposed on a body increases, it may exceed the system's ability to control shank and thigh motion, leading to excessive multi-axis rotation of the knee, and possible injury. Interpretation of joint kinetics is sensitive to the orientation of joint axes. We hypothesize that calculating functional axes during a movement may provide more accurate insight into how the net joint moment is achieved by muscles controlling the joint.

In this study, our aim is to use a quaternion parameterization of kinematics to quantify the degree of lower extremity mal-alignment during 3D tasks using model-generated and experimental data. We expect that using quaternions will allow us to determine a) the degree of hinge-like knee motion during momentum redirection, b) the orientation of the functional joint axes relative to bony landmarks assumed to represent the axes, and c) alignment of adjacent joint axes, and d) implications of lower extremity alignment on lower extremity control strategies.

## METHODS

### *Kinematic Parameterization*

Quaternions are an extension of complex numbers of the form:

$$\mathbf{q} = [\sin \varphi/2 \cdot \mathbf{n}_1 \quad \sin \varphi/2 \cdot \mathbf{n}_2 \quad \sin \varphi/2 \cdot \mathbf{n}_3 \quad \cos \varphi/2]^T$$

The four parameters define a rotation of a rigid body  $\varphi$  radians about a single axis,  $\mathbf{n}$ .

A quaternion for the relative rotation between adjacent segments was calculated based on the segment quaternions for each time step. The angular velocity vector of this relative quaternion represents the functional joint axis. Knee angular velocity results were compared to the angular velocity input data to validate our quaternion algorithm.

### *Multilink Model*

In this stage of the study, a two-segment, two-joint, velocity-driven model of the lower extremity was created with rigid links using ADAMS software (Mechanical Software, Ann Arbor, MI) (Figure 1).

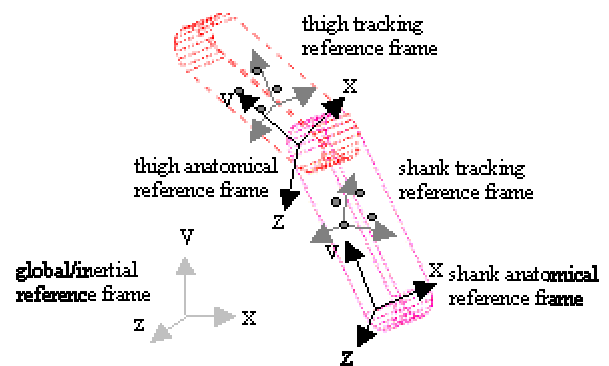


**Figure 1.** Adams model of lower extremity.

### *Experimental Design*

Simulations were run to generate kinematic data for combinations of uni-axial and multi-axial knee and ankle joints. Tracking and anatomical marker coordinates were

imported into Matlab (The Mathworks Inc, MA) for processing.

In addition, sensitivity analysis was performed using kinetic data from a 3D footwork task to see how small changes in axis orientation could affect the interpretation of the net joint moments in regard to muscles controlling joint motion.

## RESULTS AND DISCUSSION

Simulations demonstrated that hinge-like and non-hinge-like knee motion can be captured using quaternion angular velocities. Angular velocities about the knee axes matched exactly the input velocities, demonstrating the validity of our approach. Results from a simulation using a revolute joint at the knee during a 3D task are provided. Figures 3 and 4 show that the axis of rotation of the shank and thigh segments, calculated using quaternions, varies in global space during the task; whereas the knee axis is constant relative to the thigh reference frame. This is consistent with the knee being hinge-like even during a 3D task.

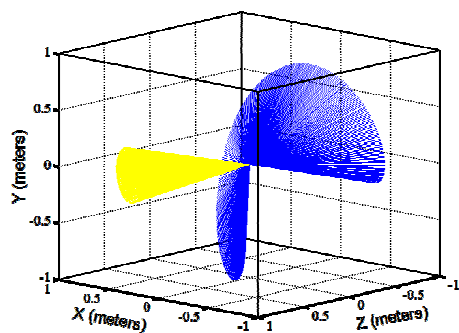


**Figure 3:** Shank and thigh axes of rotation in global reference frame during a simulation with a hinge knee joint and 3D subsystem rotation.

Sensitivity analysis demonstrated that the interpretation of net joint moments at each joint can vary significantly depending on the orientation of the joint axis relative to axes

assumed using bony landmarks. At peak ground reaction force during the footwork task, the magnitude of the net joint moment at the knee was 320 N. Changing the orientation of the flexion/extension axis by  $5^\circ$  in the horizontal plane caused a 25% decrease in the knee extensor moment, a 5% increase in the knee abductor moment, and a 26% decrease in the internal rotation moment. The discrepancy in results may affect the interpretation of which muscles are being used to control these moments. Because many of the knee muscles used to control knee motion are two-joint muscles, there are also implications for control of adjacent joints.

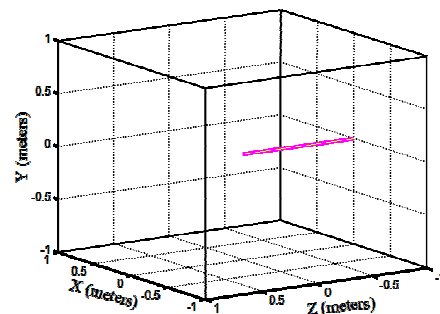


**Figure 4:** Knee axes of rotation in thigh reference frame during a simulation with a hinge knee joint and 3D subsystem rotation.

## SUMMARY/CONCLUSIONS

Interpretation of axes results, in combination with kinetic and electromyography data, will help us understand how individuals organize their systems during 3D movements.

## REFERENCES

- Zatsiorsky. (1998). *Kinematics of Human Motion*.
- Kuipers. (1999) *Quaternions and Rotation Sequences*. Princeton University Press.
- Kim, Injung et al. Kalman filtering using the quaternion extracted from vector measurements. AAS01-142. 571-8

# SAGITTAL PLANE KINEMATICS AND GAIT RECOGNITION

Adam M. Fullenkamp<sup>1</sup> and James G. Richards<sup>1</sup>

<sup>1</sup> University of Delaware, Newark, DE, USA  
E-mail: afullen@udel.edu

## INTRODUCTION

Advances in biometric technologies have improved our ability to uniquely identify individuals based upon physically acquired metrics (Jain et al., 2004). While these methods provide a reliable means of personal identification, they require a deliberate interaction between the person in question and the system attempting to establish or verify the identity (e.g. placing a thumb over a scanning device). This limitation has motivated researchers to develop methods that allow for personal identification at a distance (Sarkar et al., 2005). One of the more promising metrics for distance-based recognition is human gait.

More recent attempts to identify individuals from a distance have involved the extraction of gait related information from 2D surveillance cameras (Mowbray & Nixon, 2003). Typically, 2D silhouettes of a human subject are extracted from video footage and analyses are performed to compare those silhouettes to previously acquired template data. Such analyses have involved everything from simple silhouette matching (i.e. biometric comparison) to metrics that describe the silhouette's motion. However, to date there have been no attempts to utilize sagittal plane motion for gait recognition.

This study was designed as an initial step in the development of a video-based system for remote human identification. Because the system will use sagittal plane kinematic data for gait recognition, it was first necessary to identify the sagittal plane characteristics that are best suited to distinguish between

individuals. Specifically, those variables that show a large ratio of between to within subject variability (VR) are ideal for individual identification. The purpose of this study was to identify the sagittal plane variables that provide the largest VR's and to evaluate these measures using computer-based matching simulations. Also, two video-based anthropometrics were included to determine if they provide a distinct advantage over motion variables.

## METHODS

Gait data were collected for 50 normal subjects using a 3D motion analysis system. From these data, 10 sagittal plane variables were analyzed: thigh length, shank length, hip flexion/extension (F/E) angle and angular velocity, knee F/E angle and angular velocity, ankle F/E angle and angular velocity, and trunk lean angle and angular velocity. These variables were divided into three groups for matching algorithm analyses: anthropometrics (A), sagittal plane angles (B), and sagittal plane angular velocities (C).

First, the variability was calculated for each of the 10 observed measurements both within and between subjects. Next, a variance ratio (VR) was computed for each measure by dividing the between subject variance by the within subject variance.

To demonstrate the relationship between VR results and matching performance, Receiver Operating Characteristic (ROC) curves were generated for each of the three variable groups by programmatically implementing

each group of variables into a matching algorithm simulation. Each simulation used the same 50 subjects that were used to determine the VR's. When analyzing ROC curves, a greater area under the curve represents a more effective matching algorithm.

## RESULTS AND DISCUSSION

The VR results presented in Table 1 illustrate the uniqueness of the anthropometric measures (group A VR  $\approx$  10.5). Group B produced VR's much smaller than group A, but slightly larger than group C (group B VR  $\approx$  2.5). The VR's for each variable in the group C were slightly smaller than their counterpart in group B (VR  $\approx$  2.0 compared to VR  $\approx$  2.5).

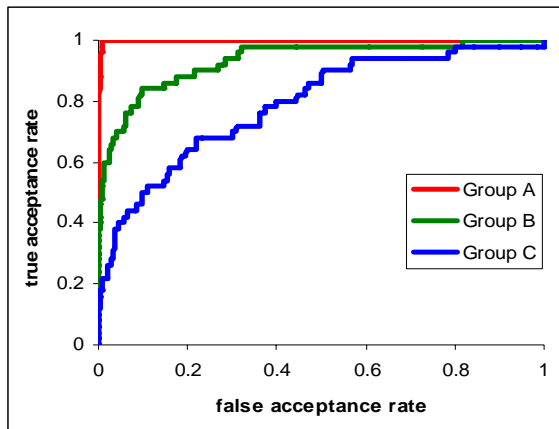


**Figure 1:** ROC for each group (group A's curve follows the top left corner).

Based on the VR results, a matching algorithm that utilizes the variables in group A would be expected to show the best matching performance. This performance

would be followed by group B, and finally group C.

The ROC curves derived from the matching simulations are consistent with the VR results (Figure 1). The ROC areas for groups A, B, and C were 0.998, 0.934, and 0.790, respectively. These results verify that matching scores based on the anthropometric variables perform better for subject matching. Specifically, the ROC curve for group A suggests that a matching score threshold can be set in the matching algorithm such that a very high true acceptance rate can be obtained while minimizing the false acceptance rate.

## CONCLUSIONS

The results of this experiment suggest that anthropometrics are more effective than sagittal kinematics in recognizing subjects. However, the sagittal angles produced promising ROC areas and may serve as a useful element in future gait matching algorithms. It is possible that a combination of anthropometric and kinematic variables will provide the best solution.

## REFERENCES

- Jain, A.K. et al. (2004). *Proceedings of Biometric Authentication*, **3087**, 259-269.  
 Mowbray, S.D. & Nixon, M.S. (2003). *Lecture Notes in Computer Science*, **2688**, 566-573.  
 Sarkar, S. et al. (2005). *IEEE Transactions on Pattern Analysis and Machine Intelligence*, **27**, 162-177.

**Table 1:** Variance ratios (VR) for each group; thigh and shank lengths (TL, SL), hip, knee, ankle, and trunk angles (HA, KA, AA, TA), and hip, knee, ankle and trunk angular velocities (HV, KV, AV, TV).

	Group A		Group B				Group C			
	TL	SL	HA	KA	AA	TA	HV	KV	AV	TV
VR	11.3	10.2	2.8	2.5	2.6	2.2	2.4	2.1	1.9	1.5

# ERGONOMIC ASSESSMENT OF LOCOMOTIVE SEATS

Tyler A. Kress<sup>1,2</sup>, Anne M. Kroman<sup>2</sup>, Logan Mullinix<sup>3</sup>

<sup>1</sup> Virginia Tech, Blacksburg, VA, USA

<sup>2</sup> University of Tennessee, Knoxville, TN, USA

<sup>3</sup> National Seating Company, USA

E-mail: kress@utk.edu

## INTRODUCTION

Similar to truck drivers, bus drivers, and heavy equipment operators, railroad engineers spend much of their workday in a seat operating their vehicle. Long-term health is influenced by design characteristics such as comfort, suspension, and adjustability. There are numerous reported back problems by locomotive engineers and assistant engineers from the virtually all of the major railroads in the United States.

Exposure to whole body vibrations can result in injury, however the vibrations themselves and ergonomic/biomechanical adverse effects can be subtle and injury development difficult to detect by the operators. In other words, operators of vehicles are often ignorant of the fact that their everyday exposure can be injurious. The cumulative problems caused by rough riding locomotives and vibrational issues resulted in a lawsuit filed by Union Pacific (UP) Railroad Company against a major U.S. locomotive manufacturer in an attempt to recover the significant costs due to injury claims by approximately fifty UP engineers and assistant engineers.

The recognition of the problem has sparked significant research regarding the issue of locomotive cab seat design. The Association of American Railroads issued a useful final report on Locomotive Cab Seat Evaluation in 1980 and the U.S. Federal

Railroad Administration has also issued numerous reports (dating back to the 1970s) regarding the need to improve locomotive cab design. Many major U.S. railroads have studied the rough-riding and vibrational problems and documented the complaints and needs for design improvement. There has been extensive engineering, medical, and epidemiology literature indicating that exposure to certain vibrations and/or poor ergonomics of seating can cause injury to the human spine and other anatomical structures.

The type of exposure in a typical railroad environment is eloquently summarized by Johanning et al (2002):

*"...these data indicate that locomotive rides are characterized by relatively high shock content (acceleration peaks) of the vibration signal in all directions. Locomotive vertical and lateral vibrations are similar, which appears to be characteristic for rail vehicles compared with many road/off-road vehicles. Tested locomotive cab seats currently in use (new or old) appear inadequate to reduce potentially harmful vibration and shocks transmitted to the seated operator, and older seats particularly lack basic ergonomic features regarding adjustability and postural support."*

The aim of this study is to further investigate vibrational/ergonomic problems

associated with locomotives by examining both seat design and level of vibration exposure in a sample of locomotives from U.S. railway fleets.

## **METHODS**

Typical locomotive seating environments were evaluated with respect to ergonomic design. The sample of examined seats was selected to be representation of the most common types currently found in United States railway fleets. Each of the seats was examined in regards to human factors characteristics and vibrational behavior. Vibrational measurements were recorded in locomotives in accordance with ISO and ANSI standards. Measurements were taken in a range of situations, such as through-freight train rides and yard environments.

## **RESULTS AND DISCUSSION**

Data can be characterized by the following numbered statements: 1) Low to moderate RMS (root-mean-squared) vibration levels; 2) High crest factors; listed in decreasing amplitude are the X, Y and Z directions 3) Low frequency side-to-side swaying/rolling that results in the body swaying or rocking; resulting in the occupant continually trying to counteract this motion; 4) Long exposure durations; 5) Most basic level seating systems present; 6) Vertical seat adjustment is oftentimes a two-person operation, requiring one person in the floor operating the pins while a second person provides lift assistance and sets the height while the pins and locks are engaged; 7) Seat fore-aft seat adjustment oftentimes relies on metal-to-metal tracks that require the weight of the seat and pedestal to be lifted and slid fore-aft; units show rust that adds to the adjustment effort; units show bent track mechanisms and missing paint that illustrate the difficulty of the adjustment and the effort that may be required if the mechanism

does not freely slide; 8) Overall, poor seats with respect to suspension and ergonomic characteristics. The evaluation indicated several characteristics in which there are significant ergonomic opportunities for design improvement, such as: 1) pad/seat cushion material and contour, 2) armrest compatibility with occupant anthropometrics, 3) vibrational performance and seat suspension, 4) seat positioning and interfacing with the control console; and 5) overall seat adjustability.

## **CONCLUSIONS**

Typical seats exhibited deficiencies in lumbar support, vibrational characteristics, vertical and fore/aft adjustment control design, and biomechanical soundness. The basic seating systems are typical of industries such as those found on lower-end school buses where driver exposure is usually 1-3 hours/day as opposed to 6-plus hours per day for railroad engineers. Detailed vibrational data, collected and analyzed in accordance with current national and international standards, show high crest factors and low frequency side-to-side swaying/rolling that results in the body swaying or rocking. As a result the occupant is continually trying to counteract this motion. This can lead to accelerated muscle fatigue and increase average disk pressure. These fatigued muscles are the ones that support the spinal column and help resist segmental buckling. Railroad companies and locomotive manufacturers should incorporate ergonomically-desirable features and air-ride suspensions into the design of their seats and reduce the injury risk to engineers.

## **REFERENCES**

Johanning, E. et al (2002). *AIHA Journal* 439-446.

# KINETIC AND KINEMATIC EFFECTS OF ALTERING CLEAT PLACEMENT DURING CYCLING

Jeff W. Frame and Eric L. Dugan

Ball State University, Biomechanics Laboratory, Muncie, IN, USA

E-mail: eldugan@bsu.edu

## INTRODUCTION

Cycling is a sport that demands the compromising relationship between man and machine in order to be successful.

Performance is dependent on a number of environmental, mechanical, and human factors. It is well known that environmental factors are critical to effective power production and movement. These include wind resistance, rolling resistance, and friction within the machinery itself.

Engineers have focused extensively on designs and developments of lighter, more aerodynamic bicycles to confront these issues while often overlooking the human component of cycling performance.

Cycling is a sport that demands the most out of the rider and bike together in order to perform optimally. Power and efficiency are the two most important factors when riding a bike. In cycling, power and efficiency are uniquely determined by the four design parameters; pelvic inclination, crank length, seat height and rate of crank rotation (Gregor et al., 1991; Too, 1990; Yoshiyuku and Herzog, 1990). Yoshiyuku and Herzog (1990) developed an optimization model explaining how power transfer could be optimized by tailoring the bicycle equipment to the individual.

Specifically, a cleat and pedal system utilizing a heel position (HP) as the point of transfer of power rather than the traditional toe position (TP) may help improve power

output and pedaling efficiency. This arrangement may assist the cyclist keep his/her heels down during the recovery phase of the pedal stroke, thus achieving a more even distribution of force to the pedals. The purpose of this study was to examine the effects of altering cleat placement on the bottom of a cycling shoe on peak power outputs, pedaling efficiency and ankle angle.

## METHODS

Ten competitive male cyclists participated in this study. Competitive 'status' was determined by minimum requirements in mileage/week, hours/week, years racing, and the number of races per year they competed in and or their category ranking (Category 5 or higher) based on United States of America Cycling Federation. The subjects' characteristics (mean  $\pm$  SD) were age  $32.5 \pm 11.2$  yrs, mass  $73.7 \pm 8.5$  kg, and height  $179.4 \pm 5.2$  cm. Each subject completed two different tests using the Computrainer (CT) per cleat position.

**Testing Protocol:** The first visit served as a familiarization session and was used to determine the subjects' anthropometrics, bike geometry, and to serve as a practice session using the CT system and software, along with becoming familiar with the shoes and cleat positions. The second session took place 1-3 days after the familiarization session and served as the data collection session in which two tests were performed

for each of the two cleat positions; Modified Wingate (MWgat) for Peak Power Output (PP) and SpinScan (SS) for pedal efficiency. The order for testing between the TP and HP conditions was randomized.

The pedaling rate for the spin scan (SS) was set at 90 rpm. The protocol for the MWgat consisted of a 55 second steady state ride at 100 W. The gearing was predetermined and consistent for all trials. The load was determined for each subject based on 9 watts/kg body weight. Kinematic data were collected using a 60 Hz digital video camera, during the SS testing sessions only, in order to determine the effects of the two cleat positions on the ankle patterns. The mean ankle angles for the four phases (0-90, 90-180, 180-270, 270-360) were calculated for one complete pedal revolution. The Statistics Package for the Social Sciences (SPSS) was used to perform a one-way ANOVA for the ankle angles among participants between conditions. A paired-sample *t*-test was used for the analysis of the peak power outputs and pedal efficiencies.

## RESULTS AND DISCUSSION

**Peak Power Output (MWgat)** – There was no significant difference ( $p = .820$ ) between PP outputs during the two cleat conditions. The mean values were 666.11 W and 661.77 W for the TP and HP respectively.

**Pedaling Efficiency (SS)** – The results obtained from the CT during the SS, however, did indicate a significant difference ( $p = .027$ ) between average TP (73.4) and HP (77.0) pedal efficiencies.

**Ankle Kinematics** - The mean ankle angle was calculated for the entire stroke resulting in angles of  $82 \pm 4.3$  and  $79.9 \pm 2.5$  for the HP and TP respectively. A break down of the pedal stroke into 4 quadrants did illustrate a significant difference in the first

half of the power phase and second half of the recovery phase seen in Table 1.

Ankle Angles	Toe	Heel
0-90	87.06 (0.93)	82.79 (0.84)*
90-180	77.98 (2.87)	77.38 (1.46)
180-270	78.83 (1.62)	78.01 (0.79)
270-360	83.84 (1.46)	80.9 (1.11)*

**Table 1:** Mean ankle angles ( $\pm SD$ ) for the four phases of the pedal stroke.

The purpose of this study was to examine the effects of altering cleat placement on the bottom of a cycling shoe on PP outputs, pedal efficiency mechanics and ankle joint angles. Placing cleats on the heel of the shoe alters the lower body kinematics during the pedal stroke which potentially affects the efficiency during cycling.

## SUMMARY/CONCLUSIONS

The results of this study indicate that while there was no significant difference in PP outputs between cleat positions, a smoother pedaling pattern does exist when using the HP position. This results in a more evenly displaced pattern of force production through the complete 360 degrees of the pedal cycle. Future studies should examine the long term effects of training with the HP cleat position on power output and muscle activation patterns.

## REFERENCES

- Gregor, R. J., Broker, J.P., and Ryan, M.M., (1991) The Biomechanics of cycling *Exercise and Sport Sciences Reviews*, 19, 127-169.
- Too, D., (1990) Biomechanics of cycling and factors affecting performance. *Sports Medicine*, 10(5) 286-302.
- Yoshihuku, Y., Herzog, W., (1990) Optimal design parameters of the bicycle-rider system for maximal muscle power output. *J Biomechanics*, 23(10) 1069- 1079.

# BIOMECHANICAL COMPARISON OF ELDERLY GAIT DURING ELEVATION CHANGES

Jeffrey B. Casebolt, Sukhoon Yoon, Sunghoon Shin and Young-Hoo Kwon

Texas Woman's University, Denton, TX, USA

E-mail: [jbcasebolt@gmail.com](mailto:jbcasebolt@gmail.com) Web : [www.twu.edu/biom/](http://www.twu.edu/biom/)

## INTRODUCTION

The elderly are often presented with elevation changes during gait. Negotiating an obstacle has been reported as a major cause of falls among the elderly (Archea, 1985). Most reported fall-related injuries occur while attempting to step onto or over an obstacle (Ellis, 2001). However, serious bodily injury is more likely to occur during the descending phase. (Svanstrom, 1974).

There are several studies comparing gait differences among elevation changes and level walking. Previous studies have investigated both kinematic and kinetic parameters for gait during elevation changes. Kinematic studies determined a 12° increase in joint flexion is needed to negotiate elevation changes when compared to level walking (Laubenthal et al., 1972 and Hoffman et al., 1977). Maximum resultant joint moments at the knee were calculated to be 12-25% greater when compared to level walking (Morrison, 1969). Maximum resultant joint moments at the knee occurred at 50° of flexion (Andriacchi, 1980). During level walking, maximum joint moments occur when the knee is near full extension (Winters, 1980). All the above mentioned studies used healthy young adults as

subjects, which may not represent the elderly population. The purpose of this study was to determine the differences in lower extremity lower-body joint angles and net joint moments among Step-Up Gait (SUG), Step-Down Gait (SDG), and Normal Gait (NG).

## METHODS

Fifteen healthy, elderly subjects volunteered for the study (Table 1). Informed consent, medical clearance, and IRB were all secured prior to data collection. Six reflective markers were placed on bony landmarks on both the right and left sides of the body.

The participants walked their preferred pace for all conditions. A 2D motion analysis was performed as cameras from both right and left sagittal plane recorded the motion at 60Hz. Two force plates recorded GRF at 240 Hz. During SDG and SUG a platform was raised to 30% of the participant's leg length (LL) - measured from floor to GT. Joint angles and net joint moments at the ankle, knee, and hip were computed. A One-Way ANOVA with repeated measures was used to determine significance among the conditions ( $p < 0.05$ ).

**Table 1:** Participant Anthropometric Information

Groups	Age (yrs)	Height (m)	Weight (kg)	Leg Length (m)	BMI
Total (15)	69.6 ± 3.5	1.73 ± 0.08	79.84 ± 14.78	0.92 ± 0.05	26.62 ± 4.17
Females (10)	69.3 ± 3.8	1.68 ± 0.03	73.25 ± 12.31	0.90 ± 0.03	25.99 ± 4.79
Males (5)	70.2 ± 3.1	1.82 ± 0.04	93.04 ± 9.88	0.97 ± 0.05	27.88 ± 2.49

## RESULTS AND DISCUSSION

The angles at the knee were computed to be 50% greater for the lead leg for stepping up or down and 25% less for the trailing leg. The peak knee flexion angles for the lead leg were  $109.9 \pm 4.4$  and  $105.6 \pm 4.2$  degrees for stepping down and stepping up, respectively, as compared to approximately  $70^\circ$  for normal walking.

Peak knee joint moments occurred during stepping down for both the lead and trail foot (Table 2). In addition, stepping up also produced increased values when compared to normal walking. Net joint moments have been estimated at 12-25% greater (Morrison, 1969) when stepping up or down, however the current research suggests lead leg values as high 80% and 50% greater for stepping down and stepping up, respectively for step heights of 30% LL. Stepping down produced net joint moments of approximately 180% to that of normal walking.

## SUMMARY/CONCLUSIONS

Joint angles and net joint moments for normal walking and stepping up and down for the elderly elicit significantly different patterns. The peak net joint moment for both the leading and trailing leg are both elevated in comparison to normal walking values,

thus indicating that stepping down may be more “strenuous” and warrant greater attention. The point in the stride of most concern during the step down occurs immediately prior to impact of the lead foot. It is at this point that the angular velocity of the lead leg is reaching maximum indicating that the individual is “dropping” down to the lower elevation. This is further emphasized with peak net joint moment also occurring just before impact of the lead foot that is attempting to support the body in this unstable position.

## REFERENCES

- Andriacchi, T.P. et al. (1980). *Journal of Bone and Joint Surgery*, **62**, 749-757.
- Archea, J.C. (1985). *Clinical Gerontology*, **1**, 555-569.
- Hoffman, R.R. et al. (1977). *In Proceedings of the 13<sup>th</sup> Annual Conference on Engineering in Medicine and Biology*, Los Angeles, California, **19**, 186-191.
- Laubenthal, K.N. (1972). *Physical Therapy*, **52**, 34-42.
- Morrison, J.B. (1969). *Biomedical Engineering*, **4**, 573-580.
- Svanstrom, L (1974). *Scandinavian Journal of Social Medicine*, **2**, 113-120.
- Winters, D.A. (1980). *Journal of Biomechanics*. **13**, 923-927

**Table 2: Net Joint Moments**

(BW·m)	Normal Walking		Step Down		Step UP	
	1 <sup>st</sup> Foot	2 <sup>nd</sup> Foot	1 <sup>st</sup> Foot	2 <sup>nd</sup> Foot	1 <sup>st</sup> Foot	2 <sup>nd</sup> Foot
APM	$1.6 \pm 0.5$ <sup>a,b</sup>	$1.5 \pm 0.2$	$1.2 \pm 0.2$ <sup>a,c</sup>	$1.6 \pm 0.3$	$1.9 \pm 0.2$ <sup>b,c</sup>	$1.4 \pm 0.2$
KEM	$0.6 \pm 0.1$ <sup>a</sup>	$0.6 \pm 0.1$ <sup>a,b</sup>	$1.1 \pm 0.2$ <sup>a,c</sup>	$1.0 \pm 0.2$ <sup>a</sup>	$0.7 \pm 0.2$ <sup>c</sup>	$0.9 \pm 0.2$ <sup>b</sup>
HFM	$1.1 \pm 0.3$	$1.0 \pm 0.3$ <sup>a</sup>	$1.1 \pm 0.2$	$0.8 \pm 0.2$ <sup>a,c</sup>	$1.1 \pm 0.2$ <sup>c</sup>	$1.1 \pm 0.3$ <sup>c</sup>
HEM	$0.5 \pm 0.1$ <sup>b</sup>	$0.5 \pm 0.1$	$0.4 \pm 0.1$	$0.4 \pm 0.2$	$0.3 \pm 0.1$ <sup>b</sup>	$0.5 \pm 0.1$

Abbreviations - APM, KEM, HFM and HEM are peak ankle plantar flexion, knee flexion and hip flexion moment during Obstacle Clearance Cycle, respectively. Significant differences are denoted by: subscript a, b, and c, which represent differences between normal walking and step down; normal walking and step up; and step down and step up, respectively.

# Seated Postural Sway is Sensitive to Local Vibration

Joseph Soltys and Sara Wilson

University of Kansas, Lawrence, KS, USA

E-mail: jsoltys@ku.edu

## INTRODUCTION

Low back pain affects up to 85% of the population at some point in their lives. This is especially true in industrialized nations like the United States where direct costs are estimated at over \$28 billion annually in lost productivity (Pai, 2004). It has been suggested that a lack of lumbar stability may increase risk of low back injury (Panjabi, 1992). It is therefore important to obtain a better understanding of the sensory mechanisms contributing to spinal stability.

Sway has been used in several studies investigating postural control and stability, primarily in standing. A few studies have attempted to isolate the postural controls of the spine by utilizing a seated sway protocol (Bennet, 2004, Cholewicki, 2000). These studies have made use of both stable and unstable seating in making traces of the center of pressure.

The purpose of this research was to use both stable and unstable sitting to isolate the postural control mechanisms of the lumbar spine. In particular, vibration of the paraspinal musculature was used to examine the role of muscle spindle organs in postural control of the trunk. It was hypothesized that local vibration applied to the lumbar spine will result in increased path lengths in both stable and unstable seated sway.

## METHODS

Three healthy subjects, with no history of low back pain or musculoskeletal disorder within the past six months, participated in

this study, which was approved by the University of Kansas Human Subjects Committee.

A force plate and amplifier were used to record ground reaction forces and calculate COP (Bertec, Columbus, OH). Force plate data were collected at 100 Hz for a 24 trials lasting 30 seconds each. During this time subjects sat quietly with back straight, arms crossed at the chest and feet crossed at the ankles. Subjects were instructed to focus their gaze forward. A short break between trials was allowed between trials to prevent fatiguing and stiffness.

Trials were performed in both stable and unstable seating. With stable seating, subjects sat on a solid platform with legs unsupported. The unstable sitting condition was created using a platform with wobble board with a rounded contact with the force plate.

Local vibration was applied at the L3 level the spinal column using an inertial vibration device worn over the right paraspinal musculature. Vibration was applied at a frequency of 44.5 Hz.

Data were collected for both no stimulus and applied local vibration conditions for both eyes open and eyes closed conditions. Three repetitions were collected for each condition resulting in 24 total trials. The trial order was randomized.

## RESULTS AND DISCUSSION

Medial-Lateral (ML) and Total COP path lengths were calculated from the resultant ground reaction forces. The path lengths for the three trials at each condition were averaged and plotted (Figure 1).

Medial-Lateral and Total path lengths increased with the application of vibrations for both the stable and unstable seated conditions. The increased path lengths with vibration can be attributed to the muscle spindle organs. Vibration can alter afferent activity from the muscle spindle organs and result in changes in perceived muscle length and muscle lengthening velocity (Roll, 1982).

Surprisingly path length was not necessarily greater for the unstable condition when compared to the stable sitting condition. In addition, vision was not found to play a major role in path length with little difference in the eyes closed and open conditions.

## SUMMARY/CONCLUSIONS

Stable seated sway was found to be appropriate for isolating lumbar postural control mechanisms. This research demonstrates the key role that proprioceptive elements and particularly the muscle spindle organs play in lumbar control and stabilization.

## REFERENCES

- Bennett, B.C., M.F. Abel, and K.P. Granata, *Spine*, (2004). **29**(20): p. E449-54.
- Cholewicki, J., G.K. Polzhofer, and A. Radebold. *J Biomech*, (2000). **33**(12): p. 1733-7.
- Pai, S. and L.J. Sundaram. *Orthop Clin North Am*, (2004). **35**(1): p. 1-5.
- Panjabi, M.M., *J Spinal Disord*, (1992). **5**(4): p. 383-9; disc. 397. 5.
- Roll, J.P. *Exp Brain Res*, (1982). **47**(2): p. 177-90.

## ACKNOWLEDGEMENTS

The authors wish to acknowledge the support of the Self Graduate Fellowship.

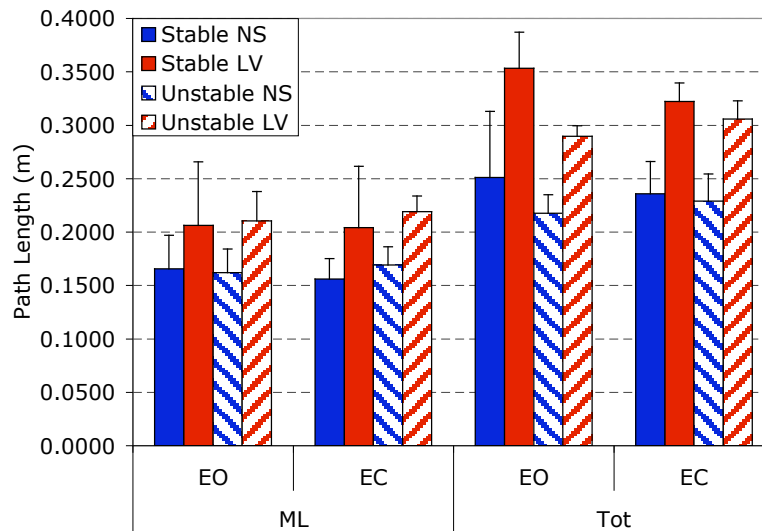


**Figure 1:** Medial-Lateral and Total path lengths in seated sway were found to increase with exposure to paraspinal muscle vibration but were not found to change with eyes closed or unstable seating conditions.

# A DIGITAL TEMPLATE OF CARTILAGE THICKNESS VARIATION IN THE ANKLE

Donald D. Anderson,<sup>1</sup> Steven A. Millington,<sup>2</sup> Bing Li,<sup>3</sup> and Thomas D. Brown<sup>1</sup>

<sup>1</sup>University of Iowa, Iowa City, IA, USA

<sup>2</sup>Medical University of Vienna, Vienna, AUSTRIA

<sup>3</sup>University of Virginia, Charlottesville, VA, USA

e-mail: don-anderson@uiowa.edu

## INTRODUCTION

Patient-specific modeling of the ankle has provided a unique opportunity to study the relationship between altered articular surface anatomy and elevated contact stress, to help elucidate the mechano-pathology of post-traumatic osteoarthritis [Anderson et al., 2006]. The source medical images for these fracture patients have been CT, rather than MRI, because of the presence of metallic hardware. Thus, cartilage layers have been modeled as of constant uniform thickness.

This abstract describes the derivation of a digital template of cartilage thickness variation in the normal ankle working from MRI datasets, to allow projection of non-uniform cartilage thicknesses upon patient-specific models derived from CT datasets.

## METHODS

Bone and cartilage boundaries of the distal tibia and the proximal talus were previously segmented from high-resolution MRI scans of eight human cadaveric ankles [Millington et al, 2005]. In the present study, these data were fitted using fourth order B-spline least-squares surface-fitting techniques [Ateshian, 1993], implemented in MATLAB. Cartilage thicknesses (defined as the length of the three dimensional vector originating on, and normal to, the subchondral bone surface and terminating at the cartilage surface) were calculated for both the tibia and talus at between 15,000 and 20,000 points across the entire subchondral bone surfaces (Figure 1).

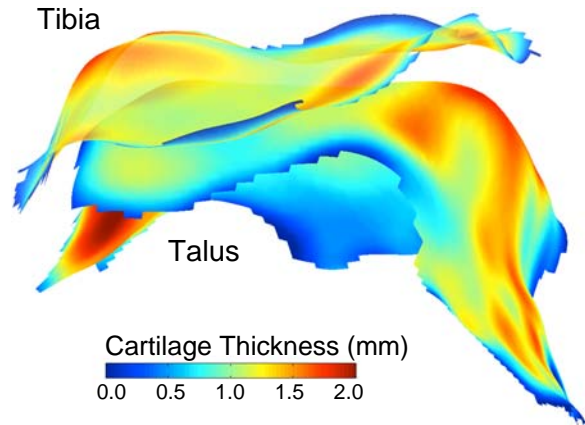


**Figure 1.** Mapping of cartilage thickness distribution upon tibia and talus for a single cadaveric ankle specimen.

In order to create thickness maps that were averages of those measured in the 8 different ankles, the three-dimensional topographical and thickness data were scaled and aligned into a parametric space [Cohen et al., 2003] based on an anatomical coordinate system. The foundation of this approach was the highly accurate fitting of a cylinder to the superior surface of each talar dome.

This parameterization of the ankle cartilage thickness mappings was selected to allow later projection of a generic normalized cartilage thickness distribution upon CT-segmented bone surfaces from fracture patients enrolled for study.

## RESULTS AND DISCUSSION

Cartilage thickness values varied gradually over the surfaces of the tibia and talus (Figure 1). Peak values were observed

anteriorly on the tibia, and at the junction between the medial malleolus and the rest of the articular surface. On the talar dome, peak cartilage thicknesses were noted along the primarily AP-directed ridges.

The parameterization of the tibial and talar surfaces allowed averaging over the eight specimens (Figure 2). Standard deviations were relatively small over most of the surface, although individual specimen variability at the periphery resulted in larger values there. These digital templates of cartilage thickness variation in the ankle provide a valuable basis for incorporation of non-uniform cartilage thickness in patient-specific computational joint models derived from source CT datasets.

## REFERENCES

- Anderson, DD et al. (2006). *Biomech Model Mechanobiol*, [Epub ahead of print].  
Ateshian G (1993) *J Biomech Eng* 115:366-73.  
Cohen ZA et al. (2003) *Osteoarthritis & Cartilage*. 11:569-79.  
Millington SA et al. (2005) *Trans ORS* 30:701.

## ACKNOWLEDGEMENTS

Funded by grants from the NIH (AR46601 and AR048939). Dr. Scott Acton provided technical assistance.

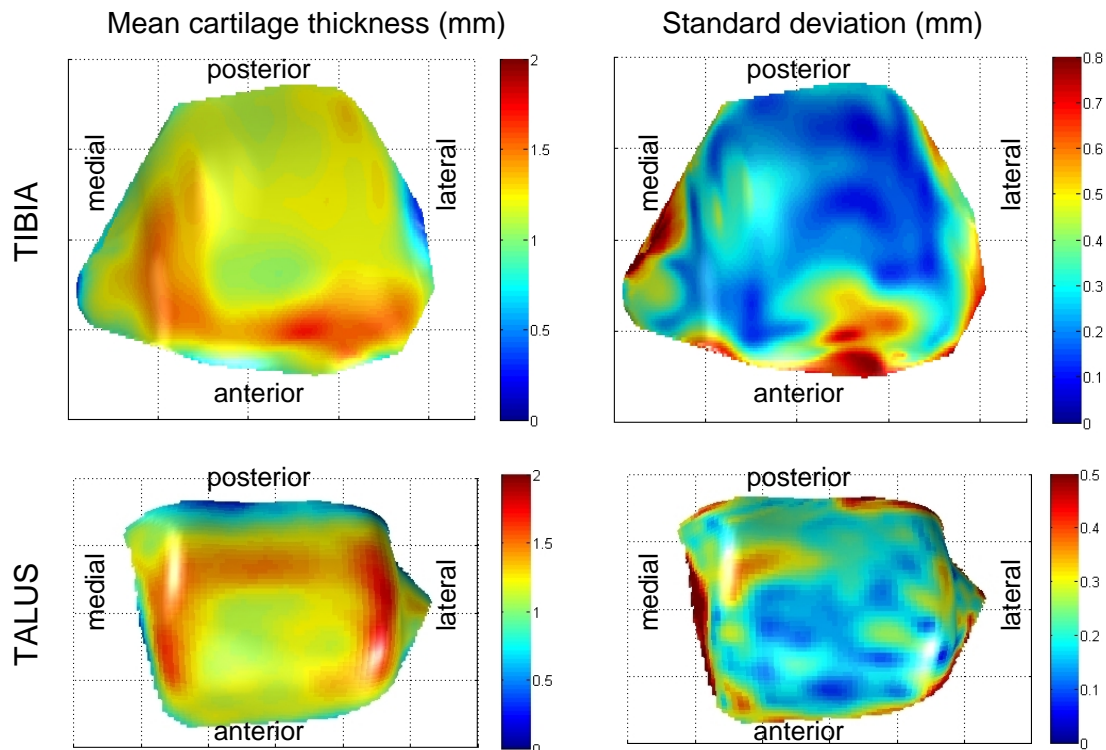


**Figure 2.** Mapping of cartilage thickness in parametric space (values are scaled in a specimen-specific manner), averaged across the eight cadaveric ankle specimens. All surfaces are visualized from superior viewpoint.

# EFFECT OF PILOT HOLE SIZE ON THE INSERTION TORQUE AND PULLOUT STRENGTH OF SELF-TAPPING CORTICAL BONE SCREWS IN OSTEOPOROTIC BONE

Suneel Battula MS <sup>1</sup>, Andrew Schoenfeld MD <sup>2</sup>, Vivek Sahai MD <sup>2</sup> and Glen O. Njus PhD <sup>1</sup>

<sup>1</sup> Department of Biomedical Engineering, The University of Akron, Akron, OH, USA

<sup>2</sup> Department of Orthopaedic Surgery, Akron General Medical Center, Akron, OH, USA

E-mail: bsuneel@uakron.edu

## INTRODUCTION

Screws are the most commonly used implants for osteosynthesis. All the surgical screws can experience failure if the torsional, tensile and flexion loads are considerably high. The use of self-tapping screws results in higher insertion torques, i.e. higher torsional loads, as these screws cut their own threads in the pilot hole drilled in the bone sample. The insertion torques (IT) and axial forces vary with respect to size of the pilot hole. Gantous et al. suggested that one way to decrease the IT was to increase the pilot hole size. Their results suggested that the pilot hole size (PHS) could be increased to 80% of the outer diameter (OD) of the screws without compromising on the pullout strength (PS) of the screws. They tested their theory using blocks of Delcron that simulated bone but what remains unknown is the validity of their theory in the presence of a cortical shell and also for osteoporotic bone.

In this study, the torque for inserting the STS into an osteoporotic bone block for different PHS was measured and the PS for extraction of the screws was determined for different depths of insertion.

## METHODS

Bone blocks simulating the osteoporotic bones were acquired from Pacific Research Laboratories (Vashon, WA). The bone blocks had a bi-cortical layer made from e-glass-filled epoxy sheets and cancellous

bone mimicked by polyurethane foam with densities 1.7 & 0.24 gms/cc and tensile moduli 12.4 GPa & 143 MPa respectively. Seventy-two Synthes stainless steel (SS) self-tapping cortical bone screws (40mm length & 3.5mm diameter) were inserted into the pilot holes, drilled into the blocks, of sizes 2.55 (A: 73% of OD), 2.50 (B: 71.5%), 2.45 (C: 70%) or 2.8mm (D: 80%). Using a digital torque screwdriver, as shown in Fig 1, screws were inserted to 0, 1 or 2 mm past the far cortex.

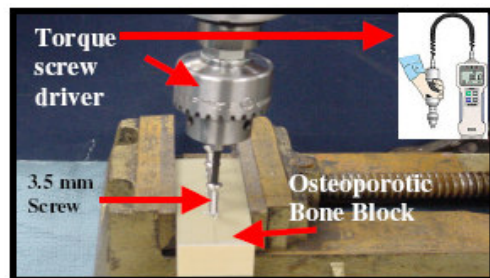


**Figure 1:** Insertion of the screws into the osteoporotic bone block using the digital torque screwdriver.

All the pullout tests were performed using a servo-hydraulic material testing system (Instron 8511). The holding fixture for the axial pullout was designed according to the *ASTM F 543-02* specifications for the metallic medical bone screws. The screws were extracted axially from the blocks under displacement control at 0.1 mm/s. The force-displacement data was digitally recorded for each of the pullout tests and the maximum value of the applied tensile force was determined as the PS of the screw. ANOVA

and SNK tests were performed to determine the effect of the depth of insertion and PHS on the loading energy (LE), PS and IT.

## RESULTS AND DISCUSSION

Fig. 2 shows comparison of the mean IT ( $\pm$  Std Dev) values of the screws for different PHS. It may be observed that IT of the screws inserted into pilot holes A, B & C were higher than those inserted into D. It was observed during screw insertion that the peak IT value was reached when it penetrated the far cortex and didn't change for 0,1 or 2mm penetration past the far cortex.

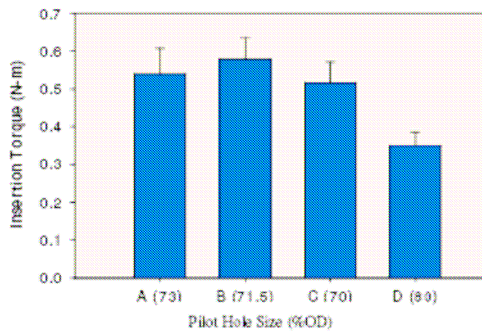


**Figure 2:** Insertion torque of the self-tapping screws inserted into 4 PHS.

Mean PS ( $\pm$  Std Dev) values for all the PHS at different insertion depths are illustrated in Fig 3. It may be observed that PS for 1 & 2 mm penetration past the far cortex are higher than that for 0mm regardless of the PHS. It may also be observed that the PS for the screws at all the depths was lower for pilot hole D when compared to the others.

LE was computed as the area under the load displacement curve up to maximum load (PS). Table.1 summarizes the results of the LE at different depths and also for all PHS.

The statistical analysis indicated that the IT for the screws inserted into A, B & C was significantly different from that of the D size pilot hole. The PS at 1 & 2mm past the far cortex was significantly different ( $P < 0.05$ )

from 0mm depth of insertion. The results also indicated a significant difference between LE for A,B & C pilot holes to be significantly different from that of D for all depths of insertion.

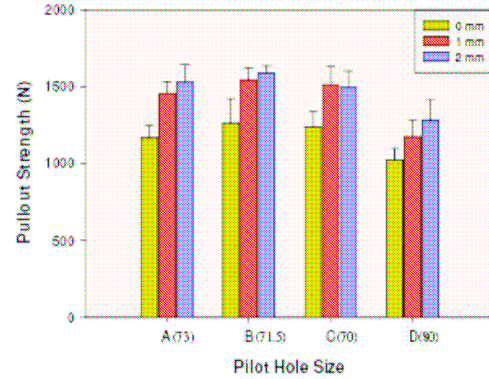


**Figure 3:** Pullout Strength of the screws inserted to different depths for 4 PHS.

**Table 1:** LE to peak force for screws inserted to different depths for 4 PHS.

	A (N-mm)	B (N-mm)	C (N-mm)	D (N-mm)
0 mm	348.1	403.0	381.9	286.9
1 mm	555.5	563.8	570.0	358.0
2 mm	657.9	693.9	648.5	430.4

## SUMMARY/CONCLUSIONS

It has been confirmed with the help of biomechanical testing that the PHS has an influence on the IT, PS and LE for cortical bone screws inserted in osteoporotic bone. It can be concluded that the recommendations made by Gantous et al. do not apply to osteoporotic bone and bones with cortical - cancellous interface. This study illustrated that an increase in the PHS to 2.8mm (80% OD) will reduce the IT but will also reduce the PS of the bone-screw construct relative to that of PHS of 2.5mm (71.5% OD), which is currently used as optimal for 3.5mm cortical screws.

## REFERENCES

- Gantous.A, Phillips. J. (1995). *Plastic and reconstructive surgery*, 1165-69.
- Heidemann W, Gerlach K.L., et al. (1998). *J Craniomaxillofac Surg*. 26(1):50-5.

# RELATIONSHIP BETWEEN THE SAGITTAL AND FRONTAL KNEE MOMENTS IN HEALTHY OBESE ADULTS WITH DIFFERENT BODY MASS DISTRIBUTION PATTERNS.

Khole Priyanka<sup>1</sup>, Segal Neil, MD<sup>2</sup>, Yack H John, PT PhD<sup>1</sup>

<sup>1</sup>Graduate Program in Physical Therapy and Rehabilitation Sciences, University of Iowa, Iowa.

<sup>2</sup>Department of Orthopedics and Rehabilitation, University of Iowa, Iowa.

john-yack@uiowa.edu or priyanka-khole@uiowa.edu

## INTRODUCTION

Osteoarthritis (OA) is a leading cause of disability amongst US adults (Felson, 1998) and obesity has been identified as an important modifiable risk factor, contributing to both the development (Gelber, 1999) and progression of knee OA (Spector, 1994). Though many researchers believe that obesity may be affecting the pathogenesis of knee OA by increasing the mechanical loading of the articular cartilage, there have been very few studies analyzing obese gait and quantifying knee kinetics in both the frontal and sagittal plane (DeVita, 2003). Obesity is highly associated with increased odds ratio for combined tibiofemoral and patellofemoral knee OA (Cicutini, 1997). External knee adduction moments are considered a reliable estimate of loading at the medial compartment of the knee joint, whereas sagittal moments contribute to the overall loading across the knee, as well as the loading through the patellofemoral joint. While investigators have speculated that high frontal moments would require stabilization by high knee extensor moments (Schnitzer, 1993), to date, the extent to which the magnitudes of these moments are synchronized has not been documented. Coloring the relationship between mechanical loading and OA is the fact that only 16% of obese adults develop knee OA (Doherty, 2001) with is a greater prevalence in obese women (Eaton, 2004). This suggests that the unexplored differences in the body mass distribution patterns amongst men and women might be

contributing to altered gait mechanics, subsequently affecting knee joint loading. The purpose of the study was to analyze the relationship between sagittal and frontal moments in obese adults with varying body mass distribution and comparing them with their normal weight peers as this might help to provide some insights into the loading mechanics of this at risk population.

## METHODS

Sixty subjects, twenty normal weight controls, twenty subjects with a lower obese pattern and twenty subjects with a central obesity pattern, between the ages of 35-55 years and with no knee, lower limb, neuromuscular or medical problems participated in the study. Obesity was defined as having a body mass index greater than or equal to 30.0 Kg/m<sup>2</sup> (BMI of controls < 25.0 Kg/m<sup>2</sup>). Women with waist: hip ratio of 0.85 or less and men with a ratio of 0.95 or less were identified to have lower obesity patterns. Standard kinetic and kinematic data was collected using an Optotrak motion analysis system and Kistler force plate as the subjects walked along a 10 m walkway at their self selected speed. Three non-collinear markers were used to track the right lower limb, pelvis and trunk. Kinematic data were collected at 60 Hz and filtered at 6 Hz. Frontal plane data were analyzed using Visual 3D (C-Motion, Inc) to obtain the external knee adduction moments. Inter-group comparisons were made using a Non-parametric equivalent of Kruskal-

Wallis test and Spearman's coefficients were calculated to assess associations.

## RESULTS AND DISCUSSION

A significant difference in peak abductor moments was found between the central obese group and controls ( $p < 0.001$ ). Also, a difference in peak extensor moments was found between both obese groups and controls ( $p < 0.01$ ). The correlations between the peak frontal and sagittal moments in the three groups were found to be weak.

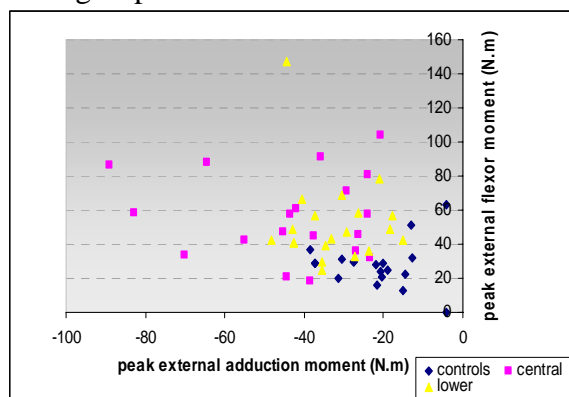


Figure 1: This scatter plot illustrates the weak correlation between the peak moments occurring in the sagittal and frontal planes.

The results of this study demonstrate that even though the peak frontal and sagittal moments are increased in obese adults, as compared to their normal weight peers, the association between these moments is weak. Hence, it is unadvisable to deduce conclusions about the overall status of knee loads based on moments in one plane alone. While the central obesity pattern appears to have a differential effect on the frontal moment, mass distribution was not an issue

in the sagittal plane where both obese groups had increased moments. It should also be noted that since the magnitude of these moments represents absolute loading at the knee, documented normalized values should otherwise be interpreted cautiously

## SUMMARY

Due to the lack of a strong association between the peak frontal and sagittal moments, it is problematic to comment on overall knee joint loads based on just the sagittal moments. Focusing strictly on the muscle loading across the knee, potentially detrimental loads in the frontal and sagittal planes would appear to be independent in the association with medial knee and patellofemoral OA.

## REFERENCES

- Cicuttini, F. M., T. Spector, et al. (1997). *J Rheumatol* **24**(6): 1164-7.
- DeVita, P. and T. Hortobagyi (2003). *J Biomech* **36**(9): 1355-62.
- Doherty, M. (2001). *Lancet* **358**(9284): 775-6.
- Eaton, C. B. (2004). *Medicine & Health, Rhode Island* **87**(7): 201-4.
- Felson, D. T. et al (1998). *Epidemiology of Osteoarthritis. Osteoarthritis*. Oxford, Oxford University Press: 12-22.
- Gelber, A. C., M. C. Hochberg, et al. (1999). *Am J Med* **107**(6): 542-8.
- Schnitzer, T. J., J. M. Popovich, et al. (1993). *Arthritis Rheum* **36**(9): 1207-13.
- Spector, T. D., D. J. Hart, et al. (1994). *Ann Rheum Dis* **53**(9): 565-8.

Table 1: Peak moments and correlations in the three groups.

Groups	Peak frontal plane moments (N.m)	Peak sagittal plane moments (N.m)	Correlation between peak frontal and sagittal moments
Obese Central	-43.3+-23.4	56.7+-24.8	-0.056
Obese Lower	-32.3 +-9.9	52.5+-26.1	-0.143
Controls	-21.9+-9.6	27.9 +-11.8	0.024

# DETERMINATION OF MAXIMUM TORQUE / ANGULAR VELOCITY RELATIONSHIP USING THE BIODEX SYSTEM 3 ISOKINETIC DYNAMOMETER

Jessica Quiroz and Pui Wah Kong

The University of Texas at El Paso, El Paso, TX, USA

E-mail: [pkong@utep.edu](mailto:pkong@utep.edu) Web: [www.utep.edu](http://www.utep.edu)

## INTRODUCTION

Isokinetic dynamometers have been widely used to measure maximum torque / angular velocity data at various joints. During concentric contraction, muscle force decreases hyperbolically with increasing velocity whereas during the eccentric contraction, muscle force increases to approximately 1.5 times the maximum isometric force and then plateaus at higher velocities. Inter-subject variations in torque / angular velocity responses limit the development of a generic model based on average data (Hawkins & Smeulders, 1999) and therefore subject-specific torque data are preferred when used in biomechanical simulation models (King & Yeadon, 2002).

Most software provided with commercial isokinetic dynamometers identifies the peak concentric and eccentric torque values throughout the whole range of movement for a given angular velocity. These peak torques are subsequently used to plot a maximum torque / angular velocity curve to represent isokinetic muscle properties. It has been shown that inertial effect of the dynamometer and body segment will influence the accuracy of the measured velocity-specific torque especially during high velocity movement (Herzog, 1988). The purpose of this study is to compare the torque / angular velocity relationship obtained from the Biodex System 3 software and that obtained from raw digital data.

## METHODS

Two physically active male subjects participated in this study. Each subject performs maximum concentric (+ve) and eccentric (-ve) knee extension at various angular velocities on the Biodex System 3 isokinetic dynamometer ( $\pm 30^\circ/\text{s}$ ,  $\pm 60^\circ/\text{s}$ ,  $\pm 120^\circ/\text{s}$ ,  $\pm 180^\circ/\text{s}$ ,  $\pm 240^\circ/\text{s}$ ,  $\pm 300^\circ/\text{s}$ ,  $+350^\circ/\text{s}$ ,  $+400^\circ/\text{s}$ ,  $+450^\circ/\text{s}$ ,  $+500^\circ/\text{s}$ ). The effect of weight due to gravity was corrected. Peak concentric and eccentric torque values were identified by the Biodex System 3 software. The raw digital torque, angle and angular velocity time histories recorded were exported for manual analysis. From the raw data, the peak concentric and eccentric torques at constant velocities were identified by visual inspection. This provided two torque / angular velocities data sets: 1) Biodex System 3 software, and 2) raw data.

A seven-parameter function (Yeadon et al., 2006) was used to obtain a torque / angular velocity relationship from each data set. This curve fitting procedure was achieved by minimizing the root mean squared differences between the data points and the fitted curve using the Simulated Annealing optimization algorithm (Corana et al., 1987). Computer programs were written in Matlab (The MathWorks) and a typical 100,000 evaluations took approximately 2 hours.

## RESULTS AND DISCUSSION

The seven-parameter fit representing the maximum knee extension torque / angular velocity relationship for subject 1 and

subject 2 are shown in Figure 1 and Figure 2 respectively. For both subjects, the raw data were very similar to the software data except for high concentric velocities of 400°/s, 400°/s and 500°/s at which the software data were systematically higher than the raw data.

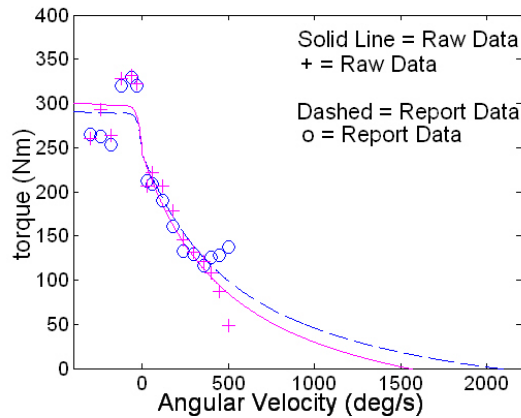


**Figure 1:** Maximum torque / angular velocity relationship for subject 1.

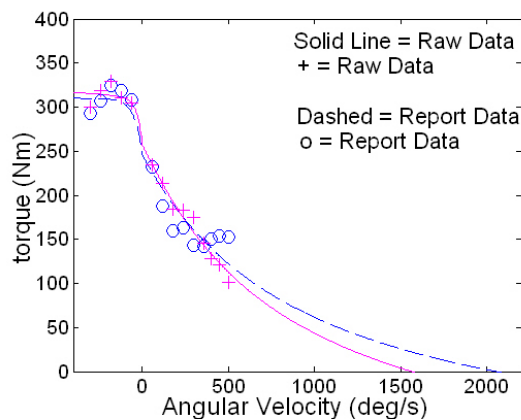


**Figure 2:** Maximum torque / angular velocity relationship for subject 2.

The seven-parameter torque / angular velocity relationship fitted closely to the experiment data. The curves obtained from the two data sets were very similar in eccentric velocities and slow concentric velocities. However, there was a substantial

discrepancy between the two curves when extrapolated to higher concentric velocities beyond the limit of the isokinetic dynamometer. The maximum torque at higher concentric velocities (500°/s to 2000°/s) predicted from the software data were higher than those predicted from the raw data. This was probably due to the higher torque values identified by the software at 400°/s, 400°/s and 500°/s. These results may have some implications in simulation models that incorporate force-velocity relationships based on experimental data obtained from dynamometry. While it is unlikely to impose a problem on simulations of sub-maximal slow movements such as walking, it will be essential to obtain an accurate relationship for maximal dynamic movement such as kicking and throwing.

## SUMMARY/CONCLUSIONS

This study compared the maximum torque / angular velocity relationship obtained from the Biodex System 3 software and raw data. Using the software data tends to over-estimate the peak torque at high concentric velocities and this may lead to errors in simulation model of maximal dynamic movement such as kicking and throwing.

## REFERENCES

- Corana, A. et al. (1987). *ACM Transactions on Mathematical Software*, **13**, 262-280.
- Herzog, W. (1988). *J. Biomechanics*, **21**, 5-12.
- Hawkins, D., Smeulders, M. (1999). *J. Applied Biomechanics*, **15**, 253-269.
- Yeadon, M.R., King, M.A. (2002). *J. Biomechanics*, **18**, 195-206.
- Yeadon, M.R. et al. (2006). *J. Biomechanics*, **39**, 476-482.

# PATELLOFEMORAL FORCES AND STRESSES DURING LUNGE EXERCISES

Rafael F. Escamilla<sup>1</sup>, Naiquan Zheng<sup>2</sup>, Alan Hreljac<sup>3</sup>, Rodney Imamura<sup>3</sup>, Toran D. MacLeod<sup>1</sup>, William B. Edwards<sup>4</sup>, Glenn S. Fleisig<sup>5</sup>, Kevin E. Wilk<sup>5</sup>

<sup>1</sup>Department of Physical Therapy, California State University, Sacramento, USA

<sup>2</sup>Orthopaedics and Rehabilitation Program, University of Florida, Gainesville, FL, USA

<sup>3</sup>Kinesiology and Health Science Department, California State University, Sacramento, USA

<sup>4</sup>Department of Health and Human Performance, Iowa State University, Ames, Iowa, USA

<sup>5</sup>American Sports Medicine Institute, Birmingham, AL, USA

e-mail: rescamil@csus.edu

## INTRODUCTION

The forward and side lunge exercises are used in both athletic training and during knee rehabilitation programs. However, it is currently unknown how patellofemoral forces and stresses change among different lunge exercises and knee angles. The purpose of this study was to compare patellofemoral forces and stresses as a function of lunge exercises and knee angles. It was hypothesized that patellofemoral forces and stresses would increase as knee flexion increased and would be greater in the short stride lunge compared to the long stride lunge.

## METHODS

Eighteen subjects (9 males and 9 females) were used with an average age, mass, and height of  $29\pm 7$  y,  $77\pm 9$  kg, &  $177\pm 6$  cm for males and  $25\pm 2$  y,  $60\pm 4$  kg, &  $164\pm 6$  cm for females. Each subject performed the forward lunge both with a long stride (knee over ankle at the bottom position) and a short stride (knee beyond toes at bottom position). A long stride side lunge was also performed (knee over ankle at bottom position). Intensity was normalized for each exercise by having each subject their 12 repetition maximum weight, which were  $49\pm 10$  kg for males and  $32\pm 7$  kg for females for the forward lunge, and  $55\pm 9$  kg for males and  $36\pm 9$  kg for females for the side lunge. Surface electrodes were placed over the vasti muscles, rectus femoris, medial & lateral hamstrings, and gastrocnemius. Reflective

markers were positioned over landmarks on the foot, ankle, knee, hip, and shoulder.

Video (60 Hz), EMG & force platform (960 Hz) data were collected during 3 repetitions of each exercise (0-90° knee flexion) and averaged. EMG data were normalized by maximum voluntary isometric contractions (MVIC).

Patellofemoral forces & stresses were calculated using a biomechanical knee model (Zheng et al., 1998; Salsich et al., 2003) with input variables consisting of resultant knee forces and moments, patellofemoral contact areas, and the muscle force function  $F_{m(i)} = k_i A_i \sigma_{m(i)} [EMG_i / MVIC_i]$ , where  $k_i$  was a muscle force-length variable,  $A_i$  was physiological cross sectional area (PCSA) per muscle,  $\sigma_{m(i)}$  was MVIC force per unit PCSA,  $EMG_i$  and  $MVIC_i$  were EMG window averages, and  $c_i$  was a weight factor adjusted in a computer optimization program. Patellofemoral forces and stresses as a function of exercise and knee angle were assessed by a two-way repeated measures analysis of variance ( $p < 0.05$ ).

## RESULTS AND DISCUSSION

Patellofemoral forces and stresses are shown in Figures 1 and 2. Both patellofemoral forces and stresses increased progressively as knee flexion increased, and these forces and stresses were significantly greater in the short stride forward lunge compared to the long stride forward lunge between 60-90° knee flexion during the ascent.

## SUMMARY/CONCLUSIONS

Performing different variations of the lunge exercise does affect the magnitude of

patellofemoral forces and stresses. In addition, both forces and stresses increased with knee flexion.

Zheng et al. (1998), *Journal of Biomechanics*, **31**, 963-967.

**REFERENCES**

Salsich et al. (2003), *Clinical Orthopaedics*, **417**, 277-284.

**ACKNOWLEDGEMENTS**

The authors would like to thank Lisa Bonacci, Toni Burnham, Juliann Busch, Kristen D’Anna, Pete Eliopoulos, & Ryan Mowbray for all their assistance during data collection and analyses.

Figure 1. Mean (SD) patellofemoral compressive force during the forward lunge and the side lunge.

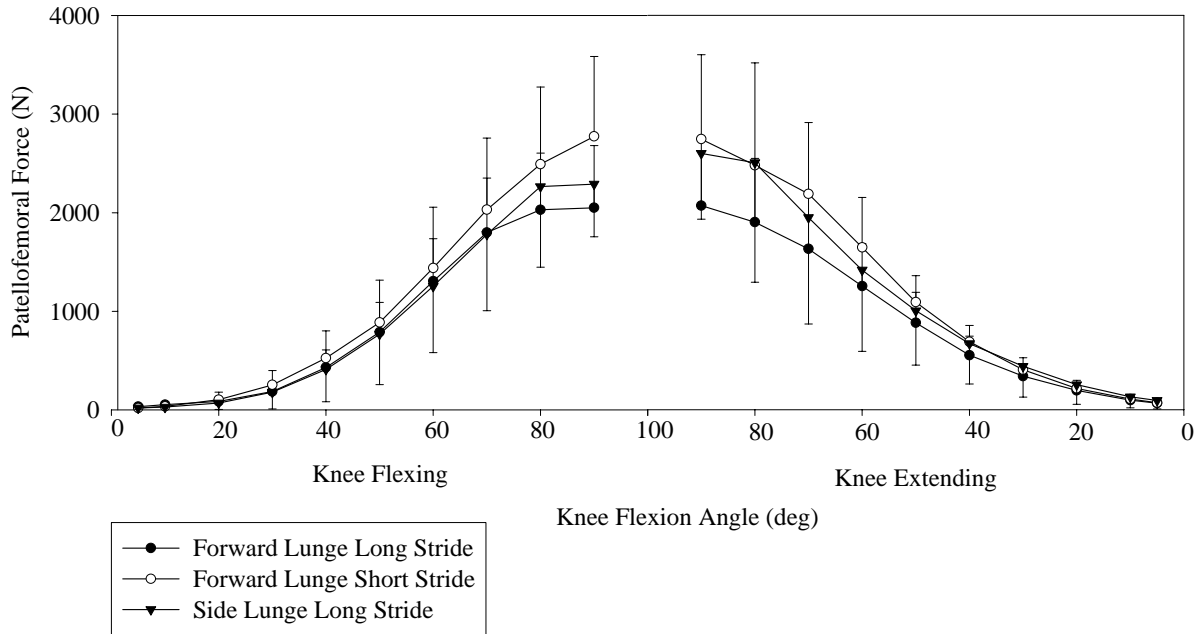
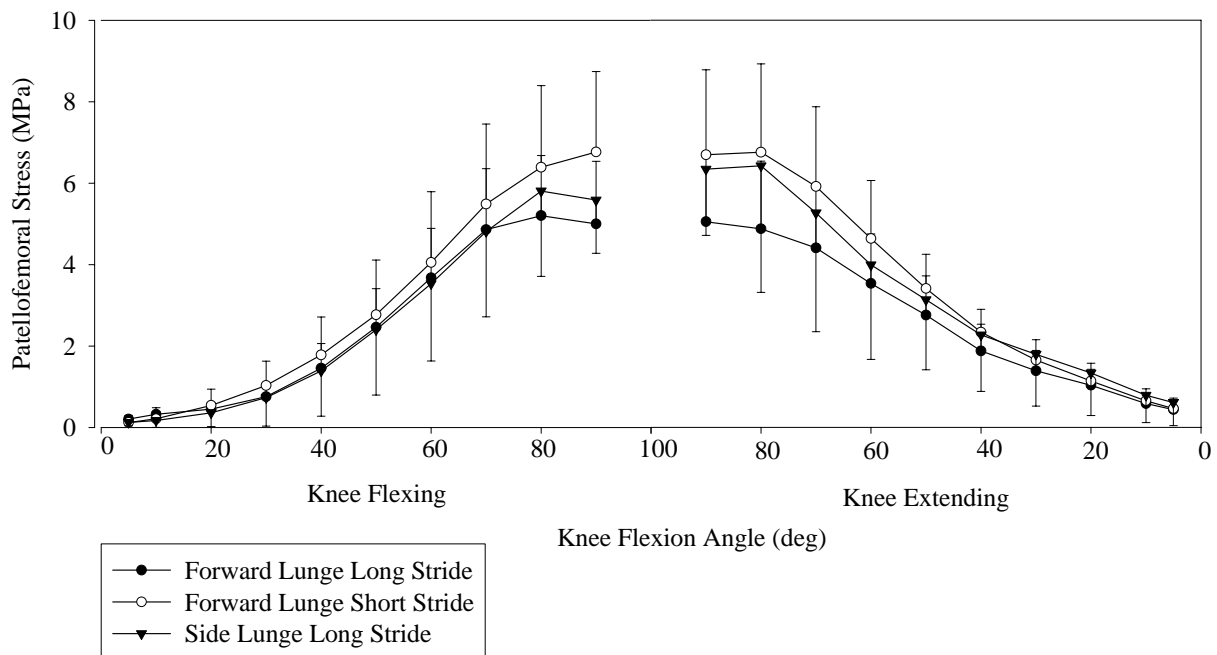


Figure 2. Mean (SD) patellofemoral stress during the forward lunge and the side lunge.



# EFFECT OF HIP ROTATION ON ANTERIOR HIP FORCE DURING STRAIGHT LEG RAISING

Cara L. Lewis<sup>1</sup>, Shirley A. Sahrman<sup>2</sup>, and Daniel W. Moran<sup>2</sup>

<sup>1</sup> University of Michigan, Ann Arbor, MI, USA

<sup>2</sup> Washington University, St. Louis, MO, USA

E-mail: caralew@umich.edu

## INTRODUCTION

Acetabular labral tears are a recently recognized source of anterior hip pain (AHP) (Lewis and Sahrman, 2006). Excessive forces have been implicated as one cause of these tears. A clinical sign of a tear is anterior hip pain during active or resisted straight leg raising (SLR).

Clinical, we have noted that when people with AHP perform SLR, the femur appears to medially rotate more than when people without AHP perform SLR. We have also noted that in some people with AHP, verbal cues to alter the muscle activation when performing SLR decreases the medial rotation and decreases the report of pain when compared to performing SLR without verbal cues regarding muscle activation. In a prior study, we found that the anterior hip joint force during SLR decreased with increasing force contribution from the iliacus and psoas muscles. In this study, we investigate the effect of hip rotation on anterior hip force while maintaining the leg in the SLR position. We hypothesize that the anterior hip force will increase with increasing degrees of hip medial rotation.

## METHODS

A three dimensional, six degree of freedom musculoskeletal model of a leg was modified to estimate hip joint forces while maintaining the leg in different hip positions in supine. Musculoskeletal parameters were adapted from Delp (1990). Kane's Method (Kane and Levinson, 1985) and AUTOLEV 3.1 (OnLine Dynamics, Inc., Sunnyvale,

CA) were used to generate the dynamic equations of motion. In this study we were interested in the anteriorly directed hip force only when the limb was held in a position, we simplified the equations of motion to include only torque due to muscle force and gravity. The general form of the simplified equations of motion is:

$$\mathbf{M}(\bar{\mathbf{Q}})\ddot{\bar{\mathbf{Q}}} = \bar{\mathbf{T}}(\bar{\mathbf{Q}}) + \bar{\mathbf{G}}(\bar{\mathbf{Q}})$$

In this equation,  $\mathbf{M}$  is the mass matrix.  $\mathbf{Q}$  is the column vector of joint angles.  $\mathbf{T}$  and  $\mathbf{G}$  are the column vectors of the net joint torques due to muscle and gravity respectively.

In this study, the hip position was varied in 1 degree increments from 10° of hip extension to 10° of hip flexion, and from 20° of hip medial rotation to 20° of hip lateral rotation. The range of simulated hip flexion started at 10° of hip extension because this is the presumed position of the hip when the lumbar spine is flat against the mat and is commonly the starting position for correct performance of a SLR. The hip was maintained in neutral adduction / abduction and the knee in full extension for all iterations. A pseudoinverse optimization routine was used to solve for the optimal set of muscle stresses (Yamaguchi et al. 1995) needed to hold the leg in the specified position. The model then calculated the resulting force in the hip joint due to the muscle stresses and resolved it into its three force components.

## RESULTS AND DISCUSSION

The anterior hip force was higher when the femur was in medial rotation than when the femur was in neutral or lateral rotation. At the starting position of 10° of hip extension, the anterior hip force was 222 N at 20° of medial rotation, 88 N at neutral rotation and 95 N at 20° of lateral rotation. At 10° of hip flexion, when the hip force was posterior for most hip rotation angles studied, the force remained anterior when in 20° of medial rotation. The anterior hip force was lowest when the femur was in flexion and between 8 and 9° of lateral rotation.

## SUMMARY/CONCLUSIONS

A 3D musculoskeletal model was modified to estimate hip forces when performing a straight leg raise at a range of hip rotation angles. The anterior hip force increased with increasing hip extension angle and with increased hip medial rotation angle. Patients with anterior hip pain or an acetabular labral tear should be instructed to avoid hip

extension and hip medial rotation when performing a straight leg raise. Initiating the SLR with the hip in slight flexion and lateral rotation would reduce the anterior hip force.

## REFERENCES

- Delp, S. L. (1990). *Surgery simulation: a computer graphics system to analyze and design musculoskeletal reconstructions of the lower limb*. Department Mechanical Engineering. Palo Alto, California, The Stanford University.
- Kane, T. R. and Levinson, D. A. (1985). *Dynamics: theory and applications*. New York, NY, McGraw-Hill.
- Lewis, C.L., and Sahrman, S.A. (2006). Acetabular labral tears. *Phys Ther*, **86**, 110-21.
- Yamaguchi, G.T, Moran, D.W. and Si, J. (1995) Computationally efficient method for solving the redundant problem in biomechanics. *Journal of Biomechanics*, **28**, 999-1005.

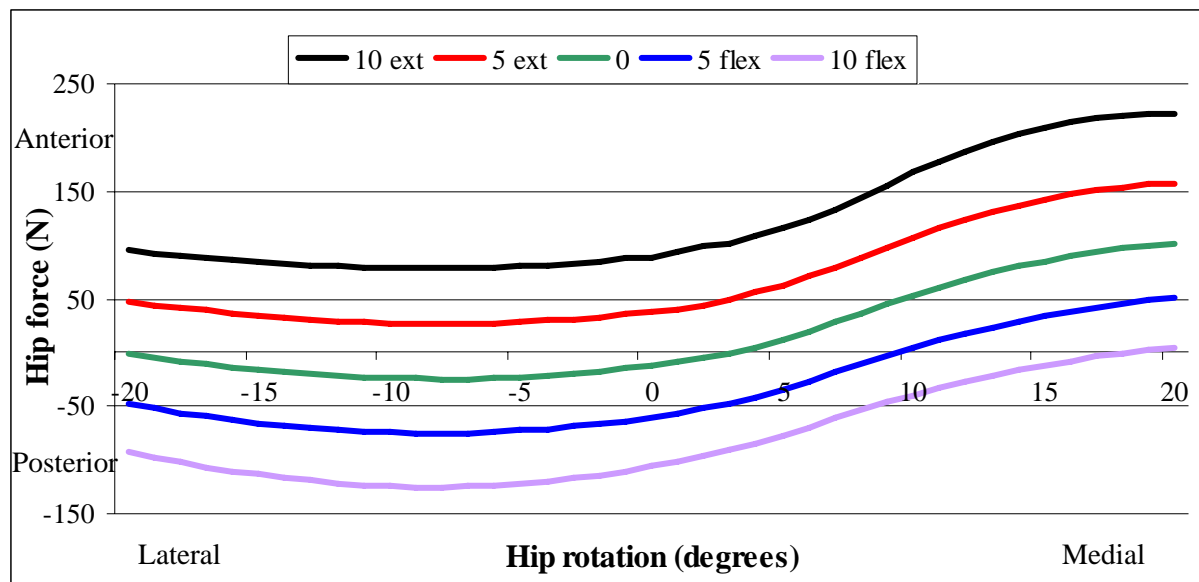


**Figure 1: Anterior hip forces.** Anterior hip joint forces at 10 and 5° of hip extension, neutral, and 5 and 10° of hip flexion, and at a range of hip rotation angles. The hip joint force is higher when the hip is in medial rotation than when in neutral or lateral rotation. The anterior hip force is lowest when the hip is in 8-9° of hip lateral rotation.

# **A KINEMATIC COMPARISON OF MANUAL AND PUSHRIM-ACTIVATED POWER-ASSISTED WHEELCHAIR PROPULSION**

John W. Chow, Mark D. Tillman, Kim A. Fournier, Srikant Vallabhajosula, Michael A. Stancil, Peter Giacobbi, Jr., and Charles E. Levy<sup>1,2</sup>

Department of Applied Physiology & Kinesiology and <sup>1</sup>Department of Occupational Therapy, University of Florida, Gainesville, FL, USA

<sup>2</sup> North Florida/South Georgia Veterans Health System, Gainesville, FL, USA  
E-mail: jchow@hhp.ufl.edu Web: www.hhp.ufl.edu/apk/ces/labs/biomech/

## **INTRODUCTION**

Pushrim-activated power-assisted wheelchairs (PAWs) are an intermediate alternative between conventional power and manual wheelchairs. PAWs require users to stroke the pushrims to activate a small, lightweight motor which then drive the wheels for a brief period of time (Levy & Chow, 2004). To keep a PAW moving, a user must continue to stroke the pushrims like propelling a standard manual chair. PAW is a relatively new technology and limited biomechanical studies have been conducted to quantify the stroking characteristics of PAW propulsion. Testing subjects on a computer-controlled dynamometer at 3 different resistance levels and 2 different speeds, Corfman et al. (2003) found significant reductions in upper extremity range of motion with the use of the PAW. Testing their subjects on a level surface, a carpet, and an incline, Levy et al. (2004) reported that the use of a PAW was associated with lower heart rate elevation, lower perceived exertion, and reduced muscular activity. To gain further insights into the biomechanics of PAW propulsion, the purpose of this preliminary study was to compare stroking kinematics of wheeling over a variety of terrains using manual and PAW wheelchairs.

## **METHODS**

Three male and 2 female full-time manual wheelchair users (age  $45.4 \pm 17.9$  yrs) who have no musculoskeletal disorders in their upper extremities served as the subjects. Each subject was asked to wheel over 3 different surfaces using his/her own manual chair and his/her own chair fitted with e.motion power-assisted wheels ([www.frankmobility.com/emotion.htm](http://www.frankmobility.com/emotion.htm)) in a laboratory setting:

- a flat vinyl floor
- a thick carpet
- a 4-m ramp ( $6^\circ$  in slope)

Two trials were completed for each chair type and surface. Wheelchair location was tracked using 7 digital Hawk cameras operated at 60 Hz and an EvaRT software (Motion Analysis Corporation, Santa Rosa, CA). Side view of the stroking motion was also recorded using a Sony digital camcorder (60 frames/s). Two consecutive strokes in each trial were analyzed. The instants of initial hand contact and release were identified from the video recordings and applied to data collected by the EvaRT system. Five parameters were determined from each stroke analyzed: stroke distance, stroke frequency, stroke speed, and contact and recovery times as a percentage of the stroke time. A stroke cycle was divided into two phases – contact and recovery phases –

using the instants of initial contact and release. For chair-surface combination, the average over 4 strokes were use in the statistical analyses. In addition to descriptive statistics, a 2 (chair type) x 3 (surface) ANOVA with repeated measures was performed for each parameter ( $\alpha = 0.05$ ).

## RESULTS AND DISCUSSION

No significant chair type main effects were detected in any of measures (Table 1). However, significant surface main effects were found in the stroke speed ( $p = 0.018$ ), stroke length ( $p = 0.005$ ), and relative contact and recovery times ( $p = 0.010$ ). No post-hoc analyses were performed since the surface effect was not the primary focus of this study.

Although the chair x surface interactions were not significant in relative contact and recovery times ( $p = 0.110$ ), PAW seems to have different effects on flat and ramp surfaces. Specifically, the use of a PAW caused a relatively large decrease in relative contact time for the flat surface and a small increase in the relative contact time for the ramp condition (Table 1). The opposite was true for the relative recovery time since these two times are inversely related.

The subjects in this study only had a few minutes to get used to the PAW. All subjects expressed that lesser effort was needed when using the PAW. They might be very conservative in wheeling a PAW when they were not fully adapted to the performance characteristics of PAW. The small sample size may also contribute to the lack of significant differences between the 2 types of chair. Future studies should examine whether stroking kinematics will change after a prolonged use of PAW.

## SUMMARY/CONCLUSIONS

No significant differences in stroking kinematics were found between manual and PAW wheelchairs. Future studies should examine the impact of PAW in different subgroups of wheelchair users.

## REFERENCES

- Corfman, T.A. et al. (2003). *J. Spinal Cord Med.*, **26**, 135-140.  
 Levy, C.E, Chow, J.W. (2004). *Am. J. Phys. Med. Rehabil.*, **83**, 166-167.  
 Levy, C.E. et al. (2004). *Arch Phys Med Rehabil.*, **85**, 104-112.

## ACKNOWLEDGEMENTS

NIH grant: R21HD046540-01A1.

**Table 1:** Mean (SD) of different measures.

Surface	Manual chair					PAW				
	Stroke speed (m/s)	Stroke Dist (m)	Stroke Freq (Hz)	Rel Cont Time (%)	Rel Recy Time (%)	Stroke speed (m/s)	Stroke Dist (m)	Stroke Freq (Hz)	Rel Cont Time (%)	Rel Recy Time (%)
Flat	1.05 (0.27)	1.23 (0.59)	1.05 (0.29)	53.5 (12.3)	46.5 (12.3)	1.04 (0.26)	1.25 (0.55)	1.06 (0.26)	44.2 (7.0)	55.8 (7.0)
Carpet	0.893 (0.23)	0.95 (0.43)	1.02 (0.22)	61.8 (10.2)	38.2 (10.2)	0.87 (0.24)	0.95 (0.38)	0.97 (0.23)	61.6 (14.4)	38.4 (14.4)
Ramp	0.75 (0.35)	0.76 (0.48)	1.06 (0.24)	64.3 (7.9)	35.7 (7.9)	0.77 (0.42)	0.84 (0.60)	0.98 (0.20)	68.1 (11.2)	31.9 (11.2)

# PATELLOFEMORAL FORCES AND STRESSES DURING SQUAT EXERCISES

Rafael F. Escamilla<sup>1</sup>, Naiquan Zheng<sup>2</sup>, Alan Hreljac<sup>3</sup>, Rodney Imamura<sup>3</sup>, Toran D. MacLeod<sup>1</sup>,  
William B. Edwards<sup>4</sup>, Glenn S. Fleisig<sup>5</sup>, Kevin E. Wilk<sup>5</sup>

<sup>1</sup>Department of Physical Therapy, California State University, Sacramento, USA

<sup>2</sup>Orthopaedics and Rehabilitation Program, University of Florida, Gainesville, FL, USA

<sup>3</sup>Kinesiology and Health Science Department, California State University, Sacramento, USA

<sup>4</sup>Department of Health and Human Performance, Iowa State University, Ames, Iowa, USA

<sup>5</sup>American Sports Medicine Institute, Birmingham, AL, USA

e-mail: rescamil@csus.edu

## INTRODUCTION

The one leg squat and wall squat exercises are used in both athletic training and during knee rehabilitation programs. However, it is currently unknown how patellofemoral forces and stresses change among one leg and wall squat exercises and knee angles. The purpose of this study was to compare patellofemoral forces and stresses as a function of these squat exercises and knee angles. It was hypothesized that patellofemoral forces and stresses would increase as knee flexion increased and would be greater in the wall squat short (feet closer to wall) compared to the wall squat long (feet further from wall) and the one leg squat.

## METHODS

Eighteen subjects (9 males and 9 females) were used with an average age, mass, and height of  $29\pm 7$  y,  $77\pm 9$  kg, &  $177\pm 6$  cm for males and  $25\pm 2$  y,  $60\pm 4$  kg, &  $164\pm 6$  cm for females. Each subject performed the wall squat long (knees over ankles at the bottom position) and the wall squat short (knees beyond toes at bottom position). A one leg squat was also performed. Intensity was normalized for each exercise by having each subject their 12 repetition maximum intensity, which were  $55\pm 9$  kg for males and  $36\pm 9$  kg for females for the wall squat and  $15\pm 3$  kg for males and  $10\pm 3$  kg for females for the one leg squat. Surface electrodes were placed over the vasti muscles, rectus femoris, medial and lateral hamstrings, and gastrocnemius. Reflective markers were positioned over landmarks on the foot, ankle, knee, hip, and shoulder.

Video (60 Hz), EMG & force platform (960 Hz) data were collected during 3 repetitions of each exercise (0-90° knee flexion) and averaged. EMG data were normalized by maximum voluntary isometric contractions (MVIC).

Patellofemoral forces & stresses were calculated using a biomechanical knee model (Zheng et al., 1998; Salsich et al., 2003) with input variables consisting of resultant knee forces and moments, patellofemoral contact areas, and the muscle force function  $F_{m(i)} = k_i A_i \sigma_{m(i)} [EMG_i / MVIC_i]$ , where  $k_i$  was a muscle force-length variable,  $A_i$  was physiological cross sectional area (PCSA) per muscle,  $\sigma_{m(i)}$  was MVIC force per unit PCSA,  $EMG_i$  and  $MVIC_i$  were EMG window averages, and  $c_i$  was a weight factor adjusted in a computer optimization program. Patellofemoral forces and stresses as a function of exercise and knee angle were assessed by a two-way repeated measures analysis of variance ( $p < 0.05$ ).

## RESULTS AND DISCUSSION

Patellofemoral forces and stresses are shown in Figures 1 and 2. Both patellofemoral forces and stresses increased progressively as knee flexion increased. Both patellofemoral forces and stresses were significantly greater in the one leg squat compared to the wall squat short between 50-90° of the descent, while both the wall squat short and long were significantly greater than the one leg squat between 50-90° of the ascent.

## SUMMARY/CONCLUSIONS

Performing variations of the squat exercise does affect the magnitude of patellofemoral forces and stresses during both the descent and ascent

phases. In addition, both forces and stresses increased with knee flexion.

**REFERENCES**

Salsich et al. (2003), *Clinical Orthopaedics*, **417**, 277-284.  
 Zheng et al. (1998), *Journal of Biomechanics*, **31**, 963-967.

**ACKNOWLEDGEMENTS**

The authors would like to thank Lisa Bonacci, Toni Burnham, Juliann Busch, Kristen D’Anna, Pete Eliopoulos, & Ryan Mowbray for all their assistance during data collection and analyses.

Figure 1. Mean (SD) patellofemoral compressive force during the one leg squat and the wall squat.

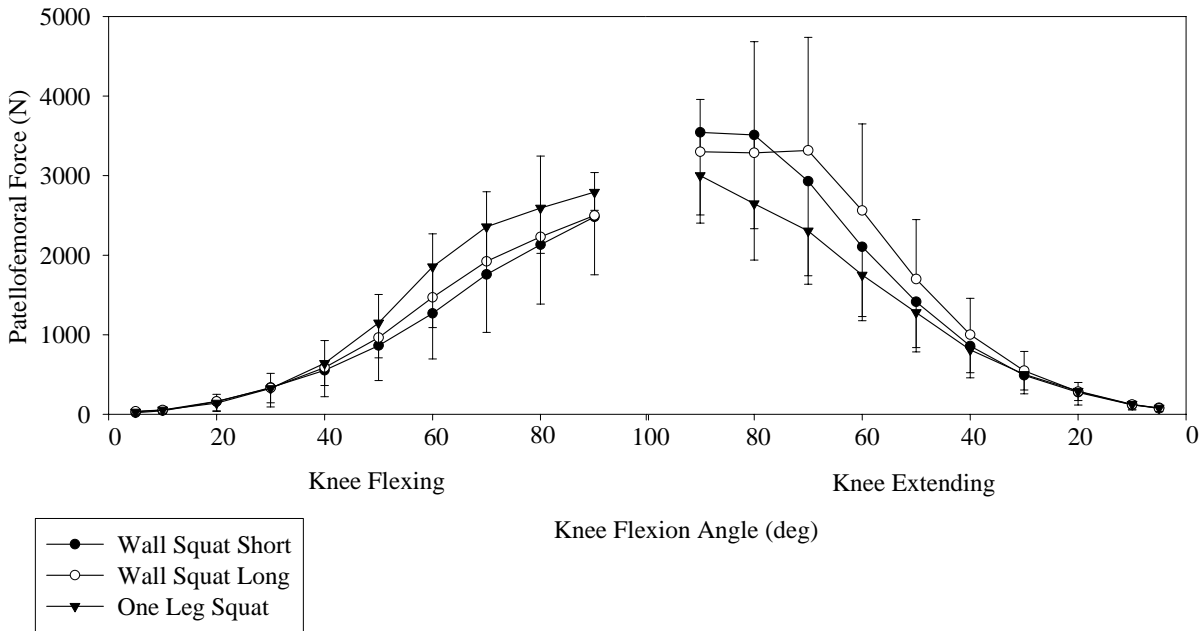
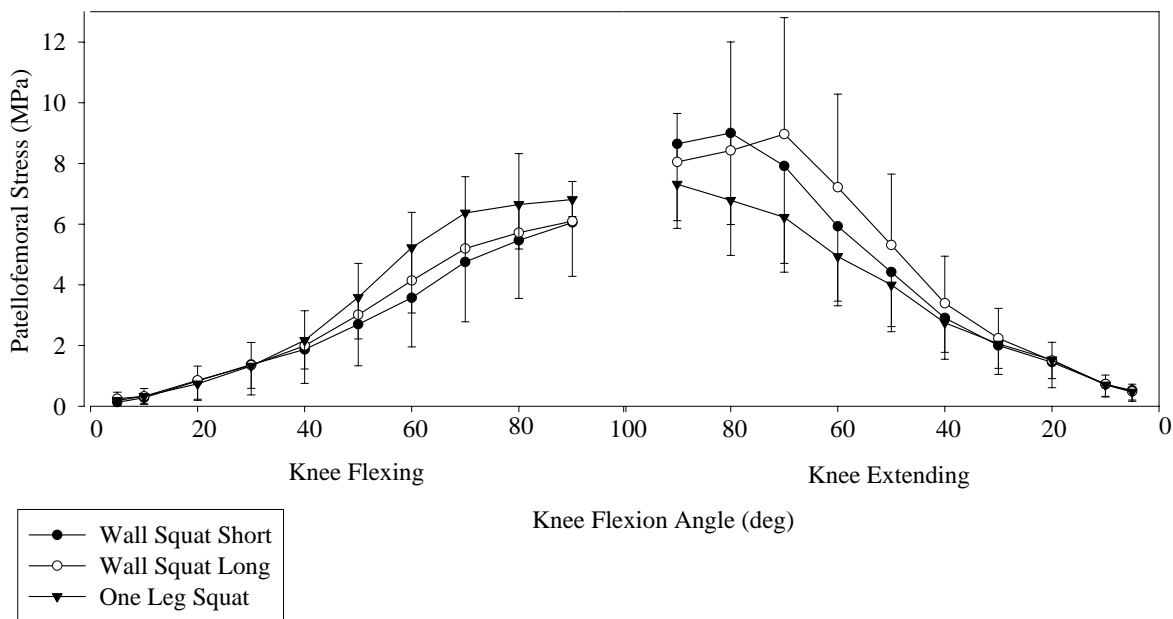


Figure 2. Mean (SD) patellofemoral stress during the one leg squat and the wall squat.



# COMPARISON OF LATERAL CUTTING ACTIVITIES USED TO ASSESS ACL INJURY RISK

Kristian O'Connor, Sarika Monteiro, Carl Johnson, and Ian Hoelker

University of Wisconsin-Milwaukee, Milwaukee, WI, USA  
E-mail: krisocon@uwm.edu Web: www.chs.uwm.edu/neuromechanics

## INTRODUCTION

Side cutting has been identified as one of the most common mechanisms of non-contact ACL injury (Boden et al., 2000). In order to understand this mechanism of injury and to develop prevention protocols, a variety of experimental protocols have been employed. Of these, the unanticipated running and cutting maneuver may best replicate the conditions encountered during a game situation. Besier et al. (2001) reported greater muscle co-activation and greater loading of the knee as compared to an anticipated cut. While potentially having greater ecological validity than more controlled tasks, this activity presents many challenges as a broad screening tool. The protocol can be time consuming and logistically difficult to conduct. An experimental protocol where speed control and foot placement are less of a concern can be more easily implemented and may be better suited to large scale screening of athletes. Drop landings and stride jumps with a 90° side cut have been used to assess joint stability, but it is unknown whether the performance on these tasks reflect an individual's ability to perform a running and cutting maneuver. Ideally, a simpler task would reflect movement patterns that under more stressful conditions would increase injury risk.

Drop landing and stride landing paradigms result in either a nearly vertical or horizontal approach velocity. Another variation of these tasks is to place the box

further from the landing target in order to generate both vertical and horizontal velocity components. This type of task may produce responses that better reflect game stresses. The purpose of this study was to compare the knee joint dynamics for individuals performing side cutting maneuvers starting from a static position to an unanticipated running and cutting maneuver.

## METHODS

Five males and six females participated in this study. All were recreationally active and free from musculoskeletal injury. Each subject was asked to perform running and cutting maneuvers where they were randomly cued to either run straight, stop rapidly, or cut 45°. Subjects also performed 90° side cuts immediately upon landing from the three approaches; a) a box height equal to their maximum jump height set close (CL) to the force plate, b) a box at the same height set far (FL) from the force plate (distance = three times box height), and c) a stride landing (SL) from level ground (maximum single stride distance). Five trials of each task were recorded.

Three-dimensional kinematic data were collected using a seven-camera Motion Analysis Eagle system (200 Hz), and force data were collected with an AMTI force platform (1000 Hz). Three-dimensional knee joint kinematics and kinetic were calculated, and touchdown angles, maximum joint excursion, range of motion,

and peak moments were extracted for each plane. A repeated measures ANOVA was performed for each dependent variable ( $p < 0.05$ ). A factor analysis was also performed in order to assess how individual performances across tasks were related to one another.

## RESULTS AND DISCUSSION

Only knee sagittal plane kinematics were significantly different between activities with the cut exhibiting a smaller range of motion than the CL, FL, and SL tasks. Peak knee extensor moments were not different, but there were greater varus moments (Figure 1) and internal rotation moments during early stance.

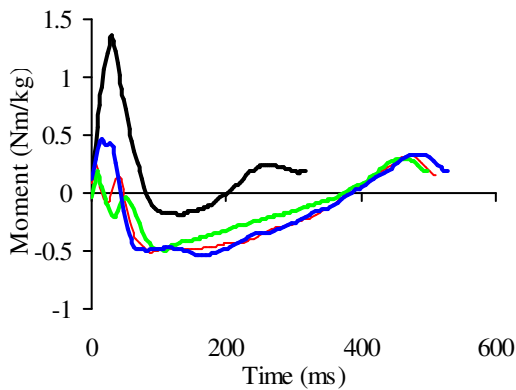


**Figure 1:** Group mean knee frontal plane moments. Black = Cut, Red = FL, Green = CL, Blue = SL. Positive values indicate a varus moment.

The factor analysis generally reported that individual performances on the four tasks were highly related. For instance, the frontal plane range of motion resulted in a single principle component explaining 78% of the variance and the loading factors ranged from 0.728-0.942 for the four tasks. This indicates that an individual's relative performance on one task was related to performance on another. Therefore, the easier landing tasks may serve as a

reasonable indicator of an individual's movement pattern during a cut. In contrast, the peak varus moment during the cut was related only to the peak varus moment observed during the SL task (Table 1).

**Table 1:** Factor analysis for the peak varus moment. Component 1 accounted for 55% and component 2 accounted for 38% of the total variance. Values indicate the loading factors.

Task	Comp. 1	Comp. 2
Cut	-0.33	0.878
CL	0.94	-0.257
FL	0.979	0.14
SL	0.489	0.807

## SUMMARY/CONCLUSIONS

Frontal plane dynamics have been identified previously as a discriminator of knee injury risk (Hewett et al., 2005). While the kinematic patterns of the cut, CL, FL, and SL tasks related to one another, only the SL produced a kinetic response in the frontal plane that related to the cut. Therefore, the stride landing may be the most appropriate of these tasks to use to characterize an individual's cutting knee joint dynamics during play.

## REFERENCES

- Besier, T.F. et al. (2001). *MSSE*, **33**, 1176-1181.
- Boden, B.P. et al. (2000). *Orthopedics*, **23**, 573-578.
- Hewett, T.E. et al. (2005). *Am. J. Sports Med.*, **33**, 492-501.

## ACKNOWLEDGEMENTS

UWM Graduate School Research Committee Award

# VALIDATION OF THE GRAVITY LINE PROJECTION TECHNIQUE AT THE LIMITS OF STABILITY

Alessandro Telonio and Cécile Smeesters

Research Center on Aging, Sherbrooke, QC, Canada  
Department of Mechanical Engineering, Université de Sherbrooke, Sherbrooke, QC, Canada  
E-mail: Cecile.Smeesters@USherbrooke.edu Web: www.cdrv.ca

## INTRODUCTION

The most common model to characterize postural control is the inverted pendulum. In this model, the center of pressure (COP) is the control variable whereas the center of mass (COM) is the controlled variable (Winter et al., 1998).

The position of the COM can be determined directly using the kinematics and the anthropometry of the participant. It can also be determined indirectly by its projection in the COP plane using the zero-point-to-zero-point double integration or gravity line projection (GLP) technique (Zatsiorsky and King, 1998). Although the GLP technique has been validated for quiet standing and voluntary oscillations (Lafond et al., 2004), it has not been validated for leaning postures at the limits of stability such as those obtained by NeuroCom (1993).

The purpose of this study was to validate the use of the GLP technique to determine the position of the COM at the limits of stability and to confirm the limit of stability total angles obtained by NeuroCom (1993).

## METHODS

Fifteen healthy and barefoot young participants (right-legged,  $24.7 \pm 3.7$  yrs,  $1.71 \pm 0.09$  m,  $67.1 \pm 10.3$  kg) first stood quietly on a force platform. They then performed 20 s leans at the limits of stability with their arms hanging at their side.

The initial angle in quiet standing and the limit of stability angles of the COM were evaluated in four directions: a) forward, b) right side, c) left side and d) backward. Three methods to estimate these angular positions of the COM were used (Figure 1):

- Kinematic method ( $\theta_{\text{Limit KIN}}$ ) using a seven segment model: 2 feet, 2 calves, 2 thighs and the head-arms-trunk complex (Winter, 2005);
- Gravity line projection technique ( $\theta_{\text{Limit GLP}}$ );
- Position of the COP ( $\theta_{\text{Limit COP}}$ ) as equal to that of the COM.

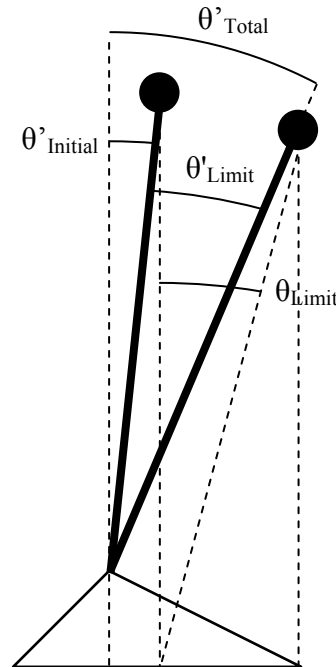


**Figure 1:** Initial angle in quiet standing ( $\theta'_{\text{Initial}}$ ) and limit of stability angles ( $\theta'_{\text{Limit}}$  and  $\theta_{\text{Limit}}$ ). For small angles,  $\theta'_{\text{Limit}} \sim \theta_{\text{Limit}}$  and thus the limit of stability total angles

$$\theta'_{\text{Total}} \sim \theta_{\text{Limit}} + \theta'_{\text{Initial}}$$

Force platform (OR6-7, AMTI, Newton MA) data were sampled at 1000 Hz and kinematic data (Optotrak, NDI, Waterloo ON) were sampled at 100 Hz.

## RESULTS AND DISCUSSION

The initial angle in quiet standing ( $\theta'_{\text{Initial}}$ ) was  $2.61 \pm 1.32$  deg and  $0.72 \pm 0.03$  deg in the anterior-posterior and medial-lateral directions, respectively. These values are in agreement with the mean values from NeuroCom (2.30 deg and 0.00 deg, respectively) but show the great variability between participants.

The RMS differences between the projections of  $\theta_{\text{Limit KIN}}$  and  $\theta_{\text{Limit GLP}}$  in the COP plane are less than 1 mm in the anterior-posterior and in the medial-lateral directions at the limits of stability.

Moreover, the limit of stability angles ( $\theta'_{\text{Limit}} \sim \theta_{\text{Limit}}$ ) estimated using the three different methods are in nearly perfect agreement (Table 1). Finally, the values of the limit of stability total angles ( $\theta'_{\text{Total}}$ ) are also in agreement with the mean values from NeuroCom but again show the great variability between participants.

## CONCLUSIONS

The GLP technique gives similar results to the KIN method. It is thus possible to

estimate the position of the COM at the limits of stability with only a force platform. Furthermore, the limit of stability total angles obtained by NeuroCom have been confirmed. To obtain these one simply needs to add the initial angles to the limit of stability angles.

## REFERENCES

- Winter, D.A., et al. (1998) *J. Neurophysiol.*, **80**(3), 1211-1221.  
 Zatsiorsky, V.M., King, D.L. (1998). *J. Biomech.*, **31**(2), 161-164.  
 Lafond, D., et al. (2004) *J. Biomech.*, **37**(9), 1421-1426.  
 NeuroCom (1993). *Instruction Manual*. NeuroCom Inc.  
 Winter, D.A. (2005) *Biomechanics and Motor Control of Human Movement*, John Wiley & Sons.

## ACKNOWLEDGEMENTS

We gratefully acknowledge the assistance of Vincent Deschamps-Sonsino, Mathieu Hamel, Myriam Jbabdi and Mathieu Rosa along with the support of the Junior I Research Fellow Grant of an FRSQ Centre 6391 and 5393 from the Research Centre on Aging to Cécile Smeesters.

**Table 1:** Limit of stability angles (mean  $\pm$  SD)

Angle (deg)	Forward	Right side	Left side	Backward
$\theta_{\text{Limit KIN}}$	$5.33 \pm 1.32$	$6.97 \pm 1.39$	$-7.48 \pm 0.93$	$-3.13 \pm 1.30$
$\theta_{\text{Limit GLP}}$	$5.33 \pm 1.32$	$6.97 \pm 1.39$	$-7.48 \pm 0.93$	$-3.14 \pm 1.30$
$\theta_{\text{Limit COP}}$	$5.33 \pm 1.32$	$6.97 \pm 1.39$	$-7.48 \pm 0.93$	$-3.14 \pm 1.30$
$\theta'_{\text{Total}}$	$8.1 \pm 1.90$	$8.00 \pm 1.62$	$-8.55 \pm 1.26$	$-1.90 \pm 1.06$
<b>NeuroCom</b>	8.85 [1]	8.00	-8.00	-1.95 [2]

[1]  $\theta'_{\text{Total}} \sim \theta_{\text{Limit}} + \theta'_{\text{Initial}} = 6.25 \text{ deg} + 2.3 \text{ deg} = 8.85 \text{ deg}$

[2]  $\theta'_{\text{Total}} \sim \theta_{\text{Limit}} + \theta'_{\text{Initial}} = -4.25 \text{ deg} + 2.3 \text{ deg} = -1.95 \text{ deg}$

# EFFECT OF AGE AND THE NATURE OF THE POSTURAL PERTURBATION ON THE THRESHOLD OF BALANCE RECOVERY

Kodjo Enyonam Moglo and Cécile Smeesters

Research Center on Aging, Sherbrooke, QC, Canada

Department of Mechanical Engineering, Université de Sherbrooke, Sherbrooke, QC, Canada

E-mail: Cecile.Smeesters@USherbrooke.edu

Web: www.cdrv.ca

## INTRODUCTION

There are only a dozen or so studies that have attempted to take tasks to the limit by using sufficiently large postural perturbations that balance recovery and avoiding a fall is not always possible. There are even fewer studies showing age-related differences in the threshold of balance recovery (Madigan and Lloyd, 2005; Pijnappels et al., 2005; Wojcik et al., 1999). Comparisons between these studies are complicated by the differences in the nature of the postural perturbations and by the differences due to the presence or absence of initial velocity. We have recently shown in young adults that although different postural perturbations are not the same, they are similar and can thus be compared using the disturbance threshold line method (Moglo and Smeesters, 2005). The purpose of this study is to determine the effect of age and the nature of the postural perturbation on the threshold of balance recovery.

## METHODS

Six healthy younger adults ( $23 \pm 2$  yrs,  $1.71 \pm 0.07$  m,  $66.8 \pm 8.7$  kg), 3 males and 3 females, and six healthy older adults ( $68 \pm 2$  yrs,  $1.65 \pm 0.09$  m,  $69.5 \pm 13.6$  kg), 2 males and 4 females, participated in this study. We determined the maximum forward lean angle that our participants could be suddenly released from and still recover balance using a single step for three pull forces with no initial velocity. We also

determined the maximum forward pull force that our participants could suddenly sustain and still recover balance using a single step for two walking velocities with no initial lean angle. Maximum lean angles, maximum pull forces, walking velocities, reaction times, angular positions, angular velocities, weight transfer times, step times, step lengths and step velocities were measured using force platforms (OR6-7, AMTI, Newton MA) and a motion measurement system (Optotrak, NDI, Waterloo ON). Data were analysed using one-way analyses of variances with repeated measures (SPSS Version 12, Chicago IL).

## RESULTS AND DISCUSSION

For both younger and older adults, increasing pull force, which in effect added initial velocity, decreased the maximum lean angle from which participants could suddenly be released (Table 1). On the other hand, increasing the walking velocity decreased the maximum pull force that participants could suddenly sustain.

During the first part of balance recovery, from the initiation of the postural perturbation to the onset of balance recovery by the participant, reaction times for the threshold of balance recovery trials were not different between younger and older adults even though they were affected by the nature of the postural perturbation for young adults only (Table 1). Furthermore, the angular positions and velocities of the lean

angle at the end of reaction time for the threshold of balance recovery trials formed a disturbance threshold line separating falls from recoveries, regardless of the postural perturbation, for both younger and older adults. Although the slopes of these lines were not significantly affected by age, the intercepts were (Table 1 and Figure 1).

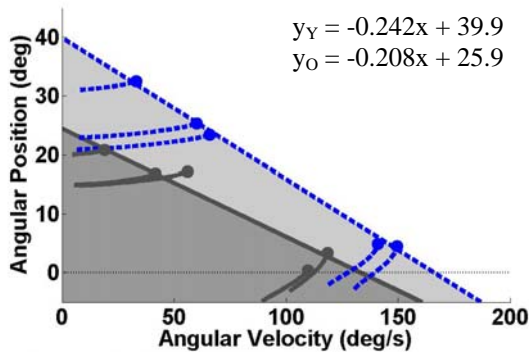


**Figure 1:** Disturbance threshold lines

During the second part of balance recovery, from the onset of balance recovery by the participant to step landing, weight transfer times, step times, step lengths and step velocities for the threshold of balance recovery trials were not affected by the nature of the postural perturbation (Table 1). However, except for step time, there was a

significant age-related decrease in all of these performance variables.

## CONCLUSIONS

The age-related decrease of the threshold of balance recovery is well illustrated by the disturbance threshold line method.

## REFERENCES

- Moglo, K.E., Smeesters, C. (2005). *Int. Soc. Biomech. XX<sup>th</sup> Congress*.  
 Madigan, M.L., Lloyd, E.M. (2005). *J. Gerontol.*, **60A**(4), M481-485.  
 Pijnappels, M., et al. (2005). *Gait Posture*, **21**(4), 388-394.  
 Wojcik, L.A., et al. (1999). *J. Gerontol.*, **54A**(1), M44-50.

## ACKNOWLEDGEMENTS

We gratefully acknowledge the assistance of José-Carl Harnois, Valérie Tremblay-Boudreault and Mathieu Hamel along with the support of grant RG-02-0585 from the Whitaker Foundation.

**Table 1:** Effect of age and the nature of the postural perturbation on the threshold of balance recovery (mean±SD)

Type of perturbation	Y/O	Leaning Trials			Walking Trials		p	
Maximum Lean Angle (deg)	Y	31.0±3.2	22.9±4.1	20.8±3.7	<b>-2.2±3.1</b>	<b>-3.0±3.2</b>	<b>0.00</b>	m 0.26
	O	20.0±3.0	14.9±4.2	14.9±4.0	<b>-4.9±2.1</b>	<b>-3.1±2.1</b>	<b>0.03</b>	
Maximum Pull Force (N)	Y	<b>0±0</b>	<b>474±36</b>	<b>605±51</b>	462±70	372±45	<b>0.04</b>	b <b>0.00</b>
	O	<b>0±0</b>	<b>371±126</b>	<b>577±87</b>	478±90	356±78	<b>0.00</b>	
Walking Velocity (m/s)	Y	<b>0.00±0.00</b>	<b>0.00±0.00</b>	<b>0.00±0.00</b>	<b>1.82±0.15</b>	<b>2.03±0.18</b>		<b>0.00</b>
	O	<b>0.00±0.00</b>	<b>0.00±0.00</b>	<b>0.00±0.00</b>	<b>1.20±0.16</b>	<b>1.53±0.15</b>		
Reaction Time (ms)	Y	73±8	76±3	76±6	55±2	55±3	<b>0.02</b>	0.51
	O	66±13	79±10	70±7	54±3	59±6	0.08	
Weight Transfer Time (ms)	Y	138±20	133±6	129±12	n/a	n/a	0.63	<b>0.00</b>
	O	206±22	179±9	170±7	n/a	n/a	0.07	
Step Time (ms)	Y	189±19	202±19	204±18	214±43	203±27	0.20	0.08
	O	202±10	206±24	214±24	260±60	206±29	0.28	
Step Length (m)	Y	1.02±0.13	1.10±0.09	1.12±0.12	1.04±0.08	1.05±0.08	0.14	<b>0.00</b>
	O	0.82±0.13	0.84±0.11	0.91±0.13	0.79±0.06	0.84±0.09	0.46	
Step Velocity (m/s)	Y	5.42±0.65	5.48±0.68	5.51±0.53	4.99±0.67	5.22±0.52	0.70	<b>0.00</b>
	O	4.09±0.65	4.14±0.72	4.26±0.68	3.17±0.61	4.12±0.53	0.20	

**Bolded** values are controlled by the nature of the postural perturbations and thus not included in the analyses.

# A NOVEL, MORE ROBUST METHOD TO QUANTIFY SYMMETRY

Becky Avrin Zifchock<sup>1</sup> and Irene Davis<sup>1,2</sup>

<sup>1</sup> University of Delaware, Newark, DE <sup>2</sup> Drayer Physical Therapy Institute, Hummelstown, PA  
E-mail: beckyaz@udel.edu

## INTRODUCTION

Measurement of gait symmetry is used for many clinical and research applications. Asymmetry is most often quantified using the symmetry index (SI) (Robinson, 1989), which is simply the percent difference between sides. This method is prone to inconsistencies based upon the choice of reference value. Further, the SI method introduces the potential for artificial inflation of the symmetry index, when the difference between sides is much larger than the side chosen as the normalization factor. Therefore, a more robust method of assessing symmetry is necessary. The purposes of this study were (1) to assess the difference in SI based upon whether the left or right side is used as the reference value and (2) to correlate the values generated using a novel measure, the symmetry angle (SA) to the more traditionally-used SI.

## METHODS

Ten rearfoot strikers, running at least 20 miles/week, with no current injuries were included in this study. Subjects ran along a 25m runway, striking two forceplates with consecutive steps. A 6-camera Vicon motion capture system tracked the motion of reflective markers mounted on the pelvis and both thighs, shanks, and rearfeet. Two kinematic and kinetic variables were assessed in both sides of each runner: hip internal rotation velocity (HIRv), rearfoot eversion velocity (REVv), impact peak of the grf along the shank (SHFz), and peak tibial shock (PPA). All variables, aside from PPA, were assessed from heel strike to vertical impact peak. Additionally, two

strength and structural measures were assessed: frontal projection knee valgus angle (KVA), hip internal rotation range of motion (HIRr), hip abduction strength (HABs), and hip external rotation strength (HERs). In order to compare between normalization methods, for each variable, the SI between consecutive footsteps was calculated as:  $SI_L = (X_R - X_L)/X_L * 100$  and  $SI_R = (X_R - X_L)/X_R * 100$ . The absolute difference between the two methods was calculated to determine the magnitude of the discrepancy. A 5 point difference between methods was considered clinically relevant.

The SI, normalized to the average of the left and right sides, was also calculated as:  $SI_{AVG} = (X_R - X_L)/avg(X_R, X_L) * 100$  for comparison to the SA. In order to calculate the SA for a given variable, the right and left sides are plotted against each other as seen in Fig. 1. Any set of values will create a vector that creates some angle,  $\alpha$ , with respect to the x axis and can be quantified as  $\alpha = \arctan(X_L/X_R)$ . In order to quantify the deviation,  $\delta$ , of this vector from the 45° vector of perfect symmetry,  $\alpha$  must be subtracted from 45:  $\delta = 45 - \alpha$ . This formula is sufficiently

robust to quantify the asymmetry between values that fall within any of the graphed quadrants. Since the maximum

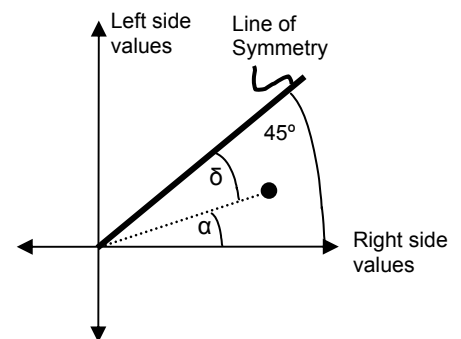


Fig. 1: Calculation of the SA

deviation from the vector of perfect symmetry is set at 90°, the following equation for SA, converted to percent of the maximum is:

$$SA = (45 - \arctan(X_L/X_R))/90 * 100$$

A linear regression was used to relate the  $SI_{AVG}$  and SA.

## RESULTS AND DISCUSSION

Seven of the eight variables were at least 5 points different when calculated as  $SI_L$  versus  $SI_R$  (see Fig. 2). The absolute difference is particularly large in the kinematic variables and KVA. These variables may be particularly prone to artificial inflation, where the difference between the sides is much larger than the side chosen as the reference value. These findings suggest that a different choice in reference value can produce alternative interpretations of the magnitude of asymmetry between two identical left and right side values.

Another limitation of the SI is highlighted in the results of the second aim. Table 1 shows the  $R^2$  values of the regressions between the  $SI_{AVG}$  and SA methods. Six of the eight variables exhibited perfect regressions. The two variables that exhibited somewhat lower  $R^2$  values were a result of artificial inflation of the SI. The  $SI_{AVG}$  values were inflated in two runners for HIRv and in one runner for KVA. Fig. 3 shows that the regression for HIRv is strongly influenced by the inflated cases, shown in gray. When those cases were removed, the regression improves to  $R^2 = 0.97$ . When the aberrant case was removed from analysis of KVA, the regression improved to  $R^2 = 1.00$ .

Table 1:  $R^2$  values of the regressions between the  $SI_{AVG}$  and SA methods

Variable	$R^2$
HIRv	0.45*
REVv	1.00
SHfz	1.00
PPA	1.00
KVA	0.89*
HIRr	1.00
HABs	1.00
HERs	1.00

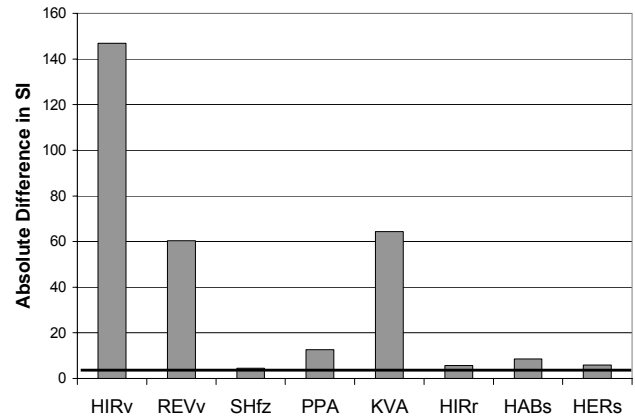


Fig. 2: Difference between assessing SI using the left versus right sides as reference values, where the bold line denotes at least 5 points difference

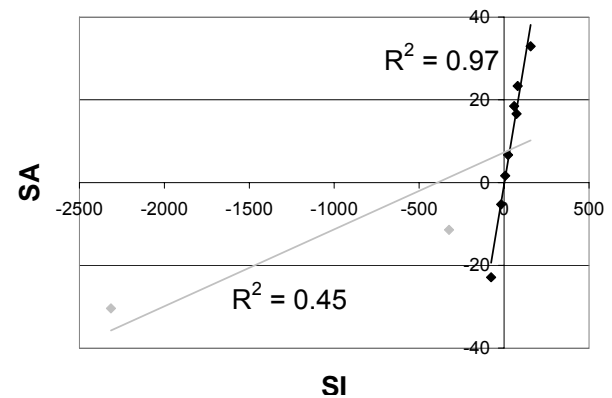


Fig. 3: Aberrant, artificially inflated SI values poorly influenced the regression between SI and SA for HIRv

## SUMMARY/CONCLUSIONS

This study demonstrates that choosing two different normalization factors can result in alternative interpretations regarding the asymmetry between sides. This can make comparisons within the biomechanics literature difficult. The SA does not require the choice of a normalization factor and is not prone to artificial inflation. Yet it yields almost identical results as compared to the SI.

## REFERENCES

Robinson, R.O. et al. (1987). *J Manipulative Physiol Ther*, **10**(4), 172-176.

# REGIONAL BONE FUSION FOR THA FEMORAL IMPACTION GRAFTS

Anneliese Heiner, John Callaghan, Thomas Brown

Department of Orthopaedics and Rehabilitation, University of Iowa, Iowa City, IA  
E-mail: [anneliese-heiner@uiowa.edu](mailto:anneliese-heiner@uiowa.edu) Web: <http://poppy.obrl.uiowa.edu/>

## INTRODUCTION

Impaction grafting for THA involves impacting morselized cancellous bone (MCB) into a cavitory defect, to build up bone stock. Ideally, the MCB is remodeled into a new cancellous lattice contiguous with the host bone.

An earlier study determined the relative stability of femoral impaction grafted constructs in which the MCB had fused, versus the freshly-impacted nonfused condition (Heiner et al., submitted). That study found that the fused femoral impaction grafts were much more stable than the nonfused grafts at the proximal stem location, but MCB fusion had a much smaller effect on distal stem stability. This indicates that steps to enhance MCB fusion are most effectively focused proximally.

Bone morphogenic proteins (BMPs) have the potential to enhance impaction graft remodeling, but they are expensive. BMP use, however, could be economized by only using it where it would do the most good.

The purpose of the current study is to determine the stability of femoral impaction grafted constructs for which only half of the MCB volume is fused, with this fused half being placed either proximally or distally, and to compare these constructs to those with fully fused or fully nonfused MCB.

## METHODS

Composite femurs were prepared in a standardized manner. A nylon abductor strap

was attached to each femur. Cavitory defects were simulated by overdrilling the femoral diaphysis and removing all proximal cancellous bone. Impaction grafts constructs were then created by impacting human MCB into the femur. A polished, collarless, triple-tapered femoral stem was then cemented into the impaction graft.

The MCB was either nonfused or fused. The nonfused MCB was typical of that used surgically. The fused MCB was mixed with an amine-based epoxy adhesive just before the impaction grafting process; after impaction grafting (and cementing in the stem), the MCB-epoxy mixture fuses into a contiguous structure biomechanically equivalent to intact cancellous bone (Heiner et al., 2005), simulating the desired end-stage of an impaction graft.

The impaction grafts were constructed with either the proximal half of the MCB fused (proximally fused) or the distal half of the MCB fused (distally fused). Equivalent volumes of fused and nonfused MCB were used in each femur; because of the femur's variation in transverse cross-section over the stem length, the distal half of the MCB covered a greater length of the femoral stem than did the proximal half (Figure 1a).

Each impaction graft construct was loaded to 250,000 complete physiologic level walking and stair climbing cycles (with both axial and torsional loads) at 50% full-scale loading (Figure 1b). Three-dimensional motion between the femoral stem and the femur was measured at the proximal and distal stem (Figure 1a) with DVRTs.

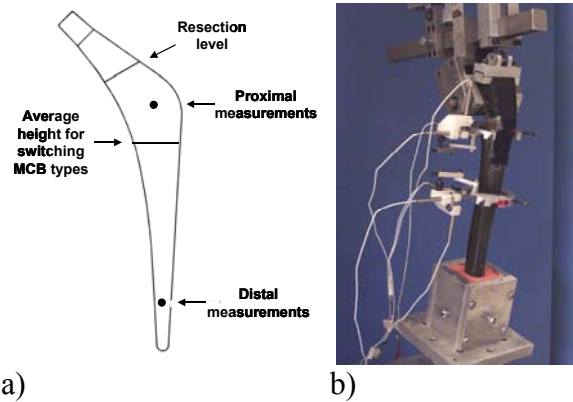


**Figure 1:** Impactation graft construct a) femoral stem and b) testing set-up.

## RESULTS AND DISCUSSION

Fusing just the proximal half of the impactation graft volume improved construct stability nearly as much as did fusing the entire graft, as compared to the nonfused impactation graft construct (Table 1). This was the case for both proximal and distal stem stability. Fusing just the distal half of the impactation graft volume did not significantly change final micromotion, as

compared to the nonfused impactation graft construct, for either the proximal or distal stem locations, although it did significantly change final migration for both stem locations.

## CONCLUSION

Fusing only the proximal half of the impactation graft volume was more effective in improving femoral stem stability than was fusing only the distal half, and fusing just the proximal half of the impactation graft volume improved stem stability nearly as much as did fusing the entire graft. The use of expensive growth factors to enhance MCB fusion could be economized by only applying them to MCB that will be impacted into the proximal portion of the graft.

## REFERENCES

- Heiner, A.D., et al. (2005). *J Biomechanics*, **38**, 811-818.  
 Heiner, A.D., et al. (submitted). *Trans 30<sup>th</sup> ASB*.

Table 1. Micromotion and migration at 250,000 cycles for nonfused, fused, proximally fused and distally fused femoral impactation graft constructs. Standard deviations are in parentheses. Groups with measurements that were not significantly different (NSD) from each other ( $\alpha = 0.05$ ) are indicated by the same number of stars.

	Level walking micromotion, $\mu\text{m}$	NSD	Stair climbing micromotion, $\mu\text{m}$	NSD	Migration $\mu\text{m}$	NSD
<b>Proximal stem</b>						
Nonfused graft	25 (11)	**	30 (13)	**	508 (178)	
Fused graft	2.4 (3.0)	*	2.5 (3.1)	*	37 (19)	*
Proximally fused graft	2.8 (1.3)	*	2.9 (1.4)	*	144 (108)	*
Distally fused graft	31 (16)	**	43 (29)	**	330 (115)	
<b>Distal stem</b>						
Nonfused graft	2.5 (1.5)	*	2.8 (1.2)	*	732 (210)	
Fused graft	2.3 (0.7)	*	2.7 (0.7)	*	248 (57)	*
Proximally fused graft	2.6 (1.0)	*	3.3 (1.7)	*	393 (97)	*
Distally fused graft	2.4 (1.3)	*	3.0 (1.7)	*	420 (156)	*

# EFFECT OF EMOTION ON THE KINEMATICS OF GAIT

Melanie B. Cluss<sup>1</sup>, Elizabeth A. Crane<sup>1</sup>, M. Melissa Gross<sup>1</sup> and Barbara L. Fredrickson<sup>2</sup>

<sup>1</sup> University of Michigan, Ann Arbor, MI, USA

<sup>2</sup> University of North Carolina, Chapel Hill, NC, USA

E-mail: mgross@umich.edu Web: www.umich.edu/~mgross

## INTRODUCTION

Emotion is expressed through multiple physiological channels including voice, facial expression, body movements, autonomic responses and subjective experience. Facial and bodily expressions of emotion can be recognized cross-culturally, suggesting a biological component (Ekman, 1971; Hejmadi, 2000). Although emotions have been recognized in individuals during walking, emotion-related gait characteristics have been described only qualitatively, e.g., “heavy-footed” for angry gait (Montepare, 1987). Such qualitative descriptions limit understanding of the biological phenomena underlying bodily expression of emotion. The effects of emotions on gait have not yet been described quantitatively.

The purpose of this study was to describe the effect of specific emotions on gait kinematics in trials in which the presence of the emotion was validated using both self-report and social consensus methods.

## METHODS

Twenty-six undergraduate students (15 females, 11 males; 20±2.3 yrs) participated after giving informed consent. Before walking, each subject recalled an experience from their own lives in which they felt angry, sad, content, joy, or no emotion at all (neutral). After recalling a target emotion, participants walked across the lab. Whole body motion data were acquired using a video-based, 6-camera system. Front and

side view videos were recorded at the same time as the motion data.

Participants performed three trials for each emotion in a block. After each trial, participants rated the intensity of eight emotions (4 target and 4 non-target) using a questionnaire. A 5-item Likert scale (0 = not at all; 1 = a little bit; 2 = moderately; 3 = a great deal; 4 = extremely) was used to score emotion intensity. Intensity scores of two (“moderately”) or greater were considered a “hit” (the subject felt the emotion). After blurring the faces so that facial expressions were not observable, the video clips were randomized and assembled into three different composite videos. The composite videos were shown to undergraduate student observers. After viewing each video clip, observers selected one of ten responses (Figure 1) corresponding to the emotion that they thought the walker felt during the trial.

Marker coordinate data were filtered at 6 Hz and gait parameters were calculated using Visual3D software. Stride length and velocity were normalized by body height. A general linear model was fitted using PROC GLM in SAS to determine the effects of emotion and gender on the dependent variables. Multiple pair-wise comparisons of the means were performed using Tukey's Honest Significant Difference test ( $p < 0.05$ ).

## RESULTS AND DISCUSSION

Emotion validation. Self-report data indicated that the walkers felt the target

emotions at levels corresponding to “moderately” or above in all trials. For the neutral emotion, however, 42% of the trials failed to meet the criterion for neutrality, i.e., at least one emotion (typically content) was felt above the threshold value.

Validation data were collected from five female observers (20.6±4.7 yrs) on gait trials from a subset of subjects (n=16) (Figure 1). Recognition rates (side view) for sad, anger, neutral and content were 45%, 25%, 20% and 16%, respectively. Joy was recognized at chance levels (10%) with side view but was improved with front view (15%).

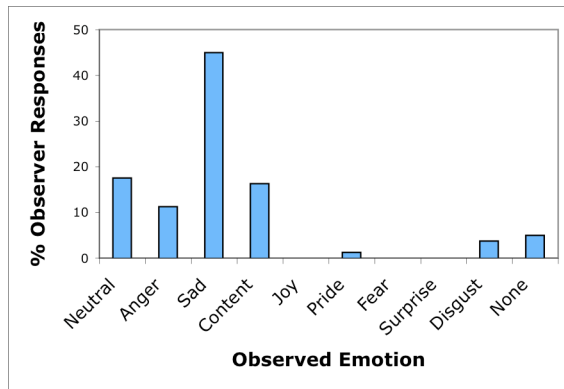


**Figure 1:** Observer responses for sad trials, viewed from the side.

Emotion kinematics. Normalized velocity, normalized stride length, cycle duration and velocity were significantly affected by emotion (Table 1). As expected for the two emotions associated with high levels of arousal (i.e., joy and anger), normalized velocities and normalized stride lengths were greater than in the neutral emotion

**Table 1:** Gait characteristics for each emotion (mean ± SD).

	Anger	Sad	Neutral	Joy	Content
Cycle Duration (s)	1.01±0.09 <sup>2</sup>	1.13±0.13	1.09±0.07	1.01±0.10 <sup>2</sup>	1.07±0.08
Velocity (m/s)	1.41±0.22 <sup>1,2</sup>	1.10±0.21	1.19±0.13	1.42±0.23 <sup>1,2</sup>	1.29±0.19 <sup>1,2</sup>
Normalized Velocity (1/s)	0.83±0.12 <sup>1,2</sup>	0.66±0.13	0.71±0.08	0.84±0.13 <sup>1,2</sup>	0.76±0.11 <sup>1,2</sup>
Normalized Stride Length	0.83±0.07 <sup>2</sup>	0.73±0.08	0.76±0.05	0.84±0.08 <sup>1,2</sup>	0.80±0.08 <sup>2</sup>

<sup>1</sup> Significantly different from neutral trials

<sup>2</sup> Significantly different from sad trials

trials. Sad trials had significantly longer cycle durations, shorter normalized stride lengths and slower normalized velocities than other emotion trials. Angular kinematic analyses are underway.

## SUMMARY/CONCLUSIONS

This study is unique in describing the effects of specific emotions on gait in individuals for whom the presence of the emotions has been validated. The preliminary results indicate that gait kinematics change with emotion. Consistent with the reports for individuals with depression (Lemke, 2000), gait speed slows markedly with sadness. Although temporal-spatial kinematics were related to arousal levels, angular kinematics are needed to distinguish emotions with similar levels of arousal.

## REFERENCES

- Ekman, P., Friesen, W.V. (1971). *J. Personality & Soc. Psychol.*, 17, 124-129.
- Hejmadi, A., et al. (2000). *Psychological Science*, 11, 183-187.
- Lemke, M.R., et al. (2000). *J. Psychiatric Research*, 34, 177-283.
- Montepare, J.M., et al. (1987). *J. Nonverbal Behavior*, 11, 33-42.

## ACKNOWLEDGEMENTS

We thank Zara Schulman, Zach Webster and Kelly Woznicki for their help with data collection and analysis.

# KINEMATIC DEFICITS IN EXECUTION OF LATERAL PINCH AFTER STROKE

Joseph D. Towles<sup>1</sup> and Derek G. Kamper<sup>1,2</sup>

<sup>1</sup> Sensory Motor Performance Program, Rehabilitation Institute of Chicago, Chicago, IL, USA

<sup>2</sup> Biomedical Engineering Department, Illinois Institute of Technology, Chicago, IL, USA  
e-mail: towles@northwestern.edu

## INTRODUCTION

Lateral pinch, a simple grasp modality in which the thumb flexes toward the side of the index finger, is useful for accomplishing many activities of daily living. A few studies have quantified deficits in the ability to independently control finger and thumb movements after stroke (e.g., Lang et al., 2003), but the impact of such deficits on the ability to perform lateral pinch movements is unclear. Thus the goal of this work was to quantify the ability to perform lateral pinch movements post-stroke and to compare the performance of the involved side to that of uninvolved side. We hypothesized that thumb movements on the involved side would be inconsistent and characterized by abnormally short path lengths and path trajectories with abnormally large out-of-plane deviations when these parameters could be calculated.

## METHODS

Four chronic (at least 6 months post-stroke), hemi-paretic stroke subjects with moderate to severe hand impairment (as classified according to the Stage of Hand section of the Chedoke-McMaster clinical scale (Gowland et al. (1993)) have participated in this study (Table 1).

**Table 1: Subject Information**

Subject	Age (y.o.)	Months post-stroke	Chedoke
A	57	27	2
B	56	126	2
C	69	52	2
D	67	124	5

Chedoke-McMaster, 7 is normal.

Each subject was seated with the shoulder abducted approximately 30°, the elbow flexed approximately 90°, and the forearm neutrally pronated and at rest on a table. A volar wrist splint was used to support the wrist in slight extension (i.e., 20°).

Each subject was asked to simulate lateral pinch by first positioning (or allowing the experimenter to position) the pad of the thumb on the lateral side of the middle segment of the index finger (Fig. 1). Second, the subject was asked to maximally extend his/her thumb and then flex it as naturally as possible until light contact was made again with the lateral side of the middle segment of the index finger. Each subject was allowed to chose his/her own movement speed. Three trials (1 trial = thumb extension followed by flexion) were performed and both hands were tested. Subjects were allowed to practice the movement before data collection began.

### *Data Collection*

Three-dimensional (3D) thumb-tip position was measured with a camera system (Optotrak 3020; Northern Digital, Inc.; Waterloo, Ontario, Canada) whose reference frame was situated at the base of the thumb. Infrared-emitting diode (IRED) markers were taped to the thumb: one onto the lateral side of the base and one onto the lateral side of the thumb-tip. The camera system collected data at 30 Hz for 30 s.

### Data Analysis

Thumb-tip position data were projected to a plane perpendicular to the table top, defined as the thumb's plane of flexion-extension. Least squares analyses were used to find a representative thumb-tip trajectory for all three trials, and representative trajectories for both the extension and flexion portions of all three trials per subject per thumb.

Path length (PL), path inconsistency (PI) and normalized peak out-of-plane deviation (PD) were used to quantify representative trajectories. Path length was computed from

$$PL = \int_{\eta_1}^{\eta_2} \sqrt{1 + \left(\frac{df}{d\eta}\right)^2} d\eta$$

where  $f$  is a mathematical description of a representative thumb-tip trajectory. Path inconsistency was defined as the maximum horizontal distance in the plane between the extension and flexion trajectories (see Fig. 1 for illustration). Normalized peak out-of-plane deviation was defined as the largest width of the trajectory (across all three trials) in a plane perpendicular to the thumb-tip (with normal vector along distal phalanx) normalized by the path length.

### RESULTS AND DISCUSSION

As expected, lateral pinch trajectories resulting from the involved side exhibited greater inconsistency, greater normalized peak out-of-plane deviations and had shorter path lengths than those resulting from the uninvolved side (Table 2). In several cases (column 3 of Table 2), path inconsistency could not be computed because trial-to-trial movements were very small (on the order of millimeters) and irregular preventing the identification of regular extension and flexion phases (Fig. 1C).

**Table 2: Kinematic measures of lateral pinch execution (involved vs. uninvolved)**

Subject	PL (cm)	PI (cm)	PD
A	1.0 vs. 9.1	NC vs. 0.49	1.0 vs. 0.16
B	1.0 vs. 9.0	NC vs. 0.20	0.80 v. 0.26
C	0.34 vs. 7.9	NC vs. 0.40	0.59 vs. 0.28
D	6.1 vs. 7.0	2.9 vs. 0.46	0.29 vs. 0.21

“NC” means the quantity could not be calculated.

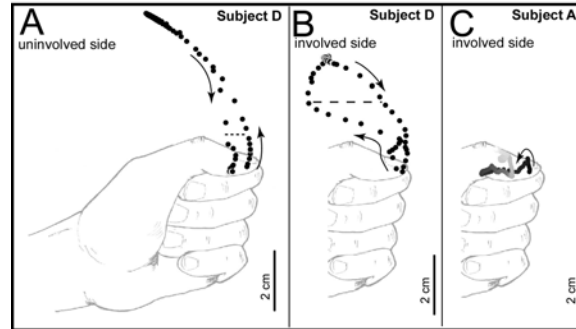


**Fig. 1: Lateral pinch execution trials (Subjects D & A).** Figures 1A and 1B illustrate one trial of lateral pinch execution for Subject D who has moderate

hand impairment. Horizontal dotted lines indicate “path inconsistency” measure in the plane of thumb flexion-extension. Figure 1C illustrates all movement trials for Subject A who has severe hand impairment. Thumb-tip position progresses from dark to light.

As expected, differences in ability to perform the task were related to the degree of hand impairment. Subjects with severe hand impairment (Chedoke-McMaster, Stage of Hand rating  $\leq 3$ ) produced very little thumb movement. Conversely the subject with only moderate hand impairment (Chedoke, 4-5) produced larger thumb movements. Further, a stroke survivor's inability to perform lateral pinch well on the involved side may be due to inappropriate activation of muscles (Kamper et al. (2001)), weakness or tightness in the thumb.

### REFERENCES

- Gowland, C. et al. (1993). *Stroke*, **24**, 58-63.
- Kamper, D. K., Rymer, W. Z. (2001). *Muscle Nerve*, **24**(5), 673-681.
- Lang, C. E., Schieber, M. H. (2003). *J. Neurophysiology*, **90**, 1160-1170.



# COMPARISON OF SHORT-RANGE STIFFNESS OF FELINE LOWER LIMB MUSCLES BETWEEN ANATOMICAL ESTIMATES AND EXPERIMENTAL MEASUREMENTS

Lei Cui<sup>1</sup>, Eric J. Perreault<sup>1,2</sup> and Thomas Sandercock<sup>3</sup>

Departments of Biomedical Engineering<sup>1</sup>, Physical Medicine and Rehab.<sup>2</sup> and Physiology<sup>3</sup>  
Northwestern University, Chicago, IL, USA

E-mail: [t-sandercock@northwestern.edu](mailto:t-sandercock@northwestern.edu)

## INTRODUCTION

The ultimate goal of our research is to study the contributions of individual muscles and muscle combinations to whole limb stiffness. A computer muscle model that is capable of predicting the short-range stiffness (SRS) of individual muscles is believed to be necessary for accomplishing this goal. Specifically, we are interested in developing a methodology for predicting SRS based only on the architectural properties of an individual muscle and the material properties common to all muscles.

The SRS of a muscle depends on the force-dependent material properties of the contractile tissue and the material properties of the passive tendinous structure (1). In contrast, SRS does not depend strongly on motor unit composition or recruitment order (2). Hence, given that the maximum tension ( $P_0$ ) of a muscle can be estimated from anatomical measurements (3), it also should be possible to make anatomically based estimates of SRS provided that muscle and tendon material properties are invariant across muscles. The purpose of this study was to evaluate the errors associated with this approach to modeling SRS.

This was accomplished by developing a simple, anatomically based model and comparing model predictions of SRS with experimental data collected from three cat hindlimb muscles. The contributions of the tendon and aponeurosis to the net SRS also were quantified experimentally.

## METHODS

Strain and SRS-force relationships were measured from medial gastrocnemius (MG), soleus (SOL) and plantaris (PLA). Each muscle was assessed in a single cat, which was anesthetized with sodium pentobarbital (i.v.). The target muscle was isolated from the surrounding tissues and the blood supply was preserved. The muscle tendon was left intact and attached to an instrumented linear motor via a bonechip from the insertion point. Force and length data were collected.

Tendon and aponeurosis strains were measured from the SOL using insect pins (10 mm long) inserted into the muscle at a depth of approximately 1 mm and oriented along the direction of muscle force. Pins were placed at multiple locations including: the tendon insertion site into the bone, the myotendinous junction site and the insertion site of the aponeurosis fibers into the muscle. Strains were calculated based on the locations of the pins measured using a 3D motion tracking system. The tendon elastic modulus was determined from the net stress and strain measurements across the length of the external tendon and aponeurosis.

The architectural parameters used in our model are fascicle length, tendon cross-sectional area and tendon length. Fascicle length was measured by microscope following dissection in a 30% nitric acid solution. Tendon cross-sectional area was measured at one location and assumed to be constant for the length of the tendon and

aponeurosis. Total tendon length was defined as the sum of the external tendon length and the aponeurosis length. Even with these simplifications, our tendon data are comparable to (4).

The model used to calculate the SRS-force relationship is similar to the alpha model described by Morgan (1). This has two components, tendon stiffness ( $K_T$ ) and muscle fiber stiffness ( $K_M$ ).  $K_T$  was estimated for each muscle based on the architectural parameters from that muscle and the net elastic modulus measured in the SOL.  $K_M$  was assumed to vary only with muscle force and fascicle length (5):

$$K_M = P / (\gamma \cdot l_f);$$

$P$  is muscle force,  $l_f$  is fascicle length and  $\gamma$  is a dimensionless constant determined from previous work (2) on the MG ( $\gamma=0.057$ ) and assumed to be constant across muscles.

## RESULTS AND DISCUSSION

During the 2 mm-perturbation, the average SOL strain was 0.3% in the external tendon and 1.7% in the aponeurosis, indicating that the external tendon was much stiffer than the aponeurosis. The estimated net elastic modulus of the SOL tendinous complex (600 MPa) was much lower than reported previously for excised tendons (6). Together, these results suggest that the stiffness of the tendinous structure ( $K_T$ ) was dominated by the aponeurosis. Figure 1 shows the predicted and measured SRS-force relationships for all muscles. Experimental data for SOL were clustered around  $P_0$  because accurate SRS measurements at lower forces were not obtained from this animal. Nevertheless, modeled and experimentally measured SRS matched well for all three muscles, even though our simplified assumption of uniform strain in the aponeurosis and

external tendon was incorrect. The success of the model may reflect the fact that external tendon contributed little to the net muscle SRS in these experiments.

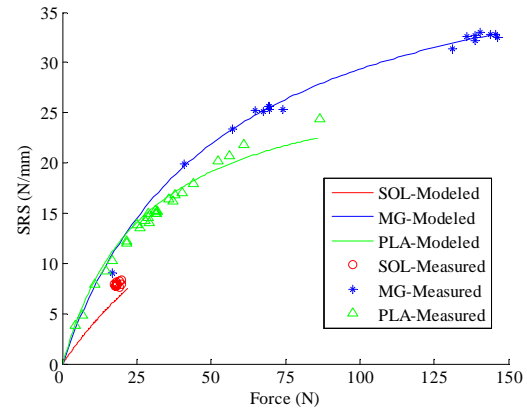


Figure 1. Modeled and measured SRS-force relationships for SOL, MG and PLA muscles

## CONCLUSIONS

1. SOL tendon stiffness is dominated by the aponeurosis.
2. For the muscles tested, the SRS-force relationship could be estimated from simple anatomical measurements.
3. A general extension of this model may require better estimates of stiffness contributions by the aponeurosis and external tendon.

## REFERENCES

1. D. L. Morgan, *Am J Physiol* **232**, C45 (1977).
2. L. Cui, T. Sandercock, *Am Soc Biomech Proceedings* (2005).
3. P. L. Powell, R. R. Roy, P. Kanim, M. A. Bello, V. R. Edgerton, *J Appl Physiol* **57**, 1715 (1984).
4. B. I. Prilutsky, W. Herzog, T. R. Leonard, T. L. Allinger, *J Biomech* **29**, 417 (1996).
5. B. Walmsley, U. Proske, *J Neurophysiol* **46**, 250 (1981).
6. C. M. Pollock, R. E. Shadwick, *Am J Physiol* **266**, R1016 (1994).

# LOAD SHARING COMPARISON BETWEEN POSTERIOR RIGID ROD AND FLEXIBLE DEVICE FIXATION SYSTEMS IN A SPINE MODEL

Jayant Jangra<sup>1</sup>, Ahmad Faizan<sup>1</sup>, Vijay Goel<sup>1</sup>, Leonora Felon<sup>1</sup>, Ashok Biyani<sup>2</sup> and Nabil A. Ebraheim<sup>2</sup>

<sup>1</sup> University of Toledo, Toledo, OH, USA

<sup>2</sup> Medical University of Ohio, Toledo, OH, USA

E-mail: Vijay.Goel@UToledo.Edu Web: [http://bioe.eng.utoledo.edu/adms\\_staffs/chair/index.htm](http://bioe.eng.utoledo.edu/adms_staffs/chair/index.htm)

## INTRODUCTION

Flexible motion preservation devices have emerged as a means to help regenerate the spinal discs and/or lessen the iatrogenic effects of fusion with spinal instrumentation. The purpose of this biomechanical study was to compare a flexible device to a rigid rod based pedicle stabilization system using a simple vertebra-disc-vertebra (VDV) and an intact spine 3-dimensional Finite Element Model.

## METHODS

A simple finite element model of Vertebra-Disc-Vertebra (VDV) segment (Figure 1) with a rigid rod system or flexible device (Sengupta, 2004) was simulated. The disc was removed from the VDV models to simulate the corresponding missing disc models. For the missing disc models, compressive loads required to touch the two vertebrae were compared for the two fixation devices. Models with disc were subjected to 450N axial loads alone or with a flexion moment of 8Nm.

Subsequently, a 3-dimensional, non-linear, ligamentous, experimentally validated, finite element model of L3-S1 spine segment was used to simulate the two stabilization systems in an intact model (Figure 2). The bottom surface of S1 vertebra was constrained. A preload of 450N alone or with a flexion moment of 8Nm was applied on the top surface of the L3 vertebra.

Biomechanically relevant parameters like motion, and disc loads were computed for each loading condition and for each model.

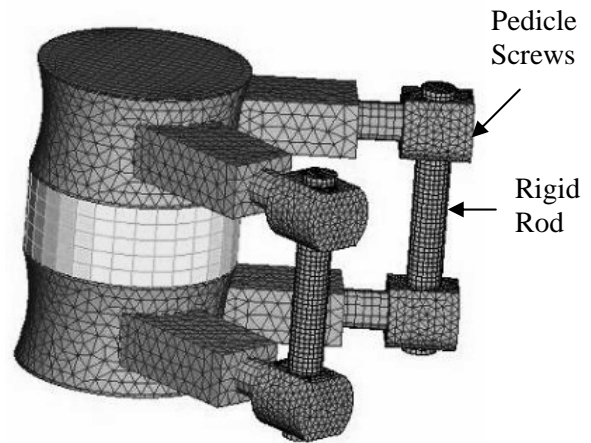


**Figure 1:** The VDV model with the Rigid Rod Fixation and

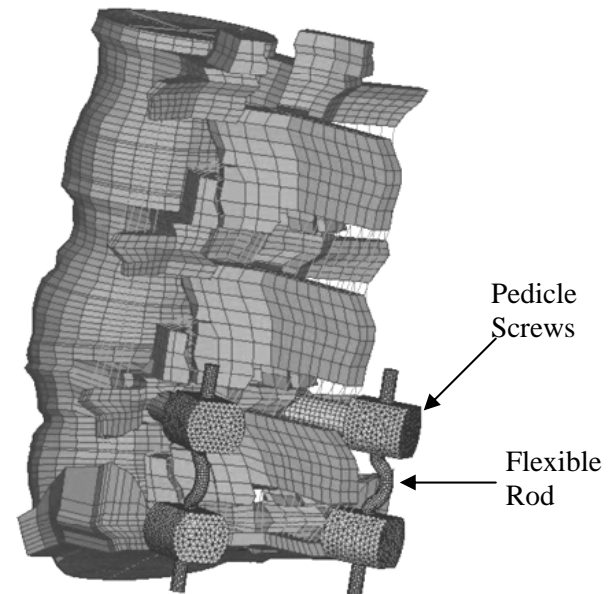


**Figure 2:** The Intact L3-S1 Spine Model with the flexible device.

## **RESULTS AND DISCUSSION**

The missing disc model showed that a compressive load of 1570N was required for the two vertebrae to touch each other with the rigid rod system as opposed to 120N with the flexible device, as expected.

However, the presence of the disc in between the two vertebrae, for the 450N axial compression case resulted in a load of 324N in the disc with the rigid rod system as compared to 424N with the flexible device, while the increase in motion of the segment with flexible device was marginal from 2.33° to 2.35°. With flexion moment of 8 Nm, the load in the disc showed an increase of 23%, from 463N with the rigid rod system to 571N with the flexible device.

The corresponding data for the motion and loads in the disc for the systems used in the intact model were similar in nature. The effect of flexion moment was to increase the overall motion and load in the disc but the trends were still similar. In the intact model also, the increase in motion was very small - from 2.3° with the rigid rod system to 2.5° with the flexible device. With flexion

moment in the intact model, the load in the disc showed an increase of 19%, from 506N with the rigid rod system to 601N with the flexible device.

## **SUMMARY/CONCLUSIONS**

The VDV and the intact spine model data indicate that the effect of increasing flexibility of the stabilization system does not lead to a significant increase in motion at the "stabilized" levels, as compared to the rigid system. However, the load in the disc increases with the use of flexible system, suggesting that the disc may regenerate itself. In the long run this may be helpful.

## **REFERENCES**

Sengupta, D.K. et al. (2004). *The Lumbar Spine*. Lippincott Williams & Wilkins.

## **ACKNOWLEDGEMENTS**

Research supported by Globus, Inc. through an unrestricted educational grant.

# NONLINEAR VERSUS LINEAR BEHAVIOR OF CALCANEAL BONE MARROW AT DIFFERENT SHEAR RATES

Brian L. Davis<sup>1</sup> and S. Solomon Praveen<sup>2</sup>

<sup>1</sup> Cleveland Clinic, Cleveland, OH, USA

<sup>2</sup> Drexel University, Philadelphia, PA, USA

E-mail: davisb3@ccf.org Web: <http://www.lerner.ccf.org/bme/davis/>

## INTRODUCTION

Despite the interest in fluid-solid interactions in bone, there are very few publications describing the rheological properties of either animal or human bone marrow obtained from cancellous specimens. Bryant et al. [1] measured the viscosity of bovine marrow obtained from the radius. They found that the viscosity varied with temperature and location (i.e., proximal versus distal). In addition, viscosity was found to be independent of shear rate after a certain temperature, and remained constant at 40 cP. In another study, Bryant [2] measured the viscosity of sheep marrow at 37°C and reported a viscosity value of 67 cP at a shear rate of 46/sec. Sobotkova et al. [3] measured the rheological properties of bone marrow obtained from the femoral diaphysis and epiphysis of fresh human cadavers, pigs, and bulls and obtained highly varying data.

The present study focused on the rheology of bone marrow present in the calcaneus.

## METHODS

The use of calcaneal specimens from patients undergoing a foot or leg amputation was the most practical way of obtaining sufficient quantities of fresh cancellous bone marrow. Immediately after harvesting the marrow, its rheological properties were measured. The Institutional Review Board (IRB) approved this approach.

### Fresh and frozen bone marrow

Nine bone marrow specimens (six from men and three from women) were harvested from the calcaneus of freshly amputated human legs within approximately 30 minutes of above- or below-knee amputation. To study the effect of freezing, eight additional bone marrow samples (four male and four female) were obtained from the calcaneus of unembalmed frozen cadaver or amputated foot specimens. The age of the specimens (fresh as well as frozen) was  $62 \pm 13$  (average  $\pm$  SD) years old.

### Method of harvesting bone marrow

Bone plugs of 8.4 mm in diameter were removed from the calcaneus, using a bone coring drill bit. After removing the skin tissue and cortical shell at the ends, bone marrow was forced out of the bone cores by using a custom-made 0.5-ton arbor press. The bone marrow was collected directly into a test tube that contained spray-dried K<sub>2</sub> EDTA, an anticoagulant. Spray-dried K<sub>2</sub> EDTA was chosen over other liquid anticoagulants to minimize dilution of the bone marrow sample. The density of bone marrow was measured by using a specific-gravity bottle.

### Viscosity measurements

The viscosity of the bone marrow and its dependence on shear rate were measured using a Vilastic-3 Viscoelasticity Analyzer (Vilastic Scientific, Inc., Austin, TX, USA). This instrument operates on the principle of controlled oscillatory flow within a straight,

cylindrical tube with circular cross section. A stainless steel, thermally jacketed measurement tube of 0.049 cm inner radius and an effective length of 1 cm was used to measure the viscosity of bone marrow. The measurement tube was maintained at a desired temperature during viscosity measurements by using a constant temperature water circulator.

## RESULTS AND DISCUSSION

Cancellous bone contains a large amount of bone marrow in its porous intertrabecular spaces. This study focused on the influence of shear rate on the viscosity of bone marrow obtained from the human calcaneus.

It was found that the influence of shear rate on viscosity depended on the state of health of the donors, with some marrow specimens behaving like a non-Newtonian fluid (Fig 1) and the yellow marrow behaving like a Newtonian fluid (Fig 2).

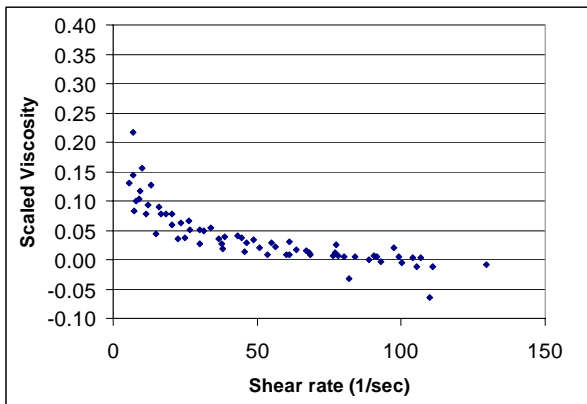


**Figure 1:** Influence of shear rate on bone marrow viscosity of bone marrow specimens containing red components in the range of 36-38°C. All the marrow samples behaved like a non-Newtonian fluid that followed a relationship of the form  $\text{Viscosity} = A/\text{shear rate} + B$ , where A and B were constants determined through a standard regression procedure. The scaled viscosity shown above was determined by computing  $(\text{Viscosity} - B)/\sqrt{A}$

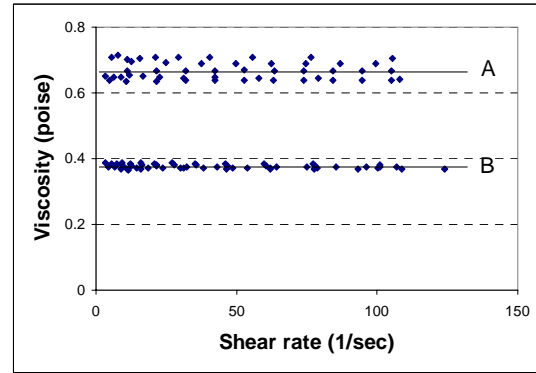


**Figure 2:** Yellow marrow viscosity from freshly amputated bone marrow specimen without any red components at 23°C (upper set, A) and at 36°C (lower set, B).

The average viscosity of yellow marrow at approximately 36°C was 37.5 cP. The temperature of the marrow during testing had a highly significant effect on viscosity, but whether or not the specimen had been frozen prior to testing had no effect on viscosity results. These data provide important information for understanding the role of bone marrow in a number of biomedical applications (including cancellous bone remodeling) and diagnostic techniques (such as calcaneal ultrasound).

## REFERENCES

1. Bryant JD, David T, Gaskell PH, King S, Lond G. Rheology of bovine bone marrow. *Proc Inst Mech Eng [H]* 1989;203:71-5.
2. Bryant JD. On the mechanical function of marrow in long bones. *Eng Med.* 1988; 17:55-8.
3. Sobotkova E, Hruby A, Keifman J, Sobotkova Z. Rheological behavior of bone marrow. *Proc. of the 2<sup>nd</sup> conference of European rheologists*, Prague, 1988;467-9.

## ACKNOWLEDGEMENTS

The authors would like to acknowledge the assistance of Dr. Victor Kashyup and Dr. Bill Smith in providing specimens and in permitting use of the viscoelastic analyzer.

# HIGH-RATE VISCOELASTIC PROPERTIES OF HUMAN CERVICAL SPINAL INTERVERTEBRAL DISCS

Scott Lucas<sup>1</sup>, Cameron Bass<sup>1</sup>, Robert Salzar<sup>1</sup>, Barry Shender<sup>2</sup>, and Glenn Paskoff<sup>2</sup>

<sup>1</sup> University of Virginia, Charlottesville, VA, USA

<sup>2</sup> NAVAIR, Patuxent River, MD, USA

E-mail: slucas@virginia.edu Web: www.centerforappliedbiomechanics.org

## INTRODUCTION

The neck is vulnerable to injury in automotive and military crash scenarios. To investigate these injuries and develop countermeasures, computational models of neck response may be used. In these models, it is imperative to have accurate material properties of the internal soft tissues derived using appropriate loading rates. The purpose of this study was to determine high-rate viscoelastic properties of human cervical spinal intervertebral discs. The viscoelastic model, derived from human experimental data, was compared based on location on the anulus and gender.

## METHODS

Ten human cadaver cervical spines (5M, 5F) were used in this study. The average male age, stature, and mass were  $60.2 \pm 10.3$  yr,  $1821 \pm 44$  mm, and  $99.2 \pm 12.2$  kg. The average female age, stature, and mass were  $43.7 \pm 17.8$  yr,  $1687 \pm 85$  mm, and  $75.4 \pm 28.1$  kg. The cervical discs were isolated from each cervical spine at C3-C4, C5-C6, and C7-T1 and localized indentation tests were performed on four sites on the anulus fibrosus (Figure 1). The inferior vertebral body remained for each disc. A total of 93 cervical intervertebral discs were tested. A 2.75 mm diameter spherical head indenter was used for all tests.

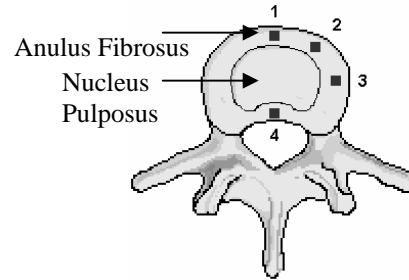


**Figure 1.** Schematic of intervertebral disc. Indentation tests were performed on the sites marked 1-4.

A series of incrementally increasing strain ramp-hold inputs were applied to each spot. The tests were performed in an environmental chamber at appropriately physiological conditions ( $\sim 99$  °F,  $\sim 100\%$  RH). An analytic solution of average true strain and average local true stress was developed. A viscoelastic material model was determined from the nonfailure tests using quasi-linear viscoelasticity theory (c.f. Lucas *et al.*, 2004). The relaxation function in the QLV model was comprised of four relaxation coefficients, with corresponding time constants, and a steady state coefficient (Table 1). The model was developed using the average true strain and average local true stress beneath the indenter.

**Table 1.** Summary of  $G_n$  and corresponding time constants.

$G_n$	$G_1$	$G_2$	$G_3$	$G_4$	$G_\infty$
Time Constant (ms)	1000	100	10	1	----

## RESULTS AND DISCUSSION

The highest weighted relaxation coefficient,  $G_4$ , corresponds to a time constant of 1 ms. This indicates that at high-rates, the intervertebral disc relaxes early in the strain ramp onset. The next highest weighted coefficient,  $G_\infty$ , is the steady state coefficient. Comparisons were made between annulus site and gender. Figure 2 is a comparison of  $G_4$  and  $G_\infty$  based on annulus site. There is no substantial difference in  $G_4$  or  $G_\infty$  between site 1 and site 4.  $G_4$  is slightly higher in site 2 and site 3, which are located on the anterior-lateral and lateral aspects of the annulus, respectively.

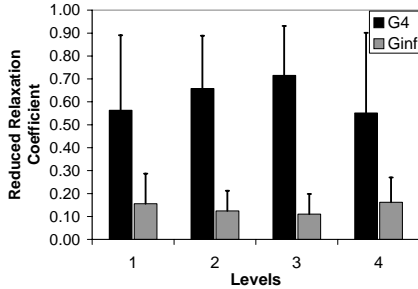


**Figure 2.** Comparison of relaxation coefficients based on annulus site

Figure 3 is a comparison of  $G_4$  and  $G_\infty$  based on gender. The male  $G_4$  is larger than the female  $G_4$ , indicating that more relaxation is occurring in the ramp onset for the male discs. Consequently, the female  $G_\infty$  coefficient is larger than the male  $G_\infty$  coefficient, since the sum of the relaxation coefficients is one. Differences in male and female relaxation coefficients may be attributed to the amount of disc degeneration. Males have a higher prevalence of disc degeneration. Additionally, the average age of male subjects in this study was larger than the average age of the female subjects. Disc degeneration is certainly exacerbated with age.

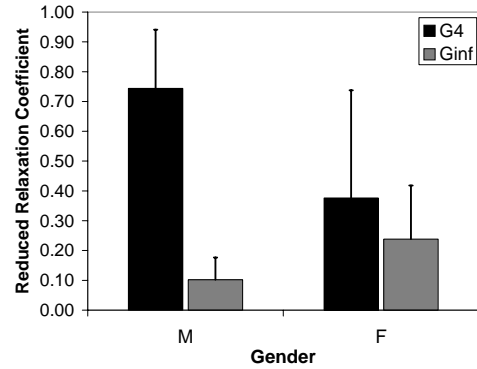


**Figure 3.** Comparison of relaxation coefficients based on gender. Annulus sites 1-4 are grouped together in this comparison.

## SUMMARY/CONCLUSIONS

The primary objective of this study was to investigate high-rate viscoelastic properties of cervical spine intervertebral discs. It has been shown that there is a large amount of relaxation early in the strain ramp onset. There are no substantial trends in the relaxation coefficients based on annulus site; however, there are discernable differences in relaxation based on gender.

## REFERENCES

- Darvish, K.K. et al. (1999). *A Nonlinear Viscoelastic Model for Polyurethane Foams*. Journal of Materials and Manufacturing, **108**, 209-215.
- Fung, Y.C. (1981). *Biomechanics: Mechanical Properties of Living Tissues*. Springer-Verlag, New York.
- Lucas, S.R., et al. (2004). *Viscoelastic Characterization of Cervical Spinal Ligaments*. Presented at the ASB 28<sup>th</sup> Annual Meeting, Portland, OR.
- Yoganandan N. et al. (2001). *Biomechanics of the Cervical Spine Part 2*. Clinical Biomechanics, **16**, 1-27.

## ACKNOWLEDGEMENTS

This study was supported by the US Office of Naval Research, the Naval Air Systems Command Patuxent River, MD and the University of Virginia School of Engineering and Applied Science.

## Estimate of Posterior Tibialis Muscle Length During the Heel Rise Test

Christopher G. Neville<sup>1</sup> Adolf Flemister<sup>1</sup> Josh Tome<sup>2</sup>  
Jeff Houck<sup>1,2</sup>

<sup>1</sup> University of Rochester, Rochester, NY, USA

<sup>2</sup> Ithaca College, Rochester, NY, USA

E-mail: christopher\_neville@urmc.rochester.edu

### INTRODUCTION

Studies have shown kinematic changes in subjects with Posterior Tibial Tendon Dysfunction (PTTD) with evidence that the Posterior Tibialis (PT) muscle plays the greatest role during gait after heel rise[1]. The impact of the kinematic changes seen in subjects with Stage II PTTD on the length of the PT muscle in-vitro has also been investigated revealing contributions from both the hindfoot and forefoot[2]. One commonly used clinical test to evaluate the integrity of the PT muscle is the heel rise test. The ability of subjects to perform this test provides insight to clinicians on the competence of the PT muscle, however the kinematics exhibited during this test are currently unknown. In addition, the impact this test has on muscle length has not been investigated. The purpose of this study was to compare PT muscle length during the heel rise test between subjects with Stage II PTTD and control subjects.

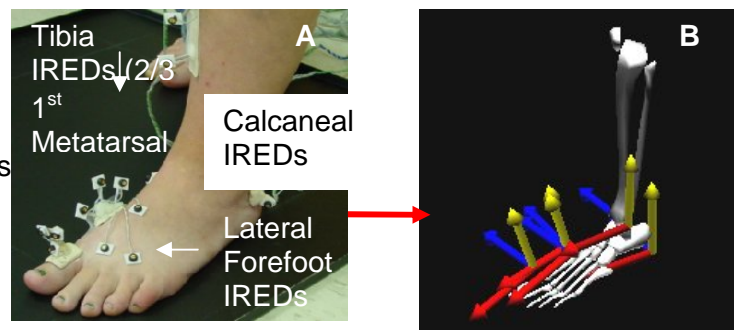
### METHODS

Kinematic data was collected from the leg, calcaneus (hindfoot) and 1st metatarsal (forefoot) while performing double limb heel rise tests using an Optotrak Motion Analysis System (Northern Digital Inc, CAN) and Motion Monitor Software

(Innsport Training Inc, USA). The data was sampled at 60 Hz and low pass filtered at 6 Hz. A Cardan angle Z-X-Y sequence of rotations was used to calculate the four angles listed below for input into a regression equation to estimate Posterior Tibialis Length ( $PT_{Length}$ ). The regression equation ( $PT_{Length}=0.747 + 0.404(\theta_{hfin/ev}) + 0.260(\theta_{ffab/ad}) + 0.143(\theta_{ffpf/df}) + 0.055(\theta_{anklepf/df})$ ) used to estimate posterior tibialis muscle length ( $PT_{Length}$ ) was determined using in-vitro kinematic measures of hindfoot inversion/eversion (hfin/ev), forefoot abduction/adduction (ffab/ad), forefoot plantarflexion/dorsiflexion (ffpf/df) and ankle plantarflexion/dorsiflexion (anklepf/df). The equation to estimate  $PT_{Length}$  showed a high  $r^2$  value (0.83) and low standard error of the estimate of 2.04 mm. Zero PT muscle length corresponds to length at sub-talar neutral position of the foot. A statistical comparison was made between peak shortening of those with PTTD and their matched controls using a two-tailed t-test for comparison between group means.

The individual contributions from each kinematic input were compared to explore which kinematic changes produced the differences in length estimates.

**Figure 1.** Infrared emitting diodes (A) and anatomic coordinate systems used to model foot movement (B).



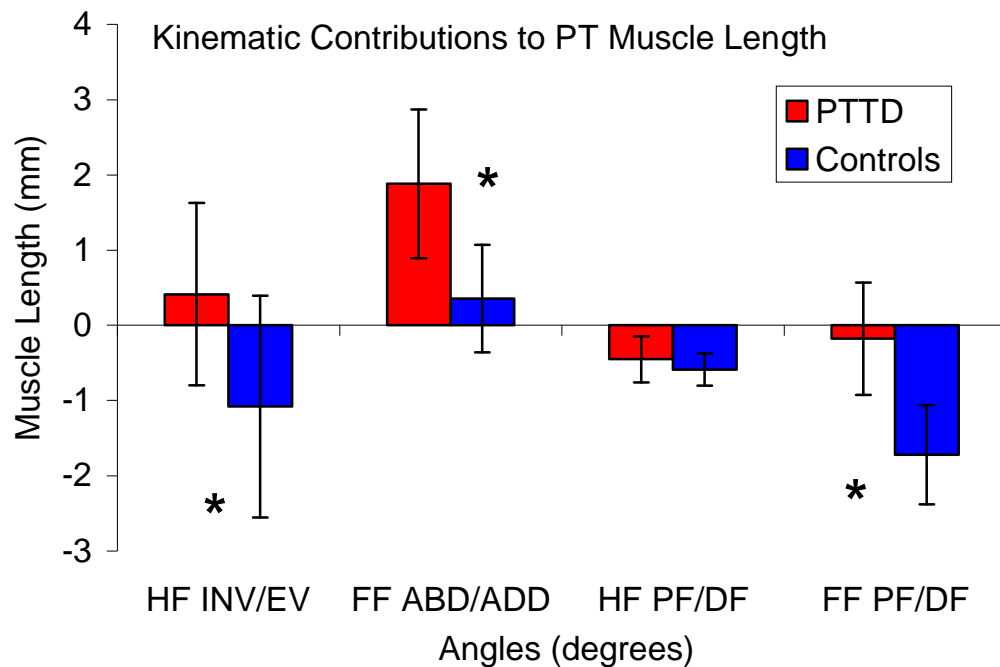


**Figure 2:** Individual foot kinematic contributions to PT muscle length at peak plantarflexion of the heel rise test..

**RESULTS AND DISCUSSION**

There was a significant difference between the PTTD group and the control group at the start ( $p=.003$ ) and peak plantar flexion ( $p=.002$ ) of the heel raise. The PTTD subjects started the test at a longer estimated muscle length, mean 8mm, versus 4.44 mm for the control group. There was a non-significant change in muscle length as both groups demonstrated shortening during the test. The PTTD group were unable to reach their zero referenced muscle length (subtalar neutral position) while the control group achieved a muscle length of 2mm shorter than the zero position. The individual foot kinematic contributions to muscle length (Figure 2) showed both the hindfoot and forefoot contributed to a longer muscle length in the PTTD subjects. This lengthening of the muscle in subjects with PTTD raises the possibility of compromised force of the muscle due to a shift in the force/length relationship.

**SUMMARY/CONCLUSIONS**

The PTTD subjects functioned at a longer muscle length throughout the heel rise test. This suggests subjects may have compromised force production due to a shift in the force length relationship. The longer length in PTTD subjects is a result of both hindfoot and forefoot kinematic changes.

**REFERENCES**

- 1.Niki, H., et al., *The effect of posterior tibial tendon dysfunction on hindfoot kinematics.* Foot & Ankle International, 2001. **22**(4): p. 292-300.
2. Neville, C, et al, *The Effect of Stage II Posterior Tibial Tendon Dysfunction on Muscle Length During Walking.* J Orthop Sports Phys Ther,2006, 36(1) p.A12-13.,

**ACKNOWLEDGEMENTS**

Supported in part by the Foundation of Physical Therapy



# INDIVIDUAL LANDING STRATEGIES IN FIGURE SKATING JUMPS

Dustin A. Bruening and James G. Richards

University of Delaware, Newark, DE USA

Email: dustinb@udel.edu

## INTRODUCTION

In a previously presented study (Bruening & Richards, 2005) we compared jump landings of figure skaters using standard skating boots and articulated skating boots (in a repeated measures design). We showed decreases in peak heel impact forces and loading rates with use of the articulated skating boot and suggested that such decreases may translate into reduced overuse injury risks.

We hypothesized that increased plantar flexion at the moment of impact would allow the triceps surae complex to slow the descent of the heel, resulting in a lower peak heel ground reaction force (Gross & Nelson, 1988; Self & Paine, 2001). Group means from our study that supported this hypothesis included increased plantar flexion angles at the moment of toe contact and increased times between toe and heel strike with use of the articulated skates.

A retrospective analysis of the landing data revealed other important insights into individual landing strategies that were masked by the group analysis. These individual landing strategies may help explain the mechanisms through which joint restrictions (such as stiff figure skates) affect landing forces as well as how training methods can be used to help lower landing forces.

## METHODS

Jumps from nine competitive figure skaters who trained in standard boots and in prototype articulated boots (Figure 1) were

analyzed. Tests consisted of off-ice simulated jump landings from a 1-ft box onto a force plate (960 Hz) covered with an acrylic sheet. An eight camera motion analysis system was used to collect three-dimensional kinematics (240 Hz).



**Figure 1:** Standard skating boot (A) and articulated skating boot prototype (B).

In the retrospective analysis, the following dependent variables were analyzed: Peak heel contact force, jump height, ankle angle at toe contact, strike time (time between toe strike and heel strike), peak ankle power, heel velocity at impact, heel impact effective mass, landing phase time, and ankle and total lower extremity excursions during the entire landing phase (toe contact to CM settling). Heel effective mass represented the amount of mass that was decelerated at heel impact.

## RESULTS AND DISCUSSION

In order to observe relationships between variables, the dependent variables were represented simply by whether there was an increase, decrease, or no change from the standard boot condition to the articulated boot condition (Table 1). The subjects are grouped by whether the heel contact force decreased (subjects 1-5) or did not decrease (subjects 6-9).

Subjects 1 and 2 illustrate the landing strategy that was expected to result in the greatest contact force decrement. They increased plantar flexion at toe contact and increased ankle power during the impact phase, resulting in a decreased strike time and heel velocity. Additionally, they lowered their effective mass at heel contact by increasing ankle and total leg excursion, prolonging the landing time.

Subject 9 represented the reverse of this situation. Although the subject increased ankle plantar flexion at toe contact, the ankle power and strike time decreased, implying decreased ankle muscle activity. The heel velocity increased as did the heel effective mass. The subject apparently attempted to follow the landing instructions (to “point the

toes and use the ankle motion”) yet did not succeed in lowering the impact force.

Between the two extremes there are many possible landing variable combinations. It may be possible to identify, based on landing kinematics, how subjects will respond to articulated skates (or in a more general sense to increased ranges of joint motion). It may also be possible to identify the type of training that may be required for an individual to develop an effective landing strategy that will result in decreased landing forces. Proper training and instruction in conjunction with equipment that allows full sagittal plane motion may help reduce the risk of overuse injuries in figure skating and perhaps other jumping activities as well.

**Table 1:** Dependent variable changes for each of nine subjects

Subject	Ankle Mechanics Variables						Effective Mass Variables			
	Heel Contact Force	Jump Height	Plantar Flexion at Toe Contact	Strike Time	Peak Ankle Power	Heel Velocity at Contact	Heel % EM	Ankle Excursion	Total Leg Excursion	Landing Time
<i>Heel Force Decreased</i>										
1	↓	-	↑	↑	↑	↓	↓	↑	↑	↑
2	↓	-	↑	↑	↑	↓	↓	↑	↑	↑
3	↓	-	↑	-	-	↑	↓	↑	↑	↑
4	↓	-	-	↑	↑	↓	↓	↑	-	-
5	↓	↓	↓	↑	↑	-	-	↓	↓	↑
<i>Heel Force Did Not Decrease</i>										
6	-	↑	↓	↑	↓	↑	↑	↓	↓	↑
7	-	-	↑	↑	↓	↓	↓	↑	↑	↑
8	-	↑	↑	↑	↑	↑	-	↑	↑	↑
9	↑	-	↑	↓	↓	↑	↑	-	-	↓

## REFERENCES

- Bruening, D., & Richards, J. (2005). *Articulated Figure Skating Boots Can Reduce Impact Forces*. Paper presented at the 7th Symposium on Footwear Biomechanics, Cleveland, OH.
- Gross, T. S., & Nelson, R. C. (1988). The shock attenuation role of the ankle during landing from a vertical jump. *Med Sci Sports Exerc*, **20**, 506-514.
- Self, B. P., & Paine, D. (2001). Ankle biomechanics during four landing techniques. *Med Sci Sports Exerc*, **33**, 1338-1344.

# ALTERATIONS IN KINEMATICS AND MUSCLE ACTIVITY DURING LOCOMOTOR TRAINING.

Gail F Forrest<sup>1</sup>, Sue Ann Sisto<sup>1</sup>, Pierre Asselin<sup>1</sup>, John Mores<sup>1</sup>, Dr Steven Kirshblum<sup>2</sup>, Janina Wilen<sup>1</sup>, Susan Harkema<sup>3</sup>

<sup>1</sup>Kessler Medical Rehabilitation Research and Education Corporation

<sup>2</sup>Kessler Institute for Rehabilitation

<sup>3</sup>Department of Neurological Surgery, University of Louisville  
email:gforrest@kmrrec.org

## INTRODUCTION

Recently new approaches to facilitate locomotor recovery have been directed away from compensatory strategies and towards Locomotor Training (LT) using body weight support (BWS) that optimizes afferent sensory information and facilitates activity-dependent plasticity in the spinal cord to control movement (Harkema et al.). LT has been studied extensively as a therapeutic intervention for individuals after spinal cord injury (SCI) and stroke (Visintin, Barbeau). Preliminary studies have shown that LT following SCI can improve muscle activity during locomotion, where individuals are able to load more on the treadmill and improve their functional walking overground (Wernig, Muller). A potential limitation of the research related to LT is the lack of normative data to validate the kinematic and electromyography (EMG) data profiles that are generated from individuals with SCI. The objective of this preliminary study is to determine the effects of LT using BWS on kinematics, and muscle activation for able-bodied controls at different BWS, at different velocities, and the effect of the harness on kinematics and muscle activation. This data is highly relevant to the research being performed in our laboratory and an understanding of the effects of changing velocity, BWS and the influence of the harness to neural activation is necessary to the design of the new protocols or when analyzing the effects of LT.

## METHODS

Four participants (3 males, 1 female, mean age: 31 ±11.03 years) walked at speeds: 0.71m/s, 0.89m/s,

1.16m/s for 60, 40, 0% BWS and without wearing a body weight support harness walked at .71m/s, .89m/s, and 1.16m/s. Each trial was collected for 20 seconds. Kinematic and EMG were collected bilaterally for each condition. A 6-camera Vicon system (sampled at 60Hz) was used to collect kinematic data. Spherical reflective markers were placed on right and left second and fifth metatarsal, calcaneus, tibial tuberosity, femoral epicondyle, greater trochanter, anterior inferior iliac spine, posterior inferior iliac spine. EMG was recorded using surface EMG for left and right medial gastrocnemius (L/R GA), tibialis anterior (L/R TA), rectus femoris (L/R RF) and biceps femoris (L/R BF). EMG were collected at a bandwidth of 10-600 Hz, and sampled at 1560 Hz. Raw EMG signals were filtered at a bandwidth of 30-150 Hz, full-wave rectified, and root mean squares (RMSs) were calculated over a 50ms window (Wilen et al.). Mean RMS EMGs were calculated as the sum of the RMS amplitudes from burst onset to burst offset divided by burst duration. Burst onset/offset was defined as time of onset/offset of EMG burst. Burst Duration (BD) was defined as time between the onset of EMG burst to the offset of EMG burst of each muscle within stance and swing phase of gait cycle (GT). EMG data was processed using MATLAB (MathWorks Inc., Version 6.1). Calculation of sagittal plane segment motion for the thigh, shank and foot was determined using MATLAB (MathWorks Inc., Version 6.1). Limb kinematics were calculated in the local moving plane. Orientation angles for each segment relative to the right horizontal. 3-8 gait cycles were analyzed per condition. Non parametric Wilcoxon signed rank

test determined if there were significant differences between different levels of BWS or different speeds.

## RESULTS AND DISCUSSION

**Stance time (ST):** Increased with decrease in BWS for all participants (.715m/s, 60%BWS:  $53 \pm 0.7\%$  GT, versus .715m/s 0% BWS:  $61\% \pm .4\%$  GC ).

**Kinematics:** Increases in angular displacement (AD) at the hip and knee (Table 1) were not significant. There does appear to be a trend with an increase in hip and knee AD at 0% BWS.

**Muscle Activation:** Not a significant increase in mean RMS LBF (Table 2). Figure 1 illustrated a trend: with a decrease in BWS there is an increase in amplitude. Similar results were shown for LGA and LTA at different BWS. Our results also indicated an increase in BD for an increase in load (Fig 1). There was also a trend to show an increase in mean RMS amplitude for LBF without harness (Table2, Fig 1). Similar results were shown for the right limb. The LRF RMS amplitudes were not significant at different BWS. BD for LRF occurred during early stance and pre swing for all individuals. Regardless of BWS LRF amplitudes were small ( $0.71\text{m/s}$  60%, 40%, 0%, and without harness:  $11.8 \pm 0.7$ ,  $10.9 \pm 0.8$ ,  $10.3 \pm 0.2$ ,  $7.8 \pm 3.9\text{uV}$ )

In general, the BD for the LRF, LBF, LTA and LG increased with increasing load.

## SUMMARY/CONCLUSIONS

At high BWS, ST was less and often heel strike was difficult to obtain. Altering BWS changes the kinematic and EMG activation patterns. The harness also seems to contribute to a change in kinematics and EMG. This study provided preliminary data relevant to able-bodied controls that we can use to compare individuals who have had a SCI and who have completed LT (Fig. 2).

This preliminary data is limited by the small sample size but does show a trend. Further data needs to be collected to increase the n size.

**Figure 1.** For one participant: EMG Activity for LBF (uV) for different velocities, BWS and no harness.

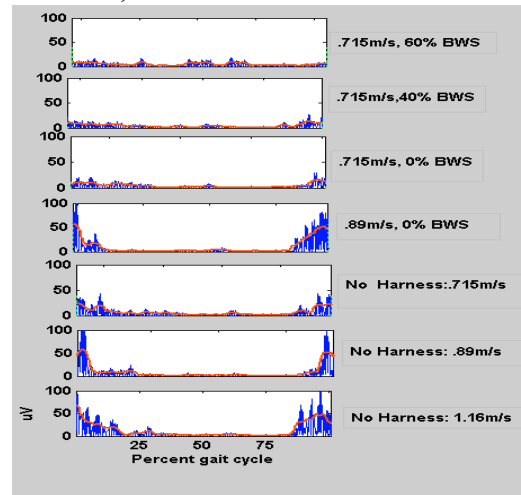


**Figure 2.** Individual with Chronic Motor Complete ASIA-B SCI. EMG data [LBF (uV)]

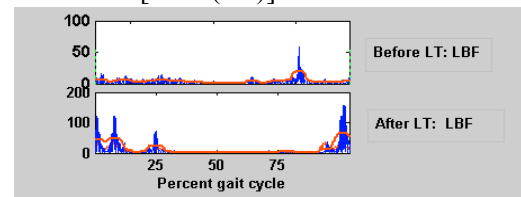


**Table 2:** Mean RMS LBF (uV): BWS (60,40,0%);

	60	40	0	NO Harness
0.71m/s	5.5±.4	10.7±1.8	10.1±2.6	20.7±8.0
0.89m/s	7.5	12.75.5±6.1	20.45.5±7.	25.5±3.2

## REFERENCES

- Harkema, S et al., *J Neurophysiol* 1997; 77: 797-811.  
 Wernig, A., S. Muller, S. Paraplegia, 30 229-238, 1992.  
 Visintin, M., Barbeau, H. *Can. J. of Neurol. Science.* 1989; 16(3) 315-325.  
 Wilen J, et al., *A of Biomed Eng.* 39:97-106, 2002

## ACKNOWLEDGEMENT

New Jersey Commission on Spinal Cord Research

**Table 1:** Angular Displacement for knee and Hip for BWS (60,40,0%) and velocities (0.71m/s, 0.89m/s).

HIP	KNEE				HIP	KNEE				
	BWS	60	40	0		W/O Harness	BWS	60	40	0
0.71m/s		31.0±.12	33.0±.2.8	43.0±1.4	28.0±12.7	0.71m/s	56.9±2.8	57.4±3.5	65.6±1.9	68.2±10.3
0.89m/s		30.5±2.1	34.0±2.3	40.5±3.5	46.0±5.66	0.89m/s	60.5±.7	59.0±2.1	69.48±3.6	67.03±7.1

# SENSITIVITY OF $\mu$ CT-DERIVED CORTICAL BONE METRICS TO SPECIMEN ORIENTATION AND IMAGE THRESHOLDING

Jane A. Casey, Douglas C. Moore, and Joseph J. Crisco

Department of Orthopaedics, Brown Medical School/RI Hospital, Providence, RI, USA

E-mail: douglas\_moore@brown.edu

## INTRODUCTION

Microcomputed tomography ( $\mu$ CT) is often used to generate morphometric data for studies aimed at identifying the influence of genetics on skeletal phenotype (Beamer 2001; Jacques 2004). Commonly reported metrics for cortical bone include cross-sectional area and moments of inertia, typically calculated from short scans at the mid-diaphysis. It is unknown how these metrics are affected by specimen alignment during scanning, or thresholding of the acquired images during analysis.

This study was performed to evaluate the sensitivity of  $\mu$ CT-derived mid-diaphyseal area and moments of inertia to specimen alignment. To do so, we compared interspecimen variability to machine, thresholding, and positioning-related variability using data from scans of mouse femurs.

## METHODS

**$\mu$ CT Scanning** Left femurs were obtained from 47 twenty-four week old female mice euthanized as part of another study (HSD:ICR, generation 38) (Morgan 2003). 6  $\mu$ m-resolution images of the femoral midshaft were acquired using a Scanco  $\mu$ CT 40 (55kVP, 145  $\mu$ A, 250 ms integration time). During scanning, the femurs were aligned with their diaphyses parallel to the scanner's built-in z-axis and the anteroposterior (AP) and mediolateral (ML) planes were aligned with the scanner's - and y- axes respectively. Alignment was

assessed subjectively using the AP scout views. For each bone, the cross-sectional area (A) and moments of inertia ( $I_{AP}$ ,  $I_{ML}$ ,  $I_{max}$ ,  $I_{min}$ ) were calculated for 10 adjacent thresholded  $\mu$ CT slices and averaged (threshold = 400).

**Interspecimen Variability** was assessed by calculating the means ( $\mu$ ), standard deviations ( $\sigma$ ), and Coefficients of Variation ( $CV=\sigma/\mu$ ) for all 47 femurs.

**Machine-Related Variability** was assessed by repeatedly (n=6) scanning a single femur, without removing it from the scanner.

**Positioning-Related Variability** was assessed by repeatedly (n=6) scanning six femurs, each of which was removed and replaced in specimen holder between scans.

**Thresholding-Related Variability** was assessed by repeatedly (n=6) processing one scan of one bone at the standard (400) and at two additional threshold values (350, 450).

**Analytical Error Estimate** The effect of small rotational misalignment was estimated by calculating cross-sectional area and moments of inertia for a hollow circular cylinder (outer radius  $r_o$ , inner radius  $r_i$ ) rotated off-axis from one to fifteen degrees ( $\alpha$ ) using the following equation:

$$I = \frac{1}{4} r_o \pi \left( \frac{r_o}{\cos(\alpha)} \right)^3 - \frac{1}{4} r_i \pi \left( \frac{r_i}{\cos(\alpha)} \right)^3$$

## RESULTS

**Interspecimen Variability** Across all 47 specimens, the variability (standard deviation) in cortical bone area was 13.4% of the mean, while the variability in the moments of inertia was approximately 21% of the mean (Table 1).

	Area <sup>(1)</sup>	I <sub>AP</sub> <sup>(2)</sup>	I <sub>ML</sub> <sup>(2)</sup>	I <sub>max</sub> <sup>(2)</sup>	I <sub>min</sub> <sup>(2)</sup>
$\mu \pm \sigma$	1.03±0.14	0.26±0.05	0.19±0.04	0.26±0.05	0.18±0.04
CV	0.134	0.214	0.205	0.208	0.211

Units: (1) mm<sup>2</sup>, (2) mm<sup>4</sup>; Coefficient Variation (CV).

	Area <sup>(1)</sup>	I <sub>AP</sub> <sup>(2)</sup>	I <sub>ML</sub> <sup>(2)</sup>	I <sub>max</sub> <sup>(2)</sup>	I <sub>min</sub> <sup>(2)</sup>
$\mu \pm \sigma$	1.06±0.008	0.27±0.007	0.20±0.005	0.28±0.004	0.19±0.002
CV	0.008	0.027	0.027	0.016	0.012

Units: (1) mm<sup>2</sup>, (2) mm<sup>4</sup>; Coefficient Variation (CV).

### Machine & Positioning-Related Variability

The machine-related variability associated with simply selecting the midpoint of the femur, scanning and running the automated cross-sectional area and MOI calculations was less than 0.5% of the mean, for all variables. When positioning specimens in the scanner was included, the variability increased only slightly, to 1-3% of the mean (Table 2). Rotational alignment about the z-axis was least consistent (CV was 0.027 for I<sub>AP</sub> and I<sub>ML</sub>, compared to 0.008 for A and 0.016 and 0.012 for I<sub>max</sub> and I<sub>min</sub>, respectively, which are independent of z-axis rotation).

**Interspecimen vs. Positioning-Related Variability** Interspecimen variability in cross-sectional area and moment of inertia was 7.5-17.5 times greater than positioning-related variability, depending on metric (Compare tables 1 and 2)

**Analytical Positioning Error Estimate** Our analytical model indicates that the errors in cross-sectional area and moments of inertia

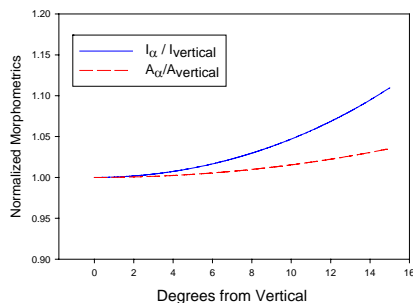


**Figure 3a** Analytical estimate of error associated with positioning in holder.

of a hollow circular cylinder remain less than 1% and 2%, for off-axis rotations of less than seven degrees.

**Thresholding-Related Variability** Varying the threshold by 12.5% did not appreciably alter morphometric calculations (CV<0.02).

## DISCUSSION

This study was performed to determine the sensitivity of  $\mu$ CT-generated midshaft cross-sectional area and moment of inertia measurements to specimen placement in the scanner. We found that the variability associated with careful, subjective alignment (positioning-related variability) was roughly 10% of the variability inherent in the sample of bones we studied. Our rotational alignment about the z-axis was the least consistent. The 2% positioning-related variability we measured is consistent with our analytical estimate of the 2% error associated with seven degrees of off-axis alignment, which is more than would be accepted with subjective alignment on a standard scout.

## CONCLUSION

Our results confirm that subjective alignment is reasonable for comparing relatively dissimilar groups of bones. Where differences are subtle, more objective methods to standardize positioning may be necessary.

## REFERENCES

- Beamer et al. (2001). *J Bone Miner Research*, **16**, 1195-1206.  
 Jaecques et al. (2004). *Biomaterials*, **25**,1683-1696.

## ACKNOWLEDGEMENTS

Funded by RIH Orthopaedic Foundation, Inc. and University Orthopedics Inc.

# THE VELOCITY OF STRETCH-SHORTENING CYCLES DURING A CHRONIC EXPOSURE AFFECTS MUSCLE PERFORMANCE DIFFERENTIALLY WITH AGE

Kenneth B. Geronilla, John Z. Wu, Brent A. Baker, and Robert G. Cutlip  
National Institute for Occupational Safety and Health 1095 Don Nehlen Drive,  
Morgantown, WV 26505

## INTRODUCTION

The age distribution of the workforce in the United States is predicted to shift to older workers (Bureau of Labor Statistics, 1999). Indeed, the 55-64 year old demographic is now the fastest growing sector of the labor force in the United States. Senescent-related changes in strength and skeletal muscle mass have been studied previously (Evans et al., 1993); however, changes in functional performance and muscle plasticity with resistance training in aged-populations are not fully understood. An effective and physiologically relevant means to study muscle function and adaptation to physical loading is via stretch-shortening cycles (SSCs). Natural muscle function during locomotion, daily lifting tasks, and sports are comprised of SSCs (reciprocal concentric and eccentric muscle actions). SSCs have been studied in the context of human locomotion and athletic performance (Komi, 2000) and have been shown to produce muscle injury due to the eccentric component of the cycle. However, the effect of age on the ability to adapt to a chronic exposure of SSCs, and how age affects performance during different SSC velocities has not been studied. We hypothesized age negatively affects the ability to adapt to repetitive exposures of SSCs, and performance is most affected during higher velocity SSCs.

## METHODS

All testing was performed on male Fischer Brown Norway Hybrid rats (F344 x BN F1, N = 11) obtained from the National Institutes on Aging colony. Young adult (N=6, 330g  $\pm$  28 g SD, 12 weeks of age) and old (N= 5, 588g  $\pm$  32 g SD, 30 months) rats were housed in an AAALAC accredited animal quarters. All testing was performed on a custom-designed rat

dynamometer (Cutlip et al., 1997). The response of the dorsiflexor muscles to isometric and stretch-shortening contractions (SSC) were quantified *in vivo*. Young and old rats underwent exposure to 8 sets of 10 SSCs, 3 times/week, for 4.5 weeks duration. Performance was assessed by pre and post isometric testing and dynamic muscle function testing via a single SSC (Table 1). The sets of SSCs were performed at an angular velocity of 60°/s from 90° to 140° ankle angle for a total of 80 SSC (see Table 1). There was a 2 minute rest period between steps in the experimental protocol to minimize fatigue.

**Table 1.** Experimental Protocol

Step	Young (N=6)	Old (N=5)
1	Isometric Test (90 deg)	Isometric Test (90 deg)
2	1 Stretch-Shortening Contraction 70°-140°-70° ankle angle @ 500 deg/s	1 Stretch-Shortening Contraction 70°-140°-70° ankle angle @ 500 deg/s
3	8 sets of 10 intermittent Stretch-Shortening Contractions at 90°-140°-90° ankle angle @ 60 deg/s	8 sets of 10 intermittent Stretch-Shortening Contractions at 90°-140°-90° ankle angle @ 60 deg/s
4	Isometric Test (90 deg)	Isometric Test (90 deg)
5	1 Stretch-Shortening Contraction 70°-140°-70° ankle angle @ 500 deg/s	1 Stretch-Shortening Contraction 70°-140°-70° ankle angle @ 500 deg/s

The performance parameters used to evaluate the force changes were: 1) peak force (i.e, the maximum force achieved in the eccentric contraction), 2) minimum force (i.e. the force value prior to the eccentric contraction), negative work (eccentric work), and positive work (concentric work). These parameters were generated from the pre-test SSC (step 2) and the first SSC of the 8 sets (step 3) at each exposure.

## RESULTS AND DISCUSSION

The peak force (@ 500 °/s) of the young group improved over the 4.5 week exposure while the old group declined. The 60 °/s performance was lower for both groups (Fig 1). The isometric pre-stretch force increased for the young group and

decreased for the old group during the chronic exposure (Fig 2). Negative work increased for the young group and decreased for the old group (@ 500 °/s) but was lower and did not change over the exposure period for the 60 °/s performance (Fig 3). Positive work also showed the same trends as the negative work (Fig 4).

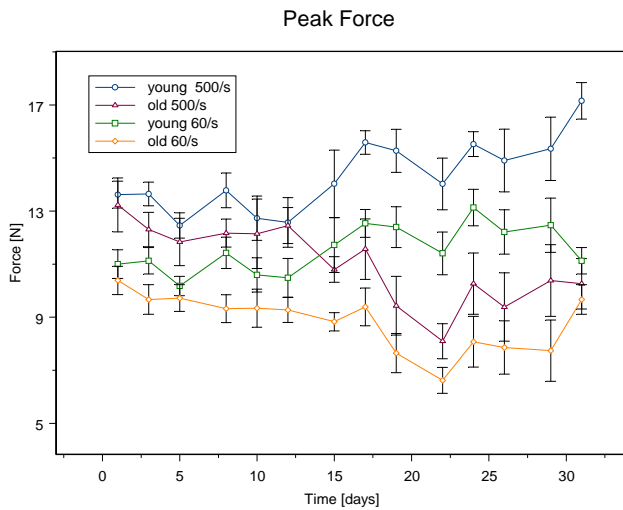


**Figure 1:** Peak Eccentric Force

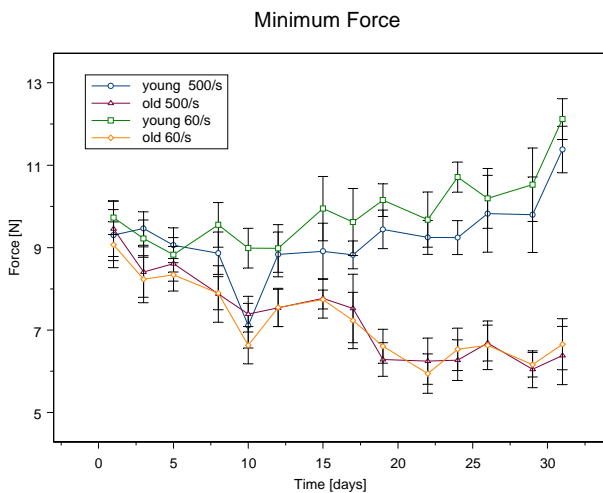


**Figure 2:** Isometric Pre-stretch force

## SUMMARY

The performance differences between age groups and during the chronic exposure period was much more magnified during higher velocity SSCs. This indicates that high velocity performance is a more sensitive measure of changes in muscle function than low velocity performance.

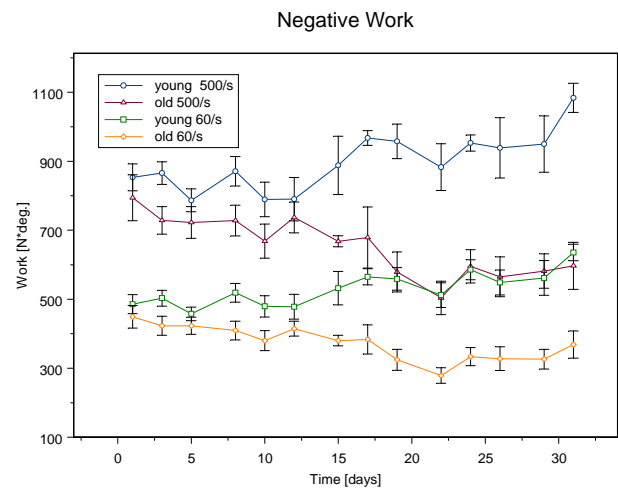


**Figure 3:** Negative Work

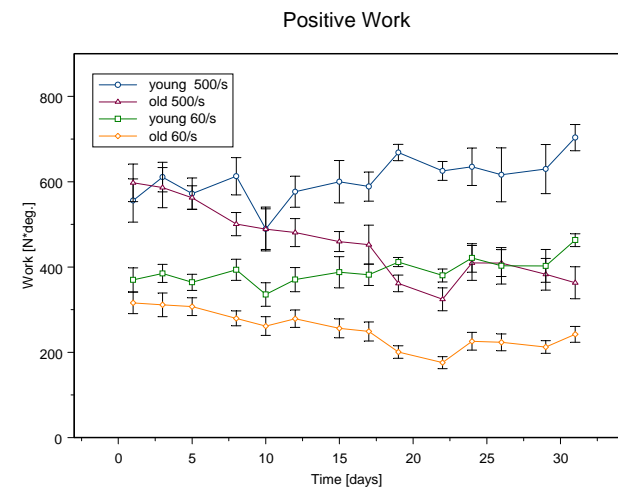


**Figure 4:** Positive Work

## DISCLAIMER

The findings and conclusions in this report are those of the authors and do not necessarily represent the views of the National Institute for Occupational Safety and Health.

## REFERENCES

- Cutlip RG et al.* (1997) Medical & Biological Engineering & Computing, 35(5):540-3.
- Evans WJ et al.* (1993) J Nutr,123(2 Suppl): 465-468.
- Komi PV.* (2000) J Biomech, 33(10):1197-206.
- Statistics BoL.* (1999) [cited; Available from: [http://stats.bls.gov/news\\_release/empsit.t12.htm](http://stats.bls.gov/news_release/empsit.t12.htm)].

# NUMERICAL ANALYSIS OF GLOTTAL DYNAMICS USING AN IMMERSED-BOUNDARY METHOD

Haoxiang Luo<sup>1</sup>, Xudong Zheng<sup>1</sup>, Rajat Mittal<sup>1</sup>, Haibo Dong<sup>1</sup>,  
Steven Bielamowicz<sup>2</sup>, Raymond Walsh<sup>3</sup>, and James Hahn<sup>4</sup>

<sup>1</sup> Department of Mechanical & Aerospace Engineering  
<sup>2</sup> Division of Otolaryngology

<sup>3</sup> Department of Anatomy & Cell Biology

<sup>4</sup> Department of Computer Science

George Washington University, Washington DC, USA

E-mail: mittal@gwu.edu Web: project.seas.gwu.edu/~fsagmae

## INTRODUCTION

A high fidelity and patient specific computer model of glottal air / vocal folds interaction is useful in helping us gain further insight into the biophysics of phonation, though much progress has been made in the past in developing models of the phonatory dynamics and investigating the function of vocal folds (e.g., Ishizaka & Flanagan, 1972; Pelorson *et al*, 1994; Alipour & Titze, 1996; Rosa *et al*, 2003). In addition, such an accurate model would have clinical applications. For example, in medialization laryngoplasty, a surgical treatment for vocal fold paresis or paralysis, surgeons have to depend on experience to determine the shape and location of the implant which is inserted into larynx to force the diseased vocal fold into a more medial position. The realistic computer model may help surgeons make decisions and therefore improve the outcome of surgeries. To guarantee model accuracy, several new features are incorporated into our approach:

1. Realistic geometry reconstructed from CT scan data of laryngeal anatomy
2. Direct numerical simulation (DNS) modeling of the glottal flow
3. Continuum model of anisotropic and non-homogeneous vocal fold tissues

At this conference, we will report our progress in developing the computer model and discuss the numerical results.

## METHODS

We employ direct numerical simulations to calculate the highly complex glottal flow during phonation including the turbulent jet at the super-glottal area. The approach can sufficiently resolve the spatial and temporal scales in the flow, and thereby improve overall fidelity, produce high-quality data, and enable us to gain deeper insight into the flow physics. The numerical method is implemented on a Cartesian grid based on the immersed boundary method (IBM). Fig. 1 shows streamlines of simulated flow through the CT data based geometric model of laryngeal airway.

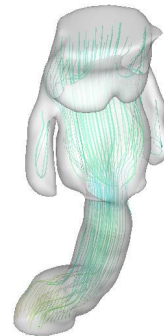


**Figure 1:** Streamline pattern at the breathing position.

Following some of the recent work in this area (e.g., Alipour, Berry, & Titze, 2000), a continuum, viscoelastic model for the vocal folds has been developed. The governing equations are solved using the finite-difference method (FDM) on a Cartesian

mesh (see Fig. 2). To deal with the complex geometry of the vocal folds, the FDM approach is combined with the immersed-boundary method that is currently used in our fluid model.

## RESULTS AND DISCUSSION

The immersed-boundary method is used to calculate the eigenmodes of linear elastic vocal folds on the Cartesian grid. Fig. 2 shows the first four vibration modes in the three-dimensional space, where the prototypical vocal folds have three material layers: cover, ligament, and body. The associated frequencies are 112 Hz, 140 Hz, 162 Hz, 171 Hz, respectively, and are approximately in the physical phonation frequency range. Note that the fourth mode represents the wavy motion on the vocal surface during phonation.

At the conference, we will also show the influence of the surgical implant on the eigenmodes.

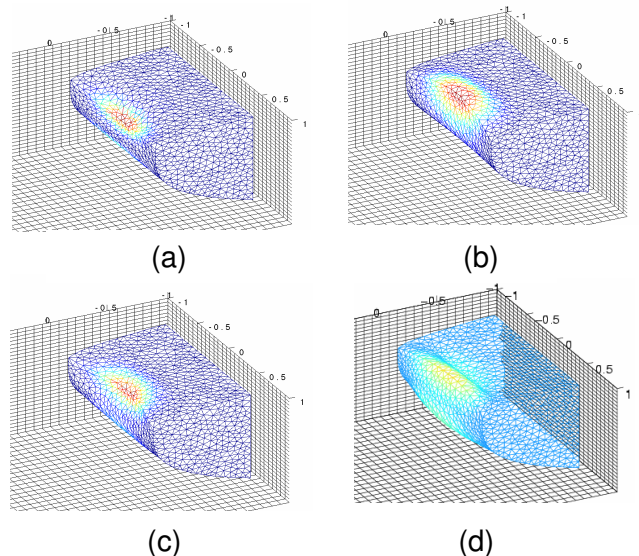


**Figure 2:** First four eigenmodes ((a) to (d)) obtained using the Cartesian grid based calculations.

The solid solver is coupled with the flow solver to compute the flow structure interaction (FSI). Fig. 3 shows a two-dimensional flow passing between two vocal fold like obstacles. The unsteady hydrodynamic force generated due to vortex shedding causes the obstacles to vibrate. Details of the nonlinear interaction, together with the vortex pattern and the structural vibration, will be discussed during the conference.

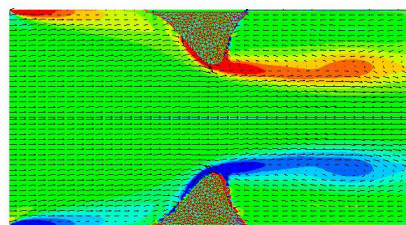


**Figure 3:** Flow field and vortex structures in a coupled flow/tissue simulation.

## REFERENCES

- Alipour, F. and Titze, I.R., (1996). *Vocal Fold Physiology: Controlling Complexity and Chaos*, 17-29
- Alipour, F., Berry, D.A., and Titze, I.R., (2000). *J. Acoust. Soc. Am.*, **14**, 442-540.
- Ishizaka, K. and Flanagan, J.L., (1972). *The Bell System Technical Journal*, **51**, 1233-1268.
- Pelorson, X., Hirschberg, A., Van Hassle, R.R., Wijnands, A.P.J., and Auregan, Y., (1994). *J. Acoust. Soc. Am.*, **96**, 3416-3431.
- Rosa, M.O., Pereira, J.C., Grellet, M., and Alwan, A., (2003). *J. Acoust. Soc. Am.*, **114**(5), 2893-2905.

## ACKNOWLEDGEMENTS

The project is supported by NIDCD grant R01 DC007125-01A1.

# METHODS FOR ANALYSIS OF DAILY WHEELCHAIR ACTIVITY DATA

Sharon Eve Sonenblum  
Georgia Institute of Technology, Atlanta, GA, USA  
E-mail: sharoneve@gatech.edu

## INTRODUCTION

Recent advances in technology, including accessibility of wireless sensors, improved memory size, low power consumption and longer battery life have resulted in the increased portability of activity monitors. Numerous commercial and custom products including pedometers, wheelchair odometers and accelerometer-based activity monitors allow research to take place beyond the laboratory. It is possible to monitor a subject in their home environment for weeks at a time. Although many medical interventions are meant to improve mobility and physical activity, improved gait in the laboratory does not necessarily translate to improved mobility at home. Therefore, the characterization of daily mobility is very important and raises many new questions including: How much data should be collected? How should it be analyzed? While common measures such as mean and standard deviation successfully describe the magnitude of the data, the temporal spread of activity may also be important. For example, 30-minute bouts of moderate to vigorous physical activity are recommended for health benefits. Alternatively, short bouts of movement may indicate environmental interactions and stationary activities. In wheelchair activity, long durations without activity may be detrimental to tissue loading and pressure ulcer outcomes.

Many methods for describing the temporal sequencing of data are described in the literature. Detrended fluctuation analyses, approximate entropy and power spectral analyses are a few examples that have been applied to gait. This discussion will be limited to the use of approximate entropy

(ApEn), a measure of predictability or regularity described by Pincus in 1991. Specifically, ApEn “measures the logarithmic probability that a series of data points a certain distance apart will exhibit similar relative characteristics on the next incremental comparison” (Stergiou 2004).

This paper addresses questions that arise when applying ApEn to daily activity data such as: What is the appropriate epoch size (i.e., time over which activity events are summed) for analyzing the data? Are there inherent properties of mobility that effect the optimal epoch size? Is ApEn too sensitive to the epoch size to use for analysis of activity data? Two conflicting hypotheses of the influence of epoch size on ApEn are: 1) With *increasing* epoch size, there is more averaging of data so the ApEn should decrease. 2) With *decreasing* epoch size, there is an increase in the number of zero-count epochs (epochs containing no movement), which are inherently more predictable so the ApEn should decrease.

## METHODS

We recruited seven upright power wheelchair users who had just been prescribed a new, tilt-in-space (TIS) wheelchair. Subjects’ wheelchairs (first the upright and then the TIS 3 months after its delivery) were instrumented with an occupancy monitor, position sensor, and wheel odometer for 2 weeks. The total number of wheel counts was recorded every two seconds on a custom data logger.

ApEn(m,r) parameters were selected according to Stergiou 2004 as  $m=2$  (observations to compare) and tolerance  $r =$

0.2\*stdev. This analysis considered the ApEn over the most active 8 hours per day for each subject. ApEn was calculated for the raw 2 second epoch, as well as for down-sampled epoch sizes of 30 sec, 1, 2, 3, 4 and 5 minutes. ApEn is meant to be used as a comparative measure (e.g. pre- and post-intervention). First, day-to-day differences were used to consider the effect of epoch size on ApEn. Then, ApEn was calculated with 1 minute epochs for the 2 subjects who have completed both phases of this study to compare ApEn across different wheelchairs.

**RESULTS AND DISCUSSION**

Subject 1’s data (Fig 1, Left) illustrated a typical response of ApEn to epoch size over most subjects. The graphs suggest that zero-count epochs dominated the ApEn analysis. Analysis at all epoch sizes should produce approximately the same results for day-to-day comparisons. A few exceptions to this are also presented in Figure 1. ApEn was robust across different phases of data collection for the same subject (Table 1).

To further understand the influence of zero-count epochs, ApEn was regressed with percent zero-count epochs at each epoch size. With increasing epochs from 30s to 300s, the slopes decreased from 0.0174 to 0.00506 while the R<sup>2</sup> decreased from 0.80 to 0.31. Thus, the influence of percent zero-counts decreased with increasing epoch size.

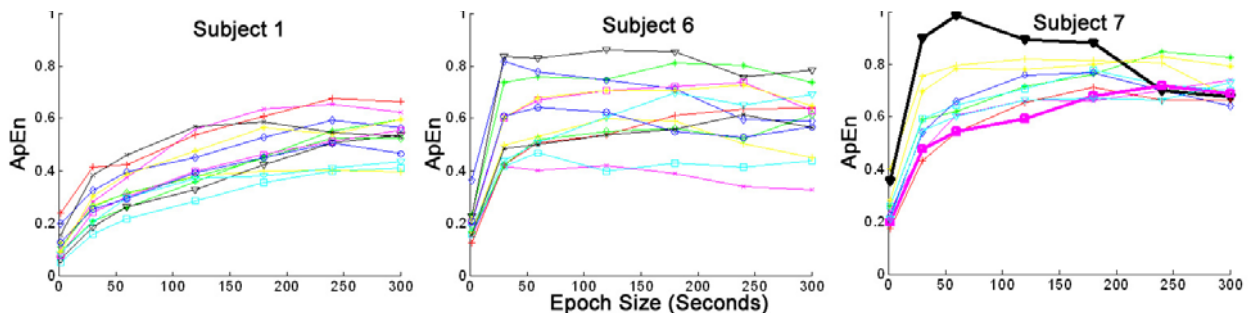


**Figure 1:** ApEn (plotted over multiple days) typically increases with epoch size (Subject 1, Left). At least one subject (6, Center), shows no increase in ApEn with epochs larger than 2s. For Subject 7 (Right), comparison of days 7 (black) and 10 (magenta) lead to different conclusions depending on epoch size.

**Table 1:** ApEn values differed between Subjects 2 and 3. Despite high day-to-day variability, ApEn was robust to two weeks in different wheelchairs and seasons.

	Subject 2		Subject 3	
	Mean	Stdev	Mean	Stdev
Pre	0.619	0.222	0.364	0.083
Post	0.647	0.183	0.365	0.105

**SUMMARY/CONCLUSIONS**

In general, ApEn was sensitive to epoch size but comparative relationships tended to be consistent across epoch sizes. It is open for discussion whether ApEn is too sensitive to use for analysis of daily activity data given the few conflicting cases. It is likely that the differences may be acceptable when taken in context of the research question. For example, large epochs might be needed to determine if wheelchair activity is sufficiently spread over the day to prevent excessive tissue loading. On the other hand, stepping activity may require smaller epochs to distinguish between simple repeated paths and more complex paths consisting of many direction and speed changes.

**REFERENCES**

Pincus, S.M. (1991) *Proc natl Acad Sci USA*, **88**(6) 2297-301.  
 Stergiou, N. ed. (2004) *Innovative Analyses of Human Movement*. Human Kinetics.

**ACKNOWLEDGEMENTS**

Funding: NIDRR RERC on Wheeled Mobility and NSF GFRP. Jim Cavanaugh, Helen Heonig, and William Del'Aune for their discussion and insight.

# SEVERITY OF KNEE OSTEOARTHRITIS AND ITS EFFECT ON GAIT MECHANICS IN WALKING

Ershela L. Sims<sup>1</sup>, Mary Beth Nebel<sup>1,2</sup>, Francis J. Keefe<sup>1</sup>, Jennifer Pells<sup>1</sup>, Jessica Tischner<sup>1</sup>, Virginia Kraus<sup>1</sup>, Farshid Guilak<sup>1</sup>, and Daniel O. Schmitt<sup>1</sup>

<sup>1</sup>Duke University, Durham, NC, USA

<sup>2</sup>University of NC at Chapel Hill, Chapel Hill, NC, USA

E-mail: [ershela.sims@duke.edu](mailto:ershela.sims@duke.edu)

Web: <http://klab.surgery.duke.edu>

## INTRODUCTION

Osteoarthritis (OA) of the knee, affecting 10% of adults ages 55 and over (Baliunas et al, 2002), is characterized by pain and lack of mobility. The etiology of knee OA is not entirely clear, however, previous research has determined a number of risk factors for the disease. These include obesity, gender, age, repeated trauma to joint tissues, and lower extremity injuries (Lohmander et al, 2004). Consequently, there is a great need to better understand how these factors may influence the severity or progression of the disease. Most often, a combination of these risk factors is present in persons with OA, which leads researchers to the question— which risk factor is most responsible for altered gait mechanics? This study addressed that question through the examination of the effects of the severity of OA on gait mechanics in a large sample of obese patients with knee osteoarthritis of varying radiographic degree.

## METHODS

The study population consisted of 137 subjects (35 men, 102 women) with radiographic OA in at least one limb. All subjects were obese (BMI ranged from 25-42; Mean= 34.12±4.36); morbidly obese were excluded from the study. Three-dimensional kinematic data was collected at 60Hz using a motion analysis system

(Motion Analysis Inc, Santa Rosa, CA).

Subjects performed three practice trials and five walking trials along a 30m walkway at three self-selected speeds (normal, fast and intermediate). Ground reaction force data was collected using two AMTI force plates. Data were processed using OrthoTrak 6.29 (Motion Analysis Inc, Santa Rosa CA). OA severity levels were established through the Kellgren-Lawrence radiographic grading system: mild (K/L =1), moderate (K/L= 2 or 3), and severe (K/L = 4); limbs with K/L<1 were excluded from analyses. Correlation between level of OA and the gait variables was evaluated using Pearson's correlation coefficient (r). A 1x3 ANOVA was used to compare means for knee range of motion (KROM), as well as means for peak vertical force (PVF), for the different levels of OA at each speed ( $\alpha=0.05$ ). Post-hoc testing (LSD) was performed when necessary.

## RESULTS AND DISCUSSION

There was an inverse correlation between K/L grade and KROM at normal ( $r= -.27$ ,  $p<.05$ ) and fast speeds ( $r=-.32$ ,  $p=.01$ ) for the left limb. An inverse correlation also existed between K/L grade and KROM in the right limb at the normal speed. Differences in KROM and PVF existed at all three speeds. There was a significant difference in KROM between subjects with mild and severe OA in their left limb at both normal and fast speeds (Figure 1).

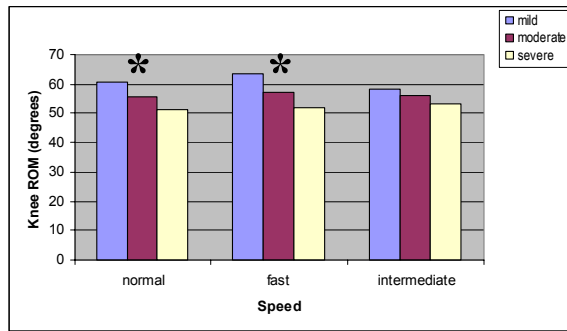


**Figure 1:** Knee ROM by level of OA at three different walking speeds. A significant difference between mild and severe OA is denoted by an \*.

None of the spatiotemporal variables showed a strong correlation with K-L grade. However a significant correlation between K-L grade and support time was displayed at fast speeds ( $r=.282$ ,  $p=.05$ ). Small correlations between K-L grade and PVF at fast speeds also existed. Average knee ROM was consistent with previous reported values in persons with OA; it was also smaller than that of persons without OA (Baliunas et al, 2002; Messier et al, 2005).

## SUMMARY/CONCLUSIONS

We hypothesized that certain biomechanical gait parameters would vary with severity of OA. Our preliminary study indicates that variation in gait could not be fully explained by K/L grade; although, when K/L grade was grouped by severity, significant differences did exist. Still, the significant associations between severity of OA and biomechanical gait parameters only account for about 10% of the variance. Therefore, other critical factors, such as level of pain or psychosocial variables, found to be important in understanding pain and disability in persons with OA may be more strongly correlated with the altered gait mechanics associated with the disease. Further research should be done in order to gain a better understanding of what factors

contribute to the majority of variation in gait associated with OA.

## REFERENCES

- Baliunas, A, et al. (2002) *Osteoarthritis and Cartilage*, **10**, 573-579.  
 Lohmander, L. S. et al (2004). *Arthritis and Rheumatism*, **50**, 3145-3152.  
 Messier, S., et al. (2005) *Arch. Phys. Med Rehabilitation*, **86**, 703-709.

## ACKNOWLEDGEMENTS

This study was supported by NIH grant AR50245.

# AN INVERTED PENDULUM MODEL FOR THE SPINE TO STUDY MUSCLE RECRUITMENT PATTERNS ON SUDDEN PERTUBATION

Anand Navalgund, Dr. Deborah G. Heiss, Dr. Eric R. Westervelt, Dr. Necip Berme

Ohio State University, Columbus, Oh, USA  
E-mail: navalgund.1@osu.edu

## INTRODUCTION

Trunk equilibrium control involves anticipatory (feedforward or open-loop) or reactive (feedback or closed-loop) or both for adjustments in muscle forces to trunk stability disturbances. Recent studies (Hodges, 2001, Hides et al., 1994) have shown the importance of deep muscles in local stability. Current optimization methods (Hughes et al., 1994, Cholewicki et al., 1995) have been open loop and have not accounted for reflexive behavior, a key to spinal stability. These methods have not been able to accurately predict muscle activity in the deep (multifidus) and the intermediate (erector spinae) muscles.

The goal of this study was to provide an anatomically and physiologically realistic model. The spine is modeled as an inverted pendulum. Proprioceptive feedback from the muscle spindle (length and velocity) and the Golgi tendon organ (force) is included in the muscle model. Muscles have different time delays present in their activation due to their location with respect to the spine. This was accounted for in the model. Results demonstrated that the optimization methods, which were closed-loop and included reflexive feedback performed better by predicting activity in the deep (multifidus) and the intermediate (erector spinae) muscles.

## METHODS

Four healthy female subjects (mean age 26 yrs, height 65 inches and weight 124 pounds) participated in the study. Subjects stood upright in a custom built frame that restricted pelvic motion. A firm plastic thoracic orthosis was applied to the subject. The orthosis was attached to the pendulum on the anterior aspect at approximately the T4 level via a Kevlar cable that was connected to the pendulum mounted on the wall. The pendulum swing provided an impulse force of 120 N. Load cell and motion analysis data from Optotrak markers were recorded. EMG was recorded from the internal and external obliques, erector spinae and the lumbar multifidus at L5/S1.

The optimization was performed using the `fmincon` function in MATLAB. Two cost functions were tested: the sum of cubed stress and square of muscle forces at L4-L5. Muscle properties were based on the Winters model (Winters, 1995) with muscle activation- to-force build up represented by a first order process with an activation time constant  $\zeta_a = 55$  ms. The muscle spindle was modeled by a transfer function that represents the Ia transduction properties with a gain and the conduction time delay  $T_d$ . Similarly Golgi tendon organs (GTO) was represented by a Ib transfer function, gain and conduction time delay.

## RESULTS

EMG results show that the lumbar multifidus responds faster (latency was 10-15 ms) than other paraspinal muscles (latency was 18-50 ms) in response to flexion impulse perturbations. Figure 1 shows a typical EMG response of a healthy subject. Simulation results demonstrated that, in the presence of reflex feedback loops, an early recruitment of the multifidus takes place. Delayed response time in muscles leads to instability in the model. Both the cost functions displayed a similar trend with the sum of cubed stress performing better in terms of the magnitude of deep muscle recruitment.

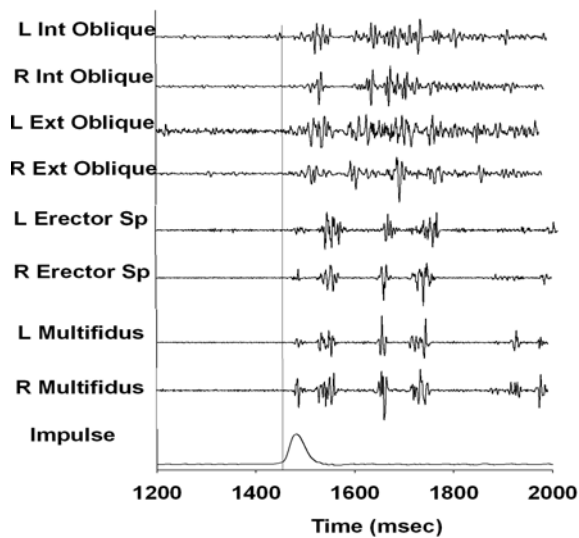


**Fig 1.** EMG response with a flexion impulse perturbation applied to the trunk. Vertical line indicates the onset of the impulse.

## CONCLUSIONS/DISCUSSION

A neuromuscular control model with a closed loop optimization method closely simulates the muscle responses to flexion perturbations recorded in healthy controls. Reflexes in the deep muscles play an important role in providing stability to the

trunk. Optimizing the muscle forces in the presence of reflex loops provides more accurate results by simulating the reflexes and recruiting all muscle groups including the deep and the intermediate muscles. Time delays affect the patterns of muscle group recruitment with longer time delays destabilizing the system. Hence, future optimization methods should include proprioceptive feedback in the muscle models to account for reflexes and their contribution to stability.

## REFERENCES

- Cholewicki, J., McGill, S. M., Norman, R. W., (1995). Comparison of muscle forces and joint load from an optimization and EMG assisted lumbar spine model: towards development of a hybrid approach. *Journal of biomechanics* **28**, 321-331.
- Hides, J. A., Stokes, M. J., Saide, M., Jull, G. A., Cooper, D. H., (1994). Evidence of lumbar multifidus muscle wasting ipsilateral to symptoms in patients with acute/subacute low back pain. *Spine* **19**, 165-172.
- Hodges, P. W., (2001). Changes in motor planning of feedforward postural responses of the trunk muscles in low back pain. *Experimental brain research. Experimentelle Hirnforschung. Experimentation cerebrale* **141**, 261-266.
- Hughes, R. E., Chaffin, D. B., Lavender, S. A., Andersson, G. B., (1994). Evaluation of muscle force prediction models of the lumbar trunk using surface electromyography. *Journal of orthopaedic research : official publication of the Orthopaedic Research Society* **12**, 689-698.
- Winters, J. M., (1995). An improved muscle-reflex actuator for use in large-scale neuro-musculoskeletal models. *Annals of biomedical engineering* **23**, 359-374.

# **DEVELOPMENT OF AN INFLATABLE HIP PROTECTION SYSTEM: DESIGN FOR HIP FRACTURE PREVENTION AND INCREASED COMPLIANCE**

Stefan Duma, PhD, John Caine, David Coleman, Melanie Langmead, Kachun Leung,  
Tracy Ng, Jeff Weatherholtz, Matt Whitehair, and Kaitlin Wilson

Virginia Tech – Wake Forest, Center for Injury Biomechanics, Blacksburg, VA, USA  
E-mail: [duma@vt.edu](mailto:duma@vt.edu) Web: <http://www.cib.vt.edu/>

## **INTRODUCTION**

Hip fractures are debilitating and the leading cause of injury deaths among persons 65 and older. Over 350,000 hip fractures occur annually in the United States, totaling \$18 billion in healthcare costs (Cummings, 1990). Developing an effective means of protection against hip fracture could prevent premature death, increase livelihood among the elderly, and reduce healthcare costs.

Most hip fractures occur due to direct trauma to the hip from falling. The use of energy shunting and/or absorbing materials to divert impact forces away from the bone has been shown to prevent the occurrence of hip fractures. Although studies have proven that the use of external hip protector pads have reduced the incidence of hip fractures by nearly 50%, non-compliance has been an issue with compliance rates of 24% (Lauritzen, 1993). In addition to the issue of non-compliance, the current commercially available hip protectors are ineffective in reducing the impact forces below the hip fracture threshold of 2100 N (Lotz, 1990). The purpose of this study to develop a hip protection system which targets the issues of force attenuation and non-compliance.

## **METHODS**

Two new designs were modeled after an inflatable airbag and utilized an energy shunting method to dissipate the fall energy away from the hip and into the surrounding soft tissue. Once a fall is detected, the hip bags will rapidly inflate with carbon dioxide gas. The first design, Prototype A, is a

garment mounted hip protection system. The hip bag is designed to be concealed within pockets which are sewn onto the user's garments and pre-positioned over the greater trochanter. The second design, Prototype B, consists of an enclosure containing a hip bag that can be clipped onto a belt. When a fall is detected, the enclosure opens and the hip bag unfolds and inflates, to protect the greater trochanter.

A vertical drop tower was used to simulate a fall in which the hip was directly impacted. Since 80% of hip fracture patients are women, it was desirable to recreate the typical fall conditions for a female. The drop tower was constructed from an impactor assembly traveling on four reciprocating roller bearings that were attached to two linear shafts. A Hybrid III dummy hip was mounted to the impactor assembly with a load cell mounted inside. The load cell was mounted on a simulated greater trochanter, so that the measured load accurately represented the force on the hip. A drop height of 0.35 m was used with an effective mass of 20 kg. This is a similar design to that presented by Robinovitch (1995).

Baseline impact tests were performed without any protective measures in place. The new hip protector designs and commercially available hip protectors were compared to the baseline tests. The peak impact forces, or greater trochanter forces, measured with the drop tower for each test condition are compared.

## RESULTS AND DISCUSSION

A plot of the measured forces on the hip from the drop tests is shown in Figure 1. A peak impact force of 8000 N was measured for an unprotected hip (no pad). This peak impact force falls within the range of average peak impact forces during a fall (Robinovitch, 1995). Although the commercial hip pads were effective in reducing the peak impact force, they were unable to reduce the force below the fracture threshold of 2100 N. In comparison, both of the new hip pad designs were able to reduce the impact force well below the fracture threshold. The peak impact forces for the garment mounted and belt mounted hip protection system were 1190 N and 1250 N, respectively. This results in a force reduction of approximately 85% for the garment mounted device and 84% for belt mounted device.

## CONCLUSIONS

The proposed hip protector designs were effective in reducing the peak impact forces below the fracture threshold. The hip bags utilize an energy shunting method to protect the hip, which has been shown to be more effective than energy absorbing hip protectors (Robinovitch, 1995). With further development, the new hip protection devices proposed in this study have the potential to significantly reduce the number of hip fractures that occur annually in the United States.

## REFERENCES

- Cummings, S.R., Rubin, S.M., Black D. (1990). *Clin Orthop Relat Res.* **252**,163-6.
- Lauritzen, J.B., Petersen, M.M., Lund, B. (1996). *Bone.* **18(1)**, 77S-86S.
- Lotz, J.C., Hayes, W.C. (1990). *J Bone Joint Surg.* **72(5)**, 689-700.
- Robinovitch, S.N., Hayes, W.C., McMahon, T.A. (1995). *J Biomech Eng.* **117**, 409-13.

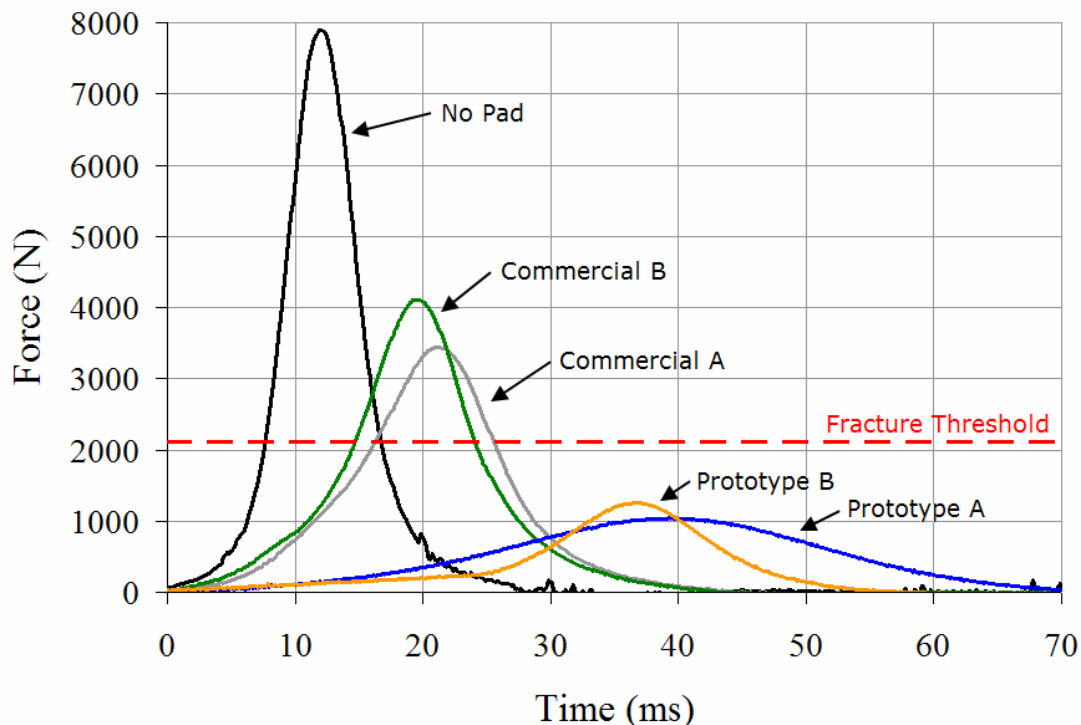


**Figure 1:** Greater trochanter force versus time curves for all hip pad tests from experimental falls. Note that impulse values are different given increased load sharing with the prototype pads.

# REDUCED INTERJOINT COORDINATION WITH AGE AND GAIT TASK DIFFICULTY

Paul DeVita, Allison Gruber, Patrick Rider, Joe Helseth & Tibor Hortobagyi

East Carolina University, Greenville, NC, USA; Email: [DeVitaP@mail.ecu.edu](mailto:DeVitaP@mail.ecu.edu)

## INTRODUCTION

While all muscles lose strength through the lifespan, distal vs. proximal muscles have greater losses (3). Physiological and neural changes underlie this pattern of force loss with age. Old vs. young muscle has a greater proportion of Type I vs. Type II muscle fibers and this reorganization is more pronounced in distal vs. proximal muscles (2,5). Motor neuron apoptosis with age is followed by collateral sprouting in surviving neurons to re-innervate muscle fibers. Sprouting capacity however is inversely related to axon length such that more distal muscles have reduced re-innervation capability (6). These adaptations provide a neurophysiological basis for our previous observation that old vs. young adults generate more torque and power with hip extensors and less with knee and ankle extensors when walking at the same speed (1). It is also well established that hip and knee joint torques are strongly inversely related in young adult walking (7). We ask therefore, is this inverse relationship retained in old adults despite the asymmetrical age-related plasticity in neuromuscular properties? The purpose of this study was to compare the relationships between hip and knee joint torques in young and old adults during three walking conditions.

## METHODS

Ground forces and sagittal plane kinematics were obtained in level walking and in ascent and descent walking on a 10° incline from 20 young and 25 old adults (mean ages of 21

& 75 years). All subjects were healthy and were able to perform all tasks without difficulty. Each subject performed multiple trials per task. Inverse dynamics were used to compute lower extremity joint torques. The relationships among average stance phase hip and knee joint torques in each age group and walking task were assessed with Pearson product moment correlations over all trials. These were tested for significant age differences with z-transforms ( $p < .05$ ).

## RESULTS AND DISCUSSION

Young and old adults had strong inverse relationships between average stance phase hip and knee torques during level walking. The correlation coefficients were  $r = -0.76$  and  $r = -0.80$  for young and old adults which were statistically identical. These values agree with results for young adults in level walking (7). Young adults also had similarly strong inverse relationships for ascent ( $r = -0.73$ ) and descent ( $r = -0.70$ ) walking. In contrast, old adults had significantly lower inverse relationships for these gait tasks (both  $r = -0.41$ ,  $p < .05$ ). More revealing however were the amounts of explained variance between hip and knee torques. Young and old adults had 56% and 63% explained variance in level walking and young adults also had 54% and 49% explained variance in ascent and descent walking. Old adults however, had only 17% explained variance between hip and knee torques in both ascent and descent walking. In total, these results indicate that healthy old adults coordinate their hip and knee torques well in level walking but they have reduced joint torque coordination and

presumably muscle force production in the more difficult tasks of walking up and down 10° inclines. This reduced coordination may be one behavioral outcome of the asymmetrical age related changes in neuromuscular physiology. We also speculate that this reduced coordination with age and gait task difficulty may be related to the increased metabolic cost of locomotion and the increased gait instability in old vs. young adults (4).

**REFERENCES**

1. DeVita et al, (2000) *J Appl Physiol* 88: 1804-1811.

2. Jennekens et al, (1971) *J Neurol Sci* 14: 259-276.  
 3. Kirkeby et al, (2000) *Histol Histopathol* 15: 61-71.  
 4. Malatesta et al, (2003) *J Appl Physiol* 95 :2248-225.  
 5. Monemi et al, (1999) *Acta Physiol Scand* 167: 339-345.  
 6. Pestronk et al, (1980) *Exp Neurol* 70:65-82.  
 7. Winter (1989) *J Mot Behav* 21 : 337-355.

**ACKNOWLEDGEMENTS:** NIH R01 AG024161.

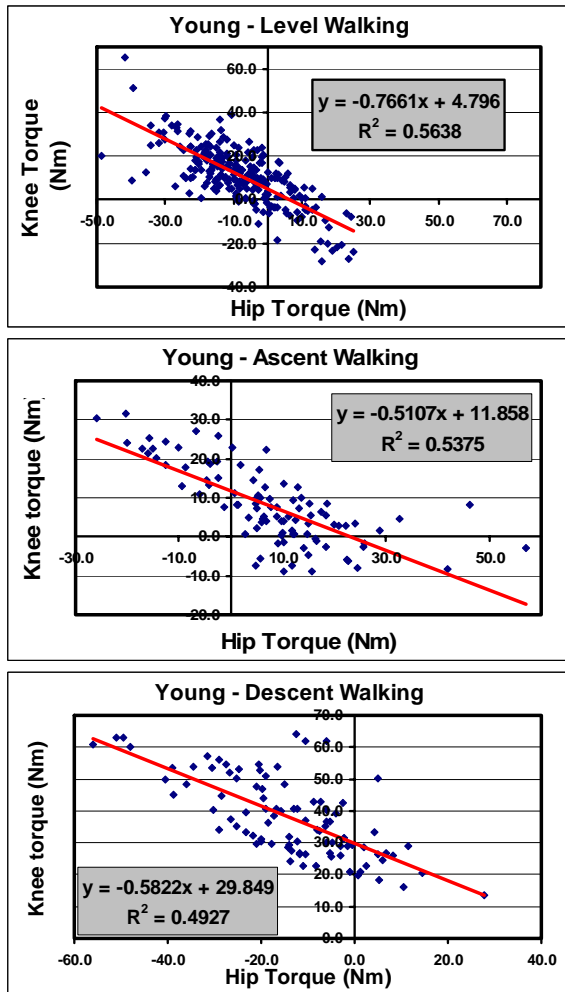


Fig 1. Relationships between hip and knee torques in young adults.

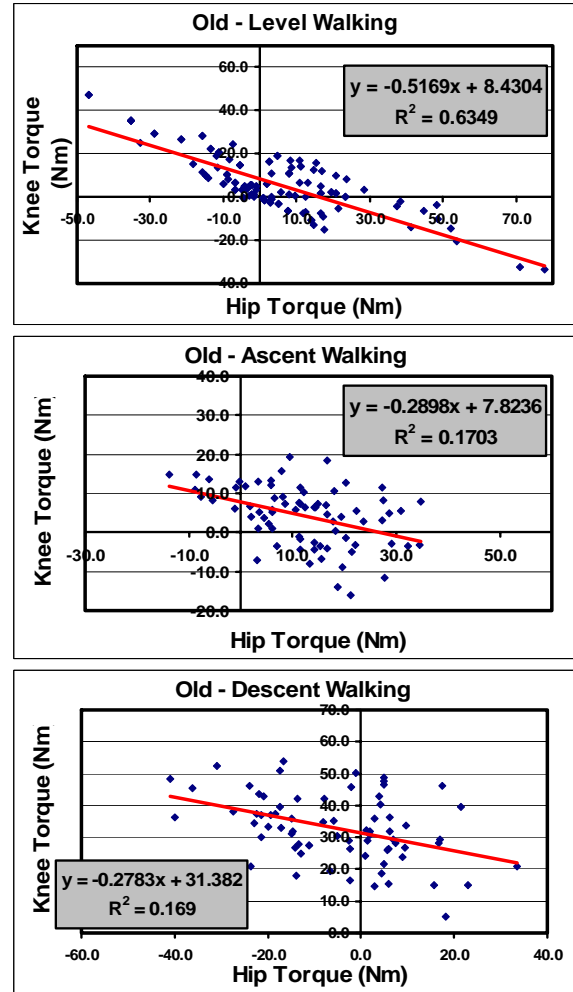


Fig 2. Relationships between hip and knee torques in old adults.

# THE ROLE OF INTERJOINT FEEDBACK IN THE CONTROL OF MULTI-LINK SYSTEMS

Nathan Bunderson and Thomas Burkholder  
Georgia Institute of Technology, Atlanta GA, USA  
E-mail: [nbunderson@gatech.edu](mailto:nbunderson@gatech.edu)

## INTRODUCTION

Non-conservative feedback is asymmetric feedback between muscles that cross different joints, for example, when feedback from a knee flexor to a hip extensor is not equal to the feedback from the hip extensor to the knee flexor. Previous work has established that pathways for non-conservative feedback exist in biological multi-link systems (Nichols, 1989) and the effects of this feedback are measurable in the net behavior of these systems (Mussa-Ivaldi et al., 1985). However, a satisfactory explanation for this feedback has not been put forth, and it has even been argued that such feedback would be detrimental to control of the system (Hogan, 1985). It has been suggested that coordination, in addition to stability, may play an important role in motor tasks such as posture, and that coordination of a multi-link system may require non-conservative feedback (Nichols et al., 2002). In addition, endpoint control tasks which are limb configuration dependent may require integrative non-conservative feedback.

**Our hypothesis is that non-conservative length and velocity feedback coordinate joint mechanics and contribute to endpoint control.** It was found that non-conservative feedback improved endpoint rigidity by 30% over a conservative controller in a kinematically redundant model.

## METHODS

The model is constructed of three identical segments connected by revolute joints with a control torque applied at each joint. The magnitude of the control torque is determined by the angle and velocity of each joint,

$$\bar{T} = -\mathbf{R}(\bar{\theta} - \bar{\theta}_0) - \mathbf{B}\dot{\bar{\theta}}.$$

Control torques are determined using the linear quadratic regulator (LQR) algorithm for two cases: joint control (J) which minimizes the angular displacement of individual joints, and endpoint control (E) which minimizes the displacement of the endpoint. To evaluate the role of interjoint feedback, nonlinear regression is used to find approximations to the LQR solution (A) under the constraints of symmetric (S) and diagonal (D) control matrices. The diagonal control matrix models a system with no interjoint feedback, the symmetric control matrix models a system with only conservative interjoint feedback and the unconstrained control matrix (A) allows non-conservative interjoint feedback.

Resulting system performance was quantified by displacement of the endpoint in response to an applied force.

## RESULTS

The unconstrained optimal joint controller (JA) is identical to the symmetric control structure (JS), suggesting that asymmetric heterogenic feedback may not be important to a joint control strategy.

The limb responses to force perturbations applied to the model are shown in Figure 1. The ED and ES models display kinematic responses (Fig. 1B) to the force perturbations similar to those of the joint models (Fig. 1A), while the EA model has a substantially different response (Fig. 1B). The magnitude of the endpoint displacement of the EA model is 42% lower than both the ED and ES models.

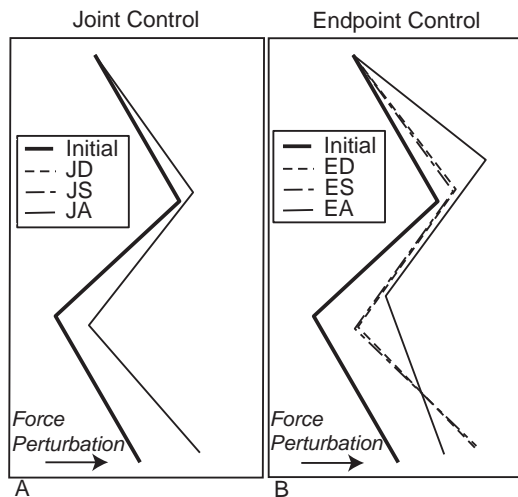


**Figure 1:** The configuration of the model before perturbation (gray dashed) and at steady-state after a step force perturbation to the right ( $0^\circ$ ) for optimal control models JD/ED (gray solid), JS/ES (black dashed), and JA/EA (black solid). The effect of non-conservative feedback was zero for the joint displacement models (A), and substantial for the endpoint displacement models (B).

The magnitude of endpoint displacement is plotted as a function of perturbation direction for ED, ES, and EA models in Figure 2. Controller EA decreases endpoint displacement (mean: 30% across directions over ES) in all directions except for a small region along the direction of the limb axis.

## DISCUSSION

In order to achieve the reduced endpoint displacement, the EA model adopts a

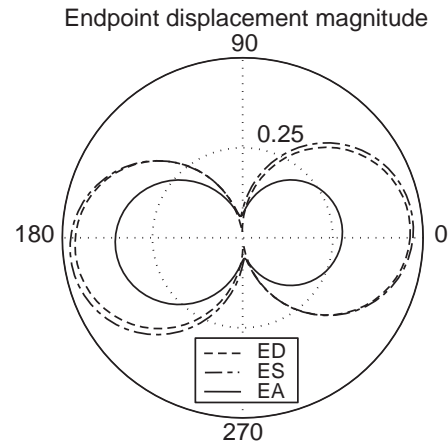


**Figure 2:** Endpoint displacement magnitudes following force perturbations in all directions for the endpoint models.

completely different coordination strategy than is possible with ED or ES; the middle joint flexes and the distal joint extends in response to the perturbation, allowing greater yield at the proximal joint and an overall decrease in endpoint displacement. The non-conservative feedback in EA, which can only result from neural mechanisms, allows the system to achieve exceptional endpoint stiffness, suggesting that non-conservative feedback may contribute to rigid endpoint posture in a kinematically redundant multi-link system.

## ACKNOWLEDGEMENTS

Dr. Lena Ting (Emory University, Georgia Institute of Technology)  
NIH Grant HD46922

## REFERENCES

- Mussa-Ivaldi, F.A., Hogan, N., & Bizzi, E. (1985). *J Neurosci.*, **5**:2732-2743.
- Nichols, T.R. (1989). *J Physiol. (London)*, **410**:463-477.
- Nichols, T.R. et al. (2002). *Progress in Motor Control-II: Structure-Function Relationships in Voluntary Movements*. Champaign: Human Kinetics, pp.179-193.
- Hogan, N. (1985). *Biol Cybern.*, **52**:315-331.

# ANKLE JOINT MOMENT DURING WALKING AFTER SELF-REINNTERVATION OF SELECTED ANKLE EXTENSORS IN THE CAT

Boris I. Prilutsky, Huub Maas and Robert J. Gregor

Georgia Institute of Technology, Atlanta, GA, USA

E-mail: boris.prilutsky@ap.gatech.edu

## INTRODUCTION

Self-reinnervation of skeletal muscles in animals (surgically cutting and reattaching the muscle nerve) has been used as a model of peripheral nerve injury (English 2005) and as a tool for removing length-dependent feedback from selected muscles (Cope et al., 1994; Abelew et al., 2000). Little is known about the effects of self-reinnervation on the gait kinetics and the mechanisms of motor compensation/adaptation to nerve injury. The aim of this study was to quantify ankle joint moments during walking after self-reinnervation of selected ankle extensors.

## METHODS

After 7 cats (2.8–4.0 kg) were trained to walk on a walkway, EMG fine wire electrodes were implanted in 4 cats under sterile conditions while the cats were deeply anesthetized. The wires were passed subcutaneously from a head-mounted multipin connector and implanted chronically in the soleus (SO), lateral (LG) and medial gastrocnemius (MG) and plantaris (PL). Following recovery, the cats walked on a walkway and were video-filmed (120 Hz; Vicon, UK), the ground reaction forces were recorded (360 Hz; Bertec, USA) and EMG signals were sampled at 3000 Hz. The recorded kinematics and ground reaction forces were used to compute joint moments (Gregor et al., 2006). A self-reinnervation procedure was performed in 7 cats under sterile conditions and deep anesthesia (In the 4 cats with implanted EMG electrodes it was performed in the same hindlimb one month after the first surgery.) The procedure consisted of exposing the tibial nerve and its

branches and then cutting and immediately reattaching (using 10-0 suture or fibrin glue) the individual nerve branches to MG and LG or to SO-LG. The second series of locomotion experiments started typically within one week after self-reinnervation and were repeated weekly (4 cats) or monthly (3 cats) for 3 to 11 months. Only walking trials with stance duration of 400 ms to 650 ms were analyzed to reduce effects of walking speed. Ankle joint angles and moments were expressed as a function of the normalized stance and swing times and were averaged within and across all cats. Peak joint moment and its relative time of occurrence were determined for each trial and subjected to one-factor repeated measures ANOVA to determine the effect of time after self-reinnervation on these variables.

## RESULTS AND DISCUSSION

Self-reinnervated muscles did not typically show substantial activity within the first month after the procedure. The activity recovered by the third month (Fig. 1). The patterns of the ankle joint moment and joint angle significantly diverged from the control patterns within the first month and almost completely recovered two months later (Figs. 2 and 3).

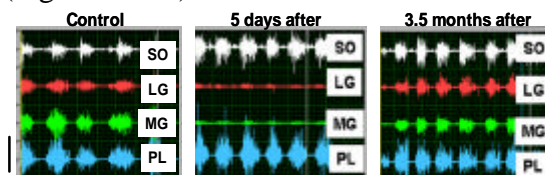


**Figure 1:** Typical EMG activity of self-reinnervated (LG and MG) and intact (SO and PL) muscles before (Control) and after (5 days and 3.5 months) self-reinnervation.

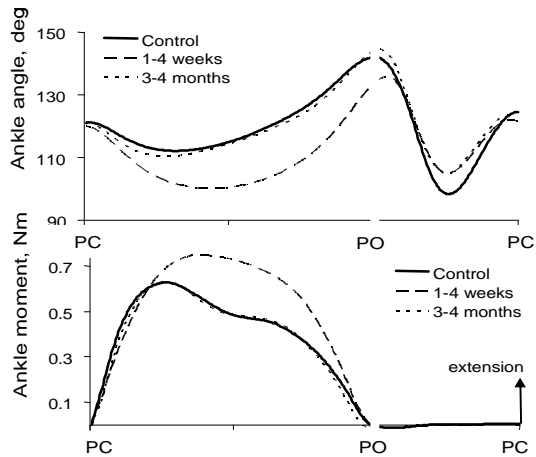


**Figure 2:** Mean patterns of joint angle and joint moment at the ankle during a walking cycle before and after self-reinnervation.

Although there was no significant decrease in peak ankle moment, the time of its appearance in stance increased significantly shortly after self-reinnervation (Fig. 3).

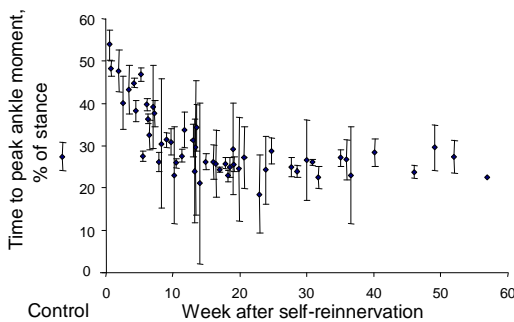


**Figure 3:** Means ( $\pm$ SD) of the normalized time to peak of the ankle joint moment before (Control) and after self-reinnervation.

Preservation of peak ankle moment and even an increase in the extensor moment magnitude in mid-stance within the first month post-injury (Fig. 2) was unexpected given little or no activity in self-reinnervated muscles (Fig. 1) which might have led to an enhanced ankle yield. These results may be partially explained by an increased contribution of passive joint structures to the ankle moment as a result of the greater ankle yield and reaching the limits of ankle joint range of motion in mid-stance. The limits of ankle dorsiflexion at the hindlimb

configuration corresponding to mid-stance shortly after injury were tested in 4 sedated cats and found consistent with this explanation. In addition, the peak of low-pass filtered SO EMG did not correlate with the peak ankle extension moment within the first month post-injury, whereas this correlation was high and significant for trials before and 3-4 months after injury (Fig. 4).

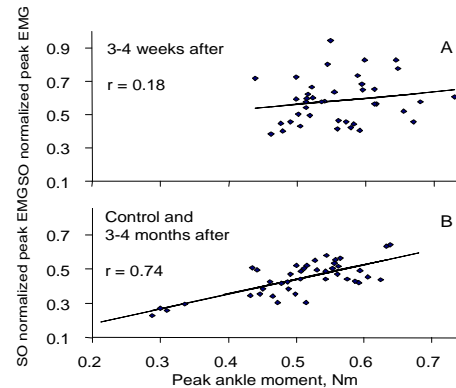


**Figure 4:** Peak normalized filtered EMG of intact SO of one cat as a function of peak ankle extension moment 3-4 weeks post (A), and before and 3-4 months post (B) MG & LG injury

## SUMMARY/CONCLUSIONS

Within one month after self-reinnervation of selected ankle extensors, the ankle moment pattern changed but subsequently recovered 3 months post surgery.

## REFERENCES

- Ablew, T.A. et al. (2000). *J Neurophysiol.* **84**, 2709-2714.
- Cope, T.C. et al. (1994). *J Neurophysiol.* **71**, 817-820.
- English, AW. (2005). *J Comp Neurol.* **490**, 427-441.
- Gregor, R.J. et al. (2006). *J Neurophysiol.* **95**, 1397-1409.

## ACKNOWLEDGEMENTS

Webb Smith, Brad Farrell, Vasiliy Buharin, Denise Larkins, Drs. Richard Nichols and Art English. Supported by NIH HD032571 and the CHMS of Georgia Tech

# REDUCING LOWER EXTREMITY LOADS THROUGH GAIT RETRAINING USING REAL-TIME FEEDBACK METHODS

Harrison Philip Crowell, III <sup>1,2</sup> and Irene S. Davis <sup>2,3</sup>

<sup>1</sup> U.S. Army Research Laboratory, Aberdeen Proving Ground, MD

<sup>2</sup> University of Delaware, Newark, DE

<sup>3</sup> Drayer Physical Therapy Institute, Hummelstown, PA

E-mail: [philip@arl.army.mil](mailto:philip@arl.army.mil)

## INTRODUCTION

Stress fractures are a common injury associated with the repetitive loads encountered during running and marching in basic combat training (BCT). A recent study of U.S. Army recruits found that 30% of the injuries sustained in BCT were stress fractures. Stress fractures are costly in terms of time and money. Rehabilitation time is 8 to 10 weeks (Hauret et al., 2001), and recruits who are discharged because they cannot complete their training cost the Army approximately \$10 M per year.

Prospective and retrospective studies have shown that subjects who sustain a tibial stress fracture have higher tibial shock than those who do not sustain a stress fracture (Milner et al., 2006; Davis et al., 2004). The rapid deceleration of the tibia at heel strike can lead to high strain rates in the bone which are suspected of being a cause of stress fractures (Fyhrie et al., 1998). Therefore, reducing these loads may result in reducing stress fracture risk.

Acute changes in lower extremity loads during running are possible in a single session of training with visual feedback (Crowell et al., 2005). However, long term retention of these changes has not been studied. Therefore, the purpose of this pilot study was to determine whether a longer period of training would result in reductions

in loading that would be evident one month after training.

## METHODS

This is an ongoing study in which five subjects (3 females, 2 males) have participated to date. All subjects were between 20 and 34 years of age, ran at least 10 miles per week, and exhibited tibial shock greater than 8.9 g. Baseline three-dimensional kinematic and kinetic data were collected as subjects ran through the laboratory at 3.7 m/s ( $\pm 5\%$ ).

For the retraining sessions, subjects ran on a treadmill at a self-selected pace. A uniaxial accelerometer was attached to the distal tibia on the side that had the highest shock, noted in the baseline data collection. Visual feedback of their tibial shock was provided on a monitor placed in front of them as they ran. Subjects were instructed to maintain their shock levels under 6 g as indicated by a line placed on the monitor.

The time for which subjects ran started at 10 minutes and increased to 30 minutes for the final sessions. Subjects were restricted from running outside the retraining sessions. Subjects received constant visual feedback for the first half of their sessions. The feedback was progressively removed over the remaining sessions such that subjects had three minutes of feedback in their final session. Immediately after the last

retraining session, kinematic and kinetic data were collected again. Then they ran on their own for four weeks and returned for a follow-up data collection. The first two subjects underwent retraining for 12 sessions over 4 weeks. However, because of the ease with which these subjects reduced their loading, the protocol was shortened to two weeks (8 sessions) for the remaining three subjects.

## RESULTS

All subjects reduced their peak tibial shock from baseline at both post training and at 1 month follow-up (Figure 1).

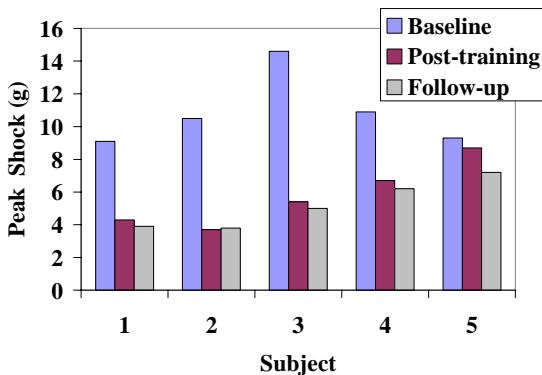


**Figure 1:** Peak shock at baseline, post-training and one month follow-up.

For the group, tibial shock decreased by approximately 50% (Table 1). Instantaneous vertical loading rate, vertical impact peak, and average vertical loading rate decreased by approximately 30%.

## DISCUSSION

As expected, both the four week and two week protocol resulted in reductions in lower extremity loading that were maintained over the one month follow-up period. Feedback was only provided on tibial shock, which exhibited the greatest reduction from baseline. However, retraining also significantly reduced the other three loading variables. The reductions in loading that the subjects achieved during this study likely reduce the strain and strain rates on their tibias, and thereby decrease their risk of stress fractures. Further analysis is underway to identify the kinematic strategies used by the subjects to reduce their lower extremity loading.

## CONCLUSIONS

Based on these preliminary results, subjects are able to reduce their lower extremity loading by retraining with real-time visual feedback. These changes were maintained at one-month follow-up.

## REFERENCES

- Hauret, K.G. et al. (2001). *Milit. Med.*, **166**(9), 820-826.
- Fyhre, D.P. et al. (1998). *Ann. Biomed. Eng.*, **26**(4), 660-665.
- Milner, C.E. et al. (2006). *Med. Sci. Sports Exercise*, **38**, 323-328.
- Davis, I.S. et al, (2004) *Med. Sci. Sports Exercise*, **36**(5) Supplement, S58.
- Crowell, H.P. et al. (2005). *Med. Sci. Sports Exercise*, **37**(5) Supplement, S346.

**Table 1.** Lower extremity loading and changes for the group.

	Baseline	Post-training	1 month follow-up	Change (Baseline to Follow-up)
Tibial Shock (g)	10.8	5.8	5.2	-52 %
Inst. Load. Rate (BW/s)	84.7	58.6	54.8	-35 %
Impact Peak (BW)	1.6	1.3	1.2	-29 %
Avg. Load. Rate (BW/s)	69.8	47.5	47.6	-32 %

# Is the Leg Most Spring-Like at the Preferred Hopping and Running Frequencies?

Nitin Moholkar and Claire T. Farley

Locomotion Lab, University of Colorado, Boulder, CO, USA

E-mail: nmoholkar@kmrrec.org

## INTRODUCTION

Humans strongly prefer particular frequencies during hopping and running. Furthermore, the metabolic cost of running at this preferred stride frequency (PSF) is near its minimum (Cavanagh, 1982). It is possible that metabolic cost is minimized at the PSF because elastic energy storage and return provides most of the mechanical work. If this is true, it would make sense that the overall leg would behave more like a spring at the PSF than at other stride frequencies. Based on this idea, we hypothesized that a spring-mass model most accurately predicts the COM motion during hopping in place and running when subjects use their PSF. In the model, the mass of the body is represented by a point mass, and the mechanical behavior of the leg is modeled as a linear spring. This model has been successfully used to represent bouncing gaits in a wide variety of animals (Farley et al., 1993), including hopping in place and running in humans.

## METHODS

Eleven males ran (2.5 m/s) and ten males hopped in place on two legs at a range of stride frequencies that were above, below, and at their PSF. We measured ground reaction force (GRF).

For each trial, leg stiffness was calculated using two methods: from the slope of the leg force-leg compression curve during stance and using a spring-mass simulation (Matlab). We calculated leg compression by twice integrating the COM accelerations,

calculated from the GRF. For the second method, we ran a simulation of a spring-mass model using initial conditions from each trial (leg length, body mass, leg angle at touchdown, COM velocity at touchdown). The simulation error was calculated as the average absolute difference between subject data and the simulation's prediction for COM displacement over the ground contact phase. For each trial, we found the spring stiffness that minimized this error ('optimal' leg stiffness for that trial). Finally, we compared this 'optimal' leg stiffness value to the value calculated from the leg's force-compression curve for the stance leg.

## RESULTS AND DISCUSSION

The leg stiffness values that optimized the spring-mass model trajectory predictions were, on average, within 0.6 kN/m of values calculated from the leg's force-compression curve for both hopping and running. The finding that two very different methods give similar leg stiffness values lends further support to the idea that the leg behaves like a spring during hopping and running.

Contrary to our hypothesis, the spring-mass model did not predict COM motion most accurately at the PSF for hopping and running (Fig. 1). Rather, its predictions improved continuously as frequency increased and were remarkably accurate at moderate and high frequencies. This observation suggests that the stance leg did indeed behave more like a spring at the PSF than at lower stride frequencies but behaved less like a spring at the PSF than at higher stride frequencies.

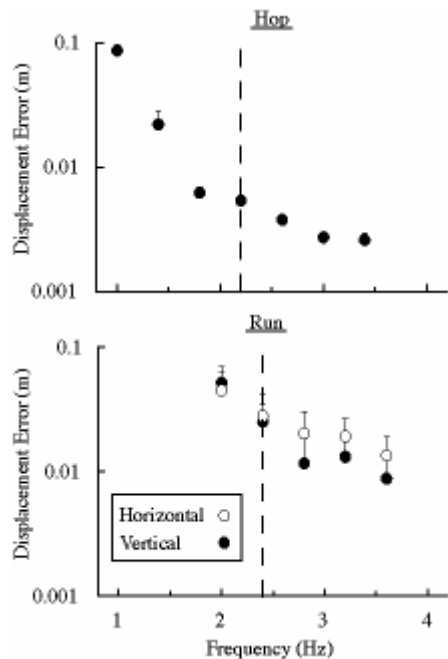


**Figure 1:** Vertical dashed lines show the average PSF. Frequency is step frequency for running. For running, the figure shows horizontal and vertical errors, while the text uses total error which is the vector sum of the two components. Error values are larger for running than for hopping because COM displacements are larger for running.

The spring-mass model did predict COM motion more accurately at the PSF than at lower frequencies for both hopping and running. The model's predictions differed the most from subject data at the lowest frequency for both hopping (8.7 cm) and running (6.9 cm). In contrast, at the PSF, the average error was lower for hopping (0.5 cm) and running (3.8 cm). This observation suggests that the leg behaved more like a spring at the PSF than at lower frequencies, which might indicate greater storage and return of mechanical energy.

Contrary to our hypothesis, the model predicted COM motions with 40-60% less error at the highest frequency (0.3 cm for hopping and 1.6 cm for running) than at the

PSF. This observation suggests that the stance legs behaved more like springs at higher frequencies than at the PSF. Consequently, spring-like behavior of the leg does not explain why runners consume less metabolic energy at the PSF than at higher frequencies.

It is possible that the metabolic cost increases at frequencies higher than the PSF because stance time becomes shorter. Shorter stance times require the use of faster muscle fibers which are metabolically more expensive for force generation (Kram, 1990). Thus, shorter stance times might explain why metabolic cost increases above the PSF.

## SUMMARY/CONCLUSIONS

Despite its simplicity, a spring-mass model predicts COM motions in human hopping and running remarkably well. Surprisingly, the body coordinates the actions of many muscle-tendon units to make the overall stance leg behave like a spring at the PSF and higher frequencies. It is likely that the energetic cost of running is minimized at the PSF due to an optimal combination of high elastic energy storage/return and a low cost of generating force.

## REFERENCES

- Cavanagh, P.R. and Williams, K.R. (1982). *Medicine and Science in Sports and Exercise*, **14**, 30-5.
- Farley, C.T. et al. *Journal of Experimental Biology*, **185**, 71-86.
- Kram, R. and Taylor, C.R. (1990). *Nature*, **346**, 265-267.
- McMahon, T.A. and Cheng, G.C. (1990). *Journal of Biomechanics*, **23**, 65-78.

# FORCE- AND MOMENT-GENERATING CAPACITY OF FLEXOR DIGITORUM LONGUS FOLLOWING TENDON TRANSFER

Nicholas A.T. Brown<sup>1,2</sup>, Joe Hui<sup>2</sup>, Timothy C. Beals<sup>1</sup>.

University of Utah, Salt Lake City, UT, USA

<sup>1</sup>Department of Orthopaedics, <sup>2</sup>Department of Bioengineering

Email: [Nick.Brown@hsc.utah.edu](mailto:Nick.Brown@hsc.utah.edu)

**INTRODUCTION:** Posterior Tibialis Tendon Dysfunction is a common condition that leads to significant morbidity of the foot (Mann et al., 1985). In conjunction with surgical lengthening of the lateral column of the foot or with calcaneal osteotomies, the flexor digitorum longus (FDL) muscle is often transferred to the medial cuneiform or navicular bones to augment the function of the deficient posterior tibialis muscle (Wacker et al., 2002). The functional success of this and other tendon transfers relies, among many factors, on the post-surgical production of appropriate muscle moments which in turn depends on donor muscle architecture, joint mechanics and transfer technique. However, knowledge of the functional capacity of native and transferred extrinsic foot muscles including the FDL is limited. The purpose of this research was to quantify the maximal isometric forces and moments that FDL is capable of producing following tendon transfer. It was hypothesized that in comparison to the native state, the hindfoot moment arm, force and moment produced by FDL would increase following tendon transfer to either the medial cuneiform or navicular bones.

**METHODS:** In six cadaveric specimens free from musculoskeletal disease, muscle moment arms for FDL and posterior tibialis (PT) were determined using the tendon-excursion method (An et al., 1984). Moment arms were measured with both muscles in their native state and with FDL transferred to either the plantar aspect of the navicular

or medial cuneiform bones. PT remained intact and served as a control.

To estimate the force FDL can produce in its native and transferred states, surgical simulations were performed in a specimen-specific musculoskeletal (MS) model of the talocrural, subtalar (STJ) and talonavicular joints. The kinematic structures of these joints were determined from the same cadaver from which bone geometry was obtained. Cardinal plane rotations and translations were measured using a joint coordinate system approach (Cole et al., 1993) and introduced into the MS model. The model was actuated by muscle-tendon units represented as three-element Hill-type muscles in series with elastic tendons. Reported muscle fiber lengths, maximal isometric forces, tendon lengths and pennation angles specified the force-producing properties of each muscle (Wickiewicz et al., 1983). Muscle paths were defined by MRI collected from the same cadaveric specimen. Via points and wrapping structures were added to maintain physiological muscle paths during joint rotations. Simulations in which muscles were maximally and isometrically activated as the STJ was rotated from  $-10^{\circ}$  of eversion to  $+15^{\circ}$  of inversion were used to examine the force- and moment-generating capacity of the PT and FDL muscles.

ANOVA was used to compare cadaveric moment arm magnitudes in the native and transferred states ( $p=0.05$ ).

**RESULTS AND DISCUSSION:** The FDL hindfoot moment arm magnitude measured in cadaveric specimens decreased by up to 40% when transferred from its native state (Table 1). These differences were not significant ( $p=0.122$ ) due to variability within specimens. Post hoc power analyses indicated that over 20 specimens would be required to detect statistical significance.

FDL muscle moment arms also decreased during the simulated transfer surgeries. FDL produced more force in both transferred conditions than in the native state when the hindfoot was inverted. However, force production for foot positions representative of the stance phase of gait ( $0-10^\circ$  eversion)

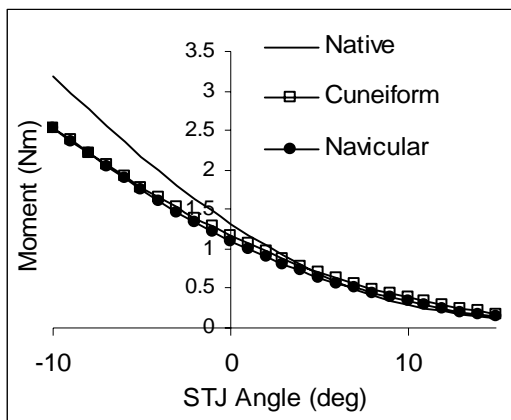


Fig 1: Simulated maximal isometric FDL muscle moments about the hindfoot for FDL tendon transfers. Eversion  $0^\circ$  to  $-10^\circ$ ; inversion  $0^\circ$  to  $+15^\circ$ .

Table 1: Individual (S1–S6) and group mean moment arms magnitudes (mm) for FDL calculated in hindfoot neutral position for the native and transferred FDL.

	S1	S2	S3	S4	S5	S6	Mean
Native	19.7	15.5	10.2	18.7	23.4	15.6	17.2
Cuneiform	16.7	15.4	7.6	16.8	5.0	8.1	11.6
Navicular	13.6	17.3	9.7	16.6	1.8	8.4	11.2

## REFERENCES

1. Mann RA, Thompson FM. (1985). *J Bone Joint Surg Am.* **67**, 556-61.
2. Wacker JT, et al. (2002). *J Bone Joint Surg Br.* **84**, 54-58.
3. An KN, et al. (1984). *J Biomech Eng.* **106**, 280–282.
4. Cole GK, et al. (1993). *J Biomech Eng.* **115**, 344–349.
5. Wickiewicz TL, et al. (1983). *Clin Orthop Rel Res.* **179**, 275-283.

was unchanged. Due to decreased moment arm magnitudes and no change in muscle force, the transferred FDL produced lower inversion moments about the hindfoot compared with its native condition for neutral to everted STJ positions (Fig 1.).

**CONCLUSIONS:** Transfer of the FDL tendon to the navicular or medial cuneiform did not increase the capacity of the FDL muscle to invert (or resist eversion of) the hindfoot. In contrast, the transferred FDL tended to be less effective in this role suggesting little functional advantage is gained through its transfer to these sites. Because muscles were fully activated and the subtalar and talonavicular joints were moved in isolation, the current simulation results cannot be directly applied to predict muscle forces or to analyze muscle function during gait. However, combined with appropriate in vivo measurements of joint kinematics, ground-reaction forces and muscle activity, the model described herein may be used to estimate muscle-tendon forces during gait.

# MECHANICAL DIFFERENCES IN ONE-LEGGED AND TWO-LEGGED HOPPING AT PREFERRED FREQUENCY

Arick Auyang<sup>1</sup>, Young-Hui Chang<sup>1,2</sup>

<sup>1</sup>Comparative Neuromechanics Lab, GeorgiaTech, Atlanta, GA, USA

<sup>2</sup>Biomedical Engineering Program, Emory Univ/GeorgiaTech, Atlanta, GA, USA

## INTRODUCTION

The dynamics of human running can be modeled as a simple spring-mass system (McMahon and Cheng, 1990; Blickhan 1989). This model is highly robust in its ability to describe the dynamics of bouncing gaits in animals with 2, 4, 6, or even 8 legs (Blickhan and Full, 1993; Cavagna, G.A. et al., 1977). Independent studies have shown that one-legged and two-legged hopping both exhibit linear relationships between vertical ground reaction force (vGRF) and vertical displacement of center of mass ( $\Delta\text{CoM}$ ; Ferris et al., 2006; Austin, 2002; Farley et al., 1991). Our objective is to determine whether the spring-mass dynamics of one-legged hopping can be simply explained as the linear sum of the two parallel springs in two-legged hopping.

## METHODS

We collected preliminary data on 3 healthy adults. Subjects gave their informed consent before participating in this study as per Georgia Tech's IRB. Subjects hopped on one and two legs at 2.2 Hz. We collected vGRF and sagittal plane kinematics for 30 hopping cycles for each condition. An average effective leg stiffness ( $k_{\text{leg}}$ ) was calculated as a ratio between the maximum change in vGRF and the maximum  $\Delta\text{CoM}$  (Figure 1).

## RESULTS AND DISCUSSION

The effective leg stiffness during one-legged hopping was on average 34.6% less than the predicted algebraic sum of the two effective leg stiffnesses in two-legged hopping (Figure 2).

Average  $\Delta\text{CoM}$  decreased only 2.3% during one-legged hopping (Figure 3).

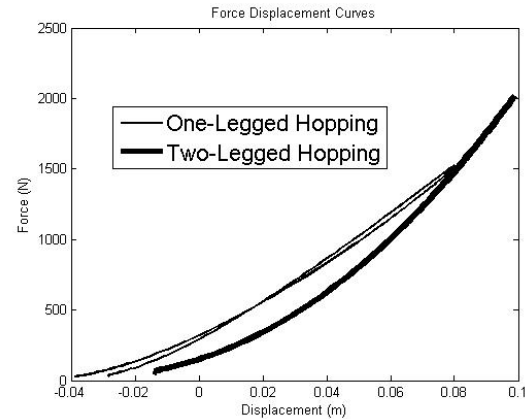


**Figure 1** Average net vGRF vs  $\Delta\text{CoM}$  curves during the stance phase of one legged (thin line) and two-legged hopping (thick line) for one subject.

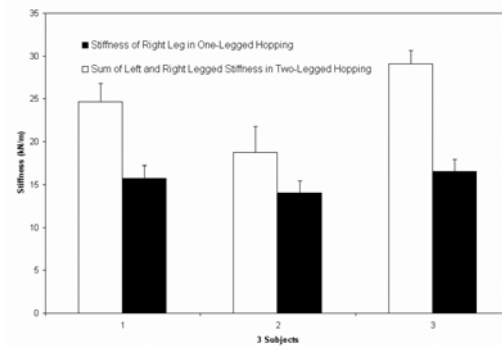


**Figure 2:** Effective leg stiffness of both legs during two-legged hopping (white) is greater than the effective leg stiffness of the one leg (black) during one-legged hopping in all three subjects ( $p < 0.05$ ).

Average peak vGRF decreased by 31% across subjects for one-legged hopping compared to two-legged hopping (Figure 4).

We saw no substantial changes in ankle angle kinematics. Peak knee flexion decreased substantially during one-legged hopping (Figure 5), which would suggest a

more extended and upright limb posture.

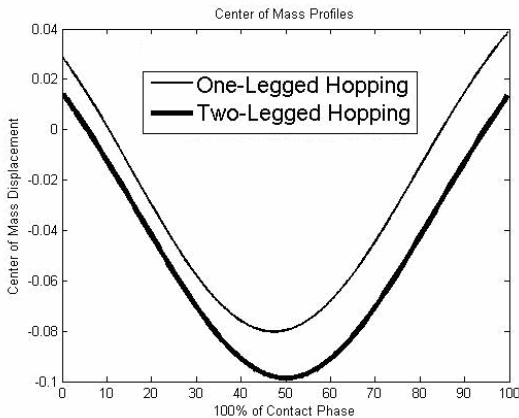


**Figure 3** Mean CoM trajectories for one legged (thin line) and two-legged hopping (thick line) during contact phase.

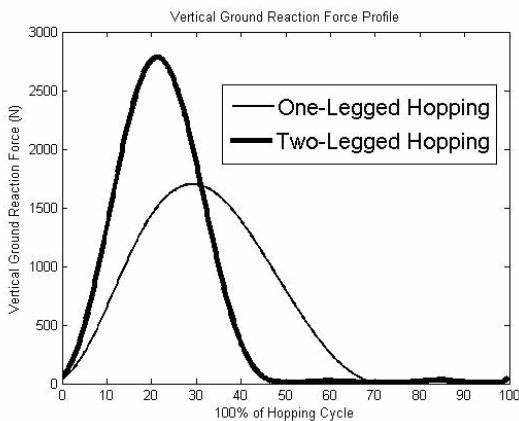


**Figure 4** Mean vGRF for one-legged (thin line) and two-legged hopping (thick line) beginning with foot contact for one subject.

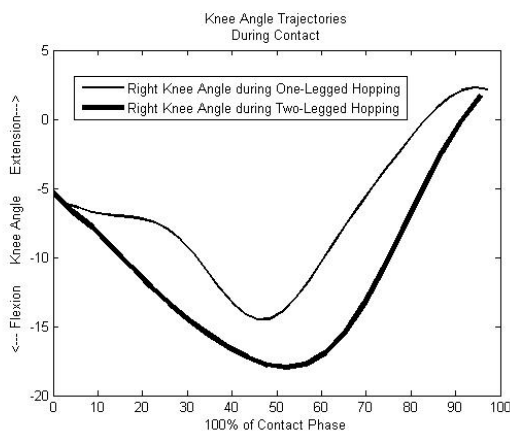


**Figure 5** Mean knee angle trajectories for one-legged (thin line) and two-legged hopping (thick line) during stance phase for one subject.

## SUMMARY

The total effective leg stiffness of one-legged hopping was less than the expected summed total effective leg stiffness of two-legged hopping. This decrease in effective leg stiffness generated lower peak vGRF and longer stance times during one-legged hopping. Overall  $\Delta\text{CoM}$  was only affected minimally. Subjects adopted more upright limb postures during one-legged hopping which has been seen to be a general mechanism among mammals for minimizing joint moments and muscle stress (Biewener et al., 1991). This may represent a fundamental strategy for minimizing musculoskeletal stress during single limb support.

## REFERENCES

- Austin et al. (2002). *Percept Mot Skills*. **94**, 834-40.
- Biewener et al. (1991). *J. Biomech.* **24**, 19-29.
- Blickhan, R. (1989). *J. Biomech.* **22**, 1217-27.
- Blickhan R., Full R. (1993). *J. Comparative Physiology*. **173**, 509-517.
- Cavagna, G.A. et al. (1977). *Am J Physiol*. **233**, 243-61.
- Farley et al. (1991). *J. Appl Physiol*. **71**, 2127-32.
- Ferris et al. (2006). *J. Appl Physiol*. **100**, 163-70.
- McMahon, T.A., Cheng, G.C. (1990). *J. Biomech.* **23 Suppl 1**, 65-78.

## Acknowledgements

Anish Ghodadra

# GROUND REACTION FORCES DURING THE STANCE PHASE OF GAIT OF YOUNG AUTISTIC CHILDREN

Kimberly Fournier<sup>1</sup>, Krestin Radonovich<sup>1</sup>, Mark Tillman<sup>1</sup>, and John Chow<sup>1</sup>

<sup>1</sup> University of Florida, Gainesville, FL, USA

E-mail: kfournier@hhp.ufl.edu

## INTRODUCTION

Autism is a neurodevelopmental disorder characterized by qualitative impairments of language, communication, social interaction in addition to stereotypic behaviors. Autism Spectrum Disorder (ASD) is used to describe children diagnosed with autism as well as those having the same core deficits, but to a lesser severity. This group also includes children diagnosed with Pervasive Developmental Disorder-Not Otherwise Specified (PDD-NOS) and Asperger Syndrome. In addition to communicative symptoms, children with ASD display a wide range of other symptoms that impair their development. Motor problems are the most frequently reported non-verbal impairments.

Motor impairments have received little attention in the autism literature, due to the fact that these impairments were considered less important and believed to belong to a co-occurring syndrome. However, recent research suggests that motor impairments may be the earliest indicators of autism and may be observed within the first few months of life (Teitelbaum et al., 1998). Although “clumsiness” is not used to diagnose autism, it is often used to describe children diagnosed with ASD. A clear definition of “clumsiness” in these children remains to be described, however, gait analysis techniques can provide an objective assessment of gait patterns seen in children with ASD.

The purpose of the current investigation was to attempt to describe “clumsiness” observed in young children diagnosed with

ASD. Thus, ground reaction forces during stance of young children with ASD were compared to those of typically developing children (TD).

## METHODS

Gait trials at self-selected walking speeds were collected for 6 children with ASD ( $5.5 \pm 1.6$  years) and 6 TD children ( $4.3 \pm 1.1$  years). Ground reaction forces in the vertical (Fz), antero-posterior (Fx) and mediolateral (Fy) directions were collected using a force plate (900Hz). Trials were considered successful if only one complete foot contact occurred on the force plate. Foot contact was determined as the point at which the ground reaction force vector was initially observed and the foot off was determined as the point at which the ground reaction vector diminished to zero. Ground reaction force data were filtered using a 7 point moving average using Microsoft Excel.

Ground reaction forces were normalized to body weight (BW) and % stance phase for all trials. The vertical ground reaction force (Fz) was characterized by Fz<sub>1</sub> (maximum force within first 50% of stance phase), Fz<sub>2</sub> (maximum within the second 50% of stance phase) and Fz<sub>0</sub> (the minimum value between opposite foot off and foot contact). The antero-posterior ground reaction (Fx) was characterized by Fx<sub>1</sub> (maximum posteriorly directed force) and Fx<sub>2</sub> (maximum anteriorly directed force). The mediolateral force (Fy) was characterized by Fy<sub>1</sub> (maximum lateral force) and Fy<sub>2</sub> (maximal medial force). See Figure 1.

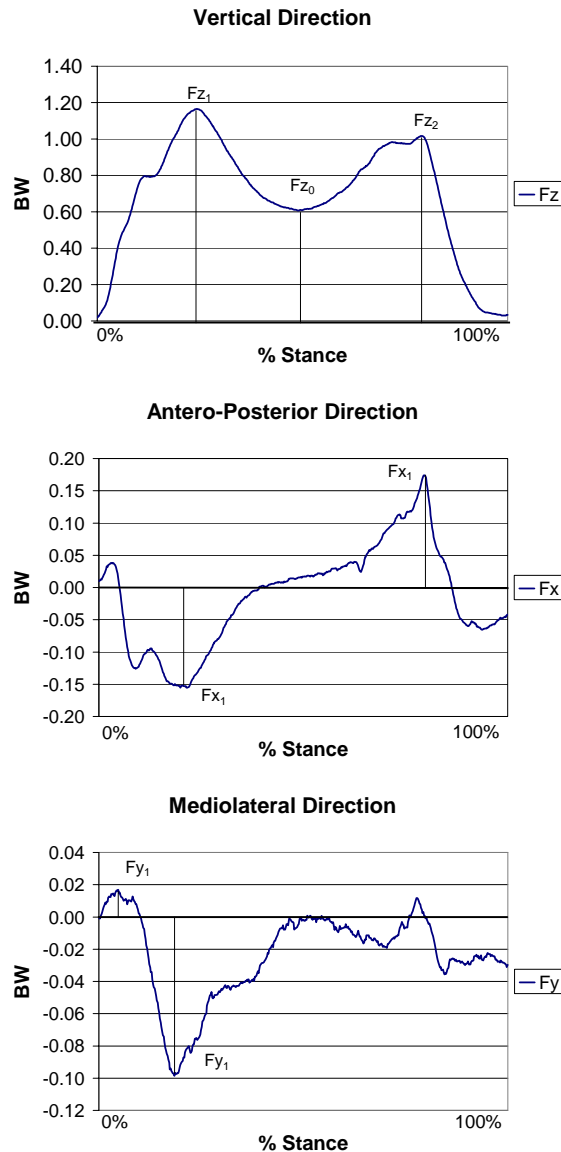


**Figure 1.** Ground Reaction Force Measures.

Two-tailed, independent t tests ( $\alpha = 0.05$ ) were performed for each of the 7 ground reaction force measures ( $Fz_1$ ,  $Fz_2$ ,  $Fz_0$ ,  $Fx_1$ ,  $Fx_2$ ,  $Fy_1$ , and  $Fy_2$ ).

## RESULTS AND DISCUSSION

Children with ASD had significantly larger  $Fz_2$  values ( $t(10) = -2.5, p < 0.05$ ) and significantly smaller  $Fy_1$  values ( $t(10) = 2.3, p < 0.05$ ). No significant differences were observed for the other measures (Table 1).

Previous research indicates that kinetic measures of gait are consistent (particularly  $Fz_1$ ,  $Fz_2$ , and  $Fx_2$ ) with  $Fz_2$  being the most reproducible force measure. Increased variability of these measures has been observed in children with cerebral palsy and may be considered an indicator of pathological gait (White et al., 1999) and an inability to modulate increasing gait speed during the first half of stance (Stansfield et al., 2001).

## SUMMARY/CONCLUSIONS

Preliminary findings suggest that children with ASD have altered gait kinetics during stance that may contribute to the appearance of “clumsiness”. Force plate data may be a useful tool for quantifying motor impairment in children with ASD. The source of these differences remains unclear. Further gait analysis, including kinematics, is warranted.

## REFERENCES

- Stansfield, B.W. et al. (2001). *J. Pediatr. Orthop.*, **21**(3), 395-402.  
 Teitelbaum, P. et al. (1998). *Proc.Natl. Acad. Sci. USA*, **95**, 13982-13987  
 White, R. et al. (1999). *Clinical Biomechanics*, **14**, 15-192.

## ACKNOWLEDGEMENTS

NIH Grant # MH073

**Table 1:** Means & SD for Ground Reaction Force Measures (\*significance  $p < 0.05$ ).

Group	$Fz_1$ (%BW)	$Fz_2$ (%BW)*	$Fz_0$ (%BW)	$Fx_1$ (%BW)	$Fx_2$ (%BW)	$Fy_1$ (%BW)*	$Fy_2$ (%BW)
TD	1.28 (0.21)	0.88 (0.19)	0.54 (0.13)	-0.22 (0.17)	0.19 (0.05)	0.07 (0.02)	-0.06 (0.02)
ASD	1.21 (0.17)	1.20 (0.26)	0.68 (0.31)	-0.15 (0.08)	0.26 (0.14)	0.03 (0.03)	-0.09 (0.06)

# UNSTABLE SINGLE-LEG LANDINGS: A CASE STUDY

Scott W. Arnett, Julie Hayes, Rachel Nelson, and Kathy Simpson

University of Georgia, Athens, GA, USA

E-mail: [sarnett@uga.edu](mailto:sarnett@uga.edu) Web: [www.coe.uga.edu/kinesiology/exs/labsbiom.html](http://www.coe.uga.edu/kinesiology/exs/labsbiom.html)

## INTRODUCTION

Movements occurring during sports participation, such as landings, can result in high-risk loading of the knee (Boden et al., 2000). Furthermore, particularly if landing on a single limb, ACL injuries can occur during atypical landings that alter the mechanics of the lower extremity.

While testing a participant performing drop landings onto her non-preferred limb, we noticed she exhibited extreme difficulty maintaining balance. What was occurring biomechanically during these 'unstable' compared to 'stable' landings? We surmise that during sports situations, such landings onto the non-preferred limb may increase the risk of ACL injury due to altered landing mechanics. Therefore, the aim of this case study was to determine this participant's kinematic and kinetic differences between stable (SL) and unstable (NSL) single-leg landings.

## METHODS

The performer (20 yr old, skilled basketball player) selected was participating in an ongoing drop landing study of females. For both landing conditions, 3 non-preferred-limb drop landing trials (ht = 42 cm) were analyzed. A SL occurred when the participant remained stationary after landing, whereas a NSL occurred when the participant had to take a step or use the arms to regain balance.

Maxima/minima and times to these events were generated for sagittal plane video data

(60 Hz) of angles and GRF data (1020 Hz). The difference for a variable between SL and NSL was statistically significant ( $p < 0.05$ ) if it exceeded the product of a weighted average of the SL and NSL standard deviations and a critical value dependent on number of trials (Bates, et al., 1992).

## RESULTS AND DISCUSSION

The magnitudes of peak VGRF, posterior A-P GRF, and peak rates of force application were greater for SL compared to NSL. Time to peak VGRF was greater for NSL compared to SL. Maximum hip flexion was greater during NSL than SL.

As the performer was only able to perform 3 SL, limited interpretation is warranted. Learning to reduce VGRF magnitudes have been recommended by some (Cowling, et al., 2003) to be a strategy to reduce a performer's risk of ACL injury. However, this participant demonstrated decreased, not increased, VGRF magnitudes and rates of application during an unstable landing suggesting that high VGRF's are not necessarily associated with atypical landings. For this landing task, the performer generated increased posterior GRF during SL in order to try and rotate the body back into an upright position. Greater maximum hip flexion may reflect a strategy of lowering the body's COM to improve stability and simultaneously served to reduce the effective mass during the impact phase, resulting in decreased VGRF's.

During practice or competition, athletes may have to land on the non-preferred limb, as was the case for the participant in this study. Of qualitative interest was the difficulty that this participant had in executing a landing onto the non-preferred limb. Of the 9 landing trials, only 3 were SL. This limits the behavioral generalizability of our participant's data. Nonetheless, greater insight is needed into the biomechanics of unstable landings and if landing onto the non-preferred limb induces greater risk for unstable landings due to lesser strength or a movement control problem.

### SUMMARY/CONCLUSIONS

We had an unforeseen opportunity to analyze non-invoked unstable landings for

this case study. Decreased VGRF's during NSL compared to SL suggest that the VGRF's are not necessarily positively correlated with atypical landings, as has been previously suggested but not proven. Stable landings are not always possible and altered biomechanics resulting in an unstable landing may occur when reacting to unfamiliar situations.

### REFERENCES

- Bates, B.T., et al. (1992). *Med Sci Sports Exerc*, **24**, 1059-1068.  
 Boden, B.P. et al. (2000). *Orthopedics*, **23**, 573-578.  
 Cowling, E.J., et al. (2003). *Br J Sports Med*, **37**, 126-130.

**Table 1:** Angles and GRF's (mean  $\pm$  SD).

Joint/ Segment	Angle	Stable	Unstable	GRF	Stable	Unstable
Trunk (0°=vertical)	Initial contact	5.1 $\pm$ 1.9	4.6 $\pm$ 0.8	Peak VGRF	2606 $\pm$ 32*	2426 $\pm$ 122*
	Max flexion	15.4 $\pm$ 1.8	19.0 $\pm$ 3.2	Peak VGRF time	.087 $\pm$ .001*	.092 $\pm$ .001*
Hip Flexion (0°=straight)	Initial contact	5.6 $\pm$ 0.7	6.7 $\pm$ 1.7	VGRF Max Slope	38946 $\pm$ 1673*	31713 $\pm$ 4213*
	Max Flexion	9.3 $\pm$ 1.1*	13.9 $\pm$ 2.0*	Peak posterior A-P force	-198 $\pm$ 11*	-178 $\pm$ 6*
Knee Flexion (0°=straight)	Initial contact	7.1 $\pm$ 3.3	7.6 $\pm$ 2.6	Peak posterior A-P max slope	-7119 $\pm$ 566*	-6186 $\pm$ 548*
	Max Flexion	47.0 $\pm$ 4.7	47.9 $\pm$ 10.8			
Ankle (+=plantar, -=dorsi)	Initial contact	27.3 $\pm$ 2.2	29.4 $\pm$ 6.5			
	Max Flexion	-24.1 $\pm$ 1.8	-23.6 $\pm$ 2.6			

Note. \* statistically different (p < 0.05).

# WHAT ARE WE MISSING WHEN USING INVERSE DYNAMICS?

Kurt Manal, Joseph Gardinier and Nicole Chimera

Center for Biomedical Engineering Research  
University of Delaware, Newark, DE, USA  
E-mail: manal@udel.edu

## INTRODUCTION

Ascending stairs is a challenging task for people with knee osteoarthritis (OA) and patellofemoral pain (PFP). The knee extensor moment has a single peak during the first half of stair ascent, with little to no extensor moment during late stance. Subjects with knee OA and PFP exhibit a smaller peak extensor moment than healthy controls when climbing stairs, which has been described as a strategy to reduce joint loading and pain during stair climbing (Salsich et al., 2001).

In contrast, the ankle plantarflexion moment during the first half of stair ascent is small; reaching a peak near the end of stance when the knee extension moment is minimal. These observations and the biarticular nature of the gastrocnemius as an ankle plantar flexor and a knee flexor raised a question about the role of the gastrocnemius during stair climbing. Although the *net* knee extension moment was minimal during late stance (Figure 1), we hypothesized that significant quadriceps force would be needed during late stance to prevent the knee from flexing as the gastrocnemius actively plantarflexes the ankle.

An EMG-driven musculoskeletal model of the knee was used to partition the net knee joint moment into separate extensor and flexor contributions. This approach allowed us to examine quadriceps force during late stance that could not be obtained using inverse dynamics alone.

## METHODS

Visual3D was used to compute ankle and knee joint moments (%BW \* Height) during stair ascent for 14 subjects with knee OA and 16 healthy controls. In addition, EMG was recorded from 10 muscles crossing the knee, including the medial and lateral heads of the gastrocnemius, the rectus femoris, and the medial and lateral heads of the vasti. A Hill-type muscle model was used to partition the net knee joint moment into extensor and flexor contributions. A review of this modeling approach and data processing methods has been described elsewhere (Buchanan et al., 2004).

## RESULTS AND DISCUSSION

Average knee extension and plantarflexion moments for each group are presented in Figures 1 and 2. Both groups had an extensor peak during the first half of ascent and a plantarflexion peak during late stance. Although peak extension and plantarflexion moments were greater for the control subjects, only the plantarflexion moment was statistically different (Table 1).

Partitioning the net joint moment into extensor and flexor contributions revealed that the quadriceps generated significant force (i.e., extensor moment) during late stance when the net joint moment was small (Figure 3). This is clinically relevant, especially when considering patellofemoral contact area decreases with decreasing knee flexion that occurs during stair ascent (Levangie & Norkin, 2005). Thus, although

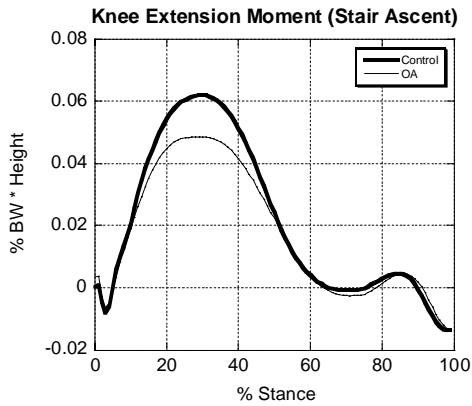


**Figure 1:** Stair ascent is characterized by a single net extension moment during the first half of stance.

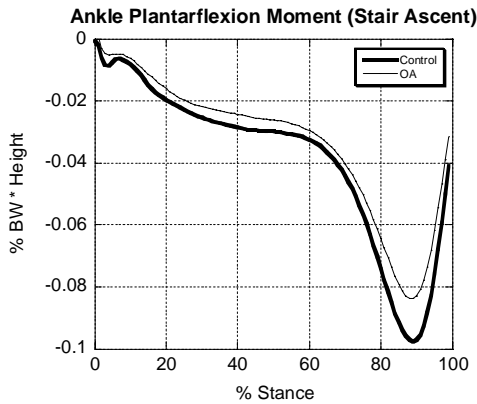


**Figure 2:** Plantarflexion moment during ascent peaks during late stance.

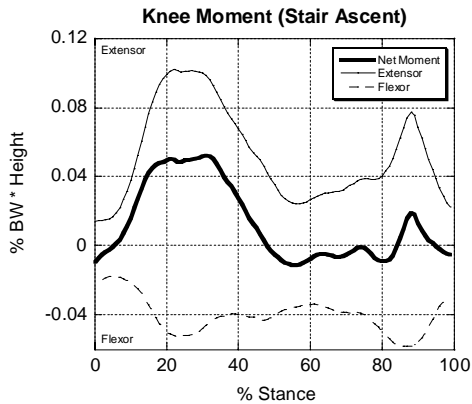


**Figure 3:** Extensor, flexor and net moment for a representative subject with OA. The extensor moment generated by the quadriceps is relatively large during late stance.

the *net* knee joint moment may be small during late stance, the quadriceps generated a significant extensor moment, which when combined with a small patellofemoral contact area may produce joint stresses similar to, or possibly even greater than during the first half of stance when the net extension moment was at its peak.

**Table 1:** Peak net moment (%BW \* Ht) during stair ascent (mean± SD). \* indicates  $p < 0.05$

Group	Knee Extension	Plantarflexion*
OA	$0.054 \pm 0.019$	$-0.086 \pm 0.014$
Control	$0.063 \pm 0.021$	$-0.098 \pm 0.013$

## SUMMARY/CONCLUSIONS

The net joint moment has been used to characterize joint loading during dynamic tasks (Hurwitz et al., 2000). However, when antagonistic muscle activity is present, inferring joint loads and patterns of loading from the net joint moment may significantly underestimate what is actually occurring at the joint.

## REFERENCES

- Buchanan, T.S., et al. (2004), *J. App Biomech*, 20,367-395.
- Hurwitz, D.E., et al. (2000), *J Orthop Res*, 18, 572-579
- Levangie, P.K. & Norkin, C.C. (2005), *Joint Structure and Function. A comprehensive analysis*, p422.
- Salsich, G.B., et al. (2001), *Clin Biomech*, 16, 906-912.

## ACKNOWLEDGEMENTS

Supported by NIH grant RR16458

# VASTUS LATERALIS FORCES DURING STAIR DESCENT

Joseph D. Gardinier and Kurt Manal

Center for Biomedical Engineering Research  
University of Delaware, Newark, DE, USA  
E-mail: joeg@udel.edu

## INTRODUCTION

Individuals with knee osteoarthritis (OA) exhibit altered lower leg kinematics and kinetics during walking and stair climbing. These include reduced sagittal plane knee excursions and joint moments and prolonged activity of key lower extremity muscles, including vastus lateralis (Childs et al., 2004). Hinman (2002) reported delayed onset of the vastus lateralis (VL) compared to control subjects during stair descent. It is difficult to appreciate the magnitude and timing of VL forces during stair descent from the data reported in these studies. In this paper, we report preliminary data for VL forces during stair descent for a small group of subjects (control & OA). In addition, peak VL forces expressed as a percentage of the total quadriceps force are reported. Muscle force estimates were computed using an EMG-driven musculoskeletal model. This approach allows us to examine individual muscle forces during dynamic activities.

## METHODS

The EMG-driven musculoskeletal model and data processing methods have been described elsewhere (Buchanan et al., 2004). Joint kinematics, kinetics and EMG signals were collected during stair descent for 2 healthy controls and 2 subjects with knee OA. Each subject performed 5 trials at a self-selected speed. Knee joint moments were computed using Visual3D and normalized to %BW\*Height. The muscle-tendon lengths and moment arms of 13

muscles crossing the knee were determined using SIMM and the lower extremity anatomical model developed by Delp (1990). Peak VL forces were expressed as a percentage of the total force generated by the quadriceps. The total quadriceps force was computed from individual force estimates for the rectus femoris, the vastus lateralis, medialis and intermedius.

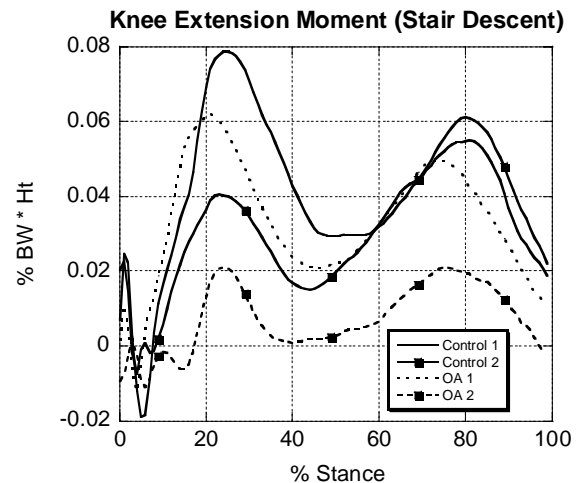


**Figure 1:** The knee extension moment has two distinct peaks. Each curve represents the average of 5 trials per subject.

## RESULTS AND DISCUSSION

Our results are consistent with previous work reporting the VL is active prior to foot contact when descending stairs. The VL force at initial contact in our study was slightly greater than 100 Newtons for all subjects. It is difficult to make direct force

comparisons between subjects because stair climbing speed was not controlled, nor were the forces adjusted for maximum quadriceps strength. Nonetheless, these data provide useful information regarding the role of the VL during stair descent. There were two distinct VL force peaks occurring at 20% and 80% of stance. Peak VL force tends to be greater during late stance even though the magnitude of the first peak extension moment was greater during early stance. In addition, from Table 1 we see that the VL generates approximately 1/3 or more of the total force generated by the quadriceps. Although individual muscle force data are not presented, the VL generated the greatest amount of force of the 4 muscles comprising the quadriceps. With only 2 subjects per group it is premature to propose potential neuromuscular differences between groups at this time. Individual subject data were presented to show that the patterns of force were similar, although the magnitudes varied markedly between subjects. In general, larger VL forces were noted for subjects that generated larger knee extensor moments. Ongoing work is investigating individual muscle force contributions during walking, stair ascent and descent in a larger group of subjects.

**SUMMARY/CONCLUSIONS**

The VL is an important knee extensor during stair descent, generating 1/3 or more of the total quadriceps force. There were 2 distinct VL force peaks occurring at the same time as the peak extension moments

(Figures 1 & 2). Musculoskeletal models that integrate kinematic, kinetic and muscle activation can lend insight into the patterns and magnitudes of individual muscle forces during dynamic movements.

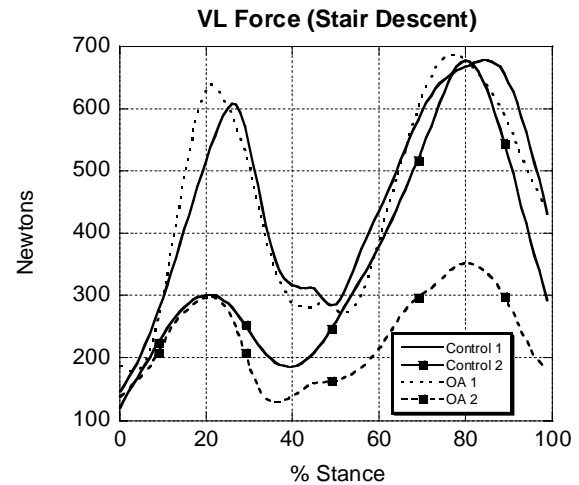


**Figure 2:** Timing of the peak VL forces coincides with the timing of the peak knee extension moments

**REFERENCES**

Buchanan, T.S., Lloyd, D.G., Manal, K., Besier, T.F. (2004), *J. App Biomech*, 20,367-395.  
 Childs, J.D., et al. (2004). *Clin Biomech*, 19, 44-49.  
 Hinman, R.S., et al. (2002). *Arch Phys Med Rehabil*, 83, 1080-1086.

**ACKNOWLEDGEMENTS**

Supported by NIH grant RR16458

**Table 1:** Percent VL contribution to the total quadriceps force during stair descent.

Subject	% VL force (1 <sup>st</sup> Peak)	% VL force (2 <sup>nd</sup> Peak)
Control 1	36%	36%
Control 2	34%	36%
OA 1	34%	33%
OA 2	48%	45%

# EFFECTS OF PARTIAL MENISCECTOMY ON THE KNEE JOINT STRESS DISTRIBUTIONS

Sharadsinh P Vadher, Hamid Nayeb-Hashemi, Paul K Canavan, Grant M Warner

Northeastern University, Boston, MA, USA  
E-mail: sharad@coe.neu.edu

## INTRODUCTION

Meniscal tears are a common occurrence in the human knee joint. Orthopedic surgeons routinely perform surgery to remove a portion of the torn meniscus. This surgery is referred to as a partial meniscectomy. It has been shown that individuals who have decreased amount of meniscus are likely to develop knee osteoarthritis. This research analyses the stresses of knee joint upon various amounts of partial meniscectomy.

## METHODS

An axisymmetric finite element model of the human knee joint was developed and analyzed in Adina8.2 on UNIX platform.

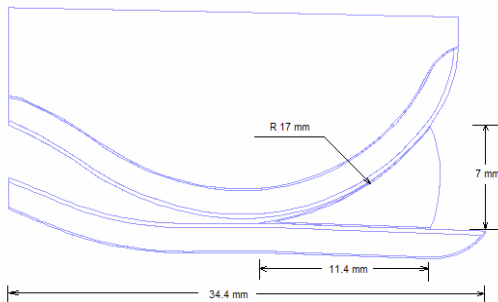


**Figure 1:** 2D axisymmetric model of knee joint consists of meniscus, tibio-femoral articular cartilage and portion of femur

The cartilage and meniscus are modeled as poroelastic materials. The articular cartilage is modeled with three layers (Adam 1998) which has been shown to be essential for proper knee joint simulation (Singh 2004). These three layers are superficial tangential layer, the middle and deep zones as one layer and the calcified part of the cartilage. Table-1 presents the material properties of

the meniscus, articular cartilage layers, and bone used in this study.

<b>Cartilage</b>	Transversely Isotropic poroelastic	$E_x=E_y=5.8\text{MPa}, E_z=0.46\text{MPa},$ $\nu_{xy}=0.0002, \nu_{yz}=0,$ $G_{xz}=0.37\text{MPa}, k=5.1 \cdot 10^{-15}$ $\text{m}^4/\text{Ns}, \Phi_m=0.25$
<b>Cartilage</b>	Isotropic poroelastic	$E=0.69\text{MPa}, \nu=0.018,$ $k=3 \cdot 10^{-15} \text{m}^4/\text{Ns}, \Phi_m=0.25$
<b>Calcified Cartilage</b>	Elastic	$E=10\text{MPa}, \nu=0.499$
<b>Meniscus</b>	Transversely Isotropic elastic	$E_x=100\text{MPa},$ $E_y=E_z=0.075\text{MPa},$ $\nu_{xy}=0.0015, \nu_{yz}=0.5,$ $G_{xy}=0.025\text{MPa}, k=1.26 \cdot 10^{-15}$ $\text{m}^4/\text{Ns}, \Phi_m=0.75$
<b>Bone</b>	Elastic	$E=400\text{MPa}, \nu=0.3$

**Table 1:** Material properties assigned to cartilage, meniscus, calcified cartilage and bone ( $E$  = Elastic modulus,  $\nu$  = Poisson ratio,  $k$  = Permeability,  $G$  = Shear modulus and  $\Phi_m$  = Solid volume fraction)

In this axisymmetric knee joint model (Fig 1), The maximum thickness of the cartilage is 2.4 mm (Eckstein 2001) in the center of the model. The thickness of the superficial tangential layer varies between 10 and 20 percent of the total thickness of the cartilage. A pressure of 0.17 MPa was applied at the top surface of the femur, which corresponds to half of the body weight of a 60 kg person. The full load was applied linearly in one second and then was kept constant for the next 59 seconds.

To consider the effect of partial meniscotomy on stress distribution, eight different cases have been analyzed. These

cases include a knee joint with an intact meniscus and a knee joint with various amount of meniscus removed from medial region (10%, 20%, 30%, 40%, 50%, 60% and 65% of total length of meniscus).

## RESULTS AND DISCUSSION

The results showed that the maximum normal stress (Contact stress) was located at the interface of bone and cartilage and Maximum normal stress in cartilage increases drastically up to 50% (Fig.2)

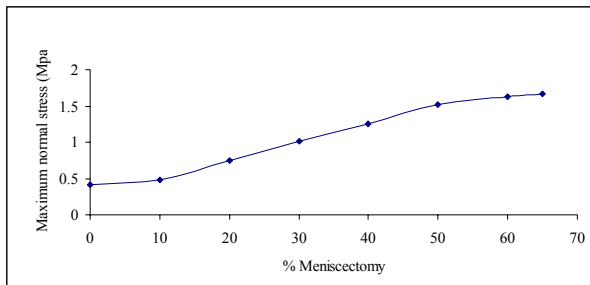


**Figure 2:** Maximum normal stress (contact stress) in the articular cartilage with respect to percentage removal of partial medial meniscectomy

The maximum shear stress was found in the meniscus because of its soft tissue material property. However, significant amount of shear stress develops in cartilage with percentage removal of meniscus.

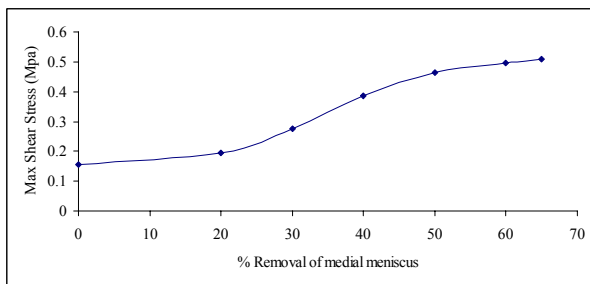


**Figure 3:** Maximum shear stress in the articular cartilage with respect to percentage removal of partial medial meniscectomy

After 65% of meniscectomy the maximal shear stress in the cartilage increased up to

225% compared to knee with intact meniscus. The contact area between femoral and tibial cartilage surface significantly increases up to 40% of the medial meniscus is removed.

## SUMMARY/CONCLUSIONS

Finite element analysis of knee joint performed to understand the effect of partial meniscectomy on stress distribution, both in cartilage and meniscus. The results showed that shear distribution of in the cartilage is little effective up to 20% medial removal of meniscus. However, with further removal, significant normal and shear stress developed in the cartilage, which could lead to its degeneration. Contact area, between tibio-femoral cartilage surfaces, also increased with percentage removed meniscus. This effect is more pronounced with 20% or more meniscus removal.

## REFERENCES

- Adam, C., Eckstein, F., Milz, S., Schulte, E., Becker, C. and Putz, R. (1998). *The distribution of cartilage thickness in the knee-joints of old-aged individuals measurement by A-mode ultrasound*. Clinical Biomechanics **13**(1): 1-10.
- Eckstein, F., Winzheimer, M., Hohe, J., Englmeier, K. H., and Reiser, M. (2001). *Interindividual variability and correlation among morphological parameters of knee joint cartilage plates: analysis with three-dimensional MR imaging*. Osteoarthritis Cartilage **9**: 101-111.
- Singh, A. (2004). *Finite Element Modeling and Analysis of the Human Knee Joint*. Computer System Engineering. Boston, Northeastern University. Master of Science.

# THE INFLUENCE OF MUSCLE LOADINGS ON DENSITY DISTRIBUTION AND EXTERNAL SHAPE OF THE PROXIMAL FEMUR

Ali Mazrban, Hamid Hashemi, Grant Warner and Paul K. Canavan

Northeastern University, Boston, MA, USA

E-mail: marzban.a@neu.edu

## INTRODUCTION

This paper presents an efficient method for simulating the bone remodeling procedure. This method is based on the trajectorial architecture theory of optimization and employs a truss-like model for bone. The truss was subjected to external loads including 5 point loads simulating the hip joint contact forces and 12 muscular forces at the attachment sites of the muscles to the bone. The strain in the links was calculated and the links with high strains were identified. The initial truss is modified by introducing new links wherever the strain exceeds a prescribed value; each link undergoing a high strain is replaced by several new links by adding new nodes around it using the Delaunay method. Introduction of these new links to the truss, which is conducted according to a weighted arithmetic mean formula, strengthens the structure and reduces the strain within the respected zone. This procedure was repeated for several steps. Convergence was achieved when there were no critical links remaining. This method was used to study the 2D shape of proximal femur in the frontal plane and provided consistent results to the CT data. The proposed method exhibited a similar capability in comparison with complicated conventional nonlinear algorithms, however, with a much higher convergence rate and lower computation costs.

## METHODS

In order to find the external shape of bone and the bone density distribution, we employ topology optimization. The initial design domain is a uniform rectangular plate which occupies a larger space than the anticipated final shape of the bone structure. The rectangle is meshed by 156 link elements and subjected to the actual loadings found on the proximal femur (Fig. 1). This consists of muscle contributions from the gluteus medius, gluteus minimus, gluteus maximus, psoas, iliacus, piriformis, adductor magnus, adductor minimus, and hip joint contact force.

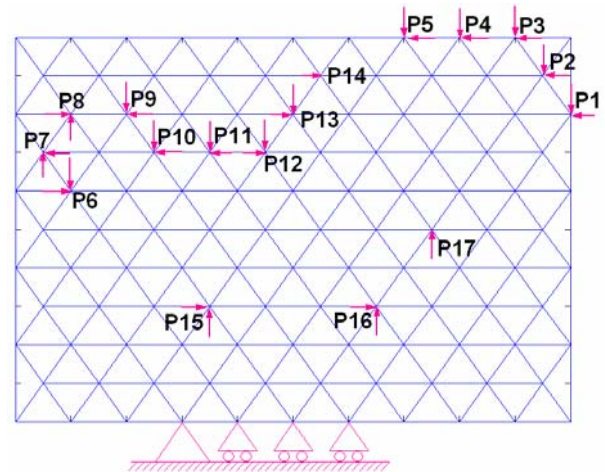


**Figure 1:** Loadings and boundary conditions

Strain in each link is calculated by using an algorithm written in Matlab. A critical strain threshold is established and links with strain above this value are identified.

Additional nodes are added near any critical link effectively stiffening the structure in the vicinity of the link. The strain is then recalculated in the structure. At each step critical links are identified and additional nodes are added. Convergence is a function of the critical strain; therefore a judicious choice of critical strain is needed to minimize computational time. We have found that the average of the absolute value of strains in the initial model is a good value for the critical strain threshold.

## RESULTS AND DISCUSSION

Figure 2 shows the model after convergence. The number of nodes after convergence is approximately 1500.

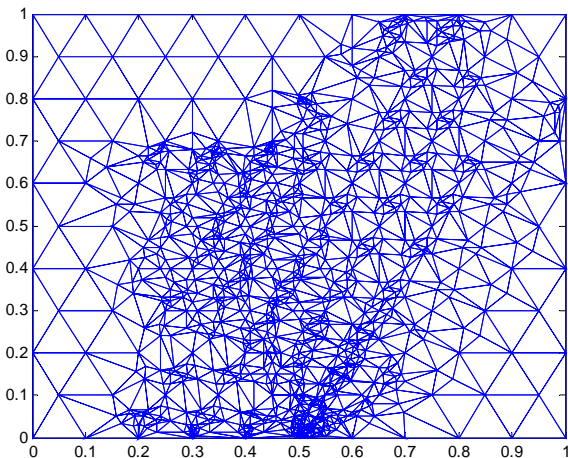


**Figure 2:** Model after the 10th run

As a final step a “density matrix” is developed to find the density distribution in the model. The model is divided into 100×100 small rectangles. The density is found by dividing the mass of the trusses in that rectangle by the volume of the rectangle, which is considered to have unit thickness. By assigning white color to the high density areas and dark color to the low density areas, a gray-scale image is generated which is shown in Fig. 3.

This image is like CT-scan images of the proximal Femur, and the density distribution

which is found by the density matrix is comparable with DEXA data. Each component of the density matrix can be compared with the density of actual bone in that zone from densitometry data.

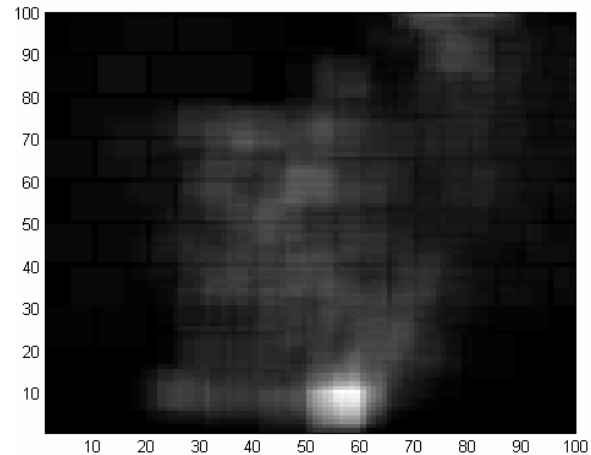


**Figure 3:** Density distribution of proximal Femur in the model after 10th Run

## CONCLUSIONS

The density distribution and the external shape of the proximal femur were predicted by this method. The effect of muscle loadings was investigated. The results are comparable with the CT-scan data.

## REFERENCES

- Wolff, J.L., (original publication in 1892)  
The law of bone remodeling (translated by Marquet, P., Furlong, R.), Springer, Berlin, 1892.
- C. Bitsakos, J. Kerner, I. Fisher, A. A. Amis, The effect of muscle loading on the simulation of bone remodeling in the proximal femur, *Journal of Biomechanics*, 38, pp. 133–139, 2005.
- Z. Xinghuaa, G. He, G. Bingzhao, The application of topology optimization on the quantitative description of the external shape of bone structure, *Journal of Biomechanics*, 38, pp. 1612–1620, 2005.

# CORRELATION BETWEEN MRI AND MECHANICAL MEASUREMENTS FOR PATELLAR STABILITY

Yiu Ming Wong<sup>1</sup> and Gabriel Ng<sup>2</sup>

<sup>1,2</sup> Hong Kong Polytechnic University, Hung Hom, Kowloon, Hong Kong  
E-mail: rswongym@polyu.edu.hk

## INTRODUCTION

Patellar instability is a common cause of patellofemoral pain. While the factors of patellar instability can be examined via mechanical and radiographic means, there is little documentation on the correlation between the imaging and mechanical findings. This study aimed to (I) develop and apply a mechanical method for quantifying passive patellar gliding, (II) record the axial and sagittal views of the knee with magnetic resonance imaging, and (III) correlate the results of I and II.

## METHODS

(I) Seventeen able-bodied volunteers (13 males, 4 females, aged 18-35 years) participated in the instrumented lateral patellar gliding test. A DC magnetic motion tracker with 1mm accuracy (pciBIRD, Ascension Technology Corp., Burlington, VT, USA) was used for this assessment. It consisted of a computer digital signal processing card, a magnetic field transmitter and a magnetic field sensor. The sensor was fixed on a patellar glide apparatus (Push-pull gage, Aikoh Engineering Co., Osaka, Japan) which was connected to a plastic linear slide and supported by a plastic lab jack. The transmitter was placed lateral to the tested knee with the subjects lying supine on a wooden bed. A laser-cross projector was located superior to the knees and emitted a cross mark on the bed for standardizing the position of subjects. With the subject's knees extended and feet together, the ankles and lower legs were secured. The patellar

glide apparatus was applied manually to glide the patella laterally in a consistent manner. The gliding force was 14.7N and both knees were tested separately with three continuous passive gliding movements. The average of the three movements was calculated to minimize random error as the linear displacement of the patella was collected for off-line analysis. In order to ensure relaxation of the vastus medialis (VM) muscle during the measurement, mechanomyogram (MMG) of VM was monitored via an air-coupled transducer (Pulse wave pickup, 21051D, Hewlett Packard, Palo Alto, CA, USA) and connected to a biofeedback unit (Myotrac, Thought Technology Ltd., Montreal, Quebec, Canada) which provided audio alarm once the MMG signal was over the preset threshold (fig 1).

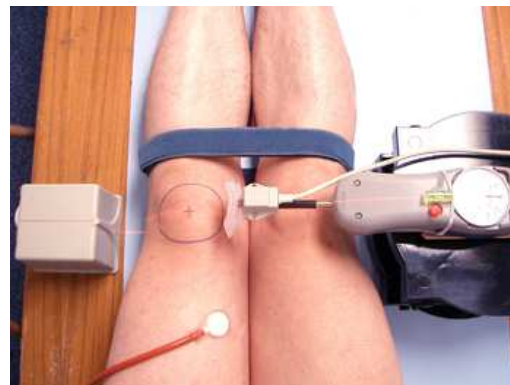


**Figure 1:** Lateral patellar gliding test

(II) Both knees of the subjects were examined with MRI (Magnetom Avanto, Siemens AG, Erlangen, Germany) for sagittal view (T1, TI: 600ms, TR: 1180ms,

TE: 4.32ms, slice thickness: 2mm) and axial view (T1, TR: 420ms, TE: 50ms, slice thickness: 3mm) in supine position with knees extended. The MR images were analyzed for the patellar tendon length/patellar length (TL/PL) ratio (Shabshin et al, 2004) and the lateral trochlear inclination (Yannick, et al 2000) (fig 2, 3).



**Figure 2:** TL/PL ratio

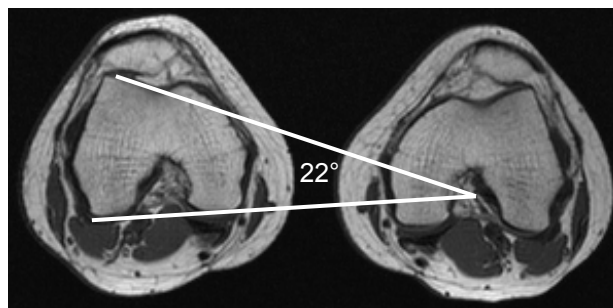


**Figure 3:** Lateral trochlear inclination

(III) Spearman's correlation coefficient was calculated to examine the relationships between the patellar gliding test and the radiographic measurements.

## RESULTS AND DISCUSSION

The results of patellar gliding were between 10.4-23.3mm. All subjects' TL/PL ratio was in the range of 0.74-1.33, and their lateral

trochlear inclinations were regarded as normal (13.5-25°). The Spearman's correlation coefficient between the lateral patellar gliding test and the TL/PL ratio was 0.125. The value between the lateral patellar gliding test and the lateral trochlear inclination was -0.458. These implied that the former has a weak association; and the latter has a moderate correlation. These results suggested that the lateral passive mobility of patella may not be related to the length of patellar tendon in terms of the TL/PL ratio among healthy subjects, but may associate with the shape of femoral trochlea in terms of the lateral trochlear inclination. As the angle of the lateral femoral trochlea appeared to be smaller, the patellar stability could be relatively compromised.

## SUMMARY/CONCLUSIONS

With the test on able-bodied subjects, the present findings seemed to suggest that the lateral trochlear inclination is a more sensitive index to reflect the lateral patellar instability than the TL/PL ratio.

The instrumented patellar gliding test was moderately correlated to the lateral trochlear inclination measured on MR images. As the gliding test is an inexpensive test for passive patellar stability when compared with the radiographic methods. Physicians may consider the quantitative patellar gliding as the first screening test for patellar disorders.

## REFERENCES

- Carrillon, Y. et al. (2000). Patellar instability: Assessment on MR images by measuring the lateral trochlear inclination-initial experience. *Radiology*, **216**, 582-585.
- Shabshin, N. et al. (2004). MRI criteria for patella alta and baja. *Skeletal Radiol*, **33**, 445-450.

# DEVELOPMENT OF A THREE-DIMENSIONAL KNEE JOINT MODEL FOR SIMULATION OF ACL INJURIES

Bhushan S. Borotikar<sup>1</sup>, Leendert Blankevoort<sup>2</sup>, Scott G. McLean<sup>1</sup>, Antonie J. van den Bogert<sup>1</sup>

<sup>1</sup>Cleveland Clinic Foundation, Cleveland, OH, USA

<sup>2</sup>Orthotrauma Research Center Amsterdam, Academic Medical Center, Amsterdam

E-mail: borotib@ccf.org

## INTRODUCTION

Rupture of the anterior cruciate ligament (ACL) remains a common sports injury, especially in females (Griffin et al., 2000). Most of these injuries are “non-contact” injuries that involve ground contact and its effect on the knee during landing tasks. Considerable differences in knee joint mechanics exist between individuals and between genders (Mizuno et al., 2005) and this may affect their risk of injury. Our long term goal is to incorporate subject-specific computational joint modeling into strategies for injury prevention. Here we present the development of such a model and we demonstrate its ability to predict ACL injury due to combined knee joint loading conditions.

## METHODS

MR images of the right knee were acquired from a human subject (male, 35 years) with no prior history of knee injury. Imaging was performed with Orthone 1.0 T extremity scanner (ONI medical systems Inc., Wilmington, MA), and with 3D Gradient Echo pulse sequence. Sagittal plane images were acquired at a resolution of 0.57mm x 0.78mm x 2.0mm (FOV = 150mm, 260x192 matrix) and with acquisition time of 4min, 51sec. Articular cartilage was segmented manually from the sagittal scans using in-house code written in Matlab 7.1 (Mathworks Inc., Natick, MA). A thin plate spline surface was fitted through the femoral, lateral tibial, medial tibial and patellar surfaces individually (Boyd et al, 1999) with smoothing adjusted to obtain a RMS fit error of 0.3mm for all the surfaces.

Anatomical insertion areas of patellar tendon, cruciate ligaments, and collateral ligaments were manually digitized. Each ligament was represented by two line elements. Force-deformation properties for ligaments and articular cartilage were taken from earlier work (Blankevoort et al., 1996). Initially, zero ligament strain was defined to occur with the joint in its imaged position. The model had 30 degrees of freedom: six for tibiofemoral joint motion, six for patellofemoral joint motion, and 18 for wrapping particles embedded in the MCL and quadriceps. Simulations were performed with software for 3D quasi-static joint modeling (Kwak et al., 1999).

To simulate ACL injury, we first applied valgus moment while the knee was constrained at 0° flexion. Valgus moment was increased in the steps of 10 Nm until the ACL reached 2000N, which was assumed to be the ACL failure load (Woo et al., 1991). We repeated the same series in the presence of anterior drawer force of 300N and 500N.



**Figure 1:** Knee joint model.

## RESULTS AND DISCUSSION

ACL force increased with valgus load and anterior drawer force (Figure 2). With anterior drawer, solutions could not be obtained at valgus loads higher than 85 Nm, possibly due to rotational instability in the model. At 85 Nm valgus and 500 N anterior drawer, ACL force was 1145 N, which approaches the failure load for young females (Chandrashekhara et al., 2005). Load sharing between MCL and ACL was influenced by loading condition (Figure 3). In combined loading, the force in the ACL often exceeded that in the MCL. After consideration of their respective failure loads, this may explain why isolated ACL injury can occur during valgus loading, leaving the MCL unharmed.

The loads applied during these simulations could potentially occur during sports movements, where valgus moments of 50 Nm valgus and 500 N anterior drawer have been reported (McLean et al., 2005; Simonsen et al., 2000).

Each ligament was represented by only two line elements, which might have caused rotational instability. Internal rotation was 28° at 85 Nm valgus and 500 N anterior drawer force. In order to obtain stable solutions at high loads, we had to increase the ACL and PCL resting lengths by 1% and 10% respectively. This may also have caused an underestimation of cruciate ligament loads.

Equilibrium states were solved in less than 8 seconds (SGI Octane), which is much less than a comparable finite element model. This allows the model to be used for post processing of dynamic simulations (200 loading states at 1 ms intervals) and Monte Carlo simulations. Further work will be aimed at obtaining subject-specific ligament properties and model validation using cadaveric experiments.

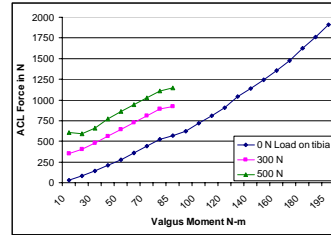


**Figure 2:** Model predicted ACL force due to valgus loading with combined anterior drawer loading.

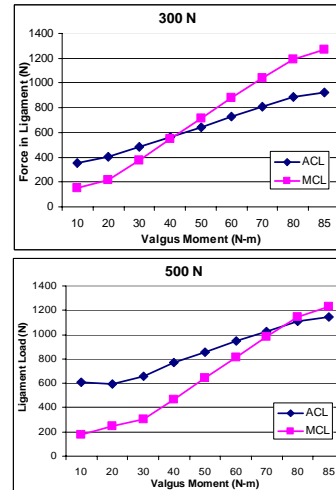


**Figure 3:** MCL-ACL load sharing at two levels of anterior drawer force.

## REFERENCES

- 1.Griffin et al., (2000). *JAAOS* **8**, 141-150.
- 2.Mizuno et al., (2005) *ORS 51<sup>st</sup> annual meeting*.
3. Boyd et al., (1999). *J Biomech Eng* **121**, 525-532.
- 4.Blankevoort et al., (1996). *J Biomech* **29**, 955-961
- 5.Kwak et al., (1999). *Comp Meth Biomech Biomed Eng* **3**, 41-64.
- 6.Woo et al., (1991). *Am J Sports Med* **29**, 217-225.
- 7.Chandrashekhara N et al. (2005) *Proceedings of XX<sup>th</sup> ISB Congress'05*, 428.
- 8.McLean et al. (2005) *Clin Biomech* **20**: 863–870.
- 9.Simonsen EB et al. (2000) *Scand J Med Sci Sports* **10** : 78-84.

## ACKNOWLEDGEMENTS

This work was supported by NIH grant R01 AR47039.

# MOTOR CONTROL IN OCCUPATIONAL BIOMECHANICS

Jaap H. van Dieën

Institute for Fundamental and Clinical Human Movement Sciences, 'Vrije Universiteit Amsterdam', the Netherlands

E-mail: j.vandieen@fbw.vu.nl Web: www.ifkb.nl

## INTRODUCTION

Variability and adaptability can be considered hallmarks of human motor behavior. In this presentation, I will argue that the conventional approach in occupational biomechanics needs to be rethought to accommodate these phenomena. Figure 1 summarizes the agenda that is implicit in most occupational biomechanics research. It should be noted that this model reflects the methodology used, i.e. inverse dynamics, but not causality. While this will probably be acknowledged by most researchers in the field, the consequences are often not sufficiently appreciated. When rearranging the model in Figure 1 to illustrate causality rather than methodology, two important aspects come to the fore (Figure 2). First, there is no deterministic relation between task and environment on one hand and motor behavior on the other hand. Second, mutual influences exist between musculoskeletal loading, musculoskeletal health, and the task.

## VARIABILITY

The term motor control suggests that a controller, the nervous system, determines motor behavior. The control exerted is dependent on demands defined by the task and the environment. Obviously, properties

of the individual performing the task, 'organismic constraints', play an additional role and introduce inter-individual variation that already presents a considerable challenge in occupational biomechanics. Moreover, motor control is determined by task, environmental and organismic constraints in a probabilistic sense only.

When an individual performs a given task repeatedly, considerable variance occurs in musculoskeletal loading, related to variations in the way the task is performed. I will present data on repetitive lifting, showing that the 95<sup>th</sup> percentile of the peak compression forces in a series of lifts performed by an individual exceeded the median by up to 39%. Obviously, this has important methodological implications. This variance must be taken into account in the design of biomechanical exposure assessment and biomechanical experiments to achieve sufficient statistical precision and power. The variance of loading in a given task also has an important conceptual consequence. A task that entails musculoskeletal loading that is on average below an injury threshold or normative guideline can and will at some point exceed this threshold, if the confidence interval is wide enough. Therefore, occupational biomechanics needs to consider the effect of constraints on both the mean and the variance of musculoskeletal loads.

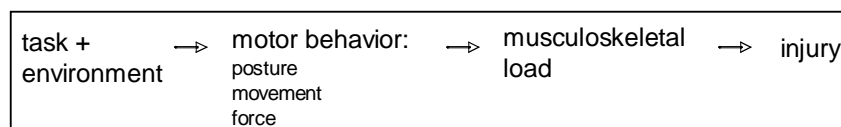


Figure 1: Implicit model underlying most occupational biomechanics studies,

## ADAPTATION

Above, motor control was described as control of the nervous system over the musculoskeletal system. It can more adequately be described as an interaction process of the nervous system, the musculoskeletal system, the task, and the environment. This implies that the task or environment can change both the behavior and the system itself (Figure 2).

Motor control can and will be adapted to changes in constraints, in a manner that may interfere with expected effects of interventions. Data from a recent mock-up study among experienced bricklayers will be presented to show that effects of ergonomic interventions on low back load are modified and mostly attenuated by behavioral modifications. Lowering the mass of sandstone blocks and optimizing their vertical position had less effect on back load than expected, because the bricklayers for example increased the horizontal distance to the blocks lifted and lifted faster.

In addition, the task and environment through musculoskeletal loading will change the state of the nervous and musculoskeletal system, e.g. due to fatigue, injury or training

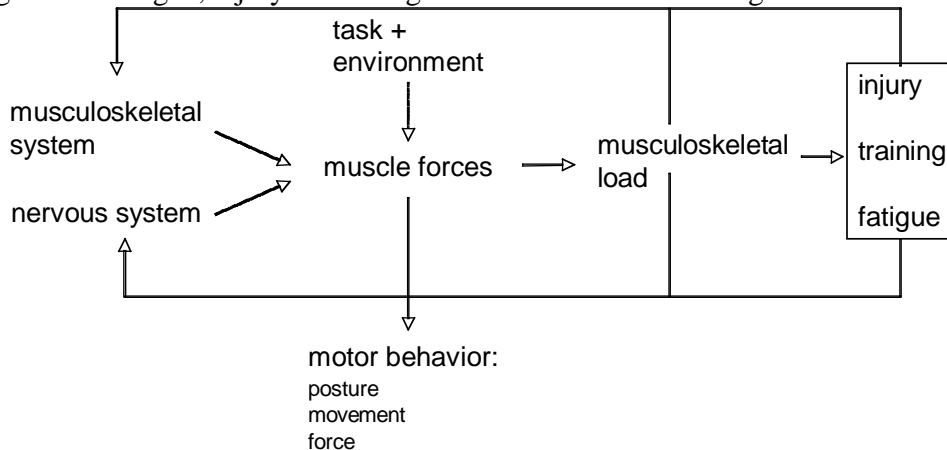


**Figure 2:** The probabilistic determination (dotted arrows) of muscle forces that in turn determine behavior and mechanical loads on the musculoskeletal system and the feedback involved.

(of skill and musculoskeletal tissues).

Especially, training effects complicate the relationship between task and injury risk and argue against the traditional view of musculoskeletal injury depicted in figure 1 and suggests that special circumstances may be needed to create an injury. These circumstances may involve perturbations e.g. due to balance loss, repeated loading as in fatigue fractures, or a temporary mismatch between the capacity of certain components of the system, e.g. due to faster adaptation of muscle than of bone.

## CONCLUSION

The relationship between task demands, mechanical loading and injury risk may be more complicated than appears implicitly assumed in occupational biomechanics. Perhaps the current approach to occupational biomechanics needs to be replaced by a more biological approach. This will complicate decision-making in ergonomic practice, but may help avoid undue claims falsified by limited success. On a more optimistic note, knowledge of motor control can also point to new interventions in ergonomics.

# Age related changes in multi-finger coordination during moment of force production tasks.

Halla Olafsdottir<sup>1</sup>, Wei Zhang<sup>1</sup>, Vladimir Zatsiorsky<sup>2</sup>, and Mark Latash<sup>1</sup>

<sup>1</sup> Motor Control Laboratory and <sup>2</sup>Biomechanics Laboratory, Department of Kinesiology  
Penn State University, University Park, PA, USA

E-mail: hbo101@psu.edu Web: <http://www.personal.psu.edu/faculty/m/l/ml111/index.htm>

## INTRODUCTION

The production of accurate rotational hand action is a component of many everyday tasks. Most previous studies of finger coordination focused on force production tasks. Unexpectedly, the studies showed better stabilization of the total moment of force by co-varied signals to individual fingers in spite of having no instruction or feedback on the moment of force (Latash, 2001). In force production tasks, elderly individuals show impaired stabilization of the moment of force in both pressing (Shinohara, 2003) and static prehension tasks (Shim, 2003). We hypothesized that elderly persons would show lower indices of a moment stabilizing synergy and higher indices of moment variability when they are explicitly required to produce accurate moment time profiles. We also expected elderly subjects to adopt an adaptive strategy involving the production of larger forces and larger antagonist moments.

## METHODS

Four piezoelectric sensors (Model 208A03, Piezotronics Inc.) were positioned on top of a wooden board and used to measure the vertical forces generated by the index ( $F_I$ ), middle ( $F_M$ ), ring ( $F_R$ ) and little ( $F_L$ ) fingers. Twelve elderly ( $77 \pm 4$  years old) and twelve young ( $26 \pm 3$  years old) subjects participated in the study. Subjects sat in a chair with their right arm resting on the table in front of them. The forearm was constrained with Velcro straps and a wooden piece placed in subjects palm helped to

maintain stable configuration of the hand and fingers. The main task required the subjects to follow an inverted trapezoidal template on a computer screen by producing a time profile of the total moment ( $M_{TOT}$ ) while pressing down on the sensors with all four fingers. Pressing down with the index and middle fingers, produced a positive (pronation; PR) moment, while pressing down with the ring and little fingers produced a negative (supination; SU) moment. Individual finger moment arms ( $d_I, d_M, d_R, d_L$ ) were defined about a point between the middle and ring fingers,  $d_I = d_L = 4.5$  cm and  $d_M = d_R = 1.5$  cm, thus  $M_{TOT} = d_I F_I + d_M F_M - d_R F_R - d_L F_L$ . The maximal pronation and supination moments were in elderly subjects set at 5% of the maximal moment produced by their index finger but for young subjects this level was set at 10%.

For each point in time the following variables were computed across trials for each subject: a) Total Force ( $F_{TOT}$ ) and its variance ( $V_F$ ) b) Total Moment ( $M_{TOT}$ ) and its variance ( $V_M$ ) c) Total agonist ( $M_{Ag}$ ) and antagonist ( $M_{Ant}$ ) moments where  $M_{Ag}$  is a moment produced that meets the task requirements but  $M_{Ant}$  opposes these requirements d) Uncontrolled manifold analysis (UCM) was used to compute  $\Delta V_F$  and  $\Delta V_M$ . All variables were further divided into five time intervals, Pre-Pronation (PR<sub>PRE</sub>), Pronation-Supination (PR-SU), Supination (SU), Supination-Pronation (SU-PR) and Post-Pronation (PR<sub>POST</sub>) and averaged across time within them.

## RESULTS AND DISCUSSION

All subjects were able to produce the required pattern of total moment (Fig. 1). In both age groups,  $F_{TOT}$  increased from the beginning to the end of the task but elderly subjects produced significantly larger  $F_{TOT}$  during supination than the younger subjects. Variance of the total force ( $V_F$ ) and of the total moment ( $V_M$ ) was larger in the elderly subject group. This difference was particularly prominent during SU and SU-PR phases for  $V_F$ , and during the ramp moment changes (PR-SU, SU-PR) for  $V_M$ .

Elderly subjects also produced larger  $M_{Ant}$  during supination, while in pronation the performance of the two groups did not differ.

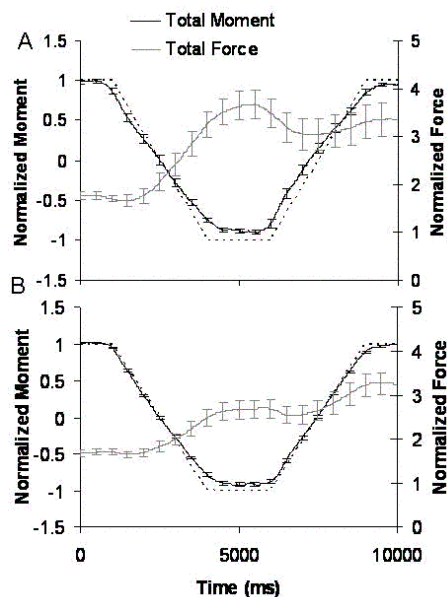


**Figure 1:** Average performance of the total moment (black lines) and total force (grey lines) of A. elderly and B. young subjects with standard error bars.

The young subjects were able to stabilize the time profile of total moment as reflected in positive  $\Delta V_M$  values across the task (Fig. 2B) while elderly subjects were on average not able to do so as is reflected in  $\Delta V_M$  value that oscillates about zero (Fig. 2A).

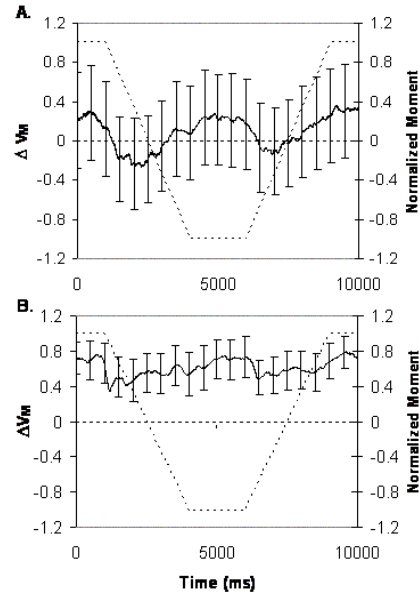


**Figure 2:** Average profile of  $\Delta V_M$  for A. elderly and B. young subjects with standard error bars.

## SUMMARY/CONCLUSIONS

We conclude that elderly subjects have impaired ability to coordinate signals to fingers in tasks that require the production of accurate  $M_{TOT}$  pattern, especially during supination. This is manifested in larger  $F_{TOT}$ ,  $V_F$ ,  $V_M$  and  $M_{Ant}$ . Young subjects showed a moment stabilizing synergy while elderly subjects did not. The lack of moment stabilizing synergies may be causally related to the documented impairment of the hand function with age.

## REFERENCES

- Latash, M.L. et al. (2002). *Exp Brain Res*, **141**, 153-165.
- Shim, J. K. et al. (2004). *J Appl Physiol*, **97**, 213-224.
- Shinohara, M. et al. (2003). *Exp Brain Res*, **156**, 282-292.

## ACKNOWLEDGEMENTS

NIH grants AG-018751, NS-035032, AR-048563, and M01 RR-10732.

# NEEDS FOR AND POTENTIAL APPLICATIONS OF BASIC BIOMECHANICS RESEARCH IN OCCUPATIONAL BIOMECHANICS

Maury A. Nussbaum

Virginia Tech, Blacksburg, VA, USA  
E-mail: nussbaum@vt.edu

## INTRODUCTION

As a sub-discipline of biomechanics, occupational biomechanics has experienced extensive growth over recent decades. Chaffin et al. (2006) have defined the area as “the science concerned with the mechanical behavior and limitations of the musculoskeletal system and component tissues when a person performs an exertion in industry (p. xiii).” As an application-oriented discipline, drawing on a broad range of basic biomechanics theory and technology, occupational biomechanics also serves as one of the major components of the ergonomics discipline, which is concerned with more general goals of improving the design of systems involving humans.

The purpose of this paper is to highlight several major topics within the occupational ergonomics discipline, specifically those that represent important current needs to advance the field, and to which research in basic biomechanics can make important contributions. Throughout, occupational biomechanics and (physical) ergonomics are treated in a broad sense, as encompassing the study of the physical (mechanical, physiological, etc.) interactions of workers with work systems (tools, material, etc.).

A major motivation for research in these fields is the continued personal, economic, and societal burden associated with work-related musculoskeletal disorders (WMSDs). Over 500,000 cases were reported in 2001,

with nearly half involving more than 20 days away from work (NIOSH, 2006). While ongoing research has led to a reduction of risk in some areas, prevalence rates overall appear to be fairly constant. As such, a need is apparent for improvement in the theory, technology, and application of occupational ergonomics and biomechanics.

## METHODS

In order to gain some understanding of current issues that may be hindering such improvement, a survey was conducted of a number of active researchers. This was in no way meant to be a comprehensive investigation, but rather to learn what these individuals believed were substantial current needs to advance understanding and prevention of WMSDs. Roughly 40 individuals were contacted, nearly half of whom responded. In order to summarize the variety of input received, I used as a framework the National Occupational Research Agenda (NORA) material that has been generated by the National Institute for Occupational Safety and Health (NIOSH). The interested reader can refer to the citations provided for additional detail (NIOSH, 1995; 2001; 2006). In the following, major categories of research priorities are taken from the NORA documents. Specific items are drawn from both the input I received as well as my own opinions and limited to those thought most relevant to the current audience.

## RESEARCH NEEDS

### Disease and Injury

- Improved understanding of injury mechanisms and subsequent pain generation
- Use of biomechanics to identify stages of injury/illness, recovery, rehabilitation, and ability to return to work
- Addressing lower extremity injuries
- Understanding the nature of WMSDs (e.g. accident vs. systematic overload)

### Work Environment and Workforce

- Assessing injury in the modern workforce (e.g. those providing service/information)
- Pathophysiological pathways of psychosocial risk factors
- Risks in ‘special populations’, such as the aged and obese (e.g. developing and adapting biomechanical models)
- Quantification of relative contribution and interactions within and between risk factor ‘domains’ (physical, personal, psychosocial)

### Research Tools and Approaches

#### *Control Technology*

- Developing ‘safe’ workload limits (e.g. posture, repetition, force),
- Tissue-specific, task-specific, and occupationally-relevant tissue tolerances and workload limits
- Relationships between short-term perceptual responses and long-term risk

#### *Exposure Assessment Methods*

- How to quantitatively describe complex tasks (e.g. peak, mean, probability dist.), and data reduction procedures for long-term or continuous exposure measures
- How to accumulate risk for jobs composed of sets of different sub-tasks
- Methods to facilitate detailed field assessment

- Determining necessary levels of accuracy in laboratory- or field-based models (e.g. sensitivity analyses)
- Using virtual reality and motion capture for proactive assessment
- Efficacy of ‘macro’ indicators or metrics of risk (e.g. fatigue, stability, technique)
- Biomarkers for musculoskeletal trauma

#### *Intervention Effectiveness Research*

- Valid and usable human simulation models
- Merging biomechanical analysis with financial estimates (cost-benefit)
- Determining necessary reductions in exposure to reduce injury risk

I hope that this paper and the symposium stimulate continued development of occupational biomechanics research and application, and also inform investigators in basic biomechanics disciplines to the potential applications of their efforts.

## REFERENCES

- Chaffin, D.B. et al. (2006). *Occupational Biomechanics (4<sup>th</sup> ed.)*, Wiley: NJ.
- NIOSH (1995) DHHS (NIOSH) Publication No. 1996-115.
- NIOSH (2001) DHHS (NIOSH) Publication No. 2001-117.
- NIOSH (2006) DHHS (NIOSH) Publication No. 2006-121.

## ACKNOWLEDGEMENTS

Thanks to the following individuals, each of whom provided fruitful ideas, that are contained in one form or other in this paper:

Kari Babski-Reeves, Don Chaffin, Rakié Cham, Kermit Davis, Patrick Dempsey, Jack Dennerlein, Kurt Hegmann, Simon Hsiang, Richard Hughes, Pete Johnson, Karl Kroemer, Paul Kuijer, Jim Potvin, David Rempel, Mark Redfern, Gary Mirka, Jaap van Dieën, Jeff Woldstad

# SIMULATION-BASED TREATMENT PLANNING FOR KNEE OSTEOARTHRITIS

Benjamin J. Fregly<sup>1</sup> and Jeffrey A. Reinbolt<sup>1</sup>

<sup>1</sup> University of Florida, Gainesville, FL, USA  
E-mail: fregly@ufl.edu Web: www.mae.ufl.edu/~fregly

## INTRODUCTION

Few clinical interventions exist that can slow the progression of knee osteoarthritis (OA). A conservative surgical intervention is high tibial osteotomy (HTO), which shifts some of the contact load from the diseased medial to the healthy lateral compartment. A more conservative intervention to achieve this goal is gait modification (e.g., toeing out). For both interventions, the peak knee adduction torque during gait has been identified as a surrogate for medial compartment load and a predictor of long-term clinical outcome (Andriacchi, 1994).

This study presents a new simulation-based method for planning conservative treatment of knee OA. The method utilizes dynamic optimization of a patient-specific full-body gait model to predict how rehabilitation or surgical intervention will alter the patient's peak knee adduction torque. First, we use the method to design a novel gait motion that significantly reduces both adduction torque peaks. Next, we extend the method to predict the peak knee adduction torque for different measured gait motions. Finally, we apply the method to predict the effect HTO surgery on knee adduction torque changes.

## METHODS

We constructed a dynamic, patient-specific, full-body gait model for a single patient with knee OA. The three-dimensional model possesses 27 degrees of freedom (DOFs) composed of gimbal (3 DOFs – hips and back), universal (2 DOFs – ankles and shoulders), and pin (1 DOF – knees and

elbows) joints, with a free joint (6 DOFs) between the ground and pelvis. We calibrated the model's joint and inertial parameters to gait and isolated joint motion data collected from the patient (Reinbolt *et al.*, 2005). The patient gave informed consent for all experimental data collection.

Using this model, we performed inverse dynamics optimizations to predict patient-specific gait modifications to reduce both knee adduction torque peaks. The cost function minimized the knee adduction torque subject to reality constraints that tracked the patient's nominal gait kinematics and kinetics. After attempting to learn the predicted gait modifications, the patient was retested to assess their effectiveness at reducing both adduction torque peaks simultaneously.

We also formulated additional optimization problems to evaluate how patient-specific cost function weights affect the prediction process. We used surrogate modeling to identify cost function weights for the individual leg control torques such that minimization of the cost function yielded the patient's adduction torque curve and motion for toe out gait given his nominal gait data as the initial guess. Next, we evaluated the resulting cost function weights by predicting the patient's wide-stance gait adduction torque curve, again starting from his nominal gait data. Finally, we utilized the same cost function weights to predict how HTO wedge angle would alter the patient's peak knee adduction torque post-surgery. All predictions were evaluating using either the patient's own experimental gait data or published data from HTO studies.

## RESULTS AND DISCUSSION

The first set of optimizations predicted “normal looking” gait motions that significantly reduced both adduction torque peaks (Fig. 1). The predicted reductions were 32 to 56% in both peaks, depending on the cost function weights. These reductions were produced by three synergistic kinematic changes that drove the knee medially. After gait retraining to learn the predicted modifications, the patient achieved reductions of 32 to 55%. The kinematic and kinetic changes achieved by the patient were generally in agreement with the optimization predictions. The main difference was in the post-training pelvis coronal tilt.

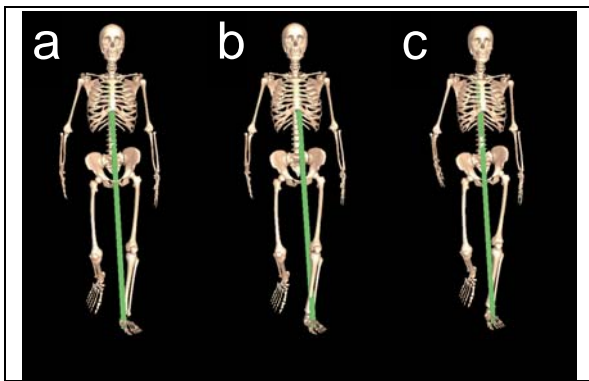


**Figure 1:** a) Nominal, b) Predicted, and c) Post-training gait motion. The moment of the patient’s ground reaction force vector about his knee center was significantly decreased.

When the cost function weights were calibrated to the patient’s toe out gait motion, the predicted adduction torque peaks were in excellent agreement with the patient’s experimental peaks (Fig. 2a). When the same weights were used to predict the patient’s experimental peaks for wide stance gait, the agreement was again excellent (Fig. 2b). Finally when the same weights were used to predict how HTO wedge angle would affect the patient’s post-surgery adduction torque peaks, the results were in good agreement with published data (Fig. 2c; Bryan *et al.*, 1997).

While these initial results are encouraging, application of the method to additional patients is needed to evaluate and refine it further prior to clinical implementation.

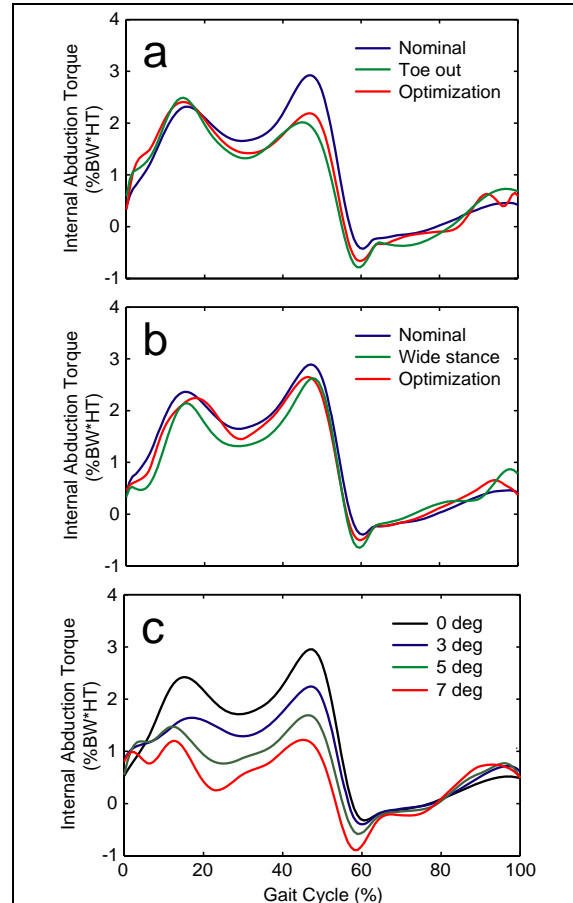


**Figure 2:** Optimization predictions of the internal abduction torque curve for a) Toe out gait, b) Wide stance gait, and c) high tibial osteotomy using the patient-specific cost function weights.

## REFERENCES

- Andriacchi, T.P. (1994) *Ortho. Clinics North America* **25**, 395-403.  
Bryan, J.M et al. (1997) *43rd ORS*, 718.  
Reinbolt, J.A. et al. (2005) *J. Biomech.* **38**, 621-626.

## ACKNOWLEDGEMENTS

This work was funded by the Whitaker Foundation



# **WHOLE BODY LOCOMOTIVE BIOMECHANICS IN SLIPS, TRIP AND FALLS.**

Mark S. Redfern

Department of Bioengineering,  
University of Pittsburgh, Pittsburgh, PA, USA  
E-mail: mredfern@pitt.edu

## **INTRODUCTION**

Slips, trips and falls continue to be a serious public health concern across the age-span. Biomechanical approaches have been used to understand the problem and reduce fall-related injuries, with some success. However, there is still much to be done. The field of biomechanics can further address the problem of slips, trips and falls and aid in further reducing the incidence of injury. This is particularly true in the workplace. The following sections describe the seriousness of the problem, with particular reference to the occupational sector. In addition, gaps in the field that need to be addressed in the future to reduce injuries are described.

## **EPIDEMIOLOGY OF OCCUPATIONAL SLIPS AND TRIPS**

Slips are recognized as a major contributor to falls. They were the most frequent event leading to fall and overexertion related injuries in the Swedish labor force (Courtney et al. 2001) and were the most common fall initiating event for employees in the UK (Gao and Abeysekera 2004). The US National Health Interview Survey questionnaire administered by the National Center for Health Statistics in 1997 revealed a clear majority (64%) of work-related falls were attributable to slipping, tripping, or stumbling and indicated that 43% of occupational same-level fatal falls were most commonly triggered by a slip (Courtney et al. 2001). According to the

Bureau of Labor Statistics (2003), nearly 30% (28.7%) of workers that sustained injuries from slips and/or falls missed 31 days of work or more. Further, 14% of accidental deaths in the workplace were reportedly caused by falls (BLS 2004). In addition to the risk of fall related injuries and fatalities, slip recovery efforts have been shown to contribute to high rates of overexertion injuries (Courtney and Webster 2001). De Laet and Pols (2000) estimated that the annual direct cost of all fall-related occupational injuries in the U.S. alone was approximately six billion dollars.

The risk of fall accidents increases with age. A 10-fold increase in the incidence of falls was reported in older adults (65+) compared to younger individuals (16-64) (Thomas and Brennan 2000) and Lloyd and Stevenson (1992) indicated that while slips and trips caused 32% of falls for young people, 67% of falls for the elderly were initiated by slips. Falls on the same level caused roughly 20% of all injuries to older workers as compared to around 10% for the general population with "floor and ground surfaces" listed as the most common source of non-fatal injuries among workers in the 55 year and older age group (Personick and Windau 1995). In 2004, over one third (39%) of the occupational fatal fall victims were 55 and older (BLS 2005), more than double that age group's share of the work force (16%) (BLS 2005).

## ERGONOMICS AND BIOMECHANICS

An ergonomics approach to reducing injuries due to slips, trips and falls is appropriate; namely, investigate the interface between the person and the environment. The principal environmental factors here are floors, shoes, contaminants, visual affordances, lighting, handrails, ramps, ladders, and steps. Human factors that are involved include postural control, motor coordination, vision, proprioception, vestibular function, and strength. Even cognitive variables, specifically attention, play an important role. However, the interactions between the human factors and environmental factors are critical.

Biomechanics has proven very useful in addressing falls from an ergonomics approach. For example, slip potentials during walking, load carrying, and other tasks have been evaluated using force plates by comparing the generated ground reaction forces to the coefficient of friction of the shoe/floor/contaminant interface. This has led to improvements in the design of workplace flooring to maintain adequate friction. Other studies have used whole-body dynamics analysis to investigate stability during various work-related tasks, leading to redesign of jobs or environments.

### FUTURE APPLICATIONS

There are a number of areas where biomechanical approaches can continue to lead to reductions of injuries due to occupational falls. The following are some specific applications:

*Slip potentials during work:* Understanding the frictional requirements for various tasks in the workplace will lead to improvements in the selection of floors and shoes towards the reduction of slips and falls.

*Ladders, Ramps, and Steps:* There is limited understanding of the biomechanical implications of these designs with respect to falls. Further study of the interface of the worker and these environments is needed.

*Population-specific studies:* Biomechanical studies of special populations are necessary to understand specific design needs to reduce injuries. The older adult population is one group in particular where studies will yield knowledge necessary to make modifications to the environment to reduce age-related falls in the workplace.

*Human/environmental factor interactions:* The previously mentioned human factors interact with environmental factors to impact the biomechanics of locomotion and task performance. Research into these effects will result in new designs to reduce high fall risk situations.

### REFERENCES

- Courtney, T et al. (2001). *Ergonomics*, **44**, 1118-1129.
- Courtney, T and Webster, B (2001), *J. AIHA*, **62**, 622-632,
- Gao and Abeysekera (2004) *Ergonomics*, **47**, 573-598.
- Bureau of Labor Statistics (2005) Report USDL-05-1598.  
BLS 2004
- De Laet and Pols (2000) *Baillieres Best Pract Res Clin Endocrinol Metab*, **14**, 171-179.
- Thomas and Brennan (2000) *BMJ*, **320**, 741-744.
- Lloyd and Stevenson (1992) *Mech Eng Trans (Australia)*, **ME17**, 99-104.
- Personick and Windau (1995) *Fatal workplace injuries in 1993*, US Dept Labor.



# THE SQUEAKS IN YOUR SNEAKS: VIBRATIONS AT THE SHOE-SURFACE INTERFACE

Martyn Shorten and Xia Xi

BioMechanica LLC, Portland, OR, USA

E-mail: Martyn.Shorten@biomechanica.com Web: www.biomechanica.com

## INTRODUCTION

Contact between rubber-soled shoes and indoor sports surfaces commonly results in brief, high-pitched “squeaks” (Fig. 1). The classical Amontons-Coulomb friction paradigm assumed by most slip-resistance research does not accommodate vibration or sound generation. Consequently, an examination of this phenomenon offers the possibility of novel insights into the mechanics of shoe-surface interaction.

During *ad hoc* experiments with human subjects performing cutting movements on a sample of wood sports flooring, we have noted that shoes with different sole patterns elicit squeaks with a characteristic frequency. Also, squeaks appear to occur only when the shoe sole is lightly loaded (at the beginning and end of ground contact) and during relative sliding of the shoe and surface.

It is known from studies of brake “squeal” and other “stick-slip” phenomena that self-induced vibrations, and audible sounds, can occur when the mechanics of contact between two surfaces involves both elasticity velocity-dependant friction. The polymers athletic shoe soles are non-linearly elastic and do not demonstrate classical linear friction behavior. (Van Gheluwe, 1983; Valiant, 1987).

This study examined the nature and provenance of the “squeaks” induced by relative sliding motion, and their consistency with stick-slip vibration theory.

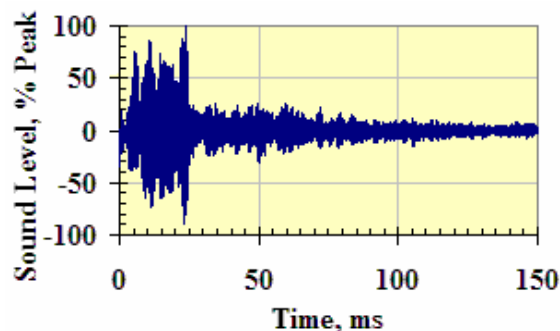


**Figure 1:** Example of a 5 kHz “squeak” elicited during a basketball play action.

## METHODS

Squeaks elicited by two basketball shoes with different “herringbone” sole patterns were digitally recorded with 24-bit resolution at a sample rate of 96 kHz and subjected to frequency spectral analysis. The sliding friction coefficients of the same shoes on a sample of polyurethane coated maple flooring were measured using a standard test method (ASTM F2333). Tests were performed with normal loads on the forefoot ranging from 50 to 1000 N and sliding velocities between 0.03 to 0.5 m s<sup>-1</sup>. Sliding motions were induced by means of computer controlled, linear actuator. Normal and tangential loads at the shoe-surface interface were recorded with an AMTI force plate, sampled at 500Hz.

## RESULTS AND DISCUSSION

Finite element models of generic herringbone structures predict natural frequencies above 4.0 kHz, with low order vibration modes clustered in a narrow range of frequencies. This prediction is consistent

with the observation that the squeaks from the two shoe samples occupy distinct, narrow frequency bandwidths centered at ~5.0 and ~6.0 kHz respectively (with harmonics observed at approximately double those frequencies; Fig. 2). Consequently the squeaks would appear to be the result of vibrations in the rubber herringbone structures rather than vibrations of the surface of other shoe components.

Traction tests results revealed a strong dependency of the sliding friction coefficient on the applied normal force and on sliding velocity at the slowest of the speeds considered (Figure 2). These nonlinear behaviors allow the possibility of audible stick-slip vibrations at the shoe-surface interface. However, basic stick-slip models (Bhushan, 1999; pp 382 &c.) must be modified to accommodate our observations. Adding non-linear dependence of the friction coefficient on normal force to basic stick-slip models has a non-linear effect on vibration amplitude, such that audible vibrations would be produced only when the normal force is within a limited, low range.

Based on our limited observations, the best explanation of the squeaks that we can offer is as follows:

The herringbone structures of the shoe outsole are induced to vibrate at their low-order natural frequencies by stick-slip contact with the surface. Their occurrence is limited to low normal force conditions by the non-linear force-dependance of the friction coefficient and by heavy damping at higher normal forces.

## REFERENCES

ASTM Standard F2333 (2001). ASTM International, West Conshohoken, PA.  
 Bhushan, B. (1999) *Principles and Applications of Tribology*. Wiley, New York.

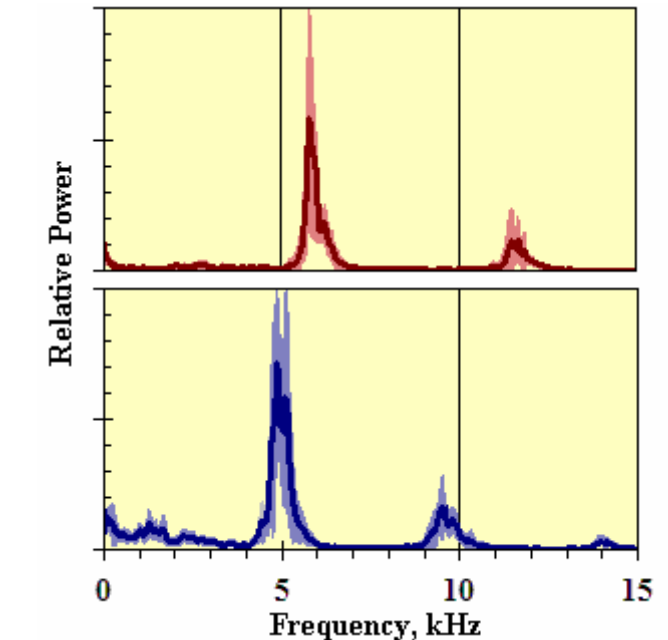


**Figure 2:** Amplitude-Frequency Spectra of squeaks from two basketball shoes with different sole patterns

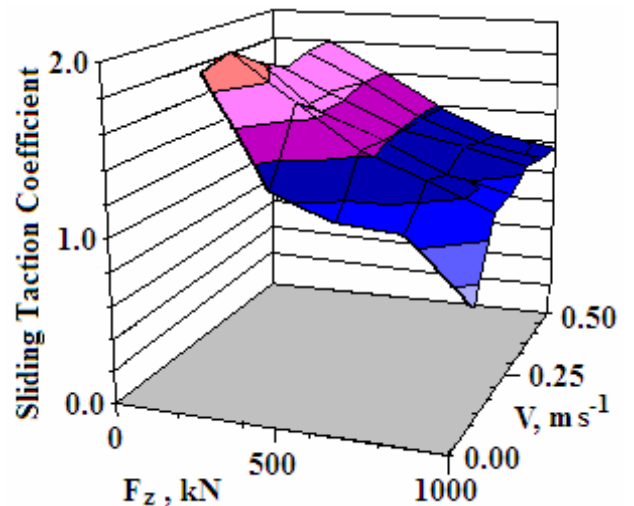


**Figure 3:** Sliding traction (friction) coefficient as a function of normal force ( $F_z$ ) and sliding velocity ( $V$ ).

Van Gheluwe, B. et al (1983). *Biomechanical aspects of sports shoes and playing surfaces*.(Ed. Nigg & Kerr) University Printing, Calgary; pp 161-168  
 Valiant, G.A. (1987). *J. Biomechanics*, **20**, 892.

## Measurement of Skeletal Kinematics from Fluoroscopy: Techniques, Validation and Accuracy for Real-World Applications

Scott Tashman<sup>1</sup>, William Anderst<sup>1</sup>, Stephanie Brock<sup>2</sup> and Michael Bey<sup>2</sup>

<sup>1</sup> University of Pittsburgh, Pittsburgh, PA, USA

<sup>2</sup> Henry Ford Health System, Detroit, MI, USA

E-mail: tashmans@upmc.edu

Accurate measures of musculoskeletal kinematics are essential for understanding the function of healthy joints, the impact of injury or disease, and the effectiveness of orthopaedic treatment. Dynamic radiography is the only currently available imaging modality that offers the potential for:

- High frame rates
- Sub-mm accuracy
- Freedom from skin motion artifact
- Testing of dynamic, functional, high-loading motion activities (e.g. walking, running, jumping, throwing, etc)

The advantages of this technology are now widely recognized, as evident from the growing number of laboratories that either have or are developing radiographic systems for kinematic studies. These vary considerably in hardware and analysis techniques, ranging from a single conventional C-arm fluoroscopy unit (commonly available in most hospitals) to custom-designed configurations that can provide biplane imaging for a wide variety of movements and joints. The accuracy of these systems varies with design and application, and has in general not been well characterized. A lack of consensus in this relatively young field as to how these systems should be evaluated has also made direct comparisons between systems difficult. The goals of this symposium talk are to discuss some of the design considerations for dynamic radiographic imaging systems, consider different approaches for evaluating measurement accuracy, and report some of our efforts to

characterize performance during real-world applications.

X-ray based motion analysis is complex, expensive and exposes subjects to ionizing radiation. Thus, its use is justified only for studies that require greater measurement accuracy than more conventional methods. Examples include investigations of in-vivo ligament function or cartilage-level interactions of the articulating surfaces of a joint. These applications require tracking six degree-of-freedom bone pose with accuracy consistently better than 1 mm/1 degree. Single-plane fluoroscopy systems have not been able to achieve this level of accuracy, due to uncertainty of position along the direction of the x-ray beam. This requires a priori assumptions to be made about the “important” movement directions, and dictates image views (e.g. sagittal) that may be prone to limb/bone overlap. Biplane systems can provide consistently high 3D accuracy and robust tracking. However, actual performance depends upon a number of factors related to the hardware design, analytical methods and specific application.

Dynamic biplane imaging system hardware should be designed to achieve:

- The best possible x-ray image quality
- The largest possible field of view
- Freedom of movement within the imaging area
- Positioning flexibility to enable imaging of a variety of joints/movements

These goals are often conflicting. C-arm systems are readily available and easy to

use, but tend to restrict freedom of movement. The gantry system used at Henry Ford offers a large area of unrestricted movement, at the cost of more limited flexibility for imaging configuration.

Image quality is highly dependent on both hardware configuration and application. It varies with imaging system properties (noise, contrast, resolution), radiographic protocol (kVp, mA), exposure time per frame, source-subject-detector distance, density of imaged tissues and limb movement speed. Higher x-ray power leads to better-quality images, particularly for fast movements where short exposure times are essential to minimize image blur. Many commercial fluoroscopy systems were designed primarily for static imaging, and are inappropriate for dynamic studies. High-power, high frequency pulsed x-ray generators can significantly reduce radiation dose while maximizing image quality.

The level of image quality necessary to achieve accurate 3D bone tracking depends upon the method used to extract 3D information from the x-ray image pairs. Radio-stereophotogrammetric (RSA) methods, employing implanted fiducial markers (e.g. tantalum beads), can achieve very good accuracy ( $\pm 0.1$  mm) even from relatively noisy, low-resolution images. However, recent efforts have focused on techniques utilizing some form of model or shape-based tracking, as they do not require an invasive procedure for marker implantation. These techniques vary considerably in technical approach, but all are much more dependent on image quality, particularly for identifying edges between bone and soft tissue as well as internal bone features. Methods previously applied for tracking metal implants (e.g. for TKA) may not be suitable for natural bone tracking, due to the huge difference in relative radiographic contrast between bone and high-density metals. Performance may also

depend on bone size, density and shape, the volume of surrounding soft tissue and the presence of overlapping objects in the image field. The influences of these various factors on tracking accuracy are difficult to predict *a priori* for a particular application.

Thus, it is essential that validations be performed to determine performance for each hardware/software system under *real-world* conditions, i.e. for the bones/joints in their natural configuration (including overlap with other bones/soft tissues, etc), moving at appropriate speeds, using radiographic protocols approved for *in vivo*, human use. Validation requires a “gold standard” for comparison; repeatability studies alone do not assess accuracy. This presents a significant challenge for *in vivo* validations. However, reasonable results can be achieved using a high-precision positioning system to move a joint *ex vivo*, provided the testing adequately simulates the real-world conditions described above.

An attractive alternative is to use a tracking technique of established accuracy for comparison with model-based radiographic tracking, enabling validation during arbitrary joint motions. Using our previously validated dynamic RSA methods, we are able to evaluate tracking performance for nearly any motion or joint, either *in vivo* or *in vitro*. We have completed accuracy studies for the tibio-femoral joint, the patello-femoral joint and the gleno-humeral joint, with demonstrated accuracy in the range of 0.2 to 0.5 mm in translation and 0.3 to 1.6 degrees in rotation. We have also shown that soft tissue/bone overlap and image quality can have a significant effect on real-world measurement accuracy. These results further support the need for joint, application and system-specific validation of x-ray based measurement methods.

# ANALYSIS AND MODELING OF GAIT DISABILITY DUE TO STROKE

D. Casey Kerrigan, Paul Allaire, and Patrick Riley

University of Virginia, Charlottesville, VA, USA

E-mail: dck7b@virginia.edu Web: <http://www.healthsystem.virginia.edu/internet/pmr/>

## INTRODUCTION

Modeling can be used to improve the effectiveness of clinical gait analysis (Cooper, Quatrano et al. 1999). We use a spectrum of models, ranging from fundamental conceptual models, e.g., the determinants of gait, to complex computer-based forward-dynamic musculoskeletal models. This presentation illustrates how we have used various models our quest to better understand and treat gait disability due to stroke.

## METHODS

The “determinants of gait,” originally described by Saunders et al. (Saunders, Inman et al. 1953) as a **conceptual model**, has value because it addresses two fundamental issues: 1) how local impairments affect global disability, and 2) how movement patterns affect and are affected by patient strength and endurance. A rigid link-segment **kinematic model** facilitated refining and quantifying the determinants of gait.

Impairments are frequently described in imprecise language, and are thus, immeasurable. The use of kinematic and **inverse dynamic models** in modern motion analysis laboratories permit, indeed force, the development of precise, quantitative definitions of gait impairments.

Using these precise measurements of impairment as a starting point, **dynamic models** can then be used to determine how impairment contributes to disability. These models allow us, in the cyber world, to isolate the effects of individual impairments that, in the real-world, only occur in the presence of other impairments or compensations. They also allow us to

estimate physical and physiological parameters that are currently immeasurable. These computer models will be the basis for **model-based design** of the next generation of prosthetics and orthotics, and of rehabilitation technology.

## RESULTS

**Determinants of Gait:** We first conducted a series of studies to quantify center of mass (CoM) excursion (Kerrigan, Viramontes et al. 1995; Kerrigan, Thirunarayan et al. 1996; Thirunarayan, Kerrigan et al. 1996), and assess its significance. (Duff-Raffaele, Kerrigan et al. 1996; Kerrigan, Thirunarayan et al. 1996) We then used rigid link-segment kinematic models to refine and quantify the determinants of gait. (Kerrigan, Della Croce et al. 2000; Della Croce, Riley et al. 2001; Kerrigan, Riley et al. 2001) The kinematic model was used to perform induced displacement analyses that quantified the relative contributions of pelvic kinematics, knee flexion, and heel rise (ankle kinematics) to CoM vertical displacement.

**Precise Characterization of Stroke Related Gait Pathology:** The effect of stroke on the determinant of gait parameters was also precisely measured and data characterizing their interactions were obtained. We quantified hip hiking and circumduction in this population. (Kerrigan, Frates et al. 2000) Stiff-legged gait, the most characteristic knee impairment in stroke was analyzed in detail. (Kerrigan, Gronley et al. 1991; Kerrigan, Frates et al. 1999; Kerrigan, Karvosky et al. 2001) Similarly, we investigated toe-walking in detail, (Kerrigan, Riley et al. 2000) elucidating a possible link

between toe-walking and stiff-legged gait. (Kerrigan, Burke et al. 2001)

**Dynamic Models:** These clinical studies highlighted the importance of kinetic parameters in characterizing the various impairments, motivating analyses based on dynamic biomechanical and musculoskeletal models. Starting with a relatively simple 2-D model of stiff-legged gait (Kerrigan, Roth et al. 1998) we progressed to 3-D forward dynamic musculoskeletal (Riley and Kerrigan 1998) and biomechanical (Riley and Kerrigan 1999) models. The latter analysis used a technique called induced acceleration analysis, which promised to be an extremely useful tool for investigating the linkage between specific impairments and disabilities. We used this technique to investigate the dynamics of CoM displacement, the kinetic determinants of gait. (Riley, Della Croce et al. 2001; Riley, Della Croce et al. 2001; Riley, Della Croce et al. 2001; Riley and Kerrigan 2001)

**Model-based Design:** We are now engaged in the development of a dynamically controlled body-weight support system to be used in the rehabilitation of stroke survivors and others. The underlying assumption of this effort is the determinants of gait in reverse, that inducing appropriate CoM excursion will facilitate treating specific impairments. The model-based controller for this system builds on our analytical models, (Lee, Allaire et al. 2004; Lee, Allaire et al. 2004) and biomechanical models are being used to guide protocol development.

## SUMMARY

Our modeling approach applied to gait disability due to stroke has been multi-modal, subject specific, data driven, and data verifiable. Our approach has been hypothesis driven and most importantly, it has been clinically focused.

## REFERENCES

- Saunders, J. B. D. V. T. Inman, H. D. Eberhart (1953) *Am J Bone Joint Surg* 35: 543-558.
- Cooper, R. A., L. A. Quatrano, et al. (1999) *Am J PM&R* 78: 278-80.
- Della Croce, U., P. O. Riley, et al. (2001) *Gait Posture* 14: 79-84.
- Duff-Raffaele, M., D. C. Kerrigan, et al. (1996) *Am J PM&R* 75: 375-9.
- Kerrigan, D. C., D. T. Burke, et al. (2001) *Am J PM&R* 80: 33-7.
- Kerrigan, D. C., U. Della Croce, et al. (2000) *Arch PM&R* 81: 1077-80.
- Kerrigan, D. C., E. P. Frates, et al. (1999) *Am J PM&R* 78: 354-60.
- Kerrigan, D. C., E. P. Frates, et al. (2000) *Am J PM&R* 79: 247-52.
- Kerrigan, D. C., J. Gronley, et al. (1991) *Am J PM&R* 70: 294-300.
- Kerrigan, D. C., M. E. Karvosky, et al. (2001) *Am J PM&R* 80: 244-9.
- Kerrigan, D. C., P. O. Riley, et al. (2001) *Arch PM&R* 82: 217-20.
- Kerrigan, D. C., P. O. Riley, et al. (2000) *Arch PM&R* 81: 38-44.
- Kerrigan, D. C., R. S. Roth, et al. (1998) *Gait Posture* 7: 117-24.
- Kerrigan, D. C., M. A. Thirunarayan, et al. (1996) *Am J PM&R* 75: 3-8.
- Kerrigan, D. C., B. E. Viramontes, et al. (1995). *Am J PM&R* 74: 3-8.
- Lee, J.-H., P. E. Allaire, et al. (2004) *Internat Soc Magnetic Bearings*, Lexington, KY.
- Lee, J.-H., P. E. Allaire, et al. (2004) *IEEE Internat Conf Control Apps*, Taipei.
- Riley, P. O., U. Della Croce, et al. (2001) *J Biomech* 34: 1669-1670.
- Riley, P. O., U. Della Croce, et al. (2001) *J Biomech* 34: 197-202.
- Riley, P. O., U. Della Croce, et al. (2001) *Gait Posture* 14(3): 264-70.
- Riley, P. O. and D. C. Kerrigan (1998) *J Biomech* 31: 835-40.
- Riley, P. O. and D. C. Kerrigan (1999) *IEEE Trans Rehab Eng* 7: 420-6.
- Riley, P. O. and D. C. Kerrigan (2001) *Clin Biomech* 16: 681-7.
- Thirunarayan, M. A., D. C. Kerrigan, et al. (1996) *Gait Posture* 4: 306-314.



# EVALUATION OF JOINT FUNCTION USING KINEMATIC MAGNETIC RESONANCE IMAGING : RESEARCH AND CLINICAL APPLICATIONS

Christopher Powers, Ph.D., P.T.

Musculoskeletal Biomechanics Research Laboratory  
Dept. Biokinesiology & Physical Therapy, University of Southern Calif., Los Angeles, CA, USA  
E-mail: powers@usc.edu Web: www.usc.edu/go/mbrl

## INTRODUCTION

While traditional kinematic analyses form the cornerstone of the biomechanical assessment of joint function, interpretation of such data is limited with respect to identifying the internal factors contributing to abnormal joint motion. Kinematic magnetic resonance imaging (KMRI) provides a means by which the intricacies of joint function can be evaluated for both diagnostic and research purposes. KMRI techniques were developed in recognition of the fact that pathologic conditions that affect joint function are position-dependent and/or associated with stressed or loaded conditions. We have used KMRI to evaluate 1) patellofemoral joint kinematics during non-weightbearing and weightbearing conditions and 2) motion of the spine in response to manually applied forces (i.e. joint mobilization). The methods used to obtain these data are described below.

## METHODS

### *Instrumentation*

Dynamic imaging of the patellofemoral joint and spine has been performed using a vertically opened (56 cm opening) MR system (0.5 T, Signa SP) developed for interventional MR procedures (General Electric Medical Systems, Milwaukee, WI, USA). This system is equipped with pulse sequence programming and real-time interactive MR imaging capabilities. The

vertically-opened design of this MR system permits subjects to be imaged during both weightbearing (standing) and non-weightbearing (seated) conditions. In addition, the opening allows the examiner access to the subject during spine imaging.

### *Patellofemoral Joint Imaging*

Axial images of the patellofemoral joint have been obtained in persons with lateral patellar subluxation using a flexible transmit-receive surface coil and a fast spoiled gradient recalled acquisition in the steady state (spoiled GRASS) pulse sequence. MR images were obtained at a rate of 1 image per 0.75 sec using the following parameters: repetition time (TR), 10.3 msec; echo time (TE), 2.7 msec; flip angle, 40°; field of view, 35 cm x 18 cm; matrix size, 256 x 128; number of excitations: 2. Images of the PFJ were obtained as subjects extended their knee from 45° to 0° during non-weightbearing (5% body weight resistance) and weightbearing (unilateral squat) conditions. Measurements of patellofemoral joint relationships (medial/lateral patellar displacement and patellar tilt) as well as femur and patella rotations relative to an external reference system (i.e. the image field of view) were obtained at 3° increments during knee extension.

### *Spine Imaging*

Sagittal plane imaging of the spine (N=20) has been performed using a flexible receive-only surface coil and the following imaging parameters: TR 200ms; TE 18 ms; matrix: 256 x 256; FOV: 28 x 21 cm; and a 7 mm section thickness with an interslice spacing of 1 mm. Posterior-anterior (PA) forces were applied at each subject's vertebrae starting at L5 and moving to L1. The manual force was aimed at reaching the end range of vertebral motion. The intervertebral angle, defined as the angle formed by lines delineating adjacent vertebral endplates, was measured. Segmental motion was defined as the difference between the intervertebral angles as measured from the resting and the end-range images. An increase in intervertebral angle between those positions was indicative of segmental extension. The superior vertebra was used to define the target segment.

## **RESULTS AND DISCUSSION**

### *Patellofemoral Joint Imaging*

During non-weightbearing knee extension, lateral patellar displacement was more pronounced than during the weightbearing condition between 30° and 12° of knee extension, with statistical significance being reached at 27°, 24°, and 21°. No differences in lateral patellar tilt were observed between conditions ( $p=0.065$ ). During the weightbearing condition, internal femoral rotation was significantly greater than during the non-weightbearing condition as the knee extended from 18° to 0°. During the non-weightbearing condition, the amount of lateral patellar rotation was significantly greater than during the weightbearing condition throughout the range of motion tested. These results of this investigation suggest that the patellofemoral joint kinematics during non-weightbearing can be characterized as the patella rotating

on the femur, while the patellofemoral joint kinematics during the weightbearing condition could be characterized as the femur rotating underneath the patella.

### *Spine Imaging*

The results of this study revealed a consistent pattern of lumbar spine motion during the PA force application. Specifically, motion at the targeted and adjacent segments always was directed towards extension. A theoretical explanation for this pattern of segmental motion can be proposed based on the morphology of the lumbar spine. For example, when a PA force is applied to the spinous processes of L3, the facet of the tested (L3) vertebra approximates the facet joint of the adjacent caudal (L4) vertebra and imposes motion to it. It is conceivable that this approximation would result in the L3 facet "pushing" on its L4 counterpart (bone on bone contact), causing a bending moment rotating L4 away from L3. The facet of L3 moves away from the facet of L2 causing tension in the joint capsule, which in turn also results in a bending moment of L2 on L3 into extension, but of lesser magnitude. The findings suggest that a PA force at one spinous process causes motion at the target vertebra and the neighboring vertebrae. Secondly, we propose a mechanism by which a PA force applied to a spinous process propagates motion caudally and cranially.

## **SUMMARY/CONCLUSIONS**

KMRI techniques can be used to test hypotheses related to normal and abnormal joint function. Information obtained from KMRI may prove to be useful in better understanding the causes of various orthopaedic disorders, thereby assisting clinicians in establishing more effective treatment options.



# **SIMULATION-BASED TREATMENT PLANNING FOR STIFF-KNEE GAIT**

Scott L. Delp, Allison S. Arnold, May Q. Liu, Frank C. Anderson and \*Darryl G. Thelen  
Departments of Bioengineering and Mechanical Engineering, Stanford University  
\*Department of Mechanical Engineering, University of Wisconsin-Madison  
Email: [delp@stanford.edu](mailto:delp@stanford.edu) Web: <http://www.stanford.edu/group/nmbl/>

## **INTRODUCTION**

Many persons with cerebral palsy walk with stiff-knee gait, a condition in which swing-phase knee flexion is substantially diminished.

Reduced knee flexion is often attributed to excessive excitation of the rectus femoris during the swing phase (Perry, 1987). However, stance-phase factors that limit knee flexion velocity at toe-off, such as excessive force in vasti or rectus femoris, or diminished force in iliopsoas or gastrocnemius, may also limit knee flexion (Goldberg et al., 2005). Determining which, if any, of these factors limit an individual's knee flexion is challenging because existing diagnostic methods cannot evaluate how forces produced by the rectus femoris or other muscles influence swing-phase knee motions.

There are several options for treatment of stiff-knee gait. One option, botulinum toxin injection, theoretically decreases the hip and knee moments generated by the rectus femoris. A second option, rectus femoris transfer, theoretically decreases the muscle's knee extension moment while leaving its hip flexion moment intact. At present, the mechanisms responsible for patients' improvements in swing-phase knee flexion following these treatments are not well understood.

Dynamic simulations provide a framework for identifying the causes of diminished knee flexion in individual subjects and for evaluating the effects of potential treatments. We have created dynamic simulations of unimpaired children and children with stiff-knee gait. This presentation will review how we generated and analyzed a dynamic simulation of a subject with stiff-knee gait to determine the biomechanical cause of his diminished knee flexion and the potential consequences of different treatment options.

## **METHODS**

We have generated and analyzed dynamic simulations of individual subjects without impairments and with abnormal gait to determine the biomechanical cause of their abnormal movements and the potential consequences of different treatment options. Each subject's musculoskeletal system was represented by a scaled, 21-degree-of-freedom linkage actuated by 92 muscles. We used "computed muscle control" to find a set of muscle excitations that produced a simulation that closely matched the measured gait kinematics and kinetics (Thelen et al., 2003). The predicted muscle excitations were generally consistent with the subjects' measured EMG activity, and the simulated joint angles reproduced the subjects measured kinematics. We identified which muscles were contributing to the abnormal moments and evaluated their relative contributions to the joint motions by altering muscle excitations in the simulation and computing the resulting changes in body motions.

Botulinum toxin injections were simulated by decreasing the excessive excitation of rectus femoris. Rectus femoris transfers were simulated by transferring the muscle's insertion in the model. Two transfer sites were evaluated: one that eliminated the muscle's knee extension moment and one that converted the muscle into a knee flexor.

We present an analysis of a 12-year-old male with cerebral palsy. His left lower limb exhibited limited peak knee flexion during swing and abnormal activity of rectus femoris (preswing and swing) and vasti (preswing). The changes in swing-phase knee flexion following each simulated treatment were compared to the subject's measured changes in knee flexion following rectus femoris transfer surgery.

## RESULTS AND DISCUSSION

Peak knee flexion was improved following each of the simulated treatments (Fig. 1). Decreasing the excessive excitation of rectus femoris in the model, simulating the effects of botulinum toxin injection, increased peak knee flexion by about 10°. Eliminating the excessive knee extension moment of rectus femoris in preswing and swing while leaving the hip moment intact, simulating a rectus femoris transfer, increased the peak knee flexion by about 30°. A substantial improvement in knee flexion was generated regardless of whether the muscle was converted to a knee flexor (i.e., curves B and C are similar in Fig. 1). The simulated improvements were similar to the subject's actual improvements following rectus femoris transfer.

Simulations of normal walking (e.g., Neptune et al, 2001, Anderson et al., 2001, Piazza et al., 1996) have enabled investigators to identify the actions of muscles with a level of specificity and certainty that surpasses insights gained with experimental methods alone. Simulations of abnormal walking offer similar potential, but are challenging to develop, in part, because they require determination of muscle excitations that generate the abnormal movement dynamics exhibited by persons with movement disorders. The computed muscle control method provides a computationally efficient means to generate these simulations.

The potential to use subject-specific simulations to better understand the causes of specific movement deviations and to assess various treatment options is exciting. This case study provides specific and useful insights into stiff-knee gait. Future studies are needed to determine if subject-specific simulations can improve treatment outcomes.

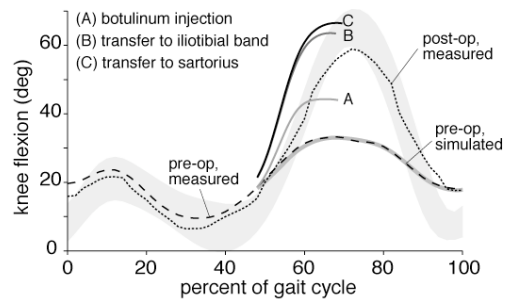


Figure 2. Knee flexion trajectories for different simulated treatments. The subject's pre- and post-operative measured knee angles are shown for comparison. Shaded area is normal mean  $\pm$  1 SD.

## REFERENCES

- Perry, J., 1987, *Developmental Medicine and Child Neurology*, 29, pp. 153-158.
- Goldberg, S.R., et al., 2004, *Journal of Biomechanics*, 37, pp. 1189-1196.
- Thelen, D.G., Anderson, F.C. and Delp, S.L., 2003, *Journal of Biomechanics*, 36, pp. 321-328.
- Neptune, R.R., Kautz, S.A., and Zajac, F.E., 2001, *Journal of Biomechanics*, 34, pp. 1387-1398.
- Anderson, F.C. and Pandy, M.G., 2001, *Journal of Biomechanical Engineering*, 123, pp. 381-390.
- Piazza, S.J. and Delp, S.L., 1996, *Journal of Biomechanics*, 29, pp. 723-733.

## ACKNOWLEDGEMENTS

The authors thank Ayman Habib and the staff of the Center for Motion Analysis at the Connecticut Children's Medical Center. Supported by NIH R01 HD45109, R01 HD38962, and the NIH Roadmap for Medical Research, U54 GM072970

On-Field Measurement of Head Impact Acceleration in Helmeted Sports  
Richard M. Greenwald<sup>1,2</sup>, Jeffrey J. Chu<sup>1</sup>, Jonathan G. Beckwith<sup>1</sup>, Joseph T. Gwin<sup>1</sup>,  
Aaron T. Buck<sup>1</sup>, Joseph J. Crisco<sup>3</sup>

<sup>1</sup> Simbex, Lebanon, NH <sup>2</sup> Thayer School of Engineering, Dartmouth College, Hanover, NH;

<sup>3</sup> Dept of Orthopaedics, Brown Medical School, Providence, RI

E-mail: rgreenwald@simbex.com

Web : www.simbex.com

## INTRODUCTION

There are approximately 300,000 sports related mild traumatic brain injuries (MTBI), or concussions, reported each year. A critical piece in the puzzle for understanding MTBI is the link between the mechanical input (trauma) that causes injury and the clinical outcome. One limiting factor in the development and validation of prevention and intervention strategies to reduce MTBI is the lack of sufficient *in vivo* biomechanical head impact data that can be correlated to clinical outcome.

In order to rapidly advance human research related to MTBI, a system capable of recording head acceleration during impacts in at-risk populations is required. Athletic environments, such as American football, hockey and boxing draw public attention to the possible effects of repeated concussive and sub-concussive events and offer a rich opportunity for collecting data on large numbers of head impacts. We developed and validated Head Impact Telemetry (HIT) System (Simbex, Lebanon, NH) (Crisco 2004, Manoogian 2006) technology to allow data collection of head acceleration due to impacts incurred on the playing field. Large-scale data collection of head impacts is required to study pathomechanics of concussion because of the relatively low incidence of MTBI per athlete exposure.

We hypothesize that head acceleration due to impact along with other independent impact measures is predictive of the type and severity of brain injury, and correlates to specific clinical measures of brain injury.

## METHODOLOGY

To date, HIT System technology has been utilized in football, ice hockey, boxing (Figure 1), and is under development for soccer and equestrian use. For each sport, commercially available helmets or headgear are modified to include six or more linear accelerometers (Analog Devices, Cambridge, MA), a microcontroller, and an RF telemetry link for real-time transmission of data to the sidelines. Data are collected at 1000 Hz per channel for 40 ms when any accelerometer detects accelerations that exceed a user-selected threshold (eg. 10g). Acceleration data are time-stamped (+/- 5 ms resolution) and wirelessly transmitted to a sideline receiver interfaced to a laptop. These data are processed using a linear least squares regression technique (Crisco, 2004) that calculates linear head acceleration and impact location. Recent improvements to the algorithm allow for computation of full six degree-of-freedom head acceleration, overcoming earlier limitations (Chu, 2006).



**Figure 1:** Instrumented football, hockey, and boxing helmets

For each sports configuration, instrumented headgear was validated using a series of impact tests with a helmet-equipped Hybrid-III dummy that featured a

3-2-2 head accelerometer array. For on-field research and clinical studies, head impact acceleration, impact location about the head, impact time, impact duration and calculated metrics including HIC and GSI are collected and correlated with clinical diagnosis of concussion, symptoms, neuropsychological testing scores, and fMRI imaging studies. Where possible, baseline scores for these clinical tests are collected on athletes at risk.

## RESULTS AND DISCUSSION

Over the course of the 2003-2006 fall and spring football seasons, 249,613 impacts from 423 players at nine colleges and high schools have been collected. In 2005 a pilot study resulted in 5,463 recorded impacts to 5 instrumented hockey players over the course of one complete season. Preliminary testing was also conducted during male and female (6 each) boxing competition before beginning a 100 boxer study scheduled to finish in spring 2007.

Most head impacts (>89%) in helmeted sports are relatively low magnitude (< 40 g's) (Figure 2). More than 3000 impacts recorded in football were greater than 98 g's, but did not result in symptoms consistent with diagnosis of concussion. A total of 11 concussions were diagnosed in players whose impacts were monitored with instrumented helmets. In general, impacts that were experienced prior to a concussion were of relatively high peak linear acceleration (peak occurrence

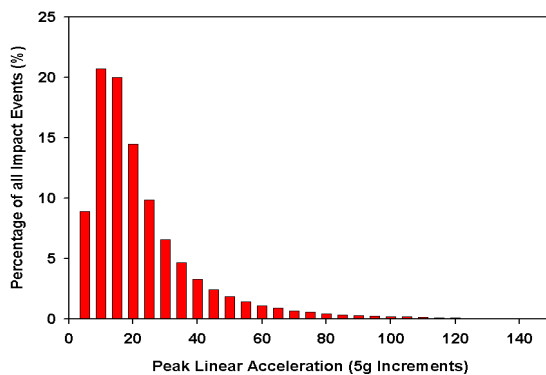


**Figure 2:** Distribution of all recorded impacts by peak linear acceleration.

between 60-180 g's). Linear acceleration magnitude correlates well with rotational acceleration magnitude, but linear acceleration alone does not appear to be predictive of concussion diagnosis. There are differences in trends for impact magnitude and impact location as a function of player position in both football and hockey.

The primary finding of this study is that this instrumented helmet system proved effective at collecting thousands of head impact events and providing real-time on-field data analysis. Results also show that players experience impact magnitudes greater than the reported 98g average concussed threshold (Pellman, 2003) without sustaining injuries. Through continued use of this system, it is anticipated that on-field impact measurements will help improve head injury criteria and clinical evaluation techniques. The long-term goal for this technology is to provide enabling data to develop strategies for reducing the incidence and severity of MTBI in the population that can be practically implemented across large numbers of athletes.

## REFERENCES

- Crisco, J.J. et al (2004) *J. Biomechanical Engineering*. 126(1), 849-854.
- Chu, J.J. et al (2006) World Congress of Biomechanics.
- Gwin, J.T. et al (2006) World Congress of Biomechanics.
- Beckwith, J.G. et al (2006) World Congress of Biomechanics.
- Manoogian, S. et al (2006) *Technical Papers of ISA: Biomedical Sciences Instrumentation*. 42: 383-288.
- Pellman, E. J. et al (2003) *Neurosurgery*. 53: 799-814.

## ACKNOWLEDGEMENTS

This work was supported in part by NIH 2R44HD40473 and various research awards from NOCSAE.

# EFFECTS OF WALKING SPEED AND VISUAL-TARGET DISTANCE ON TOE TRAJECTORY DURING SWING PHASE

Chris Miller<sup>1</sup>, Brian Peters<sup>1</sup>, Rachel Brady<sup>1</sup>, Liz Warren<sup>2</sup>, Jason Richards<sup>1</sup>,  
Ajitkumar Mulavara<sup>3</sup>, Hsi-Guang Sung<sup>2</sup> and Jacob Bloomberg<sup>4</sup>

<sup>1</sup>Neurosciences Laboratory, Wyle Laboratories, Houston, TX, USA

<sup>2</sup>Universities Space Research Association, Houston, TX, USA

<sup>3</sup>Department of Otorhinolaryngology, Baylor College of Medicine, Houston, TX, USA

<sup>4</sup>Neurosciences Laboratory, NASA Lyndon B. Johnson Space Center, Houston, TX, USA

E-mail: chris.miller-1@nasa.gov

## INTRODUCTION

After spaceflight, astronauts experience disturbances in their ability to walk and maintain postural stability (Bloomberg, et al., 1997). One of the post-flight neuro-vestibular assessments requires that the astronaut walk on a treadmill at 1.8 m/sec (4.0 mph), while performing a visual acuity test, set at two different distances (“far” and “near”). For the first few days after landing, some crewmembers can not maintain the required pace, so a lower speed may be used. The slower velocity must be considered in the kinematic analysis, because Andriacchi, et al. (1977) showed that in clinical populations, changes in gait parameters may be attributable more to slower gait speed than pathology.

Studying toe trajectory gives a global view of control of the leg, since it involves coordination of muscles and joints in both the swing and stance legs (Karst, et al., 1999). Winter (1992) and Murray, et al. (1984) reported that toe clearance during overground walking increased slightly as speed increased, but not significantly. Also, toe vertical peaks in both early and late swing phase did increase significantly with increasing speed.

During conventional testing of overground locomotion, subjects are usually asked to fix their gaze on the end of the walkway – a

“far” target. But target (i.e., visual fixation) distance has been shown to affect head and trunk motion during treadmill walking (Bloomberg, et al., 1992; Peters, et al., in review). Since the head and trunk can not maintain stable gaze without proper coordination with the lower body (Mulavara & Bloomberg, 2003), it would stand to reason that lower body kinematics may be altered as well when target distance is modified. The purpose of this study was to determine changes in toe vertical trajectory during treadmill walking due to changes in walking speed and target distance.

## METHODS

Six males and six females gave informed consent and participated in this study, and the NASA-JSC Committee for the Protection of Human Subjects approved the protocol. Subjects wore lab-supplied shoes (Converse, North Andover, MA) with footswitches (Motion Lab Systems, Baton Rouge, LA) affixed to the soles for the determination of heel contact and toe-off events. Retro-reflective markers (25 mm diameter) were taped over anatomical landmarks on the shoe of the subject’s right foot. Three-dimensional marker positions were recorded using a video-based motion capture system (Motion Analysis, Santa Rosa, CA). The toe was defined by a virtual marker computed at the location of the distal end of the shoe at the 2<sup>nd</sup> toe.

Subjects walked on a motorized treadmill at five different speeds (0.9, 1.1, 1.3, 1.6, 1.8 m/sec) while performing a visual acuity task (Peters & Bloomberg, 2005) with the optotypes shown on a visual display at two target distances from the eyes: 4 meters (“far”) and 50 centimeters (“near”). Subjects performed ten 60-second trials – one for each speed-target combination. The order of speed-target combinations was determined by a balanced-block design, and each subject was randomly assigned to one of the twelve orders.

The marker positions and footswitch data were exported and analyzed using in-house Matlab scripts (Mathworks, Inc., Natick, MA) to determine gait cycle events and kinematics of the foot. The toe’s vertical position was reported relative to that during the quiet stance (static) trial for reference. The analysis concentrated on three features of the swing toe’s vertical trajectory: minimum toe clearance (TCI), the first toe peak in early swing just after push-off (toemax1) and the second toe peak just before heel contact (toemax2). A linear random-effects model was utilized to determine changes in the parameters due to speed and target distance ( $p < 0.05$ ).

## RESULTS AND DISCUSSION

In this study, toe clearance significantly *decreased* with increasing speed (Figure 1; slope =  $-4.3$  mm/(m/sec);  $p < 0.01$ ) – a result opposite to that found by Winter (1992) and Murray, et al. (1984). However, like those studies, the toe peak just before heel contact significantly increased with speed (slope =  $59.1$  mm/(m/sec);  $p < 0.01$ ). Target-fixation distance only had an effect on the toe peak just after toe-off, where the near-target values were lower than far-target values ( $p = 0.01$ ). No significant interactions of speed and target distance were observed.

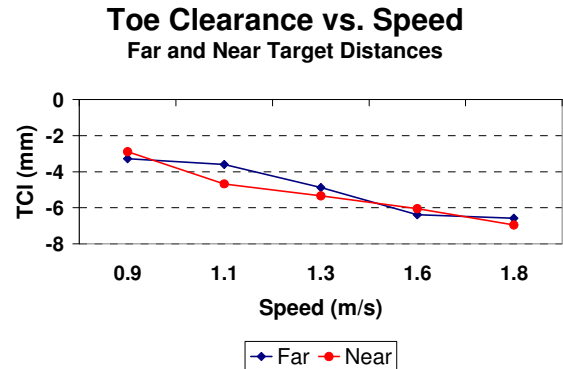


**Figure 1:** Vertical toe clearance (relative to standing) versus speed for two target distances.

## SUMMARY

As speed increased, toe clearance decreased, and vertical toe peak in late swing increased. The vertical toe peak just after push-off was lower during near-target fixation, than far. Therefore speed and visual fixation distance should be considered when analyzing toe trajectory during treadmill walking. These results will be used to enhance the assessment of lower limb control following space flight.

## REFERENCES

- Andriacchi, T.P., et al. (1977). *J. Biomech*, **10(4)**, 261-8.
- Bloomberg J.J., et al. (1992). *Ann. N. Y. Acad. Sci.*, **656**, 699-707.
- Bloomberg J.J., et al. (1997). *J. Vestib. Res.*, **7(2-3)**, 161-77.
- Karst, G.M., et al. (1999). *J. Gerontol. A. Biol. Sci. Med. Sci.*, **54(7)**, M343-7.
- Mulavara, A.P. & Bloomberg J.J. (2002-3). *J. Vestib. Res.*, **12(5-6)**, 255-69.
- Murray, M.P., et al. (1984). *J. Orthop. Res.*, **2(3)**, 272 – 80.
- Peters B.T. & Bloomberg J.J. (2005). *Acta. Oto-Laryng.*, **125**, 353 – 7.
- Peters, B.T., et al. (2006). *in review*.
- Winter D.A. (1992). *Physical Therapy*, **72(2)**, 45 – 53.

# RUNNING TO MARS: A BIOMECHANICAL ADVENTURE

Peter R. Cavanagh

Department of Biomedical Engineering, Cleveland Clinic, Cleveland, OH, USA  
Email: [cavanap@ccf.org](mailto:cavanap@ccf.org) Web: <http://www.lerner.ccf.org/bme/>

## INTRODUCTION

The opportunity to present the James Hay Memorial Award lecture is a significant honor for my colleagues and me and a particularly meaningful one for me, given my long association with Jim. I first met him in 1972 when, as the architect of the American Society of Biomechanics, he came to Penn State University to formulate a constitution for the fledgling society. In many interactions with Jim over 30 years of subsequent friendship, I developed a deep respect for his integrity, energy, intellect, and his life-long passion to bring science to sports.

The title of this talk clearly needs some explanation. In the presentation, I intend to trace some of the work of my research group in the biomechanics of running and to show how this has influenced the subsequent direction of my career and that of my students. Even though our research team is no longer active in the field of sport biomechanics, this area has informed our current interests, which are focused on bone loss during long-duration space travel and on foot disease in diabetes. My goal is not only to present some of the research that has been conducted, but also to communicate to the younger members of the Society the metaphor of a career in science as an adventure, where each new destination enables a multitude of other possible pathways. I also hope to show the critical contributions that graduate theses and dissertations make to the scientific literature.

## BIOMECHANICS OF RUNNING

An enduring issue in locomotion studies is the relationship between the mechanics and energetics of running. Studies of male and female elite distance runners indicated that “economy” is not a clear determinant of success (Cavanagh et al., 1977; Williams et al., 1987). Defining the “efficiency” of human movement has proven an elusive goal (Cavanagh and Kram, 1985; Williams and Cavanagh, 1987; van Ingen Schenau and Cavanagh, 1990). Estimates are highly dependent on methodological approaches, such as the ever-present issue of optimal filtering. Prolonged eccentric muscle action, in downhill running for example, produces delayed onset soreness and a slowly increasing oxygen uptake that remains unexplained (Dick and Cavanagh, 1987).

New insights into the role of the arms in running were provided by Hinrichs et al. (1987), and the limits of motion analysis were explored by Lafortune et al. (1992) in a study that involved inserting intra-cortical pins in the bones of the knee joint. This led to significant insight into action of the normal knee joint, which was extended to pathological subjects, using similar techniques, by McClay et al. (1991). The motion capture capability in our laboratory was also applied in studies of older individuals during standing and stair climbing (Simoneau et al., 1991; Startzell et al., 2000), including the elucidation of postural instability secondary to peripheral neuropathy (Simoneau et al., 1994).

## FOOTWEAR AND FOOT DISEASE

Studies of ground reaction forces (Cavanagh and Lafortune, 1980) and moments (Holden and Cavanagh, 1991) were accompanied by work on running shoes (Cavanagh, 1980), including an early “computer shoe” that interfaced with an Apple IIe computer (Cavanagh, 1988). The advent of devices to measure plantar pressure distribution (Hennig et al., 1982) opened new doors to the study of the foot complications of diabetes (Schaff and Cavanagh, 1990), which has since become a major focus of my laboratory’s work (Cavanagh et al, 2005).

## BONE LOSS IN SPACE

Running in space as a countermeasure to adverse musculoskeletal and cardiovascular changes was pioneered by the astronaut-physician William Thornton, who designed a treadmill for use on the space shuttle. Our own work in space started when Dr. Thornton asked us to analyze film of crew members using this device on the Shuttle (Thornton et al., 1997). We subsequently performed an in-flight evaluation of the current International Space Station (ISS) treadmill (McCrorry et al., 1999). A simulator for zero-gravity locomotion was constructed in our laboratory (Davis et al., 1996) and used to demonstrate that subjects could run with a gravity replacement system that applied full body weight loading (McCrorry et al., 2002). This work culminated in a recent experiment on the ISS implicating decrements in daily load to changes in lumbar and femoral bone mass.

## SUMMARY

Early studies in the biomechanics and energetics of distance running have informed much of the subsequent research of our group and have led to new opportunities to gain insight from

biomechanical approaches to the study of space flight and diabetic foot disease.

## REFERENCES

- Cavanagh, P.R. (1980). *The Running Shoe Book*, Anderson World.
- Cavanagh, P.R. (1988). U.S. Patent 4,771,394.
- Cavanagh, P.R. et al. (1977). *Ann. NY Acad. Sci.*, **301**, 328-345.
- Cavanagh, P.R., Kram, R. (1985). *Med. Sci. Sports Exerc.*, **17**, 304-308.
- Cavanagh, P.R., Lafortune, M.A. (1980). *J. Biomech.*, **13**, 397-406.
- Cavanagh P.R. et al. (2005). *Lancet*, **366**, 1725-1735.
- Davis, B.L. et al. (1996) *Aviat., Space Environ. Med.*, **67**, 235-242.
- Dick, R.W., Cavanagh, P.R. (1987). *Med. Sci. Sports Exerc.*, **19**, 310-317.
- Hennig, E.M. et al. (1982). *J. Biomed. Eng.*, **4**, 213-222.
- Hinrichs, R.N. et al. (1987). *Int. J. Sports Biomech.*, **3**, 222-241.
- Holden, J.P., Cavanagh, P.R. (1991). *J. Biomech.*, **24**, 887-897.
- Lafortune, M.A. et al. (1992). *J. Biomech.*, **25**, 347-357.
- McClay, I. et al. (1991) *Phys. Ther.*, **71**, S46-S47.
- McCrorry, J.L. (1999). *J. Appl. Biomech.*, **15**, 292-302.
- McCrorry, J.L. et al. (2002). *Aviat. Space Environ. Med.*, **73**, 625-631.
- Schaff, P.S., Cavanagh, P.R. (1990). *Foot & Ankle*, **11**, 129-140.
- Simoneau, G.G. et al. (1991). *J. Gerontol.*, **46**, M188-M195.
- Simoneau, G.G et al. (1994). *Diabetes Care*. **17**(12): 1411-1421.
- Startzell, J.K. (2000). *J. Am. Geriatr. Soc.*, **48**, 567-580.
- Thornton, W.E. et al. (1997). In Allard et al., eds., *Three-Dimensional Analysis of Human Locomotion*. John Wiley & Sons, pp. 375-388.
- van Ingen Schenau, G.J., Cavanagh, P.R. (1990). *J. Biomech.*, **23**, 865-881.
- Williams, K.R. et al. (1987). *Int. J. Sports Med.*, **8**(Suppl), 107-118.
- Williams, K.R., Cavanagh, P.R. (1987). *J. Appl. Physiol.*, **63**, 1236-1245.

# OF MYOSINS, MUSCLES AND MECHANISMS OF CONTRACTION

Walter Herzog

University of Calgary, Calgary, AB, Canada

E-mail: [walter@kin.ucalgary.ca](mailto:walter@kin.ucalgary.ca) Web: <http://www.kin.ucalgary.ca/HPL/content/herzog.html>

## INTRODUCTION

For the past two decades, my research has been focused on the biomechanics of the musculoskeletal system with specific interest in skeletal muscle function and contraction. In the 1980s, I tackled the distribution problem in biomechanics, theoretically and experimentally, and realized that a solution to this problem could only be achieved with a deep understanding of the mechanical properties of muscles. Investigating the force-length and force-velocity relationships, I stumbled over the phenomenon of force enhancement and force depression following stretching and shortening of activated muscles, respectively (Abbott and Aubert 1952), and realized that these history-dependent properties could not be explained within the framework of the sliding filament (Huxley and Niedergerke 1954; Huxley and Hanson 1954) and the cross-bridge theory of muscle contraction (Huxley 1957). This realization led to a body of work covering the last decade that was aimed at unraveling the mechanisms responsible for force depression and force enhancement, and in parallel, a re-evaluation of the sliding filament and cross-bridge theories of contraction.

For the purpose of the Borelli lecture, I will focus on the research on force enhancement and the implications of this work for the cross-bridge theory. Force enhancement is defined here as the extra force of an isometric, steady-state contraction that is preceded by stretching of the activated muscle, compared to the corresponding isometric, steady-state force of a purely isometric contraction (i.e., one that is not preceded by stretch – Figure 1).

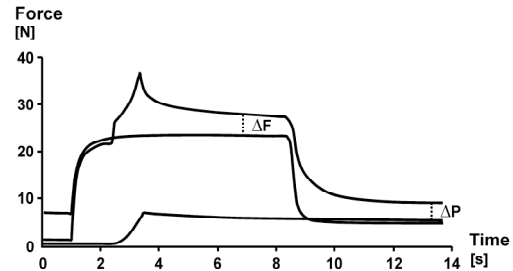


Figure 1: Definition of force enhancement ( $\Delta F$ ) and passive force enhancement ( $\Delta P$ ).

## METHODS

Force enhancement was induced in all preparations by stretching an activated muscle by various amounts and at various speeds. The preparations tested included in vivo human muscles (Lee and Herzog 2002), an in situ preparation of the cat soleus (Herzog and Leonard 2002), single fibres of the tibialis anterior and lumbrical muscles of the frogs (Rassier et al. 2003), single myofibrils from the rabbit psoas (Leonard et al. 2006), and single cross-bridge interactions with isolated actin molecules (Mehta et al. 2006). For details of the preparations, please be referred to the original papers.

## RESULTS AND DISCUSSION

Steady-state force enhancement was present in all preparations ranging from in vivo voluntary contractions to single myofibrils. Force enhancement was increased with increasing magnitudes of stretch (Figure 2), was independent of stretch speed, and was associated with an increase in muscle stiffness and a decrease in force relaxation time. Most importantly, at long muscle length, force enhancement was also

accompanied by an increase in passive force (after muscle relaxation – Figure 1) that could account in extreme cases for up to 85% of the total force enhancement measured in the activated muscle.

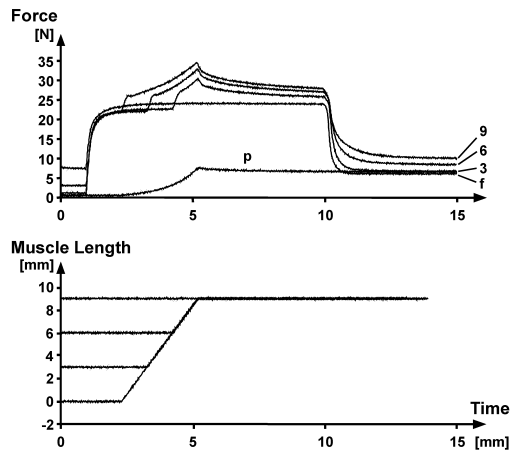


Figure 2: Force enhancement increases with increasing magnitudes of stretch

From the results of these studies, we concluded that force enhancement consists of an active and passive component. The active component was tentatively associated with a decrease in the rate of detachment of cross-bridges from actin; the passive component was hypothesized to originate from a calcium-dependent increase in stiffness of the molecular spring titin.

In order to test these two hypotheses, we first performed experiments on single cross-bridge interactions with actin and measured the duty ratio of cross-bridges subjected to stretching and shortening, and second, performed tests on single myofibrils which were activated with solutions of increasing calcium concentrations and measured the passive forces by inhibiting active forces through deletion of troponin C on actin.

The results indicated that stretched cross-bridges have a smaller duty ratio than shortened cross-bridges, therefore rejecting our first hypothesis that the active force

enhancement might be caused by an increase in the duty ratio.

The second experiment demonstrated that myofibril stiffness increased with increasing calcium concentration (in the troponin C deleted preparation), thereby supporting the hypothesis that at least part of the passive force enhancement was caused by a calcium-dependent increase in titin stiffness.

## SUMMARY/CONCLUSIONS

Force enhancement has an active and a passive component. The active component is likely associated with an as of yet unknown stretch-dependent change in the cross-bridge kinetics, while the passive force enhancement is caused in part by a calcium-dependent increase in the stiffness of the molecular spring titin.

## REFERENCES

- Abbott B.C., Aubert X.M. (1952). *J Physiol*, **117**:77-86.
- Huxley H.E., Hanson J. (1954). *Nature*, **173**:973-976.
- Huxley A.F., Niedergerke R. (1954). *Nature*, **173**:971-973.
- Huxley A.F. (1957). *Prog.Biophys.Biophys.Chem.*, **7**:255-318.
- Lee H.D., Herzog W. (2002). *J Physiol*, **545**:321-330.
- Herzog W., Leonard T.R. (2002). *J Exp Biol*, **205**:1275-1283.
- Rassier D.E., et al. (2003). *Proceedings of the Royal Society London B*, **270**:1735-1740.
- Leonard TR, et. al. (2006) 6th International Muscle Energetics Conference
- Mehta A, et. al. (2006) 6th International Muscle Energetics Conference

## ACKNOWLEDGEMENTS

CIHR, NSERC, Canada Research Chair Programme

## **That which does not stabilize will only make us stronger: The Berkeley Exoskeleton**

H. Kazerooni

University of California, Berkeley, CA, USA

E-mail: [exo@berkeley.edu](mailto:exo@berkeley.edu) Web: <http://bleex.me.berkeley.edu/>

### **INTRODUCTION**

In October 2003, the first functional load-bearing and energetically autonomous exoskeleton, called the Berkeley Lower Extremity Exoskeleton (BLEEX) was demonstrated, walking at the average speed of two miles per hour while carrying 75 pounds of load. The project tackled four fundamental technologies: the exoskeleton architectural design, a control algorithm, a body LAN to host the control algorithm, and an on-board power unit to power the actuators, sensors and the computers. This article gives an overview of the BLEEX project.

BLEEX2, developed in 2005, weighs 30 pounds and is able to carry 200 pounds. The speed of this system is limited by the wearer's speed.

### **WHAT IS A LOWER EXTREMITY EXOSKELETON?**

The primary objective of this project at U.C. Berkeley is to develop the fundamental technologies associated with design and control of energetically autonomous Lower Extremity Exoskeletons that augment human strength and endurance during locomotion. The first field-operational lower extremity exoskeleton at Berkeley (commonly referred to as BLEEX) is comprised of two powered anthropomorphic legs, a power unit, and a backpack-like frame on which a variety of heavy loads can be mounted. This system provides its wearer (i.e., its wearer) the ability to carry significant loads on his/her

back with minimal effort over any type of terrain. BLEEX allows the wearer to comfortably squat, bend, swing from side to side, twist, and walk on ascending and descending slopes, while also offering the ability to step over and under obstructions while carrying equipment and supplies. Because the wearer can carry significant loads for extended periods of time without reducing his/her agility, physical effectiveness increases significantly with the aid of this class of lower extremity exoskeletons. In order to address issues of field robustness and reliability, BLEEX is designed such that, in the case of power loss (e.g., from fuel exhaustion), the exoskeleton legs can be easily removed and the remainder of the device can be carried like a standard backpack.

BLEEX was first unveiled in October 2003, at U.C. Berkeley's Human Engineering and Robotics Laboratory. In this initial model, BLEEX offered a carrying capacity of seventy five pounds, with weight in excess of that allowance being supported by the wearer.

BLEEX's unique design offers an ergonomic, highly maneuverable, mechanically robust, lightweight, and durable outfit to surpass typical human limitations. BLEEX has numerous applications; it can provide soldiers, disaster relief workers, wildfire fighters, and other emergency personnel the ability to carry major loads such as food, rescue equipment, first-aid supplies, communications gear, and weaponry without the strain typically

associated with demanding labor. It is our vision that BLEEX will provide a versatile transport platform for mission-critical equipment.

## **CONTROL METHOD**

The effectiveness of the lower extremity exoskeleton stems from the combined benefit of the human intellect provided by the user and the strength advantage offered by the exoskeleton. The human provides an intelligent control system for the exoskeleton, while the exoskeleton actuators provide most of the strength necessary for walking. The control algorithm ensures that the exoskeleton moves in concert with the wearer with minimal interaction force between the two. The control scheme needs no direct measurements from the user or the human-machine interface (e.g. the force sensors between the two); instead, the controller estimates, based on measurements from the exoskeleton only, how to move so that the wearer feels very little force. The basic principle for the control of BLEEX rests on the notion that the exoskeleton needs to shadow the wearer's voluntary and involuntary movements quickly, and without delay. This means that the exoskeleton requires a high level of sensitivity in response to all forces and torques on the exoskeleton, in particular the forces imposed from the wearer.

One class of systems that has large sensitivity is marginally stable systems. We therefore designed a marginally stable closed loop controller system that uses the sensor information on the exoskeleton only. This is done by using the inverse of the dynamics of the exoskeleton as a positive feedback controller so the loop gain for the exoskeleton approaches unity (slightly less than 1). Obviously, to get this method working properly, one needs to understand

the dynamics of the exoskeleton quite well, as the controller is heavily model based. Our experiments with BLEEX have shown that at this time, this control scheme—which does not stabilize BLEEX—forces it to follow human wide bandwidth maneuvers while carrying heavy loads although it requires a great deal of dynamic modeling. We have come to believe that that which does not stabilize, will only make us stronger.

BLEEX2 was developed recently to create a lighter and faster system capable of carrying larger payloads. BLEEX2 weighs 30 pounds and is able to carry 200 pounds. It is electrically powered and allows its wearer to walk and even run with minimal effort over any type of terrain.

## **REFERENCES**

A. Zoss, H. Kazerooni, A. Chu "On the Biomechanical Design of the Berkeley Lower Extremity Exoskeleton (BLEEX)", IEEE/ASME Transactions on Mechatronics, Volume 11, Number 2, April 2006.

H. Kazerooni, R. Steger, "The Berkeley Lower Extremity Exoskeletons", ASME Journal of Dynamics Systems, Measurements and Control, V128, March 2006.

H. Kazerooni, R. Steger, L. Huang "Hybrid Control of the Berkeley Lower Extremity Exoskeleton, " The International Journal of Robotics Research", V25, No 5-6, May-June 2006.

## **ACKNOWLEDGEMENTS**

This work is partially funded by DARPA grant DAAD19-01-1-0509.

# Mechanics of Head Injuries in Children - Separating Fact from Fiction

Susan S. Margulies

University of Pennsylvania, Philadelphia, PA, USA

E-mail: [Margulies@seas.upenn.edu](mailto:Margulies@seas.upenn.edu) Web: [www.seas.upenn.edu/be/labs/injury/](http://www.seas.upenn.edu/be/labs/injury/)

## INTRODUCTION

Traumatic brain injury (TBI) is the most common cause of death in childhood (CDC 1990). Brain injuries resulting in hospitalization or death occur in at least 150,000 children per year, at a rate of over 200 per 100,000 children. Head injury in infancy results in higher morbidity and mortality than that seen in older children, and it has become increasingly clear that the significant incidence of inflicted injury in the youngest patients is in large part responsible for this difference (Billmire and Myers 1985; Luerssen, Huang et al. 1991; Duhaime, Alario et al. 1992; Luerssen, Bruce et al. 1993). Determination of abuse is often subjective, confounded by limited objective data regarding injury mechanisms.

Questions include whether vigorous shaking alone can cause significant brain injury, whether repeated minor head trauma in infants can lead to catastrophic outcome, and the contribution of hypoxic-ischemic injury to the clinical presentation and prognosis of affected children. Bilateral subdural hemorrhages and loss of gray-white differentiation occur more frequently in young children, and unilateral injuries are more common in older children (Gilles and Nelson 1998), suggesting that the mechanism of injury, subsequent patterns of injury and cerebral response to abusive head trauma might differ by age. Age dependent differences may also affect clinical presentation of infants and toddlers with ultimately fatal accidental or inflicted injury (Arbogast, Margulies et al. 2005).

To date, the contributions of shaking, impact injury, brainstem and cervical cord damage, and hypoxia-ischemia to infant and toddler injury are still incompletely understood, creating a maelstrom of scientific and legal controversy. In turn, accuracy of diagnosis, protection of abused children, and avoidance of erroneous

diagnoses of abuse remain a clinical and legal challenge. Equally important, because mechanisms of pathophysiology remain unclear, effective prevention strategies and animal models for testing age and injury appropriate treatments remain elusive.

## OBJECTIVES

The long-term objectives of our research program are to identify the specific injuries and mechanisms associated with traumatic brain injuries (TBI) in young children, and to develop injury prevention and treatment strategies using animal and biomechanical models of pediatric TBI.

## HYPOTHESIS

Our overall hypothesis is that rapid rotations of the immature brain without impact produce brain injury via both mechanical and biochemical signals, resulting in sustained functional and histological abnormalities.

## RESULTS AND DISCUSSION

We have established an interdisciplinary research paradigm using acute animal experiments, biomechanical tissue tests, retrospective clinical studies, anthropomorphic "doll" re-enactments of real-world events, and computational simulations. Mechanical properties of human and porcine brain and skull revealed that infant brain tissue is stiffer than adult due to its lower lipid content and, therefore, deforms less when exposed to the same force. However, infant skull stiffness (Young's modulus) was 45 times lower than adult values, and suture was able to elongate 20 times more than adult before failure. Consequently, the pediatric braincase can deform considerably more with impact than the

adult. The biomechanics data was used to assign life-like tissue properties in the human and porcine computational models.

When we compared histopathological data from our piglet experimental model of acute diffuse brain injury with our porcine computational model predictions of tissue stresses and strains, we identified tissue deformation thresholds associated with acute axonal injury. The critical level of deformation associated with axonal injury was lower in newborn piglets than in adults, underscoring the vulnerability of immature axons to mechanical insult.

Finally, instrumented anthropomorphic surrogates were used to estimate head rotations and impact forces during vigorous shakes as well as falls and inflicted head impacts onto hard and soft surfaces. The data suggest that inflicted impacts onto hard surfaces are more likely to be associated with inertial brain injuries than are falls from <1.5 meters or shaking. Currently, we are developing computational models of the infant and toddler head to estimate biomechanical responses to vigorous shaking and impact.

In summary, we have determined that the severity and extent of acute traumatic brain injury could be predicted from the distribution of deformation (strain) in the tissue, estimated with the assistance of computational models of the head. Our results demonstrate that infant brains indeed have distinct brain injury mechanisms (loading conditions, material properties, injury thresholds) that contribute to their unique vulnerability to falls, shakes and inflicted impacts. Consequently, children require age-specific injury prevention strategies and treatments.

The focus of our ongoing studies has expanded, both to deepen our understanding of basic injury mechanisms and to enhance the clinical relevance of our findings. We now supplement our current platforms with novel preparations - survival studies, porcine behavioral outcomes, cerebral blood flow measures, post-injury

respiratory insufficiency, and promising injury treatment studies - to enhance translation of research findings from the laboratory to the clinical setting.

## REFERENCES

- Arbogast, K., S. Margulies, et al. (2005). "Initial Neurological Presentation in Young Children Sustaining Inflicted and Unintentional Fatal Head Injuries." *Pediatrics* **116**: 180-184.
- Billmire, M. and P. Myers (1985). "Serious head injury in infants: accident or abuse?" *Pediatrics* **75**(2): 340-2.
- CDC (1990). "Childhood injuries in the United States." *American Journal of Diseases of Children* **144**(6): 627-46.
- Duhaime, A., A. Alario, et al. (1992). "Head injury in very young children: Mechanisms, injury types, and ophthalmologic findings in 100 hospitalized patients under two years of age." *Pediatrics* **90**(2): 179-185.
- Gilles, E. E. and M. D. Nelson, Jr. (1998). "Cerebral complications of nonaccidental head injury in childhood." *Pediatr Neurol* **19**(2): 119-28.
- Luerssen, T., D. Bruce, et al. (1993). "Position statement on identifying the infant with nonaccidental central nervous system injury." *Pediatric Neurosurgery* **19**: 170.
- Luerssen, T., J. Huang, et al. (1991). Retinal hemorrhages, seizures, and intracranial hemorrhages: Relationships and outcomes in children suffering traumatic brain injury. *Concepts in Pediatric Neurosurgery*. A. Marlin. Basel, Karger. **11**: 87-94.

## ACKNOWLEDGEMENTS

Support for studies are provided by NIH R01 NS39679, DOT/NHTSA Cooperative Agreement No. DTNH22-01-H-07551, R49/CE000411-01 and the CDC NCIPC.

# ANALYSIS OF AN ARTICULATED FIGURE SKATING BOOT

James G. Richards and Dustin Bruening  
University of Delaware, Newark, DE, USA  
E-mail: [jimr@udel.edu](mailto:jimr@udel.edu), [dustinb@udel.edu](mailto:dustinb@udel.edu)

## INTRODUCTION

In 1990, the discipline of figures (to which the sport of figure skating owes its name) was eliminated from competitions. This precipitated a shift in training time from figures to freestyle, and specifically, to jumping. The rapid increase in jump training volume over the past 15 years may be causing a similar increase in overuse injuries. Dubravcic-Simunjack et al. (2003) determined the injury incidence of elite junior level skaters over a four year period, reporting a 20% stress fracture rate in female *junior* level singles skaters.

Coaches, trainers, and medical experts are concerned that overuse injuries in figure skating appear to be escalating at an alarming rate, as evidenced in less scientific sources (Waldman, 2006). Almost all skating injury studies have suggested a connection between overuse injuries and the stiffness of the current figure skating boot (Bloch, 1999; Brock & Striowski, 1986; Dubravcic-Simunjak et al., 2003; Pecina et al., 1990; Smith, 1990). Modifying the current figure skating boot to include an ankle articulation may help reduce landing forces by increasing the ankle's range of sagittal plane motion.

The purpose of this project was to examine the effectiveness of an articulated figure skating boot prototype in enabling a skater to attenuate the impact force at landing. Kinetic and kinematic variables were compared to test the hypothesis that articulated boots can effectively help reduce jump landing forces compared to standard boots.

## METHODS

An articulated figure skating boot was designed over a one year period and working models were manufactured by Jackson Ultima Skates (Waterloo, ON) for use in the study. Nine individual figure skaters (six females, three males) competing at the US Figure Skating defined juvenile level or higher volunteered to test the boots. Both off-ice and on-ice jump analyses were first performed while the subjects were training in their own standard boots. The skaters were then fitted with articulated skating boots in which to train. After a training time that varied between 3 days and 3 weeks, the analyses were repeated using the articulated boots.

For the off-ice tests, the subjects hopped backwards off of a 30 cm high wood box and landed on one foot on an AMTI SGA6-4 force platform (Watertown, MA) covered with a 3-mm thick sheet of acrylic (artificial ice surface). Force plate data (960hz) and marker position data (240hz) were synchronized and recorded for three trials. Only marker positions (240hz) were collected for the on-ice tests as the subjects performed single axels, double toe loops, and double axels

## RESULTS AND DISCUSSION

The group kinetic results from the off-ice jumps showed a decrease in peak heel force and loading rate with use of the articulated skates (Table 1). Several kinematic variables showed significant differences between boots in the off-ice tests, but only two (heel

acceleration and heel velocity) were significantly correlated with heel force for standard boots, articulated boots, and the difference between the boots.

The on-ice kinematic analysis did not reveal any differences between boots, except for peak knee flexion and jump height. Peak knee flexion increased in all three jump types with use of the articulated skates. Jump height was lower in double axels and trended to be lower in double toe loops. Heel acceleration and heel velocity on-ice were approximately double the value measured off-ice, despite the lower on-ice jump heights.

Results from the off-ice jump simulations support the hypothesis that an articulated skate can be used to decrease landing forces, although the exact individual mechanisms for this are still unclear. While all skaters exhibited a decrease in peak impact force and loading rate in the articulated skates, each skater implemented a somewhat unique strategy to achieve their result. No combination of variables was able to explain the difference in impact forces for a majority of the skaters.

The lack of on-ice kinematic differences suggests that the skaters did not use the articulation in skating jumps. This may be due to the difficulty of the on-ice jumps and the limited training time in the articulated skates. Heel velocity and acceleration correlated well with impact force in the off-

ice tests, allowed for speculations on the magnitude of on-ice landing forces. Specifically, estimates of the on-ice impact forces from the heel accelerations yielded peak loads in the range of 8-10 BW. However, direct on-ice measures may be needed to accurately profile the ground reaction forces.

## REFERENCES

- Dubravcic-Simunjak, S. et al. (2003). The incidence of injuries in elite junior figure skaters. *The American journal of sports medicine*, **31**, 511-517.
- Bloch, R. (1999). Figure skating injuries. *Physical medicine and rehabilitation clinics of North America*, **10**, 177-188, viii.
- Brock, R. & Striowski, C. (1986). Injuries in elite figure skaters. *The Physician and sportsmedicine*, **14**, 111-115.
- Pecina, M. et al. (1990). Stress fractures in figure skaters. *The American journal of sports medicine*, **18**, 277-279.
- Smith, A. D. (1990). Foot and Ankle Injuries in Figure Skaters. *The Physician and sportsmedicine*, **18**, 73-86.
- Waldman, P. (2006, February 17). Skaters blame boot design for injury plague. *The Wall Street Journal*, pp. A1.

## ACKNOWLEDGEMENTS

The authors wish to thank Jackson-Ultima Inc. for their help in creating prototypes.

**Table 1:** Kinetic measurements from the *off-ice* tests (mean  $\pm$  SD).

Variable	Standard Boots	Articulated Boots	p-value
Peak toe force (BW)	2.6 $\pm$ 0.8	2.9 $\pm$ 1.3	0.150
Peak heel force (BW)	5.0 $\pm$ 1.0	4.1 $\pm$ 1.0	0.047*
Loading rate (BW/s)	111.2 $\pm$ 32.9	76.4 $\pm$ 41.0	0.048*

# BIOMECHANICS OF ELASTOMERIC ENGINEERED HEART VALVE TISSUES

Michael S. Sacks, Ph.D.

Department of Bioengineering  
University of Pittsburgh  
Pittsburgh, PA

## INTRODUCTION

Synthetic scaffolds for heart valve tissue engineering applications require mechanical properties comparable to the native valve leaflet tissue for at least the minimum time necessary for the seeded cells to lay down an equivalent supporting matrix (Fig. 1). To achieve maximal results in the scaffold design process, it is beneficial to know and control specific scaffold characteristics that may alter the mechanical properties of the scaffolds so that a minimal amount of parameters could be changed to achieve the characteristics of the desired scaffold (i.e. for isotropic, moderately anisotropic, or highly anisotropic tissues). One familiar characteristic in electrospun scaffolds is fiber tortuosity, which is analogous to collagen crimp in valvular tissues. One can delay the onset of scaffold stiffness by controlling the degree of tortuosity and the fiber angles at which the tortuosity is more (or less) prominent. A constitutive model that incorporates the effects of these scaffold characteristics, and that can predict the response of the scaffold without having to perform time-consuming mechanical tests, would assist in the design of the scaffold and allow for more expediently-designed and predictable custom-tailored scaffolds. In this study, we extended our previous research with electrospun poly ester (urethane) urea (ePEUUs) scaffolds to incorporate the effects of fiber tortuosity on the mechanical response of the scaffolds. We also developed a constitutive model that is dependent not only on fiber angle but also on the fiber tortuosity with respect to fiber angle.

## MATERIALS AND METHODS

**Electrospun Scaffolds.** The methods used to develop the ePEUU scaffolds have previously been reported [1]. In brief, three generators were employed with 12 kV charging the steel capillary containing the polymer solution, -7 kV charging the aluminum collection mandrel, and 3 kV charging a steel mesh screen, which acted to control the area of fiber deposition onto the aluminum mandrel. The PEUU was synthesized at a 5% wt concentration in hexafluoroisopropanol under mechanical stirring at 25°C. The PEUU solution was fed by syringe pump into the steel capillary (I.D. = 0.047) suspended vertically over the center of the cylindrical steel mesh focusing screen and aluminum rotating mandrel (4.5" diam.) The mandrel speed was varied between 0.3 and 14.0 m/s. **Mechanical Testing.** Biaxial testing was performed on the ePEUUs to determine the mechanical properties of the

scaffolds. The procedures for biaxial testing have been previously reported [1]. The specimens were tested in room-temperature water at equibiaxial tensions ( $T_{11}:T_{22}$ ) up to 90 N/m on each side, with ten cycles. The testing protocol consisted of  $T_{11}:T_{22}$  test ratios of 0.1:1.0, 0.5:1.0, 0.75:1.0, 1.0:1.0, 1.0:0.75, 1.0:0.5, and 1.0:0.1.

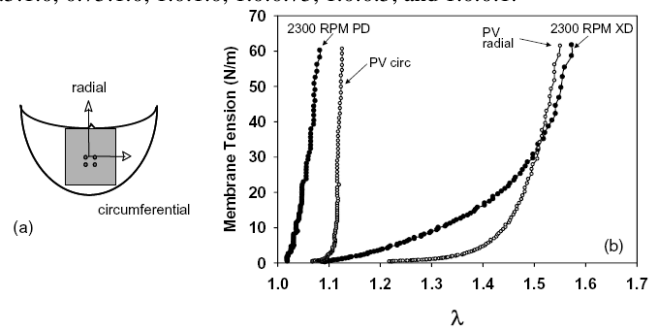


**Figure 1. (a) Biaxial mechanical specimen location of a pulmonary heart valve leaflet. (b) Resulting biaxial mechanical properties along with those of a 2300 RPM ES-PEUU scaffold.**

**Structural Characterization.** To determine the degree of alignment for the scaffolds, SEM images were obtained for the various spin speeds and analyzed using a custom image analysis software routine written in MATLAB. Two masks are created and convolved with every pixel in the image, leading to a gradient vector and angle associated with each pixel [1]. A boxsize (dimensions depending on the width of the fiber diameters) is chosen and the weighted contribution from each pixel is calculated using an accumulator function and assigned to that region. Several images were taken for each spin speed and then analyzed, with the resulting orientation data then being combined to determine the overall fiber orientation for the specimen. **Tortuosity Measures.** Tortuosity measures were performed on the SEM images of all unstrained scaffolds by tracking a fiber for the viewable length of the fiber (Fig. 2). Tortuosity was calculated by dividing the full length of the fiber by the end-to-end distance of the fiber. Twenty-five fibers were tracked on each SEM image for a total of 150 fibers for each spin speed. To better understand the change in tortuosity with deformation, a stage was designed that allowed the scaffold to be stretched and imaged using SEM. Specific regions of the scaffolds were imaged in a

unstretched reference and deformed state.

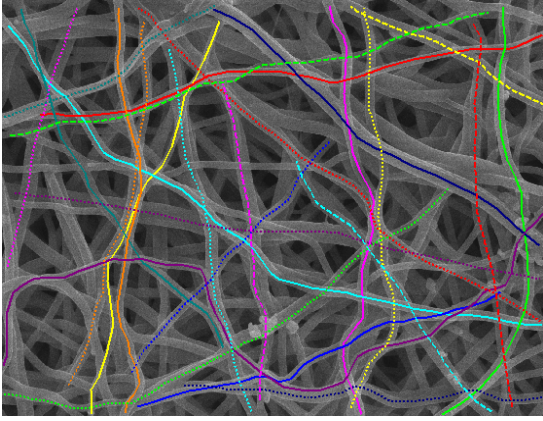


**Figure 2. Tracking of fibers to determine the degree of tortuosity with respect to angle**

The resulting fiber orientation data were normalized using,

$$R(\theta) = \frac{\bar{I}(\theta)}{\sum_{\theta=-\pi/2}^{\pi/2} \bar{I}(\theta)\Delta\theta} \quad (1)$$

where  $\theta$  is the fiber direction with respect to the preferred fiber axis. The PEUU effective fiber stress-strain properties were determined from the mechanical data using,

$$S_f(\theta) = \kappa \int_0^\varepsilon D(x,\theta) \frac{\varepsilon - x}{(1 + 2x)^2} dx \quad (2)$$

where  $S_f$  is the 2<sup>nd</sup> Piola–Kirchhoff fiber stress,  $\kappa$  is the fiber elastic modulus and  $D(x,\theta)$  is the statistical distribution accounting for the fiber recruitment.  $D(x,\theta)$  is a function of the fiber strain and orientation  $\theta$ , with the strain itself a function of fiber angle, since it was found that tortuosity varies with angle as the mandrel speed increases (Fig 2). The structural and mechanical data were then combined to determine the Lagrangian membrane stresses. Using the structural data,  $R(\theta)$ , and a single equibiaxial test for the determination of the fiber stress-strain response, the model allows one to predict the complete biaxial mechanical response of the polymer.

## RESULTS

The PEUU scaffolds displayed higher orientation with increasing stretch as tortuosity is gradually lessened. Tortuosity was higher in the direction of spin of the mandrel. The scaffolds with the most amount of variation in tortuosity were those developed at higher mandrel velocities (fig 3). Tortuosity for random (isotropic) scaffolds exhibited no dependence on fiber angle. As the mandrel speed was increased though, tortuosity was much more dependent on fiber angle. Inclusion of the tortuosity data into the constitutive model yielded a much more robust fit to the experimental data. Upon stretching the scaffolds and viewing them under the SEM, it was seen that the fibers gradually straightened (fig 4). The disappearance of tortuosity depended on the scaffold, which showed angular dependence, and also the amount of stretch. This is the first time that this angular dependence has been incorporated into a structural model developed for soft tissues or scaffolds. Also shown are dual photon images of the ES-PEUU scaffold demonstrating that this imaging technique can be utilized to quantify scaffold fiber rotation and stretch, as well as cellular deformations (Fig. 5).

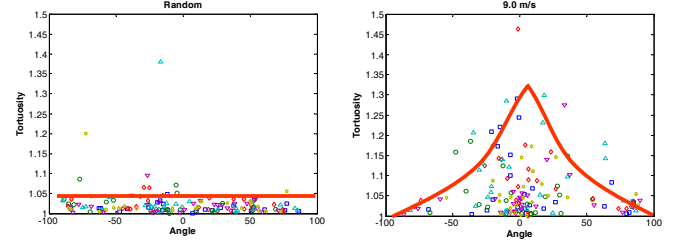


**Figure 3. Tortuosity vs. angle for (a) random (isotropic) scaffold, (b) 9.0 m/s scaffold. As mandrel speed is increased, tortuosity also increases and there is a concentration of more tortuous fibers along the direction of spin.**

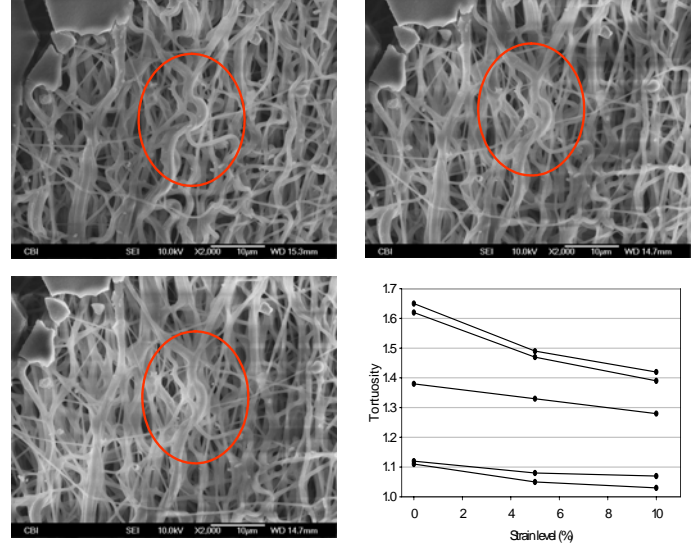


**Figure 4. Gradual straightening of fibers as the scaffold is strained. Oval region in SEM images shows the effect of strain on a fiber. (Top left-no strain, top right-5% strain, bottom left-10%strain) Bottom right figure shows the decrease in tortuosity with increasing strain.**

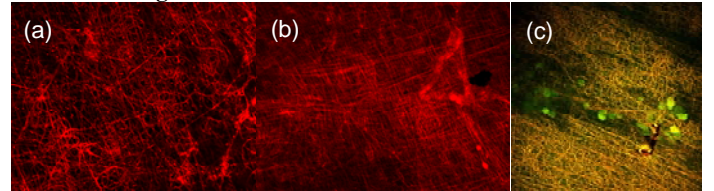


**Figure 5. Dual photon images of the ES-PEUU scaffold in the (a) unloaded, (b) loaded states, along with the integrated cells in (c).**

## CONCLUSIONS

The biaxial stretching analysis allowed for the measure of tortuosity fibers and the gradual diminishing of that tortuosity with stretch. The data allowed for a more robust constitutive model to predict the mechanical response of the scaffolds. Future work will investigate the effect of stretch on cells integrated into the scaffold and compare this with cellular deformation within the ECM.

## ACKNOWLEDGEMENTS

Funded by NIH grants HL-069368 and HL-68816

## REFERENCES

1. Sacks, MS et al. J. Biomaterials. 2006 (In press)

# A MOTORIZED FLYWHEEL FOR SKATING CROSSOVER TRAINING: DOES IT SIMULATE ON-ICE PERFORMANCE? A PILOT STUDY

Michael J. Stuart, M.D.<sup>1</sup>; Aynsley M. Smith, RN, Ph.D.<sup>1</sup>; Moira McPherson, Ph.D.<sup>2</sup>; William Montelpare, Ph.D.<sup>2</sup>; Matthew C. Sorenson, MA<sup>1</sup>; and Brian Graner, M.E<sup>1</sup>.

<sup>1</sup> Mayo Clinic College of Medicine, Rochester, MN, USA

<sup>2</sup> Lakehead University, Thunder Bay, Ontario, CA

E-mail: [stuart.michael@mayo.edu](mailto:stuart.michael@mayo.edu) Web: [www.mayo.edu](http://www.mayo.edu)

## INTRODUCTION

The skating crossover is central to on-ice agility and performance, comprising a high percentage of skating strides executed during a game. Although scientific studies have examined physiologic and kinematic variables of forward skating, no studies have analyzed these variables in hockey players during the crossover stride. Recently, a prototype skating flywheel was designed to improve on-ice cross-over technique and endurance. The 22 foot diameter polyethylene skating flywheel is capable of inclines between 5 degrees and 35 degrees, driven by a variable frequency electric motor.

## METHODS

To determine the relationship between on-ice and flywheel crossovers a pilot study of five hockey players was conducted. Kinematics, rate of perceived exertion, heart rate and cadence were tested during forward skating both directions on the flywheel and on-ice, using a circle of a similar diameter. Two digital video cameras oriented to pan and tilt through the required field width recorded skaters performing the crossover technique under on-ice and flywheel conditions. Calibration poles were filmed in the field following each session to provide the information necessary for the image to produce real life conversions. The **Peak Motus®** software was used to digitize the video and extract the 3D coordinates for the following specific kinematic parameters (1)

point of outside leg maximal extension, (2) point of outside leg contact, (3) point of inside leg maximal extension and (4) point of inside foot contact.

## RESULTS

Rate of Perceived Exertion averaged 10.0 on ice and 12.8 on the flywheel (corresponding approximate heart rate average of 100 bpm on-ice and 130 bpm on the flywheel according to the Borg Scale). The cadence, timed to on-ice contact of the crossover foot, (as set to a metronome) ranged from 42-50 on ice and 54-68 on the flywheel. The results indicated that movement similarities between the on-ice and off-ice conditions exist. There was variability within and between skaters across conditions.

Differences in preferred and non-preferred direction were more pronounced on the flywheel.

With the exception of one highly trained subject, average stride rate on the flywheel (measured as cadence with a metronome)

was 25% faster on the flywheel, and RPE was approximately three intervals higher on the flywheel, corresponding to a 30 bpm faster HR.

## CONCLUSIONS

These preliminary results suggest that Flywheel training will translate to increased on-ice crossover skating velocity and endurance. The next phase of this research is a randomized, repeated measure design that will examine changes in velocity, endurance, and kinematics as a result of adding flywheel training to the regular training regime.

## ACKNOWLEDGEMENTS

The investigators thank USA Hockey.

## REFERENCES

- Pollock, M. L, Wilmore, J.H and Fox, S.M. Exercise in Health and Disease (1984) W.B. Saunders Company, pp189-192.
- McPherson et al. (2004) The Biomechanical Characteristics of Development Age Hockey Players. Safety in Ice Hockey.

# 3D FINITE ELEMENT SIMULATIONS OF THE DYNAMIC INTERACTION BETWEEN A FINGERTIP AND A FLAT SURFACE

John Z Wu, Daniel E Welcome, and Ren G Dong

National Institute for Occupational Safety and Health, Morgantown, WV, USA  
E-mail: jwu@cdc.gov

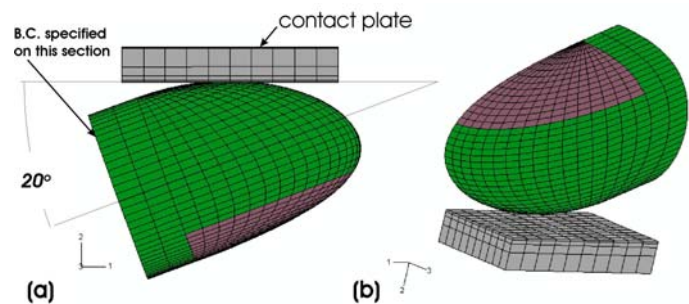
## INTRODUCTION

The contact interactions between hands and handles may influence the loading distributions in musculoskeletal systems while operating power tools (Gurram et al., 1995). Many occupation-related disorders in the hand and fingers are believed to be associated with the contact pressure between the fingers and the tool handle. The contact interactions between fingers and handle may also interfere with grasp stability, thereby affecting the manipulations of hand-held tools (Birzniaks et al., 1998). The purpose of the present study is to develop a 3D finite element (FE) model for the fingertip to simulate the nonlinear and time-dependent responses of a fingertip to static and dynamic loadings and to compare the theoretical predictions with the published experimental data.

## METHODS

The fingertip considered in the model is the distal phalanx, the portion of the finger distal to the distal interphalangeal (DIP) joint articulation, as shown in Fig. 1. The external shape of the fingertip was determined using a smooth mathematical surface fitting to the digitized fingertip shapes. The fingertip model has a length of 25 mm, a width of 20 mm, and a height of 18 mm, which are considered to be representative for a typical male index finger. The fingertip was assumed to be symmetric, such that only a half of the fingertip was considered in the modeling. The FE model incorporates the essential

anatomical structures of a finger: skin layers (outer and inner skins), subcutaneous tissue, bone, and nail. The soft tissues (inner skin and subcutaneous tissue) are considered to be nonlinearly viscoelastic, while the hard tissues (outer skin, bone, and nail) are considered to be linearly elastic. The simulations were performed using the commercial FE software package Abaqus (version 6.5). Using the proposed model, we have studied the dynamic contact interaction between the fingerpad and a flat surface. The fingertip was subjected to four different loading/unloading time-histories, as shown



in Fig. 2.

**Figure 1:** FE model of the fingertip in contact with a flat surface. (a): side view. (b): perspective view. The fingertip is in contact with a flat plate with a contact angle of  $20^\circ$ .

## RESULTS AND DISCUSSION

The predicted time-histories of the force responses agree well in trends with the corresponding data (Wu et al., 2003) for the dynamic contact of the fingertip with the flat surface (Fig. 3). At the moment when the compressed displacement was suddenly released from 2 mm to 1 mm, the model

predicts that the contact force reaches about zero and then recovers to higher levels. These simulation results are a little different from the experimental observations, which showed higher minimum force values. The difference between the theoretical prediction and experiment data at that particular point is likely due to artifacts in the experiments. The small contact forces (< 5 g) observed in the experiments may be caused by the inertia of the indentation plate, while the simulations were performed using a quasi-static scheme in which the inertial effects of the contact platen were excluded.

### SUMMARY/CONCLUSIONS

In the present study, we proposed a novel 3D FE fingertip model, which contains realistic anatomic micro structures and nonlinear viscoelastic material properties of the soft tissues. The model predictions on the time-dependent force responses of the fingertip subjected to the dynamic contact with a flat surface agree well with the published experimental observations.

### REFERENCES

*Birznieks, I. et al.* (1998). *J Neurophysiol*, 80 (4) 1989–2002.  
*Gurram, R. et al.* (1995). *Ergonomics*, 38 (4) 684–699.  
*Wu, J.Z. et al.* (2003). *Med Eng Phys*, 25, 397-406.

### DISCLAIMER

The findings and conclusions in this report are those of the authors and do not necessarily represent the views of the National Institute for Occupational Safety and Health.

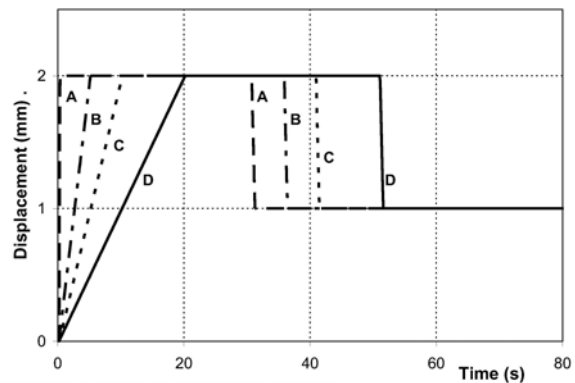


**Figure 2:** The flat contact plate was prescribed to four (A, B, C, and D) different displacement time-histories in the simulation

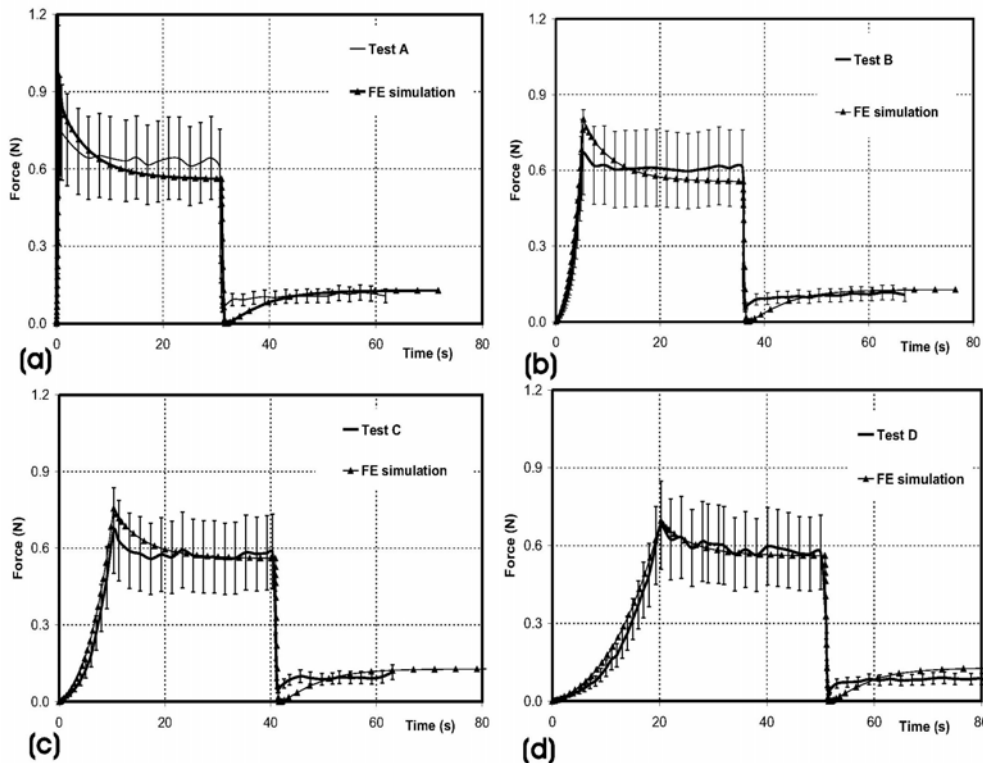


**Figure 3:** The comparison of the predicted time-dependent force responses with the experimental data (Wu et al., 2003)

# LOWER EXTREMITY JOINT ENERGETICS DURING DROP JUMPS TO DIFFERENT TARGET HEIGHTS

Steven T. McCaw and Aaron J. Decker

Illinois State University, Normal,

email: [smccaw@ilstu.edu](mailto:smccaw@ilstu.edu), web: [cast.ilstu.edu/mccaw](http://cast.ilstu.edu/mccaw)

## INTRODUCTION

Plyometric strength training incorporates the stretch-shorten cycle while providing an overload. A form of lower extremity plyometrics is the drop jump. The subject steps off a box, lands and immediately executes a vertical jump. Drop jumps are varied in training by adjusting drop height or the height of the following target jump.

Most research on drop jumps has adjusted drop height followed by a maximal vertical jump. The analysis focuses on the initial energy absorption and the latter energy generation phases of ground time (Bobbert et al, 1987a&b; Walsh et al, 2004). With increased drop height, negative work during the absorption phase increases although the duration of the phase does not change. Increased height in the subsequent jump is achieved by increasing positive work during the generation phase. Bobbert et al. (1987 a&b) showed that the ankle and knee are the primary energy absorbers, while the knee and ankle are the primary energy generators.

One version of drop jump training involves dropping from a set height but varying the target height of the subsequent jump, keeping kinetic energy at contact the same but altering the demands of the jump. We were interested in how the protocol alters individual joint contributions. The purpose of the study was to compare measures of individual joint energetics among jumps performed to different target heights after dropping from a consistent height.

## METHODS

Fourteen physically active males were subjects. Four trial blocks of drops from a 60 cm box with target jump heights of 40, 60 and 80 cm were collected in random order. Instructions were to “land and take off as quickly as possible”.

Subjects landed with the right foot on a force platform (960 Hz) with right side markers defining the trunk, thigh, shank and foot segments on high speed video (120 Hz). Custom software using an inverse dynamic analysis calculated joint torques. Joint mechanical power was calculated as joint torque\*joint angular velocity.

Ground contact consisted of two phases: energy absorption during negative joint power and energy generation during positive joint power. Negative and positive work was calculated by integrating the joint power curve during the absorption and generation phases; values were scaled to body mass (Joules/kg). The relative contribution of each joint was calculated by dividing joint phase work by total phase work (sum of all three joints' work). Each variable was entered into a repeated measures oneway ANOVA ( $\alpha = .05$ ).

## RESULTS AND DISCUSSION

Descriptive statistics of temporal and energetic variables are presented in Table 1. Similar to Bobbert et al (1987a&b), ground contact time did not differ significantly and the duration of the two phases were also similar across the three target heights.

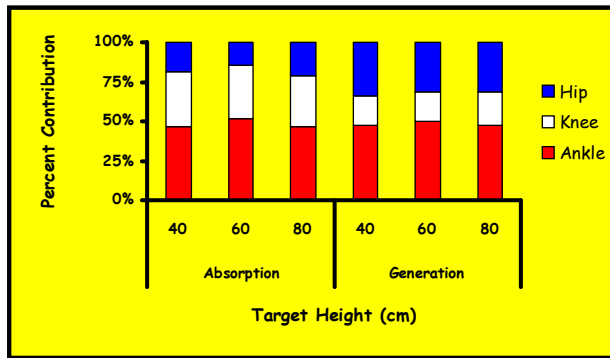


**Figure 1** Percent relative contribution of hip, knee and ankle joints to total energy absorption and generation.

The ankle and knee were primary absorbers of energy (Figure 1). The total negative work during the absorption phase was not different and the ankle joint was the primary contributor to energy absorption across the heights. There were no significant differences in the negative work at the joints or in the relative joint contributions to energy absorption. This suggests that energy absorption in a drop jump is not affected by the demands of the subsequent target jump.

Total work during absorption was significantly greater than total work during generation at all target heights. Total work during generation significantly increased

from 2.21 J/kg at 40 cm to 2.45 J/kg at 60 cm, but there was no significant change to 80 cm. Hip and knee flexion in the air, and not work during the energy generation phase, probably becomes of greater import to attain jumps heights higher than 60 cm.

The ankle and hip were primary generators of energy (Figure 1). Increasing the ankle work by ~19% was the primary source to increase total work for a 60cm jump.

### SUMMARY/CONCLUSIONS

There was little change in the energetics of the absorption phase after dropping from a consistent height. There was a significant increase in ankle joint energetics during the generation phase of jumps to different target heights, but the changes do not warrant using a target height as high as 80 cm.

### REFERENCES

- Bobbert, MF et al. (1987a). *MSSE*, **19**, 332-338.  
 Bobbert, MF et al. (1987b). *MSSE*, **19**, 339-346.  
 Walsh, M et al. (2004). *JSCR*, **18**, 561-566.

**Table 1:** Descriptive statistics of selected temporal and energetic variables

		TARGET HEIGHT						Comps
		40 cm		60 cm		80 cm		
		Mean	SD	Mean	SD	Mean	SD	
Contact	Time	0.279	0.048	0.284	0.056	0.289	0.056	NSD
	Tabs	0.135	0.023	0.135	0.028	0.138	0.027	NSD
	Tgen	0.143	0.026	0.148	0.029	0.151	0.030	NSD
Ttl Work	Abs	-3.06	0.39	-3.07	0.44	-3.12	0.37	NSD
	Hip	-0.58	0.31	-0.61	0.37	-0.67	0.35	NSD
	Knee	-1.05	0.29	-0.98	0.27	-1.00	0.27	NSD
	Ankle	-1.43	0.48	-1.48	0.44	-1.45	0.29	NSD
Ttl Work	Gen	2.21	0.42	2.45	0.34	2.54	0.28	40<60=80
	Hip	0.76	0.28	0.78	0.28	0.80	0.26	NSD
	Knee	0.42	0.18	0.46	0.11	0.54	0.14	40<80

Units: Time in seconds, Work in Joules/kilogram

# MODELING ATTENTION AND SENSORY INTEGRATION IN POSTURAL CONTROL OF OLDER ADULTS

Arash Mahboobin, Patrick Loughlin, and Mark Redfern

University of Pittsburgh, Pittsburgh, PA, USA  
E-mail: loughlin@engr.pitt.edu

## INTRODUCTION

Attention plays a role in postural control (Redfern et al. 2001; Shumway-Cook and Woollacott 2000), as does dynamic sensory integration (Horak and Macpherson 1996; Oie et al. 2002; Peterka 2002; Peterka and Loughlin 2004). However, the interaction between attention and sensory integration is an open question.

We conducted an experiment, similar to those in (Peterka 2002) but augmented to include information processing (IP) tasks, to explore this question. Data were fit to a postural control model (Peterka 2002; Peterka and Loughlin 2004). We explicitly added “attention” to the model and its influence on sensory integration via the sensory weight and time delay parameters of the model (Fig. 1). This model hypothesizes that the cognitive processing and integration of sensory inputs for balance requires time, and that attention influences this processing time, as well as sensory selection by facilitating specific sensory channels. A competing IP dual-task would compete for cognitive resources and thus increase the delay time in the model if the capacity for this processing is limited, i.e. subject to attention. We explored model response differences between young and older adults.

## METHODS

Ten healthy young adults (M = 5, F = 5, 25±3 yrs.) and five older adults (M = 3, F = 2, 73±9 yrs.) participated in this study, with their IRB-approved informed consent.

Subjects stood, while performing IP tasks, with eyes closed and arms folded across their chest on an EquiTest posture platform that rotated randomly ( $\pm 1$  deg) for 121 sec about an axis collinear with the ankle axis. Platform motion was preceded and followed by 30 seconds of no platform motion. Three trials per subject per IP task were conducted, and subjects performed the IP task throughout the 181 sec trials. IP tasks were performed on different days.

The IP tasks were: 1) None, 2) an auditory choice reaction task (CRT), in which subjects pressed a hand-held microswitch with either the left hand or right hand depending on whether they heard a high or low tone (980 Hz or 560 Hz, duration 250 msec, intensity 80 dB SPL, mean inter-stimulus interval of 4 sec), 3) an auditory vigilance task (VT), in which subjects had to remember the number of high or low tones heard during the trial. Subjects were trained in the IP tasks prior to testing. Platform movement and A-P hip position were recorded, from which least-squares fits to the postural control model were made, analogous to (Peterka 2002).

## RESULTS AND CONCLUSION

The time delay of the postural control model increased during concurrent IP tasks and postural perturbations for both the CRT and VT tasks in the older adults; young adults exhibited an increased time delay for only the more cognitively-challenging VT IP task (Table 1). Older subjects, unlike younger subjects, also exhibited changes in sensory

re-weighting during concurrent IP tasks, as manifest by a decrease in proprioceptive weight relative to no IP conditions.

These results suggest that dual-task interference impacts postural control processing time for young and older adults; however, older adults are sensitive to less challenging cognitive tasks (i.e. CRT) that do not affect young adults. Differences in attentional influences on sensory selection may also exist. Further study in a larger population is planned.

## REFERENCES

Horak, F.B. and Macpherson, J.M. (1996). In: *Handbook of Physiology*. Oxford University Press, pp. 255-292.

Oie, K.S. et al. (2002). *Brain Res Cogn Brain Res*, **14**:164-76.

Peterka, R.J. (2002). *J Neurophysiol.*, **88**:1097-1118.

Peterka, R.J. and Loughlin, P. (2004) *J. Neurophysiol.*, **91**:410-423.

Redfern, M.S. et al. (2001). *Gait Posture*, **14**:211-216.

Shumway-Cook, A. and Woollacott, M. (2000). *J Gerontol A Biol Sci Med Sci*, **55**:M10-6.

## ACKNOWLEDGEMENT

Funding provided by the Pittsburgh Claude D. Pepper Older Americans Independence Center [P30 AG024827 (NIA)].

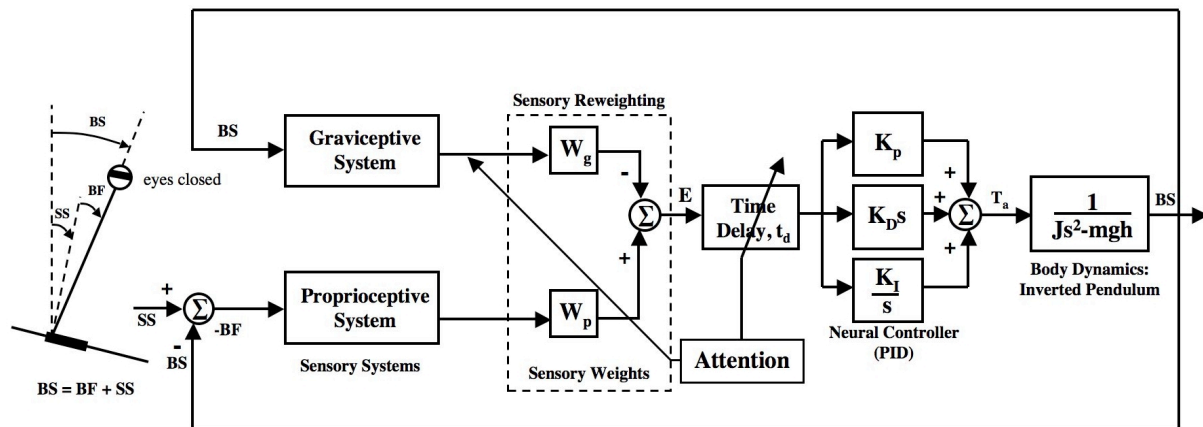


**Figure 1.** Feedback model of postural control for eyes-closed stance. The body is modeled as a linearized inverted pendulum. Sensory pathways include weights ( $W_g$ ,  $W_p$ ) that can change as environmental factors change (the “sensory re-weighting” hypothesis). Corrective ankle torque,  $T_a$ , is generated by a fixed-gain proportional-integral-derivative controller acting on the combined delayed error signal  $E$  from the sensory systems. Attentional tasks that interfere with balance are hypothesized to increase cognitive processing time involved in balance, manifest in the model as an increase in the time delay of the system. Attention may also influence sensory integration, as manifest in the model via the sensory weights ( $W_g$ ,  $W_p$ ). Modified from (Peterka 2002; Peterka and Loughlin 2004).

**Table 1:** Postural Control Time Delay for Young and Older Adults during IP tasks vs. no task (mean± SD).

IP Task	$t_d$ [msec], YOUNG	$t_d$ [msec], OLDER
NONE	153.52±11.98	155.42±11.93
CRT	153.55±18.00	165.34±20.01
VT	161.90±12.98	163.04±12.05

# CHANGES IN THE ORBITAL STABILITY OF WALKING ACROSS SPEEDS

Laura C. Marin<sup>1</sup>, Hyun Gu Kang<sup>2</sup>, and Jonathan B. Dingwell<sup>2</sup>

<sup>1</sup>Military Performance Lab, Brooke Army Medical Center, Fort Sam Houston, TX, USA

<sup>2</sup>Nonlinear Biodynamics Lab, Dept. of Kinesiology, University of Texas, Austin, TX, USA

E-mail: jdingwell@mail.utexas.edu

Web: <http://www.edb.utexas.edu/faculty/dingwell/>

## INTRODUCTION

The elderly and patients with gait pathologies walk at slow speeds and are at increased risk of falls. Properly defining and quantifying the relationship between speed and walking stability is therefore important. *Local* stability measures define how systems respond to small perturbations *in real time*. Local stability improves with slower walking speeds (Dingwell & Marin, 2006), suggesting that slowing down may be a useful strategy to improve walking stability. *Orbital* stability defines how purely *periodic* systems respond to small perturbations *discretely* after one complete cycle (i.e. one stride) and may be better suited to study strongly periodic movements like walking (Hurmuzlu & Basdogan, 1994; Full et al., 2002). While Hurmuzlu found that human walking was orbitally stable, we previously reported significant local *instability* (Dingwell & Cusumano, 2000). Therefore, we set out to determine how walking speed affects the *orbital* stability of human walking.

## METHODS

Eleven healthy subjects (age: 21-34 yr, 5 female) participated after giving informed consent. Each subject performed three treadmill trials at each of five walking speeds: their preferred walking speed (PWS), PWS  $\pm 20\%$ , and PWS  $\pm 40\%$ . 3-D kinematic data of a single marker on the first thoracic vertebrae were collected at 60 Hz using a 6-camera Vicon motion analysis system (Oxford Metrics, Oxford, UK). Because subjects tended to “wander” on the treadmill, first-

difference time series ( $\Delta$ ) were computed and analyzed to ensure improved signal stationarity (Dingwell & Marin, 2006).

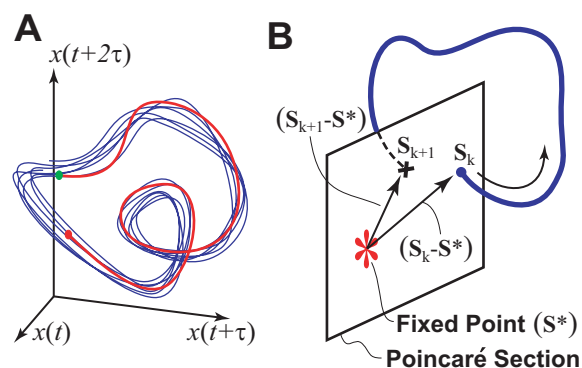


**Figure 1:** **A:** Example of a 3-D state space,  $\mathbf{S}(t) = [x(t), x(t+\tau), x(t+2\tau)]$ , constructed from a single scalar variable,  $x(t)$ , and its time-delayed copies. **B:** Floquet multipliers quantify how much small perturbations ( $S_k$ ) away from the fixed point ( $S^*$ ) grow or decay after 1 complete stride ( $S_{k+1}$ ).

Multi-dimensional state spaces,  $\mathbf{S}(t)$ , were reconstructed from each time series, using an embedding dimension of 5 (Dingwell & Marin, 2006). Orbital stability was quantified by computing the magnitudes of the maximum Floquet multipliers (Hurmuzlu & Basdogan, 1994) at each percent (0% to 100%) of the gait cycle. We defined the fixed points ( $S^*$ ) at each Poincaré section (i.e., at each % of the gait cycle) as the average trajectory across all strides within a trial. Floquet multipliers (FM) were then computed from (Fig. 1B):

$$[S_{k+1} - S^*] \approx J(S^*)[S_k - S^*]$$

where  $J(S^*)$  defined the Jacobian matrix for the system at each Poincaré section. The

Floquet multipliers are the eigenvalues of  $J(S^*)$ . They define the amount by which small perturbations grow or diminish after one cycle. If the maximum FM has magnitude  $< 1$ , perturbations decay from stride to stride and the system is orbitally stable.

The Max FM at different walking speeds were compared using repeated measures ANOVA and quadratic regression.

## RESULTS AND DISCUSSION

All subjects exhibited orbitally stable walking kinematics across the entire gait cycle (Max FM  $< 1$ ; Fig. 2), although these same kinematics were previously shown to be locally *unstable* (Dingwell & Marin, 2006).

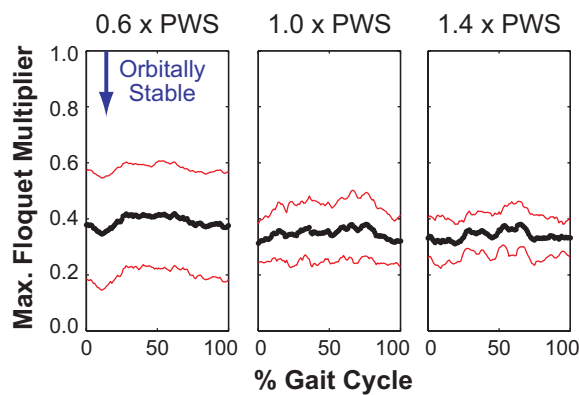


**Figure 2:** Variations in maximum FM across the gait cycle for AP trunk movements ( $\Delta_{AP}$ ). “Max FM” was defined as the largest of these maximum FM across all points during the gait cycle.

Orbital stability changed very little with speed (Fig. 3). The ANOVA revealed only 1 significant ( $p < 0.05$ ) difference: moderately slow speeds ( $0.8 \times PWS$ ) were more stable than the fast speeds ( $1.4 \times PWS$ ) for  $\Delta_{AP}$  movements. While orbital stability improved slightly with slower walking speeds, only the regression between walking speed and Max FM for  $\Delta_{AP}$  movements was statistically significant ( $p = 0.009$ ), and all regressions were generally weak ( $r^2 < 17\%$ ).

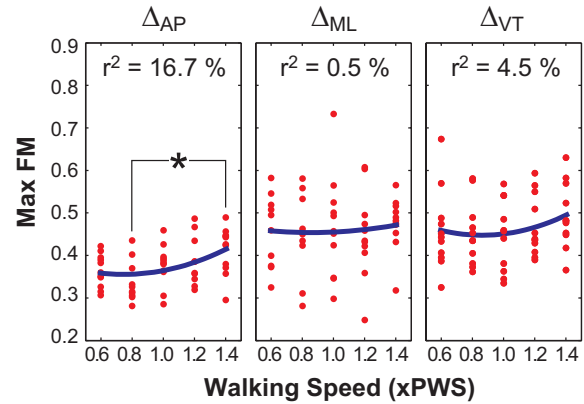


**Figure 3:** Variations in Max FM with changes in walking speed for upper body movements in all 3 directions (AP, ML, and VT). Curves are quadratic fit lines. The \* indicates a significant difference ( $p < 0.05$ ).

## CONCLUSIONS

Kinematic variability increases at slower walking speeds, even though *local* stability actually improves (Dingwell & Marin, 2006). Conversely, *orbital* stability changed very little (Fig. 3). Thus, orbital stability is not very sensitive to changes in speed. For patients at increased risk of falling, this suggests that while slowing down may help improve *local* stability, it does not yield any benefit with respect to *orbital* stability.

## REFERENCES

- Dingwell, J.B. and Cusumano, J.P. (2000) *Chaos*, **10** (4): 848-63.  
 Dingwell, J.B. and Marin, L.C. (2006) *J. Biomech.*, **39** (3): 444-52.  
 Full, R.J., et al., (2002) *Integr. Compar. Biol.*, **42** (1): 149-57.  
 Hurmuzlu, Y. and Basdogan, C. (1994) *J. Biomech. Eng.*, **116** (1): 30-36.

## ACKNOWLEDGEMENTS

Supported by Research Grant # RG-02-0354 from the Whitaker Foundation.

# OF MYOSINS, MUSCLES AND MECHANISMS OF CONTRACTION

Walter Herzog

University of Calgary, Calgary, AB, Canada

E-mail: [walter@kin.ucalgary.ca](mailto:walter@kin.ucalgary.ca) Web: <http://www.kin.ucalgary.ca/HPL/content/herzog.html>

## INTRODUCTION

For the past two decades, my research has been focused on the biomechanics of the musculoskeletal system with specific interest in skeletal muscle function and contraction. In the 1980s, I tackled the distribution problem in biomechanics, theoretically and experimentally, and realized that a solution to this problem could only be achieved with a deep understanding of the mechanical properties of muscles. Investigating the force-length and force-velocity relationships, I stumbled over the phenomenon of force enhancement and force depression following stretching and shortening of activated muscles, respectively (Abbott and Aubert 1952), and realized that these history-dependent properties could not be explained within the framework of the sliding filament (Huxley and Niedergerke 1954; Huxley and Hanson 1954) and the cross-bridge theory of muscle contraction (Huxley 1957). This realization led to a body of work covering the last decade that was aimed at unraveling the mechanisms responsible for force depression and force enhancement, and in parallel, a re-evaluation of the sliding filament and cross-bridge theories of contraction.

For the purpose of the Borelli lecture, I will focus on the research on force enhancement and the implications of this work for the cross-bridge theory. Force enhancement is defined here as the extra force of an isometric, steady-state contraction that is preceded by stretching of the activated muscle, compared to the corresponding isometric, steady-state force of a purely isometric contraction (i.e., one that is not preceded by stretch – Figure 1).

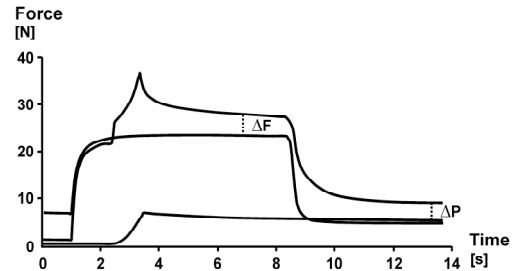


Figure 1: Definition of force enhancement ( $\Delta F$ ) and passive force enhancement ( $\Delta P$ ).

## METHODS

Force enhancement was induced in all preparations by stretching an activated muscle by various amounts and at various speeds. The preparations tested included in vivo human muscles (Lee and Herzog 2002), an in situ preparation of the cat soleus (Herzog and Leonard 2002), single fibres of the tibialis anterior and lumbrical muscles of the frogs (Rassier et al. 2003), single myofibrils from the rabbit psoas (Leonard et al. 2006), and single cross-bridge interactions with isolated actin molecules (Mehta et al. 2006). For details of the preparations, please be referred to the original papers.

## RESULTS AND DISCUSSION

Steady-state force enhancement was present in all preparations ranging from in vivo voluntary contractions to single myofibrils. Force enhancement was increased with increasing magnitudes of stretch (Figure 2), was independent of stretch speed, and was associated with an increase in muscle stiffness and a decrease in force relaxation time. Most importantly, at long muscle length, force enhancement was also

accompanied by an increase in passive force (after muscle relaxation – Figure 1) that could account in extreme cases for up to 85% of the total force enhancement measured in the activated muscle.

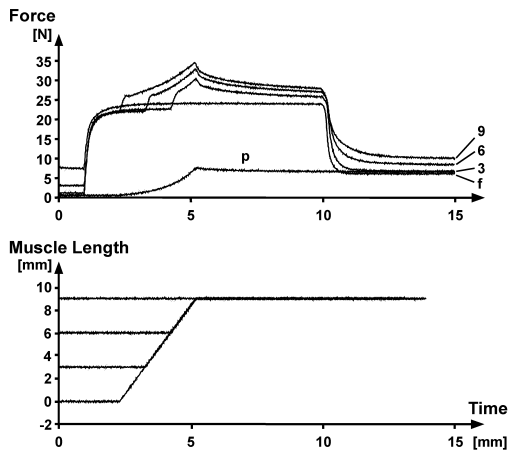


Figure 2: Force enhancement increases with increasing magnitudes of stretch

From the results of these studies, we concluded that force enhancement consists of an active and passive component. The active component was tentatively associated with a decrease in the rate of detachment of cross-bridges from actin; the passive component was hypothesized to originate from a calcium-dependent increase in stiffness of the molecular spring titin.

In order to test these two hypotheses, we first performed experiments on single cross-bridge interactions with actin and measured the duty ratio of cross-bridges subjected to stretching and shortening, and second, performed tests on single myofibrils which were activated with solutions of increasing calcium concentrations and measured the passive forces by inhibiting active forces through deletion of troponin C on actin.

The results indicated that stretched cross-bridges have a smaller duty ratio than shortened cross-bridges, therefore rejecting our first hypothesis that the active force

enhancement might be caused by an increase in the duty ratio.

The second experiment demonstrated that myofibril stiffness increased with increasing calcium concentration (in the troponin C deleted preparation), thereby supporting the hypothesis that at least part of the passive force enhancement was caused by a calcium-dependent increase in titin stiffness.

## SUMMARY/CONCLUSIONS

Force enhancement has an active and a passive component. The active component is likely associated with an as of yet unknown stretch-dependent change in the cross-bridge kinetics, while the passive force enhancement is caused in part by a calcium-dependent increase in the stiffness of the molecular spring titin.

## REFERENCES

- Abbott B.C., Aubert X.M. (1952). *J Physiol*, **117**:77-86.
- Huxley H.E., Hanson J. (1954). *Nature*, **173**:973-976.
- Huxley A.F., Niedergerke R. (1954). *Nature*, **173**:971-973.
- Huxley A.F. (1957). *Prog.Biophys.Biophys.Chem.*, **7**:255-318.
- Lee H.D., Herzog W. (2002). *J Physiol*, **545**:321-330.
- Herzog W., Leonard T.R. (2002). *J Exp Biol*, **205**:1275-1283.
- Rassier D.E., et al. (2003). *Proceedings of the Royal Society London B*, **270**:1735-1740.
- Leonard TR, et. al. (2006) 6th International Muscle Energetics Conference
- Mehta A, et. al. (2006) 6th International Muscle Energetics Conference

## ACKNOWLEDGEMENTS

CIHR, NSERC, Canada Research Chair Programme

# EFFECTS OF SENSORY LOSS ON THE ORBITAL STABILITY OF WALKING

Jonathan B. Dingwell and Hyun Gu Kang

Nonlinear Biodynamics Lab, Dept. of Kinesiology, University of Texas, Austin, TX, USA  
 E-mail: jdingwell@mail.utexas.edu Web: http://www.edb.utexas.edu/faculty/dingwell/

## INTRODUCTION

Peripheral sensory feedback is believed to contribute significantly to maintaining walking stability. Patients with diabetic peripheral neuropathy have a greatly increased risk of falling (Richardson, 2002). We previously demonstrated that slower walking speeds in neuropathic patients lead to improved *local* dynamic stability (Dingwell et al., 2000). However, all subjects exhibited significant *local instability* during walking, even though no subject fell or stumbled.

Currently there is no commonly accepted way to define or quantify walking stability. *Local* stability measures (Dingwell et al., 2000) define how aperiodic systems respond to small perturbations *in real time*. Measures of *orbital* stability that define how purely periodic systems respond to small perturbations *discretely* after one complete cycle (i.e. one stride) may be better suited to study strongly periodic movements like walking (Hurmuzlu & Basdogan, 1994; Full et al., 2002). The present study was therefore conducted to determine if and how significant changes in peripheral sensation affect *orbital* stability during walking.

## METHODS

14 diabetic patients with significant peripheral neuropathy (NP) and 12 appropriately matched controls (CO) participated. A custom-made data logger (Dingwell et al., 2000) was used to collect kinematic data during continuous walking. Electrogoniometers measured sagittal plane motions of the hip, knee, and ankle. A tri-axial accelerome-

ter mounted at the base of the sternum measured trunk motions. Data were sampled for 10 minutes at 66.7 Hz while subjects walked around a 200m level indoor walking track at their own freely chosen pace.

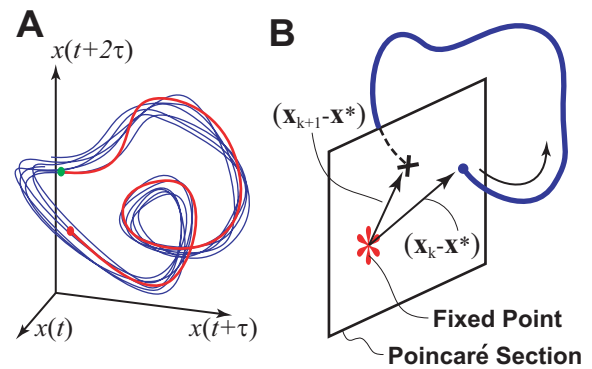


**Figure 1:** **A:** Example of a 3-D state space,  $\mathbf{S}(t) = [x(t), x(t+\tau), x(t+2\tau)]$ , constructed from a single scalar variable,  $x(t)$ , and its time-delayed copies. **B:** Floquet multipliers quantify how much perturbations ( $\mathbf{S}_k$ ) away from the fixed point ( $\mathbf{S}^*$ ) grow or decay after 1 complete stride ( $\mathbf{S}_{k+1}$ ).

Multi-dimensional state spaces,  $\mathbf{S}(t)$ , were reconstructed from each time series, using an embedding dimension of 5 (Dingwell et al., 2000). Orbital stability was quantified by the magnitudes of the maximum Floquet multipliers (Hurmuzlu & Basdogan, 1994) at each percent (0% to 100%) of the gait cycle. We defined the fixed points ( $\mathbf{S}^*$ ) at each Poincaré section (i.e., at each % of the gait cycle) as the average trajectory across all strides within a trial. Floquet multipliers (FM) were then computed from (Fig. 1B):

$$[\mathbf{S}_{k+1} - \mathbf{S}^*] \approx J(\mathbf{S}^*)[\mathbf{S}_k - \mathbf{S}^*]$$

where  $J(\mathbf{S}^*)$  defined the Jacobian matrix for the system at each Poincaré section. The

FM are the eigenvalues of  $J(S^*)$ . They define the amount by which small perturbations grow or diminish by the next cycle. If the Max FM has magnitude  $< 1$ , this indicates that perturbations decay from stride to stride and that the system is orbitally stable.

Differences in Max FM between NP and CO subjects were assessed using repeated measures ANOVA and multivariate regression (Dingwell et al., 2000).

## RESULTS AND DISCUSSION

NP subjects walked more slowly than did CO subjects (Dingwell et al., 2000). All subjects exhibited orbitally stable walking kinematics (Max FM  $< 1$ ; Fig. 2), even though these same kinematics were previously shown to be locally *unstable* (Dingwell et al., 2000). Differences between NP and CO subjects (Fig. 2) were generally very small and not statistically significant ( $0.380 \leq p \leq 0.946$ ), with the single exception of knee joint movements ( $p = 0.001$ ). Follow-up multivariate regression analyses (not shown) found that neither differences in sensory status nor walking speed predicted Max FM differences at the knee after accounting for differences in passive range of motion, and lower extremity strength. Thus, the NP patients did not gain improved orbital stability as a result of slowing down, but also did not experience any *loss* of orbital stability because of their sensory deficits.

These findings suggest that during normal *unperturbed* overground walking, sensory feedback may play a much less critical role in regulating locomotor stability than commonly believed. However, these NP subjects had been living with significant sensory loss for many years, so the present results also reflect the effects of any compensatory strategies used by NP subjects to maintain walking stability.

In either case, the increased risk of falling in NP patients is not due to their inability to generate normal and relatively stable locomotor rhythms, but is more likely due to their inability to develop and execute appropriate response strategies when faced with unexpected obstacles or *large-scale* perturbations encountered during locomotion.

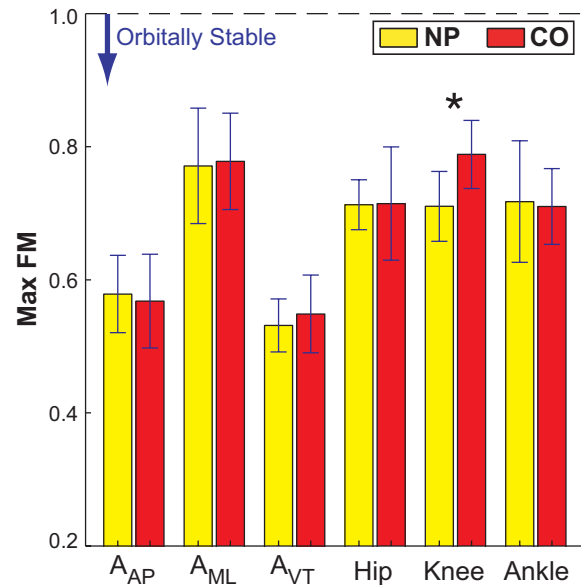


**Figure 2:** Max FM values (Mean  $\pm$  SD) for NP and CO subjects for all 6 time series measures examined. Smaller Max FM values indicate better orbital stability. The \* indicates statistically significant ( $p = 0.001$ ).

## REFERENCES

- Dingwell, J.B. et al., (2000) *J. Biomech.*, **33** (10): 1269-1277.  
 Full, R.J., et al., (2002) *Integr. Compar. Biol.*, **42** (1): 149-157.  
 Hurmuzlu, Y. and Basdogan, C. (1994) *J. Biomech. Eng.*, **116** (1): 30-36.  
 Richardson, J.K. (2002) *J. Am. Ger. Soc.*, **50** (11): 1760-1766.

## ACKNOWLEDGEMENTS

Supported by Research Grant # RG-02-0354 from the Whitaker Foundation.

# PERIPHERAL NEUROPATHY DOES NOT ALTER THE FRACTAL DYNAMICS OF GAIT STRIDE INTERVALS

Deanna H. Gates<sup>1</sup> and Jonathan B. Dingwell<sup>2</sup>

<sup>1</sup> Department of Biomedical Engineering, University of Texas, Austin, TX, USA

<sup>2</sup> Nonlinear Dynamics Laboratory, Dept. of Kinesiology, University of Texas, Austin, TX, USA

E-mail: [jdingwell@mail.utexas.edu](mailto:jdingwell@mail.utexas.edu)

Web: <http://www.edb.utexas.edu/faculty/dingwell/>

## INTRODUCTION

In healthy adults walking at a variety of speeds, the stride interval time series exhibits long-range correlations (Hausdorff, 1995). These stride intervals approach an uncorrelated (random) time series in elderly subjects, patients with Huntington's disease (Hausdorff, 1997), and healthy people who walk in time with a metronome (Hausdorff, 1996). Therefore, it has been suggested that these long-range correlations are regulated by supraspinal control mechanisms. The loss of long-range correlations would then be due to the deterioration of *central* processing mechanisms that results from aging or central nervous system disease (Hausdorff, 1997; Herman, 2005).

The question of how (if at all) changes in *peripheral* mechanisms affect long-range correlations in gait cycle timing has not been examined. To answer this question, we studied the stride time series of patients with severe peripheral sensory loss versus matched healthy controls and tested two alternative hypotheses. If the loss of long-range correlations in stride intervals reflects changes in the mechanisms that regulate gait cycle timing *in general*, then similar changes should also occur in patients with peripheral sensory neuropathy. If instead, this loss of long-range correlation structure indicates deterioration specifically of the *central* control of gait, as has been suggested (Hausdorff, 1997; Herman, 2005), then changes in peripheral sensation should not affect these long-range correlations.

## METHODS

Fourteen diabetic patients with significant peripheral neuropathy (NP) and twelve control subjects with no history of diabetes or neuropathic illness (CO) participated. All NP patients had "loss of protective sensation" as determined by touch / pressure sensation tests (Birke, 1986) and exhibited substantial sensory loss compared to CO subjects (Dingwell & Cavanagh, 2001).

Subjects wore their own comfortable low-rise rubber-soled walking shoes while walking around a 200-m open level indoor walking track at his/her self-selected speed. Data from an electro-goniometer attached over the right knee were sampled at 200 Hz for 10 minutes. The total number of strides and stride times for each subject were calculated from the points of maximum knee joint extension just prior to heel strike.

Each stride interval time series was analyzed using both power spectral density analysis (PSD) and detrended fluctuation analysis (DFA). While both methods look for correlations in data over time, DFA is more robust to noise and nonstationarities in the signal (Hausdorff, 1995). DFA and PSD each produce a scaling exponent, denoted either  $\alpha$  and  $\beta$ , respectively. This exponent indicates what type of correlation exists. The scaling exponents are theoretically related through  $\beta = 2\alpha - 1$  (Hausdorff, 1995). A value of  $\alpha = 0.5$  indicates that the time series is completely uncorrelated (i.e., white noise). Long-range correlations are present

when  $0.5 < \alpha \leq 1$  and short-range correlations exist when  $\alpha < 0.5$ . A single value each of  $\alpha$  and  $\beta$  were calculated for each subject from their stride time series.

## RESULTS AND DISCUSSION

NP patients walked 445 to 620 strides, while CO subjects walked 488 to 668 strides. NP subjects walked slower ( $p = 0.008$ ) and with greater stride time standard deviations ( $p=0.036$ ) than CO subjects (Dingwell & Cavanagh, 2001). The scaling exponents,  $\beta$ , from the PSD analysis were  $0.593 \pm 0.128$  for the NP patients and  $0.599 \pm 0.252$  for CO subjects. These values were statistically identical ( $p = 0.954$ ). The results of DFA analysis (Fig. 1) also showed no statistical differences between NP and CO subjects (CO:  $\alpha = 0.867 \pm 0.099$ , NP:  $\alpha = 0.867 \pm 0.099$ ,  $p = 0.786$ ). Thus, the structure of the long-range correlations in stride time for the NP patients, as quantified by both  $\alpha$  and  $\beta$ , were completely unaffected by the significant deterioration in peripheral sensory feedback that these patients experienced. We note, however, that these NP subjects had been living with significant sensory loss for many years, so the present results also reflect the effects of any compensatory strategies adopted by these NP patients.

## SUMMARY/CONCLUSIONS

The normal long-range correlation structure seen in stride intervals remains unaltered by substantial peripheral sensory loss, even though these sensory inputs are believed to play a significant role in regulating gait cycle timing (Zehr, 1999). The hypothesis that changes in  $\alpha$  and/or  $\beta$  reflect deterioration of the mechanisms *in general* that regulate gait cycle timing was rejected. The alternative hypothesis that loss of these long-range correlation results specifically from deterioration of the *central* mechanisms controlling

gait cycle timing was supported. While the exact origin of these long-range correlations remains unknown, distal peripheral sensory feedback is *not necessary* to generate them.

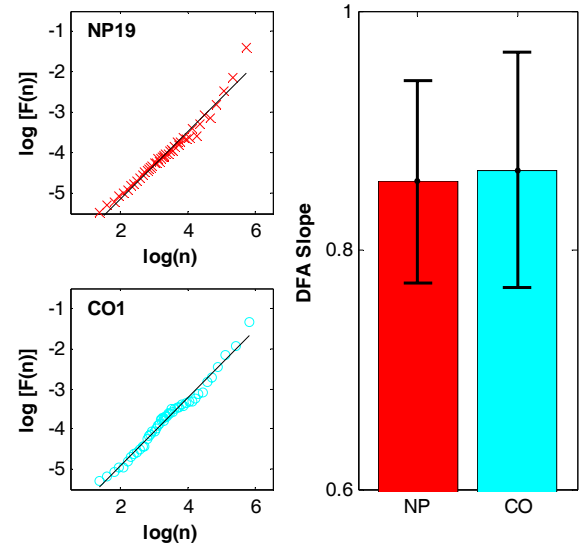


**Figure 1:** DFA results for two representative subjects (NP = x, CO = o), and results for both groups. There was no statistical difference between groups ( $p = 0.786$ ).

## REFERENCES

- Birke, J.A. and Sims, D.S. (1986). *Leprosy Review*, **57** (3): 261-267.
- Dingwell, J.B. and Cavanagh, P.R. (2001) *Gait and Posture* **14** (1): 1-10.
- Hausdorff, J.M. et al. (1995). *J. Appl. Physiol.*, **78** (1): 349-58.
- Hausdorff, J. M. et al. (1996) *J. Appl. Physiol.*, **80** (5): 1448-57.
- Hausdorff, J.M., et al. (1997). *J. Appl. Physiol.*, **82** (1): 262-9.
- Herman, T., et al. (2005) *Gait and Posture* **21** (2): 178-85.
- Zehr, E.P. and Stein, R.B. (1999). *Progress in Neurobiology* **58** (2): 185-205.

## ACKNOWLEDGEMENTS

This work was supported by Research Grant #RG-02-0354 from the Whitaker Foundation and by grant #EB003425 from the NIH.

# THE EFFECT OF BILATERAL LAMINECTOMY ON THE INSTANTANEOUS AXIS OF ROTATION OF LUMBAR SPINE IN FLEXION AND EXTENSION

Tianxia Qiu and Ee Chon Teo

Nanyang Technological University, Singapore  
E-mail: txqiu@ntu.edu.sg

## INTRODUCTION

Severe spinal stenosis or ruptured/herniated discs are often treated by dorsal decompression. Decompressive laminectomy can benefit many patients with lumbar spinal stenosis by reducing pain and increasing function. Resections of posterior bony or ligamentous parts normally alter the kinematics of the functional spinal unit (FSU) at the level. Range of motion (ROM) and Instantaneous axis of rotation (IAR) are two kinematic characteristics of a FSU in a plane under load. A number of papers have reported the degree of increased ROM caused by resecting dorsal parts [1,2]. Little is known about the alteration of IARs caused by this surgical procedure. Understanding the locations of the IARs before and after a specific injury would allow the clinician to objectively choose the best surgical approach and the appropriate instrumentation. Hence, the purpose of this study is to investigate the IARs locations and loci before and after bilateral laminectomy in flexion and extension.

## METHODS

The previously developed and validated finite element (FE) model of lumbar L2-L3 FSU (Figure 1) [2] was used to determine the IARs under flexion and extension before and after bilateral laminectomy. Figure 2 shows the extent of resection with removal of the left and right superior facets of L3, removal of the spinous process, the left and

right lamina and inferior facets of L2, as well as the supraspinous, flaval and intraspinous ligaments. To compute the IARs, the intact and resected models were subjected to a compressive preload of 400 N, and flexion and extension pure moments of 7.5 Nm uniformly applied to the top of L2 vertebral body in 10 incremental steps with L3 fully constrained. The IAR (as shown in Figure 3), defined by an intersection of two perpendicular bisectors of line segments A-A' and B-B' (A, B are two nodes on the L2 body), A, B and A', B' corresponding to the locations of these two nodes before and after rotation for flexion load increment in the sagittal plane, is computed to define as the IAR under flexion. The IARs calculated for each load step of each load type were joined to track the loci for flexion and extension.

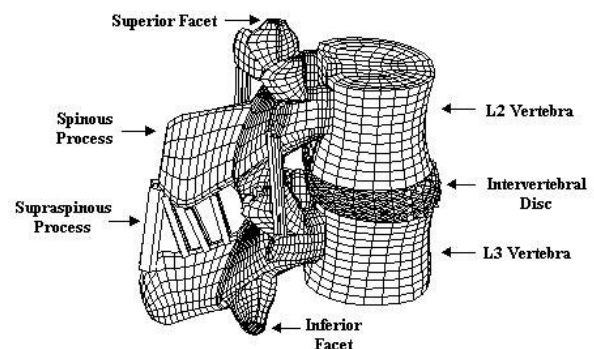
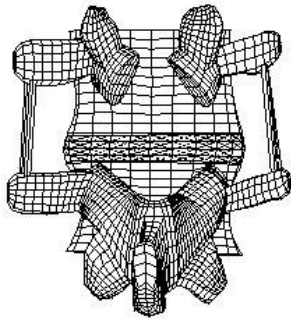
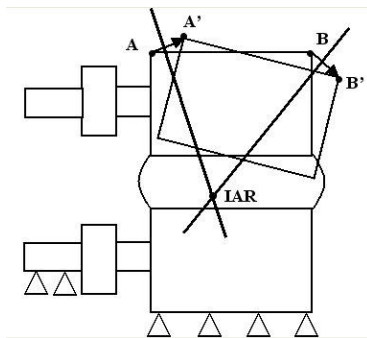


Figure 1: FE model of L2-L3 FSU.



**Figure 2:** Illustration of bilateral laminectomy.



**Figure 3: Definition of IAR shown in flexion of L2-L3.**

## RESULTS AND DISCUSSION

Within the validated range, the IARs locations and loci were found to vary with the applied pure moments for both intact and resected models (Figure 4). The locations of the IARs are located in the posterior part below the mid-height of the disc and around upper endplate of lower vertebra for the intact model and all confined around the mid-height of the disc for resected model. For intact model, the loci of the IARs were tracked to diverge in different directions depending on the type of load. The loci of IARs shifted anterosuperiorly along curve a-b towards the center of the disc for flexion and posterosuperiorly along curve c-d to the posterior mid-height of the disc for extension, respectively. For the resected model, the loci are shown to move in

opposite directions, along curves a'-b' and c'-d' for flexion and extension, respectively. The loci of the IARs were tracked to move anteriorly and posteriorly along almost straight lines for flexion and extension, respectively.

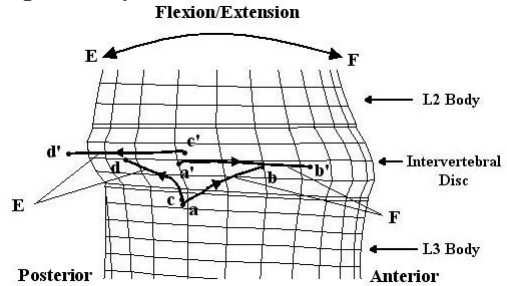


**Figure 4:** Predicted loci of IARs with increasing flexion and extension pure moments before and after bilateral laminectomy. The curves a-b and c-d are the loci for intact model under flexion and extension, respectively; the curves a'-b' and c'-d' are the loci after laminectomy under flexion and extension respectively. (F for flexion, E for extension).

After bilateral laminectomy, the locations and the loci patterns are all altered. These data provide insight into the effects of surgical procedure on lumbar spine mechanics. Changes in the IAR associated with surgical operation likely alter the length of the moment arms for the lumbar spine musculature and therefore the relative demand imposed upon the musculo-skeletal system.

## REFERENCES

- Zander T, Rohlmann A, Klockner C, Bergmann G *Eur Spine J* 12:427-34, 2003.
- Lee KK, Teo EC, Qiu TX, Yang K. *Spine* 29:1624-31, 2004.

Bone strength deficits result from delayed pubertal development caused by hypothalamic suppression in female rats.

Vanessa Yingling

Brooklyn College (CUNY), Brooklyn, NY USA

Email: [Vanessa.Yingling@Temple.edu](mailto:Vanessa.Yingling@Temple.edu)

## INTRODUCTION

Optimal bone strength is imperative in order to avoid fracture later in life. Multiple factors affect the structural development of the skeleton; in particular estrogen levels during growth are an important factor in the pathogenesis of bone fragility (Seeman, 2002). The delay of menarche and infrequent menstrual cycles decrease estrogen levels during adolescence and decrease peak bone mass (Warren, 1991). Furthermore, Warren et al. (2002) found the age of menarche to be more correlated to stress fracture occurrence than bone mineral density (BMD). Therefore, conditions that delay puberty by delaying the maturation of the Hypothalamic-Pituitary-Gonadal (HPG) axis are associated with delayed skeletal development and may affect long-term bone strength. The purpose of this study was to test the hypothesis that suppression of the HPG axis during pubertal development results in a deficit in bone strength accrual.

Gonadotropin releasing hormone antagonists (GnRH-a) have successfully delayed the onset of puberty in female rats as determined by delayed vaginal opening, lower ovarian weights and lower serum estradiol levels (Roth, 2000). This model offers an opportunity to reproduce an environment of delayed menarche and to investigate the effect on bone strength at a critical time point in bone development. The investigative hypothesis predicts that administration of a GnRH-a initiated prior to the onset of the first estrus cycle would

impede the development of cortical bone strength in female rats.

## METHODS

At 23 days of age female Sprague Dawley rats (Charles River) were randomly assigned into a control group (C) (n=15) and three experimental groups that received injections of GnRH-a (Zentaris GmbH) intraperitoneally (0.2ml) for a 29 day period. The experimental groups were separated into a group that injected 125 ug/dose daily (D1) (n-15), 250 ug/dose daily (D2) (n-15) and 500 ug/dose, 5 days per week (D3) (n-15). All animals were monitored daily for vaginal opening which is an indicator of the onset of puberty. Animals were sacrificed after the final injection, approximately 50 days of age. Uterine weights were measured. Femoral lengths were measured and then the bones were mechanically tested under 3-point bending at a loading rate of 0.1 mm/s. Differences were detected using a One-way ANOVA ( $p < 0.05$ ). The study was approved by the Institutional Animal Care and Use Committee at Brooklyn College (City University of New York).

## RESULTS & DISCUSSION

A delay in the timing of puberty through GnRH antagonist injections was confirmed by the delay in the day of vaginal opening of the experimental groups compared to control (Figure 1). 50% of the animals in D1 did not reach puberty prior to sacrifice. 93% of the animals in D2 and D3 groups did not reach puberty. The significant decrease in

uterine weight by 75.5% was a further indicator of the efficacy of the protocol to delay pubertal development (Table 1).

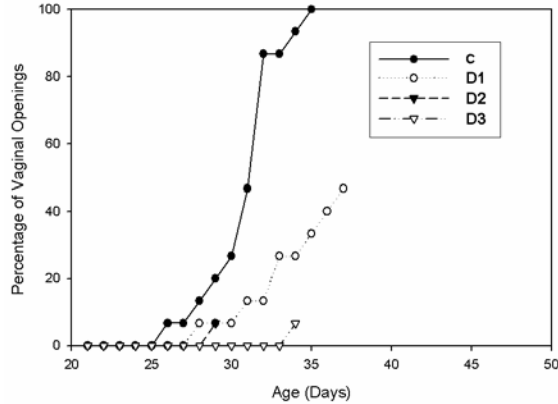


Figure 1: The cumulative percent of animals with VO is displayed per age (days).

Table 1: Summary of group differences in uterine weights, femur length and body weights at sacrifice. Mean (SD). \* p<0.05 versus C

Parameters	Groups			
	C	D1	D2	D3
Uterine Weight (g)	.347 ± .110	.079 ± .004*	.084 ± .005*	.085 ± .013*
Femur Length (mm)	28.12 ± .90	25.28 ± .40*	26.34 ± .59*	24.62 ± .83*
Body Weight at Sacrifice (g)	182.96 ± 15.85	215.75 ± 20.98	214.68 ± 20.49	214.53 ± 15.33

A significant decrease in femoral length was found (Table 1). This deficit in femoral length was accompanied by a deficit in bending strength of the femoral cortical diaphysis in the GnRH-a groups (Figure 2). Specifically, peak moment and stiffness were lower in the GnRH-a groups. However, the body weights of the experimental animals were significantly larger than control (17.9%). Body weight is often considered a correlate to bone strength. The bone strength deficit could have resulted from a decrease in the quantity

of bone, the structural arrangement of the bone from the diaphyseal center or the composition of the bone.

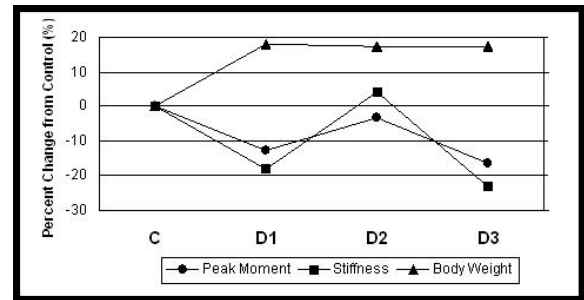


Figure 2: The percent change from C for Peak Moment, Stiffness and Body Weight for all groups.

## SUMMARY/CONCLUSIONS

GnRH antagonist administered to animals prior to the first estrus cycle at doses of 125 ug/dose and 500 ug/dose significantly decreased the bone strength in the femur at 50 days of age. The mechanisms and duration of this deficit need further investigation.

## REFERENCES

- Seeman (2002) *Lancet*, **359**:1841-1850
- Warren et al. (1991) *J Clin Endocrinol Metab* **72**:847-853
- Warren et al. (2002) *J Clin Endocrinol Metab* **87**:3162-3168
- Roth et al. (2000) *Pediatr Res* **48**:468-474

## ACKNOWLEDGEMENTS

- NIH Grant AG19654
- PSC-CUNY Grant 64293-00-33
- Zentaris GmbH

# THE EFFECT OF TRANSVERSE PLANE MECHANICAL COMPLIANCE ON AMPUTEE GAIT AND IN-SOCKET FORCES

Martin Twiste, Laurence Kenney, Chris Nester

Centre for Rehabilitation and Human Performance Research, University of Salford, Salford, UK  
E-mail: [m.twiste@salford.ac.uk](mailto:m.twiste@salford.ac.uk) Web: [www.healthcare.salford.ac.uk/crhpr/](http://www.healthcare.salford.ac.uk/crhpr/)

## INTRODUCTION

The connection between the socket and foot in a trans-tibial prosthesis is commonly based on a rigid adapter. This rigidity restricts the socket from moving significantly relative to the foot, thereby restricting movement of the residuum also. Restricting the residuum can increase residuum-socket interface forces, including shear stresses, thus increasing the risk for skin breakdown.

Instead of a rigid adapter, it is possible to connect the socket and foot via a mobile adapter that comprises a compliant element (Twiste & Rithalia, 2003). Similar to transverse rotation in the anatomic lower limb (Levens et al., 1948), a mobile adapter permits transverse rotation at the prosthesis between the socket and the foot. Compared to a rigid adapter, a mobile adapter therefore provides reduced resistance to transverse rotation of the socket/residuum.

Some prostheses manufacturers claim that their mobile adapter reduces shear stresses exerted onto the residuum. However, there appears to be a lack of evidence in the literature to support these claims. This study investigates the way in which a mobile adapter affects knee flexion, ground reaction forces (GRFs) and residuum-socket interface forces during straight, level walking.

## METHODS

Ten male, unilateral trans-tibial amputee volunteers (mean age 44, range 27-71) were

recruited for gait tests in a motion laboratory. Each amputee walked on a customised test-prosthesis with a transverse rotation adapter that could be configured to provide either a high or low degree of compliance. Two gait conditions were tested: with a rigid adapter (low degree of adapter compliance) and with a mobile adapter (high degree of adapter compliance).

Two force plates (Kistler, Switzerland) and an eight-camera motion capture system (Qualisys AB, Sweden) were used for capturing the kinetic and kinematic data, respectively. Residuum-socket interface forces were captured with six FlexiForce sensors (Tekscan, USA), which were located over soft tissue areas and bony landmarks, including the medial tibial flare, lateral tibial flare, popliteal fossa, tibial tuberosity, tibial crest and fibula head. Data were recorded over ten gait cycles for each of the two gait conditions. Customised Matlab programs (The MathWorks Inc, USA) and standard statistical software (SPSS Inc, USA) were used for subsequent data analysis.

## RESULTS AND DISCUSSION

Tests with a mobile adapter showed that, compared to tests with a rigid adapter, the socket rotated internally at early stance due to adapter compliance. Socket/residuum internal rotation made it therefore likely for the magnitude of internal rotation, and subsequently forward motion of the pelvis, to be greater than without adapter compliance. Forward motion of the pelvis is associated with greater elevation of the

centre of mass. This elevation can be compensated for by increasing and delaying the peak in knee flexion during stance.

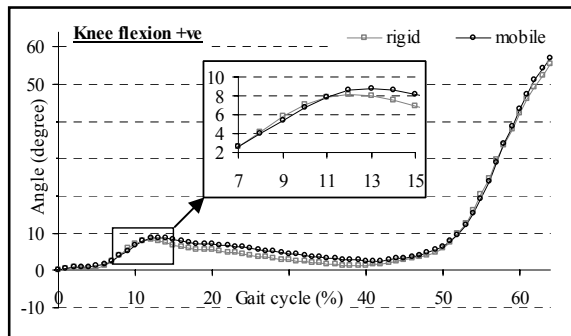


**Figure 1:** Knee angle against time graph

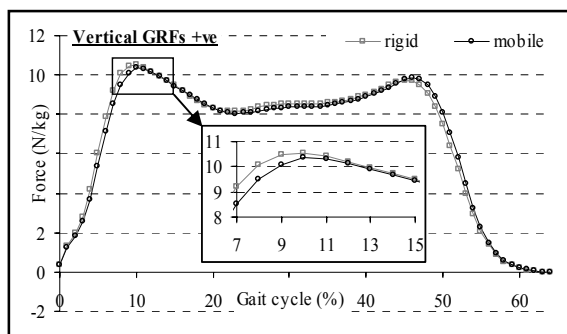


**Figure 2:** GRFs against time graph

The results showed that the introduction of a mobile adapter did not significantly increase the magnitude of peak knee flexion, but it significantly delayed the timing of peak knee flexion (by approx. 2.1% of gait cycle,  $p=0.010$ ), (Fig. 1). It should be taken into account that knee flexion is a common shock absorption mechanism, which can be considered to have an influence on lowering the vertical loading rate. A lower vertical loading rate is a consequence of reducing the magnitude and/or the timing of peak vertical GRFs.

It was established that the introduction of a mobile adapter significantly reduced the magnitude of peak vertical GRFs (by approx. 0.2N/kg,  $p=0.050$ ), and delayed the timing of peak vertical GRFs, but not significantly (Fig. 2). However, overall the

average vertical loading rate was reduced. Such a reduction should have an influence on the residuum-socket interface forces, which are therefore likely to be lower than with a rigid adapter.

An analysis of residuum-socket interface normal forces, calculated over the area of each FlexiForce sensor, and expressed as pressures, revealed that, with a mobile adapter, the majority of measured landmarks experienced lower pressures than with a rigid adapter. The peak pressures, calculated as the mean of all six landmarks' highest pressures, were reduced by approx. 6.4% with a mobile adapter. In addition, the total pressures, calculated as the mean of all six landmarks' pressure-time integral over the gait cycle, were also reduced by approx. 6.7% with a mobile adapter.

## SUMMARY/CONCLUSIONS

This study showed that the way in which a mobile adapter reduces residuum-socket interface forces is complex. It not only affects transverse plane kinematics at the prosthesis (i.e. adapter), but, in addition, affects various other aspects of lower limb kinematics also, which then influences the lower limb kinetics and subsequently reduces residuum-socket interface forces or pressures.

## REFERENCES

- Twiste, M., Rithalia, S.V.S. (2003). *J Rehab Res Dev*, **40(1)**, 9-18.  
 Levens, A.S. et al. (1948). *J Bone and Joint Surg*, **30A**, 859-872.

## ACKNOWLEDGEMENTS

- NHS North West R&D Directorate UK
- South Manchester University Hospital NHS Trust UK

# A NUMERICAL APPROACH IN ESTIMATION OF TENDON SLACK LENGTH IN INDIVIDUAL LOWER EXTREMITY MUSCLES

Miloslav Vilimek <sup>1</sup>

<sup>1</sup> Czech Technical University in Prague, Prague, Czech Republic  
E-mail: Miloslav.Vilimek@fs.cvut.cz

## INTRODUCTION

In the equations, which express dynamic conditions of musculotendon (MT) loading, are some input parameters, which are difficult to measured or simply obtain otherwise. One of these input parameters is a tendon slack length  $L_s^T$ . It is very difficult to find complete experimentally obtained data about human muscles. Therefore, some authors develop simulation methods for estimation of this value. Manal and Buchanan (Manal and Buchanan, 2004) use the numerical optimization method based on the fact, that the tendon slack length,  $L_s^T$ , is constant value when the MT length,  $L^{MT}$ , and muscle length,  $L^M$ , are different in a different joint angle and the MT length is measurable. In opposite, Garner and Pandey (Garner and Pandey, 2003) use the two phase nested optimization technique for estimation of the tendon slack length,  $L_s^T$ , together with other muscle parameters as optimal fiber length,  $L_0^M$ , and isometric muscle force,  $F_0^M$  within a group of muscles. In the Garder and Pandey's method, the obtained parameters are not independent and an error in one parameter can denote error in other parameter and it is not possible to say which MT parameter is true and which is false. The Manal and Buchanan's method is always for one muscle, it means that MT parameters are independent between muscles, and this method assumes true values of inputs. In this study, the simple simulation method for estimation of the tendon slack length was derived, which is close to Garder and Pandey's method but MT parameters are independent between muscles.

## METHODS

From the relationship between maximal and minimal MT lengths, pennation angle, optimum muscle fiber length, minimal and maximal muscle fiber length and tendon length was derived equation for calculation of tendon lengths (1). The dimensionless muscle properties were used (Zajac, 1989). The  $\tilde{L}_{\min}^M$  and  $\tilde{L}_{\max}^M$  are normalized minimum and maximum muscle fiber lengths, which are the muscle fiber length divided by the optimum muscle fiber length  $L_0^M$ . Calculation of the tendon length is in this case based on the simplification that difference between tendon slack length and instantaneous value of tendon length is neglected.

$$L_s^T = \frac{L_{\min}^{MT} \sqrt{(\tilde{L}_{\max}^M)^2 - \sin^2(\alpha_0)} - L_{\max}^{MT} \sqrt{(\tilde{L}_{\min}^M)^2 - \sin^2(\alpha_0)}}{\sqrt{(\tilde{L}_{\min}^M)^2 - \sin^2(\alpha_0)} - \sqrt{(\tilde{L}_{\max}^M)^2 - \sin^2(\alpha_0)}} \quad (1)$$

$$L_0^M = \frac{L_{\max}^{MT} - L_{\min}^{MT}}{\sqrt{(\tilde{L}_{\max}^M)^2 - \sin^2(\alpha_0)} - \sqrt{(\tilde{L}_{\min}^M)^2 - \sin^2(\alpha_0)}} \quad (2)$$

We assumed, that the theoretical values of normalized minimal and maximal muscle fiber lengths, which are  $\tilde{L}_{\min}^M = 0.5$  and  $\tilde{L}_{\max}^M = 1.5$ , is not real interval of effective operating range of muscle length, valid for every muscle. The interval, when muscle can produce active force, can be optimized. Optimization problem was to calculate new  $\tilde{L}_{\min}^{M*}$  and  $\tilde{L}_{\max}^{M*}$  parameters for each of muscle based on minimization of the error between

new normalized values and theoretical values  $\tilde{L}_{\min}^M = 0.5$  and  $\tilde{L}_{\max}^M = 1.5$ . The optimization problem was constrained by the equation (2) where  $L^M_0$  is the optimum muscle fiber length.

## RESULTS AND DISCUSSION

This approach was applied to Lower extremity muscles: Semimembranosus (SM), Biceps femoris long head (BFL), Biceps femoris short head (BFS), Tensor fasciae latae (TFL), Gracilis (GRC), Rectus femoris (RF), Vastus medialis (VM), Vastus intermedius (VI), Vastus lateralis (VL), Semitendinosus (ST), Sartorius (SAR), Medial gastrocnemius (MG), Lateral gastrocnemius (LG), Soleus (SOL), Tibialis posterior (TP), Tibialis anterior (TA). The input data as positions of muscle attachments, pennation angle, optimal muscle fibre length and measured values of tendon slack length  $L^T_s$  were taken from the lower extremity musculoskeletal model including in SIMM software (Delp et al, 1995). The maximal and minimal MT length, were derived from the combination of the knee and hip flexion/extension angles. The optimized interval of effective operating range of muscle length  $\tilde{L}_{\min}^{M*}$  and  $\tilde{L}_{\max}^{M*}$ , calculated tendon slack lengths  $L^T_s$  and error between the calculated and published data for the selected lower extremity actuators are shown in Table 1. The mean error in estimation is about 10%.

## SUMMARY/CONCLUSIONS

From the relationship between maximum and minimum length of musculotendon (MT), pennation angle, normalized muscle length and tendon slack length has been derived relation for the tendon slack length calculation. After optimizing the interval of effective operating range of muscle length

the values from this finding are close to experimentally measured and published data.

**Table 1:** Tendon slack length values calculated for some lower extremity muscles from the optimized interval of effective operating range of muscle length. The  $L^T_s^*$  values are taken from SIMM musculoskeletal lower extremity model.

Muscle	$\tilde{L}_{\min}^{M*}$	$\tilde{L}_{\max}^{M*}$	$L^T_s$ [m]	$L^T_s^*$ [m]	Error [%]
SM	0,26	2,05	<b>0,3482</b>	0,359	<b>2,99</b>
BFL	0.20	1.80	<b>0,3409</b>	0,341	<b>0,02</b>
BFS	0.83	1.10	<b>0,0808</b>	0,1	<b>19,21</b>
TFL	0.06	2.04	<b>0,3749</b>	0,425	<b>11,78</b>
GRC	0.80	1.20	<b>0,1101</b>	0,14	<b>21,35</b>
RF	0.09	1.96	<b>0,3210</b>	0,346	<b>7,21</b>
VM	0.65	1.34	<b>0,1145</b>	0,126	<b>9,16</b>
VI	0.64	1.36	<b>0,1264</b>	0,136	<b>7,04</b>
VL	0.64	1.36	<b>0,1472</b>	0,157	<b>6,22</b>
ST	0.53	1,47	<b>0,2816</b>	0,262	<b>7,47</b>
SAR	0.83	1.04	<b>0.00</b>	0,04	<b>100</b>
MG	0.31	1.79	<b>0,3933</b>	0,408	<b>3,60</b>
LG	0.41	1.59	<b>0,3689</b>	0,385	<b>4,19</b>
SOL	0.42	1.75	<b>0,2602</b>	0,268	<b>2,89</b>
TP	0.76	1.22	<b>0,3134</b>	0,31	<b>1,09</b>
TA	0.74	1.26	<b>0,2069</b>	0,223	<b>7,22</b>

## REFERENCES

- Delp, S.L., Loan, J.P., (1995). *Comput. Biol. Med.*, **25**, 21-34.
- Garner, B.A., Pandy, M.G., (2003). *Annals of Biomedical Engineering*, **31**, 207-220.
- Manal, K., Buchanan, T.S. (2004). *J. Applied Biomechanics*, **20**, 195-203.
- Zajac, F.E., (1989). *Critical Reviews in Biomedical engineering*, **17**, 359-411.

## ACKNOWLEDGEMENTS

This study was supported by grant GACR 106/06/P304 and MSM 6840770012.

# PREDICTING LOADS ON THE LOW BACK IN THE WORKPLACE: A PORTABLE POSTURE SENSOR

Tilak Dutta,<sup>1</sup> Brent Carmichael<sup>1</sup> and Geoff Fernie<sup>2</sup>

<sup>1</sup> University of Toronto, Toronto, ON, Canada

<sup>2</sup> Toronto Rehabilitation Institute, Toronto, ON, Canada

E-mail: tilak.dutta@utoronto.ca

## INTRODUCTION

Risk of back injury can be estimated using a bottom-up inverse dynamic analysis that predicts loading of the low back. This analysis requires body position data normally collected using 3D motion capture systems (eg. Vicon Peak). However, a lack of portability restricts such systems to the laboratory where it is difficult to recreate psychosocial factors that can affect loading of the spine (Davis, 2003). Therefore, it is advantageous to perform these measurements in the actual workplace. The focus of the present work is to develop a portable alternative to existing motion capture systems. Specifically, for the initial development and validation of this technique, the purpose of this study is to determine the error associated with the novel technique when compared to a traditional motion capture system.

## METHODS

**System Description** – Our portable posture sensing system (FootCam) is comprised of two Xsens MT9 inertial sensors, a video camera (calibrated for distortion) and a lightweight rigid frame. The video camera and one inertial sensor are fixed to the frame. The frame is strapped to the subject's low back such that the feet are in view of the camera (Figure 1). The second inertial sensor is attached to a harness worn on the upper back. The inertial sensor mounted to the frame (a) tracks the 3D orientation (roll, pitch and yaw) of the camera to allow for a

primary reference frame with the vertical direction defined by gravity. The second inertial sensor tracks the trunk orientation (b). Two reflective markers are attached to each foot and two other reflective reference markers are fixed to the floor 50cm apart for calculating the distance from the camera to the floor.

This setup enables us to determine the relative coordinates of the feet and L5/S1 joint of the spine. Resultant forces can then be calculated at this joint given ground reaction forces at the feet. These forces are resolved into compression and shear components and compared to accepted limits (Waters, 1993; McGill, 1998).

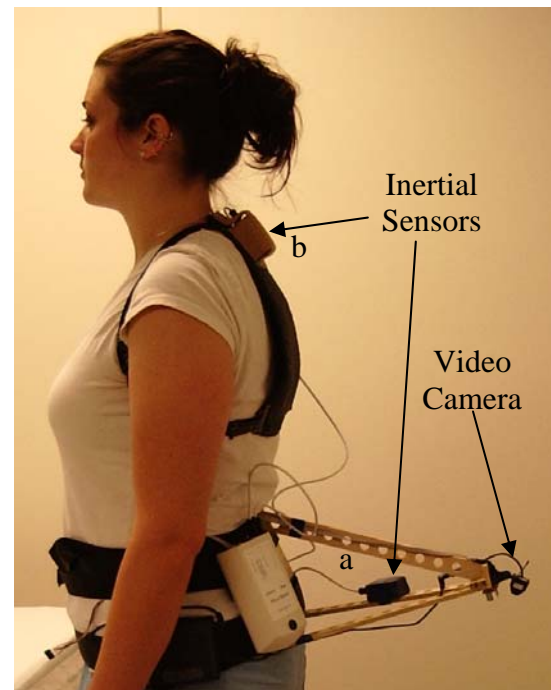


**Figure 1:** A subject wearing FootCam.

**Validation** - Our system is compared to a Peak motion capture system. This includes examining errors in the predicted x, y and z coordinates of the feet and L5/S1 joint as well as the error resulting from the use of a simplified lower body model.

The latter error is due to the fact that FootCam only predicts locations of the feet and L5/S1 joint. The Peak system predicts locations of the knees and hips in addition to these. With Peak data, the effect of gravity on the thighs and shanks can be modeled as a point load at the centre of gravity (COG) of each segment. However, there is a discrepancy with FootCam data because the COG locations are unknown. To measure the magnitude of this error, position data for all joints in the lower body was collected by a Peak motion capture system for 5 caregivers rolling a patient on a bed while ground reaction forces were collected by a pair of forceplates. Forces at the L5/S1 joint were first calculated using all markers (gold standard) (Santaguida, 2001) and again using only data from the feet and pelvis (the model to be used with FootCam).

## RESULTS AND DISCUSSION

Preliminary testing indicated the absolute errors in the x, y and z (vertical) coordinates were  $0.45\text{cm} \pm 0.39\text{cm}$ ,  $0.72\text{cm} \pm 0.12\text{cm}$  and  $0.39\text{cm} \pm 0.53\text{cm}$  respectively ( $n = 10$ ). This was the result of capturing marker locations with FootCam on a tripod at 10 different heights from 98.3cm to 144.5cm. These errors are on the same order as those from Peak (0.29cm, 0.22cm and 0.39cm in the x, y and z directions respectively).

The error in the resultant force due to missing estimates of COG locations of the thighs and shanks was  $54.1\text{N} \pm 113\text{N}$  ( $n = 5$ ). This corresponds to a  $5.75\% \pm 11.9\%$  error. This error may be reduced by

estimating the location of the knees and hips based on the locations/orientations of the feet and L5/S1 joint.

Further testing will investigate two additional sources of error. The first is due to oscillations of the frame relative to the subject's low back. The degree to which the cantilevered mass oscillates will be measured by placing the second inertial sensor on a belt around a subject's waist just above the camera assembly while she performs a task. The difference in the orientations of the two inertial sensors will indicate the magnitude of this error. Second, how closely the orientation of the L5/S1 joint follows the orientation of the low back surface will be determined. This error will be quantified with a "stand-up" MRI. A subject will be imaged while wearing a weighted plastic replica of FootCam as she flexes forward at the waist. Ultimately, the combined error in our force estimate will be found. If this total error is large, the system may be redesigned. We do expect to sacrifice some accuracy as a tradeoff to achieving portability.

## SUMMARY

Preliminary validation indicates that FootCam may be useful as a portable motion capture tool. Further testing is needed to fully determine the accuracy of FootCam compared to the Peak system.

## REFERENCES

- Davis, K.G., Marras, W.S., (2003). *Spine Journal*, **3**, 331-338.
- Waters, T.R. et al. (1993). *Ergonomics*, **36**, 749-776.
- McGill, S.M., et al. (1998). *Proceedings of 30th HFAC*, 157-161.
- Santaguida, P.L., (2001). *Doctoral Thesis* University of Toronto.

# LOWER EXTREMITY JOINT POWERS INCLUDE PASSIVE ELASTIC COMPONENTS DURING WALKING

<sup>1</sup>Ben Whittington, <sup>2</sup>Amy Silder, <sup>3</sup>Bryan Heiderscheit, <sup>1,2,3</sup>Darryl Thelen  
Departments of <sup>1</sup>Mechanical Engineering, <sup>2</sup>Biomedical Engineering, and <sup>3</sup>Orthopedics and  
Rehabilitation, University of Wisconsin – Madison  
Email: [bwhittington@wisc.edu](mailto:bwhittington@wisc.edu) Web: <http://www.engr.wisc.edu/groups/nmb/>

## INTRODUCTION

The passive stretch of soft tissues may contribute to joint moments at the hip, knee, and ankle during gait. For example, it has been suggested that passive elastic mechanisms acting about the hip may be substantial during normal walking, thereby providing an energy storage and return mechanism (Yoon, 1982). To investigate this issue, previous studies have measured passive joint moment-angle relationships while adjacent joint angles are held fixed (Edrich, 2000; Mansour, 1986; Yoon, 1982). However, such an approach does not fully capture the contributions of bi-articular muscle stretch to the passive moments observed. Furthermore, understanding the subject-specific use of passive moments during walking requires that the moment-angle characterizations take place using a consistent methodology to that used in gait. The purposes of this study were to 1) identify subject-specific hip, knee and ankle moment-angle relationships that account for bi-articular muscle stretch, and 2) estimate passive energy storage and return patterns during human gait using subject-specific walking kinematics.

## METHODS

Five healthy subjects participated in this study. The subjects were positioned on their non-dominant side with their dominant leg supported on a smooth table by low-friction carts. The hip, knee and ankle joints were systematically manipulated through full ranges of motion by a physical therapist using two handheld 3D load cells. Three-dimensional lower-extremity kinematics

were recorded throughout using 16 markers placed on anatomical landmarks. A scaled biomechanical model of the lower extremity was then used to estimate the joint angles and moments from the measured kinematics and load cell forces. Visual inspection of EMG signals from seven lower extremity muscles was used to ensure the subjects remained relaxed.

We developed an eight component exponential spring model to describe the relationship between the passive moments and angles at the hip, knee and ankle. The model accounted for the stretch of the uni-articular flexors and extensors at the hip, knee and ankle, as well as the bi-articular rectus femoris, hamstrings and gastrocnemius muscles. Bi-articular muscle functions were formulated to ensure that the energy transfer between joints was conserved. Model parameters were estimated from the subject-specific passive data using a least squares fitting method.

Kinematics and ground reactions were also collected for each subject during walking at his/her preferred speed. Hip, knee and ankle joint angles and moments during walking were then computed in a manner consistent with the passive testing. An estimate of the passive joint moments during walking was made by applying the previously derived moment-angle functions to the joint angles measured during walking. The net joint moments, passive joint moments, and joint angular velocities were then combined to distinguish the joint powers attributable to passive factors and

active muscle contractions. Positive and negative powers were then integrated to estimate the portion of the net work that was attributable to the passive stretch and release of tissues.

## RESULTS AND DISCUSSION

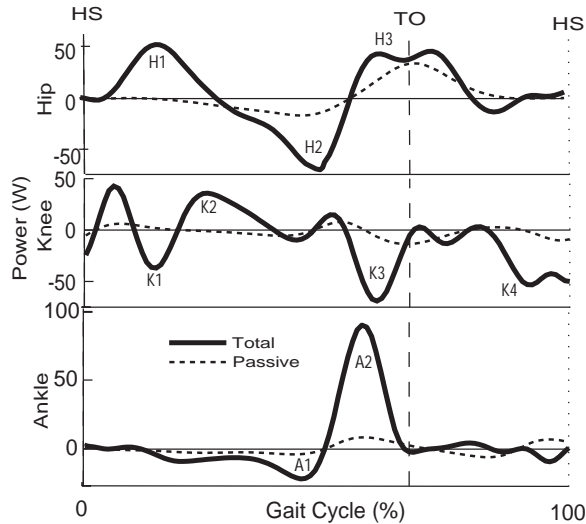


Figure 1: Total and passive hip, knee, and ankle powers through the gait cycle of a representative subject. Energy is stored passively during H2 and A1, with subsequent energy return during H3 and A2.

Both the hip and ankle exhibited passive energy storage and release characteristics from mid stance through the early swing phase of walking (Figure 1). At the hip, passive energy is absorbed (H2) while the hip is extending. This energy is returned when the hip flexes from pre-swing to just after toe-off (H3). Passive mechanisms accounted for ~30% of the total positive work done at the hip during walking (Figure 2). At the ankle, passive energy is absorbed during mid-stance (A1) and returned during pre-swing (A2). Taken together, these results suggest that swing initiation and propulsion may be aided by the stretch of passive mechanisms acting about the hip and ankle.

Although the energy due to passive stretch in the entire system is conserved, passive energy and release at isolated joints is not (Figure 2). Specifically, the hip returns more

energy than is stored, while conversely the knee absorbs more energy than it directly returns. This difference was the direct result of energy being transferred between the knee and hip through the passive stretch of the rectus femoris.

It should be noted that our analysis did not account for a slight hysteresis that was present in the passive joint moment-angle data. Such an effect would reduce the amount of energy returned from stretched tissue. Furthermore, it is challenging to determine whether the moment-angle properties measured during passive trials truly add linearly to active moments during walking. However, the close timing and magnitude between the passive and net power bursts (e.g. H3, Fig. 1) suggests that this may indeed be a mechanism that enhances the efficiency of walking. Future studies will investigate the extent to which hip flexor tightness associated with aging and disease (McGibbon, 2003) may alter the use of passive elastic mechanisms.

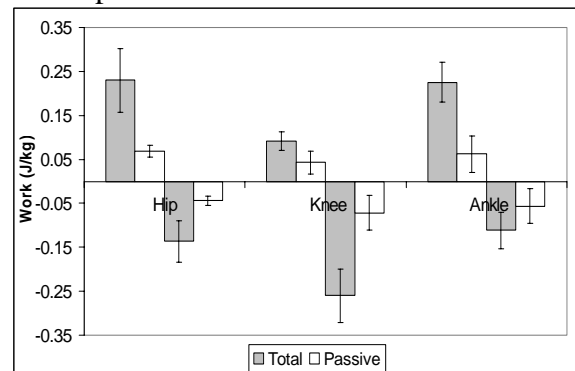


Figure 2: Total and passive energy absorption and return at the hip, knee, and ankle during preferred speed walking.

## REFERENCES

- Edrich, T. et al. (2000). *IEEE Trans Biomed Eng*, **47**, 1058-1065.
- Mansour, J.M., Audu, M.L. (1986). *J. Biomech*, **19**, 369-373.
- McGibbon, C.A. (2003). *Exerc Sport Sci Rev*, **31**, 102-108.
- Yoon, Y.S., Mansour, J.M. (1982). *J. Biomech*, **15**, 905-910.

## ACKNOWLEDGEMENTS

NIH AG023276

# The Effects of Reflex Gain and Delay on Metabolic Power in the Spine

Timothy C Franklin and Kevin P Granata

Virginia Polytechnic Institute and State University, Blacksburg, VA, USA

E-mail: granata@vt.edu Web: www.biomechanics.esm.vt.edu

## INTRODUCTION

Intrinsic stiffness and reflex response may both contribute to stability of the spine. This is related to the fact that musculoskeletal stiffness is composed of both intrinsic and reflexive components (Kearney R.E. and Stein R.B., 1997). Intrinsic stiffness is modulated through co-contraction, which has a large steady-state metabolic cost. One advantage of reflexes is that they may provide stiffness in the spine without steady-state metabolic cost. Therefore while intrinsic stiffness alone may be capable of stabilizing the spine, the inclusion of reflexes may be a more energy efficient way to stabilize the spine.

Though instantaneous reflex may aid spine stability, delay in the reflexive system may undermine this effect. In patients with low back pain abnormally large reflex delays were related to impaired postural control (Radebold et al., 2001). The effect of reflex delay on stability may additionally depend on the reflex gain. This study used a model to investigate the relationship between metabolic power, reflex gain and the maximum limit of reflex delay. It was hypothesized that 1) reflex gain decreases the metabolic power required for stability and 2) reflex delay limits the maximum tolerable reflex gain.

## METHODS

A forward dynamic model of the spine was implemented to investigate the stabilizing role of reflexes. The model represented a three dimensional 18 degree of freedom spine consisting of five lumbar vertebrae

and a thoracic segment. Passive forces included gravity and a lumped intervertebral disc model. A three dimensional anatomy of 90 muscles described origin, insertion, and via point locations in vertebral body fixed coordinate frames (Cholewicki and McGill, 1996). Two loading conditions were investigated in this study: upright unloaded, and loaded with 200N applied vertically 20cm anterior to the trunk at the T4 level.

Muscle contraction  $f_m$  was a function of muscle activation  $\alpha(t)$ , muscle length  $l_m$ , and muscle velocity  $v_m$ :

$$f_m(\alpha(t), l_m, v_m) = f_o \cdot \alpha(t) \cdot \left\{ 1 + q \cdot \left( \frac{l_m - l_o}{l_o} \right) + b \cdot \frac{v_m}{l_o} \right\}$$
$$\alpha(t) = \alpha_o + \alpha_r(t), \quad \text{where } \alpha_r(t) = \alpha_o \cdot G_R \cdot \left\{ \frac{l_m(t - \tau) - l_o}{l_o} \right\}$$

where  $f_o$  was the maximum isometric force,  $l_o$  was the muscle length at equilibrium posture,  $q$  was the intrinsic stiffness coefficient, and  $b$  was the damping coefficient. Our model implemented the average stiffness value from the literature,  $q=10$  (Crisco and Panjabi, 1991). The effects of the damping coefficient value are explored in this study. Muscle activation  $\alpha(t)$  was modeled as the sum of steady state activation,  $\alpha_o$ , and a reflex response  $\alpha_r$ . Reflex response was related to muscle strain by means of a reflex gain coefficient  $G_R$ . Reflex response was delayed by  $\tau$  seconds.

For stability analysis the dynamics were linearized about the equilibrium state

$$\dot{x}(t) = J_i \cdot x(t) + J_d \cdot x(t - \tau)$$

Jacobian  $J_i$  represented the instantaneous effects of gravity, intrinsic muscle stiffness, passive tissue forces and steady-state muscle

force. The delayed Jacobian  $J_d$  represented the delayed effects of the reflex response. Steady state muscle activations  $\alpha_0$  were established that minimized metabolic power while ensuring spinal equilibrium and stability. These activations allowed the calculation of the Jacobians. The delay margin was determined by methods developed by Chen (1995). The delay margin was defined as the maximum delay for which the system remained stable.

## RESULTS AND DISCUSSION

As reflex gain increased, the metabolic power required for stability decreased to a minimum metabolic power (Figure 1). The minimum power level was commensurate with equilibrium requirements. For small reflex gains intrinsic stiffness necessary for stability was recruited by means of co-contraction and required increased metabolic power. Metabolic power was not influenced by the damping coefficient.

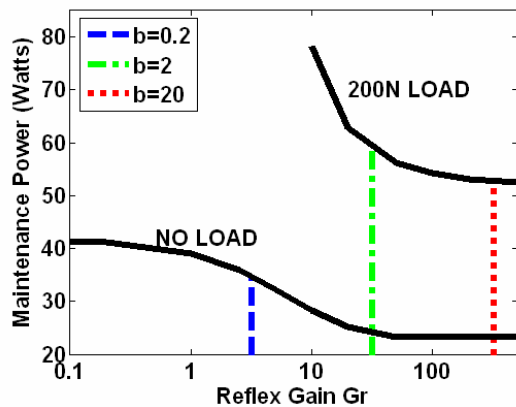


**Figure 1:** Metabolic power vs. reflex gain. Vertical lines indicate maximum reflex gain.

A physiologic reflex delay was established at 60ms based on empirical measurements. Hence, when the delay margin was less than this physiologic value results were interpreted as having no feasible stable solution. The reflex delay imposed a maximum acceptable reflex gain, beyond which the system became unstable (Figure 2). This maximum gain value was

influenced by the damping coefficient. For damping of  $b=0.2$ , this value was below the minimum gain required to stabilize the 200N load (Figure 1). Hence, there was no stable solution for this minimal damping. The presence of a maximum gain limited the benefits of reflex on metabolic cost.

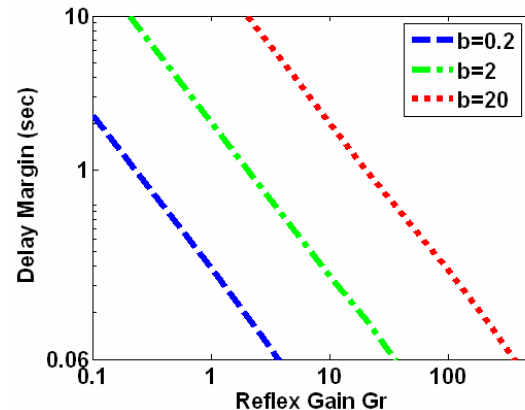


**Figure 2:** Delay margin vs. reflex gain. Relationships did not change with load.

## SUMMARY/CONCLUSIONS

The analyses demonstrated that reflexes are an important resource for stabilizing the spine and that there are advantages to recruiting reflexes. For a given physiological reflex delay this study found that a subject has an optimal reflex gain that minimizes metabolic power while assuring stability

## REFERENCES

- Chen, J. (1995). *IEEE Transactions on Automatic Control* **40**, 1087-1093.
- Cholewicki, J. and McGill, S.M. (1996). *Clin. Biomech.* **11**, 1-15.
- Crisco, J.J. and Panjabi, M.M. (1991). *Spine* **16**, 793-799.
- Kearney R.E. and Stein R.B. (1997). *IEEE Trans. Biomed. Eng* **44**, 493-504.
- Radebold, A., Cholewicki, J., Polzhofer, G.A., and Green, T.P. (2001). *Spine* **26**, 72

# DIFFERENCES IN FOREFOOT LOADING DURING THREE ATHLETIC TASKS ON FIELDTURF.

Robin M. Queen, PhD, Ershela L. Sims, PhD, Benjamin B Haynes, and  
William E. Garrett, Jr, MD, PhD

Michael W. Krzyzewski Human Performance Lab  
Duke University, Durham, NC, USA  
E-mail: robin.queen@duke.edu Web: <http://klab.surgery.duke.edu>

## INTRODUCTION

Previous research has indicated that in competitive soccer there is a performance limiting injury every 0.8 to 2 matches (Giza, et al., 2003). Over the past few years the playing surfaces used during practice and competition have shifted from being natural grass to being different synthetic turfs, one of which is FieldTurf<sup>®</sup>. One previous study examined the differences in injuries sustained on FieldTurf<sup>®</sup> versus natural grass and determined that the incidence of injuries was higher on FieldTurf<sup>®</sup> (Meyers and Barnhill, 2004). While the incidence was higher on FieldTurf<sup>®</sup>, the severity of the injuries was decreased with the increase in injuries on FieldTurf<sup>®</sup> being mostly muscle strains and spasms versus ligamentous injuries on natural grass (Meyers and Barnhill, 2004). The purpose of this study was to determine plantar loading pattern differences while performing three different athletic tasks on FieldTurf<sup>®</sup>.

## METHODS

A total of 36 subjects were recruited and tested during this study. Subjects all signed an informed consent form, which was approved by the institutional review board prior to testing. Each subject had their height and weight recorded and were fit with the proper size shoe and insole. The testing shoe was a Nike Vitoria Hard Ground Boot, with 25 molded cleats. Subjects run an agility course 5 times in each shoe while

plantar pressure data were collected on both feet at 100 Hz using the Pedar in-shoe pressure measurement system (Novel Electronics, Inc, St. Paul, MN). The left plant (cross-over cut) around the final flag, the right plant (side-cut) around the second flag, and the acceleration phase at the beginning of the agility course were used for comparison. During the three movements the peak pressure, loading rate, and contact area differences under the entire foot as well as in eight masked regions of the foot were determined. The foot was divided into eight regions for analysis, with following regions being the regions of interest: medial forefoot, middle forefoot, lateral forefoot, hallux, and the lesser toes. Each variable was analyzed using a 1X3 repeated measures ANOVA, followed by Tukey's post hoc testing when necessary ( $\alpha=0.05$ ).

## RESULTS AND DISCUSSION

Significant differences in peak pressure, contact area, and contact time beneath the entire foot existed between the three movement tasks. In addition, significant differences in peak pressure, contact area, and loading rate existed in the forefoot region between the three movements. The loading rate was highest in the medial forefoot and Hallux during the side-cut task, while the middle and lateral forefoot regions had the highest loading rate during the cross-over cutting task. The peak pressure was highest in the medial forefoot and Hallux during the side-cut task, while the

peak pressure was highest in the middle forefoot during the acceleration task, and highest in the lateral forefoot during the cross-over cutting task (Figure 1).

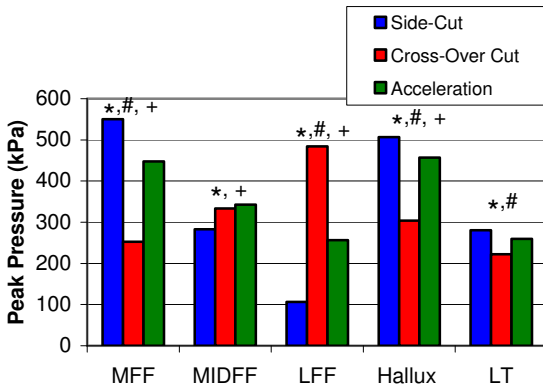


**Figure 1:** Peak Pressure comparison between three movement tasks based on foot region. (\* = significant difference between side cut and cross-over cut, + = significant difference between side-cut and acceleration, # = significant difference between cross-over cut and acceleration.) (MFF= Medial Forefoot, MIDFF=Middle Forefoot, LFF=Lateral Forefoot, LT=Lesser Toes)

The results of this study are partially supported by previous work by Elis et al, which examined plantar pressure patterns in different athletic tasks. The only comparable task between the two studies is the side-cut task. In both studies, the peak pressure was the highest in the medial forefoot during this task (Eils et al, 2004). The peak pressure values were, however, different between these two studies, with the peak pressure being higher in the study by Elis, et al (Elis et al, 2004). The differences in peak pressure between the two studies could be the result of differences between the testing surfaces used in the two studies.

## SUMMARY/CONCLUSIONS

The results of this study indicate that different cutting tasks could potentially lead to different types of injuries. In both the cross-over cut task as well as the side-cut task, the peak pressure was approximately 500kPa. With repetitive loading of this magnitude it is possible that repeated cross-over cutting could result in stress fractures of the fifth metatarsal. Future studies need to be conducted in order to gain a better understanding of potential gender differences in these loading patterns. In addition, future studies examining different cleats plate configurations could help in the prevention of stress related injuries by optimizing cleat type and cleat placement without compromising performance.

## REFERENCES

- Elis, E, et al. (2004) *American J. of Sports Medicine*, **33**, 140-145.
- Giza, E. et al. (2003) *American J. of Sports Medicine*, **31**, 550-554.
- Meyers, M., Barnhill, B. (2004) *American J. of Sports Medicine*, **32**, 1626-1638

## ACKNOWLEDGEMENTS

The authors would like to thank Nike, Inc for their support and funding of this project. This study was supported in part by NIH grant AR50245.

# INFLUENCE OF VISUAL AND SOMATOSENSORY INPUTS ON THE FREQUENCY DISTRIBUTION OF SWAY DURING QUIET STANDING

Navrag Singh <sup>1</sup> and Maury Nussbaum <sup>2</sup>

<sup>1</sup> Liberty Mutual Research Institute for Safety, Hopkinton, MA, USA

<sup>2</sup> Virginia Tech, Blacksburg, VA, USA

E-mail: [navrag.singh@libertymutual.com](mailto:navrag.singh@libertymutual.com)<sup>1</sup>; [nussbaum@vt.edu](mailto:nussbaum@vt.edu)<sup>2</sup>

## INTRODUCTION

Static posturography is a technique providing measurements of center of pressure (COP) to assess postural sway during quiet standing. Analyzing the COP in temporal, spatial and frequency domains offers insights to the control mechanisms involved in maintaining posture.

It has been extensively reported that lower frequency components of sway are influenced by visual and vestibular inputs, whereas middle and higher frequencies are influenced by somatosensory inputs (Giacomini et al., 2004; Nagy et al., 2004). There is, however, a lack of definitive recommendations in terms of the size and range of these frequency bands. Hence, this study sought to determine the influence of vision and somatosensory inputs on different frequency bands.

## METHODS

Sixteen healthy young participants (8 males and 8 females) were selected from the local community. Each participant completed an informed consent procedure approved by the local Institutional Review Board before conducting the experimental procedures.

Independent variables were vision (*eyes open and closed*), surface (*compliant and hard*), and gender. Participants performed initial practice sway trials to help familiarize them with standing on a force plate (AMTI OR6-7-1000, Watertown, Massachusetts, USA). During the trials, participants were

required to stand upright on the force plate (FP) with feet together, arms by their sides, and head straight. For the eyes open condition, a cross-mark placed 75 cm away and for the compliant surface condition, a foam board, 23mm in height, was placed on the force plate.

Each participant performed three trials in each of the four combinations of vision and surface compliance. One minute of rest was provided in between, and the presentation order of conditions was fully randomized. Each trial lasted 75 s, and was sampled for 60 s (initial 10 s and final 5 s removed). Triaxial ground reaction forces and moments were sampled at 100 Hz and transformed to obtain COP values. After zero-padding and removal of means, Fast Fourier Transform (FFT) was used to calculate the power spectra for frequencies of the COP signal in both antero-posterior (AP) and medio-lateral (ML) directions.

Dependent measures were obtained from the AP and ML power spectra, after normalizing to total power in the signal and then dividing the spectra into 30 bands of 0.05 Hz each (i.e. ranging from <0.05 to 1.5 Hz). For the purposes of analysis, bands 1 – 6 ( $\leq 0.3$  Hz) were considered low, bands 7-17 (0.35-0.85) middle and bands 18 – 30 were high frequency. Analysis of variance (ANOVA) was used to determine the effects of the sway conditions and gender on normalized power in each of the spectral bands, with significance at  $p < 0.01$ .

## RESULTS AND DISCUSSION

Absence of vision significantly increased the normalized power in almost all AP frequency bands from 0 – 1.5 Hz, except the 2<sup>nd</sup> band (0.05 - 0.1 Hz). However, in the ML direction, absence of vision significantly increased power in the only the low frequency bands ( $\leq 0.45$  Hz). These results are in contradiction with previous studies which reported that visual control influences only the lower frequencies in both the AP and ML directions (Giacomini et al., 2004; Nagy et al., 2004).

Introduction of surface compliance significantly increased normalized power in the middle frequencies (0.3 – 0.65 Hz) for both AP and ML. This is in agreement with previous reports (Giacomini et al., 2004; Nagy et al., 2004). Additionally, significant gender differences were observed in AP spectra in 2 low frequency bands ( $< 0.1$  Hz), 3 mid frequency bands (0.6-0.8 Hz), and 2 high frequency bands ( $> 0.9$  Hz).

Calculated effect sizes ( $\omega^2$ ) suggested that vision had a stronger effect on AP sway than surface compliance. This could be due to

the fact that all study participants had at least moderate levels of regular physical activity, and hence relied more on visual cues.

Effects of vision and surface on power for band 8 (0.35 – 0.4 Hz) are illustrated as an example (Figure 1). Increased power was observed in both AP and ML directions, for eyes closed vs. open, and for the compliant vs. hard surface condition.

## SUMMARY/CONCLUSIONS

Overall, vision had a stronger and more distributed effect on the spectral composition of sway as compared to surface compliance. Understanding the influence of sensory inputs on the spectral components of sway will facilitate a better mapping of the sensory systems and their roles in postural performance, and aid in developing more effective intervention strategies.

## REFERENCES

- Giacomini, P.G. et al. (2004). *European Journal of Pain*, **8**, 579-83.  
Nagy, E. et al. (2004). *European Journal of Applied Physiology*, **92**, 407-13.

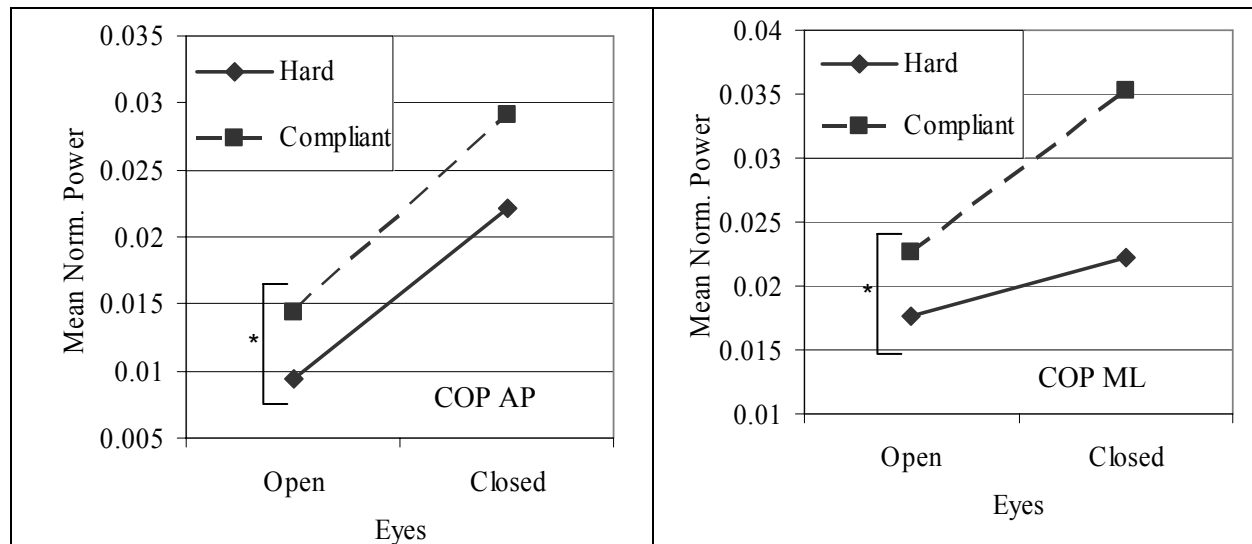


**Figure 1:** Mean AP (left) and ML (right) normalized power in the 8<sup>th</sup> frequency band (0.35 – 0.4 Hz) under different visual and surface conditions (\*  $p < 0.01$ )

# THE EFFECT OF DOWNHILL RUNNING ON IMPACT SHOCK AND ASYMMETRY

Megan L. Killian, Corrigan Nagashima, and Michael E. Hahn

Movement Science Laboratory, Montana State University, Bozeman, MT, USA

E-mail: mhahn@montana.edu

## INTRODUCTION

Impact shock during running can be measured by quantifying ground reaction forces and transient accelerations at the tibia during heel-strike. Increases in impact shock magnitude and frequency have been linked to an increased likelihood of degenerative diseases, stress fractures and other overuse injuries (Guanche and Sikka, 2005). It has also been observed that vertical impact force is greater during downhill running compared to level running (Mercer, et al., 2003), and such increases imply increased likelihood of injury during downhill running (Gottschall and Kram, 2005). Lateral asymmetry has been reported to be smaller for left-limb preferred (LP) individuals than right-limb preferred (RP) individuals because of adaptations to right-limb oriented lifestyles (Purves, et al., 1994).

The purpose of this study was two-fold: to explore if a relationship exists between lower-limb symmetry and tibial impact shock (TIS) while running downhill and to examine the tendency of limb preference to affect lower-limb symmetry. It was hypothesized that asymmetry would be greater at steeper declines (larger differentiation of TIS) and that LP would exhibit greater symmetry.

## METHODS

Six subjects were recruited for this initial study ( $24 \pm 1.9$  years,  $164.9 \pm 7.4$  cm,  $61.35 \pm 6.9$  kg). All subjects were female, heel-strike runners with no current injuries. Lower limb preference was observed by kicking a ball. Of the six subjects, one was determined to be LP and the remaining five RP.

Subjects were asked to run on a negative grade capable treadmill (Trackmaster, Newton, KS). After a familiarization period, subjects were asked to perform a self-determined warm-up on the treadmill. Following warm-up, subjects then self-selected their running speed for each of four grades (level running, -3% grade, -6% grade, and -9% grade).

Lightweight (1.7 gram) piezoelectric accelerometers (PCB Piezotronics, Depew, NY) were attached bilaterally to the antero-medial tibia. Subjects then performed four-minute phases at each of four grades. The order of grades was determined using a Latin-square technique. Four TIS samples were taken for each grade at a frequency of 1000 Hz. One sample was defined as five heel-strikes of each foot. Raw accelerometry data were filtered using a 4<sup>th</sup> order low-pass Butterworth filter (cut-off frequency = 50 Hz).

A symmetry index (SI) was calculated for each of four samples at each grade

for each subject using the following equation:

$$SI = \frac{(XR - XL)}{0.5(XR + XL)} \times 100\%$$

where XR and XL are the TIS of the right and left tibias, respectively (Herzog, et al., 1989). Mean SI were used to determine if asymmetry increased with decreasing grade.

A 2-factor ANOVA of side (right/left limb) with repeated measures of grade was performed for RP data ( $\alpha=0.05$ ).

## RESULTS AND DISCUSSION

Averaged TIS magnitudes for RP and LP are shown in Figure 1 and Table 1. TIS of RP subjects increased with decline in a linear fashion ( $p < 0.001$ ). Of the data collected, there were no trends in SI regardless of grade. There appeared to be a trend relating the difference between left and right impact shock for RP subjects, however these measures were not significant ( $p=0.074$ ). The small sample size combined with the high variability of subjects' SI is a primary limitation of this initial study. With increased subject recruitment, it is expected that the trends will show significance.

## SUMMARY

The findings of this study support Mercer et al.'s data that impact kinetics increase with downhill grade (2003). The trend relating the change between left and right TIS is promising, and future research with larger subject

recruitment is expected to reveal statistical significance. Future research will also include examination of laterality and its influence on TIS.

## REFERENCES

- Gottschall and Kram (2005). *J Biomech*, **38**, 445-452.  
 Guancho and Sikka (2005). *Arthroscopy*, **21**(5), 580-5.  
 Herzog, et al. (1989). *Med Sci Sports Exerc*, **21**(1), 110-4.  
 Mercer, et al. (2003). *Med Sci Sports Exerc*, **35**(2), 307-13  
 Purvees, et al. (1994). *Proc Natl Acad Sci U S A*, **9**(11), 5030-2.

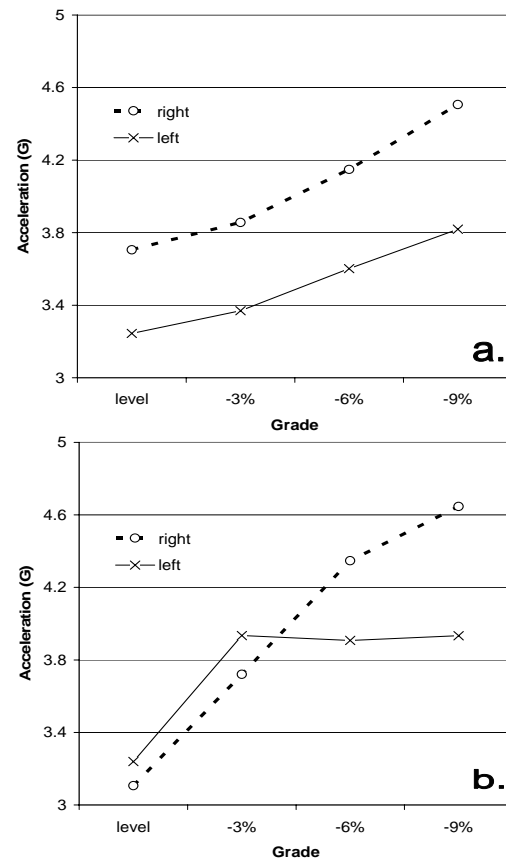


**Figure 1:** a. Averaged TIS for five RP subjects. b. TIS for both limbs of one LP subject.

**Table 1:** Mean tibial impact shock values for right and left limbs of RP subjects. (Mean  $\pm$  SD)

	Side	0% grade	-3% grade	-6% grade	-9% grade
Tibial impact shock (G)	Right limb	3.706 $\pm$ 1.08	3.856 $\pm$ 1.57	4.159 $\pm$ 1.63	4.507 $\pm$ 1.88
	Left limb	3.245 $\pm$ 0.83	3.370 $\pm$ 1.07	3.602 $\pm$ 0.93	3.819 $\pm$ 0.91
Run speed (m/s)	--	2.272 $\pm$ 0.34	2.295 $\pm$ 0.36	2.354 $\pm$ 0.33	2.377 $\pm$ 0.33

# THE EFFECTS OF HIKING POLES ON BALANCE AND VALGUS/VARUS KNEE ANGLES IN FEMALE HIKERS

Julianne Abendroth-Smith<sup>1</sup>, Winthrop Head<sup>1</sup>, and Michael Bohne<sup>2</sup>

<sup>1</sup>Willamette University, Salem OR; <sup>2</sup>Western Illinois University, Macomb, IL USA  
Email: [jabendro@willamette.edu](mailto:jabendro@willamette.edu)

## INTRODUCTION

Hiking has become an increasingly popular activity for recreation and enhancing physical fitness. Hiking pole use has increased in popularity during the past decade, partly in response to evidence that hiking poles can reduce lower extremity joint forces in both men and women (Schwameder, et al., 1999; Abendroth-Smith & Bohne, 2004). However, little is known about the more intricate aspects of hiking pole use, such as their effects on stability and frontal plane joint kinematics, particularly in women, who demonstrate a greater rate of injury while hiking (Blake & Ferguson, 1993). Yet in 2002, 29% of American women participated in hiking (Boulware, et al., 2004). The aim of this study was to examine possible relationships between static and dynamic measures of balance, frontal knee joint angles during stance, and the use of poles while hiking downhill, to prevent injury.

## METHODS

Eight women (average age = 45, ht= 1.67 m wt = 64.3 kg), all experienced hikers, walked down a 20-degree ramp in two different conditions; with and without poles. All subjects signed informed consents and approval was obtained by the University IRB. Forces were measured via a Bertec force plate set into but separately from the ramp (1000 Hz). Peak ground reaction force (Fz), peak A/P force (Fy) and the SD of the

M/L force (Fx) were examined, with Fz and Fy forces normalized to body mass (N/kg).

Self-selected speeds were maintained across conditions using an infrared timing system and all trials (ten per condition) were recorded with a digital video camera (60 Hz). Knee joint angles of one leg, during the stance phase on the force plate, were measured in the frontal plane via kinematic analysis (Datapac Software, Run Technologies). Data was filtered using a Butterworth low pass filter (7 Hz), and averaged together over the 10 trials. Three supports were examined (25%, 50% and 75% of stride) for knee valgus and varus angle differences.

Participants also completed five trials in three balance test conditions. Static balance tests included a one-legged quiet stance on the force plate for 4 second intervals, and then repeated while standing on a foam pad placed on the force plate. Dynamic balance was similarly obtained using a balance disk. All data was collected at 1000 Hz, and subsequent center of pressures (RMS) obtained via DataPac software. A final summative balance, with all three balance measures, was also used in correlations for possible relationships between changes in forces and knee angles due to pole use. Statistical significant was set at .05, and repeated measures ANOVAs were used for comparisons. Pearson coefficient (r) was used for the correlations. Effect sizes (ES) were also calculated.

## RESULTS AND DISCUSSION

GRFs demonstrated little change between the pole conditions, while braking forces were slightly greater with pole use. Fx variability was less with pole use, indicating the poles may have been used more for stability than for decreasing forces (Figure 1). No statistical significant was noted for any of the comparisons.  $ES$  were  $<.21$ .

No differences were seen in knee valgus angles in the early stance, but knee varus angles were less with pole use, though not statistically (Figure 2).  $ES$  were  $.12$ ,  $.35$ , and  $.66$ , respectively, for the three supports.

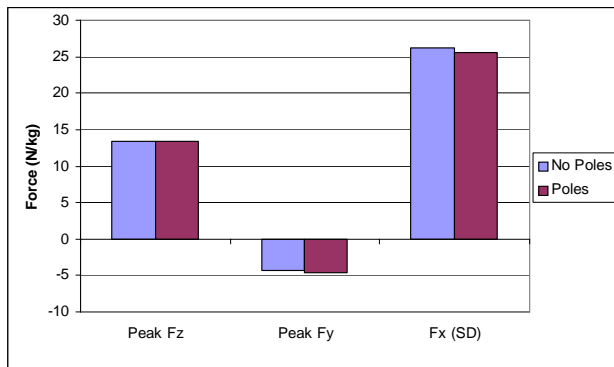


Figure 1. Change in forces with and without pole use.

Correlations between the balance tests and changes in force between pole conditions were moderate, with the highest correlation between Fz and quiet stance ( $r = .53$ ). The change in Fx correlated best with foam balance ( $r = .46$ ). Midstance changes in knee angles correlated moderately with changes in Fz ( $r = .44$ ) and with balance overall ( $r = .70$ ). All support knee joint angle changes correlated weakly with Fx ( $r = .26$  to  $.31$ ).

## SUMMARY

While some indications of the aspects of pole use on the lower extremities were noted, the participants were a more homogenous group than expected. It may be

this group of experienced women hikers were all relatively fit and comfortable enough with the hiking protocol on a 20 degree ramp, and so did not demonstrate much change in forces with pole use. A more heterogeneous group of hiking experience may reveal stronger relationships.

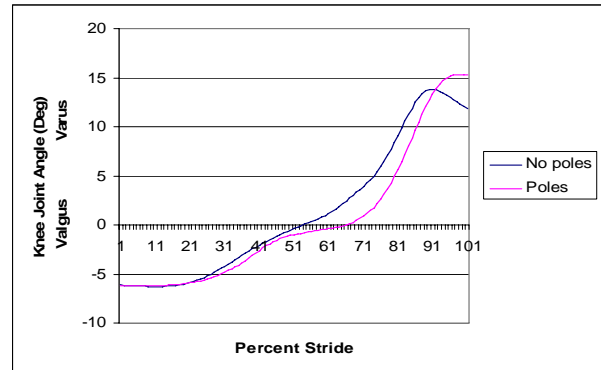


Figure 2. Average frontal plane knee joint angles over 100 % of stride.

There is some indication that good balance may be associated with the way women use the poles (stability vs. lessening forces). Finally, knee varus angles do appear to lessen slightly with pole use. This may indicate the supporting leg during stance is less likely to be subjected to certain traumatic injury, such as ankle and knee sprains, when poles are used for stability.

## REFERENCES

- Abendroth-Smith, J., & Bohne, M. (2002) *Proceedings of the Fourth World Congress of Biomechanics*, Calgary, Canada.
- Blake, R. & Ferguson, H. (1993). *J of Amer Podiatry Assoc*, **83**(9). pp. 499-503.
- Boulware, D., Forgey, W., & Martin, W. (2003) *The Amer J of Medicine*. **114**(4). pp. 288-293.
- Schwameder, H., Roithner, R., Muller, E., Niessen, W., & Raschner, C. (1999). *Journal of Sport Sciences*, **17**, 969-978.

## ACKNOWLEDGEMENTS

The Authors wish to thank Willamette University's Science Collaborative Research Program (SCRIP) for their generous support, and Lindsay Yocum who also worked on this project.

# Predicting Neck Injuries Due to Head Supported Mass

Sarah J. Manoogian<sup>1</sup>, Eric A. Kennedy<sup>1</sup>, Kaitlin A. Wilson<sup>1</sup>, Nabih M. Alem<sup>2</sup>, Stefan M. Duma<sup>1</sup>

<sup>1</sup>Virginia Tech- Wake Forest, Center for Injury Biomechanics, Blacksburg, VA

<sup>2</sup>United States Army Aeromedical Research Laboratory, Fort Rucker, AL

## INTRODUCTION

In the past 30 years, technological advances in military equipment have resulted in more devices being mounted on the helmet to enhance the capability of the soldier. They include night vision goggles (NVGs), counterbalance weights, chemical masks, oxygen masks, information display visors, communications equipment, and more. As these systems are mounted to helmets, the soldier's neck must support this head-supported mass (HSM) and the resulting dynamic characteristics of the head and neck system are changed. It has been hypothesized that these systems increase the likelihood of both low and high-severity injury, but the additional risk of neck injury that these systems create has not been fully quantified before this study. Previous research has concluded that safe limits of head-supported device mass properties, such as mass location and distribution are important design criteria, the challenge being to establish those safe limits for HSM properties that can be tolerated by aviators (1). The purpose of this study is to quantify the effect of head supported mass on neck injury risk through computational modeling.

## METHODS

The TNO MADYMO Detailed Neck model for a 50<sup>th</sup> percentile human male, presented by Van der Horst, was selected because it had been widely validated for a variety of loading scenarios, including six degree of freedom motion of individual spine segments, frontal, lateral, and rear impact

tests, both from volunteer and cadaver testing (2).

A simulation test matrix was designed to vary the impact conditions and HSM properties added to the model. These parameters included seven impact directions, three impact magnitudes, nine mass locations, and three mass magnitudes (Figure 1). Using the last three variables a central composite faced design was created to optimize simulation time. Therefore, a total of 196 simulations were completed including 28 different configurations for each of the seven impact directions.

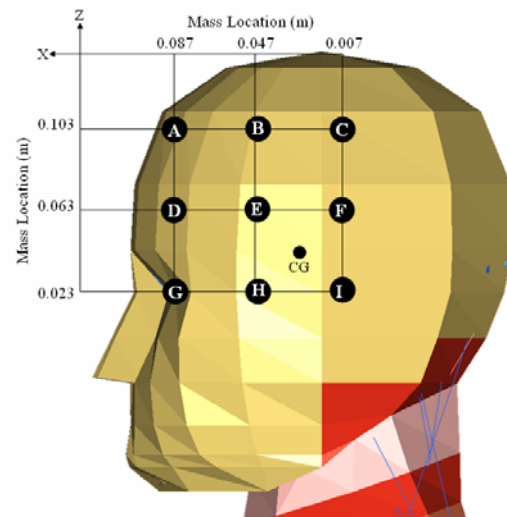


**Figure 1:** The locations for the HSM were chosen to be mostly above and in front of the head cg based on realistic equipment design.

The impact pulse for all simulations had the same shape, a half sine for 100 milliseconds, but the magnitude of the pulse varied between three different peak magnitudes for the central composite faced design. The low, medium, and high severity impacts

were modeled with 5.0 g, 13.5 g, and 22.0 g acceleration peaks respectively. These pulse durations and magnitudes are used to represent a helicopter to ground impact. While HSM injuries occur in other circumstances, a low level long duration impact is a survivable one in which the neck injuries can be prevented based on the HSM design. The outputs of the model were set so  $F_x$ ,  $F_z$ , and  $M_y$  were measured using the lower neck load cell between T1 and C7. The force and moment data from the simulations provided the necessary information to determine injury risk using a beam criterion (3).

## RESULTS

The effect of pulse magnitude is more dominant in the directions that create a flexion or lateral bending moment. These directions are negative X, positive Y, XZ 60, YZ 45, and XY 45, which all have very similar peak risk values for each simulation configuration. For these five impact directions the average risk for the lowest pulse magnitude is 2.0% ( $\pm 0.6\%$ ). The average level of risk increases to 11.8% ( $\pm 5.4\%$ ) for the medium pulse magnitude. The highest level of risk is 70.0% ( $\pm 4.6\%$ ) for a peak acceleration of 22.0 g. Note that this is not simply due to the added mass but the baseline risk increases for the higher pulse magnitudes as well.

The two directions not reported in the previous averages affect neck injury risk quite differently. The negative Z impulse direction has very low levels of injury risk for all pulse magnitudes. Because the main kinematic response from this impact direction is compression and not a flexion or lateral bending moment, the average risk for any HSM configuration is 3.3% ( $\pm 2.4\%$ ) with the highest maximum risk equal to 14.0%. Conversely, the positive X impact direction induces an extension moment for

all of the impact levels and HSM configurations. Therefore, the neck is in a weak position and the risk, even for baseline, is very high. The average risk associated with the peak beam criteria for these simulations is 93.8% ( $\pm 9.4\%$ ) with the lowest risk equal to 70.9%. For both of these impact directions the contribution of HSM location or mass to the level of risk is not a dominating factor. The extremely high or low risk is primarily associated with the impact direction.

## CONCLUSIONS

Adding HSM does increase the risk of neck injury, but the impact level the subject is exposed to is a more dominating factor in determining injury risk. The impact directions are critical in HSM evaluation because they determine the neck moment. For the highest acceleration the mass magnitude and location more drastically affect the level of risk associated with the HSM configuration than for the lower accelerations. All of these factors should be considered in designing HSM configurations for various applications.

## REFERENCES

1. Barazanji K, et al. (1998) In NATO RTO Meeting Proceedings; 19:31-1 – 31-7.
2. Van der Horst MJ, et al. (2001). In Proc of the 17<sup>th</sup> ESV, The Netherlands
3. Eppinger R, et al. (1999). NHTSA, USA, November.

## ACKNOWLEDGEMENTS

This work was funded by the United States Army Aeromedical Research Laboratory (USAARL). This paper does not represent official policy or practice of the United States Army. The authors are also thankful for the technical support provided by The Netherlands Organization for Applied Scientific Research (TNO) and Altair.

# SCAPULOTHORACIC JOINT KINEMATICS DURING CONSTRAINED AND UNCONSTRAINED MOVEMENTS

Tal Amasay and Andrew R. Karduna

University of Oregon, Eugene, OR, USA

E-mail: [karduna@uoregon.edu](mailto:karduna@uoregon.edu)

## INTRODUCTION

Scapular kinematics is a very important component of shoulder motion. Researchers trying to measure scapulohumeral kinematics typically use constrained protocols. These protocols include constraining the humeral movement to specific planes such as the scapular, frontal and sagittal planes and restricting motion of the wrist, elbow and thorax (Ludewig et al. 1996; McClure et al. 2001). In contrast, there are studies measuring scapular kinematics in unconstrained scenarios such as wheelchair propulsion (Nawoczinski et al. 2003).

To the best of our knowledge there have been no published studies comparing scapular kinematics between constrained and unconstrained humeral movements. Therefore, the purpose of this study was to test the influence of constrained and unconstrained humeral movements on scapular kinematics.

## METHODS

Five healthy subjects (3 males, 2 females) participated in this study (mean age, 30.8 years). Kinematic data were collected via the Polhemus Liberty magnetic tracking system with three receivers: thorax, scapula and humerus. The thoracic receiver was attached using double side adhesive tape to the manubrium below the jugular notch. The scapular receiver was attached using a scapula tracker jig and Velcro strips on the

scapular spine and acromion process (Karduna et al. 2001). The humeral receiver was placed over the deltoid tuberosity using a molded cuff. For all trials, data were collected at a rate of 120 Hz (Figure 1).

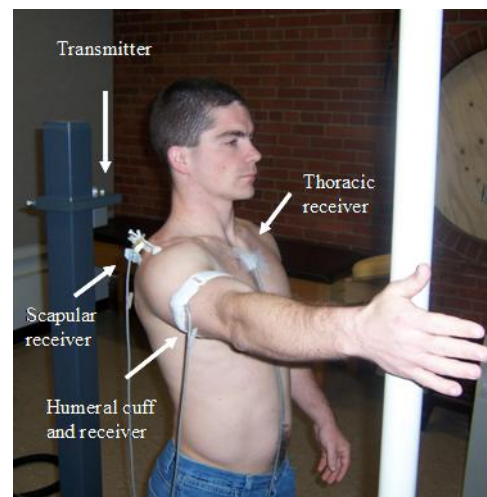


Figure 1. Experimental setup

During calibration and data collection trials subjects were in a standing position. Global and anatomical coordinate systems were based on the ISB recommendation for the upper extremity (Wu et al. 2005). Each subject performed one unconstrained movement which was reaching to a car seatbelt; we chose this natural movement because it crosses many humeral planes of elevation. After data collection for the unconstrained movement, the subject performed constrained movements consisting of arm elevation in different planes, starting with the frontal plane ( $0^\circ$ ) and ending with their maximal plane of elevation. The plane changed in increments of approximately  $10^\circ$  and a plastic pole was

used to indicate a specific plane. In the constrained trials the subjects were instructed to keep their elbow extended and thumb pointing to the ceiling.

Using the constrained data for each subject, we plotted the humeral plane of elevation and elevation. We then superimposed the unconstrained collected data of humeral plane of elevation and elevation on the constrained graph (Figure 2). Using this graph we identified crossing points of the constrained and unconstrained motions. Each one of these points was associated with three scapular angles (protraction, lateral rotation and posterior tilt). For each of these intersected points the scapular angles were compared between the constrained and unconstrained humeral movements.

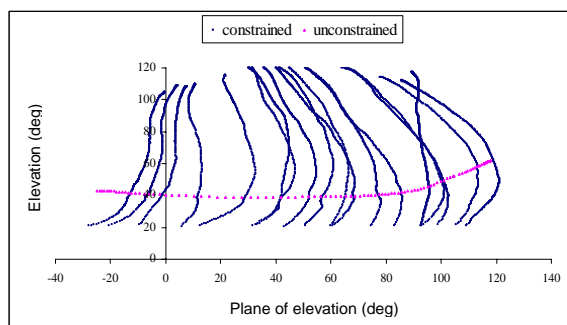


Figure 2. Representative trial of constrained and unconstrained humeral movement

## RESULTS AND DISCUSSION

The mean residuals (unconstrained minus constrained scapular angles) were  $0.2^\circ \pm 2.3^\circ$  for retraction/protraction,  $4.7^\circ \pm 4.5^\circ$  for lateral/medial rotation and  $-1.3^\circ \pm 1.6^\circ$  for anterior/posterior tilt. The residuals occurring at the measured humeral plane of elevation (Figure 3) and humeral elevation were found to be distributed over the whole measured range of motion.

Furthermore, scapular lateral rotation angles were higher in the constrained movement, in some cases by more than  $15^\circ$ . Alternatively

scapular posterior tilt angles were as much as  $5^\circ$  lower in the constrained movement. However, for scapular protraction angles there were no obvious trend to the residuals between the constrained and unconstrained movement.

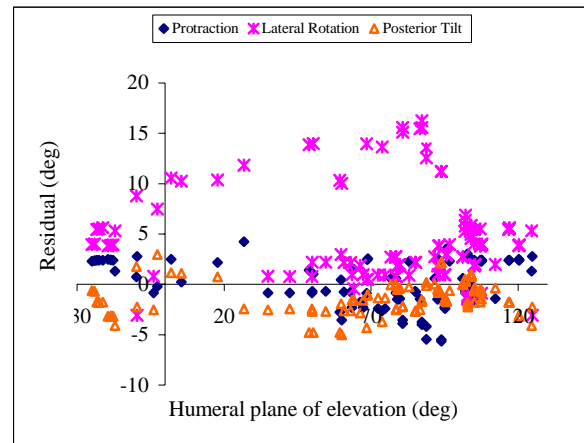


Figure 3. Effect of humeral plane of elevation on scapular residual angles

## SUMMARY/CONCLUSIONS

The results from this preliminary study demonstrate that there are differences in scapular orientations between constrained and unconstrained humeral movements. This may indicate that the use of constrained movement to represent scapular orientation in unconstrained movement may not be appropriate. Further study in this area is needed.

## REFERENCES

- Karduna, A. R., et al. (2001). *J Biomech Eng*, **123**(2), 184-90.
- Ludewig, P. M., et al. (1996). *JOSPT*, **24**(2), 57-65.
- McClure, P. W., et al. (2001). *JSES*, **10**(3), 269-277.
- Nawoczenski, D. A., et al. (2003). *Arch Phys Med Rehabil*, **84**(9), 1293-1300.
- Wu, G., et al. (2005). *J Biomech*, **38**(5), 981-992.

# NORMALIZATION OF SURFACE EMG SIGNALS - COMPARISON AMONG EFFORTS, JOINT POSITIONS AND PROCESSING METHODS

Naiquan (Nigel) Zheng<sup>1</sup>, Brian Ragan<sup>2</sup>, Paul Marvar<sup>2</sup>, and Steve Barrentine<sup>2</sup>

<sup>1</sup>University of Florida, Gainesville, FL, USA

<sup>2</sup>American Sports Medicine Institute, Birmingham, AL

E-mail: nigelz@ufl.edu Web: www.ortho.ufl.edu/BMAL

## INTRODUCTION

EMG signals have been used for diagnosis of disease, evaluation of different exercises, and estimation of muscle forces (Zheng, N et al, 1997). EMG results are affected by numerous factors during data detection and processing (De Luca, C. 1997), however these factors are often ignored and/or not reported when normalizing EMG. The objective of this study was to evaluate the effects of contraction effort, joint angle, and data processing method on EMG signal normalization. EMG signals were recorded during isometric contraction of the quadriceps muscles.

## METHODS AND MATERIALS

Ten healthy subjects (5 male, 5 female) with no history of knee injury volunteered and signed consent forms approved by the IRB. The dominant leg was tested with the subject seated. Three pairs of surface electrodes (Medicotest Marketing, Inc. Ballwin, MO) were placed on the muscle belly of the vastus medialis (VM), vastus lateralis (VL), and rectus femoris (RF). A load cell (Omega Engineering) was installed to directly measure force applied by the dominant leg near the ankle. The force signal was collected at 1000 Hz. Synchronized EMG signals from the three muscles were recorded at 1000 Hz with a Myosystem 2000 (Noraxon USA, Inc., Scottsdale, AZ). Signals were converted from analog to digital data and stored with an ADS system (Motion Analysis Corp.,

Santa Rosa, CA). Tests were conducted at 30, 60 and 90 degrees of knee flexion with maximum, 75% and 50% effort voluntary isometric contraction for 3 seconds. Each test was repeated three times. Subjects were allowed to take a 2-minute break between tests.

Data were passed through a high-pass 4<sup>th</sup> order butter filter and rectified. Four different processing methods were then used: integration (INT), low-pass filter with cut-off frequency of 25 Hz (LPS), root-mean-square (RMS) and average rectified value (ARV). For each processing method, the mean value of the middle second was calculated and averaged for the three tests each subject performed for each condition. The coefficient of variability (COV) among the three tests was also calculated. Repeated measures analysis of variance (ANOVA) was used to identify significant ( $p < 0.05$ ) differences in mean EMG and COV among effort, knee angle, and data process for each muscle (SPSS Inc, Chicago, USA).

## RESULTS AND DISCUSSION

Table 1 lists the forces recorded at different effort levels and knee flexion angles during 3 second peak (G-P), middle second peak (L-P) and the average in the middle second (L-M). Table 2 lists the mean EMG signals at different knee angles (A), effort levels (EL), data processing methods (PM), and signal origins (SO) (i.e. G-P, L-P and L-M).

The mean values and COV of EMG for the VM and VL muscles varied significantly with knee flexion angle. For the RF muscle, mean values and COV for different knee angles showed no significant differences. EMG results varied significantly among the different data processing methods. Mean values were greatest with the INT method and least with the ARV method. COV was the least with INT and no differences among others. Each of these methods has virtue and has been used in EMG analysis. The current study does not suggest that one method is superior, but that the choice of method can affect the results and should therefore be reported. Results also varied significantly due to signal origin.

EMG data is scaled commonly by the EMG magnitude of maximum voluntary isometric contraction (MVIC). While this is a common approach, Lawrence and De Luca (1983) suggested that the variability of EMG during maximum effort was high, which makes it a poor choice for normalization. As expected, the current study showed that mean values of EMG and force both were highest with maximum effort and lowest with 50% effort. However their COV were not significantly different among effort levels. Thus, the choice of effort for normalization trials would affect the magnitude but not the consistency of scaled data.

## SUMMARY

Normalization is often used in EMG data analysis. MVIC has the highest magnitude and the choice of using MVIC is no better or worse than 75% or 50% effort level. The choice of joint position and processing method should also be considered and reported. Different joint angles should be considered for different muscles to obtain MVIC or other level VIC. Because of

variability, multiple trials are always a good idea. The choice of signal origins also affects results. The choices of effort levels, joint positions, and processing methods are important, not only for the quality of an individual study, but also for comparison of various studies and clinical applications of EMG testing.

## REFERENCES

- De Luca, C (1997). *J. Appl. Biomechanics*, 13, 135-163.  
 Lawrence, J.H. and De Luca, C. *J. Appl. Physiol.* 54:1653-9.  
 Zheng, N. et al (1998) *J. Biomechanics*, 31, 963-967

Table 1 Forces recorded at different efforts and angles (mean± SD) (N)

		G-Peak	L-Peak	L-Mean
Effort Level	100%	332 ± 12	321 ± 11	301 ± 11
	75%	266 ± 11	259 ± 11	241 ± 10
	50%	203 ± 8	197 ± 8	183 ± 7
Angle (deg)	30	228 ± 8	220 ± 8	207 ± 8
	60	317 ± 14	310 ± 14	291 ± 13
	90	257 ± 10	247 ± 10	228 ± 9

Table 2 EMG Signals for RF, VM and VL (mean± SD) (mV)

		RF	VM	VL
A	30°	39.6 ± 1.5	28.9 ± 1.4	33.9 ± 1.1
	60°	43.1 ± 1.6	34.5 ± 2.2	33.7 ± 1.1
	90°	44.8 ± 1.6	56.0 ± 2.1	46.1 ± 1.4
E L	100%	54.7 ± 1.8	36.5 ± 2.1	39.2 ± 1.3
	75%	48.6 ± 1.9	39.2 ± 1.4	38.6 ± 1.3
	50%	51.3 ± 1.8	62.1 ± 2.4	52.0 ± 1.6
P M	INT	52.6 ± 2.2	51.0 ± 2.4	48.2 ± 1.7
	LPS	44.4 ± 1.9	42.2 ± 2.2	40.4 ± 1.6
	RMS	40.7 ± 1.3	37.1 ± 1.7	35.3 ± 1.1
	ARV	32.4 ± 1.3	28.9 ± 1.4	27.6 ± 0.9
S O	G-P	54.1 ± 1.8	50.1 ± 2.0	47.5 ± 1.4
	L-P	46.9 ± 1.6	44.4 ± 2.6	42.6 ± 1.2
	L-M	26.6 ± 0.9	24.2 ± 1.0	23.5 ± 0.6

# ROTATIONAL LAXITY OF THE KNEE MEASURED USING REFLECTIVE SKIN MARKERS

Naiquan (Nigel) Zheng, Bo Gao, Bryan Conrad

University of Florida, Gainesville, FL, USA  
E-mail: nigelz@ufl.edu Web: www.ortho.ufl.edu/BMAL

## INTRODUCTION

Recent studies show the necessity of understanding the three-dimensional (3-D) mechanics of the knee in order to isolate the functions of knee ligaments and their roles in mechanical instability and progressive osteoarthritis. Using bone pins with an optical motion analysis system, the Roentgen stereometric analysis (RSA), and a combined fluoroscopic imaging and MR image-based 3-D computer modeling technique, 3-D mechanics of the knee have been studied in both cadavers and patients (Li et al 2005, Tashman et al, 2004). However, these research tools cannot be used clinically due to radiation, and their complexity and invasive nature. Almquist et al (2002) developed an external device measuring knee joint rotation, but the device overestimated the joint rotation about 100%. Non-invasive optical tracking systems have been used for gait analysis. The tibial rotation has been calculated but it is influenced by soft tissue artifacts. Deficient of the anterior cruciate ligament may increase the rotational laxity of the knee. The purpose of this study is to study the rotational laxity of the knee using reflective skin markers.

## METHODS AND MATERIALS

Both left and right knees from four healthy subjects and four patients with reconstructed anterior cruciate ligament were tested using an IRB approved protocol. They were three females and 5 males. Subjects sat on a chair with knee flexed 90 degrees. Reflective

markers (10 mm sphere) were attached to the anterior superior iliac spine, middle anterior thigh and distal thigh, medial and lateral femoral epicondyle, medial and lateral tibia tubercle, and proximal and distal shank anterior. Extended wand markers were attached also to the bony and flat anteromedial surface of the tibia. The inferior wand marker was placed at the mid-shank. The superior wand marker was placed about 25% of the shank length from the knee. Three-dimensional coordinates were determined with an 11-camera motion analysis system (Motion Analysis Co. Santa Rosa, CA), while the rotational torque was recorded from a JR3 universal load cell (67M25, JR3 Inc., Woodland, CA). This system is capable of tracking reflective markers with an accuracy of approximately 0.5 mm. The load cell was attached to the foot through a custom-made adapter (Fig. 1). The motion data were collected at 60 Hz. The force and torque data were recorded at 1200 Hz and later reduced to 60 Hz to synchronize with the motion data.

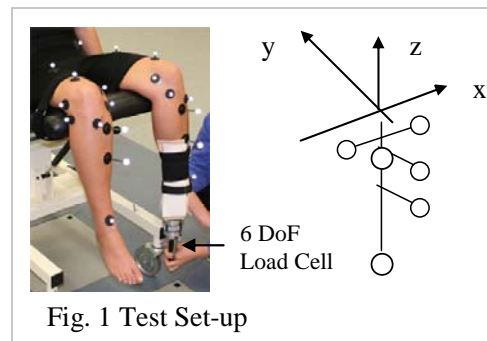


Fig. 1 Test Set-up

Subjects were instructed to relax during the test. Data from three trials were collected from both legs during internal and external rotation. A local reference system was created based on the markers attached to the thigh (Fig. 1), with

x axis pointing to the lateral, y axis to the proximal of the thigh, and z axis to the superior and aligned with the long axis of the shank. Tibial rotation was calculated from markers on the tibia: the two markers on the tibia tubercles ( $\alpha_t$ ), the superior extended wand marker ( $\alpha_s$ ), the inferior extended wand marker ( $\alpha_i$ ) and all markers with optimization ( $\alpha_o$ ) (Spoor and Veldpaus, 1980). The rotational laxity of the knee was measured at 7 Nm torque (Mill and Hull, 1991). A repeated measure ANOVA (SPSS) was used to test the differences.

## RESULTS AND DISCUSSION

Figure 2 shows four rotation angle curves vs. the rotational torque. There was no significant thigh movement during the tests. The skin movement of the tibia had a significant effect on the rotational angle measurement. The angles determined from the two tibial markers were significantly less than the angle calculated from the wand markers. Although the tibial markers were attached directly to the bony landmarks, they had relatively less movement than the underlying tibia. Therefore the rotational angle ( $\alpha_t$ ) was underestimated. The inferior wand marker had the most skin artifact error in determining the rotational angle during the laxity test. The angle ( $\alpha_i$ ) was overestimated. The angle determined from all markers with optimization ( $\alpha_o$ ) was very close to that from the superior wand marker ( $\alpha_s$ ).

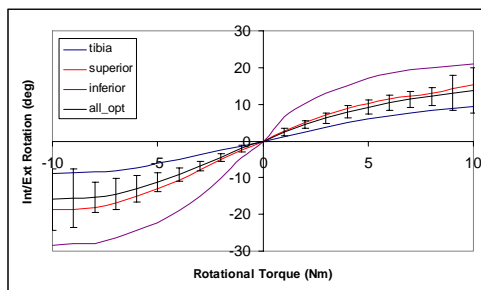


Fig. 2 Rotational Angle-Torque

There was a significant differences ( $p < 0.01$ ) in internal and external rotation calculated from the tibial plateau, all markers with optimization, superior and inferior wand markers (Fig. 3). The mean internal rotation at 7 Nm rotational torque was 7.6, 11.4, 12.3 and 19.4 degrees for  $\alpha_t$ ,  $\alpha_o$ ,  $\alpha_s$  and  $\alpha_i$  respectively. The mean external rotation at 7 Nm rotational torque was 8.1, 14.4, 16.7 and 26.5 degrees for  $\alpha_t$ ,  $\alpha_o$ ,  $\alpha_s$  and  $\alpha_i$  respectively.

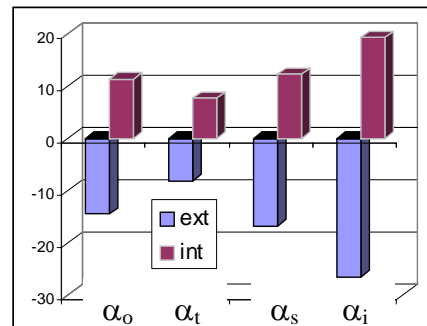


Fig. 3 Angles using different marker sets

## SUMMARY

Soft tissue artifacts affected the rotational laxity measurement of the knee. When the rotational laxity is compared between healthy and non-healthy subjects or between involved and non-involved legs, soft tissue artifacts become one of the major systematic errors. Reflective markers must be placed carefully. Slight changes of the marker placement may affect the laxity measurement. Future studies will be focused on removal of the soft tissue artifacts during the rotational laxity measurement.

## REFERENCES

- Almqvist PO et al, J Orthop Res. 20:427, 2002
- Li G et al, J. Orthop Res. 23:340, 2005
- Mills OS & Hull ML. J. Biomech, 24:673, 1991
- Spoor CW & Veldpaus FE, J. Biomech, 13:391 1980
- Tashman S et al, J Orthop Res. 22:931, 2004

# UPPER EXTREMITY ELECTROMYOGRAPHIC ACTIVITY IN RESPONSE TO BICEPS TO TRICEPS TRANSFER SURGERY

Richard T. Lauer, Carole A. Tucker, MJ Mulcahey, Sudarshan Dayanidhi, Carrie Stackhouse, David Hutchinson, Scott Kozin

Shriners Hospitals for Children, Philadelphia, PA  
Email:rlauer@shrinenet.org

## INTRODUCTION

Published outcomes of upper extremity (UE) reconstruction in persons with cervical level spinal cord injuries (SCI) are overwhelmingly positive. Tendon transfer surgeries for active grasp have been shown to increase hand function, and improve social, emotional, and vocation status (Freehafer 1991; Hentz et al.,1992). An important outcome of UE reconstruction also concerns the pivotal role of elbow extension. The biceps to triceps tendon transfer surgery has successfully restored elbow extension in persons with tetraplegia (Kozin et al, 2002). However, there is a lack of data in supporting this intervention as the best means for restoring elbow extension. Key to addressing this question is to understand how well the nervous system re-learns the use of the muscle in its new role as elbow extensor. Insight into the re-learning process by the nervous system may be accomplished through a quantitative analysis of electromyographic (EMG) activity of the transferred muscles.

## METHODS

EMG data with concurrent motion analysis (Vicon, Lake Forest CA) of the upper extremity was collected from one participant (Female, 16 years of age) SCI who underwent a biceps to triceps transfer two years prior to data collection. Fine wire EMG electrodes were inserted into the brachialis and biceps muscles, with surface electrodes placed on the biceps, triceps, and

brachioradialis. The data were collected at 3.0 kHz, with bandwidth filtering between 20 and 1500 Hz and anti-alias filtering with a cut-off of 350 Hz using Motion Lab Systems MA-310 system (Baton Rouge, LA).

The individual was asked to perform a series of concentric/eccentric flexion/extension movements with the forearm pronated at two self selected speeds. Processing of the data involved identifying three complete flexion/extension movements with concurrent EMG activity. The signals were rectified, smoothed with a moving average window, and averaged over the three trials. EMG and elbow joint angle were time normalized, and divided into the flexion stage of movement and the extension stage of movement. Activity of the sEMG signal was determined if values exceed three times the minimal level of EMG activity during the movement given that no baseline data was available. Analysis involved examination of the average EMG signals by calculating the percentage of the flexion/extension movement that a muscle was active, and the level of co-activation between the biceps and the remaining elbow flexors as a way to quantify selective control post-transfer.

## RESULTS AND DISCUSSION

Biceps muscle activity was restricted primarily to the extension phase of movement, with increases in activity for

faster movement speeds in the extension phase of movement. Brachialis activity increased in the flexion and extension phases of movement with increased movement speed, indicating increased overall joint stiffness to stabilize the elbow during rapid movements. This is supported by increased co-activation of the biceps and brachialis at the transition of flexion to extension phases of movement.

Brachioradialis activity decreases, most likely in response to increased brachialis activity. Co-activation for biceps and brachioradialis was not present except for the slow movement speed in flexion.

This pilot study represents the first attempt to understand nervous system re-education after a tendon transfer surgery using measurements of muscle activity. The fast and slow speeds of movement, which attempted to assess whether using the biceps as an elbow extensor required concentration on the part of the individual or have become part of the motor program demonstrates that the muscle can be retrained completely to act in its new role and that it does not require conscious effort on the part of the individual. This will require testing on a larger sample size to determine how effective this re-learning is, and how additional therapies might be imposed early on to help facilitate the motor re-education.

**Table 1:** EMG activity in relation to the flexion and extension phases of elbow movement. In rows where two muscles are listed, percent values indicate the percent of the repetition that muscles overlap in activity.

	<b>Flexion – Slow</b>	<b>Flexion - Fast</b>	<b>Extension – Slow</b>	<b>Extension – Fast</b>
<b>Biceps</b>	<b>8.4 %</b>	<b>8.4 %</b>	<b>47.2%</b>	<b>80.8%</b>
<b>Brachialis</b>	<b>96.8 %</b>	<b>100%</b>	<b>25.6%</b>	<b>56.4%</b>
<b>Brachioradialis</b>	<b>99.6%</b>	<b>53.6%</b>	<b>58.4%</b>	<b>14.8%</b>
<b>Biceps/Brachialis</b>	<b>8.4%</b>	<b>8.4%</b>	<b>21.6%</b>	<b>37.2%</b>
<b>Biceps / Brachioradialis</b>	<b>8.4 %</b>	<b>0%</b>	<b>0 %</b>	<b>0%</b>

## SUMMARY / CONCLUSIONS

Biceps to triceps tendon transfer surgeries are a means to restore elbow extension in individuals with a cervical level spinal cord injury (SCI). However, it is unclear as to whether this is the best rehabilitation option as compared to other surgical measures. One way to establish the effectiveness of this procedure is to determine how well the biceps muscle can be re-educated to perform elbow extension. Results of this preliminary pilot study demonstrate that the muscle can be completely readapted to its new role, as tested through alternating speed and position. Further study is required on a larger sample size to verify this preliminary finding

## REFERENCES

- Freehafer A. (1991). *J Hand Surg* **16A**:804-809.  
 Hentz V., et al (1992). *J Hand Surg* **17A**:964-967.  
 Kozin S., et al. (2002). *J Hand Surg* **27**:666-669.

## ACKNOWLEDGEMENTS

Funding was provided by The American Society for Surgery for the Hand Outcome Studies Grant and the Shriners Hospitals for Children.

# BIOMECHANICAL RISK ESTIMATES FOR CONCUSSION IN COLLEGIATE FOOTBALL PLAYERS

James R. Funk<sup>1</sup> and Stefan M. Duma<sup>2</sup>

<sup>1</sup> Biodynamic Research Corporation, San Antonio, TX, USA

<sup>2</sup> Virginia Tech-Wake Forest Center for Injury Biomechanics, Blacksburg, VA, USA

E-mail: jfunk@brconline.com

## INTRODUCTION

Past efforts to determine head injury tolerance have been hampered by the need to study injury in cadavers or primates. American football presents a unique opportunity to study concussion, or mild traumatic brain injury (MTBI), in living humans.

Based on video footage of NFL games, Pellman et al. (2003) reconstructed 31 head impacts, 25 of which resulted in a player sustaining a concussion, using helmeted Hybrid III dummies. King et al. (2003) presented risk curves for MTBI based on logistic regressions of the NFL data. However, the NFL data was intentionally biased towards injurious impacts, and was not intended to document the head impact exposure experienced by players in the NFL. The purpose of the present study was to analyze the risk of MTBI in the collegiate football setting in light of more complete head impact exposure data.

## METHODS

Head impact data obtained from instrumented helmets worn by Virginia Tech (VT) football players during the 2003 and 2004 seasons were analyzed. The helmets were instrumented with the Head Impact Telemetry (HIT) System (Simbex, Lebanon, NH), which consisted of six spring-mounted accelerometers designed to stay in contact with the player's head. The methodology

and validation of the HIT system are described by Duma et al. (2005).

The risk of MTBI was analyzed in terms of peak resultant linear head acceleration, the head injury criterion (HIC), and peak resultant rotational head acceleration. A biomechanical data set was generated that included all injurious head impacts as well as the most severe non-injurious head impact sustained by each instrumented player. Risk curves for MTBI were calculated using the consistent threshold (CT) estimate for doubly censored data (Nusholtz and Mosier, 1999). The CT estimate is a non-parametric maximum likelihood estimate.

## RESULTS AND DISCUSSION

The total data set included 11,605 head impacts sustained by 52 players. Although most impacts were of low severity, there were 993 impacts over 4500 rad/s<sup>2</sup>, 225 impacts over 80 g, and 114 impacts with a HIC greater than 250. Only three concussions were recorded (Table 1). All three concussions resulted from impacts to the front of the head. For two of the injured players, the concussive impacts were the second-most severe impact recorded. For the other (MTBI #1), there were 6 – 13 more severe impacts recorded, depending on the severity measurement used. However, all three concussive impacts were the most severe frontal impact recorded for that player.

In spite of the small sample size, the results of the present study are in general agreement with the results of Pellman et al. (2003), at least with regard to injury data. The average peak linear acceleration and HIC associated with MTBI are similar in both studies. The average peak rotational acceleration associated with MTBI was somewhat higher in the VT data than the NFL data.

**Table 1:** Summary of VT injury data.

MTBI #	$a_{res}$ (g)	HIC	$\alpha_{res}$ (rad/s <sup>2</sup> )
1	56	121	5165
2	118	366	10776
3	137	518	11727
Mean	103	332	9223
S.D.	42	200	3546

With regard to non-injury data, the VT data is markedly different from the NFL data. The VT data is a random collection of head impacts, and is therefore an unbiased sample of the head impact exposure experienced by VT football players. As a result, the VT data includes a large number of non-injurious impacts, most of which are of low severity. However, a surprising number of high severity non-injurious impacts were recorded in the VT data that were not found in the NFL data. As a result, the CT estimate of MTBI risk using the VT data was considerably lower than the MTBI risk estimated from the logistic regression (LR) of the NFL data (Figures 1, 2, and 3).

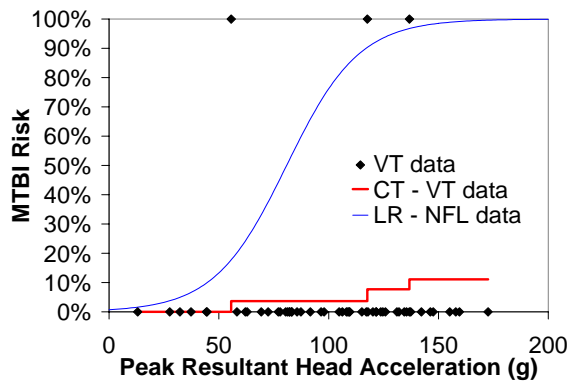


**Figure 1:** MTBI risk vs. head acceleration.

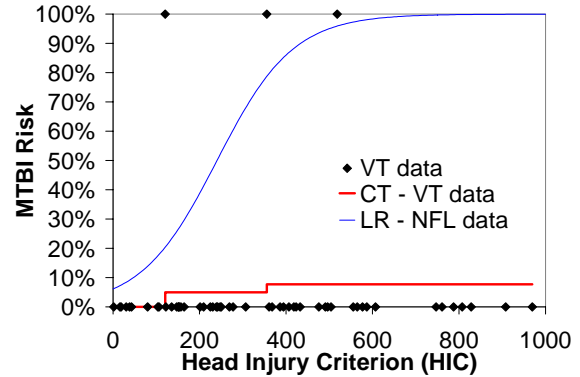


**Figure 2:** MTBI risk vs. HIC.

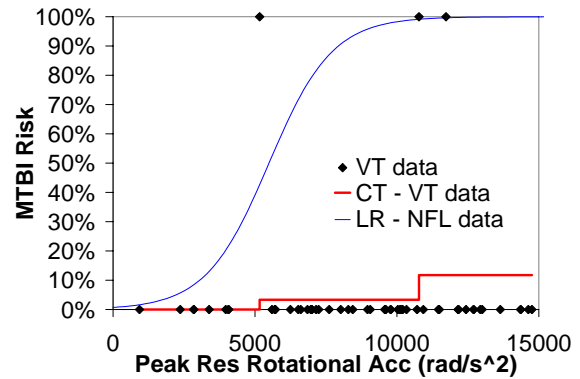


**Figure 3:** MTBI risk vs. rotational head acceleration.

## SUMMARY AND CONCLUSIONS

MTBI risk curves were estimated from data obtained from VT football players wearing instrumented helmets. These unbiased head impact exposure data complement the injury data from Pellman et al. (2003), and allow for a more accurate determination of concussion risk. These data may be useful in designing equipment to protect football players and the general public.

## REFERENCES

- Duma, S.M. et al. (2005). *Clin J Sports Med*, **15**(1): 3-8.
- King, A.I. et al. (2003). *IRCOBI*.
- Nusholtz, G., Mosier, R. (1999). *SAE*, paper 1999-01-0714, 1-14.
- Pellman, E.J. et al. (2003). *Neurosurgery*, **53**(4): 799-814.

# A FREQUENCY-BASED ELECTROMYOGRAPHIC INDEX FOR USE IN CEREBRAL PALSY

Richard Lauer<sup>1</sup>, Carrie Stackhouse<sup>1</sup>, Brian Smith<sup>1</sup>, Patricia Shewokis<sup>1,2</sup>, Carole Tucker<sup>1</sup>, James McCarthy<sup>1</sup>

<sup>1</sup> Shriners Hospitals for Children, Philadelphia, PA, USA

<sup>2</sup> College of Nursing and Health Professions, Drexel University, Philadelphia, PA, USA  
Email: rlauer@shrinenet.org

## INTRODUCTION

Surface electromyography (sEMG) is a typical part of instrumented gait assessment for the child with cerebral palsy (CP). Numerous methods exist to characterize the sEMG in order to gain insight into the neuromuscular impairments that exist in CP, including the use of muscle onset and offset and amplitude. However, these methods have focused upon one aspect of the sEMG to characterize the signal. The sEMG could potentially be better utilized clinically if multiple characteristics are examined concurrently. The introduction of time-frequency analysis provides a method of extracting more information from the sEMG in CP (Lauer et al 2005), and thus potentially gaining further insight into the neuromuscular system. The purpose of this study was to apply these techniques to the analysis of sEMG during gait in children with CP to derive an index that may be used to track and categorize muscle activity.

## METHODS

A retrospective study was conducted with 33 children. The group consisted of sixteen children with typical development (TD) to act as a control group (mean age 10.8 years, age range: 7-14 years). The remaining data set consisted of five children with spastic, hemiplegic CP and 16 children with spastic, diplegic CP (mean age at 10.4 years, age range: 6-20 years).

The sEMG signals were acquired during a standard gait analysis as individuals walked across a 10 meter (28 foot) walkway barefoot at a self-selected pace. The activity of the following muscles was recorded bilaterally: the vastus lateralis (VL), the medial hamstring (MH), the medial gastrocnemius (MG) and the tibialis anterior (TA). A representative time-frequency pattern was extracted from the sEMG for each muscle using the continuous wavelet transform applied using the Morlet wavelet with a linear scale of 1 to 126. The result of the analysis, the scalogram, for each trial for each muscle was averaged and the representative value of the scalogram at each gait interval was calculated using the instantaneous mean frequency (IMNF) (Lauer et al., 2005).

The resulting IMNF curves were plotted as a series of muscle-muscle plots representing interlimb muscle symmetry (right versus left side) and intralimb muscle co-activation. Analysis of the muscle-muscle plots was performed using functional data analysis (FDA) techniques (Ramsay and Silverman 2005). The FDA was selected for use as it allowed for a principal component analysis of the entire plot, allowing for better assessment of the sEMG characteristics. The harmonic output from the FDA, after normalization using the values from the control group, was used to generate the index.

The EMG index was compared to several kinematic measurements, a Gait Index, (Schutte et al., 2000) and several clinical assessment scales. Correlations were performed using either Pearson Product Moment or Spearman's rho with a two-tailed test for a 0.05 significance criterion. Normality of data was assessed and confirmed using the D'Agostino-Pearson test for normal distribution. In addition, 95% confidence intervals were calculated.

## RESULTS AND DISCUSSION

The EMG indexes demonstrated an increase in the value with an increasing level of motor impairment. On an initial breakdown of the groups into children with spastic, hemiplegic CP (Hemi), and children with spastic, diplegic CP grouped according to their GMFCS level (Palisano et al., 1997), Level 1, Level 2 or Level 3, the average scores (STD) were as follows: Hemi: 13.23 (4.5); Level 1: 15.6 (3.5); Level 2: 16.5 (14.2); Level 3: 52.41 (28.8). No distinction at this time is made between right and left hemiplegia given the small sample size and the variability in the data.

**Table 1:** Correlation analysis with upper and lower limits confidence intervals for  $r$  for the EMG index ( $p < 0.01$ ,  $p < 0.001$ ).

Measure	EMG Index	
	$r$	95% CI
Cadence	-0.74	-0.89 to -0.46
Step Length	-0.38	-0.70 to 0.06
Velocity	<b>-0.62</b>	-0.83 to -0.25
Gillette Index	<b>0.62</b>	0.26 to 0.83
GMFCS	<b>0.65</b>	0.30 to 0.84
GMFM-D	<b>-0.70</b>	-0.87 to -0.38
GMFM-E	<b>-0.65</b>	-0.85 to -0.31
POSNA-Global	-0.36	-0.69 to 0.08
POSNA_Mobility	<b>-0.43</b>	-0.73 to 0.01

The correlation analyses between the EMG index and the selected kinematic parameters and clinical assessment scales are summarized in Table 1. In addition, represented are the upper and lower limits for the 95% confidence interval. For the index, significant moderately high ( $r = -0.43$  to  $-0.74$  and  $r = 0.56$  to  $0.65$ ) correlations were achieved for all parameters and scales compared except for step length ( $r = -0.38$ ) and the POSNA global score ( $r = -0.36$ ).

## SUMMARY/CONCLUSIONS

A new method of processing the sEMG data acquired during a standard gait analysis, and reduction of the data to a meaningful scale has been described. The end stage of the analysis, an EMG index, correlated significantly to existing clinical measurements of motor impairment in cerebral palsy. This methodology has the potential to provide additional insight into the outcome of a clinical intervention that was not available previously, and may find use as a predictive tool that can be utilized for clinical decision making. Future avenues of investigation for this scale involve refinement of the index to determine sensitivity to spasticity, muscle weakness, and fatigue, as well as testing on prospective data to examine reliability.

## REFERENCES

- Lauer, R.T. et al. (2005) *J Biomech*, **38(6)**, 1351-1357.
- Palisano, R., et al. (1997) *Dev Med & Child Neurol*, **39**, 214-223.
- Ramsay, J., Silverman, B., (2005). *Functional Data Analysis*, 2<sup>nd</sup> ed. Springer, New York.
- Schutte, L. et al. (2000) *Gait & Posture*, **11**, 25-31.

## ACKNOWLEDGEMENTS

Funding for this study was provided by Shriners Hospitals for Children, Grants #8520 and #8540.

# **GENDER DIFFERENCES IN PLANTAR LOADING DURING THREE ATHLETIC TASKS ON FIELDTURF.**

Robin M. Queen, PhD, W. Mack Hardaker, BS, and William E. Garrett, Jr, MD, PhD

Michael W. Krzyzewski Human Performance Lab

Duke University, Durham, NC, USA

E-mail: robin.queen@duke.edu Web: <http://klab.surgery.duke.edu>

## **INTRODUCTION**

Soccer is one of the most popular sports in the world with approximately 200,000 professional players and 240 million recreational players. Athletes who participate in sports involving running, jumping, and cutting are at risk for knee, ankle, and forefoot injuries (Giza and Micheli, 2005; Hockenberry, 1999; Malinzak, et al, 2001) Athletes who abruptly increase their training, either in terms of mileage changes, or with a change in the frequency of the activity are more susceptible to stress fractures.(Kennedy et al, 2005) Stress fracture account for approximately 10% of all sports injuries and are most common in the tibia (49.1%), followed by the tarsals (25.3%), the metatarsals (8.8%) and finally the femur (7.2%) and the fibula (6.6%) ( Korpelainen, et al, 2001; Matheson, et al, 1987). The purpose of this study was to determine the differences in plantar pressure distribution patterns between men and women when performing three different athletic tasks during the completion of an agility course.

## **METHODS**

A total of 34 (17 female, 17 male) subjects were recruited and tested during this study. Subjects all signed an informed consent form, which was approved by the institutional review board prior to testing. Each subject had his/her height and weight recorded and were fit with the proper size shoe and insole. The testing shoe was a

Nike Vitoria Hard Ground Boot, with 25 molded cleats. Subjects ran an agility course 5 times in each shoe while plantar pressure data were collected on both feet at 100 Hz using the Pedar in-shoe pressure measurement system (Novel Electronics, Inc, St. Paul, MN). The left plant (cross-over cut) around the final flag, the right plant (side-cut) around the second flag, and the acceleration phase at the beginning of the agility course were used for comparison. During the three movements the peak pressure, maximum force, loading rate, and contact area differences under the entire foot and in the following eight foot regions were determined: heel, medial and lateral midfoot, medial forefoot, middle forefoot, lateral forefoot, hallux, and the lesser toes. The maximum force was normalized to the subject's body weight and the contact area was normalized to the contact area of the insole to allow for comparisons between genders. Each variable was analyzed using paired t-tests to determine significant gender differences ( $\alpha=0.05$ ).

## **RESULTS AND DISCUSSION**

During the side cut task there were significant gender differences in the peak pressure beneath the entire foot ( $p=0.017$ ) as well as the medial midfoot ( $p=0.039$ ), the medial forefoot ( $p=0.004$ ), and the middle forefoot ( $p=0.0001$ ), with the men demonstrating increased pressure in each of these foot regions during the side cut task.. The gender difference in peak pressure could be the result of differences in body

weight between genders. The maximum force beneath the middle forefoot was significantly different between genders ( $p=0.028$ ) with the men having a larger maximum force during the side cut task. No statistically significant differences existed between genders for any of the foot regions for either the contact area or the loading rate during the side cut task.

During the cross-over cut task, statistically significant differences existed between genders in the peak pressure beneath the entire foot ( $p=0.018$ ), the lateral midfoot ( $p=0.022$ ), lateral forefoot ( $p=0.021$ ), hallux ( $p=0.05$ ), and the lesser toes ( $p=0.021$ ), with the men demonstrating increased pressure in each of these comparisons. The maximum force beneath the lateral forefoot ( $p=0.009$ ) and the lesser toes ( $p=0.017$ ) were significantly different between genders with the men having a larger maximum force. The contact area beneath the lesser toes were significantly different between genders ( $p=0.028$ ) with the men having an increased contact area when compared to the women. Significant differences existed between genders in the loading rate beneath the lateral midfoot ( $p=0.032$ ), lateral forefoot ( $p=0.002$ ), hallux ( $p=0.035$ ), and the lesser toes ( $p<0.0001$ ), with the men having an increase in the loading rate compared to women.

During the acceleration task, significant differences existed between genders in the peak pressure ( $p=0.005$ ), maximum force ( $p=0.003$ ), and the contact area ( $p<0.0001$ ) beneath the entire foot. The maximum force and contact area were significantly greater for the men when compared to the women. Significant gender differences in peak pressure existed beneath the lateral midfoot ( $p=0.038$ ), middle forefoot ( $p=0.025$ ), lateral forefoot ( $p=0.006$ ), hallux ( $p=0.028$ ), and the lesser toes ( $p=0.046$ ), with the men

demonstrating increased pressure in each of these foot regions. The maximum force beneath the middle forefoot ( $p=0.014$ ), lateral forefoot ( $p<0.0001$ ), hallux ( $p=0.024$ ), and the lesser toes ( $p=0.004$ ) were significantly different between genders with the men having a larger maximum force in these regions of the foot. The contact area beneath the middle forefoot ( $p<0.0001$ ), lateral forefoot ( $p=0.002$ ), and the lesser toes ( $p=0.005$ ) were significantly different between genders. Significant differences existed between genders in the loading rate beneath the lateral forefoot ( $p=0.030$ ) with the men having an increase in the loading rate compared to women.

## SUMMARY/CONCLUSIONS

Based on the results of this study, it is important to consider gender differences in loading patterns when comparing different movements and to examine different movement tasks when considering injury risks for both genders. The significant difference in the normalized maximum force between genders in the lateral forefoot could be one explanation for the increased number of fifth metatarsal stress fractures in men.

## REFERENCES

- Giza, E., Micheli, L.J. (2005) *Med. & Science in Sports & Exer.* **49**:140-169.
- Hockenberry, RT. (1999) *Med. & Science in Sports & Exer.* **31**:S448-S458.
- Kennedy, J, et al. (2005). *Current Opinion in Pediatrics.* **17**:34-42.
- Malinzak, R. et al. (2001) *Clinical Biomechanics.* **16**:438-445.
- Matheson, G, et al. (1987) *American J. of Sports Med.* **15**:46-58.

## ACKNOWLEDGEMENTS

The authors would like to thank Nike, Inc for their support and funding of this project.

# EFFECTS OF LIMITED LOWER BACK MOTION ON SOFT LANDING MECHANICS

Soo-An Park, Mark D. Tillman, John W. Chow

University of Florida, Gainesville, FL, USA  
E-mail: parksa@ufl.edu

## INTRODUCTION

The flexibility of the spine in vivo is measured by the ROM of the spine, and is determined as the angular change of each region of the spine. Lumbar flexibility is a critical factor to maintain balanced locomotion between the upper body and lower extremities. The population of patients who have undergone spinal fusion surgery is getting larger and younger and they demand active lives. However, very few studies have examined the effects of a stiff lower back on the mechanics of other regions of the body during physical activities.

Landing from a jump demands large eccentric muscle forces during the control of motion in many load-bearing joints. It is not known whether landing mechanics is influenced by lumbar spinal flexibility.

Therefore it was the purpose of this study to investigate the kinematic, temporal and kinetic characteristics of lower extremity joints during soft landing in three different lower back brace conditions simulating various lumbar spine flexibilities.

## METHODS

Twelve healthy active males (ages:  $23.4 \pm 2.1$  yrs) and 13 females (ages:  $21.7 \pm 1.7$  yrs) participated in this study. Before landing trials, sagittal lumbar ROM (flexibility index) was measured based on the American medical association (AMA) guide to ROM assessment using a BROM II (a modified double inclinometer).

During each landing trial, the subject descended from a 50-cm height platform and landed on two force plates with each foot at the center of force plate. The kinematic, temporal and kinetic data were collected using a 3-D Motion Analysis system and a force plate. All the same procedures were repeated with the different brace conditions.

The dependent variables for the flexibility tests were as follows: (1) Flexion ROM (FROM), (2) Extension ROM (EROM), (3) Sit-and-reach value (SNR). Dependent variables were submitted to three separate 2 (gender)  $\times$  3 (brace type: no\_brace, lumbar corset: LC, semirigid lumbosacral orthosis: LSO) ANOVA with repeated measures on the brace type.

The kinematic and kinetic dependent variables were submitted to two separate 2 (gender)  $\times$  3 (brace type) MANOVA with repeated measures on the last factor, and the time to maximal joint flexion was submitted to a 2 (gender)  $\times$  3 (brace type)  $\times$  3 (lower extremity joints: ankle, knee, hip) ANOVA with repeated measures on the last two factors. A nonparametric binomial test was performed to determine whether overall sequences of maximal joint flexion varied according to gender and brace type.

## RESULTS AND DISCUSSION

LSO significantly limited FROM, EROM and SNR compared to the other conditions (Table 1).

Significant main effects of brace type for the kinematic (angular displacement of knee ( $\phi_{K(LP)}$ ) ( $p=0.026$ ) and hip ( $\phi_{H(LP)}$ ) ( $p=0.036$ ) joints during the landing phase) and kinetic (peak vertical ground reaction force ( $VGRF_P$ ) ( $p=0.001$ ) and peak axial hip joint force ( $AHF_P$ ) ( $p<0.001$ )) variables were detected:  $\phi_{H(LP)}$  and  $\phi_{K(LP)}$  of LC and  $\phi_{K(LP)}$  of no\_brace were significantly decreased and  $VGRF_P$  and  $AHF_P$  of no\_brace were significantly increased in LSO condition. A significant interaction of knee extensor moment between gender and brace type was observed ( $p=0.044$ ) (Figure 1). The binomial test revealed that the typical sequential joint flexion from distal to proximal (i.e., ankle  $\rightarrow$  knee  $\rightarrow$  hip) was disrupted in the majority of females (85%) in LSO ( $p=0.003$ ) (Figure 2).

**Table 1:** Lumbar flexibility indices across brace type (mean  $\pm$  SD).

	FROM ( $^{\circ}$ )	EROM ( $^{\circ}$ )	SNR (cm)
No_Brace	30.2 $\pm$ 6.5*	15.0 $\pm$ 5.3*	5.1 $\pm$ 10.4*
LC	29.4 $\pm$ 7.5#	15.7 $\pm$ 4.4#	4.0 $\pm$ 11.2#
LSO	17.5 $\pm$ 3.8*#	10.2 $\pm$ 2.8*#	-9.1 $\pm$ 12.8*#

\* # significant differences ( $p<0.001$ )

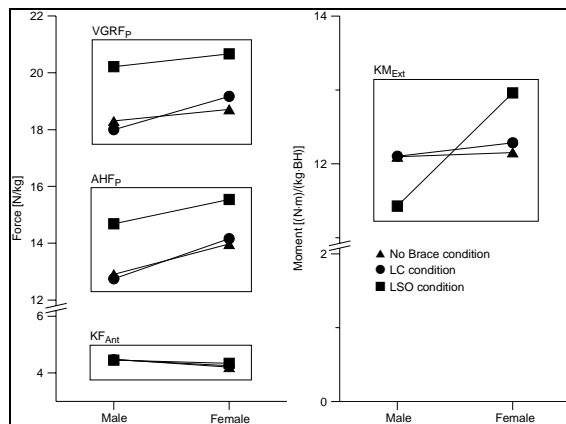


**Figure 1:** Significant main effects of brace type for  $VGRF_P$  and  $AHF_P$ ; Significant interaction of knee extensor moment between gender and brace type.

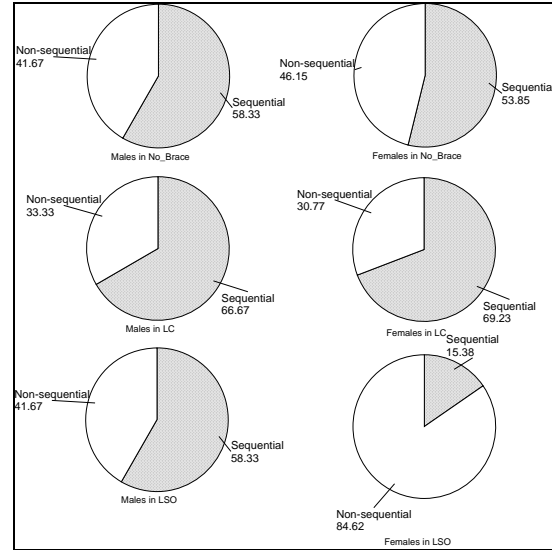


**Figure 1:** Sequence of maximal joint flexion across gender and brace type: sequential (ankle  $\rightarrow$  knee  $\rightarrow$  hip) and non-sequential.

## SUMMARY/CONCLUSIONS

LSO significantly restricted sagittal lumbar ROM. The altered spinal kinematics by the LSO caused limitations of knee and hip joint motions during the landing phase and an increase of peak vertical ground reaction force. The uses of LSO significantly disrupted sequential joint motions from distal to proximal and increased knee extensor moment in females. It seems that lower back motion is one of the factors in determining landing mechanics, and a stiff lower back causes a stiff landing. More decelerating torque might be concentrated on the knee extensors for females, and more axial loads be transmitted to the proximal body segments of males during soft landings in LSO (stiff lower back) conditions.

## ACKNOWLEDGEMENTS

Braces (LSO) were supplied by Boston Brace International, Inc. (Avon, MA).

# GROUND REACTION FORCES IN PATIENTS WITH UNILATERAL PERIPHERAL ARTERIAL DISEASE

Sara A. Myers<sup>1</sup>, Jessie M. Huisinga<sup>1</sup>, Jason Johanning<sup>2,3</sup>, Iraklis Pipinos<sup>2,3</sup>, and Shing-jye Chen<sup>1</sup>

<sup>1</sup>University of Nebraska at Omaha, Omaha, NE, USA

<sup>2</sup>University of Nebraska Medical Center, Omaha, NE, USA

<sup>3</sup>Veterans Affairs Medical Center, Omaha, NE, USA

E-mail: sfagan@mail.unomaha.edu Web: www.unocoe.unomaha.edu/hper/bio/home.htm

## INTRODUCTION

Peripheral arterial disease (PAD) is a manifestation of systemic atherosclerosis significantly reducing arterial blood to the lower extremities. Up to 12 million people in the USA suffer from PAD with claudication as the most common clinical manifestation. These claudicants have an inability to ambulate with a normal gait secondary to pain and fatigue of ischemic muscles. As the affected muscle becomes progressively ischemic, ambulation becomes impaired and eventually must cease to allow for reperfusion. This moderate to severe claudication limits a person's ability to walk and perform activities of daily living (McCully et al., 1999). Our previous work has established that biomechanical differences exist in the gait patterns of bilateral PAD patients as compared to controls (Scott et al, 2005). Unilateral PAD is a common clinical condition where patients experience claudication solely in one leg. Research involving other unilateral pathologies has demonstrated that asymmetries exist due to compensations of the unaffected leg (Schmid et al, 2005; Viton et al, 2000). However, no such information is available for unilateral PAD. The purpose of this study was to investigate potential gait adaptations occurring in unilateral PAD patients. Specifically, we compared the selected parameters of ground reaction forces (GRF) in the vertical (Fz), the anterior-posterior (Fy) and the medio-

lateral (Fx) directions between (a) the claudicating and the contralateral healthy leg in unilateral PAD patients, and (b) both legs of unilateral PAD patients and healthy controls.

## METHODS

Eight unilateral PAD patients and five healthy controls walked through a 10 meter runway over an embedded Kistler force plate while kinetics (600 Hz) were recorded using a Motion Analysis system. Five trials were captured for each leg during pain free and pain (claudication) conditions. Claudication was induced in the patients by using a common clinical protocol in which the patient walked on a treadmill which was set at 10 percent grade and .67 m/sec speed until the onset of muscle ischemia and pain. The GRF data was evaluated using a discrete point approach. Thus, the group means of all local maximums and minimums as well as their differences and their times of occurrence during stance, were calculated. Impulses were also calculated. Statistics included a repeated 2X2 ANOVA to compare the claudicating to contralateral healthy leg under the two pain conditions. Independent t-tests were also used to compare both legs of the PAD patients under the pain-free condition to the healthy controls.

## RESULTS AND DISCUSSION

Significant differences were found for several parameters in all GRF directions for the pain factor. Specifically, these differences were located at: a) Fx<sub>min</sub> (the Fx minimum; p=0.022), b) FxD (the difference between Fx max and Fx<sub>min</sub>; p=0.024), and c) DF2-Fz<sub>min</sub> (p=0.026). A significant interaction was found for FyP (p=0.035) and TF2 (p=0.022). These findings collectively showed that pain resulted in decreased fluctuations on the Fz and Fx curves, indicating less sideway movements and decreased time in single support. The claudicating PAD leg demonstrated reduced forward push compensated by the contralateral healthy leg pushing harder. The lack of any significant main effects between the two legs clearly indicated the existence of additional adaptation at the contralateral leg.

Both legs of the PAD group revealed significant differences compared to controls for several Fz and Fy parameters (Table 1), but not for the Fx. These findings collectively showed the diminished ability of the PAD group to properly push forward, and even brake naturally with the PAD leg, when compared to healthy controls. This was evident from the decreased values observed in the PAD group for all parameters evaluated. Furthermore, the decreased amount of curve fluctuations was

again observed for the PAD group as compared to controls, indicating decreased time in single support and diminished anteriorposterior movement.

## SUMMARY/CONCLUSIONS

PAD unilateral patients have an altered gait compared to healthy controls during pain free walking which is increased when claudicating pain is induced. However, unilateral patients seem to experience significant adaptations at the contralateral healthy leg. The claudicating PAD leg demonstrated reduced forward push compensated by the contralateral healthy leg pushing harder. Our data suggests these adaptations are the result of maintaining a stable gait. Future studies will further explore these phenomena by increasing our sample sizes and examining differences in terms of kinematics and joint moments.

## REFERENCES

- McCully, K. et al. (1999). *J. Gerontol: Biol Sci*, **54A**, B291-B294.  
 Schmid, M. et al. (2005). *Gait Posture*, **21**, 255-262.  
 Scott, M. et al. (2005). *Proceedings of ISB'05*. Cleveland, OH.  
 Viton, J. et al. (2000). *Arch Phys Med Rehabil*, **81**, 194-200.

**Table 1:** T-test results for selected GRF parameters; Direction of differences are indicated in parenthesis.

GRF parameters	PAD healthy leg vs. Control	PAD leg vs. Control
Fz local minimum at midstance (Fz <sub>min</sub> )	p=0.002 (PAD > Control)	p=0.052 (PAD > Control)
Fz difference between first maximum and Fz <sub>min</sub> (DFz1-F <sub>min</sub> )	p=0.013 (PAD < Control)	p=0.009 (PAD < Control)
Fz difference between second maximum and Fz <sub>min</sub> (DFz2-Fz <sub>min</sub> )	p=0.003 (PAD < Control)	p=0.105 (PAD < Control)
Fz time to second maximum (TF2)	p=0.041 (PAD < Control)	p=0.028 (PAD < Control)
Fy maximum braking (FyB)	p=0.101 (PAD < Control)	p=0.037 (PAD < Control)
Fy maximum propulsion (FyP)	p=0.002 (PAD < Control)	p=0.034 (PAD < Control)
Fy difference between FyB and FyP (FyD)	p=0.005 (PAD < Control)	p=0.016 (PAD < Control)
Fy propulsion impulse IP	p=0.006 (PAD < Control)	p=0.093 (PAD < Control)

# ORBITAL STABILITY OF PASSIVE DYNAMIC WALKING ON A BUMPY SURFACE

Jimmy Li-Shin Su<sup>1,2</sup> and Jonathan B. Dingwell<sup>1</sup>

<sup>1</sup> Nonlinear Biodynamics Lab, Dept. of Kinesiology, University of Texas, Austin, TX, USA

<sup>2</sup> Dept. of Biomedical Engineering, University of Texas, Austin, TX, USA

E-mail: [jdingwell@mail.utexas.edu](mailto:jdingwell@mail.utexas.edu)

Web: <http://www.edb.utexas.edu/faculty/dingwell/>

## INTRODUCTION

Passive dynamic walkers (PDWs) can walk down shallow slopes with no motors or feedback controllers, using gravity as their only source of power input into the system. These systems have been used to examine the stability of human locomotion. The orbital stability of these systems under “ideal” conditions has been well established (Goswami 1997). However, like humans, these PDWs can fall over if subjected to sufficiently large perturbations. Little has been done to quantify the stability properties of PDWs under non-ideal conditions.

For humans, walking on bumpy terrain causes increased variability (Menz 2003, 2004). This infers that increased variability may indicate increased instability. In mechanics, stability is quantified by how a *system* responds to perturbations. In this sense, stability is an inherent property of the system and not based on perturbations applied. For limit cycle systems, *orbital stability* is defined from Floquet theory describing how a system responds to small perturbations from one cycle to the next (Garcia 1998). We hypothesized that at given perturbation levels, the orbital stability of the system would be uncorrelated to locomotor variability.

## METHODS

We modified the “simplest” 2D model of passive dynamic walking (Garcia 1998) to simulate walking down a shallow, bumpy slope. The heelstrike transition was modified to be  $\phi(t) - 2\theta(t) = \delta = \varepsilon \cdot U[-0.5, +0.5]$ , where

$\phi$  and  $\theta$  were defined as in Fig. 1. Uniform white noise,  $U$ , was applied to the system with amplitude,  $\varepsilon$  (in rad). Ten trials of 300 strides were simulated for each of 6 perturbation amplitudes ( $0 \leq \varepsilon \leq 0.1$ ). All trials simulated walking down a slope of angle  $\gamma = 0.009$  rad, which corresponded to a stable period-1 limit cycle.

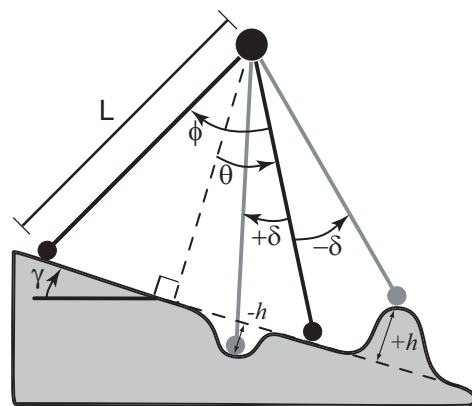


**Figure 1** - Random perturbations applied to the leg angle at heelstrike.

Since Floquet theory assumes the system is purely periodic, the data for each stride were normalized to 101 samples (0% to 100%). Orbital stability was quantified by calculating the Floquet Multipliers (FM) based on standard techniques at each % of the gait cycle (Hurmuzlu 1994). For an orbitally stable system, these complex-valued FM must lie inside the unit circle. We extracted the maximum FM occurring at any point in the gait cycle, because the system can only be as stable as when it is most unstable. We then performed a linear regression between the Max FM and the perturbation amplitude,  $\varepsilon$ . Variability was computed as the average standard deviation across 10 trials at the same perturbation,  $\varepsilon$ .

## RESULTS AND DISCUSSION

The PDW remained orbitally stable (Max FM < 1) across all perturbation magnitudes. The Max FM remained approx. constant as  $\varepsilon$  were increased ( $r^2 = 0.0\%$ ;  $p = 0.95$ ) (Fig. 2). Thus, the system's stability remained unchanged. The lack of correlation between Max FM and  $\varepsilon$  indicated that the orbital stability of the PDW was largely independent of the amplitude of applied perturbations. By contrast, mean kinematic variability increased exponentially with  $\varepsilon$  ( $r^2 = 98.3\%$ ;  $p \leq 0.001$ ) (Fig. 3).

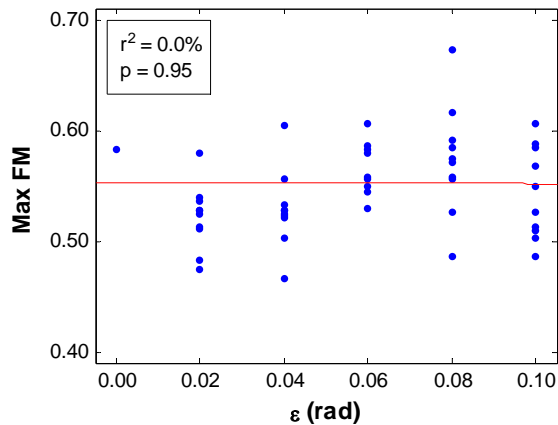


**Figure 2** - Linear regression between  $\varepsilon$  and Max FM occurring at any point in gait cycle.

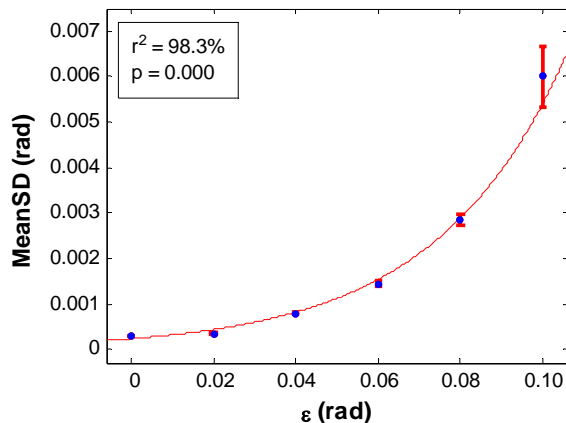


**Figure 3** - Increased perturbation amplitude causes increased variability for  $\theta$  (all state variables also showed a similar trend).

The variability data were similar to those results from recent studies which report that elderly and diabetic subjects walking over

bumpy surfaces showed increased variability (Menz 2003, 2004), yet did not fall over. In the same way, all PDW simulations were able to continue walking and therefore remained orbitally stable at all times.

## CONCLUSIONS

Our results supported the hypothesis that orbital stability is not related to the perturbation magnitude applied to the system, and also not related to the variability magnitude exhibited by the system. By examining how orbital stability varies as the surface bumpiness increases, we can better understand walking stability. Our results imply that walking stability can be studied without using a wide range of perturbations.

Our findings suggest that falls are not directly caused by increased variability. The results are confirmed by previous experimental studies (Dingwell 2001) which conclude that increases in kinematic variability do not directly correspond to a loss of local dynamic stability.

## REFERENCES

- Dingwell, J.B. et. al. (2001) *J. Biomech. Eng.* **123**, 27-32.
- Garcia, M. et. al. (1998) *J. Biomech. Eng.* **120**, 281-288.
- Goswami, A. et. al. (1997) *Auton. Robots* **4**, 273-86.
- Hurmuzlu, Y., Basdogan, C. (1994) *J. Biomech. Eng.* **116**, 30-6.
- Menz, H.B. et. al. (2004) *Arch. Phys. Med. Rehabil.* **85**, 245-52.
- Menz, H.B. et. al. (2003) *Age Ageing* **32**, 137-42.

## ACKNOWLEDGEMENTS

Supported by Research Grant #RG-02-0354 from the Whitaker Foundation

# ACCELERATION OF A SIMULATED HUMAN HEAD DURING IMPACTS WITH A PICKUP REAR WINDOW

Sean D. Shimada, PhD, Michael Turkovich, BS and Ken W. Heichman  
Biomechanical Consultants of California, Davis, CA, USA  
E-mail: drs@davis.com

## INTRODUCTION

Traumatic brain injury can occur when there is either direct or indirect contact to the head. Even though a skull fracture is absent, the brain may still sustain an injury. In situations like these, the brain injury is due to an acceleration of the head and its resulting inertial loading (Schmitt, 2004). The resulting concussion is often an indication of the brain injury tolerance being reached or exceeded (Ono et al. 1980). There have been several standards that have been accepted as threshold levels for brain injury. The most common is the Wayne State Tolerance Curve (WSTC), illustrated in figure 1.

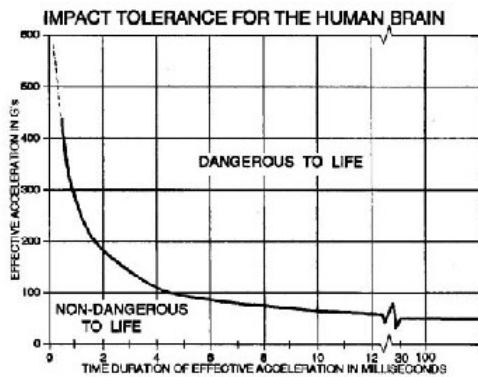


**Figure 1.** Wayne State Tolerance Curve

Accelerations above the curve can cause irreversible brain damage. Below the curve may cause transitory injury (Schmitt, 2004). The curve was later adjusted and a value of 80 g was determined to be the threshold for serious brain injury (Patrick et al, 1965). In another study, human head concussion parameters were extrapolated from research on monkeys. The study revealed that severe concussions occurred at 100 g with a

duration of 10 ms (Ono et al. 1980). When the impact time was shortened to the 2-4 ms range, severe concussions were recorded between 150 g and 300 g (Ono et al. 1980). Research has pointed to an injury threshold of approximately 80-100 g for brain injury (Gurdjian et al. 1966, Patrick et al, 1965). The purpose of this study was to determine whether a simulated human head experiences sufficient acceleration to cause a brain injury when the head fractures a rear window of a 1988 Chevrolet S-10 pickup.

## METHODS

A synthetic skull covered with bovine hide, which simulated a 50<sup>th</sup> percentile female, was utilized for the study. The skull was impacted on the posterior aspect, and dropped from specified heights to simulate various changes in velocities ( $\Delta v$ ) experienced during low-speed rear-end accidents. A tri-axial accelerometer (Crossbow Technology Inc., San Jose, CA) was securely fastened to the skull at the approximate center of mass, and recorded the accelerations as it passed through the window. The window was mounted as specified by the manufacture in the rear window frame of a 1988 Chevrolet S-10 pickup.

Eleven 3-segment windows, with the middle segment being a sliding window, were utilized for this study. The trials were performed on the driver segment of the window. 500 Hz data were obtained from the tri-axial accelerometer data collection system. The data were then analyzed using Matlab software (The Math Works, Inc.,

Natick, MA) to obtain skull resultant acceleration and change in velocity ( $\Delta v$ ) values.

## RESULTS/DISCUSSION

The resulting impact velocities with the windows were between 4.9 m/s (10.9 mph) and 7.3 m/s (16.4 mph). Peak skull resultant accelerations were found to be between 1.8 g and 7.5 g as it contacted the window. The resultant change in velocity ( $\Delta v$ ) of the skulls as it passed through the window ranged from 0.43 m/s (0.97 mph) to 2.14 m/s (4.79 mph). Peak resultant acceleration, impact duration ( $\Delta t$ ), and changes in velocities are listed in table 1.

**Table 1.** Skull resultant accelerations, impact duration, and changes in velocity as a result of fracturing the window.

Trial #	Impact Time ( $\Delta t$ ) (sec)	Peak Resultant Acceleration (g)	$\Delta v$ (m/s)
1	0.048	5.9	1.38
2	0.068	4.4	1.45
3	0.060	4.8	1.41
4	0.052	2.7	0.68
5	0.034	4.9	0.82
6	0.052	2.1	0.54
7	0.050	1.8	0.43
8	0.056	3.8	1.05
9	0.048	2.4	0.56
10	0.036	4.7	0.83
11	0.058	7.5	2.14
Avg.	0.051	4.1	1.03

The resultant accelerations obtained from this study were well below current proposed threshold values for mild traumatic brain injury. The peak resultant accelerations in this experiment did not exceed 7.5 g. The current accepted threshold is approximately 80-100g, interpreted from the WSTC. This value is significantly greater than the peak 7.5 g value obtained during this study. The

accelerations associated with this specific study were found to be insufficient to cause a mild traumatic brain injury when compared to tolerance levels.

## CONCLUSIONS

The results of this study revealed that head impacts greater than 5 m/s will fracture a rear window of a 1988 Chevrolet S-10 pickup. Despite this fact, it was found that the head would experience very low linear accelerations and changes in velocity during the time when the window fractures. Therefore, this study revealed that it is unlikely that a human head breaking a window experiences sufficient acceleration to cause a mild traumatic brain injury.

## REFERENCES

- Gurdjian E., Robert V., and Thomas L. (1966). Tolerance curves of acceleration and intercranial pressure and protective index in experimental head injury. *J. Trauma*, **6** (5), pp. 600-604.
- Lissner, H., Lebow, M., and Evans, F. (1960). Experimental studies on the relation between acceleration and intracranial pressure changes in man. *Surg Gynecol Obstet*, **111**, pp.320-338.
- Ono et al. (1980). Human head tolerance to sagittal impact reliable estimation deduced from experimental head injury using subhuman primates and human cadaver skulls. *Proc. 24<sup>th</sup> Stapp Car Crash Conf.*, SAE 801303.
- Patrick, L.M., Lissner, H.R., and Gurdjian, E.S. (1965). Survival by Design-Head Protection. *Proc. 7<sup>th</sup> Stapp Car Crash Conf.* SAE J885
- Schmitt, K.-U., Niederer, P., and Walz, F. (2004). *Trauma Biomechanics*. Springer, New York, pp. 39-56.

# SUPRASCAPULAR NERVE BLOCK RESULTS IN A COMPENSATORY INCREASE IN DELTOID MUSCLE ACTIVITY

Sean P M<sup>c</sup>Cully<sup>1</sup>, David N Suprak<sup>1</sup>, Peter Kosek<sup>2</sup>, Andrew R Karduna<sup>1</sup>

<sup>1</sup>Department of Human Physiology, University of Oregon, Eugene, Oregon, USA,

<sup>2</sup>Pain Consultants of Oregon, Eugene, Oregon, USA

email: karduna@uoregon.edu

## INTRODUCTION

During normal shoulder function, there exists a delicate balance between the forces exerted by the deltoid and rotator cuff muscles. It has been established in cadaver (Sharkey et al., 1994; McMahon et al., 1995) and computer (Magermans et al., 2004) models that reducing the contribution of the rotator cuff muscles places a higher demand on the deltoid. Since the line of action of the deltoid is directed more superiorly, this increase in deltoid force results in a more superiorly directed joint reaction force at the glenoid.

The aim of this study was to examine the *in-vivo* consequences of rotator cuff dysfunction by studying the effects of a suprascapular nerve block on shoulder muscle activity. We hypothesized that this block would result in a compensatory increase in deltoid activity, similar to what has been observed in cadaver models.

## METHODS

Ten subjects with no reported shoulder pathology successfully completed a nerve block protocol (age range 23-33). EMG, kinematic and isometric strength data were collected prior to and immediately after a suprascapular nerve block.

A Myopac Jr. (RUN Technologies, Mission Viejo, CA) unit with dual lead channels was used for collection and processing of EMG

recordings from the upper and lower trapezius; anterior, middle, and posterior portions of the deltoid; serratus anterior; and infraspinatus. EMG data were normalized to a maximum voluntary contraction (MVC) for each muscle. The 3Space Fastrak (Polhemus, Colchester, VT) was used to collect humerothoracic motion. A thoracic receiver was placed over T3 with double sided tape and a humeral receiver was mounted on a molded cuff strapped to the distal humerus. Kinematic and EMG data were collected simultaneously during scapular plane elevation. Isometric strength during shoulder external rotation was assessed with the arm at the side with a 50 lb (22.7 kg) capacity load cell (Lebow, Troy, MI).

The suprascapular nerve block was performed by an anesthesiologist (PK) who administered lidocaine 100 mg after motor stimulation confirmed needle placement by the nerve.

## RESULTS AND DISCUSSION

The nerve block resulted in a mean external rotation force level that was 25% of the original baseline measurement. All three heads of the deltoid demonstrated an increase in activation following the nerve block ( $p < 0.002$ ). Follow-up t-tests indicated that there was an increase in muscle activation at all angles, except for 120 degrees of elevation for the anterior deltoid and 20 degrees of elevation for the

posterior deltoid (figure 1). There was no significant effect of the nerve block on activity of the upper and lower trapezius, serratus anterior and infraspinatus.

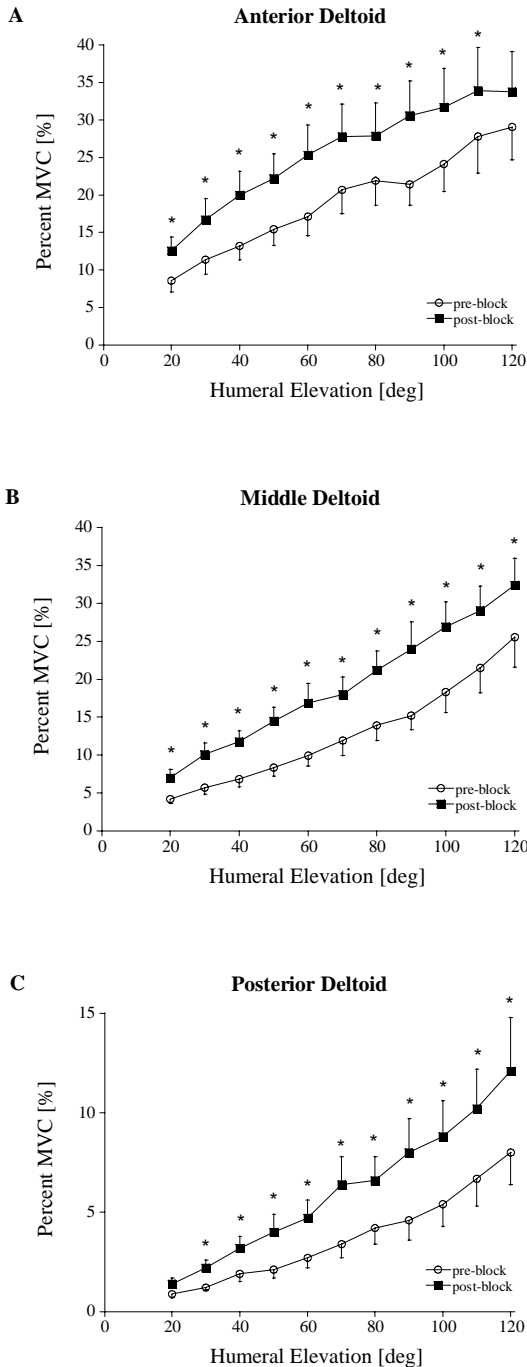


**Figure 1:** Deltoid EMG activity as a function of humerothoracic elevation. \* p < 0.05

A comparison was made with two cadaver models that simulated paralysis of cuff muscles (Sharkey et al., 1994; McMahon et al., 1995) and a computation based on moment arm data (Liu et al., 1997). Despite the disparity between the models (cadaver, computational and in-vivo), they all show the same general trend of a large percent increase from baseline at low elevation angles that decreased as the arm was elevated (figure 2).

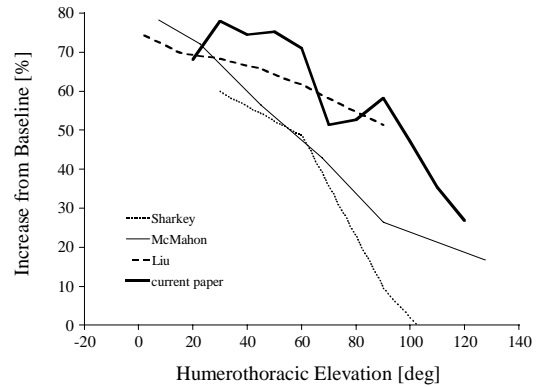


**Figure 2:** Percent increase in middle deltoid activity as a function of humerothoracic elevation

## SUMMARY/CONCLUSIONS

Our results provide *in-vivo* evidence that the central nervous system compensates for the loss of rotator cuff function with an increase in deltoid activity. Future studies examining the EMG activity of the deltoid and rotator cuff muscles in patients with rotator cuff pathology is warranted.

## REFERENCES

- Liu, J.et al. (1997). *Clin Biomech* **12**, 32-38.  
 Magermans, D.J.et al. (2004). *Clin Biomech* **19**, 116-22.  
 McMahon, P.J.et al. (1995). *J Shoulder Elbow Surg* **4**, 199-208.  
 Sharkey, N.A.et al. (1994). *J Orthop Res* **12**, 699-708.

# THE EFFECTS OF AGE AND PARTIAL BODY WEIGHT SUPPORT ON KINEMATIC VARIABILITY DURING TREADMILL WALKING

Anastasia Kyvelidou<sup>1</sup>, Julie L. Ehlers<sup>1</sup>, Max J. Kurz<sup>1,2</sup>, and Nicholas Stergiou<sup>1</sup>

<sup>1</sup>University of Nebraska at Omaha, Omaha, NE, USA

<sup>2</sup>University of Houston, Houston, TX, USA

E-mail: akyvelidou@mail.unomaha.edu Web: www.unocoe.unomaha.edu/hper/bio/home.htm

## INTRODUCTION

Recent studies have shown that variability in gait kinematics is increased in the elderly (Maki, 1997; Buzzi *et al.*, 2003; Kurz & Stergiou, 2003; Owings & Grabiner, 2004). These findings have been demonstrated with both linear and nonlinear evaluations of the variability present in gait patterns of the elderly. It has been suggested that these changes in variability are due to increased randomness in the elderly gait patterns (Buzzi *et al.*, 2003). Physiological aging may degrade the natural deterministic patterns present in locomotion resulting in more “noisy” movements. This may be the reason for the increased chance of falling in the aging (Buzzi *et al.*, 2003). Thus, it makes sense to retrain the aging neuromuscular system with hopes of diminishing noise and reintroducing normal gait patterns. It is possible that such a task can be accomplished with recent technological advances, such as the usage of a partial body weight support system (BWS). It has already been shown that such systems are successful in retraining gait in stroke patients (Hesse and Werner, 2003). Similarly, BWS training could possibly improve gait function and reduce the incidence of falling in the elderly. However, the effect of BWS on elderly gait patterns and specifically on kinematic variability is currently unknown. Therefore, the purpose of this study was to evaluate sagittal plane angular kinematic variability of the lower extremity joints in young and elderly healthy

females at different levels of BWS during treadmill walking.

## METHODS

Twenty young and elderly females from the Omaha community were recruited for this study. Ten subjects were between the ages of 20-35 years, while the other ten were 70 years or older. Each subject walked at their self-selected pace on the treadmill under four different conditions, 0%, 10%, 20% and 30% BWS. Lower extremity kinematics (60Hz) were acquired for two minutes of continuous walking under the respective conditions. The speed was kept constant across conditions and the level of BWS for the first condition was always set at 0%. Thereafter, the presentation of the BWS condition were randomized. The time series from the hip, knee and ankle sagittal (flexion/extension) joint angles were calculated for the two minutes of continuous walking. The minimum and maximum joint angular values were identified, as well as the maximum range of motion, for each gait cycle. For these parameters, the linear measures of standard deviations (SD) and coefficients of variation (COV) were estimated. In addition, the largest Lyapunov exponent (LyE), a nonlinear measure, was also estimated from the continuous gait data of the gait cycles using the *Chaos Data Analyzer* (Sprott and Rowlands, 1995). LyE is a measure of the stability of a dynamical system and its dependence on initial conditions. All calculations were performed using 7 embedded dimensions. The

embedded dimension, a description of the number of dimensions needed to unfold the structure of a given dynamical system, was calculated from a Global False Nearest Neighbor (GFNN) analysis (Abarbanel, 1996). Mean group values were calculated for all linear and nonlinear parameters and analyzed statistically with a two way analysis of variance with repeated measures.

## RESULTS & DISCUSSION

Linear analysis revealed no significant interactions between the two factors, age and level of BWS. However, both age and level of BWS did have an effect on the kinematic variability, with the elderly subjects demonstrating higher values. Specifically, age significantly increased variability of the range of motion and the maximum angle of both the knee and the hip. These findings are in accordance with Buzzi *et al.* (2003). Increased variability at the hip and knee joint in the elderly has been attributed to less certainty in the aged nervous system to select hip and knee range of motion during gait (Kurz and Stergiou, 2003). BWS significantly increased variability of the hip range of motion, the maximum hip angle, the minimum knee angle and the ankle range of motion, with the BWS at 30% having the largest values. This was attributed to the balance component of gait being stressed at higher levels of BWS. Nonlinear analysis presented significant differences only among BWS levels. No interaction or aging effects were found. Specifically, all joints had significantly larger values for the LyE, with the 30% BWS level having the largest values. This result is in agreement with the linear analysis. In addition, LyE values tended to be larger in the elderly subjects than the young, although not significantly. This result is contradictory to previous findings (Buzzi *et al.*, 2003; Kurz &

Stergiou, 2003) where aging increased variability as measured with nonlinear tools. In the present study it is possible that this effect was diminished due to the stabilization provided by the BWS. It should also be noted that the results of the present study are derived from a relatively small sample size. Measures of variability may be more conclusive using a larger number of subjects.

## SUMMARY/CONCLUSIONS

Increased variability of gait parameters has been found to be a predictor of falls in the elderly (Maki, 1997). BWS has been used successfully as a gait retraining tool in pathological populations. In this preliminary work, we hypothesized that BWS may also improve gait in the elderly by decreasing variability. We found that different levels of BWS and aging affected kinematic variability. The elderly had the higher values as expected. However, increased levels of BWS also increased kinematic variability. If the intent of BWS training is to decrease variability in gait patterns, certainly this does not seem to be feasible. However, this conclusion needs to be tested with an actual training trial. In addition, it is possible that BWS training can have a positive transfer effect by bringing overground kinematic variability to healthy normative levels.

## REFERENCES

- Buzzi, U. *et al.* (2003). *Clin. Biomech*, **18**, 435-443.
- Hesse, S., & Werner, C. (2003). *Adv Neurol*, **92**, 423-428.
- Kurz, M. J., & Stergiou, N. (2003). *Neurosci Lett*, **348**, 155-158.
- Maki, B. E. (1997). *J Am Geriatr Soc*, **45**, 313-320.
- Owings T. M. & Grabiner M .D. (2004). *J. Biomech*, **37** (6), 935-938.

# CASTING FOR DISTANCE: EFFECTS OF LINE LENGTH ON KINEMATICS OF FLY-CASTING

Joshua R. Allen<sup>1</sup> and Michael E. Hahn<sup>1,2</sup>

<sup>1</sup> Montana State University, Bozeman, MT

<sup>2</sup> Fly Casting Institute, Missoula, MT

E-mail: mhahn@montana.edu

## INTRODUCTION

Outdoor enthusiasts have long been attracted to the leisure of fly fishing and the skill that drives the motion of casting. A recent study revealed shoulder and elbow pathologies associated with repetitive, high velocity, overhand movements common to fly-casting (McCue et al., 2004). However, little research exists that focuses on the motions and coordination common to fly-casting. The purpose of this study was to determine the kinematic and joint coordination changes necessary to cast lines of different length. Documenting the movement patterns needed to cast varying lengths of line should allow for greater understanding of the underlying mechanisms of upper extremity pathologies. It was hypothesized that kinematic casting parameters would increase in order to cast lines of different length, and that time between peak joint velocities would decrease as length of line increased.

## METHODS

Eighteen male subjects participated in the study (Table 1). Experience ranged from intermediate to expert, with a number of the subjects being professional fly-fishing guides. Prior to data collection, subjects signed an informed consent, and completed

**Table 1:** Subject characteristics; Mean (SD).

Age	32.7 (8.4)
Height (cm)	180.1 (6.4)
Mass (kg)	80.2 (7.9)
Days fishing/year (past 5 years)	98.9 (70.2)
Casting experience (years)	19.4 (10.4)

a brief medical history. Twenty three reflective markers were placed on bony landmarks of the upper body. A 6-camera Vicon® 460 system (ViconPeak, Lake Forest, CA) sampled marker position data at 200 Hz (Woltring filter, MSE = 30).

Shoulder motion was calculated with respect to the trunk. Euler angle rotation order was sagittal, frontal, transverse. The elbow was modeled as a uni-axial pin joint and the wrist as a bi-axial pin joint. Total ROM and peak angular velocity were examined for the following range of motion (ROM): shoulder flex/extension (F/E), ab/adduction (AB/AD), int/external rotation (IR/ER); elbow F/E; wrist F/E, radial/ulnar deviation (RD/UD).

Subjects performed five casts at each of four distance conditions (20, 40, 60, and 80 ft; C1- C4, respectively) for a total of twenty casts. Instructions were given to perform a series of “false casts” (usually 1-2), followed by the “shooting” cast. Distance of line cast was the independent variable. Dependent variables were the kinematic parameters for each joint. A single factor MANOVA was used to assess effect of line distance on dependent variables.

## RESULTS AND DISCUSSION

The fly casting motion was divided into three primary phases. The first phase (P1), the “back cast,” is a movement from anterior to posterior; primarily including shoulder F, AB, and ER combined with elbow F, and wrist RD. At the end of the back cast, there

is a pausing phase (P2) in which the caster waits for the line to load the rod. In phase 3 (P3), the “forward cast,” primary motions included shoulder IR, AD, and E, combined with elbow E and wrist UD (Figure 1).

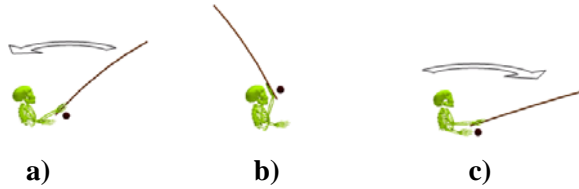


**Figure 1:** Phases of casting; a) Back cast, b) Pause, and c) Forward cast.

Overall, total ROM increased with increased length of line cast, supporting the first part of the hypothesis. However, wrist RD/UD total ROM changed little across all distances. Wrist F/E total ROM decreased with increased line length (Figure 2). Similar to other throwing motions (Cook and Strike, 2000), timing of peak angular velocity exhibited a proximal-to-distal trend

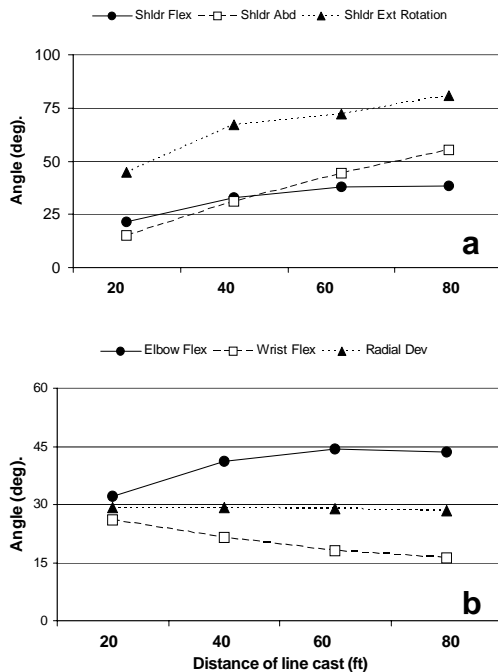


**Figure 2:** Total ROM for the shoulder (a) and the elbow/wrist (b) during fly casting. Significant effect of line distance on all shoulder joint actions ( $p < 0.005$ ).

for all four casting distance conditions. During P3, peak shoulder IR velocity occurred first, followed by elbow E velocity, and wrist UD velocity (Table 2).

Data from this study did not support the second part of the hypothesis. The only significant difference was an increase in the time between peak shoulder and elbow angular velocities ( $p = 0.037$ ) as line length increased. This may be due to the tendency of the caster to lean the trunk forward, immediately preceding the forward cast, forcing the shoulder to generate velocity earlier in P3 (with respect to the elbow, see Table 2).

**Table 2:** Peak angular velocity timing (% of P3); Mean (SD).

Cond	Sh. IR	Elb. Ext	Wr. UD
C1	38 (10)	47 (10)	76 (24)
C2	46 (9)	57 (9)	80 (20)
C3	48 (11)	67 (9)	82 (17)
C4	49 (13)	69 (8)	81 (15)

## CONCLUSIONS

Findings from this study indicate that significant changes in total ROM were needed to accommodate the demands of casting greater lengths of line. Also, joint velocity coordination patterns of fly-casting appear to follow a proximal-to-distal pattern, similar to other throwing motions (Cook and Strike, 2000). Finally, time between peak joint velocities did not decrease with increased line length. Parallel analyses are currently focusing on joint dynamics, with emphasis on motion efficiency and injury prevention.

## REFERENCES

- Cook and Strike. *J Sports Sci.* **18**, 965-973, 2000.  
 McCue, et al. *Wilderness Environ. Med* **15**, 267-273, 2004.

# EFFECTS OF SELECTED SAGITTAL PLANE LANDING BIOMECHANICS ON ACL LOADING IN A STOP-JUMP TASK

Cheng-Feng Lin<sup>1</sup>, Bing Yu<sup>1</sup>, William E. Garrett<sup>2</sup>

<sup>1</sup>The University of North Carolina at Chapel Hill, Chapel Hill, NC, USA

<sup>2</sup>Duke Sports Medicine Center, Duke University, Durham, NC, USA

E-mail: [feng1368@email.unc.edu](mailto:feng1368@email.unc.edu)

## INTRODUCTION

Altered lower extremity motion patterns in athletic tasks have been proposed as factors of sustaining non-contact ACL injuries. How peak ground reaction force, knee flexion angle, and landing style affect ACL loading was still unclear. Understanding the effects of lower extremity motion patterns in athletic tasks on ACL loading is important for understanding non-contact ACL injury mechanisms and risk factors. The purpose of this study was to determine the effects of peak posterior ground reaction force, knee flexion angle, and landing style on ACL loading in the stop-jump task using a biomechanical modeling approach.

## METHODS

A total of 10 male and 10 female recreational athletes without known history of knee disorders were recruited for knee radiographic data collection. Side-view x-ray films of the knee were obtained for each subject from 0 to 90° knee flexion bearing 50% of the total body weight. Patella tendon-tibia shaft angles (PTTS), hamstring tendon-tibia shaft angle (HTTS), and actual knee flexion angles were measured from the x-ray films. Multiple regression analyses with dummy variables were performed to express the PTTS and HTTS as functions of knee flexion angle and gender. Quadriceps and hamstring muscle moment arms and ACL elevation angles from the literature were also expressed as functions of knee flexion angle using regression analyses. A

sagittal plane biomechanical model of the knee was developed using these knee geometric data for inverse dynamic calculation of ACL loading.

A total of 40 male and 40 female recreational athletes without known history of knee disorders were recruited for in-vivo motion data collection. Each subject was asked to perform five trials of a stop-jump task with maximum effort. Three-dimensional coordinates of lower extremity landmarks and ground reaction forces were collected for each trial. Lower extremity segment and joint angles, and knee joint resultants were reduced. The location of center of pressure (COP) relative the ankle joint center was used as a measure of landing style. The mean and standard deviation of each variable were calculated and used to determine the ranges of inputs for a computer simulation of ACL loading. The peak posterior ground reaction force, knee flexion angle at peak posterior ground reaction force, and the location of COP relative to the ankle joint were altered systematically in the computer simulation of ACL loading.

## RESULTS AND DISCUSSION

Peak posterior ground reaction force significantly affects ACL loading in the stop-jump task (Figure 1). The greater the posterior ground reaction force is, the greater the ACL loading is. Knee flexion angle also significantly affects ACL loading (Figure 2). The smaller the knee flexion

angle is, the greater the ACL loading is. Landing style significantly affects ACL loading as well (Figure 3). Landing on the heel significantly increases ACL loading in comparison to landing on the toe. The gender differences in the PTTS is the explanation of the gender differences in the effects of posterior ground reaction force, knee flexion angle, and landing style on ACL loading.

The results of this study are consistent with those of in-vitro studies in the literature, and demonstrated that sagittal plane biomechanics significantly affect ACL loading in athletic task. The results of this study suggest that large posterior ground reaction force, small knee flexion angle, and landing on the heel may be important ACL injury mechanisms and risk factors of sustaining non-contact ACL injuries. Gender differences in these relationships may be explanations for gender difference in ACL injuries.

### SUMMARY/CONCLUSIONS

Decreasing peak posterior reaction force, increasing knee flexion angle, and landing on the toe can significantly reduced ACL loading and may assist in prevention of non-contact ACL injuries.

### REFERENCES

- Boden, B.P., et al. (2000). *Orthop*, **23**: 573-578.  
 Cerulli, G., et al. (2003). *Knee Surg Sports Traumatol Arthrosc*, **11**: 307-311.  
 Li, G.A., et al. (2005). *J Orthop Res*, **23**: 340-344.  
 Nunley, R.M. et al. (2003). *Res Sports Med*, **11**: 173-185.  
 Yu, B., et al. (2006). *Am J Sports Med*, **34**: 312-315.

Yu, B., et al. (2006). *Clin Biomech*, **21**: 297-305.

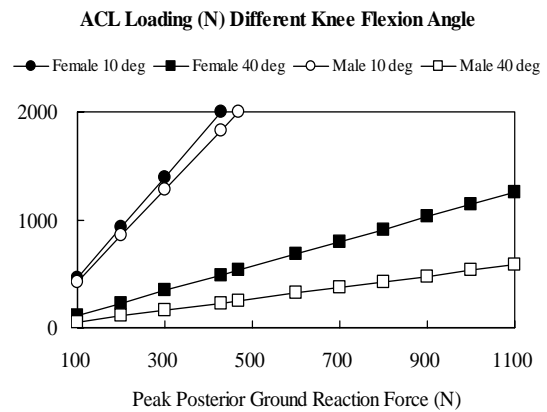


Figure 1. Effect of posterior ground reaction force on the ACL loading.

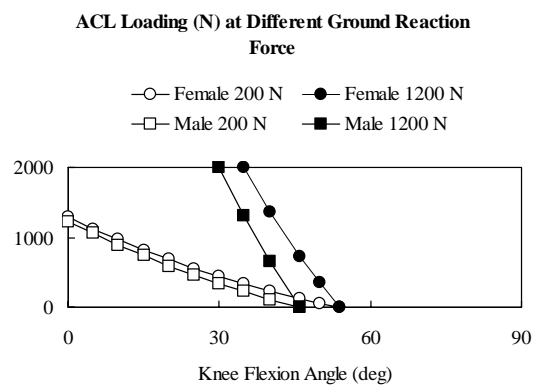


Figure 2. Effect of knee flexion angle on the ACL loading.

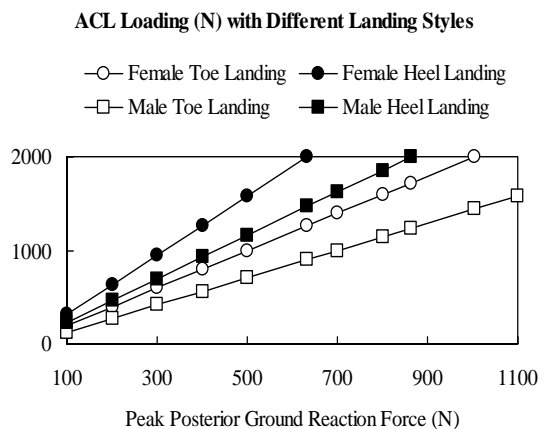


Figure 3. Effect of landing style on the ACL loading.

# EFFECTS OF A KNEE EXTENSION CONSTRAINT BRACE ON LANDING BIOMECHANICS

Bing Yu<sup>1</sup>, Cheng-Feng Lin<sup>1</sup>, William E. Garrett<sup>2</sup>

<sup>1</sup> University of North Carolina at Chapel Hill, Chapel Hill, NC, USA

<sup>2</sup> Duke University, Durham, NC, USA

E-mail: byu@med.unc.edu

## INTRODUCTION

Acute anterior cruciate ligament (ACL) rupture is one of the most commonly seen injuries in sports. The majority of ACL injuries occurred with non-contact mechanisms. Literature indicates that small knee flexion angle in landing tasks is likely to be a risk factor for non-contact ACL injuries. A knee extension constraint brace was recently developed as a training tool for prevention of non-contact ACL injuries. The purpose of this study was to determine the immediate effects of the new knee brace on lower extremity motion patterns in a stop-jump task in which non-contact ACL injuries frequently occur.

## METHODS

A total of 40 male and 40 female college aged recreational athletes without known lower extremity disorders were recruited as subjects. Each subject was asked to perform five trials of the stop-jump task under each of the three brace conditions: (1) no brace, (2) with a non-constraint brace, and (3) with the constraint brace. The order of brace conditions was randomized. The non-constraint knee brace had the same appearance as the constraint knee brace.

Three-dimensional (3-D) coordinates of 15 reflective markers on the pelvis and lower extremities, and ground reaction forces were collected using six cameras and two force plates. The 3-D coordinates of critical lower extremity landmarks were estimated from

the coordinates of reflective markers. Knee joint angles were determined as Euler angles. Approach and takeoff velocities were estimated from the horizontal velocity of the mid hip at initial foot contact with the ground and the vertical velocity of the mid hip at the takeoff. Ground reaction forces were normalized to subjects' body weight.

One-way ANOVAs with repeated measures were performed to compare knee flexion angles at initial foot contact with the ground and peak posterior ground reaction force, peak impact posterior and vertical ground reaction forces, and approach and takeoff velocities among three brace conditions. A 0.05 Type I error rate was used as indication of statistical significance.

## RESULTS AND DISCUSSION

Subjects significantly increased their knee flexion angle at landing of the stop jump task with the knee extension constraint brace ( $p = 0.00$ ) (Figure 1). Subjects also significantly increased their knee flexion angle at the peak posterior ground reaction force with the knee extension constraint brace ( $p = 0.00$ ) (Figure 2). The non-constraint brace did not show significant effect on the knee flexion angles at initial foot contact with the ground and at the peak posterior ground reaction force.

Subjects significantly decreased the impact peak posterior ground reaction force during the landing of the stop jump task with knee braces ( $p = 0.00$ ) (Figure 3). Knee braces

did not show significant effect on the peak vertical ground reaction force during the landing of the stop-jump task. Knee braces did not show significant effects on approach and takeoff velocities

The results of this study suggest that knee extension constraint brace can increase knee flexion angles and decrease impact peak posterior ground reaction force during landing of the stop-jump task. The effect of the knee extension constraint brace on knee flexion angle is a constraint effect while the effect on peak impact posterior ground reaction force is a brace effect.

Increasing knee flexion angle at the peak impact posterior ground reaction force and decreasing posterior ground reaction force during landing should assist in reducing peak ACL loading and thus the risk of non-contact ACL injuries. The knee extension constraint brace may be a useful training tool in future ACL injury prevention programs. Future studies are needed to investigate the training effects of the knee extension constraint brace.

## CONCLUSIONS

The constraint to knee extension significantly increased knee flexion angle while the brace significantly decreased peak impact posterior ground reaction force during the landing of the stop-jump task.

## REFERENCES

- Malinzak, R.A. et al. (2001). *Clin Biomech* **16**: 438-445.  
 Markolf, K.L. et al. (1995). *J Orthop Res*, **13**: 930-935.  
 Nunley, R.M. et al. (2003). *Res Sports Med*, **11**: 173-185.  
 Yu, B. et al. (2004). *Am J Sports Med*, **32**: 1136-1143, 2004.

## ACKNOWLEDGEMENT

This study was financially supported by a research grant from dj Orthopedics, Inc.

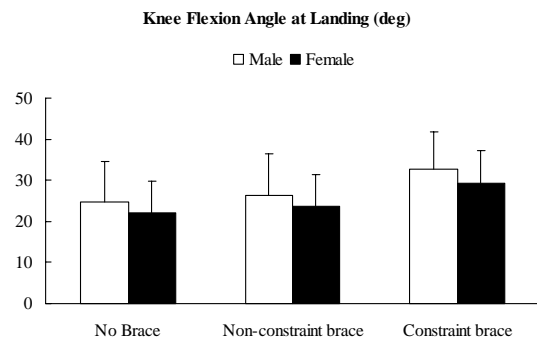


Figure 1. Knee flexion angles at initial foot contact with the ground.

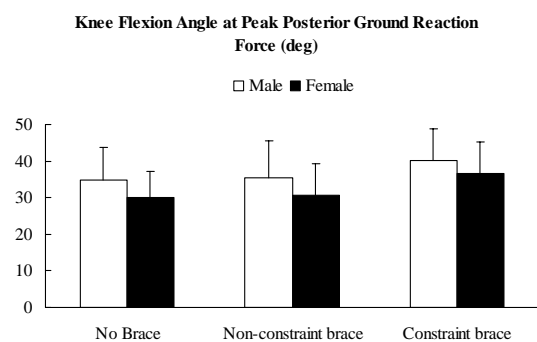


Figure 2. Knee flexion angles at peak impact posterior ground reaction force.

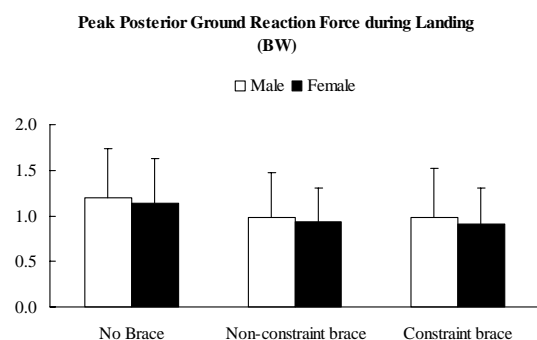


Figure 3. Peak impact posterior ground reaction force.

# THE KNEE JOINT PIVOTS ON THE LATERAL COMPARTMENT DURING AMBULATION

Seungbum Koo<sup>1</sup> and Thomas P. Andriacchi<sup>1,2</sup>

<sup>1</sup> Stanford University, Stanford, CA, USA

<sup>2</sup> VA RR&D Center, Palo Alto, CA, USA

E-mail: skoo@stanford.edu Web: biomotion.stanford.edu

## INTRODUCTION

Knee joint kinematics and its influence on the movement of tibiofemoral contact have been suggested as an important consideration in analysis of factors leading to the initiation of knee osteoarthritis [Andriacchi, 2004]. While the movement of tibiofemoral contact for non-ambulatory activities such as chair rising, deep knee bending and lunging, have been extensively studied [Komistek, 2003, Li, 2005, Banks 2004] using radiographic methods, there is limited information on tibiofemoral contact movement during walking in spite of the fact that walking is the most frequent activities of daily living. When considering reports that knee joint kinematics differs between activities [Dyrby, 2004], it is important to evaluate the tibiofemoral contact movement during walking. In this study, we investigated the movement of tibiofemoral contact in the medial compartment relative to the lateral compartment and tested the hypothesis that the movement is different than the patterns reported for non-ambulatory activities.

## METHODS

Twenty six healthy subjects (age  $39.3 \pm 13.6$  years, 17 males, BMI  $23.8 \pm 2.3$  kg/m<sup>2</sup>) without any previous knee injuries underwent gait test after IRB approval and informed consent were obtained. The six degree of freedom knee joint kinematics were measured during ambulation using the point cluster technique [Andriacchi, 1998] at self-selected normal walking speed for

bilateral limbs of the subjects (#knees=52). The motion of the femoral anatomical axis was described relative to the tibial anatomical axis. A generic three-dimensional geometric model of the femur was used to reconstruct the motion of the femur relative to the tibia. The tibial surface was assumed to be flat to calculate the tibiofemoral contact points. The lowest points of medial and lateral condyle of the geometric femur model were found throughout the stance phase of ambulation. The contact points were projected on to the flat tibia surface. A line connecting the medial and lateral contact points were drawn at each instance during stance phase of ambulation. Anterior-posterior ranges of movement (ROM) of the medial and lateral contact points were calculated for each knee [Figure 1].

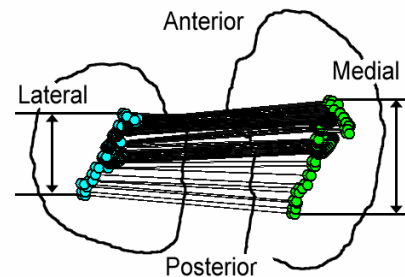


**Figure 1:** Anterior-posterior ROM of the contact points in medial and lateral compartments were measured.

Paired Student's t-test was used to test the difference of ROMs of contact points between the medial and lateral compartments at  $\alpha=0.05$ .

## RESULTS AND DISCUSSION

The tibiofemoral contact points in the medial compartment moved significantly more than those in the lateral compartment in the anterior-posterior direction according to paired Student's t-test ( $p < 0.01$ , 95% CI: 3.7~ 6.4 mm).

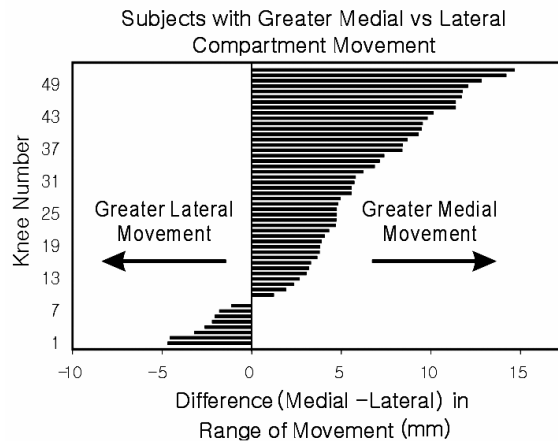


**Figure 2:** ROM of contact points was larger in medial than lateral compartments.

Forty three knees out of 52 knees (83%) had larger contact point movement in medial than lateral compartment [Figure 2]. The fact that the majority of subjects had greater movement in the medial rather than lateral compartments during walking supports the conclusion that knee joint kinematics is highly dependent on physical activities [Dyrby, 2004]. These results are consistent with the reports [Lafortune, 1992] of anterior-posterior (AP) translation and internal-external (IE) rotation at the knee during walking, where at heel strike the femur is posterior and internally rotated relative to tibia. The femur moves anterior and rotates externally during stance phase thus creating greater movement in the medial compartment and pivoting in the lateral compartment [Figure 3]. The fact that previous studies have reported that the knee joint pivots on the medial compartment for non-ambulatory activities such as chair rising, deep knee bending [Komistek, 2003], and lunging [Li, 2005]

motions for normal subjects or unrealistically slow walking speeds [Komistek, 2003], suggest the importance of describing knee kinematics in the context of a specific activity or the constraints of the test conditions.

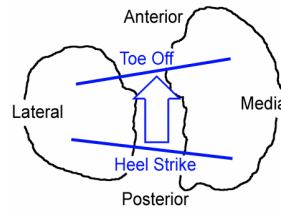


**Figure 3:** Lines connecting contact points at heel strike and toe off were drawn.

The finding of greater medial compartment movement of the knee during walking is an important consideration in evaluating knee pathology. In particular, the prevention and treatment of osteoarthritis would benefit from a better understanding of the knee kinematics during the walking. In addition, these results suggest that it is not possible to extrapolate knee kinematics from non-ambulatory activities to ambulatory kinematics.

## REFERENCES

- Andriacchi, T.P., Mündermann, A., Smith, R.L., Alexander, E.J., Dyrby, C.O., Koo, S. (2004). *Ann Biomed Eng.* 32:447-457.
- Komistek, R.D., Dennis, D.A., Mahfouz, M. (2003). *Clin Orthop Relat Res.* 410:69-81.
- Li, G., DeFrate, L.E., Park, S.E., Gill, T.J., Rubash, H.E. (2005). *Am J. Sports Med.* 33:102-107.
- Banks, S.A., Hodge, W.A. (2004). *J. Arthroplasty.* 19:809-816.
- Dyrby, C.O., Andriacchi, T.P. (2004). *J. Orthop Res.* 22:794-800.
- Andriacchi, T.P., Alexander, E.J., Toney, M.K., Dyrby, C., Sum, J. (1998). *J. Biomech Eng.* 120:743-749.
- Lafortune, M.A., Cavanagh, P.R., Sommer, H.J. 3rd, Kalenak, A. (1992). *J. Biomech.* 25:347-357.

## ACKNOWLEDGEMENTS

NIH grant # 1R01AR0497902.

# TEMPORAL EMG MEASURES EXPLAIN INTERINDIVIDUAL DIFFERENCES IN THE RUNNING ECONOMY OF WOMEN

Gary D. Heise, Laura Binks, Lauren Rapacki, and Piyachaet Dounglomchunt

University of Northern Colorado, School of Sport & Exercise Science, Greeley, CO, USA  
E-mail: gary.heise@unco.edu Web: www.unco.edu

## INTRODUCTION

Running economy (RE) is strongly associated with distance running performance (Conley & Krahenbuhl, 1980). Researchers from various disciplines have had limited success explaining the inter-individual variability in RE. Biomechanists have identified kinematic and kinetic descriptors of the running cycle which are related to RE (Saunders et al., 2004).

EMG analysis offers great potential in addressing this interindividual variability. For example, Heise et al. (1996) identified several temporal EMG measures which were related to RE. In addition, they observed a trend in which more economical runners displayed greater coactivation between biarticular muscles during stance. This proposed metabolic savings may come from increased elastic energy, which is a result of greater muscle coactivation. This is indirectly supported by findings from studies examining the associations between RE and flexibility and between RE and lower extremity stiffness (Butler et al., 2003; Saunders et al., 2004).

The present study was designed to re-examine the trend highlighted above and to address the paucity of research on the inter-individual variability of RE in women. Specifically, our purpose was to examine the relations between RE and temporal measures of lower extremity muscle activity during the stance phase of running. The muscle forces during stance have been identified as important contributors to the

interindividual variability in RE (Saunders et al., 2004).

## METHODS

Sixteen women, who were part of a larger study, ran for 30 min on a treadmill at a speed designed to elicit a rating of perceived exertion of 6 (out of 10) at the end of the run (Mean  $\pm$  SD: Age = 24.4  $\pm$  5.8 yrs; Body Mass = 59.7  $\pm$  5.0 kg). After appropriate skin preparation, electrodes were placed over the lateral head of gastrocnemius (G), vastus lateralis (VL), rectus femoris (RF), and the long head of biceps femoris (BF).

During the final 4 min of the run, expired gasses were collected and  $\dot{V}O_2$  was determined using standard methods of indirect calorimetry.  $\dot{V}O_2$  was normalized to running speed and expressed in  $ml \cdot kg^{-1} \cdot km^{-1}$ . Four, 60 Hz digital camcorders recorded the motion of running while EMG data (1020 Hz) were collected (Myopac Jr). Video and EMG data were synchronized with an audio signal (Vicon-Peak Motus).

EMG data were full-wave rectified and low-pass filtered ( $f_c=15$  Hz). Muscle onset and cessation from late swing through stance were identified manually by a single experimenter using the method of Heise et al. (1996). Muscle on-time durations during stance, coactivation durations during stance, and muscle onset with respect to foot contact were calculated. Nonparametric correlations were used to relate EMG measures to RE, with  $\alpha = .05$ .

## RESULTS AND DISCUSSION

The range of RE, expressed as a percent of the mean, was 22.4% (Mean  $\pm$  SD:  $\dot{V}O_2 = 214 \pm 13 \text{ ml}\cdot\text{kg}^{-1}\cdot\text{km}^{-1}$ ). This falls within the 20-30% range reported by previous studies (Saunders et al., 2004). The temporal EMG measures, as shown in Table 1, were similar to values reported by Heise et al. (1996) in their study of nine men. A longer duration of RF activity during stance and an earlier onset time of VL were significantly associated with lower  $\dot{V}O_2$  (see Table 1).

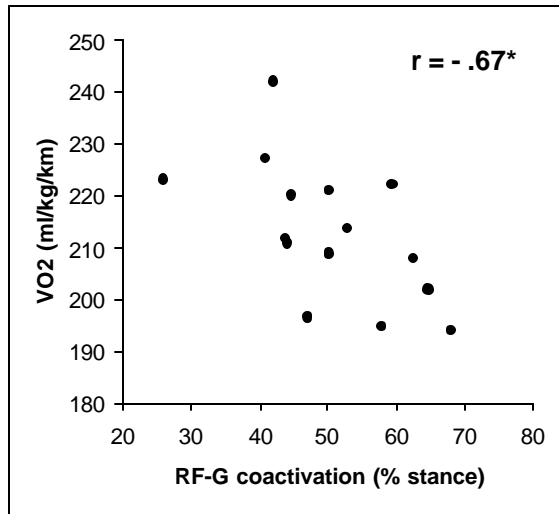


**Figure 1:** Scatterplot of RF-G coactivation versus RE. \* $p < .05$

The duration of coactivation between RF and G during stance was the only coactivation measure significantly related to RE (see Figure 1). Coactivation between G and BF and between RF and BF were not

significantly related to  $\dot{V}O_2$  ( $r = .21$  and  $.19$  respectively).

The significant, negative correlation shown in Figure 1 is consistent with the trend identified by Heise et al. (1996); greater coactivation is associated with better economy (i.e., lower  $\dot{V}O_2$ ). Both G and RF are biarticular muscles that cross the knee joint. More economical runners displaying longer durations of muscle coactivation during stance may provide a better metabolic solution for knee joint stability. The earlier onset of VL in more economical runners may also support this contention.

In summary, several temporal EMG measures of muscles crossing the knee joint during the stance phase of running explained a significant amount of interindividual variability in the RE of women.

## REFERENCES

- Butler, R.J. et al. (2003). *Clin Biomech*, **18**, 511-517.  
 Conley, D. & Krahenbuhl, G. (1980). *Med Sci Sports*, **12**, 357-360.  
 Heise, G.D. et al. (1996). *Int J Sports Med*, **17**, 128-133.  
 Saunders, P.U. et al. (1998). *Sports Med*, **34**, 465-485.

## ACKNOWLEDGEMENTS

Study funded by Wacoal, Inc. via a sub-contract with University of Colorado.

**Table 1:** Mean Temporal EMG Measures and Correlations with RE (Mean  $\pm$  SD).

Muscle	Duration (%stance)	r	Onset time wrt FC <sup>1</sup> (s)	r
gastrocnemius	65.6 $\pm$ 11.6	.02	.006 $\pm$ .065	.46
vastus lateralis	58.2 $\pm$ 17.8	-.34	-.040 $\pm$ .081	.70*
rectus femoris	52.6 $\pm$ 12.5	-.62*	-.054 $\pm$ .068	.01
biceps femoris	40.2 $\pm$ 26.2	.36	-.131 $\pm$ .104	.27

<sup>1</sup>wrt FC = with respect to foot contact; time = 0 at FC. \* $p < .05$ .

# RELATIONSHIP BETWEEN VEHICLE AND RESULTING OCCUPANT DYNAMICS DURING LOW-SPEED REAR-END IMPACTS

Sean D. Shimada, PhD, Brent Edwards, MS, and Michael Turkovich, BS  
Biomechanical Consultants of California, Davis, CA, USA  
E-mail: drs@davis.com

## INTRODUCTION

It is the job of a Biomechanist or Automotive Safety Engineer to determine whether the reported injuries are consistent with the kinematic and kinetic response of the occupant during a motor vehicle collision. The Biomechanist or Automotive Safety Engineer must draw a conclusion based predominately on the collision dynamics of the involved vehicles. Therefore, it was the purpose of this preliminary study to determine the strength of the relationship between the vehicle and resulting occupant dynamics during low-speed rear-end collisions. If a significant correlation can be found to exist between occupant and vehicle dynamics, that information may serve to more accurately predict the potential for whiplash injuries following a rear-end collision.

## METHODS

An experimental design was adopted to simulate a real world situation in which a stopped vehicle (target), with the brake applied by the occupant, was struck from the rear by another vehicle (bullet) at low velocities. Two vehicles were used for the study, a 2001 Ford Taurus 4-door sedan and a 2000 Mercury Sable 4-door sedan. Both vehicles had an identical mass of 1,507 kg according to Expert Autostats (Forensic Expert Software, La Mesa, CA).

Two male subjects free from any history of cervical, thoracic, or lumbar injury volunteered for the study. Subject number one stood 182.9 cm tall, had a mass of 90.9 kg, and was 40 years of age. Subject number two stood 172.7 cm tall, a mass of 81.8 kg, and was 45 years of age. Each subject

completed 10 trials positioned in the driver seat. The subjects were instructed to position themselves as they would have been under normal driving conditions. The subjects were exposed to changes in velocity ( $\Delta v$ ) less than 5 km/h, as these velocities fell below the range suggested as being tolerable for normal human subjects (McConnell et al., 1993; Watts et al., 1999).

Occupant and vehicle accelerations were measured using an accelerometry system composed of two tri-axial 10g accelerometers (Crossbow Technology, Inc., San Jose, CA). Each subject was instrumented with one US Digital Inclinometer (US Digital Corporation, Vancouver, WA) attached to a "friction" type head arrangement that also housed the head accelerometer. The head accelerometer (measuring along local head x-axis only for this preliminary study) and inclinometer (measuring anatomical flexion/extension) was centered on each subject's tragus, representing the center of mass of the head. The second accelerometer was securely fastened to the center of mass of the vehicle found according to Expert Autostats. The vehicle accelerometer was utilized to measure the horizontal (forward) acceleration only. All data were collected at 500 Hz.

Data were analyzed using Matlab software (The Math Works, Inc., Natick, MA). A frequency/power spectrum analysis was first performed on the acceleration data in order to obtain frequency cut-off characteristics. It was determined that a cut-off frequency of 25 Hz should be used. These cut-off

frequencies were then implemented into an 8<sup>th</sup> order Butterworth filter for its steep cut-off characteristics. The vehicle acceleration data were then integrated to determine the vehicles' maximum change in velocity ( $\Delta v$ ).

## RESULTS/DISCUSSION

The calculated average peak head acceleration (local x-axis) obtained for all trials was 3.4 g, while the head accelerations ranged from 0.68 to 5.09 g. The relative neck extensions ranged from 3.3-33.7 degrees, with an average of 12.1 degrees. Vehicle, head, and neck dynamics are described in table 1.

**Table 1.** Vehicle, head, and neck dynamics for 20 trials

vehicle $\Delta v$ (km/h)	vehicle 'g'	head 'g'	neck ext (deg)
0.81	1.13	0.95	6.5
0.54	0.72	0.82	5.0
0.92	1.47	1.19	7.1
0.55	0.70	0.68	3.3
1.56	2.32	3.16	17.3
1.52	2.37	3.46	15.4
1.91	2.76	4.46	33.7
1.89	2.69	4.01	11.0
1.86	2.53	4.25	17.5
1.79	2.60	3.88	18.2
1.34	1.71	3.31	9.0
1.24	1.56	3.84	6.5
1.49	2.10	3.91	10.0
1.46	2.00	4.50	8.5
1.82	2.58	5.01	17.5
1.76	2.42	5.09	8.5
1.12	1.43	3.28	8.5
1.51	2.10	4.27	7.3
1.16	1.48	3.67	9.8
1.16	1.59	3.40	12.1

When the head accelerations were compared with the change in velocities ( $\Delta v$ ) of the target vehicle, a strong relationship ( $r=0.88$ ) was found. This resulted in an  $r^2=0.77$ , meaning that 77% of the variance in the occupant head acceleration can be accounted by the  $\Delta v$  of the target vehicle. Comparison of peak neck extension with the  $\Delta v$  of the

target vehicle was somewhat weaker with a moderate relationship of  $r=0.66$  and an  $r^2=0.43$ .

Head acceleration values for this study were consistent with those of West et al. (1993) and Matsushita et al. (1994). During 14 of the 20 trials for the present study, vehicle  $\Delta v$ 's were below 4 km/h (2.5 mph). A maximum peak head acceleration of 3.8 g was found during these trials. Six trials during the present study were between 4 km/h to 4.8 km/h change in vehicle velocity, resulting in a maximum peak head acceleration of 5.1 g.

## CONCLUSIONS

Occupant head acceleration and neck extension were both found to be related to the  $\Delta v$  of the target vehicle. None of the resulting occupant kinematics were found to be within injury producing levels reported by previous researchers. However, these results should be interpreted with caution. It may be that the relationships found in this investigation apply only to vehicles similar in structure and mass, as well as occupants of comparable inertial characteristics.

## REFERENCES

- Matsushita, T. et al. (1994). X-ray study of the human neck motion due to head inertia loading. *SAE*, Paper No. 942208.
- McConnell, W. E. et al. (1993). Analysis of human test subject kinematic responses to low velocity rear end impacts. *SAE*, Paper No. 930889.
- Watts, A., Atkinson, D., & Hennesey, C., (1999). Low speed automobile accidents: Accident reconstruction and occupant kinematics, dynamics and biomechanics (2<sup>nd</sup> ed.). Tuscon: Lawyers and Judges Publishing Company.
- West, D. H., Gough, J. P., & Harper, T. K., (1993). Low speed rear-end collision testing using human subjects. *Accident Reconstruction Journal*, **5** (3), 22-26.

# THE EFFECT OF COLD-WATER IMMERSION ON THE BIOMECHANICS OF DROP-LANDING MOVEMENT

H. Wang, M.M. Toner, T.J. Lemonda, and M. Zohar  
Queens College of the City University of New York, Flushing, NY, USA  
E-mail: he.wang@qc.cuny.edu

## INTRODUCTION

Cold has been shown to decrease maximal muscle force and increase time to peak tension and relaxation (Bergh, et al. 1979 & Bigland-Ritchie, et al. 1992) and neuromuscular performance (Oksa, et al. 2002). The stiffness of the muscles, tendons and joints also increase under cold condition (Hunter, et al. 1952 & Rice, 1967).

Although cold can affect muscular performance, it is not known whether it affects kinetic and kinematic patterns of dynamic movements, e.g. drop-landing movement. Many winter sports (e.g. football, soccer, and cross country skiing) and occupational outdoor activities (e.g. railroad workers jump off a box-cart) have landing components. Exposure to cold during such activities may impose an increased risk to musculoskeletal system of lower extremities. Therefore, it is important to investigate how cold affects the mechanics of landing. Furthermore, it is of interest to know the kinetic and kinematic patterns of landing following cooling at different levels of the lower body (ankle, knee, and hip levels). The purpose of the study was to investigate the kinetic and kinematic patterns of drop-landing movement after cold-water immersion to ankle, knee, and hip joint levels.

## METHODS

Ten healthy males volunteered to participate in the study. Participants' age, body weight, and body height (means and standard

deviations) were 23.5 (2.8) years, 74.7 (8.3) kg, and 1.71 (0.07) m, respectively.

After familiarization, subjects performed drop-landing tests following still immersion in water at neutral (34 °C) temperature (control condition) (*N*) to hip level (immersion to the anterior iliac spine), and cold water (20 °C) to the ankle (20 mm above the malleolus) (*A*), knee (40 mm above the femoral epicondyles) (*K*) and hip (*H*) levels. Kinematic and kinetic analyses were performed following drop-landing from a platform situated 0.6 m above a force plate. The four tests and treatment conditions were administered on separate days and presented in a counterbalanced fashion.

Two high speed video cameras (120 Hz) were used to track participants' motion. A force platform (1080 Hz) was used to monitor ground reaction force (GRF). Inverse dynamic method was used to calculate joint reaction forces (JRF), moments, and powers of ankle, knee, and hip joints. Repeated measure ANOVAs were used to determine the kinematic, kinetic, differences between the *N* and the other three cold-water immersion conditions (*A*, *K*, and *H*) ( $\alpha = 0.05$ ).

## RESULTS AND DISCUSSION

There were kinematic and kinetic differences between the control condition and the three cold water conditions. The *A* condition showed greater knee and hip joint flexion velocities (3.4 % and 6 % greater, respectively) than the *N* condition ( $P <$

0.05). The *K* condition showed greater hip flexion velocity (9 % greater) than the *N* condition ( $P < 0.05$ ). Most importantly, the *H* condition showed greater hip and trunk flexion (11 ° and 10 ° greater, respectively) and less anteroposterior (AP) and vertical ground reaction forces (10 % and 8 % lesser, respectively) than the *N* condition during landing ( $P < 0.05$ ).

Increasing joint flexion velocity activates the stretch reflex (Duncan, et al. 2000) and increase the eccentric force (Katz, 1939). In the present study, the increasing knee and hip joint flexion velocities seen in the *A* condition appears to use to compensate the reduction of impact absorption of the cooled-ankle joint during landing. Similarly, the *K* condition increased the hip joint flexion velocity to compensate for the reduction of impact absorption from the cooled-ankle and knee joints, as well as lower-leg muscles. Moreover, the *H* condition used kinematic adaptation by increasing hip and trunk flexion to dissipate the landing impact.

The findings concerning various levels of cold-water immersion show that, during drop-landing movement, local cooling of the ankle showed no kinematic changes at the ankle, while changes were demonstrated at the non-affected (non-cooled) muscle/joint

complexes of the knee and hip. During cold-water immersion to the knee, kinematic changes were noted at the ankle, which appear to be the result of cooling the muscles supporting the ankle; similar to the results during ankle immersion, kinematic changes were observed in the non-affected hip joint. Finally, the most pronounced effects on kinematic and kinetic changes were seen following hip immersion. These data suggest that the kinematic changes noted during cold are more the result of muscle-tissue cooling, rather than changes in joint-tissue stiffness.

## REFERENCES

- Oksa, J. et al. (2002) *J Appl Physiol.*, **92**, 354-361.  
Bergh, U. et al. (1979) *Acta physiol Scand.* **107**, 33 – 37.  
Bigland-Ritchie, B. et al. (1992) *J Appl Physiol.*, **73**, 2457 – 2461.  
Hunter, J. et al. (1952) *Can J Med Sci.*, **30**, 367-377.  
Rice, M. H. C. (1967) *J Physiol.*, **188**, 1 – 2.  
Katz, B. (1939) *J Physiol.*, **96**, 45.  
Duncan A, et al. (2000) *J Physiol.*, **526**, 457-468.

## ACKNOWLEDGEMENTS

This study was funded by CUNY Research Foundation.

# Vertical Ground Reaction Force During Trunk-flexed Gait

D. Saha, B.S<sup>1</sup>; S. Gard<sup>1,2,3,4</sup>, Ph.D., S. Fatone<sup>1,3</sup>, Ph.D.

<sup>1</sup>Northwestern University Prosthetics Research Laboratory and Rehabilitation Engineering Research Program; <sup>2</sup>Jesse Brown VA Medical Center; <sup>3</sup>Northwestern University Department of Physical Medicine and Rehabilitation; <sup>4</sup>Northwestern University Department of Biomedical Engineering, Chicago IL.  
Email: d-saha@northwestern.edu

## INTRODUCTION:

The ground reaction force vector generated during gait is equal to the sum of the masses of each body segment multiplied by their respective accelerations. Compared to other body segments, the trunk is the primary contributor of vertical force during gait (Gillet, 2003). However, few studies have investigated the role of trunk posture on the characteristics of the vertical ground reaction force (vGRF). To better understand the kinetics associated with forward trunk posture, this study examined the vGRF of able-bodied subjects walking with trunk-flexed postures.

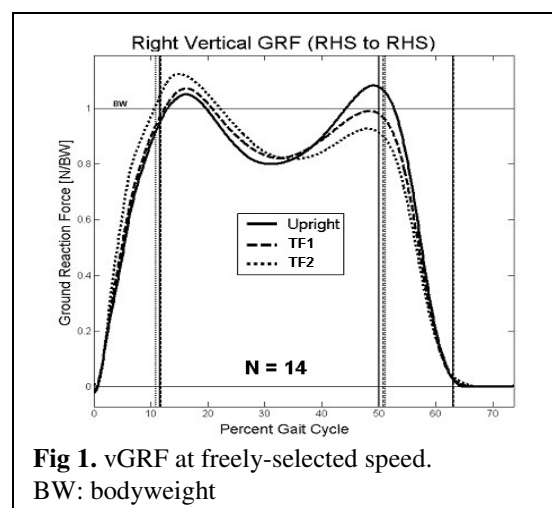
## METHODS:

Quantitative gait analyses were conducted on 14 able-bodied subjects walking upright and with  $25 \pm 7^\circ$  (TF1) and  $50 \pm 7^\circ$  (TF2) of trunk-flexion from the vertical. Trunk flexion was monitored in real time. Feedback in the form of auditory cues helped subjects maintain their trunk flexion angle within the desired range. Motion analysis was conducted using retro-reflective markers arranged on the body according to the Helen Hayes marker set, with additional markers on the head and trunk. Subjects walked at their self-selected slow, normal, and fast walking speeds across a 10-meter walkway with six force plates<sup>1</sup> Orthotrak software<sup>2</sup> was used to calculate joint kinematics, the body's center of mass (BCOM) position based on kinematic data

(Gard, 2004), and the magnitude of the vGRF. Discrete double differentiation of the BCOM position was used to determine the vertical acceleration of the body. The vGRFs were normalized by body weight and expressed as a function of the gait cycle. The magnitude of the vGRF peaks and the average rate of loading (ROL) were compared between postures. The ROL was computed during the weight acceptance phase by taking the slope of the vGRF profile from initial contact to the first peak of the vGRF (Gard, 2003). A two-way repeated measures ANOVA ( $\alpha = 0.05$ ) was used to analyze the data.

## RESULTS & DISCUSSION:

Walking speed was not significantly different between postures ( $p=0.343$ ). The ROL was significantly greater with trunk-flexed postures than with upright posture ( $p_{up:TF1}=0.009$ ,  $p_{up:TF2}<0.029$ ). At freely-selected walking speed the ROL was 22% greater with TF2 than in upright posture (Fig



<sup>1</sup> Advanced Technology Inc., Watertown, MA.

<sup>2</sup> Motion Analysis Corporation, Santa Rosa, CA

1). At freely-selected walking speed the first vGRF peak of TF2 was significantly greater (7%,  $p=0.003$ ) than in upright posture. With increasing trunk flexion there was a significant decrease in the magnitude of the second vGRF peak ( $p<0.002$  for all postures). In trunk-flexed postures the second peak failed to rise above body weight.

An increase in stance-phase knee flexion during trunk-flexed gait may be related to the changes observed in the vGRF. During upright gait, the BCOM reached its peak vertical position and its lowest vertical acceleration in midstance when the stance leg hip joint was in line over the ankle in the sagittal plane. Due to an increase in knee flexion during trunk-flexed gait the hip joint center was shifted posteriorly (relative to its position in upright posture) and was not aligned over the ankle until later in the gait cycle. In trunk-flexed gait the peak vertical BCOM position occurred after mid stance (Fig 2). The phase shift in the vertical position of the BCOM was associated with a corresponding shift in its vertical acceleration (Fig 3) and in the vGRF.

The second peak of the vGRF indicates that in upright walking positive acceleration of the BCOM was achieved prior to contralateral initial contact. Hence, at the end of single support the BCOM was *decelerating* downward. However, due to the phase lag that occurred with trunk flexion, positive acceleration was achieved closer to or at initial contact (Fig 3, circle). This implies that at the end of single support the BCOM was *accelerating* downward. Contact of the leading limb during trunk-flexed gait may have been necessary to “catch” the downward fall of the trunk and reverse its acceleration. Greater downward trunk accelerations at initial contact may be responsible for the higher impact forces and faster loading rates during trunk-flexed gait.

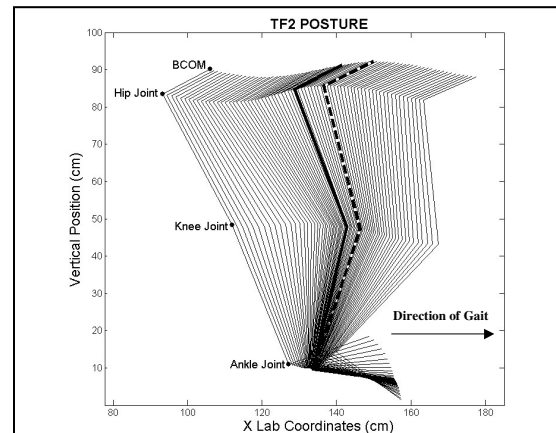


**Fig 2.** Orientation of the stance limb with TF2 during gait, particularly in mid stance (bold line) and when the BCOM is at its highest vertical position (dashed line).

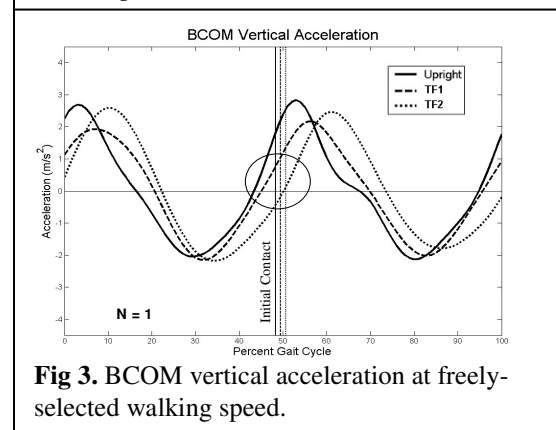


**Fig 3.** BCOM vertical acceleration at freely-selected walking speed.

## CONCLUSION:

Attenuation of the second vGRF peak accompanied by higher impact forces and increased ROL during initial contact are associated with forward trunk lean. These changes may be related to a posterior shift in the hip joint center of the stance limb during trunk-flexed gait.

## REFERENCES:

- Gillet C., et al.(2003). *Am J Phys Med Rehabil*, 82(2), 101-109.
- Gard S, Konz R (2003). *J Rehabil Res Dev*, 40(2), 109-124.
- Gard et al. (2004). *Hum Mov Sci*, 22(6), 597-610.

**FUNDING:** National Institute on Disability and Rehabilitation Research and Medtronic-Sofamor Danek, Inc.

# DYNAMIC STABILITY OF MOTION IMPAIRED ELDERLY ASSESSED BY E-TEXTILE PANTS

Jian Liu <sup>1</sup>, Thurmon E. Lockhart <sup>1</sup>, Mark Jones <sup>2</sup>, Tom Martin <sup>2</sup>, and Christopher Einsmann <sup>2</sup>

<sup>1</sup> ISE Department, Virginia Tech, Blacksburg, VA, USA

<sup>2</sup> ECE Department, Virginia Tech, Blacksburg, VA, USA

E-mail: [lockhart@vt.edu](mailto:lockhart@vt.edu) Web: [www.locomotion.ise.vt.edu](http://www.locomotion.ise.vt.edu)

## INTRODUCTION

Fall induced injury has been a prevalent problem, especially for the elderly. Approximately one-third of adults over 70 years fall in a given year, with one-fourth of those falls resulting in fall-related injuries (CDC, 2000). Thus, effective fall prevention, detection and intervention solutions are in great need for such situation.

Age- and disease- associated degradation of an individual's ability to ambulate in a repetitive and stable manner is regarded as an apparent sign of many gait pathologies leading to falls. It was suggested that individuals with step variability fell more often than non-faller in a study of older adults who were hospitalized after falls (Guimaraes & Isaacs, 1980). Furthermore, researchers also demonstrated that gait variability is linked to falls in the elderly (Imms & Edholm, 1979). Therefore, effective and timely assessment of gait stability of the elderly could help detect individual's stability change and differentiate fall-prone individuals with higher instability.

Local dynamic stability measure, which is based on nonlinear dynamic theory, has been proposed as a more precise measurement of individuals' resistance to perturbations. Up to now, however, the application of local dynamic stability is still constrained in the laboratory with no attempt for everyday field assessment, which is greatly needed for fall prevention solutions.

Recent advances of wearable computing makes possible the application of context awareness in human activity. While monitoring daily activities can be useful, it is our belief that by integrating local dynamic stability assessment capability in the context awareness of human activity monitoring, it would be more appealing, in terms of being able to differentiate fall-prone elderly by detecting individual's stability change. Such integration would eventually contribute to fall prevention solutions.

Therefore, the objective of current study was to demonstrate the e-textile pants' capability of assessing and differentiating motion impaired individuals based on their local dynamic stability measures. Specifically, it was first hypothesized that the local dynamic stability measures obtained from motion capture system and e-textile pants were equivalent for each individual. Furthermore, it was hypothesized that motion impaired old individuals would have higher local dynamic stability measures, which represent lower walking stability, than their healthy counterparts.

## METHODS

5 healthy young, 3 healthy old and 3 motion impaired old individuals, whose anthropometric information were summarized in Table 1, were involved in current study. Informed consent was reviewed by IRB in Virginia Tech and

obtained from every participant before data collection. Motion impaired old individuals are characterized as weak and/or with major injury/surgery conditions like knee-replacement, recovery from stroke, etc.

**Table 1 – Participants’ anthropometric information**

Group	Age (years)	Weight (kg)	Height (cm)
HY*	26.4 (2.3)**	71.0 (13.6)	176.8 (7.4)
HO	71.3 (6.5)	71.2 (7.3)	164.7 (9.3)
UO	71.0 (3.0)	88.6 (10.4)	172.3 (10.8)

\* HY = healthy young; HO = healthy old; UO = motion impaired old

\*\* mean (standard deviation)

An e-textile garment was developed to collect acceleration, angular velocity and piezoelectric data. The e-textile is a pair of pants (Fig.1) comprised of numerous e-TAGs, which are small printed circuit boards with some combination of microcontrollers, sensors and communication devices (Lehn, Neely, Schoonover, Martin, & Jones, 2004). Technical details will be detailed in full paper.

Ten infrared-reflective markers were placed over participant’s bony landmarks of lower body for kinematic motion capture, together with a six-camera ProReflex system (Qualysis Medical AB, Gothenburg, Sweden).

During the data collection, participants were instructed to walk on the Parker PM treadmill (Parker Treadmill Co., Auburn, AL) at the speed remotely controlled by the experimenter. Three speed levels (100%, 110% and 120% of individual’s normal speed) were tested for each participant sequentially. At each speed level, a 50-second dataset was taken from both motion analysis system and e-textile system.

Local dynamic stability was quantified by maximum Lyapunov Exponent (max-LE) from nonlinear dynamic approach. Computation detailed will be shown in full

paper. All the computations were achieved in MATLAB 7.0 (The MathWorks Inc., Natick, MA, USA) and TSTool (Merkwirth, Parlitz, Wedekind, & Lauterborn, 1997).

Paired-t tests on AV (Angular Velocity) based max-LE and VA (Vertical Acceleration) based max-LE for three participant groups and three speed conditions were performed at different locations. Significant level  $\alpha = .01$ , instead of .05, was adopted to reduce possibly inflated Type I error caused by multi t-tests.

## RESULTS AND DISCUSSION

Due to the space limitation, only results at one location (left ankle joint) were reported in here.

E-textile (ET) pants were found to produce equivalent local dynamic stability measures as MC. Based on results from paired-t tests, AV based and VA based max-LE from both systems were not found to be significantly different.

In summary, current study demonstrated the capability of e-textile pants to assess local dynamic stability, which were comparable to those obtained in motion capture system. Future studies incorporating more participants with improved control of noise influences, it was still expected that e-textile pants should be able to detect stability change associated with motion impaired and healthy individuals.

## REFERENCES

CDC (2000), *CDC Facts Book 2000/2001*  
 R. M. Guimaraes and B. Isaacs, "Characteristics of the gait in old people who fall," *International Rehabilitation Medicine*, vol. 2, pp. 177-180, 1980.

(complete references will be provided in full paper)

# KNEE STRENGTH AND SLIP SEVERITY IN YOUNG AND OLDER ADULTS

Sarah Wyszomierski, April J. Chambers and Rakié Cham

Human Movement and Balance Laboratory,  
Department of Bioengineering, University of Pittsburgh, Pittsburgh, PA, USA  
email: saw6@pitt.edu, web: www.engr.pitt.edu/hmbl

## INTRODUCTION

Falls initiated by slips are a major cause of serious injury in the elderly population (Moyer, 2005). Studies have shown a possible correlation between lower extremity muscle strength, which decreases with age, and slip severity (Lockhart, 2005). However, these studies did not focus on the knee, which plays an important role in slip-recovery attempts (Moyer, 2005/2006). Thus, the goal of this study was to investigate the relationship between knee flexion/extension (KF/KE) strength and slip severity in young and older adults.

## METHODS

Ten young (Y) ( $24 \pm 3.0$  yrs) and ten older subjects (O) ( $57 \pm 5.1$  yrs), screened for neurological and orthopedic abnormalities, participated. In Visit 1, isometric KF and KE strength was collected at 1000 Hz using a Biodex AP System 2. Subjects were instructed to contract for five seconds then relax for ten seconds over three repetitions. In Visit 2, subjects were instructed to walk at a self-selected pace across a vinyl tile walkway. Whole body motion data was recorded at 120 Hz using a Vicon 612 motion capture system. After two to three baseline dry trials, the left force plate was covered with a glycerol-water solution (75:25%) without the subject's knowledge, creating an unexpected slippery condition.

Strength data of the left/stance (slipping) leg was lowpass filtered at 20 Hz using a fourth-order zero phase Butterworth filter (Winter, 1990). Peak torque and rate of force development (RFD), defined as the slope of

the torque-time curve, were determined for each repetition. RFD was calculated in incrementing time periods of 0-10, 0-20,..., 0-300 ms from the onset of the contraction (Andersen, 2006). Repetition was determined to be insignificant; therefore, the mean value of across each repetition was used for this analysis.

Slip trials were categorized as non-hazardous (NH) and hazardous (H) by considering the peak slip velocity (PSV) of the heel during a slip. PSV was identified as the first local maximum of horizontal heel velocity after 50 ms from heel strike using the velocity of the left heel marker. Hazardous slips were defined as having a PSV of greater than 1.0 m/s (Moyer, 2005). To achieve the goal of this study, linear ANOVA models were used to compare differences in knee strength characteristics (peak torque magnitude and RFD) between 2 fixed effects and their interactions, i.e. slip severity (NH/H) and age (Y/O). A significance level of  $p < 0.05$  was used.

## RESULTS AND DISCUSSION

Peak isometric strength was not different between H/NH slips across both age groups (Table 1). This is somewhat expected, as exerting peak strength is not required when reacting to an unexpected slip.

**Table 1:** Peak Torque Mean (Std Dev)

	Young		Older	
	NH	H	NH	H
KF	63.84 (21.73)	65.82 (22.08)	57.73 (24.38)	64.19 (6.26)
KE	98.69 (20.44)	90.13 (36.82)	73.98 (19.31)	81.51 (24.09)

A significant NH/H x age interaction effect was noted for KF RFD from 0-100 to 0-180 ms (Figure 1). KE RFD demonstrated near significant interaction effects later, between 0-140 and 0-250 ms (Figure 2). These effects were due to young adults who experienced H slips having lower RFD values than those who experienced NH slips. RFD in older adults did not affect slip severity. This may be attributed to older adults generally adopting “safer” gait styles, while younger adults must overcome initial conditions with quick, powerful reactions to reduce slip severity. Initial reaction to a slip consists of a KF moment, 120 ms, followed by a KE moment, 180 ms (Moyer, 2005/2006). These temporal reactions correspond to the RFD time intervals reported here that significantly impacted slip severity. The RFD intervals are also equivalent to the time span during which responses to a slip occur (Andersen, 2006; Moyer, 2006).

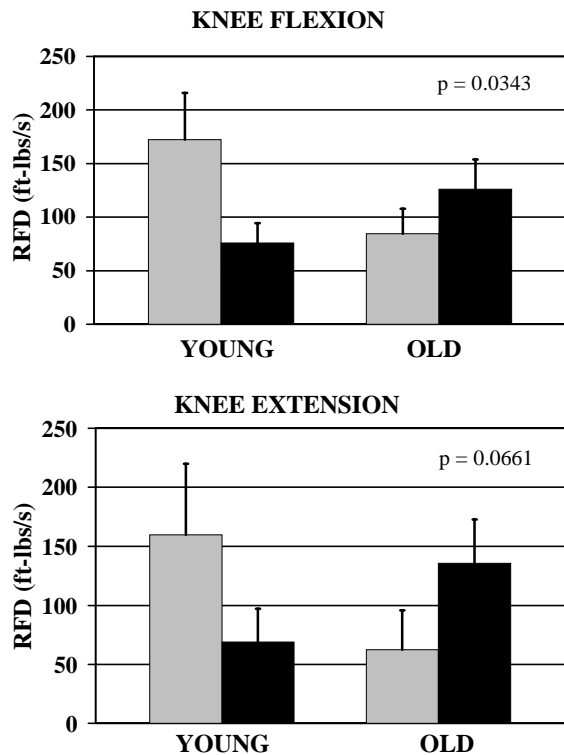


**Figure 1:** RFD of NH (gray) and H (black) from 0-120 ms for Y/O. Interaction effects are shown in the upper right corner.

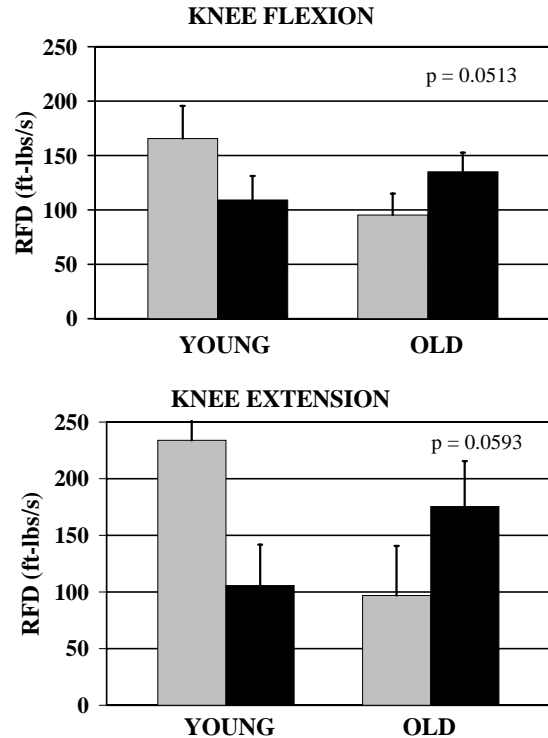


**Figure 2:** RFD for NH (gray) and H (black) from 0-190 ms for Y/O. Interaction effects are shown in the upper right corner.

## SUMMARY/CONCLUSIONS

In summary, RFD, and not peak torque, at the knee was noted to be an important factor in slip severity. The temporal aspects of RFD were determined critical at the same time as corrective reactions to slips and suggest that age-related strength differences may impact slip severity.

## REFERENCES

1. Andersen, L, et al. *Eur J Appl Physiol* (2006) 96: 46-52.
2. Lockhart, T, et al. *Human Factors* (2005) 47: 708-729
3. Moyer, BE, et al. *Ergo* (2005), in press.
4. Moyer, B.E., et al. (2006), in preparation.
5. Winter, D.A. *Biomechanics and motor control of human movement*. (1990).

## ACKNOWLEDGEMENTS

NIOSH R01 OH007592  
Joseph Furman & Kathy Brown

# IMPORTANT KINEMATIC FACTORS FOR FEMALE VOLLEYBALL PLAYERS IN THE PERFORMANCE OF A SPIKE JUMP

Chengtu Hsieh and Gary D. Heise

School of Sport and Exercise Science, University of Northern Colorado, Greeley, CO, USA  
E-mail: hsie6169@unco.edu Web: www.unco.edu

## INTRODUCTION

Numerous researchers have investigated vertical jump mechanics and determinant factors of jump performance in the field of sport biomechanics (Vint & Hinrichs, 1996). These studies have concluded that segmental and whole body mechanical power were the best predictors for vertical jump performance (Argón-Vargas & Gross, 1997). However, few of them have examined a jump in the context of competition (e.g., volleyball spike jump). In addition, the analysis of a simple vertical jump may have limited pedagogical usefulness for young athletes in competitive settings.

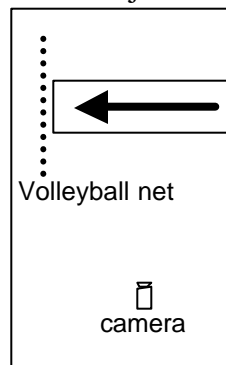
From the perspective of a sport scientist, the most important goal of biomechanical analysis is the ability to offer constructive feedback to athletes (Dowling & Vamos, 1993). For example, while the maximum mechanical power of the center of mass (COM) at takeoff accounts for 86% of the variability in jump height, the researcher can do little with this information to improve the jump performance because it is a difficult variable to use as a diagnostic indicator (Dowling & Vamos, 1993).

Therefore, the purpose of this study was to identify the crucial kinematic factors that contribute to a successful volleyball spike jump from the onset of approach to the peak of the jump height. Specifically, we investigated the factors that can be used for pedagogical purposes.

## METHODS

Fifty female volleyball players (mean body height =  $1.72 \pm 0.08$  m; mean body mass =  $64.5 \pm 11.0$  kg) were recruited from high school and college-level teams. All policies and procedures for the use of human subjects were followed and approved by the local Institutional Review Board.

Each subject was required to warm-up for at



least 5 min by stretching all major muscle groups for jump performance and practicing several normal spike jumps in front of a net and camera (see Figure 1). All subjects performed 10 volleyball spike jumps.

**Figure 1.** Experimental set-up showing one camera and volleyball net.

Two-dimensional coordinate data from one side of the body were obtained with a 60-Hz video camera in conjunction with a motion analysis system (Vicon-Peak). Data were collected from movement onset until after the peak of the jump. Coordinate data were filtered and then kinematic variables (see Table 1) were calculated to describe the volleyball spike jump performance. Various multiple regression model-selection methods were used to identify the most important variables for spike jump performance. The following methods were used: best subsets; stepwise; forward selection; and backward elimination techniques.

## RESULTS AND DISCUSSION

Regression analysis identified six kinematic measures which accounted for 59% of the variability in spike jump height. In order of importance, these variables were  $X_{10}$ ,  $X_4$ ,  $X_8$ ,  $X_6$ ,  $X_1$ , and  $X_5$  as defined in Table 1. Table 2 shows the correlation of each variable with jump height. Moreover, the three best variables for predicting jump height were average angular velocities at hip, shoulder, and ankle joints during the arm swing and takeoff phases. These accounted for 51% of the variation in jump height and are shown schematically in Figure 2.

	r		r
$X_{10}^*$	.6309	$X_6$	-.1184
$X_4^*$	.4923	$X_1$	.0241
$X_8$	-.0014	$X_5$	-.2289

**Table 2.** Correlation coefficients of six variables from significant regression model. \* ( $p < 0.05$ )

Surprisingly, the results drew attention to an unexpected finding which is that the average angular velocity of knee extension during the takeoff period was not a significant predictor for jump height. The volleyball spike jump may place different demands on the lower extremity musculature as compared to the much-studied, simple

vertical jump. The importance of the arm swing is also recognized in these results.

Pedagogically, instructors, coaches, and trainers may want to focus on the speed of the hip, ankle, and shoulder joints during the performance of a volleyball spike jump. This contradicts present conventional instruction (e.g, Weishoff, 2002).

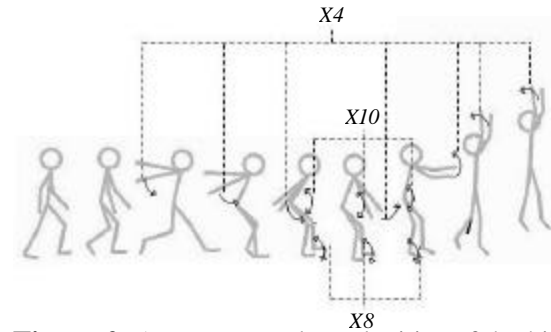


**Figure 2.** Average angular velocities of the hip ( $X_{10}$ ), shoulder ( $X_4$ ), ankle ( $X_8$ ) were best kinematic predictors of jump height.

## REFERENCES

- Argón-Vargas, L.F., & Gross, M.M. *J of App Biomech*, **13**, 24-44, 1997.
- Dowling, J. J., & Vamos, L. *J of App Biomech*, **9**, 95-110, 1993.
- Weishoff, P. *The Volleyball Coaching Bible*, Human Kinetics, 2002.
- Vint, P.F. & Hinrichs, R.N. *J of App Biomech*, **12**, 338-358, 1996.

**Table 1:** Kinematic variables in three phases of a volleyball spike jump

Phases	Approach	Arm Swing	Takeoff
Variable Name [Variable code]	Avg. Horizontal Velocity of CM [ $X_1$ ]	Max. Shoulder Joint Angle at Forward Swing [ $X_2$ ] Max. Shoulder Joint Angle at Backward Swing [ $X_3$ ] Avg. Shoulder Joint Angular Velocity [ $X_4$ ]	Max. Negative Vertical Velocity of CM [ $X_5$ ] Time of Downward motion of CM [ $X_6$ ] Time of Upward motion of CM [ $X_7$ ] Avg. Ankle Joint Angular Velocity [ $X_8$ ] Avg. Knee Joint Angular Velocity [ $X_9$ ] Avg. Hip Joint Angular Velocity [ $X_{10}$ ]

# ESTIMATION OF CHANGING MUSCLE ACTIVATION PATTERNS TO ACHIEVE A SPECIFIC JOINT MOMENT PROFILE

Qi Shao, Daniel N. Bassett, Thomas S. Buchanan

Center for Biomedical Engineering Research  
University of Delaware, Newark, DE, USA  
E-mail: shaoq@me.udel.edu Web: www.cber.udel.edu

## INTRODUCTION

EMG biofeedback training has been used among individual muscles of patients with neurological disorders (Wolf, 2001). Since the muscles of these patients are inappropriately activated, it is important to know how much activity should be added or reduced during muscle training. In this preliminary study, we have created a biomechanical model to estimate the corrective changes in muscle activation patterns that would enable a subject to achieve a new joint moment profile during walking.

## METHODS

A forward dynamics model was developed based on a Hill-type muscle model (Buchanan et al., 2004). The electromyographic (EMG) and kinematic data were used to calculate the joint moments. Inverse dynamics was also used to calculate the joint moments for comparison. An optimization algorithm was then employed, and the parameters in the forward dynamics model were adjusted or *tuned* to minimize the difference between the forward and inverse dynamic joint moments. Once the parameters were tuned, the model could then be used to predict joint moments for new muscle activation patterns.

Using the tuned forward dynamics model, we constructed an optimization model using constrained simulated annealing (Wah and Chen, 2000). Different cost functions were

used for different joint moment profiles. The new EMG pattern was optimized to minimize the cost function so that it may achieve the new joint moment profile. The new EMG should be in the range of [0, 1]. In this paper, "EMG" connotes the normalized, rectified and filtered EMG. Ankle joint and knee joint were treated separately in this model.

## RESULTS AND DISCUSSION

Data were collected from one healthy subject's walking trials, including the EMGs from major muscles, joint positions, and force plate data. Maximum voluntary contraction trials were collected for the normalization of EMG. In this paper we use the ankle joint as an example. We included the four main muscles: tibialis anterior (TA), medial and lateral gastrocnemius (GM and GL), and soleus (Sol). The data of interest are from heel-strike to toe-off.

Firstly, the forward dynamics model was tuned using the subject's gait trial. The tuned forward dynamics model predicted the ankle joint moment well, as shown in Figure 1. Through the comparison of calculated joint moment from original EMG with inverse dynamic joint moment, we found that the  $R^2$  value was 0.928, root mean square (RMS) error was 5.98 N·m, and the average stress cubed per muscle was  $64561.4 \text{ N}^3/\text{cm}^6$ .

The new EMG patterns were then calculated through the optimization model. Here we

show the results using the sum of muscle stresses cubed as a cost function (Crownshield and Brand, 1981). We kept the joint moment and kinematics unchanged, and the EMGs of the four muscles were altered individually. The calculated joint moment from the new EMG was also compared with the inverse dynamic joint moment, as shown in Figure 1. The  $R^2$  value was 0.965, RMS error was 2.85 N·m, and the average stress cubed per muscle was  $6676.3 \text{ N}^3/\text{cm}^6$ . With the new EMG patterns, the sum of stresses cubed was greatly reduced.

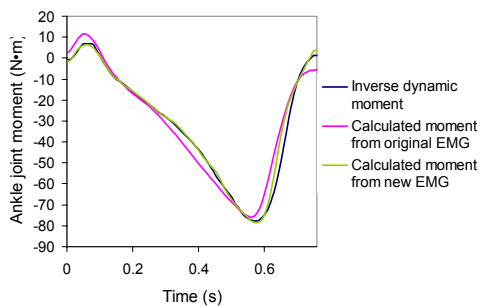


**Figure 1:** The ankle joint moment patterns

Figure 2 shows the calculated  $\Delta\text{EMG}$  patterns. As a part of a rehabilitation protocol, a subject could increase his EMG through functional electrical stimulation or decrease his EMG through biofeedback training (of course, biofeedback training could be used to increase muscle activity as well).

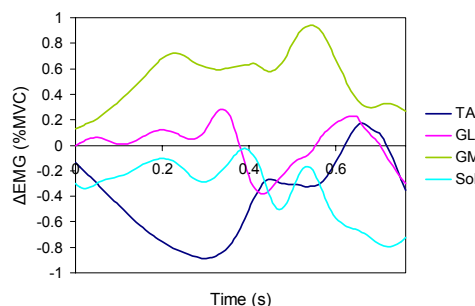


**Figure 2:** The change of EMG patterns

Figure 3 shows the calculated muscle forces from the original and new EMG. Note that

in the original gait trial, the soleus was highly activated, producing much bigger force than gastrocnemius; while in the new gait trial, the soleus force was reduced, and gastrocnemius forces were increased. With the forces distributed evenly across the plantarflexors, decreases in fatigue and lower muscle activations might be expected.

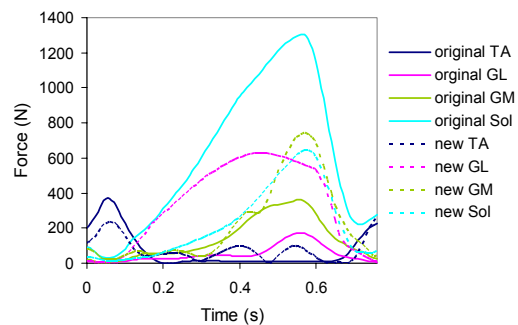


**Figure 3:** The calculated muscle forces with the original and new EMG patterns

## SUMMARY/CONCLUSIONS

Through this modeling work, we determined changes in muscle activation patterns for the subject that would decrease the sum of muscle stresses cubed. This approach to optimize muscle activity could be used in the rehabilitation of patients with neurological disorders to achieve specific joint moment profiles.

## REFERENCES

- Buchanan, T.S. et al. (2004), *J. Applied Biomechanics*, 20, 367-395.  
 Crownshield, R.D., Brand, R.A. (1981), *J. Biomechanics*, 14, 793-801.  
 Wah, B.W., Chen, Y.X. (2000) *Proceedings of CP 2000*, 425-440.  
 Wolf, S.L. (2001). *Applied Psychophysiology and Biofeedback*, 26, 155-174.

## ACKNOWLEDGEMENTS

NIH R01-HD38582 and P20-RR16458

# **MUSCLE SYNERGIES DURING VOLUNTARY BODY SWAY: COMBINING ACROSS-TRIALS AND WITHIN-A-TRIAL ANALYSES**

Yun Wang, Tadayoshi Asaka, Vladimir M. Zatsiorsky, Mark L. Latash

Department of Kinesiology, The Pennsylvania State University, University Park, PA 16802  
E-mail: [yunwang70@hotmail.com](mailto:yunwang70@hotmail.com)

## **INTRODUCTION**

We investigated co-varied changes of muscle activity during voluntary sway tasks that required a quick shift of the center of pressure (COP). We hypothesized that multi-muscle synergies (defined as task-specific covariation of elemental variables) stabilize a COP location in the anterior-posterior direction prior to a voluntary COP shift and that during the shift the synergies would weaken.

The first purpose of the current study has been to develop and test a new method to identify M-modes (leg and trunk muscles organized into groups with parallel scaling of muscle activation level within a group) based on only a handful of trials during voluntary sway. This method combines across-trials and within-a-trial analyses.

The second purpose of the study has been to apply this method to analysis of muscle synergies associated with COP shifts during a quick targeted body sway. This action is common in everyday activities such as reaching for an object, avoiding being hit by an object or a person, leaning to pick up something from the floor, etc.

Our third purpose has been to compare time profiles of an index of a hypothetical multi-muscle postural synergy during voluntary sway performed under the self-paced and reaction-time instructions. We hypothesized that baseline values of a synergy index

reflecting the difference between “good variability” and “bad variability” would be weaker under the reaction time instruction than under the self-paced manner.

## **METHODS**

Eight healthy subjects participated in the experiment. A force platform recorded the reactive forces and moments. Disposable self-adhesive electrodes (3M) were used to record the surface EMG of the following postural muscles from the right side of the body: lateral head of gastrocnemius, medial head of gastrocnemius, soleus, semitendinosus, biceps femoris, gluteus medius, erector spinae, tibialis anterior, vastus lateralis, rectus femoris, tensor fasciae latae, and rectus abdominis. Standing subjects performed two tasks, a cyclic COP shift over a range corresponding to 80% of the maximal amplitude of voluntary COP shift and a unidirectional quick COP shift over the same nominal amplitude. The cyclic sway task was used to define M-modes and the relations between small changes in the gains at M-modes and COP shifts.

A novel approach was used involving principal component analysis applied to indices of muscle integrated activity measured both within a trial and across trials. The unidirectional sway task was performed in a self-paced (SP) manner and under a typical simple reaction time (RT) instruction. M-modes were also defined along trials at those tasks. They are shown to be similar to

M-modes defined in the first task by analysis of angles between pairs of vectors in the muscle space. Integrated indices of muscle activity in the SP-Sway and RT-Sway tasks were transformed into the M-modes.

Variance in the M-mode space was partitioned into two components, one that did not affect the average value of COP shift ( $V_{UCM}$ ) and the other that did ( $V_{ORT}$ ). An index ( $\Delta V$ ) corresponding to the normalized difference between  $V_{UCM}$  and  $V_{ORT}$  was computed.

## RESULTS AND DISCUSSION

We hypothesized that multi-muscle synergies stabilize a COP location in the anterior-posterior direction prior to a voluntary COP shift and that during the shift these synergies would weaken. Our experiments provided support for the hypotheses. In particular, we documented multi-muscle (more exactly, multi-M-mode) synergies stabilizing location of the center of pressure (COP) in the anterior-posterior direction in the steady-state phase of the tasks. Voluntary quick sway was shown to be associated with a drop in the magnitude of the synergy index ( $\Delta V$ ) close to zero, which may be interpreted as disappearance of the pre-existent synergy. There were differences between  $\Delta V$  magnitudes prior to voluntary sway actions performed under the self-paced (SP) and simple reaction time (RT) instruction; these differences were significant prior to sway in the forward direction.

There is also an important methodological aspect to the study, namely the fact that for

the first time, we used only a handful of trials to identify muscle modes. This is a potentially important development that may allow using this method for studies of subpopulations who cannot perform numerous trials involved in the earlier used methods.

## CONCLUSIONS

We conclude that M-mode synergies stabilize COP location during quiet standing, while these synergies weaken or disappear during fast voluntary COP shifts. Under RT conditions, the COP stabilizing synergies were weaker supposedly to facilitate a quick COP shift without time for preparation. The suggested method of M-mode identification may potentially be applied to analysis of postural synergies in persons with impaired postural control such as elderly persons, persons with atypical development, or in the course of rehabilitation after an injury.

## REFERENCES

- Wang Y, Zatsiorsky VM, Latash ML (2005) Muscle synergies involved in shifting the center of pressure while making a first step. *Exp Brain Res*, 167: 196-210.
- Wang Y, Zatsiorsky VM, Latash ML (2006) Muscle synergies involved in preparation to a step made under the self-paced and reaction-time instructions. *Clin Neurophysiol*, 117: 41-56.

## ACKNOWLEDGEMENTS

We appreciate the helpful suggestions of Dr. Kazuhiko Watanabe. Preparation of this paper was supported in part by NIH grants AG-018751, NS-35032, and AR-048563.

# MUSCLE SYNERGIES DURING THE INDUCED FORWARD SHIFTS OF THE CENTER OF PRESSURE FROM A NARROW SUPPORT

Yun Wang, Tadayoshi Asaka, Vladimir M. Zatsiorsky, Mark L. Latash

Department of Kinesiology, The Pennsylvania State University, University Park, PA 16802  
E-mail: [yunwang70@hotmail.com](mailto:yunwang70@hotmail.com)

## INTRODUCTION

Upright human posture is inherently unstable due to the difficulty in maintaining the high center of gravity on the relatively small base of support provided by the feet. Voluntary movements such as forward body sway and interactions with external objects challenge the whole-body's equilibrium and threaten vertical postural balance. Obviously, when voluntary movements are made while standing, the center of pressure (COP) cannot be shifted beyond the available dimensions of the support area. In particular, when standing on boards with a decreased dimension of the support area in the anterior-posterior (AP) direction or in the medio-lateral (ML) direction ("unstable boards"), the activity of postural muscles has to be adjusted to constrain COP shifts and maintain the whole-body balance.

We used the framework of the uncontrolled manifold (UCM) hypothesis to analyze multi-muscle synergies involved in the induced forward shifts of the center of pressure on a narrow support. We hypothesized that leg and trunk muscles are organized into stable groups (muscle modes, M-modes) related to shifts of COP with a decreased dimension of the support area in the AP direction. Another hypothesis was that multi-muscle synergies stabilize a COP location in the AP direction in the steady-state phase of the tasks and that during the shift the synergies would weaken.

## METHODS

Eight healthy subjects participated in the experiment. A force platform recorded the reactive forces and moments. Disposable self-adhesive electrodes were used to record the surface EMG of the following postural muscles from the right side of the body: lateral head of gastrocnemius, medial head of gastrocnemius, soleus, semi-tendinosus, biceps femoris, gluteus medius, erector spinae, tibialis anterior, vastus lateralis, rectus femoris, tensor fasciae latae, and rectus abdominis.

Six types of tasks were used. The first task required the subject to release the load (load release task, LR) suspended behind his/her body using the pulley system while standing on the force plate ("normal support" condition, LR<sub>N</sub>). The second task required the subject to release the load suspended behind his/her body using the pulley system from the board fitted with the narrow beam in the AP direction ("AP narrow support" condition, LR<sub>NAR\_AP</sub>). And the third task required the subject to release the load suspended behind his/her body using the pulley system from the board fitted with the narrow beam in the ML direction ("ML narrow support" condition, LR<sub>NAR\_ML</sub>). These three tasks were used to explore EMG combinations responsible for COP shifts in AP direction under the different support conditions. The other three tasks required the subjects to push a load forward. The load was suspended via a pulley system in front

of the subject's extended arms about 5 cm away. The subject was asked to begin each trial by standing naturally and quietly, with the arms extending in front of the body. One of them required the subject to push load from quiet stance in "normal support" condition ( $LP_N$ ). Another task required the subjects to push load forward in "AP narrow support" condition ( $LP_{NAR\_AP}$ ). Within the final task, the subjects were to push load in "ML narrow support" condition ( $LP_{NAR\_ML}$ ).

Variance in the M-mode space was partitioned into two components, one that did not affect the average value of COP shift ( $V_{UCM}$ ) and the other that did ( $V_{ORT}$ ). An index ( $\Delta V$ ) corresponding to the normalized difference between  $V_{UCM}$  and  $V_{ORT}$  was computed.

## RESULTS AND DISCUSSION

M-modes were defined using principal component analysis applied to indices of changes in the EMG activity prior to releasing variable loads that were held by the subject using a pulley system with different decreased dimension of the support area. To further analyze the M-modes defined in the three LP tasks, we performed analysis of cosines of the angles between vectors in the muscle space corresponding to modes in individual subjects and "central vectors" ( $M_{CVi}$ ). We used two types of comparisons, across subjects (within-a-task) and across tasks (within-a-subject). We found larger cosine values for the angles between each individual  $M_i$ -modes with  $M_{CVi}$  of the same number. Both types of analysis suggest that the similarity among M-modes across subjects was similar to their similarity across tasks.

We hypothesized that multi-muscle synergies stabilize a COP location in the AP direction prior to the induced forward COP

shifts and that during the shift these synergies would weaken. Our experiments provided support for the hypotheses. In particular, we documented multi-muscle (more exactly, multi-M-mode) synergies stabilizing COP location in the AP direction in the steady-state phase of the tasks.  $LP_{NAR\_ML}$  was shown to be associated with a early drop in the magnitude of the synergy index ( $\Delta V$ ) close to zero or even negative values, which may be interpreted as disappearance of the pre-existent synergy.

## CONCLUSIONS

The findings corroborate both main hypotheses. The study supports a view that control of whole-body actions involves grouping the muscles, using fewer elemental variables to scale the muscle activity, and forming synergies in the space of the elemental variables that stabilize time profiles of important performance variables.

## REFERENCES

- Wang Y, Zatsiorsky VM, Latash ML (2005) Muscle synergies involved in shifting the center of pressure while making a first step. *Exp Brain Res*, 167: 196-210.
- Wang Y, Zatsiorsky VM, Latash ML (2006) Muscle synergies involved in preparation to a step made under the self-paced and reaction-time instructions. *Clin Neurophysiol*, 117: 41-56.
- Wang Y, Asaka T, Zatsiorsky VM, Latash ML Muscle synergies during voluntary body sway: combining across-trials and within-a-trial analyses. *Exp Brain Res*, (Under review)

## ACKNOWLEDGEMENTS

Preparation of this paper was supported in part by NIH grants AG-018751, NS-35032, and AR-048563.

# CONTINUOUS RELATIVE PHASE WITHIN THE LOWER EXTREMITY IN RUNNERS WITH PATELLOFEMORAL PAIN DURING A PROLONGED RUN

Tracy A. Dierks<sup>1</sup>, Irene S. Davis<sup>2,3</sup>, John P. Scholz<sup>2</sup>, and Joseph Hamill<sup>4</sup>

<sup>1</sup>Department of Physical Therapy, Indiana University, Indianapolis, IN, USA

<sup>2</sup>Department of Physical Therapy, University of Delaware, Newark, DE, USA

<sup>3</sup> Drayer Physical Therapy Institute, Hummelstown, PA, USA

<sup>4</sup>Department of Exercise Science, University of Massachusetts, Amherst, MA, USA

E-mail: tdierks@iupui.edu <http://www.shrs.iupui.edu/pt/content/bios/dierks.php>

## INTRODUCTION

Patellofemoral pain (PFP) syndrome is the most common running related injury. However, little progress has been made in understanding the etiology of PFP. Recent literature suggests that the patellofemoral joint may be influenced by the coupling of the segments that are both distal and proximal to the knee (Tiberio 1987; Powers, 2003). One way to assess joint coupling is through the measurement of the continuous relative phase (CRP). The CRP is a continuous measure of coordination between two oscillatory components, such as rearfoot eversion/inversion and tibial rotation (Hamill et al, 1999). A CRP of 0° corresponds to in-phase coupling, meaning the phase angles for the two motions are identical, and a potentially stable coupling pattern exists as they are behaving similarly. As the CRP moves away from 0° in either a positive or negative direction, the two motions become more out-of-phase and are behaving in a less similar fashion.

The knee pain experienced by runners with PFP is generally not present at the beginning of a run. Instead, the onset is subtle and progressively worsens throughout the run. Yet no studies have examined joint coupling in runners with PFP at the end of a prolonged run, where pain is likely to be present. Therefore, the purpose of this study was to investigate lower extremity CRP in runners with PFP over the course of a prolonged run. It was hypothesized that the PFP group would exhibit more out-of-phase

CRP coupling across stance when compared to controls. In addition, it was expected that the PFP group would become out-of-phase to a greater extent than the controls at the end of the run.

## METHODS

Twenty runners with PFP and 20 uninjured runners participated in the study. All were between the ages of 18 and 45 and ran at least 10 miles per week. All subjects performed a prolonged run on a treadmill at a self-selected pace. 3D kinematic data (120 Hz) of the leg with the most painful knee (random for controls) were collected for 20 footfalls at the beginning and at the end. The prolonged run ended when one of three events occurred: 1) 85% heart rate maximum was reached, 2) 17 was reached on the rating of perceived exertion scale, and 3) for the PFP group, 7 was reached on a visual analog pain scale.

The CRP relationships of interest included: 1) rearfoot eversion/inversion and tibial internal/external rotation ( $RF_{(ev/in)}-T_{(rot)}$ ), 2)  $RF_{(ev/in)}$  and knee flexion/extension ( $RF_{(ev/in)}-K_{(f/e)}$ ), and 3)  $RF_{(ev/in)}$  and knee internal/external rotation ( $RF_{(ev/in)}-K_{(rot)}$ ). For each joint motion, the angles and velocities during stance were used to construct a phase plot (Hamill et al, 1999). The phase plot was normalized and phase angles were calculated. The CRP was then calculated from the two joint motions (i.e.  $RF_{(ev/in)}-T_{(rot)}$ ) as the difference between each phase angle throughout stance. The CRP

was assessed over four periods that were based on vertical ground reaction force events. A two-factor ANOVA for each period of stance (group by time) was used to assess the CRP with a Tukey post-hoc for follow-up comparisons. Alpha was set at 0.05 and trends were identified for p values between 0.05 and 0.10.

## RESULTS AND DISCUSSION

No interactions were detected for any of the CRP relationships, suggesting that both groups exhibited similar changes in CRP

coupling over time (Figure 1). For the main effect of group, the PFP group was more out-of-phase during periods 1 and 2, where loading forces on the leg occur, for  $RF_{(ev/in)}-T_{(rot)}$  and  $RF_{(ev/in)}-K_{(f/e)}$  (Figure 1). This may have been related to a prolonged eversion difference that was observed in the PFP group. However, more in-phase coupling was found for  $RF_{(ev/in)}-K_{(rot)}$  during periods 1 and 2. This may have been a result of an observed earlier peak knee internal rotation in the PFP group, which would be related to motion of the femur. Since the femur articulates with both the patella and the tibia, these atypical CRP coupling patterns may have resulted in abnormal patellofemoral contact pressure. For the main effect of time, decreases in the CRP occurred during periods 1 and 2 at the end of the run (Figure 1). This resulted in downward shifts of the CRP curves in both groups. Interestingly, the CRP patterns in the PFP group at the end of the run resembled those of the uninjured group at the beginning of the run. The PFP group may have changed their coupling patterns in order to reproduce those associated with uninjured runners in a pain-free and non-exerted state. While this compensatory strategy did not reduce pain at the end of the run, it may have been successful in slowing the progression of the pain throughout the run.

## SUMMARY/CONCLUSIONS

These findings demonstrate that runners with PFP display atypical CRP coupling patterns throughout the entire lower extremity when compared to uninjured runners during a prolonged run. These differences were primarily observed during the first half of stance and may have been adopted to slow knee pain progression.

## REFERENCES

- Hamill, J. et al. (1999). *Clin. Biomech.*, 14, 297-308.  
 Powers, CM. (2003). *J.O.S.P.T.*, 33, 639-646.  
 Tiberio, D. (1987). *J.O.S.P.T.*, 9, 160-165.

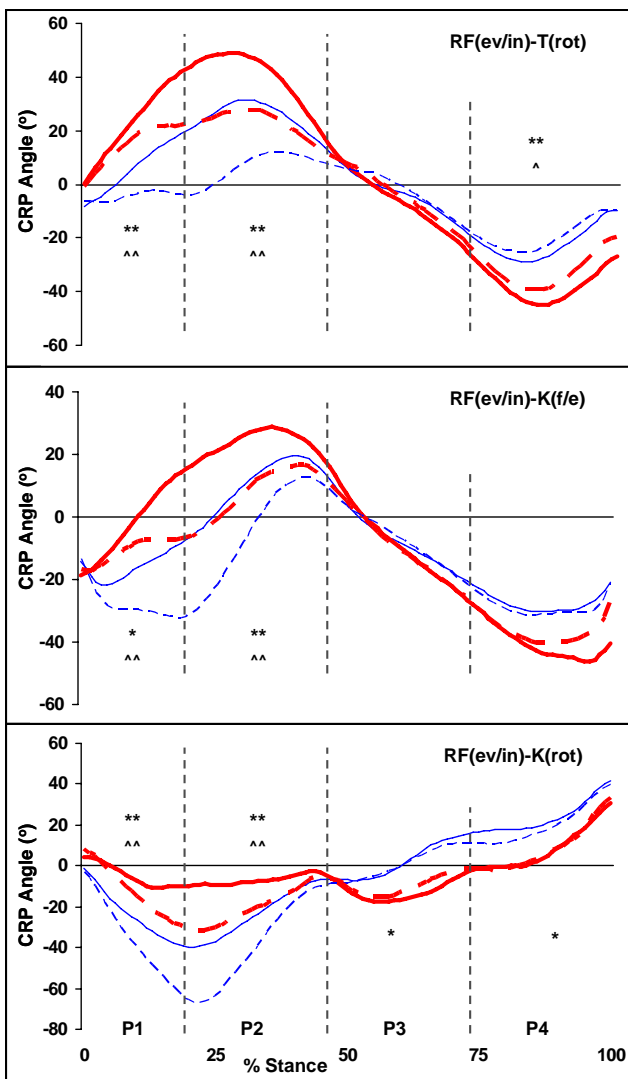


**Figure 1.** Group CRP curves at the beginning and end of the run. Vertical dashed lines divide the curves into the periods of stance (P1-P4). Solid line = begin, dashed line = end, thick/red = PFP, thin/blue = Uninjured. \*\*Significant group effect,  $p < 0.05$ ; \*Trend towards a significant group effect,  $p < 0.10$ . ^^Significant time effect,  $p < 0.05$ ; ^Trend towards a significant time effect,  $p < 0.10$ .

# TRACKING KINEMATIC CHANGES IN ELITE CYCLISTS DURING FATIGUE

Jason E. Joubert and Jonathan B. Dingwell

Nonlinear Biodynamics Lab, Dept. of Kinesiology, University of TX, Austin, TX, USA  
E-mail: [jdiningwell@mail.utexas.edu](mailto:jdiningwell@mail.utexas.edu) Web: <http://www.edb.utexas.edu/faculty/dingwell/>

## INTRODUCTION

Recent popularization has drawn more people into recreational and competitive cycling. This has led to an increase in cycling injuries that may be due to biomechanical inefficiencies (Asplund 2004). At 85 rpm, a cyclist performs over 5000 revolutions every hour. As fatigue sets in, changes in muscle activation patterns may *cause* changes in kinematics. Alternatively, these changes may reflect a strategy used to maintain performance while trying to *minimize* fatigue. In both cases, non-optimal kinematics could cause joint mal-alignments that have a large cumulative effect over frequent long rides.

Typical “pre. vs. post” experimental designs assume one kinematic strategy exists prior to fatigue and a second exists following fatigue. Such experiments cannot quantify changes in kinematics *across* the experiment. In an upper extremity repetitive lifting task, untrained subjects exhibited continuous changes in coordination over time that varied greatly both within and between subjects (Voge 2004). These variations suggest subjects tried a wide variety of strategies to combat progressing muscle fatigue. However, they may instead have been due to either the unconstrained nature of the task, the untrained nature of the subjects, or both.

The present study tested elite cyclists cycling on a stationary bicycle. We tested the hypothesis that even highly trained elite athletes performing a more kinematically constrained task would also exhibit varying and non-monotonic changes in movement kinematics in response to fatigue onset.

## METHODS

Ten elite (USCF Category 3 or higher level of competition ) male cyclists, age 18 – 45 yrs, participated. Each subject was marked with reflective markers (Fig. 1) to collect sagittal plane kinematic data. Participants cycled to exhaustion on a Lode Excalibur Sport bicycle ergometer at a pre-calculated work load equivalent to 100% of their  $VO_{2max}$ . Subjects were given vigorous verbal encouragement throughout the trials, which lasted 4 – 10 min. Kinematic data were sampled at 120 Hz continuously throughout each trial using a Vicon Motion Analysis system (Oxford Metrics, Oxford, UK). The variations exhibited in different joint angles (Fig. 1) were examined *within* subjects to assess nonstationarities that occurred as fatigue progressed and *across* subjects to determine what kinematic changes were common among elite cyclists.

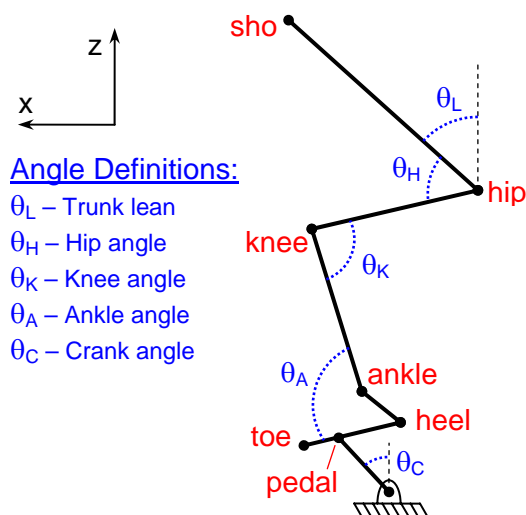


**Figure 1:** Left sagittal plane view of the cyclist showing locations of reflective markers and definitions of joint angles computed.

## RESULTS AND DISCUSSION

All joint angles in all subjects exhibited non-monotonic and non-stationary behaviors in response to the fatigue protocol. Different joint angles exhibited different *types* of non-stationarities. While there were differences *between* subjects, several trends *across* subjects were evident. For example, all subjects increased their trunk flexion as time progressed (Fig. 2). This likely reflected a strategy to increase the stretch response of the hip extensors to maintain total power output. However, at various times in the fatigue protocol, different subjects made noticeable shifts in trunk flexion and shortly after returned towards the trend line.

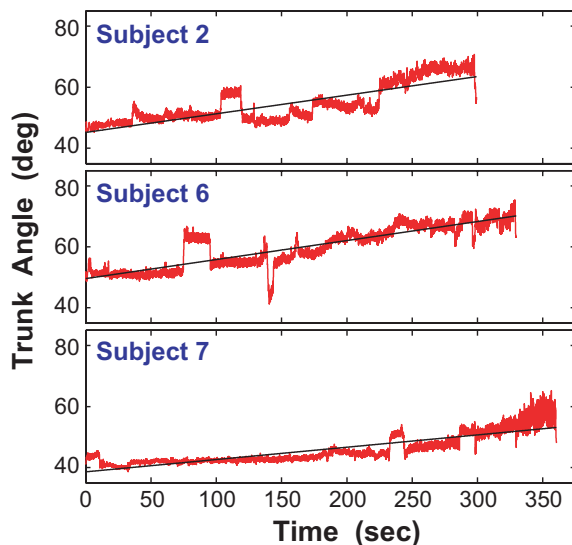


**Figure 2:** Changes in trunk flexion angles ( $\theta_L$ ; in red) over the entire trial for 3 representative subjects. Linear regression lines (in black) show positive trends.

All subjects generally showed a smooth decreasing trend in ankle angle ( $\theta_A$ ) as time progressed (Fig. 3). However, there were also changes in the *range* of ankle motion *within* each subject that differed in direction *between* subjects. For example, Subject 2 tended to use *less* ankle range of motion, whereas Subject 6 tended to use *more* range of motion as fatigue progressed (Fig. 3).

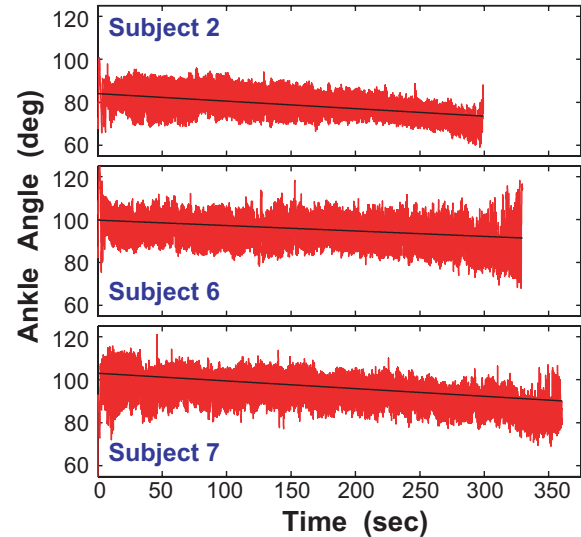


**Figure 3:** Changes in ankle angles ( $\theta_A$ ; in red) over the entire trial for 3 representative subjects. Linear regression lines (in black) show negative trends.

## SUMMARY/CONCLUSIONS

As hypothesized, elite cyclists changed their kinematics in non-monotonic ways. While there were differences across joint angles and across individuals for each angle, those changes were generally consistent with the idea that subjects were trying to prevent the progression of muscle fatigue. These findings extend the work of Voge (2004) by demonstrating that even highly trained elite athletes executing a far more kinematically constrained task still exhibit multiple and continuous changes in their kinematics to maintain power output while delaying the effects of fatigue for as long as possible.

## REFERENCES

- Asplund C., St. Pierre, P. (2004). *Physician and Sportsmedicine*, 32 (4): 23-30.
- Voge K.R., Dingwell J.B. (2004) *Proceedings of ASB '04*, 2 pgs.

## ACKNOWLEDGEMENTS

This work was supported by supplemental grant #EB003425-01A1S1 from the NIH.

# A MUSCLE FORCE PREDICTION BY ARTIFICIAL NEURAL NETWORK FOR GENERAL MUSCLE

Miloslav Vilimek<sup>1</sup>, Jana Vejpuskova<sup>1</sup>, Miroslav Sochor<sup>1</sup>

<sup>1</sup> Czech Technical University in Prague, Prague, Czech Republic  
E-mail: Miloslav.Vilimek@fs.cvut.cz

## INTRODUCTION

The first objective of our research was to establish the possibility of a general artificial neural network (NN) object in the musculoskeletal system of the human elbow joint as a function of the muscle activity, musculotendon (MT) physiological properties and the joint kinematics. The object of backpropagation (BPG) NN with supervised learning algorithm was suggested, in order to fast, accurately and simply predict the muscle forces in the 7 elbow actuators during flexion/extension movement activities. The second objective was to evaluate 14 input muscle parameters which influence the resulting muscle forces. The last objective was to simplify the proposed NN object by the sensitivity analysis to the muscle input parameters. It was studied, because some of the inputs were more sensitive to the results and the network topology than others. The most insensitive inputs need not to be applied to the NN object and it would be made easier to use.

## METHODS

The approach is based on the non-knowledge of relation between input parameters, the MT morphological and physiological data and the muscle fiber recruitment, and the output parameter the muscle force. To train the proposed neural network object was necessary to know the input and output parameters. The direct measurement of muscle force is in most cases extremely invasive approach, therefore

the *Virtual Muscle System* (Cheng et al., 2000) was used in order to relate this to the real muscle force. The input muscle parameters utilized in this investigation result from the Hill-type muscle model including active and passive components (Zajac., 1989). The input parameters express the passive and active muscle force-length factors. Third input was the force-velocity factor. Next were five constant MT parameters, physiological crosssectional area, optimal muscle fiber length, tendon slack length, maximal isometric muscle force and optimum pennation angle. The (MT) length and the velocity of muscle shortening were input parameters estimated from anatomical positions of the muscle attachments and recorded kinematic data in various movement conditions. Last inputs were the muscle electrical activities of the observed muscles recorded by surface electromyography (EMG). The processed EMG's were filtered, rectified, smoothed and normalized. The processed EMG signal was taken as the input of the muscle activity and the three levels of history of muscle activity. The history of muscle activity ensures direct expression of time, thereby dynamic of the object of neural network.

The neural network architecture was the feedforward multilayer network (BPG), in this case consisting of three layers (input layer and two hidden layers followed by an output layer). The feedforward multilayer network was fully connected, that means the each neuron in a given layer was connected to every neuron in the next layer, neurons in the same layer were not connected. The

network object with 30 neurons in the 1<sup>st</sup> hidden layer and 24 neurons in the 2<sup>nd</sup> hidden layer was proposed. Between input layer and 1<sup>st</sup> hidden layer and between 1<sup>st</sup> and 2<sup>nd</sup> hidden layer were used sigmoidal transfer functions. Between 2<sup>nd</sup> hidden layer and output layer was used linear transfer function. In the course of the (BPG) learning, the main goal was to find out the solution having the smallest error and the fastest convergence with respect to the network's weight and biases. By adjusting network's weights, network object was trained to predict muscle forces.

The measurement and calculation of some NN inputs is not trivial and the more inputs make a solving the more complicated. Therefore, the network object was used to evaluate the sensitivity to the inputs. Here was an effort to examine if some inputs were possible to eliminate without increasing the network error.

## RESULTS AND DISCUSSION

Several variants were performed according to the sensitivity analysis to the inputs. Primary variant was for the general muscle with all of the 14 inputs. The cross-correlation coefficient to the force prediction for the 14 inputs variant is 0.97 (97% of prediction). The force-velocity factor input had coefficient of non-sensitivity very high, hence in the next variant this "insensitive" input was left out. This way the possible simplification of calculation and inputs reduction was studied. The cross-correlation coefficient for the variant without force-velocity factor was 0.98. Here also one of the inputs had very high coefficient of non-sensitivity, the velocity of shortening which was reduced in the next variant too. By this way were reduced several inputs and still the network cross-correlation coefficients for the force prediction were good. In one

variant was studied influence of muscle activation level and its history. In the one of variants were aside from the activation input eliminated also history of activation inputs. The ability of proposed NN object to predict muscle force without activation and activation history was much lower, the correlation coefficient was 0.87. The achievement of the smallest error depends several limitations. The first limitation is the knowledge of the true output of the network training data. The training outputs were calculated musculotendon forces and not directly measured, for example by using optic fiber sensors (Komi, et al., 1987; Finni et al., 2000). In our case the output data were calculated but we suppose the training process would be similar but with directly estimated muscle forces. Second limitation is the number of training datasets. In our case the sets of input/target pairs data were only from four 4 elbow flexion/extension movement conditions, which is smaller than full real motion spectrum in elbow. Third limitation is a correct preprocessing and choice of representative set of input/target pairs. Performed and early stopping algorithm and with data preprocessed by principal component analysis were provided good results.

## REFERENCES

- Cheng, E.J. et al. (2000). *J. Neuroscience Methods*, **101**, 117-130..
- Finni, T. et al. (2000). *European Journal of Applied Physiology*, **83**, 416-426.
- Komi, P.V. et al. (1987). *International Journal of Sports Medicine*, **8**, 3-8.
- Zajac, F.E. (1989). *Critical Reviews in Biomedical engineering*, **17**, 359-411.

## ACKNOWLEDGEMENTS

This study was supported by grant No.: MSM 6840770012.

# THE RELATIONSHIP OF MEDIOLATERAL MOTION AND VO<sub>2</sub> DURING RUNNING

Gannon A. White and Gary D. Heise

University of Northern Colorado, Greeley CO, USA  
E-mail: uncbiomechanics@yahoo.com

## INTRODUCTION

Biomechanical variables which describe “good running form” help explain the interindividual variability in running economy (RE). These include vertical oscillation, wrist excursion, and measures of symmetry (Saunders et al., 2004). Excessive vertical oscillation and wrist excursion, for example, are considered wasteful because they contribute little to forward motion. In addition, the majority of research examining RE and biomechanics analyze 2-D, sagittal-plane motion. Williams and Cavanagh (1987) measured 3-D motion and are the only researchers, to our knowledge, that reported wrist excursion over the entire running stride.

Excessive mediolateral (ML) motion of the arms, legs, and the body’s center of mass (COM) also may be considered metabolically wasteful. This ML motion of the body and body segments may compromise forward momentum necessary for economical running. The purpose of the present study was to focus on the ML motion of the COM, and the upper and lower extremities during running and determine if these kinematic measures are related to RE. Secondly, the symmetry in ML motion of the upper and lower extremities was also examined.

## METHODS

The subjects in this study were participants in a larger multi-visit study. Seventeen healthy, active women participated (Mean  $\pm$

SD: Age =  $24.4 \pm 5.8$  yrs; Body Mass =  $59.7 \pm 5.0$  kg). All subjects were regular runners and were free from injuries during the time of data collection.

For the present study, subjects performed a 30-min treadmill run. The final speed was chosen by the subject during the first 8-min to elicit a 6 on the Borg RPE 10-pt scale by the end of the run. Prior to the treadmill run the subjects completed other various physically demanding tests but were given sufficient rest time before starting the run.

The other tests were physical enough to constitute a proper warm-up. Four 60-Hz Panasonic digital, video camcorders were placed around the treadmill to record the runner’s gait kinematics (see Figure 1). Direct linear transformation was used to calibrate the volume (overall error < 0.5%).

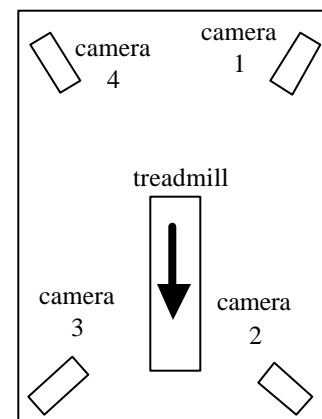


**Figure 1:**  
Experimental set-up.

The range of ML motion of the wrists, ankles, and body COM were quantified for a complete running cycle. In addition, the left wrist and ankle values were divided by the right-side values and expressed as a percent difference from 100 (i.e., perfect symmetry). Nonparametric correlations were used to relate kinematic measures to RE.

## RESULTS AND DISCUSSION

The range of RE, expressed as a percent of the mean, was 22.4% (Mean  $\pm$  SD: RE =  $214 \pm 13 \text{ ml}\cdot\text{kg}^{-1}\cdot\text{km}^{-1}$ ). This falls within the 20-30% range reported by previous studies (Saunders et al., 2004). COM mediolateral motion had a significant negative correlation with oxygen consumption (see Table 1, Figure 2). Most other ML motion measures resulted in negative correlation coefficients, however none reached statistical significance. The observed ranges for ankle ML values were similar to those reported by Heise et al. (2003). Symmetry values for the wrist and ankle (Mean  $\pm$  SD:  $40.8 \pm 33.8\%$ ;  $27.2 \pm 18.2\%$ ) were highly variable and not related to oxygen consumption ( $r = -.07, .09$  respectively).

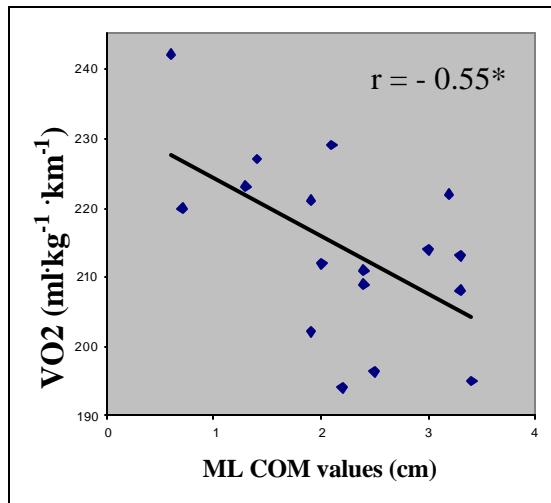


**Figure 2:** Scatterplot of  $\dot{V}O_2$  and COM mediolateral values. \*  $p < 0.05$

The negative relation between ML motion of the COM and oxygen cost was unexpected. It seems counterintuitive that more ML motion is associated with better economy (Figure 2). The ML motion of the lower extremities may have been the greatest influence to COM motion based on the nearly similar correlation of left ankle ML motion to  $\dot{V}O_2$ . Further study of this potential relationship is warranted. The least economical runner appears to be an outlier (Figure 2), however removal of this data point did not change the correlation.

In conclusion, ML motion of the COM was the only variable significantly related to RE. Although it has been thought that excessive motion which does not contribute to forward motion may be metabolically wasteful, our result contradicts this claim.

## REFERENCES

- Cavanagh, P.R. et al. (1977). *Ann N Y Acad Sci*, **301**, 328-345.  
 Heise, G.D. et al. *Proceedings of ASB*, Abstract, 2003.  
 Saunders, P.U. et al. (1998). *Sports Med*, **34**, 465-485.  
 Williams, K.R., & Cavanagh, P.R. (1987). *J. Applied Physiology*, **63** (3), 1236-1245.

## ACKNOWLEDGEMENTS

Study funded by Wacoal, Inc. via a sub-contract with University of Colorado.

**Table 1:** Mean data values and correlations of biomechanical measures with  $\dot{V}O_2$ . \*  $p < 0.05$

	Mean $\pm$ SD	Range	$r_{\dot{V}O_2}$
$\dot{V}O_2$ (ml·kg <sup>-1</sup> ·km <sup>-1</sup> )	$214 \pm 13$	194 – 242	-----
COM (cm)	$2.2 \pm 0.9$	0.6 – 3.4	- .55*
R-Ankle (cm)	$8.4 \pm 4.6$	4.7 – 20.5	- .17
L-Ankle (cm)	$6.6 \pm 2.2$	3.5 – 11.7	- .46
R-Wrist (cm)	$17.4 \pm 7.0$	10.6 – 34.7	- .14
L-Wrist (cm)	$18.1 \pm 7.9$	7.5 – 39.9	.13

# SEGMENTAL FOOT MOBILITY IN INDIVIDUALS WITH AND WITHOUT DIABETES AND NEUROPATHY

Smita Rao<sup>1</sup>, Charles Saltzman<sup>2</sup> and John Yack<sup>1</sup>

<sup>1</sup> University of Iowa, Iowa City, IA, USA

<sup>2</sup> University of Utah, Salt Lake City, UT, USA

E-mail: smita-rao@uiowa.edu

## INTRODUCTION

Plantar ulcers develop in an estimated 15% of patients with Diabetes Mellitus (DM) (Gordois, Scuffham et al. 2003). Along with grave consequences in terms of health and functional abilities (Mueller, Sinacore et al. 2004), foot ulcers and amputation are often harbingers of personal and financial hardship. Factors contributing to increased loading on the plantar aspect of the foot and thus the potential development of foot ulcers are therefore of considerable interest.

Clinical studies have reported an association between factors intrinsic to the foot and plantar loading in subjects with DM. Limitations in subtalar (Delbridge, Perry et al. 1988) and first metatarsal mobility (Birke, Franks et al. 1995) have been reported in individuals with DM. However, evidence confirming the functional consequences of limited joint mobility in the foot is limited. The purpose of our study was to examine segmental foot mobility during gait in subjects with and without DM and neuropathy. These results are important because they may help uncover mechanisms underlying segmental foot function and plantar loading in individuals with DM.

## METHODS

All procedures were approved by the Institutional Review Board at the University of Iowa Hospitals and Clinics. 15 subjects with DM and neuropathy and 15 non-diabetic control subjects (Ctrl) participated

(Summarized in Table 1). Inclusion criteria for subjects with DM: diagnosis of DM (ADA criteria), no current foot ulcer, great toe or transmetatarsal amputation, absence of Charcot neuroarthropathy. Subjects in the control group were screened for diabetes and matched in age ( $58\pm 11$  and  $56\pm 12$  years, DM and Ctrl) and gender to subjects with DM.

	DM	Ctrl
Height (m)	$1.77\pm 0.11$	$1.75\pm 0.10$
Mass (kg)	$90.6\pm 13.8$	$74.6\pm 13.3$
VPT	$48\pm 5$	$13\pm 6$
HbA1C	$8.1\pm 1.1$	
Type 2	12 (80%)	
Duration (yrs)	$19\pm 6$	

Table 1: Summary of Subject characteristics

A multi-segment kinematic foot model (Wilken, Saltzman et al. 2004) was used. Kinematic data were collected at 120 Hz using an active marker system (Optotrak, NDI, Waterloo, Canada) for each of the following segments: first ray, forefoot, calcaneus and leg. Kinetic data were collected at 360 Hz using a forceplate embedded in the walkway (Kistler Inc, NY). Motion of the distal segment was expressed relative to the proximal segment as well as to the lab and was calculated using Euler angles (Visual 3D, C-Motion Inc) with the following sequence of rotations: sagittal, frontal and transverse. A two-sample t-test was used to assess differences between the two groups ( $\alpha=0.05$ ).

## RESULTS AND DISCUSSION

Subjects in both groups walked with similar speed ( $0.89\pm 0.13$  and  $0.93\pm 0.11$  m/s, DM and Ctrl,  $p=0.169$ ) and stride length ( $1.08\pm 0.15$  and  $1.12\pm 0.10$  m, DM and Ctrl,  $p=0.166$ ).

Segmental kinematics expressed relative to the proximal segment: Subjects with DM showed reduced sagittal and frontal plane excursion of the calcaneus relative to the tibia (Figure 1). Subjects with DM showed decreased excursion of the first metatarsal relative to the calcaneus in the frontal ( $9.8\pm 3.6^\circ$  and  $12.3\pm 3.2^\circ$  degrees, DM and Ctrl,  $p=0.03$ ) as well as transverse ( $7.1\pm 3.1^\circ$  and  $9.6\pm 3.6^\circ$ , DM and Ctrl,  $p=0.03$ ) plane.

Segmental kinematics expressed relative to the lab: The first metatarsal ( $68.8\pm 12.5^\circ$  and  $81.1\pm 8.8^\circ$ , DM and Ctrl,  $p<0.01$ ) as well as the forefoot ( $68.4\pm 12.4^\circ$  and  $81.4\pm 8.7^\circ$ , DM and Ctrl,  $p<0.01$ ) in subjects with DM showed less sagittal plane excursion through stance. In addition, the forefoot showed decreased frontal plane excursion ( $12.1\pm 3.2^\circ$  and  $16.6\pm 4.6^\circ$ , DM and Ctrl,  $p<0.01$ ) in subjects with DM. Subjects with DM showed less sagittal ( $64.1\pm 10.4^\circ$  and  $72.8\pm 7.2^\circ$ , DM and Ctrl,  $p<0.01$ ) as well as frontal plane excursion ( $9.7\pm 7.5^\circ$  and  $12.6\pm 4.6^\circ$ , DM and Ctrl,  $p=0.02$ ) of the calcaneus.

### SUMMARY AND CONCLUSIONS

Our results revealed significant differences in patterns of segmental mobility between the two groups, with DM subjects showing lower magnitudes of motion. The reductions in motion were not generalized – they were particularly dramatic in the calcaneus (20%) compared to the forefoot and first metatarsal.

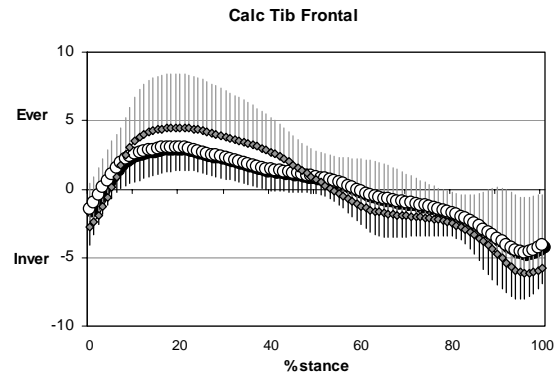


Figure 1: Ensemble averaged kinematics of the calcaneus relative to the tibia. Circles = DM, Diamonds = Ctrl; Error bars represent  $\pm 1SD$ .

Decreases in frontal plane calcaneal motion were accompanied by reduced midfoot mobility, discerned as reduced first metatarsal and forefoot motion. Our results underscore the complexity of segmental foot function during gait; motion at one joint has important consequences on motion at neighboring joints. Our findings provide new insights on the nature of impairments in segmental foot function in individuals with DM and indicate that there are dramatic differences in foot function in early stance in shock absorption and in propulsion in terminal stance.

### REFERENCES

- Birke, J. A., B. D. Franks, et al. (1995). *FAI* 16(5): 277-84.
- Delbridge, L., P. Perry, et al. (1988). *Diabet Med* 5(4): 333-7.
- Gordois, A., P. Scuffham, et al. (2003). *Diabetes Care* 26(6): 1790-5.
- Mueller, M. J., D. R. Sinacore, et al. (2004). *Diabetes Care* 27(7): 1559-64.
- Wilken, J., C. Saltzman, et al. (2004). *Summer Meeting, AOFAS, Seattle, WA.*

### ACKNOWLEDGEMENTS

This work was partially funded by NIH (RO1 NR07721-03)

## CENTER OF MASS ACCELERATION AND SLIP OUTCOME

Kurt Beschoner<sup>1</sup> and Rakié Cham<sup>1</sup>

<sup>1</sup>Department of Bioengineering, University of Pittsburgh, Pittsburgh, PA, USA

E-mail: [keb52@pitt.edu](mailto:keb52@pitt.edu)

Web: <http://www.engr.pitt.edu/hmbl/>

### INTRODUCTION

Slip, trip, and fall accidents result in 20-40% of disabling injuries in industry with as many as half of these coming from slipping alone (Courtney et al., 2001). The number of incidences and resulting injury severity increases with age (Courtney et al., 2001).

Center of mass (COM) position and velocity with respect to the base of support (BOS) are important in recovery from a slip perturbation during sit to stand tasks (Pai and Patton, 1997) and walking (Bhatt et al., 2006). Bhatt and colleagues have used an inverted pendulum model of the body to show that the sagittal plane angle and angular velocity of the COM with respect to the BOS are important predictors of “stability” during slipping (Bhatt et al., 2006). Intuitively, angular acceleration of the COM with respect to the BOS at heel contact (HC) may also be important as it affects angle and angular velocity measures. Yet, this variable has not been investigated in previous research.

Thus, the purpose of this study is to examine differences in COM angular acceleration at HC between slip-recovery and slip-fall outcomes in young and older adults.

### METHODS

*Subjects:* The study included 18 young subjects (10 female, 8 male) aged 20-35 years old and 13 older subjects (8 female and 5 male) aged 55-70 years old.

Written informed consent was obtained and subjects were excluded based on

neurological, orthopedic, cardiovascular, and pulmonary abnormalities that would affect balance or gait.

*Equipment:* Subjects walked across a vinyl tile floor wearing the same brand/model polyvinyl chloride soled work shoes. Slips were induced using a diluted glycerol contaminant (75% glycerol/25% water). Motion of 79 markers was captured using an 8 M2-camera Vicon 612 motion capture system with a sampling rate of 120 Hz. Subjects were harnessed to prevent contact with the ground in case of an irrecoverable balance loss.

*Protocol:* In order to induce an unexpected slip, subjects were told that the first few trials would be dry. After three dry trials and without the subjects' knowledge, the glycerol contaminant was applied to the floor inducing an unexpected slip.

*Data processing:* Marker data was low-pass filtered using a zero-phase 6 Hz elliptical filter. The body was modeled as a rigid body link of 15 segments and the body COM position was derived from the weighted average of the individual segments' COM. The BOS was determined as the projection of the heel marker onto the plane of the floor. The vector from the BOS to COM is projected into the sagittal plane and the angle from the resulting vector to vertical is  $\theta$  (Fig 1).

Slips were categorized as falls if the midpoint of their hips fell below 5% of

their local minimum during dry trials similar to work done by Pai and Patton (1997).

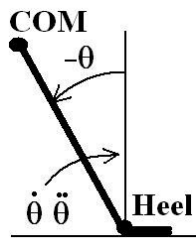


Fig. 1: Inverted pendulum model used to determine angle ( $\theta$ ) and its derivatives

## RESULTS AND DISCUSSION

Four subjects were excluded from the analysis for various experimental or technical problems. Subjects who fell during the slip had larger deviations in the profile of their angle, angular velocity and angular acceleration from baseline dry (Fig. 2). Also, initial conditions at HC were different between fall and recovery events (Fig. 2).

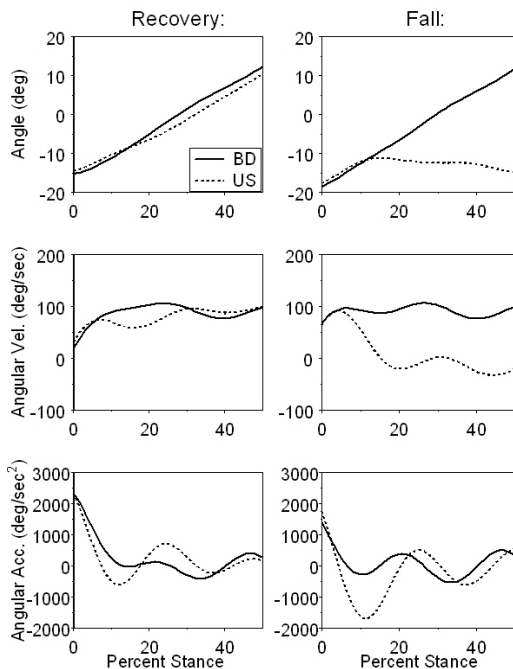


Fig 2: Typical angle, angular velocity, and angular acceleration. BD is baseline dry (solid) and US is unexpected slip (dashed). HC is 0% stance.

As mentioned previously, the focus of this abstract is on angular acceleration at HC. ANOVA was used to compare angular acceleration at HC between outcomes and age groups.

An average 34% reduction in angular acceleration at HC was found in fallers compared to non-fallers ( $p < 0.05$ ) (Fig. 3). Age group and its interaction with outcome were not significant effects. Thus, fall-recovery differences in angular acceleration at HC were similar in both age groups.

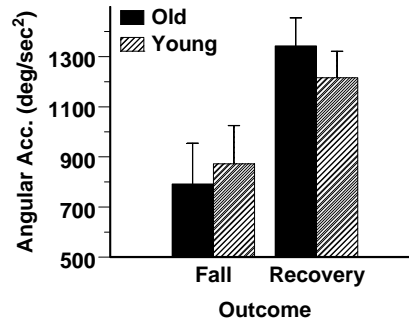


Fig 3: Angular acceleration stratified by age and outcome (SE bars)

“Thrust” push off force generated by the trailing leg produces forward and upward COM acceleration. This may be the underlying reason for the differences in angular acceleration at HC between recovery and fall outcomes, i.e. a potential predictor of slip and fall events is reduced push off thrust needed to move the COM over the BOS.

## SUMMARY/CONCLUSIONS

The results of this study demonstrate that angular acceleration at HC may be a predictor of the outcome of a slip.

## REFERENCES

- Bhatt et al. (2006). *Exp Brain Res*, **107** (1), 61-73.  
 Courtney, T.K. et al. (2001). *Ergonomics*, **44** (13), 1118-1137.  
 Pai, Y.C., Patton, J. (1997). *J. Biomechanics*, **30** (4), 347-354.

## ACKNOWLEDGEMENTS

NIOSH R03 OH007533 and Dr. Furman.

# VALIDATION OF ULTRASOUND FOR THE ESTIMATION OF MUSCLE VOLUME *IN VIVO*

Benjamin W. Infantolino<sup>1</sup>, Daniel J. Gales<sup>1,2</sup>, and John H. Challis<sup>1</sup>

<sup>1</sup> Biomechanics Laboratory, Department of Kinesiology, The Pennsylvania State University, University Park, PA, USA

<sup>2</sup> Lock Haven University of Pennsylvania, Lock Haven, PA, USA  
E-mail: bwi100@psu.edu

## INTRODUCTION

Muscle volume is correlated to the potential of a muscle to produce maximal power. *In vivo* estimation of muscle volume via the Cavalieri method has been accomplished using magnetic resonance imaging (e.g., Lund et al., 2002), computed tomography scans (e.g., Mitsiopoulos et al., 1998), and ultrasonography (e.g., Esformes et al., 2002). The Cavalieri method uses the cross-sectional area (CSA) of a muscle measured from the digitized cross-sectional views of the muscle produced by an imaging technique. Serial cross-sectional images are produced and sectional volumes are estimated using two serial CSA's and the distance between the cross-sections. The segment volumes are then summed to estimate the total muscle volume.

Muscle volume has been estimated *in vivo* using ultrasound (US), but in the current literature there is no validation of this technique for human muscle. The purpose of this study was to validate ultrasound muscle volume estimation *in vivo*. To examine validity, vastus lateralis ultrasound images were collected from cadavers before muscle dissection, after dissection the volumes were determined by hydrostatic weighing.

## METHODS

The vastus lateralis muscles of four cadavers were scanned with US prior to dissection

using a 7.5 MHz ultrasound probe (SSD-1000, Aloka, Japan) in B-mode. A standoff pad was used to optimize the US image. The scans were performed at 2 cm intervals along the muscle, except for the terminal scan, which was the length required to accommodate the remainder of the muscle. Metal guides were placed on the skin to aid in the accurate positioning of the US probe. The CSA of each US slice was recorded and then measured using Scion Image digitizing software (NIH Image, version Beta 4.0.2, National Institutes of Health, Bethesda, MD, USA). The muscle volumes (V) were estimated from the cross-sectional area using the formula,

$$V = \frac{1}{3} \sum_{i=1}^{n-1} (CSA_i^2 + 2CSA_i CSA_{i+1} + CSA_{i+1}^2) h_i$$

where  $CSA_i$  and  $CSA_{i+1}$  are successive CSA's,  $n$  is the number of CSA's and  $h_i$  is the distance between pairs of CSA's.

Three operators each performed four digitizations of one set of images of a vastus lateralis. After initial practice there was no statistical difference between operators or trials ( $p < 0.05$ ). All data reported are therefore the results of one operator.

After US imaging the eight muscles were dissected from the cadavers, and sealed in polyethylene bags to prevent fluid loss. The volumes of these muscles were determined using hydrostatic weighing.

## RESULTS

There was no statistically significant difference between the US estimation of muscle volume and that estimated using hydrostatic weighing ( $p < 0.05$ ). The mean percentage error between the two volume estimates was  $-0.4 \% \pm 5.8$ . Bland and Altman (1986) presented a graphical method for assessing the correspondence between two measures; using this method there was good correspondence between the US and hydrostatic weighing estimates of muscle volume (Figure 1).

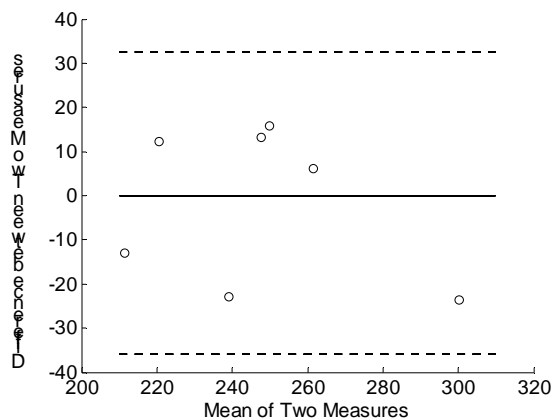


**Figure 1:** Hydrostatic weighing direct measure compared to US estimation using graphical method of Bland and Altman (1986). Upper and lower dashed lines represent the 95% confidence interval, and the solid line represents the line of identity.

## DISCUSSION

Muscle volume is an important parameter for examining the function of muscle *in vivo*, therefore it is important to have methods available for its estimation *in vivo*. This study has demonstrated that accurate estimation *in vivo* is possible using US imaging. The vastus lateralis muscle volumes ( $246.4 \text{ ml} \pm 28.1$ ) were comparable with those previously reported by Friedrich and Brand (1990) for example.

Some limitations to the study include inability to precisely control the position of the US probe, although metal guides were used to reduce this problem. It is not uncommon for the vastus lateralis to be fused to the vastus intermedius (Willan et al., 2002), which was the case in six of the eight samples. Identification of the border of the vastus lateralis did not prove problematic as evidenced by the good correspondence between the measurements made by different operators. The results were obtained in cadavers, the quality of images obtained on these specimens compares favorably with those obtained *in vivo*.

The results of this study indicate that US is an accurate method for estimating muscle volumes *in vivo*. Future studies include estimating the volume of other muscles, and the examination of atrophy and hypertrophy due to disease or injury, and training respectively.

## REFERENCES

- Bland, J. M., Altman, D. G. (1986). *Lancet*, **1**(8476), 307-310.
- Esformes, J., et al. (2002). *Eur. J. App. Physiol.*, **87**(1), 90-92.
- Friedrich, J.A., Brand R.A. (1990). *J. Biomech.*, **23**(1), 91-95.
- Lund, H., et al. (2002). *Eur. Radiol.*, **12**(12), 2982-2987.
- Mitsiopoulos, N. et al., (1998). *J. App. Physiol.*, **85**(1), 115-122.
- Willan, P. L. et al. (2002). *Clin. Anat.*, **15**(2), 116-128.

## ACKNOWLEDGEMENTS

The support of ALOKA, USA is gratefully acknowledged.

# PROFILES OF THE ATHLETICS' MARATHON COURSES

Patrycja Lipinska, Włodzimierz S. Erdmann

Sniadecki University of Physical Education and Sport, Gdansk, Poland, EU  
E-mail: werd@awf.gda.pl

## INTRODUCTION

Tactics of individual sports includes several items, e.g. use of proper garments, equipment, technique. Another important factor is knowledge of terrain and its configuration. In athletics' marathon there is important proper distribution of effort taking into account course profile. This effort is described in a way of distribution of the velocity of running. Usually a second half of a marathon is run with bigger velocity. But only by the few first runners at the finish (Lipinska, 2006). Wrong tactics, i.e., wrong distribution of running's velocity might lead to the exhaustion, contusions, or even to death.

The legend has it Greek soldier ran in full gear from Marathon, where Greeks defeated Persian Army, to Athens with a news of victory. The legend has it also he died afterward. One must say his tactics of running was wrong. In contemporary times some competitors end running in a very bad state (Figure 1) or does not end running at all (e.g. Paula Radcliffe – who holds the best world result – at Olympic Games Athens 2004).

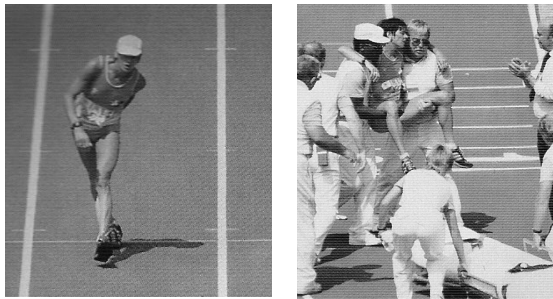


**Figure 1:** Wrong tactics of running leads to exhaustion (photos from: Moore, 1984).

The aim of the entire scientific work was investigation of running tactics of the best marathon runners taking into account geometry of the running course. The aim of this paper is presentation of the running courses' profiles of the important world marathons and their evaluation.

Since 2004 International Association of Athletics Federations (IAAF) gathers the best world times of marathon runs and considers them as the world records. In order to validate the record the distance and its measurement has to conform special requirements. Regulations are as follow: 1) distance in a straight line between start and finish points shall not be further apart than a half of a marathon distance; 2) decreasing in elevation between the start and finish shall not exceed an average of one in a thousand, i.e. 1 m vertical per 1 km horizontal; 3) it is necessary to verify a course by the IAAF or AIMS (Association of International Marathon and Road Races) at least two weeks before the run or just after the run; 4) it is necessary to mark every 5 km of a marathon distance and a half of a distance with an error not exceeding 0.1 %, i.e. 42 m for the whole marathon distance.

## MATERIAL AND METHODS

The following marathon courses were taken into account: 1) Athens (GRE), 2) Berlin (GER), 3) Boston (USA), 4) Edmonton (CDN), 5) Fukuoka (JAP), 6) Los Angeles (USA), 7) Paris (FRA), 8) Stockholm (SWE), 9) Tokyo (JAP). For all courses profiles were presented, i.e. vertical elevation (m) vs. distance

(hypotenuse, km). The profiles were obtained from the web pages of the marathon's organizers.

In order to describe difficulty of a course a coefficient of a course difficulty (Ccd) was calculated:  $Ccd = [\sum (p \times tg \alpha)] \times 100$  where: p – parameter for 1 km course's fragment (a = 1.0 for horizontal, b = 0.8 for descending, c = 1.6 for ascending (Costill, 1976)),  $\alpha$  - angle of hypotenuse of a course's fragment (Lipinska 2006). Acceptance according to IAAF / AIMS rule no. 2 was presented as „A”.

## RESULTS AND DISCUSSION

Figures 2 – 10 present profiles of investigated marathon courses. Ccd values and „A” marks were added. The lightest marathon course was that of Fukuoka, and the toughest was that of Athens. Of all investigated courses only Boston marathon course can not be accepted for world record results according to rule no. 2.



**Figure 2:** Fukuoka (JAP), Ccd = 3.0.

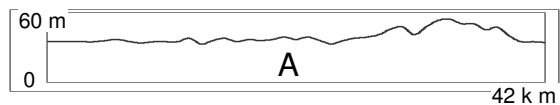


**Figure 3:** Berlin (GER), Ccd = 3.7

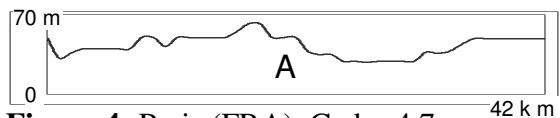


**Figure 4:** Paris (FRA), Ccd = 4.7.

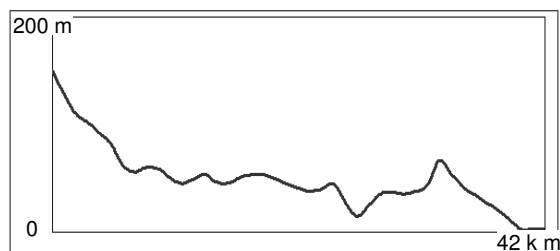


**Figure 5:** Boston (USA), Ccd = 5.4.



**Figure 6:** Tokyo (JAP), Ccd = 5.6.

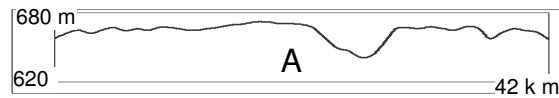


**Figure 7:** Edmonton (CDN), Ccd = 8.3.

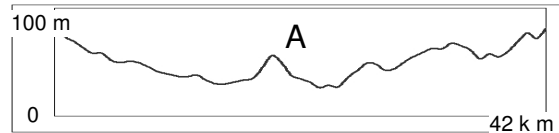


**Figure 8:** Los Angeles (USA), Ccd = 10.3.



**Figure 9:** Stockholm (SWE), Ccd = 13.2.

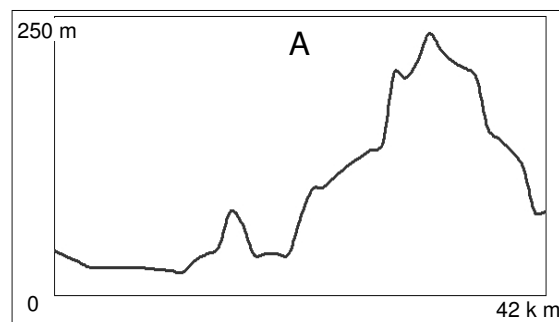


**Figure 10:** Athens (GRE), Ccd = 23.4.

## CONCLUSIONS

American marathon runners made their training runs on high altitude on the course similar to that of Athens 2004 (Wilber, 2005). During Olympic runs they obtained silver (male) and bronze (female) medals. This shows that knowing a course profile is worthwhile.

## REFERENCES

- Costill, D. L. (1976) *Competitive Sport* (in Polish), **9**, 1-76.
- Lipinska, P. (2006) *Kinematic quantities and geometry of a course and tactics of marathon run* (in Polish). Doctoral dissertation, Sniadecki University of Physical Education and Sport, Gdansk.
- Moore, K. (1984) *Sports Illustrated*, **Aug.** **13<sup>th</sup>**, 60-81.
- Wilber, R. (2005) *First ASPIRE Sport Science Conference*, Doha, Qatar.

# DO HOURS SPENT ON SPORTING ACTIVITIES INFLUENCE POSTURAL SWAY?

Ai Choo Lee, DJ. Magee, S. Warren, M. Haykowsky, T. Manns, and DC. Reid

University of Alberta, Edmonton, Alberta, Canada  
E-mail: ail@ualberta.ca Web: www.ualberta.ca

## INTRODUCTION

Postural control is an integral component of all movement. (Westcott et al., 1997) Postural control has been defined as the ability to maintain the center of body mass or center of gravity (CG) over the base of support (BS) to attain the desired positions or movement without falling. (Westcott et al., 1997) Deviation from this center of balance in any direction represents postural sway. (Winter et al., 1990), (Horak, 1987).

Ability to maintain postural control under dynamic conditions is an important underlying component of physical activity or performance. (Irrgang et al., 1994) Dysfunction in postural control may cause function loss as well as restricted mobility. Decline in postural control is influenced by inactivity, yet several studies have shown that the practice of sporting activities at various levels of skill improves postural performances and reduces the number of falls in elderly. (Perrin et al., 1999)(Lord & Castell, 1994)

Investigations on the effects of sporting activities on postural sway have rarely been performed. Based on the premise that practicing sporting activities had a positive effect on postural control on elderly, the question considered by the present research was whether and to what extent hours spent on sporting activities influenced postural sway of healthy young females.

The purpose of this study was to determine if females who were vigorously practicing sporting activities five hours or more per

week (Group 1) have better postural sway control when compared with those who were moderately practicing sporting activities less than five hour per week (Group 2) in competition or as an active pastime pleasure.

## METHODS

A total of 40 healthy young females age ranging from 20 to 49 years were recruited in this study. They had all engaged in some sporting activities weekly. They were free from lower limbs injuries, had normal visual and vestibular functions, and did not show any musculoskeletal disorder of all joints. The subjects comprised 20 vigorously active healthy females and 20 moderately active healthy females with average age of  $30 \pm 7$  years. Before the evaluation process, a self-reported questionnaire was administered to record the types of sporting activities and hours spent on sporting activities weekly.

To quantify the amount of postural sway in three postural sway measures i.e. overall sway, anterior-posterior sway, and medial-lateral sway, subjects were required to evaluate on six combine conditions included: 1) bilateral on stable platform with eyes-closed, 2) bilateral on platform moving up and down with eyes-open, 3) right leg on stable platform with eyes-closed, 4) left leg on stable platform with eyes-closed, 5) left leg on platform moving linearly with eyes-open, and 6) right leg on platform moving linearly with eyes-open, using the Chattecx Dynamic Balance System. All subjects were tested for their static and dynamic balance. Each subject was evaluated twice for a 10-

second evaluation. Average scores from two repetitions were used for data analysis.

## RESULTS AND DISCUSSION

Study findings indicated that vigorously active females sway lesser than moderately active females for all three postural sway measures when testing on static balance and dynamic balance. But, the difference did not show statistically significant for both static and dynamic balance (Table 1).

The findings were contradictory with the previous studies. The authors concluded that practicing physical and sporting activities had a positive effect on balance and postural control of elderly, thus reducing the risk of falling significantly. (Perrin et al., 1999)(Lord & Castell, 1994) We noted that it was due to the different study population of interest. According to literatures, the effects of training on postural stability are related to the degree of the initial instability. Generally, the elderly adults (over 60 years) demonstrated poorer initial postural stability compared with young adults. Therefore, it is assumed that the elderly adults would show greater effect after sporting activities due to their initial instability. The healthy young adults might need to exercise to a higher threshold for improvement.

## SUMMARY/CONCLUSIONS

The study findings suggested that the hours spent on sporting activities did not influence the amount of postural sway in all three measures i.e. overall sway, anterior-posterior sway and medial-lateral sway on

healthy young females when testing on static and dynamic balance.

## REFERENCES

- Horak FB. (1987). Clinical measurement of postural control in adults. *Phys Ther*, **27** (12):1881-5.
- Irrgang JJ, Whitney SL, Cox ED. (1994). Balance and proprioceptive training for rehabilitation of the lower extremity. *Journal of Sport Rehabilitation*, **3**:68-83.
- Lord S, Castell S. (1994). Effect of exercise on balance, strength and reaction time in older people. *Australian Physiotherapy*, **40**:83-8.
- Perrin P, Gauchard G, Perrot C, Jeandel C. (1999). Effects of physical and sporting activities on balance control in elderly people. *Br J Sports Med*, **33**:121-6.
- Westcott S, Lowes L, Richardson P. (1997). Evaluation of postural stability in children: Current theories and assessment tools. *Phys Ther*, **77**:629-45.
- Winter D, Patla A, Frank J. (1990). Assessment of balance control in humans. *Medical Program of Technology*, **16**:31-51.

## ACKNOWLEDGEMENTS

Ai Choo Lee was supported by the “The Canadian Commonwealth Scholarship and Fellowship Program”, “The Malaysian Academic Training Scholarship”, and “The Delta Kappa Gamma World Fellowships for Key Women Educators, USA”.

**Table 1:** Postural sway measures for static and dynamic balance with mean  $\pm$  SD and t-test between Group 1 and Group 2

<b>Postural Sway Measures for Static Balance</b>				
<b>Variables</b>	<b>Group 1 (cm)</b>	<b>Group 2 (cm)</b>	<b><i>t</i></b>	<b><i>*p</i></b>
Overall Sway	M $\pm$ SD 0.88 $\pm$ 0.17	M $\pm$ SD 0.94 $\pm$ 0.22	-0.859	0.40
Anterior-posterior Sway	M $\pm$ SD 3.51 $\pm$ 0.77	M $\pm$ SD 3.76 $\pm$ 1.11	-0.837	0.41
Medial-lateral Sway	M $\pm$ SD 1.96 $\pm$ 0.29	M $\pm$ SD 2.09 $\pm$ 0.38	-1.162	0.25
<b>Postural Sway Measures for Dynamic Balance</b>				
<b>Variables</b>	<b>Group 1 (cm)</b>	<b>Group 2 (cm)</b>	<b><i>t</i></b>	<b><i>*p</i></b>
Overall Sway	M $\pm$ SD 1.00 $\pm$ 0.12	M $\pm$ SD 1.07 $\pm$ 0.18	-1.445	0.16
Anterior-posterior Sway	M $\pm$ SD 4.59 $\pm$ 0.60	M $\pm$ SD 4.63 $\pm$ 0.71	-0.164	0.87
Medial-lateral Sway	M $\pm$ SD 1.30 $\pm$ 0.19	M $\pm$ SD 1.34 $\pm$ 0.28	-0.546	0.59

# THE EFFECT OF TORQUE DIRECTION ON HAND-OBJECT COUPLING

Na Jin Seo and Thomas J. Armstrong

University of Michigan, Ann Arbor, MI, USA  
E-mail: najins@umich.edu

## INTRODUCTION

Torque is applied with the hands in many activities at work, daily living and recreation. Some examples are joining and removing threaded and non-threaded parts such as containers and vacuum hoses, using hand tools, and using controls.

Torque that can be produced on a handle is related to the radius of the handle and the friction force acting tangentially to the surface. Previous studies have shown that friction is related to the normal force and coefficient of friction between the hand and the handle (Pheasant and O'Neill 1975). The coefficient of friction itself is related to contact force, handle material (Buchholz et al. 1988) and texture and the presence of lubrications (Bobjer et al. 1993). The normal force is related to the grip strength of the individual. It is hypothesized that skin friction produced by twisting an object in the direction of the fingertips causes palmar flexion of the phalanges and increases grip force and torque (see Figure 1).

## METHODS

To test the proposed hypothesis, an experiment was conducted in which 12 subjects (6 females and 6 males, age = 21 to 35, mean age = 26.7) performed isometric maximum torque exertions on a cylindrical handle in the counter-clockwise and clockwise direction when viewed from the lateral side of the hand (see Figure 2).

Two halves of the cylindrical handle were

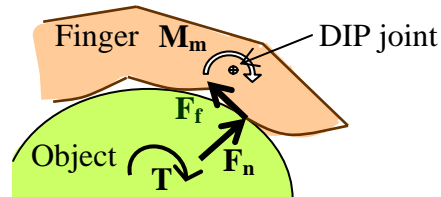


**Figure 1:** Friction force ( $F_f$ ) causes increase in normal force ( $F_n$ ), thus increased torque ( $T$ ), for a given muscle strength ( $M_m$ ).

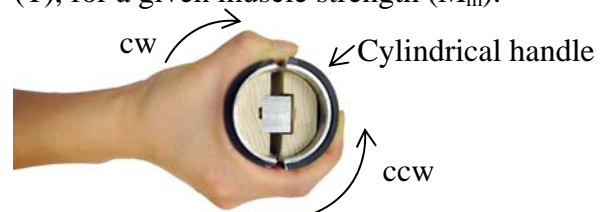


**Figure 2:** Direction of the counter-clockwise (ccw) and clockwise (cw) rotation

separated via a force transducer. The handle was covered with a pressure sensitive pad (Tekscan Pressure Measurement System) that recorded normal pressure at each 5.08 by 5.08mm sensor. The pressure pad was covered with a 3.5 mm-thick sheet of rubber. Handle diameters of 38.1, 50.8 and 76.2mm were tested. This presentation will discuss the results for the 50.8mm handle.

Subjects' grip strength measured with a Jamar dynamometer (2<sup>nd</sup> position) and wrist strength measured using a BTE Work Simulator (wrist neutral) is summarized in Table 1. All exertions were performed with a right hand in a random order.

**Table 1:** Grip strength, wrist flexion and extension strength by gender (mean  $\pm$  SD)

	Male	Female
Grip (N)	442 $\pm$ 107	215 $\pm$ 101
Flexion (Nm)	15.6 $\pm$ 5.1	6.2 $\pm$ 3.2
Extension (Nm)	11.6 $\pm$ 3.6	5.0 $\pm$ 2.0

## RESULTS

The maximum torque, grip force, contact area, total normal force (arithmetic sum of normal forces around the handle) and fingertip force (normal forces on the index to little fingers' distal phalanges) for the clockwise and counter-clockwise rotations are shown by gender in Table 2. The maximum torque was 33% greater for the counter-clockwise rotation than clockwise rotation (gender pooled,  $p < 0.05$ ). Total normal force and fingertip force were 25% and 42% greater, respectively, for the counter-clockwise rotation than for clockwise rotation (gender pooled,  $p < 0.05$ ).

Figure 3 shows a representative recording of the pressure distribution for a clockwise and counter-clockwise rotation. Forces were concentrated on the index to little fingers' fingertips more so for the counter-clockwise rotation than for the clockwise rotation. More contact and force were observed on the thenar area for the clockwise rotation than for the counter-clockwise rotation.

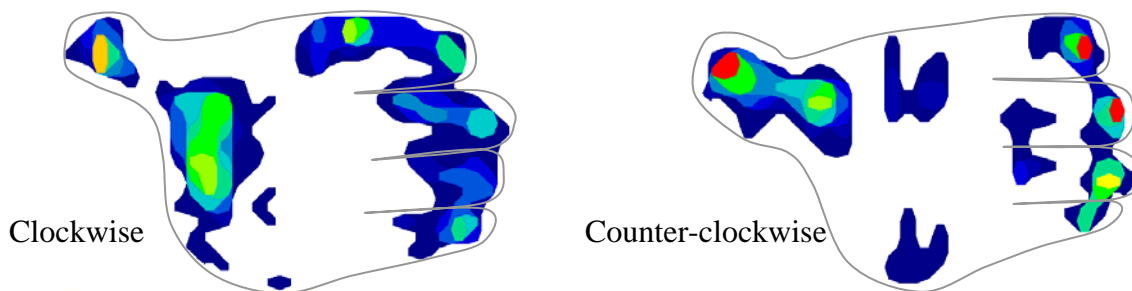


**Figure 3:** A typical force distribution during the clockwise and counter-clockwise rotation

**Table 2:** The maximum torque, grip force, contact area, total normal force (arithmetic sum of normal forces around the handle) and fingertip force (normal forces on the index to little fingers' distal phalanges) for clockwise (cw) and counter-clockwise (ccw) rotations (mean  $\pm$  SD)

Gender	Direction	Torque (Nm)	Grip force (N)	Contact area (cm <sup>2</sup> )	Total normal force (N)	Fingertip force (N)
Male	cw	5.3 $\pm$ 1.3	173 $\pm$ 41	63 $\pm$ 19	261 $\pm$ 99	116 $\pm$ 52
	ccw	7.2 $\pm$ 1.7	198 $\pm$ 91	65 $\pm$ 14	342 $\pm$ 123	172 $\pm$ 65
Female	cw	2.2 $\pm$ 1.5	106 $\pm$ 87	62 $\pm$ 19	145 $\pm$ 27	67 $\pm$ 21
	ccw	2.9 $\pm$ 2.5	107 $\pm$ 94	60 $\pm$ 18	168 $\pm$ 48	88 $\pm$ 24

## DISCUSSION AND CONCLUSIONS

By comparing wrist strengths (Table 1) and maximum torques, it can be seen that the coupling between the hand and the work object is the limiting torque factor – not the wrist. The increase in torque, total normal force and fingertip force for the counter-clockwise exertion supports the proposed hypothesis: the maximum torque is greater for the counter-clockwise than the clockwise rotation.

Forces were concentrated on the distal phalanges, thumb and thenar area. For the counter-clockwise rotation, greater forces were concentrated on the index to little fingers' fingertips.

## REFERENCES

- Pheasant, S., O'Neill, D. (1975). *Applied Ergonomics*, **6**, 4, 205-208.  
 Buchholz, B. et al. (1988). *Ergonomics*, **31**, 317-325.  
 Bobjer, O. et al. (1993). *Applied Ergonomics*, **24**, 190-202.

# TEST-RETEST REPEATABILITY OF KINEMATICS AND RANGE OF MOTION IN CHILDREN DIAGNOSED WITH HYPERMOBILITY SYNDROME

F. Fatoye<sup>1</sup>, F. Macmillan<sup>1</sup>, S. Palmer<sup>2</sup>, P. Rowe<sup>3</sup>, M. van der Linden<sup>1</sup>, S. Wilkinson<sup>4</sup>.

<sup>1</sup>Physiotherapy Subject Area, Queen Margaret University College, Edinburgh, UK; <sup>2</sup>Faculty of Health & Social Care, University of the West of England; <sup>3</sup>Bioengineering Unit, University of Strathclyde, Glasgow, UK; <sup>4</sup>Physiotherapy Department, Royal Hospital for Sick Children, Edinburgh, UK. Email: [ffatoye@qmuc.ac.uk](mailto:ffatoye@qmuc.ac.uk)

## INTRODUCTION

Gait analysis and passive ROM are frequently assessed in patients with knee complaints and gait abnormalities have been observed in children with hypermobility syndrome (HMS) (Adib et al 2005). Repeatability of walking patterns has been described in healthy children (Gorton et al 1997) but not in children with HMS. Therefore, this study investigated the test-retest repeatability of knee kinematics during walking and also knee ROM measurements in both healthy children and those with HMS.

## METHODS

Ten healthy children (mean age  $\pm$  SD =  $9.9 \pm 2.1$  years, range 8-15 years) and ten children with HMS (mean age  $\pm$  SD =  $11.8 \pm 1.3$  years, range 9-13 years) were examined. Sagittal motion during walking and passive ROM of the knee joint were assessed on two separate occasions, one week apart. The study was approved by the City of Edinburgh Council Education Department, and the QMUC and NHS Lothian Ethics Committees. Informed written consent was obtained from the participants and their parents. In healthy children the test knee was chosen at random, while the most painful knee was examined in children with HMS. Sagittal knee motion was recorded using a VICON camera

system (Oxford Metrics, England) while participants walked six times barefoot on a 7 meter walkway at their self-selected speed. Average knee joint angles were calculated for each participant. Passive knee ROM (flexion and extension) was measured with a universal goniometer. Intraclass correlation coefficient (ICC) and 95% limits of agreement (LOA) were used for data analysis.

## RESULTS AND DISCUSSION

Tables 1 and 2 demonstrate the ICC values and 95% LOA for all the variables in healthy children and the HMS cohort respectively. Repeatability of passive ROM measurements was excellent in both groups. Based on the ICC, repeatability of KFLR in the healthy group and MKF in the HMS group was excellent. However, KEMS and MKF were measured with low to moderate repeatability in healthy children. The repeatability of KEMS and KFLR was also low to moderate in the HMS cohort. 95% LOA revealed a small variation between repeated measurements of knee passive ROM and kinematics in both groups except for MKF in healthy children. Therefore, these findings indicate good agreement between the measurement parameters except for MKF in healthy children.

Table 1. ICC and 95% limits of agreement for sagittal knee motion and passive flexion in healthy children.

	Sagittal knee motion (°)			Passive Knee ROM (°)	
	KEMS	KFLR	MKF	Extension	Flexion
ICC	0.74	0.84	0.48	0.95	0.96
95% LOA (°)	-7.75 - 10.28	-6.15 - 7.59	-12.91 - 17.42	-1.07 - 1.47	-1.95 - 1.35

ICC = Intraclass correlation coefficient, KEMS = knee extension in mid stance, FLR= Knee flexion during loading response, MKF = Maximum knee flexion during swing phase, LOA = Limits of agreement.

Table 2. ICC and 95% limits of agreement for sagittal knee motion and passive knee flexion for children with HMS.

	Sagittal knee motion (°)			Passive Knee ROM (°)	
	KEMS	KFLR	MKF	Extension	Flexion
ICC	0.68	0.48	0.81	0.90	0.96
95% LOA (°)	-5.74 - 7.38	-8.50 - 8.95	-4.07 - 4.86	-1.47 - 1.07	-1.38 - 1.78

ICC = Intraclass correlation coefficient, KEMS = knee extension in mid stance, FLR= Knee flexion during loading response, MKF = Maximum knee flexion during swing phase, LOA = Limits of agreement.

## SUMMARY/CONCLUSION

Between days repeatability of kinematics and passive ROM of the knee joint was investigated in healthy children and those with HMS. Based on the ICC values, this study suggests that PROM can be measured repeatedly in children using a universal goniometer while knee kinematics data (MKF in healthy children and KFLR in those with HMS) are not very repeatable. However, 95% LOA showed good agreement between repeated measurements of all the

parameters in both groups except for MKF. Therefore, the findings of the present study suggest that major clinical decisions can be based on one assessment of knee kinematics and passive ROM in children.

## REFERENCES

- Adib et al (2005). Rheumatology 44: 744 – 750  
 Gorton et al (1997). Gait and Posture 5 (2): 155

# UNCONSTRAINED SHOULDER JOINT POSITION SENSE IMPROVES WITH EXTERNAL LOAD

David N. Suprak, Louis R. Osternig, Paul van Donkelaar, and Andrew R. Karduna

University of Oregon, Eugene, OR, USA  
Email: karduna@uoregon.edu

## INTRODUCTION

Joint position sense (JPS) contributes to the maintenance of muscle stiffness and coordination about a joint to produce smooth limb movements and prevent injury. It is afforded by afferent signals from capsuloligamentous and musculotendinous mechanoreceptors in and around the joint. Musculotendinous mechanoreceptors (muscle spindles and golgi tendon organs, GTO) are the primary contributors to JPS, especially in the middle ranges of motion (Shields, 2005).

Both the GTOs and muscle spindles increase firing with increases in muscle activation levels (Gregory, 2002). The elevation of gamma motoneuron firing frequency enhances the sensitivity of the muscle spindle afferents to a given change in muscle length (Durbaba, 2001).

Previous data from our laboratory indicate that shoulder JPS improves as the position approaches 90° of elevation (Suprak, 2006). These results suggest that increases in muscle activation levels may result in improved JPS, since external shoulder torque and muscle activation increase as shoulder elevation angles approach 90°. However, the direct effects of muscle activation on JPS acuity remain to be elucidated. The purpose of the present study was to directly examine the effect of external load on unconstrained JPS.

## METHODS

Twenty-four subjects (10 males, 14 females) participated in the study. Following a standardized warm-up procedure, subjects were fitted with a head-mounted display and asked to remove shirts (females wore sports bras) to minimize visual and tactile cues (Figure 1). Kinematic data were collected via the Polhemus Fastrak magnetic tracking system, with one receiver on the thorax and one on the humerus.

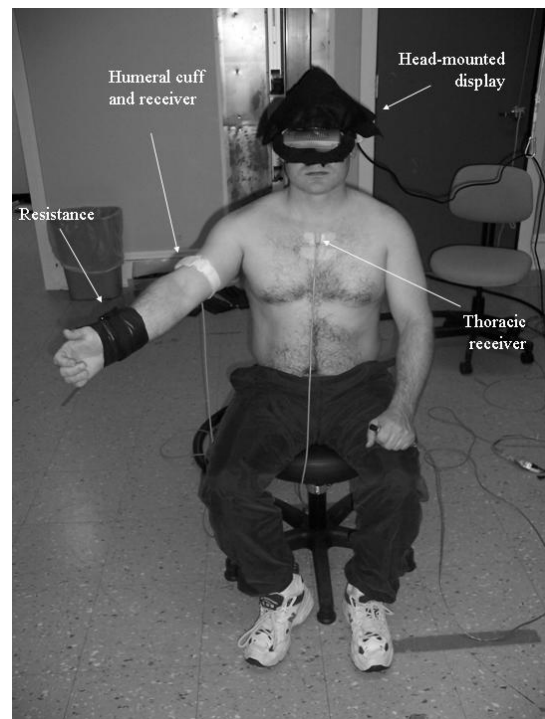


Figure 1. Experimental Set-up

Five conditions of external loading were presented. These conditions were based on the resistance (placed at the wrist) required to create an external shoulder torque

equivalent to 0% (no resistance), 10%, 20%, 30%, and 40% of the baseline torque due to the mass and length of the unloaded arm, forearm, and hand at 50° of elevation.

Within each condition, subjects were presented with a target shoulder position consisting of 50° of elevation in a plane 35° anterior to the coronal plane (scapular plane), via custom-made Labview software through the head-mounted display. Once the target position was achieved, the display turned black and remained so for the remainder of the trial. Subjects held the position for five seconds, and returned to the side. Subjects then attempted to replicate the target position in three dimensions, in the absence of visual cues. Two repositioning trials were recorded under each loading condition.

## RESULTS AND DISCUSSION

Vector repositioning error (angle between humerus at presented and reproduced positions) decreased linearly as external resistance increased ( $p = 0.019$ ) (Figure 2). However, a repeated measures analysis of variance (ANOVA) revealed no significant main effect of resistance on vector error ( $p = 0.09$ ).

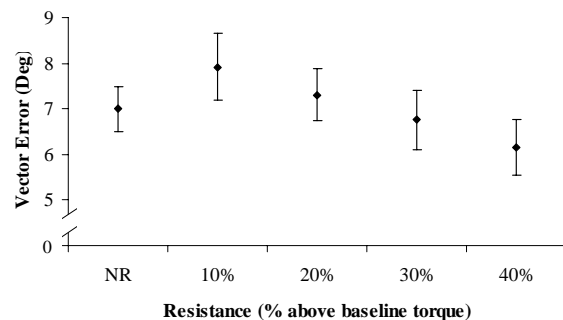


Figure 2. Effect of load on vector error

No significant main effect or linear contrast was found with respect to the repositioning error in the plane angle ( $p = 0.51$  and  $p = 0.39$ , respectively). However, elevation

angle error was significantly affected by external resistance ( $p = 0.02$ ) (Figure 3). Also, elevation angle error decreased linearly with increases in resistance ( $p = 0.02$ ).

Since no effect or significant linear contrast was found in plane error, adding this element into the vector error may have contributed only random error to the signal. The effect of resistance on error in elevation angle, together with the data from vector and plane angle errors, suggest that JPS is improved with increases in load, presumably owing to enhanced musculotendinous mechanoreceptor sensitivity. In addition, it appears that this improved JPS is only evident in the direction coincident with the load.

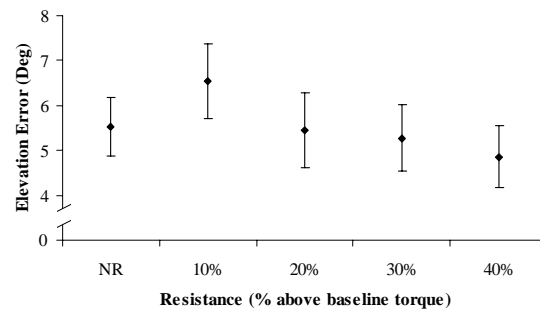


Figure 3. Effect of load on elevation error

## SUMMARY/CONCLUSIONS

Our results indicate that JPS improves with increasing resistance, but only in the direction of the load.

## REFERENCES

- Durbaba, R. et al. (2001). *J Physiol*, **532**, 563-74.
- Gregory, J.E. et al. (2002). *J Physiol*, **538**, 209-18.
- Shields, R.K. et al. (2005). *J Orthop Sports Phys Ther*, **35**, 443-51.
- Suprak, D.N. et al. (2006). *J Orthop Res*, **24**, 559-68.

# RELATIONSHIP BETWEEN KNEE KINAESTHESIA AND JOINT POSITION SENSE IN HEALTHY CHILDREN

F. Fatoye<sup>1</sup>, F. Macmillan<sup>1</sup>, S. Palmer<sup>2</sup>, P. Rowe<sup>3</sup>, M. van der Linden<sup>1</sup>, S. Wilkinson<sup>4</sup>.

<sup>1</sup>Physiotherapy Subject Area, Queen Margaret University College, Edinburgh, UK; <sup>2</sup>Faculty of Health & Social Care, University of the West of England; <sup>3</sup>Bioengineering Unit, University of Strathclyde, Glasgow, UK; <sup>4</sup>Physiotherapy Department, Royal Hospital for Sick Children, Edinburgh, UK. Email: [ffatoye@qmuc.ac.uk](mailto:ffatoye@qmuc.ac.uk)

## INTRODUCTION

Joint kinaesthesia (JK) and joint position sense (JPS) are two techniques commonly used for testing proprioception of the knee joint (Corrigan et al 1992). The two proprioceptive tests have been shown to elicit different responses in the same group of subjects (Friden et al 1997). Moreover, in adults, lack of correlation has been observed between the two tests (Grob et al 2002). It is currently unknown whether, in children, similar disparities are evident in the relationship between the two techniques. Therefore, this issue was examined in healthy children.

## METHODS

Thirty-seven healthy children (mean age  $11.5 \pm SD 2.6$  years) participated in this investigation. The study was approved by the City of Edinburgh Council Education Department and Queen Margaret University College Ethics Committee. Informed written

consent was obtained from the participants and their parents. Knee JK was assessed at 60 degrees of knee flexion and JPS was examined at both 25 and 10 degrees of knee flexion using a motorised proprioception assessment device. JK was calculated as the threshold for passive movement while absolute angular error (AAE) was calculated as the difference between the target and perceived angles for JPS tests. Spearman Rho Correlation analysis was used to determine the relationship between the measures of proprioception.

## RESULTS AND DISCUSSION

In Table 1 the findings of this study demonstrated a weak correlation between JK and the JPS test at 25°. A slightly stronger and statistically significant relationship was found between JK and JPS at 10°. A weak negative correlation was observed between JPS tests at the two test angles.

Table 1: Spearman Correlation between proprioceptive measures

Variables	r values	p values
JK at 60° and JPS 25°	0.150	0.374
JK at 60° and JPS at 10°	0.385	0.019*
JPS at 25° and 10°	-0.116	0.495

r = Spearman correlation coefficient; \*statistically significant at  $\alpha < 0.05$ .

(JK = joint kinaesthesia; JPS = joint position sense).

## **SUMMARY/CONCLUSIONS**

The relationship between JK and JPS was examined in healthy children in this study. The findings indicate no strong correlation between these two proprioceptive measures. Given the results of the present investigation, the findings of one proprioceptive test in children cannot be substituted for the other. Clinicians are to be aware of this and should not make clinical judgement based on independent tests of either joint kinaesthesia or position sense. Therefore, these findings

provide justification for continual use of both tests for knee proprioception assessment as they are assessing two different proprioceptive systems, both of which might be important for normal function.

## **REFERENCES**

- Corrigan et al (1992): *Journal of Bone and Joint Surgery* 74B (2): 247 – 250.  
Friden et al (1997): *Journal of Orthopaedic Research* 15: 637 – 644.  
Grob et al (2002): *Journal of Bone and Joint Surgery* 84B: 614 -618.

# KINEMATIC ANALYSIS OF THE 100-METER WHEELCHAIR RACE

John W. Chow<sup>1</sup> and Woen-sik Chae<sup>2</sup>

<sup>1</sup> Department of Applied Physiology & Kinesiology, University of Florida, Gainesville, FL, USA

<sup>2</sup> Department of Physical Education, Kyungpook National University, Daegu, Korea

E-mail: jchow@hhp.ufl.edu Web: www.hhp.ufl.edu/apk/ces/labs/biomech/

## INTRODUCTION

In general, an able-bodied runner can reach the maximum speed in about 30-50 m and can maintain the maximum speed for 20-40 m before decelerating toward the end of a 100-m run. Although the speeds of able-bodied subjects during sprinting are well-documented, the corresponding data for the wheelchair racers are not currently available. The purpose of this study was to compare the speed and selected stroke cycle characteristics during different phases of the 100-m wheelchair race.

## METHODS

Four male and 2 female T4 (functional upper extremities, abdominal, and lower back muscles) and 1 male and 3 female T3 (same as T4 except no functional abdominal and lower back muscles) highly-trained track athletes served as the subjects (age  $15.2 \pm 1.9$  and  $19.2 \pm 4.7$  yrs for females and males, respectively). Trials were conducted on a synthetic-surfaced track and each subject was asked to complete two 100-m races. Two subjects were tested at one time and competed in adjacent lanes.

Two S-VHS camcorders (Panasonic AG455, 60 fps) were used to cover the 1st and 2nd 50 m of the 100-m race, respectively. Forty-two background markers were placed at 5-m intervals along lanes 5 and 8. The cameras were panned horizontally to follow both subjects in each trial.

For the purpose of this study, a *stroke cycle* begins at the instant of initial hand contact with the handring and ends at the next initial contact. The instant the hands break contact with the handring (hand release) is used to divide a stroke into 2 phases — the *push* and *recovery phases*. The contact distance of a stroke is defined as the shortest distance between the location of the bottom of the front wheel and the starting line at the instant of initial hand contact (Figure 1). The trial with the shorter 100-m time from each subject was selected for subsequent analysis. For each trial being analyzed, the video fields for the instants of initial contacts were analyzed. A Peak motion measurement system was used to extract coordinate data from the video recordings. The contact distance of a stroke was determined using the procedures described by Chow (1987) and Hay and Koh (1988).

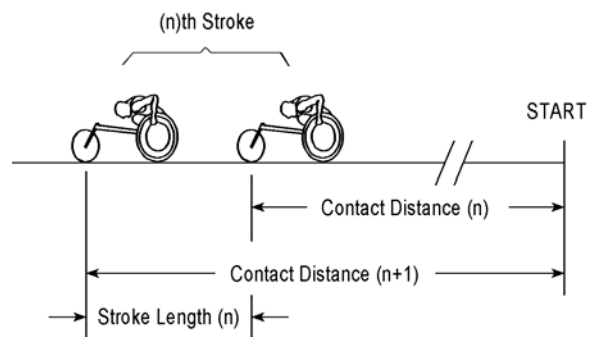


**Figure 1:** Contact distances were used to determine stroke lengths.

Stroke, push and recovery times were determined using field numbers for initial hand contacts and hand releases, and the known video field rate. The average speed

of a stroke was obtained by dividing the stroke length by the stroke time.

The maximum speed phase (MSP) is defined as the part of the 100-m race that consists of the five consecutive strokes that together have the largest average speed value. For each kinematic parameter, the average value during the first 10 m (initial phase, IP), the MSP, and the last 10 m (final phase, FP) of the race were determined. For each parameter, an ANOVA with repeat measures was performed and Tukey HSD post-hoc tests were completed when a significant main effect was found.

## RESULTS AND DISCUSSION

The 100-m times for the trials analyzed ranged from 16.10 s (a T4 male) to 22.18 s (a T3 female) (mean  $18.95 \pm 1.97$  s). Except for stroke frequency and stroke time, significant differences were found between IP and MSP and between IP and FP in all other parameters. No significant differences were found between MSP and FP in any of the measures.

The distance and time needed to reach the beginning of the MSP ranged from 48.4 m and 11.92 s (a T4 female) to 88.1 m and 18.77 s (a T3 female). Two of the subjects did not reach their maximum speed until the end of the 100 m. Comparing to able-bodied runners, wheelchair racers generally

need longer time and distance to reach their maximum speeds. The lower maximum speed and the longer time needed to reach the maximum speed explain why wheelchair racers have much greater 100-m times than able-bodied runners.

There was a significant decrease in push time (or increase in recovery time) when going from IP to MSP. However, stroke frequency (reciprocal of stroke time) values were relatively constant for different phases. This may suggest that racing wheelchair athletes like to maintain the same stroking rhythm throughout a 100-m race.

## SUMMARY/CONCLUSIONS

Wheelchair 100-m is a race of acceleration. Athletes should focus on training methods that will shorten the duration of acceleration. The maximum speed values can be useful in determining the load setting in training on a roller system.

## REFERENCES

- Chow, J.W. (1987). *Int. J. Sports Biomech.*, **3**, 110-127.  
 Hay, J.G., Koh, T.J. (1988). *Int. J. Sports Biomech.*, **4**, 372-392.

## ACKNOWLEDGEMENTS

Wheelchair Sports, USA (WSUSA).

**Table 1:** Means (SDs) of different kinematic characteristics during different phases.

Phase	Speed (m/s)	Stroke length (m)	Stroke frequency (Hz)	Stroke Time (s)	Push Time (s)	Relative push time (%)	Recovery time (s)	Relative recovery time (%)
IP	2.69 <sup>*#</sup> (0.22)	1.463 <sup>*#</sup> (0.101)	1.85 (0.16)	0.545 (0.048)	0.274 <sup>*#</sup> (0.021)	50.4 <sup>*#</sup> (3.1)	0.271 <sup>*#</sup> (0.036)	49.6 <sup>*#</sup> (3.1)
MSP	6.60 <sup>*</sup> (0.71)	3.419 <sup>*</sup> (0.656)	1.97 (0.21)	0.514 (0.052)	0.117 <sup>*</sup> (0.020)	22.8 <sup>*</sup> (5.5)	0.398 <sup>*</sup> (0.063)	77.2 <sup>*</sup> (5.5)
FP	6.46 <sup>#</sup> (0.82)	3.562 <sup>#</sup> (0.570)	1.84 (0.18)	0.546 (0.041)	0.116 <sup>#</sup> (0.078)	21.6 <sup>#</sup> (5.7)	0.430 <sup>#</sup> (0.059)	78.4 <sup>#</sup> (5.7)

Note: Significant difference between <sup>\*</sup>IP and MSP or <sup>#</sup>IP and FP ( $p < 0.001$ ).

# ANALYSIS OF JOINT KINEMATICS DURING QUIET STANDING FOLLOWING LOCALIZED LUMBAR EXTENSOR FATIGUE

Bradley S. Davidson, Michael L. Madigan, Maury A. Nussbaum

Virginia Tech, Blacksburg, VA, USA

E-mail: [bsd@vt.edu](mailto:bsd@vt.edu) Web: [www.biomechanics.esm.vt.edu](http://www.biomechanics.esm.vt.edu)

## INTRODUCTION

In recent years, many studies have reported increases in postural sway with localized muscle fatigue. Results of these studies have shown increases in sway based on characteristics of the center of pressure (COP) and center of mass (COM) trajectories. While these measures are certainly important in assessing postural stability and control (Maki et al., 1991), they are limited in discerning postural strategies and movement patterns (Kuo et al., 1998). Therefore, in order to advance our understanding of these reported changes in postural sway following fatigue, it is necessary to employ measures which are more sensitive to subtle changes in body movements.

The purpose of this investigation was to characterize changes in postural sway and postural control during quiet standing using joint kinematics. It is not clear what changes in body movements contribute to the reported increases in COP and COM-based measures of sway. Are the effects local to the site of fatigue? Is there any evidence of changes in postural strategy which are indicative of changes in postural control? To answer these questions, changes in COP, COM, and joint kinematics were analyzed during quiet standing following localized lumbar extensor fatigue.

## METHODS

Twelve physically active males with no reported history of low back pain

participated in the experiment. Participants attended three experimental sessions. During each session, postural sway was recorded before and after a lumbar extensor fatiguing protocol. This protocol consisted of lumbar extensor exercises performed on a 45° roman chair with intermittent assessment of fatigue level by measuring the maximum possible torque exerted around the low back, approximately L3 (Davidson et al., 2004).

Body position and COP data during quiet standing were collected for 30 seconds both before and after the lumbar fatigue protocol. During these collections, instructions were given to “stand as still and as quietly as possible” with feet together, eyes closed, and arms at their sides.

Posture in the anterior-posterior (AP) plane was described using (1) mean COM and COP position; (2) mean joint angles. Postural sway was described using (1) standard deviation (SD) of COM and COP position; (2) SD of ankle, knee, hip, and back angles; and (3) SD of ankle, knee, hip, and back angular velocities. Cross correlations of selected variables were also performed to quantify AP postural strategy in terms of the so-called ankle strategy and hip strategy: (1) ankle angle and COM position; (2) hip angle and COM position; (3) ankle and angle and hip angle. A two-way repeated measures ANOVA was used to determine the significant effects of fatigue on the dependent variables.

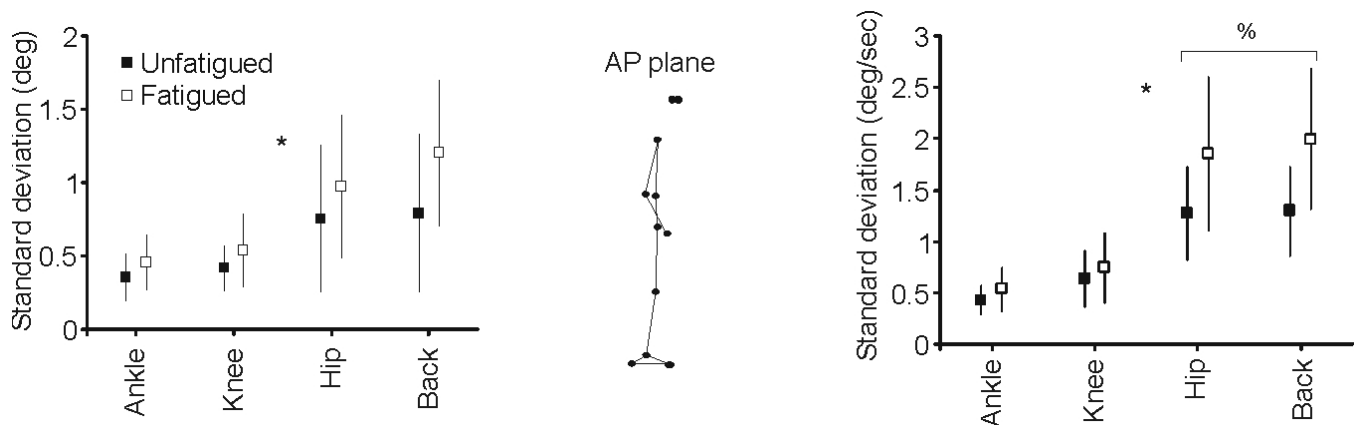


**Figure 1:** Effects of fatigue on joint kinematics. Left plot shows SD of joint angles and right plot shows SD of joint angular velocities. \* indicates significant fatigue effect ( $p < 0.001$ ). % indicates increases in hip and back were more pronounced than at ankle and knee ( $p < 0.05$ ).

## RESULTS AND DISCUSSION

Three main findings emerged from this investigation. First, participants adopted a slightly forward lean when fatigued. Second, changes in sway involved increased variability in joint kinematics at different joints, including joints distal to the fatigued musculature. Despite these changes, ankle angle correlated well with AP COM position. Third, global measures of COM and COP did not reveal localized changes in sway such as joint kinematics.

The slight forward lean adopted by participants may represent a strategic change in posture which is beneficial to balance control. A slight forward lean necessitates an increase in muscle activity and concurrent increased ankle stiffness thus reducing reliance on sensory feedback control.

Qualitatively, the increase in kinematic variability in joints distal to the feet (Figure 1) is consistent with previous work by Gatev et al. (1999). Variability increases following low back fatigue are indicative of more erratic sway. Despite these changes, ankle angle remained highly correlated with COM position, suggesting that an ankle strategy

remained the predominant strategy after fatigue.

In addition, no changes were found in COM or COP displacements with fatigue in spite of simultaneous increases in joint kinematic variability. COM and COP variables are traditionally the most commonly used means of assessing sway. However, the results of this study indicate that additional or multivariate measures of sway are necessary to understand how fatigue affects movement patterns during quiet standing.

## REFERENCES

- Davidson, B.S. et al. (2004). *Eur. J. Appl. Physiol.*, **93**, 183-189.  
 Gatev, P. et al. (1999). *J. Physiol.*, **514**, 915-928.  
 Maki, B.E. et al. (1991). *J. Gerontol.*, **46**, M123-M131.  
 Kuo, A.D. et al. (1998). *Exp. Brain Res.*, **122**, 185-195.

## ACKNOWLEDGEMENTS

This work was supported by grants from the Jeffress Memorial trust, Richmond, VA, and Centers for Disease Control and Prevention.

# **CERVICAL SPINE GEOMETRY: FEMALE VERTEBRAE CANNOT BE SCALED FROM MALE VERTEBRAE**

Amber R. Bonivtch<sup>1</sup>, W. Loren Francis<sup>1</sup>, Donald E. Moravits<sup>1</sup>, Ben H. Thacker<sup>1</sup>, Frank Pintar<sup>2</sup>,  
Narayan Yoganandan<sup>2</sup>, and Daniel P. Nicolella<sup>1</sup>

<sup>1</sup>Southwest Research Institute, San Antonio, TX

<sup>2</sup>Medical College of Wisconsin, Milwaukee, WI

E-mail: amber.bonivtch@swri.org Web: www.swri.org

## **INTRODUCTION**

It is estimated that whiplash-related trauma resulting from low-speed rear impacts make up approximately 25% of all injuries resulting from automobile accidents (NHTSA). Statistically, females have twice the risk of receiving a whiplash injury as males do in automobile accidents (Mordaka, 2003). Finite element (FE) models of the cervical spine have been used since the 1980's (Brolin, 2004); however, models in which the geometry is described parametrically from easily obtained CT scans do not exist. The development of parametric and anatomically accurate finite element models representative of the human cervical spine for both genders provided the motive for this study.

Basic differences between the male and female cervical spine geometry have been noted in the literature. In studies performed by Katz (1975) and Liguoro (1994), the mean width and height of male vertebral bodies were found to be significantly larger than female vertebral bodies. In 2004, Klinich confirmed the findings of previous studies. However, in all of the cited studies, measurements were taken from lateral x-rays, computed tomography (CT) scanning would yield three dimensional results and more geometric measurements could be made. While knowledge of the differences between the male and female cervical spine exists, it is not documented in sufficient detail to create gender representative FE models.

The objective of this study is to measure the dimensions of the cervical vertebrae (C3-C7) from high fidelity CT images that can then be used to create a parametric finite element model of the cervical spine. A database will be created of the vertebral dimensions at each vertebral level of the cervical spine for both genders. A statistical comparison will also be made between the male and female values to determine which parameters are statistically different.

## **METHODS**

CT scans of the cervical spine of 73 healthy young volunteers (23 female and 50 male) were obtained in digitized format. For each cervical vertebra C3 through C7, 35 parameters were measured describing the vertebral geometry; a total of 175 parameters were measured for each volunteer. The CT image stacks were re-sliced to allow measurements on four different planes. All of the measurements were made in ImageJ (ImageJ 1.34, National Institutes of Health, USA) by a single researcher trained in reading cervical spine CT images to minimize error.

A statistical t-test procedure was used to compare the sample means of the two groups (male vs. female) for each of the 175 parameters in order to test the hypothesis that the population means are the same. An equal variance check was used to determine the type of t-test. A confidence level of 95 % (a p-value of less than 0.05)

was considered to be significant. The statistical procedure was then repeated controlling for subject weight.

## RESULTS AND DISCUSSION

A database was created containing measurements for the male and female vertebral geometry parameters at each vertebral level C3 through C7. Significant differences were found between the male and female parameters at all of the cervical levels (Table 1). The parameters were divided into five groups by the region they define: articular process (ap), pedicle (pd), spinous process (sp), transverse process (tp), and vertebral body (vb). Significant differences were found between the genders in each of these regions. A majority of the differences remained after controlling for subject weight (77 of 175 measurements), including vertebral width and height, which is in agreement with the literature.

## CONCLUSIONS

This study shows that the female cervical spine is significantly different from the male cervical spine; the female cervical spine is not simply a scaled version of the male cervical spine. Significant geometrical differences occur between the genders at each of the vertebral levels from C3 to C7. The geometry parameters found in this study are currently being used to generate parametric FE models of both genders.

## REFERENCES

- Brolin, K., Halldin, P. (2004). *Spine*, **29**(4), 376-85.
- Katz, P.R. et al. (1975). *Am J Phys Anthropol*, **43**, 319-26.
- Klinich, K.D. et al. (2004). *Proc 48th Stapp Conf*, SAE Paper No: 2004-22-0014.
- Liguoro, D. et al. (1994). *Surg Radiol Anat*, **16**, 149-55.
- Mordaka, J., Gentle, C.R. (2003). *Proc 4<sup>th</sup> European LS-DYNA Users Conference*.

**Table 1:** Measured Parameters by Vertebral Level (shaded cells, female v. male  $p < 0.05$ ).

C3	C4	C5	C6	C7
ap1	ap1	ap1	ap1	ap1
ap2	ap2	ap2	ap2	ap2
ap3	ap3	ap3	ap3	ap3
ap4	ap4	ap4	ap4	ap4
ap5	ap5	ap5	ap5	ap5
ap6	ap6	ap6	ap6	ap6
ap7	ap7	ap7	ap7	ap7
ap8	ap8	ap8	ap8	ap8
pd1	pd1	pd1	pd1	pd1
sp1	sp1	sp1	sp1	sp1
sp2	sp2	sp2	sp2	sp2
sp3	sp3	sp3	sp3	sp3
sp4	sp4	sp4	sp4	sp4
sp5	sp5	sp5	sp5	sp5
sp6	sp6	sp6	sp6	sp6
sp7	sp7	sp7	sp7	sp7
tp1	tp1	tp1	tp1	tp1
tp2	tp2	tp2	tp2	tp2
tp3	tp3	tp3	tp3	tp3
vb1	vb1	vb1	vb1	vb1
vb2	vb2	vb2	vb2	vb2
vb3	vb3	vb3	vb3	vb3
vb4	vb4	vb4	vb4	vb4
vb5	vb5	vb5	vb5	vb5
vb6	vb6	vb6	vb6	vb6
vb7	vb7	vb7	vb7	vb7
vb8	vb8	vb8	vb8	vb8
vb9	vb9	vb9	vb9	vb9
vb10	vb10	vb10	vb10	vb10
vb11	vb11	vb11	vb11	vb11
vb12	vb12	vb12	vb12	vb12
vb13	vb13	vb13	vb13	vb13
vb14	vb14	vb14	vb14	vb14
vb15	vb15	vb15	vb15	vb15
vb16	vb16	vb16	vb16	vb16

NHTSA (2006). *NASS-GES*.  
ftp.nhtsa.dot.gov/GES.

## ACKNOWLEDGEMENTS

The authors would like to thank the Naval Air Warfare Center Aircraft Division (NAWCAD) for their continuing support of this project.

# SELECTION OF A SIMULATION MODEL FOR ASSESSING INJURY RISK IN GYMNASTICS LANDINGS

Matthew Pain, Chris Mills and Fred Yeadon

Loughborough University, Loughborough, UK  
E-mail: [m.t.g.pain@lboro.ac.uk](mailto:m.t.g.pain@lboro.ac.uk) Web: [www.lboro.ac.uk](http://www.lboro.ac.uk)

## INTRODUCTION

Landing from a dismount in Artistic Gymnastics aims to reduce the velocity of the mass centre to zero within a single foot placement. The gymnast must trade off increased technical difficulty with decreased probability of a successful landing and increased risk of injury. The landing surface and the landing control strategy adopted by the gymnast contribute to the dissipation of forces at landing (McNitt-Gray et al. 1994). Optimizing landing technique using a computer simulation model of a gymnast and landing mat could be a useful tool when attempting to safely assess injury risk.

Simulation time is critical when attempting to optimize a landing technique since many iterations must be run. The model complexity used to generate the joint motion could influence simulation time and simpler models that run faster may lack some reality, therefore model evaluation is important. This study has two aims: The first is to investigate whether a torque or muscle driven model of a gymnast and landing mat is best at matching ground reaction forces. The second is to determine what level of model complexity is required to simulate landings from different skills with the intention of assessing injury risk.

## METHODS

A subject-specific 7 link wobbling mass model of a gymnast was developed using Visual Nastran4D. Three variants of this

model were implemented: a torque driven model, torque driven model with series elastic component and a lumped linear muscle with series elastic component (Model 1, Model 2 Model 3). Torque-angle-angular velocity functions for the model's joint torque generators or lumped muscles were derived from isokinetic dynamometer measurements of the gymnast. A landing mat model based on independent mat testing (Mills et al., 2006) was also developed in Visual Nastran 4D. These models were used to simulate the gymnast landing.

Landings from two vaults were recorded, vault with a backward somersault (BS), and a vault with a forward somersault (FS). Sixteen Vicon cameras (250Hz), a Phantom (v5) high-speed camera (1000Hz), a Kistler force plate (1000Hz) and a Biovision surface EMG system (250Hz) were used to collect data.

Torque activation histories were optimized using a Simplex algorithm. Weighted root mean square differences between experimental and simulated ground reaction forces, joint angle time histories and trunk orientation time history were minimized.

## RESULTS AND DISCUSSION

Model 3 performed best (Table 1) but took the longest to run a simulation and required the longest optimization time. Model 2 did not perform as well. For this activity the effect of the series elastic component could be replaced with different activation profiles

in a simpler model. For evaluation against external parameters Models 1 and 3 were very similar (Figure 1). However the internal joint reaction forces were, as expected, much higher due to the lumped muscle model producing a moment rather than a torque (Figure 2).

The simulations performed with similar accuracy to other subject specific model evaluations of dynamic activities. The single largest error was in the horizontal ground reaction force for the backward somersault and was due to a mat-force plate interaction that could not be modeled here.

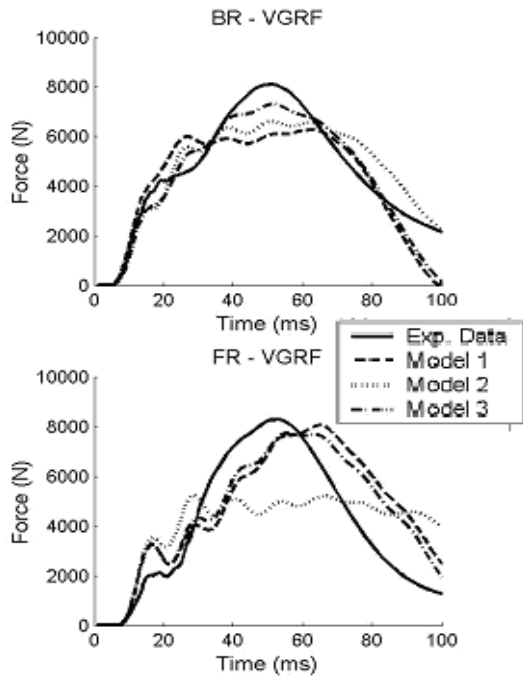


**Figure 1:** A comparison of the vertical ground reaction forces for the gymnast-mat models and equivalent experimental data.

**Table 1:** Evaluation score breakdown for the three gymnast-mat models.

Model	Skill	Total Score	VGRF	HGRF	Trunk	Joint Angles
1	BS	18.2 %	15.0 %	36.0 %	1.0°	15.0 %
	FS	11.9 %	21.0 %	15.0 %	4.0°	8.0 %
2	BS	17.6 %	14.9 %	35.8 %	0.8°	19.0 %
	FS	13.9 %	25.7 %	12.7 %	5.1°	12.3 %
3	BS	16.2 %	12.1 %	36.1 %	0.8°	15.7 %
	FS	10.1 %	16.8 %	12.3 %	4.6°	6.6 %

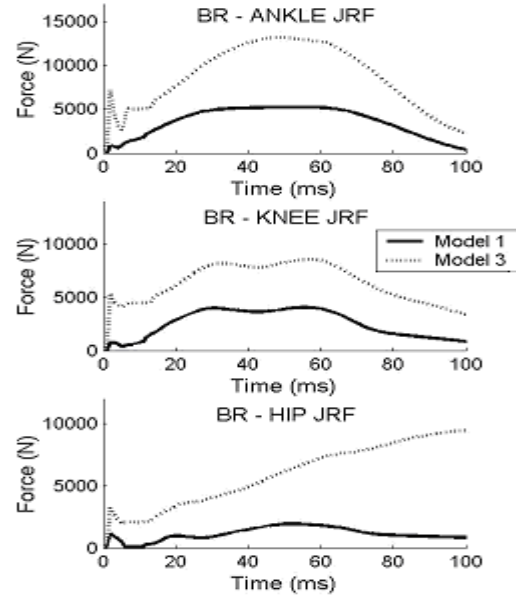


**Figure 2:** Calculated joint reaction forces using models one and three.

### SUMMARY/CONCLUSIONS

External performance criteria were similar for Models 1 and 3. For performance analysis Model 1, which runs faster, would be suitable. For injury assessment Model 3 is needed as Model 1 underestimates the internal loading on joints and bones. Model 1 and 2 always gave values way below those associated with acute injury levels. In this case the need for more realistic internal forces offsets the reduction in the number of simulation studies that can be performed.

### REFERENCES

- McNitt-Gray, J., et al. (1994). *J. App Biomech*, **10**, 237-252.  
 Mills; C., et al. (2006). *J. App Biomech*, **22**, 103-111.

# BILATERAL COMPARISON OF KNEE EXTENSOR MECHANISM AND PATELLAR TENDON LENGTH IN YOUNG ADULTS WITH HEALTHY KNEES

John W. Chow, Jeff T. Wight, Ryan A. Mizell, and Mark D. Tillman

Department of Applied Physiology & Kinesiology, University of Florida, Gainesville, FL, USA  
E-mail: jchow@hhp.ufl.edu Web: www.hhp.ufl.edu/apk/ces/labs/biomech/

## INTRODUCTION

To examine the effect of injuries and surgical interventions on knee biomechanics, the non-injured knees of the patients were commonly used as controls for comparison purposes in previous studies. For example, using radiography and MRI techniques, respectively, Breitfuss et al. (1996) and Meisterling et al. (1993) explored possible changes in patellar tendon length due to anterior cruciate ligament (ACL) reconstruction by comparing the data collected from the operated knee with the non-operated knee of the same subject. These authors assumed that there were minimum bilateral differences in knee geometry before the ACL injury. However, the validity of such an assumption has not been examined. Therefore, the purpose of this study was to investigate whether significant bilateral differences in knee extensor mechanism and patellar tendon length existed in individuals with healthy knees.

## METHODS

Sagittal knee radiographs of both knees at 4 different knee flexion angles ( $40^\circ$  to  $85^\circ$  at intervals of  $15^\circ$ ) were obtained from 6 males and 6 females (age  $22.4 \pm 1.9$  yrs, height  $172 \pm 10$  cm, weight  $782 \pm 121$  N) who had no history of major knee injuries or surgery. To load the knee joint, the subject sat on a stool located next to an x-ray film and performed isometric knee extensions with maximal effort when the radiographs were taken. To provide the resistance to knee

extension, a steel cable with one end connected to an ankle strap and the other end fastened to an angle iron fixed to the bottom of the stool was used (Figure 1). A metal pin with a length of 10.15 cm was placed on the anterior surface of the patella tendon for spatial reference.

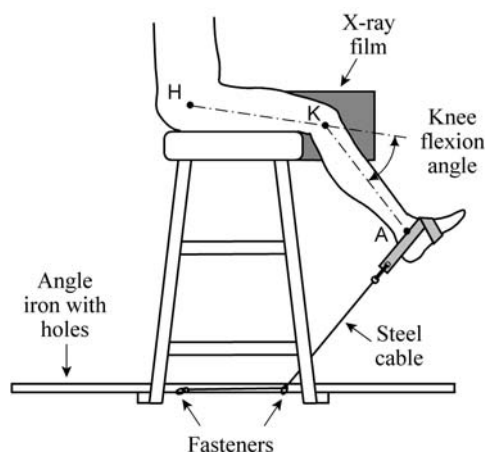


**Figure 1:** Schematic showing the stool used for radiographic data collection.

Each radiograph was analyzed by 3 analysts independently using the same procedures/instructions. The detail procedures and its reliability were reported in Chow et al. (2006). In essence, each analyst identified different landmarks on a radiograph for the determination of the lines of action of the patellar tendon, quadriceps tendon, and patellofemoral joint contact forces and the patellofemoral and tibiofemoral contact points. The effective moment arm of the quadriceps was computed as the product of the moment arm of the patellar tendon force about the tibiofemoral contact and the mechanical

advantage of the patellar mechanism (the ratio of the moment arms of the patellar tendon and quadriceps tendon force acting on the patellofemoral joint) (Grood et al., 1984).

The proximal attachment of the patellar tendon is the midpoint between the most inferior point of the anterior surface of the patella and the most inferior aspect of the patella. The distal attachment of the patellar tendon is the midpoint between the deepest superior tibial indentation and the farthest tibial protrusion. The patellar tendon length is the shortest distance between the proximal and distal attachments. The average values over 3 analysts were used in subsequent statistical analyses. In addition to descriptive statistics, bilateral differences were examined using t-tests with repeated measures. To adjust for multiple tests, the alpha level was set at 0.00625 (0.05/8).

## RESULTS AND DISCUSSION

No significant bilateral differences were found in any of the effective moment arm and patellar tendon length measures. The relatively large SD values indicate large individual differences in knee geometry (Table 1).

The effective moment arm values are within the range of values reported in the literature (Chow et al., 1999). The results also agree with previous findings that the effective

moment arm decreases with increasing knee flexion for knee flexion angles greater than 40°.

Though not statistically significant, the average patellar tendon length of the right knee is greater than the left side in all knee flexion angles included in this study. Future studies should investigate whether such trend is just a coincidence.

## SUMMARY/CONCLUSIONS

The lack of significant bilateral differences suggests that the non-operated healthy knee can serve as the control for examining the effect of injuries and surgical interventions on knee biomechanics if measures before injuries and surgeries are not available.

## REFERENCES

- Breitfuss, H. et al. (1996). *Knee Surg. Sports Traumatol. Arthrosc.*, **3(4)**, 194-198.  
 Chow, J.W. et al. (1999). *J. Appl. Biomech.*, **15**, 166-174.  
 Chow, J.W. et al. (2006). *Knee*. (in press)  
 Grood, E.S. et al. (1984). *J. Bone Joint Surg.*, **66-A**, 725-734.  
 Meisterling, R.C. et al. (1993). *Clin. Orthop. Relat. Res.*, **289**, 208-212.

## ACKNOWLEDGEMENTS

We appreciate the assistance of Stacy Colon, Lindsay Dole, and Kim Fournier.

**Table 1:** Mean (SD) effective moment arm and patellar tendon length values.

Knee flexion angle (°)	Effective moment arm (cm)			Patellar tendon length (cm)		
	Left	Right	p-value	Left	Right	p-value
40	4.38 (0.36)	4.23 (0.30)	0.113	5.32 (0.66)	5.47 (0.50)	0.229
55	3.88 (0.46)	4.01 (0.36)	0.193	5.25 (0.68)	5.46 (0.46)	0.127
70	3.24 (0.40)	3.26 (0.46)	0.784	5.28 (0.64)	5.54 (0.38)	0.051
85	2.63 (0.28)	2.69 (0.45)	0.587	5.29 (0.64)	5.43 (0.49)	0.265

# PROELASTIC FINITE ELEMENT MODEL TO PREDICT THE FAILURE PROGRESSION IN A LUMBAR DISC DUE TO CYCLIC LOADING

R.N Natarajan (1,2), J.R Williams (1), S.A Lavender (3), G. BJ Andersson (1)

(1) Rush University Medical Center, Chicago, Illinois. (2) University of Illinois at Chicago, Chicago, Illinois, (3) Ohio State University, Columbus, Ohio  
E-mail: raghu\_natarajan@rush.edu

## INTRODUCTION

The intervertebral disc is susceptible to ruptures and degenerative processes. Autopsy studies have shown that the formation of annular tears, dehydration of the nucleus pulposus, and fissure formation in the cartilage endplate are the main early macroscopic features that characterize disc degeneration. Understanding how failure originates and progresses in a motion segment subjected to cyclic loading conditions is thus important to understand the process of disc degeneration.

Initiation and propagation of different types of events that lead to disc degeneration and the effect of the degenerative process on the disc mechanical performance is difficult to study by experimental techniques. Therefore, the aim of this investigation is to model the development of annular tears and endplate fissures and study the propagation of these degenerative processes in a lumbar motion segment subjected to cyclic loading that correspond to a certain heavy physical work activity. The hypothesis of this study is that the failure progression due to cyclic loading increases exponentially as the drained elastic modulus of the failed disc components decreases (as compared to modulus of the intact portion) due to presence of failure.

## METHODS

A previously validated three-dimensional poro-elastic finite element model of the L4-L5 motion segment including biological parameters (swelling pressure and strain dependent permeability

and porosity) was used [1]. Elastic and poro-elastic material properties for the nucleus, inner annulus and outer annulus were varied regionally according to values taken from the literature. The annular fibers were modeled using several layers of large number of “re-bar” elements that accurately model the bulging of the annulus due to large compression and shear loads experienced during the heavy physical work activities.

Failure initiation and progression was modeled using a “user-supplied-material” function available in the finite element code (ADINA). Failure initiation and progression in all the disc components was modeled as follows: due to the applied load if at any integrating point in an element representing the disc the von-Mises stress is greater than the corresponding failure stress, the drained elastic modulus of material at that integrating point is reduced by an assumed percentage of the intact elastic modulus value and used for subsequent analyses. This method allows prediction of the location of failure initiation in any component of the disc and follows the failure progression continuously as the cyclic loading continues.

The physiological loading conditions used in this investigation involved pulling a box with a force of 140 N using a handle at 142 cms above the ground. A muscle optimization model using EMG and kinematics data collected in a lifting laboratory was used to calculate spinal loads as a function of time. Five cycles of activity per minute was modeled in the current

study. During each cycle, push-pull activity was completed in 5 seconds followed by a rest for 7 seconds. The rest period was simulated by applying an axial compressive load of 400 N.

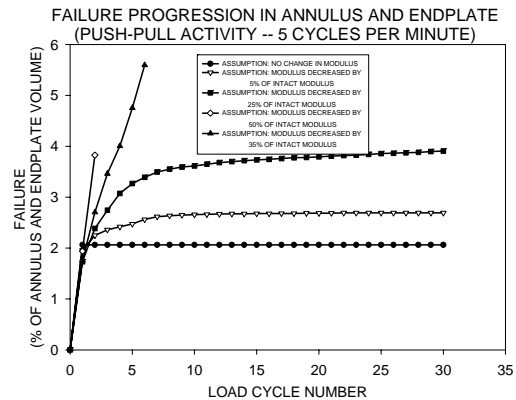
The number of integrating points where failure occurred in various elements representing different components of the disc was collected at the end of each load cycle. Percentage of disc failure volume at the end of each load cycle was calculated by dividing the number of failed integrating points by the total number of integrating points in the disc.

## RESULTS

The failure initiated both in the endplate and annulus during the first load cycle. Annular failure initiated on the interface surface between the bottom endplate and inner annulus. On the other hand, endplate failure initiated at the top endplate. Both annular and endplate failure initiations occurred in the right lateral quadrant of the disc. As the load cycle increased, endplate failure progressed towards the center of the endplate as well as along the anterior quadrant of the top endplate. Failure in the annulus progressed outward as the number of load cycles increased.

There was no change in disc failure volume as the load cycle increased (Figure) when it was assumed that the drained elastic modulus of failed disc components were not altered (due to failure) in the subsequent load cycle analyses. On the other hand, when the drained elastic modulus of the failed disc components were decreased in the subsequent analyses by 30% of the corresponding intact drained elastic modulus, failure was found to propagate. The analyses also showed that the rate at which the disc failure volume increased as the load cycle progressed (slope of the curve) was greater as the assumed decrease

in drained elastic modulus due to failure increased. The result showed that the disc failure volume increased exponentially as the reduction in drained elastic modulus at the failure locations in the disc components increased.



## SUMMARY/CONCLUSIONS

The results of the current study support our hypothesis that the failure progression due to cyclic loading exponentially increases as the assumed drained elastic modulus of the failed disc components decrease. Since the failed portion of the disc was able to carry a much smaller share of the load (due to larger percentage reduction in drained elastic modulus in such regions) progression of failure was exponential. The results presented here is a conformation that the current concepts used in modeling the failure progression in a lumbar disc are reasonable.

## REFERENCES

1. Natarajan, R. N., Williams J. R., and Andersson G. B. J., 2004, "Recent Advances in Analytical Modeling of Lumbar Disc Degeneration", *Spine*: 29(23), pp. 2733-2741.

## ACKNOWLEDGEMENTS

NIH: AR48152-02.

# DISTINCT WAVEFORM CHARACTERISTICS OF PULSED ELECTROMAGNETIC FIELDS UNDERLIE POST-EXPOSURE CHANGES IN $\alpha 1(I)$ COLLAGEN CONCENTRATION IN CONDITIONED MEDIUM OF MOUSE OSTEOBLASTS

Mark D. Grabiner<sup>1</sup>, Yoshi Sakai<sup>3</sup>, Thomas A. Patterson<sup>2</sup>,  
Alan Wolfman<sup>2</sup>, Maciej Zborowski<sup>2</sup>, Ronald J. Midura<sup>2</sup>

<sup>1</sup>University of Illinois at Chicago, Chicago, Illinois USA

<sup>2</sup>The Cleveland Clinic Foundation, Cleveland, Ohio USA

<sup>3</sup>Kobe University, Kobe, Japan

grabiner@uic.edu

## INTRODUCTION

The mechanisms by which pulsed electromagnetic fields (PEMF) influence osteoblast biology have not been elucidated. In addition, the physical properties of PEMF that induce these influences have not been characterized. In mouse pre-osteoblasts, the reduction of mature,  $\alpha 1(I)$  collagen in the extracellular matrix (ECM) and the conditioned medium was mediated by a distinct time-amplitude characteristic of the three PEMF waveforms used in that study (Sakai et al., 2006). This provided support for the hypothesis that osteoblasts are sensitive to specific waveform characteristics. The present study further tested this hypothesis by the addition of a PEMF waveform having considerably different characteristics in the time-amplitude domain.

## METHODS

After passaging and growing for 5 days MC3T3-E1 subclone 30 cells were exposed to PEMF. Culture dishes were placed in an incubator between a pair of 29.5 x 29.5 cm Helmholtz coils. Sham controls were placed in an identical incubator with unpowered coils. Four pulsed electromagnetic fields having substantial between-waveform differences in the time-amplitude and frequency-amplitude domains were used in this study (Figure 1, Table 1).

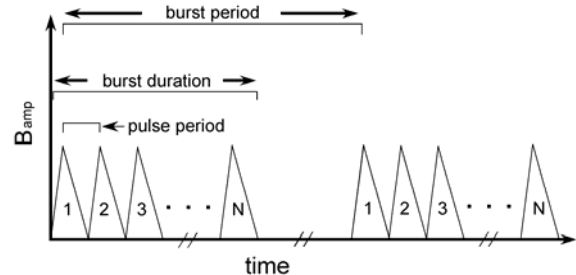


Figure 1: Diagram of the temporal variables of the PEMF waveforms.

Waveform	Bamp (mT)	pulse period ( $\mu$ s)	burst duration (ms)	burst period (ms)
A	0.4	260	5.46	67.1
B	0.3	260	25.48	671
C	0.015	16	25.90	671
D	1.2	260	66.66	4.6

Table 1: Values for the temporal variables of each PEMF waveform.

Cells were exposed to PEMF waveforms generated by coils oriented such that the induced magnetic field was parallel (horizontal) relative to the surface of the culture dishes. The magnetic field intensity and the rate of change of the magnetic field to which the cells were exposed were controlled by placing the culture dishes at two different locations within the coil volume.

The extracellular matrix was isolated by exhaustively rinsing the cell layers with PBS at room temperature followed by three repeated treatments (10 minutes each) with

0.5% sodium deoxycholate (10 mM Tris-Cl buffered saline, pH 8.0, 1 mM phenylmethylsulfonyl fluoride) at 4°C. The dishes were then treated 3 successive times with 2 mM Tris-Cl, pH 8.0 containing 1 mM PMSF for 10 minutes at 4°C. After each incubation the aqueous phase was carefully removed by aspiration. The remaining matrix was scraped into 1 ml of Lysis Buffer (20 mM MOPS, pH 7.0, 5 mM EDTA, 2 mM EGTA, 2 mM sodium orthovanadate, 40 mM  $\beta$ -glycerophosphate, 10 mM sodium pyrophosphate, 30 mM sodium fluoride, 1 mM phospho-Ser, 0.5 mM phospho-Tyr, 0.5 mM phospho-Thr, 1 mM PMSF, 10  $\mu$ M leupeptin and 5  $\mu$ M pepstatin A containing 0.5% TX-100) and sonicated. The ECM extracts were centrifuged at 13,000 x g for 30 minutes at 4°C and the supernatant was retained for further analysis.

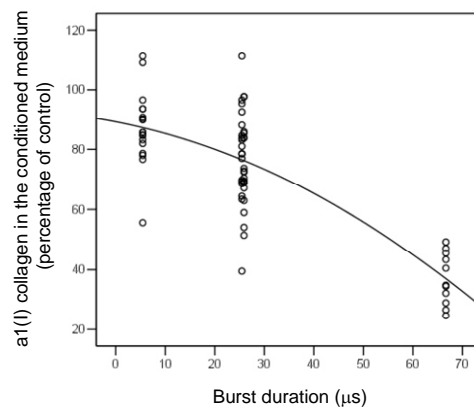
The spatial field distribution between the field-generating coils was measured using an inductive search coil that detected the local value of the magnetic field time derivative, dB/dT. This signal was amplified, digitized (bandwidth: 500 MHz, sampling rate of 1 GHz) and stored for off-line analysis. The field was mapped by positioning the search coil along the three axes of symmetry of the coil system, in spatial increments of 2.54 cm.

The independent variable in the statistical design was the concentration of  $\alpha 1(I)$  collagen in the conditioned medium ( $\alpha 1(I)_{\text{medium}}$ ) subsequent to PEMF exposure. The significance of the main effects terms from a 4 by 2 (waveform by amplitude) ANOVA provided guidance for subsequent regression analyses. Ultimately, a series of stepwise multiple linear regression models using the  $\alpha 1(I)_{\text{medium}}$  as the dependent variable were used to test the hypothesis that a significant proportion of the variance of  $\alpha 1(I)_{\text{medium}}$  following PEMF exposure would

be explained by the selected waveforms characteristics. The independent variables were the amplitude of the magnetic field, the pulse period, the burst period, the burst duration, and the frequencies of the latter three variables. The statistics were performed using SPSS 12.0 (Chicago, IL).

## RESULTS

The between-signal differences in  $\alpha 1(I)_{\text{medium}}$  were significant ( $p < 0.001$ ). The regression analyses revealed a quadratic relationship between burst duration and  $\alpha 1(I)_{\text{medium}}$ . The quadratic term of burst duration accounted for 62 percent of the variance in  $\alpha 1(I)_{\text{medium}}$  ( $p < 0.001$ , standard error of the estimate = 13.22).



## DISCUSSION

The results demonstrate the statistical and biological importance of specific waveform characteristics with regard to the influence of PEMF on mouse pre-osteoblasts. In particular, burst duration appears to exert a strong influence of the biological response of osteoblasts to PEMF treatment.

## REFERENCES

Sakai et al. (2006) *J Orthop Res*, 24:242-53.

## ACKNOWLEDGMENT

The authors gratefully acknowledge funding from OREF and Orthofix, Inc.

# AN INTEGRATED APPROACH FOR IMPROVING GAIT IN A STROKE POPULATION: COMBINING ROBOTICS, FES AND NEUROMUSCULOSKELETAL MODELING

Daniel L Benoit, Vijaya Krishnamoorthy, Sai Banala, Wei-Li Hsu, Ramu Perumal, Trisha Kesar, John P. Scholz, Sunil K Agrawal, Stuart Binder-MacLeod, and Thomas S Buchanan

University of Delaware, Newark, DE, USA  
Center for Biomedical Engineering Research  
E-mail: benoit@me.udel.edu

## INTRODUCTION

Stroke is one of the leading causes of functional disability among American adults. The effects of post-stroke hemiparesis include reduced muscular strength and endurance as well as diminished mechanical work output and altered muscular activation patterns during gait. These combined effects lead not only to reduced mobility but may also contribute to increased injuries from falls in this population (Nyberg et al 1995).

The overall goal of this project is to assist patients with CNS dysfunction to produce improved walking patterns through a combination of functional electrical stimulation (FES), robotic-assistive training and biomechanical modeling.

## METHODS

This project combines the resources of the mechanical engineering and physical therapy departments at the University of Delaware to develop and integrate a robotic gait rehabilitation device with an intervention strategy to progressively facilitate hemiparetic patients during gait. This will be combined with an electrical stimulation protocol developed with a minimal intervention strategy based on musculoskeletal modeling and gait simulation.

**I. Robotic device:** This project required the creation of a novel robotic assistive device capable of providing varying and adjustable degrees of assistive intervention throughout

the gait cycle. The first prototype achieved this by compensating for the effect of gravity on the subject's affected limb through the use of adjustable springs and pulleys<sup>1</sup>. The second generation device uses motorized joints that allow the subject to move within acceptable boundaries, or virtual walls, before assistance is provided within a dynamic control environment.

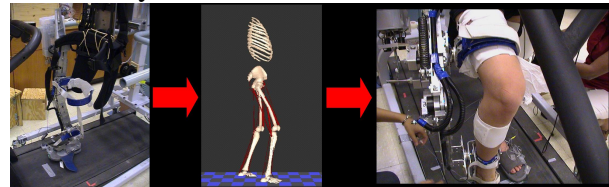


**Figure 1:** Organization of the research approach: from left, a robotic assistive device is combined with subject-specific musculoskeletal modeling and simulation in order to improve gait.

**II. Intervention strategy:** Since the robotic device is designed to be minimally assistive, the patient is required to initiate and correct their motions throughout the gait cycle while being guided through a movement pattern progressively more similar to the correct pattern. The level of assistance provided by the device can be adjusted to optimize learning and take advantage of the plasticity inherent in the central nervous system.

**III. Electrical stimulation:** Fatigue is a major concern when applying FES. A minimally invasive approach is therefore desired and can be achieved when the stimulation is meant to compliment, rather than replace, existing voluntary muscle activation. The

assistance provided by the electrical stimulation will vary according to the real-time needs of the patient to augment the volitional activity. The level of stimulation needed is based on that determined through modeling and simulation in order to minimize the intervention.

**IV. Modeling and simulation:** We have created a biomechanical model of the ankle to estimate the corrective increases in muscle activation patterns that would enable post-stroke patients to walk normally. This information will be used to control the stimulation device and will be optimized for each patient, thus providing the minimal additional activation required by the stimulator to achieve the desired joint motions.

## RESULTS AND DISCUSSION

### Robotic device and intervention:

Preliminary results indicate that hemiparetic stroke patients using the device have increased joint excursions during gait (figure 2) when the effect of limb weight is reduced<sup>2</sup>. This improved range of motion is more similar to the motion of healthy controls using the device.

**Muscle stimulation and modeling:** We have found that the original ankle joint moment of the stroke patients can be ‘morphed’ to

produce a healthy joint moment profile by increasing ankle and plantar flexor activity. The electrical stimulation model developed for this project also predicts joint torque outputs based on electrical stimulation and the additive effect of electrical stimulation on volitional activation is currently being explored.

## SUMMARY/CONCLUSIONS

As all phases of the project move forward, integration of each component is taking place. This unique and multi-disciplinary approach promises to provide novel rehabilitation alternatives to patients exhibiting hemiparetic gait impairment.

## REFERENCES

1. Banala S.K., Agrawal S.K., Fattah A., Rudolph K., Scholz J.P., "Gravity Balancing Leg Orthosis for Robotic Rehabilitation", *IEEE Proc. Int. Conf. of Robotics and Automation*, 2004, 2474-2479
2. Banala, S. K., Agrawal, S. K., Fattah, A., Scholz, J. Krishnamoorthy, V., Rudolph, K., and Lie, W., "Gravity Balancing Orthosis and Its Performance Evaluation", *IEEE Trans. on Robotics*, 2006 (In Review).

## ACKNOWLEDGEMENTS

The following people have greatly contributed to this project: Drs. J. Higginson, K Manal, K Rudolph, A. Fattah, and D. Bassett, Q. Shao, C. Crabtree. This project is funded by NICHD (R01-HD38582).

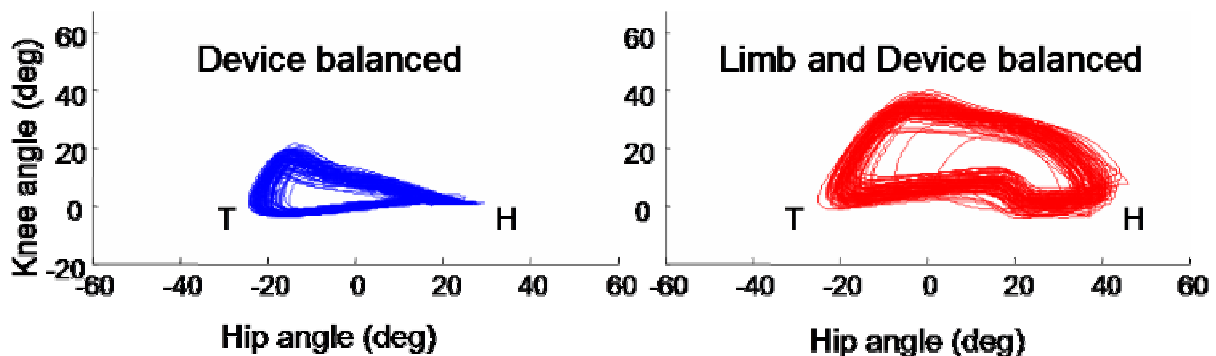


Figure 2: Hip and knee joint excursions of a representative stroke subject throughout the gait cycle. T and H represent toe-off and heel-strike respectively. In ‘Device balanced’ only the weight of the assistive device is removed; in ‘Limb and device balanced’ both the device and the limb weight are removed, reducing the work required by the patient to produce motion.

# LOADED PATELLAR TENDON LENGTHS IN ACL RECONSTRUCTED KNEES

John W. Chow, Jeff T. Wight, Ryan W. Johnson, and Mark D. Tillman

Department of Applied Physiology & Kinesiology, University of Florida, Gainesville, FL, USA  
E-mail: jchow@hhp.ufl.edu Web: www.hhp.ufl.edu/apk/ces/labs/biomech/

## INTRODUCTION

A possible change in patellar tendon length due to anterior cruciate ligament reconstruction (ACLR) has been a topic of interest for many years and inconsistent findings have been reported. For example, Meisterling et al. (1993), Shelbourne et al. (1995), and Krosser et al. (1996) found no significant change in patellar tendon length after ACLR. Alternatively, Breitfuss et al., (1996) found an average patellar tendon shortening of 3 mm (9.8%) on the donor site in 41 ACLR knees by evaluating bilateral knee radiographs. Using MRI to evaluate patellar tendon lengths during the first year after ACLR, Bernicker et al. (1998) found the length decreased significantly (by 8%) over 12 months. It is worth noting that patellar tendon lengths were measured while the tendon is not loaded in these studies. The purpose of this study was to investigate whether significant differences in patellar tendon length existed between ACLR and non-operated knees when the tendon was maximally loaded during knee extensions.

## METHODS

Sagittal knee radiographs of both knees at 5 different knee flexion angles (25° to 85° at intervals of 15°) were obtained from 6 males (age 21.2±2.3 yrs, 3.4±2.1 yrs post-op; 3 patellar tendon, 2 hamstring, 1 allograft) and 7 females (age 20.0±2.0 yrs, 2.9±3.0 yrs post-op; 4 patellar tendon, 3 allograft) who had unilateral ACLR. To load the knee joint, each subject sat on a stool located next to an x-ray film and performed isometric knee extensions with maximal effort when

the radiographs were taken. A steel cable with one end connected to an ankle strap and the other end fastened to an angle iron fixed to the bottom of the stool was used to provide resistance to knee extension (Figure 1). A metal pin with a length of 10.15 cm was placed on the anterior surface of the patella tendon for spatial reference.

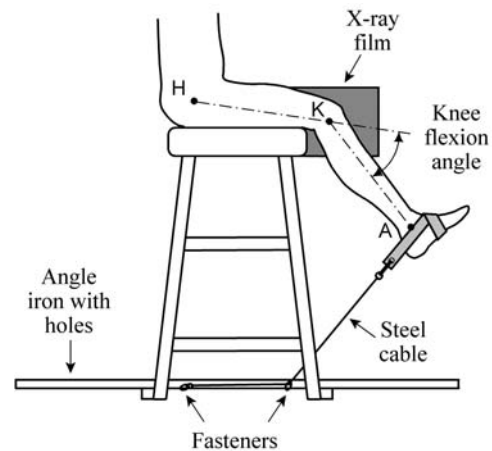


**Figure 1:** Schematic showing the stool used for radiographic data collection.

Each radiograph was analyzed by 2 analysts independently using the same guidelines. Specifically, each analyst identified 4 points on a radiograph (Figure 2):

- Ends of the metal pin.
- The proximal attachment of the patellar tendon – the midpoint between the most inferior point of the anterior surface of the patella and the most inferior aspect of the patella.
- The distal attachment of the patellar tendon – the midpoint between the deepest superior tibial indentation and the farthest tibial protrusion.

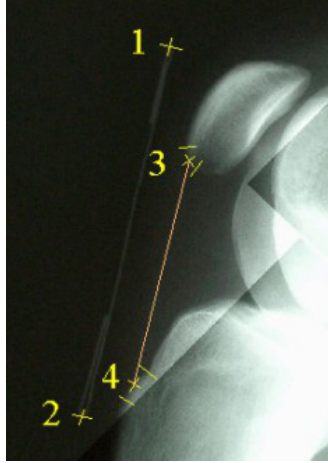


**Figure 2:** Points identified on each X-ray.

The patellar tendon length is the shortest distance between the proximal and distal attachments. The average values over 2 analysts were used in subsequent statistical analyses. For each knee flexion angle, 2 paired t-tests, one using data from all 13 subjects and the other with data from 7 patellar tendon autograft subjects, were performed to compare patellar tendon lengths of the ACLR and uninvolved knees. The alpha level was set at 0.005 (0.05/10) to adjust for multiple tests.

## RESULTS AND DISCUSSION

No significant differences were found between ACLR and involved knees (Table 1). Our results support the findings of Meisterling et al. (1993), Shelbourne et al. (1995), and Krosser et al. (1996). However, these results must be interpreted with caution. There are several limitations in the

current study. Because subjects were recruited from a general student population, ACLR surgical procedures and rehabilitation programs were not controlled. The small sample size is another limitation.

## SUMMARY/CONCLUSIONS

The lack of significant differences between ACLR and non-operated knees suggests that ACLR surgeries do not significantly affect the length of the patellar tendon regardless of graft type. Changes in knee extensor function as a result of ACLR are not likely due to a change in patellar tendon length. To confirm these speculations, a larger sample size for each graft type should be used in future studies.

## REFERENCES

- Bernicker, J.P. et al. (1998). *Arthroscopy*, **14**, 804-809.  
 Breitfuss, H. et al. (1996). *Knee Surg. Sports Traumatol. Arthrosc.*, **3(4)**, 194-198.  
 Krosser, B.I. et al. (1996). *Am. J. Knee Surg.*, **9**, 158-160.  
 Meisterling, R.C. et al. (1993). *Clin. Orthop. Relat. Res.*, **289**, 208-212.  
 Shelbourne, K.D. et al. (1995). *Orthopedics*, **18**, 1073-1077.

## ACKNOWLEDGEMENTS

We appreciate the assistance of John D. Garbrecht and Michelle Davis.

**Table 1:** Mean (SD) patellar tendon length values (cm).

Knee flexion angle (°)	Overall: 13 subjects			Patellar tendon autograft: 7 subjects		
	ACLR	Uninvolved	p-value	ACLR	Uninvolved	p-value
20	4.89 (0.56)	5.16 (0.77)	0.040	5.24 (0.31)	5.48 (0.73)	0.304
40	4.76 (0.48)	4.71 (0.59)	0.511	5.16 (0.33)	5.16 (0.42)	0.971
55	4.84 (0.59)	4.78 (0.59)	0.442	5.17 (0.54)	5.12 (0.48)	0.729
70	4.86 (0.60)	4.65 (0.69)	0.081	5.17 (0.39)	4.80 (0.86)	0.178
85	4.81 (0.51)	4.64 (0.64)	0.246	5.11 (0.19)	4.97 (0.59)	0.571